



Moscow International Symposium on Magnetism

29 June – 3 July 2014

Book of Abstracts

M.V. Lomonosov Moscow State University, Faculty of Physics

Main Topics

Spintronics and Magnetotransport
Magnetophotonics (linear and nonlinear magneto-optics, magnetophotonic crystals)
High Frequency Properties and Metamaterials
Diluted Magnetic Semiconductors and Oxides
Magnetic Nanostructures and Low Dimensional Magnetism
Magnetic Soft Matter (magnetic polymers, complex magnetic fluids and suspensions)
Soft and Hard Magnetic Materials
Magnetic Shape-Memory Alloys and Magnetocaloric Effect
Multiferroics
Magnetism and Superconductivity
Magnetism in Biology and Medicine
Theory

Editors: N. Perov
V. Samsonova
A. Kharlamova
L. Loginova
A. Semisalova

Moscow 2014

С623
УДК 537
ББК 22.334

**Moscow International Symposium on Magnetism
(MISM)**

29 June – 3 July 2014, Moscow

Book of Abstracts

The text of abstracts is printed from original contributions.

Faculty of Physics M.V. Lomonosov MSU

Физический факультет МГУ имени М.В. Ломоносова

“Moscow International Symposium on Magnetism”
is included in the list of events of the EU-Russia Year of Science



ISBN 978-5-91978-025-0

© MISM - 2014

Contributors to MISM 2014

Moscow International Symposium on Magnetism expresses its warmest appreciation on the following organizations for their generous support

	Lomonosov Moscow State University
	Russian Foundation for Basic Research
	Faculty of Physics
	Japan Society for the Promotion of Science
	Institute for Theoretical and Applied Electromagnetics of Russian Academy of Sciences
	Russian Academy of Science (RAS)
	Moscow Government Department of Science
	Dynasty Foundation (Moscow)
	German Houses for Research and Innovation

Organizing Committee

Chairmen: A. Vedyayev
A. Granovsky
N. Perov

Secretary: A. Semisalova

International Advisory Committee

M. Barandiaran	<i>Bilbao</i>	X. Jin	<i>Shanghai</i>
A. Buzdin	<i>Bordeaux</i>	D. Khomskii	<i>Koeln</i>
B. Dieny	<i>Grenoble</i>	D. Khmel'nitskii	<i>Cambridge</i>
D. Givord	<i>Grenoble</i>	C. Lacroix	<i>Grenoble</i>
B. Hernando	<i>Oviedo</i>	S. Maekawa	<i>Tokai</i>
M. Farle	<i>Duisburg</i>	D. Mapps	<i>Plymouth</i>
A. Fert	<i>Orsay</i>	S. Nikitov	<i>Moscow</i>
D. Fiorani	<i>Rome</i>	S. Ovchinnikov	<i>Krasnoyarsk</i>
A. Freeman	<i>Evanston</i>	S. Parkin	<i>San Jose</i>
J. Gonzalez	<i>San Sebastian</i>	H. Szymczak	<i>Warsaw</i>
B. Heinrich	<i>Burnaby</i>	V. Ustinov	<i>Ekaterinburg</i>
M. Inoue	<i>Toyohashi</i>	M. Vazquez	<i>Madrid</i>

National Advisory Committee

Chairman: N. Sysoev

A. Fedyanin	A. Lagar'kov	L. Prozorova	A. Vasiliev
M. Chetkin	S. Maleev	V. Prudnikov	V. Veselago
D. Khokhlov	S. Nikitin	V. Shavrov	N. Volkov

Program Committee

Chairman: A. Granovsky

Secretary: A. Semisalova

M. Acet	<i>Duisburg</i>	Yu. Pastushenkov	<i>Tver</i>
B. Aktas	<i>Gebze</i>	N. Pugach	<i>Moscow</i>
B. Aronzon	<i>Moscow</i>	A. Pyatakov	<i>Moscow</i>
N. Bebenin	<i>Ekaterinburg</i>	A. Radkovskaya	<i>Moscow</i>
D. Berkov	<i>Jena</i>	Yu. Raikher	<i>Perm</i>
V. Chernenko	<i>Moscow</i>	K. Rozanov	<i>Moscow</i>
M. Chshiev	<i>Grenoble</i>	E. Shalygina	<i>Moscow</i>
E. Gan'shina	<i>Moscow</i>	E. Shamonina	<i>Erlangen</i>
A. Gencer	<i>Ankara</i>	A. Smirnov	<i>Moscow</i>
O. Kazakova	<i>London</i>	L. Tagirov	<i>Kazan</i>
Cheol Gi Kim	<i>Daejon</i>	N. Usov	<i>Moscow</i>
A. Kimel	<i>Nijmegen</i>	A. Vinogradov	<i>Moscow</i>
A. Kirilyuk	<i>Nijmegen</i>	A. Zhukov	<i>San Sebastian</i>
K. Kugel	<i>Moscow</i>	M. Zhuravlev	<i>Moscow</i>
G. Kurlyandskaya	<i>Ekaterinburg</i>	V. Zubov	<i>Moscow</i>
X. Li	<i>Singapore</i>	M. Yamaguchi	<i>Sendai</i>
L. Nikitin	<i>Moscow</i>		
V. Novosad	<i>Argonne</i>		

Local Committee

Chairman: N. Perov

N. Abrosimova	D. Krasil'nikova	I. Rodionov
T. Andrianov	A. Kudakov	V. Samsonova
S. Granovsky	Yu. Kurbatova	A. Semisalova
E. Gan'shina	L. Loginova	T. Shapaeva
Yu. Gritsenko	A. Loseva	N. Strelkov
D. Isaev	L. Mironova	N. Svechkina
E. Feoktistova	L. Nikitin	I. Titov
D. Kadyshev	A. Novikov	A. Titova
M. Khairullin	E. Pan'kova	V. Tyablikov
A. Kharlamova	Ya. Pile	E. Shalygina
I. Kovaleva	V. Prudnikov	V. Zubov
S. Koptsik	M. Prudnikova	G. Zykov
O. Kotel'nikova	A. Radkovskaya	A. Yakushechkina

CONTENTS

30 JUNE	9
PLENARY LECTURES.....	9
ORAL SESSION.....	13
“Spintronics and Magnetotransport”.....	13
“Magnetism and Superconductivity”.....	23
“Magnetophotonics and Optomagnetism”.....	33
“Magnetic Shape Memory and Magnetocaloric Effect”.....	37
“Multiferroics”.....	47
“Soft and Hard Magnetic Materials”.....	57
“Magnetic Oxides”.....	71
“Magnetic Soft Matter (magnetic polymers, fluids and suspensions)”.....	75
“Magnetism of Nanostructures”.....	81
“Low Dimensional Magnetism”.....	93
“High Frequency Properties and Metamaterials”.....	99
“Diluted Magnetic Semiconductors”.....	105
“Magnetoplasmonics”.....	113
“Theory”.....	121
POSTER SESSION.....	129
“Magnetic Nanostructures and Low Dimensional Magnetism”.....	129
“Magnetism and Superconductivity”.....	169
“Diluted Magnetic Semiconductors and Oxides”.....	201
“Magnetism in Biology and Medicine”.....	217
“Spintronics and Magnetotransport”.....	229
“Multiferroics”.....	257
“Soft and Hard Magnetic Materials”.....	281
1 JULY	301
PLENARY LECTURES.....	301
ORAL SESSION.....	305
“Spintronics and Magnetotransport”.....	305
“Magnetism and Superconductivity”.....	317
“Materials & Nanostructures”.....	331
“Magnetic Shape Memory and Magnetocaloric Effect”.....	339
“Magnetism in Biology and Medicine”.....	351
“Diluted Magnetic Semiconductors”.....	363
“Magnetism of Nanostructures”.....	369
“Magnetophotonics”.....	381
“Multiferroics”.....	391
“Low Dimensional Magnetism”.....	397
“Soft and Hard Magnetic Materials”.....	403
“Magnetic Soft Matter (magnetic polymers, fluids and suspensions)”.....	413
“Magnetic Oxides”.....	421
“Topological Insulators”.....	427
POSTER SESSION.....	435
“Magnetic Nanostructures and Low Dimensional Magnetism”.....	435
“Magnetic Shape Memory and Magnetocaloric Effect”.....	471
“Diluted Magnetic Semiconductors and Oxides”.....	507
“Theory”.....	527
“Spintronics and Magnetotransport”.....	533
“High Frequency Properties and Metamaterials”.....	561
“Soft and Hard Magnetic Materials”.....	577
2 JULY	605
PLENARY LECTURES.....	605
ORAL SESSION.....	609
“Spintronics and Magnetotransport”.....	609
“Magnetism and Superconductivity”.....	625
“Diluted Magnetic Semiconductors”.....	639
“Magnetophotonics”.....	645

“Theory”	649
“Magnetism of Nanostructures”	665
“Magnetic Soft Matter (magnetic polymers, fluids and suspensions)”	679
“Multiferroics”	693
“Magnetic Oxides”	699
“Magnetic Shape Memory and Magnetocaloric Effect”	711
“Magnetoplasmonics”	717
“High Frequency Properties and Metamaterials”	727
“Low Dimensional Magnetism”	735
POSTER SESSION	743
“Magnetic Nanostructures and Low Dimensional Magnetism”	743
“Magnetophotonics (linear and nonlinear magneto-optics, magnetophotonic crystals)”	781
“Magnetic Soft Matter (magnetic polymers, fluids and suspensions)”	813
“Multiferroics”	837
“High Frequency Properties and Metamaterials”	859
3 JULY.....	879
PLENARY LECTURES	879
ORAL SESSION	883
“Spintronics and Magnetotransport”	883
“Magnetism and Superconductivity”	893
“Magnetophotonics”	911
“Magnetism of Nanostructures”	919
“High Frequency Properties and Metamaterials”	927
“Multiferroics”	935
AUTHOR INDEX.....	945

30 June

Monday

10:00-11:30

plenary lectures
30PL-A

30PL-A-1

INTERFACE-DRIVEN MAGNETISM: FROM CHIRAL DOMAIN WALLS TO SPIN SPIRALS AND MAGNETIC SKYRMIONS

Wiesendanger R.*

Institute of Applied Physics and Interdisciplinary Nanoscience Center Hamburg
University of Hamburg, D-20355 Hamburg, Germany

Magnetism in ultrathin films can significantly deviate from commonly known bulk magnetism due to low dimensionality, hybridization effects, changes of the lattice constant, stacking dependencies, and broken inversion symmetry at interfaces. This can lead to non-collinear spin states such as spin spirals or skyrmions. Especially magnetic skyrmions with their nontrivial topology are interesting objects for both fundamental as well as application-oriented research due to their possible utilization in future magnetic data storage.

Based on the development of atomic-resolution spin-polarized scanning tunneling microscopy (SP-STM) [1], we have discovered chiral domain walls in ultrathin Fe films on W(110) substrates [2-4], spin spiral states in various transition metal thin films [5-7] and quasi-one-dimensional magnetic chains [8] on different W and Ir single-crystal substrates, as well as nanoskyrmion lattices with a periodicity of only one nanometer in single atomic layers of Fe on Ir(111) [9]. In all these cases, the Dzyaloshinskii-Moriya interaction combined with the breaking of inversion symmetry at surfaces and interfaces plays a crucial role for the stability of the observed non-collinear spin textures.

More recently, we have made use of multiple interface engineering in bilayer and multilayer systems in order to demonstrate the direct observation and manipulation of individual skyrmions of single-digit nanometer-scale size [10]. By locally injecting spin-polarized electrons from an atomically sharp SP-STM tip, we were able to write and delete individual skyrmions one-by-one, making use of spin-transfer torque exerted by the injected high-energy spin-polarized electrons [10]. Switching rate and direction can then be controlled by the parameters used for current injection. The creation and annihilation of individual magnetic skyrmions demonstrates their great potential for future nanospintronic devices making use of individual topological charges as information carriers [11].

- [1] R. Wiesendanger, *Rev. Mod. Phys.*, **81** (2009) 1495.
- [2] O. Pietzsch et al., *Science*, **292** (2001) 2053.
- [3] A. Kubetzka et al., *Phys. Rev. B*, **67** (2003) 020401.
- [4] S. Meckler et al., *Phys. Rev. Lett.*, **103** (2009) 157201.
- [5] M. Bode et al., *Nature*, **447** (2007) 190.
- [6] P. Ferriani et al., *Phys. Rev. Lett.*, **101** (2008) 027201.
- [7] Y. Yoshida et al., *Phys. Rev. Lett.*, **108** (2012) 087205.
- [8] M. Menzel et al., *Phys. Rev. Lett.*, **108** (2012) 197204.
- [9] S. Heinze et al., *Nature Physics*, **7** (2011) 713.
- [10] N. Romming et al., *Science*, **341** (2013) 6146.
- [11] A. Fert et al., *Nature Nanotechnology*, **8** (2013) 152.

* Work in collaboration with: K. von Bergmann, S. Blügel, J. Hagemeister, Ch. Hanneken, S. Heinze, J. Hermenau, S. Krause, A. Kubetzka, M. Menzel, N. Romming, A. Sonntag, E. Vedmedenko.

30PL-A-2

FEMTOSECOND OPTO-MAGNETISM: CONTROLLING AND HARNESSING FUNDAMENTAL FORCES IN MAGNETS*Kimel A.V.*

Radboud University Nijmegen, Nijmegen, The Netherlands
Moscow State Technical University MIREA, Moscow, Russia
a.kimel@science.ru.nl

In magnetic nanostructures, there are two conservation laws between the conduction electrons and the magnetic moment [1]. The first is the angular momentum conservation which brings about the spin angular momentum transfer between them. The other is that of energy between them. The magnetic energy stored in the conduction electrons is released as the spin motive force. The spin-motive force is derived by extending the Faraday's law of electro-magnetism. The non-conservative force acting on the spins of conduction electrons causes the work, which brings about the spin-motive force [2]. A variety of the phenomena due to the spin motive force [3, 4] are presented.

- [1] *Concepts in Spin Electronics*, ed. S. Maekawa (Oxford University Press, 2006).
- [2] S. E. Barnes and S. Maekawa: *Phys. Rev. Lett.* **98**, (2007) 246601.
- [3] J. Ohe, S. E. Barnes, H. W. Lee and S. Maekawa. *Appl. Phys. Lett.* **95**, (2009) 123110.
- [4] P.N. Hai, S. Ohya, M. Tanaka, S.E. Barnes and S. Maekawa. *Nature* **458**, (2009) 489.

30 June

Monday

12:00-13:30

15:00-17:15

oral session

30TL-A

30RP-A

30OR-A

**“Spintronics and
Magnetotransport”**

30TL-A-1

SPIN WAVE MANIPULATION IN FERROMAGNETIC METALS: MAGNON SPINTRONICS

Sekiguchi Koji^{1,2}

¹ Department of Physics, Keio University, Yokohama, Japan

² JST-PRESTO, Kawaguchi, Japan

koji_s@phys.keio.ac.jp

Spin wave devices have been the most promising candidate for the realization of ultralow-power consumption devices. The key concept is the control of spin current. The spin current can be classified into two different types; a coherent spin-current (magnons) and a diffusive spin-current (the flow of electron spin). By utilizing the coherent spin-current [1, 2], we can design a new class of spin devices: all magnon processing and information transferring. For the magnon processing, the binary 1/0 outputs can be realized by spin-wave interference in metallic nanostructures [3]. Compare to the yttrium iron garnet (YIG) based magnonics, we can fabricate a much smaller device down to the order of spin-wave wavelength. We demonstrate that the interfered amplitude of the spin wave is perfectly controllable by changing a phase of incident spin waves. The destructive and constructive interferences lead to 0 and 1 logic operation. We have further proved that the 1/0 outputs can be generated with no external phase control.

This work was supported by the Japan Science and Technology Agency, Precursory Research for Embryonic Science and Technology (JST-PRESTO). K.S. also acknowledges a Grant-in-Aid for Young Scientists (A) from the MEXT, Japan.

[1] Y. Kajiwara, K. Harii, S. Takahashi, J. Ohe, K. Uchida, M. Mizuguchi, H. Umezawa, H. Kawai, K. Ando, K. Takanashi, S. Maekawa, and E. Saitoh, *Nature*, **464** (2010) 262.

[2] K. Sekiguchi, K. Yamada, S.-M. Seo, K.-J. Lee, D. Chiba, K. Kobayashi, and T. Ono, *Phys. Rev. Lett.*, **108** (2012) 017203.

[3] N. Sato, K. Sekiguchi, and Y. Nozaki, *Appl. Phys. Express*, **6** (2013) 063001.

30TL-A-2

LARGE EXTRINSIC SPIN HALL EFFECT IN GOLD DOPED WITH TUNGSTEN

Laczkowski P.¹, Rojas-Sánchez J.C.¹, Savero-Torres W.², Reyren N.¹, Deranlot C.¹, George J.M.¹, Jaffrès H.¹, Notin C.², Beigne C.², Marty A.², Attané J.P.², Vila L.², Fert A.¹

¹ UMR/CNRS-Thales and Université Paris-Sud, 91767, Palaiseau, France

² INAC/SP2M, CEA-Université Joseph Fourier, F-38054 Grenoble, France

piotr.laczkowski@gmail.com

The spin Hall effect (SHE) [1] allows for a reciprocal conversion between charge and spin currents using the spin orbit coupling. This conversion, and eventually produced spin torque, can be at the core of several promising spintronics devices. The spin orbit interaction is used to produce a transverse flow of spin or charge in response to a longitudinal excitation, these are the direct or inverse SHE. The spin Hall angle (SHA), the ratio of longitudinal and transverse electronic conductivities, is the characterizing parameter of this conversion. So far, large SHA have been reported in transition metals like Pt, Pd, W, Beta-Ta and in a few alloys with large spin orbit coupling impurities: CuIr, CuBi or CuPb [2]. In this presentation we will report on a large SHE induced in Au using resonant scattering on W impurities. We have used two different techniques to characterize the SHA. The first technique is based on lateral spin valves consisting of two ferromagnetic electrodes connected by a non magnetic wire. These nano-structures enable injecting and detecting spin currents to study the direct and inverse SHE (Fig1 (a)). The second technique is based on spin pumping at ferromagnetic resonance (FMR) and inverse SHE [3]. Pure spin currents are injected by the spin pumping effect from a ferromagnet into the material and the corresponding inverse SHE voltage is measured (Fig2 (b)). We have found a relatively short spin diffusion length of the order of 2nm and the spin Hall angle of 10% in both experiments, the total resistivity of the alloy being 57 uOhm.cm. Combining this large SHA and short spin diffusion length with stability at room temperature and chemical inertia makes the AuW alloy technologically relevant.

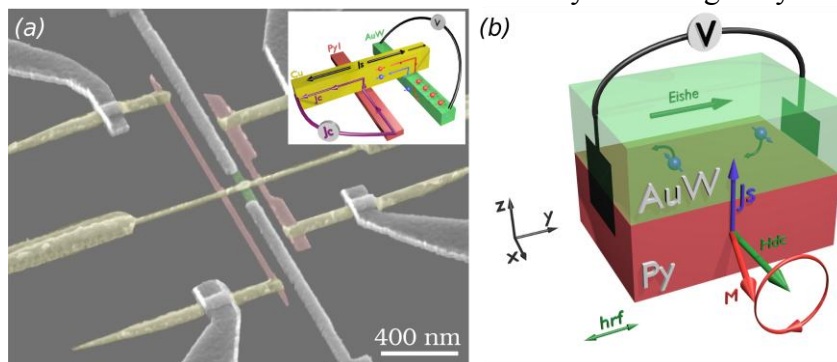


Fig. 1. SEM image of a Lateral Spin Valve nano-device with inserted AuW nano-wire and (b) a sketch of Py/AuW bilayer used in the spin pumping-FMR experiment.

[1] J.E. Hirsch, *PRL* **83** (1999) 1834.

[2] Y. Niimi et al., *PRL* **106** (2011) 126601, *PRL* **109** (2012) 156602, *PRB* **89** (2014) 054401.

[3] E. Saitoh, et al., *APL* **88** (2006) 182509.

30TL-A-3

SPIN TO CHARGE CURRENT CONVERSION USING RASHBA COUPLING AT THE INTERFACE BETWEEN NONMAGNETIC MATERIALS

Vila L.¹, Rojas-Sanchez J.C.^{1,3}, Oyarzun S.¹, Savero-Torres W.¹, Laczkowski P.^{1,3}, Marty A.¹, Vergnaud C.¹, Jamet M.¹, Attané J.P.¹, De Teresa J.M.², Fert A.³

¹ Institut Nanosciences et Cryogénie, CEA, and Université Joseph Fourier, Grenoble, France

² Instituto de Ciencia de Materiales de Aragón (ICMA), Univ. de Zaragoza-CSIC, Spain

³ Unité Mixte de Physique CNRS/Thalès, Palaiseau, and Université Paris-Sud, Orsay, France

laurent.vila@cea.fr

New horizons for Spintronics can be foreseen by taking further advantage of spin dependent transport phenomena in novel heterostructures. Efficient charge to spin current conversion has to be achieved for novel electrical operation scheme of devices. Several routes exist: in lateral spin valves, using thermal gradient or by Spin-Orbit interaction such as the spin Hall and Rashba effects. In this presentation we will focus on experiments realizing charge to spin conversion using Edelstein Rashba effect at the interface between nonmagnetic materials.

The Rashba effect is an interaction between the spin and the momentum of electrons induced by the spin-orbit coupling (SOC) in surface or interface states. Its potential for conversion between charge and spin currents has been theoretically predicted but never clearly demonstrated for surfaces or interfaces of metals. Edelstein has shown that a charge current carried by a Rashba 2DEG is automatically associated to a nonzero spin density (spin accumulation). We present experiments evidencing a large spin-charge conversion by the Bi/Ag Rashba interface (the inverse effect). We use spin pumping to inject a spin current from a NiFe layer into a Bi/Ag bilayer and we detect the resulting charge current. As the charge signal is much smaller (negligible) with only Bi (only Ag), the spin to charge conversion can be unambiguously ascribed to the Rashba coupling at the Bi/Ag interface. This result demonstrates that the Rashba effect at interfaces can be used for efficient charge-spin conversion in Spintronics [1].

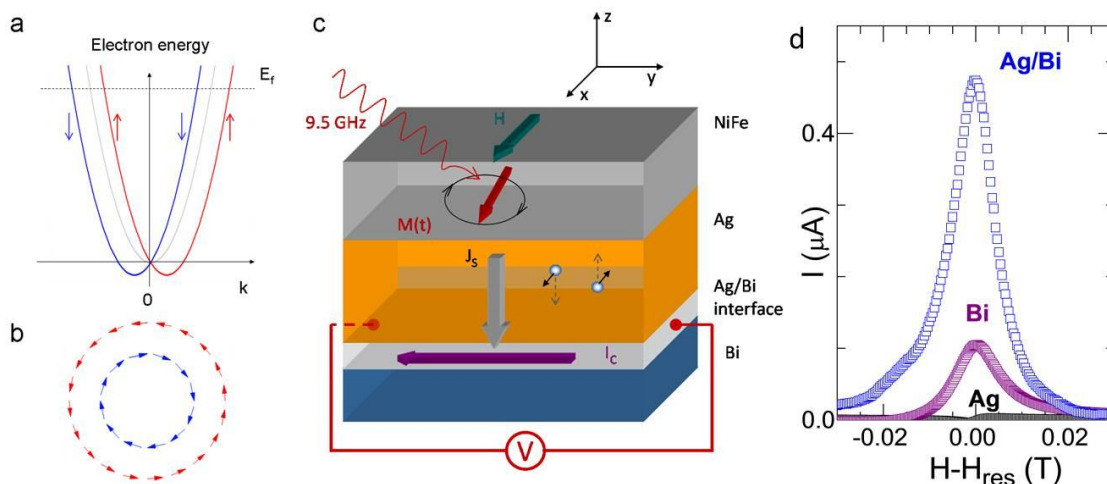


Fig. 1. (a) Typical spin-split dispersion curves of a Rashba 2DEG and (b) typical Fermi contours. (c) Scheme of the NiFe/Ag/Bi samples under resonance. J_s is the vertical DC spin current injected into the Ag/Bi interface states. (d) Charge current produce at the resonance condition in spin pumping experiments for NiFe/Ag, NiFe/Bi and NiFe/Ag/Bi samples.

[1] J. C. Rojas Sanchez et al. Nat. Commun. 4:2944 doi: 10.1038/ncomms3944 (2013).

30TL-A-4

FERROELECTRIC AND MULTIFERROIC TUNNEL JUNCTIONS

Tsymbal E.Y.

Department of Physics and Astronomy, University of Nebraska, Lincoln, Nebraska, USA
tsymbal@unl.edu

The phenomenon of electron tunnelling has been known since the advent of quantum mechanics, but continues to enrich our understanding of many fields of physics, as well as creating sub-fields on its own. Spin-dependent tunnelling in magnetic tunnel junctions has aroused considerable interest and developed into a vigorous field of research.¹ In parallel with this endeavour, recent advances in thin-film ferroelectrics have demonstrated the possibility of achieving stable and switchable ferroelectric polarization in nanometre-thick films. This discovery opened the possibility of using thin-film ferroelectrics as barriers in magnetic tunnel junctions, thus merging the fields of magnetism, ferroelectricity, and spin-polarized transport into an exciting and promising area of novel research.^{2,3} This talk will overview recent developments in ferroelectric and multiferroic tunnel junctions. We will discuss the recent demonstration of giant resistive switching effects observed in ferroelectric tunnel junctions, physical mechanisms responsible for this behaviour, and the interplay between ferroelectricity and magnetism in controlling the transport spin polarization in magnetic tunnel junctions with ferroelectric barriers.

- [1] E.Y. Tsymbal and I. Žutić, Eds., *Handbook of Spin Transport and Magnetism* (CRC press, Boca Raton, FL, 2011).
- [2] E.Y. Tsymbal and H. Kohlstedt, Tunneling across a ferroelectric. *Science*, **313** (2006) 181.
- [3] E.Y. Tsymbal, A. Gruverman, V. Garcia, M. Bibes, and A. Barthélémy, Ferroelectric and multiferroic tunnel junctions. *MRS Bulletin*, **37** (2012) 138.

30TL-A-5

ELECTRICAL DETECTION OF MAGNETIZATION DYNAMICS

Hu Can-Ming

Department of Physics and Astronomy, University of Manitoba, Winnipeg, Canada
hu@physics.umanitoba.ca

Via the interplay between electrons and photons, charge transport in semiconductor materials can be manipulated and controlled by using light. It enables electrical detection of charge dynamics in the optical and infrared frequency regimes, which is well known to the semiconductor research community. Recently, this technique has received increasing attention of the spintronics and magnetism research communities. By utilizing the interplay of spins, charges, and photons, electrical detection of magnetization dynamics in the microwave regime becomes a powerful new tool for dynamics spintronics research. In this talk, I will review our work in this frontier of spintronics by addressing:

- 1) Electrical detection of ferromagnetic resonance using spin dynamos (Fig. 1) [1].
- 2) Electrical detection of nonlinear magnetization dynamics and foldover effect [2].
- 3) Probing the phase of magnetization dynamics via spintronic Michelson interferometry [3].
- 4) Universal method for separating spin pumping from spin rectification voltage [4].
- 5) Electrical detection of dynamically generated DC and AC spin currents [5].

These results will be presented and discussed in comparison with relevant intriguing results obtained from the semiconductor spintronics community.

Support by NSERC and CFI is acknowledged. For more information and references, please check at:

<http://www.physics.umanitoba.ca/~hu/>

- [1] Y.S. Gui, et al., *Phys. Rev. Lett.*, **98** (2007) 107602.
 [2] Y.S. Gui, et al., *Phys. Rev. B*, **80** (2009) 060402(R).
 [3] A. Wirthmann, et al., *Phys. Rev. Lett.*, **105** (2010) 017202.
 [4] Lihui Bai, et al., *Phys. Rev. Lett.*, **111** (2013) 217602.
 [5] P. Hyde, et al., *arXiv:1310.4840*, (17 Oct 2013).

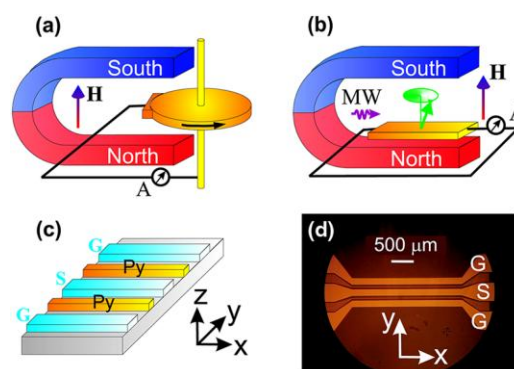


Fig. 1 (a) Faraday's dynamo with a revolving copper disk converts energy from rotation to a current of electricity. (b) Spin dynamo with a FM strip converts energy from spin precession to a bipolar current of electricity. (c) Diagram of the spin dynamo structure with Py strips placed in slots between the ground (G) and signal (S) lines of a coplanar waveguide. (d) Top view micrograph of a device.

30TL-A-6

PERPENDICULAR STT-MRAM: ORIGINS OF ANISOTROPY, SCALABILITY AND CHALLENGES

Apalkov D.¹, Khvalkovskiy A.¹, Chepulskyy R.¹, Nikitin V.¹, Butler W.², Krounbi M.¹

¹Samsung Electronics, Semiconductor R&D Center, San Jose, CA, USA

²Physics and Astronomy Department, University of Alabama, Tuscaloosa, AL, USA
d.apalkov@ssi.samsung.com

Recent observation of strong perpendicular anisotropy in ultrathin CoFeB layers adjacent to an MgO barrier has spurred activity in perpendicular STT-MRAM devices [1]. This breakthrough opens a new way to achieve stable and reliable STT-MRAM memory at small dimensions. Previously perpendicular anisotropy required bulk perpendicular materials (e.g. L1₀ FePt), which are typically associated with high damping and compatibility issues with MgO barrier for high TMR requirements.

In our talk, we will start by discussing how the information is stored in a magnetic state of a free (or storage) layer in STT-MRAM [2]. We will introduce interfacial perpendicular magnetic anisotropy (I-PMA), which can be subdivided into three equally important contributions:

hybridization of Fe and O orbitals at the interface, symmetry breaking, and lattice distortion. Then, we will discuss how I-PMA translates into stability of the storage layer. Using nudged elastic band (NEB) method we studied energy barriers in our free layer and observed two distinct switching paths: (a) quasi-uniform rotation and (b) domain-wall nucleation and propagation with a crossover region between the two. We will discuss dependence of crossover region on system parameters (magnetic and spatial) and compare the modeling predictions to available experimental observations [2].

Next, we will go over how the information is written into STT-MRAM free layer and explain spin transfer torque switching in various time scales. For fast memory operation, reliable switching in nanosecond regime is of crucial importance.

We will explain stages of switching, presence of domain-wall state during switching and discuss write error rates (probability of not switching). We will show that getting low write error rates with small current is one of the challenges for fast and reliable STT-MRAM designs and introduce a novel solution by engineering perpendicular anisotropy angular dependence. Our solution utilizes higher-order anisotropy terms to achieve a special type of anisotropy: easy-cone anisotropy:

$$E(\theta) = K_1 \sin^2(\theta) + \beta K_1 \sin^2(2\theta)$$

In easy-axis (EA) anisotropy, the equilibrium state of magnetization is at along a special (easy) axis. For easy-cone (EC) anisotropy, this special direction degenerates into a circular projection, as shown on the Fig. 1. This results in presence of very strong initial spin transfer torque, which significantly enhances not only average switching speed but also strongly improves write error rates (Fig. 1) – solving one of the challenges of STT-MRAM.

[1] S. Ikeda, et al., *Nature materials*, **9** (2010) 8, 1–4.

[2] A.V. Khvalkovskiy et al., *J. Phys. D: Appl. Phys.*, **46** (2013) 074001.

[3] M. Gajek et al., *Appl. Phys. Lett.*, **100** (2012) 132408.

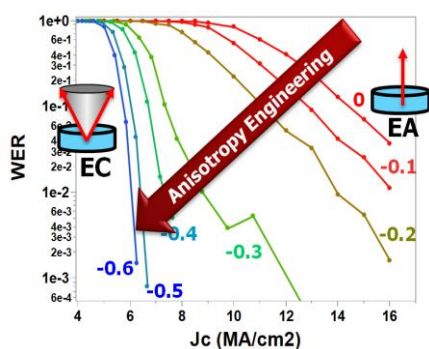


Fig. 1. Write Error Rates (WER) for 2 ns STT switching. Anisotropy engineering (β values are given next to data) allows reducing current density J_c needed for reliable switching.

30RP-A-7

NANOMAGNET-BASED SHIFT REGISTER AND UNIDIRECTIONAL TRANSMISSION WIRE

Nomura H., Miura S., Moria A., Nakatani R.

Division of Materials and Manufacturing Science, Osaka University, Suita-city, Japan
nomura@mat.eng.osaka-u.ac.jp

A nanomagnetic logic (NML), also called as a magnetic quantum cellular automata (MQCA) [1], is one of a magnetic field-coupled devices. NML elements are composed of nanoscale magnets. In the NML, binary information of "0" and "1" are stored as a magnetization direction of the nanomagnets. A logic operation or signal propagation is performed via magnetostatic interaction between the nanomagnets. NML has advantages of high integration density, low-energy dissipation and high resistivity to an ionized particle. Transmission wire, inverter and majority logic gate have been demonstrated experimentally [2,3].

In general, NML elements are composed of equally-sized cylindroid nanomagnets, and magnetically easy axis of the nanomagnets are designed to be parallel to each other. Thus, neighbouring nanomagnets shows symmetrical structure along an expected signal propagation direction. However, according to the symmetrical structure, signal can easily propagate in undesirable directions. This signal back-flow causes a serious error in a sequential logic circuit.

Here we propose and demonstrate a shift register and a unidirectional data transmission wire which can define a signal propagation direction. A combination of the unidirectional data transmission wire and NML NAND/NOR logic gates are also studied.

Figures 1(a) and (b) show schematic illustration of the shift register and unidirectional transmission wire, respectively. As a sample, Ni-20at.%Fe nanomagnets with thickness of 20 nm were fabricated on a thermally oxidized Si(100) substrate with electron-beam lithography, ion beam sputtering, and lift-off technique. All experiments were performed in vacuum condition at room temperatures with a commercial scanning probe force microscope (SII-A300) and originally developed magnetic force microscope (MFM) controlled by LabVIEW. To write digital information to nanomagnets, we applied a magnetization manipulation technique based on MFM. To execute a data transfer, we used spatially uniform external magnetic field with angle of 45 degrees with respect to the magnetically easy axis of the nanomagnets. With various initial states of the wire, we confirmed that the shift register and the wire can transfer the stored data unidirectionally. These results show good agreement with micromagnetic calculation.

With the shift register and the unidirectional transmission wires, sequential logic circuits based on NML will be realized in near future.

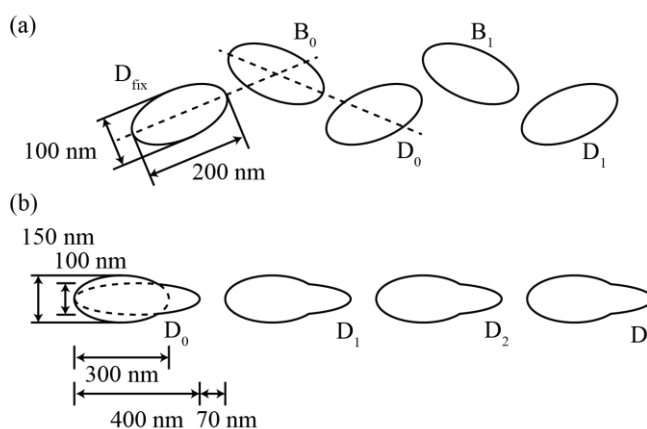


Fig. 1 Schematic illustration of (a) NML shift register and (b) NML unidirectional transmission wire.

[1] R. P. Cowburn and M. E. Welland, *Science*, **287** (2000) 1466.

[2] A. Imre, G. Csaba, L. Ji, A. Orlov, G. H. Bernstein and W. Porod, *Science*, **311** (2006) 205.

[3] H. Nomura and R. Nakatani, *Appl. Phys. Express*, **4** (2011) 013004.

30OR-A-8

NONRECIPROCAL SCATTERING OF NEUTRONS BY NONCOPLANAR MAGNETIC SYSTEMS

Nikitenko Yu.V.¹, Petrenko A.V.¹, Tatarsky D.A.², Udalov O.G.², Vdovichev S.N.², Fraerman A.A.²

¹JINR, Joliot-Curie 6, 141980 Dubna, Moscow region, Russia

²Institute for physics of microstructures RAS, GSP-105, Nizhny Novgorod, Russia
andr@ipm.sci-nnov.ru

It is well known that time reversal symmetry of the particle motion equations leads to the following equality for the elastic scattering cross section $\sigma(\vec{k}, \vec{k}', \vec{B})$

$$\sigma(\vec{k}, \vec{k}', \vec{B}) = \sigma(-\vec{k}', -\vec{k}, -\vec{B}), \quad (1)$$

where \vec{k} and \vec{k}' are wave vectors of the incident and scattered particles, and \vec{B} is the magnetic field in the system. Further assume that the scattering of neutrons is weak enough to be expanded in a series over the magnetic induction. Requirement of invariance with respect to rotation of \vec{B} strongly restricts possible form of neutron scattering cross section. Particularly $\sigma(\vec{k}, \vec{k}', \{\vec{B}(\vec{r})\}) = \sigma_0(\vec{k}, \vec{k}') + \int Q_1(\vec{k}, \vec{k}'; \vec{r}_1, \vec{r}_2)(\vec{B}_1 \cdot \vec{B}_2) d\vec{r}_1 d\vec{r}_2$

$$+ \int Q_2(\vec{k}, \vec{k}'; \vec{r}_1, \vec{r}_2, \vec{r}_3)(\vec{B}_1 \cdot [\vec{B}_2 \times \vec{B}_3]) d\vec{r}_1 d\vec{r}_2 d\vec{r}_3 + \dots, \quad (2)$$

where $Q_{1,2}$ are scalar functions, $\vec{B}_j \equiv \vec{B}(\vec{r}_j)$. $\sigma_0(\vec{k}, \vec{k}')$ is a part of cross section independent on the magnetic field. It can be seen from Eq. (2) that non-reciprocity of unpolarized neutron elastic scattering exists only in a system with a non-coplanar magnetic field spatial distribution, for which the mixed product $(\vec{B}(\vec{r})[\vec{B}(\vec{r}_1) \times \vec{B}(\vec{r}_2)])$ is not zero.

For verification of the non-reciprocity we suggested a following experiment. Two mirrors are used as polarizers, external field between ferromagnetic mirrors (induced by coil with electrical current) is used as polarization rotator. Magnetization of the first mirror (\mathbf{M}_1) is perpendicular to magnetization of second one (\mathbf{M}_2) and external magnetic field (\mathbf{B}_{ext}) is perpendicular to magnetization vectors of both mirrors. Nonreciprocal transmission means the dependence of the transmitted intensity on the sign of external magnetic field or the changing of the intensity under the interchange of neutron source and detector. In the experiment we changed the sign of external magnetic field.

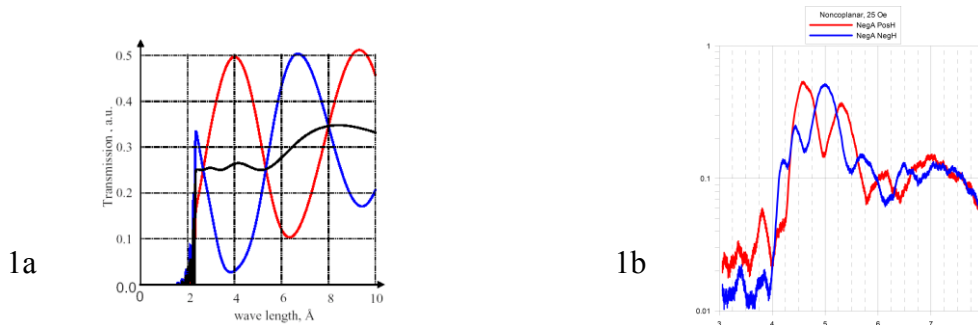


Fig. 1a - calculated transmission of unpolarized neutrons as function of wave length for different sign of the mixed product ($\mathbf{B}_{\text{ext}}[\mathbf{M}_1 \times \mathbf{M}_2]$) (red and blue curves), black curve for $B_{\text{ext}} = 0$; 1b – experimental results for transmission of unpolarized neutrons as function of wave length for different sign of the mixed product ($\mathbf{B}_{\text{ext}}[\mathbf{M}_1 \times \mathbf{M}_2]$) (red and blue curves).

30RP-A-9

UNIVERSAL HELIMAGNON AND SKYRMION EXCITATIONS IN METALLIC, SEMICONDUCTING, AND INSULATING CHIRAL MAGNETS

Schwarze Th.¹, Waizner J.⁴, Garst M.⁴, Bauer A.², Stasinopoulos I.¹, Berger H.³, Pfeleiderer Ch.², Grundler D.^{1,5}

¹ Physik Department E10 TU München, Garching, Germany

² Physik Department E21 FG Magnetische Materialien TU München, Garching, Germany

³ Institut de physique de la matière complexe EPFL, Lausanne, Switzerland

⁴ Institute for Theoretical Physics Univ. Köln, Köln, Germany

⁵ STI, EPFL, Lausanne, Switzerland

dirk.grundler@ph.tum.de

A detailed understanding of the collective spin excitations and damping mechanisms in chiral magnets [1] is of great interest if one thinks about the application of the hexagonally ordered magnetic Skyrmion-lattice phase in spintronics and magnonics. We have used cryogenic broadband GHz spectroscopy based on a coplanar waveguide (CPW) and a vector network analyzer [2] to explore the magnetization dynamics across the entire magnetic phase diagrams of a metallic (MnSi), a semiconducting ($\text{Fe}_{0.8}\text{Co}_{0.2}\text{Si}$) and an insulating chiral magnet (Cu_2OSeO_3). The CPW excites and simultaneously probes the spin excitations in the helimagnets [3] (Fig.1). For the metallic, semiconducting, and insulating chiral magnets the spin excitations occur at different GHz frequencies depending on the material and applied magnetic field. Still we provide a unified quantitative account of their field dependent resonance frequencies across the whole magnetic phase diagram. The universal behavior of these excitations sets the stage for purpose-designed applications based on the resonant response of chiral magnets with tailored electric conductivity offering an unprecedented freedom for integration with electronics. Financial support by the DFG via TRR80 and the German excellence cluster “Nanosystems Initiative Munich (NIM)” is acknowledged.

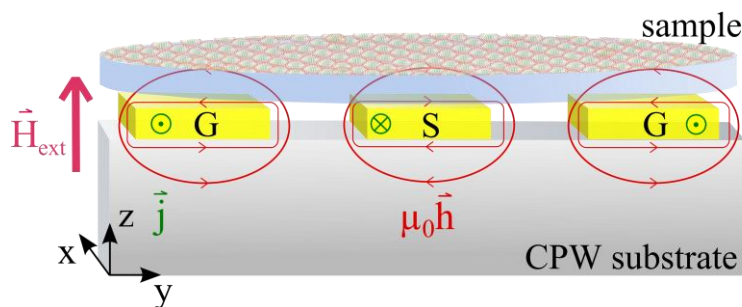


Fig. 1: A CPW consisting of metallic ground (G)-signal (S)-ground (G) lines carries a rf current j and provides an excitation field h for a helimagnet (sample) mounted on the top. The field H_{ext} is applied along the z direction.

[1] Y. Onose et al., *PRL*, **109**, 037603 (2012).

[2] S. S. Kalarickal et al., *JAP*, **99**, 093909 (2006).

[3] T. Schwarze et al., submitted.

30 June

Monday

12:00-13:30

15:00-17:00

oral session

30TL-B

30RP-B

30TL-LT

30RP-LT

30OR-LT

**“Magnetism and
Superconductivity”**

30TL-B-1

SPIN FILTER JOSEPHSON JUNCTIONS

Pal A., Muduli P., Robinson J.W.A., Blamire M.G.

Department of Materials Science, University of Cambridge, U.K.

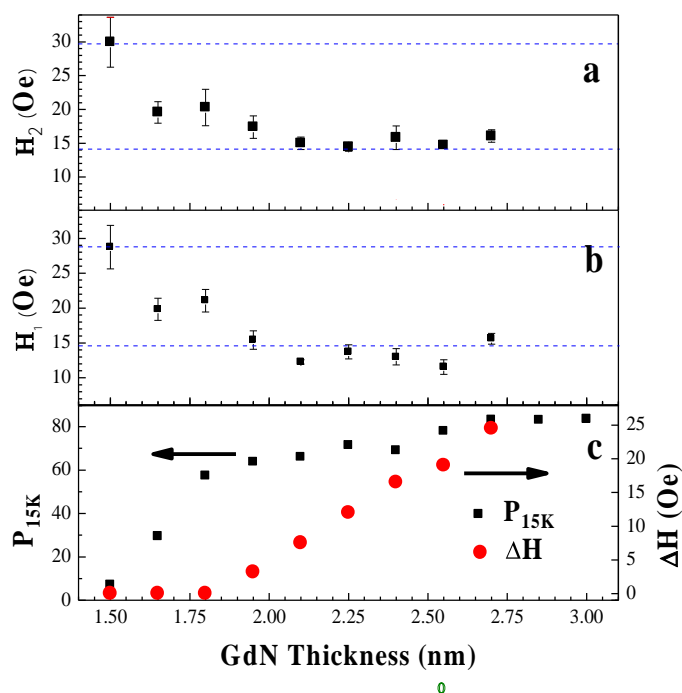
mb52@cam.ac.uk

The exchange-splitting of the density of states in a ferromagnetic insulator results in differing tunneling probabilities for the two electron spin directions and can result in substantial spin polarisation of the tunneling current so that the devices operate as spin filter tunnel junctions. Over the past five years we have developed the fabrication of NbN/GdN/NdN tunnel junctions. Although the tunneling of singlet pairs through the ferromagnetic GdN barrier is expected to be strongly suppressed by spin-filtering, we showed that superconducting tunnel junctions containing such barriers could show a significant Josephson supercurrent [1].

Subsequent work has shown that the normal-state tunneling properties of such devices differ strongly from the behaviour expected for a simple metal-insulator-metal tunnel junction and that the barrier is probably better understood as a double-Schottky type [2] in which the thinnest barriers have zero- or strongly-suppressed magnetisation because of the effective depletion of the defect states which are believed to mediate magnetism in the rare-earth nitrides.

More recent work has shown that, although junctions with thin, barely magnetic barriers, behave conventionally, the dependence of the critical current on field ($I_c(H)$) for Josephson junctions containing strongly magnetic barriers are consistent with a current-phase relationship $I = I_0 \sin(2\hat{f})$: i.e. the 2nd harmonic of the conventional form [3]. This behaviour, together with significant asymmetry in the quasiparticle conductance-voltage characteristic, suggests that the triplet pairs mediate the Josephson current in such devices.

Fig. 1. The evolution of magnetic GdN barrier junction properties with thickness: (a) the field-width of the second lobe of the $I_c(H)$ pattern, (b) half the field-width of the main peak of the $I_c(H)$ pattern, (c) the hysteresis (ΔH) in $I_c(H)$ which is proportional to the barrier moment and the spin polarization at 15K (P_{15K}).



Support by the ERC is acknowledged.

[1] K. Senapati, M. G. Blamire, and Z. H. Barber, *Nature Mater.* **10** (2011) 849-852.

[2] A. Pal, K. Senapati, Z. H. Barber, and M. G. Blamire, *Adv. Mater.* **25** (2013) 5581–5585.

[3] A. Pal, Z. H. Barber, J. W. A. Robinson, and M. G. Blamire, *Nat. Commun.* **in press** (2014).

30RP-B-2

ENGINEERING MAGNETIC STRUCTURES FOR GENERATING SPIN-POLARISED SUPERCURRENTS

Robinson J.W.A.

Department of Materials Science, University of Cambridge, U.K.
jjr33@cam.ac.uk

Upon injection into a ferromagnet from a superconductor, spin-singlet supercurrents rapidly decay within a few nanometers unless the superconductor / ferromagnet interface (S/F) allows spin-aligned triplet Cooper pairs to form [1]. It is now established that such triplet pairs form when the magnetisation at the S/F interface is non-collinear with respect to the magnetisation in the F layer [2]. Because triplet pairs carry spin in addition to charge it is possible that triplet supercurrents could be used in spintronics in order to control the electronic state of a device [2] (a superconducting spintronic device"); unlike non-superconducting spin-polarised currents, triplet currents are dissipationless and so could offer an energy efficient solution for low-temperature applications such in large scale data handling facilities.

Our group has discovered a variety of ways to generate spin-triplet pairs [3-7] and in this talk I will provide an overview of our recent experimental work in this area; in particular, I will discuss spin-selectivity of triplet Cooper in superconducting spin-valves devices [7].

This work is funded by the UK Royal Society through a University Research Fellowship and the Leverhulme Trust through an International Network Grant.

- [1] F.S. Bergeret, et al., *Rev. Mod. Phys.*, **77** (2005) 1321.
- [2] M Eschrig, *Phys. Today*, **64** (2011) 43–49.
- [3] J.W.A. Robinson, G.B. Halász, A.I. Buzdin, M.G. Blamire, *Phys. Rev. Lett.*, **104** (2010) 207001.
- [5] J.W.A. Robinson, JDS Witt, M.G. Blamire, *Science*, **359** (2010) 1189246.
- [6] J.D.S. Witt, J.W.A. Robinson, M.G. Blamire, *Phys. Rev. B*, **85** (2012) 84526.
- [8] J.W.A. Robinson, F. Chiodi, M. Egilmez, G.B. Halász, MG Blamire, *Nature Sci. Rep.* **2**, **699** (2012).
- [7] N. Banerjee, C.B. Smiet, R.G.J. Smits, A. Ozaeta, F.S. Bergeret, M.G. Blamire, J.W.A. Robinson, *Nature Communications* **5**, **3048** (2014).

30RP-B-3

I-V CHARACTERISTICS IN Nb/Py BILAYERS WITH THICK Py LAYER

Attanasio C.¹

¹ CNR-SPIN Salerno and Dipartimento di Fisica "E.R. Caianiello", Università degli Studi di Salerno, Fisciano (Sa) I-84084, Italy
attanasio@sa.infn.it

The dynamic instability of the moving vortex lattice at high driving currents has been studied in Nb/Permalloy(=Py=Ni_{0.8}Fe_{0.2}) bilayers when the thickness of the Py layer, d_{Py} , is in the range 50-350 nm. For small and large values of d_{Py} the critical velocity v^* for the occurrence of the instability is consistently found to be larger in the bilayers than in the single Nb layer. When d_{Py} is around 200 nm interesting features appear in the I-V characteristics which could be connected to the presence of spin-triplet correlations in the superconductor.

30TL-B-4

TRIPLET PAIRING EFFECTS IN SUPERCONDUCTOR-FERROMAGNET NANOLAYERED HETEROSTRUCTURES

Zdravkov V.I.^{1,2}, Morari R.^{2,3}, Obermeier G.¹, Lenk D.¹, Seidov Z.^{1,4}, Krug von Nidda H.-A.¹, Müller C.¹, Kupriyanov M.Yu.⁵, Sidorenko A.S.², Horn S.¹, Tidecks R.¹, Tagirov L.R.^{1,3}

¹ Institut für Physik, Universität Augsburg, D-86159 Augsburg, Germany

² Institute of Electronic Engineering and Nanotechnologies ASM, 2028 Kishinev, Moldova

³ Solid State Physics Department, Kazan Federal University, 420008 Kazan, Russia

⁴ Institute of Physics, Azerbaijan National Academy of Science, AZ-1143 Baku, Azerbaijan

⁵ Skobeltsyn Institute of Nuclear Physics, Moscow State University, Moscow 119992, Russia

ltagirov@mail.ru

The theory of superconductor-ferromagnet (S-F) heterostructures with two and more ferromagnetic layers predicts generation of long-range, odd-in-frequency triplet pairing at non-collinear alignment of magnetizations of the F-layers ([1] and references therein). As a consequence, the triplet spin-valve effect has been predicted in [2]. To observe this effect experimentally we realized Nb/Cu₄₁Ni₅₉/Nb/Co/CoO_x and Co/CoO_x/Cu₄₁Ni₅₉/Nb/Cu₄₁Ni₅₉ superconducting spin-valve type proximity-effect heterostructures [3,4].

In the first, adjacent type spin-valve structure, a weak ferromagnet – Cu₄₁Ni₅₉ alloy was used as a propagator layer adjacent to the bottom niobium layer – a conventional S-wave superconductor. An antiferromagnetic cobalt oxide layer provided the exchange bias of the in-plane magnetization of the underlying cobalt layer, which played a role of mixer of the triplet and singlet pairing channels.

In the second, interleaved type spin-valve structure, the functional superconducting Nb layer was sandwiched between two ferromagnetic copper-nickel alloy layers. The auxiliary Co/CoO_x bilayer served for exchange biasing the adjacent Cu₄₁Ni₅₉ alloy layer to create non-collinear magnetic configurations in the system in the external magnetic field.

Our FMR and SQUID measurements confirmed that the Cu₄₁Ni₅₉ layer has easy magnetization axis perpendicular to the film plane, while the metallic Co layer always has in-plane alignment of the magnetization.

The magnetoresistance measurements in Nb/Cu₄₁Ni₅₉/Nb/Co/CoO_x system at temperatures close to the superconducting (SC) transition temperature T_c , and magnetic field applied in the in-plane direction, have shown a sequence of transitions from the normal to the SC state and vice versa when sweeping the magnetic field. We refer this unusual magnetoresistance behavior to the indication of the triplet pairing generation at the non-collinear alignment of magnetizations in the Nb/Cu₄₁Ni₅₉/Nb/Co/CoO_x heterostructure [3]. A memory effect, *i.e.* zero-field resistance, depending on a magnetic pre-history, has been observed experimentally in Co/CoO_x/Cu₄₁Ni₅₉/Nb/Cu₄₁Ni₅₉ heterostructure [4] which is also referred to generation of the triplet pairing at non-collinear magnetic configurations.

The support by DFG, and RFBR, grants Nos. 14-02-90018 (M.Yu.K) and 14-02-00793-a (L.R.T.), is gratefully acknowledged.

1. F. S. Bergeret, A. F. Volkov, and K. B. Efetov, *Rev. Mod. Phys.* **77**, 1321 (2005).
2. Ya. V. Fominov, *et al.*, *JETP Lett.* **91**, 308 (2010).
3. V. I. Zdravkov, *et al.* *Phys. Rev. B* **87**, 144507 (2013).
4. V. I. Zdravkov, *et al.* *Appl. Phys. Lett.* **114**, 0339903 (2013).

EXPERIMENTS WITH SIFS φ JOSEPHSON JUNCTIONS

Goldobin E.¹, Sickinger H.¹, Weides M.², Kohlstedt H.³, Lipman A.⁴, Mints R.⁴, Koelle D.¹,
Kleiner R.¹

¹ University of Tübingen, Tübingen, Germany

² Karlsruhe Institute of Technology, Karlsruhe, Germany

³ University of Kiel, Kiel, Germany

⁴ Tel Aviv University, Tel Aviv, Israel
gold@uni-tuebingen.de

Josephson junctions (JJs) with a ferromagnetic interlayer can be used to fabricate π JJs, which have a phase drop of π in the ground state in comparison to conventional JJs having a phase drop of 0 (0 JJs)[1–3]. One can use these π JJs in superconducting circuits as a device providing a constant phase shift, i.e. as a π phase battery[4, 5]. A generalization of a π JJ is a φ JJ[6], which has the phase $\pm\varphi$ in the ground state. The value of φ can be chosen by design and tuned in the interval $0 < \varphi < \pi$. The φ JJs used in our experiment are fabricated as superconductor-insulator-ferromagnet-superconductor (SIFS) $0-\pi$ JJs[3] with asymmetric current densities in the 0 and π facets [7]. This system can be described by an effective current phase relation, which is tunable by an externally applied magnetic field[8]. We present several recent experiments with such a φ JJ[9]. First, we demonstrate that the unknown state can be read out by measuring the critical current I_{c+} or I_{c-} and written in by applying a magnetic field. Thus, φ JJ can be used as a memory cell. Second, we study the retrapping of the phase by the φ JJ and discover a butterfly effect not accompanied by chaos.

Support by DFG is acknowledged.

- [1] V. V. Ryazanov, V. A. Oboznov, A. Yu. Rusanov, A. V. Veretennikov, A. A. Golubov, and J. Aarts, *Phys. Rev. Lett.*, **86** (2001) 2427.
- [2] T. Kontos, M. Aprili, J. Lesueur, F. Genêt, B. Stephanidis, and R. Boursier, *Phys. Rev. Lett.*, **89** (2002) 137007.
- [3] M. Weides, M. Kemmler, E. Goldobin, D. Koelle, R. Kleiner, H. Kohlstedt, and A. Buzdin, *Appl. Phys. Lett.*, **89** (2006) 122511.
- [4] T. Orllepp, Ariando, O. Mielke, C. J. M. Verwijs, K. F. K. Foo, H. Rogalla, F. H. Uhlmann, and H. Hilgenkamp, *Science*, **312** (2006) 1495.
- [5] A. K. Feofanov, V. A. Oboznov, V. V. Bol'ginov, J. Lisenfeld, S. Poletto, V. V. Ryazanov, A.N. Rossolenko, M. Khabipov, D. Balashov, A. B. Zorin, P. N. Dmitriev, V. P. Koshelets, and A.V. Ustinov, *Nat. Phys.*, **6** (2010) 593.
- [6] A. Buzdin and A. E. Koshelev, *Phys. Rev. B*, **67** (2003) 220504(R).
- [7] M. Kemmler, M. Weides, M. Weiler, M. Opel, S. T. B. Goennenwein, A. S. Vasenko, A.A. Golubov, H. Kohlstedt, D. Koelle, R. Kleiner, and E. Goldobin, *Phys. Rev. B*, **81** (2010) 054522.
- [8] E. Goldobin, D. Koelle, R. Kleiner, and R. G. Mints, *Phys. Rev. Lett.*, **107** (2011) 227001.
- [9] H. Sickinger, A. Lipman, M. Weides, R. G. Mints, H. Kohlstedt, D. Koelle, R. Kleiner, and E. Goldobin, *Phys. Rev. Lett.*, **109** (2012) 107002.

30TL-LT-2

SPIN AND CHARGE DYNAMICS IN A HYBRID CIRCUIT QED ARCHITECTURE

Viennot J.J., Delbecq M.R., Dartiailh M.C., Cottet A., Kontos T.

Laboratoire Pierre Aigrain, Ecole Normale Supérieure, CNRS UMR 8551, Laboratoire associé aux universités Pierre et Marie Curie et Denis Diderot, 24, rue Lhomond, 75231 Paris Cedex 05, France
kontos@lpa.ens.fr

The recent development of hybrid cQED allows one to study how cavity photons interact with a system driven out of equilibrium by fermionic reservoirs. We study here one of the simplest combination: a double quantum dot coupled to a single mode of the electromagnetic field. We are able to couple resonantly the charge levels of a carbon nanotube based double dot to cavity photons. We perform a microwave read out and spectroscopy of the charge states of this system which allows us to unveil features of the out of equilibrium charge dynamics, otherwise invisible in the DC current. We develop a theory explaining our measurements and extract relaxation rate, dephasing rate and photon number of the hybrid system. These findings open the path for manipulating other degrees of freedom e.g. the spin and/or the valley in nanotube based double dots using microwave light [1,2]. Preliminary results demonstrating the spin/photon coupling in such an architecture will also be presented.

[1] J.J Viennot, J. Palomo and T. Kontos, *APL* (2014).

[2] J.J. Viennot et al. *PRB* (2014).

30RP-LT-3

EXPERIMENTS WITH SUPERCONDUCTORS SEPARATED BY A MAGNETIC BARRIER

Weides M.P.

Karlsruhe Institute of Technology, Karlsruhe, Germany
Martin.Weides@KIT.edu

In superconductor/ferromagnet (S/F) systems the Cooper pair wave function extends into the ferromagnet with a decaying amplitude and spatially dependent oscillatory phase. The pair's total angular momentum depends on the magnetic profile. These systems provide interesting physics, such as a non-monotonic dependence of the critical current I_c on temperature T or ferromagnetic layer thickness d_F , formation of triplet Cooper pairs, or the realization of π -coupling in SFS-type Josephson junctions with a ferromagnetic interlayer. To explore the Josephson dynamics, and to obtain higher $I_c R_n$ products, an additional tunnel barrier (I) next to the ferromagnetic barrier is required, i.e. SIFS-type junctions [1].

Properties like the Josephson phase inversion or generation of spontaneous flux render the π -junctions important phase-shifting elements for utilization in superconducting circuits. π -Josephson junctions have been proposed as new, central elements in superconducting devices such as Rapid Single Flux Quantum (RSFQ)-architecture or quiet qubits, where a phase shift of π is necessary to produce a degenerate double-well potential without applying an external bias. For logic operations, the weak dissipation in superconducting circuits facilitates relevant features such as high-speed operation with low power consumption per gate operation.

We investigated transport properties in SIFS-type junctions using CuNi, Ni, CoFe, Cu₂MnAl and Cr barriers while varying T , d_F or the in-plane magnetic field [1-4]. Combined 0 and π coupling of the same junction has been systematically studied by varying the junction's shape, dimension and number of phase-steps [5]. Under certain conditions junctions with a doubly degenerated ground state of Josephson phases $\psi = \pm\phi$ have been observed (so-called ϕ Josephson junctions) and demonstrated as a memory cell (classical bit) [6,7].

- [1] M. Weides, M. Kemmler, E. Goldobin, *et al.*, *Appl. Phys. Lett.* **89**, 122511 (2006).
- [2] A. A. Bannykh, J. Pfeiffer, V. S. Stolyarov, *et al.*, *Phys. Rev. B* **79**, 054501 (2009).
- [3] M. Weides, M. Disch, H. Kohlstedt, *et al.*, *Phys. Rev. B* **80**, 064508 (2009).
- [4] D. Sprungmann, K. Westerholt, H. Zabel, *et al.*, *Phys. Rev. B* **82**, 60505 (2010).
- [5] M. Weides, U. Peralagu, H. Kohlstedt, *et al.*, *Supercond. Sci. Technol.* **23**, 095007 (2010).
- [6] H. Sickinger, A. Lipman, M. Weides, *et al.*, *Phys. Rev. Lett.* **109**, 107002 (2012).
- [7] E. Goldobin, H. Sickinger, M. Weides, *et al.*, *Appl. Phys. Lett.* **102**, 242602 (2013).

30OR-LT-4

ROLE OF NORMAL INTERLAYER IN FERROMAGNETIC JOSEPHSON JUNCTIONS

Pugach N.G.^{1,2}, Heim D.M.³, Kupriyanov M.Yu.¹, Goldobin E.⁴, Koelle D.⁴, Kleiner R.⁴

¹SYNP, M. V. Lomonosov Moscow State University, Moscow, Russia

²Royal Holloway University of London, UK

³Institut für Quantenphysik and IQST, Universität Ulm, Germany

⁴Physikalisches Institut and CCQP, Universität Tübingen, Germany

pugach@magn.ru

The coexistence and competition of ferromagnetic (F) and superconducting (S) ordering leads to a rich spectrum of unusual physical phenomena, intensively studied during the recent years. One of the consequences is the so-called π Josephson junction with phase shift π in the ground state. One or two insulating (I) barriers may be introduced at the SF interfaces as well, in order to enlarge the product $J_c R_N$ in the π -phase. Here J_c is the critical current density of the junction and R_N is its normal resistance.

Nowadays, the development of magnetic memory cells for rapid single flux quantum (RSFQ) logics becomes more and more actual. Only recently, a new type of magnetic memory element based on a junction with a complex ferromagnet-superconductor-insulator weak link (SIFS) was proposed. One of the aims of our calculation is to study the behaviour of such SIFS junctions when their middle superconducting layer is in the normal state. Introducing a normal metal (N) layer between the F layer and the S electrode into a ferromagnetic Josephson junction (FJJ) is technologically necessary. Such an additional N layer was used in many FJJs. However, it was not taken into account by any theoretical explanation of these experiments [1].

We calculate the critical current density J_c of FJJs containing ferromagnetic, normal, and insulating layers in the weak link region. We determine the Green's functions with the help of the Usadel equations, which we use in theta parametrization. The Kupriyanov-Lukichev boundary conditions at all interfaces were used.

It was shown earlier that insulating barriers decrease the critical current density and shift the $0-\pi$ transitions to smaller values of the ferromagnet thickness d_F [2,3]. A thin N layer inserted between S and I layers does not significantly influence the Josephson effect. However, if the N layer is inserted between I and F layers, it can have a large effect on the Josephson current. The presence of the N layer may increase the amplitude of $J_c(d_F)$ and shift the first $0-\pi$ transition to larger d_F . The oscillation period of $J_c(d_F)$ is still determined by the relation of the magnetic exchange energy H and the diffusion coefficient in the dirty limit.

It is shown that even a thin additional N layer may change the boundary conditions at the IF boundary depending on the value of its conductivity. We conclude that it effectively mitigates the effect of the insulating barrier on the decaying oscillations of the critical current density $J_c(d_F)$. Even technological thin N layers, which almost do not suppress the superconducting correlation, have to be taken into account for the explanation of experimental results concerning the Josephson effect in FJJs. For example, the 0 and π states of multilayered FJJs containing few normal layers, proposed recently as basis for a cryogenic magnetic memory, should be determined very carefully. Using the developed approach we explain the existing experiments on SIFS and SINFS FJJs [1].

Support by RFBR (13-02-01452, 14-02-91350), SFB-TRR21, EP/J010618/1 is acknowledged.

[1] M. Weides, M. Kemmler, E. Goldobin, et.al. *Appl. Phys. Lett.* **89**, 122511 (2006).

[2] A. S. Vasenko, A. A. Golubov, M. Y. Kupriyanov, et. al. *Phys. Rev. B* **77**, 134507 (2008).

[3] A. Buzdin, *JETP Lett.* **78**, 1073 (2003).

30RT-LT-5

VORTEX MAGNETIC RESPONSE OF QUANTUM METAMATERIAL WITH SUPERCONDUCTING QUBITS

Asai H.^{1,2}, *Kawabata S.*¹, *Savel'ev S.*², *Zagoskin A.*²

¹ Electronics and Photonic Research Institute (ESPRIT), National Institute of Advanced Industrial Science and Technology (AIST), Tsukuba, Ibaraki 305-8568, Japan

² Department Physics, Loughborough University, Loughborough LE11 3TU, UK
hd-asai@aist.go.jp

Metamaterials have been intensively studied as a new way for controlling electromagnetic (EM) field. Metamaterials are artificial electromagnetic materials consisting of artificial atoms, that is, artificial structures whose sizes are small compared to the wavelength of respective EM wave. We can manipulate effective permittivity and permeability of metamaterials at will by changing shapes and arrangements of the artificial atoms. However, conventional metamaterials composed of “classical” elements cannot control EM waves beyond the framework of classical electrodynamics. Recently, quantum metamaterial(QMM), which utilizes superconducting qubits as artificial atoms, has been theoretically proposed [1] and its first prototype fabricated [2]. QMMs are expected to show unique characteristics reflecting quantum superposition and/or entanglement of the qubit states.

In this presentation, we discuss the EM field response of the QMM, which utilize the superconducting charge qubits as its artificial atoms. We numerically calculate the distribution of magnetic field inside the QMM in the presence of an external magnetic field. We find the spontaneous formation of the quantized magnetic flux in the QMM. This peculiar flux states come from the superposition states of the qubits. Based on the above results, we also discuss the kinematic superconducting states in the QMM induced by the applied magnetic field.

[1] A.Rakhmanov et al., *Phys. Rev. B* **79**, 184504 (2009).

[2] P. Macha et al. (arXiv:1309.5268).

30RT-LT-6

2D MAGNETIC NANOPARTICLE IMAGING USING SECOND HARMONIC OF MAGNETIZATION RESPONSE

Tanaka S.¹, Murata H.¹, Ohishi T.¹, Zhang Y.²

¹ Toyohashi University of Technology, 1-1 Hibarigaoka Tempaku-cho Toyohashi, Aichi 441-8580 Japan

² Peter Gruenberg Institute, Forschungszentrum Juelich, Juelich, D-52425 Germany
tanakas@ens.tut.ac.jp

Magnetic particle imaging (MPI) introduced by Gleich and Weizenecker is based on utilizing the non-linear magnetic response M for detection of super-paramagnetic iron oxide nanoparticles (MNP) [1]. A number of magnetic detection methods have been developed to determine the MNP volume (or mass) for different applications, such as immunoassay [2, 3]. In the MNP detection and the MPI technique, the most commonly employed method is the detection of the odd harmonics of the M response. We employed a method to improve the detection sensitivity for the magnetization M of superparamagnetic nanoparticles (MNP). The M response of MNP to an applied magnetic field H (M - H characteristics) could be divided into a linear region and a saturation region, which are separated at a transition point H_k . When applying an excitation AC magnetic field (H_{ac}) and an additional DC bias field $H_{dc} = H_k$ as shown in Fig.1, the second harmonic of M reaches the maximum due to the nonlinearity of the M - H characteristics. It is stronger than any other harmonics including a third harmonic [4, 5]. The advantage of the use of the second harmonic response is that the response can be taken for even in small H_{ac} . The M response of MNP was systematically analyzed and experimentally proven. In the case of the conventional detection using a third harmonic, the amplitude of the H_{ac} must be larger than the threshold level, which is almost the same as H_k . The detection method using a second harmonic can be applied to MPI (Magnetic Particle Imaging). A high sensitive device, SQUID magnetometer was also applied to the MPI. Then we could successfully demonstrate the 1D and 2D image of a bottle-shaped sample filled with MNP using a lock-in amplifier technique.

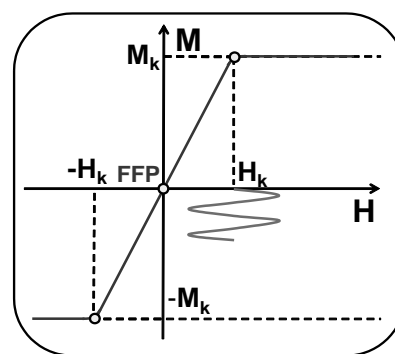


Fig.1. Principle of the detection using a 2nd harmonic with dc bias field of H_k .

- [1] B. Gleich and J. Weizenecker, *Nature*, **435** (2005) 1214-1217.
- [2] H.-J. Krause, N. Wolters, Y. Zhang, A. Offenhaeusser, P. Miethe, M. H. F. Meyer, et al., *J. Magn. Magn. Mater.*, **311** (2007) 436-444.
- [3] P. W. Goodwill and S. M. Conolly, *IEEE TRANSACTIONS ON MEDICAL IMAGING*, **30** (2011) 1581-1592.
- [4] T. Yoshida, K. Ogawa, T. Tsubaki, and N. B. O. a. K. Enpuku, *IEEE Trans. Magn*, **47** (2011) 2863-2866.
- [5] Yi Zhang, Hayaki Murata, Yoshimi Hatsukade and Saburo Tanaka, *Review of Scientific Instruments*, **84** (2013) 094702.

30 June

Monday

12:00-13:30

oral session

30TL-C

**“Magnetophotonics
and Optomagnetism”**

30TL-C-1

SPIN-PHOTONICS*Munekata H.*

Tokyo Institute of Technology, Yokohama 226-8503, Japan

hiro@isl.titech.ac.jp

Since the demonstration of light-induced magnetic phase transition in (In,Mn)As [1], the first III-V-based magnetic semiconductor epitaxial layer [2], the author has been elaborating the concept of spin-photonics on the basis of influence between photons and ordered spins with various experiments [3]. Interaction rate between photons and electron is determined by the frequency of the photon field, being 10^{15} Hz and higher, which suggests that magnetism, through the spin-orbit interaction, can be excited and controlled with the frequency beyond the limit of magnetization precession. Spin-photonics also gives us the opportunity of studying a new type of information processing in which spin/magnetization dynamics is used to input, processed, and output electromagnetic signals without displacement of electrons.

At the present stage, it is very important to establish reliable techniques for manipulating spins in magnetic materials with photons, and demonstrate prototype devices for mutual conversion between photons and ordered-spins. To this end, the author, with his colleagues, study experimentally the photo-induced ferromagnetic resonance (phi-FMR) with various III-V ferromagnetic metals and semiconductors [4,5,6], circularly polarized light emitters/detectors [7], and preparation and characterization of hybrid structures composed of magnetic films and optical waveguides [8]. At the time of presentation, the author will review thermal and non-thermal aspect of excitation referring experimental data of phi-FMR in (Ga,Mn)As [9] and Co/Pd multilayers [6], and spin light emitting diodes incorporation the ability of helicity switching [7].

[1] S. Koshihara, *et al.*, *Phys. Rev. Lett.* **78**, 4617 (1997).

[2] H. Munekata *et al.*, *Phys. Rev. Lett.* **63**, 1849 (1989).

[3] H. Munekata, *Concepts in Spin Electronics* (ed. S. Maekawa, Oxford Science Publications, 2006) 1 - 42.

[4] Y. Hashimoto, *et al.*, *Phys. Rev. Lett.* **100**, 067202 (2008).

[5] Y. Hashimoto and H. Munekata: *Appl. Phys. Lett.* **93**, 202506 (2008).

[6] K. Yamamoto, *et al.*, *IEEE Trans. Mag.* **49**, 3155 (2013).

[7] N. Nishizawa *et al.*, *Appl. Phys. Lett.*, accepted March 6th (2014); N. Nishizawa and H. Munekata, *J. Appl. Phys.* **114**, 033507 (2013).

[8] K. Nishibayashi, *et al.*, *MORIS-2013*, Omiya, Dec.4th, 2013.

[9] T. Matsuda *et al.*, *UMC-2013*, Strasburg, Oct. 28th, 2013.

30TL-C-2

BREAKING INTRA-ATOMIC EXCHANGE IN GADOLINIUM METAL*Frietsch B., Bowlan J., Carley R., Teichmann M., Weinelt M.*Fachbereich Physik, Freie Universität Berlin and Max-Born-Institut, Berlin, Germany
weinelt@physik.fu-berlin.de

The exchange interaction is the defining element in the formation of magnetic order in atoms and solids and thus plays a decisive role in ultrafast magnetization dynamics. We investigate the magnetization dynamics in lanthanide metals by time- and angle-resolved photoemission using higher-order harmonic radiation [1]. In the atomic magnetism of lanthanide metals localized 4f and itinerant 5d orbitals contribute to the overall magnetic moment. In general it is assumed that the intra-atomic exchange coupling is fast enough to be treated as an instantaneous process. We have studied the magnetization dynamics in gadolinium and terbium metal recording in parallel 4f magnetic linear dichroism and 5d exchange splitting. We observe distinct spin dynamics in Gd, which prove the breakdown of the intra-atomic exchange upon femtosecond laser excitation. While the Gd exchange splitting drops with a time constant of about 800 fs [2], it takes more than 10 ps for the 4f spin-order to reduce. An orbital-resolved Heisenberg model [3] explains the state-dependent two timescales of magnetization dynamics in Gd metal. Due to its much stronger spin-lattice coupling, Tb shows a distinctly different magnetization dynamics.

Support by the Deutsche Forschungsgemeinschaft, the Leibniz Graduate School *Dynamics in New Light* and the Helmholtz Virtual Institute *Dynamic Pathways in Multidimensional Landscapes* is gratefully acknowledged.

- [1] B. Frietsch, R. Carley, K. Döbrich, C. Gahl, M. Teichmann, O. Schwarzkopf, Ph. Wernet, and M. Weinelt, *Rev. Sci. Instrum.* **84** (2013) 075106.
- [2] R. Carley, K. Döbrich, B. Frietsch, C. Gahl, M. Teichmann, O. Schwarzkopf, P. Wernet, and Martin Weinelt, *Phys. Rev. Lett.* **109** (2012) 057401.
- [3] S. Wienholdt, D. Hinzke, K. Carva, P. M. Oppeneer, and U. Nowak, *Phys. Rev. B* **88** (2013) 020406(R).

30TL-C-3

ALL-OPTICAL CONTROL OF FERROMAGNETIC THIN FILMS AND NANOSTRUCTURES

Mangin S.^{1,2}

¹ Center for Magnetic Recording Research, University of California San Diego, La Jolla, USA

² Institut Jean Lamour, UMR CNRS 7198 –Université de Lorraine- BP 70239, F-54506 Vandoeuvre, France

The interplay of light and magnetism has been a topic of interest since the original observations of Faraday and Kerr where magnetic materials affect the light polarization. While these effects have historically been exploited to use light as a probe of magnetic materials there is increasing research on using polarized light to alter or manipulate magnetism. For instance deterministic magnetic switching without any applied magnetic fields using laser pulses of the circular polarized light has been observed for specific ferrimagnetic materials [1]. Here we demonstrate, for the first time, optical control of ferromagnetic materials ranging from magnetic thin films to multilayers and even granular films being explored for ultra-high-density magnetic recording [2]. Our finding shows that optical control of magnetic materials is a much more general phenomenon than previously assumed. These results challenge the current theoretical understanding and will potentially have a major impact on data memory and storage industries via the integration of optical control of ferromagnetic bits

[1] S. Mangin, M. Gottwald, C.-H. Lambert, D. Steil, V. Uhlíř, L. Pang, M. Hehn, S. Alebrand, M. Cinchetti, G. Malinowski, Y. Fainman, M. Aeschlimann, and E.E. Fullerton, *Nature Materials*, PUBLISHED ONLINE: 16 FEBRUARY 2014 | DOI: 10.1038/NMAT3864 (2013).

[2] C. Lambert, S. Mangin, B. S. D. Ch. S. Varaprasad, Y.K. Takahashi, M.Hehn, M.Cinchetti, G.Malinowski, K.Hono, Y.Fainman, M.Aeschlimann, E.E.Fullerton, <http://arxiv.org/abs/1403.0784>.

30 June

Monday

12:00-13:30

15:00-17:00

oral session

30TL-D

30RP-D

**“Magnetic Shape
Memory and
Magnetocaloric Effect”**

30TL-D-1

ADVANCED MAGNETOCALORIC MATERIALS FOR POWER-EFFICIENT REFRIGERATION TECHNOLOGY AND BIOMEDICAL APPLICATIONS

Tishin A.M.^{1,2}, *Spichkin Y.I.*¹, *Zverev V.I.*^{2,3}

¹ Advanced Magnetic Technologies and Consulting LLC 142190, Troitsk, Moscow, Russia

² Faculty of Physics, M.V. Lomonosov Moscow State University 119991, Moscow, Russia

³ Pharmag LLC 142190, Troitsk, Moscow, Russia

spichkin@amtc.org

Magnetocaloric effect (MCE) is considered to be one of the key fundamental physical effects to be employed in various technological applications nowadays [1]. Among them are the environmentally-friendly magnetic refrigeration technology [2], the controllable delivery and release of drugs and biomedical substances [3], the achievement of extremely low temperatures, etc.

Here we review the recent progress in magnetocaloric effect (MCE) studies. One of the most important aspects in design of MCE-based equipment is the correct choice of the magnetocaloric material. The last decades have shown the real ‘boom’ in research activity and the attempts to find the ‘best’ MCE material which reveals the highest value of the effect. Here we point out the importance of theoretical models’ development which demonstrates the interactions between magnetic and structural subsystems of the magnetic material in the vicinity of magnetic phase transitions. The ability to control these interactions by changing the composition of the material or its chemical purity, for example, is one of the possibilities to essentially increase MCE values [4]. Secondly, it is important to notice that MCE reaches its highest values in the vicinity of the critical points of magnetic material. Thus it is extremely important to learn to control these points’ location on the temperature scale and to know their dependence on the ‘external’ properties of the material (e.g. shape, anisotropy etc. [5]). After it has been cleared which material and in what conditions should be studied to obtain the maximum possible MCE value it is essential to discuss the existing and perspective methods of MCE measurements. The advantages of investigation of MCE parameters in dynamic mode and necessity of its measurements in low fields have been discussed [6]. In conclusion some possible practical applications of MCE, such as magnetic refrigeration, local hyperthermia and drug delivering, have been considered.

Work in Advanced Magnetic Technologies and Consulting LLC is supported by Skolkovo Foundation, Russia. Authors acknowledge support by the AMT&C Group Ltd., UK.

[1] A.M. Tishin, Y.I. Spichkin, *Intern. Journ. Refrig.* **37** (2014) 223.

[2] C. Zimm, A. Sternberg, V. K. Pecharsky, K. A. Gschneidner, Jr., M. Osborne, A. Jastrab, and I. Anderson, *Adv. Cryog. Eng.* **43** (1998) 1759.

[3] A.M. Tishin, J.A. Rochev, and A.V. Gorelov. 2006, Magnetic carrier and medical preparation for controllable delivery and release of active substances, a method of production and method of treatment using thereof. Patent GB 2458229.

[4] V.I. Zverev, A.M. Tishin, A.S. Chernyshov, Ya. Mudryk, K.A. Gschneidner, V.K. Pecharsky, *J. Phys.: Cond. Matter* **26** (2014) 066001.

[5] V.I. Zverev, R.R. Gimaev, A.M. Tishin, Ya. Mudryk, K.A. Gschneidner, V.K. Pecharsky, *Journ. of Magn. and Magn. Mater.*, **323** (2011) 2453.

[6] Y.I. Spichkin, R.R. Gimaev, *Intern. Journ. Refrig.* **37** (2014) 230.

30TL-D-2

GIANT MAGNETOCALORIC EFFECT IN INHOMOGENEOUS FERROMAGNETS

Bebenin N.G., Zainullina R.I., Ustinov V.V.

Institute of Metal Physics UB RAS, Ekaterinburg, Russia

bebenin@imp.uran.ru

Magnetocaloric effect (MCE) attracts attention because of possible application in refererators. MCE is more pronounced when a ferromagnet undergoes a transition from one magnetic state to another. The main features can be described, at least qualitatively, in the frame of Landau theory. The free energy can be written as:

$$F = \frac{1}{2}AM^2 + \frac{1}{4}BM^4 + \frac{1}{6}DM^6 + 2\pi NM_z^2 - M_z H_z, \quad (1)$$

where A is a function of temperature while B and D are assumed to be independent of T , M is modulus of magnetization, N is demagnetizing factor. If $B > 0$ the second order phase transition takes place in zero magnetic field; when $B = 0$, one deals with the tricritical point; if $B < 0$, the transition is discontinuous. In the latter case, the transition temperature is increased and the jump ΔM in magnetization is decreased with increasing magnetic field. Finally, at the critical temperature T_{crit} and critical field H_{crit} the jump disappears. Therefore there are four special cases that should be considered separately.

We start with considering MCE in an homogeneous ferromagnet near the second order transition temperature because in such a case we can compare the phenomenological approach with the results obtained in the frame of simple models; further another special cases are analyzed. The results are given in terms of the magnetic-field-induced entropy change ΔS .

As most of the ferromagnets are complex compounds for which the tendency to formation of inhomogeneous states is a characteristic feature the effect of inhomogeneity on MCE needs special consideration. First we discuss in what terms one can describe an inhomogeneous ferromagnet and what scientists call "Curie temperature" in this case; then we report the theory of the magnetocaloric effect together with some experimental data. It is shown that the magnetic inhomogeneity reduces MCE in all the cases except the vicinity of the critical point. The detectable decrease of ΔS due to demagnetizing field is shown to take place even when this field is noticeably less than an external field. At the tricritical point, the effect of the inhomogeneity is stronger than in the case of the second order transition. The most essential is the effect of the inhomogeneity when the transition is of the first order because, in this case, a great value of ΔS can be achieved in a weak magnetic field. The temperature dependence of ΔS at a given applied field is shown to be determined by the shift of the transition temperature in the field and the Curie temperature distribution function, so that the narrower the transition region, the lower magnetic field in which the entropy change is maximum.

This work was supported by RAS Program "Quantum mesoscopic and disordered structures" (project 12-P-2-1034) and RFBR grant 12-02-00208.

30RP-D-3

FIRST-PRINCIPLES CALCULATION OF THE INSTABILITY LEADING TO GIANT INVERSE MAGNETOCALORIC EFFECT

Entel P.¹, Gruner M.E.¹, Comtesse D.¹, Grünebohm A.¹, Sokolovskiy V.V.^{2,3}, Buchelnikov V.D.²

¹ Faculty of Physics, University Duisburg-Essen, 47048 Duisburg, Germany

² Condensed Matter Physics Dept., Chelyabinsk State University, 454001 Chelyabinsk, Russia

³ National University of Science and Technology "MIS&S", 119049, Moscow, Russia
entel@thp.uni-duisburg.de

Magnetic cluster glass induced by competing magnetic interactions and strain glass formed by kinetic arrest of first-order structural phase transition [1,2] are discussed on the basis of first-principles calculations. The main emphasis is on multi-functional properties such as magnetocaloric effect in disordered magnetic Heusler alloys Ni-(Co)-Mn-(Ga, In, Sn) with Mn-excess, where the martensitic transformation is accompanied by a large jump of the magnetization from long-range ferromagnetic austenite to ferromagnetic/antiferromagnetic or superparamagnetic martensite and a subsequent spin-glass and strain-glass phase at low temperature. We show that this variety of phases is to a large extent influenced by the intrinsic magnetic interactions of frustrated Mn spins, nesting property of the Fermi surface (in spite of disorder) and softening of Ni-Mn bonds. As an example of the outstanding properties of these alloys, we show in Fig. 1 the characteristic jump of magnetization curves for Ni-Co-Mn-In in different external magnetic fields [3], which do not saturate in large fields and where the size of the jump determines the size of the magnetocaloric effect.

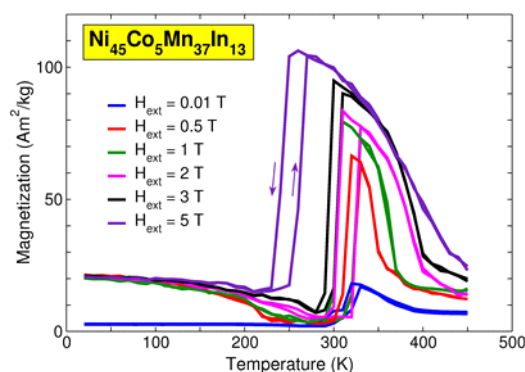


Fig. 1. Results of Monte Carlo simulation of isofield magnetization curves of Ni-Co-Mn-In across the magneto-structural transition in different magnetic fields. Exchange parameters used in the simulations are from ab initio calculations.

We acknowledge support by DFG (SPP 1599) and thank R. Arroyave, N. Singh, T. Gottschall, O.Gutfleisch, V.A. Chernenko, F. Albertini and A. Maslovskaia for discussion.

[1] P. Entel et al., *Eur. Phys. J. B*, **86** (2013) 65.

[2] S.B. Roy, *J. Phys.: Condens. Matter*, **25** (2013) 183201.

[3] J.M. Barandiaran et al., *Appl. Phys. Lett.*, **102** (2013) 071904.

30RP-D-4

MAGNETOCALORIC EFFECT: MICROSCOPIC APPROACH WITHIN TYABLIKOV APPROXIMATION FOR ANISOTROPIC FERRO- AND ANTIFERROMAGNETS

Kotelnikova O.A.¹, Prudnikov V.N.¹, Rudoy Yu.G.²

¹ Lomonosov MSU, Moscow, Russian Federation

² People's Friendship University, Moscow, Russian Federation

rudikar@mail.ru (Rudoy Yu.G.)

Magnetocaloric effect (MCE) has become the object of intensive studies – experimental as well as theoretical – in the past decade (see, e.g., comprehensive review articles [1,2]). The main reason is, of course, the perspective of practical use of MCE for magnetic refrigeration purposes, but our report will be concerned only with theoretical aspects of MCE. It appears [1,2] that rather perspective class of materials for MCE are the rare earths (e.g., Gd) and their compounds, which belong to the various types of anisotropic ferro- and antiferromagnets.

Most theoretical considerations up to now were carried only in the Weiss–Neel, or mean-field approximation (MFA), which is not sufficiently accurate. Fortunately, starting from 1959 there exists another approach, i.e. Tyablikov approximation (TA), known also as random phase approximation (RPA) which exceeds MFA significantly. TA gives renormalized magnon spectrum and thus the magnetic state equation $M(T,H)$ which mainly defines the MCE; M is magnetization, T – Kelvin temperature, H – magnetic field.

To our knowledge, up to now there exists only one sufficiently full TA calculation which is restricted only to the case of isotropic ferromagnet [3] as well as antiferromagnet [4] with arbitrary spin S . In this report we generalize these results on the anisotropic case and apply it to MCE.

[1] N.A. de Oliveira, P.J. von Ranke, *Phys. Rep.* **489** (2010) 89-159.

[2] K.A. Gschneider, V.K. Pecharsky, *J. of Rare Earths* **24** (2006) 641- 647.

[3] E.E. Kokoreva, M.V. Medvedev, *Physica B* **416** (2013) 29-32.

[4] F.A. Kassan-Ogly, E.E. Kokoreva, and M.V. Medvedev, private communication (2013).

30TL-D-5

RECENT RESULTS ON TRANSITION METAL BASED MAGNETOCALORIC MATERIALS

Brück E., Guillou F., Caron L., Yibole H., Miao X.F.

Fundamental Aspects of Materials and Energy, RST TU Delft, Delft, NL
e.h.bruck@tudelft.nl

Modern society relies on readily available refrigeration. Magnetic refrigeration has three prominent advantages compared to compressor-based refrigeration. First there are no harmful gasses involved, second it may be built more compact as the working material is a solid and third magnetic refrigerators generate much less noise. Additionally a higher energy efficiency is expected for magnetic refrigerators compared to small compressors or thermoelectric refrigerators.

Recently, a new class of magnetic refrigerant-materials for room-temperature applications was discovered. These new materials have important advantages over existing magnetic coolants: They exhibit a large magnetocaloric effect (MCE) in conjunction with a magnetic phase-transition of first order. This MCE is, larger than that of Gd metal, which is used in most demonstration refrigerators built to explore the potential of this evolving technology [1].

An optimized magneto-caloric material can be seen as an extremely efficient converter for energy from the spin sector (magnetization, magnetic field) to phonons (thermal energy) and vice versa. Due to the microscopic quantum nature of the spin system in a solid-state material, and its coupling to the lattice, this energy transfer possesses an inherently high efficiency.

Thus, given the right magneto-caloric system, we can use heat flow between the material and its surroundings to switch a suitable material across a magneto-caloric transition and thus we are able to convert this thermal energy efficiently into a change in magnetic field. The latter needs only to be 'picked up' in a solenoid and the transfer of heat to electrical current is complete. Alternatively, one may switch magnetic fields that are applied on a magnetocaloric material, which will result in a change of temperature. This change of temperature can be employed in a heat pump.

First principle electronic structure calculations on hexagonal MnFe(P,Si) reveal a new form of magnetism: the coexistence of strong and weak magnetism in alternate atomic layers. The weak magnetism of Fe layers (disappearance of local magnetic moments at the Curie temperature) is responsible for a strong coupling with the crystal lattice and thus large thermal effects while the strong magnetism in adjacent Mn-layers ensures Curie temperatures high enough to enable operation at and above room temperature [2]. Varying the composition on the magnetic and nonmagnetic sublattices gives a handle to tune the working temperature and to achieve a strong reduction of the undesired thermal hysteresis. In this way we design novel materials based on abundantly available elements with properties matched to the requirements of an efficient refrigeration or energy-conversion cycle.

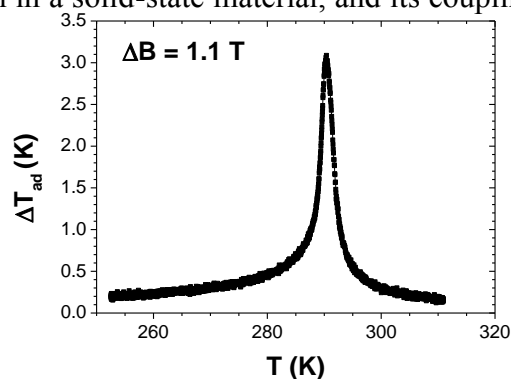


Fig. 1. Adiabatic temperature change of $\text{MnFe}_{0.95}\text{P}_{0.58}\text{B}_{0.08}\text{Si}_{0.34}$ from direct measurement.

[1] Brück E., *J. Phys. D-Appl. Phys.* **38**(2005) R381-91.

[2] Dung NH, Ou ZQ, Caron L, Zhang L, Thanh DTC, de Wijs GA, de Groot RA, Buschow KHJ, Brück E. *Adv. Energy Mat.* **1**(2011) 1215.

30TL-D-6

MAGNETIC PHASE TRANSITIONS IN 4f-3d INTERMETALLIC COMPOUNDS WITH LOW CONTENT OF RARE-EARTH ELEMENTS

*Mushnikov N.V., Kuchin A.G., Gerasimov E.G., Terentev P.B.,
Gaviko V.S., Serikov V.V., Kleinerman N.M., Vershinin A.V.*
Institute of Metal Physics UB RAS, Ekaterinburg, Russia
mushnikov@imp.uran.ru

It is well-known that, for the 4f-3d intermetallic compounds, the rare earth (R) atoms are responsible for appearance of large magnetic anisotropy, while high magnetic ordering temperatures are due to a strong exchange interaction in the 3d-sublattice. Therefore, ferromagnetic (F) intermetallic compounds with low content of R elements can show very high Curie temperatures. However, this is not always valid. In the compounds with iron and manganese, decrease in the distances between the 3d-atoms leads to increase in the negative exchange interactions. For such compounds, magnetic ordering temperature is lowered, and antiferromagnetic (AF) or non-collinear magnetic (helimagnetic) states are frequently formed. The magnetic state appears to be very sensitive to the external parameters (magnetic field, temperature, pressure), which enables their use in magnetocaloric and magnetoresistive applications [1].

In this work, in order to elucidate the mechanism of change in the type of magnetic ordering, we studied the structure, magnetic and magnetothermal properties of several intermetallic systems with competitive exchange interactions. The F-AF transitions upon changing concentration were found in $\text{La}(\text{Fe}_{0.88}\text{Si}_x\text{Al}_{0.12-x})_{13}$, $\text{R}_2(\text{Fe}_{1-x}\text{Mn}_x)_{17}$ ($\text{R} = \text{Ce}, \text{Lu}$), $\text{Y}_{1-x}\text{Tb}_x\text{Mn}_6\text{Sn}_6$, $\text{La}_{1-x}\text{R}_x\text{Mn}_2\text{Si}_2$ ($\text{R} = \text{Gd}, \text{Tb}, \text{Dy}$) and some other systems. We determined the temperatures of magnetic phase transitions and plotted magnetic phase diagrams (Fig. 1). Using both steady and high pulsed magnetic fields, we determined characteristic parameters of metamagnetic transitions for the AF phases and first-order magnetization processes for the F compounds with anisotropic R ions.

Although the magnetic phase diagrams have similar features for all the studied compounds, each system has specific origin of magnetic phase transitions. Using the obtained data, we suggest models of the formation of magnetic structures in these systems with competitive exchange interactions.

This work has been partially supported by RFBR (projects 12-02-00864 and 13-02-96022) and by Program of UB RAS (project 12-T-2-1012).

[1] N.V. Mushnikov, *Physics-Uspekhi*, **55**(2012) 421-425.

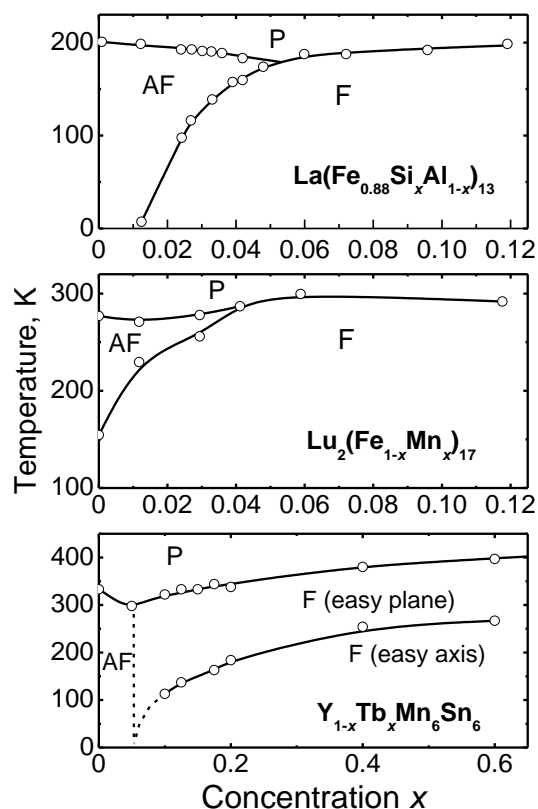


Fig. 1. Magnetic phase diagrams of several of R-Fe and R-Mn intermetallic systems

30TL-D-7

MAGNETIC AND CRYSTALLOGRAPHIC DOMAINS IN MnV_2O_4 *Murakami Y.*^{1,2}, *Murai S.*¹, *Tanigaki T.*², *Nii Y.*², *Arima T.*^{2,3}, *Shindo D.*^{1,2}¹ IMRAM, Tohoku University, Sendai, Japan² CEMS, RIKEN, Wako, Japan³ Dept. Adv. Mater. Sci., University of Tokyo, Kashiwa, Japan

murakami@tagen.tohoku.ac.jp

A spinel-type compound MnV_2O_4 undergoes a cubic-to-tetragonal displacive transformation at approximately 53 K [1,2]. Due to the interplay between the lattice and spin degrees of freedom, this compound shows the functionalities such as magnetic field-induced shape deformation (on the order of 0.1% [1,2]) and magnetocaloric effect [3]. For understanding of the underlying physics and/or optimization of these materials functionalities, a key examination is to reveal the relationship between the magnetic domains and the crystallographic domains (tetragonal domains). We have studied this essential problem by cryogenic transmission electron microscopy.

As shown in the Lorentz micrograph of Fig. 1(b), the ferrimagnetic, tetragonal phase shows micrometer-scaled magnetic domains: refer to the contrast of magnetic domain walls (*i.e.*, bright and dark lines), which are absent in the paramagnetic, cubic phase at 56 K [Fig. 1(a)]. The magnetic domain structure in the tetragonal phase dramatically changes by cooling to 6 K, as shown in Fig. 1(c). In the regions labeled by X and Y, the magnetic domains show 'one-to-one correspondence' with the twinning plates of crystallographic domains (20-30 nm width), due to the magnetocrystalline anisotropy enhanced by cooling. However, the magnetic domain structure remains almost unchanged in the region Z, in which extremely narrow crystallographic domains (10-14 nm width) are present. The observations indicate that the one-to-one correspondence (*i.e.*, a configuration widely observed in magnetic shape memory materials) cannot be achieved for those thin crystallographic domains, the plate width of which is smaller than the magnetic exchange length. The observations provide useful information for the micromagnetics of densely twinned magnetic systems.

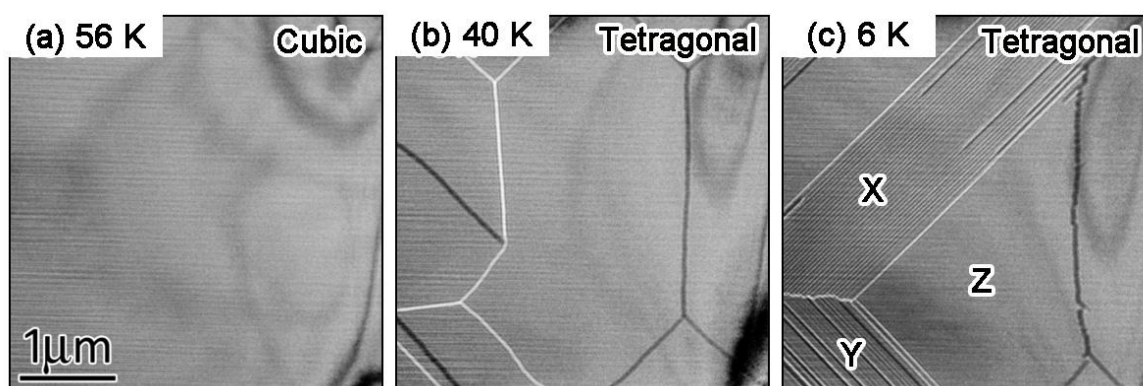


Fig. 1 Change in Lorentz micrographs of MnV_2O_4 with cooling. In the ferrimagnetic state [(b) and (c)], magnetic domain walls are imaged in bright and dark lines.

[1] T. Suzuki et al., *Phys. Rev. Lett.*, **98** (2007) 127203(1)-127203(4).

[2] Y. Nii et al., *Appl. Phys. Lett.*, **100** (2012) 051905(1)-051905(3).

[3] X. Luo et al., *Appl. Phys. Lett.*, **96** (2010) 062506(1)-062506(3).

30RP-D-8

MATERIAL CHALLENGE FOR HIGH PERFORMANCE MAGNETIC REFRIGERATION

Lyubina J.^{1,2}

¹ Evonik Industries AG, Hanau, Germany

² Department of Physics, Imperial College London, London, UK

y.lyubina@imperial.ac.uk

Near room temperature magnetic refrigeration, based on the magnetocaloric effect (MCE), is an emerging technology that has the potential to reach higher efficiency than the conventional vapour compression. The future of the magnetic refrigeration relies heavily on the availability and ease of processing of magnetic refrigerant materials [1,2]. For optimum performance the magnetic refrigerant materials should have a large MCE, low hysteresis, appropriate thermal and mechanical properties, and tunable Curie temperature T_c which determines the operating temperature range [1-3].

A large MCE can be obtained in materials undergoing a first order magnetic phase transition. The first order character of the transition sharpens the response so that the entropy change is concentrated in a relatively narrow temperature range. The gain in the MCE magnitude is often offset by such detrimental effects as large hysteresis and poor mechanical stability. Extensive research activity has been concentrated on optimising the magnetic properties of these materials by chemical composition modification, while little effort has been made in terms of microstructure design to overcome these problems. On the example of the $\text{La}(\text{Fe},\text{Si})_{13}$ -type system, one of the front-runner materials for the use as magnetic refrigerant, it will be shown how the introduction of porosity and the use of composite materials can be used to improve the performance of refrigerant materials. Moreover, MCE characterisation in light of the non-uniform first order magnetic transition in polycrystalline materials as well as appropriate methods for assessing materials and their suitability for the use in magnetic cooling systems will be presented.

[1] J. Lyubina, U. Hannemann, M.P. Ryan, L.F. Cohen, *Adv. Mater.*, **24** (2012) 2042.

[2] J. Lyubina, *J. Appl. Phys.*, **109** (2011) 07A902.

[3] J. Lyubina, U. Hannemann, L.F. Cohen, M.P. Ryan, *Adv. Energy Mater.*, **2** (2012) 1323.

30RP-D-9

METASTABILITIES ACROSS FIRST-ORDER TRANSITIONS IN MAGNETIC FUNCTIONAL MATERIALS

Siruguri V.

UGC-DAE Consortium for Scientific Research Mumbai Centre, R-5 Shed, BARC Campus,
Mumbai – 400 085, INDIA

A variety of magnetic functional materials like CMR manganites, magnetic shape memory alloys, magnetocalorics, multiferroics, etc., exhibit first order phase transitions and have been subject of intense experimental research in the recent times. These materials typically exhibit hysteresis when supercooled. It has been observed that the kinetics of the phase transformation can be influenced critically by an external magnetic field. For example, the high temperature magnetic phase can be kinetically arrested when cooled under an appropriate external magnetic field, thereby inhibiting the transformation to the low temperature equilibrium phase. Thus, a kinetically arrested state could have magnetically ordered coexisting meta-stable or glass-like arrested states (GLAS) and equilibrium (transformed) phases and has been termed as a magnetic glass. The phase coexistence is established by using a novel measurement protocol called CHUF (Cooling and Heating in Unequal Fields) and the metastable and equilibrium phases of the kinetically arrested state can be distinguished. Hence, magnetic field can be used as a useful thermodynamic variable, in addition to temperature, to study magnetic first-order transitions and their kinetic arrest. This protocol has also been used to demonstrate that the kinetically arrested state devitrifies at a characteristic temperature, $T_K(H)$, thereby qualifying it to be called a magnetic glass. Neutron diffraction is considered as an ideal technique to probe magnetic and chemical structures of materials and is capable of detecting the simultaneous presence of ferromagnetic (FM) and antiferromagnetic (AFM) order in a material in the form of unique magnetic reflections for the AFM order. We have used this technique along with the CHUF protocol, for the first time [1], to show the phenomenon of kinetic arrest of (i) the austenite to martensite transformation in a magnetic shape memory alloy (MSMA) and (ii) the ferromagnetic to CE-type antiferromagnetic transition in the well-studied compound $\text{La}_{0.5}\text{Ca}_{0.5}\text{MnO}_3$ (LCMO). The devitrification of the arrested austenite and FM phases into the low temperature equilibrium martensite and AFM phases at the characteristic temperature $T_K(H)$ for MSMA and LCMO, respectively, and their subsequent reentrant transition to the high temperature, high entropy austenite and paramagnetic phases, unambiguously demonstrate the glassy nature of the arrested states. The use of magnetic field as a second thermodynamic control variable via the CHUF protocol to observe arrest and de-arrest of a magnetic glass could help in drawing analogies on the pressure-induced transitions in structural glasses.

[1] V. Siruguri, P.D. Babu, S.D. Kaushik, A. Biswas, S.K. Sarkar, K. Madangopal and P. Chaddah, *J. Phys.: Condens. Matter* **25** (2013) 496011 and references therein.

30 June

Monday

12:00-13:30

15:00-17:00

oral session

30TL-E

30RP-E

30OR-E

“Multiferroics”

30TL-E-1

MULTIFERROIC MATERIALS AND DEVICES FOR ADVANCED APPLICATIONS

Vopson M.M.

University of Portsmouth, Faculty of Science, Portsmouth PO1 3QL, UK
melvin.vopson@port.ac.uk

The worldwide surge of interest in multiferroic materials over the past 15 years has been driven by their fascinating physics and properties, as well as their huge potential for technological applications. Materials science is one of the factors driving development and economic growth. Since the silicon industrial revolution of the 1950s, research and developments in materials science have radically impacted and transformed our society through the emergence of the computer technologies, wireless communications, Internet, digital data storage technologies and widespread consumer electronics. Today's emergent topics in materials science research such as nano-materials, carbon based graphene and nano-tubes, smart and multifunctional materials, spintronic materials, bio-materials and multiferroic materials, promise to deliver a new wave of technological advances and economic impact, comparable to the silicon industrial revolution of the 1950s.

Potential application of multiferroic materials cover a wide range of topics and technologies including sensors, microwave devices, energy harvesting, photo-voltaic technologies, solid-state refrigeration, data storage recording technologies, random access multi-state memories, magneto-electric opto-electronic modulators, to name a few. In this lecture, some of the most interesting and high impact proposed applications of multiferroic materials are presented in detail, with emphasis on potential improvements of the state-of-the-art technologies and material synthesis challenges that must be further addressed.

30TL-E-2

MAGNETO-IONICS: A NEW APPROACH TO MAGNETOELECTRIC MATERIALS

Beach G.

MIT Dept. of Materials Science and Engineering, Cambridge, MA 02139, USA
gbeach@mit.edu

Voltage control of magnetism has the potential to substantially reduce power consumption in spintronic memory and logic devices, while offering new functionalities through field-effect operation [1-4]. Magneto-electric coupling has most often been achieved using complex oxides such as ferroelectrics, piezoelectrics, or multiferroic materials. Here I describe a new approach, based on voltage-controlled ionic displacements at the interface between a metallic ferromagnet and a simple oxide dielectric [2,4]. Interfacial perpendicular magnetic anisotropy (PMA) at metal/oxide interfaces such as CoFe/MgO arises from interfacial hybridization between the ferromagnetic metal and oxygen ions. By using a solid-state ionic conductor with high oxygen ion mobility as a gate oxide, one can electrically displace O^{2-} at the ferromagnet/oxide interface to achieve extremely large changes in interfacial PMA [4]. I will describe our work on Co/GdOx bilayers [2-4], in which GdOx acts as a gate oxide that permits efficient oxygen exchange. By tailoring the gate structure, we engineer strong voltage-controlled domain wall traps that are nonvolatile, programmable to pinning strengths of at least 650 Oe, and switchable over many cycles without device degradation. We exploit this functionality to demonstrate a prototype nonvolatile memory device based on voltage-controlled magnetic bit selection in a magnetic nanowire. By further enhancing the ionic mobility, we show that fast, reversible switching of interfacial PMA by an amount $\sim 1 \text{ erg/cm}^2$, can be achieved. The metal/oxide heterostructures described here thus represent an alternative approach to traditional voltage-controlled multifunctional composites, providing similar functionality but based on materials amenable to integration with conventional semiconductor processing.

Support by NSF ECCS-1128439 and the Samsung SGMi Program is acknowledged.

- [1] U. Bauer, M. Przybylski, J. Kirschner, and G. S. D. Beach, *Nano Lett.* **12**, 1437 (2012).
- [2] U. Bauer, S. Emori, and G. S. D. Beach, *Appl. Phys. Lett.* **100**, 192408 (2012).
- [3] U. Bauer, S. Emori, and G. S. D. Beach, *Appl. Phys. Lett.* **101**, 172403 (2012).
- [4] U. Bauer, S. Emori, and G. S. D. Beach, *Nature Nanotechnology* **8**, 411 (2013).

30TL-E-3

TOWARD THE ELECTRICAL CONTROL OF MAGNETISM: SPECTROSCOPY AND MAGNETISM @ APE BEAMLINE

Torelli P.

TASC laboratory, IOM-CNR, s.s. 14 km 163.5, 34149 Basovizza, Trieste, Italy
piero.torelli@elettra.eu

The possibility of control the magnetic properties of a device by an electric impulse has attracted a great attention from the scientific community due to the important application that will find in electronics. Up to now important steps toward the control of magnetoelectric coupling in suitable nanostructures has been realized[1], however the current research is mainly based on transport measurements and magnetic measurements such as SQUID and MOKE which can address the magnetic response but not the electronic structure of the materials.

In this work we present an experimental set-up which permits the simultaneous investigation of the magnetic and electronic structure of materials and nanostructures by performing XMCD under applied bias voltage. Advanced Photoemission Experiment (APE beamline at Elettra the Italian synchrotron radiation facility [2]) consists of two independent beamlines, one for the VUV energy range and one for the soft X-ray range. The High Energy beamline (APE-HE) is optimized for soft-X-ray absorption (XAS) and magnetic dichroism (XMCD) and we recently developed a set-up for the investigation of the magnetic properties of thin films and nanostructures under an applied electrical bias field. To illustrate the possibility of this setup, and the experimental procedure (see fig.) needed to perform such experiments, we will present few examples recently performed at APE:

in a first example we show how magnetoelectric coupling effect can be controlled in a hybrid ferromagnetic(FM)/ferroelectric(FE) interfaces. In this experiment we observed that a sharp magnetic transition from ferromagnetic to antiferromagnetic state can be induced in thin Fe oxide, at the Fe/BTO interface, by the strain of the BTO layer when the BTO is subject to an electrical polarization [3]. As a second example we show the influence of the BTO strain on LSMO films.

The beamline is always open for proposals for experiment and in search of valuable collaboration in the field of spintronic and magnetism.

Support by NFFA DEMONSTRATOR is acknowledged.

[1] Y. W. Yin et al. *Nature Mater.* **12**, 397 (2013).

[2] G. Panaccione et al., *Rev. Sci. Instrum.* **80**, 043105 (2009).

[3] G. Radaelli et al. *Nature Communications* **5**, 3404 (2014).

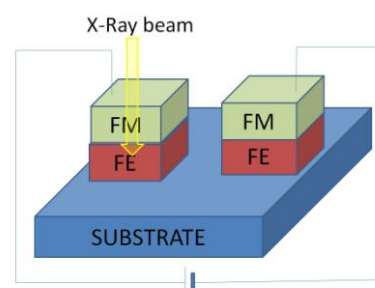


Fig. 1. Sample structure for in-operando experiment: Ferromagnetic layer is deposited onto Ferroelectric layer.

30TL-E-4

MULTIFERROIC CHROMITES: A COMPARISON BETWEEN $M\text{Cr}_2\text{O}_4$ SPINELS, CuCrO_2 DELAFOSSITES AND LnCrO_3 PEROVSKITES

Maignan A., Martin C., Preethi Meher K.R.S.

Laboratoire CRISMAT UMR 6508 ENSICAEN/CNRS, ENSICAEN, UCBN 6 boulevard du Maréchal Juin, 14050 Caen cedex 4 – France
antoine.maignan@ensicaen.fr

This presentation will focus on systems containing Cr^{3+} ($S=3/2$) magnetic cations, for which ferroelectricity has been recently reported [1]. The CuCrO_2 delafossite illustrates the improper ferroelectricity: it crystallizes in the centrosymmetric $R\bar{m}$ space group but becomes ferroelectric below $T_N = 25$ K, i.e. in its screw antiferromagnetic structure. In comparison, the AgCrS_2 sulfide, with a delafossite-like $R3m$ polar structure, exhibits a polarization below $T_N = 42$ K; for which a structural transition from $R3m$ to Cm (also polar) is concomitant.

Different origins can be inferred to explain the ferroelectricity in the antiferromagnetic states of these layer chromites.

Ferroelectricity induced by ferrimagnetic ordering has been also measured in FeCr_2O_4 , NiCr_2O_4 and CoCr_2O_4 spinels [2]. The presence of a Jahn-Teller cation (Ni^{2+} or Fe^{2+}) at the tetrahedral site leads to higher polarization values as compared to CoCr_2O_4 . For these oxides, the observation of polarization below T_C cannot be simply understood as their magnetic structures are collinear. Similar observations below T_N have been made for LuCrO_3 and ErCrO_3 orthochromites, which are not compatible with the models for improper ferroelectricity - spin current or exchange striction. These examples will give an overview of the variety of the magnetic behaviors and possible ferroelectric properties in Cr^{3+} based antiferromagnetic or ferrimagnetic compounds.

[1] For a review, K.R.S. Preethi Meher, A. Maignan, C. Martin, V. Caignaert, F. Damay, *Chem Mater*, **26** (2014) 830.

[2] For a review, A. Maignan, C. Martin, K. Singh, Ch. Simon, O.I. Lebedev, S. Turner, *J. Solid State Chem.*, **195** (2012) 41.

30TL-E-5

MULTIFERROICS AND CHIRAL MAGNETS UNDER HIGH PRESSURE AS STUDIED BY NEUTRON DIFFRACTION

*Mirebeau I.*¹, *Makarova O.L.*², *Deutsch M.*¹, *Hansen T.C.*³, *Fernandez-Diaz M.T.*³,
*Sidorov V.A.*⁴, *Tsvyashchenko A.V.*^{4,5}, *Fomicheva L.N.*⁴, *Porcher F.*¹, *Petit S.*¹

¹ Laboratoire Leon Brillouin, CEA-Centre de Saclay, 91191 Gif sur Yvette, France

² National Research Center Kurchatov Institute, 123182 Moscow, Russia

³ Institut Laue Langevin, F38042 Grenoble France

⁴ Vereshchagin Institute for High Pressure Physics, RAS, 142190, Troitsk, Moscow, Russia

⁵ Skobeltsyn Institute of Nuclear Physics, MSU, 119991 Moscow, Russia

isabelle.mirebeau@cea.fr

Insulating multiferroics and metallic itinerant magnets both show chiral spin structures, usually helicoidal or cycloidal. These structures are highly tunable and potentially interesting for industry. The magnetic frustration and inherent complexity are the source of original effects, suggesting new applications in the fields of data storage, information transfer or spintronics. Recent examples are the tuning of the magnetization by an electric field in insulating TbMnO₃ and BiFeO₃ multiferroics, and the manipulation of vortex-like chiral textures in MnSi or FeGe itinerant magnets in thin film form. The magnetic frustration comes from the competition of near neighbour interactions or from the influence of weak anisotropic perturbations. In both cases, the subtle energy balance of the magnetic interactions can be destabilized by applying pressure, yielding new magnetic phases, and informing about the energy scheme at play. High pressure neutron diffraction allows one to characterize magnetic phases at a microscopic level [1]. Recent results will be shown in two topical systems involving Mn magnetism, the multiferroic TbMnO₃ and the itinerant chiral magnet MnGe.

In TbMnO₃ at ambient pressure, a longitudinal modulation of the Mn moments occurs below 43K, followed by a cycloidal modulation below 28K. The spiral order is destabilized under pressure and a commensurate spin structure settles in, akin to that of HoMnO₃ with smaller ionic radius. Concomitantly, a change of phase of the modulation between cycloidal Mn chains occurs, and the Mn moments reorient [2]. The results imply both a change in the relative magnitude of the Mn near neighbor interactions, and a strengthening of the Tb ones.

In MnGe at ambient pressure, an helical order occurs below 170 K, induced by the Dzyaloshinskii-Moriya anisotropy and spin-orbit coupling. The short helical pitch (29 Å with regards to 180 Å in MnSi and about 700 Å in FeGe) is the source of a giant Topological Hall Effect [3,4]. We recently observed deep changes in the Mn magnetic order of MnGe under applied pressure, with the onset of pressure induced quantum critical points [5]. The two step pressure induced collapse of Mn magnetism suggests a profound change in the band structure under pressure, as predicted by *ab initio* calculations [6].

[1] I. N. Goncharenko High Pressure Research **24** (2004) 193.

[2] O. L. Makarova *et al* Phys. Rev. B **84** (2001) 020408 R.

[3] O. L. Makarova *et al* Phys. Rev. B **85**, (2012) 205205.

[4] N. Kanazawa *et al* Phys. Rev. Lett., **106** (2011) 156603.

[5] M. Deutsch *et al* to be published (2014).

[6] U. K. Roessler *et al* J. Physics Conf. Series, **391** (2012) 012104.

CHIRAL SPIN STRUCTURES IN THIN FILMS OF MAGNETIC METALS AND MULTIFERROICS

Pyatakov A.P.^{1,2}, Sergeev A.S.¹, Zvezdin A.K.²

¹ Physics Department, M.V. Lomonosov Moscow State University, Moscow, Russia

² A.M. Prokhorov General Physics Institute of the Russian Academy of Science, Moscow, Russia
pyatakov@physics.msu.ru

Chiral magnetic structures observed in thin films of magnetic metals such as spin cycloids [1], domain walls [2] and skyrmions [3] have inspired intensive research during the last few years. These topological objects demonstrate unusual properties promising for spintronics applications, such as high sensitivity of skyrmion to spin polarized currents [3] or an emergent feature of electric field induced magnetic domain wall motion [4]. The various aspects related to the chiral magnetic structures can be viewed from the perspective of a general concept of *flexomagnetism* [5]. From the symmetry standpoints there is analogy between magnetic structures in thin films, the crystal subjected to flexural strain, the fan-shaped molecular structures in liquid crystals, and spin cycloids in multiferroics [6].

Conventional approach to the microscopic analysis of origin of the chiral magnetic structures is based on the three-site indirect exchange interaction [7]. However in magnetic metal films another scenario is possible based on the exchange interaction through the conduction electrons in 2 dimensional electron gas (2DEG). The spin precession of conduction electrons in 2DEG due to the spin-orbit coupling gives rise to the so-called twisted RKKY interaction in a “twisted” spin space where the spin quantization axis rotates from point to point [8]. It is shown that starting from a conduction electron Hamiltonian with Rashba spin-orbit coupling the Dzyaloshinskii-Moriya terms in exchange interaction can be obtained accounting for the presence of the spin cycloid as well as other chiral structures like Neel type domain walls and skyrmions in thin magnetic metal film. It is also shown that in high magnetic field of an order of 30 Tesla the phase transition into the homogenous magnetic state with spin cycloid suppression is possible.

Support by Russian Foundation for Basic Research RFBR ## 13-02-12443 ofi_m2 is acknowledged. AKZ acknowledges support from 14-02-91374 ST_a grant.

- [1] M. Bode, M. Heide, K. von Bergmann, P. Ferriani, S. Heinze, G. Bihlmayer, A. Kubetzka, O. Pietzsch, S. Blügel, and R. Wiesendanger, *Nature*, **447** (2007) 190-193.
- [2] M. Heide, G. Bihlmayer, and S. Blügel, *Physical Review B*, **78** (2008) 140403.
- [3] A. Fert, V. Cros, and J. Sampaio, *Nature nanotechnology*, **8** (2013) 152-156.
- [4] A. P. Pyatakov, G. A. Meshkov, and A. K. Zvezdin, *JMMM*, **324** (2012), 3551–3554.
- [5] R. Hertel, “Curvature-Induced Magnetochirality,” *Spin*, **3** (2013), 1340009.
- [6] A. P. Pyatakov and A. K. Zvezdin, *The European Physical Journal B*, **50** (2009), p. 419-427.
- [7] Fert A and Levy P M, *Phys. Rev. Lett.* **44** (1980) 1538-1541.
- [8] Imamura H., Bruno P., Utsumi Y., *Physical Review B* **69** (2004) 121303(R).

30RP-E-7

CHIRAL CATASTROPHE OF THE BAK-JENSEN MODEL IN SPIRAL STRUCTURE OF $\text{Fe}_{1-x}\text{Co}_x\text{Ge}$

Grigoriev S.V.^{1,2,*}, *Siegfried S.-A.*³, *Altynbayev E.V.*^{1,2}, *Heinemann A.*³, *Dyadkin V.A.*⁴,
Moskvin E.V.^{1,2}, *Menzel D.*⁵, *Tsvyashchenko A.V.*⁶

¹ Petersburg Nuclear Physics Institute, Gatchina, 188300 St-Petersburg, Russia

² Faculty of Physics, Saint-Petersburg State University, 198504 Saint Petersburg, Russia

³ Helmholtz Zentrum Geesthacht, 21502 Geesthacht, Germany

⁴ Swiss-Norwegian Beamlines at the ESRF, Grenoble, 38000 France

⁵ Technische Universität Braunschweig, 38106 Braunschweig, Germany

⁶ Institute for High Pressure Physics, 142190, Troitsk, Moscow, Russia

* grigor@pnpi.spb.ru

We have synthesized under high pressure the solid solutions of $\text{Fe}_{1-x}\text{Co}_x\text{Ge}$ compounds with x running from 0.0 to 1.0. Samples are in a polycrystalline powder form with a crystallite size of order of 10 microns. Small-angle neutron scattering and magnetization measurements have shown that the magnetic system in the $\text{Fe}_{1-x}\text{Co}_x\text{Ge}$ compounds is ordered into the spin helix structure, which is characterized by several parameters of the Bak-Jensen model [1,2]: T_C , S , k , and H_{C2} . The ordering temperature T_C and the average spin of the unit cell S decreases smoothly with concentration x from the maximum for FeGe to zero for the compound with $x = 0.9$. The value of the wavevector k changes from 0.09 nm^{-1} for pure FeGe, through its minimum ($|k| \rightarrow 0$) at $x_C = 0.6$, to the value of 0.14 nm^{-1} for $x = 0.8$. Similar to the recent work with the $\text{Mn}_{1-x}\text{Fe}_x\text{Ge}$ compounds [Phys. Rev. Lett. **110** (2013) 207201] we observe a transformation of the helix structure to the ferromagnet at $x \rightarrow x_C$, which is explained by different signs of chirality for the compounds with $x > x_C$ and $x < x_C$. The critical field of transformation into collinear state, H_{C2} , decreases linearly with concentration x to its minimum at x_C , then increases, duplicating the dependence $k(x)$.

It is known that the parameters magnetic system k , and H_{C2} are interconnected via the exchange integral J and Dzyaloshinskii constant D in the Bak-Jensen model: $k = D/J$ and $SJk^2 = g\mu_B H_{C2}$ [1, 2]. We estimated the values of the exchange integral J and Dzyaloshinskii constant D from the experimental data. It is found that the modulo of the D does not depend on x within error bars, but changes its sign at x_C . The exchange integral J is a diverging function of the argument $|x-x_C|$, that is tend to infinity at x_C . Nevertheless, the ordering temperature T_C of the compound at x_C is finite and equals to 120 K. The very fact of J tending to infinity in the vicinity of x_C , accompanying step-like abrupt change of the sign of D was named as a ‘‘chiral catastrophe of the Bak-Jensen model’’ in $\text{Fe}_{1-x}\text{Co}_x\text{Ge}$. One may doubt in the applicability of the Bak-Jensen model, nevertheless, it gives the value of the Dzyaloshinskii constant with great confidence $D/a \approx 1 \text{ meV}$ for the whole series of the $\text{Fe}_{1-x}\text{Co}_x\text{Ge}$ compounds. The same value $D/a = 1.15 \pm 0.10 \text{ meV}$ was found earlier for $\text{Mn}_{1-x}\text{Fe}_x\text{Si}$ and $\text{Fe}_{1-x}\text{Co}_x\text{Si}$ [Phys.Rev. B **79** (2009) 144417].

The magnetic peculiarities close to x_C should be possible to explain within the microscopic theory, where both exchange and DM interactions are taken into account for the first, second, and third magnetic neighbors. The interplay between the exchange parameters of several magnetic shells is, probably, responsible for the observed chiral catastrophe.

[1] P. Bak and M. H. Jensen, *J. Phys. C: Solid St. Phys.* **13** (1980) L881.

[2] S.V. Maleyev, *Phys.Rev. B*, **73** (2006) 17440.

30OR-E-8

CRITICAL BEHAVIOR OF RMn_2O_5 MULTIFERROICS IN VICINITY OF MAGNETIC TRANSITION FROM PARAMAGNETIC TO LONG-PERIOD STRUCTURE

Men'shenin V.V.

Institute of Metal Physics of the Ural Division of RAS, Yekaterinburg, Russia

menshenin@imp.uran.ru

In recent years, much attention has been devoted to studying the physical properties of RMn_2O_5 oxides, where R is a rare earth element. This interest is related primarily to the discovery of strong coupling between the long range magnetic order and electric polarization [1]. A magnetic phase transition from the paramagnetic state to a long period magnetic structure in RMn_2O_5 multiferroics (R = Eu, Er) has been studied [1]. According to experimental data, the wave vector star corresponding to the transition is $\mathbf{k} = \{1/2, 0, \mu\}$, where $\mu = 0.3$ for EuMn_2O_5 . An effective Hamiltonian for this system has been constructed, which allows this transition to be analyzed in the framework of the RG approach. This effective Hamiltonian for a four component order parameter, in view of a low (orthorhombic) symmetry, involves four (in the general case, different) parameters g_i ($i = 1, \dots, 4$) related to fourth order invariants in the thermodynamic potential. In the case where $g_2 = g_4$, this effective Hamiltonian coincides with that used for studying magnetic transitions in transition metal oxides. If $g_3 = 0$, the effective Hamiltonian is equivalent to that used for studying magnetic transitions to incommensurate structures in compounds such as TbAu_2 and DyC_2 .

It has been established that there are three other critical points in the event that four values of g_i ($i = 1, \dots, 4$) are nonzero. An analysis of the stability of these points leads to the following results. There are two stable critical points. At these points, a second order phase transition takes place from the paramagnetic state to a long-period magnetic structure incommensurate along the crystallographic z axis. However, one of this transition can only take place provided that the orthorhombic symmetry in the system is present as a small distortion of the cubic symmetry.

It has been found that the transition from the paramagnetic phase occurs to a long-period structure that has the wave vector $\mathbf{k} = (\beta, 0, \kappa)$ and is incommensurate in two spatial directions in the compounds RMn_2O_5 (R = Tb, Ho, Dy). This phase transition has been studied also [2]. An effective Hamiltonian for this system has been constructed in order to analyze this transition on the base of the RG approach. This effective Hamiltonian for a four component order parameter, involves three (in the general case, different) parameters g_i ($i = 1, \dots, 3$) related to fourth order invariants in the thermodynamic potential. The coefficients g_1 and g_2 satisfy the relationship $g_2 = 2g_1$. It should be noted that this effective Hamiltonian differs from the Hamiltonian describing the phase transition in RMn_2O_5 oxides with the star of the wave vector $\mathbf{k} = (1/2, 0, \kappa)$ in that it does not contain an invariant of the form $\zeta_1(x)\zeta_2(x)\zeta_3(x)\zeta_4(x)$, where $\zeta_i(x)$ ($i=1,\dots,4$) are the components of the order parameter.

It has been shown that, upon the transition corresponding to the star of the wave vector $\mathbf{k} = (\beta, 0, \kappa)$ in the studied oxides, there is only one fixed critical point of the renormalization group transformation. It is a stable point of this transformation, at which there occurs a second order phase transition to the magnetic structure incommensurate in two spatial directions. The critical points which arise upon the transition corresponding to the star of the wave vector $\mathbf{k} = (1/2, 0, \kappa)$, do not coincide with this critical point. Thus, the conditions for the occurrence of second order phase transitions differ for the wave vectors with the incommensurability in one and two spatial coordinates.

This work is partly supported by grant 12-П-2-1041 UB RAS.

[1] V.V. Men'shenin. *JETP*, **116** (2013) 980–986.

[2] V.V. Men'shenin. *PSS*, **55** (2013) 2051–2056.

30 June

Monday

12:00-13:45

15:00-17:15

oral session

30TL-F

30RP-F

30OR-F

**“Soft and Hard
Magnetic Materials”**

30TL-F-1

MAGNETIC PECULIARITIES OF PLUTONIUM AND COMPOUNDS

Kassan-Ogly F.A.¹, Korolev A.V.¹, Ustinov V.V.¹, Zuev Yu.N.², Arkhipov V.E.¹

¹ Institute of Metal Physics, Ural Division, RAS, Ekaterinburg, Russia

² Russian Federal Nuclear Center - Institute of Technical Physics, Snezhinsk, Russia
felix.kassan-ogly@imp.uran.ru

The peculiarities of plutonium crystal structures, their distinguishing features from metals are discussed in the report. They are found to be in close interdependence with the intricate problem of localized magnetic moments and magnetic ordering in plutonium and its numerous compounds. Multifarious physical models suggested for determining the nature and origins of these peculiar features, based on the well-known concepts and approaches and on novel very original and exotic ideas, are considered. The detailed comparative analysis of experimental achievements and numerous papers in various versions of numerical computations in “the first principles (*ab initio*)” approach is carried out. Some new effects recently discovered and not yet comprehended are regarded as well [1].

In many papers, in different versions of numerical computations of Pu magnetic moment in the framework of the first-principles approach different results were obtained, and the scatter of magnetic moment value constitutes the wide range from 0.25 up to 5.0 μ_B , and the magnetic ordering appears either to be antiferromagnetic or it is absent at all. Several papers are also available in which either magnetic ordering is denied or even magnetic moment of plutonium is entirely negated. Plutonium has atypically high magnetic susceptibility, but even at the lowest temperatures, plutonium never settles down to a state of magnetic long-range order as other metals do. In the case of even great antiferromagnetic interaction, magnetic ordering may be lacking at all, which is related to the frustration phenomenon. Thus, the absence of magnetic ordering in pure Pu and plutonium monochalcogenides is explained.

In plutonium mononictides a wide diversity of magnetic structures are observed. Plutonium mononitride PuN is an antiferromagnet, undergoing a transition from paramagnetic state to the structure of AI type that has an arrangement of ferromagnetic sheets of a (001) type, alternating in the [001] direction in a simple consequence $+ - + - + -$. Plutonium mononictides PuP and PuAs are ferromagnets. In plutonium monoantimonide PuSb, two magnetic phase transitions take place: first, from paramagnetic phase to an incommensurate phase and then from incommensurate to ferromagnetic phase. Plutonium monobismuthide PuBi is an antiferromagnet with an incommensurate structure. All these structures are explained by taking into account the competing interactions between nearest and next-nearest neighbors. A formula that describes the temperature behaviour of incommensurate wave-vector is proposed.

One more effect - changing of 5f electron localization degree with temperature in plutonium-gallium alloys and in plutonium monochalcogenides is discovered and explained in the framework of modified Curie-Weiss law.

Support by project of Integrated Fundamental Research of UD RAS no.12-I-2-2020 and project of Presidium of RAS no. 12-P-2-1041 is acknowledged.

[1] F.A. Kassan-Ogly, A.V. Korolev, V.V. Ustinov, Yu.N. Zuev, V.E. Arkhipov, *Phys. Met. Metallogr.*, **114** (2013) 1155-1181.

[2] V.E. Arkhipov, F.A. Kassan-Ogly, A.V. Korolev, S.V. Verkhovskii, Yu.N. Zuev, I.L. Svyatov, *J. Magn. Magn. Mater.* **385** 42-45 (2009).

30TL-F-2

FLAT MAGNETOIMPEDANCE NANOSTRUCTURES: NEW TOPOLOGICAL APPROACHES

Kurlyandskaya G.V.^{1,2,}, Chlenova A.A.², Lodewijk K.J.^{1,3}*

¹ University of the Basque Country UPV-EHU, Bilbao, Spain

² Ural Federal University, Ekaterinburg, Russia

³ University of Groningen, Groningen, Holland

* galina@we.lc.ehu.es

Magnetoimpedance (MI) is the change in electrical impedance of a ferromagnetic conductor under application of an external magnetic field [1]. MI research is of great interest due to its present and potential applications for magnetic field sensors [2]. Special efforts were made in the development of magnetic thin film sensitive elements including biosensor prototypes [3-4]. Classic flat MI film structures consist of top and bottom ferromagnetic parts of equal thickness (either thin film or multilayered structure) separated by Cu, Al or Au conductive lead. Therefore, in all previous studies only symmetric MI structures were considered for the following selected reasons: symmetric MI film structures with both open and closed magnetic flux provide the highest sensitivity with respect to uniform external magnetic fields. At the same time, there are a number of particular applications (biosensing is among one of them) where non-uniform magnetic fields of complex configurations must be detected and evaluated. Here we describe our experience in design, fabrication and characterisation of highly sensitive symmetric and non-symmetric MI multilayers with open magnetic flux deposited by rf-sputtering onto rigid and flexible substrates. In some cases micro-meanders were fabricated using optical lithography. Non-symmetry of the structures was obtained by the deposition of top and bottom ferromagnetic parts of MI element of different thickness. Another way of fabrication of non-symmetric MI structures is a special surface modification [5] of the top layer by aromatic organic compounds resulting in formation of irregular polycyclic structures. Finally, it is possible to change the MI response by utilization of polymer/magnetic nanoparticle composite thin films spread onto the surface of flat MI sensitive element. Top and bottom layers of MI multilayers deposited onto flexible substrates tend to be very different even if they are deposited in similar conditions and special efforts are necessary to obtain requested sensitivities of the order of 50%/Oe (sensitivities of 100 %/Oe correspond to the same MI layered structures deposited onto rigid substrates).

This work was supported by SAIOTEK-REMASEN grant and by a grant CRDF – UB RAS RUE2-7103-EK-13 from the U.S. Civilian Research & Development Foundation (CRDF Global) with funding from the United States Department of State. The opinions, findings and conclusions stated here in are those of the authors and do not necessarily reflect those of CRDF Global or the United States Department of State. We thank A.V. Svalov, A.García-Arribas, E. Fernández, I.V. Beketov, A.P. Safronov, A.M. Murzakaev S.O. Volchkov, V.N. Lepalovskij and B.J. Kooi for special support.

- [1] A.S. Antonov, S.N. Gadetskii, A.B. Granovskii, A. L. Diackov, V.P. Paramonov, N. S. Perov, A.F. Prokoshin, N. A. Usov, A. N. Lagar'kov, *Phys. Met. Metal.*, **83** (1997) 612.
- [2] V.E. Makhotkin, B.P. Shurukhin, V.A. Lopatin, P.Y. Marchukov, Y.K. Levin, *Sens. Actuators A*, **759** (1991) 759.
- [3] L.V. Panina, K. Mohri, *Sens. Actuators A*, **81** (2000) 71.
- [4] G.V. Kurlyandskaya, D. de Cos, S.O. Volchkov, *Russian J. Nondestr. Test.*, **45** (2009) 377.
- [5] I.V. Beketov, A.P. Safronov, A.V. Bagazeev, A. Larrañaga, G.V. Kurlyandskaya, A.I. Medvedev, *J. All. Comp.*, **586** (2014) S483.

30OR-F-3

MAGNETIC PROPERTIES OF MECHANICALLY ALLOYED (NANOSTRUCTURED) AND ANNEALED CEMENTITE

Yelsukov E.P.

Physical-Technical Institute UrB RAS, 132, Kirov St., 426000 Izhevsk, Russia
e_yelsukov@mail.ru

The structure of cementite, which is one the most important structural constituent of steels and cast irons, has been analyzed in a great number of papers during a more than eighty-year history of its study. Nevertheless, to date there are no unambiguous viewpoints on the localization of C atoms in the unit cell and its influence on magnetic properties of cementite. X-ray diffraction, Mössbauer spectroscopy and magnetic measurements were used to study cementite produced by mechanical alloying and followed by annealing.

The cementite prepared by mechanical alloying (MA) is in a nanostructural state (3 nm) and is characterized by strong lattice microdistortions and large line width of Mössbauer spectrum. Being in the strained state, C atoms occupy not only prismatic, but also octahedral interstices. This structure is called here the deformed cementite (Fe₃C)_D. At the annealing temperature 775 K C atoms are localized only in the prismatic interstices. This local structure is characterized by the low values of the lattice microdistortions and line width in the Mössbauer spectrum of cementite. We call this structure the non-distorted cementite Fe₃C. At all the stages of the local atomic structure evolution the cementite has an orthorhombic lattice (space group Pnma). The Fe₃C and (Fe₃C)_D are characterized by close Curie temperatures of 500 K, magnetic moments per Fe atom (\bar{m}_{Fe}) and average hyperfine magnetic fields (\bar{H}). Under other conditions being equal, the coercivity H_C of the Fe₃C cementite can be three times higher than that of the (Fe₃C)_D cementite due to a larger magnetocrystalline anisotropy constant [1,2].

Parameters \ Sample	MA(16h) (Fe ₃ C) _D	MA(16h)+775 K(1h) Fe ₃ C	T _{meas} , K
\bar{m}_{Fe} , μ_B	1.71 ± 0.03	1.64 ± 0.03	77
\bar{m}_{Fe} , μ_B	1.46 ± 0.03	1.42 ± 0.03	300
\bar{H} , T	24.3 ± 0.2	24.6 ± 0.2	77
\bar{H} , T	20.4 ± 0.2	20.6 ± 0.2	300
H _C , Oe	226 ± 2	691 ± 2	77
H _C , Oe	106 ± 2	320 ± 2	300

The work has been supported by the Russian Fund for Basic Research (project No. 13-03-00039).

[1]. E.P. Yelsukov et al. in Proceed. Intern. Conf. MSMS'08. *AIP Conference Proceedings*, Melville, New York, **1070**(2008)53-63.

[2]. A.K. Arzhnikov, L.V. Dobysheva, *J. Phys.: Cond. Matter*, **19**(2007)196214.

30OR-F-4

ELECTROCHEMICAL CORROSION OF THIN FERROMAGNETIC Fe-N FILMS IN NEUTRAL SOLUTION

Maklakov S.S.¹, Maklakov S.A.¹, Amelichev V.A.², Naboko A.S.¹, Ryzhikov I.A.¹

¹ Institute for Theoretical and Applied Electromagnetics of the Russian Academy of Sciences
(ITAE RAS), Moscow, Russia

² SuperOx, Moscow, Russia
squirrel498@gmail.com

Thin Fe films are of prime interest for microwave applications both as shielding media and active material for microwave devices [1]. Doping with trace amounts on nitrogen increases stability and influences magnetic properties of Fe films [2]. Studying of a corrosion behavior of thin films is of importance as it allows revealing fundamental physical and chemical phenomena [3] and as it provides evaluation of corrosive destruction for thin film materials.

Corrosion behavior is reported for *Fe-N* films ($h = 150$ and 300 nm) deposited onto polymer (*Fe-PET*) and glass (*Fe-glass*) substrates via DC magnetron sputtering (90 % Ar - 10 % N₂ gas mixture). Polarization curves are obtained in 0.1 M Na₂SO₄ under ongoing Ar bubbling.

Film's surface is covered with an oxide layer. *Fe-PET* films show lesser free surface energy in comparison with *Fe-glass* films (H₂O wetting angle is $\theta = 77 \pm 5^\circ$ and $\theta = 87 \pm 2^\circ$, which gives adhesion energy $W_a = 89.1 \cdot 10^{-3}$ J/m² and $W_a = 76.6 \cdot 10^{-3}$ J/m², respectively). Initial corrosion stage for films on the rigid substrate goes slower than for the polymer substrate: corrosion currents for oxide dissolution and stationary potentials are $i_{corr} = 5 \cdot 10^{-7}$ A/cm², and $E_0 = -0.050$ V (vs SHE) for *Fe-glass*; $i_{corr} = 7 \cdot 10^{-6}$ A/cm², and $E_0 = -0.465$ V for *Fe-PET*.

Film's thickness influences corrosion rate, but rigidity of substrate does not. Increase in thickness results in increase in corrosion current: $i_{corr} = 1 \cdot 10^{-5}$ A/cm² for $h = 150$ nm, and $i_{corr} = 8 \cdot 10^{-5}$ A/cm² for $h = 300$ nm. Stationary, passivation and repassivation potentials for *Fe-N* films after oxide layer removal are $E_0 = -0.575$ V, $E_{pass} = -0.500$ V, and $E_{repass} = +1.350$ V. In the case of $h = 150$ nm, films show localized corrosion. In a passive state, *Fe-glass* films are more stable than *Fe-PET* films.

The phenomena observed are probably the results of a mechanical stresses within metal film [3]. In the case of flexible and plastic substrate these stresses are partially decreased due to sample bend. The rigid substrate produces mechanical stress excess which increases oxide layer thickness and increase initial corrosion durability. The results reported are of practical interest for thin film materials and devices [4].

[1] I.T. Iakubov, A.N. Lagarkov, et.al., *JMMM*, **316** (2007) e813.

[2] A.N. Lagarkov, I.T. Lakubov, et.al., *Phys. B: Condensed Matter*, **394** (2007) 159-162.

[3] A.V. Agaponova, I.V. Bykov, et.al., *Phys. Solid State*. **53** (2011) 1013-1016.

[4] S.S. Maklakov, S.A. Maklakov, et.al., *Nanotechnologies in Russia*, **7** (2012) 255-261.

30RP-F-5

MAGNETIC BEHAVIOR OF SYSTEMS BASED ON YCo_2 PAULI PARAMAGNET IN DIFFERENT NANOCRYSTALLINE STATES

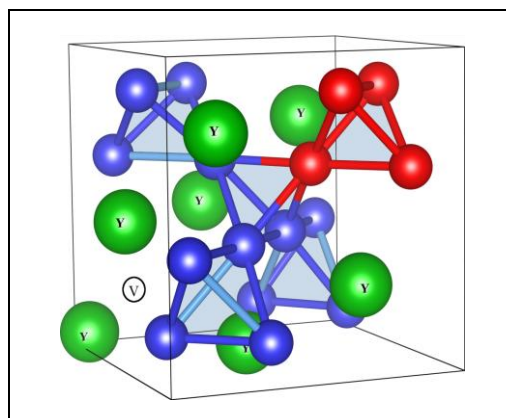
Idzikowski B., Śniadecki Z., Werwiński M., Szajek A.

Institute of Molecular Physics, Polish Academy of Sciences, Poznań, Poland
idzi@ifmpan.poznan.pl

The YCo_2 intermetallic compound is a Pauli exchange-enhanced paramagnet. In a fine crystalline form it becomes magnetically ordered in the whole volume of the grains. Also in amorphous state the ferromagnetism appears. In our studies the magnetic properties of rapidly quenched YCo_2 -type compositions are described for the nanocrystalline state produced by rapid quenching at an appropriate cooling rates.

The intermetallic compounds YCo_2 , $Y_{0.9}Nb_{0.1}Co_2$ and $Y_{0.9}Ti_{0.1}Co_2$ studied were examined with X-ray diffraction (XRD) and vibrating sample magnetometry (VSM). The samples with up to 10 at.% substitution consist of a single phase which grows after partial replacement of Y atoms in the initial YCo_2 by Nb or Ti. These compounds crystallize in $MgCu_2$ -type phase with lattice constant changing from 7.223 Å for YCo_2 , through 7.213 Å for $Y_{0.9}Nb_{0.1}Co_2$ to 7.192 Å for $Y_{0.9}Ti_{0.1}Co_2$, where Y atoms are replaced by Nb or Ti atoms.

The electronic band structures of YCo_2 systems with point defects were calculated using FP-LAPW (Full Potential–Linearized Augmented Plane Wave) method. Nb and Ti substitutions and also vacancies were considered as a point defects. Theoretically predicted ferrimagnetic ground states for the YCo_2 system with Y atoms replaced by Ti and Nb find experimental confirmation in $Y_{0.9}Ti_{0.1}Co_2$ and $Y_{0.9}Nb_{0.1}Co_2$. Calculations show that ferrimagnetic ground states are energetically more stable for systems with point defects at the sites of Y atoms than at the sites of Co ones. Reduction in the magnetic moment values of Co to about 1 μ_B for compounds with point defects (see Figure of Y_7Co_{16} supercell) at cobalt sites is found.



All investigated compounds show a broad maximum of the magnetization vs temperature $M(T)$ curves similar to polycrystalline YCo_2 behaving as exchange-enhanced Pauli paramagnets. But there is clear increase of magnetization at lower temperatures and hysteresis loops are visible in $M(H)$ curves. By replacing of Y by Ti or Nb, the overall magnetization in low magnetic field increases about two times. This feature along with observed changes in $M(H)$ curves are due to the appearance a magnetically ordered phase. Its origin is connected with point defects and/or an expanded lattice structure of the YCo_2 phase.

The results of theoretical calculations for $Y_{0.9}Ti_{0.1}Co_2$ show that magnetic moments on Co and Ti are oriented antiparallel with values of 1.1 μ_B /atom and -0.9 μ_B /atom [1]. When taking into account magnetic moment of -0.3 μ_B /atom induced on Y it gives total magnetic moment equal to 1.84 μ_B /f.u. For $Y_{0.9}Nb_{0.1}Co_2$ system, the total energy for nonmagnetic state is lower by about 5.5 meV/f.u compared to the spin-polarized state. Hence, the substitution effect alone does not explain the enhanced magnetic ordering in both alloys, which rather appears to be driven by an increased density of lattice defects and decreased grain sizes.

[1] Z. Śniadecki, M. Werwiński, A. Szajek, U.K. Röbller, B. Idzikowski, *J. Appl. Phys.*, **115** (2014) 17E129.

30TL-F-6

MANIPULATION OF MAGNETIC PROPERTIES OF GLASS-COATED MICROWIRES BY ANNEALING

Zhukov A.^{1,2}, Chichay K.³, Talaat A.¹, Rodionova V.³, Blanco J.M.⁴, Ipatov M.¹, Zhukova V.¹

¹ Dpto. Física de Materiales, Fac. Químicas, UPV/EHU, 20009 San Sebastian, Spain

² IKERBASQUE, Basque Foundation for Science, 48011 Bilbao, Spain

³ Immanuel Kant Baltic Federal University, 236041 Kaliningrad, Russia

⁴ Dpto. Física Aplicada, EUPDS Basque Country University UPV/EHU, Spain

arkadi.joukov@ehu.es

Studies of amorphous magnetically soft glass-coated microwires have attracted considerable interest in the field of applied magnetism because of their reduced dimensions (metallic nucleus diameter ranging between 0.5 and 30 μm), cheap and simple fabrication method and outstanding soft magnetic properties, such as giant magnetoimpedance, GMI, effect and the magnetic bistability and related fast domain wall propagation [1]. Magnetic sensors developed using amorphous wires with GMI effect allow achieving pT magnetic field sensitivity. The shape of magnetic field dependence of the GMI effect is intrinsically related to the magnetic anisotropy and peculiar surface domain structure of amorphous wires.

The interest on DW propagation in magnetic wires is related with proposals for magnetic logic and memory devices. Naturally the DW speed is one of most important factors affecting the viability of aforementioned potential applications.

Generally soft magnetic properties of amorphous ferromagnetic microwires are affected by the magnetoelastic energy related to quenching stresses distribution arising during rapid solidification from the melt.

Consequently optimization of the GMI effect and DW dynamics is essential for the applications of glass-coated magnetic microwires.

Fast magnetization switching and related fast DW propagation are typically observed microwires with positive magnetostriction coefficient exhibiting rectangular hysteresis loops [1]. But considerable GMI effect is usually observed in microwires with low and negative magnetostriction constant [1]. From the point of view of applications creation of the samples exhibiting both aforementioned properties simultaneously is very attractive.

Therefore, we performed studies of the effect of magnetoelastic anisotropy on magnetic properties, GMI effect and DW propagation in amorphous magnetically soft microwires paying attention to find the conditions for observation of these two effects simultaneously.

We studied GMI effect and magnetic properties of amorphous Fe-Co rich as-prepared and annealed microwires. We measured the GMI magnetic field and frequency dependences, hysteresis loops and DWs dynamics in Co-rich and observed that these properties can be tailored either controlling magnetoelastic anisotropy of as-prepared CoFeBSiC microwires or controlling their magnetic anisotropy by heat treatment. High GMI effect has been observed in as-prepared Co-rich microwires. High DW velocity and rectangular hysteresis loops we observed in heat treated Co-rich microwires. At certain annealing conditions we observed coexistence of GMI effect and fast DW propagation in the same annealed sample.

Support by by EU under FP7 “EM-safety” project, by Spanish and by the Basque Government is acknowledged.

[1] A. Zhukov and V. Zhukova, *International Frequency Sensor Association Publishing*, Barcelona, (2014) 164

30OR-F-7

EFFECT OF CURRENT ANNEALING ON DOMAIN WALL DYNAMICS IN BISTABLE FeCoMoB MICROWIRES

Klein P.¹, Varga R.¹, Badini-Confalonieri G.A.², Vazquez M.²

¹ Faculty of Science, Institute of Physics, UPJS, Park Angelinum 9, 041 54 Košice, Slovakia

² Instituto de Ciencia de Materiales de Madrid, CSIC, Sor Juana Inés de la Cruz 3, 28049 Cantoblanco, Madrid, Spain
rvarga@upjs.sk

Domain wall dynamics is used in many modern spintronic devices to transfer or store information [1,2]. The operating speed of such devices depends on the domain wall velocity.

Very fast domain wall velocities have been observed in amorphous microwires, but dynamics is very unstable with time (ageing) or temperature [3,4]. One possible solution is to use the nanocrystalline materials, which are prepared by controlled annealing from amorphous precursors [5].

In the previous work [6], stable and very fast domain wall up to 3 km/s was observed in nanocrystalline FeCoMoB microwires annealed in furnace for 1 hour at 500 °C.

In the given contribution, we present very fast method of thermal treatment based on current annealing. It will be shown that 10 minutes of current annealing corresponds to 1 hour of classical annealing in furnace. Moreover, current flowing through microwire produces Oersted magnetic field and therefore circular magnetic anisotropy is induced during current annealing. As a result, circular magnetic anisotropy prefers vortex domain wall with velocities up to 10 km/s that can be observed in the current annealed nanocrystalline FeCoMoB microwires with much higher thermal stability.

This study was supported by the project NanoCEXmat Nr. ITMS 26220120019, Slovak VEGA grant. No. 1/0060/13, APVV-0027-11 and APVV-0266-10.

[1] S.S.P. Parkin, M. Hayashi, and L. Thomas, *Science*, **320** (2008) 190.

[2] D.A. Allwood, G. Xiong, C.C. Faulkner, D. Atkinson, D. Petit, R.P. Cowburn, *Science*, **309** (2005) 1688.

[3] G. Infante, R. Varga, G.A. Badini-Confalonieri, and M. Vazquez, *Appl. Phys. Lett.*, **95** (2009) 012503.

[4] R. Varga, K.L. Garcia, M. Vazquez, and P. Vojtanik, *Phys. Rev. Lett.*, **94** (2005) 017201.

[5] G. Herzer, *Acta. Mater.*, **61** (2013) 718.

[6] P. Klein, R. Varga, and M. Vazquez, *J. Alloys. Comp.*, **550** (2013) 31-34.

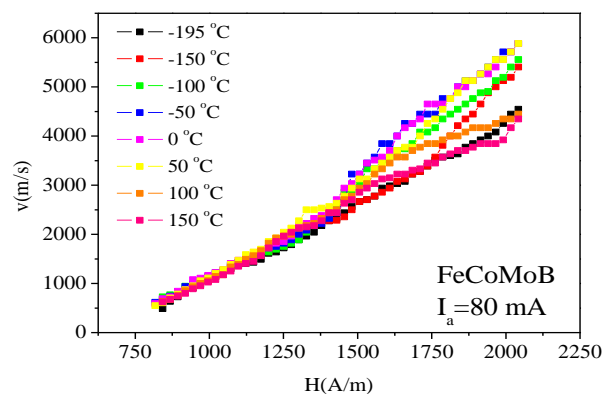


Fig. 1. Domain wall dynamics in FeCoMoB microwire annealed at 80 mA for 10 minutes.

30OR-F-8

STRUCTURAL AND MAGNETIC PROPERTIES OF $\text{Fe}_{73,5}\text{Si}_{13,5}\text{B}_9\text{Nb}_3\text{Cu}_1$ MICROWIRES, PRODUCED BY MODERNIZED ULITOVSKY-TAILOR METHOD

Shalygina E.E.¹, Shalygin A.N.¹, Kharlamova A.M.¹, Molokanov V.V.², Chueva T.R.², Umnov P.P.², Umnova N.V.²

¹ Faculty of Physics, M.B. Lomonosov Moscow State University, Moscow, 119991 Russia

² A.A. Baikov Institute of Metallurgy and Materials Science, Moscow, 119991 Russia
shal@magn.ru

It is known that the $\text{Fe}_{73,5}\text{Si}_{13,5}\text{B}_9\text{Nb}_3\text{Cu}_1$ microwires (Finemet) exhibit the unique magnetic properties after thermal treatment. At the same time the existence of a glass cover caused the strong heterogeneity of magnetic properties along their length. Recently, “thick” $\text{Fe}_{73,5}\text{Si}_{13,5}\text{B}_9\text{Nb}_3\text{Cu}_1$ amorphous microwires with diameter of the metallic core up to 50 microns were prepared with the help of the modernized Ulitovsky–Taylor method [1]. The study of the physical properties of such microwires deserved attention as from the scientific and practical points of view. In this work, results on the investigation of the mechanical, elastic and magnetic characteristics of the “thick” $\text{Fe}_{73,5}\text{Si}_{13,5}\text{B}_9\text{Nb}_3\text{Cu}_1$ amorphous microwires, produced by the modernized Ulitovsky–Taylor method, are presented.

The amorphous state of the as-cast microwires was checked with the help of X-ray diffraction (XRD). The plasticity level of the microwires was estimated by its ability to be tied into a knot without fracture. The bulk and near-surface magnetic characteristics of the microwires were measured employing the vibration and magneto-optical magnetometers, respectively. The influence of the stretching tension and tension of torsion on the magnetic properties of microwires was studied by using the special laboratory setup.

The following peculiarities of the microwires under study were established. The cores of the $\text{Fe}_{73,5}\text{Si}_{13,5}\text{B}_9\text{Nb}_3\text{Cu}_1$ microwires have the stable geometric parameters along their length and the smooth (almost without defects) surfaces. The microwires are characterized by the high plasticity and the high strength. They don't be destroyed even after a full tightening into a knot. The distinction of the magnetic characteristics of the microwires with the glass shell and without it does not exceed 10%. The values of the saturation field and the coercivity increase with the growth of the microwire diameter. The stable geometric parameters of the $\text{Fe}_{73,5}\text{Si}_{13,5}\text{B}_9\text{Nb}_3\text{Cu}_1$ microwires along their lengths cause the slight dispersion of magnetic anisotropy of the near-surface layers. As a result, the microwires exhibit the high homogeneity of the near-surface local magnetic properties.

The measurement of the Villari effect showed the strong influence of the stretching tension and tension of torsion on the remagnetization signal of the microwires. It was found that the signals of remagnetization of the microwires increase strongly at their torsion on 4 turns and are slowed down after 8 turns. In the case of the stretching tension, the remagnetization signals of the microwires linearly grow with increasing in loading up to 40 grams. The subsequent increase in the stretching tension is accompanied by the signal decrease. Thus, the high sensitivity of the $\text{Fe}_{73,5}\text{Si}_{13,5}\text{B}_9\text{Nb}_3\text{Cu}_1$ amorphous microwires to elastic deformations of stretching and torsion in the magnetic field was experimentally established. The discovered properties of the amorphous microwires make these materials promising for practical applications.

[1] P.P. Umnov, V.V. Molokanov, Yu. S. Shalimov, N.V. Umnova, T.R. Chueva, V.T. Zabolotnyi, *Journal of Perspective materials*, **2** (2010), 87-91 (in Russian).

30OR-F-9

KINETICS OF LOW TEMPERATURE TRANSFORMATIONS IN SOFT MAGNETIC AMORPHOUS ALLOYS

Kaloshkin S.¹, Churyukanova M.¹, Zhukova V.², Zhukov A.^{2,3}

¹ National University of Science and Technology «MISIS», Moscow, Russia

² Dpto. Fisica de Materiales, UPV/EHU, 20009, San Sebastian, Spain

³ IKERBASQUE, Basque Foundation for Science, 48011 Bilbao, Spain

kaloshkin@isis.ru

Structural state of amorphous magnetic materials is very important for practical application especially considering their soft magnetic properties. Curie temperature, T_c , is very sensitive to structural changes in amorphous ferromagnetic alloys, which accompany relaxation and crystallization processes during annealing. So the measurement of T_c may give much information about kinetic parameters of these processes and in combination with structural investigation it becomes a powerful method of kinetic analysis of all kinds of transformations in alloys with amorphous or partially amorphous structures. It is possible to study kinetics of relaxation, distinguish the processes of relaxation and crystallization.

One of the main fundamental properties that define soft magnetic behavior of amorphous alloys is the value of magnetostriction. Describing the change in average interatomic distances between atoms, the value of magnetostriction should have relationship to another fundamental characteristic of the material – heat of capacity. An experimental study of the relationship of these parameters during the transition from the ferromagnetic to the paramagnetic state at the Curie temperature is one of the tasks of this research. Coercivity and the heat capacity in vicinity of Curie temperature of soft magnetic materials exhibit correlation.

30OR-F-10

STRUCTURAL AND MAGNETIC PROPERTIES OF ANNEALED VAPOR DEPOSITED $\text{Co}_x\text{Cr}_{1-x}$ THIN FILMS

Kharmouche A.

Laboratory of Surfaces and Interfaces Studies of Solid Materials,
 Laboratoire d'Etudes des Surfaces et Interfaces des Matériaux Solides (L.E.S.I.M.S.)
 Department of Physics, Ferhat Abbas University Sétif1, 19000, Sétif, Algeria
 kharmouche_ahmed@yahoo.fr & kharmouche_ahmed@univ-setif.dz

We prepared, under vacuum and onto monocrystalline silicone substrate, series of $\text{Co}_x\text{Cr}_{1-x}$ thin films, with x ranging from 0.80 to 0.88. The structural and magnetic properties of the as deposited films have been performed using Rutherford backscattering spectrometry (R.B.S.), X-ray diffraction (X.R.D.), Alternating Gradient Field Magnetometer (A.G.F.M.), and Brillouin Light Spectrometry (B.L.S.) techniques. Once the films being annealed under vacuum, for 1 h at 700°C , in a pre-heated furnace, their structural and magnetic properties have been performed, by these tools, as well.

Significant results have been found. The as deposited films present only an HCP structure and show a preferred orientation. The annealed films present both HCP and FCC structures. The annealed films possess cell parameters greater than the bulk ones which infer that they are under a tensile stress. The cell parameters of the as deposited films are lower than the bulk ones which infer that they are under a compressive stress. Up to the annealing temperature the films are still ferromagnetic and some decrease of the magnetic moment is noticed. In addition, coercivity and squareness have been strongly improved in the annealed films comparatively to the as deposited films (figure1). Moreover, the stiffness constant, computed using Brillouin light scattering measurements and after adjustment of theoretical and experimental results, is found to be far lesser than pure Co one (figure2). These results and others will be presented and discussed.

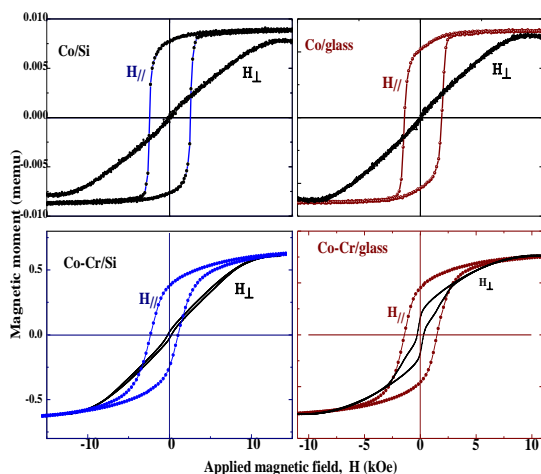


Fig. 1.

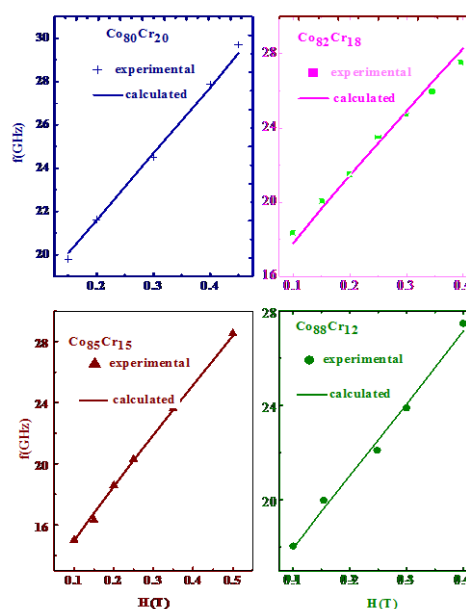


Fig. 2.

30OR-F-11

CURRENT-INDUCED CHANGE OF MAGNETIC ANISOTROPY IN CO-RICH AMORPHOUS MICROWIRES

Popov V.V.¹, Khatsaiuk V.V.¹, Berzhansky V.N.¹, Qin F.X.², Gomonay H.V.³

¹ Taurida National V. I. Vernadsky University, Simferopol, Ukraine

² 1D Nanomaterials Group, National Institute for Material Science, Tsukuba, Japan

³ National Technical University of Ukraine 'KPI', Kyiv, Ukraine

slavapop@gmail.com, faxiang.qin@gmail.com.

Glass-coated amorphous magnetic microwires possess strong dependence of their impedance on applied dc magnetic fields, which is known as giant magnetic impedance (GMI) effect. In the present work, we have investigated experimentally and theoretically various complex effects produced by DC current on GMI response of Co-rich microwires.

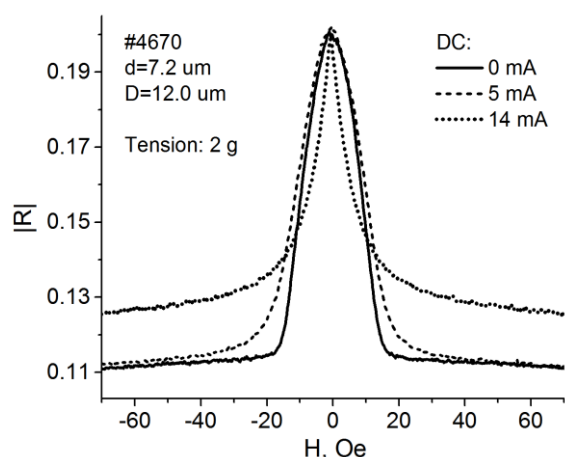


Fig. 1. Measured GMI profiles.

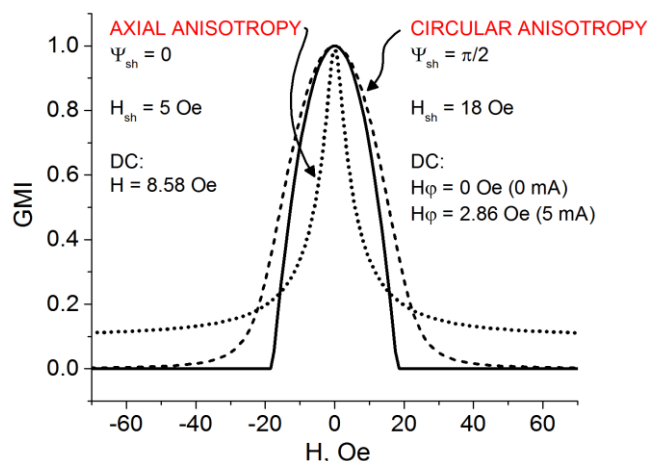


Fig. 2. Modeled GMI profiles.

It has been found that the application of the current leads to two well-distinguished scenarios depending on the current amplitude. For relatively small currents (0 and 5 mA in Fig. 1) GMI has a typical ‘valve-like’ profile corresponding to the longitudinal magnetization process. Additional circular magnetic field of the current enlarges total anisotropy of the sample while preserves smooth shape and amplitude of the peak. For larger currents (i.e., 14 mA in Fig. 1) the GMI profile changes abruptly from of broad peaks to of sharp peaks, indicating that thermo-magnetic annealing produced by current significantly modifies magnetic structure of the wire.

According to the *core-shell model* [1], the shape of the GMI peak is mainly determined by the amplitude H_{sh} and direction Ψ_{sh} of the anisotropy field for the shell layer of the wire’s metallic core. As-received Co-rich microwire has negative magnetostriction and circular anisotropy in the outer shell, i.e., $\Psi_{sh} = \pi/2$, which results in a smooth shape of the GMI profile. The circular magnetic field generated by the weak current H_{ϕ} contributes additively to the total energy, but has little influence on Ψ_{sh} and hence the broad peak feature remains.

To understand sharp peaks observed for large currents, we propose that they are attributed to the compositional and topological short range ordering processes activated during Joule-heating and the magnetostriction constant of the wire increasing towards positive values. In this case an axial anisotropy $\Psi_{sh} = 0$ is realized. Fig. 2 depicts modeled GMI profiles, which shows good agreement with experimental results in terms of the current effect on the shape of curves.

[1] V.V. Popov, et al. *J. Appl. Phys.*, **113** (2013) 17A326.

30OR-F-12

MANIPULATION OF MAGNETIC PROPERTIES AND DOMAIN WALL DYNAMICS OF AMORPHOUS FERROMAGNETIC $\text{Co}_{68.7}\text{Fe}_4\text{Ni}_1\text{B}_{13}\text{Si}_{11}\text{Mo}_{2.3}$ MICROWIRE

Chichay K.¹, Rodionova V.^{1,2}, Ipatov M.³, Zhukova V.³, Zhukov A.^{3,4}

¹ Immanuel Kant Baltic Federal University, 236041 Kaliningrad, Russia

² National University of Science and Technology "MIS&S", Moscow 119049, Russia

³ Dpto. Física de Materiales, Fac. Químicas, UPV/EHU, 20018 San Sebastian, Spain

⁴ IKERBASQUE, Basque Foundation for Science, 48011 Bilbao, Spain

ks.chichay@gmail.com

Amorphous ferromagnetic glass coated microwires are very interesting materials because of their unusual micromagnetic structure and magnetic properties [1]. Moreover there are many ways to manipulate the magnetic properties and the domain wall dynamics such as annealing, applying of the mechanical stresses, changing of the ρ -ratio of the metallic nucleus diameter, d , to the diameter of the glass coated microwire, D [2] and etc. This makes them very perspective and promising objects for coding system, magnetic memory applications and logical devices [1, 3].

In this work we studied the influence of annealing and applying of mechanical stresses on magnetic properties and the domain wall dynamics of glass-coated $\text{Co}_{68.7}\text{Fe}_4\text{Ni}_1\text{B}_{13}\text{Si}_{11}\text{Mo}_{2.3}$ amorphous ferromagnetic microwire ($d = 17.0 \mu\text{m}$, $D = 23.6 \mu\text{m}$, $\rho = 0.72$). The samples were annealed at annealing temperatures 300, 350 and 400° C without stress and under different applied stresses up to 300 MPa for different time.

The magnetic properties were investigated by induction method for as-cast and annealed samples. As-cast microwires had S-shape hysteresis loop, but after annealing the microwires became bistable. The domain wall velocity of bistable microwires was measured using Sixtus-Tonks technique. During the measuring of velocity of the domain wall propagation the axial mechanical stresses were applied. And it is found that the domain wall velocity can enhance with increasing of axial stresses value.

Also we measured the magnetostriction coefficient of studied microwires and investigated the influence of magnetostriction coefficient on magnetic properties for as-cast and annealed samples. We obtained the changing of magnetostriction coefficient sign from negative to positive after annealing that explains the changing of micromagnetic structure and hence the shape of hysteresis loop.

Resuming, we studied the magnetic properties and domain wall dynamics of $\text{Co}_{68.7}\text{Fe}_4\text{Ni}_1\text{B}_{13}\text{Si}_{11}\text{Mo}_{2.3}$ microwire. We showed that there are a lot of ways to tailor the magnetic properties that can be very useful for future applications.

[1] A. Zhukov, et al., *Encyclopedia of Nanoscience and Nanotechnology*, 2004, V.X.– P.23.

[2] K. Chichay, V. Zhukova, V. Rodionova, M. Ipatov, A. Talaat, J. M. Blanco, J. Gonzalez, and A. Zhukov, *J. Appl. Phys.* **113**, 17A318 doi:10.1063/1.4795617 (2013).

[3] M. Vazquez, *Handbook of Magnetism and Advanced Magnetic Materials 4: Novel Materials.*– John Wiley & Sons, Ltd., 2007.–P.2192-2226.

30OR-F-13

COMPONENTS OF MAGNETIC ANISOTROPY OF SOFT MAGNETIC NANOCRYSTALLINE Fe-BASED FILMS

Sheftel E.N., Harin E.V.

A.A. Baikov Institute of Metallurgy and Material Science RAS, Moscow, Russia
harin-eugene@ya.ru

The nanocrystalline films of quasi-binary alloys Fe-ZrN obtained by magnetron sputtering represent the new type of magnetically soft ferromagnetic materials, characterized by high magnetization and thermal stability [1]. Magnetic softness is explained in terms of random anisotropy model [2] where magnetization of single grains is randomly inhomogeneous and can be described by a magnetization autocorrelation function. An important parameter of this function is magnetic autocorrelation length R_L which is a typical magnetic microstructure radius, at which magnetization is relatively uniform. The model is applicable in cases when R_L is greater than grain radius R_C and there is exchange interaction between grains. In that case the hysteresis properties are defined by micromagnetic structure parameters: R_L , effective anisotropy $\langle K_{eff} \rangle$ on the scale R_L , and effective anisotropy K_{eff} on the grain scale R_C .

We present quantitative evaluation results of micromagnetic structure parameters of nanocrystalline films Fe, Fe₉₅Zr₅, Fe₉₀N₁₀, and Fe₈₅Zr₅N₁₀ obtained by magnetron sputtering. The structure of the films (phase composition, lattice parameter a , grain radius R_C , microstrains ε , and residual macrostresses σ) was studied by XRD. Saturation magnetization M_s was measured from Akulov's saturation approach law. The micromagnetic structure parameters (K_{eff} , $\langle K_{eff} \rangle$, and R_L) were evaluated by correlation magnetometry method [3]. Magnetostriction curves of films on substrates have been measured directly on atomic force microscope using cantilever technique [4]. Saturation magnetostriction λ_s has been obtained out of the dependence on magnetic field $\lambda \sim H^{-1/2}$ using correlation magnetometry method.

Based on the executed measurements local magnetoelastic anisotropy $K_{ME} = (3/2) \varepsilon \lambda_s E_f / (1 + \nu_f)$ (where E_f and ν_f are the Young's modulus and Poisson's ratio of the films respectively), local magnetostatic anisotropy $K_{MS} = (3/2) M_s^2 V_{nonfer}^{2/3}$ (where V_{nonfer} is volume fraction of nonferromagnetic phases in the films), and local surface anisotropy $K_{a,s} = 3K_s V_{nonfer} / R_C$ (where $K_s = (3/8 \cdot 2^{1/2}) a \lambda_s E_f / (1 + \nu_f)$ is surface anisotropy energy) were calculated. It is shown that quantities of magnetocrystalline K_1 , magnetoelastic K_{ME} , magnetostatic K_{MS} and surface $K_{a,s}$ anisotropies are components of experimentally measured effective local anisotropy K_{eff} . Differential susceptibility dM/dH of the films is well described by the sum of two Lorentz functions with peaks at magnetic fields H_C и σH_C :

$$\frac{dM}{dH} = \frac{2V_1}{\pi} \frac{\omega_1^2}{4(H - H_C)^2 + \omega_1^2} + \frac{2V_2}{\pi} \frac{\omega_2^2}{4(H - \sigma H_C)^2 + \omega_2^2},$$

where ω_1 and ω_2 – integral peak widths, V_1 and V_2 – peak areas. Based on this it is concluded that the shape of the hysteresis loops of the films is determined by the presence of two main macroscopic effective magnetic anisotropies, one of which is the anisotropy field $\langle H_a \rangle = 2 \langle K_{eff} \rangle / M_s \approx 2H_C$ of stochastic domains, and the second is the magnetoelastic anisotropy field $\sigma H_C = (3/2) \lambda_s \sigma / M_s$ due to residual macrostresses σ .

Support by RFBR (12-02-00116a) and Presidential grant supporting leading scientific schools (NSh-6207.2014.3) is acknowledged.

[1] E. N. Sheftel, *Inorganic Materials: Applied Research*, **1** (2010) 17-24.

[2] G. Herzer, *Acta Materialia*, **61** (2013) 718-734.

[3] R.S. Iskhakov, S.V. Komogortsev, *Phys. Met. Metallogr.*, **112** (2011) 666-681.

[4] E.V. Harin, E.N. Sheftel, A.I. Krikunov, *Solid State Phenomena*, **190** (2012) 179-182.

30 June

Monday

12:00-13:30

oral session

30TL-G

“Magnetic Oxides”

30TL-G-1

EMERGENT PHASES NEAR QUANTUM CRITICAL TRANSITIONS*Saxena S.S.*

Cavendish Laboratory, University of Cambridge, Cambridge, UK

This talk will focus on experimental search and discovery of novel forms of quantum order in metallic and insulating magnets, intercalated compounds, ferroelectric systems and multi-ferroic materials. Particularly discussed will be the pressure-induced superconductivity and critical phenomena in the vicinity of quantum phase transitions.

Materials tuned to the neighbourhood of a zero temperature phase transition often show the emergence of novel quantum phenomena. Much of the effort to study these new emergent effects, like the breakdown of the conventional Fermi-liquid theory in metals has been focused in narrow band electronic systems. But Spin or Charge ordered phases in insulating systems can also be tuned to absolute zero using hydrostatic pressure. Close to such a zero temperature phase transition, physical quantities like resistivity, magnetisation and dielectrics constant change into radically unconventional forms due to the fluctuations experienced in this region giving rise to new kinds ordered states including superconductivity in the metallic systems.

30TL-G-2

ON NANOENGINEERING OF NEW HIGH- T_c OXIDE HETEROSTRUCTURES: THE ROLE OF DOPING, STRAIN AND THE FIELD EFFECT

Pavuna D.¹, Dubuis G.^{1,2}, Božović I.²

¹ Physics of Complex Matter, EPFL, Lausanne, Switzerland

² Brookhaven National Laboratory, Upton, New York, USA

davor.pavuna@epfl.ch

We have heteroepitaxially grown high- T_c and related oxide films under different degree of epitaxial (*compressive vs tensile*) strain and systematically probed low energy electronic structure and properties [1]. In in-plane compressed LSCO-214 films we doubled T_c , from 20K to 40K, yet Fermi surface (FS) remained essentially two-dimensional (2D). In contrast, *tensile* strained films exhibit 3D dispersion; T_c is drastically reduced [1]. It seems that the in-plane compressive strain pushes the apical oxygen away from the CuO_2 plane, enhances the 2D character of the dispersion and enhances T_c , while the tensile strain seems to act in the opposite direction and the resulting dispersion is 3D. Subsequently, by using ionic liquid gating method, we have studied the electric field effect in cuprates and observed striking superconductor-insulator transition (SIT) in $\text{La}_{2-x}\text{Sr}_x\text{CuO}_4$ films (see Fig. 1) [2].

As we reviewed recently [3], in several *p*-type cuprates, the SIT occurs at the critical sheet resistance approximately equal to the quantum resistance of pairs, $R_Q = h/4e^2 = 6.5 \text{ k}\Omega$. In a relatively broad range of temperatures and doping levels near the quantum critical point, the sheet resistance shows universal behavior and scaling characteristic of two-dimensional quantum phase transition. These phenomena and novel magnetism related effects (spin-spin correlations) will be critically discussed.

The support by the EPFL and the Swiss National Science Foundation is gratefully acknowledged.

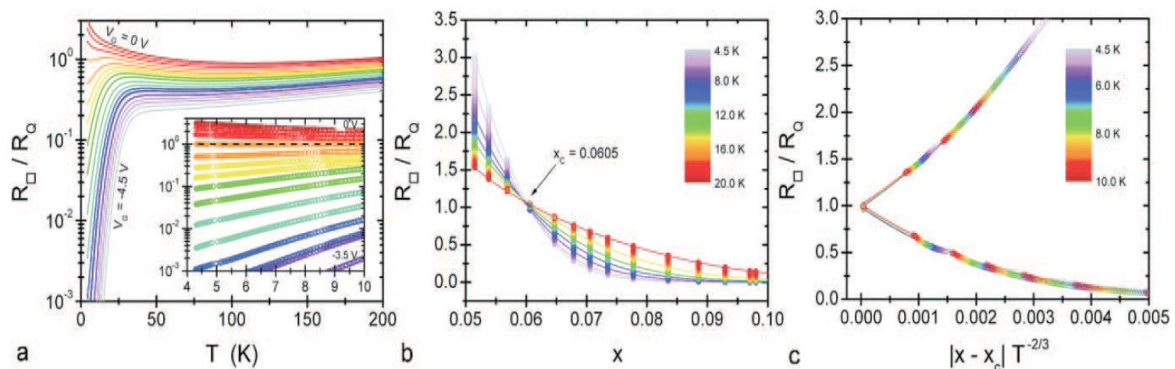


Fig. 1. Thin LSCO film is turned superconducting by applying gate voltage of -4.5V . The crossing of the SIT shows a quantum critical point at $6.5 \text{ k}\Omega$. (a) Sheet resistance normalized by the quantum one for pairs at various value of gate voltage; (b) the same data plotted as a function of the doping level at various temperatures; (c) collapse of the resistance data for a number of doping levels and temperatures onto a universal double-valued function showing a quantum critical point [2].

[1] D. Pavuna et al., *J. Phys.: Conf. Ser.*, **108**, (2008) 012040 and references therein.

[2] A.T. Bollinger et al., *Nature*, **472**, (2011) 458 and references therein.

[3] G. Dubuis, *EPFL doctoral thesis* (2014) and references therein.

30TL-G-3

ORBITAL-SELECTIVE BEHAVIOR IN DIMERIZED SYSTEMS*Streltsov S.V.^{1,2}, Khomskii D.I.³*¹ Institute of Metal Physics, Ekaterinburg, Russia² Ural Federal University, Ekaterinburg, Russia³ University of Cologne, Cologne, Germany

streltsov@imp.uran.ru

We show that in transition metal compounds containing structural metal dimers there may exist in the presence of different orbitals a special state with partial formation of singlets by electrons on one orbital, while others are effectively decoupled and may give e.g. long-range magnetic order or stay paramagnetic. Similar situation can be realized in dimers spontaneously formed at structural phase transitions, which can be called orbital-selective Peierls transition. This can occur in case of strongly nonuniform hopping integrals for different orbitals and small intra-atomic Hund's rule coupling J_H . Yet another consequence of this picture is that for odd number of electrons per dimer there exist competition between double exchange mechanism of ferromagnetism, and the formation of singlet dimer by electron on one orbital, with remaining electrons giving a net spin of a dimer. The first case is realized for strong Hund's rule coupling, typical for 3d compounds, whereas the second is more plausible for 4d-5d compounds. We discuss some implications of these phenomena, and consider examples of real systems, in which orbital-selective phase seems to be realized.

Support by RFBR 13-02-00374 and Ministry of education and science through MK-3443.2013.2 is acknowledged.

30 June

Monday

12:00-13:30

oral session

30TL-H

30OR-H

**“Magnetic Soft Matter
(magnetic polymers,
fluids and
suspensions)”**

30TL-H-1

SIMULATION MODELS FOR MAGNETIC GELS

Weeber R.¹, Kantorovich S.S.^{2,3}, Holm C.¹

¹ Institute for Computational Physics, University of Stuttgart, 70569 Stuttgart, Germany

² Ural Federal University, Lenin av. 51, 620083 Ekaterinburg, Russia

³ Universität Wien, Sensengasse 8, 1090 Wien, Austria

holm@icp.uni-stuttgart.de

Ferrogels, i.e., hydrogels that additionally contain magnetic single-domain particles, are interesting materials. Their properties can be controlled by tailoring the polymer network forming the gel and by using external magnetic fields to change the interaction of the imbedded magnetic particles. Magnetic gels are considered for applications, e.g., as artificial muscles or drug delivery systems, to name just a few examples. While many variants of ferrogels can be synthesized today, the detailed microstructure and microdynamics is often unknown.

In our contribution we investigate the microstructure, the magnetic behavior, and the mechanical and elastic properties of 3D magnetic gels on the basis of microscopic particle models. The network structure of the gel is modeled as a network of connected bead-spring chains. We will consider essentially two models: in one only the network nodes consist of magnetic (dipolar) particles, in the other model the nano-magnets are part of the chains. Both models have experimental realizations. The focus will be on magnetic field-actuated changes in the microstructure of the gel and correspondingly on the change in elastic behavior, magnetic response, and elastic properties. We will first summarize 2d computer models for the deformation by a change in the interaction between magnetic nano-particles [1]. Then, we will present results for the 2d and 3d models where the rotation induced deformation of the gel is triggered by torque transmission. In these systems, the polymer network is cross-linked by magnetic nanoparticles. When the magnetic particles rotate in response to an externally applied field, they exert a stress on the polymer chains and thus deform the gel. In a two-dimensional system, there is only one relevant axis of rotation, namely the axis perpendicular to the plane. This means that the deformation of the gel will always be isotropic, because the stress exerted on the polymer chains is independent of the chain's orientation. In the three-dimensional case, on the other hand, there are three rotation axes. While the magnetic particles can freely rotate around the axis parallel to the field, any rotation around the other two axes would reduce the Zeeman energy and is therefore unlikely in a strong external field. Hence, the orientational fluctuations are different, depending with respect to which axis they are regarded. This leads to an anisotropic deformation of the gel. If time permits we will also present recent results on magnetic polymers or dipolar shifted particles [2].

Support by the German Science Foundation SPP 1681 and the SimTech Cluster of excellence is gratefully acknowledged.

[1] R. Weeber, S. Kantorovich, C. Holm, *Soft Matter* **8** (2012) 9923-9932.

[2] R. Weeber, M. Klinkigt, S. Kantorovich, C. Holm, *Journal of Chemical Physics* **139** (2013) 214901.

30OR-H-2

STRUCTURAL EFFECTS IN THE MAGNETOMECHANICS OF FERROGELS

Melenev P.V.^{1,2}, Ryzhkov A.V.^{1,2}, Weeber R.³, Raikher Yu.L.^{1,2}

¹ Institute of Continuous Media Mechanics, UrB RAS, Perm, Russia

² Perm National Research Polytechnic University, Perm, Russia

³ Institute for Computer Physics, University of Stuttgart, Stuttgart, Germany
melenev@icmm.ru

Ferrogels (FG) are smart composite materials emerging from combining soft (elastic modulus below 10 kPa) polymer matrices with nanodisperse ferromagnetic filler. An external magnetic field of a moderate magnitude is able to considerably rearrange of the spatial distribution of the grains and, thus, to tune the mechanical characteristics and change the overall shape of FG samples [1]. Therefore, to build up a theoretical description of FGs, one should have a clear knowledge of their local internal structure under various magneto-mechanical conditions.

We approach this subject via computer experiments in the framework of molecular dynamics (MD) that is nowadays a conventional instrument in polymer science. The MD technique allows one to account for diverse types of interactions between the model elements and, thus, is very suitable for complex magneto-polymer materials like FGs. With the aid of multiprocessor computers (and/or distributed calculations) it is possible to consider relatively large samples, which contain thousands of magnetic particles. In our work we use the open source ESPResSo package [2], a powerful MD-implementation successfully applied to the simulations of FGs [3].

In the simulations, a FG sample is presented as a fragment of a polymer mesh whereto the magnetic single-domain particles are embedded. The nodes are linked by the chains of hard spheres coupled by pair-wise potentials. The latter are either of an isotropic type (e.g. Lennard-Jones) or allow for finite bending stiffness of the chain. The magnetic nanoparticles are taken to be spherical, and their diameters are greater than the size of the chain elements.

Initially generated mesh has quasi-regular structure: the nodes are arranged in a simple cubic pattern but bounds are not straight which models the real polymer conformation and gives additional flexibility for the chains. With regard to real FGs [1] we consider two types of magnetic inclusions: (i) the grains not linked to the polymer and, thus, confined just topologically, and (ii) the particles are anchored to the gel chains. In the latter case, both translational and rotational motions of the magnetic particles induce polymer network deformation. Therefore, the magnetic anisotropy of the grains plays a notable role in the material behavior.

The simulations are carried out for both types of the particle binding types at several particle concentrations and different ratios between characteristic energies of the magnetic interactions and mechanical bonding. The dependencies of the magnetic and mechanical response of the material to the applied magnetic field are investigated.

Support by RFBR grants # 13-01-96056 and 14-02-96003, Ural Branch of RAS Programme #10 (12-P-01-108) and project MIG S26/617 from Ministry of Education and Science of Perm Region is acknowledged.

[1] L. Yuhui et al. *Adv. Funct. Mater.* **23** (2012) 660-672.

[2] <http://espressomd.org>.

[3] R. Weeber, S. Kantorovich, C. Holm, *Soft Matter* **38** (2012) 9923-9932.

30OR-H-3

MOLECULAR DYNAMICS SIMULATION OF SMALL FERROGEL OBJECTS

Ryzhkov A.V.^{1,2}, Melenev P.V.^{1,2}, Holm C.³, Raikher Yu.L.^{1,2}

¹ Institute of Continuous Media Mechanics, UrB RAS, Perm, Russia

² Perm National Research Polytechnic University, Perm, Russia

³ Institute for Computer Physics, University of Stuttgart, Stuttgart, Germany

ryzhkov_alexandr@mail.ru

Embedding nanogranular ferromagnetic materials in gels, either by adding them inside the net or by chemical binding, produces soft magnetically sensitive materials with wide prospects. One of the most interesting trends in the ferrogel science is the preparation and study of submicron-size isolated entities containing a countable number (tens or hundreds) of particles [1]. The main practical use foreseen for microgels are theranostics and nanomedicine, where they facilitate immuno-probing and targeted drug delivery and/or release. This by no means exhausts the list.

The macromolecule mesh is relatively weak, making the structure of microferrogels (MFG) rather labile and facilitating loading them with biomarkers, immune complexes, etc. On the other hand, this ensures a strong effect of the field on the mesh density and overall shape of MFGs.

Molecular dynamics simulations provide a powerful tool to study the magneto-deformational response of MFGs since they enable one to simultaneously take into account a large number of structure units, whose motions and interactions determine the behavior of the ferrogel object. We use the open-source software ESPResSo package[2], which has already proven its efficiency in numerical simulations of ferrohydrogels [3]. The problem under study is especially advantageous as the MFG is considered as such, no ambiguities due to periodic boundary conditions arise.

The coarse-grain MFG model is initially generated as a cubic “brick” of a simple cubic lattice with 125 nodes. The particle sitting in each node site is ascribed a “frozen-in” magnetic moment of a fixed magnitude with a given probability. The chains connecting the nodes consist of a number of non-magnetic particles interacting via hard-sphere and bonded potentials, representing the blobs of a real gel inter-node chain. First the sample is equilibrated at a finite temperature under a given intensity of steric and magnetodipole interactions. Then a uniform field is imposed step-wise. We are interested in finding the main types of the field-induced shape and structure changes of MFG and the effect of particle aggregation on the magnetization curve of the sample. Our results are presented with respect to the magnetic particle size (in fact, the magnetic moment magnitude), concentration of the magnetic grains and temperature.

Support by RFBR grants # 13-01-96056 and 14-02-96003, Ural Branch of RAS Programme #10 (12-P-01-108) and project MIG S26/617 from Ministry of Education and Science of Perm Region is acknowledged.

[1] J. Thévenot, H. Oliveira, O. Sandre, S. Lecommandoux, *Chem. Soc. Rev.* **42** (2013) 7099-7116.

[2] <http://espressomd.org/>

[3] R. Weeber, S. Kantorovich, C. Holm, *Soft Matter* **38** (2012) 9923-9932.

30OR-H-4

NMR IN COBALT-CONTAINING MAGNETIC NANOMATERIALS

Matveev V.V., Shmyreva A.A.

Saint-Petersburg State University, Saint Petersburg, Russia

vmatveev@nmr.phys.spbu.ru

A short introduction is presented to a technique known as “NMR-in-magnetics” or “spin-echo”. The technique is very effective in testing and certification of magnetic (nano)materials of various kinds, e.g. bulk materials, thin films, multilayers and other nanostructures, molecular magnets, etc. The represented data demonstrate convincingly that NMR experiments allow one to get highly informative and reliable results concerning local magnetic structure and properties of the investigated systems: hyperfine fields, a temperature behavior of the magnetization, etc. Therefore, the technique can be the useful addition to well-known diagnostic methods and reveal the unique information which cannot be reached by other methods.

As an illustration of the usefulness of the technique we describe its application to a few sets of cobalt-containing magnetic nanostructures where ^{59}Co spectra allowed us to obtain an information concerning the structure of metallic cobalt clusters as well as their local magnetic properties [1-3]. Namely we could observe such effects as:

- 1) A dependence of local structure and the metal/oxide ratio on preparation conditions of a nanocomposite;
- 2) aging of the samples during several months (short-term aging) and during several years (long-term aging);
- 3) An increase of magnetic moment of some part of atoms of metallic cobalt which is manifested in the appearance of additional lines at higher frequencies.

No ready equipment for NMR-in-magnetics is produced by industry. As the result only a few spectrometers exist in Europe and not more than few tens in the whole world – the situation is absolutely opposite to conventional NMR. However, the modern spectrometer for NMR-in-magnetics can be assembled using available industrial modules/units.

In addition to NMR experiments the NMR-in-magnetics equipment is suitable to use for investigation of acoustical absorption in superconductors. Namely, an observation of so-called “phonon echo” in superconductors was demonstrated for MgB_2 powder [4].

Support by research programs of Saint-Petersburg State University is acknowledged.

[1] G.A. Nikolaychuk, A.V. Lukashin, V.V. Matveev, I.V. Pleshakov, In: *Lecture Notes in Physics*, Springer—Veltag, **593** (2002) 203-219.

[2] V.V. Matveev et. al., *Chem.Phys. Lett.*, **422** (2006) 402-405.

[3] V.V. Matveev, A.A. Shmyreva et. al., *Phys. Rev. Lett.*, submitted.

[4] I.V. Pleshakov et.al., *Europhys. Lett.*, **85** (2009) 67001-67004.

30OR-H-5

MAGNETIC DENDRIMERS AND SPIN-CROSSOVER DENDRIMERIC IRON(III) COMPLEXES

Domracheva N.E.¹, Vorobeva V.E.¹, Pyataev A.V.², Gruzdev M.S.³, Chervonova U.V.³, Kolker A.M.³

¹ Zavoisky Kazan Physical-Technical Institute, Kazan, Russia

² Kazan Federal University, Kazan, Russia

³ Institute of Solution Chemistry, Ivanovo, Russia

domracheva@mail.knc.ru

Two types of magnetic dendrimeric systems - the liquid-crystalline poly (propylene imine) (PPI) dendrimer with γ -Fe₂O₃ nanoparticles (NPs) and spin-crossover ($S = 1/2 \leftrightarrow 5/2$) iron(III) dendrimeric complex have been synthesized and studied for the first time. Investigation of the first system has shown that NPs fabricated into dendrimer have an average diameter about 2.5 nm, the magnetic moment about 350 Bohr magnetons, possess the uniaxial magnetic anisotropy and "core/shell" structure [1]. A temperature-driven transition from superparamagnetic to ferrimagnetic state was observed by EPR spectroscopy with the blocking temperature about 60 K. The influence of pulsed laser irradiation on the superparamagnetic properties of γ -Fe₂O₃ NPs was also studied by EPR spectroscopy. It has been shown that irradiation of the sample held in vacuo and cooled in zero magnetic field to 6.9 K leads to the appearance of a new EPR signal, which decays immediately after the irradiation is stopped. The appearance and disappearance of this new signal can be repeated many times at 6.9 K when we turn on/turn off the laser. We suppose that the generation of conduction band electrons by irradiation into the band gap of the semiconductor γ -Fe₂O₃ NPs changes the superparamagnetic properties of NPs.

Investigation of the second system – the spin-crossover (LS, $S = 1/2 \leftrightarrow S = 5/2$, HS) iron(III) dendrimeric complex allowed us to detect a novel phenomenon: magnetic - ferroelectric (MFCO) crossover, where the change of the spin state comes simultaneously with the change of the ferroelectric properties of Fe (III) centers [2]. Analysis of the magnetic behavior reflected by I versus T (where I is the EPR lines integrated intensity of the spectrum) demonstrates that iron(III) dendrimeric complex has significantly different behavior in three temperature intervals. The first (4.2-70 K) interval corresponds to the antiferromagnetic exchange interactions between LS-LS, LS-HS and HS-HS centers. The appearance of presumable magnetoelectric (ME) effect is registered in the second (70-200 K) temperature interval, whereas a spin transition process between LS and HS centers occurs in the third (200-330 K) one. The coexistence of the magnetic ordering, presumable magnetoelectric effect and spin crossover in one and the same material has been detected for the first time. The Mössbauer spectroscopy data completely confirm the EPR results.

Support by RAS Presidium program No. 24 is acknowledged.

[1] N.E. Domracheva, A.V. Pyataev, R.A. Manapov, M.S. Gruzdev, *ChemPhysChem*, **12** (2011) 3009-3019.

[2] N.E. Domracheva, A.V. Pyataev, V.E. Vorobeva, E.M. Zueva, *J. Phys. Chem. B*, **117** (2013) 7833-7842.

30 June

Monday

12:00-13:30

15:00-17:00

oral session

30TL-O

30OR-O

30TL-B

30RP-B

30OR-B

**“Magnetism of
Nanostructures”**

30TL-O-1

LOCAL MODIFICATION OF MAGNETIC FILMS BY ION BEAMS

Potzger K.¹, Bali R.^{1,2}, Heidarian A.¹, Wintz S.¹, Meutzner F.³, Hübner R.¹, Ünal A.A.⁴, Valencia S.⁴,
Boucher R.³, Neudert A.¹, Grenzer J.¹, Bauch J.³, Kronast F.⁴, Facsko S.¹, Lindner J.¹,
Fassbender J.¹

¹ Institut für Ionenstrahlphysik und Materialforschung, Helmholtz-Zentrum Dresden-Rossendorf,
Dresden 01328, Germany

² School of Physics, University of Western Australia, 35 Stirling Highway, Crawley 6009, Australia

³ Institut für Werkstoffwissenschaft, Technische Universität Dresden, Helmholtzstr. 10, Dresden
01069, Germany

⁴ Helmholtz-Zentrum-Berlin, Berliner Elektronen-Speicherring Gesellschaft für
Synchrotronstrahlung (BESSY), Albert-Einstein-Strasse 15, Berlin 12489, Germany
k.potzger@hzdr.de

Binary chemically ordered metallic alloys which show drastically varying magnetic properties upon chemical disordering are potential candidates for lateral spintronics. Among them, ion-beam patterned FeAl and FeRh binary alloys are of particular interest due to disorder induced para- to ferromagnetic and antiferro- to ferromagnetic transitions, respectively. For FeAl we demonstrate the chemical order \rightarrow disorder phase transition in thin films of Fe₆₀Al₄₀, leading to increased ferromagnetism [1, 2]. Disorder is induced by exposure to impinging ions. The ion-induced saturation magnetization (M_s) is a function of the displacements per atom. Very small amounts of atomic displacements are necessary to reach the maximum M_s . This implies that depth homogeneity of M_s is achieved at low-fluence and –energy, and deleterious effects such as interface intermixing and surface-sputtering are avoided. Irradiation through shadow masks is employed to induce ferromagnetism selectively and fabricate a magnetic pattern with sub-50 nm resolution possessing binary stable and switchable magnetic configurations. Discrete magnetic elements are thus embedded within topographically flat thin films (Fig. 1). For FeRh thin films we show the potential of ion implantation on tuning the antiferromagnetic-ferromagnetic transition temperature.

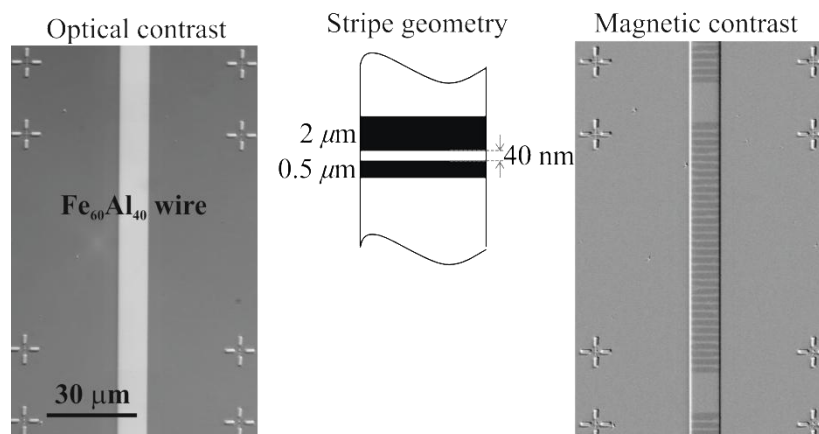


Fig. 1: Magnetic stripes patterned on to Fe₆₀Al₄₀ wire

[1] R. Bali *et al.*, *Nano Letters*, **14** (2014) 2, 435.

[2] Enric Menéndez *et al.*, *Small*, **5** (2009) 229.

30TL-O-2

SHAPE INDUCED MAGNETISM IN 2 DIMENSIONAL NANOSTRUCTURE*Hong J.-Il.*Department of Emerging Materials Science
Daegu Gyeongbuk Institute of Science and Technology (DGIST) Daegu, Korea

In addition to the well-known “size effect” of nanomaterials, it is generally accepted that the shape of nanomaterial may affect the electronic states in nanomaterials. Carbon nanotube and graphene are exemplary materials for such effect. However, there has been relatively less effort toward 2D nanostructures of inorganic materials, mainly because of the difficulty in syntheses compared with graphenes.

Due to the highly asymmetric crystal structure of ZnO, thin graphene like nanostructure was synthesized in epitaxy with the $(10\bar{1}0)$ surface of GaN.¹ The role of interface strain is examined in regard to the growth of ZnO in 2D geometry. Further controls of synthesis conditions are explored for the control of aspect ratios and the thickness of nanoplates. Thickness appears to serve as a key parameter for the emergence of magnetism in a nominally nonmagnetic ZnO. Electric polarizations at the $\{0001\}$ surfaces of ZnO cause an extremely high effective electric field across the nanoplate whose magnitude depends on the thickness and atomic structure of the nanoplates. The behavior of electrons and their band structure adjust to the modified environment, during which the balance between up and down spin densities of states breaks and nanoplates exhibit unexpected magnetism. Measured magnetic behaviors of the nanoplates will be correlated with the first principle calculation results in order to achieve comprehensive understanding on the origin of modified electronic behaviors under the influence of strong electric field.

[1] J. I. Hong, J. Choi, S.S. Jang, J. Gu, Y.Chang, G. Wortman, R. L. Snyder, Z. L. Wang, *Nano Lett.* **12** (2012) 576.

30OR-O-3

MULTICOMPONENT MAGNETOOPTICAL DOMAIN STRUCTURE IMAGING IN A Pt/Co/Pt FILM DRIVEN BY FIB IRRADIATION

Mazalski P.¹, Urs N.O.², Dobrogowski W.¹, Ferré J.³, Gierak J.⁴, Baczewski L.T.⁵, Wawro A.⁵, McCord J.², Maziewski A.¹,

¹ Faculty of Physics, University of Białystok, Białystok, Poland

² Institute for Materials Science, Kiel University, Kiel, Germany

³ Laboratoire de Physique des Solides, Université Paris-Sud, Orsay, France

⁴ Laboratoire de Photonique et de Nanostructures, CNRS UPR 20, Marcoussis, France

⁵ Institute of Physics, Polish Academy of Sciences, Warszawa, Poland

piotrmaz@uwb.edu.pl

The phase diagram depending of the fluence F of uniformly Ga^+ -irradiated Pt/Co/Pt films has been recently determined [1]. Two branches with out-of-plane magnetization have been identified. Combining uniform irradiation and Ga^+ Focused Ion Beam (FIB) lithography allows to create patterned magnetic structures on a scale of tens of nanometers up to microns. FIB lithography is particularly attractive because of its “direct-write” nature, allowing relatively fast patterning without requiring masks or resists. Polar (PMOKE) and longitudinal magneto-optical (LMOKE) Kerr effect investigations proved to be very useful for the magnetic characterization of the fabricated FIBed nanostructures. Especially promising is a recently developed method allowing for the simultaneous investigation of two magnetization components [2].

FIB-induced magnetization reorientation was studied in a MBE grown Pt/Co/Pt film with in-plane magnetization in its as-deposited state. For that purpose, several square ($50 \times 50 \mu\text{m}^2$) regions have been quasi-uniformly irradiated by scanning a FIB spot over all the sample and with different fluences F ranging between $5 \cdot 10^{13}$ and $2 \cdot 10^{16}$ ions/cm². Simultaneous in-plane and out-of-plane magnetization measurements were performed in both LMOKE and PMOKE configurations. PMOKE studies reveal the existence of 2 branches with out-of-plane magnetization similar as in Ref. 1. The domain structure of a FIB-irradiated region with oblique magnetization is visualized in Fig. 1. An in-plane domain structure is visible in the as-deposited region, outside the FIBed square. The dependence of field-induced magnetization curves and magnetic domain structures on the in-plane field orientation and fluence F will be discussed.

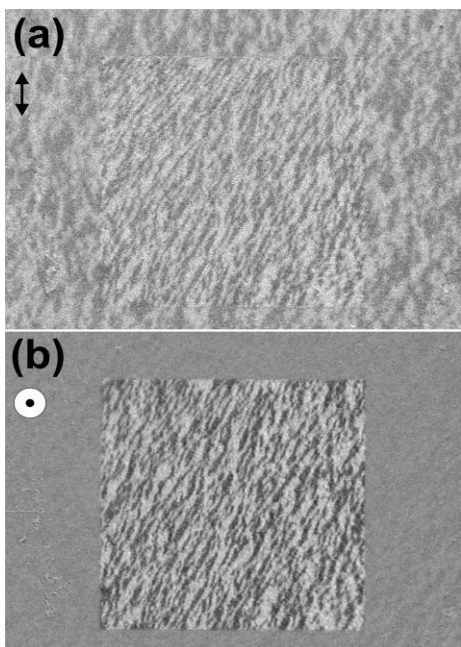


Fig.1. Exemplary magnetic domain structures in a $50 \times 50 \mu\text{m}^2$ FIB-irradiated square (fluence $F = 6 \times 10^{15}$ ions/cm²) with oblique magnetization, imaged by LMOKE (a) and PMOKE (b) configuration. Arrows indicate sensitivity for selected component of magnetization.

Work supported by the Team SYMPHONY project of the FNP, co-financed by the EU from ERDF, OPIE 2007–2013, the Polish National Science Centre - HARMONIA project (DEC-2012/06/M/ST3/00475), the Preludium project (DEC-2011/03/N/ST3/02408) and the DFG Heisenberg Programme (MC9/9-1).

- [1] A. Maziewski, *et al.*, *PRB* **85**, 054427 (2012).
 [2] T. von Hofe, *et al.*, *APL* **103**, 142410 (2013).

30OR-O-4

PERSPECTIVES OF MICROMAGNETIC MODELING OF NANOCOMPOSITES

Erokhin S.¹, Berkov D.², Gorn N.¹, Michels A.³

¹ Innovent Technology Development, Jena, Germany

² General Numerics Research Lab, Jena, Germany

³ Physics and Materials Science Research Unit, University of Luxembourg, Luxembourg
se@innovent-jena.de

We have developed a new micromagnetic methodology for numerical simulations of magnetic nanocomposites consisting of magnetically ‘hard’ grains surrounded by an amorphous magnetic matrix. This methodology overcomes the difficulties of micromagnetic simulation methods available up to now and has the following features:

(a) Generated mesh consists of polyhedral finite elements, obtained from closely packed spheres with the sizes and positions adjusted to structural and magnetic parameters of each magnetic phase. This procedure assures that the shape of all polyhedrons is close to spherical and that their spatial arrangement is random.

(b) Magnetodipolar interaction energy of this system of polyhedrons is calculated in the point dipole approximation using the FFT-based lattice Ewald method. This approximation is exact for interacting spheres, and is thus sufficiently accurate in our case, where the shape of polyhedra is close to spherical.

(c) The exchange interaction is computed using the Heisenberg form, where the exchange constant is proportional to the volumes of neighbouring finite elements and the spacing between their centres.

In this talk we present physical examples, demonstrating the power and accuracy of our method, simulating the magnetic structure of magnetic nanocomposites and corresponding small-angle neutron scattering (SANS) cross section, e.g. the study of nanocomposite of the Nanoperm type. This nanocomposite consists of iron-based crystallites with typical size of ~ 10 nm, embedded in an amorphous magnetically soft matrix. The unusual angular anisotropy in the SANS cross-section is explained with the help of the developed method and is attributed to the internal magneto-dipolar field arising around hard crystallites.

We have applied our method to simulations of nanocomposites employed in permanent magnets, that enables us to study (Fig. 1) the dependence of the macroscopic magnetic properties of such materials on the structural and magnetic parameters of the constituting phases, performing the simulations of ‘samples’ containing ~ 1000 hard grains, thus achieving a high statistical reliability of results. Our simulations allow the optimization of permanent magnet

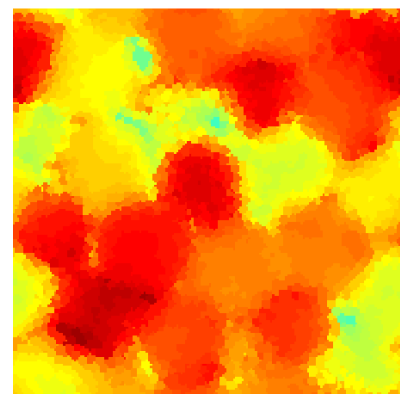


Fig. 1. Remanent magnetization distribution of a nanocomposite with a very high hard phase concentration.

This research was supported by the DFG Project BE 2464/10-3 and EU-FP7 NANOPYME Project (No. 310516), see also <http://nanopyme-project.eu/>.

30TL-B-5

SPIN AND ORBITAL MAGNETISM AT THE TRULY ATOMIC LEVEL: XMCD OF SIZE-SELECTED FREE METAL AND BINARY CLUSTERS

Lau J.T.¹

¹ Institut für Methoden und Instrumentierung der Forschung mit Synchrotronstrahlung, Helmholtz-Zentrum Berlin für Materialien und Energie GmbH, Berlin, Germany
tobias.lau@helmholtz-berlin.de

The investigation of the magnetic properties of size-selected free clusters and complexes constitutes a tremendous challenge and has only become possible with the recent introduction of ion traps for core-level spectroscopy [1,2]. This technique allows to follow spin and orbital magnetic moments of highly dilute (10^{-6} monolayer equivalent) but unperturbed samples at controlled temperature down to 4 K and magnetic field up to 5 T. This talk will summarize recent highlights and developments.

These studies show that Fe_n^+ , Co_n^+ , and Ni_n^+ clusters in the size range of ≤ 15 atoms are strong ferromagnets with $1 \mu_B$ spin moment per unoccupied 3d state in general [4] but reveal a particular behavior of Fe_{13}^+ [1,3] whose surprisingly reduced spin magnetic moment might be related to the bulk phase diagram of iron. Beyond pure clusters, the investigation of single impurities in size-selected metal and semiconductor hosts showed a coordination-driven quenching of high-spin states at the transition from exohedral to endohedral doping [4]. In addition, these studies indicate a possible dependence of the dopant magnetic moment on the energy gap of the finite free electron gas of the host cluster [5]. Finally, an outlook will be given on the properties of magnetic transition metal oxide clusters and on experimental studies of the magnetic anisotropy energy of transition metal molecules and complexes.

Support by DFG, BMBF, Genesis Research Institute, and Toyota Technological Institute is acknowledged.

- [1] M. Niemeyer, K. Hirsch, V. Zamudio-Bayer, A. Langenberg, M. Vogel, M. Kossick, C. Ebrecht, K. Egashira, A. Terasaki, T. Möller, B. v. Issendorff, and J. T. Lau, *Phys. Rev. Lett.*, **108** (2012) 057201.
- [2] S. Peredkov, M. Neeb, W. Eberhardt, J. Meyer, M. Tombers, H. Kampschulte, and G. Niedner-Schatteburg, *Phys. Rev. Lett.*, **107** (2011) 233401.
- [3] A. Langenberg, K. Hirsch, A. Ławicki, V. Zamudio-Bayer, M. Niemeyer, P. Chmiela, B. Langbehn, A. Terasaki, B. v. Issendorff, and J. T. Lau, *submitted for publication, arXiv preprint 1402.0701* (2014).
- [4] V. Zamudio-Bayer, L. Leppert, K. Hirsch, A. Langenberg, J. Rittmann, M. Kossick, M. Vogel, R. Richter, A. Terasaki, T. Möller, B. v. Issendorff, S. Kümmel, and J. T. Lau, *Phys. Rev. B*, **88** (2013) 115425.
- [5] K. Hirsch, V. Zamudio-Bayer, A. Langenberg, M. Niemeyer, B. Langbehn, T. Möller, A. Terasaki, B. v. Issendorff, and J. T. Lau, *submitted for publication, arXiv preprint 1304.7173* (2013).

30OR-B-6

SPIN GLASS BEHAVIOR IN CO₃O₄ POWDER SAMPLES*von Dreifus D.¹, Pereira E. C.², de Oliveira A.J.A.²*¹ Physics Department – Federal University of São Carlos, São Carlos-SP, Brazil² Chemistry Department – Federal University of São Carlos-SP, Brazil
adilson@df.ufscar.br

Spin-glass system is an important class of magnetic materials due to complex behavior and observed in different types of materials (metallic, semiconductors, organic and oxides). The competition between the ferromagnetic / antiferromagnetic interactions is a fascinating field for both theoretical and experimental investigations. However, size effects of particles in spin-glass systems are not explored and open the possibility for understand spin-glass behavior. For example, Co₃O₄ is an antiferromagnetic oxide with Néel temperature (T_N) around 32K. Lin He et al. [1] have observed that by reducing the particle size in Co₃O₄ samples, an intrinsic finite size effect causing a reduction on the magnetic ordering temperature [1]. Tang et al. observed the same effect, where nanoparticles of ferrimagnetic MnFe₂O₄ were studied. The authors admit that this effect could affect both the critical ordering temperatures of ferro and antiferromagnetic nanoparticles [2]. According to Resnick et al. Co₃O₄ nanoparticles presented T_N = 30K when they have 8nm but T_N is about 15K when they present 4.3nm [3].

From these previous works our group synthesized Co₃O₄ powder samples by Pechini method, a sol-gel route. The samples were characterized by X-ray diffraction analysis using Rietveld refinement that confirmed that the sample composition is exclusively of Co₃O₄. Scanning Electron Microscopy image show that the samples presents an large distribution of particles size (10nm to 160 nm).

Magnetization measurements as a function temperature and applied magnetic field show that the samples exhibit peaks in 14K and another at 32K. Nevertheless the transition at 14K vanishes when applied a field of 30 kOe. This result is similar to observed by Mousavand et al. in Co₃O₄ samples with 25nm particle size where a field of 30kOe is enough to vanish the peak at 10K [4]. The AC magnetic susceptibility at 10 Oe with different frequencies (10, 100 and 500 Hz) show that the peak observed at 14K exhibit a dependence with frequency, as expected for spin-glass system. We conclude that there is a competition between the magnetic moments of the antiferromagnetic grains leading to the establishment of spin-glass behavior.

This work was support by Brazilians agencies FAPESP is acknowledged.

[1] L. He, C. Chen, N. Wang, W. Zhou and L. Guo. *J. of Applied Physics*, **102** (2007) 103911.

[2] Z. X. Tang, C. M. Sorensen, K. J. Klabunde, and G. C. Hadjipanayis, *Phys. Rev. Lett.rs.*, **67** (1991) 3602.

[3] D. A. Resnick, K. Gilmore, Y. U. Idzerda, M. T. Klem, M. Allen, T. Douglas, E. Arenholz, and M. Young, *Journal Applied Physics*, **99** (2006) 08Q501.

[4] T. Mousavand, T. Naka, K. Sato, S. Ohara, M. Umetsu, S. Takami, T. Nakane, A. Matsushita, and T. Adschiri. *Physical Review B*, **79** (2009) 144411.

30OR-B-7

MAGNETIC ANISOTROPY OF ELECTRODEPOSITED CoP NANOWIRES WITH COAXIAL CORE-SHELL STRUCTURE

Samardak A.S.¹, Ognev A.V.¹, Sukovatitsina E.V.¹, Chebotkevich L.A.¹, Komogortsev S.V.², Bending S.J.³, Peighambari S.M.⁴, Nasirpouri F.⁴

¹ Laboratory of Thin Film Technologies, Far Eastern Federal University, Vladivostok, Russia

² Institute of Physics, SB Russian Academy of Sciences, Krasnoyarsk, 660036 Russia

³ Department of Physics, University of Bath, Bath BA2 7AY, UK

⁴ Department of Materials Engineering, Sahand University of Technology, Tabriz, Iran
samardak.as@dvfu.ru

Co_{100-x}P_x alloy nanowires have been prepared using alternating current (AC) electrodeposition in highly ordered anodic aluminum oxide (AAO) templates. Results show that AC frequency and waveform significantly change the microstructure and composition of alloy nanowires. In addition, the phosphorous content of the electrolyte influences the growth, microstructure and magnetic properties of the nanowires. Co_{100-x}P_x alloy nanowires electrodeposited under 200 Hz 15 V sinusoidal waveforms, with different P (x<10%) composition, exhibit significant changes in structure from uniform amorphous to an unusual coaxial core-shell form. Analyzing the magnetization data for Co_{100-x}P_x alloy nanowires indicates that a ferromagnetic core is surrounded by a weakly ferromagnetic or non-magnetic CoP phase, depending on the P content. The magnetic anisotropy of the investigated Co_{100-x}P_x alloy nanowire arrays is controlled by their microstructure and the template porosity. The temperature dependence of the magnetization indicates the presence of an antiferromagnetic component in the Co_{100-x}P_x nanowires.

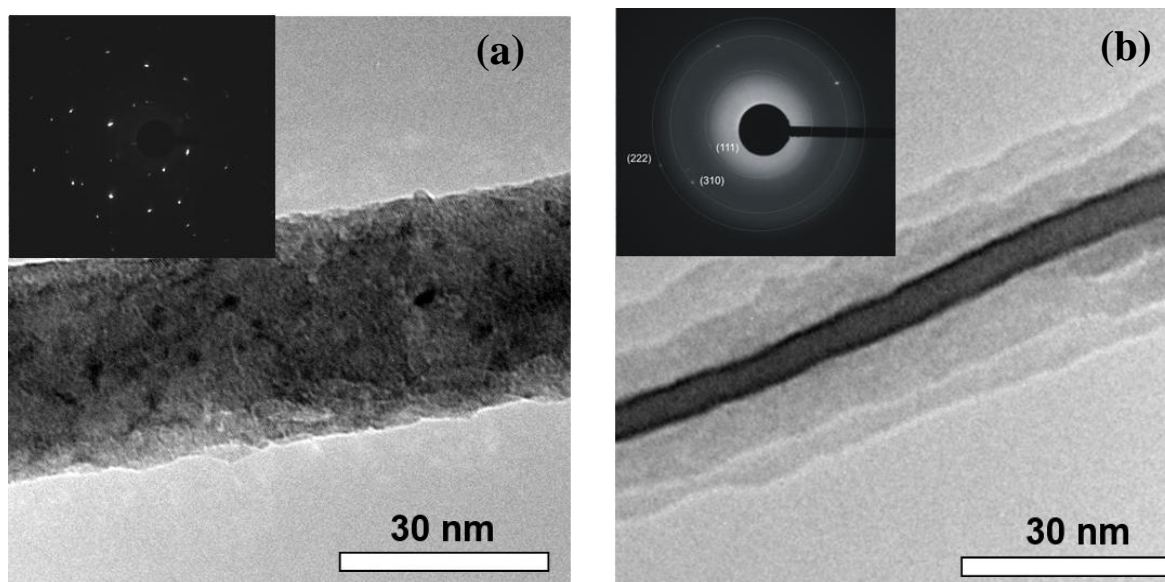


Fig. 1. Typical TEM images and selected area diffraction patterns for (a) Co and (b) Co_{100-x}P_x (x=6.8 wt.%) nanowires electrodeposited in AAO templates using a 15V, 200Hz sinusoidal waveform.

Support by the Russian Ministry of Education and Science and the Scientific Fund of Far Eastern Federal University is acknowledged.

30OR-B-8

DIAMAGNETIC-FERROMAGNETIC TRANSITION IN SILVER NANOPARTICLES OBTAINED FROM SILVER OXALATE DECOMPOSITION AT LOW TEMPERATURE

Le Trong H.^{1,2,3}, Baco V.^{1,2}, Gougeon M.^{1,2}, Tailhades Ph.^{1,2}

¹ Université de Toulouse, UPS, INP, Institut Carnot CIRIMAT, Université Paul Sabatier, Toulouse, France

² CNRS, Institut Carnot CIRIMAT, Toulouse, France

³ Ho Chi Minh City University of Science, Vietnam National University Ho Chi Minh City, Ho Chi Minh City, Vietnam

tailhades@chimie.ups-tlse.fr

The decomposition of silver oxalate starts at about 100 °C to give metallic silver nanoparticles. The ability to sintering of such nanoparticles makes them very interesting for the soldering of electronic devices below 300 °C [1]. However, a heat treatment carried out at only 125 °C for 200 hours, allows to reach the complete decomposition of the oxalate, on the one hand, and to stabilize pure silver nanoparticles, on the other hand (fig. 1). Such particles are diamagnetic at room temperature with a susceptibility of $-1.8 \cdot 10^{-7}$ emu/Oe/g, close to that of bulk silver. However, the curve of the magnetization at 20 k.Oe versus temperature, does not display the conventional diamagnetic behavior. A sharp magnetic transition is observed in the range 40 to 60 K (fig. 2). Below these temperatures the magnetization strongly increases to reach about 0.9 emu/g at 2 K and its variation with the magnetic field follows an hysteresis curve (fig. 2 inset). The anomaly observed at 40-60 K for the first time with pure silver nanoparticles, was then ascribed to an unusual diamagnetic-ferromagnetic transition.

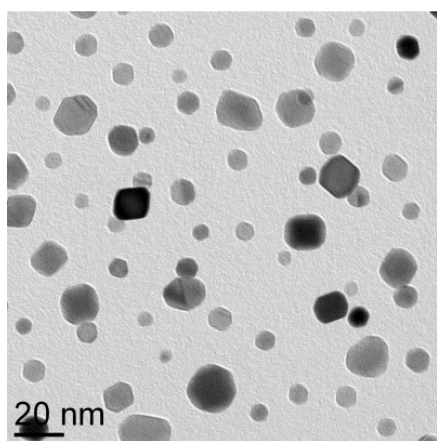


Fig. 1: TEM image of Ag nanoparticles obtained after a heat treatment at 125 °C for 200 h in vacuum.

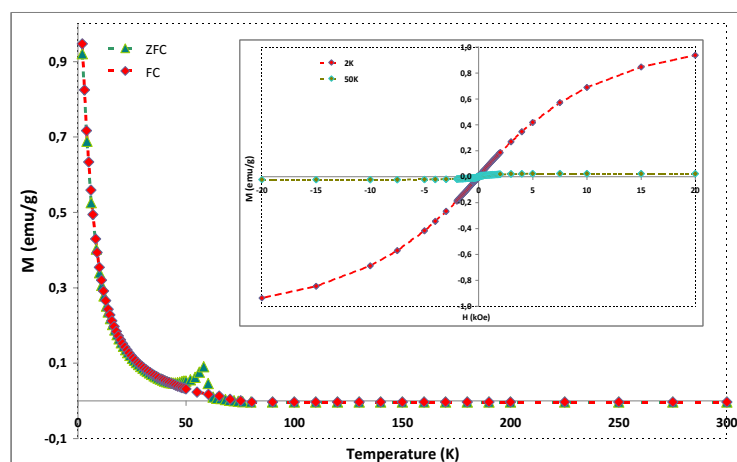


Fig. 2: Magnetization versus temperature (ZFC and FC) for Ag nanoparticles obtained after a heat treatment at 125°C for 200 h in vacuum. Upper inset, hysteresis loop at 2 K and 50 K.

[1] K. Kiryukhina, H. Le Trong, Ph. Tailhades, J. Lacaze, V. Baco, M. Gougeon, F. Courtade, S. Dareys, O. Vendier, L. Raynaud, *Scripta Mater.*, **68** (2013) 623–626.

30RP-B-9

EXCHANGE BIAS IN OXIDISED COBALT NICKEL NANORODS

Spasova M.¹, Liébana-Viñas S.^{1,2}, Perl J.¹, Elsukova A.¹, Zingsem B.¹, Salgueiriño V.², Farle M.¹

¹Fakultät für Physik and CENIDE, Universität Duisburg-Essen, Duisburg, Germany

²Departamento de Física Aplicada, Universidade de Vigo, Vigo, Spain

marina.spasova@uni-due.de

Tuning of nanoparticle shape opens the possibility to tailor their properties to the requirements of various applications. Particularly, elongated magnetic nanoparticles allow to utilize their shape anisotropy as an additional source of magnetic anisotropy energy in order to create magnetically hard Rare-Earth-free materials for permanent magnets.

CoNi nanorods with a diameter of 6.5 nm and a length of 55 nm have been prepared by polyol reduction of mixed cobalt nickel acetates involving the encapsulation of the nanorods in an organic shell (oleic acid) [1]. Transmission Electron Microscopy (TEM) and spatially resolved Energy Dispersive X-Ray (EDX) spectroscopy studies show that the rods consist of a metallic single-crystal hcp Co₈₀Ni₂₀ core covered with a polycrystalline 1.5 nm thick oxide shell (Fig. 1a). The long axis of the nanorod corresponds to the <0001> crystallographic direction which is an easy magnetization axis of the hcp Co₈₀Ni₂₀ alloy.

Cooling the nanorods in a magnetic field induces an unidirectional (horizontal shift of the hysteresis) and an uniaxial (broadening of the hysteresis) magnetic anisotropy. The exchange bias field, which is a measure of unidirectional anisotropy, rapidly decreases with increasing temperature and vanishes above 175 K. A field-cooled (FC) induced uniaxial anisotropy appears below 100K. An unusual non-monotonic temperature dependence of the coercive field is observed for both zero-field cooled (ZFC) and FC data (Fig. 1b). A minimum in H_c(T) is observed at 175 K and it increases by 60 mT with further temperature rise up to 250 K. This behaviour is specific for 1D geometries with large anisotropy energy of a ferromagnetic (FM) core and a wide distribution of anisotropy energy of antiferromagnetic (AFM) grains in a polycrystalline shell [2]. The magnetic behaviour of FM-AF hybrid nanostructures is governed by the interplay of FM, AFM anisotropy energies and interfacial coupling of FM and AFM spins in the hybrid material.

Financial Support by EU Network “REFeePerMag” and the Xunta de Galicia (Regional Government, Spain) is acknowledged.

[1] Y. Soumare, J.Y. Piquemal, T. Maurer, et al., *J. Mater. Chem.*, **18** (2008) 5696-5702.

[2] Th. Maurer, F. Zighem, F. Ott, et al., *Phys. Rev. B*, **80** (2009) 064427-9.

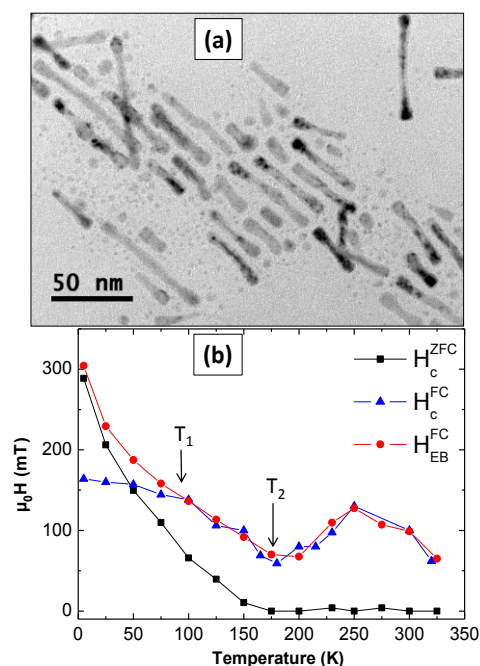


Fig. 1. (a) TEM image of Co₈₀Ni₂₀ nanorods. (b) Temperature dependence of exchange bias field H_{EB}, ZFC (H_c^{ZFC}) and FC (H_c^{FC}) coercive fields.

30RP-B-10

MACROSCOPIC BEHAVIOR AND MICROSCOPIC MAGNETIC PROPERTIES OF NANOCARBON

*Lähderanta E.*¹, *Ryzhov V.A.*^{1,2}, *Lashkul A.V.*¹, *Galimov D.M.*^{1,3}, *Titkov A.N.*^{1,4}, *Matveev V.V.*^{1,5},
*Mokeyev M.V.*⁶, *Kurbakov A.I.*², *Molkanov P.L.*², *Kiselev I.A.*², *Lisunov K.G.*^{1,7}

¹ Lappeenranta University of Technology, PO Box 20, FIN-53581 Lappeenranta, Finland

² St. Petersburg Nuclear Physics Institute, 188300 Gatchina, Leningrad province, Russia

³ South Ural State University, 454080 Chelyabinsk, Russia

⁴ A. F. Ioffe Physico-Technical Institute, 194021 St. Petersburg, Russia

⁵ St. Petersburg State University, 198504 Petergof, St. Petersburg, Russia

⁶ Institute of Macromolecular Compounds, St. Petersburg, Russia

⁷ Institute of Applied Physics, MD-2028 Kishinev, Moldova

Erkki.Lahderanta@lut.fi

Carbon-based nanomaterials represent a novel class of high-temperature ferromagnetic (FM) matter, which does not contain basically any FM metal compounds [1]. This makes them attractive for applications not only in technique, but also in biology and medicine, which is connected with low toxicity due to vanishing concentration of metallic elements [1]. Here are presented investigations of macroscopic behavior and microscopic magnetic properties of powder and glass-like samples containing carbon nanoparticles, including those doped with Ag, Au and Co. The atomic-force microscopy measurements give evidence for a broad size distribution of the assembly of carbon particles, characterized by the average and the maximum radii of ~ 60 and 110 nm, respectively. Magnetization $M(T)$ in low dc magnetic fields of $B = 1 - 50$ mT demonstrates strong irreversibility, which is suppressed above $B \sim 1$ T. The dependence of M on B exhibits saturation above 2 T at high temperatures. Magnetic hysteresis, observed already at 300 K, is characterized by a power-law temperature dependence of the coercive field, $B_c(T)$. According to the neutron diffraction data, the structure of the samples doped with Au and Co has the amorphous character, containing nanoporosity. NMR investigations of the local structure of the samples permit us to conclude, that they are (i) the products of partial carbonization of initial aromatic compounds and (ii) these products have not reach a state of glassy carbon. The main result of the ac magnetization investigations of samples doped with Au and Co is the establishment of their inhomogeneous phase-separated magnetic state, which depends on temperature. This state contains the system of the FM clusters and the magnetic matrix. The latter is formed by paramagnetic centers located outside the FM clusters. The magnetic characteristics and their temperature behavior, as well as structure of the compounds depend appreciably on the doping material. The complex temperature behavior of the magnetization in the Au-doped sample suggests changing of a mutual arrangement of magnetic moments of the matrix and the FM cluster system from an almost opposite orientation near the FM Curie temperature $T_C \approx 210$ K to an almost parallel one at low temperatures. Only the last stage of this process has been observed in the Co-doped sample within the investigated temperature interval. This stage is accompanied probably by formation of an almost homogeneous FM state, as follows from the neutron diffraction investigations.

[1] T. Makarova and F. Palacio (eds.), *Carbon-Based Magnetism*, Elsevier, North-Holland, 2006.

30 June

Monday

12:00-13:30

oral session

30TL-Q

30OR-Q

**“Low Dimensional
Magnetism”**

30TL-Q-1

MAGNETIC HEAT TRANSPORT IN SPIN-ICE MATERIALS

Lorenz T.¹, Breunig O.¹, Cho V.¹, Frielingsdorf J.¹, Hiertz M.¹, Kolland G.¹, Laschitzky P.¹, Scharffe S.¹, Valldor M.^{1,2}

¹ II. Physikalisches Institut, Universität zu Köln, 50937 Köln, Germany

² now at: Max-Planck-Institut für Chemische Physik fester Stoffe, 01187 Dresden, Germany
tl@ph2.uni-koeln.de

The spin-ice materials $\text{Dy}_2\text{Ti}_2\text{O}_7$ and $\text{Ho}_2\text{Ti}_2\text{O}_7$ crystallize in a pyrochlore lattice with the magnetic ions, Dy^{3+} or Ho^{3+} , forming a network of corner-sharing tetrahedra. The crystal electric field causes strong Ising anisotropy of the magnetic moments, which align along their local easy axis in one of the $\{111\}$ directions such that the moments point either into or out of the tetrahedron. This results in a geometric frustration with a ground-state degeneracy described by the so-called "2in/2out ice-rule", meaning that 2 spins point into and 2 out of each tetrahedron, which is equivalent to the hydrogen displacement in water ice. Excited states are created by single spin flips resulting in "3in/1out" and "3out/1in" pairs, which, in zero magnetic field, fractionalize and are described as magnetic (anti-)monopoles propagating independently [1,2]. This raises the question how these excitations influence the phonon thermal conductivity and whether the monopole excitations themselves contribute to the heat transport. In order to clarify these issues, we studied the thermal conductivity of spin ice as a function of magnetic field applied along different high-symmetry directions, which lift the ground-state degeneracy and suppress the monopole mobility. In addition, we studied various magnetic and nonmagnetic reference compounds in order to separate the phononic and the magnetic contributions to the total heat transport. For $\text{Dy}_2\text{Ti}_2\text{O}_7$ both contributions are strongly magnetic-field dependent, but these effects can be rather well separated [3,4]. The phonon contribution decreases for fields above about 1.5 T, while the magnetic contribution shows a significant decrease in the low-field range and correlates with the corresponding magnetization data reflecting the different magnetic-field induced spin-ice ground states. The anisotropic field dependence as well as various hysteresis effects [5] suggest that the magnetic heat transport is essentially determined by the mobility of the monopoles. Such a clear separation of phononic and magnetic contributions is not possible in $\text{Ho}_2\text{Ti}_2\text{O}_7$. Here, the overall low-temperature heat conductivity is significantly reduced and our data on corresponding reference systems reveal that the phonon contribution increases with magnetic field suggesting that the scattering of phonons via magnetic excitations is more pronounced in the Ho-based than in the Dy-based materials. This may cause rather different low-temperature dynamics of the magnetic excitations in both types of spin-ice materials as has been already observed in AC susceptibility data [6].

This work is supported by the Deutsche Forschungsgemeinschaft via SFB 608 and the project LO 818/2-1.

[1] I. A. Ryzhkin, *J. Exp. Theor. Phys.*, **101** (2005) 481.

[2] C. Castelnovo, R. Moessner, and S. L. Sondhi, *Nature* (London), **451** (2008) 42.

[3] G. Kolland *et al.*, *Phys. Rev. B*, **86** (2012) 060402(R).

[4] G. Kolland, *et al.*, *Phys. Rev. B*, **88** (2013) 054406.

[5] S. Scharffe, *et al.*, arXiv:1311.1139 (2013).

[6] G. Ehlers, *et al.*, *J. Phys.: Condensed Matter*, **16** (2004) S635.

30OR-Q-2

ESR STUDY OF FRUSTRATED CHAIN MAGNET LiCuVO_4 IN SPIRAL AND SPIN-MODULATED PHASES.

Svistov L.E.¹, Prozorova L.A.¹, Prokofiev A.²

¹ P.L. Kapitza Institute for Physical Problems RAS, 119334 Moscow, Russia

² Institut für Festkörperphysik Technische Universität Wien, A-1040 Wien, Austria

svistov@kapitza.ras.ru

Frustrated quantum-spin chains take up significant space in both experimental and theoretical research in condensed matter physics of the past decade: unconventional magnetic phases appear in these systems as a result of a fine balance of exchange interactions influenced by fluctuations and much weaker forces. LiCuVO_4 is an example of quasi 1D magnets whose unconventional magnetic phases are provided by competing interactions, when the intra-chain nearest-neighbor (NN) exchange is ferromagnetic and the next-nearest neighbor (NNN) exchange is antiferromagnetic. This particular type of exchange interactions results in the formation of a helical incommensurate structure undergoing a sequence of phase transformations under applied magnetic fields [1,2,3]. At higher fields $\mu_0 H_c$ around 7.5 T, was established a subsequent transition into an unusual phase with a collinear spin-modulated structure. A weak anisotropy of H_c indicated an exchange nature of this transition. All spins were found to align with the applied magnetic field independently on its direction with respect to the crystal axes. For magnetically frustrated spin $S = 1/2$ chains the theory predicts strong spin-density wave correlations in a broad range of applied magnetic fields [e.g., 4]. These correlations transformed into a long-range magnetic order due to interchain exchange interactions are, probably, the reason for the spin-modulated phase to occur in LiCuVO_4 in applied magnetic fields above H_c . The field dependency of wave vector of magnetic structure of LiCuVO_4 in high field phase also confirmed this hypothesis [4].

We report on the ESR study of LiCuVO_4 within spiral and spin-modulated phases ($0 < \mu_0 H < 14$ T). All branches of the specter in field range of spiral phase ($0 < \mu_0 H < 7.5$ T) can be satisfactorily described by uniform oscillations of planar spin structure [3]. The ESR specter observed in spin-modulated phase ($\mu_0 H > 7.5$ T) has two branches. One of them can be explained by uniform oscillations of spin structure, where as the second branch observed in experiment we associated with soliton excitation mode predicted in [5].

This work is supported by the Grants 12-02-00557-`a, 13-02-00637 of the Russian Foundation for Basic Research, Program of Russian Scientific Schools.

- [1] B.J. Gibson, et al., *Physica B*, **350** (2004) 253.
- [2] M. Enderle, et al., *Europhys. Lett.*, **70** (2005) 237.
- [3] N. Büttgen, et al., *Phys. Rev. B*, **76** (2007) 014440.
- [4] T. Hikihara, et al., *Phys. Rev. B*, **78** (2008) 144404.
- [4] M. Mourigal, et al., *Phys. Rev. Lett.*, **109** (2012) 027203.
- [5] Oleg A. Starykh and Leon Balents, *Phys. Rev. B*, **89** (2014) 104407.

30OR-Q-3

STRIPY SPIN-ORDER AND FIELD-INDUCED MAGNETIC PHASE TRANSITIONS IN 2D HONEYCOMB LATTICE TELLURATE $\text{Na}_2\text{Co}_2\text{TeO}_6$

Zvereva E.A.¹, Nalbandyan V.B.², Whangbo M.-H.³, Koo H.-J.⁴, Büchner B.⁵, Vasiliev A.N.¹

¹ Physics Faculty, Moscow State University, Moscow, Russia

² Chemistry Faculty, Southern Federal University, Rostov-on-Don, Russia

³ Department of Chemistry, North Carolina State University, Raleigh, USA

⁴ Department of Chemistry and Research Institute for Basic Sciences, Kyung Hee University, Seoul, Republic of Korea

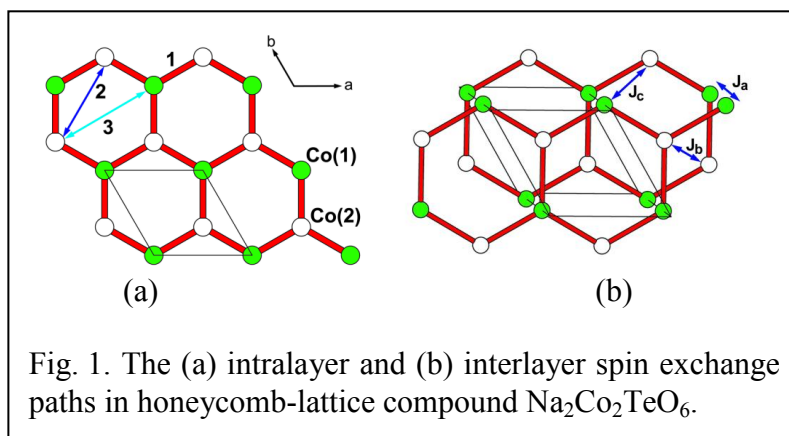
⁵ Leibniz Institute for Solid State and Materials Research IFW Dresden, Germany

zvereva@mig.phys.msu.ru

Magnetic properties of $\text{Na}_2\text{Co}_2\text{TeO}_6$ were studied comprehensively employing magnetic susceptibility, heat capacity, magnetization, electron spin resonance (ESR) as well as density functional theory calculations. The compound orders antiferromagnetically with Neel temperature ~ 26 K, however both antiferromagnetic and ferromagnetic interactions are found to be present being in delicate balance and resulting in a complicated quantum ground state. The magnetic susceptibility confirmed by specific heat data distinctly displays two-step successive phase transition at low temperature with $T_N \sim 26$ and $T_2 \sim 13$ K. The magnetization curves revealed a field-induced (spin-flop type) transition below T_2 temperature in relatively weak magnetic fields of ~ 0.3 T at $T=2$ K. Electron spin resonance (ESR) spectra show a single strongly anisotropic absorption line attributed to Co^{2+} ion in octahedral coordination with almost temperature independent effective g-factor $g=2.40\pm 0.05$. In the paramagnetic phase the temperature dependence of the magnetic susceptibility nicely follows the Curie-Weiss law with a positive value of Weiss temperature Θ of about 5 K, indicating a predominance of ferromagnetic correlations and effective magnetic moment $\mu_{\text{eff}} \approx 6.9 \mu_B/\text{f.u.}$, which is in reasonable agreement with theoretically estimated value assuming high-spin state for Co^{2+} ions ($S = 3/2$). Spin exchange interactions have been obtained from GGA+U calculations.

Theoretical calculations show that the interlayer interaction is ferromagnetic, while the intralayer interactions lead to the stripe antiferromagnetic structure

within each layer with preferred spin orientation to be parallel to c -axis. Based on the results of magnetic and thermodynamic studies in applied fields up to 9 T we propose the magnetic phase diagram in agreement with our experimental findings. Rich variety of the anomalies in magnetic properties makes quasi 2D compound $\text{Na}_2\text{Co}_2\text{TeO}_6$ an interesting system to investigate the multiple phase transitions triggered by complex interplay between competing exchange interactions on honeycomb-lattice.



Support by RFBR (grants 14-02-00245, 14-03-01122, 13-02-00374) is acknowledged.

300R-Q-4

PHASE TRANSITIONS IN PYROCHLORES $Gd_2Ti_2O_7$ AND $Er_2Ti_2O_7$ PROBED BY TRANSVERSE MAGNETIZATION MEASUREMENTS

Sosin S.S.¹, Glazkov V.N.¹, Prozorova L.A.¹, Petrenko O.A.²

¹ P.L. Kapitza Institute for physical problems, Moscow, Russia

² University of Warwick, United Kingdom

sosin@kapitza.ras.ru

Rare-earth antiferromagnets on a pyrochlore fcc-lattice are a well known example of strongly frustrated spin structures where conventional magnetic ordering is suppressed due to nontrivial topology of nearest neighbor exchange bonds. Ordered states appear in these systems as a result of competition between weaker interactions or may be stabilized by fluctuations. Fine balance of acting forces induces a variety of phase transitions of different origins, which may be effectively probed by measuring transverse magnetization (TM). Gadolinium titanate $Gd_2Ti_2O_7$ is a realization of a Heisenberg antiferromagnet whose magnetic structure remains a pending challenge for more than a decade. Our studies [1] have revealed that a sequence of phase transitions induced by magnetic field $H//[100]$ is remarkably different from those observed in any other field direction. Breaking of the initial cubic symmetry of magnetic structure is found to occur at a finite field of 10 kOe via a first order transition (see Fig. 1). Possible connection between this transition and crystal structure distortions is discussed.

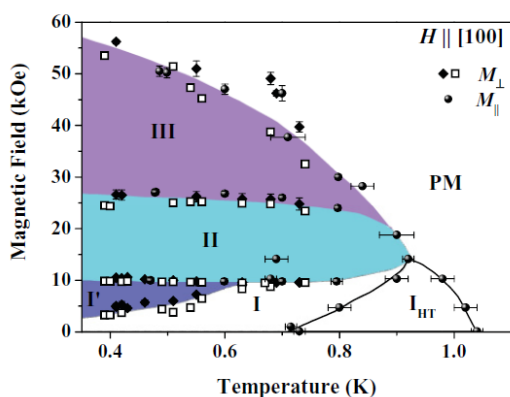


Fig. 1. Phase diagram of $Gd_2Ti_2O_7$ obtained by measuring transverse and longitudinal components of magnetization at $H//[100]$ axis.

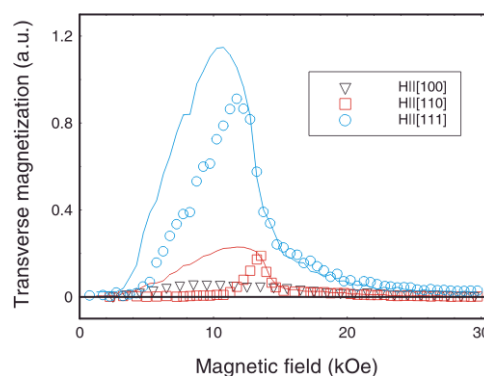


Fig. 2. TM in $Er_2Ti_2O_7$ induced by magnetic field applied along various directions; points—field increasing, solid lines—field decreasing; $T=0.4$ K.

Another compound in this series $Er_2Ti_2O_7$ is known by its nontrivial magnetic ordering which is supposedly stabilized by fluctuations (“order by disorder effect”). The proximity of the system to an XY model of effective spin Hamiltonian was assumed to put this effect on theoretical ground [2]. Our measurements show that the TM component is induced in a low field ordered phases by external field applied in all directions except for [100] (Fig. 2). The field dependence of TM and the influence of cooling prehistory can help to model magnetization process of the spin structure. One can also obtain g -tensor components and spin-Hamiltonian parameters useful for further theoretical studies of the critical behavior of the system.

[1] O.A. Petrenko *et al.*, *Phys. Rev. B* **85**, 180412(R) (2012).

[2] M.E. Zhitomirsky *et al.*, *Phys. Rev. Lett.* **109**, 077204 (2012).

30OR-Q-5

MAGNETIC RESONANCE IN THE TWO-DIMENSIONAL ELECTRON GAS AT THE INTERFACE $\text{GdMnO}_3/\text{SrTiO}_3$?

Eremina R.M.^{1,2}, *Gavrilova T.P.*¹, *Fazlizhanov I.I.*¹, *Yatsyk I.V.*^{1,2}, *Mamedov D.V.*², *Chichkov V.I.*³,
*Krug von Nidda H.-A.*⁴, *Loidl A.*⁴

¹ Zavoiisky Physical -Technical Institute RAS, Kazan, Russia

² Kazan (Volga Region) Federal University, Kazan, Russia

³ National University of Science and Technology MISiS, Moscow, Russia

⁴ EP V, Center for ECM, Augsburg University, Augsburg, Germany

The present work was stimulated by the discovery of the popular phenomena, including superconductivity and magnetism, in the two-dimensional electron liquid (2-DEL) at the interface between the insulators lanthanum aluminate (LaAlO_3) and strontium titanate (SrTiO_3) [1]. The origin of this 2-DEL, however, is highly debated, with focus on the role of defects in the SrTiO_3 , while the LaAlO_3 has been assumed perfect. Authors [1] demonstrated through experiments and first-principle calculations, that the cation stoichiometry of the nominal LaAlO_3 layer is key to 2-DEL formation; although extrinsic defects, including oxygen deficiency, are known to render $\text{LaAlO}_3/\text{SrTiO}_3$ samples conducting, their results show that in the absence of such extrinsic defects an interface 2-DEL can form.

Within this research the thin film of the multiferroic GdMnO_3 of thickness about 100 nm was deposited onto ferroelectric material SrTiO_3 ($\text{GdMnO}_3/\text{SrTiO}_3$). $\text{GdMnO}_3/\text{SrTiO}_3$ was investigated using electron spin resonance (ESR) in the wide temperature range.

The most interesting result was observed in the temperature range from 40 K to 100 K where except the exchange-narrowed line from GdMnO_3 we observed the oscillations of the absorption power. The intensity of the oscillations increases with increasing the external magnetic field or with decreasing the temperature. Chen et al. observed similar oscillations in the magnetic field dependence of resistance in the two-dimensional electron gas at the spinel/perovskite interface of $r\text{-Al}_2\text{O}_3/\text{SrTiO}_3$ [2] and V.F. Gantmakher and E.A. Kaner observed in the magnetic field dependence of the radio-frequency absorption in the tin metallic samples [3].

The reported study was partially supported by RFBR, research project No. 13-02-97120.

[1]. M.P. Warusawithana, C. Richter, J.A. Mundy, et al. *Nature Communications* **4**, Article number: 2351 (2013).

[2]. Y.Z. Chen, N. Bovet, F. Trier, et al. *Nature Communications* **4**, Article number: 1371 (2013).

[3]. V. F. Gantmakher and E. A. Kaner. *Soviet Physics JETP* **21**, 1053-1060 (1965).

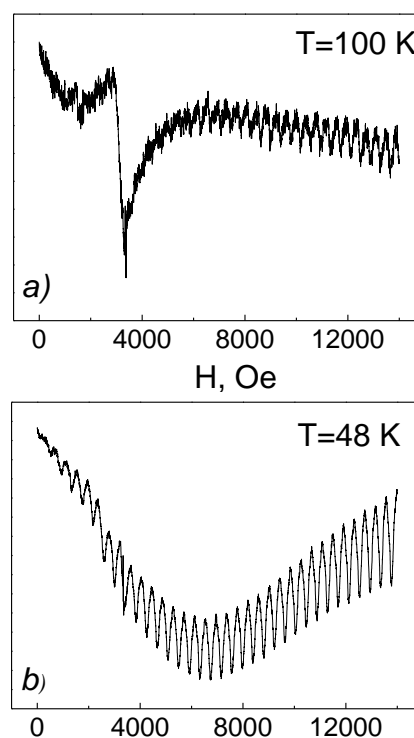


Fig. 1. ESR spectra in $\text{GdMnO}_3/\text{SrTiO}_3$ at $T=100$ K - a) и $T=48$ K - b).

30 June

Monday

15:00-17:00

oral session

30TL-C

**“High Frequency
Properties and
Metamaterials”**

30TL-C-4

**DYNAMIC MAGNETIC PROPERTIES OF SOFT MAGNETIC THIN FILMS
AND EXCHANGED BIAS MULTILAYERS***Ong C.K.¹, Phuoc N.N.², Soh Wee Tee¹*¹ Center for Superconducting and Magnetic Materials, Department of Physics, National University of Singapore, 2 Science Drive 3, Singapore 117542² Temasek Laboratories, National University of Singapore, 5A Engineering Drive 2 Singapore 117411

In this talk, I shall discuss our systematic investigation of soft magnetic thin films and exchanged bias multilayers using comprehensive vector network analyser (VNA) based ferromagnetic resonance (FMR) measurements. Specially, dynamic and static magnetic properties of the films with various types of magnetic anisotropies such as unidirectional magnetic anisotropy, static and dynamic uniaxial magnetic anisotropy, rotatable magnetic anisotropy and magneto-elastic anisotropy will be discussed in connection with the thermal stability and resonance frequency of the films. The experimental results will be analyzed together with the theoretical approach based on Landau-Lifshitz-Gilbert equation. Moreover, the hysteretic FMR line width and the spin rectification current characterization will be used to quantify different physical relaxation processes in the films and multilayers.

30TL-C-5

LAMINATED MAGNETIC MATERIAL FOR HIGH FREQUENCIES

*Iakubov I.T., Lagarkov A.N., Maklakov S.A., Osipov A.V., Rozanov K.N., Ryzhikov I.A.,
Starostenko S.N., Zezyulina P.A.*

ITAE RAS, Moscow, Russian Federation

k_rozanov@mail.ru

It is well known that thin ferromagnetic films allow high microwave permeability to be obtained [1]. This is true for film thickness of several sub-micrometers or less; with larger thickness, the microwave permeability diminishes because of the effect of eddy currents and deviation of magnetic structure from the in-plane anisotropy. For most technical applications requiring high-permeable magnetic materials, massive samples, of several millimeters or thicker, are needed. To overcome the thickness limitation in ferromagnetic films, structured multilayered magnetic materials have been suggested [2], in which the magnetic layers are separated by non-magnetic and non-conducting interlayers of. These plane-parallel laminates are advantageous over conventional composites filled with magnetic powders due to the uniformity of the elements and spatial ordering. Namely, the laminates do not possess spectrum broadening caused by dispersion of filler particles; these have low specific weight and good machineability, etc.

The presentation describes a massive magnetic material based on permalloy multilayer films and having large permeability at frequencies below 1 GHz. The rationale is performed for the selection of a magnetic material and structural parameters (the number and thickness of layers). The massive laminate is made of 20-layer films placed in stack and glued together to comprise a sample of 0.4 mm in thickness and $5 \times 40 \text{ mm}^2$ in transversal size. The content of magnetic phase in the sample is about 22% vol. The measured permeability of the sample reveals the static permeability of 60 and the imaginary permeability peak having the amplitude of about 50 and located near 1 GHz, see Fig. 1. Developed material may be useful for many technical applications that require magnetic materials with high permeability at high frequencies.

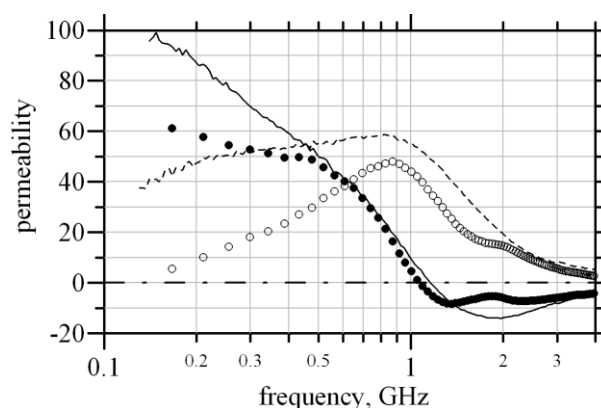


Fig. 1. The measured frequency dependence of the permeability for the laminate (filled dots are the real part and empty dots are the imaginary part) and the simulation based on the measured permeability of the coaxial washers made of the initial 20-layer film (solid curve is the real part, dashed curve is the imaginary part)

[1] A.N. Lagarkov, S.A. Maklakov, A.V. Osipov, et al, *J. Commun. Technol. Electron.*, **54** (2009) 5, 596-603.

[2] R.M. Walser and R.J. Hach, *US Patent 350047* (1970) No.10.

30TL-C-6

EDDY CURRENT EFFECT ON HIGH-FREQUENCY PERMEABILITY OF Fe-BASED NANOCOMPOSITES

*Han M.*¹, *Rozanov K.N.*², *Zezyulina P.A.*²

¹ State Key Laboratory of Electronic Thin Films & Integrated Devices, University of Electronic Science and Technology of China, Chengdu, China

² Institute for Theoretical and Applied Electromagnetics, Russian Academy of Sciences, Moscow, Russia
mangui@gmail.com

Fe-based nanocrystalline alloys are one of important ferromagnetic materials with excellent soft magnetic properties. Recently, studies showed that these materials can be good candidates for electromagnetic noise attenuation application above 1 GHz [1, 2]. For such applications in gigahertz range, the eddy current effect should be considered for ferromagnetic alloys with low resistivity values [3-4]. In this contribution, we will report the effect of eddy current on the high frequency permeability of Fe-Cu-Nb-Si-B nanocomposites flakes, in which the α -Fe(Si) nanocrystalline phase with an average grain size of 14 nm is well-dispersed in the amorphous matrix. In order to study the eddy current effect on high frequency permeability, two classes of flakes have been fabricated via a ball attrition process for 10 and 30 hours respectively. The microwave permeability spectra of composites containing 28.6 % (volume fraction) flakes particles have been measured within a frequency range of 0.5 to 10 GHz. Large effective permeability losses have been found in these two composites, which indicate that the flakes can find applications in electromagnetic noise attenuation. The feature of wide permeability dispersion has been found for the composites. There are two possible origins for the observed large dispersion in permeability: eddy current effect or distribution of magnetic anisotropy field. The initial magnetization curves have been measured for the electromagnetic composites to study the dispersion of magnetic anisotropy field, which will be used to explain the dispersion of permeability. A criterion will also be employed to check the contribution of eddy current [5].

Besides, Transmission Mössbauer Spectroscopy has been employed to study the differences in the hyperfine interactions in the as-prepared ribbons and two classes of flakes.

Supported by NSFC (Grant No. 61271039), the Scientific Foundation of Outstanding Young Scientists in Sichuan Province (Grant No. 2013JQ0006) and RFBR (Grant No. 13-08-00103) is acknowledged.

- [1] Mangui Han, Difei Liang, and Longjiang Deng, *Appl. Phys. Lett.*, **99** (2011) 082503.
- [2] Mangui Han, Haipeng Lu, and Longjiang Deng, *Appl. Phys. Lett.*, **97** (2010) 192507.
- [3] L. B. Kong, Z. W. Li, L. Liu, R. Huang, M. Abshinova, Z. H. Yang, C. B. Tang, P.K.Tan, C.R.Deng and S.Matitsine, *Intl. Mater. Rev.* **58**(2013)203.
- [4] A. N. Lagarkov, K. N. Rozanov, *J. Magn. Magn. Mater.* **321**(2009)2082.
- [5] M. Z. Wu, Y. D. Zhang, S. Hui, T. D. Xiao, S. H. Ge, W. A. Hines, J. I. Budnick, G. W. Taylor, *Appl. Phys. Lett.*, **80**(2002)4404.

30TL-C-7

DOUBLE NEGATIVE ELECTROMAGNETIC PROPERTY OF GRANULAR COMPOSITE MATERIALS IN THE MICROWAVE RANGE

Tsutaoka T.¹, Kasagi T.², Yamamoto S.³, Hatakeyama K.³

¹ Hiroshima University, Higashi-Hiroshima, Japan

² Tokuyama College of Technology, Shunan, Japan

³ University of Hyogo, Himeji, Japan

tsutaok@hiroshima-u.ac.jp

The development of left-handed metamaterials (LHM) which simultaneously have negative permittivity (ENG) and permeability (MNG) spectra in the microwave or optical range has been the subject of considerable interest in recent years. As a real electromagnetic material, several granular composite materials having the double negative (DNG) electromagnetic property have been studied [1, 2]. We reported that the copper and yttrium iron garnet (Cu/YIG) hybrid granular composites show DNG property under external magnetic field in the several GHz range [2]. In this report we would like to discuss the complex permeability ($\mu_r = \mu_r' - i\mu_r''$) and permittivity ($\varepsilon_r = \varepsilon_r' - i\varepsilon_r''$) spectra of DNG composite materials in the microwave range.

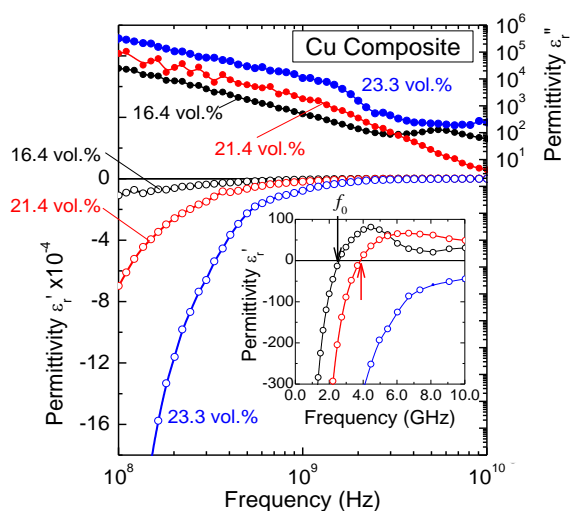


Fig.1 Complex permittivity ε_r spectra of Cu composite materials.

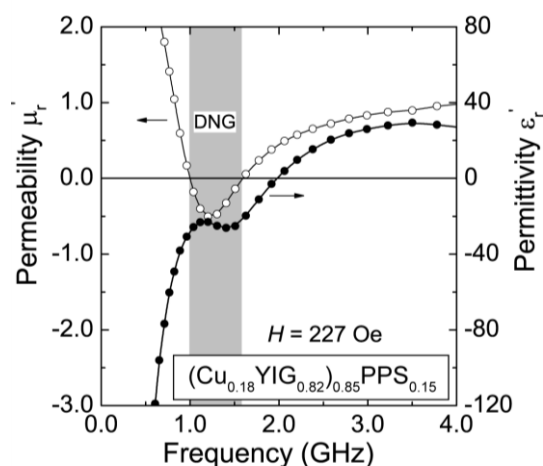


Fig.2 The ε_r' and μ_r' spectra of a Cu/YIG composite under $H = 227$ Oe.

High conductive metal granular composite materials containing Ag or Cu particles show the low frequency plasmonic property in the microwave range above the percolation threshold content [1, 2]. Figure 1 shows the ε_r spectra of Cu composites indicating the ENG property below characteristic frequency f_0 . On the other hand, the MNG property can be obtained by the magnetic resonance of ferromagnetic materials in the microwave range. Combining these ENG and MNG properties, DNG characteristic can be obtained in the several hybrid composites. Figure 2 shows the DNG electromagnetic property of a Cu/YIG granular composite under external magnetic field H of 227 Oe. Therefore, the many combinations of the metal/ferromagnet granular composite structures can be considered to realize the DNG property in the microwave range by use of the low frequency plasmonic state and the ferromagnetic resonance. In the composite structure, since the eddy current effect can be suppressed, the ferromagnetic metal such as Fe-Ni alloy particles can be used for the MNG composites.

[1] Z.-C. Shi *et al.*, *J. Mater. Chem. C*, **1** (2013) 1633-1637.

[2] T. Tsutaoka *et al.*, *Appl. Phys. Lett.*, **103** (2013) 261906.

30 June

Monday

15:00-17:00

oral session

30OR-G

30RP-G

**“Diluted Magnetic
Semiconductors”**

30OR-G-4

DEFECT-INDUCED MAGNETISM IN TITANIUM DIOXIDE

*Smekhova A.*¹, *Yildirim O.*^{2,4}, *Butterling M.*², *Cornelius S.*², *Mikhailovsky Yu.*¹, *Novikov A.*¹,
Semisalova A.^{1,5}, *Orlov A.*³, *Gan'shina E.*¹, *Perov N.*¹, *Anwand W.*², *Wagner A.*², *Potzger K.*²,
*Granovsky A.B.*¹

¹ M.V. Lomonosov Moscow State University, Moscow, Russia

² Helmholtz-Zentrum Dresden-Rossendorf, Dresden, Germany

³ Federal State Research and Design Institute of Rare Metal Industry, Moscow, Russia

⁴ Institute for Physics of Solids, Technical University Dresden, Dresden, Germany

⁵ Lappeenranta University of Technology, Lappeenranta, Finland

smeal@physics.msu.ru

The tuning of physical properties of solids to realize a desired functionality is always a challenge. In case of semiconductors the last decades were devoted to the creation, understanding and manipulation of ferromagnetism in doped semiconducting materials. In spite of great advances in recent years in this area [1] the origin of above and below room temperature ferromagnetism in different DMS and oxides remains a controversial issue [2] in majority of cases. A number of models of a long-range ferromagnetic order in different DMS systems are reported in the literature (see *e.g.* [3] and references therein). In the case of 3d doped titanium dioxide the most popular but competitive points of view on origin of RTFM are carrier-mediated and defect-induced models. Many recent published results show the strong dependence of RTFM on the preparation method, so different types of structural defects have to be taken into account for the explanation of this phenomenon. Nevertheless, most of authors are concentrated only on the importance of oxygen vacancies [4] and their complexes or the type of the crystal structure (anatase or rutile).

We discovered recently [5] that negatively charged structural defects in V- doped TiO₂ (1at%) play an important role and should be considered separately from an influence of oxygen vacancies. A ratio of saturation magnetizations in semiconducting and insulating films (a difference in resistivities is about 13 orders of magnitude) was found to be 0.7 while a ratio of defects concentrations in both films was estimated from Positron Annihilation Spectra (PAS) spectra as 0.67. For both films neither MO spectra nor AHE has been found. So, defect-induced model of RTFM is assumed for Ti_{0.99}V_{0.01}O_{2-δ} without involvement of free charge carriers or the local magnetic moment of V ions.

Contrary to that samples with 3at% of V doping exhibit the strong MO signal and the shape of MO spectra is conductivity dependent. We suppose that this is the evidence of new spin-polarized states appeared inside the band-gap due to the incorporation of V ions into the octahedral complex of oxygen. Also, a tiny signature of AHE signal has been found for one of these samples. So, we expect that RTFM in 3at% V doped TiO₂ is related somehow with a local magnetic polarization of V ions that could create a spin-polarization of the carriers. The results of PAS are also discussed.

Support by a German-Russian joint research group HRJRG-314 & RFBR 12-02-91321-SIGa is acknowledged.

[1] H. Ohno, *J. Appl. Phys.* **113** (2013) 136509.

[2] T. Dietl, *Nat. Mater.* **9** (2010) 965.

[3] J.M.D. Coey, M. Venkatesan and C.B. Fitzgerald, *Nature* **4** (2005) 173.

[4] J. Lu, K. Yang, H. Jin et al., *J. Sol. St. Chem.* **184** (2011) 1148.

[5] O. Yildirim et al., accepted to PSS, will be published in 2014.

30OR-G-5

FROM A NON-MAGNET TO A FERROMAGNET: Mn IMPLANTATION INTO DIFFERENT TiO₂ STRUCTURES

Yildirim O.^{1,2}, *Cornelius S.*^{1,2}, *Butterling M.*³, *Anwand W.*³, *Wagner A.*³, *Smekhova A.*⁴, *Baehz C.*^{1,5},
*Potzger K.*¹

¹ Institute of Ion Beam Physics and Materials Research, Helmholtz-Zentrum Dresden-Rossendorf e.V., Dresden, Germany

² Technische Universität Dresden, D-01062 Dresden, Germany

³ Institute of Radiation Physics, Helmholtz-Zentrum Dresden-Rossendorf e.V., Dresden, Germany

⁴ Lomonosov Moscow State University (MSU), Faculty of Physics, Moscow, Russia

⁵ Rossendorf Beamline, European Synchrotron Radiation Facility, Grenoble, France
o.yildirim@hzdr.de

As one of the most promising candidates for a diluted magnetic oxide material for spintronic and magneto optic applications, transition metal (TM) doped titanium dioxide (TiO₂) has been extensively studied for last two decades. Up to date room temperature ferromagnetism (RTFM) has been reported for different types of TM dopants and also different types of preparation methods, such as ion implantation [1] or magnetron sputtering [2]. There is an ongoing debate on the origin of the ferromagnetic properties of TM doped TiO₂, whether RTFM arises from unwanted clustering of the TM atoms, magnetic contamination from sample handling or the desired substitution of Ti by the TM dopants.

We have investigated Mn implanted TiO₂ films with respect to the effect of the crystalline structure of the pristine film on the magnetic properties of the doped films. The films were prepared by DC magnetron sputtering using a high purity oxygen deficient ceramic TiO_{2-x} target in Ar/O₂ atmosphere. SrTiO₃ (100) single crystals were used as substrates. In order to achieve different structures of TiO₂, namely amorphous, polycrystalline anatase and epitaxial anatase, different substrate temperatures and post-growth annealing were applied. The as-prepared TiO₂ samples have been implanted with Mn ions of 30 keV to 190 keV kinetic energy and variable fluence resulting in a homogenous Mn concentration of 5 at.% within a 150 nm thin layer below the film surface.

The structural changes upon implantation were followed by means of X-ray diffraction (XRD) measurements. Comparison of the diffraction patterns indicates ion-induced damage in the epitaxial film and the formation of Mn containing secondary phases in the polycrystalline material. Depth resolved defect concentration profiles of as-grown and Mn implanted films were determined by means positron annihilation spectroscopy (PAS) measurements based on Doppler broadening spectroscopy. Magnetometry measurements of Mn implanted films reveal ferromagnetism for amorphous and polycrystalline films whereas paramagnetism is observed for epitaxial films. The local environments of implanted Mn ions in different TiO₂ structures were probed by X-ray absorption spectroscopy (XAS) in fluorescence mode.

In summary, we have found a significant influence of the as-grown film structure on the magnetic properties of Mn:TiO₂. During the presentation the PAS and XAS data will be discussed with respect to the presence of defects and secondary phases in the Mn doped TiO₂ films.

The work was supported by Initiative and Networking Fund of the German Helmholtz Association, Helmholtz-Russia Joint Research Group HRJRG-314, and the Russian Foundation for Basic Research, RFBR #12-02-91321-SIG_a.

[1] V. Shutthanandan et al. *Appl. Phys. Lett.* **84**, 22 (2004).

[2] F.M. Liu et al. *Nuc. Ins. and Met. in Phys. Res. B* **267**, 3104-3108 (2009).

30RP-G-6

FERROMAGNETIC BEHAVIOUR OF NANOGRAINED ZnO DOPED BY Mn, Fe, Co, Cr AND Ni

*Straumal P.B.^{1,2}, Stakhanova S.V.², Mazilkin A.A.^{3,5}, Protasova S.G.^{3,5}, Straumal B.B.²⁻⁴, Schütz G.⁵,
Tietze Th.⁵, Goering E.⁵, Baretzky B.⁴*

¹ A.A. Baikov Institute of Metallurgy and Materials Science, Russian Academy of Sciences,
Leninsky prospect 49, 117991 Moscow, Russia

² National University of Science and Technology “Moscow Institute of Steel and Alloys – MISiS”,
Leninsky prospect 4, 119991 Moscow, Russia

³ Institute of Solid State Physics, Russian Academy of Sciences, Chernogolovka, Moscow district,
142432 Russia

⁴ Karlsruher Institut für Technologie, Institut für Nanotechnologie, Hermann-von-Helmholtz-Platz
1, 76344 Eggenstein-Leopoldshafen, Germany

⁵ Max-Planck-Institut für Intelligente Systeme (former MPI Metallforschung), Heisenbergstrasse 3,
70569 Stuttgart, Germany

The nanograined thin films of undoped ZnO and ZnO doped by Mn, Fe, Co, Cr and Ni were synthesized by the wet chemistry (“liquid ceramics”) method from butanoate precursors. Films consist of the dense equiaxial nanograins, and possess ferromagnetic properties. The ferromagnetism appears only in ZnO polycrystals with a quite high density of grain boundaries. The critical size of grains is about 20 nm for pure ZnO. It increases if nanograined ZnO is doped by Mn, Fe, Co, Cr or Ni. Most effective is the doping by iron (the critical grain size in this case is above 40 μm). The addition of 0.1-1 at. % of Mn, Fe, Co, Cr or Ni to pure ZnO increases the saturation magnetization 3 to 10 times. Further increase of dopant content leads to the decrease of magnetization. Total solubility of Mn, Fe, Co, Cr or Ni in ZnO drastically increases with decreasing grain size.

The financial support of Russian Foundation for Basic Research (grants 10-02-00086, and 12-08-31185) is acknowledged.

30OR-G-7

MAGNETOTRANSPORT OF InSb/MnSb COMPOSITES

Kochura A.V.^{1,2}, *Lisunov K.G.*^{2,3}, *Aronzon B.A.*^{2,4}, *Lahderanta E.*², *Khmelevskoi D.V.*¹,
*Fedorchenko I.V.*⁵, *Marenkin S.F.*⁵

¹ South – West State University, 50 let Oktjabrja str. 94, 305040 Kursk, Russia

² Lappeenranta University of Technology, PO Box 20, FIN-53851, Lappeenranta, Finland

³ Institute of Applied Physics, Academy of Science of Moldova, MD-2028 Kishinev, Moldova

⁴ P.N. Lebedev Physical Institute RAS, Moscow 119991, Russia

⁵ Institute of General and Inorganic Chemistry of Russian Academy of Sciences, Leninskii pr. 31, 119991, Moscow, Russia

akochura@mail.ru

At present time, investigations of structural, magnetic and, especially, electronic properties of the group III-V compounds doped with manganese are undertaken actively. In particular, indium antimonide attracts attention as a material with the narrowest band gap and the highest electron mobility among III-V semiconductors. This stimulates our interest to InSb bulk samples and films doped with manganese and prepared by different methods. We have investigated magnetotransport of InSb:Mn polycrystals, InSb-MnSb eutectic compositions and InSb:Mn films. To synthesise polycrystalline InSb:Mn samples, the solid state reaction method has been used [1]. Single crystals of eutectic composition were obtained by Bridgman method [2] and InSb:Mn films by laser ablation. The magnetotransport properties were investigated between 1.6 and 320 K using the standard six-point geometry in pulsed magnetic fields up to 20 T. It was found, that high-temperature ferromagnetism ($T_C \sim 600$ K) in InSb:Mn crystals and films appears due to formation of MnSb micro- and nanosize inclusions. The non-linear dependence of the Hall resistivity on the magnetic field is observed up to the room temperature, suggesting presence of the normal and the anomalous components. The anomalous contribution is attributable to the effect of the ferromagnetic MnSb phase. The normal Hall constant is affected by the nanosize MnSb inclusions, as well. The negative magnetoresistance (MR) takes place below ~ 10 K (Fig. 1) and is interpreted by spin-dependent scattering of the holes by the localized magnetic moments. Oscillations of MR have been observed and attributed to the Shubnikov-de Haas effect of the light holes.

This work is supported by Russian Foundation for Basic Researches (grant 13-02-011105a, 14-02-00586, 13-02-92694).

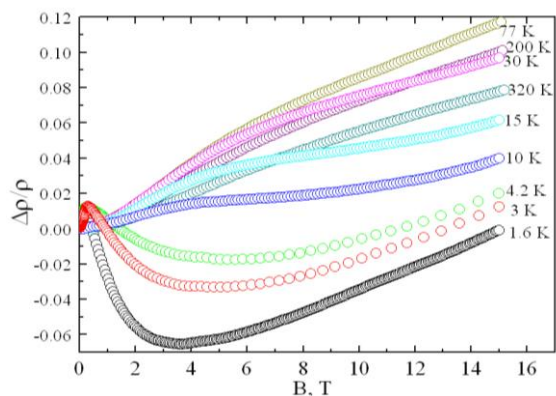


Fig. 1. Magnetic field dependence of the magnetoresistance in single crystals of the InSb-MnSb eutectic composition.

[1] A.V. Kochura, B.A. Aronzon, K.G. Lisunov et al., *JAP* **113**, 083905 (2013).

[2] V.M. Novotortsev, A.V. Kochura, S.F. Marenkin et al. *Russian Journal of Inorganic Chemistry*, 1951 (2011).

30OR-G-8

EFFECT OF CHARGE CARRIERS ON MAGNETIZATION OF FERROMAGNETIC CLUSTERS IN GaSb (59 %) – MnSb (41 %) FILMS

*Talantsev A.¹, Polyakov A.², Dmitriev A.¹, Koplak O.¹, Morgunov R.¹, Kochura A.^{3,4},
Fedorchenko I.⁵, Novodvorskiy O.⁶, Parshina L.⁶, Lahderanta E.³, Aronzon B.^{2,3}*

¹ IPCP RAS, Chernogolovka, Russia

² NRC "Kurchatov Institute ", 1 Kurchatov Sq., 123182 Moscow, Russia

³ Lappeenranta University of Technology, PO Box 20, FIN-53851, Lappeenranta, Finland

⁴ South – West State University, 50 let Oktjabrja str. 94, 305040 Kursk, Russia

⁵ Institute of General and Inorganic Chemistry RAS, 119991, Moscow, Russia

⁶ Institute of Laser and Information Technologies, RAS, 140700 Shatura, Moscow region, Russia
artgtx32@mail.ru

Semiconductor films containing ferromagnetic clusters are very promising objects for spintronics because they provide injection of the spin polarized charge clusters to the crystal lattice and can be considered as a basis of spin battery [1-3]. In our work interplay between concentration of charge carriers and parameters of the magnetic hysteresis of the ferromagnetic clusters in GaSb (59 %) – MnSb (41 %) thin films were studied. Obvious correlation between saturation magnetization and concentration of the charge carriers were found at room temperature as well as at 2 K temperature (fig.1).

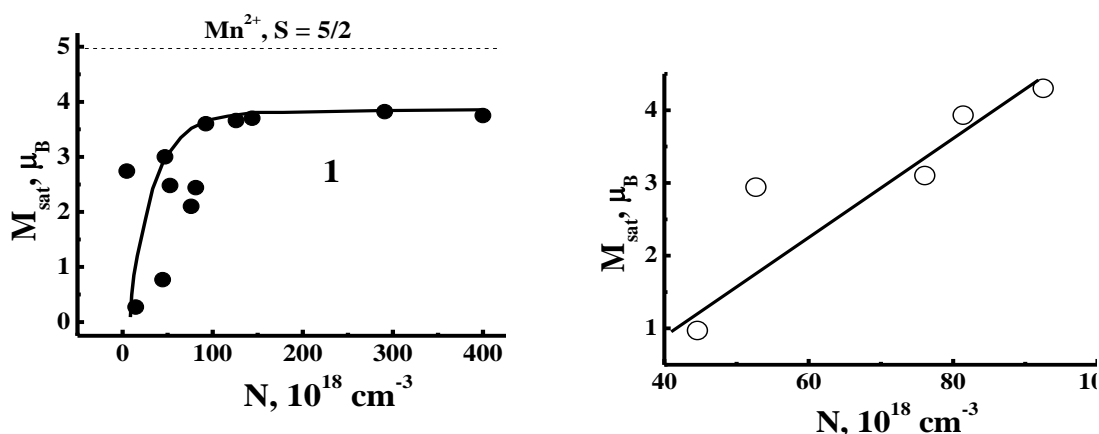


Fig.1. Dependencies of the saturation magnetic moment M_{sat} on charge carrier concentration at: $T = 300$ K (a), $T = 2$ K(b).

Derivation of the effective magnetic moment of the clusters from theoretical predictions (shown by horizontal dashed line) was discussed in the terms of antiferromagnetic interaction of the charge carriers and Mn ions. Effect of concentration of the charge carriers on Schottky barrier between clusters and semiconductor crystal lattice was discussed.

This work is supported by Russian Fund for Basic Researches (grant 13-07-12027a, 13-02-011105a) and Grant of the President of Russia MK-1598.2014.3.

[1] A.V. Kochura, B.A. Aronzon, K.G. Lisunov et al., *JAP* **113**, 083905 (2013).

[2] B.A. Aronzon, V.V. Rylkov, S.N. Nikolaev, et al., *PRB* **84**, 075209 (2011).

[3] V.V. Rylkov, S.N. Nikolaev, K.Yu.Chernoglazov, B.A. Aronzon et al., *JETP letters* **96**(4) (2012), 255-262.

30RP-G-9

NANOWIRES AND QUANTUM DOTS BASED ON $(A_3,Mn)B_5$ DILUTED MAGNETIC SEMICONDUCTORS

*Bouravleuv A.D.*¹⁻⁴, *Cirlin G.E.*¹⁻³, *Samsonenko Yu.B.*¹⁻³, *Khrebtov A.I.*¹⁻², *Sapega V.F.*¹, *Savin A.*⁴,
*Lipsanen H.*⁴, *Werner P.*⁵, *Nevedomskiy V.N.*¹

¹ Ioffe Physical Technical Institute RAS, St.Petersburg, Russia

² St.Petersburg Academic University RAS, St.Petersburg, Russia

³ Institute for Analytical Instrumentation RAS, St.Petersburg, Russia

⁴ Aalto University, Espoo, Finland

⁵ Max Plank Institute of Microstructures Physics, Halle, Germany

bour@mail.ioffe.ru

The $(A_3,Mn)B_5$ semiconductors, which can exhibit ferromagnetic properties, have attracted increasing attention over the last decades since the combination of semiconductor and ferromagnetic properties makes it possible to achieve radically new functionality in novel nano- or optoelectronic devices. At the same time, the nanostructures such as quantum dots and nanowires based on so called diluted magnetic semiconductors (DMS) deserve special attention because such low-dimensional structures can exhibit unique properties even due to their unique geometrical shape, not to mention the localization effects and so on.

Here we report on the comprehensive study of the properties of $(Ga,Mn)As$ nanowires (NWs) and $(In,Mn)As$ quantum dots (QD) grown by molecular-beam epitaxy (MBE) at intermediate temperatures higher than the ones used for low-temperature (LT) MBE growth of $(Ga,Mn)As$ and $(In,Mn)As$ thin films, respectively.

The $(Ga,Mn)As$ NWs were grown by MBE on $GaAs(100)$ substrates using Mn as a catalyst. In turn, $(In,Mn)As$ QDs have been obtained by different methods such as the Mn selective doping of the central or upper parts of $InAs$ QDs during their growth.

It was shown, that majority of $(Ga,Mn)As$ NWs have preferential growth direction along $\langle 111 \rangle$ and $\langle 110 \rangle$. The structural and chemical characterization of the samples performed by transmission electron microscopy (TEM) has revealed that NWs did not have any extended defects, such as dislocations or precipitates. However, it was found that during the MBE growth of $(Ga,Mn)As$ NWs, the segregation of α - $MnAs$ precipitates in a hemispherical shape occurred between the NWs near/at the surface of the grown $GaAs$ layer. The magnetic properties of the samples have been investigated using SQUID. $(Ga,Mn)As$ NWs, which have been peeled off from the substrate, demonstrate ferromagnetic behaviour up to 70K. PL measurements of the sample with $(Ga,Mn)As$ NWs exhibit broad emission bands around 1.411 eV and the corresponding TA-phonon and LO-phonon replica consisting of two series of lines which can be caused by the recombination of the equilibrium photoexcited free electrons with holes bound to neutral Mn acceptors.

The TEM investigation of the samples with $(In,Mn)As$ QDs has shown, that Mn doping Mn during the final stage of QD growth brings about the formation of misfit dislocations parallel to the $\{111\}$ planes. At the same time, upon doping of the central part of the QDs, no extended structural defects are observed in the sample. The samples had a good crystalline quality. As it was shown by PL, in this case, Mn atoms occupy the cation sites in the crystal lattice.

30OR-G-10

BASED ON GaSb, Ge AND Si DOPED BY MANGANESE IMPURITY LASER DEPOSITED HIGH TEMPERATURE FERROMAGNETICS

*Demidov E.S.¹, Podolskii V.V.¹, Lesnikov V.P.¹, Karzanov V.V.¹, Tronov A.A., Sapozhnikov M.V.²,
Gribkov B.A.²*

¹ Nizhny Novgorod State University, Nizhny Novgorod, Russia

² Institute for Physics of Microstructures, RAS, Nizhny Novgorod, Russia
demidov@phys.unn.ru

Coexistence of magnetism and semiconducting properties in diluted magnetic semiconductors (DMS) increases functionalities of spin-electronics. The possibility of the laser synthesis of thin 30-110 nm layers of DMS GaSb:Mn and InSb:Mn with the Curie temperature T_C above 500 K and Ge:Mn, Si:Mn, Si:Fe with T_C up to 400, 500, 250 K respectively was earlier demonstrated [1-4]. Recently [5], the crystal structure of Si:Mn DMS was investigated by HRTEM and LED. The laser technology allows to reach of solid solution of 15%Mn in silicon of DMS Si:Mn (or $\text{Si}_{3-x}\text{Mn}_x$) with high electrical and magnetic activity, conservation of diamond like crystal structure and epitaxy growth of Si:Mn on GaAs with self-organized formation of superlattice. This report represents the comparison analysis of properties of laser synthesized magnetic GaSb:Mn, Ge:Mn, Si:Mn layers grown at temperatures $T_g=200-400^\circ\text{C}$ on single crystal GaAs, Si:Mn on Si and for the first time on Ge substrates. The ferromagnetism of layers was controlled by ferromagnetic resonance (FMR), magneto-optical and magneto-transport measurements. The surface profile and distribution of magnetization were determined by atomic and magnetic force probe microcopies.

The method of pulse deposition from laser plasma is possible to synthesize rather thick layers of the silicon DMS Si:Mn up to 100 nm as on the single crystal GaAs, Si substrates and for the first time on Ge. The FMR spectra, resulted in Fig.1, testify about magnetic uniformity of layers, show comparable on intensity of resonant peaks magnetization. Most strongly angular anisotropy is shown in case of Si:Mn/GaAs, the least - for Si:Mn/Si. Detailed analysis of angular dependences and intensities of FMR spectra of magnetically soft GaSb:Mn, Ge:Mn and Si:Mn DMSs have shown the similar for $\text{Ga}_{1-x}\text{Mn}_x\text{As}$ in [6] reduced value of the g-factor <2 , the negative contribution of lateral anisotropy and the lowered saturation magnetization. It related as well as in [6] to the contribution of mobile holes in the valence band of semiconductor. At least in case of the Si:Mn DMS an alternative to RKKY the band mechanism of spin ordering can be more probable.

Support by RFBR 11-02-00855a is acknowledged.

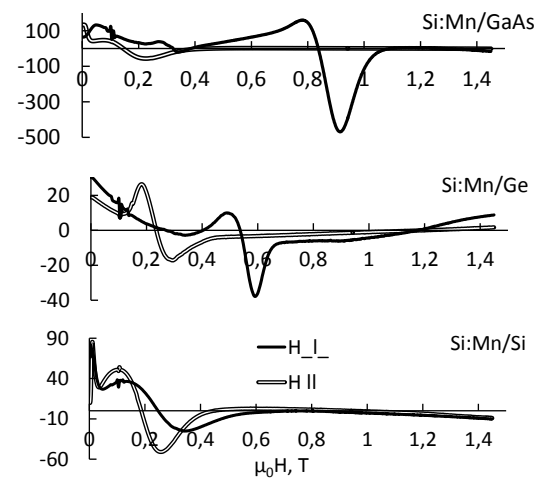


Fig. 1. FMR spectra of DMS Si:Mn on GaAs, Ge and Si substrates at 293K.

- [1] E.S. Demidov, V.V. Podolskii, V.P. Lesnikov et al, *JETP Letters*, **83** (2006) 568–571.
 [2] Yu.A. Danilova, E.S. Demidov, Yu.N. Drosdov et al, *JMMM*, **300** (2006) e24–e27.
 [3] E.S. Demidov, V.V. Podolskii, V.P. Lesnikov et al., *JETP*, **106** (2008) 110–116.
 [4] E.S. Demidov, B.A. Aronzon, S.N. Gusev et al, *JMMM*, **321** (2009) 690–694.
 [5] E.S. Demidov, E.D. Pavlova, A.I. Bobrov, *JETP Lett.*, **96** (2012) 706-709.
 [6] Xinyu Liu and J. K. Furdyna, *J. Phys.: Condens. Matter*, **18** (2006) R245–R279.

30 June

Monday

15:00-17:00

oral session

30TL-H

30RP-H

30OR-H

“Magnetoplasmonics”

30TL-H-6

BI-SUBSTITUTED $R_3Fe_5O_{12}$ (R=Y, Gd AND Nd) FILMS PREPARED BY METAL-ORGANIC DECOMPOSITION METHOD

Ishibashi T.¹, Yoshida T.¹, Lou G.¹, Nishi T.²

¹ Nagaoka University of Technology, Niigata, Japan

² Kobe City College of Technology, Hyogo, Japan

t_bashi@mst.nagaokaut.ac.jp

Bi-substituted iron garnet films, $R_{3-x}Bi_xFe_5O_{12}$ (Bi:RIG), have been attracting great attention because of exciting discoveries of inverse Faraday effect, spin Hall effect, spin Seebeck effect, spin wave phenomena in addition to its well-known huge magneto-optical (MO) effect. High quality Bi:RIG films with various magnetic and magneto-optic properties are strongly required to study those phenomena and realize applications utilizing those phenomena. For the purpose, we are developing garnet films by the metal-organic decomposition (MOD) method [1,2].

Bi:RIG (R=Y, Gd and Nd, $x = 0 - 3.0$) films were prepared on GGG and glass substrates by the MOD method using metal-organic solutions produced by Kojundo Chemical Laboratory Ltd. MOD process consists of spin coating of MOD solution (3000 rpm, 60 seconds), drying (100°C, 30 minutes), pre-annealing (450°C, 10 minutes), annealing for crystallization (700°C, 3 hours).

Figure 1 shows Faraday spectra of $Y_{3-x}Bi_xFe_5O_{12}$ (Bi:YIG) films. It is observed that Faraday rotation angle increases with Bi composition, and it reaches -2.4×10^5 degree/cm at a wavelength of 525 nm. Bi:YIG films with in-plane magnetic anisotropy shows good MO property that is suitable for MO indicator film. Magnetic recording marks in a magnetic card are clearly observed by using an MO indicator film of Bi:YIG ($x=2.5$) as shown in Fig.2. In addition, several kinds of garnet films will be discussed.

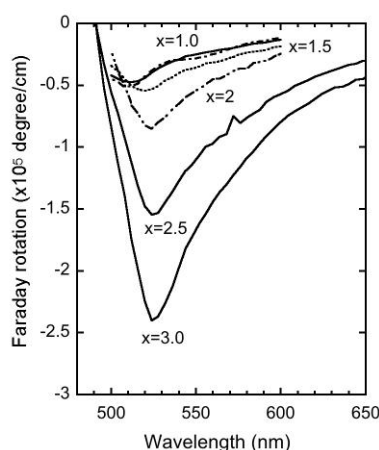


Fig. 1. Faraday rotation spectra of Bi:YIG films with $x = 1.0 - 3.0$.

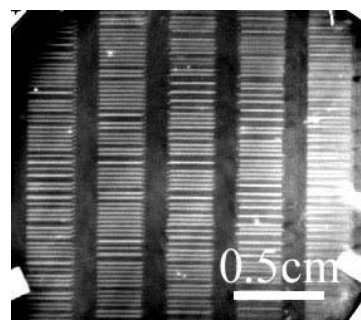


Fig. 2. A magnetic images of a magnetic card measured with Bi:YIG ($x=2.5$) films.

This work was partly supported by the National Institute of Information and Communications Technology (NICT).

[1] T. Ishibashi, A Mizusawa, M. Nagai, S. Shimizu, K. Sato, N. Togashi, T. Mogi, M. Houchido, H. Sano, and K. Kurimiya, *J. Appl. Phys.*, **97** (2005) 013516.

[2] T. Ishibashi, T. Yoshida, T. Kobayashi, S. Ikehara, and T. Nishi, *J. Appl. Phys.*, **113** (2013) 17A926.

30TL-H-7

FEASIBILITY OF MONOLITHIC INTEGRATION OF MAGNETO-OPTICAL PLASMONIC WAVEGUIDE INTO PHOTONIC INTEGRATED CIRCUIT

Zayets V.¹, Baryshev A.², Saito H.¹, Ando K.¹, Yuasa S.¹

¹ Spintronics Research Center, AIST, Tsukuba, Japan

² Toyohashi University of Technology, Toyohashi, Japan

v.zayets@aist.go.jp

An optical isolator is an important component of an optical network. At present, there is a significant commercial demand for an optical isolator, which can be integrated into the Photonic Integrated Circuits (PIC). An optical isolator utilizing surface plasmons propagating at a surface of a transition metal is a good option for such integration. Important advantages of the proposed plasmonic isolator are a small size of only a few micrometers and the good technological compatibility with the fabrication technology of a PIC.

We studied experimentally optical and magneto-optical properties of a Fe plasmonic waveguide integrated with an AlGaAs rib waveguides and a Co plasmonic waveguide integrated with Si wire waveguides.

It was demonstrated experimentally that by utilizing a double-dielectric plasmonic waveguide it is possible to reduce significantly the optical loss in a plasmonic waveguide. For Fe/SiO₂/AlGaAs double-dielectric plasmonic waveguide the low optical loss of 0.03 dB/μm is obtained. As far as we know at present it is a lowest optical loss demonstrated for a plasmon propagating at a surface of a ferromagnetic metal.

Figure 1 illustrates a monolithical integration of Si nanowire waveguide with Co:SiO₂ plasmonic waveguide. The designs of an isolator utilizing a ring resonator (Fig. 1(c)) or a non-reciprocal coupler were studied. For an efficient coupling between a plasmonic waveguide and a rib waveguide, a side-coupler (Fig. 1(e)) was utilized.

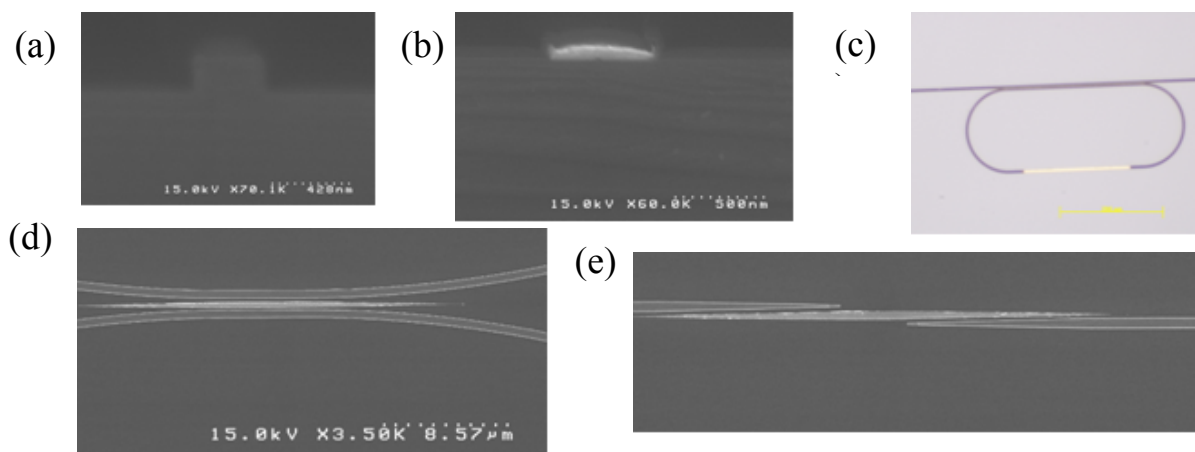


Fig.1. SEM image of monolithically integrated a Si nanowire waveguide and a Co/SiO₂ plasmonic waveguide. Cross-sectional images of (a) a Si nanowire waveguide and (b) plasmonic waveguide. Top-view images of (c) plasmonic waveguide integrated into a ring resonator; (d) non-reciprocal coupler with a 100-nm-wide plasmonic waveguide (e) plasmonic-waveguide/ Si-wire-waveguide side-coupler. In all pictures the plasmonic waveguides are whiter.

[1] V. Zayets, H. Saito, S. Yuasa, and K. Ando: *J. Appl. Phys.* **111** (2012) 023103.

[2] V. Zayets, H. Saito, S. Yuasa, and K. Ando: *Materials* **5** (2012) 857.

30RP-H-8

MAGNETO-OPTICAL SPASER

*Lisyansky A.A.*¹, *Baranov D.G.*^{2,3,4}, *Vinogradov A.P.*^{2,3,4}

¹ Department of Physics, Queens College of the City University of New York, Queens, NY USA

² Moscow Institute of Physics and Technology, Dolgoprudniy, Moscow Reg., Russia

³ Institute for Theoretical and Applied Electromagnetics, Moscow, Russia

lisyansky@qc.edu

We suggest a magneto-optical (MO) spaser – a subdiffractive source of coherent circularly polarized light operating in the near field. Unlike a non-magnetic spaser, this light source has two spasing modes with left and right circular polarizations of the dipole moments. Each of the modes has different pumping threshold. A MO spaser consists of an amplifying core, e.g. a quantum dot or active molecules, coated by a metallic layer, such as silver, exhibiting MO response at optical frequencies. To overcome large Ohmic damping, a silver shell is coated with another shell of cobalt or YIG (see a schematic drawing in Fig. 1). Thanks to the presence of the silver shell, such a structure forms a high- Q plasmonic resonator exhibiting MO properties.

To describe the MO spaser theoretically, we approximate the gain medium by the nonlinear Lorentzian profile with “negative” losses and anti-resonance dispersion. The evolution of the electric field is related to the macroscopic polarization of a gain subsystem via classical Maxwell’s equation, while the dynamics of the polarization and the population inversion of active atoms is governed by the equations following from the density matrix formalism (see [1] for detailed derivation). The gain atoms embedded into the host medium are modeled as two-level systems with transition dipole moment spread in the host matrix. Dielectric properties of the MO metal are described with the permittivity tensor having off-diagonal elements accounting for the MO effect.

We show that such a system has two spasing modes with circular polarizations. The mode dependence on gain exhibits the Hopf bifurcation which is typical for spasers (Fig. 2). The threshold gain of these structures depends on the radii of the gain core and silver and MO shells and the background permittivity of gain medium. Gain required for spasing can be minimized by choosing optimal parameters for both structures. In addition, one should keep in mind that the plasmon resonance of core/shell nanoparticles has to be tuned to the frequency range of the MO resonance of MO material.

Thus, the suggested light source has two spasing modes with left and right circular polarizations of the dipole moments. Each of the modes has different pumping threshold. Due to the competition of modes, only the mode with the lower pumping threshold survives. As a result, a specific circular polarization is realized.

Support by RFBR, Dynasty Foundation, and NSF is acknowledged.

[1] A.V. Dorofeenko, A.A. Zyablovsky, A.A. Pukhov, A.A. Lisyansky, and A.P. Vinogradov, *Phys. Usp.*, **55** 1080-1097 (2012).

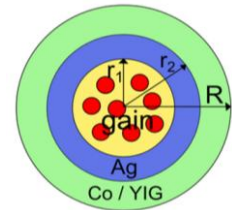


Fig. 1. A schematic drawing of the core-shell MO spaser.

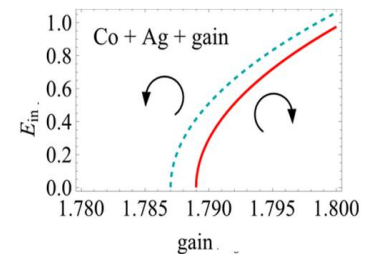


Fig. 2. Amplitudes of spasing modes versus gain near the bifurcation point.

30RP-H-9

ENHANCEMENT OF FARADAY EFFECT IN Au/GARNET COMPOSITE STRUCTURES

Uchida H.¹, Saito S.², Fedyanin A.A.³, Inoue M.⁴

¹ Tohoku Institute of Technology, Taihaku, Sendai 982-8577, Japan

² Tohoku University, Aoba, Sendai 980-8578, Japan

³ Moscow State University, Leninskie Gory, Moscow 119991, Russia

⁴ Toyohashi University of Technology, Toyohashi 441-8580, Japan
uchida_hn@tohtech.ac.jp

Faraday effect is enhanced in the composite structures of Au nanoparticles with bismuthsubstituted yttrium iron garnet (Bi:YIG) film [1]. In the nanoparticles, localized surface plasmon resonance (LSPR) is excited at a specific resonant wavelength; Faraday rotation changes from the native value of a Bi:YIG. The magnitude of enhanced Faraday rotation angle depends on the feature of the Au nanoparticles, such as size, shape, number density and volume.

Fig. 1 shows SEM images of the Au nanoparticles with different mean diameter on quartz substrates fabricated by repetitive formation method using deposition of 5 nm Au films and heating at 1000 °C [1]. Composite structures were formed by depositing Bi:YIG film on the particles. Fig. 2 shows transmissivity and Faraday rotation spectra of the composite structures. Large absorption of light was observed in case of large repetitive number around 600 nm; Faraday rotation was enhanced from the curve of Bi:YIG single film at the wavelength.

Since Au nanoparticles have an important role for the enhancement of rotation angle, we tried to develop structures with suitable mean diameter and density by self-organizing methods. Push coating method [2] and so on were attempted. Structures and optical properties are discussed.

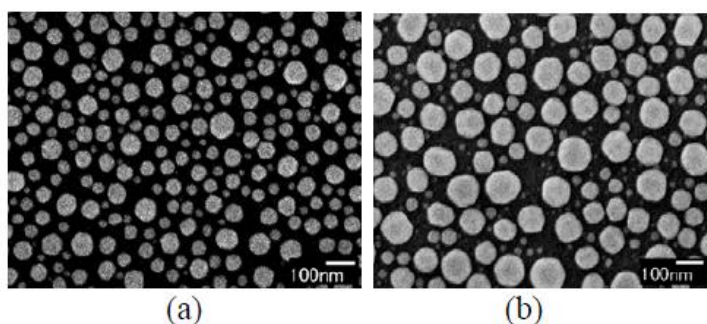


Fig. 1. SEM image of Au nanoparticles fabricated by a repetitive formation. (a) 3 and (b) 6 times repetitions.fabricated by the repetitive formation method.

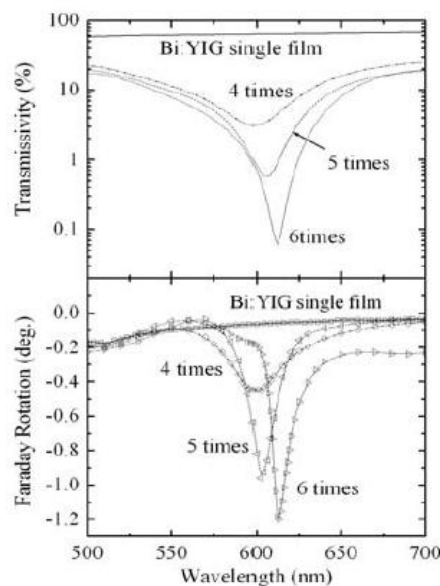


Fig. 2. Transmittance and Faraday rotation spectra of Au/Bi:YIG composite structures fabricated by the repetitive formation method.

[1] H. Uchida, Y. Mizutani, Y. Nakai, A. A. Fedyanin and M. Inoue, *J. Phys. D: Appl. Phys.* **44**, 064014 (2011).

[2] T. Kraus, L. Malaquin, H. Schmid, W. Reiss, N. D.

30OR-H-10

OPTICAL SECOND HARMONIC GENERATION IN NANOSTRUCTURES WITH INHOMOGENEOUS MAGNETIZATION

Kolmychek I.A.¹, Krutyanskiy V.L.¹, Murzina T.V.¹, Karashtin E.A.², Sapozhnikov M.V.²,
Skorohodov E.V.², Fraerman A.A.²

¹ Department of Physics, Moscow State University, Moscow, Russia

² Institute of microstructures, Nizhniy Novgorod, Russia
murzina@mail.ru

Magnetic nanostructures reveal rich variety of properties that originate from their design, composition and arrangement. One of the attracting tasks here is the realisation of various types of magnetic ordering states, which can find potential applications and are rare to be observed in natural materials. In this talk, our recent results on optical second harmonic generation (SHG) effects in nanostructures with inhomogeneous magnetization, such as planar trilayer magnetic structures that support the antiferromagnetic state, and regular arrays of triangular-shaped cobalt nanostructures with vortex magnetization are described. We demonstrate that the usage of circular polarization of the probe beam allows to visualise the vortex magnetization and second-order magnetization-induced effects.

Trilayer magnetic structures of the composition CoFe(20 nm)/Al₂O₃(2nm)/CoFe(10 nm)Py were made by *rf* sputtering technique. 2D lattice of triangular-shaped cobalt dots with the side length of 700 nm on a glass substrate was fabricated by the electron-beam lithography and a lift-off technique [3], the schematic view of the structure is shown on the inset in Fig.1. Regular arrangement of noncentrosymmetric magnetic particles results in the residual macroscopic vortex magnetization after the external DC magnetic field applied along the sides of the triangular particles is removed, as shown on the Figure. The SHG experiments were performed using linearly or circularly polarized output radiation of a femtosecond Ti-sapphire laser at 800 nm wavelength. The dependencies of the SHG intensity on the applied magnetic field, i.e. SHG magnetic hysteresis loops, were studied.

We demonstrate that when using the circularly polarized fundamental radiation in these types of magnetic nanostructures, the SHG hysteresises reveal additional effects except nonlinear magneto-optical Kerr effect that is odd with respect to the magnetization reversal. First, we demonstrate that in the case of triangular-shape magnetic particles, the macroscopic vortex magnetic state can be visualised due to the existence of a new contribution to the SHG polarization induced by the magnetic toroid moment. Typical SHG hysteresis loop obtained in such a case is shown in Fig. 1. Nonzero width of the SHG hysteresis for zero magnetic field is an evidence of such nonlinear contribution. Second, the dependencies of the SHG intensity on the DC magnetic field in the case of antiferromagnetic bilayer structures and for circular pump polarization reveal the existence of second-order in magnetization terms in the nonlinear polarization, that were not observed before. The symmetry analysis of the SHG process for the two types of magnetic nanostructures supports the results obtained in the experiment.

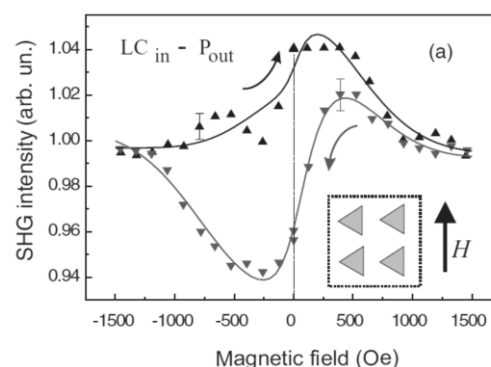


Fig. 1. SHG magnetic hysteresis loop for the array of triangular nanoparticles; inset: schematic view of the sample.

Support by RFBR grants is acknowledged.

30OR-H-11

MAGNETO-OPTICAL EFFECTS IN MAGNETOPHOTONIC CRYSTALS WITH PLASMONIC GRATINGS

Khokhlov N.E.^{1,2}, *Belotelov V.I.*^{1,2}, *Bykov D.A.*³, *Berzhansky V.N.*⁴, *Shaposhnikov A.N.*⁴,
*Mikhailova T.V.*⁴, *Prokopov A.R.*⁴, *Karavainikov A.V.*⁴, *Kharchenko Yu.M.*⁵

¹ Lomonosov Moscow State University, Moscow, 119991, Russia

² Russian Quantum Centre, Skolkovo, Moscow Region, 143025, Russia

³ Image Processing Systems Institute, Russian Academy of Sciences, Samara, 443001, Russia

⁴ Taurida National V.I. Vernadsky University, Simferopol, 95007, Russia

⁵ Institute for Low Temperature Physics and Engineering of the NASU, Kharkov 61103, Ukraine
n.e.khokhlov@yandex.ru

Modern requirements for optical signals processing rates stimulate the research of new ways for light manipulation at submicron spatial and time scales. Magneto-photonic crystals (MPCs) – periodic dielectric structures with magnetic constituents are one of the best candidates to answer these challenges. The MPCs provide significant enhancement of the magneto-optical effects, such as Faraday effect, within thin magnetic dielectric layers with relatively small optical losses [1]. These unique properties of MPCs have origin in light concentration due to Fabri-Perot resonances or optical Tamm states [2]. Another type of the structures for magneto-optical effects enhancement are plasmonic crystals where there is a concentration of light as well [3].

In this work we propose the concept of the combination of the MPCs and plasmonic structure for magneto-optical effects enhancement. Considered type of MPCs consists of a magnetic layer sandwiched between two dielectric Bragg mirrors. Plasmonic grating is placed on MPC's top and provides the excitation of surface plasmon resonances and waveguiding modes inside the magnetic layer additionally to Fabri-Perot resonances. It increases effective length of light propagation inside the magnetic medium and therefore provides magneto-optical effects enhancement.

We have found by numerical simulations that the magneto-optical Faraday and Kerr effects resonantly increase with respect to the effects in the bare magnetic film and thus plasmonic grating provides additional enhancement. In particular, Faraday rotation in MPC is increased by several times with respect to bare magnetic film and transverse magneto-optical Kerr effect reaches 20% in the case of surface plasmon and magnetic layer modes hybridization.

In order to conduct experiments the MPCs with double layer Bi: YIG films on the substrates of fused quartz: $KU-1/(TiO_2/SiO_2)^4/M1/M2/(SiO_2/TiO_2)^4$ were fabricated. Here M1 and M2 are the magneto-active layers of content $Bi_{1.0}Y_{0.5}Gd_{1.5}Fe_{4.2}Al_{0.8}O_{12}$ and $Bi_{2.8}Y_{0.2}Fe_5O_{12}$. The selected compositions for double iron garnet layers showed a significant increase of the Faraday rotation angle and magneto-optical figure of merit Q of microcavity structures [4]. Experimental demonstration of the aforementioned effects is expected in the nearest future.

[1] M. Inoue, R. Fujikawa, A. Baryshev, A. Khanikaev, P. B. Lim, H. Uchida, O. Aktsipetrov, A. Fedyanin, T. Murzina, and A. Granovsky, *J. Phys. D*, **39** (2006) R151.

[2] T. Goto, A. V. Baryshev, M. Inoue, A. V. Dorofeenko, A. M. Merzlikin, A. P. Vinogradov, A. A. Lisyansky, and A. B. Granovsky, *Phys. Rev. B*, **79** (2009) 125103.

[3] V.I. Belotelov, L.E. Kreilkamp, I.A. Akimov, A.N. Kalish, D.A. Bykov, S. Kasture, A.V. Gopal, M. Nur-E-Alam, M. Vasiliev, L.L. Doskolovich, D.R. Yakovlev, K. Alameh, A.K. Zvezdin, and M. Bayer, *Nature Communications*, **4** (2013) 2128.

[4] V. Berzhansky, T. Mikhailova, A. Karavainikov, A. Prokopov, A. Shaposhnikov, I. Lukienko, Yu. Kharchenko, O. Miloslavskaya, N. Kharchenko, Microcavity One-Dimensional Magnetophotonic Crystals with Double Layer Iron Garnet, *J. Magn. Soc. Jpn.*, **36** (2012) 42.

30 June

Monday

15:00-17:00

oral session

30TL-Q

30RP-Q

30OR-Q

“Theory”

30TL-Q-6

PHASE SEPARATION INSTABILITIES AND MAGNETISM IN TWO DIMENSIONAL SQUARE AND HEXAGONAL HUBBARD MODEL

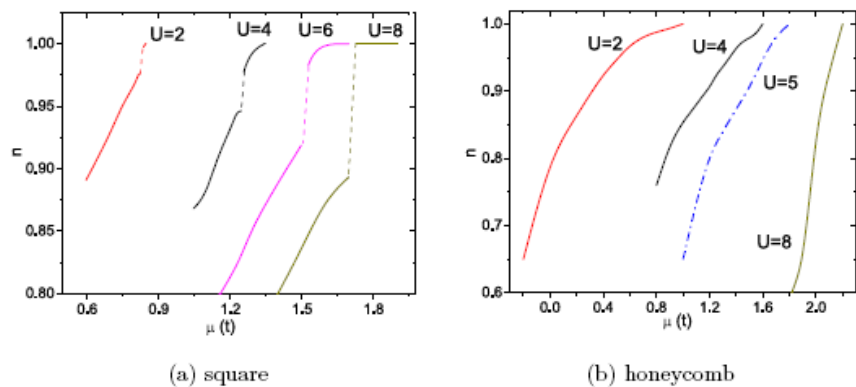
Kocharian A.N.¹, Kun Fang², Fernando G.W.¹, Balatsky A.F.^{1,2}

¹ Department of Physics, California State University, Los Angeles, CA 90032, USA

² Department of Physics, University of Connecticut, Storrs, CT 06269, USA

² Theoretical Division/Center for Integrated Nanotechnologies, LANL, Los Alamos, NM, USA
armen.kocharian@calstatela.edu

The Variational Cluster Approximation (VCA) in the two-dimensional (2D) Hubbard model with repulsion of electrons is used to rigorously calculate the intrinsic cooperative effects in strongly correlated materials with bipartite square and honeycomb lattice geometries. The Mott-Hubbard gap, manifested itself as a smooth metal-insulator transition, both in square and honeycomb lattices at half filling ($n = 1$), is in agreement with the generic 2D phase diagram. However, a density variation with the chemical potential shows their distinct structural differences away from the half filling. For example, at doping in equilibrium we found discontinuous transition (see the figure). The electronic densities n as a function of chemical potential μ for Hubbard model in a square



in the material. (b) The plots for honeycomb lattice are smooth without any discontinuities, which means that the phase separation is absent in this lattice. The density anomaly in square lattices is also signaling a phase separation instability and discontinuous transition into inhomogeneous state with hole rich (metallic) and hole poor (insulating) regions. In contrast, honeycomb lattice does not exhibit the density anomaly, but instead the density displays a smooth transition and describes a continuous evolution of homogenous (metallic) state. The implication of VCA results to HTSCs, layered graphene, topological insulators as well as comparison to other studies are discussed. The VCA provides a strong support to the spontaneous phase separation instability found in our quantum cluster calculations [1-2].

[1] A.N. Kocharian, G.W. Fernando, K. Palandage, and J. W. Davenport, *Phys. Rev. B*, **74** (2006) 024511-1 - 024511-9.

[2] A.N. Kocharian, G.W. Fernando, K. Palandage, and J. W. Davenport, *Phys. Rev. B*, **78** (2008) 075431-1 - 075431-6.

30OR-Q-7

AN ALGEBRAIC SPIN LIQUID IN THE HEISENBERG MODEL ON THE KAGOME LATTICE

*Iqbal Ya.*¹, *Becca F.*², *Poilblanc D.*³, *Sorella S.*²

¹ International Centre for Theoretical Physics (ICTP), Trieste, Italy

² International School for Advanced Studies (SISSA), Trieste, Italy

³ Laboratoire de Physique Théorique (CNRS and Université de Toulouse), Toulouse, France
yiqbal@ictp.it

It is well established that the spin-1/2 quantum Heisenberg antiferromagnetic model on the kagome lattice hosts an exotic quantum paramagnetic phase. However, the journey towards the precise identification of the nature of the ground state of this model has been long and arduous, and till date represents a critically outstanding problem. I will address this problem within the Abrikosov pseudo-fermion slave particle approach, using Gutzwiller projected variational wave functions. A state-of-the-art implementation of sophisticated numerical techniques such as variational and Green's function Monte Carlo supplemented by the application of Lanczos steps enables us to filter out the true ground state properties. Our study provides strong numerical evidence for the true ground state to be a gapless (algebraic) U(1) Dirac spin liquid [1,2] and also establishes the remarkable stability of this, otherwise, critical phase towards a large class of potential instabilities such as topological spin liquids, chiral spin liquids, and valence bond crystals [3,4,5]. The competition with a gapped (topological) spin liquid is also discussed.

Support by ANR, and CALMIP supercomputer (Toulouse, France) is acknowledged.

- [1] Y. Iqbal, F. Becca, S. Sorella, D. Poilblanc, Phys. Rev. B, **87** (2013) 060405.
- [2] Y. Iqbal, D. Poilblanc, F. Becca, Phys. Rev. B, **89** (2014) 020407.
- [3] Y. Iqbal, F. Becca, D. Poilblanc, Phys. Rev. B, **84** (2011) 020407.
- [4] Y. Iqbal, F. Becca, D. Poilblanc, Phys. Rev. B, **83** (2011) 100404.
- [5] Y. Iqbal, F. Becca, D. Poilblanc, New J. Phys., **14** (2012) 115031.

30RP-Q-8

FOUR-STATE STANDARD POTTS MODEL

Proshkin A.I., Kassan-Ogly F.A.

Institute of Metal Physics, Ural Division, RAS, Ekaterinburg, Russia
al.pro@list.ru

There is now a great interest devoted to the multi-k structures in monochalcogenides and mononictides of lanthanides and actinides. Normile with co-authors [1] showed that the identification of USb neutron diffraction pattern in the 3-k model gives better results than in the collinear one. This 3-k structure has no antiparallel directions of magnetic moments and is equal to the 4-state standard Potts model.

In this paper, we investigated ferro- and antiferromagnetic one-dimensional 4-state standard Potts model with interactions between nearest and next-nearest neighbors. In addition, the polycrystalline case was studied. The magnetization, magnetic susceptibility, capacity, magnetocaloric effect were investigated. It was shown that in the case of a single crystal, this magnet could have up to three frustration fields in which magnetization has jumps, plateaus, and entropy tends to nonzero values. Fig.1a demonstrates the result of such calculation. It is seen that this model shows the magnetization behavior almost coinciding with the experimental one shown in fig.1b.

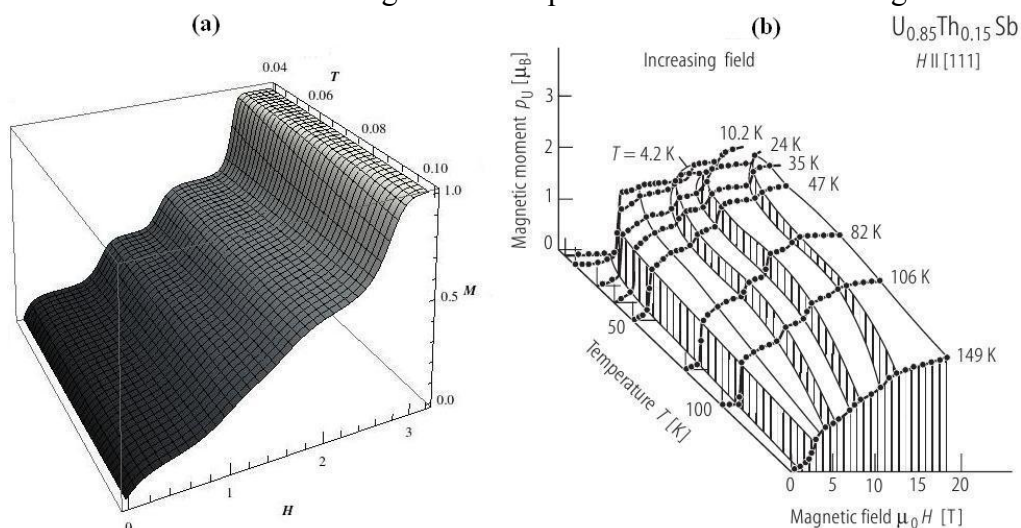


Fig. 1. (a) Calculated magnetization in 4-state Potts model, (b) the experimental one.

Polycrystalline model also has peculiarities such as the impossibility to align all spins along the direction of the applied magnetic field which leads to the fact that magnetization do not reach the value what it has in the case of a single crystal with field directed along easy axis. The asymptotic values of magnetization were analytically calculated. It is known that there exists a distinction between magnetic moments measured by asymptotic magnetization method and by neutron diffraction experiments from which they always have bigger values [2]. Our investigation explains this phenomenon.

It should be noted that the results of investigation are very useful. The 4-state Potts model can be applied as a prototype when one needs to choose the structure when identifying neutron diffraction patterns and the magnetization peculiarities allow predicting the 3-k structures.

Support by projects no. 12-P-2-1041k and no. 12-I-2-2020 is acknowledged.

[1] Normile P.S., Stirling W.G. et al, *Phys. Rev. B*, **66** 014405 (2002) 1-10.

[2] Vogt O., *Physica B*, **102** (1980) 206-211.

30OR-Q-9

**ANTIFERROMAGNETIC STATES AND PHASE SEPARATION IN
AA-STACKED GRAPHENE BILAYERS***Sboychakov A.O.*^{1,2}, *Akzhanov R.S.*^{1,3}, *Rozhkov A.V.*^{1,2}, *Rakhmanov A.L.*^{1,2}, *Nori F.*^{2,4}¹ Institute for Theoretical and Applied Electrodynamics, Moscow, Russia² Advanced Science Institute, RIKEN, Wako-shi, Japan³ Moscow Institute of Physics and Technology, Dolgoprudnyi, Russia⁴ Department of Physics, University of Michigan, Ann Arbor, USA

sboycha@mail.ru

We study electronic properties of AA-stacked graphene bilayers. In the single-particle approximation such a system has one electron band and one hole band crossing the Fermi level. If the bilayer is undoped, the Fermi surfaces of these bands coincide. Such a band structure is unstable with respect to a set of spontaneous symmetry violations. Specifically, strong on-site Coulomb repulsion stabilizes antiferromagnetic order. At small doping and low temperatures, the homogeneous phase is unstable and experiences phase separation into an undoped antiferromagnetic insulator and a metal. The metallic phase can be either antiferromagnetic (commensurate or incommensurate) or paramagnetic depending on the system parameters. The incommensurate AFM phase is mathematically equivalent to the Fulde-Ferrel-Larkin-Ovchinnikov state in superconductors. We derive the phase diagram of the system on the doping-temperature plane and find that under certain conditions, the transition from the paramagnetic to the antiferromagnetic phase may demonstrate reentrance. When disorder is present, phase separation could manifest itself as a percolative insulator-metal transition driven by doping. The application of the transverse voltage induces the exciton order parameter on the antiferromagnetic background. The value of this second order parameter is proportional to the biased voltage and the value of the nearest-neighbor interplane Coulomb repulsion.

30OR-Q-10

THE CORRELATIONS BETWEEN DYNAMIC INTERACTIONS IN ANTIFERROMAGNETIC MULTIFERROICS

Sharafullin I.F., Kharrasov M.Kh., Kyzrgulov I.R., Nugumanov A.G.

Bashkir State University, 450074, Ufa, Russia

SharafullinIF@yandex.ru

Multiferroics, which include a number of alloys and compounds, are quite promising materials for creating functional parts of modern micro- and nanoelectronic devices. Therefore, an interest for analysis of model ferroelectromagnetic systems with strongly correlated elastic, magnetic and ferroelectric subsystems has increased nowadays [1, 2]. In this work we have researched the features of dynamic magnetoelectric and magnetoelastic interactions in multiferroic crystal, influenced by various external fields, with the group of symmetry D_{4h}^{16} , which is taken into consideration when invariants in the Hamiltonian are being chosen. Analyzed multiferroic possesses strongly correlated elastic, magnetic and ferroelectric subsystems.

Based on the integrated approach, which combines N. N. Bogolyubov's quantum-statistic methods, Green's temperature functions, diagram technique and symmetry analysis, it was calculated the dependence of energy spectrum and static spin susceptibility on the temperature and external fields. Taking into account Green's anomalous functions, which are emerging because of gradient invariance breaking, damping coefficients for magnetoelectric and magnetoelastic interactions were calculated. The effective parameters' of magnetoelectric and magnetoelastic interactions dependences on the external fields' intensities were analyzed. It is shown that these parameters have a distinct maximum in the resonance value of wave vector $k = k_r$. (Fig.1-2)

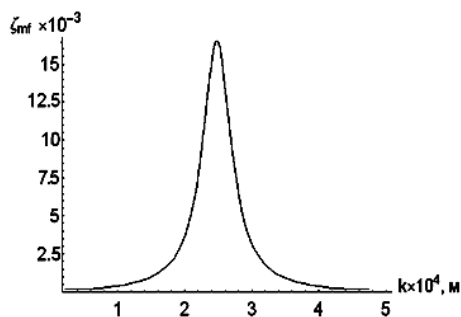


Fig. 1. Dependences of the parameter of magnetoelectric interactions on the wave vector.

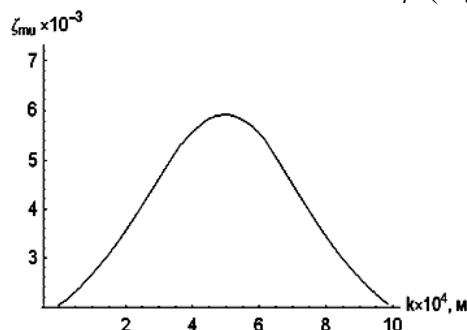


Fig. 2. Dependences of the parameter of magnetoelastic interactions on the wave vector.

As was shown, it is possible to enhance the interactions among spins, ferroelectric and fonons subsystems in multiferroics by applying the external fields in different crystallographic directions. It was discovered that external voltage influence shifts the resonance frequencies of magnetoelastic and magnetoelectric interactions.

[1] S.S. Krotov, I.V. Shnaidshtein, *M.: Department of Physics MSU* (2011) 111.

[2] A.M. Savchenko, M.A. Dergachyov, B.I. Sadovnikov, *Mathematical Notes* **93** (2013) 3, 477-482.

30OR-Q-11

CRITICAL BEHAVIOUR OF ULTRATHIN MAGNETIC FILMS

Prudnikov P.V., Medvedeva M.A., Elin A.S., Soldusova A.P.

Omsk State University, Mira 55A, Omsk, Russia

prudnikp@univer.omsk.su

An understanding of critical phenomena in low dimensional structures can be acquired from a study of ultrathin films in which one dimension, the film thickness N , is systematically reduced. Magnetic order in ultrathin ferromagnetic films is very complex due to a strong influence of the shape and the magnetocrystalline anisotropies of the sample. A considerable amount of experimental results on different aspects of magnetism in ultrathin films has appeared [1,2]. Nevertheless it is difficult to reach general conclusions even in seemingly basic things such as the kind of magnetic order at low temperatures. In view of this complexity, theoretical work on simplified models and computer simulations are essential for rationalizing and guiding new experimental work.

We have studied the magnetic behavior of anisotropic Heisenberg thin films using extensive Monte Carlo simulations. We have found the dimensional crossover of magnetization m and magnetic susceptibility χ from 2D to 3D like with increasing film thickness. Estimated values of the critical exponent β for different thickness demonstrates crossover from 2D Ising universality class to 3D Heisenberg through 3D Ising class (Fig 1).

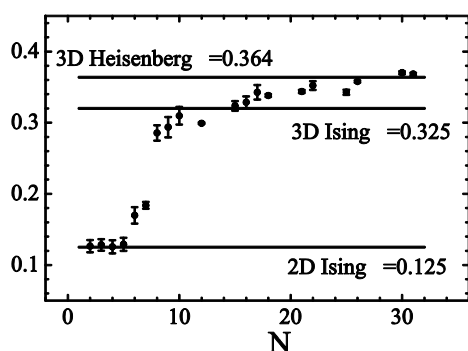


Fig. 1. Dimensional crossover in values β as function of the film thickness N

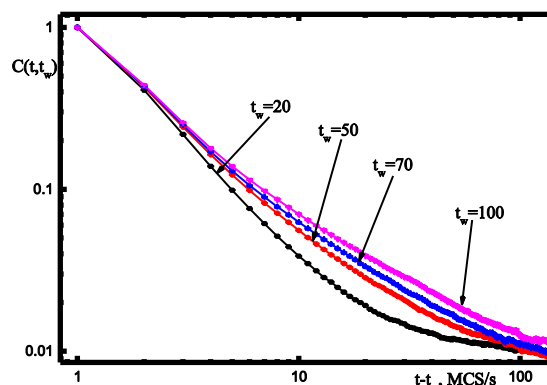


Fig. 2. Aging in autocorrelation function $C(t, t_w)$ for $N=6$

Presence of surfaces breaks lattice symmetries, and this can lead to many surprising and unexpected effects in critical dynamics and out of equilibrium [3,4]. The influence of non-equilibrium initial states on critical dynamic behavior of ultrathin magnetic and metamagnetic films have studied by short-time dynamics method [5]. Aging effects were discovered for non-equilibrium regime $t-t_w \gg t_w$ (Fig 2).

This work was supported in part by Ministry of Education and Science of Russia Federation through project no. 1627. Studies were performed using the supercomputer system resources of the Moscow State University and Joint Supercomputer Center of the Russian Academy of Sciences.

- [1] C.A.F. Vaz, J.A.C. Bland, G. Lanhoff, *Rep. Prog. Phys.*, **71** (2008) 056501.
- [2] R. Wiesendanger, *Rev. Mod. Phys.*, **81** (2009) 1495-1550.
- [3] H. Park, M. Pleimling, *Phys. Rev. Lett.* **109** (2012) 175703.
- [4] L. Bergqvist, et al., *Phys. Rev. B*, **87** (2013) 144401.
- [5] P.V. Prudnikov, M.A. Medvedeva, *Progr. Theor. Phys.* **127** (2012) 369.

30OR-Q-12

EMERGENCE OF SPIN-FILTER STATES IN Pt-Fe NANOWIRES

Smelova E.M., Tsysar K.M., Saletsky A.M.

Lomonosov Moscow State University, Faculty of Physics, Moscow, Russia

smelova_e_m@mail.ru

Our theoretical study predicts the emergence of spin-filter state in one-dimensional Pt-Fe bimetallic nanowires. The results show the existence of two transmission regime in contracted “zig-zag” Pt-Fe nanowires with low and high transmission $1G_0$ and $3G_0$ “low transmission state” and spin polarized state - “high transmission state” correspondingly and one transmission regime in linear stretched nanowires with conductance $2G_0$. Our transmission spectra calculations revealed that “low transmission state” of Pt-Fe nanowires represents the spin-filter system. We found the dependence of quantum conductance of Pt-Fe nanowire on its atomic structure. Our study shows the

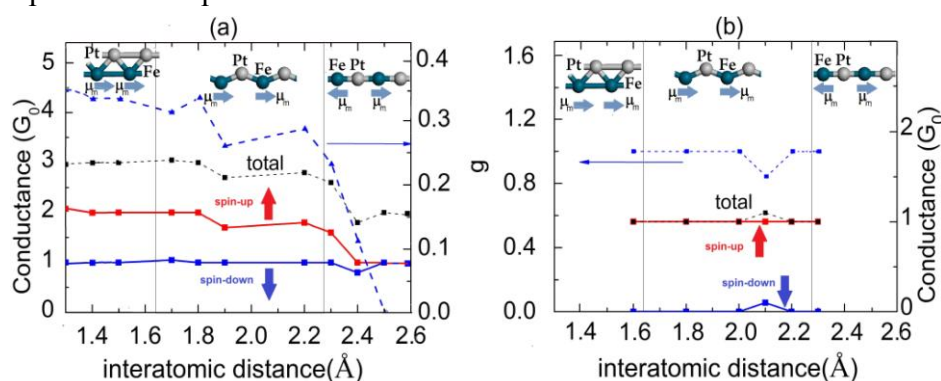


Fig.1 Total quantum conductance of Pt-Fe nanowire (dotted line), spin-polarized conductance of spin-up (solid red line) and spin-down (solid blue line) channels and also the degree of spin polarization of quantum electron transport (g) as a function of average interatomic distance (dashed blue line): (a) “high transmission state”, (b) “low transmission state”.

emergence of a magnetic transition from ferromagnetic to antiferromagnetic states under wire stretching to interatomic distance 2.3\AA accompanied by the transition of the wire from “zig-zag” to the linear configuration. In contracted Pt-Fe nanowire magnetic moment of Pt atoms is about $0.6\mu_B$ which is in good agreement with our recent studies of

magnetic properties of Pd and Pd-Fe nanowires [1,2]. However the magnetic moments of Pt atoms decreases drastically to $0\mu_B$ in linear stretched Pt-Fe nanowires in antiferromagnetic states. Our study revealed the strong correlation between transport and magnetic properties of the Pt-Fe nanowires. We found that the *spin-filter* state exists only in “zig-zag” Pt-Fe nanowires in ferromagnetic state. Moreover, the spin-polarization of quantum electron transport through Pt-Fe nanowires vanishes totally in linear stretched nanowires in antiferromagnetic state. For quantitative estimation of spin polarization of the electron transport through nanowire, we introduce a term - degree of polarization $g = \frac{G_{\uparrow} - G_{\downarrow}}{G_{\uparrow} + G_{\downarrow}}$ [3]. The value of g is about 0.33 (see Fig.1a, dashed line) and this ratio remains practically unchanged in all range (1.5\AA - 2.3\AA) corresponding to the area of “zig-zag” Pt-Fe nanowire existence. The degree of spin polarization increases to 0.99 for nanowires in “low transmission state” (see Fig.1b, dashed line), which corresponds to “spin-filter” conductive system. The value of g drastically decreases under wire stretching to ~ 0 for linear nanowire (Fig.1a, dashed line).

[1] E.M. Smelova, et. al., *JETP Lett.*, **93**, 3 (2011) 129-132; K.M. Tsysar, et. al., *JETP Lett.*, **94**, 3 (2011) 228-232.

[2] K.M. Tsysar, et. al., *Physics of Solid State*, **52** 3 (2010) 593.

[3] G.A. Nemnes, *Journal of Nanomaterials*, **2013** (2013) 408475.

30 June

Monday

17:30-19:00

poster session
30PO-I1

**“Magnetic
Nanostructures and
Low Dimensional
Magnetism”**

30PO-I1-1

MAGNETIC CLUSTERS IN NATURAL FERRO-CHROMIAN SPINELS

Sherendo T.A.¹, Vdovin V.G.¹, Martyshko P.S.¹, Mitrofanov V.Ya.¹, Alexeev A.V.², Zamyatin D.A.²,
Vazhenin V.A.³, Pamyatnykh L.A.³

¹ Institute of Geophysics, Ural Branch of the Russian Academy of Sciences (UB RAS),
Amundsena st. 100, Yekaterinburg, Russia

² Institute of Geology and Geochemistry, UB RAS, Pochtovyi per. 7, Yekaterinburg, Russia

³ Ural Federal University, Institute of Natural Sciences, Lenin Av. 51, Yekaterinburg, Russia
Tatyana_Sherendo@mail.ru; Lidia.Pamyatnykh@urfu.ru

The results of detailed laboratory investigations of ore-forming and accessory Fe-Cr-spinels, disseminated in host rocks, of one magmatic genotype, in southern part of the Klyuchevsky alpine-type chromite-bearing massif (the Middle Urals) are presented. It has been established, that the principal magnetization carriers on the studied section of the massif are accessory ferro-chromian spinels of the variable composition $\text{Fe}^{2+}(\text{Cr}_{2-x}\text{Fe}_x^{3+})\text{O}_4$.

According to a microprobe and magnitomineralogical studies the accessory Fe-Cr-spinels have an inhomogeneous microstructure with separations of the secondary microphases, enriched with cation Fe^{3+} , in the matrix of the primary nonmagnetic spinel. It is manifested as a set of magnetic phases with different temperatures of magnetic phase transitions T_c on the thermomagnetic curves over a wide temperature range (from 4 to 1000 K).

Parameters and form of magnetic resonance absorption spectra reflect the structural and magnetic microinhomogeneities in the accessory Fe-Cr-spinels, formed as a result of post-magmatic processes. This allows us to differentiate ore-forming (Kl 2-2) and accessory chrome spinels (Kl 0, Kl 1-1, Kl 2-1), having a different microstructure and magnetic properties (Fig. 1). During investigations of magnetic structure on the atomic force microscope (method of magnetic force microscopy) magnetic clusters that play an important role in the formation of the magnetic properties of the host rocks were detected in an accessory chrome spinel grains. Separations of magnetic microphases/nanophases were detected in structurally homogeneous nonmagnetic grain areas, where mineralogical changes are not observed by optical method (Fig. 2).

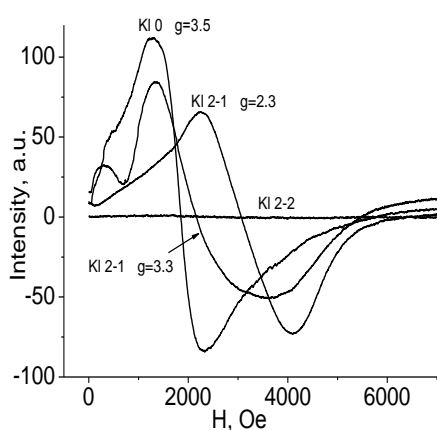


Fig.1. Magnetic resonance absorption spectra of ore-forming and accessory Fe-Cr-spinels at room temperature, in a magnetic field range 0 - 7000 Oe, operating frequency 9.86 GHz.

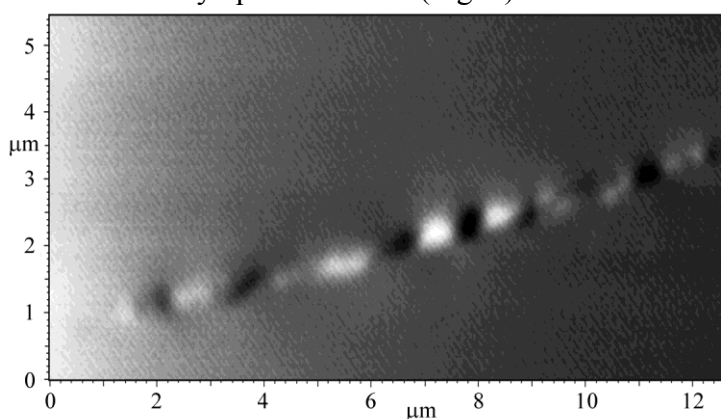


Fig. 2. Magnetic force microscopy image of the surface of the scanned area of the relict grain areas of accessory Fe-Cr-spinel.

30PO-I1-2

MAGNETIC PROPERTIES OF CuGeO₃ NANOWIRES

*Semeno A.V.*¹, *Gilmanov M.I.*^{1,2}, *Samarin A.N.*^{1,2}, *Grigorieva A.V.*³, *Gudilin E.A.*³, *Barulin A.V.*³
*Demishev S.V.*¹

¹ Prokhorov General Physics Institute RAS, Moscow, Russia

² Moscow Institute of Physics and Technology, Dolgoprudny, Russia

³ Moscow State University, Moscow, Russia

gilmanov@lt.gpi.ru

We report the results of electron spin resonance (ESR) and susceptibility measurements of CuGeO₃ nanowires [1] including samples prepared with different hydrothermal time treatment (24 and 96 hours) and samples doped with nickel (2%, 10%, 20%). The average length of crystallites in the direction along Cu chains is about several hundreds nanometers with the aspect ratio of the rod-like particles from 5 to 17 for different samples. The reduction of the sample size to nanometer scale leads to drastic change of the system magnetic properties. Full suppression of spin-Peierls (SP) transition which is peculiar for macroscopic CuGeO₃ below $T=14\text{K}$ takes place in the case of undoped nanowires. At the same time antiferromagnetic low temperature state intrinsic for macroscopic Ni doped CuGeO₃ is fully suppressed in Ni doped nanowires. ESR linewidth enhancement as well as widening of Raman peaks corresponds well to the behavior of doped macroscopic CuGeO₃ systems with disorder driven Griffiths phase. Magnetic properties of CuGeO₃ nanowires are discussed in the framework of quantum critical behavior model developed for disordered CuGeO₃ systems [2].

Support by RFBR 12-03-00800 is acknowledged.

[1] L.Z. Pei, L.J. Yang et al., *Materials chemistry and physics*, **130** (2011) 104-112.

[2] S.V. Demishev, *Physics of the Solid State*, **51** (2009) 547-551.

30PO-I1-3

INVESTIGATION ON MAGNETIC PROPERTIES OF FeCoAlON THIN FILMS WITH STRIPE DOMAIN STRUCTURE

Kamzin A.S.², Wei Fulin¹, Ganeev V.R.³, Valiullin A.A.³, Cao Jiangwei¹, Bai Jianmin¹, Zaripova L.D.³

¹ Key Laboratory for Magnetism and Magnetic Materials of the Ministry of Education, Research Institute of Magnetic Materials, Lanzhou University, Lanzhou 730000, China

² Ioffe Physico-Technical Institute of RAS, St. Petersburg 194021, Russia

³ Kazan Federal University, Kazan, Tatarstan, 420008, Russia

kamzin@mail.ioffe.ru

Soft magnetic thin films as Fe_{100-x}Co_x at X around 30 have saturation magnetic flux density (B_s) more than 2.4T has be used to fabricate inductor devices in communication apparatus, electrical power and computers. However, the coercivity of FeCo alloy films prepared by a conventional sputtering method is quite high 50-100 Oe and such films are not suitable to be used as a magnetic core of inductor. Therefore, it is necessary to find out a method to prepare FeCo films with good soft magnetic properties and high B_s . One way to get good soft magnetic properties of FeCo films is adding the third element, such as N, C to FeCo alloy films.

In this paper were studied effects of adding Al, O or/and N, influence of film thickness and annealing temperature on structure and magnetic properties of FeCo films.

The FeCoAlON thin films were fabricated by reactive RF magnetron sputtering of a 6-in Fe₇₀Co₃₀ alloy disk covered with 12 pieces of Al₂O₃ (10×10×2 mm²) chips. The sputtering gas was a mixture of Ar+N₂. The background pressure in the chamber was below 5.0×10⁻⁷ Torr and depositing pressure was 4 mTorr. The sputtering power density was 14.2 W/in². A DC magnetic field of 1500 Oe was utilized to induce a uniaxial anisotropy.

The magnetic properties of the films were measured using Vibrating Sample Magnetometer (VSM). The film structures were identified by X-ray diffraction (XRD) with Cu K_α radiation. The magnetic structure was measured by Conversion Electron Mössbauer Spectroscopy (CEMS) with ⁵⁷Fe at room temperature. The magnetic domain structure was observed using Magnetic Force Microscopy (MFM).

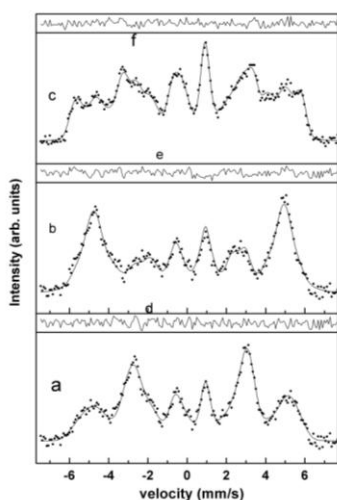


Fig. 1. Mössbauer spectra FeCoAlON thick films (a) 55 nm, (b) 320 nm and (c) 550 nm. Curves (d, e, f) is the deviation from the experimental model spectra.

Analysis of anisotropy of FeCoAlON films shown that if the film thickness smaller than 55nm, the magnetization vector lay in film plane. As the film thickness increased to 210 nm, there was a fine irregular dense stripe domain, but it was not continuation in length direction. With a further increasing of the film thickness, the clear and regular stripe domain structure formed, and the width of stripe became wide.

Mössbauer study of the properties of the films on the annealing temperature, held to 300 °C, showed a complex dependence of the film properties of the duration and the annealing temperature.

30PO-I1-4

MAGNETIC PROPERTIES OF AMORPHOUS HYDROGENATED CARBON NANOSTRUCTURED THIN FILMS

Lukitsa I.G., Nikolaychuk G.A.*, Moroz O.Yu., Smirnov V.M.

Ferrite Domen Co., 25 Tsvetochnaya st., bld.3, 196084 St. Petersburg, Russia

* niko@domen.ru

In this paper the interesting microwave properties such as high permittivity and permeability of the material based on amorphous hydrogenated carbon with nanostructured thin films are presented. These materials can characterize by perfect absorption of electromagnetic radiation (EMR) in microwave frequency range.

Obtained a-C:H:Ni material is amorphous hydrogenated carbon thin film with nanoclusters of Ni 3d metal. Thin film was deposited by the method of reactive ion-plasma magnetron sputtering on Si and glass-ceramic substrates [1]. Thin films have a high complex permittivity ϵ^* and permeability μ^* ($\epsilon' \approx 1000 - 10000$, $\epsilon'' \approx 100 - 1500$, $\mu' \approx 10 - 70$, $\mu'' \approx 0.4 - 10$) at the thickness up to 2 μm , what can stipulate by anomalous EMR absorption effect. The mechanism of absorption in the material under study is determined by three components: the attenuation of electromagnetic waves in the thin film, the interference effects and the scattering phenomena.

The permittivity and permeability of the thin film were measured by especially developed cavity method using waveguide resonators. The determination of film's parameters was carried out from waveguide's frequency characteristics [2]. Insertion of dielectric samples under study into the cavity lead to the change of resonance frequencies and Q-factors of the cavities. Parameters of ϵ^* and μ^* were calculated from frequency shifts and decreasing of Q-factors according to [3].

The magnetic parameters such as shape of hysteresis loop, values of coercive force, remanence and saturation magnetization were determined from vibrating-coil magnetometer measurements, results shows what a-C:H:Ni is a hard magnetic ferromagnetic material. The remanence per sample area was $0.45 \times 10^9 \text{ A/m}^3$ for the film deposited on glass-ceramic substrate and $0.44 \times 10^9 \text{ A/m}^3$ for the film deposited on Si substrate. The saturation magnetization per sample area was found equal to $6.71 \times 10^9 \text{ A/m}^3$ for the sample deposited on glass-ceramic substrate and equal to $4.61 \times 10^9 \text{ A/m}^3$ for the sample deposited on Si substrate (see Fig. 1).

Obtained results demonstrate a good promise to use a-C:H:Ni thin films for the absorption of electromagnetic microwave radiation.

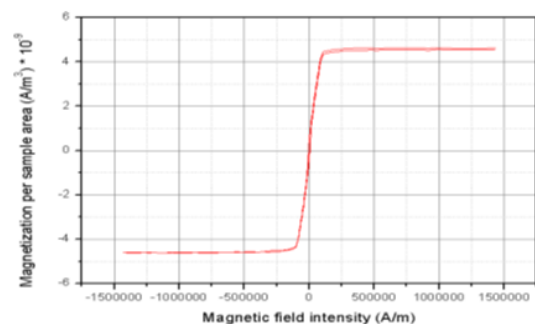


Figure 1. Saturation magnetization per sample area of a-C:H:Ni film on Si substrate at $1.5 \times 10^6 \text{ A/m}$ intensity of applied magnetic field.

[1] L.V. Lutsev, S.V. Yakovlev, T.K. Zvonareva, et al, *J. Appl. Phys.*, **97** (2005) 104327 (6).

[2] G.A. Nikolaychuk, S.V. Yakovlev, V.P. Ivanov, *Proc. XVII-th Int. Conf. "Magnetism, long-range and short-range spin-spin interaction"*, Moscow (Firsanovka), November 20-22, 2009, 257-260.

[3] I.G. Lukitsa, G.A. Nikolaychuk, O.Yu. Moroz, *Abstr. Donostia Int. Conf. "Nanoscaled magnetism and applications"*, San Sebastian, Spain, September 9-13, 2013, 250.

30PO-I1-5

SPIN CONFIGURATIONS OF HEMISPHERICAL NANOPARTICLES AND GRANULAR FILMS FORMED BY ELECTRODEPOSITION OF NICKEL

*Samardak A.S.¹, Sukovatitsina E.V.¹, Ognev A.V.¹, Steblyi M.E.¹, Davydenko A.V.¹,
Chebotkevich L.A.¹, Kim Y.K.², Nasirpouri Forough³, Janjan S-M.⁴, Nasirpouri Farzad⁴*

¹ Laboratory of Thin Film Technologies, Far Eastern Federal University, Vladivostok, Russia

² Department of Materials Science and Engineering, Korea University, Seoul, Korea

³ Department of Physics, University of Tabriz, Tabriz, Iran

⁴ Department of Materials Engineering, Sahand University of Technology, Tabriz, Iran
samardak.as@dvfu.ru

Magnetic states of nickel nanogranular films were studied in two distinct structures obtained by electrodeposition on Si (111) surface from a modified Watts bath at a low pH of 2 exhibiting the formation of individual nanoparticles and agglomerated granules. Based on the defined electrodeposition mechanism, a systematic study was conducted to exploit the change of magnetization mode of hemispherical nanoparticles and granular nickel electrodeposited on silicon. The electrodeposition of nickel at a distinct potential starts with the formation of partly isolated hemispherical nanoparticles which subsequently tend to coalesce forming a continuous granular film. Our preliminary calculations showed that preferential magnetization reversal mechanism in isolated nanoparticles is a vortex state formation. Magnetic force microscopy confirmed the three-dimensional out-of-plane magnetic vortex states and multidomain patterns in isolated hemispherical nanoparticles and its agglomerates, respectively, at zero field. Once the nanoparticles coalesced into small chains and clusters, the coercivity values increased due to the reduction of interparticle spacing and strengthening of the magnetostatic interaction. Further growth leads to the formation of a continuous granulated film which strongly affected the coercivity and remanence exhibiting an in-plane easy axis of magnetization. This was characterized by the domain wall motion and stripe-like domain pattern. Magnetoresistance measurements as a function of external magnetic field are indicative of anisotropic magnetoresistance (AMR) for the continuous films electrodeposited on Si substrate.

This work was supported in part by the Russian Ministry of Education and Science, the Scientific Find of Far Eastern Federal University, and the Joint Research Program by the National Research Foundation of Korea (2013K2A1A7076318) and Russian Foundation for Basic Research (14-02-91701).

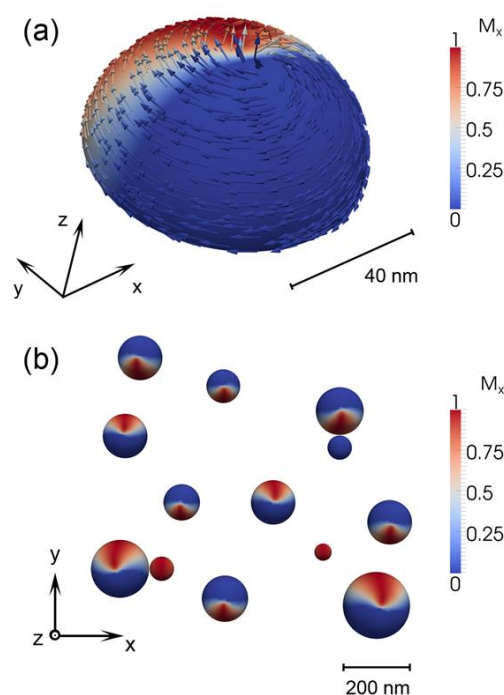


Fig. 1. Micromagnetic simulation results. (a) single hemisphere in the out-of-plane vortex state. (b) ensemble of nanoparticles in vortex and single domain states.

30PO-I1-6

GROUND STATE QUASI-DOUBLET OF Ho^{3+} ION IN $\text{Ho}_2\text{BaNiO}_5$ AND ITS CONTRIBUTION TO MAGNETIC AND THERMODYNAMIC PROPERTIES

Galkin A.S.^{1,2}, Klimin S.A.², Mill B.V.³

¹ FSBI TISNCM, Centralnaya street 7a, Troitsk 142190, Moscow region, Russia

² Institute of Spectroscopy RAS, Fizicheskaya 5, Troitsk 142190, Moscow region, Russia

³ Moscow State University, Physics Department, 119899 Moscow, Russia
klimin@isan.troitsk.ru

The transmission spectroscopy data are presented for $\text{Ho}_2\text{BaNiO}_5$. The quasideublet ground state of non-Kramers Ho^{3+} ion, previously predicted theoretically, was confirmed experimentally for the first time. Its temperature-dependent manifesting magnetic ordering at the Neel temperature $T_N = 49$ K is discussed in the frame of perturbation and mean-field approaches. Holmium contribution into magnetic susceptibility χ (T) and heat capacitance $C(T)$ calculated with the use of spectroscopic data describes well available literature experimental data. Particular shift of Ho^{3+} energy levels manifests magnetostriction in $\text{Ho}_2\text{BaNiO}_5$ in AFM state.

Transmittance spectra of the polycrystalline $\text{Ho}_2\text{BaNiO}_5$ in a broad range of frequencies (2000-20000 cm^{-1}) and temperatures (4.2÷300K) were measured using Fourier-transform spectrometer BRUKER IFS 125HR. Fig. 1 shows transmission spectra in the region of 5F_5 multiplet of Ho^{3+} ion. Temperature behavior of spectral lines is typical for all multiplets measured. Observed splitting of spectral line arising at T_N unambiguously evidences the existence of ground-state quasideublet for non-Kramers Ho^{3+} ion. Temperature dependence of ground-state quasideublet as well as experimental information on the energies of excited levels were used to calculate holmium contribution into susceptibility χ (T) and heat capacitance $C(T)$

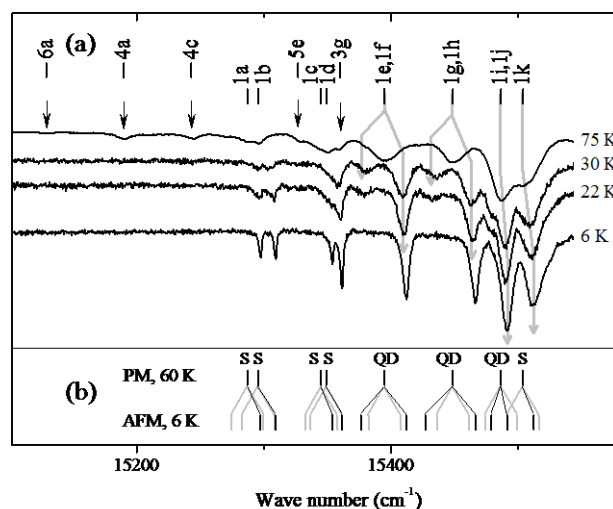


Fig. 1. (a) Transmission spectra of $\text{Ho}_2\text{BaNiO}_5$ in the region of $\text{Ho}^{3+} 5I_8 \rightarrow 5F_5$ transition at different temperatures. Arrows show spectral lines corresponding to the transitions from excited levels of ground multiplet (b) Schematic spectral line splitting: gray – expected line positions for singlet states of excited multiplet and split ground doublet, black – experimental positions.

This work was supported by RFBR (grant №12-02-00858).

30PO-I1-7

MAGNETIC PROPERTIES OF Co/CaF₂/Si HETEROSTRUCTURES: "HENKEL-PLOT" APPROACH

Gastev S.V., Baranov D.A., Kashina N.V., Fedorov V.V., Sokolov N.S.

Ioffe Physical -Technical Institute, St. Petersburg, Russia

gastev@fl.ioffe.ru

Henkel's idea to analyse the difference between isothermal remanence magnetization (IRM) and the direct current demagnetization (DCD) curves [1] to identify the type of magnetic interaction in ferromagnetic particle arrays still looks quite attractive for studies of new systems. In this study, suggested in Ref.[1] and afterwards developed for more convenient comparison with the experiment [2] approach have been applied for the arrays of cobalt nanoparticles epitaxially grown on CaF₂ surfaces.

One can expect that the sign of $\Delta M(H) = DCD(H) - [1 - 2 \cdot IRM(H)]$ has to be negative for the arrays, in which the magnetic dipole (MD) interaction prevails and positive for the case when the exchange interaction between the particle dominates.

It was shown [2] that $\Delta M/2$ is equivalent to $\Delta m(H) = LM(H) - IM(H)$. Here LM-curves were calculated as the average (half of sum) of ascending and descending branches of the magnetic hysteresis loop and IM is the initial magnetization curve.

In this work, Δm analysis was performed for characterization of magnetic properties of Co single domain nanoparticle arrays grown by molecular beam epitaxy on CaF₂/Si(111) and CaF₂/Si(001). The structures were characterised with atomic force (AFM) and scanning electron microscopies (SEM). It was found that Co forms separated nanoparticles on CaF₂ surfaces. Depending on Co exposure the islands had a lateral size from several to tens nm. The hysteresis loops and IM-curves for all structures investigated were measured with longitudinal magneto optical Kerr effect (LMOKE) setup at room temperature. The structures have been demagnetized by decreasing AC magnetic field before IM(H) recording.

The equivalence of $\Delta M(H)/2$ and $\Delta m(H)$ [2] was checked in our experiments for a sample with 30 nm effective thickness of Co layer grown on CaF₂/Si(111). For this purpose, a number of minor loops was recorded to get IRM(H) and DCD(H) curves to enable the $\Delta M(H)$ difference analysis. It was found that the signs of $\Delta M(H)$ and $\Delta m(H)$ were negative.

The negative sign of $\Delta m(H)$ was observed for all Co/CaF₂/Si(111) structures investigated regardless the different effective thickness of Co layer. The existence of the magnetic dipole interaction between Co nanoparticles in these samples is not so unexpected. The positive sign of $\Delta m(H)$ was observed for Co layer where the magnetic domain structure was reliably confirmed.

The $\Delta m(H)$ also was analyzed for several Co/CaF₂/Si(001) structures with corrugated CaF₂ buffer layers. It was found that in these structures with well pronounced uniaxial magnetic anisotropy the $\Delta m(H)$ sign depends on sample orientation in magnetic field. However no magnetic domains in these Co layers were detected. Some considerations for explanations of such behavior of $\Delta m(H)$ are suggested.

[1] O. Henkel, *Phys. Stat. solidi (b)*, **7** (1964) 919.

[2] S. Thamm and J. Hesse, *JMMM*, **184** (1998) 2, 245–255.

30PO-I1-8

EXCHANGE BIAS IN NiFe/IrMn/NiFe TRILAYER STRUCTURES WITH DIFFERENT THICKNESS OF FERROMAGNETIC AND ANTIFERROMAGNETIC LAYERS

Dzhun I.O.¹, Chechenin N.G.¹, Rodionova V.V.^{2,3}

¹ Skobeltsyn Institute of Nuclear Physics, Lomonosov Moscow State University, Moscow, Russia

² Immanuel Kant Baltic Federal University, Kaliningrad, Russia

³ National University of Science and Technology "MIS&S", Moscow, Russia

irina.dzhun@gmail.com

Exchange bias phenomenon in ferromagnetic/antiferromagnetic (F/AF) thin film structures is still of a great interest due to its potential applications such as magnetic sensory devices which are based on giant magnetoresistance effect. Along with technological applications there are also interesting fundamental aspects of this phenomenon, like relative orientation of F- and AF- magnetic moments. Here we report on investigations of exchange bias in ferromagnetic/ antiferromagnetic/ ferromagnetic (F/AF/F) trilayer structures with different thickness of F and AF layers. Two sets of experimental samples Si/Ta 30nm/NiFe t_F /IrMn 15nm/NiFe t_F /Ta 30nm, where $t_F = 7$ nm and 10 nm, and Si/Ta 30nm/NiFe 10 nm/IrMn t_{AF} /NiFe 10 nm/Ta 30nm, where $t_{AF} = 10, 20, 30, 40$ and 50 nm, were deposited by magnetron sputtering in argon at pressure of $3 \cdot 10^{-3}$ Torr with magnetic field of 420 Oe applied in plane of substrate during the deposition. The ferromagnetic resonance (FMR) spectra normally contained two peaks corresponding to upper (AF/F) and lower (F/AF) interfaces and were measured at different angles between directions of external FMR field and magnetic field, \mathbf{H}_{dep} , applied during the samples depositions. Both F/AF and AF/F interfaces in the sample with $t_F = 7$ nm had a non-symmetric FMR field angular distributions. This result is also confirmed by vibrating sample magnetometer measurements, where a shift of hysteresis loop in perpendicular to \mathbf{H}_{dep} direction was observed in case of this sample. The data assume that the exchange bias direction is not parallel to \mathbf{H}_{dep} . The estimated misalignment angles were 20° and 24° for upper and lower interfaces, respectively. The exchange bias values for the interfaces in the structure with $t_F = 7$ nm were 67 and 70 Oe, in the case of the structure with $t_F = 10$ nm the exchange bias value increased to 110 and 114 Oe for upper and lower F/AF/F interfaces, respectively. For trilayers with 10 nm F-layer thickness and various AF-layer thickness the direction of exchange bias was strongly parallel to \mathbf{H}_{dep} while a misalignment between uniaxial magnetic anisotropy and \mathbf{H}_{dep} directions was observed. Exchange bias magnitude changes non-monotonically in range of 25-58 Oe for left FMR absorption peak and 40-65 Oe for right absorption peak. The behavior of exchange bias thickness dependence is similar for both interfaces but in all thickness range AF/F interface is characterized by larger exchange bias than F/AF one. Along with larger exchange bias the coercivity of AF/F interface along \mathbf{H}_{dep} direction is averaged two times greater than that of F/AF. In direction perpendicular to \mathbf{H}_{dep} coercivity of investigated samples was about 3 Oe.

The work is supported by RFBR grant № 12-02-31541. The FMR study was performed at User Facilities Center of M.V. Lomonosov Moscow State University.

30PO-I1-9

ENHANCEMENT OF EXCHANGE BIAS IN NiFe/IrMn AND IrMn/NiFe STRUCTURES WITH DIFFERENT THICKNESS OF ANTIFERROMAGNETIC LAYER

Rodionova V.^{1,2}, Dzhun I.³, Chichay K.¹, Chechenin N.³

¹ Immanuel Kant Baltic Federal University, 236041 Kaliningrad, Russia

² National University of Science and Technology "MIS&S", Moscow 119049, Russia

³ Skobeltsyn Institute of Nuclear Physics Lomonosov MSU, 119991 Moscow, Russia
vrodionova@innopark.kantiana.ru

The phenomenon of exchange bias has been known for over 50 years. It is caused by exchange interaction which occurs at the boundary between ferromagnetic (FM) and antiferromagnetic (AFM) materials [1]. This phenomenon manifests itself as a shift of the ferromagnetic hysteresis loop along the field axis. Although many works were aimed to study exchange biased spin-valve like multilayers (for example, [2]), their properties have not been explained completely yet and the topic of active investigation remains. One of very important challenge from both, fundamental and applications, points of view is to find the ways of enhancements of exchange bias field.

In this work influence of the thickness of antiferromagnetic (AFM) layer on magnetic properties of bilayered structures with two types of deposition order (FM/AFM, AFM/FM) was studied. Angular dependences of the coercive force and exchange bias field were analyzed for structures with different thickness of AFM layer. The layers thicknesses of samples (2 – 40 nm) were determined through deposition rates of calibrating samples obtained by Rutherford backscattering. The hysteresis loops in film plane were obtained at different orientations of the magnetization easy axis of samples relative to the direction of magnetic field: 0, 45, 90, 135, 180, 225, 270, 315 degrees, with help of vibrating sample magnetometer by LakeShore, 7404 System. Magnetic field was varied in the range of -500 - +500 Oe with increment of 5 Oe. In some samples we observed the maximal values of the exchange bias field in the directions different from the magnetic easy axis. It could be explained by the different surfaces conditions of AFM and FM layers and the formation of a granular structure in AFM structures with certain thickness.

The work is supported by RFBR grant № 12-02-31541.

[1] W.H. Meiklejohn and C.P. Bean, *Phys. Rev.* **102** (1956) 1413.

[2] Sara Laureti, Y.Suck Sarah, Haas Helge, Eric Prestat, Olivier Bourgeois, Dominique Givord, *Physical review letters*, **108** (2012) 7, 077205.

30PO-I1-10

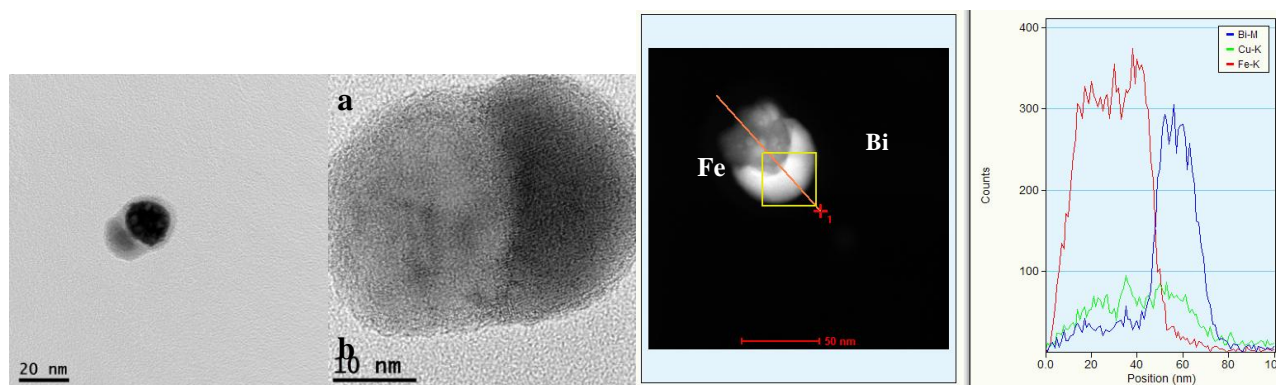
Fe-Bi DUMBELL NANOPARTICLES FROM THE GAS PHASE

Ünlü G.¹, Acet M.², Li Z.-A.², Farle M.²

¹ Pamukkale University, Faculty of Technology, Department of Biomedical Engineering, 200070, Denizli, Turkey

² Universität Duisburg-Essen, Fakultät für Physik Lotharstr. 1, 47048 Duisburg, Germany
cunlu@pau.edu.tr

In this study, Fe-Bi nanoparticles have been prepared by magnetron sputtering with subsequent in-flight annealing. A Fe-Bi patched target have been used. The primary particles generated in the nucleation chamber were travel with Ar/He carrier gas through a sintering furnace at 773 K. Particles deposited onto Cu grids are examined by electron diraction and energy dispersive x-ray line-scans using high resolution transmission electron microscopy. The results show that the sintered particles at 773 K have dumbbell morphology.



The Figure 1 shows (a) high resolution transmission electron microscopy image of sintered particles in-flight annealed at 773 K, (b) line-scan profile and elemental distribution within the particles was probed by EDX line-scans.

30PO-I1-11

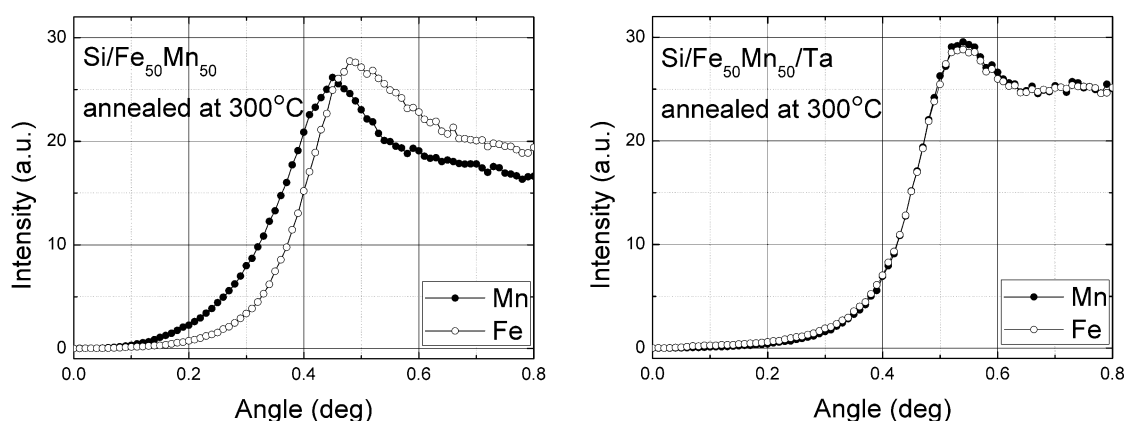
STUDY OF COMPOSITIONAL DELAMINATION OF Fe-Mn LAYER AND ITS INFLUENCE ON MAGNETIC PROPERTIES OF Fe-Mn-BASED MULTILAYERS

Kulesh N.A.¹

¹ Dept. Magnetism and Magnetic Nanomaterials, Ural Federal University, Ekaterinburg, Russia
nikita.kulesh@urfu.ru

Spin valves based on exchange coupled ferromagnetic and antiferromagnetic layers are basic elements of magnetic sensors and more complex magneto-electronic devices. Despite having some disadvantages like low blocking temperature, FeMn continues to be one of the most popular antiferromagnetic materials used as a pinning layer in spin valves as well as other exchange-coupled layered systems. It is known, that the exchange bias field depends strongly on the structural state of the FeMn layer and its oxidation as a result of the direct contact with atmosphere [1]. In this work we investigated process of FeMn delamination with increasing temperature of annealing on unshielded films as well as layers covered by protective Ta layer by grazing incidence x-ray fluorescent (GIXRF) spectroscopy. Effect of heat treatment of FeMn pinning layer on magnetic properties of adjoining ferromagnetic layer was studied on Fe₂₀Ni₈₀/FeMn based systems.

Samples were obtained by magnetron sputtering of alloyed Fe₂₀Ni₈₀ and Fe₅₀Mn₅₀ targets on the glass substrates in presence of technological magnetic field of 150 Oe. Magnetic properties were measured by vibrating sample and MOKE magnetometry. Crystal structure of the layers was analyzed by x-ray diffractometry, GIXRF experiment was performed by using desktop TXRF spectrometer Nanohunter. In the figure below dependencies of normalized x-ray fluorescent yields of Mn and Fe on angle of incidence measured on FeMn(12nm) and FeMn(12nm)/Ta(2nm) films after annealing at 300 C are presented. The obtained results confirmed separation FeMn by migration of Mn atoms to the surface, which can be seen as a separation of Mn and Fe peaks observed for unshielded layer. Magnetic measurements performed on FeMn and Fe₂₀Ni₈₀/FeMn films were in good agreement with the results of GIXRF experiment.



This work was supported by RFBR and the Government of Sverdlovsk Region (grant № 13-02-96027), UrFU under the Framework Program of development of UrFU through the «Young scientists UrFU» competition.

[1] A.V. Svalov, P.A. Savin, V.N. Lepalovskij, et al. *AIP Advances*, **3** (2013) 092104.

30PO-I1-12

DEPENDENCE OF THE HYSTERESIS CHARACTERISTICS OF THE CORE-SHELL NANOPARTICLES ON THEIR SIZE

Chernova M.A.¹, Afremov L.L.

Far Eastern Federal University (FEFU), Vladivostok, Russia

¹cmariaa@mail.ru

Numerous studies of nanoparticles led to the development of new structures, so-called core-shell nanoparticles. Co-Au occupies a special place among these nanoparticles, which due to their unique properties are widely used in biomedicine [1]. Feature of the magnetic properties of Co-Au core-shell nanoparticles is determined by the exchange interaction at the core-shell interface [2]. This thesis is devoted to the theoretical study of the influence of core size and exchange interaction on the hysteresis characteristics of Co-Au core-shell nanoparticles.

The following model was used in calculations [3]: 1) Co-Au core-shell nanoparticle with a volume V has ellipsoid-shape with elongation q_1 contain uniformly magnetized ellipsoidal core Co with a volume $v = \varepsilon V$ and elongation q_2 long axis of which parallel to the long axis of core-shell nanoparticle oriented along Oz . 2) It's believed, that crystallographic anisotropy axis is parallel to the Oz , and vectors of spontaneous magnetization of both phases $I_s^{(Au)}$ and $I_s^{(Co)}$ are located in the yOz plane comprising long axes of magnetic phases and make angles $\vartheta^{(Au)}$ and $\vartheta^{(Co)}$ with axis Oz , respectively. It's believed that $I_s^{(Au)} \approx 10^{-2} I_s^{(Co)}$ [2]. 3) External magnetic field is applied along Oz .

Dependencies of the coercive field H_c and residual saturation magnetization I_{rs} on Co core size b and interphase exchange interaction A_{in} for core-shell nanoparticles were obtained during measurements, and showed on the Fig.1. The figure shows that the size of the core and the coercive force of the spontaneous magnetization are reduced, due to the increased role of thermal fluctuations in the system. These results are in qualitative agreement with experiment [4].

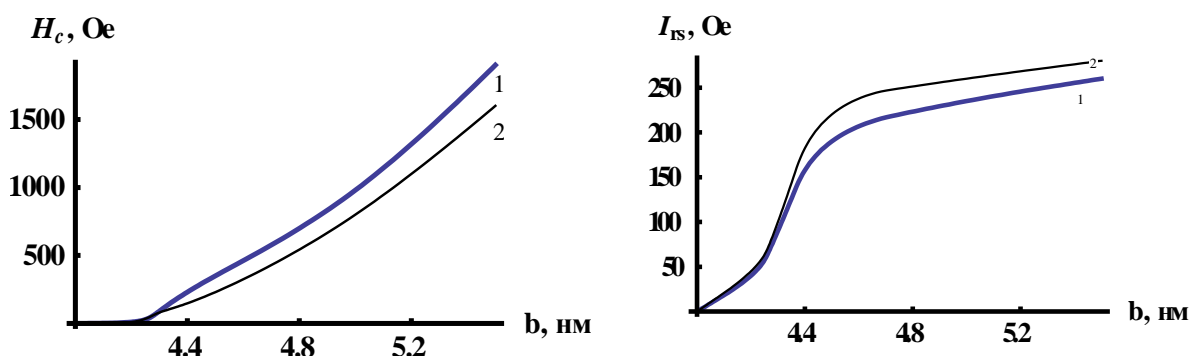


Fig. 1. Dependencies of the (a) coercive field H_c and (b) spontaneous magnetization I_{rs} on size of the Co core b and interphase exchange interaction A_{in} . For the left curve $A_{in} = -10^{-8} \text{ erg/cm}$, for the right curve $A_{in} = 10^{-8} \text{ erg/cm}$.

- [1]. Q A Pankhurst, J Connolly, S K Jones and J Dobson. // *J. Phys. D: Appl. Phys.*, **36** (2003) R167–R181.
 [2]. Tianlong Wen and Kannan M. Krishnan. *Journal of applied physics* **109** (2011) 07B515.
 [3]. Afremov L.L., Ilyushin I.G // *Journal of Nanomaterials* (2013) **2013** 687613, 15.
 [4]. Gh. Bahmanrokha, M. Hashimb, N.Soltania, I. Ismailb, P. Vaziric, M Navaseria, R. Sabbaghizadeh. *Digest Journal of Nanomaterials and Biostructures* **7** (2012) 4,1799 – 1810.

30PO-I1-13

SUPERPARAMAGNETIC PROPERTIES OF CoFe_2O_4 AS A FUNCTION OF SIZE (6-10 nm) AND COATING (OLEIC/CITRIC ACID OR TiO_2)

Repko A.¹, Vejpravová J.², Vacková T.³, Nižňanský D.¹

¹ Charles University in Prague, Faculty of Science, Hlavova 8, Prague 2, Czech Republic

² Institute of Physics AS CR, v.i.i., Na Slovance 2, Prague 8, Czech Republic

³ Institute of Macromolecular Chemistry AS CR, v.v.i., Heyrovského namesti 2, 16206 Prague 6
anton@a-repko.sk

We studied magnetic properties of cobalt ferrite nanoparticles prepared by hydrothermal hydrolysis of Co-Fe oleate in the presence of pentanol/octanol/toluene and water at 180 or 220°C. The particle size (6, 8 or 10 nm) was controlled by the organic solvent and temperature as was reported previously in [1,2]. The inter-particle distance was varied by the surface coating.

The as-prepared nanoparticles were hydrophobic due to coating by the oleic acid, which implied inter-particle distance of 2-3 nm (see Fig. 1). Their blocking temperature (estimated as a maximum of the ZFC) was 180 K, 280 K and 330 K, respectively (Fig. 2). The particles formed stable dispersions in hexane, cyclohexane and toluene.

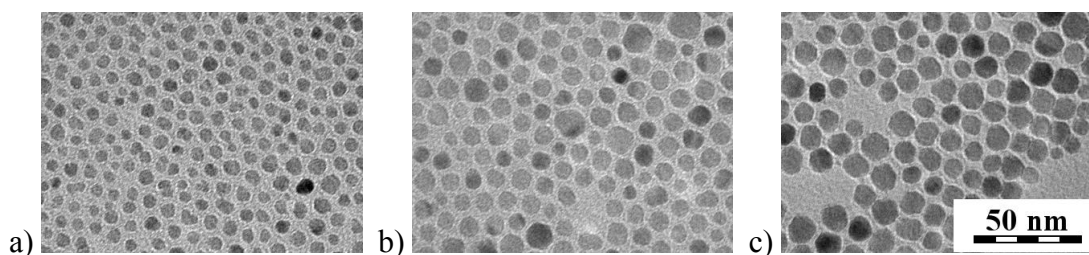


Fig. 1. CoFe_2O_4 nanoparticles of the diameter 6 nm (a), 8 nm (b), 10 nm (c).

After replacing the oleic acid by citric acid, the particles became hydrophilic and their inter-particle distance decreased to almost zero. The blocking temperature increased by approximately 10 K, which is a consequence of stronger dipolar inter-particle interactions. Their dispersion in water was stable for one week; the dispersion in methanol seems to be stable indefinitely.

Another modification was achieved by coating with titanium dioxide. The increased inter-particle distance (weight ratio of the CoFe_2O_4 was 16%) implied lowering of the blocking temperature by ca. 20 K. The $\text{CoFe}_2\text{O}_4@\text{TiO}_2$ nanoparticles were sufficiently stable in water, methanol and ethanol.

The effect of dipolar interactions on relaxation phenomena of the nanoparticles of different size and coating was finally addressed by a.c. susceptibility measurements.

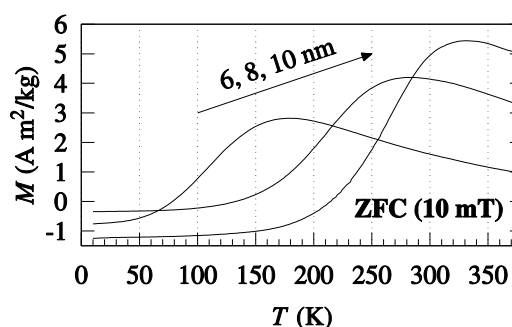


Fig. 2. Zero-field-cooled (ZFC) temperature dependence of magnetization of the CoFe_2O_4 nanoparticles coated by oleic acid.

[1] A. Repko, D. Nižňanský, J. Poltírová-Vejpravová, *Journal of Nanoparticle Research* **13** (2011) 5021-5031.

[2] A. Repko, D. Nižňanský, I. Matulková, M. Kalbáč, J. Vejpravová, *Journal of Nanoparticle Research* **15** (2013) 1767.

30PO-I1-14

MAGNETIC STATE OF THE IRON WITH CHROME AMORPHOUS ALLOY

Pechnikov V.S.¹

¹ Far Eastern Federal University, 8 Sukhanova St., Vladivostok 690950, Russia
pech_vs@mail.ru

Some amorphous alloys of iron with chrome have unusual magnetic properties (usual are f.e. in [1]). We investigated an alloy about 80% of iron and 20% of chrome. Magnetic parameters of samples of this alloy were measured by the vibration magnetometer. The device allows measurements of the magnetic moment of a sample in fields to 130 mT at any temperature from room (20°C) to 800°C. In fig.1 the main curve of magnetization and the left branch of a hysteresis loop, measured at t_0 is shown.

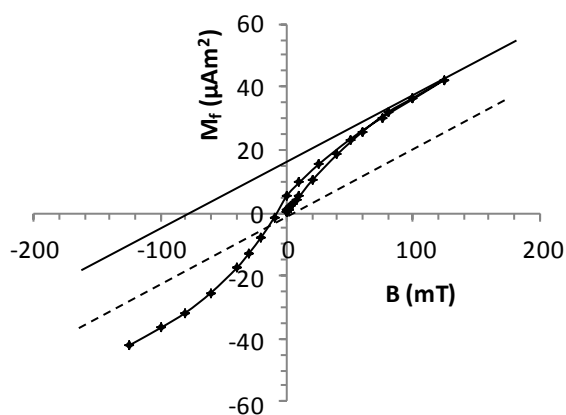


Fig. 1. The magnetic moment (M_f) dependence on induction of an external field

It is visible that characteristic for ferromagnetic material the saturation magnetic moment isn't present. The rectilinear part of the curve is at the field from 60 to 500 mT (in fig. is only to 125 mT). Rectilinear dependence of the magnetic moment on induction of an external field is characteristic for paramagnetic material and passes through zero (a dotted straight line in drawing). The type of a curve to 60 mT is characteristic for a ferromagnetic phase. Having taken away from the measured M values of the moments the paramagnetic moments (dotted line) we fined curve $M(B)$ for only a ferromagnetic phase. The part of the main curve on an interval of fields 0-0,5

mT, showed that in a sample there is a low-coercive ferromagnetic phase with a field of saturation 0,2 mT. The temperature investigation shows, that the Curie's temperature near 140°C. One can see on the fig.1 the high coercive ferromagnetic phase (the saturation field near 60 mT, saturation magnetic moment 11.5 μAm^2). From the full measured moment at different temperatures the size of the ferromagnetic moment was taken away. The curve of dependence of the paramagnetic moment from temperature was so received. It appeared, this dependence submits to Curie-Weyss law, and $1/M$ crosses an axis of temperatures approximately at 200 K (-73°C). So, the magnetic state of an alloy at the room temperature is characterized by two ferromagnetic phases low-coercive (a field of saturation 0,2 mT, the Curie point is about 140 °C, the moment of saturation is 0,4 μAm^2) and high-coercive with a field of saturation 60 mT, the moment of saturation 11.5 μAm^2 , the Curie temperature isn't defined. The main part of the magnetic moment belongs to a paramagnetic "tail" of a ferromagnetic phase with Curie's point near a minus 70 °C.

[1] E.Shalygina, N.Abrosimova, M.Komarova, V.Molokanov. *J.Techn.Phys.*, **74**(9) (2004) 127-130.

30PO-I1-15

MOSSBAUER STUDY OF FERRO-ANTIFERROMAGNETIC PHASE TRANSITION IN [001]-ORDERED $L1_0$ FePt_{1-x}Rh_x FILMS

Kamzin A.S.¹, Ishio S.², Hasegawa T.², Valiullin A.A.^{3*}, Ganeev V.R.³, Tagirov L.R.³, Zaripova L.D.³

¹ Ioffe Physical-Technical Institute, Russian Academy of Sciences, St. Petersburg, 194021 Russia

² Department of Materials Science and Engineering, Akita University, 1-1 Gakuen-machi, Tegata, Akita 010-8502, Japan

³ Kazan Federal University, Kazan, 420008, Republic of Tatarstan, Russia

* fess98@rambler.ru

The $L1_0$ FePt alloy with a face-centered tetragonal (fct) structure ($a = b > c$) has a high magnetization ($M_s \approx 1100$ emu/cm³) and a high magnetocrystalline anisotropy ($K_u \approx 7.0 \times 10^7$ erg/cm³). The [001]-oriented $L1_0$ FePt film has attracted much interest because the perpendicular magnetization is expected to have applications for high-density magnetic storage media and spintronic devices due to its good thermal stability. By substituting Rh for Pt in the equiatomic alloy, the $L1_0$ phase is stabilized. The FePt_{1-x}Rh_x bulk alloy with $x < 0.8$ has the $L1_0$ structure, and it exhibits three different magnetic phase transitions depending on the temperature: (1) a second-order ferromagnetic (FM)-paramagnetic (PM) transition ($0 < x < 0.19$), (2) a first-order antiferromagnetic (AF)-FM transition ($0.19 < x < 0.28$), and (3) a first-order AF-PM transition ($0.28 < x < 0.80$) [1,2]. The physical properties of a thin film frequently differ from the bulk behavior due to dimensionality effects.

In this work, we report the magnetic properties of a thin [001]-oriented $L1_0$ FePtRh film ($t_{\text{FePtRh}} = 20$ nm) and the FM-AF transition. FePt_{1-x}Rh_x films were deposited onto MgO(100) single crystal substrate by a magnetron sputtering method. The composition (x) of the FePt_{1-x}Rh_x films was controlled by changing the Rh thickness (t_{Rh}). An energy dispersive X-ray spectroscopy, a transmission electron microscopy, X-ray diffraction (XRD), a vibrating sample magnetometer (VSM), a superconducting quantum interference device (SQUID) magnetometer, an X-ray magnetic circular dichroism (XMCD) and Conversion Electrons Mossbauer Spectroscopy (CEMS) were used for studying film properties. The temperature variation of the hyperfine field was investigated in the films in range $0 < x < 0.40$.

The conclusions: [001]-oriented $L1_0$ FePt_{1-x}Rh_x films with a degree of long-range chemical order parameter of $S \approx 0.83$ were prepared. At room temperature, the films with $0 < x < 0.32$ showed ferromagnetism ($800 \leq M_s \leq 1100$ emu/cm³) with a high magnetocrystalline anisotropy, and the films with $0.34 \leq x \leq 0.40$ were in an antiferromagnetic (AF) phase. At $x = 0.32$, M_s were about 500 emu/cm³.

This materials system has enough thermal stability for future use in high-density magnetic storage media, and its K_u can be controlled easily by changing x .

This work was supported by the Russian Foundation for Basic Research (project No. 14-02-91151 GFEN_a).

[1] T. Hasegawa, J. Miyahara, T. Narisawa, S. Ishio, H. Yamane, Y. Kondo, J. Ariake, S. Mitani, Y. Sakuraba, and K. Takanashi, *J. Appl. Phys.* **106** (2009) 103928.

[2] S. Yuasa, H. Miyajima, and Y. Otani, *J. Phys. Soc. Jpn.* **63** (1994) 3129.

30PO-I1-16

MAGNETIC BEHAVIOR AND ASSYMETRY OF HYSTERESIS LOOPS OF SUPERLATTICES FE/PT

Kornilov A.A.¹, Antipov S.D.¹, Gorunov G.E.¹, Senina V.A.¹, Smirnitskaya G.V.¹, Moosaeva S.M.¹
¹ M.V. Lomonosov Moscow State University, GSP-1, Leninskie Gory, build.2, Physics Department,
 Moscow, Russia
 Vera_sen@mail.ru

Studies of magnetic properties of nanoparticles in superlattices, multilayers and various cluster formations based on 3d transition elements with 4d, 5d elements: 3d/4d, 3d/5d have been spurred by possibility of their practical applications in advanced magnetic storage devices and also by desire to understand fundamental interactions responsible for their unusual magnetic behaviour.

We report on the investigation of magnetic behaviour of two-component superlattices Fe/Pt, which is perspective materials with perpendicular magnetic anisotropy (PMA).

Magnetic superlattices (MSL) [Fe(14Å)/Pt(x Å)]*100 (x=4÷25) were synthesized by use of cathode sputtering in discharge with oscillating electrons at pressure of working gas Kr 10^{-5} torr, anode voltage $U_a=2$ kV and magnetic field $H=320$ Oe. Mica (muscovite thickness 0.1 mm) was used as a substrate. X-ray diffraction studies were performed on the diffractometer "STOE STADI P" and did not reveal the presence of coherent reflections. That is to say, all MSLs Fe/Pt are x-ray amorphous.

Measurements of magnetization curves and hysteresis were performed at the room temperature with the use of vibrating magnetometer with sensitivity up to $2 \cdot 10^7$ emu. We have found that the spontaneous magnetization I_{S0} and coercive force H_C in dependence of Pt layers thickness have oscillatory behaviour with period ~ 10 Å. Investigations were performed with the samples in initial state and after annealing at pressure 10^{-5} Topp in magnetic field $H=320$ Oe. After annealing we observed increase in values of I_{S0} , H_C , B_R and the effective anisotropy constant, which become equal $K_{eff} \approx 10^6 \text{ erg/cm}^3$. We also observed asymmetric forms of hysteresis loops for some samples MSLs Fe/Pt.

We discuss our results and reasons of arising the gigantic values K_{eff} and asymmetric forms of hysteresis loops.

30PO-I1-17

FIELD DEPENDENCE OF MAGNETISATION OF QUASI-ONE-DIMENSIONAL SYSTEM $(Y_{1-x}Nd_x)_2BaNiO_5$

Popova E.A.¹, Klimin S.A.², Popova M.N.², Klingeler R.³, Büchner B.⁴, Vasiliev A.N.⁵

¹ National Research University Higher School of Economics, Moscow, Russia

² Institute of Spectroscopy RAS, Troitsk, Moscow, Russia

³ Kirchhoff Institute for Physics, University of Heidelberg, Heidelberg, Germany

⁴ Leibniz-Institute for Solid State and Materials Research IFW Dresden, Germany

⁵ Low Temperature Physics Department, Moscow State University, Moscow, Russia

eapopova@yahoo.com

The crystal structure of the $(Y_{1-x}Nd_x)_2BaNiO_5$ compounds contains spin- $S=1$ chains composed of flattened NiO_6 octahedra sharing their corners. The chains are interconnected through the Nd^{3+}/Y^{3+} and Ba^{2+} ions. Y_2BaNiO_5 is a well-known Haldane-gap system, which does not order down to the lowest temperatures [1]. Members of the family R_2BaNiO_5 containing magnetic rare-earth R^{3+} ions order antiferromagnetically, however, the Haldane gap survives in both paramagnetic and ordered states [2]. In the series of compounds $(Y_{1-x}Nd_x)_2BaNiO_5$, the Neel temperature depends on x . In the ordered state, the magnetic moments of the Nd^{3+} ions are oriented along the c -axis, those of the Ni^{2+} ions lie in the (ac) plane.

In the present work, magnetic properties of $(Y_{1-x}Nd_x)_2BaNiO_5$ powder samples with different Nd concentrations were studied by means of spectroscopic and magnetization (with fields up to 50 T) measurements in the temperature range 2 – 300 K. We observed two anomalies in the field dependence of magnetization, $M(B)$, of Nd_2BaNiO_5 at 4.2 K. The values of critical fields ($B_{cr1} = 9.6$ K and $B_{cr2} = 16.4$ T) and of magnetization are in good agreement with the magnetization data on single crystal [3]. For compounds with $0.075 < x < 0.25$, only one anomaly in $M(B)$ takes place, while no anomalies are observed for compounds with $x < 0.05$. The critical fields (for $x=1$) increase with heating, and the first anomaly disappears at $T = 15$ K $< T_N = 48$ K. The critical field for other compounds decreases with increasing temperature.

We calculate a contribution of the Nd subsystem into magnetization using the values of the splitting of the ground Kramers doublet of the Nd^{3+} ion found from spectroscopic data at different temperatures ($B=0$) for each compound. In the case of $B||c$, both the internal and external magnetic fields lead to a decrease of the Nd^{3+} magnetic moments directed opposite to the direction of the external field. At the critical field B_{cr} , the magnetic moments of both Nd sublattices orientate along the magnetic field. The initial internal magnetic field (at $B=0$) decreases with increasing the temperature, it causes the shift of the B_{cr} to lower fields. For Nd_2BaNiO_5 , the same transition occurs through an intermediate phase. There are no transitions in the cases of $B||a$, $B||b$, because of a strong anisotropy of the Nd^{3+} ion.

The system of chain segments caused by uncontrolled defects inside the Ni chain can be described by the fourfold degenerate ground state which is split by both external and internal magnetic fields. The magnetization of the chain segments leads to an increase of the magnetic moments of both Ni sublattices, although the magnetic field from one of the Nd subsystems decreases. The one-dimensional character of the nickel subsystem plays, possibly, the main role in the observed transitions.

[1] J. Darriet and L. P. Regnault, *Solid State Commun.*, **86** (1993) 409.

[2] T. Yokoo, Z. Zheludev, M. Nakamura, and J. Akimitsu, *Phys.Rev. B*, **55** (1997) 11516.

[3] S. Okubo, H. Ohta, T. Tanaka, T. Yokoo, J. Akimitsu, *Physica B*, **284** (2000) 1475.

30PO-I1-18

APPLYING OF NELDER-MEAD'S ALGORITHM FOR SIMULATION OF THE HYSTERESIS CURVES Fe/SiO₂/Co STRUCTURES

Orlova A., Sinyukhin A., Kupriyanova G.S.

Immanuel Kant Baltic federal university, Kaliningrad, Russia
aorlova56@mail.ru

Magnetic tunnel junctions (MTJ) consisting of two ferromagnetic (FM) layers separated by the ultrathin tunnel barrier are the main elements of the random access memory of novel generation. The main requirements to the materials combination for MTJ were derived from the basic principles of the MTJ concept. They are the following: 1) high conductivity electrons polarization in the ferromagnetic electrode; 2) a possibility of an independent magnetization switching in two ferromagnetic electrodes for example, due to the difference in coercive force or exchange bias. The aim of this work is the development of numerical model for extracting of FM/TI/FM structures parameters. Mathematical model is based on standard thermodynamical approach. The equilibrium state of magnetization is achieved at minimum of free energy. This approach has been described in details in [1].

Extracting of unknown model parameters leads to inverse problem. Initial data is consist of depth of thin ferromagnetic films d_1 , d_2 , experimental hysteresis loop and some estimations for magnetizations M_1 and M_2 . This technique allows to extract such parameters as coercivity and anisotropy constants H_{k1} , H_{k11} , H_{k2} , H_{k22} , magnetizations M_1 , M_2 , constants of bilinear and biquadratic exchange J_1 , J_2 , angles of easy-axis orientation Δ_1 , Δ_2 . There is not guaranty that solution of inverse problem is exist. In this paper reverse problem has been reduced to optimization problem for non-analytical objective function in the space of input parameters of model. Algorithm applied for three-layer structures. In this work we investigated three-layer structures Fe/SiO₂/Co with different thicknesses of the insulating layer. The Fe/SiO₂/Co multilayer structures have been studied by the VSM technique. Magnetic parameters of the films studied experimentally were also theoretically modeled.

Advantages of the method are the simplicity of implementation, acceptable results of the algorithm and easy code parallelization (process of searching can be performed independently from different initial simplexes). Extracted parameters correlate with values obtained by FMR researches. Mathematical validity of the Nelder –Mead's method is guaranteed finding at least one local extremum. Unlike other numerical optimization techniques, the Nelder-Mead's method does not require computation of the gradient (pseudogradient) of function. This method typically requires onle one or two function evaluations [2]. Unlike gradient descent this method can be used for non-analytical functions.

The disadvantages of this method are decent runtime (depends on the number of starting points of search and required accuracy), presence of many local extremum and insecurity to find the absolute extremum even on constrained region (this is a problem of all numerical optimization methods).

- [1] A.V. Astashenok, G.S. Kupriyanova, A.U. Goikhman et al., *Vestnik I. Kant SU* **5** (2011) 60-68.
[2] Jeffrey C. Lagarias, James A. Reeds, Margaret H. Wright, Paul E. Wright. Convergence properties of the Nelder–Mead simplex method in low dimensions. *SIAM J. OPTIM*, **9** (1998) 1, 112–147.

30PO-I1-19

ELECTRON SPECTRUM AND MAGNETISM IN SILICON NANOCCLUSERS AND ORGANIC MOLECULES DOPED BY 3D TRANSITION METAL ATOMS

Tikhonov E.V.¹, Uspenskii Yu.A.², Matsko N.L.²

¹ M.V. Lomonosov Moscow State University, Physics Department, Moscow, Russia

² P.N. Lebedev Physical Institute, Russian Academy of Sciences, Moscow, Russia
e.tikhonov@physics.msu.ru

Electronic, optical and magnetic properties of nanoclusters and organic molecules are of key importance for many applications, including nano- and optoelectronics and spintronics. In this presentation we report ab initio calculations of the quasiparticle electron spectrum in many silicon nanoclusters and organic molecules (a part of them is doped by transition metal atoms) and their magnetic characteristics. The subjects of our particular interest are the dependence of nanoobject properties on their size and composition, as well as the role of many-electron effects.

Spectral properties of large organic molecules are known rather well from numerous experiments, which include the measurement of photoemission and inverse photoemission spectra. Our first-principles calculations of metal phthalocyanine, PTCDA and poly-aromatic hydrocarbon molecules were performed by DFT, hybrid functional and GW methods. They showed that DFT poorly reproduces the electron spectrum of molecules, while the hybrid functional approach gives rather precise spectra of the valence and conducting bands, but underestimates the HOMO-LUMO gap width. To get correct gap values, we used Lehman's approach, utilizing DFT total energies for the systems with N-1, N and N+1 electrons. Obtained results are in good agreement with available experimental data and the results of our several GW calculations.

Our study of magnetic nanoobjects included the phthalocyanine molecules with Ni, Co, Fe, Mn and Cr atoms, as well silicon clusters doped by Fe atoms. Calculated magnetic moments and spin splitting of electron spectra are compared with available experimental data. We notice a high sensitivity of the spin splitting to the description of many-electron effects and a too small spin splitting in DFT. The most interesting is the strong dependence of magnetization on the position of Fe atom, which was found in silicon clusters. In this connection we consider correlation between magnetic moment formation and electron spectrum.

This research was supported in part by RFBR (grants 13-02-00655a and 14-02-00583a) and RAS Programs.

30PO-I1-20

SURFACE MAGNETOPLASMONS IN METAL NANOWIRES

Gusev N.A.^{1,2}, *Belotelov V.I.*^{1,3}, *Kalish A.N.*^{1,3}, *Zvezdin A.K.*^{1,2}

¹ Russian Quantum Center, Moscow, Russia

² A.M. Prokhorov General Physics Institute, Russian Academy of Sciences, Moscow, Russia

³ M.V. Lomonosov Moscow State University, Moscow, Russia

nagusew@gmail.com

Nowadays, materials with optical properties tuned by switching the magnetization are of practical interest for telecommunication devices and magnetic field sensors. An important role is played here by the possibility of tuning eigenfrequencies of magnetic nanostructures. For example, shift of the eigenfrequencies of plasmonic modes due to magnetization reversal leads to the enhancement of the transverse magneto-optical Kerr effect [1].

Most of the publications about the interplay between magnetic and optical properties of nanostructures have been devoted to the properties of uniformly magnetized periodic structures of a rectangular or, rarely, a circular cross-section. For example, a one dimensional array of longitudinally magnetized nanocylinders is studied in Ref. [2]. In Ref. [3] authors study light scattering on magnetic particles with vortex magnetization but without taking into account surface plasmon-polariton (SPP) excitation. The problem of thermo-modulation nonlinearity in a gold plasmonic nanowire was studied by Marini [4].

This work is devoted to an effect of the vortex magnetization on dispersion properties of the SPP modes of metallic nanorods with circular cross-section in dielectric environment (see Fig.1). We consider two types of structure: nickel nanowire in air, (Fig. 1a), and golden nanowire surrounded by bismuth iron garnet (Fig. 1b). In both cases, the magnetic material is circularly magnetized. We study dispersion of SPPs propagating along the cylinder axis.

The typical analysis of the corresponding eigenwaves-eigenfrequency problem shows that cylindrical symmetry of the SPP leads to a significant deviation of dispersion curve from the planar case. Moreover, a magnetization induced shift of the propagation constant is about ten times greater than that for the planar case.

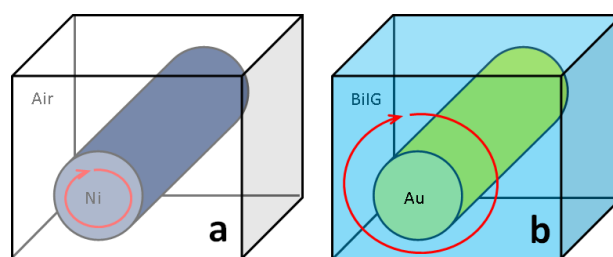


Fig. 1. The structure under investigation.

Support by RFBR is acknowledged.

[1] V.I. Belotelov et al, *Nature Nanotech.*, **6.6** (2011) 370-376.

[2] I. Pimenov, V. Kurin, *JOSA B*, **29.7** (2012) 1815-1821.

[3] E.A. Karashtin, *Phys. Rev. B*, **87.9** (2013) 094418.

[4] A. Marini et al., *New Journal of Physics*, **15.1** (2013) 013033.

30PO-I1-21

INVESTIGATION AND MODELING OF THE FERROMAGNETIC RESONANCE PROPERTIES IN COMPOSITE FERROMAGNETIC FILMS

Razmyslov I.N.¹, Vlasov V.S.¹, Turkov V.K.¹, Popova A.S.¹

¹ SyktSU, Syktyvkar, Russian Federation
z-project@bk.ru

The composite metal dielectric films are metal particles they are distributed randomly or orderly in a dielectric medium on substrate. The like structures may be used in device for recording and storing information for protective coatings, wireless device and medical equipment [1]. Therefore these structure are studied widely.

We investigated films witch composition $(\text{Co-Fe-Zr})_x(\text{CaF}_2)_y$, $(\text{Co-Fe-Zr})_x(\text{Al}_2\text{O}_3)_y$, $(\text{Co-Ta-Nb})_x(\text{SiO}_2)_y$, $0.3 < x < 0.62$, $3 < y < 12$. Films were prepared by ion-beam sputtering method. The materials of substrate were polycrystalline glass and polyethylene (PET). The films were investigated by X-ray and atomic force microscopy (AFM) [1].

For description of the ferromagnetic resonance properties these films we had developed the model. The basis of our model is the approaches of Netzelmann and Dubowik [2,3].

According to the model as the films are ensembles of identical interacting ferromagnetic particles. The shape of the particles is ellipsoid. The expression for the free energy is sum demagnetization energy of particles and demagnetization energy of ensembles as a whole.

We investigated the ferromagnetic resonance (FMR) spectra of metal-dielectric compose films. We compared experimental angular and metal concentration dependences of resonance magnetic field witch the theoretical model calculation.

Magnetic field and the magnetization of the sample were averaged over the volume. We have received evaluation for changing of the shape for effective particles when concentrations of metal are different. In the work qualitative explanation of FMR properties of thin granular composite films was proposed a by varying the concentration. The formation of columnar structures was modelled by stretching the shape of particles. Changing of the shape of the metal particles was shown by AFM [1].

Support by RFBR (grant 13-02-01401)

[1] L.N. Kotov, V.K. Turkov, V.S. Vlasov, A.V. Golov, *Nanomaterialys and nanostrukturys 21 vek.*, **4** (2011).

[2] U. Netzelmann, *J. Appl. Phys.*, **68** (1990) 1800.

[3] J. Dubowik, *Phys. Rev.*, **54** (1996) 1088.

30PO-I1-22

SPECTRAL ELLIPSOMETRY OF COBALT-IONS IMPLANTED SILICON SURFACE

Bazarov V.V.¹, Valeev V.F.¹, Nuzhdin V.I.¹, Osin Yu.N.^{1,2}, Gumarov G.G.^{1,2}, Stepanov A.L.^{1,2}

¹ Zavoisky Physical-Technical Institute of RAS, Kazan, Russia

² Kazan Federal University, Kazan, Russia

vbazarov1@gmail.com

Nanometer size structures synthesized by ion implantation dictate the need to use special control methods to study their parameters such as composition, thickness, and morphology. One of the most promising method for studying of the implanted surface structure is optical ellipsometry. Ellipsometry is based on measuring changes in polarization of light due to its interaction with the analysing sample [1].

Samples of the present experiments were monocrystalline silicon wafers with crystallographic orientation (111) and *p*-type conductivity. Ion implantation was carried out with ILU-3 ion accelerator by cobalt ions with energy of 40 keV at a fluence range of 6.6×10^{12} - 2×10^{17} Co⁺-ions/cm² at room substrate temperature. Ion current density does not exceed 5 μA/cm².

Calculation with the SRIM-2010 code [2] for 40 keV Co⁺ ion implantation into the Si substrate gives a mean projected range 40 nm with a straggling of 15 nm.

Measurements of the ellipsometric angles ψ and Δ were carried out in the optical wavelength range (380-1050 nm) by spectral ellipsometer “ES-2” with a binary modulation of the polarization state (designed and manufactured in IRE of RAS, [3]).

After spectral measurements of ψ_{exp} and Δ_{exp} , values of ψ_{th} and Δ_{th} parameters of heterogeneous multilayer structures were calculated. According to the convergence between the calculated and experimental spectra it could be concluded about the correct choice of the model and definitions of suited parameters. In the presence of the two different substances in the applied layer software allows to calculate the optical constants of mixtures of these substances in accordance with the effective medium approximation of Bruggeman [4].

It is found that a fluence of complete amorphization of Si surface layer is in a range of $(2-6) \times 10^{14}$ Co⁺-ion/cm². At fluencies in range of $(1-10) \times 10^{16}$ Co⁺- ion/cm² it needs to use a more complicated model of three films in implanted layer for convergence of experimental and calculated ellipsometric spectral dependencies. At fluencies exceeded 10^{17} Co⁺- ion/cm² a matching of the experimental and calculated values of the ψ and Δ angles throughout the used wavelength range cannot be reached. This may be due to the fact that at the indicated implantation fluencies silicon surface gets relief or porous structures. Additional cause of the discrepancy between the experimental and calculated spectra could be started from process of phase formation of cobalt silicide (Co₂Si, CoSi, CoSi₂) with optical constants, which are different from the optical constants of a statistical mixture of cobalt and silicon substances.

The magnetic properties of the surface layers were also analysed by surface-scanning magneto-optical Kerr polarimeter in the longitudinal mode. It was shown that both the coercive field and the residual magnetization of silicon surface layer were increased with fluence growth.

The work was partially supported by the RFBR, project No. 13-02-12012 ofi_m.

[1] R.M.A. Azzam, N.M. Bashara, *North-Holland Pub. Co.* (1977) 529.

[2] J.F. Ziegler, J.P. Biersack, U. Littmark, *Pergamon Press*, New York (1985) 465.

[3] A.V. Khomich, V.I. Kovalev, E.V. Zavedeev et. al. *Vacuum* **78** (2005) 583-587.

[4] Bruggeman D.A.G. *Ann. Phys. (Leipzig)* **24** (1935) 636-679.

30PO-I1-23

MAGNETIC PHASE DIAGRAM OF 2D HONEYCOMB LATTICE SILVER DELAFOSSITE $\text{Ag}_3\text{Co}_2\text{SbO}_6$

*Zvereva E.A.*¹, *Ermolov A.S.*¹, *Nalbandyan V.B.*², *Strelsov S.V.*^{3,8}, *Ushakov A.V.*³, *Silhanek A.V.*⁴, *Abdel-Hafiez M.*⁴, *Moshchalkov V.V.*⁵, *Feng H.-L.*⁶, *Yamaura K.*⁶, *Büchner B.*⁷, *Vasiliev A.N.*^{1,8}

¹ Physics Faculty, Moscow State University, Moscow, Russia

² Chemistry Faculty, Southern Federal University, Rostov-on-Don, Russia

³ Institute of Metal Physics, Ekaterinburg, Russia

⁴ Département de Physique, Liège University-Belgium, Liege, Belgium

⁵ INPAC – K. U. Leuven, Leuven, Belgium

⁶ National Institute for Materials Science, Ibaraki, Japan

⁷ Leibniz Institute for Solid State and Materials Research IFW Dresden, Germany

⁸ Theoretical Physics and Applied Mathematics Department, Ural Federal University, Ekaterinburg, Russia

zvereva@mig.phys.msu.ru

We report on the static and dynamic magnetic properties of quasi-two dimensional honeycomb-lattice silver dellafossite $\text{Ag}_3\text{Co}_2\text{SbO}_6$. The magnetic susceptibility and specific heat data are consistent with the onset of antiferromagnetic long range order at low temperatures with Néel temperature $T_N \sim 25$ K. In addition the magnetization curves revealed a field-induced (possibly spin-flop type) transition below T_N in moderate magnetic fields, suggesting that the magnetic ground state is complicated. The LDA+U calculations corroborate this finding and show that the intralayer exchange J is antiferromagnetic and exceeds 4.5 K. This exchange coupling is likely to be related with superexchange between half-filled t_{2g} and e_g orbitals. Electron spin resonance (ESR) spectra have revealed a Gaussian shape line attributed to Co^{2+} ion in octahedral coordination with average effective g-factor $g=2.3\pm 0.1$ at room temperature and shown strong divergence of ESR parameters below ~ 120 K, which imply an extended region of short-range order correlations in the compound studied. Based on the results of magnetic and thermodynamic studies in applied fields up to 9 T we propose the magnetic phase diagram in agreement with our experimental findings.

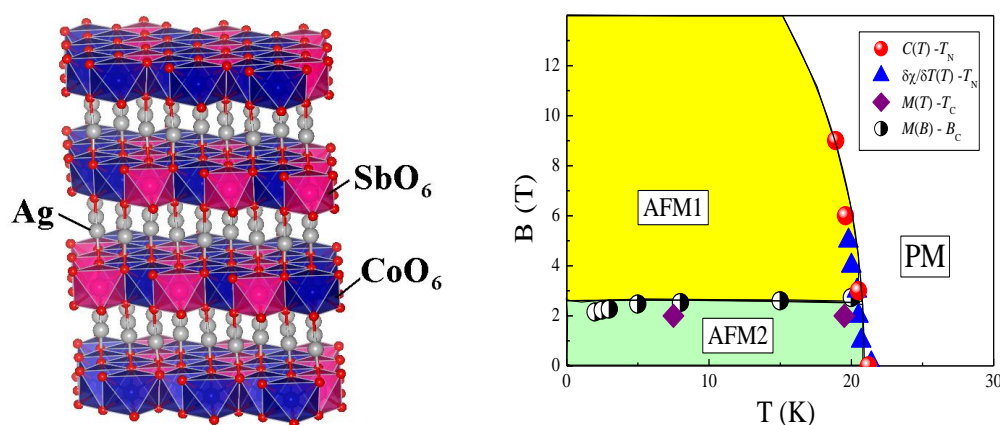


Fig. 1. Polyhedral view of a layered crystal structure (left) and magnetic phase diagram (right) for quasi-two dimensional honeycomb oxide $\text{Ag}_3\text{Co}_2\text{SbO}_6$

Support by RFBR (grants 14-02-00245, 14-03-01122, 13-02-00374), Samsung GRO and FNRS is acknowledged.

30PO-I1-24

STATIC AND DYNAMIC MAGNETIC PROPERTIES OF LAYERED HONEYCOMB LATTICE ANTIMONATES $A_3Ni_2SbO_6$ (A=Li, Na)

Zvereva E.A.¹, Kudryashov V.Y.¹, Nalbandyan V.B.², Evstigneeva M.², Lin J.-Y.³, Vavilova E.L.⁴, Abdel-Hafiez M.⁵, Silhanek A.V.⁵, Li J.⁶, Yamaura K.⁷, Stroppa A.⁸, Valenti R.⁹, Vasiliev A.N.¹

¹ Physics Faculty, Moscow State University, Moscow, Russia

² Chemistry Faculty, Southern Federal University, Rostov-on-Don, Russia

³ National Chiao Tung University, Hsinchu, Taiwan

⁴ Zavoisky Physical-Technical Institute (ZPhTI) of the Kazan Scientific Center of the Russian Academy of Sciences, Kazan, Russia

⁵ Département de Physique, Liège University-Belgium, Liege, Belgium

⁶ INPAC – K. U. Leuven, Leuven, Belgium

⁷ National Institute for Materials Science, Ibaraki, Japan

⁸ CNR-SPIN, L'Aquila, Italy

⁹ Institut für Theoretische Physik, Goethe-Universität Frankfurt, Frankfurt am Main, Germany
zvereva@mig.phys.msu.ru

We report on the static and dynamic magnetic properties of quasi-two dimensional honeycomb oxides $A_3M_2SbO_6$ ($A = Li, Na$), which can be potentially interesting for the application in electrochemical power devices. Both compounds order antiferromagnetically with the Néel temperature ~ 15 and 17 K respectively. At high temperatures, the magnetic susceptibility follows the Curie-Weiss law with positive values of Weiss temperature ~ 8 K for Li sample and ~ 12 K for Na sample indicating predominance of ferromagnetic interactions. The effective magnetic moment is $4.3 \mu_B/f.u.$ and agrees satisfactorily with theoretical estimations using determined in our work effective g-value ~ 2.15 and assuming high-spin state of Ni^{2+} .

Summarizing the data, the magnetic phase diagram for $A_3Ni_2SbO_6$ were suggested (Fig. 1). With increasing magnetic field the T_N phase transition boundary shifts slowly to lower temperature side. In addition, the field-induced spin-reorientation (spin-flop) phase is likely to be realized at low temperatures. The main superexchange interaction via half-occupied Ni e_g ($d_z^2, d_{x^2-y^2}$) orbitals is appears to be ferromagnetic. This assumption is in accordance with predominance of ferromagnetic coupling at high temperatures. At the same time, the observation of long range antiferromagnetic order implies antiferromagnetic interactions between the ferromagnetic layers providing the antiferromagnetic ground state of this compound.

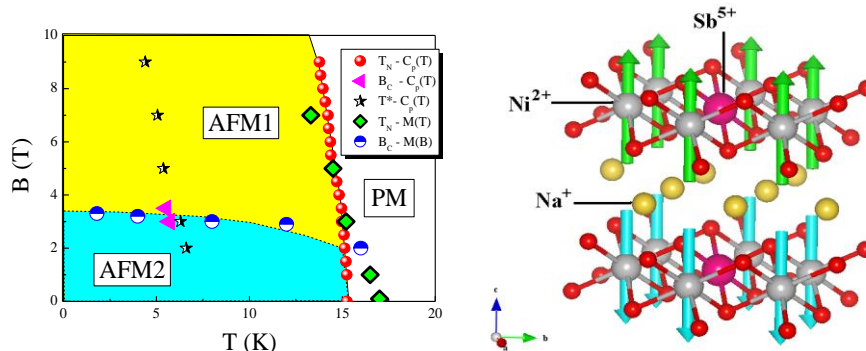


Fig. 1. Magnetic phase diagram (left) and possible spin-configuration model (right) for quasi 2D honeycomb oxide $Na_3Ni_2SbO_6$

The main superexchange interaction via half-occupied Ni e_g ($d_z^2, d_{x^2-y^2}$) orbitals is appears to be ferromagnetic. This assumption is in accordance with predominance of ferromagnetic coupling at high temperatures. At the same time, the observation of long range antiferromagnetic order implies antiferromagnetic interactions between the ferromagnetic layers providing the antiferromagnetic ground state of this compound.

Support by RFBR (grants 14-02-00245, 14-03-01122) is acknowledged.

30PO-I1-25

MAGNETIC PROPERTIES OF Co/Cu MULTILAYERED WIRES ELECTROLESS DEPOSITED IN DIFFERENT POROUS TEMPLATE

Chekanova L.A.¹, Denisova E.A.¹, Melnikova S.V.², Iskhakov R.S.¹, Komogortsev S.V.¹, Velikanov D.A.^{1,2}, Nemtsev I.V.³

¹ Kirensky Institute of Physics SB RAS, Krasnoyarsk, Russian Federation

² Siberian Federal University, Krasnoyarsk, Russian Federation

³ Krasnoyarsk Scientific Center SB RAS, Krasnoyarsk, 660036, Russian Federation
rauf@iph.krasn.ru

Metal nanowires are promising materials for a variety of applications, ranging from magnetic, high-frequency, optical, and electronic devices to chemical, biological and optomagnetic improved sensing devices [1]. Arrays of parallel magnetic nanowires embedded in a dielectric insulating material are very attractive regarding microwave devices. It should be noted that full microwave penetration is assured in nanowires when the diameter is less than the penetration depth, typically in the range 0.3–1 μm at 10 GHz for ferromagnetic metals. On the other hand, extensive measurements have shown that nanowire arrays present strong absorption peaks in the absence of an applied magnetic field in the gigahertz range due to the ferromagnetic resonance.

In this paper, the magnetic anisotropy and the dynamic magnetic properties of 10 - 20 μm long electroless deposited Co/Cu wires with diameters ranging from 50 to 500 nm are studied.

Co(P) homogeneous wires and Co(P)/Cu multilayered wires were fabricated in the anodized aluminium templates using the electroless deposition technique and also in ion-track etched polycarbonate templates (PKTM) and porous silica for comparison. The thicknesses of the Cu and Co layers were controlled in the range of 6 to 240 nm by varying each deposition time. The effects of the synthesis parameters on the structural and magnetic properties in arrays of electroless deposited Co/Cu wires and rods have been studied combining ferromagnetic resonance, magnetometry and electron microscopy. Magnetization curves were measured as functions of thicknesses of the Cu and Co(P) layers, field orientation, and template materials. Information on local anisotropy field and the grain size in the Co(P) wires was obtained from investigation of approach magnetization to saturation law. It is shown that, depending on the synthesis parameters, the average crystallographic structure can be controlled, giving rise to sensible changes in the effective crystal anisotropy field. It is found that the easy axis of the all samples is along the wires. All wires reveal a very similar behavior of the resonance field (H_r) vs angle, independent of the wire diameter and wire density, corresponding to the uniform precession mode of an infinite cylinder including the shape demagnetization anisotropy and a uniaxial anisotropy contribution. It is observed that the H_r value decreases with a reduction in Cu layer thickness (fig.1). The effects of different materials of matrices on the FMR-spectra characteristics are studied.

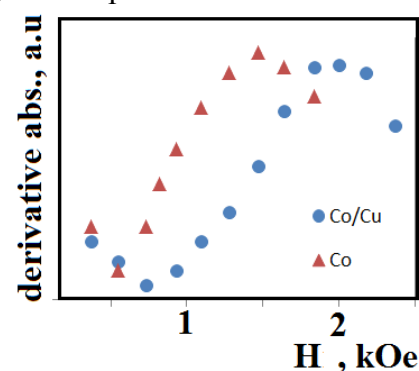


Fig.1. FMR derivative spectra for Co and Co/Cu wires embedded into PKTM with nominal pores diameter 500-nm at 9.2 GHz.

Support by RFBR 13-03-00476-a is acknowledged.

[1] L. Piraux, A. Encinas, L.Vila, S. Matefi-Tempfli, M. Matefi-Tempfli, M. Darques, F.Elhoussine, S. Michotte, *JNN*, **5** (2005) 372–389.

30PO-I1-26

THERMODYNAMIC PROPERTIES OF LOW DIMENSIONAL MAGNETIC MINERAL SHATTUCKITE

Koshelev A.V.¹, Golovanov A.N.¹, Zvereva E.A.¹, Chareev D.A.², Volkova O.S.¹, Vymazalova A.³

¹ MSU, Moscow, Russia

² IEM, Chernogolovka, Russia

³ Czech Geological Survey, Praha, Czech Republic

anatolkosh@mail.ru

Rare mineral shattuckite with chemical formula $\text{Cu}_5(\text{OH})_2(\text{SiO}_3)_4$ has an interesting and exotic topology of magnetic sub-system, constituted by both two-dimensional brucite-like patterns and one-dimensional ferromagnetic chains of divalent copper ions in planar surrounding of oxygen atoms.

As shown in Fig. 1, the magnetic susceptibility exhibits a transition to magnetically ordered state at 7K. The magnetically ordered state possesses small uncompensated magnetic moment. Taking into account the negative Weiss temperature of $\Theta = -13.5\text{K}$ one can assume the predominance of antiferromagnetic exchange in paramagnetic state. The Curie constant $C = n g^2 \mu_B^2 S(S+1) = 2.2 \text{ emu K}$ is in agreement with number of divalent copper ions ($n=5$) in the formula unit of shattuckite and g-factors of copper determined by ESR measurements.

In the upper inset to Fig. 1 the hysteresis loops are shown taken in temperature range from 2 K to 12 K, which proves the presence of finite magnetization at low temperatures. In the lower inset to Fig.1 the temperature dependence of the Curie constant $C=(\chi-\chi_0)(T-\Theta)$ is shown indicating strengthening of antiferromagnetic correlations.

Measurements of specific heat in shattuckite evidences a rounded maximum at $T_N=7\text{K}$, corresponding to the transition into magnetically ordered state.

The ESR measurements, performed at temperature range of 8-300K show the anisotropic g-factors $g_{\parallel} = 2.19$ and $g_{\perp} = 2.07$.

So, taking into consideration this measurements of magnetization, ESR, hysteresis loops and specific heat we can assume that the long-range magnetic order establishes at $T_N=7\text{K}$ and has ferrimagnetic nature.

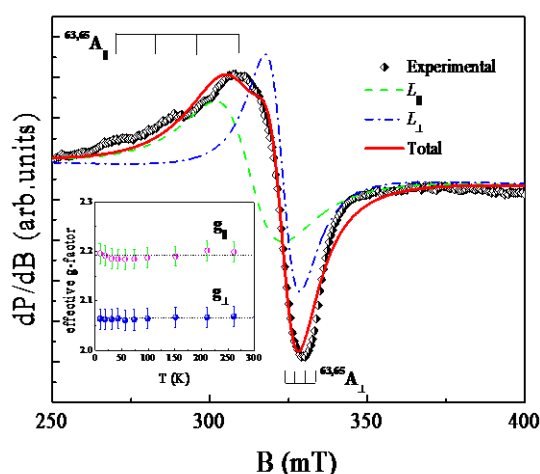
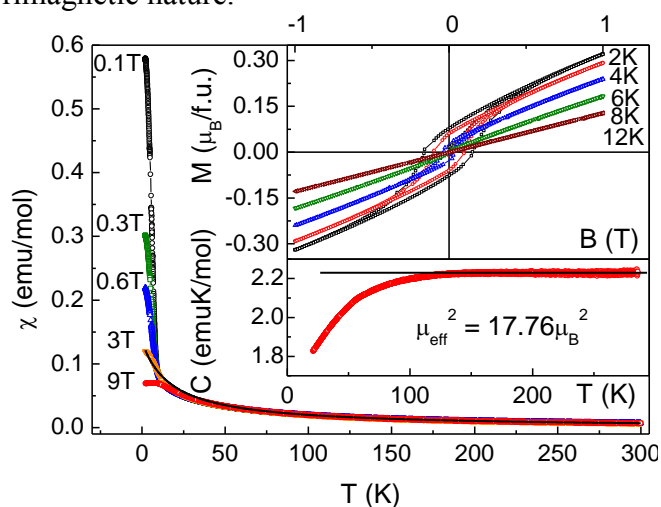


Fig. 1. Magnetic susceptibility, hysteresis loops and Curie constant. Fig. 2. ESR spectrum of shattuckite at 8K.

Support by grant of president of Russian Federation MK-7138.2013.2.

30PO-I1-27

DEPENDENCE OF THE COERCIVE FIELD ON THE SIZE OF CORE-SHELL NANOPARTICLES

Anisimov S.V.¹, Afremov L.L.², Iliushin I.G.³

Far Eastern Federal University (FEFU), Vladivostok, Russia
1ahriman25@gmail.com, 2afremov.ll@dvf.ru, 3futed@gmail.com

The interest in studying core-shell nanoparticles is due to the wide use in such areas as development of storage devices, sensors, electronic, optoelectronic and catalysis, medical biotechnologies and drug delivery [1-3].

Magnetic properties of heterophase nanoparticles may vary with size, that can be due to change of magnetic characteristics (spontaneous magnetization, magnetic anisotropy constant etc.), and the influence of thermal fluctuations. In this paper we represent theoretical analysis of size dependence of coercive field.

The following model was used in calculations [4]:

1. Uniformly magnetized nanoparticle (phase (1)) which has the shape of an ellipsoid of rotation comprises uniformly magnetized ellipsoidal inclusion (phase (2)), the long axis of which coincides with the long axis of the particle;

2. It is considered that the axis of anisotropy both uniaxial ferromagnetics are parallel to the long axis of the nanoparticle.

According to [4] core-shell nanoparticle can be in one of four states: 1 - magnetic moments of both phases of the magnetic moments are parallel and directed along an axis Oz; 2 - phases of the magnetic moments are antiparallel, the magnetic moment of the first phase is directed along the axis Oz; 3 - magnetic moments of both phases are antiparallel relative to the axis Oz; 4 - a magnetic moment of second phase oriented along the axis Oz, and first - against the axis Oz.

Magnetization of this kind of nanoparticles is defined by occupation probabilities vector of these states $\mathbf{n}(t) = \{n_1(t), n_2(t), n_3(t), n_4(t)\}$, which can be written as $dn(t)/dt = \bar{W} \mathbf{n}(t)$ with initial conditions $\mathbf{n}(0) = \mathbf{n}_0$. In this equation \bar{W} - matrix of transition probabilities between these states, matrix elements are the barriers separating corresponding states.

Fig. 1 shows H_c calculation for Fe-Fe₃O₄ nanoparticles. The figure shows that calculated dependence of the coercive field on the particle size agrees qualitatively with the experimental results [5].

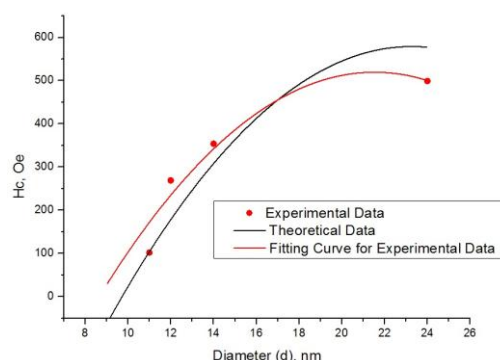


Fig. 1. Dependence of the coercive field H_c on size d for Fe-Fe₃O₄ nanoparticles.

- [1] Wei Wu, Quanguo He, Changzhong Jiang, *Nanoscale Res. Lett.*, **3** (2008) 397-415.
 [2] F. Frederix, J. M. Friedt, K. H. Choi et al., *Analytical Chemistry*, **75** (2003) 24.
 [3] J. Neamtu, N. Vegra, *Journal of Nanomaterials and Biostructures*, **6** (2011) 3, 969-978.
 [4] Afremov. L.L., Ilyushin I.G., *Journal of Nanomaterials*, **2013** (2013) 687613, 15.
 [5] Maninder Kaur, John S. McCloy, Weilin Jiang, Qi Yao, You Qiang, *J. Phys. Chem. C*, **116** (2012) 12875–12885.

30PO-I1-28

RELAXATION PROCESS IN Co/Au MAGNETIC NANOPARTICLES

Zeľňáková A.¹, Hrubovčák P.¹, Zeľňák V.², Kováč J.³

¹ Department of Solid State Physics, P.J. Šafárik University, Košice, Slovakia

² Department of Inorganic Chemistry, P.J. Šafárik University, Košice, Slovakia

³ Institute of Experimental Physics, Slovak Academy of Sciences, Košice, Slovakia

hrubovcak.pavol@gmail.com

Dynamic properties and relaxation processes in Co/Au core/shell nanoparticles system were investigated. Particles of average diameter $d \sim 8$ nm were observed employing transmission electron microscope and the presence of two separate phases of Co and Au was confirmed utilizing high energy powder X-ray diffraction. Series of magnetic measurements were carried out in static (DC) and alternating (AC) magnetic field utilizing SQUID MPMS 5XL magnetometer in temperature range of 2 - 300 K. The dependence of magnetization on temperature recorded at zero external magnetic field revealed the presence of one maximum around the temperature of 6 K, what can be regarded as the experimental blocking temperature T_B [1]. Measurements of the dependence of both contributions (in-phase and out-of-phase) of magnetic complex susceptibility on temperature at different frequencies of alternating magnetic field (0.1 Hz - 1 kHz) also displayed one maximum for each frequency, Fig. 1. The shift of the maximum of the in-phase susceptibility towards higher temperature with increasing frequency in conjunction with its decrease with the frequency increment point out the relaxation process of magnetic moments of individual particles [2].

The quantitative analysis of experimental data by means of The Model Independent Classification of the Blocking/Freezing Process via C_I parameter [3], by Critical Slowing Down theory [4] and by the Cole-Cole diagrams suggest the collective freezing processes predominate over the blocking of magnetic moments of individual particles in the system.

This work was supported by the Slovak Research and Development Agency under the contract APVV-0222-10 and VEGA (No. 1/0583/11, No. 1/0861/12) projects of Ministry of Education of the Slovak Republic and by the ERDF EU grant under No. ITMS 26220220105. The authors (A.Z and V.Z) would like to thank DESY/HASYLAB project under No. I-20110282 EC.

[1] C. Vázquez-Vázquez, M. A. López-Quintela, M. C. Buján-Núñez, J. Rivas, *J. Nanopart. Res.*, **13** (2010) 1663.

[2] F. Jimenez-Villacorta, *Phys. Rev. B*, **82** (2010) 134413.

[3] M. Tadić, D. Marković, V. Spasojević, V. Kusigerski, M. Remškar, J. Pirnat, Z. Jagličić, *J. All. Comp.*, **441** (2007) 291.

[4] C. Djurberg, P. Svedlindh, P. Nordblad, *Phys. Rev. Lett.*, **79** (1997) 5154–5157.

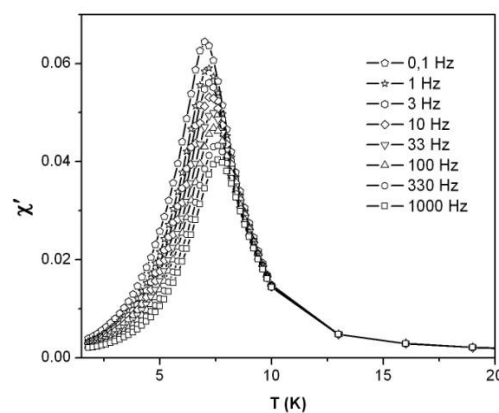


Fig. 1. The dependence of in-phase contribution of complex magnetic AC susceptibility on temperature at different frequencies.

30PO-I1-29

CALCULATION OF ENERGY AND MAGNETIC CHARACTERISTICS FOR MULTILAYER MAGNETIC FILMS ON METAL SURFACES

Mamonova M.V.¹, Prudnikov V.V.¹, Pilipenko D.V.¹

¹ Omsk State University, Omsk, Russia

mamonova_mv@mail.ru, prudnikov@univer.omsk.su, virgo54@mail.ru

At present time, a large number of experimental works have been devoted to the study of magnetic ordering in Fe, Co, and Ni ultrathin films [1]. The investigation of a nature of magnetism in these structures has a large fundamental interest through an observable dimensionality crossover of magnetic characteristics from three dimensional values for films with thickness $d \geq 10$ nm to two dimensional values for films with thickness $d \leq 1-2$ nm. It has been established that the long-range ferromagnetic order arises in films at some effective film thickness. However, the nature and regularities of this phenomenon remain not quite clear.

In this work, we use the spin-density functional method for theoretical description of multilayer ferromagnetic film formation in process of Fe, Co, and Ni transition metal ions adsorption on a nonmagnetic metal substrate. We include into consideration the thermal effects of transition metal ions intermixing inside film and their substitution with atoms of substrate surficial layer. The energy and magnetic characteristics of multilayer films were calculated for surface systems Fe(110)/W(110), Fe(110)/Ag(111), Ni(111)/Cu(111), and Co(111)/Cu(111) in dependence on their thickness in the units of number N monolayers for different temperatures (Fig.1).

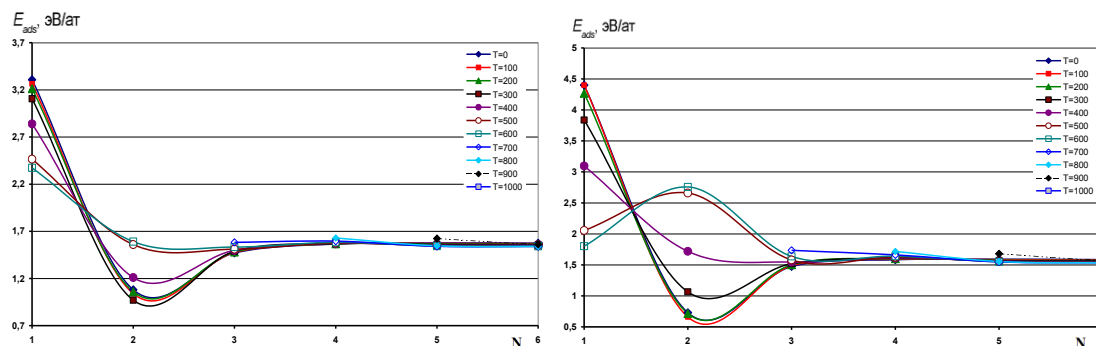


Fig.1. The dependence of adsorption energy for Fe(110)/W(110) and Fe(110)/Ag(111) systems on thickness N for Fe film.

It was shown that the energy of interfacial interaction per unit area and adsorption energy considerably depend on the thickness films, temperature, and properties of metal substrate with significant difference of the monolayer film properties from properties of films with large thicknesses. The energy and magnetic characteristics demonstrate that for film thickness $N \geq 5$ their values cease to depend on properties of metal substrate and further begin to depend on surface properties of films.

Support by Ministry of Education and Science of Russia through project No. 1627 is acknowledged.

[1] C.A.F. Vaz, J.A.C. Bland, G. Lanhoff, *Reports Progr. Phys.*, **71** (2008) 056501.

30PO-I1-30

ADSORPTION AND MAGNETIC PROPERTIES OF ULTRATHIN Fe AND Ni ALLOY FILMS WITH AN INHOMOGENEOUS MAGNETIZATION DISTRIBUTION.

Mamonova M.V., Prudnikov V.V., Pilipenko D.V.

Omsk State University, Omsk, Russia

virgo54@mail.ru, mamonova_mv@mail.ru, prudnikov@univer.omsk.su

The physical properties of ultrathin magnetic films are the subject of intense research investigations [1, 2], which are determined by many their applications in microelectronics and computer technology. For example, permalloy $\text{Fe}_{20}\text{Ni}_{80}$ is used in transformer laminations and magnetic recording heads. In this work, the spin density functional method was used for description of the temperature and ferromagnetic ordering influence on the adsorption properties of $\text{Fe}_x\text{Ni}_{1-x}$ alloy films on the nonmagnetic material surfaces. We used two-dimensional XY model for description of the temperature dependence of the relative magnetization with taking into consideration the inhomogeneous distribution of magnetization in surficial region. For theoretical description we applied the method of multi-parameter probe functions [3] the parameters of which are determined by the numerical minimization procedure of the interfacial energy functional in the subsurface region. The conditions for the formation of ultrathin ferromagnetic films stable with respect to island adsorption with a change in the coverage parameter θ are revealed. The equilibrium vacuum gap which simulates the effective influence of the atomic roughness of the substrate is determined from the minimum of the total interfacial energy. This approach makes it possible to predict the formation of stable $\text{Fe}_x\text{Ni}_{1-x}$ coatings or to reveal their absence in depending on concentration x .

T,K	Θ	X, %
0	0.7	[30-100]
	[0.8-1]	[50-100]
200	0.8	[50-100]
	[0.9-1]	All concentration
600	0.9	[17-100]
	1	All concentration

Table 1. Formation conditions of stable $\text{Fe}_x\text{Ni}_{1-x}$ film on W[110] substrate.

T,K	Θ	X, %	T,K	Θ	X, %
0	[0.5-0.7]	All concentration	200	0.7	[40-100]
	0.8	[0-60]		0.8	[60-100]
	0.9	[0-20]		0.9	[0-60]
	1	0		1	[0-20]
100	[0.7, 0.8]	All concentration			
	0.9	[0-40]			
	1	[[0-20]			

Table 2. Formation conditions of stable $\text{Fe}_x\text{Ni}_{1-x}$ film on Cu[111] substrate.

Some results of calculations are given in Tables 1 and 2. Note, that the stable monolayer film on W[110] substrate begins to form for values of $\theta \geq 0.7$ at $T=0$ K, and for $\theta \geq 0.8$ only at $T \geq 100$ K. For samples with boundary values of θ , the stable films are realized for high iron concentrations. It was found that stable $\text{Fe}_x\text{Ni}_{1-x}$ film on Cu[111] substrate is not realized also in the region of small $\theta < 0.7$ ($T > 0$ K), but samples with the values of coverage $\theta = 0.9-1.0$ are realized for low concentrations of iron only.

[1] C.A.F. Vaz, J.A.C. Bland, G. Lauhoff, *Reports on Progress in Physics*. **71** (2008) 056501.

[2] M.V. Mamonova, N.S. Morozov, V.V. Prudnikov, *Physics of the Solid State* **51** (2009) 10, 2169–2177.

[3] M.V. Mamonova, V.V. Prudnikov, and I.A. Prudnikova. *Surface Physics. Theoretical Models and Experimental Methods*. - CISP, CRC Press, Taylor & Francis Group, Boca Raton-London-New York, (2013) 384.

30PO-I1-31

LOW TEMPERATURE ANOMALIES OF THE HEAT CAPACITY OF $\text{Ho}_x\text{Lu}_{1-x}\text{B}_{12}$

*Khoroshilov A.L.^{1,2}, Sluchanko N.E.², Bogach A.V.², Glushkov V.V.^{1,2}, Demishev S.V.^{1,2},
Samarin N.A.², Shitsevalova N.Y.³, Filippov V.B.³, Gabani S.⁴, Flachbart K.⁴*

¹ Moscow Institute of Physics and Technology, Dolgoprudny, Russia

² A.M. Prokhorov General Physics Institute of RAS, Moscow, Russia

³ Institute for Problems of Materials Science, NAS of Ukraine, Kiev, Ukraine

⁴ Institute of Experimental Physics, SAS, Košice, Slovakia

Heat capacity measurements on high quality single crystals of $\text{Ho}_x\text{Lu}_{1-x}\text{B}_{12}$ ($x \leq 1$) have been carried out in a wide range of temperatures (0.07 – 300 K) and in external magnetic field up to 90 kOe. For concentrations with $x \geq 0.2$ antiferromagnetic phase transitions with T_N in the range of 1-7.7 K have been detected (Fig 1a).

Detailed investigations of received heat capacity dependencies within the framework of approach developed in [1] allowed us to separate the contributions to heat capacity. From this analysis it follows that in $\text{Ho}_x\text{Lu}_{1-x}\text{B}_{12}$ compounds there are two magnetic contributions to heat capacity. The first one may be described as a magnetic three-level Schottky anomaly attributed to Γ_5 triplet ground state of holmium Ho^{3+} ions [2] splitted by external magnetic field. The second component appears due to hyperfine splitting of holmium nuclear levels, and it can be approximated by a nuclear multi-level Schottky anomaly (see Figs 1b, 1c). The performed analysis allowed us to estimate the hyperfine field on holmium sites and the effective g-factor for all investigated Ho-concentrations.

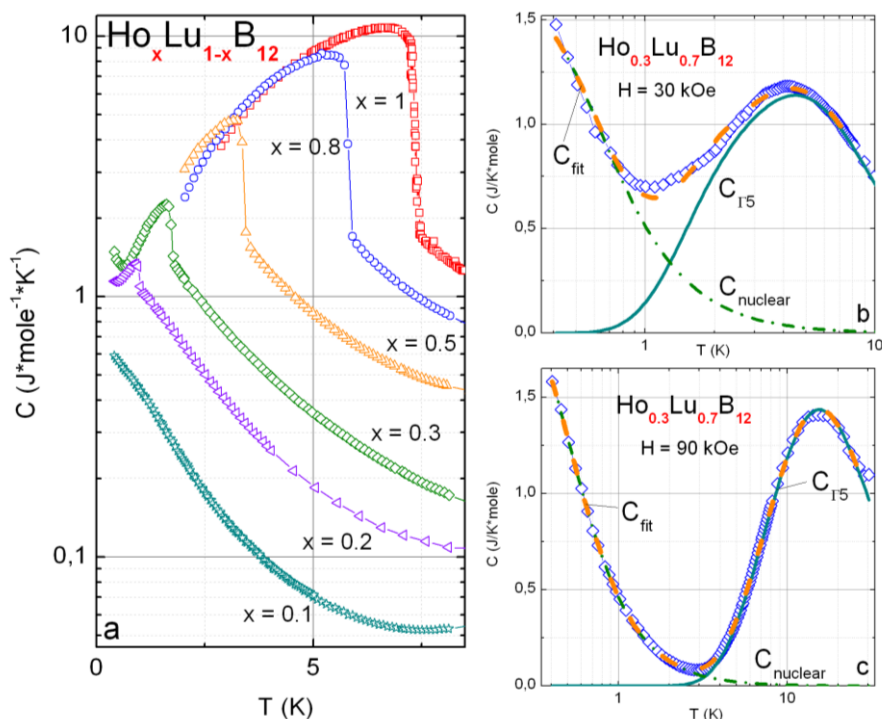


Fig 1. Low temperature heat capacity of $\text{Ho}_x\text{Lu}_{1-x}\text{B}_{12}$ (a), of $\text{Ho}_{0.3}\text{Lu}_{0.7}\text{B}_{12}$ in magnetic field of $H = 30$ kOe (b), and $H = 90$ kOe (c).

[1] N.E. Sluchanko, *JETP*, **140** (2011) 536-552.

[2] K. Siemensmeyer, *J. Low Temp. Phys.*, **146** (2007) 581-605.

30PO-I1-32

INFLUENCE OF THE SIZE EFFECT ON THE THERMODYNAMIC CHARACTERISTICS OF THE PHASE TRANSITION IN ULTRATHIN FILMS

Petrov A.A.¹, Afremov L.L.¹

¹ Far Eastern Federal University, Vladivostok, Russia
aleksandr.al.petrov@gmail.com

It is known that such characteristics of the phase transition as critical temperature T_c , heat capacity c_p and magnetic susceptibility χ have a significant influence of the ultrathin film thickness [1 – 4].

There is the magnetic susceptibility χ to be calculated depending on the thickness of the film in the approximation of the “average spin” [3, 4] in the framework of the following model:

- Ultrathin film consist of N monolayers;
- The direct exchange interaction occurs only between the nearest neighbors; moreover, interaction fields h between spin magnetic moments of atoms are distributed in a random manner;
- Spin magnetic moments are oriented along an axis Oz (approximation of the Ising model).

The calculation results are presented in the Fig. 1 and illustrate the dependence of the relative heat capacity c_p/k (k – the Boltzmann constant) per atom of the film thickness N . The calculated dependence $c_p(N)$ of the heat capacity of the film thickness is in qualitative agreement with experimental data [1]. The «average spin» method has made it possible to investigate the influence of the size effect on the ultrathin film magnetic susceptibility. We note that results are in good agreement with experimental data [2].

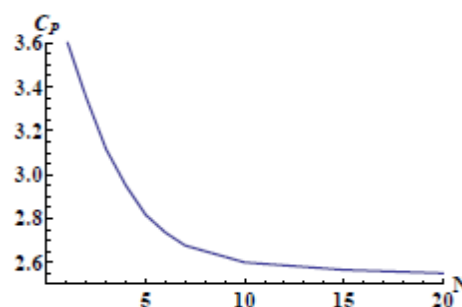
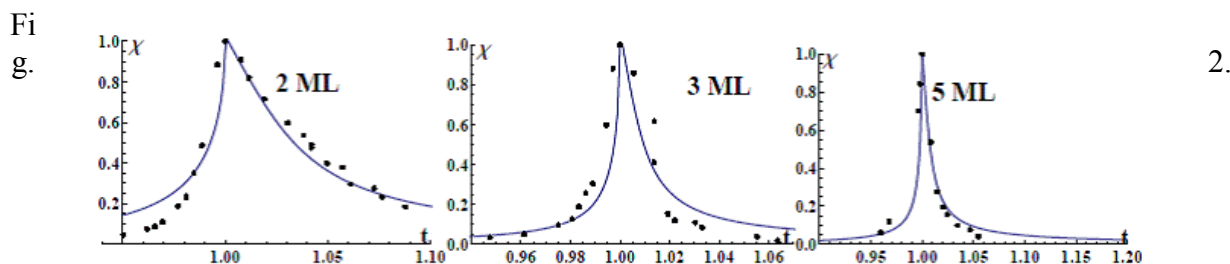


Fig. 1. The dependence of the relative heat capacity c_p/k per atom of the film thickness N .



Dependence of magnetic susceptibility of the relative temperature for $Ni_{50}Fe_{50}$ films of 2 ML, 3 ML, 5 ML. Dots show the experimental data [2].

- [1] A.F. Lopeandia, F. Pi, J. Rodriguez-Viejo, *Appl. Phys. Lett.*, **92** (2008) 122503.
 [2] R. F. Willis, T.S. Bramfeld, K.R. Podolak, *J. Appl. Phys.*, **101** (2007) 07C718.
 [3] L.L. Afremov, Yu. V. Kirienko, *Advanced Materials Research*, **683** (2013) 69-72.
 [4] L.L. Afremov, A.A. Petrov, *Advanced Materials Research*, **813** (2013) 319-322.

30PO-I1-33

Ab INITIO STUDY OF THE OXYGEN EFFECT ON MAGNETIC INTERACTIONS WITHIN 3d-METAL NANOWIRES ON THE VICINAL Rh(553) SURFACE

Kamynina I.A.¹, Bazhanov D.I.¹, Korobova J.G.¹

¹ Faculty of Physics, M.V. Lomonosov Moscow State University, Moscow, 119991, Russia
kamyninaia@gmail.com

Recently intensive theoretical and experimental research was focused on the study of linear nanostructures due to exceptional physical and chemical properties of low-dimensional systems and, consequently, their possible applications in the development of advanced technologies [1, 2]. One-dimensional nanostructures exhibit qualitatively different electronic and magnetic properties as compared to the same materials in larger scales. The different behavior can be used in developing of novel materials with the specific magnetic and electronic properties.

Recent experimental work showed the possible formation of one-dimensional metal-oxide structures (1D-oxide) during the oxidation of bimetallic Ni-Rh nanowires on stepped Rh(553) surface [3]. Besides, in the work [4] 1D- Mn oxides were produced on vicinal Pd surfaces. Such interesting experimental results motivated us to carry out *ab initio* study of oxygen effect on the electronic and magnetic properties of Mn and Ni nanowires on the vicinal Rh(553) surface. Our calculations were performed within the framework of density functional theory (DFT).

Our electronic structures calculations showed that electronic states of Ni and Mn atoms in the nanowires are weakly hybridized at the step edge with electronic states of Rh(553) substrate atoms and have distinct magnetic properties. It was found that Ni and Mn atoms in the nanowires have local magnetic moment values of $\sim 3.75\mu_B$ and $\sim 0.62\mu_B$ respectively. Investigation of the magnetic interactions showed that the atomic spins of Mn atoms in the nanowire demonstrate sustainable antiferromagnetic coupling with an energy $\Delta E = E^{FM} - E^{AFM} = 277.8$ meV. In contrast, the spins of Ni atoms in the nanowire prefer the ferromagnetic (FM) alignment with a small difference in energy $\Delta E = E^{FM} - E^{AFM} = -27.4$ meV. Then we performed calculations of one-dimensional metal-oxides Mn-O and Ni-O on the Rh(553) surface with submonolayer quantities of 0.1 ML and 0.4 ML oxygen. (Fig.1.). We obtained that one-dimensional Ni-O nanowires are in a stable paramagnetic state. Strong hybridization between Ni and O atoms and the changes in the band structures of nickel atoms lead to a quenched magnetic moment for the nickel atoms. The study of the magnetic properties of Mn-O showed that the manganese atoms retain magnetic moment slightly reducing its value to $\sim 3.42\mu_B$ and $\sim 3.11\mu_B$ due to the interaction with oxygen for 0.1 ML and 0.4 ML coverage respectively. We also found that manganese atoms in Mn-O nanowires retain antiferromagnetic coupling with an energy $\Delta E = E^{FM} - E^{AFM} = 328.2$ meV and $\Delta E = E^{FM} - E^{AFM} = 90.2$ meV for 0.1 ML and 0.4 ML respectively. The obtained results are applying for to further study of the oxygen effect on magnetic anisotropies of 3d-metal nanowires on the vicinal Rh(553) surface.

Support by the Russian Foundation for Basic Research (Grant № 13-02-01322-a).

- [1] K. Kuhnke, K. Kern, *J. Phys. Condens. Matter*, **15** (2003) S3311.
 [2] A. Mugarza, J.E. Ortega, *J. Phys. Condens. Matter*, **15** (2003) S3281.
 [3] J. Schoiswohl et al., *Phys.Rev. Lett.*, **97** 126102 (2006).
 [4] C. Franchini et al., *J. Phys.: Condens. Matter*, **24** 042001 (2012).

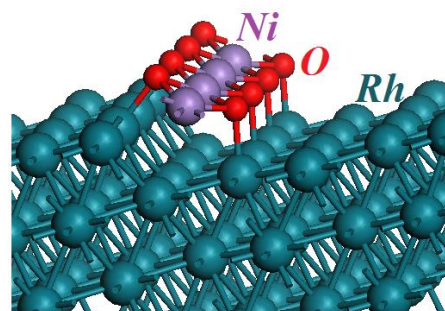


Fig. 1. One-dimensional metal-oxides Ni-O on the Rh(553) surface with submonolayer quantities of 0.4 ML oxygen.

30PO-I1-34

THICKNESS DEPENDENCE OF THE CRITICAL FIELDS IN THE FERROMAGNETIC INVERSE OPAL-LIKE STRUCTURES BY SANS AND SQUID-MAGNETOMETRY

*Shishkin I.S.*¹, *Mistonov A.A.*¹, *Grigoryeva N.A.*¹, *Menzel D.*², *Napolskii K.S.*³, *Sapoletova N.A.*³,
*Eliseev A.A.*³, *Grigoriev S.V.*^{1,4}

¹ Faculty of Physics, Saint Petersburg State University, Saint Petersburg, Russia

² Institut für Physik der Kondensierten Materie Technische Universität, Braunschweig, Germany

³ Department of Materials Science, Moscow State University, Moscow, Russia

⁴ Petersburg Nuclear Physics Institute, Gatchina, Russia

shishkin-ivan@list.ru

Inverse opal-like structures (IOLS) can be synthesized by filling the voids of opal templates with suitable structure-forming precursors and subsequent removal of the initial microspheres to leave three-dimensionally ordered porous materials. The inverse opals based on the ferromagnetic metals (Ni, Co, etc), represent a new class of the 3-dimensional nanoscale ferromagnetic structures, which are geometrically frustrated at room temperature. Its structure is an array of quasicubes and quasitetrahedra (which were the octahedral and tetrahedral voids in initial opal template,

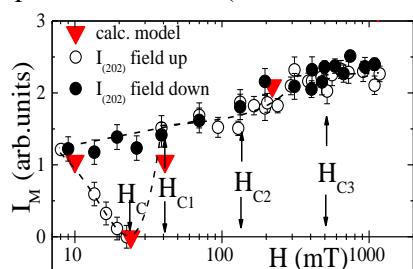


Fig. 1 The dependence of intensity on the external magnetic field for the sample

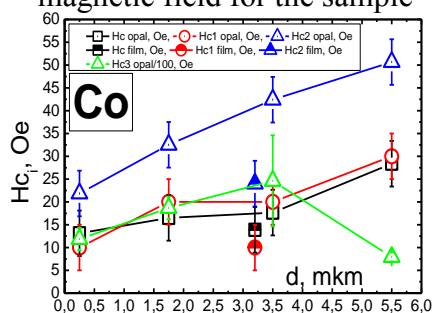


Fig. 2 Dependence of the value of critical fields on the thickness

respectively), connected via “bridges” along $\langle 111 \rangle$ -type axes of fcc structure. Because of that, it is assumed that the magnetic structure of the IOLS is a system of 4 magnetic subsystems, directed along these $\langle 111 \rangle$ axes. Diffraction patterns of IOLS based on cobalt with thickness of 8.5 microns by method of small-angle neutron scattering in the research center Geesthaht, Germany, were obtained. Coinciding of positions of magnetic and structural Bragg reflections indicates a strong correlation of magnetic and spatial structures of the IOLS. The intensity of the Bragg peak, corresponding to magnetic neutron scattering is determined by the total magnetization of the scattering crystallographic plane, that is, the sum of the magnetic subsystems projections on this plane. Thus, by analyzing the intensity of the different peaks one can obtain the magnetization distribution in the sample. In Fig. 1 an example of the dependence of magnetic intensity of the $(20\bar{2})$ reflex on the external magnetic field is presented. Since magnetizing of each subsystem takes place in different critical fields, this dependence is stepped and one can distinguish critical values of the magnetic field H_C , H_{C1} , H_{C2} , H_{C3} . Remagnetization curves of the IOLS with thicknesses in the

range from 0.25 mkm to 5.5 mkm, and at angles in the range from 0° to 90° (between the normal to the sample plane and the vector of the external magnetic field) have been measured by SQUID magnetometry. For each sample were determined critical fields mentioned above which are corresponding to coercivity, inflection point, point of divergence of forward and backward branches of the hysteresis loop and saturation point. In Fig. 2 dependencies of the critical fields values on the thickness, when the magnetic field vector is perpendicular to the plane of the sample are presented. The values of fields H_C , H_{C1} , H_{C2} for IOLS increase with the thickness increasing, indicating the link between the layers and substantial anisotropy in the structure. At the same time, the saturation field H_{C3} increases with sample thickness up to 1 mkm, and then decreases, most likely, indicating the presence of the transition from two-dimensional to three-dimensional structure of the sample.

30PO-I1-35

RESONANT DYNAMICS OF THE DOMAIN WALLS IN MULTILAYER FERROMAGNETIC STRUCTURE

Ekomasov E.G., Gumerov A.M., Murtazin R.R., Kudryavtsev R.V., Ekomasov A.E., Abakumova N.N.

Bashkir State University, Ufa, Russia

ekomasoveg@gmail.com

Multilayer magnetic structures have been widely studied recently in connection with the opportunity of their practical application [1]. Frequently, these are periodically alternating layers of two materials with different physical properties. The dynamics of spin waves and magnetic inhomogeneities that are extended in such systems in directions perpendicular to the layer interfaces are studied intensely at present. Note that, frequently, the study of one-dimensional models makes it possible to understand the influence of various magnetic parameters. It has been shown [2-4] that the presence of a thin layer with the magnetic anisotropy parameters, smaller than those in the adjacent layers, can lead to new dynamic effects, e.g., the appearance of a nucleus of a new magnetic phase or the reflection of a moving DW from the attracting potential. In this work, we have studied the effect of spatial modulation of the parameters of magnetic anisotropy and exchange on the nonlinear resonant dynamics of DWs in a three- and five-layered ferromagnetic with allowance for the opportunity of the excitation of localized magnetic inhomogeneities, internal modes of DW oscillations, and the emission of bulk waves.

The possible oscillation frequencies are found generated in the thin layers of localized magnetic inhomogeneities. Using as an example two identical thin layers in a five-layered ferromagnetic we showed that the collective effects of the layers influence on the DW dynamics are largely connected with the resonant energy exchange between the localized waves. The presence of a critical distance is discovered between the thin layers separating the two regions with qualitatively different system behavior. The possibility of the existence of a settings range, in which to pass through both layers of a DW requires significantly less energy, is proved. We demonstrated that damping and external force counteract the onset of the DW resonant reflection from the attracting thin layer, but its initiating cause – resonant energy exchange between the localized waves still takes place. For the experimental observation of the reflections and DW quazitunnelling resonance effects in real physical experiments, we suggested a method of measuring the amplitude of the DW center oscillations, and the use of physical systems with sufficiently weak damping.

- [1] A. Hubert, R. Schafer Magnetic domains. Springer-Verlag, Hedelberg, Berlin, (1998).
- [2] E.G. Ekomasov, R.R. Murtazin, O.B. Bogomazova, A.M. Gumerov, *J. Magn. Magn. Mater.*, **339** (2013) 133-137.
- [3] E.G. Ekomasov, Sh.A. Azamatov, R.R. Murtazin, *PMM*, **105** (2008) 313-321.
- [4] E.G. Ekomasov, Sh.A. Azamatov, R.R. Murtazin, *PMM*, **108** (2009) 532-537.

30PO-I1-36

THE INFLUENCE OF Si ON MAGNETIC AND MAGNETO-OPTICAL PROPERTIES OF Co/Si/Co THIN-FILM SYSTEMS

Shalygina E.E.¹, Gan'shina E.A.¹, Kharlamova A.M.¹, Mukhin A.N.¹, Kurlyandskaya G.V.², Svalov A.V.²

¹ Faculty of Physics, M.V. Lomonosov Moscow State University, Moscow, 119991 Russia

² Ural Federal University, Yekaterinburg, 620002 Russia

shal@magn.ru

The physical properties of thin magnetic films of 3d transition metals and multilayer structures consisting of alternating magnetic and non-magnetic layers with sub-micron thick are the most interesting objects of the physics of magnetic phenomena. This interest is related to the wide use of these systems in numerous devices of modern micro- and nanoelectronics, based on the discovery of phenomena of giant magnetoresistance and oscillating exchange coupling between ferromagnetic layers. It is known that Si is a base element for modern micro and nanoelectronics. Thus, the study of magnetic properties of systems consisting of magnetic metal layers with Si spacers is of the special importance. In this work the results on the investigation of the magnetic and magneto-optical properties of the Co/Si/Co thin-film systems are presented.

The Co/Si/Co samples were grown by magnetron deposition of Co and Si layers onto glass substrates at room temperature. The thickness of Co layers, t_{Co} , was equal to 5 nm, and the Si spacer, t_{Si} , was varied from 0.2 up to 3.2 nm. According to XRD data, the Co layers had a nanocrystalline structure with grain dimensions (calculated by the Scherer method) of an order of layer thickness. The magnetic characteristics and magneto-optical spectra of the Co/Si/Co systems were measured employing the magneto-optical magnetometer and spectral magneto-optical equipment with the help of Transverse Kerr effect (TKE). The following main results were received.

The Co/Si/Co thin-film systems are characterized by in-plane magnetic anisotropy with an axis of easy magnetization (AEM) parallel to the orientation of the magnetic field, applied for deposition process of the samples. The hysteresis loops, measured for the samples with $t_{Si} < 1.6$ nm and $t_{Si} > 1.6$ nm in magnetic fields parallel to AEM, have almost rectangular and two-step forms, respectively. Analysis of these data showed that the values of the saturation field, H_S , of the Co/Si/Co samples oscillates as a function of the Si layer thickness. The investigation of the magneto-optical properties of the Co/Si/Co samples showed that TKE values oscillate also with changing the Si layer thickness, and the shape of these oscillations and their values depend on light wave length. The above data were explained by structural peculiarities of the Co/Si/Co systems [1-3], the changes of their electronic structure and also the exchange coupling between Co layers through the Si spacer.

Moreover, the strong difference of TKE spectra was discovered for the two-layer Si/Co and Co/Si systems. In the case of the Co/Si sample, the significant increase of the TKE values is observed at $\hbar\omega > 2.2$ eV. This fact can be explained by increasing the magneto-optical signal due to the presence of the upper semiconductor layer.

[1] A. Sagdeo, S. Rai, A.K. Srivastava, G.S. Lodha, R. Guen Rawat, K. Le, P. Jonnard, *J. Phys.: Condens. Mater.*, **23** (2011) 246004- 240011.

[2] M. V. Gomoyunova, G. S. Grebenyuk, I. I. Pronin, S. M. Solov'ev, O. Yu. Vilkov, D. V. Vyalykh, *Physics of the Solid State*, **55**, №2 (2013) 437-442.

[3] V. O. Vas'kovskiy, G. S. Patrin, D. A. Velikanov, A. V. Svalov, P. A. Savin, A. A. Yuvchenko, N. N. Shchegoleva, *Physics of the Solid State*, **49**, №2 (2007) 302-307.

30PO-I1-37

OPTICAL SPECTROSCOPY OF PHASE TRANSITIONS IN DyVO₄ NANOPARTICLES

Pytalev D.S.¹, Popova M.N.¹, Dramicanin M.D.², Jovanovic D.²

¹ Institute of Spectroscopy, RAS, Moscow, Troitsk, Russia

² University of Belgrade, Vinca Institute of Nuclear Sciences, Belgrade, Serbia
pytalev@isan.troitsk.ru

In this work, DyVO₄ crystalline nanoparticles of different sizes have been prepared by reverse micelle method and co-precipitation. Optical spectra of Dy³⁺ have been obtained in wide spectral (3000 – 15000 cm⁻¹) and temperature (2.2 – 300 K) ranges. As previously reported (e.g. [1]), the crystallographic phase transition (a cooperative Jahn-Teller transition) followed by antiferromagnetic ordering have been detected in the low-temperature spectra. The influence of the particle size on the phase transition temperatures is discussed in details. Crystal-field levels of Dy³⁺ have been derived for both tetragonal and orthorhombic crystal phases.

[1] J.C. Wright and H.W. Moos, *J. Appl. Phys.*, **41** (1970) 1244-1245.

30PO-I1-38

FMR AND MAGNETIC PROPERTIES OF $(\text{CoFeB})_m(\text{SiO}_2)_{1-m}$ NANOCOMPOSITE

Vyzulin S.A.¹, Lebedeva E.V.², Syr'ev N.E.², Shlapakov M.S.³

¹ Krasnodar University of the Ministry of the Interior of Russia, 350005 Krasnodar, Russia

² Lomonosov Moscow State University, 119991 Moscow, Russia

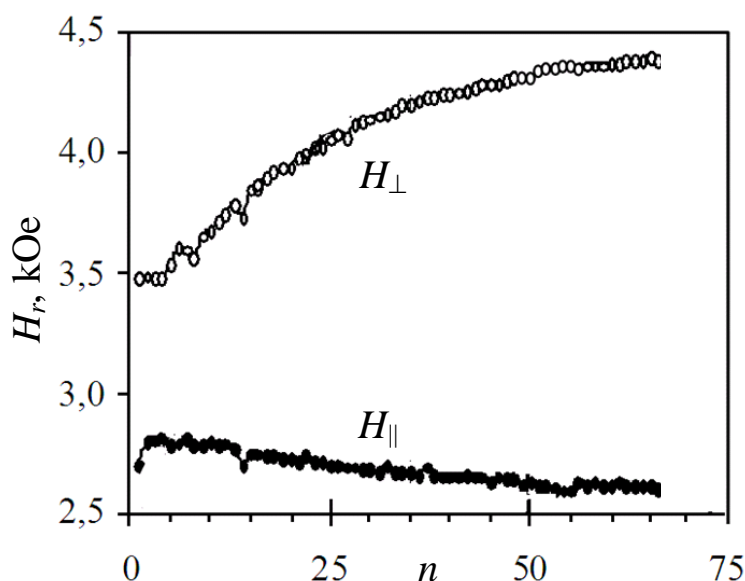
³ Kuban State University, 350040 Krasnodar, Russia

We have investigated FMR in granular film nanocomposites composed of amorphous CoFeB granules in a non-magnetic SiO₂ matrix. The samples have been prepared in Voronezh state technical university by ion-beam sputtering of CoFeB and SiO₂ samples in argon on glassceramics substrate by a consecutive layer-by-layer deposition. The film sample was 240 mm long and along it the thickness of the layers varied from 1,0 to 2,6 nm, the overall thickness changing from 160 to 400 nm. The magnetic phase concentration was 33,9 at.% (the percolation threshold being 49 at.% [1]). The performed elemental analyses, as well as the data of the manufacturer, prove the homogeneity of the magnetic phase concentration along the structure. The sample was then transversally cut into 80 small specimens with progressively increasing layer thicknesses.

The FMR spectra were measured at room temperature on the "JEOL JES FA-300" EPR spectrometer at 9.1 GHz. From the FMR data the resonance fields H_r were obtained.

The figure shows the dependence of the resonance fields H_r on the sample number n for the in-plane (H_{\parallel}) and normal (H_{\perp}) magnetization. H_r is found to depend on layer thickness, and this dependence becomes weaker when the layer thickness increases.

The observed results can be explained by progressive changes of the shapes and sizes of the spheroidal magnetic granules within layers taking place when the layer thickness increases [2]. This is also confirmed by the data obtained on the composites of the same composition (with CoFeB concentration 44 at.%), prepared by a continuous or layer-by-layer deposition. In the continuously deposited (i.e. homogeneous) samples resonance fields H_r do not depend on the film thickness and are smaller than the ones in the layer-by-layer deposited samples. The difference may be also caused by additional magnetostatic interaction due to the presence of interlayer boundaries.



[1] S.A. Vyzulin, A.V. Gorobinskii, E.V. Lebedeva, N.E. Syr'ev, M.S. Shlapakov. *Bulletin of the Russian Academy of Sciences: Physics*, **74** (2010) 1652–1654.

[2] S.A. Vyzulin, E.V. Lebedeva, D.A. Lysak, N.E. Syr'ev. *Bulletin of the Russian Academy of Sciences: Physics*, **74** (2010) 1687–1689.

30PO-I1-39

MAGNETIC, MAGNETOTRANSPORT AND STRUCTURAL PROPERTIES OF Co₂(Fe, Ti)Ga THIN FILMS

Rodionova V.¹, Shevyrtalov S.¹, Chichay K.¹, Gan'shina E.², Novikov A.², Zikov G.², Okubo A.³, Kainuma R.³, Umetsu R.Y.⁴, Ohtsuka M.⁵, Bozhko A.⁶, Golub V.⁷, Gorshenkov M.⁸, Lyange M.⁸, Khovaylo V.⁸

¹ Immanuel Kant Baltic Federal University, Kaliningrad, Russia

² Lomonosov Moscow State University, Moscow, Russia

³ Graduate School of Engineering, Tohoku University, Sendai, Japan

⁴ Institute for Material Research, Tohoku University, Sendai, Japan

⁵ Institute of Multidisciplinary Research for Advanced Materials, Tohoku University, Sendai, Japan

⁶ A.M. Prokhorov General Physics Institute of RAS, Moscow, Russia

⁷ Institute of Magnetism, NASU and MESYSU, Kyiv, Ukraine

⁸ National University of Science and Technology "MIS&S", Moscow, Russia

Shevyrtalov@gmail.com

Among a variety of half metallic ferromagnetic alloys and compounds, Co-based Heusler alloys possess the highest Curie temperature T_c , the highest magnetization saturation and the highest spin polarization at Fermi level. These properties have great importance for spintronic applications.

We investigated magnetic, magnetotransport and structural properties of the Co₂(Fe,Ti)Ga thin films with different chemical composition, prepared by a magnetron sputtering technique in Ar atmosphere. Chemical composition was controlled by the changing of the sputtering power of the targets. The measurements were performed on as-prepared and annealed samples. Energy dispersive spectrometer (Oxford X-Act) was used to detect the composition of thin films. The structure of prepared samples was examined by XRD analysis using a Rigaku diffractometer with CuK α radiation. Magnetic measurements were performed by vibration sample magnetometer (Lakeshore 7400) in a temperature range of 100-450K. In-plane hysteresis loops were measured for two different orientations of the samples in relation to the direction of the magnetic field (0, 90 grad) at different temperatures. Magnetoresistance of Co₂(Fe, Ti)Ga thin films was obtained in magnetic field up to 10 kOe in a temperature range 100-450 K.

The presence of well-defined (220) and (422) peaks corresponding to the principal reflection of the Heusler structure were revealed by XRD analysis. We found that the magnitude of the Magnetoresistance increases with increasing temperature. Measured in-plane hysteresis loops show anisotropic behavior in some samples and demonstrate step-like shape. Obtained results indicate that magnetic properties of Co₂(Fe, Ti)Ga thin films strongly depend on the Fe and Ti concentrations.

30 June

Monday

17:30-19:00

poster session

30PO-I2

**“Magnetism and
Superconductivity”**

30PO-I2-1

STRUCTURE AND UNUSUAL LINEAR AND NONLINEAR MAGNETIC PROPERTIES OF $\text{Nd}_{0.7}\text{Ba}_{0.3}\text{MnO}_3$ CRYSTAL WITH FERROMAGNETIC METAL GROUND STATE

Ryzhov A.V.¹, Molkanov P.L.¹, Chernenkov Yu.P.¹, Khavronin V.P.¹, Lazuta A.V.¹,
Kiselev I.A.¹, Runov V.V.¹, Smirnov O.P.¹, Troyanchuk I.O.²

¹ PNPI NRC “Kurchatov Insitute”, Gatchina, St. Petersburg, Russia

² IPSS NAS, Minsk, Belarus
yucher@pnpi.spb.ru

Results of structural neutron diffraction study, magnetization, transport, electron spin resonance (ESR) as well as linear and nonlinear (second and third order) *ac* susceptibilities measurements are presented for $\text{Nd}_{1-x}\text{Ba}_x\text{MnO}_3$ ($x = 0.3$) with the Curie temperature $T_C \approx 140$ K and insulator-metal transition at $T_{IM} \approx 129.5$ K.

Detailed analysis of the data is performed by using *Pbnm* space group in a temperature range 85 - 300 K. No Jahn-Teller (JT) transition is found in the compound, a rotation of MnO_6 octahedrons near T_C being only observed. The change of Mn-O-Mn bond angles is observed in the range 100 – 160 K (Fig. 1). The field cooled magnetization data are in a reasonable agreement with the predictions for a 3D isotropic ferromagnet above T_C . These measurements, however, reveal a difference between the field cooled and zero field cooled data in the paramagnetic region.

The ESR results also correspond to behavior of a 3D isotropic ferromagnet above $T^* \approx 143$ K ($\tau^* \approx 0.12 \leq \tau < 1$, $\tau = (T - T_C)/T_C$). It is shown that an anisotropic exchange coupling of the Mn and Nd magnetic moments can give a substantial contribution in ESR linewidth masking its critical enhancement. The different temperature treatments (slow/fast cooling/heating, with/without external magnetic field) of the sample reveal a temperature hysteresis of the ESR spectra below T^* indicating an anomalous response in the paramagnetic region. The study of the magnetic phase transition in the $x = 0.23$ and 0.25 manganites suggests change in its character from the second to first order at T^* . However, the conventional functional of free energy taking into account the presence of magnetic field does not describe this first order transition. This suggests that the charge, orbital, and JT phonon degrees of freedom, in addition to magnetization, may be the critical variables, the unusual character of the transition being determined by their coupling. The unconventional critical behavior is attributed to an orbital liquid metallic phase that begins to coexist with the initial orbital ordered phases below T^* .

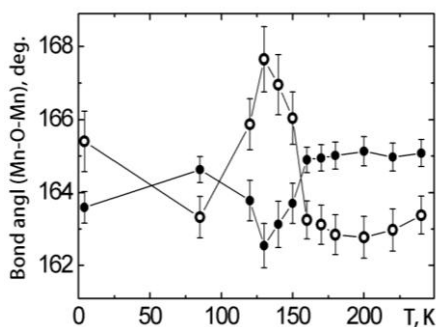


Fig. 1. Mn-O-Mn bond angles.

30PO-I2-2

SUPERCONDUCTING AND MAGNETIC PROPERTIES OF Fe(S,Se,Te) COMPOUNDS WITH TERNARY MIXTURE OF CHALCOGENS

Abouhaswa A.S.¹, Merentsov A.I.^{1,2}, Selezneva N.V.², Baranov N.V.^{1,2}

¹ Institute of Natural Sciences, Ural Federal University, 620083, Ekaterinburg, Russia

² Institute of Metal Physics, Russian Academy of Science, 620990, Ekaterinburg, Russia
aliabohaswa@hotmail.com

Iron-based layered compounds like iron oxypnictides and iron chalcogenides [1] exhibit unusual high-temperature superconductivity. Among these materials iron selenide has a simplest crystal structure and, as compared with pnictides. In previous studies, the substitution effects on the crystal structure and properties of iron chalcogenide superconductors were investigated in the compounds with different binary mixtures of chalcogens (Se-Te, Se-S, Te-S). The aim of the present work is to study how the presence of all three chalcogens will affect the crystal structure and superconducting properties of FeSe-type compounds bearing in mind that the chalcogen ions have not only different radii but also different electronegativities and polarizabilities and, therefore, may form chemical bonds with different covalency/ionicity ratio and varying strength.

A series of $\text{Fe}_{1.02}\text{Te}_{0.5}\text{Se}_{0.5-x}\text{S}_x$ ($x = 0, 0.1, 0.2, 0.3, 0.4$ and 0.5) samples has been synthesized by solid state reaction. Keeping the tellurium content unchanged the influence of the substitution of sulfur for selenium on the crystal structure and superconducting properties of synthesized samples has been studied by means of X-ray diffraction, electrical resistivity and magnetic susceptibility measurements. Effect of the presence of all three chalcogen ions in such materials on the crystal lattice and the superconducting properties is studied for the first time. The substitution of S for Se keeping the constant tellurium concentration in $\text{Fe}_{1.02}\text{Te}_{0.5}\text{Se}_{0.5-x}\text{S}_x$ is found to expand the crystal lattice despite the lower ionic radius of sulfur in comparison with selenium (see Inset in Fig 1). The maximal expansion nearly 4 % is observed for $x = 0.5$ in the c direction as compared with non-substituted $\text{Fe}_{1.02}\text{Se}_{0.5}\text{Te}_{0.5}$. The large tellurium ions bonded with iron are suggested to form in $\text{Fe}_{1.02}\text{Te}_{0.5}\text{Se}_{0.5-x}\text{S}_x$ a skeleton of the lattice. The expansion of the unit cell with increasing sulfur content may be ascribed to the softening of the lattice due to the growing amount of more ionic Fe-S bonds and weakening of the van der Waals interactions between chalcogen layers [2].

The results of the magnetization measurements show that the materials exhibit bulk superconductivity (Fig.1). The shielding volume fractions is estimated to be about 90 % and 21 % for $x = 0.1$ for $x = 0.4$, respectively. The results obtained in the present work show that the variation of S, Se and Te concentrations in the ternary chalcogen mixture can be used to control the lattice, superconducting and magnetic properties of iron-chalcogen based superconductors.

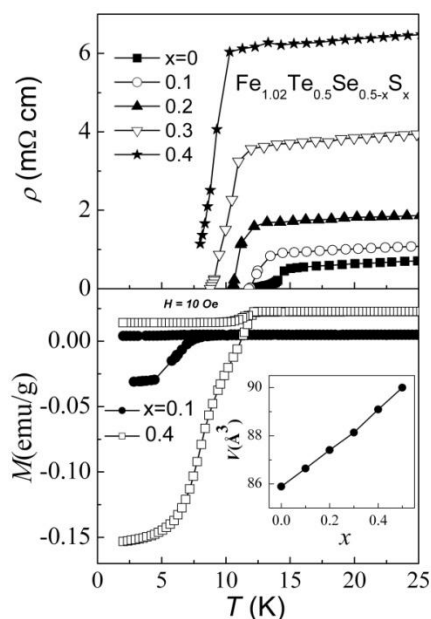


Fig.1. Temperature dependences of the resistivity and magnetization for $\text{Fe}_{1.02}\text{Te}_{0.5}\text{Se}_{0.5-x}\text{S}_x$ samples with various sulfur content. Inset shows the unit cell volume of the tetragonal phase for the $\text{Fe}_{1.02}\text{Te}_{0.5}\text{Se}_{0.5-x}\text{S}_x$ samples as a function of the sulfur concentration.

[1] Y. Kamihara et al., *J. Am. Chem. Soc.*, **130** (2008) 3296-3297.

[2] S. Margadonna et al., *Phys. Rev. B*, **80** (2009) 064506.

30PO-I2-3

A SIMPLE MODEL FOR INVESTIGATION OF THE PAIR BREAKING EFFECT ON THE PARAMETERS OF HTS/FM THIN FILMS

Nurgaliev T.C.¹, Uspenskaya L.S.^{1,2}

¹ Institute of Electronics, Bulgarian Academy of Sciences, 72 Tsarigradsko Chausse, 1784 Sofia, Bulgaria

² Institute of Solid State Physics, Russian Academy of Sciences, 142432 Chernogolovka, Moscow, Russia

timur@ie.bas.bg

A transfer of spin-polarized carriers from ferromagnetic (FM) manganites into high temperature superconductors (HTS) by diffusion process may reduce the superconducting order parameter in HTS/FM multilayer structures due to breaking of Cooper pairs. It is also known that the spin-polarized current injected into a superconductor layer may effectively suppress the superconductivity. Various spintronic devices are believed to be constructed on the basis of this effect, although the description of the effect is very complicated and possible only in the framework of the quantum theory.

In this paper a simple model is considered for investigation of Cooper pair breaking effect, which can be caused by transfer of spin-polarized carriers from FM manganites into HTS, on the critical current density and the microwave surface resistance of the HTS/FM thin film structure. It was assumed for this purpose that the concentration of quasiparticles, generated by above mechanism, changes as an exponential function inside the HTS film on dependence on the distance from the HTS/FM interface. The parameter of this exponential function and its changes in the spin injection process can be evaluated from the experimental data, concerning, for example, the dependence of the critical current density or the microwave surface resistance of the structure on the injected current density. The paper considers and discusses some experimental data as well from the point of view of the proposed model.

30PO-I2-4

SCREENING EFFECT OF MAGNETIC EXCHANGE INTERACTION IN THE U- AND Gd-BASED INTERMETALLIC COMPOUNDS

Krylov V.I.¹, Sechovský V.², Andreev A.V.³

¹ SINP, Lomonosov Moscow State University, Moscow 119991, Russian Federation

² DSMP, Charles University in Prague, Ke Karlovu 5, 12116 Prague 2, Czech Republic

³ Institute of Physics ASCR, Na Slovance 2, 18221 Prague 8, Czech Republic

vkrylovmag@gmail.com

For the whole region of x , the ^{119}Sn Mössbauer spectra of $\text{UCuGe}_{1-x}\text{Sn}_x$ compounds ($x=0.01 - 1.0$) represent a superposition of two magnetic sextets with two sets of hyperfine parameters. Two subspectra with significantly different values of the magnetic hyperfine fields (B_{hf}), B_1 and B_2 , correspond to the two local magnetic states: low-field (LF) and high-field (HF).

The LF-component corresponds to the ^{119}Sn atoms which interact only with the three nearest uranium magnetic moments. The magnetic exchange of this group of ^{119}Sn atoms with the other three more distant uranium moments is shielded by the Cu-layer and does not contribute to B_1 . The HF-component B_2 corresponds to other group of ^{119}Sn atoms which have a magnetic exchange with all six uranium ions around the tin atoms. The structural (Ge-Cu) and (Sn-Cu) defects or vacancies in Cu-layers of the $\text{UCuGe}_{1-x}\text{Sn}_x$ compounds lead to disruption of the shielding Cu-layer and creation of bonds of the Sn atoms with all the six uranium ions.

In the ferromagnetic (FM) and antiferromagnetic (AFM) Gd - X (X is a p-, s-element) compounds, the B_{hf} values on ^{119}Sn nuclei extrapolated to 0 K can be expressed as $B_{\text{hf}} = \Delta B \times N$, where $\Delta B = -4.5(5) \text{ T}/\mu_{\text{Gd}}$ is a contribution of each Gd-moment to B_{hf} , and N is the number of uncompensated Gd magnetic moment in the nearest neighborhood of tin atoms.

In the AFM GdCuSn , GdAgSn , and GdCuGe compounds crystallizing in the hexagonal GaGeLi -type of structure, the hexagonal layers of atoms Gd, Cu(Ag) and Sn(Ge) alternate in the sequence Gd-Sn(Ge)-Cu(Ag)-Gd along the c axis. The tin atoms are surrounded by six atoms of Gd (3Gd atoms are located in the lower layer and 3Gd ones in the more distant upper layer).

We have found that B_{hf} on the ^{119}Sn nuclei in GdCuSn and GdAgSn is oriented along the c -axis. The B_{hf} values at 5 K are equal to 5.31(1) T and 5.04(2) T, respectively. These values correspond to the contribution of only one Gd magnetic moment to the B_{hf} on ^{119}Sn nuclei. It is possible if only the three nearest Gd magnetic moments are involved in the magnetic exchange with the Sn atoms, the contributions from two of them mutually compensate. The three more distant Gd moments are shielded by a Cu-layer. The Cu-vacancies and partial Cu-Ge disorder in the compound GdCuGe lead to penetration of the magnetic exchange from three more distant Gd atoms through the Cu-layer. Therefore for the part of the ^{119}Sn probe nuclei in GdCuGe , B_{hf} is formed by two uncompensated Gd magnetic moments and reaches of 10 T.

Conclusions:

1). The investigation of B_{hf} on the ^{119}Sn probe nuclei in uranium and RE-based compounds have shown that in the compounds with layered crystal structure the screening effect of the magnetic exchange interaction by layers of p- or s-, d-nonmagnetic atoms is observed.

2). In magnetically ordered compounds this effect can lead to the appearance of selected layers, free of magnetic exchange and of transferred (induced by this exchange) electron polarization.

3). The presence of the vacancies in the shielding layer can lead to a creation of new magnetic bonds between the components of the alloy. This in turn leads to a significant change in magnetic properties of a compound and coexistence of two (or more) local magnetic states with different temperatures of local magnetic ordering.

30PO-I2-5

STATES OF THE SPIN SWITCHES ON THE BASE OF SUPERCONDUCTOR/FERROMAGNET MULTILAYERED STRUCTURES

Kushnir V.N.

BSUIR, P. Browka 6, 220013 Minsk, Belarus
vnkushnir@gmail.com

The critical state of superconductivity in multilayers consisting of alternate ferromagnet (F) and superconducting (S) layers, $F_0/S/F_2/\dots/S/F_N$, with F-layers magnetizations \mathbf{M}_k ($k = 0, \dots, N$) collinear to the given vector \mathbf{M} ($\mathbf{M}_k = \pm \mathbf{M}$) has been investigated on the base of the matrix solution of the boundary problem for the linearized Usadel equations [1]. The critical temperatures T_c and the diffusive limit Green functions have been calculated for different bilayers number N and the layer thicknesses. For regular structures, $F/N \times (S/F)$, the conditions of maximal effect of switching between three experimentally realizable configurations $\{\mathbf{M}_k\}$ (“spin switch with ternary logic”) have been determined. The amplitude-phase relations have established, namely:

1) the superconducting condensate tends to be localized in S-layer situated between F-layers with antiparallel magnetizations (see also the explanations in Ref. 2);

2) the imaginary part of the critical state function has the node in this S-layer.

Fig. 1, demonstrating first property, shows the Usadel’s Green functions (condensate wave functions) of critical states of 5-bilayer structure

$F/2 \times (S/F)/S_c/F/2 \times (S/F)$ with narrow central S-layer calculated in single mode approximation for two configurations of $\{\mathbf{M}_k\}$ (the material and geometrical parameters of the structure are quoted in Ref. 1). As follows from Fig. 1 a, the superconductivity in the central S-layer is almost damped for \mathbf{M} given in all F-layers. The upturn of the magnetization vectors in 4th, 5th and 6th F-layers induces the infill of the layer S_c by Cooper pairs (Fig. 1 b). Further, the imaginary part of the wave function is almost invariable in this case, but the real part transforms its symmetry to opposite.

In the given example, the critical temperature effect is order of 0.25 K but the amplitude-phase effect of magnetization directions switching seems more important for applications.

In the given example, the critical temperature effect is order of 0.25 K but the amplitude-phase effect of magnetization directions switching seems more important for applications.

Support by BFFR, grant F14R-020 is acknowledged.

[1] V.N. Kushnir, M.Yu. Kupriyanov, *JETP Letters*, **93** (2011) 539.

[2] L.R. Tagirov, *Phys. Rev. Lett.*, **83** (1999) 2058-2061.

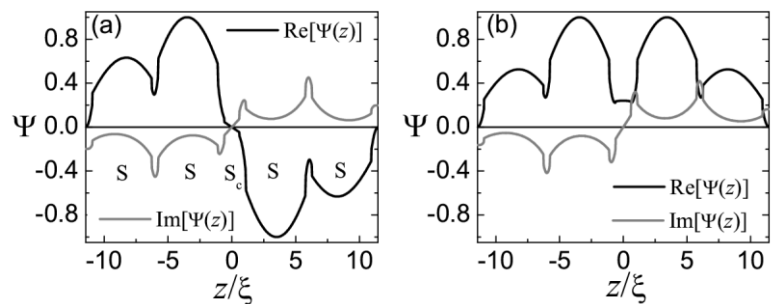


Fig. 1. The condensate wave function $\Psi(z)$ of critical state of 5-bilayer S/F structure in the case of $\mathbf{M}_k = \mathbf{M}$, $k = 1, \dots, 6$ (a), and the case of $\mathbf{M}_k = \mathbf{M}$, $k = 1, 2, 3$ and $\mathbf{M}_k = -\mathbf{M}$, $k = 4, 5, 6$. Axis OZ is orthogonal to the structure surfaces, the parameter ξ is the coherence length in S-material

30PO-I2-6

Ce_xLa_{1-x}B₆: THE ANISOTROPY OF *H* - *T* MAGNETIC PHASE DIAGRAMS

*Krasnorussky V.N.¹, Bogach A.V.¹, Glushkov V.V.^{1,2}, Demishev S.V.^{1,2}, Shitsevalova N.Yu.³,
Levchenko G.V.³, Filipov V.B.³, Sluchanko N.E.¹*

¹ Prokhorov General Physics Institute, Russian Academy of Sciences, Moscow, Russia

² Moscow Institute of Physics and Technology, Dolgoprudny, Russia

³ Frantsevich Institute for Problems of Material Science, Kiev, Ukraine

krasnorussky@mail.ru

Angular, temperature and magnetic field dependences of electrical resistivity ρ (φ , T , H) of Ce_xLa_{1-x}B₆ ($x = 1, 0.97, 0.9, 0.8, 0.7$) high quality single crystals have been measured under the external magnetic fields H up to 80 kOe at low temperatures (T) down to 1.85 K, and H - T - x magnetic phase diagrams were obtained. As a result of investigation the new features have been observed in the suppression with x and H of the antiferromagnetic (phase III) and so-called antiferroquadrupolar (phase II) states. The transverse magnetoresistance study for $x \geq 0.9$ and low H allows to conclude about considerable anisotropy of phase II - III boundary. Anisotropic behavior of magnetoresistance goes down both with increasing of substitutional disorder and external magnetic field, and the anisotropy becomes negligibly small at the phase II. The reconstructed here 3D plots of the magnetoresistance anisotropy are presented for different magnetic phases of H - T - x diagrams (see e.g. Figs. 1, 2). It has also been established that Yosida model [1] describes very well the negative magnetoresistance in II phase providing us with arguments in favor of the spin-polaron effect in Ce_xLa_{1-x}B₆. Both local spin polarization of conduction band 5d-states in the vicinity of 4f-centers as well as indirect exchange interaction (RKKY – mechanism) are essential for the formation of the ground magnetic state in the archetypal heavy fermion antiferromagnet.

[1] K. Yosida, *Phys. Rev.*, **107** (1957) 396-403.

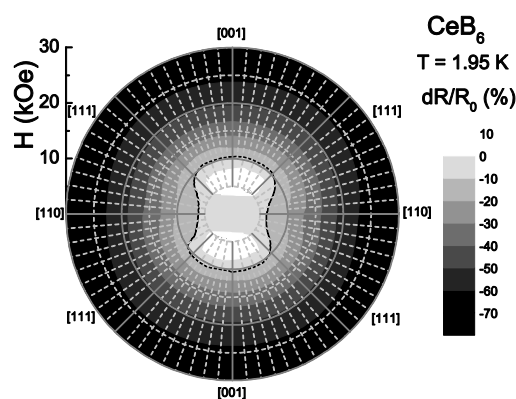


Fig. 1. The angular dependence of the transverse magnetoresistance (dR/R_0) in CeB₆ from the direction and amplitude of the magnetic field H .

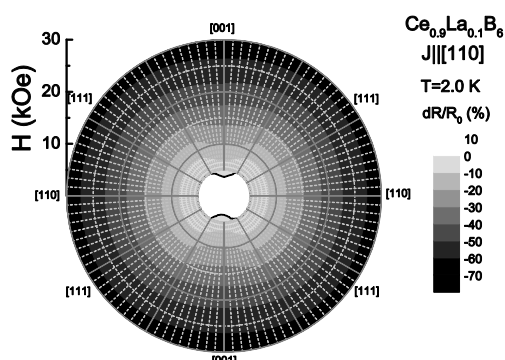


Fig. 2. The angular dependence of the transverse magnetoresistance (dR/R_0) in Ce_{0.9}La_{0.1}B₆ from the direction and amplitude of the magnetic field H .

30PO-I2-7

OBSERVATION OF PINNING STRENGTHENING IN “MgB₂ – CNT – α-Fe” NANOCOMPOSITES STUDIED BY MICROWAVE ABSORPTION TECHNIQUE

Bazarov V.V.¹, Togulev P.N.¹, Nizamov F.A.¹, Lyadov N.M.¹, Ivicheva S.N.², Suleimanov N.M.¹

¹Zavoisky Physical-Technical Institute RAS, Kazan, Russia

²A.A. Baikov Institute of Metallurgy and Material Science RAS, Moscow, Russia
vbazarov1@gmail.com

Practical applications of superconducting materials depend on the value of critical current density, which is determined by pinning of vortices. The pinning can be enhanced by creation of artificial defects, which act as additional pinning centers. Investigation of a such kind of defects has shown that the most effective ones are nanosized columnar and magnetic defects. In this report the results of investigation of pinning properties in “MgB₂-CNT- α-Fe” superconducting nanocomposites are presented (where CNT - carbon nanotubes and α-Fe - iron nanoparticles).

The process of nanocomposites preparation consists of two main steps: deposition of α-Fe nanoparticles on the surface of CNT by means of method developed in [1] and mixing of MgB₂ with CNT- α-Fe. Following the above procedure, several composites with an average iron nanoparticles diameter of 8 nm were prepared.

Thus, the measurements were carried out on initial MgB₂ and series of composites «MgB₂ - CNT», «MgB₂ - CNT-α-Fe». The experiments on «MgB₂-graphene – α-Fe» composites where instead of carbon nanotubes the graphene was used as the support for metal nanoparticles were also performed. To determine the vortex pinning force the magnetically modulated microwave absorption (MMA) technique has been used.

The method is based on the following: when a superconductor in the superconducting state is placed to a microwave cavity of electron paramagnetic resonance (EPR) spectrometer and the sweep of the magnetic field in the forward and backward direction is carried out, the so-called hysteresis loop of MMA is registered the amplitude of which is proportional to the pinning force [2]. Measurements showed that the greatest increase in the pinning force is observed in the composite «MgB₂ - CNT-α-Fe» (Fig. 1). It is found that the “MgB₂-graphene-α-Fe” composites with relatively large iron nanoparticles does not demonstrate the enhancement of pinning properties.

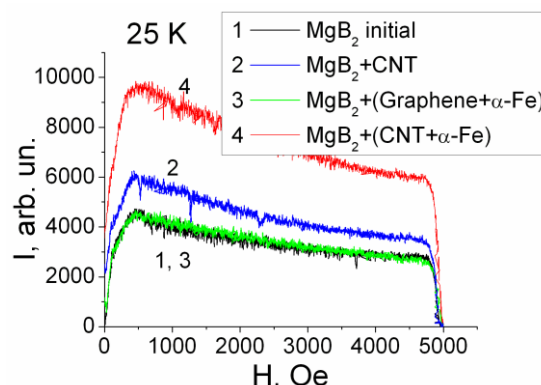


Fig. 1. The field dependence of the MMA loop amplitude at 25 K of MgB₂, «MgB₂-CNT», «MgB₂ - CNT + α-Fe» and «MgB₂ - graphene + α-Fe» composites.

The reported study was partially supported by RFBR, research projects No. 13-08-00906-a and 12-02-00563-a.

[1] S.N. Ivicheva, Yu.F. Kargin, E.A. Ovchenkov, Yu.A. Koksharov and G.Yu. Yurkov, *Physics of the Solid State*, **53** (2011) 1114-1120.

[2] V.V. Bazarov, J. Ćwik, D. Gajda, P.N. Togulev, N.M. Lyadov, V.A. Shustov and N.M. Suleimanov, *Journal of Superconductivity and Novel Magnetism*, **25** (2012) 1689-1694.

30PO-I2-8

COMPETITION OF CHARGE AND SPIN ORDERINGS IN MODEL CUPRATES

Chikov A.A.¹, Avvakumov I.L.¹, Moskvin A.S.¹

¹Department of Theoretical Physics, Ural Federal University, Ekaterinburg, Russia
alex.chikov@yandex.ru

We address the effects of the competition between the charge and spin orderings in model cuprates like $\text{La}_{2-x}\text{Sr}_x\text{CuO}_4$ whose charge transfer instability [1] implies the three effective valence centers $[\text{CuO}]_4^{7-,6-,5-}$ (nominally $\text{Cu}^{1+,2+,3+}$) should be considered on equal footings. To this end we introduce a minimal model for the cuprates with the constrained on-site Hilbert space reduced to only these three valence centers and make use of the $S=1$ pseudospin formalism [2] with correspondence: $\text{Cu}^{1+,2+,3+}$ to $M_S=-1, 0, +1$, respectively. The $\text{Cu}^{1+,3+}$ ions ($M_S=-1, +1$) in cuprates are spinless while Cu^{2+} ion has $s=1/2$, so that the projection operator $(1 - \hat{S}_z^2)$ defines the on-site spin density. The simplest model Hamiltonian describing the competition of the charge and spin degrees of freedom can be represented as follows:

$$\hat{H} = \sum_i \Delta_i \hat{S}_{iz}^2 - \sum_i h_i \hat{S}_{iz} + \sum_{i>j} V_{ij} \hat{S}_{iz} \hat{S}_{jz} + \sum_{i>j} I_{ij} (\hat{s}_i \cdot \hat{s}_j) (1 - \hat{S}_{iz}^2) (1 - \hat{S}_{jz}^2),$$

where Δ determines the energy (2Δ) of the disproportionation: $\text{Cu}^{2+} + \text{Cu}^{2+} - \text{Cu}^{1+} + \text{Cu}^{3+}$, the second term describes the effect of a pseudomagnetic field, or the chemical potential, the third term defines the attraction of electronic (Cu^{1+}) and hole (Cu^{3+}) centers, the fourth term describes the Heisenberg exchange $\text{Cu}^{2+} - \text{Cu}^{2+}$. Within the framework of the Monte Carlo (MC) technique and mean-field approximation (MFA) we calculated the correlation functions that determine both the “antiferromagnetic” pseudospin (charge) and antiferromagnetic spin orders for different values of the parameters. The phase diagrams calculated both in MC and MFA techniques distinctly demonstrate an anticorrelation effect between charge and spin ordering in model cuprates.

The RFBR grant No. 12-02-01039 is acknowledged for providing financial support.

[1] Moskvin A.S., *Phys.Rev. B* **84**, (2011) 075116.

[2] Moskvin A.S., *The Physics of Metals and Metallography*, **95**, (2003) 41.

30PO-I2-9

QUANTUM MONTE-CARLO PHASE DIAGRAM FOR A MODEL CUPRATE*Moskvin A.S.¹, Konev V.V.¹, Korolev A.V.¹*¹ Department of Theoretic Physics, Ural Federal University, Ekaterinburg, Russia
alexander.moskvin@urfu.ru

We introduce a minimal model for CT (charge transfer) unstable 2D cuprates with the on-site Hilbert space reduced to only three effective valence centers, nominally Cu^{1+,2+,3+} ions and make use of the S=1 pseudospin formalism. Focusing on the unconventional bosonic-like physics of the model cuprate we neglect the one-particle transport (on-site terms) we write out the effective S=1 pseudospin Hamiltonian for the CuO₂ plane of the model cuprate as follows:

$$\hat{H}_{ch} = \sum_i \left(\Delta_i \hat{S}_{iz}^2 - (\mu - h_i) \hat{S}_{iz} \right) + \sum_{i<j} V_{ij} \hat{S}_{iz} \hat{S}_{jz} + \sum_{i<j} t_{ij}^b \left(\hat{S}_{i+}^2 \hat{S}_{j-}^2 + \hat{S}_{i-}^2 \hat{S}_{j+}^2 \right) \quad (1)$$

with a charge density constraint: $\frac{1}{2N} \sum_i \langle \mathcal{S}_{iz} \rangle = \Delta n$,

where Δn is the deviation from a half-filling.

The first single-site term describes the effects of a bare pseudo-spin splitting, or the local energy of centers and relates with the on-site density-density interactions. The second term may be related to a pseudo-magnetic field $h_i \parallel Z$, in particular, a real electric field which acts as a chemical potential (μ is the hole chemical potential, and is h_i a (random) site energy). The third term in \hat{H}_{ch} describes the effects of the short- and long-range inter-site density-density interactions including screened Coulomb and covalent couplings. The fourth term describes the two-particle bosonic transport. It is worth noting that in the limit of large negative Δ we arrive at the Hamiltonian of the hard-core bosons. The effect of the nonisovalent substitution in the model cuprate La₂CuO₄ was modeled via a Sr²⁺ induced impurity potential region within CuO₂ plane with varied parameters Δ and V . Despite its seeming simplicity the model is believed to capture the salient features both of the hole- and electron-doped cuprates. Concept of the electron and hole centers, differing by a composite local boson, and electron-hole pairing are shown to explain central points of the cuprate puzzles, in particular, the HTSC itself and pseudogap phenomena.

Making use of two different QMC methods, the standard stochastic series expansion (SSE) with loop updates and a continuous time world-line QMC, we studied the ground-state and finite-temperature properties of the Hamiltonian (1) given different parameters values. Our QMC calculations for the model CT unstable cuprates shows a step-by-step evolution under doping of the parent insulating state into an uncoventional inhomogeneous supersolid (mixed charge order - Bose superfluid, or CO+BS) phase formed by electron and hole CuO₄ centers. The simulation does reproduce main features of the T-x phase diagrams for doped cuprates, in particular, the suppression of antiferromagnetism, a pseudogap regime due to charge ordering, formation of a local superconductivity at $T > T_c$, and global 2D superconductivity.

The work was partially supported by RFBR Grant No.~12-02-01039.

30PO-I2-10

CHARACTERISTICS OF THE COMPOSITE MgB_2 - LCMO AS AN JOSEPHSON STATE

Kononenko V.V., Tarenkov V.Yu., D'yachenko A.I., Varyukhin V.N.

A.A.Galkin Donetsk Institute for Physics and Engineering of NAS of Ukraine

Donetsk, Ukraine.

vkkononenko@gmail.com

The influence of electromagnetic noise on the transport characteristics of a composite consists of superconductor MgB_2 and of nanopowder $\text{La}_{0.7}\text{Ca}_{0.3}\text{MnO}_3$ (LCMO) are investigated. Manganite LCMO was nanopowder with an average grain size $d = 50$ nm (high-resistance phase) and low-resistance phase MgB_2 was a powder with grains of $d = 5-10$ μm . After thorough mixing the composites were pressed into the plates with size of $S=0.1 \times 1 \times 10$ mm^3 . Current and voltage leads ($r \sim 10^{-3}$ Ohm) were prepared by adding of the finely-divided silver powder on the area of the plates. It has observed that with 25% volume content of LCMO the resistance of the composite starts to increase sharply and significantly broaden the superconducting $R(T)$ transition, which means breaking of the MgB_2 percolation cluster and the current flow through the chains MgB_2 -LCMO- MgB_2 etc [1]. The current-voltage characteristics $I(V)$ of these samples showed the excess current I_{exc} which is characteristic of Josephson S-N-S junctions structure. Ability of supercurrent flow in such superconductor - ferromagnet - superconductor heterostructures has been shown in [2]. Fig. 1 shows the effect of electromagnetic noise (~ 100 mV) to $R(T)$ dependence of the composite MgB_2 -LCMO (27% LCMO) at different signal amplitudes. Note that at $R(T)$ dependence of pure MgB_2 the noise had no effect. The temperature dependences of the resistivity were recorded at transport currents $\sim 10 \mu\text{A}$. The noise signal is supplied with generator G2-37 in the band 6.5 MHz to the sample via capacitive coupling. Small amplitude of the noise signal significantly influenced at $R(T)$ transition of the composite. The noise signal affected on the current-voltage characteristic of the sample (insert Fig.1) also.

The high sensitivity of the transport characteristics of the MgB_2 -LCMO composite to the influence of a noise can be related to the dynamics of Josephson hypervortices formed in the S-N-S contacts structure. By the alternating signal of sufficiently small amplitude an oscillation of the vortices cause the phase shift in the Josephson S-N-S structures which leads to the dissipative processes. According to modern views, [3] the proximity effect in superconductor - ferromagnet - superconductor is possible if the interface between the MgB_2 -LCMO is a spin - active surface which converts Cooper pairs from s-wave symmetry of the order parameter in MgB_2 to triplet correlations in LCMO which provide supercurrent flow through the ferromagnetic LCMO.

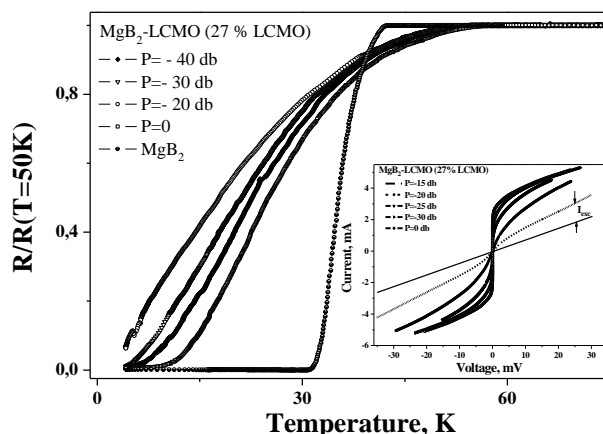


Fig. 1 Influence of electromagnetic noise (~ 100 mV) on $R(T)$ dependence of the composite MgB_2 -LCMO (27 vol. % LCMO) and MgB_2 . Inset: the influence of electromagnetic noise on $I(V)$ dependence of the MgB_2 -LCMO composite.

The high sensitivity of the transport characteristics of the MgB_2 -LCMO composite to the influence of a noise can be related to the dynamics of Josephson hypervortices formed in the S-N-S contacts structure. By the alternating signal of sufficiently small amplitude an oscillation of the vortices cause the phase shift in the Josephson S-N-S structures which leads to the dissipative processes. According to modern views, [3] the proximity effect in superconductor - ferromagnet - superconductor is possible if the interface between the MgB_2 -LCMO is a spin - active surface which converts Cooper pairs from s-wave symmetry of the order parameter in MgB_2 to triplet correlations in LCMO which provide supercurrent flow through the ferromagnetic LCMO.

[1] V.V.Kononenko, V.Yu.Tarenkov, A.I.D'yachenko, *XPPT* **23**, 3 (2014) 39-45 (in Russia).

[2] G. A. Jvsiannikov, A.E. Sheierman, *Jetph Letters*, **97**, 3 (2013) 165 - 169.

[3] F. S. Bergeret, A. F. Volkov, *Rev. Mod. Phys.* **77**, (2005) 1321-1327.

30PO-I2-11

INTERPLAY BETWEEN SUPERCONDUCTIVITY AND INHOMOGENEOUS EFFECTIVE EXCHANGE FIELD

Tumanov V.A., Proshin Yu.N.

Institute of Physics, Kazan Federal University, Kazan, Russian Federation
tumanvadim@yandex.ru

We study the superconducting state against the background of an inhomogeneous rotation of effective exchange field vector [1]. In contrary to usual approaches [1,2] we use a local unitary rotation in the spinor space to diagonalize the term in BCS Hamiltonian, that corresponds the exchange field direction inhomogeneity. After the transformation the Hamiltonian can be rewritten in terms of covariant derivatives $\mathbf{D} = \nabla + \mathbf{A}(\varphi, \theta, \xi)$ where $\mathbf{A}(\varphi, \theta, \xi)$ is an effective tensor field and it contains in general all components. φ and θ are the spherical angles defining the magnetization direction, $\xi(\mathbf{r})$ is an arbitrary real function. The effective field $\mathbf{A}(\varphi, \theta, \xi)$ is defined ambiguously: $\xi(\mathbf{r})$ is chosen arbitrarily. This ambiguity leads to invariance responsibility of equations under transformations $\mathbf{A}(\varphi, \theta, \xi) \rightarrow \mathbf{A}(\varphi, \theta, \xi')$. Due to the locality of such transformations the gradient and the effective field must be in combination $\nabla + \mathbf{A}(\varphi, \theta, \xi)$.

In many (symmetric) cases this approach permits a simplification of Gor'kov equations. The Gor'kov equations allow us to find the Green's functions and then the critical temperature of the magnetic superconductor. In Fig.1 the critical temperature of the magnetic superconductor as a function of effective exchange in the case of helicoidal magnetization is shown.

In framework of suggested approach the Usadel and Eilenberger equations can be also rewritten. Relative to known quasiclassical approach [3] we do not need to assume that the effective exchange field along with the superconducting order parameter is changed slowly in comparison with the superconducting coherence length. In this sense our approach is more consistent: the magnetization inhomogeneity on correlation length is responsible for the appearance of the triplet component of the superconducting condensate.

The work is partially supported by the Ministry of Education and Science of the Russian Federation and the RFBR (13-02-01202).

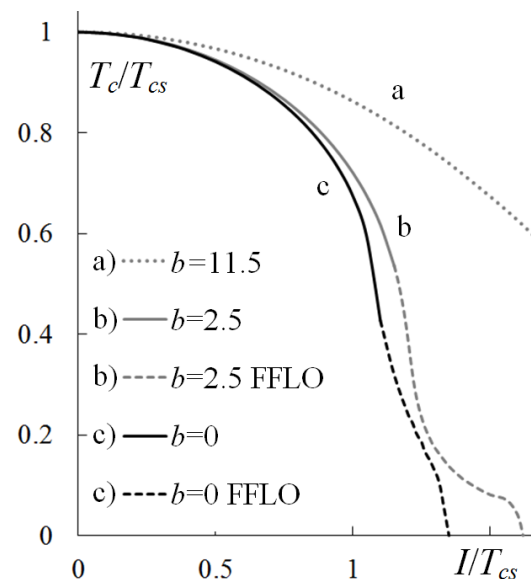


Fig.1. Dependence of the critical temperature T_c/T_{cs} as a function the average exchange field I/T_{cs} with various intensities of rotation $b = v_f \text{grad}(\theta/T_{cs})$, the dashed lines correspond to the Fulde-Ferrell-Larkin-Ovchinnikov (FFLO) states. T_{cs} is the critical temperature of bulk superconductor, v_f is the Fermi velocity.

[1] Ya.V. Fominov, A.F.Volkov, K.B.Efetov, *Phys. Rev. B.*, **75** (2007) 104509.

[2] A. F. Volkov, *Phys. Rev. B.*, **77** (2008) 064521.

[3] E.A. Demler, G.B. Arnold, M.R. Beasley, *Phys. Rev. B.*, **55** (1997) 15174.

30PO-I2-12

CURRENT-PHASE RELATION OF SFS JUNCTIONS WITH A COMPOSITE INTERLAYER

Sheyerman A.E.^{1,2}, Kislinskii Yu.V.¹, Shadrin A.V.^{1,3}, Constantinian K.Y.¹, Ovsyannikov G.A.^{1,3}

¹ Kotel'nikov IRE RAS, Moscow, Russia

² Moscow Institute of Physics and Technology, Dolgoprudny, Russia

³ MC2, Chalmers University of Technology, Gothenburg, Sweden

sasha@hitech.cplire.ru

A domination of second harmonic of the current-phase relation (CPR) was predicted [1] for SFS junctions with non-collinear magnetizations in composite interlayer. The second harmonic component in CPR could be experimentally evaluated via measurements of either Shapiro steps or detector response at microwave frequencies [2]. Au/Nb/La_{0.7}Sr_{0.3}MnO₃/ SrRuO₃/YBa₂Cu₃O_{7- δ} mesa-structures with a composite oxide ferromagnetic bilayer with non-collinear magnetizations are considered [3]. Microwave measurements with applied magnetic field demonstrate enhancement of Shapiro step amplitudes. Moreover, we observed an enhanced I_I/I_C ratio influenced by dc magnetic field, being even slightly higher than the one predicted by modified resistively shunted junction model taking into account second harmonic of CPR. Note, the sample was magnetic field cooled at $H=15$ Oe perpendicular to the substrate plane. Under external magnetic field $I_C(H)$ functions have oscillating behaviour with higher maxima.

This work was supported by the Division of Physical Sciences, Russian Academy of Sciences; Russian Federation President Grant for Support of Leading Scientific Schools NSh4871.2014.2; and RFBR project 14-07-00258.

[1] C. Richard, M. Houzet, and J.S. Meyer, *Phys. Rev. Lett.*, **110** (2013) 217004.

[2] P.V. Komissinskiy et al, *Phys. Rev. B*, **78** (2008) 024501.

[3] G.A. Ovsyannikov, A.E. Sheyerman, et al., *JETP Letters*, **97** (2013) 145.

30PO-I2-13

CRYSTAL GROWTH, MICROSTRUCTURE AND PHYSICAL PROPERTIES OF THE MIXED ALKALI METAL $(K_{1-z}Na_z)_xFe_{2-y}Se_2$ IRON SELENIDE

Liu M.¹, Roslova M.V.¹, Ovchenkov Y.A.², Kuzmichev S.A.², Kuzmicheva T.E.², Trifonov A.S.², Gippius A.A.², Lue C.S.³, Presniakov I.A.¹, Morozov I.V.¹, Boltalin A.I.¹, Shevelkov A.V.¹, Vasiliev A.N.²

¹ Department of Chemistry, Lomonosov Moscow State University, Leninskiye Gory, 119991, Moscow, Russian Federation

² Department of Physics, Lomonosov Moscow State University, Leninskiye Gory, 119991, Moscow, Russian Federation

³ Department of Physics, National Cheng Kung University, 1-Ta-Hsueh Road, 70101, ROC Tainan, Taiwan
lmdlut@gmail.com

In our work, superconducting mixed alkali metal $(K_{1-z}Na_z)_xFe_{2-y}Se_2$ iron selenide were synthesized for the first time. It was found that the maximum degree of substitution z is not more than 0.35. Using the self-flux technique we grew superconducting $(K_{1-z}Na_z)_xFe_{2-y}Se_2$ single crystals ($z=0$ ($T_c=24K$), 0.15 (14K), 0.21 (31K), 0.32 (32K), 0.4 (26K)). Properties of the sample with a degree of substitution $z = 0.32$ were studied in more detail.

The EDX mapping revealed the nearly uniform elements distribution on the crystal surface while the XRD measurements indicate that the crystals are compositionally inhomogeneous on nanoscale. Our STM studies suggest that at room temperature the sample shows spatial variations of the local electronic properties and has regions with a significantly different conductivity. The observed regions have dimensions in the range of one micrometer and indicate a phase separation in the sample. Partial sample degradation was observed to lead to formation of nanometer sized particles uniformly distributed throughout the cleaved sample surface.

The physical properties of the as-prepared sample are characterized by electrical resistivity, magnetization and specific heat measurements. Resistivity measurements show the onset of the superconducting transition at 33 K and zero resistivity at 31.7 K. The large upper critical field $H_{c2}(0)$ was estimated as high as about of 140 T for the in-plane field and 38 T for the out-of-plane field. The anisotropy of $H_c^{ab}(0)/H_c^c(0)$ and coherence lengths $\xi^c/\xi^{ab}(0)$ was found to be around 3.7. The pioneer studies by multiple Andreev reflections effect spectroscopy (“break-junction” technique) revealed the presence of two anisotropic superconducting gaps.

$\Delta_L = (9.3 \pm 1.5)$ meV, $\Delta_S = (1.9 \pm 0.4)$ meV, and provided measuring of the $\Delta_L(T)$ temperature dependence. The BCS-ratio for the large gap $2\Delta_L/k_B T_c^{bulk} \approx 6.3$ points to a strong electronboson coupling in the “driving” condensate characterized by Δ_L order parameter.

The properties of the $(K_{1-z}Na_z)_xFe_{2-y}Se_2$ samples seem to be rather similar to those of undoped potassium iron selenide $K_xFe_{2-y}Se_2$. This may point to minor variations in superconducting phase composition under K by Na substitution, which is possible, for example, in the case of irregular sodium distribution in the coexisting phases on nanoscale revealed by our XRD measurement. For a deeper understanding of the role of sodium in formation of microstructure of the sample the ^{23}Na -NMR method was used. In addition, features of local iron atoms environment were studied by ^{57}Fe Mossbauer spectroscopy.

The authors would like to acknowledge the financial support by the Russian Foundation for Basic Research (ref. No.12-03-01143-a).

30PO-I2-14

MAGNETIC ORDERING OF IRON IONS IN Fe-Se-Te SUPERCONDUCTORS

*Frolov K.V.¹, Vasyukov D.M.¹, Perunov I.V.¹, Naumov P.G.¹, Korotkov N.Yu.¹, Lyubutin I.S.¹,
Belikov V.V.², Kazakov S.M.², Pudalov V.M.³, Gavrilkin S.Yu.³*

¹ Shubnikov Institute of Crystallography RAS, Moscow, Russia

² Lomonosov Moscow State University, Chemistry Department, Moscow, Russia

³ Lebedev Physical Institute RAS, Moscow, Russia

green@crys.ras.ru

Discovery of the iron-based superconductors [1-4] has initiated intensive studies of these materials and resumes the discussion about magnetic mechanisms of the high temperature superconductivity. The FeSeTe compounds are structural simplest among new superconductors and they can be considered as convenient modelling objects for the studies of interplay between superconductivity and magnetic order of iron ions. Absence of superconductivity in the bulk FeTe compound and its presence in the isostructural FeSe and FeSeTe systems attract special interest. In this work we present the results of studies of the Fe_{1+x}Te and $\text{FeSe}_{1-y}\text{Te}_y$ compounds by the absorption ^{57}Fe Mössbauer spectroscopy in the temperature range of 5 – 295 K.

The ^{57}Fe Mössbauer spectra of the Fe_{1+x}Te and $\text{FeSe}_{1-y}\text{Te}_y$ powder samples were recorded in the transmission geometry with a standard MS-1100Em spectrometer operating in the constant accelerations regime and equipped with a special closed-cycle helium cryostat RTI CryoFree-104. The source of γ -quanta [$^{57}\text{Co}(\text{Rh})$] was at room temperature. Isomer shifts values were measured relative to the reference α -Fe sample at room temperature. The temperature dependences of specific heat $C_p(T)$ and magnetic susceptibility $\chi(T)$ was measured using a Quantum Design PPMS.

The Mössbauer spectra of the non-superconducting Fe_{1+x}Te samples ($x = 0.075, 0.100, 0.125, 0.175, 0.225$) have paramagnetic shape at room temperature and can be well fitted to superposition of doublets corresponding to the Fe ions in different structural positions. Below 70 K spectra of all samples show complex magnetic splitting which corresponds to strong magnetic ordering of the Fe ions. Mössbauer spectra of the superconducting $\text{FeSe}_{1-y}\text{Te}_y$ ($y = 0.5, 0.8$) samples mainly have a paramagnetic shape in the all temperature range of 5 – 295 K and can be well fitted to superposition of doublets too. But in low temperature spectra only small magnetic components appear even for $\text{FeSe}_{0.2}\text{Te}_{0.8}$ sample which is chemical closest to the binary FeTe compound. We assume that only interplanar Fe ions are responsible for strong magnetic ordering in the Fe_{1+y}Te system.

Support by Russian Science Foundation and “Strongly correlated electronic systems” program of the Russian Academy of Sciences is acknowledged.

[1] J. Kamihara, T. Watanabe et al, *J. Am. Chem. Soc.*, **130** (2008) 3296.

[2] R. Liu, G. Wu et al, *Phys. Rev. Lett.*, **101** (2008) 087001.

[3] F. Hsu, J. Luo et al., *PNAS USA*, **105** (2008) 14262.

[4] K. Yeh, T. Huang et al, *EPL*, **84** (2008) 37002.

30PO-I2-15

MÖSSBAUER STUDIES OF GdO_{0.79}F_{0.21}FeAs SUPERCONDUCTOR*Korotkov N.Yu.¹, Frolov K.V.¹, Lyubutin I.S.¹, Khlybov E.P.², Pudalov V.M.³,
Sadakov A.V.³, Pervakov K.S.³*¹ Shubnikov Institute of Crystallography, Russian Academy of Science, 119333 Moscow, Russia² Institute for High Pressure Physics, Russian Academy of Sciences, 142190 Troitsk, Russia³ Lebedev Physical Institute, Russian Academy of Sciences, 119333 Moscow, Russia

korotkov.nk@gmail.com

The recent discovery of a new class of layered high temperature superconductors based on iron with T_C up to 56 K [1] is currently in the focus of research interest. The theoretical suggestion that the superconductivity is unconventional and induced by spin fluctuations [2-3] and the fact that there is an unusual combination of magnetic ordering and superconductivity in the same material [4] stimulate high interest and intensive studies of these compounds. The Mössbauer spectroscopy is one of the most powerful methods of studying the structural, electronic and spin states of Fe ions and their magnetic order below T_C .

Until now the Mössbauer data on REOF_{1-x}FeAs with RE = Gd and doped with F are practically absent. Meanwhile this information is very important to understand the relationship between superconductivity and magnetism because it can be obtained without application of an external magnetic field.

In our studies, the GdO_{0.79}F_{0.21}FeAs sample was prepared by the solid state synthesis under high pressure [5]. The sample was optimally doped and its critical temperature was $T_C = 53$ K. The absorption ⁵⁷Fe-Mössbauer spectra were recorded at temperatures between 5 K and 295 K in the transmission geometry with a standard spectrometer operating in the constant accelerations regime. All measurements were performed using a ⁵⁷Co γ -quanta source in a Rh matrix. The isomer shift values of the experimental Mössbauer spectra were measured relative to standard α -Fe absorber at room temperature.

The computer analysis shows that low temperature Mössbauer spectra can be represented as a superposition of two paramagnetic doublets which correspond to iron ions of the main superconducting phase and one magnetic sextet which transforms to third doublet at temperatures above 77 K. This component corresponds to the iron ions of the nonsuperconducting impurity phase FeAs [6,7]. The superconducting phase doublets have almost equal isomer shifts δ but different quadrupole splitting ε values. We assume that two nonequivalent positions of Fe²⁺ ions in low ($S = 0$) or intermediate ($S = 1$) spin state exist in the superconducting phase.

This work is supported by Russian Foundation for Basic Research #14-02-31647

- [1] T. Watanabe, Y. Kamihara, M. Hirano and H. Hosono: *J. Am. Chem. Soc.* **130** (2008) 3296.
- [2] G. F. Chen, Z. Li, D. Wu, G. Li, W. Z. Hu, J. Dong, P. Zheng, J. L. Luo and N. L. Wang: *Phys. Rev. Lett.*, **100** (2008) 247002.
- [3] I. I. Mazin, D. J. Singh, M. D. Johannes, M. H. Du: *Phys. Rev. Lett.*, **101** (2008) 057003.
- [4] D. R. Sanchez et al. Baggio-Saitovitch: *J. Phys.: Condens. Matter*, **21** (2009) 455701.
- [5] E. P. Khlybov, O. E. Omelyanovsky, A. Zaleski, A. V. Sadakov, D. R. Gizatuln, L.F. Kulikova, I. E. Kostuleva, and V. M. Pudalov: *JETP Letters.*, **90** (5) (2009) 387.
- [6] L. Haggstrom, A. Gustavsson-Seidel and H. Fjellvag: *Europhys. Lett.*, **9** (1) (1989) 87-92.
- [7] N. Y. Korotkov, K. V. Frolov, I. S. Lyubutin, E. P. Khlybov and V. M. Pudalov *Journal of Superconductivity and Novel Magnetism*, **26** (9) (2013) 2877-2879.

30PO-I2-16

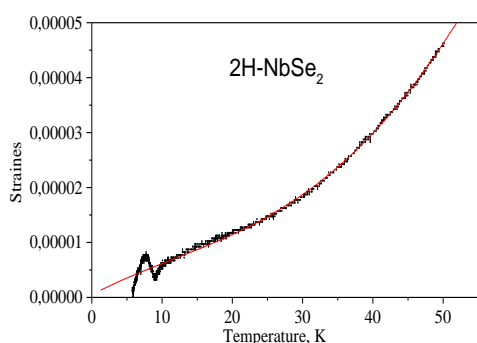
THE LOW TEMPERATURE THERMAL EXPANSION OF NIOBIUM DICHALCOGENIDE

Krynetskii I.B.¹, Kulbachinskii V.A.¹, Golubkov M.V.², Kaluzhnaya G.A.², Rodin V.V.²,
Shabanova N.P.², Kovalenko V.I.²

¹ M.V.Lomonosov Moscow State University, 119991 GSP-1, Moscow, Russia

² P.N.Lebedev Physical Institute of Russian Academy of Sciences, 119991 GSP-1, Moscow, Russia

The study of layered compound 2H-NbSe₂ is of great importance due to the variation of its electronic state with temperature. First at T=33 K a phase transition to an incommensurate charge density wave (CDW) state occurs. Then the transition into superconducting state is happened at T=7.2 K. The CDW order in 2H-NbSe₂ arises in the layer planes as determined by the single nonzero component of the vector of propagation $q=[0.329, 0, 0]$ [1]. Usually, in nonsuperconducting materials with CDW ordering the very low temperature state of electron system is the commensurate CDW order. In materials with CDW state for understanding the nature of CDW is very important to study its thermal expansion.



We have performed high precision study of thermal expansion in (001)-plane of 2H-NbSe₂ in temperature interval from T=5.7 K to T=50 K using the home-made strain gauge dilatometer. The experimental curve of the linear thermal expansion in some direction in basal plane of 2H-NbSe₂ is shown at the figure, The solid line is the Debye approximation. The very surprising anomaly of thermal expansion is observed at temperatures below ~ 10 K. Note that the experimental curve in this temperature interval is reproducible and has been observed for different samples. It is seen that the found

anomaly consists of two portions. The lower portion of the anomaly reflects the thermal expansion of the superconducting state of 2H-NbSe₂ which ended at T=7.2 K. The portion of the curve between T=7.2 K and T \approx 10 K testifies some additional phase transition other than the transition into superconducting state. The features of this portion of the curve allow us to conclude that this phase transition is more of the nature of the first order. We compare our results with the thermal expansion study of layered compound 1T-TaSe₂ in which the transition from the incommensurate CDW to the commensurate CDW is of the first order [2] and may suppose that the found anomaly of thermal expansion of 2H-NbSe₂ owes its origin to the first order phase transition into the commensurate CDW state. Thus our data indicate, that first the transition from the incommensurate CDW state to the commensurate CDW state occurs just above the temperature of superconducting transition. And after that the transition into superconducting state in 2H-NbSe₂ takes place at T=7.2 K from the commensurate CDW state.

[1] F.Weber, S.Rosenkranz, J.-P.Castellan et al., *PRL.*, **107** (2011) 107403.

[2] O.Sezerman, A.M.Simpson, and M.N.Jericho, *Solid State Commun.*, **36** (1980) 737.

30PO-I2-17

MAGNETIC JOSEPHSON JUNCTIONS FOR REVERSIBLE COMPUTATIONS

*Soloviev I.I.¹, Klenov N.V.², Shegolev A.E.², Bakurskiy S.V.^{2,4}, Golubov A.A.^{3,4}, Pankrstov A.L.⁵,
Il'ichev E.V.⁶, Kupriyanov M.Yu.^{1,4}*

¹ Skobeltsyn Institute of Nuclear Physics Lomonosov Moscow State University, Moscow, Russian Federation

² Physics Department Lomonosov Moscow State University, Moscow, Russian Federation

³ Faculty of Science and Technology and MESA+ Institute for Nanotechnology, University of Twente, The Netherlands

⁴ Moscow Institute of Physics and Technology, State University, Dolgoprudniy, Moscow region, Russian Federation

⁵ R. E. Alekseev Nijniy Novgorod, Minsk, Belarus

⁶ Institute of Photonic Technology, Jena, Germany
igor.soloviev@gmail.com

We present the possibilities to construct principal logic cell for reversible (adiabatic) computing by implementation of magnetic Josephson junction in usual dc-SQUID.

The interest to this problem is motivated by extremely small energy dissipation per operation in the mentioned reversible SQUID-based logic circuits. The currently demonstrated specific energy dissipation per elementary operation for semiconductor technology is of the order of $10^6 kT$, where k is the Boltzmann constant and T is the temperature. However, the thermodynamic threshold per logic operation, known as the Landauer limit, is equal to $kT \ln 2$ [1, 2]. And this limit can be achieved and outperformed due to *reversible* controllable evolution of current states in arrays of magnetically coupled pi-shifted bi-SQUIDs.

The suggested bi-SQUID is a two-junction interferometer, where geometric inductance is shunted with Josephson π -junction in superconducting state. This shunt is based on a heterostructure with *negative critical current*, which consists of superconductor (S), insulator (I), and ferromagnetic (F), and normal (N) metal (e.g. SFS, SIsFS, SINFS et cetera). Fabrication and utilization of the suggested structure proved to be much more easier, then for the known Josephson reversible cells (based on SQUIDs with negative inductances and quantum parametron) [2, 3].

We start with the brief discussion of impact of magnetic Josephson junction on dc-SQUID potential energy. Then we present the analysis of reversible dynamics in single cell, in the cells, coupled in the transition line and in simple shift register. As a conclusion, we compare main characteristics (such as energy dissipation per operation and size) of the bi-SQUID-based adiabatic circuits with the same characteristics of the mentioned competing structures.

Support by RFBR grants 14-02-90018, 14-02-31002_mol_a, Ministry of Education and Science of the Russian Federation, President grant MK-1841.2014.2, and RFBR grant F14R-020 and Dynasty foundation.

[1] D. S. Holmes, A.L. Ripple, M.A. Manheimer, *IEEE Trans. on Appl. Supercond.*, **23** 1701610 (2013).

[2] J. Ren, V.K. Semenov, *IEEE Trans. on Appl. Supercond.*, **21**(3) (2011) 780.

[3] N. Takeuchi, D. Ozawa, Y. Yamanashi et al., *Supercond. Sci. Technol.*, **26** (2013) 035010.

30PO-I2-18

AGING PROPERTIES OF THE DISORDERED ISING-LIKE FERROMAGNETS AT CRITICAL POINT

Pospelov E.¹, Prudnikov V.¹, Prudnikov P.¹, Malyarenko P.¹

¹Omsk State University, Omsk, Russia

posevg@yandex.ru

A spin system quenched to below or exactly at its critical temperature T_c undergoes aging that is time-translation invariance is broken and observables such as correlation or response functions display dynamical scaling [1,2]. Originally, these features were founded in complex glassy systems but the main properties of slow dynamics can be observed in simpler systems with second-order phase transition near critical point, because of the relaxation time diverges as $t_{rel} \sim |T - T_c|^{-z\nu}$ with $z, \nu > 0$ and equilibrium state is never achieved. During this out-of-equilibrium stage aging phenomena occurs with two-time dependence of correlation $C(t, t_w)$ and response $R(t, t_w)$ functions characterized by two times: waiting time t_w and observation time $(t - t_w)$ with $t > t_w$ and $t, t_w \ll t_{rel}$.

Non-equilibrium dynamic shows the violation of the fluctuation-dissipation theorem (FDT). It connects the correlation $C(t, t_w)$ and response $R(t, t_w)$ functions by relation:

$$TR(t, t_w) = X(t, t_w) \frac{\partial C(t, t_w)}{\partial t_w}.$$

The asymptotic limit $X^\infty = \lim_{t_w \rightarrow \infty} \lim_{t \rightarrow \infty} X(t, t_w)$ which called fluctuation-dissipation ratio (FDR) is a new independent characteristic of the out-of-equilibrium stage.

Ageing properties of the three-dimensional ferromagnetic pure and diluted Ising models were investigated at critical point. The model Hamiltonian is $H = -J \sum_{\langle i, j \rangle} p_i p_j S_i S_j$ with $J > 0$ is the

exchange interaction integral between nearest neighbours, p_i is the disorder distribution and S_i is the i -th spin value. The simulations were made by Monte Carlo method. We have considered the dynamics of the model both high temperature initial state with small magnetisation $m_0 \ll 1$ and low temperature initial state with $m_0 = 1$. Two-times autocorrelation and response functions for the systems with spin concentrations $p = 1.0, 0.8$, and 0.6 were computed and analysed. It was shown that the decay of the functions is slowed down with increasing t_w .

The FDR depends on system initial state. The mean-field theory without fluctuation contribute gives the value $X^\infty = 0.8$ in case of low temperature initial state and $X^\infty = 0.5$ in case of high temperature one [3]. Taking fluctuation into account the FDR values is decreased. Our MC investigation of the 3D Ising model leads to the values $X^\infty(p = 1) = 0.381(16)$, $X^\infty(p = 0.8) = 0.413(10)$ and $X^\infty(p = 0.6) = 0.446(10)$ for the with $m_0 \ll 1$ initial state, and $X^\infty(p = 1) = 0.77(6)$ for the $m_0 = 1$ initial state. It was proved the violation of the FDT.

The reported study was supported in part by Ministry of Education and Science of Russia through project No. 2.3046.2011 and by grant MU-4/2013 of OmSU. The simulations were supported by the Moscow State University Lomonosov Supercomputing Center and Joint Supercomputer Center of the Russian Academy of Sciences.

[1] N. Afzal, M. Pleimling, *Phys. Rev. E* **87** (2013) 012114.

[2] V.V. Prudnikov, P.V. Prudnikov, E.A. Pospelov, *JETP*, **118** (2014) 401-409.

[3] P. Calabrese, A. Gambassi, *J. Phys. A* **38** (2005) R133.

30PO-I2-19

MAGNETIC PREHISTORY IN THE HEAT CAPACITY OF THE LOW-TEMPERATURE SUPERCONDUCTORS

Podgornykh S.M.

Institute of Metal Physics, Ural Division of the Russian Academy of Sciences,
S.Kovalevskya st., 18, 620990 , Ekaterinburg, Russian Federation
sp@imp.uran.ru

Effect of the magnetic prehistory on the temperature dependence of the heat capacity of the superconducting *Pb*, *La*, *Sn* was studied. We observed a difference between of the heat capacity in the zero field cooled (ZFC) state and in the field cooled (FC) state in zero magnetic field for the ring specimens. The normal (*N*) state was formed by applied external magnetic field H larger than H_C . Earlier we observed the same feartures of the low-temperature heat capacity of the superconducting *Pb* [1]. The trapped flux was produced in the specimen after cooling under magnetic field (FC state) through T_C and then magnetic field was turned off. In this case the specimen has an intermediate state which is characterized by a subdivision into superconducting (*S*) and *N* regions with the surface between them. Fig.1 and Fig.2 show temperature variations of the heat capacity C_p for the specimen of *La*. One can see the difference between the heat capacity in ZFC and FC states in zero magnetic field for the ring specimens: the FC heat capacity is smaller than both in *N* and *S* states. There is an instability of the *S* state of the specimen with trapped flux when the temperature increases. We believe that the surface energy between the normal and superconducting phases changes and gives rise to the changes of the elastic energy and as well the heat capacity of the specimen. The pressure of the electron gas as the cause of the surface energy is under discussion. This result is the experimental evidence of the surface energy contribution to the heat capacity of the low-temperature superconductors.

Support by the Russian Foundation for Basic Research, project No. 13-02-96022r-ural-a is acknowledged.

[1] S.M. Podgornykh, V.P. Dyakina, A.F. Prekul, *MISM-2008, Book of Abstracts*, (2008) 427-428.

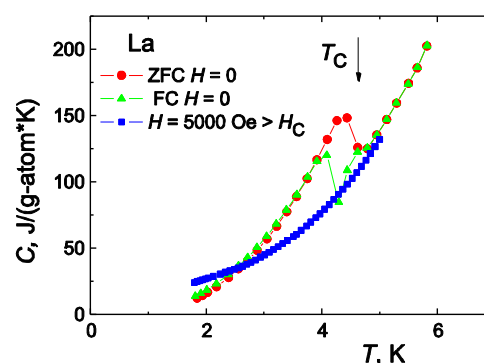


Fig. 1. Temperature dependence of the heat capacity $C_p(T)$ of *La* ($H_C= 808$ Oe): ■- normal state; ●- and ▲ - superconducting state ($T_C = 4.9$ K).

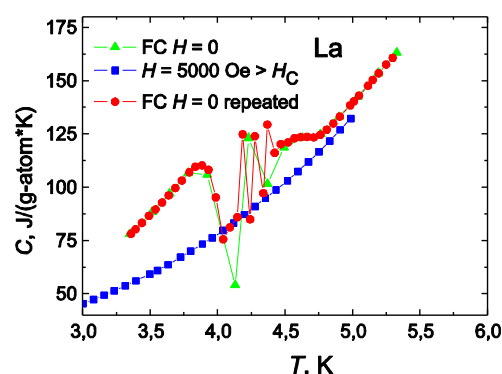


Fig. 2. Heat capacity $C_p(T)$ of *La* in detail: ■- normal state; ●- and ▲ - superconducting state after cooling at $H_{ex} = 5000$ Oe. The FC measurements were performed at zero external magnetic field $H_{ex} = 0$. The repeated measurements were made with a smaller temperature step than the first case.

30PO-I2-20

TWO SOURCES OF PARAMAGNETIC CURIE-TYPE CONTRIBUTION TO THE NORMAL STATE MAGNETIC SUSCEPTIBILITY OF HTSC $\text{YBa}_2\text{Cu}_3\text{O}_{6+\delta}$

Mamsurova L.G.¹, Trusevich N.G.¹, Pigalskiy K.S.¹, Vishnev A.A.¹, Mamsurov I.V.^{1,2}

¹ N.N. Semenov Institute of Chemical Physics RAS, Moscow, Russia

² Moscow State University, Faculty of Physics, Moscow, Russia

mamsurova@chph.ras.ru

The comparative study of the temperature dependence of the normal (non-superconducting) state magnetic susceptibility $\chi(T)$ for the two series of $\text{YBa}_2\text{Cu}_3\text{O}_{6+\delta}$ ($0.6 < \delta \leq 1$) samples in the range $67 \leq T \leq 400$ K was performed. Experimental evidence for the existence of two paramagnetic Curie-type contributions ($\chi = C_{\text{Curie}}/T$) of different nature was obtained. In addition to the usually mentioned in literature contribution due to the presence of a magnetic impurity in the samples (Fig. 1), the other Curie-type contribution has been revealed. Its nature, as it was shown, is related to the contribution from chains Cu1-O4 in the basic crystallographic planes. This contribution is clearly evident for pure samples ($\delta < 1$) at low temperature $T < 150$ K (Fig. 2). It increases with oxygen decreasing in the chains Cu1-O4 (curves 1-3) and depends on the way of the oxygen vacancies ordering (curves 3a and 3b). In addition the value $C_{\text{Curie}}(\delta)$ correlates with the lattice parameter $b(\delta)$ along which the chains Cu1-O4 are arranged.

The obtained quantitative information about chain contribution to the normal state magnetic susceptibility for the system $\text{YBa}_2\text{Cu}_3\text{O}_{6+\delta}$ allows to make a conclusion about the spin state of copper in the chains, and furthermore it is necessary for the subsequent identifying of the part of experimental dependence $\chi(T)$ which is due to the contribution from the superconducting CuO_2 -planes (see Fig.2 at $T > 150$ K) and for which the generally accepted theoretical description is still absent.

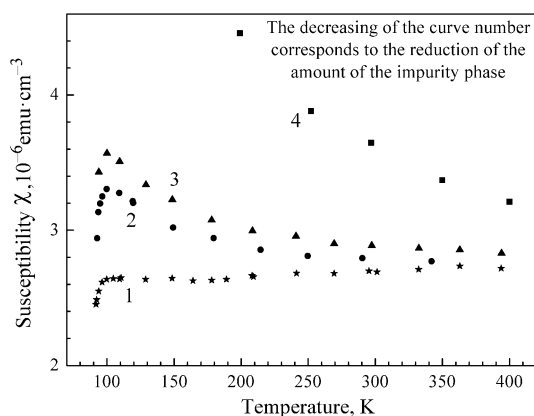


Fig. 1 demonstrates decrease of C_{Curie} with decreasing impurity phase (BaCuO_2) in sol-gel samples $\text{YBa}_2\text{Cu}_3\text{O}_{6.94}$.

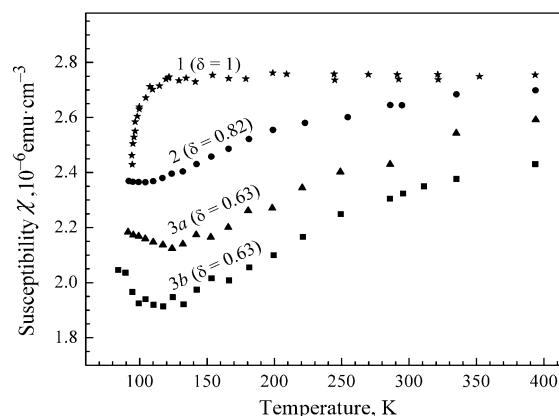


Fig. 2 demonstrates the variation of C_{Curie} in pure samples $\text{YBa}_2\text{Cu}_3\text{O}_{6+\delta}$ with different oxygen amount δ in Cu1-O4 chains.

30PO-I2-21

ANOMALOUS TEMPERATURE DEPENDENCE OF THE UPPER CRITICAL MAGNETIC FIELD IN ELECTRON-DOPED HIGH- TEMPERATURE SUPERCONDUCTOR

Charikova T.B.¹, Shelushinina N.G.¹, Harus G.I.¹, Neverov V.N.¹, Petukhov D.S.¹, Ivanov A.A.²

¹ Institute of Metal Physics RAS, Ekaterinburg, Russia

² Moscow Engineering Physics Institute, Moscow, Russia

shel@imp.uran.ru

The case of electron doping on high-temperature cuprate superconductors provides an important additional example of introducing charge into the CuO_2 planes. The antiferromagnetic (AFM) phase in the electron-doped material persists to much higher doping levels than in the hole-doped systems, and superconductivity (SC) occurs in a doping range that is almost five times narrower. In addition, these two ground states (AFM and SC) occur in much closer proximity to each other and may even coincide unlike in the hole-doped materials.

We have synthesized a good quality single crystal films of electron-doped cuprate superconductor $\text{Nd}_{2-x}\text{Ce}_x\text{CuO}_{4+\delta}$ near antiferromagnetic-superconducting phase boundary ($x = 0.14$) with different degree of disorder (δ) and made precise temperature measurements of the resistivity in external magnetic field up to 9T. The upper critical field as a function of temperature was determined by the resistivity method. It was found that temperature dependence of the upper critical field, $H_{c2}(T)$, for underdoped $\text{Nd}_{1.86}\text{Ce}_{0.14}\text{CuO}_{4+\delta}$ have an anomalous upward curvature. For an interpretation of our experimental data we explore theoretical considerations about temperature dependence of the upper critical field in two-gap dirty superconductor [1]. This model has been successively used to describe non - BCS behavior of $H_{c2}(T)$ in such diverse superconductors as MgB_2 , FeAs – systems and optimally doped $\text{Nd}_{1.85}\text{Ce}_{0.15}\text{CuO}_{4+\delta}$ system (see [2] and references therein).

The clue to understand the electron-doped cuprate comes from two doping-dependent parts of Fermi surface (FS) as revealed by ARPES investigations [3]. These are well explained in terms of the bandfolding effect associated with an AFM order fluctuations - spin density wave (SDW). The SDW correlation splits the band into upper and lower branches that results in a coexistence of electron-like and hole-like FS pockets. In the SC state, the quasiparticles could pair each other within the same band that leads naturally to a two-band / two-gap model.

We regard an investigated system as a superconductor with two FS sheets on which the superconducting gaps take the values Δ_1 and Δ_2 and the intraband diffusivities are D_1 and D_2 (indices 1 and 2 correspond to electrons and holes, respectively). It was found that the observed anomalous $H_{c2}(T)$ dependences can be consistently described by the two-band/two-gap model [1] with $\Delta_1 > \Delta_2$ for the diffusivity ratio $D_1/D_2 \gg 1$ (for optimally reduced sample $\Delta_1 = 1.6 \Delta_2$ and $D_1/D_2 = 5.4$). In accordance with analysis of [1] the critical temperature T_c corresponds to the maximum Δ (i.e. to the electron gap Δ_1) and in a case of different diffusivities the limiting value of $H_{c2}(0)$ is determined by the minimum diffusivity (i.e. by holes).

Thus, we obtain that in nominally electron-doped cuprate superconductor $\text{Nd}_{2-x}\text{Ce}_x\text{CuO}_{4+\delta}$ with $x = 0.14$ (in the close proximity of the antiferromagnetic phase) superconductivity is realized out both by electrons and holes due to the interplay of the SC order with AF order.

[1] A.Gurevich, *Phys.Rev.B*, **67** (2003) 184515(13).

[2] T.B.Charikova, N.G.Shelushinina, G.I.Harus et al., *Physica C*, **488** (2013) 25-29.

[3] N.P.Armitage, P.Fournier, R.L.Green, *Rev.Mod.Phys.*, **82** (2010) 2421-2487.

30PO-I2-22

THEORETICAL STUDY OF THE MAGNETIZATION OF RARE EARTH PYROCHLORES $\text{RE}_2\text{Ti}_2\text{O}_7$ (RE=Tb, Dy, Ho)

Klekovkina V.V.¹, Malkin B.Z.¹

¹ Kazan Federal University, Kazan, Russia
vera.klekovkina@kpfu.ru

Cubic rare earth titanates crystallizing in the pyrochlore lattice contain four magnetically non-equivalent rare earth sublattices which form a corner sharing tetrahedral network (local point symmetry of RE^{3+} ions is trigonal D_{3d}). These compounds refer to the class of geometry frustrated magnets and exhibit a wide variety of magnetic properties at low temperatures. Magnetic moments of rare earth ions in $\text{Dy}_2\text{Ti}_2\text{O}_7$ and $\text{Ho}_2\text{Ti}_2\text{O}_7$ compose a magnetic structure called Spin Ice. $\text{Tb}_2\text{Ti}_2\text{O}_7$ exhibits a spin liquid behaviour.

In this work the magnetic field and temperature dependences of magnetization of single crystals and powder samples of pyrochlores $\text{RE}_2\text{Ti}_2\text{O}_7$ (RE=Tb, Dy, Ho) in paramagnetic phase are simulated. Energy spectra of RE^{3+} ions were calculated in the framework of exchange charge model in the crystal field theory. Calculations of magnetization were performed with taking into account magnetic dipole and anisotropic exchange interactions within a mean field approximation. For $\text{Tb}_2\text{Ti}_2\text{O}_7$, magnitudes and directions of individual magnetic moments of the Tb^{3+} ions in magnetic fields along rhombic, tetragonal and trigonal crystallographic axes were computed.

Local lattice deformations induced by point defects of crystal lattice modify essentially magnetic properties of $\text{Tb}_2\text{Ti}_2\text{O}_7$ due to strong 4f-electron-strain interactions in this system. Magnetization of $\text{Tb}_2\text{Ti}_2\text{O}_7$ at low temperatures was calculated with taking into account impact of the random low-symmetry crystal fields induced by lattice deformations on the energy spectrum of terbium ions [1]. Parameters of the Hamiltonian of electron-deformation interaction were estimated in the framework of exchange charge model and verified by the analysis of magnetoelastic effects (magnetostriction and softening of the crystal lattice). The consideration of the effects due to random lattice deformations allows successful description of the $\text{Tb}_2\text{Ti}_2\text{O}_7$ magnetization (Fig. 1) in relatively weak magnetic fields (below 1 Tesla) at low temperatures when the corresponding shifts and splittings of the crystal field levels of the Tb^{3+} ions are comparable to energies of thermal excitations.

Results of simulations are in agreement with experimental data available from literature.

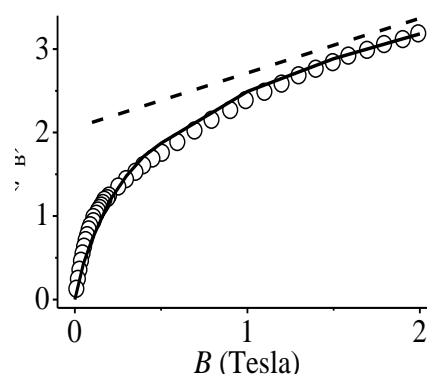


Fig. 1. Magnetization of $\text{Tb}_2\text{Ti}_2\text{O}_7$ for magnetic field along [111] axis at temperature 80 mK: mean field calculations (dashed line) and calculations with taking into account random deformations (solid line). Experimental data (symbols) are digitized from [2].

Support by RFBR (grant №14-02-00826) is acknowledged.

[1] B.Z. Malkin, D.S. Pytalev, M.N. Popova et al., *Phys. Rev. B*, **86** (2012) 134110.

[2] E. Lhotel, C. Paulsen, P. Dalmas de Reotier et al., *Phys. Rev. B*, **86** (2012) 020410.

30PO-I2-23

MAGNETIC PROPERTIES OF $\text{Pr}_x\text{Y}_{1-x}\text{Fe}_3(\text{BO}_3)_4$

Pankrats A.I.^{1,2}, Demidov A.A.³, Velikanov D.A.^{1,2}, Tugarinov V.I.¹, Temerov V.L.¹

¹ Kirensky Institute of Physics SB RAS, Krasnoyarsk, Russia

² Siberian Federal University, Krasnoyarsk, Russia

³ Bryansk State Technical University, Bryansk, Russia

vitugus@gmail.com

The $\text{Pr}_x\text{Y}_{1-x}\text{Fe}_3(\text{BO}_3)_4$ compound belongs to the family of rare-earth ferrobates which exhibit a variety of phase transitions and some multiferroic features. In $\text{PrFe}_3(\text{BO}_3)_4$ the magnetic moments of Pr and Fe are directed along the trigonal c -axis at $T < T_N \approx 39$ K [1, 2] and it shows the spin-flop transition for $\mathbf{B} \parallel \mathbf{c}$ [1, 3]. In $\text{YFe}_3(\text{BO}_3)_4$ at $T < T_N \approx 37$ K, the magnetic moments of Fe lie in the basal plane ab . Thus, as a result of competition of different contributions to the magnetic anisotropy of $\text{Pr}_x\text{Y}_{1-x}\text{Fe}_3(\text{BO}_3)_4$, the rearrangement of the magnetic structure between the easy-axis (EA) and easy-plane (EP) states appears to be possible.

In this work the experimental and theoretical investigations of the field and temperature dependences of magnetization $M_{c,\perp c}(B)$ and the temperature dependences of the initial magnetic susceptibility $\chi_{c,\perp c}(T)$ of $\text{Pr}_x\text{Y}_{1-x}\text{Fe}_3(\text{BO}_3)_4$ have been performed.

In the calculations we used a theoretical approach which has been successfully applied for description of the magnetic and magnetoelastic properties of $\text{PrFe}_3(\text{BO}_3)_4$ [3]. In order to determine the parameters of the crystal-field and the exchange parameters we have used the experimental data on the temperature dependence of $\chi_{c,\perp c}(T)$, the field and temperature dependences of $M_{c,\perp c}(B, T)$ and existing information on the structure of the ground multiplet of Pr^{3+} ion in $\text{PrFe}_3(\text{BO}_3)_4$. Good agreement of experimental and calculated magnetization curves $M_{c,\perp c}(B)$ at $T = 2$ -60 K and the temperature dependences $\chi_{c,\perp c}(T)$ in the ordered and paramagnetic regions was achieved. It is seen from Fig. 1 that the experimental (symbols) and calculated (lines) magnetization curves $M_c(B)$ of $\text{Pr}_{0.75}\text{Y}_{0.25}\text{Fe}_3(\text{BO}_3)_4$ at $T = 2$ and 20 K show magnetization jumps at the magnetic fields $B_{\text{SF}} \approx 2.2$ and 3.0 T, respectively. These jumps are caused by the spin-flop transition in the Fe subsystem from the initial EA state to the spin-flop phase. The investigations of magnetic and resonance properties showed that in $\text{Pr}_x\text{Y}_{1-x}\text{Fe}_3(\text{BO}_3)_4$ compounds at low temperatures and $B = 0$, the magnetic moments of the Pr and Fe-subsystems are oriented along the c -axis (for $x \approx 1$ -0.75, EA state), are inclined from the c -axis (for $x \approx 0.67$ -0.45, inclined state) and lie in the basal ab -plane (for $x \approx 0.25$ -0, EP state).

This work was supported by the RFBR (project no. 13-02-12442 ofi_m2).

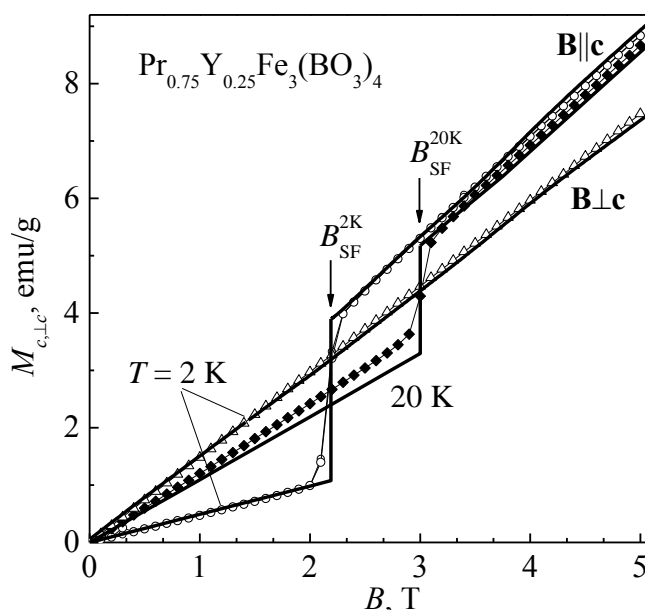


Fig. 1. Magnetization curves for $\mathbf{B} \parallel, \perp \mathbf{c}$.

[1] A.M. Kadomtseva, Yu.F. Popov, G.P. Vorob'ev et al., *JETP Lett.*, **87** (2008) 45-50.

[2] C. Ritter, A. Vorotynov et al., *J. Phys.: Condens. Matt.*, **22** (2010) 206002-206010.

[3] A.A. Demidov, N.P. Kolmakova, D.V. Volkov et al., *Physica B*, **404** (2009) 213-216.

30PO-I2-24

PHASE-SLIP LINE AS JOSEPHSON ELEMENT: OSCILLATIONS OF INSTABILITY CURRENTS IN MAGNETIC FIELDS

Kulikovskiy A.V.

Prokhorov General Physics Institute of RAS, Tarusa department, Moscow, Russia
kuliko@ran.gpi.ru

We studied experimentally resistive state properties of wide superconducting films of tin. This state is associated with the phase-slip lines (PSLs) arising against a dynamic vortex state due to evolution of the vortex instability. Temperature and magnetic field dependencies of the critical current I_c (current of the PSL formation) were analyzed. Application of a magnetic field resulted in a randomly oscillating $I_c(H)$ curve. The heights of the peaks and troughs were very variable, and no definite oscillation period was observed. There were no central peaks in the curves. Nevertheless, such apparently random curves were in general reproducible.

PSL is considered as Josephson junction with the length equal to the film's width w , the width equal to the film's thickness d , and the thickness equal to 2ξ , where ξ is the coherence length. An important test of the uniformity of the Josephson junction is the effect of an external magnetic field H parallel to the plane of contact on the critical current. When one applies an external field to the uniform junction with a dimension (perpendicular to the field) small compared to the Josephson penetration depth, the result is a single slit Fraunhofer diffraction pattern. External field transverse to the film surface was parallel to the plane of the phase-slip line as small Josephson contact.

Let's use the model considering the PSL as a large number of small individual contacts of characteristic width w_0 , and suppose that there is enough trapped flux present to make the phases of the different contacts random in zero applied fields. This explains why there was no central peak in the $I_c(H)$. In an external field the phases of the different contacts change, but they remain random, so $I_c(H)$ does not change in any systematic way with H .

We checked this model quantitatively by Fourier analysis. In the general case

$$I_c(H) = \left| \int J(x) \exp(i2\pi Hax/\Phi_0) dx \right|,$$

where $J(x)$ is a complex supercurrent density per unit width, and a is the magnetic thickness of the junction. Because experimental curve $I_c(H)$ does not contain phase information, one cannot deduce $J(x)$ directly. However, by taking the transform of $I_c^2(H)$, one can obtain $F(x)$ – the autocorrelation function of $J(x)$. $F(x)$ is also complex, and it is convenient to consider $|F(x)|^2$.

Taking a model of small contacts with random phase spread uniformly over a junction of size w one can show that except for $x < w_0$ one expects $|F(x)|^2$ to be a random function with exponential distribution at each value of x . The mean of the distribution is a triangular function of x with the width $2w$. For $x < w_0$, the phases cease to be random, leading to a large central peak.

The widths of the individual contacts for different samples and different temperatures obtained from the Fourier analysis were of the correct order and coincided with those predicted by the model of phase-slip regions.

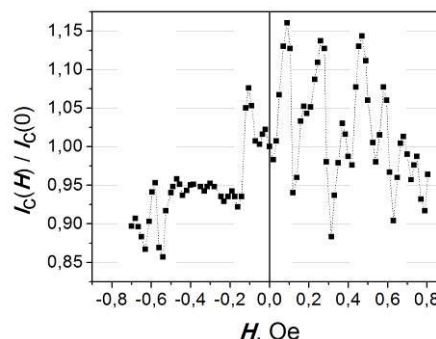


Fig. 1. Experimental $I_c(H)$ curve.

30PO-I2-25

OSCILLATION INHARMONIOUS MODEL SUPERCONDUCTING CRYSTAL*Netesova N.P.*M.V. Lomonosov Moscow State University, Physics Faculty, Moscow, Russia
nnp@mig.phys.msu.ru

The microscopic theory on the Hubbard model basis explains the main superconductor properties. HTSC is concerned to strongly electron correlated systems. In case of the one oscillation crystal model the equations of dielectric function real component [1] are assumed

$$\varepsilon_r = 1 + \omega_p^2 (\omega_c^2 - \omega^2) [(\omega_c^2 - \omega^2)^2 + 4\gamma^2 \omega^2]^{-1}, \quad \omega_p^2 = (4\pi e^2 \cdot m^{-1}) \cdot N_e \cdot q^{-1},$$

$$N_e = N_a \cdot s \cdot \rho \cdot M^{-1}, \quad \omega_p^2 = (4\pi e^2 \cdot m^{-1}) \cdot N_a \cdot M^{-1} \cdot s \cdot \rho \cdot q^{-1}, \quad \omega_c^2 = \omega_o^2 - \beta \cdot \omega_p^2, \quad (1),$$

where e , m , N_e , s are the charge, mass, density and valency number electron, accordingly; ω_c , ω_o , ω_p , γ , q , are effective natural, natural, plasma and radiant friction frequencies, the interaction parameter, accordingly, β is Lorentz factor, ρ is mass density, M is molecular mass, N_a is the Avogadro number. We consider basic and isotope crystals (Table 1).

Table 1. Isotope effect in superconducting crystals.

Formula	Explanation
$(T-T_c) \cdot C^{-1} = (\omega_{c12}^2 - 4\delta^2) \cdot \omega_{p12}^{-2}$ (2)	T_c , T_{ci} - superconducting phase transition temperatures; C , C_i - the Curie-Weiss factors; ω_{o12} , ω_{o12i} , ω_{c12} , ω_{c12i} , ω_{p12} , ω_{p12i} - effective natural, natural, plasma frequencies; q_{12} , q_{12i} - the interaction parameters, δ , δ_i - parameters, β , β_i - Lorentz factors, V_r , V_{ri} , $S_r = S_{ri}$ - volumes and molecule numbers in crystal lattices for basic and isotope crystals, accordingly, ρ_r is x-ray density.
$(T-T_{ci}) \cdot C_i^{-1} = (\omega_{c12i}^2 - 4\delta_i^2) \cdot \omega_{p12i}^{-2}$ (2i)	
$\frac{(T_{ci}-T_c) \cdot C^{-1} = (\omega_{c12}^2 - 4\delta^2) \cdot \omega_{p12}^{-2} - \omega_{c12}^2}{\omega_{c12i}^2 - 4\delta_i^2} \cdot \omega_{p12i}^{-2}$ $\omega_{c12}^2 = \omega_{o12}^2 - \beta \cdot \omega_{p12}^2,$ $\omega_{c12i}^2 = \omega_{o12i}^2 - \beta_i \cdot \omega_{p12i}^2$ $(T_{ci}-T_c) \cdot C^{-1} = \omega_{o12}^2 (\omega_{p12}^{-2} - \omega_{p12i}^{-2})$ (3)	Approaches
$\rho_r = N_a^{-1} \cdot M \cdot S_r \cdot V_r^{-1}$ (4)	1). $C \approx C_i$
$\omega_p^2 = (4\pi e^2 \cdot m^{-1}) \cdot s \cdot S_r \cdot V_r^{-1} \cdot q^{-1}$ $(T_{ci}-T_c) \cdot C^{-1} = m \cdot (4\pi e^2)^{-1} \cdot \omega_{o12}^2 \cdot s^{-1} \cdot S_r^{-1} \cdot (q_{12} \cdot V_r - q_{12i} \cdot V_{ri})$	2). $\delta \approx \delta_i$
	3). $\beta \approx \beta_i$
	4). $4\delta^2 \omega_{p12}^{-2} \approx 4\delta_i^2 \omega_{p12i}^{-2}$
	5). $\omega_{o12}^2 \approx \omega_{o12i}^2$
$(T_{ci}-T_c) \cdot C^{-1} = B \cdot (q_{12} \cdot V_r - q_{12i} \cdot V_{ri})$ (5)	6). $B = m(4\pi e^2)^{-1} s^{-1} S_r^{-1} \omega_{o12}^2$

The isotope phase transition temperature shift (Eq.3) is connected with the natural and plasma energies. Superconducting phase transition temperature (Eq.5) depends on the interaction and crystal lattice parameters. The plasma oscillations play a dominant role in producing superconducting phase transition. Superconducting crystals exist at room temperature.

[1] N.P. Netesova, *Physica C*, **2** (2007) 918-919.

30PO-I2-26

INSTABILITY OF INFINITE STRAIGHT DOMAIN WALL IN ELECTRIC CURRENT

Karashitin E.A.^{1,2}, Fraerman A.A.^{1,2}, Sapozhnikov M.V.^{1,2}

¹ Institute for Physics of Microstructures RAS, Nizhny Novgorod, Russia

² N. I. Lobachevsky State University of Nizhny Novgorod, Nizhny Novgorod, Russia
eugenk@ipmras.ru

It is well-known that the ferromagnet changes its magnetization in a spin-polarized electric current [1]. Thus if we take a Bloch domain wall in an infinite ferromagnet with the "light axis" anisotropy and add the electric current \mathbf{j} applied perpendicular to it the domain wall moves with velocity $\mathbf{V} \sim (\mathbf{j}, \mathbf{n})\mathbf{n}$ where \mathbf{n} is a normal to the surface of the domain wall. Here we consider the quasistatic case. The domain wall velocity is proportional to the square of the normal and thus does not depend on its direction. On the other hand, it is known that the infinite straight domain wall is stable with respect to harmonic oscillations of its shape while the magnetostatic term leads to the instability if a ferromagnetic slab is considered [2].

In this work we suggest an additional mechanism of the domain wall instability induced by the external electric current applied in its plane. We start from the Landau-Lifshitz-Gilbert (LLG) equation [3] for an infinite ferromagnet:

$$\frac{\partial \mathbf{M}}{\partial t} = \gamma \left[\mathbf{M}, \frac{\delta E}{\delta \mathbf{M}} \right] + \alpha \left[\mathbf{M}, \frac{\partial \mathbf{M}}{\partial t} \right] - b [\mathbf{M}, [\mathbf{M}, (\mathbf{j}, \nabla) \mathbf{M}]] - c [\mathbf{M}, (\mathbf{j}, \nabla) \mathbf{M}],$$

where \mathbf{M} is the magnetization vector normalized to unit, E is the energy functional, $\alpha, \gamma, b, c > 0$, b describes the adiabatic term while c determines the non-adiabatic term, $b \gg c$. The magnetization $\mathbf{M} = (\sin \theta \cos \varphi, \sin \theta \sin \varphi, \cos \theta)$ in the Cartesian coordinate system chosen as shown in Fig. 1; the domain wall is assumed to keep its shape:

$$\varphi = \varphi_1(x, z, t) + \varphi_2(x, z, t),$$

$$\theta = 2 \arctan \left(\exp \left(\frac{y - q_1(x, z, t) - q_2(x, z, t)}{\Delta} \right) \right),$$

where Δ is the domain wall thickness, φ_1, q_1 describe its movement caused by j_y , φ_2, q_2 stand for the deviations of shape in its plane.

Supposing $\varphi_2, q_2 \sim \cos(\omega t - k_x x - k_z z) \exp(\eta t)$, we calculate frequency $\omega(k_x, k_z)$ and increment $\eta(k_x, k_z)$ and show that if the current \mathbf{j} has non-zero component j_x or j_z there are parameters k_x, k_z for which the increment is positive. Thus, even an infinite domain wall becomes unstable in the presence of external electric current in its plane.

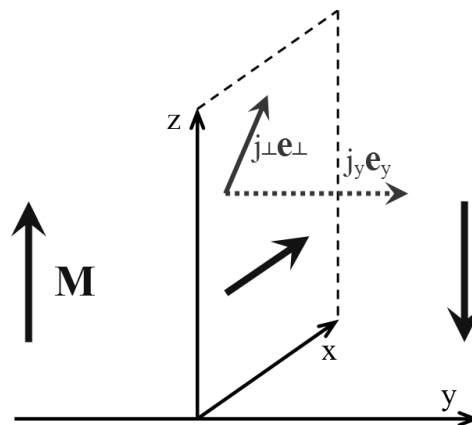


Fig. 1. The domain wall in an infinite ferromagnet.

This work was partly supported by Russian Foundation for Basic Research (Contract No.14-02-00448), the "Dynasty" foundation and the OPTEC grant for young scientists.

[1] J.C. Slonczewski, *J. Magn. Magn. Mater.*, **159** (1996) L1-L7.

[2] F.B. Hagedorn, *J. Appl. Phys.*, **41** (1970) 1161-1162.

[3] S. Zhang, Z. Li, *Phys. Rev. Lett.*, **93** (2004) 127204.

30PO-I2-27

CRITICAL BEHAVIOR OF GALLIUM DOPED OF $\text{La}_{0.7}\text{Ca}_{0.3}\text{MnO}_3$

Nanto Dwi, Hwang Jong-Soon, Oh Suhk-Kun, Yu Seong-Cho

Dept. of Physics, Chungbuk National University, Cheongju, 361-763, Korea

Potential applications in spintronics due to tunnel magnetoresistance (CMR) in hole-doped manganites $R_{1-x}M_x\text{MnO}_3$ (R = rare-earth ion; M = divalent alkali) has attracted special experimental and theoretical attention. A complete information of nature of phase transitions in numerous manganites perovskite structure has been continuously developed in the condensed state physics. Thus, issue of phase transition from paramagnetic (PM) insulator to ferromagnetic (FM) and common universality class are important to be understood by means critical exponents study around Curie temperature, T_C .

Recently, critical behavior in Ga-doped manganites $\text{La}_{0.75}(\text{Sr,Ca})_{0.25}\text{Mn}_{1-x}\text{Ga}_x\text{O}_3$ ($0 \leq x \leq 0.1$) tends towards mean-field with long-range interaction might be due to the random dilution of the Mn sublattice by non-magnetic Ga^{3+} and/or the development of the physical size of the clusters, which enhance the dipole-dipole interaction [1]. By using the modified Arrott plot method, the critical parameters 5 and 7 percent of Ga doped in LCMO were obtained to be T_C of 159.76 K, $\beta = 0.233 \pm 0.021$, $\gamma = 1.011 \pm 0.020$, for 5 percent doped, and T_C of 135.64 K, $\beta = 0.501 \pm 0.010$, $\gamma = 1.026 \pm 0.022$ for 7 percent doped as one can see in Fig.1. With these critical exponents, the isothermal magnetization data of the samples around T_C fall into two branches of a universal function $M(H, \varepsilon) = |\varepsilon|^\beta f_\pm(H/|\varepsilon|^{\beta+\gamma})$, where $\varepsilon = (T - T_C)/T_C$ is the reduced temperature, f_+ for $T > T_C$, and f_- for $T < T_C$. This proves that the critical exponents determined are reliable, and in good accordance with the scaling hypothesis. In current work, the values of β obtained for our samples are located in those expected for the Tricritical mean-field theory ($\beta = 0.5$) and the mean-field model ($\beta = 0.365$). Such results demonstrate an existence of ferromagnetic short-range order in LCMO doped with Ga due to it occurs at a tricritical point brought about by competing degrees of freedom, which are also responsible for the short range correlations. Notably, the doping at high contents has a tendency leading to long-range ferromagnetic order.

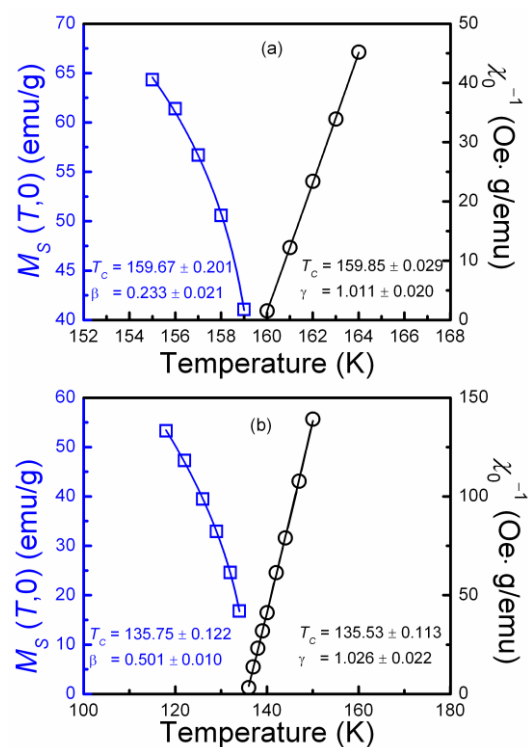


Fig. 1 Temperature dependences of $M_S(T)$ and $\chi_0^{-1}(T)$ for $\text{La}_{0.7}\text{Ca}_{0.3}\text{Mn}_{1-x}\text{Ga}_x\text{O}_3$ together with fitting curves based on the critical laws with Ga-doping concentrations of (a) $x = 0.05$ and (b) $x = 0.07$.

[1] A. Omri, A. Tozri, M. Bejar, E. Dhahri, and E. K. Hlil, *J. Magn. Magn. Mater.*, **324** (2012) 3122-3128.

30PO-I2-28

THE INVESTIGATION OF PHASE TRANSITIONS IN 2D SITE-DILUTED 3-STATE ANTIFERROMAGNETIC POTTS MODEL

Murtazaev A.K.^{1,2}, Babaev A.B.^{1,3*}, Murtazaliev R.A.²

¹ Kh.I. Amirkhanov Institute of Physics, Daghestan Scientific Center, Russian Academy of Sciences, Makhachkala, Russia

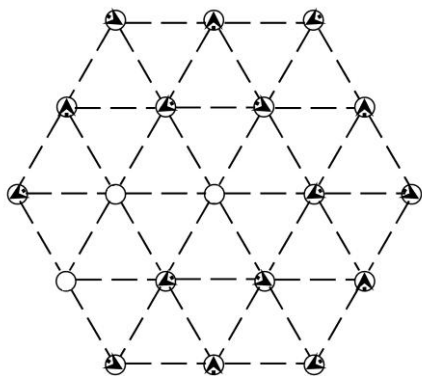
² Daghestan State Universities, Makhachkala, Russia

³ Daghestan State Pedagogical Universities, Makhachkala, Russia

* b_albert78@mail.ru

An influence of impurities and different defects on the phase transitions and critical phenomena of magnetic systems is one of more actual subjects of the phase transition theory [1]. The majority of real solids contain impurities and other structure defects which influence on their thermodynamic characteristics, particularly, on a behavior of systems at the phase transitions. Therefore, in recent times the researchers have directed the efforts to understanding how the structure defects influence on a behavior of different systems at the phase transitions. When studying the critical properties of disordered spin systems, are distinguished the systems with quenched and annealed impurities are distinguished. In solids, the impurities are usual quenched. A presence of quenched impurities is revealed as random disturbance of the local critical temperature. In the case of spin systems, experiencing the first order phase transitions in a homogeneous state, the nonmagnetic impurities lead to softening of this transition close to the induction of second order phase transition in them [2].

In this work, the influence of quenched nonmagnetic impurities on the phase transitions in the two-dimensional 3-state site-diluted antiferromagnetic Potts model on a triangular lattice is studied by the Monte-Carlo method.



In the construction of two-dimensional 4-state Potts models on a triangular lattice, one should remember that spins S_i , which can be in one of $q \geq 2$ states (see Fig.1), and nonmagnetic impurities (vacancies) locate in sites of the lattice; nonmagnetic impurities are distributed randomly and fixed in different sites of the lattice (quenched disorder).

The Hamiltonian of studied system can be written as [1]:

$$H = -\frac{J}{2} \sum_{i,j} \rho_i \rho_j \cos \theta_{i,j}, \quad (1)$$

where $\rho_i=1$, if a site i is occupied by the magnetic atom, and $\rho_i=0$, if the nonmagnetic impurity locates in a site i , J is the exchange interaction ($J < 0$), $\theta_{i,j}$ is angles between interacting spins $S_i - S_j$, $S_{ij}=1, 2, \dots, q$, $q=3$. The investigation is carried out on the basis of Monte-Carlo method. The systems of non-linear sizes $L \times L = N$, $L=20 \div 144$ at spin concentrations $p=1.00; 0.90; 0.70$, are researched. In terms of the forth order Binder cumulants method, the second order phase transition is shown to be observed in this model at spin concentrations $p=0.90; 0.70$ and the first order phase transition to be occurred for pure model ($p=1.00$).

The study was supported by the Russian Foundation for Basic Research (project nos. 13-02-00220).

[1] F.Y. Wu, *Rev. Mod. Phys.*, **54** (1982) 235.

[2] M. Aizenman, J. Wehr, *Phys. Rev. Lett.*, **62** (1989) 2503.

30PO-I2-29

INVESTIGATION OF THE ELECTRONIC AND STRUCTURAL INSTABILITY IN NONCENTROSYMMETRIC $\text{Mo}_3\text{Al}_2\text{C}$

Lue C.S.¹, Kuo C.N.¹, Kuo Y.K.²

¹Department of Physics, National Cheng Kung University, Tainan 70101, Taiwan

²Department of Physics, National Dong Hwa University, Hualien 97401, Taiwan
kuochianung@gmail.com

We report the comparative study of noncentrosymmetric compounds $\text{Mo}_3\text{Al}_2\text{C}$ (carbon-deficiency) and $\text{Mo}_3\text{Al}_2\text{C}_{1.1}$ (carbon-rich) by using x-ray diffraction (XRD), electrical resistivity, thermal conductivity, Seebeck coefficient, specific heat, as well as ^{27}Al nuclear magnetic resonance (NMR) measurements [1]. Both samples were prepared by means of the arc-melting method with different carbon concentrations. Although the XRD pattern of $\text{Mo}_3\text{Al}_2\text{C}_{1.1}$ exhibits more impurity phases, phase transition features have been observed in the specific heat and Seebeck coefficient which are invisible in $\text{Mo}_3\text{Al}_2\text{C}$. The anomalous NMR features have been found to appear at different characteristic temperatures of 197 K and of 140 K for $\text{Mo}_3\text{Al}_2\text{C}$ and $\text{Mo}_3\text{Al}_2\text{C}_{1.1}$, respectively. These observations can be associated with the change in the electronic states driven by structural instability. With such a comparison, we conclude that the noncentrosymmetric β -Mn phase in $\text{Mo}_3\text{Al}_2\text{C}$ is more stable than that in $\text{Mo}_3\text{Al}_2\text{C}_{1.1}$. It is consistent with the prediction from the recent DFT calculations that the β -Mn phase of $\text{Mo}_3\text{Al}_2\text{C}$ could be stabilized by the carbon deficiency.

[1] C. N. Kuo, H. F. Liu, and C. S. Lue, *Phys. Rev. B*, **85** (2012) 052501.

30PO-I2-30

INVESTIGATION OF ANOMALOUS PHASE TRANSITION FEATURES IN $\text{Sr}_3\text{Ir}_4\text{Sn}_{13}$

Lue C.S.¹, Kuo C.N.¹, Lue C.Y.¹, Liu H.F.¹

¹ Department of Physics, National Cheng Kung University, Tainan 70101, Taiwan
cslue@mail.ncku.edu.tw

In order to assess the phase transition nature in $\text{Sr}_3\text{Ir}_4\text{Sn}_{13}$, we have carried out the electrical resistivity, Hall coefficient, Seebeck coefficient, thermal conductivity, specific heat, and nuclear magnetic resonance (NMR) measurements, mainly focusing on the signatures around the phase transition temperature $T^*=147$ K. The phase transition has been characterized by marked features near T^* in all measured physical quantities. In particular, the Hall measurement reveals the abrupt change in both magnitude and sign of the charge carriers below T^* , providing strong evidence for the Fermi surface reconstruction associated with this phase transition. Moreover, the NMR observations indicate the presence of the splitting of the resonance lines below T^* which could be accounted for by the local distortion of the Sn_2 icosahedra within the $\text{Pm}3\text{n}$ phase. The NMR Knight shift analysis further provides microscopic evidence for the reduction in both Sn 5s and Ir 5d electronic states near the Fermi surfaces of $\text{Sr}_3\text{Ir}_4\text{Sn}_{13}$. With these respects, it suggests that the strong interplay between electronic and structural instability is responsible for the peculiar phase transition in $\text{Sr}_3\text{Ir}_4\text{Sn}_{13}$.

30PO-I2-31

ON THE SUPERCONDUCTIVITY OF PLANAR CARBON COMPOUNDS

Zaitsev R.O.

Moscow Institute of Physical Technology, 141700, Dolgoprudny, Moscow region, Russia

Zaitsev_Rogdai@mail.ru

The possibility of the existence of Cooper instability in a systems of carbon cations that form a honecomb lattice has been established based on an idea about the strong interaction in one atom of the unit cell. The phase diagram of the existence of the superconducting ordering and the BCS-constant has been calculated for various filling factor of the σ -shell.

The strong electron-electron interaction existing in high-temperature superconducting systems is responsible for the so-called kinematic interaction and finally determinates a new kinematic mechanism of superconductivity [1,2].

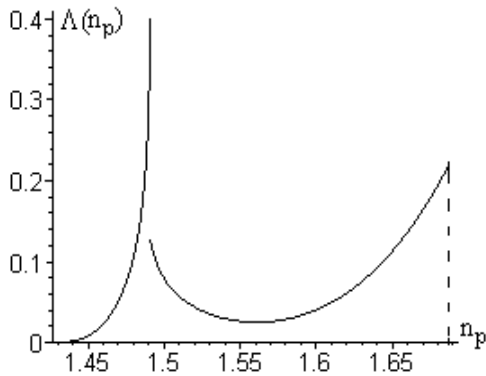
The temperature of superconductivity transition is given to the BCS formula: $T_c = \bar{\varepsilon} \exp(-1/\Lambda(n_p))$, where for $1 < n_p < 2$:

$$\Lambda(\varepsilon) = \frac{g(\varepsilon)}{4f(n_p)\sqrt{1+4\varepsilon(2-\varepsilon)^2}}, \quad f(n_p) = \frac{2+n_p}{12},$$

$g(\varepsilon)$ is the scattering amplitude:

$$g(\varepsilon) = 2(\varepsilon+1)(2\varepsilon+1)R_0^{(2)} - (2+7\varepsilon+18\varepsilon^2+16\varepsilon^3)R_0^{(1)}(\varepsilon) + 48\varepsilon^2R_2^{(0)}(\varepsilon) + \varepsilon(1+28\varepsilon+40\varepsilon^2+16\varepsilon^3)R_0^{(0)}(\varepsilon) - 4\varepsilon^2(7+12\varepsilon+14\varepsilon^2)R_1^{(0)}(\varepsilon), \quad -1/4 < \varepsilon < 2.$$

$$R_n^{(k)}(\varepsilon) = \frac{1}{\pi^2} \Re \int \frac{z^k dz}{(1+z)^n \sqrt{(1-z^2)(1+4\varepsilon-4\varepsilon^2+4\varepsilon z-z^2)}}.$$



The function $\Lambda(n_p)$ has the maximum (see Fig. 1), which is related to the van-Hove's singularity.

The results may be compared with experimental data for graphite intercalation compounds (GiCs) [3]: NaC_2 , CaC_6 .

Fig. 1. The concentration dependence of the BCS-constant

[1] R. O. Zaitsev, *JETP Letters*, **94** (2011) 206-214.

[2] R. O. Zaitsev, *JETP*, **142** (2012) 770-782.

[3] M. Sutherland, N. Dorion-Leyuand et al., *Phys. Rev. Lett.*, **98** (2007) 067003-067005.

30 June

Monday

17:30-19:00

poster session
30PO-J1

**“Diluted Magnetic
Semiconductors and
Oxides”**

30PO-J1-1

FEATURES OF THE MAGNETIC PROPERTIES OF THE FERRITE NANOPARTICLES

Svechkina N.B.¹, Berestovaya A.A.²

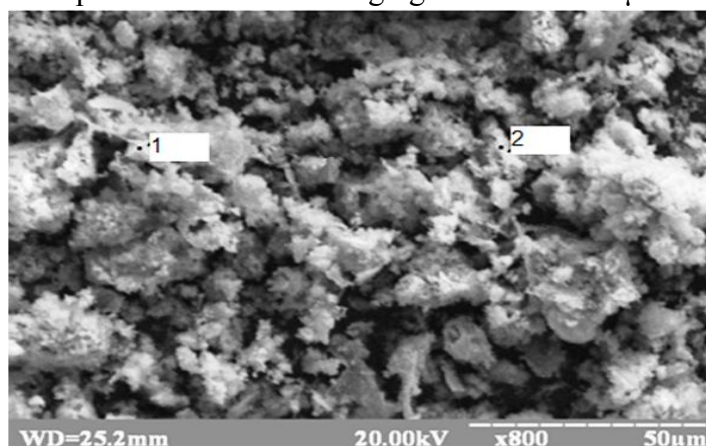
¹ Lomonosov Moscow State University, Faculty of Physics, Moscow, Russia

² Donetsk National Technical University, Donetsk, Ukraine

n.svechkina@mail.ru

Magnetic nanoparticles (MNP) for many years are of the great scientific and practical interest. MNP have some unique properties that are radically different from the properties of the bulk sample. Metal nanoparticles are unstable in the atmosphere, so scientific attention is paid to the ferromagnetic oxides nanoparticles, in particularly ferrites.

This paper presents the results of investigation of the magnetic properties of cobalt ferrite (CoFe_2O_4) and nickel ferrite (NiFe_2O_4) powders. Samples were obtained by self-propagating exothermic reaction in solid systems $\text{CoSO}_4\text{-Fe}_2(\text{SO}_4)_3\text{-NaO}_2$ and $\text{NiSO}_4\text{-Fe}_2(\text{SO}_4)_3\text{-NaO}_2$. Samples of the cobalt ferrite have different synthesis conduction, namely the velocity of propagation of the reaction front. The reaction product was milled. The resultant powder was a rather heterogeneous system, which consists of particles with sizes ranging from 0.1 to 10 μm .



Pic. 1 SEM – image of the product particles system $\text{CoSO}_4 - \text{Fe}_2(\text{SO}_4)_3 - \text{NaO}_2$

Magnetic measurements were performed on a magnetometer VSM LakeShore model 7407 in field up to 10 kOe in the temperature range from 80°K to 350°K.

It is found that the coercive force of the cobalt ferrite nanoparticles samples differs almost by 10 times, the technical saturation magnetization also doesn't coincide.

The measurement data were compared with the magnetic properties of the nickel ferrite sample. Values of the coercivity and magnetization for this sample were in-between to the values of the same parameters for the sample №1 and №2.

On the thermomagnetic curves in the temperature range from 80 to 350 K for samples №1 and №2 the blocking temperature isn't attained. It is supposedly related to the presence of the large particles in the considered samples. Thermomagnetic curves of nickel ferrite sample №2 and the sample №1 coincide.

Anisotropy constant for sample №3 found to be equal $3 \cdot 10^5 \text{ Erg/cm}^3$. Blocking temperature was assumed equal to 350°K. The obtained value of the anisotropy constant turned significantly less value of the constant for a bulk sample.

Support by RFBR (Grant No 13-02-90491).

30PO-J1-2

FERROMAGNETISM IN InFeAs LAYERS, FORMED BY LASER DEPOSITION

Danilov Yu.A.¹, Drozdov Yu.N.², Kudrin A.V.¹, Lesnikov V.P.¹, Pitirimova E.A.¹, Vikhrova O.V.¹, Yunin P.A.², Zvonkov B.N.¹

¹ N.I. Lobachevsky State University, Nizhny Novgorod, Russia

² Institute for Physics of Microstructures, RAS, Nizhny Novgorod, Russia
danilov@nifti.unn.ru

Indium arsenide highly doped with iron (InFeAs) is a promising ferromagnetic semiconductor for spintronics [1]. The key feature of this material is the ability to be ferromagnetic at n-type doping. The InFeAs, grown by molecular-beam epitaxy, has the Curie temperature no more than 70 K. Fabrication of InFeAs by other methods may be of practical interest.

We used two modifications of a laser deposition (LD) method: 1) LD in vacuum chamber ($\sim 10^{-6}$ Torr), and 2) LD in horizontal quartz reactor at low pressure (~ 50 mTorr) in flow of H_2 and AsH_3 . Pulses of YAG:Nd laser were directed alternately on Fe metallic and undoped InAs targets. The Fe relative content in deposited layer was estimated by the relationship $Y_{Fe} = t_{Fe} / (t_{Fe} + t_{InAs})$, where t_{Fe} and t_{InAs} is the sputtering time for corresponding target. Wafers of GaAs(100) or (111) and Ge(111) were used as substrates. Temperature of deposition was varied from 200 to 400°C. The content of Fe (Y_{Fe}) was in the range between 0.04 and 0.6. The deposition rate was about 5 nm/min.

Electron-diffraction examination (in reflection geometry with accelerating voltage of 50 kV) showed monocrystal structure of layers up to the highest Fe content. X-ray diffraction study (in $\Theta/2\Theta$ geometry) revealed, besides GaAs substrate peak, the maximum from relaxed InAs layer, which for $Y_{Fe} > 0.4$ shifted to GaAs peak. Appearance of mechanical stresses was noted for high contents of Fe in InAs.

Thermoprobng showed n-type conduction of the InFeAs layers. Hall effect measurements supported this conclusion. Electron concentration changed from 1.5×10^{18} to $5 \times 10^{18} \text{ cm}^{-3}$ at variation of Y_{Fe} from 0.2 to 0.6. Hall mobility of electrons varied in this Fe content range from 270 to 85 $\text{cm}^2/\text{V}\cdot\text{s}$. Magnetization measurements (by method of alternating gradient of magnetic field) at room temperature revealed ferromagnetic hysteresis (Fig.1) with coercivity around of 30 Oe.

We suppose that n-type conductivity is derived from native defects, formed in InAs at laser plasma exposure. Ferromagnetism in InFeAs layers, deposited by the laser method, has most probably cluster origin.

Support by RFBR (grants 13-07-00982 and 13-0297140) is acknowledged.

[1] M. Tanaka, S. Ohya, P.N. Hai, *Appl. Phys. Rev.*, **1** (2014) 011102.

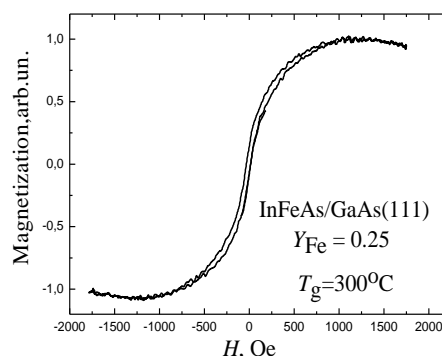


Fig. 1. Magnetization vs. magnetic field for the sample with InFeAs layer, grown by vacuum laser deposition. Measurement temperature is 300 K; magnetic field lies in the layer plane.

30PO-J1-3

ULTRATHIN FILMS OF YTTRIUM IRON GARNET GROWN BY LASER MOLECULAR BEAM EPITAXY

Fedorov V.V.¹, Korovin A.M.¹, Baranov D.A.¹, Maksimova K.Y.², Grunin A.I.²,
Zamoranskaya M.V.¹, Lutsev L.V.¹, Suturin S.M.¹, Sokolov N.S.¹

¹Ioffe Physical-Technical Institute, St. Petersburg, Russia

²Immanuel Kant Baltic Federal University, Kaliningrad, Russia
amkorovin@gmail.com

For many years yttrium iron garnet (YIG, $Y_3Fe_5O_{12}$) films are used in microwave devices. However, a new trend associated [1] with a possibility of garnet film integration with semiconductor microelectronic devices has recently appeared. It has also been shown [2] that in thin (<100 nm) films a substantial reduction of spin wave damping constant can be expected, that is of considerable interest for modern microwave devices (filters, delay lines).

In the presented work YIG layers with thickness from 12 to 84 nm were grown on (111) gadolinium gallium garnet (GGG; $Ga_3Gd_5O_{12}$) substrate. Iron and yttrium contents in the films were measured by X-ray fluorescence (XRF) and it was found that they coincide with the bulk values (5:3). Crystal structure of the films was studied by grazing incident x-ray diffraction (GIXRD) with use of synchrotron radiation. It was shown that interplane distance along the normal to the sample surface ($d_{444} = 1.807 \text{ \AA}$) increased compared to that of bulk YIG crystals ($d_{444} = 1.787 \text{ \AA}$) and depends on the oxygen pressure during the deposition (fig. 1). Analysis of off-specular reflections showed that the films are pseudomorphic. It was also found that the saturation magnetization ($\sim 1500 \text{ G}$) measured by the vibrating magnetometer (VSM) is quite

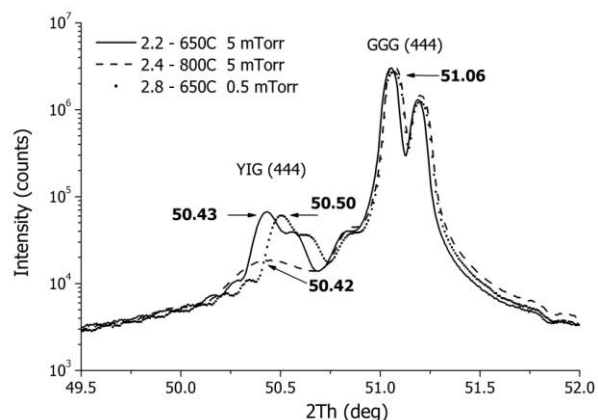


Fig. 1. θ - 2θ curves from the samples grown in different oxygen pressure and growth temperature

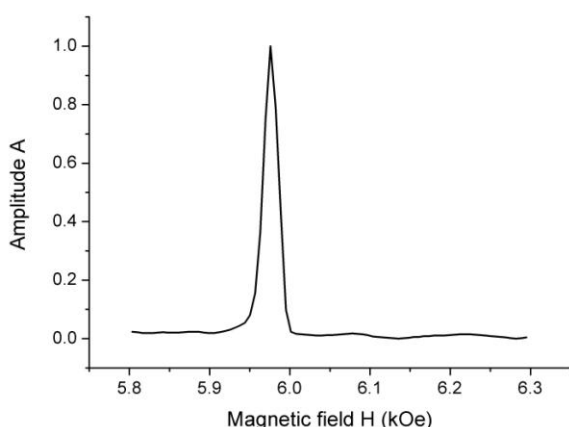


Fig. 2. FMR curve of 84 nm thick YIG film grown in 5 mTorr O_2 at 650 °C

close to that of bulk material (1750 G). Ferromagnetic resonance measurements at the frequency $F = 9.645 \text{ GHz}$ show high value of the easy plane magnetic anisotropy ($H_a = -818 \text{ Oe}$). Rather narrow FMR line ($\Delta H = 17 \text{ Oe}$), Fig. 2, indicates high quality of the YIG films grown and characterized in this work.

It has been shown that high quality YIG ultrathin films can be grown by laser molecular beam epitaxy. Varying oxygen pressure during the growth process one can control the strain and magnetic anisotropy of the epitaxial layers.

[1] Žutić H. Dery, *Nature Materials*, **10** (2011) 647–648.

[2] L.V. Lutsev, *Physical Review B*, **85** (2012) 21, 214413.

30PO-J1-4

ELECTROMAGNETIC PROPERTIES OF La-Sr MANGANITE DEPENDING ON COMBINED DIVALENT-QUADRIVALENT IONS SUBSTITUTION FOR MANGANESE

Karpasyuk V.K.¹, Badelin A.G.¹, Merkulov D.I.¹, Estemirova S.Kh.²

¹ Astrakhan State University, 414056, Astrakhan, Russia

² Institute for Metallurgy, Ural Division of RAS, 620016, Yekaterinburg, Russia
alexey_badelin@mail.ru

The aim of the study is to examine and to compare the influence of paired substitution of ($\text{Zn}^{2+} + \text{Ge}^{4+}$) and ($\text{Mg}^{2+} + \text{Ti}^{4+}$) for 2Mn^{3+} on magnetic and electrical properties of La-Sr manganites. The study and comparison of these substituents effects is of interest from the viewpoint of charge compensation and spatial charge distribution in manganites with simultaneously introduced divalent and quadrivalent ions having different electron configuration: Zn^{2+} and Ge^{4+} have completely filled d-electron shell, while Mg^{2+} and Ti^{4+} have completely filled p-shell.

Polycrystalline samples of $\text{La}_{0.8-x}\text{Sr}_{0.2+x}\text{Mn}_{1-x}(\text{Zn}^{2+}_{0.5}\text{Ge}^{4+}_{0.5})_x\text{O}_{3+\gamma}$ and $\text{La}_{0.8-x}\text{Sr}_{0.2+x}\text{Mn}_{1-x}(\text{Mg}^{2+}_{0.5}\text{Ti}^{4+}_{0.5})_x\text{O}_{3+\gamma}$ systems ($x=0.05; 0.10; 0.15$) were prepared by ceramic processing. The final sintering step was performed at 1200°C for 10 h, and the samples were cooled together with the furnace. The systems of chemical compositions are designed so that the Mn^{4+} concentration rises with increasing of substituent amount. Sintered manganites had overstoichiometric content of oxygen ($\gamma > 0$). After annealing at 950°C and partial pressure of oxygen $P_{\text{O}_2} = 10^{-1}$ Pa for 96 h they became stoichiometric, that results in decreasing of Mn^{4+} content and of cation vacancies concentration.

Regularities in the concentration dependences of phase composition, unit cell volume, magnetization in the field of 5.6 kOe at 80 K, Curie point, and temperature behavior of resistivity at the interval 100 – 290 K were established. All synthesized manganites were rhombohedral, and unit cell volume (v) of (Zn,Ge)-substituted manganites was smaller than v of analogous compositions with (Mg,Ti). Simultaneously, (Zn,Ge)-contained manganites had essentially higher values of magnetization and Curie temperature. From the temperature dependencies of magnetic permeability it was concluded that there is the evidence for the presence of magnetic inhomogeneities in (Mg,Ti)-substituted manganites, so that temperature interval of “ferromagnetic-paramagnetic” transition is overextended over one in analogous (Zn,Ge)-compositions.

All (Zn,Ge)-contained manganites had metallic type of conductivity, while manganites of other compositions exhibited semiconducting features.

On the whole, obtained ratio of parameters of the systems investigated here corresponds to the ratio of the same parameters of Ge- and Ti-substituted manganites [1].

Possible approach to the interpretation of established regularities is discussed in terms of diamagnetic dilution of octahedral Mn sublattice, decreasing of Jahn-Teller distortions, formation of clusters due to the difference of charges and radii of the ions, Coulomb interaction and mechanical stresses.

This research was performed within the framework of the State order of the Ministry of Education and Science of RF (project 334).

[1] A.G.Badelin, Z.R.Datskaya, I.Yu.Epifanova, S.Kh. Estemirova, V.K.Karpasyuk, A.M.Smirnov, *EPJ Web of Conf.*, **40** (2013) 15004-4.

30PO-J1-5

MANIFESTATION OF DONOR HYBRIDIZED ELECTRON STATES IN MAGNETISM OF NICKEL IMPURITIES IN MERCURY SELENIDE CRYSTALS

Govorkova T.E.¹, Gubkin A.F.¹, Lonchakov A.T.¹, Okulov B.I.¹, Andriichuk M.A.², Paranchich L.D.²

¹ Institute of Metal Physics Urals Branch of RAS, 620990, Ekaterinburg, Russia

² Chernovtscy National University, 58012, Chernovtscy, Ukraine

okulov@imp.uran.ru

In narrow-gap semiconductors, electron states by impurity atoms of 3d-transition metals can hybridize with the states of conduction band. Electron density of such hybridized states includes the contributions relating to both free motion of current carriers and partial localization by impurities. Localized contribution manifests itself in temperature and concentration dependences of magnetic susceptibility. In [1,2] one developed simple theoretical description of such dependences which were observed experimentally in studying magnetic susceptibility of iron and cobalt impurities of low concentration in mercury selenide crystals. Analysis of observed concentration dependence of the Curie constant compounded with measured Hall concentration of electrons allowed us to determine effective values of magnetic moments localized by impurities and degree of ionization of impurity electron states, characterizing donor properties of such states. Along with well known fact of one-fold ionization of iron impurities in experiments therewith one justified two-fold ionization of cobalt impurities in conduction band of a crystal. The

development of such investigations as applied to another 3d-impurities is essential for physics of diluted magnetic semiconductors. In this connection we undertook study of magnetic properties of nickel impurities in mercury selenide crystals. The temperature dependences of magnetic susceptibility with concentration of impurities from $1 \cdot 10^{18}$ to $1 \cdot 10^{19} \text{ cm}^{-3}$ have been studied. The measurements were performed by magnetometer MPMS-XL-5 at the temperature range of (1.8÷300) K in magnetic field of 0.5T. The concentration dependence 3 of the Curie constant is presented in Fig. 1. It has been analyzed on the base of the approach applied in [2] to analogous dependences (see 1, 2 Fig. 1), relating to the impurities of iron and cobalt. In the final analysis there have been determined effective spin of nickel impurity, ($S_i \approx 1.01$) and resonance concentration of donor electrons, ($n_{0d} \approx 0.19 \cdot 10^{18} \text{ cm}^{-3}$). It was also established that electron states of nickel impurity atoms are three-fold ionized in conduction band of the HgSe crystal, what is in conformity with ion core spin value closed to 5/2. This result means that mechanisms of forming donor energy levels of Fe, Co, Ni impurities in conduction band of the HgSe crystal are like in nature.

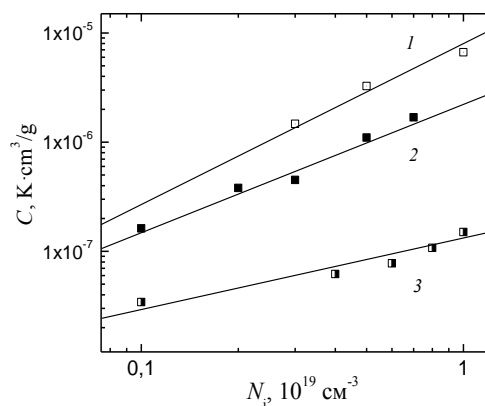


Fig.1. Concentration dependences of the Curie constant for crystals of HgSe with the 3d-impurities (1 - Fe, 2 - Co, 3 - Ni).

Work supported by RFBR (Grant No 12-02-00530) and Program of RAS (Grant №12-02-T-1016)

[1] V.I.Okulov, E.A.Pamyatnykh et al., *Low Temperature Physics*, **30** (2004) 417.

[2] V.I.Okulov, T.E.Govorkova et al., *The Physics of Metals and Metallography*, **108** (2009) 116.

30PO-J1-6

MAGNETIC STATES OF IMPURITY IRON IONS IN THE $\text{La}_{0.75}\text{Sr}_{0.25}\text{Co}_{0.98}\text{Fe}_{0.02}\text{O}_3$ PEROVSKITE

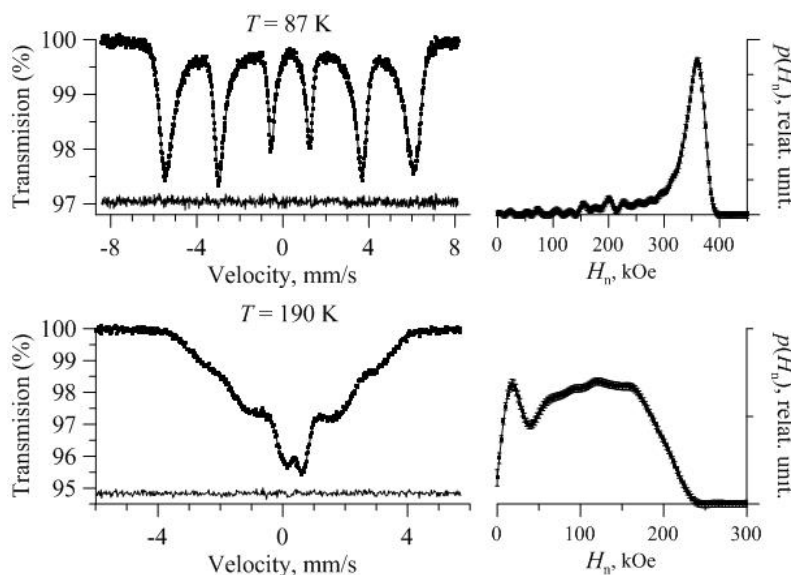
Makarova A.O.¹, Pokatilov V.S.¹, Rusakov V.S.², Sigov A.S.¹, Pokatilov V.V.¹

¹ Moscow State Institute of Radio Engineering, Electronics, and Automation (Technical University),
Moscow, 117454 Russia

² Lomonosov Moscow State University, Moscow, 119991 Russia
pokatilov@mirea.ru

The magnetical ordered $\text{La}_{1-x}\text{Sr}_x\text{CoO}_3$ compounds ($x = 0 - 0.5$) attract great research attention since these perovskites exhibit interesting electrical and magnetic properties, for example, giant magnetoresistance and large values of the Hall coefficients. According to the literature data, these compounds are heterogeneous in terms of their electronic, atomic, and magnetic structure. It was also found that the magnetic regions exhibit long-range ferromagnetic order in the composition range $x = 0.20 - 0.30$. The available experimental results do not give an unambiguous picture of the states of the cobalt ions and the local atomic, electronic, and magnetic structures in the $\text{La}_{1-x}\text{Sr}_x\text{CoO}_3$ compounds. In this work the local states of the impurity iron ions in the $\text{La}_{0.75}\text{Sr}_{0.25}\text{Co}_{0.98}\text{Fe}_{0.02}\text{O}_3$ compound were studied in the temperature range 5 – 295 K using ^{57}Fe Mossbauer spectroscopy. Techniques of recovery of hyperfine magnetic field H_n distribution $p(H_n)$ and model fitting based on the MSTools program [1] in the temperature range $5 \text{ K} \leq T < T_N < 300 \text{ K}$ were used for processing and analysis of the spectra.

X-ray studies of the crystal structure and phase state revealed that the sample was single-phase and had a rhombohedral structure with lattice parameters: $a = 5.444 \text{ \AA}$ и $c = 13.174 \text{ \AA}$. The temperature of the magnetic phase transition (Curie point) $T_C = 212 \pm 2 \text{ K}$ was determined. At room temperature the iron ions are in a single crystallographic state with hyperfine-interaction parameter values of the trivalent Fe^{3+} ions in an octahedral oxygen environment. In the temperature range 87 – 293 K it was shown that the iron ions were only in one (octahedral) state with a valence of +3. In the temperature range 180 – 212 K (see figure) two magnetic states of the Fe^{3+} ions were observed: one state in magnetically ordered microregions and another in paramagnetic microregions. In the temperature range 5 – 180 K the Mossbauer spectra are complex (see figure). These spectra are noticeably asymmetric that indicates distribution of the hyperfine fields at the ^{57}Fe nuclei sites. As the temperature decreases from 180 K, the spectra shift toward higher fields and the distribution width decreases sharply. At $T > 87 \text{ K}$ the $p(H)$ distribution has a comparatively narrow peak and a wide tail. These states are caused by an atomic heterogeneity. The Fe ion are in microregions (with different contents of Sr^{2+} and La^{3+} in the compound considered).



This work is supported by the RFBR grant № 14-02-01147.

[1]. M.E. Matsnev and V.S. Rusakov. AIP Conference Proceedings, **1489** (2012) 178-185.

30PO-J1-7

LOW TEMPERATURE ANTIFERROMAGNETISM OF THE SINGLE CRYSTAL Mn_2BO_4

Kazak N.V.¹, Platunov M.S.¹, Knyazev Yu.V.², Ivanova N.B.², Bayukov O.A.¹, Bezmaternykh L.N.¹, Nizhankovskii V.I.³, Lamonova K.V.⁴, Ovchinnikov S.G.^{1,2,5}

¹ Institute of Physics SB RAS, Krasnoyarsk, Russia

² Siberian Federal University, Krasnoyarsk, Russia

³ International Laboratory of High Magnetic Fields and Low Temperatures, Wroclaw, Poland

⁴ O.O. Galkin Donetsk Institute of Physics and Engineering NAS of Ukraine, Donetsk, Ukraine

⁵ Siberian State Aerospace University, Krasnoyarsk, Russia

nat@iph.krasn.ru

Mn_2BO_4 is a mixed valent oxyborate with warwickite structure (monoclinic, space group $P2_1/a$). The crystal structure is characterized by the presence of the flat *ribbons* of edge sharing MnO_6 octahedra. The Mn^{2+} and Mn^{3+} ions occupy inequivalent crystallographic site 1 and 2, respectively, that leads to the charge ordering of the kind $\text{Mn}^{2+}(2)\text{-Mn}^{3+}(1)\text{-Mn}^{3+}(1)\text{-Mn}^{2+}(2)$ in the *ribbon*. Strong Jahn-Teller distortion of MnO_6 octahedra suggests a d_z^2 orbital ordering at the Mn1 site. The magnetic data on Mn_2BO_4 are contradictory. The magnetic study has been done only for the polycrystalline Mn_2BO_4 [1, 2]. The magnetic ordering temperature (T_N) was found to be ~ 105 K [1] from the magnetic measurements and ~ 26 K [2] from the neutron diffraction data. The authors have marked the presence of a small amount of Mn_2O_3 and Mn_3O_4 impurities. The present work is devoted to the magnetic study of the quality single crystals Mn_2BO_4 . No impurity phases have been detected by means of X-ray diffraction. The magnetization has been measured as a function of the temperature and applied field for two orthogonal crystallographic directions. The measurements have shown a long antiferromagnetic order with the AF vector lying in the crystallographic *ab*-plane. The ordering temperature is $T_N=28$ K. A pronounced lambda-peak in the heat capacity temperature dependence at $T_N=23$ K is in agreement with magnetization data. The reduced effective magnetic moment value points out the considerable orbital component of Jahn-Teller Mn^{3+} ions. The obtained results confirm the available neutron diffraction data. The integrals of indirect exchange interactions have been calculated. The exchange interactions appeared to be negative between every two neighboring manganese ions proving the antiferromagnetic character of magnetic ordering in the presence of noticeable frustrations.

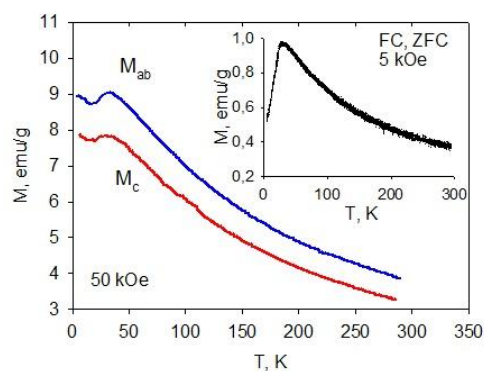


Fig. 1. The temperature dependencies of *dc* magnetization of Mn_2BO_4 single crystal. The insert shows FC and ZFC magnetizations M_{ab} measured in lower field.

This work has been financed by the programs Leading Scientific Schools NSch 2886.2014.2, RFBR № 12-02-00175, 14-02-31051-mol-a, 13-02-00958, 13-02-00358-a, Siberian Federal University Grant F11.

[1] M.A. Continentino, A.M. Pedreira, et al., *Phys. Rev. B*, **64** (2001) 014406.

[2] R.J. Goff, A.J. Williams, J.P. Attfield, *Phys. Rev. B* **70** (2004) 014426.

30PO-J1-8

MAGNETISM OF BISMUTH(III) OXIDE-BASED COMPOUNDS

Kravchenko E.A.

Institute of General & Inorganic Chemistry, Russian Academy of Sciences, Moscow, Russia
ekravchenko@igic.ras.ru

Unique magnetic properties were found by NQR in some bismuth(III) oxide-based compounds of general composition $\text{Bi}_k\text{A}_l\text{O}_m\text{X}_n$ ($A = \text{Al, B, Ge, Ba}$; $X = \text{Cl, Br}$) which are incompatible with their classification as diamagnetic compounds. The ^{209}Bi NQR experiments involved a study of the zero-field line shape, analysis of the Zeeman-perturbed patterns in the fields below 500 Oe and examination of the spin-echo envelope (SEE) in zero field, followed by theoretical treatment of the results within the density matrix formalism. The results indicated the presence in the compounds $\alpha\text{-Bi}_2\text{O}_3$, $\text{Bi}_4\text{Ge}_3\text{O}_{12}$ (BGO), $\text{Bi}_3\text{O}_4\text{Br}$, $\text{Bi}_3\text{O}_4\text{Cl}$, $\text{Bi}_2\text{Ge}_3\text{O}_9$, BaBiO_2Cl , $\text{Bi}_3\text{B}_5\text{O}_{12}$ of internal (local) magnetic fields (H_{loc}) of various strength and orientation ($5 < H_{\text{loc}} < 250$ G). In addition, a strong increase in the NQR line intensity in weak external magnetic fields (H_{ext}) was observed. The effect was shown to relate to the spin dynamics of the compounds, namely, to the influence of H_{ext} on the nuclear spin-spin relaxation. Thus in BGO ($H_{\text{loc}} \sim 25$ G), the effective time T_2^* of nuclear quadrupole spin-spin relaxation markedly elongated in external magnetic fields: the fourfold growth of the spin echo amplitude occurred in the fields as small as $H_{\text{ext}} \sim 15$ Oe at the pulse separation $\Delta\tau \sim 125$ μsec . Moreover, even minor amounts (several tenths of mol%) of magnetic atoms (Cr, Pr, Nd, Gd), inserted into the samples, resulted in a strong (up to the 8-fold) elongation of the SEE decay (Fig. 1), whereas the values of e^2Qq_{zz}/h and EFG asymmetry parameter η at the Bi nucleus remained unchanged. Such an increase in the spin-spin relaxation time as a result of doping the BGO crystals with paramagnetic atoms finds its explanation if a weakening of fluctuations in the electronic system of the crystal is suggested under the influence of H_{loc} and H_{ext} . Unlike T_2^* , the effective spin-lattice relaxation time T_1^* at room temperature differed insignificantly for both, doped and pure samples. But at lower temperatures, different contributions to the relaxation process by the dopant atoms was observed. The SQUID measurements of $\alpha\text{-Bi}_2\text{O}_3$ revealed in this crystal unisotropic paramagnetism, the magnetization markedly increasing after cooling the crystal in magnetic field. The unconventional electronic and magnetic properties of the bismuth oxy compounds are understood as resulted from an interplay of a number of contributions: features of crystal structure, electron correlations, exchange and superexchange interactions, orbital degrees of freedom.

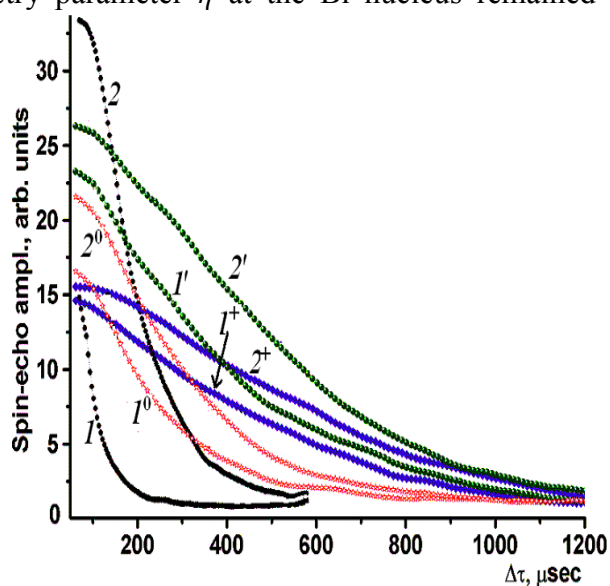


Fig.1. SEE curves for the ν_2 transition in the ^{209}Bi NQR spectrum of the BGO single crystals for non-doped ($I, 2$), doped with Pr ($I', 2'$), Nd ($I^+, 2^+$), Gd ($I^0, 2^0$) samples in $H_{\text{ext}} = 0$ (I), 30 Oe (2).

30PO-J1-9

FERROMAGNETISM IN GaAs/InAs/GaAs QUANTUM DOT LAYER DELTA-DOPED WITH Mn

Kulbachinskii V.A., Oveshnikov L.N.

M.V. Lomonosov Moscow State University, Low Temperature Physics Department, Moscow
119991, Russia
kulb@mig.phys.msu.ru

Transport, magnetotransport and magnetic properties of structures with GaAs/InAs/GaAs quantum dot (QD) layer in GaAs have been measured in the temperature interval $4.2 < T < 300$ K. The structures were δ -doped by Mn with different sheet concentration up to $3.4 \cdot 10^{14} \text{ cm}^{-2}$ from one side, to provide magnetic properties, and by carbon from another side, to enhance the p -type conductivity. The ferromagnetic phase with $T_c > 400$ K was detected by SQUID magnetometer. As an example a magnetization loop at $T=10$ K for sample with a maximal Mn concentration is shown in fig. 1. The anomalous Hall-effect (AHE) was observed at low temperatures in all samples. As an example in fig. 2 we plotted temperature dependencies of the AHE resistance R_a for two samples with different Mn concentration. As it shown in fig. 2, the AHE is visible only at the temperature interval $20 < T < 75$ K. Negative magnetoresistance was detected in the temperature interval $4.2 < T < 30$ K. In fig. 3 as an example we plotted data on the magnetoresistance for the structure with the Mn concentration $0.23 \cdot 10^{14} \text{ cm}^{-2}$ at different temperatures. Positive magnetoresistance dominates at $T > 25$ -35 K for all samples. The influence of the additional disorder in the conducting channel for samples with conducting QD layer was compared to Mn-doped quantum well structures investigated earlier in Ref. [1]. It is shown a principal role of a fluctuation potential of Mn layer, separated from the conducting QD layer by spacer, in anomalous transport properties of structures. Occurrence of negative magnetoresistance is caused by the reduction of the spin-flip scattering, related to the spin aligning in magnetic field.

[1] V.A. Kulbachinskii, P.V. Gurin, L.N. Oveshnikov, *Nanoscience & Nanotechnology Letters*, **4** (2012) 634–640.

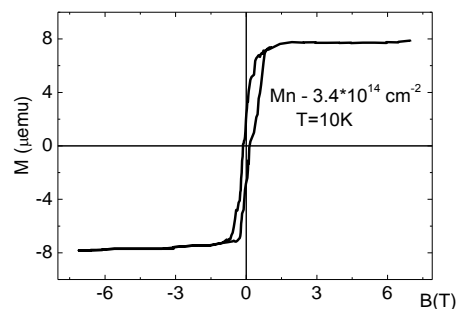


Fig. 1. Magnetization loop at $T=10$ K for one of the Mn-doped sample

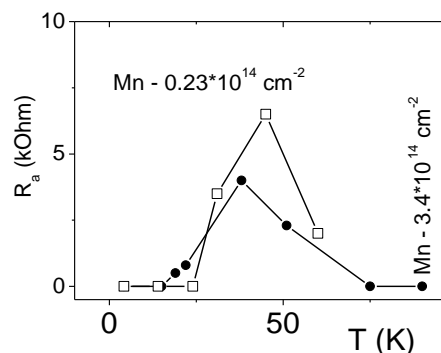


Fig. 2. Temperature dependencies of the AHE magnitude R_a for two samples with different sheet Mn concentration

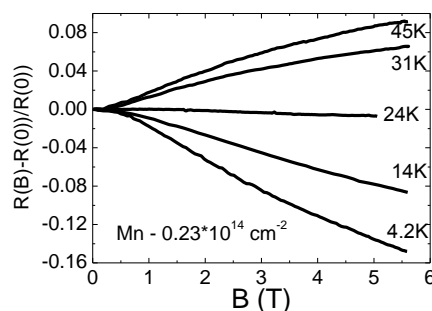


Fig. 3. Relative magnetoresistance for one sample at different temperatures

30PO-J1-10

DIFFERENT STRUCTURAL DEFECTS IN 3d IONS IMPLANTED TiO₂*Baulin R.¹, Smekhova A.¹, Yildirim O.^{2,4}, Butterling M.², Cornelius S.², Orlov A.³, Anwand W.², Wagner A.², Potzger K.²*¹ M.V. Lomonosov Moscow State University, Moscow, Russia² Helmholtz-Zentrum Dresden-Rossendorf, Dresden, Germany³ Federal State Research and Design Institute of Rare Metal Industry, Moscow, Russia⁴ Institute for Physics of Solids, Technical University Dresden, Dresden, Germany
smeal@physics.msu.ru

Titanium dioxide is in the focus of research activity for several decades since it is considered as a perspective material for a wide range of applications in optoelectronic devices, transparent conductors, gas sensors, photocatalytic devices, *etc.* Being a wide band gap semiconductor it became a very promising candidate for the special class of materials called as Diluted Magnetic Semiconductors (DMS) which exhibits room temperature ferromagnetism (RTFM) phenomenon after doping of 3d transition metals. Nevertheless, the origin of RTFM in this material is still a controversial issue.

Many recent published results declare the strong dependence of RTFM on the preparation method, thus, the influence of different defects created during the sample preparation should not be ignored. The most obvious types of defects that could be considered are: oxygen vacancies and their complexes [1], type of the crystal structure (anatase or rutile) [2] and negatively charged point defects created by Ti⁺ or 3d ions [3,4] when they are leaving the correct site positions in the host matrix.

Among different preparation techniques the ion implantation has some privileges: by variation of the ion energies the different implantation depths could be achieved allowing the creation of a homogeneous profile of ion distribution inside the host matrix. But this process *a priori* bears a lot of defects, which could be only partially removed by annealing afterwards. So, the quantitative and qualitative analysis of different defect distributions would be valuable. A successful application of ion implantation for creation of other DMS materials is already confirmed [5].

We have analyzed the amount of different defects created during 3d ion implantation in the TiO₂ semiconducting matrix. As a result, the Ti and O defect depth profiles as well as 3d ions interstitials and ion fluences have been calculated for five different energies needed to create a box-like profile of implanted ions. The analysis has been done with the help of the TRIM program package [6]. The amount of defects is compared with results of Positron Annihilation Spectroscopy (PAS) performed on the TiO₂ thin films doped with Co and V (1÷3at%) and SQUID magnetometry data. The average distances between 3d impurities in the host matrix are estimated.

Support by a German-Russian joint research group HRJRG-314 & RFBR 12-02-91321-SIGa is acknowledged.

[1] K. Griffin, M. Varela, S. Rashkeev, et al., *Phys. Rev. B*, **78** (2008) 014409.

[2] D. Kim, J. Hong, Y.R. Park, K.J. Kim, *J. of Phys.: Condens. Matter*, **21** (2009) 195405.

[3] J.O. Guillen, S. Lany, A. Zunger, *Phys. Rev. Lett.*, **100** (2008) 036601.

[4] B.J. Morgan, D.O. Scanlon, G.W. Watson, *J. Mater. Chem.*, **19** (2009) 5175.

[5] K. Potzger, *Nucl. Instr. and Meth. in Phys. Research B*, **272** (2012) 78.

[6] www.srim.org

30PO-J1-11

NMR STUDY OF THE SPIN-KAGOME COMPOUND YBaCo₃AlO₇*Iakovleva M.F.^{1,2}, Vavilova E.L.¹, Grafe H.-J.³, Valldor M.⁴, Kataev V.^{1,3}, Buechner B.³*¹Zavoisky Physical-Technical Institute, Pionerskaya str., Kazan, Russia²Kazan (Volga region) Federal University, Kremlevskaya str., Kazan, Russia³IFW Dresden, Dresden, Germany⁴Max-Planck-Institut für Chemische Physik fester Stoffe, Nöthnitzer Str., Dresden, Germany
ymf.physics@gmail.com

The frustrated spin kagome lattice may exhibit unconventional ground states such as a spin liquid. YBaCo₃AlO₇ is a metal oxide compound with a magnetic kagome substructure. We have investigated the ground state and low energy spin dynamics of this material by nuclear magnetic resonance spectroscopy.

A single crystal of YBaCo₃AlO₇ was studied at different temperatures and different magnetic fields and frequencies. The absence of a well resolved structure of ²⁷Al NMR line at low temperatures and characteristic features of the temperature dependences of the relaxation rates confirm the scenario [1] that only short-range quasi static correlations occur in the system but not a long-range antiferromagnetic ordering. The realisation of a spin-liquid state is not evident in our data.

Our conclusions are supported by earlier AC susceptibility measurements [1] and static magnetization data. We argue that the structural disorder caused by a partial Al/Co site inversion is a reason for the realisation of a spin glass state.

[1]. M. Valldor et al., *Phys.review B*, **78** (2008) 024408.

30PO-J1-12

ROLE OF Mn IN A MAGNETIC SEMICONDUCTOR: InMnP*Khalid M.¹, Weschke E.², Skorupa W.¹, Helm M.^{1,3}, Zhou Sh.¹*¹ Helmholtz-Zentrum Dresden Rossendorf, Institute of Ion Beam Physics and Materials Research, Bautzner Landstrasse 400, D-01328 Dresden, Germany² Helmholtz-Zentrum Berlin für Materialien und Energie, Wilhelm-Conrad-Röntgen-Campus BESSY II, D-12489 Berlin, Germany³ Technische Universität Dresden, D-01062 Dresden, Germany
m.khalid@hzdr.de or s.zhou@hzdr

We have synthesized ferromagnetic InMnP, a member of the III-Mn-V ferromagnetic semiconductor family, by Mn ion implantation and pulsed laser annealing. Clear ferromagnetic hysteresis loops and a perpendicular magnetic anisotropy are observed up to a Curie temperature of 42 K. Large values of negative magnetoresistance and magnetic circular dichroism as well as an anomalous Hall effect are further evidence of a ferromagnetic order in InMnP. An effort is made to understand the transport mechanism in InMnP using the theoretical models. We find that the valence band of InP does not merge with the impurity band of the heavily doped ferromagnetic InMnP. Our results suggest that impurity band conduction is a characteristic of Mn-doped III-V semiconductors which have deep Mn-acceptor levels [M. Khalid *et al.* PRB **89**, 121301(R) (2014)]. Recently, we are investigating the Mn-concentration dependent electrical, magnetic, magnetotransport etc. properties of InMnP. The preliminary results will also be presented in this contribution.

30PO-J1-13

EFFECT OF ANNEALING ON MAGNETIC PROPERTIES OF GaSb-MnSb THIN FILMS

Talantsev A.¹, Polyakov A.², Dmitriev A.¹, Koplak O.¹, Morgunov R.¹, Kochura A.^{3,4}, Fedorchenko I.⁵, Marenkin S.⁵, Novodvorskii O.⁶, Mikhalevsky V.⁶, Lahderanta E.³

¹ IPCP RAS, Chernogolovka, Russia

² P.N. Lebedev Physical Institute RAS, Moscow 119991, Russia

³ Lappeenranta University of Technology, PO Box 20, FIN-53851, Lappeenranta, Finland

⁴ South – West State University, 50 let Oktjabrja str. 94, 305040 Kursk, Russia

⁵ Institute of General and Inorganic Chemistry RAS, 119991, Moscow, Russia

⁶ Institute of Laser and Information Technologies, RAS, 140700 Shatura, Moscow region, Russia
artgtx32@mail.ru

Ferromagnetic clusters incorporated in the semiconductor crystal lattice can be applied as nano-scale spin injectors providing spin polarization of charge carriers [1]. Thermal control of the cluster sizes and their magnetic phases is traditionally most effective method to reach necessary characteristics convenient for practical applications. In our work series of the couples of the annealed and “as grown” GaSb (59 %) – MnSb (41 %) films with correspondent saturation magnetic moments M_{ann} and $M_{\text{as grown}}$ was studied. Annealing temperature was 623 K, duration was 30 min. For the films prepared at the same temperature 373 K dependencies of the saturation magnetic moments in annealed and as grown samples were different. To characterize this difference relation $M_{\text{ann}}/M_{\text{as grown}}$ was studied as function of the measurement temperature (Fig.1a). Effect of annealing on saturation magnetization was largest at high temperatures (Fig.1a).

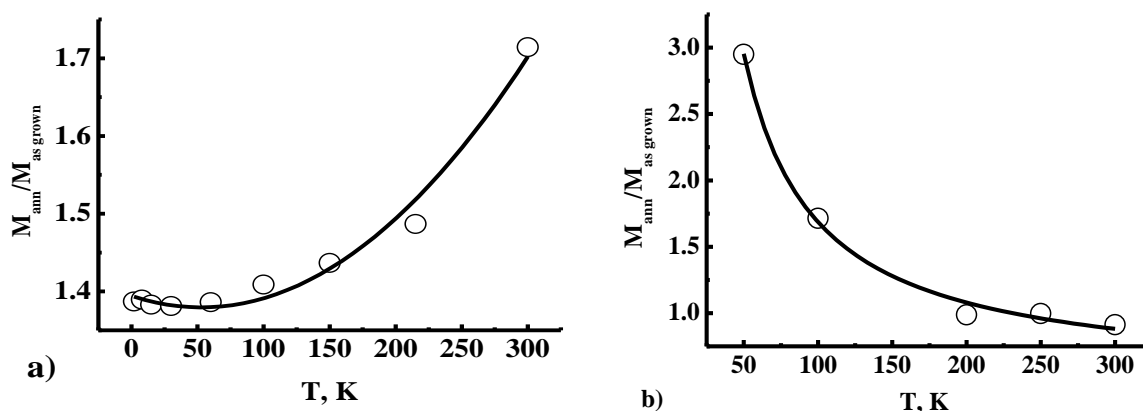


Fig. 1. (a) – Dependence of the $M_{\text{ann}}/M_{\text{as grown}}$ parameter on the measurement temperature for the samples grown in the same conditions, (b) – dependence of the $M_{\text{ann}}/M_{\text{as grown}}$ parameter on the growth temperature.

Annealing effect on magnetic properties is stronger in those samples which were grown at low temperatures (Fig.1b). These results may be explained by re-crystallization of the amorphous magnetic phase which dominates in the sample grown at the low temperatures

This work is supported by Russian Fund for Basic Researches (grant 13-07-12027, 13-02-011105a) and Grant of the President of Russia MK-1598.2014.3.

[1] A.V. Kochura, B.A. Aronzon, K.G. Lisunov et al., *JAP*, **113** (2013) 083905.

30PO-J1-14

GALVANOMAGNETIC AND MAGNETIC PROPERTIES OF $\text{Pb}_{1-y}\text{Sc}_y\text{Te}$

Skipetrov E.P.¹, Markina M.M.¹, Zakharov K.V.¹, Skipetrova L.A.¹, Solovev A.A.¹, Knotko A.V.², Slynko E.I.³, Slynko V.E.³

¹ Faculty of Physics, Moscow State University, Moscow, Russia

² Faculty of Chemistry, Moscow State University, Moscow, Russia

³ Institute of Materials Science Problems, Chernovtsy, Ukraine
skip@mig.phys.msu.ru

Lead telluride-based alloys doped with 3d-transition metal impurities (Ti, Cr, V, ...) are diluted magnetic semiconductors whose magnetic properties are dependent on their electronic structure [1]. Substituting Pb^{2+} ions in the lattice these impurities initially exist in electrically neutral Im^{2+} states. But if the impurity-induced deep level is situated above the Fermi level, transitions to the electrically active Im^{3+} states due to the self-ionization processes ($\text{Im}^{2+} \rightarrow \text{Im}^{3+} + e_{\text{band}}$) take place. An increase of impurity content leads to the filling of allowed bands lying under the level with electrons up to the pinning of the Fermi level by the impurity level. Thus, in heavily doped alloys densities of occupied and empty states in the impurity band should correspond to concentrations of impurity ions in 2+ and 3+ states with different electrical and magnetic activities.

In order to reveal a new Sc impurity level in PbTe and to establish correlation between its electronic structure and magnetic properties we have studied galvanomagnetic and magnetic properties ($2 \leq T \leq 300$ K, $B \leq 9$ T) of $\text{Pb}_{1-y}\text{Sc}_y\text{Te}$ under variation of the alloy composition ($y \leq 0.02$).

$\text{Pb}_{1-y}\text{Sc}_y\text{Te}$ single-crystal ingot with nominal Sc content $y=0.01$ was grown along $\langle 111 \rangle$ crystallographic axis by the vertical Bridgman technique. It was cut perpendicular to the growth axis into wafers about 1.5 mm thick using wire cutting. The crystal structure and the chemical composition were controlled at the cleavage surfaces of wafers by the scanning electron microscopy and X-ray fluorescence analysis. It is shown that concentration of Sc impurity exponentially increases from the end of ingot to its beginning ($y \leq 0.02$) and there are no noticeable inclusions of secondary phases in all investigated samples.

It is found that an increase of Sc impurity content leads to a monotonous growth of the free electron concentration (approximately from 10^{16} cm^{-3} to 10^{20} cm^{-3}). In heavily doped alloys ($y > 0.01$) electron concentration at $T=4.2$ K tends to saturation, indicating the pinning of the Fermi level by the Sc resonant impurity level located on the background of the conduction band. Using the six-band Dimmock dispersion relations for IV-VI semiconductors, dependence of the Fermi energy on the Sc impurity content are calculated and the energy of the resonant level is estimated to be $E_{\text{Sc}} \approx E_{\text{c}} + 280 \text{ meV}$.

In lightly doped samples the magnetic field and temperature dependences of magnetization M contain two contributions: diamagnetic contribution of the host semiconductor lattice and paramagnetic Curie-Weiss contribution ($T < 50$ K) due to the presence of magnetic Sc^{2+} ions. An increase of scandium content leads to the appearance and gradual increase of additional temperature independent paramagnetic share, connected obviously with the increase of the free electron concentration in the samples. Approximations of $M(B)$ and $M(T)$ dependences by the Brillouin function are performed and the main magnetic parameters of investigated alloys are obtained. Experimental results are discussed in the framework of the electronic structure model, assuming varying electrical and magnetic activities of Sc ions with doping.

Support by RFBR (Grant No 11-02-01298) is acknowledged.

[1] T. Story, E. Grodzicka, B. Witkowska et al., *Acta Phys. Polon. A*, **82** (1992) 879-881.

30PO-J1-15

LOW-TEMPERATURE TRANSPORT PROPERTIES OF FERROMAGNETIC SEMICONDUCTOR $\text{In}_{1-x}\text{Mn}_x\text{Sb}$

Yakovleva E.^{1,2}, *Kochura A.*^{3,4}, *Lisunov K.G.*^{3,5}, *Aronzon B.*^{2,6}, *Lahderanta E.*³

¹ Moscow Institute of Physics and Technology, Dolgoprudnyi, Moscow region, Russia

² P.N. Lebedev Physical Institute RAS, Moscow 119991, Russia

³ Lappeenranta University of Technology, PO Box 20, FIN-53851, Lappeenranta, Finland

⁴ South – West State University, 50 let Oktjabrja str. 94, 305040 Kursk, Russia

⁵ Institute of Applied Physics, Academy of Science of Moldova, MD-2028 Kishinev, Moldova

⁶ NRC "Kurchatov Institute", 1 Kurchatov Sq., 123182 Moscow, Russia

aronzon@mail.ru

Up to now, the strategy of creation of systems possessing both semiconducting and magnetic properties is based on incorporation of local magnetic moments into well-known semiconductors. The resulting new class of materials is known as diluted magnetic semiconductors (DMSs). However, the Curie temperature of such magnetically homogeneous DMSs is still insufficient, not exceeding 200 K in the most popular material GaMnAs. The alternative way is to prepare inhomogeneous DMSs with embedded ferromagnetic (FM) nanoclusters of another magnetic phase, as MnSb [1]. The special interest to InSb as a prototype DMS material is connected to its small band gap and high carrier mobility. The magnetic and transport properties of InSb:Mn, containing both the substitutional Mn atoms on In sites of the $\text{In}_{1-x}\text{Mn}_x\text{Sb}$ matrix and the nanosize MnSb precipitates, have been investigated recently [2, 3]. This DMS exhibits a FM behavior up to ~ 580 K namely due to presence of MnSb nanoinclusion [2]. However, the hump on the temperature dependence of the resistivity, widely accepted as a sign of the FM ordering, occurs at a much lower temperature $T_c < 10$ K. On the other hand, the nonlinear magnetic field dependence of the Hall resistivity, attributed usually to the anomalous Hall effect, demonstrates a behavior contradicting to this assumption. The nonlinear part of the Hall resistivity saturates in fields of $\sim 4 - 5$ T, exceeding considerably the magnetization saturation field of ~ 0.5 T. In addition, its behavior is quite different above and below T_c (inset to Fig. 1), which is attributable to the following reason. The nonlinear Hall behavior can be connected to two types of carriers; at $T > T_c$ it is determined by heavy and light holes contributing to the net conductivity [3]. These contributions depend on temperature only weakly, so the difference of the Hall resistivities at 16 K and 4.2 K gives the field dependence of the anomalous contribution to the Hall resistivity (red symbols in Fig. 1).

This work is supported by the Russian Foundation for Basic Researches (grants 14-02-00586, 13-02-92694 and 13-02-01105).

[1] V.V. Rylkov, B.A. Aronzon, Yu.A. Danilov *et al.*, *JETP* **100**, 742 (2005).
 [2] A.V. Kochura, B.A. Aronzon, K.G. Lisunov *et al.*, *JAP* **113**, 083905 (2013).
 [3] E. Lahderanta, A.V. Lashkul, A.V. Kochura *et al.*, *Phys. Stat. Sol. (a)*, in press (2014).

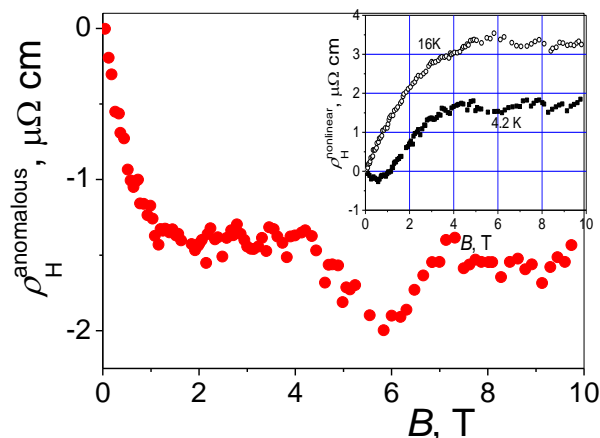


Fig. 1. Anomalous contribution to the Hall resistivity vs. B (red symbols). Inset: the Hall resistivity at $T = 16$ K and 4.2 K.

30PO-J1-16

AB INITIO STUDY OF GaSb–3d-METAL COMPOUNDS SYNTHESIZED AT HIGH PRESSURE*Magnitskaya M.V.*¹, *Kulatov E.T.*², *Uspenskii Yu.A.*³¹ Institute for High Pressure Physics, Russian Academy of Sciences, Troitsk, Russia² General Physics Institute, Russian Academy of Sciences, Moscow, Russia³ P.N. Lebedev Physical Institute, Russian Academy of Sciences, Moscow, Russia
magma@gmail.com

Ab initio calculations are reported of the electronic and magnetic properties of $MGaSb$ and MGa_2Sb_2 compounds, where M is a magnetic 3d element. These new compounds have been synthesized from magnetic and semiconducting constituents under high pressure/temperature conditions. Experimentally, most of these metastable high-pressure phases are above-room-temperature ferromagnets with rather high electrical resistivity. This combination of properties is of interest for spintronics applications, which provides a motivation for our study. The results of calculations are partly published in paper [1]. The analysis of obtained results allows us to estimate trends in the properties of bulk 3d–GaSb compounds under change of the 3d constituent. It is shown that $CrGa_2Sb_2$ differs from the other studied compounds by specific features of its electronic structure, which lead to very low and anisotropic conductivity. Owing to these features, $CrGa_2Sb_2$ appears to be close to spintronics-related materials.

Partial support by RAS and RFBR is acknowledged. The numerical calculations are performed at the Joint Supercomputer Center of RAS and the Supercomputing Center of RRC “Kurchatov Institute”.

[1] E. Kulatov, M. Magnitskaya, Yu. Uspenskii, S. Popova, V. Brazhkin, E. Maksimov, *Int. J. Quant. Chem.*, **113** (2013) 820-829.

30 June

Monday

17:30-19:00

poster session

30PO-J2

**“Magnetism in Biology
and Medicine”**

30PO-J2-1

THE SIGNALS OF ELECTRON MAGNETIC RESONANCE IN BIOLOGICAL SYSTEMS

Yurtaeva S.V.¹, Efimov V.N.²

¹ KFTI of Kazan SC, RAS, Kazan, Russia

² Institute of Physics, KFU, Kazan, Russia
yurtaeva@mail.knc.ru, vefimov.51@mail.ru

Presently there are many experimental facts of observation of electron magnetic resonance (EMR) signals in biological systems. The wide anisotropic signals were detected in late 1950's - early 1960's in DNA samples. Lately such signals were observed in cultures of dividing cells, in magnetotactic bacteria, in organs of navigation and magnetoreception in insects, birds and fish, in mammal and human tissues (nerve, brain, heart, liver, placenta, blood etc.) in cancer cell cultures, in tumours. Up to now the nature of such signals is not quite clear despite of heated discussions. The understanding of their origin is very important for many medical-biological problems such as the understanding of molecular mechanisms of brain functioning, the origin of neurodegeneration, the mechanisms of different pathologies and mechanisms of cell division.

Magnetic resonance characteristics of such signals are widely investigated only in magnetotactic bacteria. It is known the origin of the signal: the chains of magnetite nanoparticles of 20-150 nm size. Concerning the other systems the scientific discussion is being continued.

Previously we have conducted the investigation of EMR signals characteristics for the samples of human tumors [1] and nervous tissues in laboratory models [2]. Our research data and literature data allowed us to determine the following characteristics of the signals.

1) One or two line components with g-value higher than 2.1 of symmetric or asymmetric Lorentz shape (in different temperature intervals) are usually observed.

2) Characteristic non-monotonic temperature dependencies of resonance field (H_{res}), linewidth (ΔH) and integral intensity (I) with maximum for H_{res} , I and local minimum for ΔH near the temperatures 120-130 K is observed.

3) Anisotropic H_{res} behaviour of EMR signals was detected, which is character for ferrimagnetic resonance of magnetite crystals and which disappears near 130 K.

4) The correlations between the temperature dependence of the $H_{res}(T)$ and $\Delta H(T)$ and temperature dependence of magnetite magnetocrystalline constant $|K_1|$ are detected. To our opinion all the enumerated characteristics correspond to crystalline magnetite characteristics.

Sometimes wide EMR signals with $g \sim 5$ and intensive zero field signals are observed.

Detected EMR characteristics in different tissues and cells are similar to the characteristics of the signals in extracted DNA [3]. Coincidence of EMR characteristics for very different biologic systems allows us to suppose, that there is any universal phenomenon in all these cases.

Till nowadays there is no consensus on this question. On the one hand there are many facts demonstrating that EMR signals are due to magnetic impurities of biogenic magnetite, produced in the process of biomineralization in living systems, but on the other hand, magnetism of biological systems may be connected with the intrinsic structural characteristics of DNA, in which mesoscopic ring currents occur, that may produce magnetic moments and lead to resonant microwave absorption.

The present report represents a review of experimental results in investigation of EMR signals in biological systems. The main approaches in interpretation of signals are also discussed.

[1] S.V. Yurtaeva, V.N. Efimov, N.I. Silkin, et al. *Appl.Magn.Res.*, **42** (2012) 299-311.

[2] S.V. Yurtaeva, V.N. Efimov, V.S. Iyudin et al. *KFTI Annual.*, (2013) 29-33 (in Russian).

[3] A. Omerzu, B. Anzelak, et al. *Physical Review Letters*, **104** (2010) 156804(1-4).

30PO-J2-2

HEATING OF Zn-SUBSTITUTED MANGANESE FERRITE MAGNETIC NANOPARTICLES IN ALTERNATING MAGNETIC FIELD

*Elkhova T.M.*¹, *Salakhova R.T.*², *Vylegzhanin A.G.*², *Pyatakov A.P.*^{2,3}, *Yakushechkina A.K.*²

¹Physikalische Chemie Technische Universitaet, Dresden, Germany

²M.V. Lomonosov Moscow State University, Moscow, Russia

³Pharmag LLC, Troitsk, Moscow, Russia

alpya@newmail.ru

Nowadays magnetic nanoparticles (MNp) are being used in increasing number of application including biomedical ones due to the possibility of MNp injection and accumulation in the target tissue [1]. Heating of MNp in alternating (AC) magnetic field leads to the therapeutic effect either through direct thermal treatment or due to the release of the drug encapsulated in the nanoparticles.

In this report the heating capability of MNp made from Zn-substituted manganese ferrite compounds $Zn_xMn_{1-x}Fe_2O_4$ with Zn content varying from 0 to 90%. The magnetic nanoparticles of diameter 5-25 nm were synthesized in Prof. Gounko lab (Trinity College Dublin) by co-precipitation of metal salt solution with NaOH solution.

To measure the heating rate of the nanoparticles we developed the setup comprising the magnetic field generator that provides the AC magnetic field of 72 Oe with the frequency 380kHz. To measure the temperature of the sample the differential thermocouple, voltmeter Agilent 34410A and computer data acquisition system were used. Cooling system was developed to prevent the parasitic heating of the sample through the direct heat exchange with the coil.

The results of the measurements are presented in the Figure 1. In spite of the special efforts to therally isolate the test tube the residual parasitic heating was observed even in the case of the empty test tube (see Fig.1 line 1 – empty test tube).

The test tubes loaded with $Zn_xMn_{1-x}Fe_2O_4$ MNp always demonstrate larger temperature change than in the case of empty test tube while the amount of extra heating varied with the Zn content. The maximum temperature change exceeding by 40 degrees Celsius the heating of empty test tube was observed for 20% Zn-substituted MNp while the samples with higher or lower Zn content demonstrate moderate heating (see Fig.1). Various factors that might influence on heating efficiency (size, saturation magnetization, coercitivity) are analyzed. The first two factors were shown to be the crucial for heating efficiency.

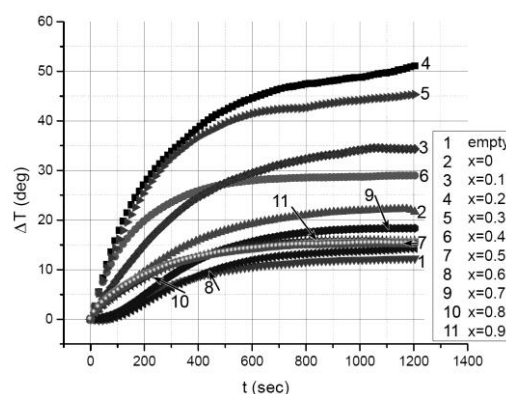


Fig. 1. The time dependence of temperature change for compounds $Zn_xMn_{1-x}Fe_2O_4$ with various Zn content $x=0-0.9$ subjected to AC magnetic field ($H=72$ Oe, $f=380$ kHz)

Support by Russian Scientific Foundation and Russian Federal Targeted Program is acknowledged.

[1] A. Ito, M. Shinkai, H. Honda, T. Kobayashi, *Journal of bioscience and bioengineering*, **100** (2005) 1–11.

[2] C.S.S.R. Kumar and F. Mohammad, *Advanced drug delivery reviews*, **63** (2011) 789–808.

30PO-J2-3

EXCHANGE ANISOTROPY IN NATURALLY OCCURRED BIOGENIC LAYERED NANOSTRUCTURES

Gendler T.S.¹, Novakova A.A.², Antonov A.N.²

¹ Institute of physics of the Earth RAS, Moscow, Russia

² Moscow State University, Physics Department, Moscow, Russia

gendler06@mail.ru, novakova.alla@gmail.com

Unusual magnetic behavior typical for layered synthesized nanostructures was found in naturally occurring system consisting from two phases -goethite (α -FeOOH) and hematite (α -Fe₂O₃) in variable proportions. Natural samples visually looked as zonal concretions or layered pigmented structures were collected from zone of lateritic bauxite of weathering crusts in basalt from South Vietnam. The abundance of microbial forms (bacteria, biofilms, bacterial mats, glycocalyx) founded in these sediments [1] suggest two-step biotic-abiotic pathway of secondary mineralization which is dictated by a complex interplay between microbial metabolism, aqueous chemistry and kinetically regulated iron oxide and hydroxide precipitation.

The samples compositions were determined from XRD, Mossbauer spectroscopy and thermomagnetic measurements. Mossbauer spectra at room temperature reveal sum of typical sextets from hematite (H) and goethite (G) with distribution of hyperfine fields along with superparamagnetic (SP) doublet. The fitting area percentages assigned with H, G and SP were variable. Magnetic measurements of real cut out samples of 0.9x 0.9x0.9 cm in size were made in two orthogonal directions using Vibrating Sample Magnetometer (LTD ORION, Borok) for the hysteresis loops and temperature dependence of the magnetization. Maximal applied field was 0.85T. In initial state VSM room-temperature hysteresis loops do not saturate at maximal applied field and display variable and complicated forms: inclined and linear, habitual, constricted, pot-bellied. Remarkable asymmetry of the magnetization reversal for direct and backward branches has been also observed. Some correlation was determined between the hysteresis loop shapes and relative content of H, G sextets and SP doublet areas fitted from the Mossbauer spectra. Both these magnetic phases are basically antiferromagnetic (AF) with weak ferromagnetism (WF) so it is not the classical case of soft and hard magnetic phase interaction.

After heating-cooling circle (20-750-20⁰C) in maximal field the large exchange bias and vertical shifts of the FC loops were observed for all the studied samples at room temperature along the applied field direction only. According to XRD and Mossbauer spectroscopy all the samples after annealing contained one crystallographic phase - α -Fe₂O₃ because of (G) dehydration. Really the annealed system consisted from two hematite of different origin: naturally formed in situ and crystallized as a result of (G) thermal transformation in external magnetic field. Thermomagnetic curves of cooling and following heating in magnetic field showed a reversible pure (AF) behavior in field direction and usual for (WF) phase in orthogonal one. Thereby within one crystallographic structure there is coexistence of two exchange coupled at room temperature magnetic phases (AF and WF). According to the model suggested by Shcherbakov et al. [2] the exchange bias in similar system originates from the formation of a quasi-spherical domain wall inside the (AF) matrix when the (WF) nanodot moment rotates under the influence of an external magnetic field.

[1] N.S. Bortnikov, V.M. Novikov, T.S. Gendler, et al. *Dokl. Earth Sci.* **441** (2), (2011) 1719-1723.

[2] V.P. Shcherbakov, K. Fabian and S. A. McEnroe. *Phys. Rev. B* **80** (2009) 174419 (1-10).

30PO-J2-4

BIOGENIC IRON-CONTAINING MAGNETIC NANOPARTICLES. MÖSSBAUER STUDY

Shapkin A.A.¹, Chistyakova N.I.¹, Zhilna T.N.², Zavarzina D.G.², Rusakov V.S.¹

¹ M.V. Lomonosov Moscow State University, Faculty of Physics, Moscow, Russia

² Institute of Microbiology, Russian Academy of Science, Moscow, Russia
alexeyshapkin@gmail.com

The iron-containing nanoparticles common use in sphere of technologies and as model objects in fundamental investigations. There are different pathways of nanoparticles synthesis such as: by chemical synthesis and by biogenic synthesis. The first method is well-known, but there are some problems such as toxic and expensive. On the other hand, the biosynthesis has not got these problems, but the quality of forming nanoparticles is not rather good [1]. The biogenic nanoparticles are formed as a result of ferric ions reduction (for example in the structure of iron hydroxide). The bacterium transports an electron from organic compound to ion in the structure of hydroxide and a new phase is formed as a result.

In case of iron oxides nanoparticles with linear size less than 30 nm the surface atoms energy contribution could not be neglected and the superparamagnetism phenomenon exists. Therefore, the Mössbauer spectroscopy method becomes useful for investigation of iron-containing nanoparticles (see for example [2]). This method has high energy resolution, hence the charge, spin state of iron in the structure could be investigated. Also, the application of special fitting models and techniques can get the size of nanoparticles, the relaxation time and the energy of the interparticle interaction.

The goal of this work was to investigate the influence of additional substances (ethanol and acetone) on biogenic iron-containing nanoparticles. The synthesised ferrihydrite was used by bacterium as electron acceptor and acetate – an electron donor. The magnetite was formed during iron reduction (a little amount of siderite was also formed).

The Mössbauer measurements were carried out in low temperature range from 80 K to 300 K and in external magnetic field up to 1.03 T at 300 K. The spectra were fitted with the many-state superparamagnetic relaxation model by program SpectrRelax [3]. The addition of ethanol and acetone lead to particle size decreasing.

[1] J.M. Byrne, N.D. Telling, V.S. Coker et al. *Nanotechnology* **22** (2011) 455709 (9).

[2] N.I. Chistyakova et al. *Hyperfine Interactions*, DOI 10.1007/s10751-013-0952-0 (2013).

[3] M.E. Matsnev and V.S. Rusakov. *AIP Conference Proceedings*, **1489** (2012) 178-185.

30PO-J2-5

IMPROVEMENT OF THE EFFICIENCY OF A SUPERCONDUCTING FILM MAGNETIC FLUX TRANSFORMER FOR A MAGNETIC FIELD SENSOR

Ichkitidze L.P.

National Research University of Electronic Technology “MIET”, MIET, Zelenograd, Moscow,
124498 Russian Federation

leo852@Inbox.ru

Wide application of SQUIDs is limited by many factors, such as high cost, brittleness, and complexity of measuring the absolute value of a magnetic field. The magnetic sensitivity of SQUIDs is often enhanced by using magnetic flux transformers (MFTs) based on superconducting films. The main function of the MFTs is transformation of a magnetic flux to a magnetic field, which is concentrated on a magnetosensitive element (MSE). The higher the magnetic field concentration F_{mag} , the more effective the MFT is.

The efficiency of the MFTs should be enhanced in order to increase magnetic sensitivity of an MSE, which can be a SQUID, a granular superconductor (Josephson medium), a sensor with the giant magnetoresistance (GMR), a Hall sensor, etc. Previously, we considered a combined magnetic field sensor (CMFS) consisting of an MFT with the nanostructured active strip (AS) and a GMR sensor-based MSE [1,2]. It was demonstrated that nanostructuring of the MFT active strip makes it possible to increase F_{mag} by 1–2 orders of magnitude and, thus, significantly improve the characteristics of a CMFS. The CMFS construction is a sandwich: an MSE is placed under the MFT active strip between insulating films.

In this work, we investigate a planar CMFS in which an MSE is placed between two MFT strips (see the **Figure**).

We calculated F_{mag} for the presented CMFS construction and compared it for the cases when the strip is continuous and fragmented by cuts with the width $w_p = 50 \div 5000$ nm. We investigated the CMFS (variant 1) with the AS width $w_s = 30$ μm , a gap between the AS and the MSE of 10 μm , an MSE width of 1 μm , and the AS and MSE thickness $d \approx 50$ nm.

In the approximation of the screening current homogeneously distributed over the AS surface, we have $F_{\text{mag}} \sim 120$. However, in the AS with the above-mentioned parameters, the current is distributed inhomogeneously, so $F_{\text{mag}} \leq 40$, since the AS is a wide superconducting film, i.e., $w_s \gg 2\lambda^2/d$, where $\lambda \sim 250$ nm is the London magnetic field penetration depth for the HTS material. Fragmentation of the AS into alternating regions of superconducting branches and cuts (**Figure, b**) additionally increases F_{mag} by a factor of F . In particular, at $w_p = 1000$ nm, we have $F \sim 4$ and at $w_p = 100$ nm, $F \sim 10$.

In variant 2, $w_s = 1$ μm was allowed; the rest widths were scaled relative to variant 1; at $w_p = 50 \div 200$ nm, we had $F < 2$.

Thus, fragmentation of the active strip by micro- or nano-cuts increases the magnetic field concentration on the MSE and thus enhances the efficiency of the MFT and CMFS.

[1] L.P. Ichkitidze, A.N. Mironyuk, *J. Phys.: Conf. Ser.*, **400** (2) (2012) 022032 (4).

[2] L.P. Ichkitidze, *AIP Advances*, **3**(6) (2013) 062125 (8); <http://dx.doi.org/10.1063/1.4812700>

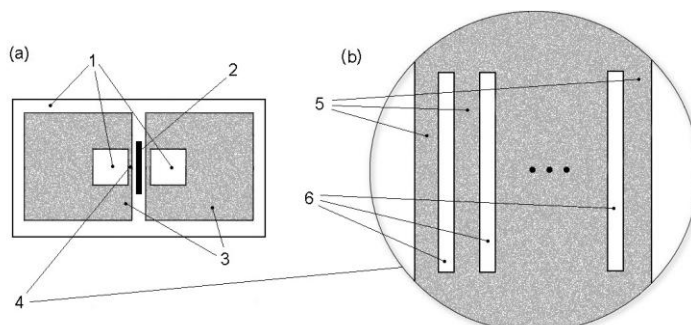


Figure. Layout of the MFT and MSE: (a) – substrate 1, MSE 2, and superconducting MFT loops 3; (b) – MFT active strip 4 consisting of numerous branches (enlarged). The shaded and unshaded areas show superconducting branches 5 and slits 6, respectively.

30PO-J2-6

COMBINED PHOTODYNAMIC THERMOCHEMOTHERAPY OF ONCOLOGICAL DISEASES CONTROLLED BY MRI AND ELECTRONIC SENSOR

*Brusentsov N.A.^{1,2}, Polianskiy V.A.², Zhukov A.V.², Khohlov A.R.³, Anisimov N.V.³, Gulyaev M.V.³,
Pirogov Y.A.³, Nikitin M.P.⁴, Nikitin P.I.⁴, Brusentsova T.N.⁵, Kuznetsov V.D.⁵, Bocharova O.A.¹,
Baryshnikov A.Y.¹*

¹ Blokhin Russian Cancer Research Center RAS, Moscow

² Institute of Mechanics, MSU, Moscow

³ Fundamental Medicine Faculty of M.B.Lomonosov Moscow State University, Moscow, Russia

⁴ Prokhorov General Physics institute, RAS, Moscow, Russia

⁵ Mendeleev University of Chemical Technology of Russia, Moscow, Russia

brusentsov2005@yandex.ru

The early revealing of proliferation by contrast MRI is an important problem in the detection of malignant tumors. In the present work, we continued investigation of early contrast MRI and magnetohydrodynamic thermochemotherapy (MTC) of malignant tumors by BIOSPEC BC 70/30 (Bruker) and scanning electronic sensor (ES) of magnetic carriers by their non-linear magnetization. Neovascularization and early pretumoral changes of outlines of structures of biological tissues under action of malignant cells are a display of first attributes of proliferation which we revealed by contrast MRI with Dextran-ferrite sol (DFS) [1, 2]. Accumulation of DFS and bracing in the healthy tissues were visualized by MRI and quantified by the ES scanning. Experiments showed that DFS appears to be a promising MRI-negative contrast agent for detection of malignant tumors.

The next step was treating the tumors by combination of chlorines (CH) with several procedures and drugs. We used Radachlorin (RCH), Cisplatin (CP), Mitoxantron (MX), Melphalan (MP), Dacarbazine (DC) and Docetaxel (DT). Besides, the effect of RCH's, CP's, MX's, MP's, DC's and DT's can be increased by combining them with DFS. A complex treatment, which combines the magnetically controlled anticancer drugs such as CP and MP containing DFS, targeting them to the tumor tissue by a gradient magnetic field produced by magnetic NdFeB bandages (0.2 T) or by cryomagnet (7.0 T) [3, 4], heating tumor by AC magnetic field with necrotic slime aspiration, and with intraperitoneal and intracavitary introduction of Cyclophosphan, was performed. The experiments were carried out for development of such complex MTCs of the rat glioma C 6, murine B 16 melanoma, mammary Ca 755 adenocarcinoma and Lewis lungs carcinoma (LLC), based on our methods for quantification of magnetic agents [3-5] and optimization of the treatment by 3D near-real-time MRI that controls MTC. Application of DFS as the diagnostic agents for MRI contrast purposes, as well as heating agents combined with chemotherapeutic preparations are promising for the combined diagnosis and therapy of tumors. Early revealing of tumor proliferation by combination of MRI contrast agents such as dextran-ferrite and Magnevist increased the therapy efficiency. Quantitative real-time detection of DF in tumor and liver by an electronic detector allowed definition of preferable therapy, enhanced the effect of photodynamic therapy combined with magnetohydrodynamic thermochemotherapy at rodent models and led to increase of life span for glioma C6 and glioblastoma 101.8 up to 47% and up to 34%, respectively.

The work was supported by RFBR, No. 13-01-00035, 14-01-00056, 13-02-011260, 13-03-12468, 14-02-00840.

[1] N.A. Brusentsov, Y.A. Pirogov, V.A. Polyanskiy et al., *Solid State Phenomena*, **190** (2012) 717.

[2] N.A. Brusentsov, *Rus.J. Gen. Chem.*, **83** (12), (2013) 2548, DOI 10.1134 /S1070363213120530.

[3] M.P.Nikitin, P.M.Vetoshko, N.A.Brusentsov, P.I.Nikitin, *J.Magn.Magn. Mat.*, **321**(2009) 1658.

[4] U.O. Häfeli, K. Gilmour, A. Zhou, S. Lee, M.E. Hayden, *J. Magn. Magn. Mat.*, **311** (2007) 323.

[5] N. A. Brusentsov, Yu. A. Pirogov, A.A. Uchevatkin, et al, *Pharm. Chem. J.*, **45** (2011) 2, 84.

30PO-J2-7

MAGNETIC AND STRUCTURAL PROPERTIES OF NANOPARTICLES IN SHELLS OF POLYELECTROLYTE MICROCAPSULES STUDIED BY MÖSSBAUER SPECTROSCOPY

*Starchikov S.S.*¹, *Lyubutin I.S.*¹, *Bukreeva T.V.*¹, *Lysenko I.A.*², *Sulyanov S.N.*¹, *Korotkov N.Yu.*¹,
*Rumyantseva S.S.*¹, *Marchenko I.V.*¹, *Funtov K.O.*¹, *Vasiliev A.L.*^{1,2}

¹ Shubnikov Institute of Crystallography, Russian Academy of Sciences, Moscow, Russia

² NRC “Kurchatov Institute”, Moscow, Russia

sergey.s.starchikov@gmail.com

Magnetic nanostructures are considered as promising materials in high-density magnetic storage and spintronic devices, magnetic heads, sensors. Recently, more attention was paid to the application of magnetic nanostructures in biology and medicine and focused mainly on the targeted drug delivery, hyperthermia treatment, magnetic resonance imaging (as contrast media), separation of biochemical products and gene manipulation and immunoassays [1-3]. In this work hollow microcapsules from biodegradable polyelectrolytes were fabricated by layer-by-layer adsorption technique. The capsule shells were modified with the maghemite nanoparticles by *in situ* synthesis. Such capsules can be assigned for the target drug delivery. Different and complementary techniques were used for the evaluation of their structural, physicochemical, and magnetic properties. A particular effort was devoted to distinguish between magnetite Fe_3O_4 and maghemite $\gamma\text{-Fe}_2\text{O}_3$ nanoparticles as well as to study the effect of the size and coating on the magnetic behavior of the nanoparticles. The low temperature Mössbauer spectroscopy was applied as one of the most adequate techniques for determining the oxidation degree and cation distribution in $\gamma\text{-Fe}_2\text{O}_3$ nanoparticles.

The sediment of the capsules was observed to move in the magnetic field of a constant magnet. XRD, electron microscopy, Raman and Mössbauer spectroscopy data revealed that the iron oxide nanoparticles have the crystal structure of maghemite $\gamma\text{-Fe}_2\text{O}_3$. An average diameter of the capsule is about 6.7 μm while the average thickness of the capsule shell is 0.9 μm . The maghemite nanoparticles formed in the capsule shell are rather monodisperse with the medium size of 8 nm. The Mössbauer spectroscopy data revealed that the spin blocking temperature T_B for particles with the size of 5 and 6 nm is about ≈ 70 and ≈ 250 K, respectively. The fraction of these particles is about 15% of the total iron content in the sample. Furthermore, about 80% of all maghemite nanoparticles with the size of 7-10 nm have marked superparamagnetic behavior which is retained up to room temperature due to slow spin relaxation. Because of that, the microcapsules with maghemite nanoparticles in their shells, coated by an organic media of polyelectrolyte, can be handled by an external magnetic field which is important for target drug delivery. It seems that interparticle interactions are decreased due to the coating by polyelectrolyte media. Based on the Mössbauer spectroscopy data, the anisotropy constants K were determined for the particles with the size of 5, 6 and 8 nm using the superparamagnetic approximation and in the low temperature approximation of collective magnetic excitation.

Support by the Russian Scientific Foundation (Grants #14-12-00848) is acknowledged.

[1] H.-S. Cho, Z. Dong, G. M. Pauletti, J. Zhang, H. X, *et al*, *ACS Nano*, **4** (2010) 5398–5404.

[2] H. Xu, M. Shao, T. Chen, *et al*, *Microporous Mesoporous Mater.*, **153** (2012) 35 – 40.

[3] G. H. Jaffari, A. Ceylan, C. Ni, and S. I. Shah, *J. Appl. Phys.*, **107** (2010) 013910.

30PO-J2-8

MAGNETIC PROPERTIES OF FERRIHYDRITE NANOPARTICLES OF BACTERIAL ORIGIN

Balaev D.A.^{1,2}, Krasikov A.A.^{2,*}, Dubrovskii A.A.¹, Semenov S.V.^{1,2}, Bayukov O.A.¹, Stolyar S.V.^{1,2}, Iskhakov R.S.¹, Ladygina V.P.³, Ishchenko L.A.²

¹ Kirensky Institute of Physics, Russian Academy of Sciences, Siberian Branch, Krasnoyarsk, 660036, Russia

² Siberian Federal University, Krasnoyarsk, 660041, Russia

³ International Research Center for Studies of Extreme States of the Organism, Presidium of the Krasnoyarsk Research Center, Siberian Branch, Russian Academy of Sciences, Krasnoyarsk, 660036, Russia

*AK9891@yandex.ru

Antiferromagnetic (AF) nanoparticles (NPs) possess spontaneous magnetic moment due to incomplete compensation of the sublattices or spins [1]. Among variety of AF materials ferrihydrite NP with the general formula $\text{FeOOH} \cdot n\text{H}_2\text{O}$ have attracted great attention, see for example [2]. It was shown [3,4] that ferrihydrite particles obtained in the process of cultivation of *Klebsiella oxytoca* bacteria [5] demonstrate magnetic properties very close to that observed on well-known horse-spleen ferritin [2].

Here we report on the modification of magnetic properties of ferrihydrite NPs (product of vital functions of *Klebsiella oxytoca* bacteria) due to thermal treatment. Two samples were studied: the “as prepared” powder [4], and powder undergone thermal treatment at 140°C for 3 hours in air (hereafter denoted as “annealed” sample).

The SP blocking temperature T_B is found to increase due to thermal treatment: $T_B \approx 23$ K for “as prepared” sample and $T_B \approx 49.5$ K for “annealed” sample.

Fitting of the magnetization curves $M(H)$ obtained in a temperature range above T_B by superposition of Langevin function (the SP contribution) and the $\chi_{AF} \times H$ term (χ_{AF} - is the AF susceptibility) allowed to derive the average magnetic moment of the particle $\langle \mu_p \rangle$. The $\langle \mu_p \rangle(T)$ dependences are found to follow $\sim \langle \mu_p \rangle(T=0) \times (1 - T^a)$ law with $a \approx 2$ and $a \approx 1.5$ for “as prepared” and “annealed” samples respectively. The $\langle \mu_p \rangle(T=0)$ value for “annealed” sample is 1.4 times higher than that for “as prepared” sample. We deduce that the growth of mean particle size during thermal treatment procedure used takes place.

Basing on these results and results of study of morphology of such NPs [6] one can conclude that uncompensated magnetic moment of ferrihydrite NP is proportional to $N_{\text{Fe}}^{1/2}$ spins of Fe^{3+} atoms (where N_{Fe} – is the total amount of Fe^{3+} atoms in NP). This is in accordance with Néel’s hypothesis of the random decompensation of the magnetic moments of magnetically active ions located both on the surface and in the bulk of a small AF particle [1].

[1] L. Néel, *C.R. Acad. Sci. Paris* **252** (1961) 4075.

[2] N.J.O. Silva, V.S. Amaral, and L.D. Carlos, *Phys. Rev. B* **71** (2005) 184408.

[3] Yu. L. Raikher, V. I. Stepanov, S. V. Stolyar, et al, *Phys. Solid State* **52** (2010) 298.

[4] D.A. Balaev, A.A. Dubrovskii, A.A. Krasikov, et al, *JETP Letters* **98** (2013) 139–142.

[5] S. V. Stolyar, O. A. Bayukov, Yu. L. Gurevich, et al, *Inorg. Mater.* **41** (2007) 638.

[6] M. Balasoiu, S. V. Stolyar, R. S. Iskhakov, et al., *Rom. J. Phys.* **55** (2010) 782.

30PO-J2-9

MAGNETIC PROPERTIES OF BIOGENIC NANOPARTICLES

Stolyar S.V.^{1,2,*}, *Bayukov O.A.*², *Balaev D.A.*², *Iskhakov R.S.*², *Ishchenko L.A.*², *Ladygina V.P.*³,
Antonov A.I.

¹Siberian Federal University, Svobodny 79, Krasnoyarsk, 660041, Russia

²Kirensky Institute of Physics, SB RAS, Akademgorodok, 50/38, Krasnoyarsk, 660036, Russia

³International scientific centre for organism extreme states research attached Presidium of KSC, SB RAS Akademgorodok 50, Krasnoyarsk, 660036, Russia

*stol@iph.krasn.ru

Antiferromagnetic (AF) nanoparticles exhibit magnetic properties significantly different than properties of the bulk materials. In present work the magnetic properties of biomineral ferrihydrite nanoparticles (massa), produced by *Klebsiella oxytoca* strain [1] and the nanoparticles obtained by drying the sol (zol), made on the basis of biomineral ferrihydrite nanoparticles have been studied. Temperature dependence of magnetization M (T) for the nanoparticles (zol) in ZFC (zero field cooling) regime show distinct maximum at 23 K [2]. There is no maximum in ZFC curve of ferrihydrite nanoparticles (massa) and it demonstrates steep decreasing with temperature from 4 to 300 K. This means that Blocking temperature is less than 4 K [3]. Mossbauer spectra of biomineral nanoparticles ferrihydrite (massa) and dried sol nanoparticles (zol) are shown in the Figure 1.

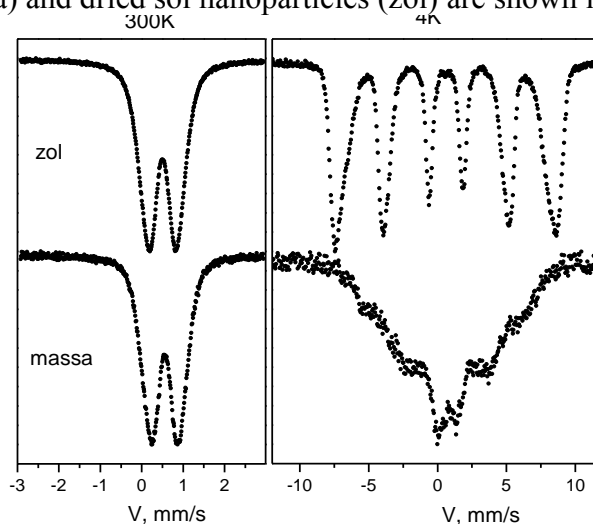


Fig . 1. Mossbauer spectra of the nanoparticles at a temperature of 300K and 4 K.

Parameters of the spectra dramatically differ that indicate the structures of the studied nanoparticles differ too.

Support by State Ministry of Education and Science is acknowledged.

[1] S.V.Stolyar, O.A.Bayukov, Yu.L.Gurevich, E.A.Denisova, R.S.Iskhakov, V.P.Ladygina, *Inorganic. materials.* **42**, **7** (2006) 1-6 .

[2] D.A. Balayev, A.A. Dubrovsky, A.A. Krassikov, S.V. Stolyar, R.S. Iskhakov, V.P. Ladygina, E.D. Hilazheva , *JETP Letters* **98**, **3**(2013), 160-164.

[3] Yu.L. Raikher, V. I. Stepanov, S. Stolyar, V. P. Ladygina, D.A.Balaev, L.A. Ishchenko, M. Balasou. *Physics of the Solid State.* **52**, **2**(2010), 277-284.

30PO-J2-10

NEW MAGNETIC NANOPARTICLES FOR BIOMEDICAL APPLICATIONS*Kamzin A.S.¹, Zaripova L.D.², Romachevskii K.E.¹*¹ Ioffe Physical Technical Institute of RAS, St. Petersburg, 194021, Russia² Kazan Federal University, Kazan, Tatarstan, 420008 Russia

kamzin@mail.ioffe.ru

Magnetic nanoparticles, due to their properties, attracting attention in the fields of medical and biological applications, including magnetic separation of biological, therapeutic drug delivery, hyperthermia for the treatment of tumors and for contrast enhancing of a magnetic resonance imaging. One area of research is the magnetic treatment of cancer tumors with hyperthermia using termograins, representing a two phase composite ceramic consisting of biologically active components, typically bioglass or ceramic based on calcium phosphates and the magnetic components in the form of ferrimagnetic nano- or microparticles. Composite ceramic injected into cancerous tissue and can heat it without wire connections to the desired temperature, depending on the force applied external alternating magnetic field. When the temperature reached 42 C, usually damaged and killing cancerous cells, healthy cells while minimally injured.

More complex view is self-regulating magnetic hyperthermia process which requires magnetic materials the Curie temperature (TC) which should be in the range from 315 to 320K. To create magnets with self-regulating heating process required technology which gives possibilities to control the magnetization and coercivity of nanoparticles - parameters that allow control TC of substance and efficiency of its heating, thus avoiding overheating during hyperthermic therapy.

In this paper, have been shown that it is possible to substantially improve the magnetic characteristics of the biomagnetic materials creating them especially for biomedical applications. As a result, ceramic implants have been designed based on the carbonated hydroxyapatite (CHA) as the biologically active matrices. As magnetic components used modified hexagonal ferrite particles $\text{BaFe}_{12}\text{O}_{19}$, spinel CoMFe_2O_4 ($M = \text{Zn}$ or Ti) and perovskite $\text{La}_{0.7}\text{Sr}_{0.3}\text{MnO}_3$.

Studies of created biocomposites made by using X-ray diffraction, infrared absorption, Mossbauer spectroscopy, electron microscopy and magnetostatic methods. Improvement of bioactive properties and biocompatibility of created magnetic bioceramics due to using of matrix CHA which have excellent bio properties. It has been established that the introduction of a significant amount of the magnetic component does not significantly influence the phase composition of the bioactive CHA matrix at both structural and molecular levels and, hence, the initial high biocompatibility of CHA is retained. Ferrite particles provided magnetic properties obtained bioceramics necessary for optimal magnetic therapy and thermal effects. The generation of heat in an alternating magnetic field created biocomposites meets magnetotherapy treatment.

Thus, the composite ceramics represents a new magnetic bioceramics that combine excellent biological activity of CHA and high magnetic characteristics of created magnetic particles of hexagonal ferrite particles M-type, Co spinel ferrite or perovskites $\text{La}_{0.7}\text{Sr}_{0.3}\text{MnO}_3$. The created composite bioceramics are a promising materials for medical applications, in particular, as thermosteds in treatment of hyperthermia.

30 June

Monday

17:30-19:00

poster session

30PO-K

**“Spintronics and
Magnetotransport”**

30PO-K-1

FEATURES OF A LASER REMAGNETIZATION OF TbCoFe BASED MAGNETIC JUNCTIONS

Krupa M.¹, Kostishyn V.^{2}, Korostil A.¹*

¹ Institute of Magnetism, 03142, Kyiv, Ukraine

² National University of Science and Technology «MISiS», 119991, Moscow, Russia

* drvgkostishyn@mail.ru

Physical limits of the minimal remagnetization time and minimal sizes of a remagnetization media represent one of fundamental problems of the physics of magnetism, which has a crucial significance for realization of ultra-fast and ultra-dense recording and readout of information. Growing attention to this problem is related to modern achievements of nanotechnologies, possibility to produce of new magnetic nanostructures with given physical properties and the novel development of ultra-fast laser sources. Today, prospects of the solution this problem associates with the use of the impact of short-time laser impulses on the ferrimagnetic multilayered nanostructures, specifically, tunnel magnetic junctions, that can lead to magnetic state variations and the remagnetization effect.

The laser-induced remagnetization of a ferrimagnetic nanolayer is characterized by its initial laser-induced swift heating, thermal demagnetization with different speeds of ferrimagnetic sublattices with subsequent a magnetic bias that can be caused both laser-induced electron excitations (the inverse magneto-optical Faraday effect) and nonequilibrium transitional ferromagnetic-like magnetic states of ferrimagnetic sublattices

We have investigated features of the laser-induced remagnetization of magnetic tunnel junctions on the basis of the RE-TM amorphous compounds, TbCoFe with strong enough perpendicular magnetic anisotropy and the magnetic compensation temperature and the Curie temperature, which can be tuned in wide temperature range by varying its composition. The tunnel barrier nanolayer consisted of PrO compound representing a wide-gap semiconductor. By the all optic pump-probe technique we investigated the laser-induced remagnetization of the TbCoFe-based magnetic junctions under picosecond and femtosecond pulsed laser radiation. We have researched the dependence of the laser-induced remagnetization on parameters of the pulsed laser radiation. It was established the role of the laser-induced effective internal magnetic fields related to the magneto-optical inverse Faraday effect and the laser-injection spin nonequilibrium redistribution in the magnetization reverse of the investigated magnetic junctions. The influence of a transient ferromagnetic-like state on the magnetization switching in the ferrimagnetic junctions was studied with and without transition across compensation points. At power enough laser pulses, such transient states lead to internal bias which in combination with the exchange interaction relaxation can results in the pure laser-induced remagnetization. The action of different remagnetization mechanisms depends on the composition TbCoFe-based ferrimagnetic, determining the compensation points.

The laser-induced remagnetization depends on laser pulse duration and the laser intensity. The corresponding phase diagram obtains on the basis of the Landau-Lifshitz-Bloch equation with temperature dependent parameters of longitudinal and transverse susceptibilities, which are calculated using Langevin dynamics combined with a Landau-Lifshitz-Gilbert equation for each spin.

Investigated ferrimagnetic TbCoFe compounds in contrast to well-known ferrimagnetic compounds, GdFeCo, which were wide used as the physical model for the investigation of mechanisms of ultra-fast laser-induced remagnetization, possess strong enough perpendicular magnetic anisotropy that determine their practical applications for high-speed and high-dense recording of information, that is characterized by thermal stability for archival storage and maintain signal to noise ratios.

30PO-K-2

SPIN-POLARIZED TUNNELING IN MULTIFERROIC TUNNEL JUNCTIONS*Demin G.D.¹, Popkov A.F.¹, Suhetsky A.A.¹*¹ National Research University of Electronic Technology (MIET), Moscow, Russia
gddemin@gmail.com

Recently, great attention in nanomagnetism is focused on the study of multiferroics as a promising class of materials for a new generation of solid-state memory devices, characterized by the presence of multiple logic states due to the coexistence of ferroelectric and ferromagnetic ordering [1,2]. In this vein, their use as tunnel barrier layers in the magnetic tunnel junctions is of particular interest, in analogy with the magnetoresistive memory STT-MRAM [3]. However, the mechanisms of spin transport in such heterostructures require more detailed consideration.

In this work we have studied the characteristics of the spin- polarized tunneling in ferromagnet - multiferroic – ferromagnet (FM-MF-FM) tunnel junctions taking into account the screening spin-split potential at the interfaces, arising from the built-in charge in multiferroic tunnel layer in the presence of spontaneous polarization. It is shown that the asymmetry of screening lengths in semi-infinite magnetic electrodes strongly affects the tunnelling behaviour of spin-polarized electrons through the multiferroic tunnel barrier with a different direction of the polarization and magnetization vectors.

The obtained results can be further used to study the effect of spin-transfer torque on the magnetization dynamics in the multiferroic tunnel layer for determining the conditions of current-induced switching between different logic states at a fixed mutual orientation of the magnetizations of the magnetic electrodes.

From a practical point of view, this work may also be useful for the optimization of parameters of multiferroic tunnel structures in the development of the energy-efficient multibit memory.

This work was supported by RFBR (Grant No 13-07-12405).

[1] M. Gajek, M. Bibes, S. Fusil, K. Bouzehouane, J. Fontcuberta, A. Barthélémy, A. Fert, *Nat. Mater.*, **6** (2007) 296-302.

[2] D. Pantel, S. Goetze, D. Hesse, M. Alexe *Nat. Mater.*, **11** (2012) 289-293.

[3] E.Y. Tsymbal, A. Gruverman, V. Garcia, M. Bibes, A. Barthélémy, *MRS Bulletin*, **37** (2012) 138-143.

30PO-K-3

QUANTUM DOTS ON 2D AND 3D TOPOLOGICAL INSULATORS WITH MAGNETIC BARRIERS: ELECTRONIC AND SPIN STRUCTURE

Konakov A.A., Chubanov A.A., Kozulin A.S., Khomitsky D.V.

University of Nizhniy Novgorod, 603950 Nizhniy Novgorod, Russia
anton.a.konakov@gmail.com

Topological insulators (TIs) remain to be one of the hottest topics of both experimental and theoretical research in condensed matter physics during the last years [1, 2]. Existence of topologically protected gapless current states makes them promising for next generation of electronic devices. Furthermore the spin polarization of these states is of a great interest in spintronics applications. Magnetic field breaks time-reversal symmetry and induces the gap in the Dirac-like spectra of edge (in the case of 2D TI) or surface (in the case of 3D TI) states. Using gapped barrier regions one can confine massless Dirac fermions in finite size [3]. Thereby new types of confined states can be formed in TIs with the use of magnetic barriers such as the states in recently proposed quantum dots at the edge of quantum spin Hall insulators [4, 5]. In this work we develop theory of localized states at the edge of 2D TI and at the surface of 3D TI produced by magnetic barriers with finite values of magnetization.

First we consider quantum dot (QD) formed at the edge of 2D topological insulator (TI) such as HgTe quantum well with inverted band structure. Free electrons at the quantum spin Hall edge are described by the 1D Weyl Hamiltonian [1, 2]. To localize electron into a single dot we assume that two magnetic barriers are positioned along the propagation direction of edge states. In the most general case absolute values and orientations of the magnetizations in barrier regions can be different. Taking into account only Zeeman energy of electrons in magnetic barrier regions one can obtain the effective Hamiltonian of 2D TI QD with finite magnetic barriers, acting on the envelope function (in [4, 5] such Hamiltonian is presented for a case of impenetrable barriers).

We calculated the electronic states in 2D TI QDs with different relations between absolute values and orientations of barriers' magnetizations. In the case of symmetric barriers single-particle energies depend on the difference between magnetic fields' directions in barriers. This fact opens a specific for discussed system possibility to manage electronic states: one can not only change a barrier height and QD size, but also manipulate relative orientation of the barriers' magnetizations. When the magnetizations of the barriers have the same orientation, energy spectrum are symmetric with respect to the Dirac point. We also computed space distribution of spin density in the stationary states and found oscillations of their spin polarization as a function of the principal quantum number.

We also investigated electronic and spin structure of rectangular QDs formed at the surface of 3D TIs, such as Bi₂Se₃. We found that magnetic field in the barrier regions can mix orthogonal spin and momentum variables and lead to nontrivial space oscillations of spin density in QD.

Support by RFBR (grants N 13-02-00717-a and 13-02-00784-a) is acknowledged.

[1] M.Z. Hasan, C.L. Kane, *Rev. Mod. Phys.*, **82** (2010) 3045-3067.

[2] X.-L. Qi, S.-C. Zhang, *Rev. Mod. Phys.*, **83** (2011) 1057-1110.

[3] M.I. Katsnelson, K.S. Novoselov, A.K. Geim, *Nature Phys.*, **2** (2006) 620-625.

[4] C. Timm, *Phys. Rev. B*, **86** (2012) 155456 (6).

[5] G. Dolcetto, N. Traverso Ziani, M. Biggio, F. Cavaliere, M. Sassetti, *Phys. Rev. B*, **87** (2013) 235423 (6).

30PO-K-4

LIGHT-EMITTING GaAsSb/GaAs STRUCTURES WITH GaMnAs FERROMAGNETIC INJECTOR

Kalenteva I.L., Vikhrova O.V., Dorokhin M.V., Danilov Yu.A., Zvonkov B.N., Kudrin A.V.

Physical–Technical Research Institute, Lobachevsky State University, Nizhny Novgorod, Russia
 istry@rambler.ru

Previously, the possibility of creating the diode structures with quantum well (QW) InGaAs/GaAs and GaMnAs injector was shown [1]. Application of GaAsSb/GaAs QW as an active region for light-emitting diode structures allows achieving the most relevant fiber-optic range near 1.3 μm . It is expected that using a suitable ferromagnetic injector, and fabrication of spin light emitting diodes on this basis may increase the speed of information transfer through the fiber lines. Such structures were studied in this work.

The studied structures contain a buffer n -GaAs layer with a thickness $\sim 0.4 \mu\text{m}$ and QW $\text{GaAs}_{1-x}\text{Sb}_x/\text{GaAs}$ ($x \sim 15\text{-}20\%$) grown by MOCVD at a temperature $T_g = 580\text{-}600^\circ\text{C}$. Under the same conditions GaAs spacer layer with varying thickness ($d_s = 25\text{-}150 \text{ nm}$) between QW and magnetic semiconductor GaMnAs was formed. The ferromagnetic semiconductor GaMnAs layer ($\sim 100 \text{ nm}$) p -type conductivity was obtained by laser sputtering (LS) at $T_g = 350^\circ\text{C}$ [2]. Diodes were fabricated with use of photolithography and chemical etching after formation of ohmic contacts. A control sample containing only GaMnAs layer on i -GaAs was also fabricated by LS.

The emission characteristics were studied via photo- (PL) and electroluminescence (EL) spectroscopy. The galvanomagnetic properties of the control sample, voltage-current and polarization characteristics were examined in the temperature range 10–300 K.

EL of quantum well is observed for all samples with different GaAs spacer at temperatures below 80 K. It is found that reduction of spacer thickness from 150 to 25 nm leads to a decrease of PL and EL (I_{EL}) intensity, corresponding to in QW, due to increase of nonradiative recombination centers number near QW. EL peak shift to higher energies (Fig. 1) with an increase of pump current ($\sim 4 \text{ meV}$ with increasing current 2.5 times) suggests that emission of GaAsSb quantum well is observed due to indirect transitions in real space.

Both negative magnetoresistance and nonlinear dependence of Hall resistance on the magnetic field ($R_H(H)$) are observed for the control sample GaMnAs on i -GaAs at temperatures below 40 K (inset in fig.1). This indicates its ferromagnetic properties.

Thus, the light-emitting diode structures with quantum well GaAsSb/GaAs as an active region and ferromagnetic injector GaMnAs were fabricated and investigated. The observation of electroluminescence emission of similar structures was no reported earlier.

This work was supported by the Russian Foundation for Basic Research (project nos. 13-07-00982 and 13-02-97140).

[1] M.M. Prokof'eva *et al.* // *Semiconductors*, **44**, (2010) 1398-1401.

[2] B.N. Zvonkov *et al.* // *J. Opt. Technol*, **75** (2008) 389-393.

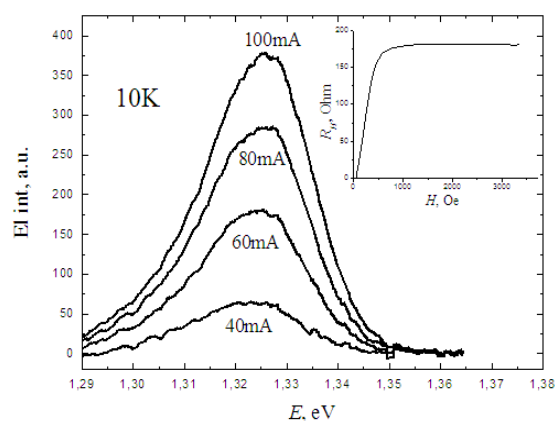


Fig. 1. Dependences of I_{EL} on pump current for sample with $d_s = 50 \text{ nm}$. The dependence $R_H(H)$ for the control sample is shown on inset.

30PO-K-5

ANOMALOUS GALVANOMAGNETIC EFFECTS DUE TO SPONTANEOUS SPIN POLARIZATION OF ELECTRONS IN CRYSTAL WITH LOW CONCENTRATION OF 3d-TRANSITION ELEMENT IMPURITIES

*Lonchakov A.T.¹, Okulov V.I.¹, Pamyatnykh E.A.², Govorkova T.E.¹, Andriichuk M.A.³,
Paranchich L.D.³, Bobin S.B.², Deryushkin V.V.²*

¹ Institute of Metal Physics Urals Branch of RAS, 620990, Ekaterinburg, Russia

² Ural Federal University, Ekaterinburg, Russia

³ Chernovtscy national university, 58012, Chernovtscy, Ukraine

okulov@imp.uran.ru

In physics of semiconductors with magnetic impurities there may become perspective the investigations of low-gap semiconductor crystals doped by 3d-impurities of low concentration. Donor 3d-states of impurity electrons in such systems prove to be hybridized in conduction band of a crystal, what results in spontaneous spin polarization of current carriers [1]. Anomalous Hall effect, connected with this phenomenon, in the systems with low ($10^{-1} - 10^{-2}$ at. %) concentration of magnetic impurity was first observed by us at room temperature in mercury selenide crystals doped by iron [2]. One revealed non-linear dependence of Hall resistivity on the magnetic field with the features characteristic of anomalous Hall effect. The same effect was observed at $T=300$ K in the HgSe crystals with impurities of cobalt and nickel [3]. In the report advanced we present the data about observing at room temperature anomalous Hall effect and, consequently, about existing spontaneous spin polarization of conduction electrons in the HgSe crystals doped by chromium and vanadium in concentration interval from $1 \cdot 10^{18}$ to $1 \cdot 10^{19}$ cm⁻³. Comparison of the data obtained shows that relative contribution to the Hall effect is maximal for the vanadium impurity (≈ 13 %) and minimal for the iron impurity (≈ 5 %). In our experiments at room temperature we have brought out transverse magnetoresistance with specific dependence on the magnetic field, what gives evidence also of manifesting spontaneous magnetization in conductivity of the crystals studied. It is specially important to note that unusual hysteresis in field dependence of magnetoresistance was therewith observed. It has been established that at switching off magnetic field at magnetic field strength values below saturation magnetization, determined in [2] by the Hall resistivity, the magnetoresistance value exceeds its values measured at switching on the magnetic field and, as a consequence, takes place residual resistance in zero magnetic field strength limit. Long-time relaxation processes (decay up to zero) are characteristic of hysteresis contribution to magnetoresistance. This indicates of the relation to relaxation of non-equilibrium magnetization in spontaneously polarized system.

Theoretical interpretation of specific behaviors observed in experiments is developed on the base of the approach expounded in [2]. This approach is based on known fact of exciting magnetization current in electron system in passing the conduction current in magnetic field.. Subtraction of magnetization current, giving no contribution to the Hall conductivity, from total current found in theory leads to explanation of anomalous Hall resistance. Anomalous contribution to magnetoresistance arises because of the appearance of energy contribution of magnetization current to the energy of locally equilibrium electron system.

Work supported by RFBR (Grant No 12-02-00530) and Progr. of RAS (Grant №12-02-T-1016).

[1] V.I.Okulov, Pamyatnykh E.A., V.P. Silin, *Low Temp. Phys.* **37** (2011) 798.

[2] A.T. Lonchakov, V.I.Okulov, et al., *JETP Letters*, **96** (2012) 405.

[3] A.T. Lonchakov, V.I.Okulov, et al., *Proc. of Int. Conf. "Actual Problems of Solid State Physics"*, Minsk, Belarus, **2** (15-18 oct 2013) 220.

30PO-K-6

IMPEDANCE OF AMORPHOUS SOFT MAGNETIC WIRE UNDER BIASING OF DIRECT ELECTRICAL CURRENT

*Semirov A.V. *, Moiseev A.A., Derevyanko M.S., Bukreev D.A., Vasuhno N.V.*

East-Siberian State Academy of Education, Irkutsk, Russia,

* semirov@igpu.ru

An influence of bias current on an impedance of the amorphous soft magnetic $\text{Co}_{66}\text{Fe}_4\text{Nb}_{2,5}\text{Si}_{12,5}\text{B}_{15}$ wire was investigated. Wire's diameter and length were 170 μm and 30 mm respectively. The wire was prepared by rapid quenching from the melt technique and wasn't subjected any treatment. The method of X-ray diffraction showed that state of tested wires is amorphous. The impedance measurements were carried out on the automated measuring complex of magnetoimpedance spectroscopy in the alternating current (ac) frequency range $f = (0.1 - 100)$ MHz for effective current of 1 mA. The used in the complex precision impedance analyzer Agilent 4294A allowed creating the direct electrical current I_{DC} in the sample with intensity till ± 100 mA.

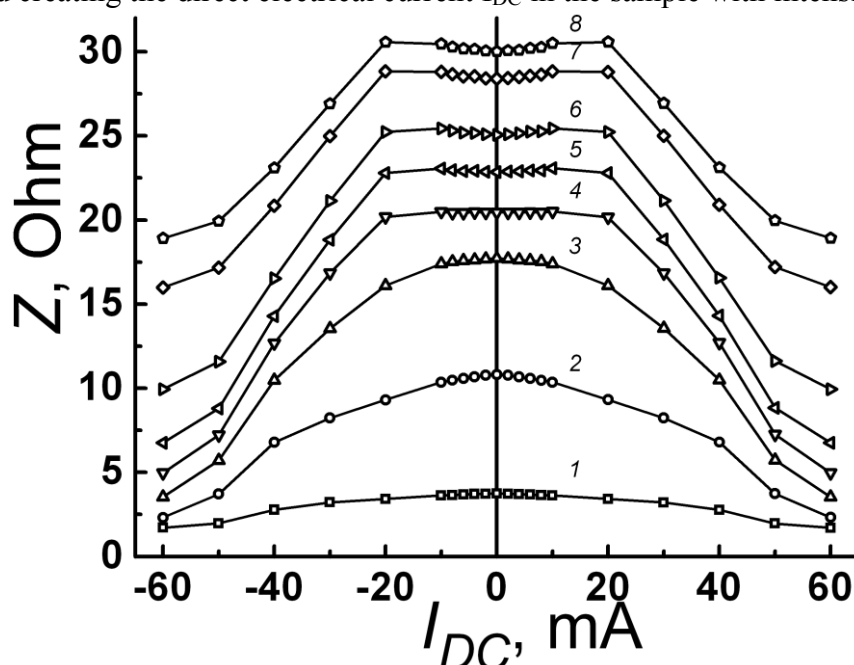


Fig.1. The impedance dependences of amorphous $\text{Co}_{66}\text{Fe}_4\text{Nb}_{2,5}\text{Si}_{12,5}\text{B}_{15}$ wire on bias current intensity at ac frequencies: 1 – 0,1 MHz, 2 – 1 MHz, 3 – 4 MHz, 4 – 10 MHz, 5 – 20 MHz, 6 – 40 MHz, 7 – 80 MHz, 8 – 100 MHz.

Frequency changes of the dependencies $Z(I_{DC})$ are explained by a presence of a combined type of the magnetic anisotropy in the amorphous soft magnetic wire and by multidomain structure of its outer shell. An influence of a circumferential permeability of the wire volume with axial magnetic anisotropy on the impedance Z is significant and Z monotonously decreases with I_{DC} increase (fig. 1). At the frequencies above the 8 MHz the wire's outer shell with helicoidal anisotropy type influences on the Z due to decrease of a skin depth. A region with small changing of the impedance under impact of the bias current points out multidomain structure of the outer shell. A probable reason of the change in $Z(I_{DC})$ dependence character at the frequencies above 8 MHz at $I_{DC} \sim 20$ mA is I_{DC} magnetic field achievement of a value of starting field of domain boundary and transition of the wire's outer shell to a single-domain state.

30PO-K-7

DOMAIN WALL'S STABILITY AND EXCITATION IN NANOWIRE WITH PERPENDICULAR MAGNETIC ANISOTROPY

Tihomirova K.A.^{1,2}, *Skirdkov P.N.*^{1,2}, *Zvezdin K.A.*^{1,2}, *Belanovsky A.D.*^{1,2}, *Grollier J.*³, *Cros V.*³,
*Ross C.A.*⁴, *Zvezdin A.K.*^{1,2}

¹ A.M. Prokhorov General Physics Institute, Russian Academy of Sciences, Moscow, Russia

² Moscow Institute of Physics and Technology, Dolgoprudny, Russia

³ Unite Mixte de Physique CNRS/Thales and Universite Paris-Sud 11, Palaiseau, France

⁴ Massachusetts Institute of Technology, Cambridge, USA

petr.skirdkov@phystech.edu

Recently, studies of the domain wall's dynamics attract great attention. This is substantially caused by the fact that apart from the purely fundamental interests, the controlled dynamic of the DW underlies most promising spintronic devices. It was initially supposed to excite the DW motion by an external magnetic field. Later it was shown theoretically [1] and experimentally [2] that the perpendicular current injection can also initiate the DW dynamics.

Recently, materials with a perpendicular magnetic anisotropy are of considerable interest. Magnetic tunnel junctions (MTJs) with a perpendicular magnetic easy axis have a potential for realizing next-generation high-density non-volatile memory and logic chips with high thermal stability and low critical current for current-induced magnetization switching [3,4].

In this work the stability of different magnetic domain wall's types in dependence on its parameters was studied in a magnetic nanowire. The possibility of excitation of each DW's type by the action of an external magnetic field as well as spin-transfer effect was studied. Dynamic properties of the DW (critical current, etc.) under the action of external influences are analyzed in detail.

Financial support by the RFBR Grants No. 12-02-01187 and No. 14-02-31781 and Skolkovo Inst. of Technology.

[1] A.V. Khvalkovskiy et al, *Phys. Rev. Lett.*, **102** (2009) 067206.

[2] A. Chanthbouala et al, *Nature Physics*, **7** (2011) 626–630.

[3] S. Ikeda et al, *Nature Materials*, **9** (2010) 721–724.

[4] H. Meng and J.-P. Wang, *Appl. Phys. Lett.*, **88** (2006) 172506.

30PO-K-8

SPIN POLARONS AND MAGNETIC GROUND STATE IN PrB₆

*Anisimov M.A.¹, Glushkov V.V.^{1,2}, Bogach A.V.¹, Demishev S.V.^{1,2}, Hairullin E.²,
Shitsevalova N.Yu.³, Filipov V.B.³, Kuznetsov A.V.⁴, Gabani S.⁵, Flachbart K.⁵, Sluchanko N.E.¹*

¹ A.M. Prokhorov General Physics Institute of RAS, Moscow, Russia

² Moscow Institute of Physics and Technology, Dolgoprudnyi, Russia

³ Frantsevich Institute for Problems of Materials Science, NASU, Kiev, Ukraine

⁴ National Research Nuclear University "MEPhI", Moscow, Russia

⁵ Institute of Experimental Physics of SAS, Košice, Slovakia

anisimov.m.a@gmail.com

Praseodymium hexaboride (PrB₆) exhibits a rather complex magnetic H-T phase diagram and considerable anisotropy of its transport and magnetic properties. In zero magnetic field this system is characterized by two successive antiferromagnetic (AFM) transitions into incommensurate (IC1) and commensurate (C) phases at $T_{N1} \approx 6.7\text{K}$ and $T_{N2} \approx 4.6\text{K}$, respectively. The strong anisotropy in PrB₆ is traditionally explained by the competition between O_{xy}-type antiferroquadrupolar and indirect exchange interactions. However, the nature of the ground state of PrB₆ is still under discussion.

In current work we present a complex investigation of magnetic (magnetization, susceptibility), transport (magnetoresistance, Hall effect) and thermal (specific heat, Seebeck coefficient) properties of PrB₆. The measurements have been performed on high quality single crystals of Pr^NB₆ with various isotope content (N=11, nat.) of boron, and before and after high temperature annealing. In order to investigate the magnetic anisotropy of PrB₆, specific heat, magnetoresistance (MR) and magnetization have been measured in external magnetic field oriented along main axis $\mathbf{B} \parallel \langle 100 \rangle$, $\langle 110 \rangle$, $\langle 111 \rangle$.

Based on our measurements, several fundamental results have been obtained for the first time. (i) - above Neel temperature in the range $T_{N1} - 21\text{K}$ an unusual low temperature maximum of resistivity ($\Delta\rho_{\text{max}} \approx 0.03\mu\Omega\cdot\text{cm}$) was observed in combination with spontaneous magnetization $M_{sp} \sim 1.6\text{emu/mol}$ on the initial state (before annealing) of PrB₆ samples. The anomalies detected may be explained in terms of ferromagnetic (FM) fluctuations and itinerant ferromagnetism developed in the presence of $n_{\text{vac}} \approx 1-2\%$ boron vacancies in the PrB₆ matrix. Moreover, it was found that this FM state is totally destroyed by annealing at $T_{\text{an}} \approx 1700^\circ\text{C}$ ($t \approx 10\text{hours}$). (ii) - below T_{N1} , in the IC1 phase, a second harmonic contribution ρ_{H2} to Hall resistivity $\rho_H(\varphi)$ was observed in magnetic fields $B \leq 2.5\text{T}$. It was also found that the increase of external magnetic field in the range 2.5-8T leads to a depression of the ρ_{H2} amplitude which results into a drastic switch-on of angular dependences of both Hall resistivity $\rho_H(\varphi)$ and magnetoresistance $\rho(\varphi)/\rho(0)$. (iii) - the vicinity of temperature T_{N2} is characterized by considerable hysteresis of $\Delta\rho/\rho(H)$ curves. The performed study of $\Delta\rho/\rho(H)$ allowed us to estimate the magnetic parameters including the local susceptibility $\chi_{\text{loc}}(T)$ and the effective magnetic moment μ_{eff} . The calculated effective magnetic moment depends on the orientation of magnetic field and reaches the maximal values $\mu_{\text{eff}} = 2.5\mu_B$ for $\mathbf{B} \parallel \langle 110 \rangle$, $\langle 111 \rangle$ and $\mu_{\text{eff}} = 4\mu_B$ for $\mathbf{B} \parallel \langle 100 \rangle$, whereas the value of inherent moment of Pr³⁺ ions is expected to be $\mu(\Gamma_5) = 2\mu_B$. The results obtained may be attributed to the formation of magnetic clusters which are constructed from magnetic moments of Pr³⁺ ions and spin polarized domains in the conduction band of PrB₆ (5d-component of magnetism). These spin polarons of small radius $a_{sp} \sim 5\text{\AA}$ appear below 21K and are responsible for the itinerant ferromagnetism in PrB₆. Moreover, the anisotropy of PrB₆ may be explained in terms of coexistence of 4f- (local) and 5d- (itinerant) components of the magnetic structure of this unusual antiferromagnet.

30PO-K-9

ANOMALOUS HALL EFFECT AND MAGNETIC ANISOTROPY IN GdB₆

*Anisimov M.A.¹, Glushkov V.V.^{1,2}, Bogach A.V.¹, Demishev S.V.^{1,2}, Samarin N.A.¹,
Shitsevalova N.Yu.³, Levchenko A.V.³, Filipov V.B.³, Kuznetsov A.V.⁴, Sluchanko N.E.¹*

¹ A.M. Prokhorov General Physics Institute of RAS, Moscow, Russia

² Moscow Institute of Physics and Technology, Dolgoprudnyi, Russia

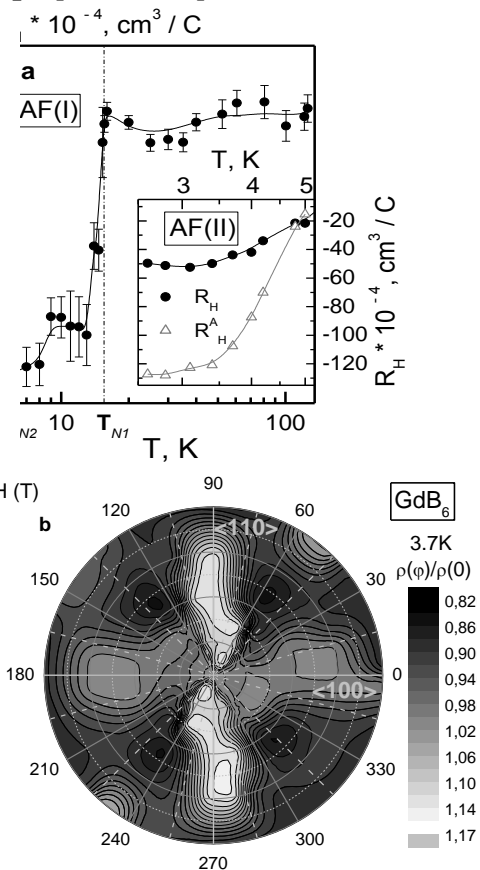
³ Frantsevich Institute for Problems of Materials Science, NAS of Ukraine, Kiev, Ukraine

⁴ National Research Nuclear University "MEPhI", Moscow, Russia

anisimov.m.a@gmail.com

Gadolinium hexaboride (GdB₆) fills the important place among the all magnetic hexaborides (RB₆) since it is considered as the system without orbital degrees of freedom ($L=0$, $S=7/2$). However at low temperatures this compound undergoes two successive phase transitions with simultaneous structural distortion and antiferromagnetic (AF) ordering. Below Neel temperature $T_{N1} \approx 15.5$ K (AF I phase) a magnetic structure is characterized by the wave vector $\mathbf{k}_m = [1/4, 1/4, 1/2]$ and a structural modulation by $\mathbf{q}_I = [0, 0, 1/2]$. The modulation is slightly suppressed at $T_{N2} \approx 4.7$ -9 K (AF II phase), involving another modulated structures with $\mathbf{q}_2 = [0, 1/2, 1/2]$. Nevertheless the nature of magnetic ground state in GdB₆ is still under discussion [1].

In current work we present the angular dependences of Hall resistivity $\rho_H(\varphi)$ and magnetoresistance $\rho(\varphi)/\rho(0)$ measured in the temperature range 2-120 K and magnetic fields up to 4 T. The data obtained allow to detect the several fundamental results. (i) In paramagnetic (P) state R_H takes the constant value $-4 \cdot 10^{-4}$ cm³/C ($n/n_{4f} \sim 1$). (ii) On the contrary it changes drastically ($\Delta R_H/R_H \sim 68\%$) in AF I phase below T_{N1} (Fig.a). The subsequent transition at T_{N2} to AF II state is accompanied by (iii) the emergence of the anomalous component of Hall effect R_H^a which drops with temperature and reaches a huge value $R_H^a(1T) \approx -120 \cdot 10^{-4}$ cm³/C at 2 K (see the symbols Δ on the inset of Fig.a). The rise of external magnetic field at $B > 1.5$ T is followed by both (iv) the depression of R_H^a 's amplitude and (v) by the anisotropic behaviour of the magnetoresistance (MR). The angular distribution of the scattering reconstructed from MR data takes the form of cross with maximal scattering along $\mathbf{B} \parallel \langle 110 \rangle$ and four satellites along $\mathbf{B} \parallel \langle 111 \rangle$. In our opinion above-mentioned anomalies may indicate on the several subsequent metamagnetic transitions in magnetic fields 0.7-1.7 T ($\mathbf{B} \parallel \langle 111 \rangle$) and 1.7-4 T ($\mathbf{B} \parallel \langle 111 \rangle$, $\langle 100 \rangle$). The data obtained in combination with the results of previous MR study allow to propose the complex scenario including the spin polarons formation in P and AF phases. The spin polarons along with additional coherent displacement of Gd³⁺ ions from their centrosymmetric positions inside the boron cages are responsible for the anisotropy in both AF I and II states of GdB₆.



[1] M. Amara, S.E. Luca et al., *Phys. Rev. B*, **72** (2005) 064447.

30PO-K-10

THE MAGNETIC-RESONANCE PROPERTIES TEMPERATURE STUDY OF Fe/Ni MULTILAYER THIN FILMS BY FMR

Zubin A.Y., Kupriyanova G.S.

Immanuel Kant Baltic Federal University, Kaliningrad, Russia
azubin@mail.ru

One of the important tasks today is to create new materials for the applications of spintronics. The magnetic tunnel junctions (MTJ) are of a very special interest. The perspective class of materials for the application is Fe/NM/Ni structures at different substrates [1].

The temperature study of Fe/NM/Ni thin film systems with MgO, Si/SiO₂ interfaces was done by ferromagnetic resonance (FMR). Thin film systems realized in the polycrystalline multilayer structures, synthesized on amorphous Si/SiO₂ substrate by pulsed laser deposition technique are presented in this work [2]. The temperature dependence of Gilbert damping constant, linewidth, interlayer exchange coupling and other FMR parameters on Fe/MgO/Ni, Fe/Si/SiO₂/Ni systems were investigated both X-band and Q-band FMR frequencies. These systems are investigated to estimate their applicability in model creation experiments for spintronics devices research [3].

Ferromagnetic resonance spectra of the films were taken using Bruker electron spin resonance spectrometer operating at the X-band and Q-band frequencies and the modulation frequency 100 kHz. The first field derivative of the microwave power absorption was registered as a function of applied steady magnetic field at the different temperature.

The in-plane and out-of-plane temperature dependences of FMR signal position have been measured for Fe/NM/Ni samples with MgO and Si/SiO₂ interfaces in position of 0 and 90 degrees rotation angle to the external static magnetic field. The extracted magnetic parameters such as linewidths, Gilbert damping constant, parameters of interlayer exchange coupling and anisotropy constants were calculated.

The present work was supported by Russian Ministry of Education and Science within the frames of the Federal Special-Purpose program of Education at the Contract No.02.740.11.0550.

[1] G. Kupriyanova, A. Zyubin, A. Astashonok, A Orlova and E. Prokhorenko, *Journal of Physics: Conference Series* **324** (2011) 012012.

[2] A. Zenkevich, Y. Y. Lebedinskii, A. Goikhman, V. Nevolin, P. Chernykh, V. Kulikauskas, R. Mantovan, and M. Fanciulli, *Journal of surface investigation-x-ray synchrotron and neutron techniques*, **3**, 173–178 (2009).

[3] A.Goikhman, G. Kupriyanova, E. Prokhorenko, A, Chernenkov, *Vestnik I. Kant SU*, **4** (2010), 81-88.

30PO-K-11

MAGNETORESISTIVITY OF $\text{Bi}_{93.99}\text{Mn}_6\text{Fe}_{0.01}$ SINGLE CRYSTAL

Ivasishin O.M.¹, Shevchenko A.D.¹, Kovalyuk Z.D.², Terekhov A.V.^{3,4,5}, Zaleski A.J.⁴, Los A.S.⁵, Cwik J.⁵

¹ G.V. Kurdyumov Institute of Metal Physics National Academy of Sciences of Ukraine, 36 Vernadsky blvd., Kyiv 03142, Ukraine

² Frantsevich Institute for Problems of Materials Science NAS of Ukraine, Chernivtsi Branch, 5 I. Vil'dy str., Chernovtsy 58001, Ukraine

³ B. Verkin Institute for Low Temperature Physics and Engineering of the National Academy of Sciences of Ukraine, 47 Lenin Ave., Kharkov 61103, Ukraine

⁴ W. Trzebiatowski Institute of Low Temperature and Structure Research, Polish Academy of Sciences, P.O. Box 1410, Wroclaw 50-950, Poland

⁵ International Laboratory for High Magnetic Fields and Low Temperatures, Gajowicka 95, Wroclaw 53-421, Poland
admit@imp.kiev.ua

Researches of magnetic properties of materials based on bismuth and manganese show that these compounds at room temperatures possess high values of coercivity, thus making them perspective for production of high-temperature permanent magnets. However, the study of the magnetoresistant properties of these materials is not paid sufficient attention, and such researches are actual.

In this paper temperature dependences of the single crystals resistivity ρ of $\text{Bi}_{93.99}\text{Mn}_6\text{Fe}_{0.01}$ are researched within the temperature range 5-300K and magnetic fields up to 9T with the magnetic field parallel and perpendicular to the crystallographic c axis.

It is found that with the temperature decrease ρ decreases linearly throughout the interval. In the magnetic field of 9T ohmic losses increase with the decrease of temperature, reaching a maximum at $T \approx 150\text{K}$ for $I \perp H \parallel c$ and at $T \approx 200\text{K}$ for $I \parallel H \perp c$, and then ρ decreases. Figure 1 shows the dependence of the relative magnetoresistance ($\Delta\rho/\rho_0 = [(\rho(9\text{T}) - \rho(H=0))/\rho(H=0)] \times 100\%$) of the value of the magnetic field at fixed temperatures for $I \perp H \parallel c$ (Fig. 1a) and $I \parallel H \perp c$ (Fig. 1b). It is set that at two orientations of magnetic field the magnetic-field dependences are qualitatively similar, and magnetoresistance is positive on a sign. Thus, there is an anisotropy of magnetoresistance: at 300 K the maximum value of $\Delta\rho_{\parallel}/\rho_{0\parallel}(H=0)$ is 2365 % for $I \perp H \parallel c$ and $\Delta\rho_{\perp}/\rho_{0\perp}(H=0)$ is 417 % for $I \parallel H \perp c$, that is the magnetoresistance for the case $I \perp H \parallel c$ is higher in about 6 times.

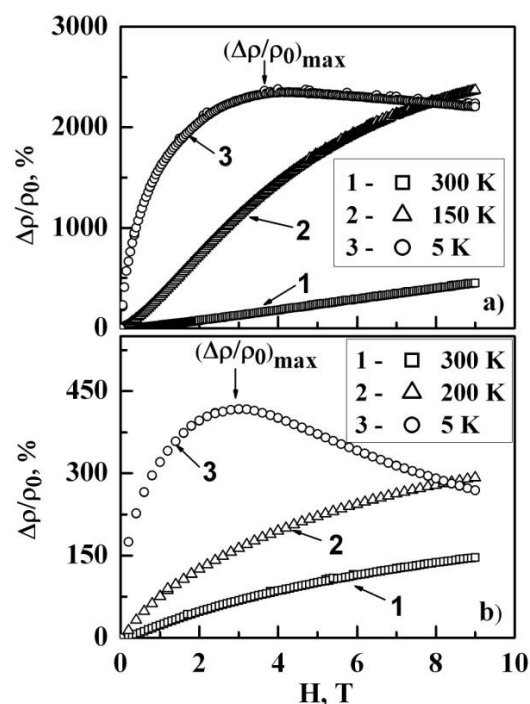


Fig. 1. Magnetoresistance of single crystals $\text{Bi}_{93.99}\text{Mn}_6\text{Fe}_{0.01}$ for different orientations $I \perp H \parallel c$ (a) and $I \parallel H \perp c$ (b).

30PO-K-12

DYNAMICS OF DOMAIN WALLS IN RARE-EARTH ORTHOFERRITES UNDER THE ACTION OF PULSE AND GRADIENT MAGNETIC FIELDS

Ekomasov E.G.¹, Shapaeva T.B.², Murtazin R.R.¹, Bogomazova O.B.¹

¹Bashkortostan State University, Ufa, Russia

²Moscow State University, Moscow, Russia

boksanab@rambler.ru

As is known, the dynamics of domain walls (DWs) in plates of rare-earth orthoferrites (REOs) can be effectively studied using high-speed photography [1, 2]. To processing of experimental data, it is necessary to have a theory that allows us to describe nonlinear DW dynamics at given parameters of a system and an external magnetic field. The equation of Landau-Lifshitz that describes the nonlinear dynamics of REO, in the one-dimensional case can be reduced to the dimensionless nonlinear modified sine-Gordon equation (MSG) [1, 2]:

$$u_{tt} - u_{xx} + \sin u = f + \Phi(x,t) \sin \frac{u}{2} + \alpha u_t \quad (1)$$

where u - is the angle that describes the deviation of an antiferromagnetism vector from axis of easy magnetization, $\Phi(x,t) = h_{pulse}(t) + h_{grad}(x)$ - is an normalized external magnetic field, $f = \dot{h}_t$ - the time derivative component of the external magnetic field, α - is a damping constant normalized. In orthoferrites there are two types of DW ac- and ab - type. In the case of DW ac - type equation (1): $\Phi = h_z$, $f = \dot{h}_y$; in the case of DW ab - type: $\Phi = h_z$, $f = \dot{h}_z$.

In the work analytically and experimentally considered dynamics of a single 180 - degree DW of REO in high-temperature magnetic phase for the following cases: DW ac - type $h_y = 0$, $f = 0$; $\Phi = h_z$, $h_z(x,t) = h_{pulse} + h_{grad}$; DW ac - type $h_y \neq 0$, $f \neq 0$; $\Phi = 0$; DW ac - type $h_y \neq 0$, $f \neq 0$; $\Phi \neq 0$, $\Phi = h_z$; DW ab - type $h_z \neq 0$, $f \neq 0$; $\Phi \neq 0$, $\Phi = h_z$, $f = \dot{h}_z$.

At the initial moment in time, the DW is under the action of a gradient magnetic field, stabilizing its position. The pulse magnetic field is then switched on, and the DW begins to move under the action of the field. After the magnetic field's pulse action is terminated, the DW continues its motion and, reaching the position of maximum deviation, returns to the initial state under the action of the gradient magnetic field. We found a connection between the parameters of the field (pulse amplitude and the length of a pulse and its leading edge) and the characteristics of DW motion (initial acceleration, time required to attain constant motion, constant velocity, and the maximum shift from the equilibrium position). The experimental data agree qualitatively with the results from our numerical simulations. The initial acceleration was shown to be linearly dependent on the pulse field amplitude. The time required to attain constant motion under experimental conditions is comparable to the duration of the leading edge of the magnetic field pulse and its decline with an increase in the pulse amplitude. The velocity of DW constant motion is determined only by the pulse field amplitude and does not depend on the duration. The maximum DW shift from the equilibrium position is determined by the relationship between the gradient and pulse magnetic fields. If the motive pulse is too short, the DW has no time to shift to the maximum possible distance during the length of the pulse's action.

[1] V.G. Bar'jakhtar, M.V. Chetkin, B.A. Ivanov, et al., Dynamics of Topological Magnetic Solitons. Experiment and Theory (Springer tracts in modern physics, Berlin), **129** (1994).

[2] T.B. Shapaeva, R.R.Murtazin, E.G.Ekomasov, *Bull. Russ. Acad. Sci. Phys.*, **78** 2 (2014) 88-91.

30PO-K-13

STUDY OF FACTORS THAT INFLUENCE ON THE WORK OF LIGHT-EMITTING SPINTRONIC DIODES WITH InGaAs/GaAs QUANTUM WELLS

Danilov Yu.A., Dorokhin M.V., Zdoroveishev A.V., Saeid S.

Lobachevsky State University of Nizhni Novgorod, Nizhny Novgorod, Russia
s.saeed34@yahoo.com

Spin injection light-emitting diodes based on InGaAs/GaAs quantum wells (QW) and the ferromagnetic metal layer as Co are considered as the source of circularly polarized light and promising for coding, conservation data and encryption [1]. Metal layer plays the role of the injector for the spin-polarized charge carriers, which recombine with the opposite carriers within the QW and results in circularly polarized electroluminescence. In our study we used structures containing three QWs with different contents of In ($x=0.25, 0.20$ and 0.15) and located at different depths (30, 70, and 110 nm, respectively) from the surface. The QWs emit photo- or electroluminescence with different intensity and then it enables us to measure the penetration of Co atoms into structure. We used substrates of n-GaAs (001), so that the circular polarization is due to spin-polarized holes injection from ferromagnetic contact into a semiconductor. Heterostructure was prepared by metalorganic chemical vapour deposition (MOCVD) method under atmospheric pressure of hydrogen. The ferromagnetic metal layer (Co) was prepared by the electron-beam evaporation method in vacuum. Fig.1, curve 1 shows the spectrum of photoluminescence (PL) of the structure, PL peaks at 1.28, 1.34 and 1.39 eV correspond to the energies of the basic transitions in WQs with $x=0.25, 0.20$ and 0.15 .

The deposition and removal of cobalt layer leads to a change in spectrum, namely, to a reduction by two orders of the PL peak intensity for the QW-1 with $x=0.25$, close to the surface (Fig.1, curve 3). The intensity of the other peaks remained practically without changes. It indicates the diffusion penetration of Co atoms in quantum well structure and formation of nonradiative recombination centers that leads to quenching of photoluminescence. Incorporation of a tunnel-thin (1-1.2 nm thick) diffusion barrier of Al_2O_3 dielectric layer between the ferromagnet and the semiconductor leads to reduce influence Co on the luminescence intensity, which indicates the reduction of penetration and defects in the structure. We also investigated the influence of the cover layer thickness and deposition temperature and found that the thickness of the cover layer (up to 30 nm) and the deposition temperature ($630-650^\circ\text{C}$) are optimal for structure. Also we confirmed the data obtained in the investigation of structure by transmission electron microscopy (JEM-2100F) on cross-sectional samples and measuring the degree of polarization of the circularly polarized electroluminescence.

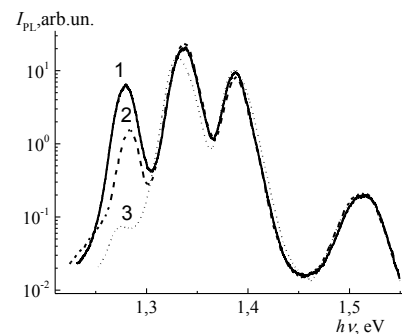


Fig.1. The photoluminescence spectra of the structure with three quantum wells:
1 - the initial sample;
2 - after deposition of $\text{Al}_2\text{O}_3/\text{Co}$;
3 - after Co deposition.

[1] I. Zutic, J. Fabian, S. DasSarma // *Rev. Mod. Phys.* **76** (2004) 323-410.

30PO-K-14

NUMERICAL SIMULATION OF SPIN HALL EFFECT IN CuPt/Fe HETEROSTRUCTURE

Andrianov T.¹, Gritsenko Y.¹, Strelkov N.¹, Ryzhanova N.¹, Vedyayev A.¹

¹ M.V. Lomonosov Moscow State University, Faculty of Physics, Leninskie Gory 1, 119991,
Moscow, Russia
timofey.andrianov@gmail.com

The existence of Spin Hall Effect (SHE) in paramagnetic metal without applying external magnetic field under influence of spin-orbit interaction was predicted by Dyakonov and Perel [1]. It is considered that SHE may be very effective tool for the manipulation with spin current and spin accumulation. For the calculation both spin accumulation and spin polarized current spin diffusion equation used taking into account both SHE for the paramagnetic metals and processes governing spin transport in ferromagnetic metals [2, 3]:

$$\vec{j}_e = -\sigma_0 \vec{\nabla} \varphi - \beta \frac{\sigma_0}{ev} \vec{\nabla} (\vec{U}_M, \vec{m}) + a_0^3 \sigma_{SH} [\vec{m} \times \vec{\nabla} \varphi] \quad (1)$$

$$\vec{j}_m^{(i)} = -\beta \sigma_0 \vec{\nabla} \varphi \vec{U}_M^{(i)} - \frac{\sigma_0}{ev} \vec{\nabla} \vec{m}^{(i)} - \sigma_{SH} \vec{U}_m^{(i)} [\vec{U}_m \times \vec{\nabla} \varphi] \quad (2)$$

$$\begin{cases} \text{div} \vec{j}_e \\ \text{div} \vec{j}_m^{(i)} = -\frac{\sigma_0}{e^2 v l_J^2} [\vec{m} \times \vec{U}_M]^{(i)} - \frac{\sigma_0}{e^2 v l_{sf}^2} \vec{m}^{(i)} \end{cases} \quad (3)$$

Where φ – electric potential, σ_0 is the conductivity, β is the spin-asymmetry parameter of conductivity, σ_{SH} is the Spin Hall conductivity, $\vec{U}_M = \vec{M}/M_s$, where \vec{M} is magnetization vector in FM, $\vec{U}_m = \vec{m}/|\vec{m}|$, where \vec{m} is spin accumulation vector, index i is a component of vectors \vec{m} , \vec{j}_m and \vec{U}_M in spin space, l_{sf} – spin diffusion length, l_J – exchange spin diffusion length and v – density of states. To study the possibility to manipulate with magnetization of small ferromagnetic dots under influence of SHE current we have calculated the field induced by SHE in the small ferromagnetic dot situated on the surface of paramagnetic metallic layer with SHE. The direction of magnetization of the ferromagnetic dot changes from $\vec{M} \parallel z$ to $\vec{M} \parallel y$ (Fig. 2a) or $\vec{M} \parallel x$ (Fig. 2b).

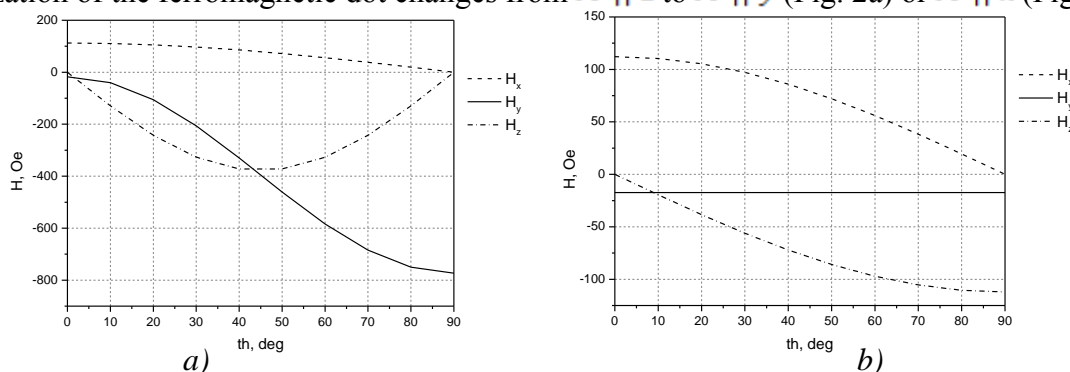


FIG. 2: Dependence of effective fields induced by CuPt SHE in Fe averaged over the volume of Fe from rotation of magnetization: a) from state when $\vec{M} \parallel z$ to $\vec{M} \parallel y$, b) from state when $\vec{M} \parallel z$ to $\vec{M} \parallel x$.

[1]. M. I. Dyakonov and V. I. Perel, *Phys. Lett. A* **35**, 459 (1971).

[2]. R.V. Shchelushkin and A. Braatas, *Phys. Rev. B* **72**, 073110 (2005).

[3]. S. Zhang, P. M. Levy and A. Fert, *Phys. Rev. Lett.* **88**, 236601 (2002).

30PO-K-15

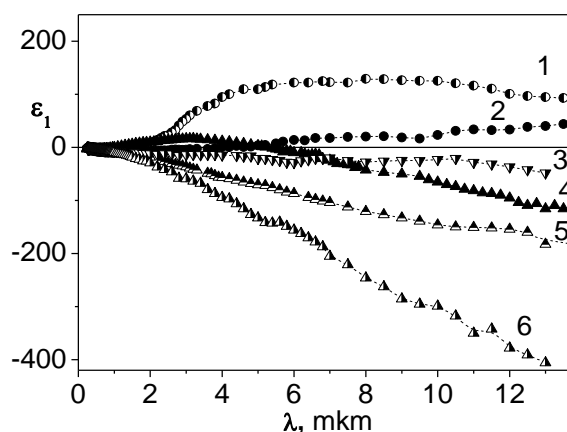
EVOLUTION OF THE ELECTRONIC STRUCTURE AND OPTICAL PROPERTIES OF FERROMAGNETIC Fe-BASED HEUSLER ALLOYS

Svyazhin A.D., Shreder E.I.

Institute of Metal Physics, Kovalevskaya Str. 18, Ekaterinburg 620990, Russia
shreder@imp.uran.ru

During last years, a lot of attention has been paid to the Fe_2MeAl Heusler alloys, where Me is a 3d transition metal, due to anomalous behavior of magnetic, optical and transport properties [1,2]. According to the band structure calculations, substitution of one transition metal with another is accompanied by electronic structure transformations. The spin-up and spin-down DOS's possess very different shapes, this case is of interest for the general theory of the magnetism of itinerant electrons. Here, we present the results of investigation of influence of the Me constituent (Me =Ti, V, Cr, Mn, Fe, Ni) on optical properties of the alloys in the spectrum range $\lambda = (0.3 - 13) \mu\text{m}$ at room temperature. Effective concentration of free carries N_{eff} was estimated using $1/(1-\varepsilon_1) = f(\omega^2)$ relation.

In the fig.1, the real part of a complex dielectric function for the investigated alloys is shown. The negative values of the real part of the dielectric constant ε_1 characterizes the metallic type of the substance. The alloys containing V and Cr demonstrate positive values of ε_1 . According to the ab-initio band structure calculations, Fe_2CrAl is a half-metallic ferromagnet (HMF). In the case of Fe_2VAl the Fermi level is inside a deep pseudogap in both spin subbands, we estimated the effective concentrations of charge carriers $N_{\text{eff}} \sim 10^{19} \text{ cm}^{-3}$. Fe_2TiAl and Fe_2MnAl , predicted to be HMF as well, reveal negative but small for metals absolute values of ε_1 . In contrast, in Fe_3Al and Fe_2NiAl the Fermi level lies in the region of a high density of d-states in spin-down subbands and in the region of a low density of p-states in spin-up subbands, resulting in the $N_{\text{eff}} \sim 10^{22} \text{ cm}^{-3}$. As compared to normal metals, these values are lower by one–two orders of magnitude.



Fe_2VAl (1), Fe_2CrAl (2), Fe_2MnAl (3),
 Fe_2TiAl (4), Fe_3Al (5), Fe_2NiAl (6)

This work was partly supported by the UB RAS Program (project Nos 12-T-2-1011 and 12-Y-2-1036) and RFBR (project No 12-02-00271).

[1] V. Yu. Irkhin and M. I. Katsnelson. *Phys._Usp.* **37** (1994) 659–676.

30PO-K-16

INFLUENCE OF SPIN-ORBIT INTERACTION ON SPIN-TRANSPORT

Titova M.S.¹, Vedyayev A.V.¹, Ryzhanova N.V.¹, Zhuravlev M.Ye.², Strelkov N.V.¹

¹ Moscow State University, Physics Department, Moscow, Russia

² Kurnakov Institute for General and Inorganic Chemistry, RAS, Moscow, Russia
maryartster@gmail.com

In our paper the theory of tunneling anisotropic magnetoresistance (TAMR) in magnetic tunnel junction due to spin-orbit interaction of Rashba type was developed. This type of spin-orbit is proportional to the gradient of voltage drop across the barrier. It was demonstrated that in adopted spin-polarized free electron model TAMR is closely related to the usual tunnel magnetoresistance, and in case of half-metallic ferromagnetic electrodes having antiparallel orientation of magnetizations the value of TAMR reaches 100%. Moreover, it was shown that due to SO interaction the relative TMR value is finite even for half-metallic FM electrodes and reaches $10^3 - 10^5$ (in experiment 10^3 was observed [1]).

Also anomalous and spin Hall effects for a magnetic tunnel junction (MTJ) where Rashba spin-orbit coupling within the tunneling barrier layer was produced by applied voltage were theoretically investigated. The ferromagnetic electrodes are the source of the spin-polarized current.

Tunneling electrons experience a spin-orbit coupling inside the barrier due to the applied electrical field. Charge and spin Hall currents as functions of the position inside the barrier and the angle between the magnetizations of the electrodes were calculated. It was found out that both charge and spin Hall currents were located inside the barrier near the interfaces. The currents' dependence on magnetic configuration of the MTJ makes it possible to manipulate the Hall currents via rotation of the electrodes' magnetizations.

[1] Tanja Graf, Stuart S. P. Parkin, and Claudia Felser, Heusler Compounds — A Material Class With Exceptional Properties // *IEEE Transactions on Magnetics* **47** (2011) 367

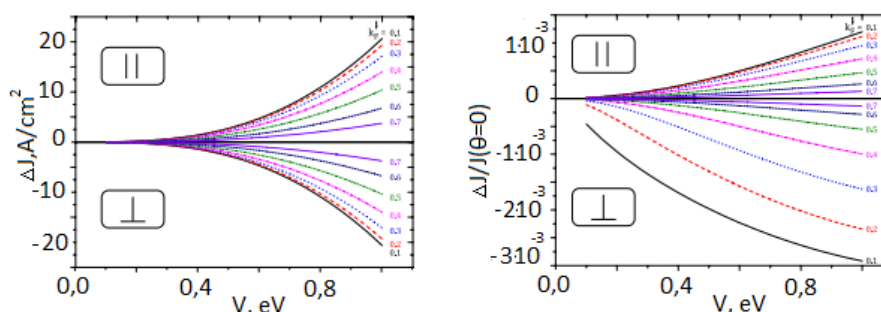


Fig.1 Absolute (a) and relative (b) TAMR values for P and AP configurations

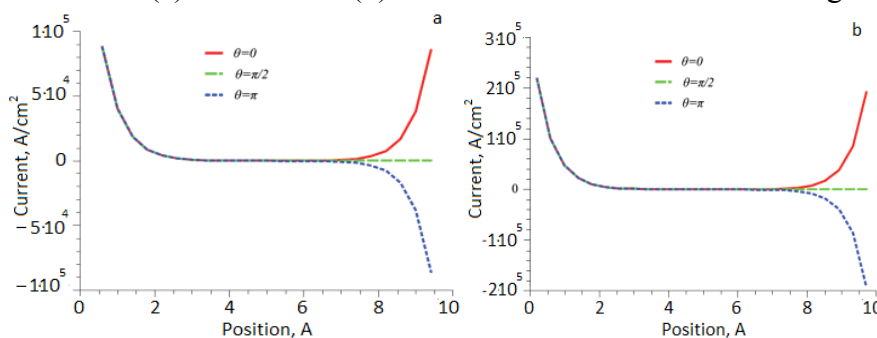


Fig.2 Charge (a) and spin (b) Hall currents dependence on position inside the insulating layer.

30PO-K-17

SPIN STRUCTURE OF GRAPHENE/PT INTERFACE FOR SPIN CURRENT FORMATION AND INDUCED REMAGNETIZATION IN DEPOSITED (Ni-Fe)-NANODOTS

Klimovskikh I.I.¹, Shikin A.M.^{1}, Rybkina A.A.¹, Rybkin A.G.¹, Skirdkov P.N.^{2,3}, Zvezdin K.A.^{2,3}, Zvezdin A.K.^{2,3}*

¹ Saint Petersburg State University, Saint Petersburg, Peterhof, Ulyanovskaya str. 1, 198504 Russia

² A.M. Prokhorov General Physics Institute, Russian Academy of Sciences, Moscow, Vavilova str. 38, 119991 Russia

³ Moscow Institute of Physics and Technology, Dolgoprudny, Institutskiy per. 9, 141700 Russia
klimovskih_ilya@mail.ru

Investigations of spintronics, have become last time a considerable interest motivated by new physical effects (spin Hall effect, spin-orbit torque) concerning coupling of spin and charge currents in magnetic films and nanostructures with the aim to improve existing and create new spin devices. Up to now the investigations in the field of spintronics were restricted mainly by magnetic systems with exchange coupling. Here, we present the results of experimental study of features of spin structure caused by spin-orbit coupling in two-dimensional layered graphene-derived Rashba systems in contact with Pt and the idea, how to use the forming spin structure for creation of spin current developed in such systems based on spin-orbit interaction with their following application for reverse magnetization of ferromagnet (FM) nanostripes contacting with them. For excitation of the magnetization dynamics of FMs we propose to use the spin-orbit torque effect induced by spin current developed in these graphene-derived two-dimensional systems due to applied potential gradient.

Generally speaking, Pt is one of the mostly spreading metals in spintronics which effectively used both as a spin current adsorber, so as a spin current source. The spin-Hall conductivity in Pt is significantly larger than that in semiconductor systems. Moreover, Pt is often and successfully used in the experiments related to the spin-orbit induced magnetization manipulation in FMs contacting with Pt layers [1], because it demonstrates strong spin-orbit interaction on the interface.

In the current work we demonstrate the features of the spin electronic structure of graphene synthesized on Pt(111) surface and analyze their formation in the framework of spin-dependent avoided-crossing effects. We show that the spin structure of the graphene - states is characterized by the Dirac-cone like states with localization of the Dirac-point in the region of the Fermi level with the value of the induced spin-orbit splitting of the -states near the Fermi level of about 60 meV. Similar effect was also demonstrated last time for graphene in contact with Au [2], but Au d-states are localized below Fermi level, so Pt is more appropriate for using in spintronics. We propose the idea, how such spin structure can be used for application in caloritronics for creation of spin current followed by the induced remagnetization of array of FM-nanostripes contacting with the Graphene/Pt interfaces. For estimation of spin current and of efficiency of remagnetization of FM-nanostripes the corresponding theoretical analysis and estimations are presented.

[1] Miron, I.M. et al. Current-driven spin torque induced by the Rashba effect in a ferromagnetic layer. *Nature Materials* **9**, 230-234 (2010).

[2] Marchenko, D. et al. Giant Rashba splitting in graphene due to hybridization with gold. *Nature Commun.* **3**, 1232 (2012).

30PO-K-18

MAGNETIC INFORMATION STORAGE IN ANTIFERROMAGNETIC-ONLY-BASED SPINTRONIC DEVICES

Cantoni M.¹, Petti D.¹, Albisetti E.¹, Bertacco R.¹, Stroppa A.², Picozzi S.²

¹ LNESS center, Physics Department, Politecnico di Milano, Como, Italy

² CNR-SPIN-L'Aquila-Italy

alessandro.stroppa@spin.cnr.it

Spintronics explores phenomena that interlink the charge and spin degrees of freedom, aiming to develop novel devices where the spin, in addition or in substitution of the charge, is employed in order to store and manipulate information. For a long time spintronics was essentially focused on “Mott” devices, made by two ferromagnetic (FM) layers whose relative magnetization directions (parallel/antiparallel) lead to different resistance states (low/high). However, very recently, “Dirac” devices came to the attention of the scientific community: in these devices, the key role is played by the spin-orbit coupling that makes the device conductivity depending on the orientation of the spin direction, with respect to crystal structure or current direction, in a single ferromagnetic or antiferromagnetic layer [1].

The latter opportunity is strongly preferable, because the absence of a ferromagnetic layer leads to two main advantages: i) due to the absence of magnetic stray fields, the device packaging density can be strongly increased with respect to FM-based cells; ii) antiferromagnets (AFMs) are more stable versus external perturbations (such as magnetic fields) with respect to FMs.

A paradigmatic work [2] demonstrating the opportunity of magnetic information storage in antiferromagnetic-only-based spintronic devices is described in this contribution. An innovative memory cell based on a IrMn/MgO/Ta Antiferromagnetic Tunneling Junction (ATJ), *without any ferromagnetic element*, will be described; the information is written in the cell by field cooling under an external applied field and read by the Tunneling Anisotropic Magneto Resistance (TAMR) effect.

Transport experiments revealed that the set-in of antiferromagnetic ordering plays a role in electron tunneling, also coexisting with the strain effects induced by the structural transitions of the SrTiO₃ substrate below 100 K. We show that the magnetic field-cooling procedure and the strain induced by the phase transitions are suitable tools to manipulate the otherwise elusive antiferromagnetic moments in spintronic devices without net magnetic moment.

Experimental work is in progress in order to integrate the device on a Silicon platform and extending the working regime up to room temperature, paving the way towards to the realization of tunable spintronic devices only comprising antiferromagnetic layers.

Density functional theory calculations have been performed to interpret the experimental data.

[1] J. Sinova and I. Zutic, *Nat. Mat.* **11**, **368** (2012).

[2] D. Petti, E. Albisetti, H. Reichlová, J. Gazquez, M. Varela, M. Molina-Ruiz, A. F. Lopeandía, K. Olejník, V. Novák, I. Fina, B. Dkhil, J. Hayakawa, X. Mart, J. Wunderlich, T. Jungwirth and R. Bertacco, *Appl. Phys. Lett.*, **102** (2013) 192404.

30PO-K-19

THE INFLUENCE OF THE MAGNETIC FIELD ON ELECTRICALLY INDUCED DOMAIN WALL MOTION

Sechin D.A., Nikolaeva E.P., Pyatakov A.P., Nikolaev A.B., Kosykh T.B.

M.V. Lomonosov Moscow State University, Physics Department, Moscow, Russia
nikolaevaep@phys.msu.ru

The inhomogeneous distribution of the magnetization may lead to the appearance of the electric polarization. An example of such sort of magnetic inhomogeneity possessing electric polarization is Neel domain wall [1]. It was experimentally demonstrated that these walls react on electric field applied [2]. With the application of a permanent magnetic field it is possible to modify the domain wall internal structure and, in turn, its polarization. As it was revealed previously, domain wall displacement caused by electric field depends on the strength and the direction of the magnetic field [3].

In this work we continue investigations started in [3] with studying the dynamics of the electrically induced domain wall motion. Experiments were carried out with external magnetic field applied in the direction parallel to the magnetic film plane and perpendicular to the domain walls.

Samples used are $(\text{BiLu})_3(\text{FeGa})_5\text{O}_{12}$ garnet films liquid-phase epitaxially grown on GGG substrates. The films crystallography orientations are (210) and (110). Non-uniform high strength electric field an order of 1 MV/cm is induced by the voltage applied to the sharpened copper tip touching the sample. The electric signal is 1 microsecond rectangular pulse with 1.6 kV amplitude. Domain walls displacement is observed in transmission mode Faraday microscopy. With the use of the illuminating laser pulses we are able to observe instant positions of the domain wall before the application of the electric pulse and with a variable delay after the start of the electric field pulse.

The experiments reveal that with the growth of the magnetic field strength, the velocity of the electrically induced domain wall motion increases at least with one order of the magnitude (fig. 1). The measurements are carried out at the two adjacent domain walls.

The suggested model for the electrically induced domain wall motion assumes that the domain wall velocity is determined by the wall magnetic structure. Computer simulation based on this model is in the qualitative agreement with the experiment.

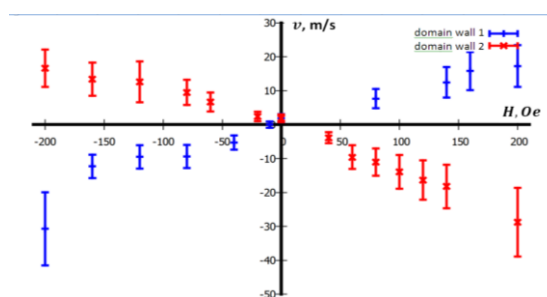


Fig.1. Magnetic field dependence of the electrically induced domain wall displacement velocity.

Work was partially supported by RFBR #13-02-12443-ofi-m2

[1] V.G. Bar'yakhtar, V.A. L'vov, D.A. Yablonskii, *JETP Letters*, **37** (1983) 673.

[2] A.S. Logginov, G.A. Meshkov, A.V. Nikolaev, A.P. Pyatakov *JETP Letters*, **86** (2007) 2, 115.

[3] A.S. Sergeev, D.A. Sechin, O.B. Pavlenko, E.P. Nikolaeva, A.B. Nikolaev, T.B. Kosykh, A.P. Pyatakov, *Izvestiya RAN, seriya Fizicheskaya*, **77** (2013) 10, 1541.

30PO-K-20

THE TEMPERATURE AND MAGNETIC FIELD CHANGE OF POLARON SIZE AS THE REASON OF CMR-EFFECT IN LAYERED MANGANITES

Solin N.I., Naumov S.V., Patrakov E.I.

Institute of Metal Physics, S.Kovalevskaya str.18, Yekaterinburg, 620990, Russia
solin@imp.uran.ru

Studies are dedicated at explaining the nature of colossal values (of the order 10³) of magnetoresistance of layered manganites La_{1,2}Sr_{1,8}Mn₂O₇ close to $T_C \approx 125$ K [1]. Manganites are heavily doped semiconductor with intrinsic disorders. Their transport properties can be understood in the context of physics of disorder medium. When substituting La⁺³ for Me⁺² the excess electron is localized on 8 Mn ions to form the polaron with the size $2R_{pol} \approx \sqrt{3} a \approx 7A^\circ$ with $a_{Mn-Mn} \approx 4A^\circ$. The conductivity is caused by the activation of holes to the mobility edge, $\sigma_0 = \sigma_{min} \exp(-\Delta E/kT)$, $\sigma_{min} \approx 300$ cm/Ohm. The Fermi level and the activation energy of jump ΔE are defined by the energy of Coulomb's blocking $E_{cut} \sim 1/2R_{pol}$. Due to the gain in the exchange energy an electron polarizes the neighboring ions of Mn, the polaron size rises, ΔE decreases with the temperature lowering or with the magnetic field action.

The magnetotransport properties of La_{1,2}Sr_{1,8}Mn_{1-x}O₇ with deficit of Mn ($x \approx 0.1$, $T_C \approx 60$ K) are discussed on a basis of this model. The chemical analysis was performed by an electron probe microanalysis on a scanning microscope Inspect F (EDAX). The electrical resistance on the *ab* plane has the form which is characteristic for layered manganites (Fig.1): at $T_{IM} = 75$ K ρ decreases sharply, below ~ 40 K ρ again increases. Electrical resistance decreases in the magnetic field at all the temperatures (by the factor ≈ 1250 at $T_{IM} = 75$ K and $H = 9$ T). From ΔE values (inset of Fig.1) the relative changes of polaron sizes $\Delta R_{pol}/R_{pol}^0 \equiv [R_{pol}(H) - R_{pol}(H=0)]/R_{pol}(H=0)$ are defined (inset of Fig.2).

The weak change of the polaron size above T_C and its sharp decrease below T_C explain the behavior of $\rho(T, H=0)$ (Fig.1). The regularities of polaron size change depending on the temperature and magnetic field are alight described in the model of phase separation into metallic drops of a small radius in paramagnetic matrix

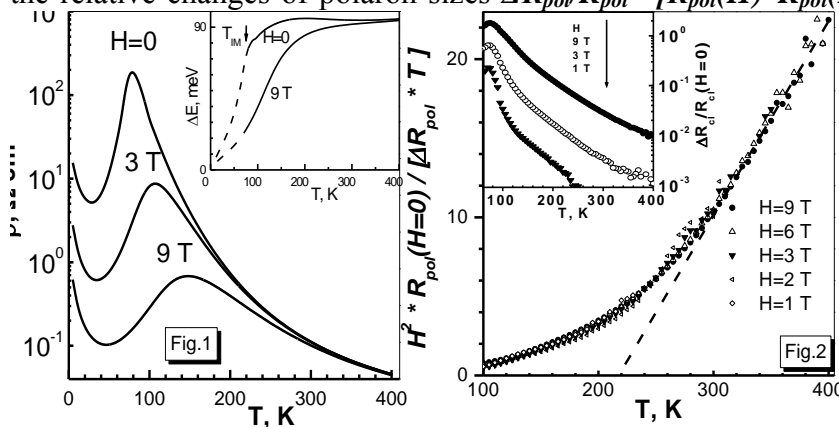


(Fig.2): $\Delta R_{pol}/R_{pol}^0 = bH^2/[5T(T-\theta)]$, with θ is Weiss temperature [3,4].

Model explains the increase of magnetoresistance (*MR*) under reduced Curie temperature T_C [4]. $MR(T=T_C, H) \equiv \rho(T_C, H=0) / \rho(T_C, H) \approx \exp[(C_0 * T_0/T_C) * (1 - R_{pol}(T_C, H=0)/R_{pol}(T_C, H))]$, with $C_0 \approx 0,8-0,9$, $T_0 \approx 10^3$ K $\approx \Delta E_0/k$ is the energy of jump activation at high ($T \approx 400$ K) temperature. An increase of the polaron size by the factor 2-3 in the magnetic field can explain the observed values of *MR* $\sim 3, 10, 10^2, 10^3, 10^4$ at $T_C = 350, 300, 200, 100$ and 60 K respectively.

This work was financially supported by the project 12 C-2-1026.

- [1]. Y. Moritomo et all, *Nature*, **380** (1996) 141-144.
- [2]. M. Yu. Kagan, K. I. Kugel', *Phys. Usp.*, **44** (2001) 553-572.
- [3]. N. I. Solin, *JETP Lett.*, **91** (12) (2010) 676-681.
- [4]. K. Khazeni et all, *Phys.Rev. B*, **76** (1996) 235.

30PO-K-21

THERMO-SPIN EFFECT IN A FERROMAGNETIC METAL / INSULATING FERROMAGNETIC JUNCTION

Lyapilin I.I., Okorokov M.S.

Institute of Metal Physics, Yekaterinburg, Russia
lyapilin@imp.uran.ru

Recently, spin Seebeck effect (SEE), a phenomenon that temperature bias can produce a spin current and associated spin voltage, has been observed in magnetic metals, semiconductors, insulators and even non-magnetic materials with spin-orbit coupling. These observations indicate that the SEE is a universal phenomenon in magnetic materials. Besides the SEE, there are several intriguing phenomena in which the interplay of spin and heat plays a crucial role. The SEE is crucial in spintronics and spin caloritronics since it enable a simple and versatile generation of spin currents from heat. Of particular interest is the SEE in the insulating magnetic interface. The reason is that different from spin dependent Seebeck effect in metallic materials. SEE allows heat to generate a pure flow of spin angular momentum, a flow of spins without electron currents. This becomes obvious only after the observation of the SEE through magnetic insulators-metal interface. Insulating ferromagnets have unique properties is that they are electrically inactive with frozen charge degrees of freedom, but magnetically active due to the spin degrees of freedom of localized spins; low-lying excitation in spin wave (magnon) which carries integer spin angular momentum. The spin flip scattering of conduction electrons through the exchange interaction with the local moments at the interface, creates a magnon excitation in ferromagnet.

As rule, the physics of the nonmagnetic (ferromagnetic) metals is described by the itinerant spin density \mathbf{s} , and its dynamics is modelled by the Bloch equations. The physics of the insulating ferromagnet (IF) is described by the localized moment M , for which the dynamics is modelled by Landau-Lifshitz-Gilbert equation. These calculations, for the most part involving a phenomenological collision integral. However, such a semi-phenomenological technique, obviously, cannot give theoretical estimates for the magnitude of kinetic coefficients, their dependence on temperature, magnetic field strength, etc. Answers to these questions can be found only within the microscopic theory that relates the spin relaxation and diffusion with certain mechanisms of the electron scattering.

One of the best ways to obtain closed expressions for the transport coefficients appearing in the equations for the density components of the spin magnetization is to apply the nonequilibrium statistical operator (NSO) method. Due to this method both the spin relaxation time and the components of the spin diffusion of the conduction electrons can be calculated by using temporal integration of mechanisms of the electron-lattice interaction.

Using NSO method, the macroscopic equations of motion for the spatial density of the spin magnetization of the localized electrons and phonon subsystem were constructed and an effect of heat on the magnon subsystem on the SSE has been studied. Studied the role of small deviations of the mean density of a spin magnetization of localized electrons at IF from the equilibrium values, due to the free electron spin-flip scattering at the F/IF interface. A nonequilibrium distribution magnon subsystem by the temperature $\beta_m^{-1} = T_m$ has been described, that differs from an equilibrium lattice temperature. Effect of nonequilibrium phonons on the SSE effect as a deviation of a magnons from equilibrium distribution through the magnon-phonon interaction has been studied.

30PO-K-22

EXCHANGE BIAS PROPERTIES OF X/CoO (X: PtCo, Co, Ni) FILMS*Erkovan M.¹, Parlak U.², Öztürk M.², Demirci E.², Öztürk O.², Aköz M.E.², Akdoğan N.²*¹Sakarya University, Department of Metallurgy and Materials Engineering, Sakarya, Turkey²Gebze Institute of Technology, Department of Physics, Kocaeli, Turkey

merkovan@sakarya.edu.tr

Exchange Bias effect has been observed in several nano-structures since it was first discovered in Co/CoO powders[1]. However, thin films are the desired candidates for the applications such as sensors and data-storage technologies.

Exchange Bias effect is considered as a key phenomenon that results spin-dependent scattering due to its unidirectional character. In this manner, exchange bias is required in order to provide a pinned layer in the spin-valve structures[2, 3]. The exchange layers are commonly consisted of a ferromagnetic and an antiferromagnetic layer, and are exposed to field cooling process to hold unidirectional magnetic anisotropy.

We carried out a comparative study on different ferromagnetic layers coupling with cobalt oxide as antiferromagnetic layer. X/CoO (X = PtCo, Co, Ni) [4,5]samples were compared with respect to their exchange bias field and blocking temperature values.

In this study, all samples were prepared by magnetron sputtering on Si(100) substrates, in ultra-high vacuum conditions. Since the thickness is a key feature for magnetic properties, the deposition rate must be well-controlled. For that purpose, thickness calibration was performed by using X-Ray Photoelectron Spectroscopy. XPS was also used for chemical characterization of the PtCo and CoO layers.

Magnetic properties were investigated by both magneto-optical Kerr effect (MOKE) and vibrating sample magnetometer (VSM). Magnetic hysteresis loops were measured by MOKE at room temperature. Exchange bias measurements were done by using the VSM, from 10 K to RT at an interval of 10 K step.

This work was supported by TÜBİTAK (The Scientific and Technological Research Council of Turkey) through project numbers 112T857, 106T576, 212T217 and 114F004.

[1] W.H. Meiklejohn, C.P. Bean, *Physical Review*, **102** (1956) 1413.

[2] J. Kools, *Magnetics, IEEE Transactions On*, **32** (1996) 3165-3184.

[3] J. Nogués, I.K. Schuller, *Journal of Magnetism and Magnetic Materials*, **192** (1999) 203-232.

[4] M. Ozturk, E. Sınır, E. Demirci, M. Erkovan, O. Ozturk, and N. Akdoğan, *Journal Of Applied Physics*, **112** (2012) 093911.

[5] E Demirci, M Öztürk, E Sınır, U Ulucan, N Akdoğan , Öztürk , M Erkovan, *Thin Solid Films* **550** (2014) 595–601.

30PO-K-23

ANISOTROPY OF MAGNETIC INTERACTIONS AND H-T-X MAGNETIC PHASE DIAGRAM OF ANTIFERROMAGNETIC STATE IN $Tm_{1-x}Yb_xB_{12}$

Azarevich A.N.^{1,2}, Sluchanko N.E.², Bogach A.V.², Glushkov V.V.^{1,2}, Demishev S.V.^{1,2}, Gavrilkin S.Yu.³, Gabani S.⁴, Flachbart K.⁴, Shitsevalova N.Yu.⁵, Filippov V.B.⁵, Vanaken J.⁶, Moshchalkov V.V.⁶

¹ Moscow Institute of Physics and Technology, Dolgoprudny, Russia

² A.M. Prokhorov General Physics Institute of RAS, Moscow, Russia

³ P.N. Lebedev Physical Institute of RAS, Moscow, Russia

⁴ Institute of Experimental Physics of SAS, Košice, Slovakia

⁵ Institute of Problems of Materials Science, NAS of Ukraine, Kiev, Ukraine

⁶ Institute for Nanoscale Physics and Chemistry of KU Leuven, Leuven, Belgium

azarevich@lt.gpi.ru

Antiferromagnetic-paramagnetic (AF-P) and metal-insulator transitions [1-2] have been studied in $Tm_{1-x}Yb_xB_{12}$ solid solutions with $x \leq 0.81$ and in the external magnetic field up to 12 T. Measurements of resistivity, heat capacity and magnetization have been carried out on high quality single crystals of $Tm_{1-x}Yb_xB_{12}$ at helium and intermediate temperatures. As a result, magnetic phase H - T - x diagram of AF-state has been constructed for compounds with $x \leq 0.1$. On the basement of transverse magnetoresistance measurements significant anisotropy of phase boundaries has been found both for AF-P and AF1-AF2 spin-orientation transition in AF-state for these magnetic metals with simple *fcc* crystalline structure [3]. For AF-state 3D-diagrams of the magnetoresistance anisotropy has been constructed for different magnetically ordered phases (Fig. 1). Negative magnetoresistance in $Tm_{1-x}Yb_xB_{12}$ has been shown to be determined by destroying of on-site *4f-5d* spin fluctuations in the external magnetic field (spin-polaron effect). Moreover, it was shown, that the magnetic structure in the ground AF-state of the rare-earth dodecaborides under study is influenced by induced local spin polarization of *5d*-states in conduction band in close surrounding of *4f*-centers, and these nanosize magnetic domains (ferrons) participate in the formation of complex magnetic structure in combination with indirect exchange (RKKY-mechanism) of *4f*-based localized magnetic moments.

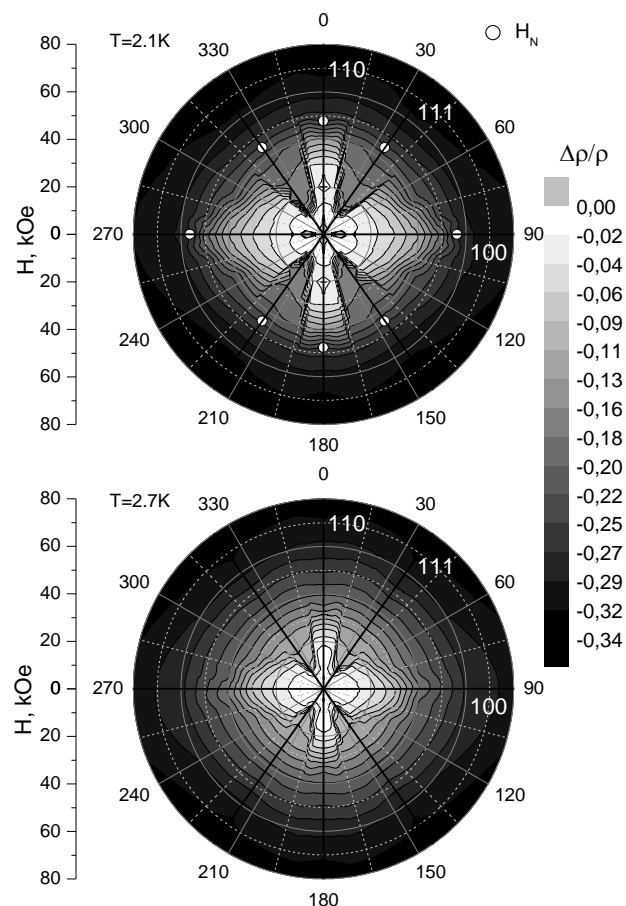


Fig.1. 3D view of $\Delta\rho/\rho(\mathbf{H})$ for $x=0.004$ at $T=2.1K$ and $2.7K$

[1] N.E. Sluchanko, A.N. Azarevich, A.V. Bogach et al., *JETP Letters*, **89** (2009) 298.

[2] N.E. Sluchanko, A.N. Azarevich, A.V. Bogach et al., *JETP*, **142** (2012) 574.

[3] N.E. Sluchanko, A.N. Azarevich, A.V. Bogach et al., *JETP*, **143** (2013) 998.

30PO-K-24

EPITAXY OF MnGa FERROMAGNETIC FILMS ON GaAs (100) FOR SPINTRONIC APPLICATIONS

Dorokhin M.V.^{1,2}, Pavlov D.A.², Bobrov A.I.², Danilov Yu.A.^{1,2}, Zvonkov B.N.¹, Zdoroveushev A.V.¹, Kudrin A.V.², Malekhonova N.V.², Malysheva E.I.¹

¹ Physical Technical Research Institute of Nizhny Novgorod State University, 603950
Nizhny Novgorod, Gagarin Av., 23/3, Russia

² Physical Department of Nizhny Novgorod State University, 603950
Nizhny Novgorod, Gagarin Av., 23/3, Russia
dorokhin@nifti.unn.ru

The latest development of the spintronics implies the fabrication of diode structures with the option for spin-polarized carrier injection from ferromagnetic layer to non-magnetic semiconductor [1]. One of the major requirements for ferromagnetic layer is an ideal interface quality providing the highest spin injection efficiency. In the present paper, the results of investigation of Mn₃Ga₅/GaAs epitaxial structure are discussed. The metallic-type conductance of Mn₃Ga₅ layers provide possibility for the fabrication of diode contacts and the ferromagnetic properties make these structures attractive for the investigation of spin-related phenomena.

The structures for investigation were fabricated by means of two-stage epitaxial growth method. Buffer GaAs layer, undoped GaAs layer, an In_xGa_{1-x}As quantum well (QW) and 30 nm cap GaAs layer were sequentially grown at 600°C on n-GaAs (100) substrate by means of a vapor phase epitaxy. At the next stage, the Mn₃Ga₅ layer was grown at 300°C by means of laser sputtering of MnGa target. For the fabrication of diode structure Au contact was deposited on the surface of the sample. Ferromagnetic properties were investigated within the reference samples consisting of a single Mn₃Ga₅ layer grown on i-GaAs substrate.

The crystalline structure and the composition of cross-section of the sample were carried out by means of JEM-2100F transmission electron microscope (TEM) equipped with energy-dispersive detector. The diode structures were investigated via measurements of electroluminescence spectra in the temperature range of 10-300 K.

The TEM measurements of the sample showed that the fabricated Mn₃Ga₅ is crystalline and coherently aligned with GaAs. The crystalline structure derived from the analysis of the diffraction pattern corresponds to the material with the Mn vs. Ga composition being close to the one adjusted technologically (Mn₃Ga₅) [2]. Note that material with Mn:Ga=3:5 composition is ferromagnetic as shown in [2].

The I-V characteristics of the diodes with Au contacts were measured at 77 K and 300 K. The exponential forward current growth with the increase of the voltage was obtained. The forward bias corresponds to a positive potential to a Au/Mn₃Ga₅. On the EL spectra the peak at ~ 1.35 eV was detected. The peak corresponds to the radiative transition in the quantum well.

Thus, we have investigated the light-emitting diodes with Mn₃Ga₅/GaAs epitaxial layers. High crystalline quality of the fabricated structures make them attractive for the spin injection investigations.

The work was supported by RFBR (13-02-97140, 13-07-00982, 14-07-31280), Grant of the RF President (MK-2708.2013.2)

[1] M. Holub, P. Bhattacharya, *J. Phys. D: Appl. Phys.*, **40** (2007) R179–R203.

[2] J.S. Wu, K.H. Kuo, *Metallurgical and Materials Transactions A*, **28** (1997) 729-742.

30PO-K-25

INTERLAYER EXCHANGE COUPLING IN FERRO/ANTIFERROMAGNETIC 3d-METALS BASED FILM STRUCTURES

Lepalovskij V.N., Gor'kovenko A.N., Savin P.A., Svalov A.V., Vas'kovskiy V.O.

Dept. Magnetism and Magnetic Nanomaterials, Ural Federal University, Ekaterinburg, Russia
vladimir.lepalovsky@urfu.ru

Interlayer exchange coupling is interesting as a source of magnetic bias in the magnetic sensory elements based on giant magnetoresistance, giant magnetic impedance and anisotropic magnetoresistance [1]. Generally, in sensory structures the antiferromagnetic Fe₅₀Mn₅₀ is used as the material of pinning layer and permalloy (Fe₁₉Ni₈₁) is pinned ferromagnetic layer [2]. In this paper, we investigate the effectiveness of the interlayer coupling in the Fe₅₀Mn₅₀/T films, where T is permalloy, Fe, Ni, Co or their alloys.

The multilayer films were prepared by magnetron sputtering using ATC Orion system. The films were deposited on the glass substrates in the presence of a uniform magnetic field (250 Oe) at Ar pressure of 1.6 mTorr. The preparation conditions for steadily formation of the fcc lattice which is responsible for antiferromagnetic ordering in the Fe₅₀Mn₅₀ layers have been defined in preliminary experiments. These include the existence of a high frequency electric bias on substrate during film deposition and the presence of buffer seed layers separating the Fe₅₀Mn₅₀ layer from the SiO₂ substrate. The Ta(5 nm)/Fe₁₉Ni₈₁(5 nm)/Fe₅₀Mn₅₀ (20 nm) multilayer is optimal basic structure on which the T layers were deposited.

Coercive force (H_c) and exchange bias field (H_{ex}) were determined from magnetometric hysteresis loops. Fig. 1 shows a typical hysteresis loop for the studied samples. Spontaneous magnetization (M_s), H_c , H_{ex} and interface coupling constant ($K_{ex} = M_s \cdot H_{ex} \cdot L$) are shown in the table 1. for the metals and alloys which were used as pinned ferromagnetic layer. In this paper we analyzed the reasons of the significant differences of K_{ex} for the ferromagnetic layers of different composition. The emphasis was laid on the features of crystal structure of the conjugation layers which were determined by means of X-ray diffraction.

This work was supported by the Scientific researches of higher educational institutions the State

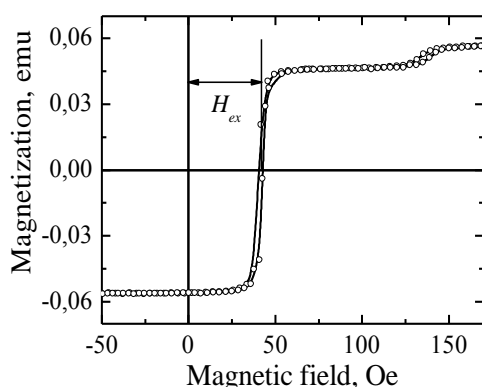


Table 1.

T	H_{ex} , Oe	H_c , Oe	M_s , Gauss	K_{ex} , erg/cm ²
Fe ₁₉ Ni ₈₁	42	3.0	810	0.136
Co	22	18.6	1422	0.125
Ni	60	28	484	0.116
Fe ₁₁ Ni ₈₉	36	6.5	630	0.091
Co ₃₀ Ni ₇₀	23	14.6	788	0.072
Fe	5	14.3	1717	0.034

Fig. 1. Hysteresis loop for Ta(5 nm)/Fe₂₀Ni₈₀/(5 nm)/Fe₅₀Mn₅₀(20nm)/Fe₁₉Ni₈₁(40 nm)/Ta(5 nm) film
task of the Russian Federation contract № 2014/236.

[1] B. Dieny, *Magnetoelectronics*, ed. by M. Johnson, (2004) 67-149.

[2] R. Coehoorn, *Handbook of magnetic materials*, ed. by K.H.J. Buschow, **15** (2003) 1-198.

30PO-K-26

SPIN GLASS STATE INFLUENCE ON ELECTRIC PROPERTIES IN SOME La-Pb MANGANITES

Craus M.-L.^{1,2}, *Anitas E.M.*^{1,3}, *Cornei N.*⁴, *Bobrikov I.*¹, *Turchenko V.*¹, *Simkin V.*¹

¹ Joint Institute for Nuclear Research, Dubna, Russia

² National Institute of Research and Development for Technical Physics, Iasi, Romania

³ Horia Hulubei National Institute for Physics and Nuclear Engineering, Bucharest-Magurele, Romania

⁴ "Al. I. Cuza" University, Iasi, Romania

kraus@nf.jinr.ru

The manganites were intensively studied in the past two decades, their properties allowing applications as magnetoresistive sensors. Magnetic structure of manganites, specially the origin of magnetic frustration is probably connected with the incoherent displacement of oxygen anions, due to the different radii of A cations. This implies incoherent positions of oxygen anions also, in agreement with the Mn cations, which could lead to the stabilization of the Jahn-Teller distorted $Mn^{3+}O_6$ octahedra and the resulting random magnetic anisotropy [1].

Some La manganites doped with Pb exhibit interesting electrical characteristics at temperatures near room temperature. We decided to obtain and investigate La manganites, where La was substituted with Pr, Pb and Sr. The $La_{0.5}Pr_{0.2}Pb_{0.3-x}Sr_xMnO_3$ manganites ($x=0.0 \div 0.20$) were synthesized by ceramic technology at Laboratory of Neutron Physics, JINR, Dubna, Russia. The samples were finally treated in air at 1200°C in a closed vessel to prevent Pb evaporation. The phase composition, lattice constants, position of the cations (A= La, Pr, Pb and Sr; B=Mn) and anions in ABO_3 lattice, tolerance factor, chemical disorder degree, average length of coherent blocks and microstrains were determined by XRD and ND methods. Data on magnetic and transport properties were obtained at temperatures between 77 and 300 K. We found that the substitution of Pb with Sr leads to important structural changes and we show that a transition from cubic to rhombohedral structure occurs for $x>0.05$. With the variation of Pb/Sr concentrations the magnetic moment of metallic phase, based on double exchange interaction between Mn^{3+} and Mn^{4+} remains constant at $3.7 \mu_B$, when the oxygen concentration corresponds to stoichiometry and the concentrations ratio of Mn^{4+} and Mn^{3+} cations is 3/7. On other hand, we observed at low magnetic fields a dependence of specific magnetization on temperature typical for a spin-glass state (s. Fig.1). We observed an important magnetoresistance near room temperature for the samples corresponding to $x=0.05$, 0.10 and 0.15.

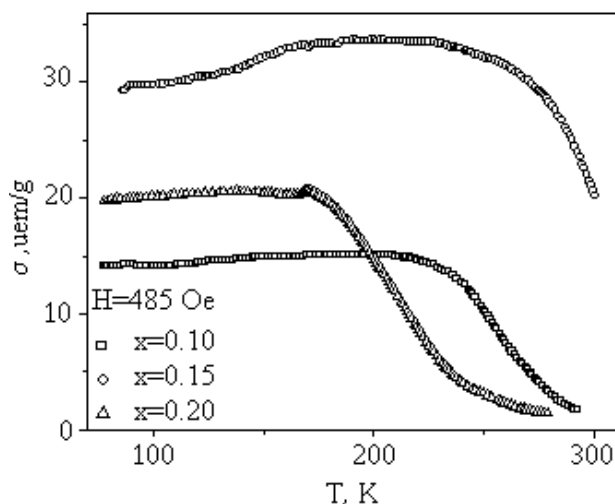


Figure 1 Variation of specific magnetization (σ) with temperature (T) and Sr concentration (x) (zero field cooling)

Support by FLNP – JINR Dubna and Romanian Council for JINR is acknowledged.

[1] A. Maignan, C. Martin G. Van Tendeloo, M. Hervieu and B. Raveau, *Phys. Rev. B*, **60** (1999) 15214-15219.

30 June

Monday

17:30-19:00

poster session

30PO-M

“Multiferroics”

30PO-M-1

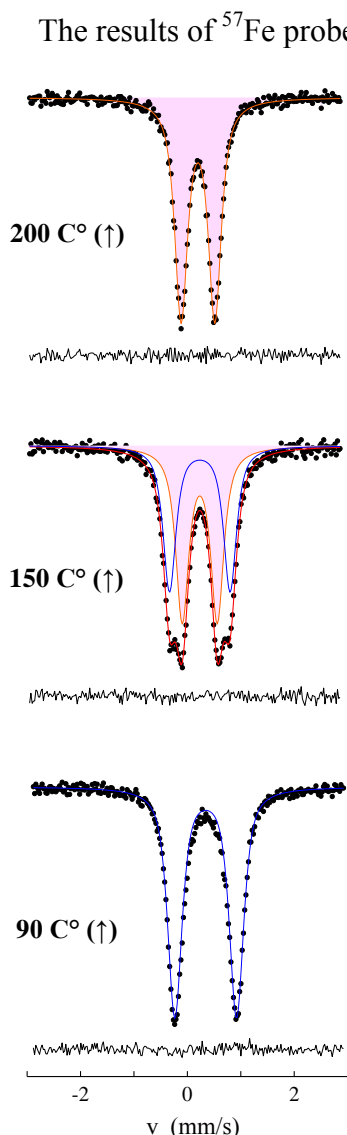
 ^{57}Fe PROBE MOSSBAUER INVESTIGATION OF BiMnO_3 MULTIFERROIC*Glazkova I.a.S.¹, Belik A.², Sobolev A.V.¹, Presnyakov I.A.¹*¹ Lomonosov Moscow State University, Moscow, Russia² National Institute for Materials Science (NIMS), Tsukuba, Japan
janglaz@bk.ru

Fig. 1. MS spectra of $\text{BiMn}_{0.96}\text{Fe}_{0.04}\text{O}_3$ measured in the "heating"-mode.

The results of ^{57}Fe probe Mossbauer studies of $\text{BiMn}_{0.96}\text{Fe}_{0.04}\text{O}_3$ multiferroic are represented.

Considered manganite refers to a large class of perovskite-like BiMO_3 bismuth oxides ($M = \text{Cr}, \text{Mn}, \text{Fe}$), where the spontaneous electric polarization occurs due to the stereochemical activity of the Bi^{3+} ions lone sp^n -hybrid pair [1]. In addition, this compound has attracted a wide interest due to its constituent Jahn-Teller Mn^{3+} ions, which demonstrate cooperative orbital ordering effects [2].

The results of semiempirical calculations of the electric field gradient (EFG) at the ^{57}Fe nuclei discusses in present work, allowing, in particular, to explain the observed high values of the quadrupole splittings in MS spectra measured below and above structural phase transition at $T_{\text{OO}} \approx 140^\circ\text{C}$ (Fig. 1) associated with orbital ordering (OO) in manganese sublattice. Analysis of the temperature dependence of the spectra showed the presence

of wide range ($\Delta T_{(\uparrow)} \approx 65^\circ\text{C}$ and $\Delta T_{(\downarrow)} \approx 50^\circ\text{C}$) of temperatures of two BiMnO_3 phases coexistence between, $3d$ -orbital-disordered ($T > T_{\text{OO}}$) and ordered ($T < T_{\text{OO}}$).

MS spectra measurements at "heating"-mode (\uparrow) and "cooling"-mode (\downarrow) showed hysteresis in the temperature dependence of the partial intensity (I) of the corresponding phases (Fig. 2), which is specific for the first order phase transitions.

In magnetically-ordered region of temperatures ($T < T_{\text{N}}$) MS spectra represent a superposition of several Zeeman components with relaxation hyperfine structure. It was assumed that the observed complex magnetic hyperfine structure of ^{57}Fe atoms caused by the formation of frustrated states of impurity centers Fe^{3+} .

This study was supported in part by the Russian Foundation for Basic Research, project no. 14-03-00768.

[1] A. Belik, *J. Solid State Chemistry*, **195** (2012) 32.

[2] I.V. Solovyev et al., *New J.Phys.*, **10** (2008) 073021.

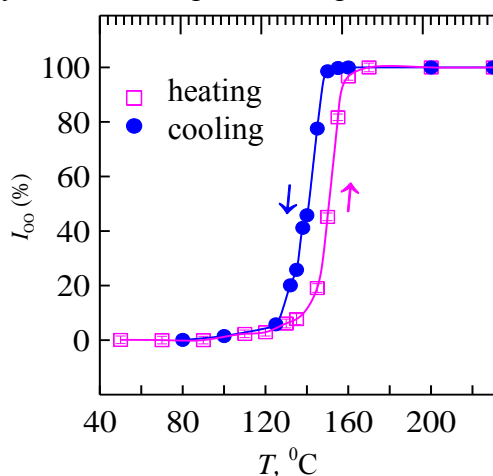


Fig. 2. Temperature dependence of the partial contribution (I_{OO}) of ^{57}Fe spectrum for orbitally ordered phase of $\text{BiMn}_{0.96}\text{Fe}_{0.04}\text{O}_3$ in MS measurements (\uparrow) and (\downarrow) modes.

30PO-M-2

MÖSSBAUER STUDY OF LOCAL STRUCTURE AND MAGNETIC HYPERFINE INTERACTIONS OF ^{57}Fe NUCLEI IN FERRITE BiFeO_3

Sobolev A.V.¹, Presniakov I.A.¹, Rusakov V.S.¹, Belik A.V.², Matsnev M.E.¹, Gorchakov D.S.¹, Glazkova Ia.S.¹

¹Lomonosov Moscow State University, Moscow, Russia

²National Institute for Materials Science (NIMS), Tsukuba, Japan

alex@radio.chem.msu.ru

The antiferromagnet ferrite BiFeO_3 is a “proper” multiferroic in which ferroelectricity and magnetism have different microscopic sources. The ferroelectricity is considered to primarily originate from displacements of the Bi^{3+} ions due to the stereochemically active $6s^2$ lone pair. It was found that the G -type antiferromagnetic structure of BiFeO_3 is subjected to a long-range modulation of cycloidal-type with the period ~ 620 Å. The temperature-dependent evolution of the magnetic structure in BiFeO_3 is important subject with several currently unresolved issues. We report new results of ^{57}Fe Mössbauer studies on BiFeO_3 powder sample performed at various temperatures above and below of the point $T_N \approx 640$ K of magnetic phase transitions.

The ^{57}Fe Mössbauer spectra measured at $T > T_N$ consist of doublet with quadrupole splitting $\Delta_{660\text{K}} \approx 0.43$ mm/s corresponding to the Fe^{3+} sites in rhombohedral perovskite-like BiFeO_3 lattice with a strong electric field gradient (EFG) at ^{57}Fe nuclei. We have performed self-consistent calculations of the lattice contributions to the EFG tensor, taking into account dipole moments of the O^{2-} and Bi^{3+} ions. It was found that the induced dipolar moments of the oxygen and bismuth ions make a substantial contribution to the EFG. From a comparison with experimental results, a coherent ranges of variation of the dipole polarizabilities, $\alpha_{\text{O}} \approx 0.5 \div 1.0$ Å³ and $\alpha_{\text{Bi}} \approx 2.5 \div 6.5$ Å³, were determined. Using the parameters of the crystal structure of BiFeO_3 for temperatures from 5 K to 923 K, we found the dependence $\alpha_{\text{Bi}}(T)$ reflecting that the displacement of the Bi^{3+} from the FeO_6 polyhedra, which influence the electric polarization, decreases with temperature. According to our calculations, the principal EFG tensor component V_{zz} has the positive sign and is directed along c -axis of hexagonal unit cell coinciding with the direction of easy-axis magnetic anisotropy $[111]_{\text{hex}}$ in bismuth ferrite.

Low-temperature ^{57}Fe spectra recorded at $T < T_N$ were analyzed assuming an anharmonic cycloidal modulation of the Fe^{3+} magnetic moments. The cycloidal modulation of the iron spin was described with the elliptic Jacobi function $sn[(\pm 4K(m)/\lambda)x, m]$ (where m is its anharmonicity parameter, $K(m)$ is the complete elliptic integral, λ is the modulation period, x is coordinate along the propagation direction). The good fit of the experimental spectra was obtained for the anharmonicity $m = 0.36 \pm 0.04$ ($T = 4.9$ K) resulting from easy-axis magnetic anisotropy, which was previously suggested by NMR and neutron diffraction studies [1, 2]. On the basis of single-ion approximation we described the experimental temperature dependence $m(T)$ in terms of the parameters of spin Hamiltonian of the Fe^{3+} ions and magnetization of the lattice. One of the unusual results is associated with strong temperature dependence of anisotropy of the magnetic hyperfine field H_{hf} at ^{57}Fe nuclei: $\Delta H_{\text{an}} = 2/3(H_{\parallel} - H_{\perp})$, where H_{\parallel} and H_{\perp} are the values of H_{hf} along and perpendicular to the direction V_{zz} ($H_{\parallel} = 545.5 \pm 0.3$ kOe and $H_{\perp} = 541.2 \pm 0.3$ kOe, at $T = 4.9$ K). This ΔH_{an} value decreases with increasing temperature, changing sign at $T^* \approx 610$ K ($\Delta H_{\text{an}} < 0$). We discuss possible mechanisms of such unusual behavior, including a so-called spin reorientation phase transitions previously observed for rare-earth orthoferrites.

This work is supported by the RFBR grant No. 14-03-00768a and No. 14-02-01109a.

[1] A.A. Bush, A.A.Gippius, A.V.Zaleskii, and E.N. Morozova, *JETP Lett.*, **78** (2003) 389.

[2] I. Sosnowska, T. Peterlin-Neumair and E. Steichele, *J. Phys. C*, **15** (1982) 4835.

30PO-M-3

COMPARATIVE ^{57}Fe MÖSSBAUER STUDY OF TRIANGULAR-LATTICE FERRITES AgFeO_2 AND CuFeO_2

Presniakov I.A.¹, Rusakov V.S.¹, Sobolev A.V.¹, Gapochka A.M.¹, Matsnev M.E.¹, Belik A.V.²,
Glazkova Ia.S.¹, Lekina Yu.V.¹

¹Lomonosov Moscow State University, Moscow, Russia

²National Institute for Materials Science (NIMS), Tsukuba, Japan

ipresniakov@rambler.ru

The ferroelectricity in triangular-lattice ferrites $A\text{FeO}_2$ ($A = \text{Ag}, \text{Cu}$) with delafossite-like structure appears as a result of the phase transition inducing an unusual magnetic structure that breaks the crystal symmetry. In this work, we present the results of the ^{57}Fe Mössbauer (MS) study of AgFeO_2 and CuFeO_2 ferrites. The MS spectra were measured in temperature range including the points of two successive magnetic phase transitions: $T_{\text{N1}} = 14 \div 15$ K (Ag, Cu), and $T_{\text{N2}} \approx 9$ K (Ag), 11 K (Cu) [1, 2].

The ^{57}Fe MS spectra of both $A\text{FeO}_2$ ferrites measured at temperatures above T_{N1} consist of single doublets with almost the same high quadrupole splitting $\Delta \approx 0.66$ mm/s indicating that all ferric ions occupy in the rhombohedral delafossite-like lattice ($R\bar{3}m$) equivalent crystal positions with a strong electric field gradient (EFG) at ^{57}Fe nuclei. We calculated the lattice contributions to the EFG tensor using a monopole-dipole model. The calculations emphasized the importance of the major dipolar contribution to the EFG which is induced from the oxygen. The symmetry lowering to monoclinic $C2/m$ ($T \leq T_{\text{N1}}$) revealed no noticeable changes in the magnitudes of the EFG tensor. These results emphasize that, in spite of the qualitative different character of the lattice distortions in the AgFeO_2 and CuFeO_2 delafossites [1], the local crystal structure of Fe^{3+} ions in their hexagonal and monoclinic phases are equivalent.

The ^{57}Fe MS spectra measured at low temperatures $T < T_{\text{N2}}$ demonstrate very different magnetic behavior of iron sublattices in two ferrites. In the case of AgFeO_2 , the spectra consist of Zeeman magnetic hyperfine pattern with inhomogeneous line broadenings and sizeable spectral asymmetry. It has been shown that the observed spectral shape is consistent with a phase transition to the space modulated cycloidal magnetic structure of AgFeO_2 ($T \leq T_{\text{N2}}$) [1]. The observed complex hyperfine structure for AgFeO_2 significantly differs from a single symmetrical Zeeman sextet for CuFeO_2 ferrite which is characterized by a collinear magnetic structure $\uparrow\uparrow\downarrow\downarrow$ excluding any possibility of spontaneous electric polarization [2]. Analysis of the experimental spectra for AgFeO_2 ferrite was carried out assuming the modulation of the electric hyperfine interactions when the Fe^{3+} magnetic moment rotates with respect to the principal axis of the EFG tensor V_{zz} , and the slight anisotropy of the magnetic hyperfine field $H_{\text{hf}}(\vartheta)$ at the ^{57}Fe nuclei (ϑ is the angle between the direction of the hyperfine magnetic fields H_{hf} and V_{zz} at ^{57}Fe nuclei). The obtained from the experimental spectra large temperature independent anharmonicity parameter ($m \approx 0.78$) of cycloidal spin structure results from easy-axis anisotropy in the plane of the iron spin rotation.

In the intermediate temperature range of $T_{\text{N2}} < T < T_{\text{N1}}$, the ^{57}Fe Mössbauer spectra for both ferrites can be described in terms of collinear spin-density-waves (SDW) with inclusion of many high-order harmonics, indicating that the real magnetic structure of AgFeO_2 and CuFeO_2 appears to be more complicated than previously suggested pure sinusoidally modulated SDW [1, 2].

This work is supported by the RFBR grant No. 14-03-00768a and partially No. 14-02-01109a.

[1] N.Terada, D.Khalyavin, P.Manuel et al., *Physical Review Letters*, **109**(2012) 097203.

[2] T.Nakajima, S.Mitsuda, K.Takahashi et al., *Physical Review B*, **79** (2009) 214423.

30PO-M-4

**THE MAGNETO-ELECTRIC EFFECT IN ORTHORHOMBIC
YbMnO₃ THIN FILMS**

*Andreev N.V.¹, Volodin A.P.², Sviridova T.A.¹, Chichkov V.I.¹, Van Haesendonck C.²,
Mukovskii Ya.M.¹*

¹ National University of Science and Technology "MISIS", Moscow, Russia

² KU Leuven, Lab. Solid State Phys & Magnetism, Leuven, Belgium

andreevn.misa@gmail.com

Epitaxial thin film growth on some single crystal substrates allows obtaining a material in structural modification different from a bulk one. The orthorhombic (perovskite-like) modification YbMnO₃ (o-YbMO) that is hexagonal in bulk was epitaxially stabilized on conductive Nb-doped SrTiO₃ (STO(:Nb)) substrate. The o-YbMO films are ferroelectric at low temperatures with the saturation polarization value of ~ 300 nC/cm². The magneto-electric effect in o-YbMO films consisting in increasing of polarization magnitude in an applied external magnetic field has been demonstrated. The magnetic field induced charge ordering on microscopic level in the o-YbMO films was displayed by the low temperature electrostatic force microscopy. The presence of electrostatic domains with different polarization signs of typical size of about 200 nm was revealed. It was suggested that the electrostatic domains correspond to the varying transverse orientation crystalline domains. The existence of the polarization itself induced by the magnetic field was attributed to the emergence of a manganese cycloidal magnetic structure in the o-YbMO films and to interaction of magnetic and charge subsystems.

The work has been supported by the RFBR grant № 14-07-00258.

30PO-M-5

DOES FERROELECTRICITY EXIST IN THE RARE EARTH ORTHOCHROMITES RCrO_3 ?

Ivanov V.Yu.¹, Mukhin A.A.¹, Popov Yu.F.², Vorob'ev G.P.², Pyatakov A.P.²

¹ Prokhorov General Physics Institute of the Russian Acad. Sci., 119991, Moscow, Russia

² Faculty of Physics, M.V. Lomonosov Moscow State University, 119992 Moscow, Russia

ivanov@ran.gpi.ru

Recently several papers [1-4] have reported on the observation of spontaneous electric polarization in some ceramic samples of rare-earth orthochromites RCrO_3 ($\text{R}=\text{Gd}, \text{Sm}, \text{Tb}, \text{Er}, \dots$) at high temperatures (near or even above Neel temperature of the Cr-subsystem 120-200 K). However, these findings contradict with the well known symmetry properties of these compounds, which do not allow spontaneous electric polarization because of their crystal structure (Pbnm space group) and Cr^{3+} magnetic ordering (G-type) are centrosymmetrical.

In order to check and clarify the “high temperature” magnetoelectric properties in orthochromites, we have carried out pyroelectric study of the single crystalline orthochromite samples RCrO_3 (Gd, Tb, Er, Y, Dy, Ho et al.). Due to higher electric resistance of the single crystalline samples as compared to ceramic ones it is possible to more accurately elicit the useful pyroelectric signal from the background of parasitic ones caused by leakage currents. Besides, we have performed the pyroelectric measurements along different crystallographic directions in order to determine geometrical conditions for appearance and anisotropy of the electric polarization in case it exists. However, we have not observed any noticeable anomalies of pyroelectric current near or below the Neel temperature in the studied crystals, except for SmCrO_3 where the electric resistance was not big enough for the reliable pyroelectric measurements. Increase of pyroelectric current with increasing temperature was observed as a rule at the temperatures higher the Neel temperature, for which the electric resistance of the samples was reduced and a “discharge” of the electric charge stored during a preliminary cooling down in an electric field occurred. A change of the heating regime to the cooling down one was not accompanied by a change of the pyroelectric current sign just as it occurs in case of true spontaneous electric polarization. We have not also observed an effect of magnetic field (at least up to 14 kOe) on the pyroelectric current value after cooling down of the samples in the electric field, which was observed for ceramic samples.

Thus our results show that the electric polarization is not probably an intimate feature of the rare-earth orthochromite crystals. The origin of the electric polarization in the ceramic samples likely has an improper character and could be due to local distortions at crystal grain boundaries affected by a treating in the electric field during cooling down of the samples.

This work was partially supported by RFBR (13-02-01093).

[1] C.R. Serrao et al. *Phys Rev.* **B 72** (2005) 220101.

[2] Z.X. Cheng, et al. *J. Appl. Phys.*, **107** (2010) 09D905.

[3]. B. Rajeswaran et al. *Phys. Rev.*, **B 86** (2012) 214409.

[4]. K.R.S.P. Meher, C. Martin, et al., *Chem. Mater.*, **26** (2014) 830-836.

30PO-M-6

TEMPERATURE CHARACTERISTICS OF RESONANT MAGNETOELECTRIC EFFECT IN BILAYER STRUCTURES

Burdin D.A., Chashin D.V., Economov N.A., Fetisov Y.K.

Moscow State Technical University of Radio Engineering, Electronics and Automation, Moscow, Russia
phantastic@mail.ru

Composite structures containing ferromagnetic and piezoelectric layers are the basis for high-sensitivity magnetoelectric (ME) magnetic field sensors [1]. For applications it is very important to know temperature characteristics of the devices.

This paper describes measured temperature characteristics of resonant ME interactions in bilayer piezoelectric-ferromagnetic (PE-FM) structures. We used a PZT ceramics ($\text{PbZr}_{0.52}\text{Ti}_{0.48}\text{O}_3$) or a langatate crystal ($\text{La}_3\text{Ga}_{5.5}\text{Ta}_{0.5}\text{O}_{14}$) for the PE layer. The FM layer was made from Ni or Metglas (FeBSiC). All samples had in-plane dimensions of $23.6 \times 5 \text{ mm}^2$, the thickness of PE layer was $b_p = 0.5 \text{ mm}$, and the thickness of FM layer was $b_m = 0.05 \text{ mm}$. The PE and FM layers were glued together with a fast dry epoxy.

An automated system was assembled for measurements. The samples were placed in a thermo-cell and their temperature was changed in the $T = 100 \dots 400 \text{ K}$ range using a nitrogen flow. The thermo-cell in its turn was placed in ac magnetic field $h \cos(2\pi ft)$ ($f = 0.1 \dots 200 \text{ kHz}$, $h = 0 \dots 3 \text{ Oe}$) and dc bias field H , parallel to each other. The ME voltage u generated across the PE layer was measured at a longitudinal acoustic resonance frequency for different T and fields H : 7 Oe for PZT-Metglas structures and 80 Oe for PZT-Ni structures.

Fig.1 shows a set of amplitude-frequency ME voltage dependencies measured for the PZT-Ni structure at different temperatures. By processing these data, we got the voltage-temperature and frequency-temperature curves, which are shown in Fig.2. Similar data were obtained for other composite structures. Results of our investigations showed that temperature dependencies of ME characteristics in studied samples were determined mainly by the PE layer's properties.

The research was supported by the Ministry of Education and Science of Russia and the Russian Foundation for Basic Research.

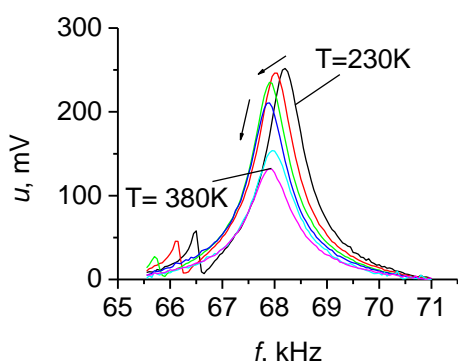


Fig.1. A set of amplitude-frequency dependencies for the PZT-Ni structure.

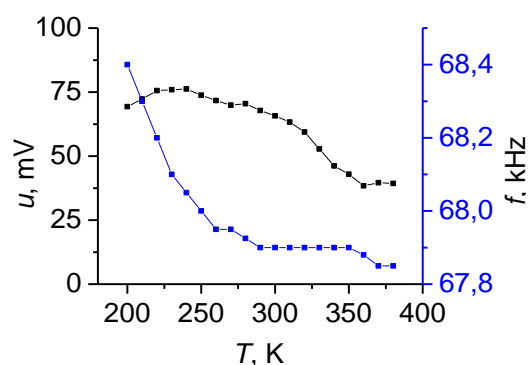


Fig.2. Temperature dependencies of ME voltage u and frequency f for the PZT-Ni structure.

[1] D.A. Burdin, Y.K. Fetisov, D.V. Chashin et al., *Appl. Phys. Lett.*, **100** (2012) 242902.

30PO-M-7

SYNTHESIS AND MAGNETIC PROPERTIES OF POLYCRYSTALLINE $\text{Cr}_2\text{O}_3/\text{CoFe}_2\text{O}_4$ MULTIFERROIC FILMS

Polyakova K.P.¹, Polyakov V.V.¹, Velikanov D.A.^{1,2}, Patrin G.S.^{1,2}

¹Kirensky Institute of Physics, Krasnoyarsk, Russia

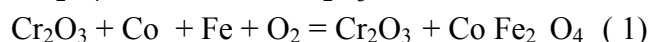
²Siberian Federal University, Krasnoyarsk, Russia

pkp@iph.krasn.ru

Of interest are composite multiferroics with the Cr_2O_3 antiferromagnet characterized by the magnetoelectric effect. As is known, the specific feature of the structures antiferromagnet–ferro(ferri)magnet is the unidirectional anisotropy and exchange bias. Under the action of an electric field, such structures reveal a number of intriguing phenomena offering new opportunities for application. In particular, in the $\text{Cr}_2\text{O}_3/\text{CoPt}$ heterostructures, the bias field switching effect under the action of an electric field was found [1].

In this study, we investigate for the first time the magnetic properties of the layered $\text{Cr}_2\text{O}_3/\text{CoFe}_2\text{O}_4$ composite multiferroic structure.

The $\text{Cr}_2\text{O}_3/\text{CoFe}_2\text{O}_4$ film structure was formed as follows. The Cr_2O_3 films were prepared on a quartz substrate by the oxidation Cr layer in air at a temperature of 870 K. After that, the Co and Fe layers were deposited on the Cr_2O_3 film. The CoFe_2O_4 cobalt ferrite film was obtained by solid-state reaction (1) in the regime of self-propagating high-temperature synthesis with an initiation temperature of 620 K. It was shown that at this temperature, only the CoFe_2O_4 film form on Cr_2O_3 film.



To observe the exchange bias, we measured the magnetization reversal curves $M(H)$ upon cooling from the Neel temperature of Cr_2O_3 to 4 K. The samples were cooled in the zero field cooling (FZC) and 1-kOe-field cooling (FC) modes. The magnetic field was applied in the film plane along the chosen direction.

The magnetic measurements confirmed the existence of the exchange coupling in the $\text{Cr}_2\text{O}_3/\text{CoFe}_2\text{O}_4$ bilayer. Figure 1 shows the hysteresis loops obtained using a SQUID magnetometer at a temperature of 4.2 K. It can be seen that the FC-curve shifts toward negative magnetic fields. The exchange bias field is 90 Oe. Temperature dependences of the magnetic moment at (FZC) and (FC) cooling it possible to determine the Neel temperature layer Cr_2O_3 (330 K).

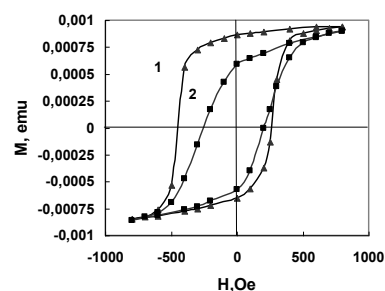


Fig. 1. FZC(2) and FC(1) hysteresis loops of the $\text{Cr}_2\text{O}_3/\text{CoFe}_2\text{O}_4$ multiferroic film.

[1] P. Borisov, A. Hochstrat, Xi. Chen, W. Killeman, Ch. Benik, *Phys.Rev. Lett.*, **94** (2005) 117203-117206.

[2] K.P. Polyakova, V.V. Polyakov, V.A. Seredkin, G.S. Patrin, *Pisma v Zhurnal Tekhnicheskoi Fiziki* **37** (2011) 30-35.

30PO-M-8

STRUCTURE AND MAGNETIC PARAMETERS OF COMPOSITE MULTIFERROICS $x(\text{MFe}_2\text{O}_4) + (1-x)\text{BaTiO}_3$

Nosov A.P.¹, Semkin M.A.², Teplykh A.E.¹, Bogdanov S.G.¹, Urusova N.V.², Pirogov A.N.^{1,2}

¹Institute of Metal Physics of UB of RAS, Ekaterinburg, Russia

²Ural Federal University, Ekaterinburg, Russia

mihail.semkin@mail.ru

Effective interplay between magnetic and ferroelectric degrees of freedom, which can be realized both in homogenous single phase and composite multiferroics, permits to control magnetization by external electric field or electric polarization by external magnetic field. The efficiency of magnetoelectric interaction at room temperature in homogenous single phase multiferroic materials is low, which hinders their potential technical applications. In contrast, composite multiferroics can have the values of magnetoelectric constant at room temperature of the order of 1 V/cm·Oe, which are much greater than the ones for the homogenous single phase materials. Such materials are of great interest for potential technical applications.

The aim of the present work is to study the crystal and magnetic states of heterogeneous multiferroic material of the $x(\text{MFe}_2\text{O}_4) + (1-x)\text{BaTiO}_3$ composition, where $M = \text{Ni}$ and Co . In this materials the MFe_2O_4 spinel has magnetostrictive properties while barium titanate has the ferroelectric properties.

The bulk polycrystalline samples of the $x\text{NiFe}_2\text{O}_4 + (1-x)\text{BaTiO}_3$, with $x = 0.2, 0.3$ and 0.4 , and $x\text{CoFe}_2\text{O}_4 + (1-x)\text{BaTiO}_3$, with $x = 0.2$, and 0.4 , compositions were prepared by mixing and pressing the corresponding powders. Powder neutron diffraction patterns (PNDP) were recorded in the $\Theta - 2\Theta$ mode using the D2 and D3 diffractometers at neutron wavelengths of $\lambda = 1.805$ and 2.43 \AA , respectively. Small angle neutron scattering experiments were made using the D6 diffractometer at $\lambda = 4.5 \text{ \AA}$. All diffractometers are installed at the IVV-2M reactor (Zarechny, Russia).

Intensive nuclear and magnetic reflections (see Fig. 1) from spinel does not overlap with reflections from barium titanate. This favorable circumstance allows to determine structural and magnetic parameters of both subsystems with good accuracy (global $\chi^2 = 3.1$). Iron ions occupy the $8a$ position in the nickel ferrite lattice, while the Fe and Ni ions are located in the $16d$ sites (space group $Fd\bar{3}m$). The sizes of nuclear and magnetic unit cells coincide, therefore, the wave vector of a magnetic structure $\mathbf{k} = 0$. Spins of ions in the $8a$ position are antiparrallel to those in the $16d$ sites. In cobalt ferrite the Fe ions occupy half of sites in the $8a$ position and 67% in the $16d$ one, the Co ions are located in the rest sites. Both nickel and cobalt ferrites have magnetic structure described by the vector $\mathbf{k} = 0$. Magnetic moments of ions in the $8a$ and $16d$ positions are equal to 3.5 and $3.1 \mu_B$, respectively, and are mutually antiparrallel.

The BaTiO_3 ferroelectric subsystem has the tetragonal structure (space group $P4/mmm$) in which the Ba, Ti, O1 and O2 occupy the $1a$, $1b$, $1b$, and $2c$ positions, respectively.

This work is supported by the RFBR 13-02-00720 and 12-U-2-1010 projects.

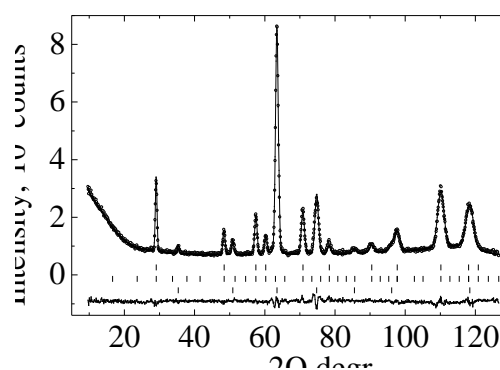


Fig. 1. Observed (points), calculated (line), and differential PNDP of $0.2(\text{CoFe}_2\text{O}_4)+0.8(\text{BaTiO}_3)$ at external magnetic field $\mu_0H = 4$ Oe. Bars show angle positions of the nuclear and magnetic reflections.

30PO-M-9

^{57}Fe NMR AND MÖSSBAUER DIAGNOSTICS OF SPATIAL SPIN-MODULATED STRUCTURE IN MULTIFERROIC BiFeO_3

Rusakov V.S.¹, Pokatilov V.S.², Sigov A.S.², Matsnev M.E.¹, Gubaidulina T.V.¹

¹Lomonosov Moscow State University, Moscow, 119991 Russia

²Moscow State Institute of Radio Engineering, Electronics, and Automation (Technical University), Moscow, 117454 Russia

rusakov@phys.msu.ru

Bismuth ferrite BiFeO_3 is multiferroic, with ferroelectric and magnetic properties. It has high antiferromagnetic Neel temperature (643 K) and ferroelectric Curie temperature (1103 K). Thanks to the exceptional features of its physical properties BiFeO_3 evoke the great interest in many areas of science and technology. Currently, the study of multiferroic acquire great significance methods which allow to diagnose and study the spatial spin-modulated structure (SSMS). Such methods, along with neutron diffraction are nuclear magnetic resonance (NMR) and Mossbauer spectroscopy (MS). At the same time, the experimental data on the parameters of the hyperfine interaction and the degree of anharmonicity of the spin wave, obtained by means of neutron diffraction, NMR and MS are quite controversial.

The paper deals with methods of diagnostics SSMS cycloid type in multiferroics based on nuclear magnetic resonance and Mossbauer spectroscopy. Studies by NMR and MS were performed on a ceramic sample of BiFeO_3 , with relative abundance stable isotope ^{57}Fe at 10 %. For processing and analysis of the NMR and Mossbauer spectra we used methods of accounting of transverse spin-spin relaxation, recovery hyperfine parameter distributions and fitting in the SSMS cycloid type model implemented in the program SpectrRelax [1].

On the example of ferrite BiFeO_3 it is shown that when using NMR techniques one must consider the dynamic effects, primarily the transverse spin-spin relaxation, that significantly affects the measurement result. It is established that by means of Mossbauer spectroscopy the anharmonicity parameter of SSMS cycloid type can be determined with not a less accuracy than by NMR, which has higher resolution (see Table). MS methods with sensitivity to the hyperfine quadrupole interaction of the nucleus in an excited state provide additional information about the features of SSMS.

The table presents the results of fitting the NMR and MS spectra in the SSMS cycloid type model, where δ and ε_{lat} are isomer and quadrupole shifts, ν_{\parallel} (H_{\parallel}) and ν_{\perp} (H_{\perp}) are NMR frequency (hyperfine magnetic field at the ^{57}Fe nuclear) in the case of the magnetic moment of Fe atom, oriented parallel and perpendicular to the axis of symmetry of the crystal, respectively, $\Delta\nu = \nu_{\parallel} - \nu_{\perp}$ ($\Delta H = H_{\parallel} - H_{\perp}$), m is anharmonicity parameter of SSMS cycloid type.

Table. The results of fitting the NMR and MS spectra in the SSMS cycloid type model.

Spectrum	δ , mm/s	ε_{lat} , mm/s	ν_{\parallel} , MHz	H_{\parallel} , kOe	ν_{\perp} , MHz	H_{\perp} , kOe	$\Delta\nu$, MHz	ΔH , kOe	m
NMR (4.2 K)	—	—	2 75.568	1 547.00	2 74.884	2 542.05	3 0.684	2 4.95	9 0.13
MS (4.85 K)	10 0.5054	2 0.254	15 75.555	11 546.90	17 74.953	12 542.54	25 0.602	18 4.36	6 0.26

This work is supported by the RFBR grants No. 14-02-01109a and No. 13-02-00690a

[1] M.E. Matsnev and V.S. Rusakov. *AIP Conference Proceedings*, **1489** (2012) 178-185.

30PO-M-10

MAGNETIC AND MAGNETOELECTRIC PROPERTIES OF $\text{Sm}_{1-x}\text{La}_x\text{Fe}_3(\text{BO}_3)_4$

Eremin E.V., Gudim I.A., Temerov V.L., Volkov N.V.

Kirensky Institute of Physics, Russian Academy of Sciences, Krasnoyarsk, Russia
eev@iph.krasn.ru

In recent years, there has been a great interest in studying multiferroic crystals, including the crystals of rare-earth ferrobates $\text{RFe}_3(\text{BO}_3)_4$ with the non-centrosymmetric trigonal structure. Below the temperature of the antiferromagnetic ordering $T_N \sim 30\text{-}40$ K, some of them exhibit the spontaneous or/and magnetic-field-induced electric polarization. The variety of characteristics of ferrobates is due to the presence of two magnetic subsystems: iron ions and rare-earth ions. In the crystal structure of ferrobates, the direct Fe–Fe exchange dominates and exceeds by far the indirect exchange between rare-earth ions. This is indicated, in particular, by the closeness of the Neel temperature of ferrobates to that of different rare-earth elements.

This study is aimed at investigation of the magnetic, magnetodielectrical, and magnetoelectric properties of single crystals of the mixed rare-earth ferrobates $\text{Sm}_{1-x}\text{La}_x\text{Fe}_3(\text{BO}_3)_4$ ($x = 0, 0.5,$ and 0.75).

The single crystals were grown by spontaneous crystallization from the flux. Below the temperature of the magnetic ordering, spontaneous polarization occurs under the action of factors that reduce the crystal symmetry. One of such factors can be the anisotropy induced by stresses caused by the magnetoelastic interactions [1]. This polarization can be controlled by an external magnetic field. It was established in the experiment that as the lanthanum concentration is increased, the spontaneous polarization drops. The maximum value of the magnetic-field-induced polarization changes insignificantly. However, the value of the magnetic field at which the polarization saturates decreases with increasing x . This behavior is apparently related to the fact that a lanthanum ion has a larger radius as compared with a samarium ion. Therefore, upon partial substitution of lanthanum for samarium ($x > 0$), the mobility of ions grows, which leads to a decrease in the saturation field. The establishment of the magnetic order is accompanied by the anomaly in the temperature dependence of permittivity. Being nearly constant in the paramagnetic region, permittivity strongly grows below the Neel temperature. This growth is suppressed by a magnetic field (Fig. 1).

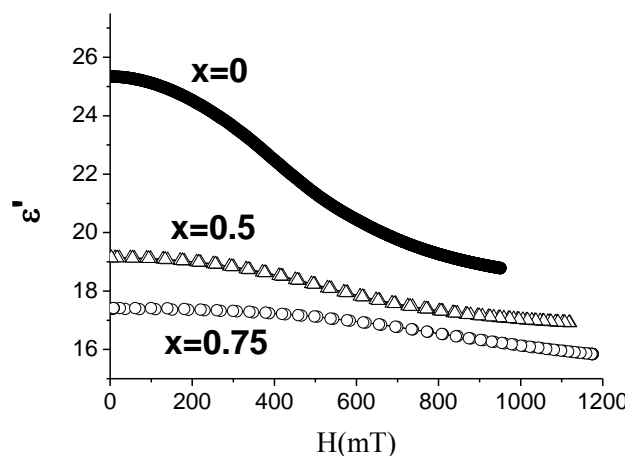


Fig.1. Field dependences of permittivity of $\text{Sm}_{1-x}\text{La}_x\text{Fe}_3(\text{BO}_3)_4$ at 10 K.

This work was supported by the RFBR (project no. 14-02-00307).

[1] Y.F. Popov, A.P. Pyatakov, A.M. Kadomtseva et al. *JETP*, **138** (2010) 229.

30PO-M-11

THIN-FILM FERRITE-FERROELECTRIC STRUCTURES FOR MICROWAVE PHASE SHIFTERS

Nikitin A.A., Ustinov A.B., Semenov A.A., Kalinikos B.A.

Saint Petersburg Electrotechnical University "LETI", St. Petersburg, Russia
and.a.nikitin@gmail.com

Rapidly growing interest to the artificial multiferroic structures is driven by a possibility to use them for various applications, in particular, to create frequency agile microwave devices. A distinctive feature of the multiferroic materials is dual electric and magnetic tunability of their physical properties (see e.g. [1,2]). One way to create structures with the multiferroic properties is to use multilayered structures composed of ferrite and ferroelectric materials. In these structures the multiferroic properties are due to a hybrid nature of their eigen-wave excitations named spin-electromagnetic waves (SEWs). They form as a result of electrodynamic coupling between the spin waves localized mainly in the ferrite layer and the electromagnetic waves propagating mostly in the ferroelectric layer [2]. Electric tuning of the SEW spectrum is possible due to a dependence of dielectric permittivity from bias electric field whereas magnetic tuning is provided by a dependence of magnetic permeability from bias magnetic field.

This work reports for the first time the experimental and theoretical investigations of spin-electromagnetic waves propagating in a thin-film multiferroic phase shifter composed on a slot-line. In contrast to earlier works, the spin-electromagnetic wave (SEW) in the present device is originated from the electrodynamic coupling of the electromagnetic wave localized mainly in the slot-line with the spin wave excited mostly in the ferrite film. For theoretical analysis of SEWs in such kind of structures a theory of their Eigen-wave spectrum was developed. Spectrum of SEW in the investigated structures was calculated and analysed. The range of electric and magnetic tunability of dispersion characteristic was investigated.

We fabricated multiferroic phase shifter composed by a slot-line waveguide with a ferroelectric film 2 μm thick and a single-crystal yttrium iron garnet film of thickness 13.6 μm . The performance characteristics of the phase shifter were measured. The device pass-band was 5.711-5.950 GHz. The minimum insertion loss of -20 dB was observed at 5.8 GHz. The electric field induced phase shift depended on the signal frequency. The maximum value of the phase shift variation of 54° was obtained for 30 kV/cm applied across the slot at the frequencies around 5.74 GHz.

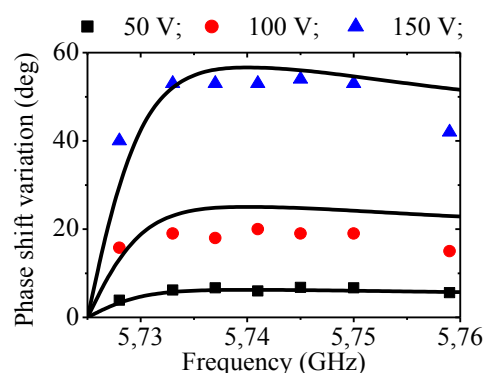


Fig. 1. Comparison of the experimental and the theoretical results.

Support by the Russian Foundation for Basic Research is acknowledged.

- [1] U. Ozgur, Ya. Alivov, H. Morkoc, *J. Mater. Sci.: Mater. Electron.*, **20** (2009) 911-952.
[2] V. E. Demidov, B. A. Kalinikos, P. Edenhofer, *J. Appl. Phys.*, **91** (2002) 10007-10016.

30PO-M-12

CHARGE ORDERING IN MULTIFERROIC LuFe_2O_4 : INFLUENCE OF DOPING AND ELECTRIC FIELD

Maslov D.A.^{1,2}, *Kudasov Yu.B.*^{1,2}

¹ Russian Federal Nuclear Center – VNIIEF, Sarov, Russian Federation

² SarFTI, National Research Nuclear University “MEPhI”, Sarov, Russian Federation

maslov_dem@mail.ru

Multiferroic LuFe_2O_4 is a hexagonal layered compound with variable valence of iron ions $\text{Fe}^{2+}/\text{Fe}^{3+}$ [1]. Then the mean valence is +2.5. Due to this feature ferroelectricity of this substance is given rise by charge ordering in contrast to common ferroelectrics where lattice distortion takes place. All iron sites are crystallographically equivalent and form triangular bilayers (W layers).

Below 500 K a two-dimensional charge order (2D-CO) appears, that is, the Fe^{2+} and Fe^{3+} ions form a 2D superstructure within individual W layers although the W layers remain uncorrelated between each other. This high-temperature 2D-CO is characterized by the wave vector $k = (1/3, 1/3)$ [2]. That is why a six-sublattice (6-SL) model of CO was proposed: in each layer of the W layers, two-thirds of all iron ions form the honeycomb structure with alternating Fe^{2+} and Fe^{3+} positions. A state of the other one-third has not been clearly identified [2]. At approximately 320 K a transition from the 2D-CO to three-dimensional charge order (3D-CO) takes place. It was supposed that in LuFe_2O_4 the W layers are stacked up in the ferroelectric order which causes the bulk ferroelectric state. But recent investigations [3] have cast doubt on the bulk nature of the ferroelectricity in LuFe_2O_4 assuming antiferroelectric arrangement of the W layers.

We have investigated charge ordering of LuFe_2O_4 by means of Ising model [4]. It is shown that a high-temperature ordered phase on a triangular bilayer (W layer) is a dimer partially disordered antiferroelectric (DPDA) state. The DPDA state is stable against a variation of interaction parameters in a wide range. It is also shown that 3D-CO can be stabilized by interbilayer interaction [4] (Fig. 1).

Properties of nonstoichiometric crystals of LuFe_2O_4 differ from common samples [5]. Behavior of this substance under electric field also should be investigated [5]. The developed Ising model of W layers can be generalized to include influence of doping and electric field into consideration. The results of treatment of generalized model are discussed.

The work was supported by the Russian Foundation for Basic Research (Project No. 13-02-01194).

[1] N. Ikeda, H. Ohsumi, K. Ishii et al., *Nature (London)*, **436** (2005) 1136.

[2] Y. Yamada, K. Kitsuda, S. Nohdo, and N. Ikeda, *Phys. Rev. B*, **62** (2000) 12167.

[3] D. Niermann, F. Waschkowski, J. de Groot et al., *Phys. Rev. Lett.*, **109** (2012) 016405.

[4] Yu.B. Kudasov, D.A. Maslov, *Phys. Rev. B*, **86** (2012) 214427.

[5] M. Angst, *Phys Status Solidi RRL*, (2013) 1-18.

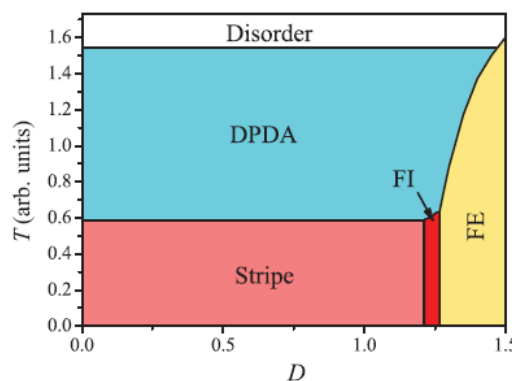


Fig. 1. Phase diagram of stacked W layers. D is an interbilayer coupling constant. FE, FI and Stripe are ferroelectric, ferrielectric and stripe phases correspondingly.

30PO-M-13

INFLUENCE OF DIFFERENT SPACERS ON THE PROPERTIES OF MULTILAYER STRUCTURES BASED ON $(\text{Co}_{41}\text{Fe}_{39}\text{B}_{20})_{33.9}(\text{SiO}_2)_{66.1}$ COMPOSITE

Kalinin Yu.E., Kashirin M.A., Sitnikov A.V.
Voronezh Technical State University, Voronezh, 394026, Russia
kalinin48@mail.ru

The authors report experimental data for the influence of different spacers on the electrical and magnetic performance of multilayer structures based on $(\text{Co}_{41}\text{Fe}_{39}\text{B}_{20})_{33.9}(\text{SiO}_2)_{66.1}$ composite are presented. Multilayer nanostructures made up of $(\text{Co}_{41}\text{Fe}_{39}\text{B}_{20})_{33.9}(\text{SiO}_2)_{66.1}$ composite layers with different spacers were obtained by ion-beam sputtering of two targets on a rotating substrate [1]. As a metallic component, readily amorphizable and well-studied $\text{Co}_{41}\text{Fe}_{39}\text{B}_{20}$ alloy was used. To deposit composite–semiconductor (metal) multilayer structures, a composite target and a semiconductor (metallic) target were applied. In the course of sputtering, a V-shaped screen was placed between the semiconductor target and the substrate. Numbers after curly brackets indicate the number of bilayers.

The dependence of the resistivity of the multilayer structures on the parameters of the layers was studied. It is found that the resistivity of the $\{[(\text{Co}_{41}\text{Fe}_{39}\text{B}_{20})_{33.9}(\text{SiO}_2)_{66.1}]/[\text{Si}]\}_{94}$, $\{[(\text{Co}_{41}\text{Fe}_{39}\text{B}_{20})_{33.9}(\text{SiO}_2)_{66.1}]/[\text{C}]\}_{46}$, $\{[(\text{Co}_{41}\text{Fe}_{39}\text{B}_{20})_{33.9}(\text{SiO}_2)_{66.1}]/[\text{Cu}]\}_{93}$, $\{[(\text{Co}_{41}\text{Fe}_{39}\text{B}_{20})_{33.9}(\text{SiO}_2)_{66.1}]/[\text{Bi}_2\text{Te}_3]\}_{101}$ heterostructures decreases by three to four orders of magnitude in the presence of a continuous spacer. Presumably, this is because the lower resistivity spacer has an effect on electrotransport. The resistivity of the $\{[(\text{Co}_{41}\text{Fe}_{39}\text{B}_{20})_{33.9}(\text{SiO}_2)_{66.1}]/[\text{SiO}_2]\}_{93}$, $\{[(\text{Co}_{41}\text{Fe}_{39}\text{B}_{20})_{33.9}(\text{SiO}_2)_{66.1}]/[\text{Sn}_{29}\text{Si}_{4.3}\text{O}_{66.7}]\}_{48}$, $\{[(\text{Co}_{41}\text{Fe}_{39}\text{B}_{20})_{33.9}(\text{SiO}_2)_{66.1}]/[\text{In}_{35.5}\text{Y}_{4.2}\text{O}_{60.3}]\}_{47}$ heterogeneous systems is comparable to that of the composite matrix, and therefore the influence of the spacer is more complicated: the $\rho(h)$ curve has a minimum.

The dependences of the real and imaginary parts of the complex magnetic permeability of superparamagnetic multilayer $(\text{Co}_{41}\text{Fe}_{39}\text{B}_{20})_{33.9}(\text{SiO}_2)_{66.1}$ films with different spacers on the thickness of the layers were taken at a frequency of 50 MHz. It was found that when a continuous spacer forms and the resistivity is on the order of 0.01 Ω m, the superparamagnetic state changes to a ferromagnetic one. These findings are associated with indirect exchange interaction between individual $\text{Co}_{41}\text{Fe}_{39}\text{B}_{20}$ ferromagnetic granules through conduction electrons in the spacer.

The $\{[(\text{Co}_{41}\text{Fe}_{39}\text{B}_{20})_{33.9}(\text{SiO}_2)_{66.1}]/[\text{Si}]\}_{94}$, $\{[(\text{Co}_{41}\text{Fe}_{39}\text{B}_{20})_{33.9}(\text{SiO}_2)_{66.1}]/[\text{C}]\}_{46}$, $\{[(\text{Co}_{41}\text{Fe}_{39}\text{B}_{20})_{33.9}(\text{SiO}_2)_{66.1}]/[\text{Cu}]\}_{93}$, $\{[(\text{Co}_{41}\text{Fe}_{39}\text{B}_{20})_{33.9}(\text{SiO}_2)_{66.1}]/[\text{Bi}_2\text{Te}_3]\}_{101}$ multilayer heterogeneous structures are promising materials for rf and microwave functional devices.

Support by the Russian Foundation for Basic Research (Grant N 13-02-97511-r-tsentra-a) is acknowledged.

[1] A.V. Sitnikov, *Al'ternat. Energ. Ekolog.*, **4** (2004) 28-30.

30PO-M-14

MAGNETOELECTRIC POLARIZATION OF PARAMAGNETIC $\text{HoGa}_3(\text{BO}_3)_4$ SINGLE CRYSTALS

Gudim I.A., Eremin E.V., Molokeev M.S., Temerov V.L., Volkov N.V.

L.V. Kirensky Institute of Physics, Russian Academy of Sciences, Siberian Branch, Krasnoyarsk, Russia
bezm@iph.krasn.ru

The origin of the magnetoelectric effect in multiferroic single crystals with the huntite structure ($\text{RM}_3(\text{BO}_3)_4$, where $\text{R} = \text{RE} + \text{Y}$ and $\text{M} = \text{Fe}, \text{Al}, \text{Ga}, \text{or Cr}$) is one of the urgent problems of modern physics of magnetic phenomena. These crystals [1] possess the noncentrosymmetric trigonal structure. Below the antiferromagnetic ordering temperature $T_N \approx (30\text{--}40)$ K, some of them, e.g. the ferroborate, exhibit spontaneous or/and magnetic-field-induced electric polarization. Recently, it has been established that the paramagnetic trigonal rare-earth alumoborates $\text{RAl}_3(\text{BO}_3)_4$ ($\text{R} = \text{Ho}, \text{Tm}, \text{or Er}$) [2] also exhibit the magnetoelectric polarization, which can exceed the values obtained earlier on ferroborates. The largest polarization value ($P \approx 4500 \mu\text{C}/\text{m}^2$) was obtained for $\text{HoAl}_3(\text{BO}_3)_4$.

In this work, we report the data on the magnetic and magnetoelectric properties of the $\text{HoGa}_3(\text{BO}_3)_4$ single crystal. In this compound, the system of small cations is presented by Ga^{3+} ions with a larger ionic radius as compared with Al^{3+} and different electronic structure. $\text{HoGa}_3(\text{BO}_3)_4$ single crystals were grown from bismuth trimolibdate-based fluxes. The crystal growth techniques used were described in detail in [3].

The magnetic and magnetoelectric properties were investigated on a PPMS-9 facility in the temperature range 3–300 K and magnetic fields up to 90 kOe. Magnetization of holmium galloborate crystals attains 30000 emu/mol, which is slightly lower than that of holmium alumoborate. The magnetoelectric polarization of the $\text{HoGa}_3(\text{BO}_3)_4$ crystals is $\sim 1000 \mu\text{C}/\text{m}^2$, which is second only to the value for holmium alumoborates. Thus, the behavior of the temperature and field dependences of magnetization and electric polarization is nearly invariable (Fig. 1).

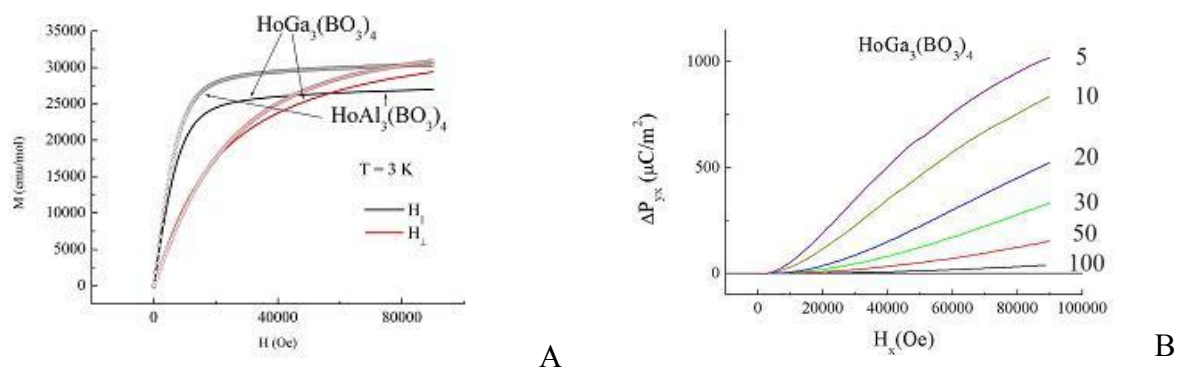


Fig. 1. (A) Field dependence of magnetization for the grown $\text{HoGa}_3(\text{BO}_3)_4$ single crystals in comparison with those for the $\text{HoAl}_3(\text{BO}_3)_4$ single-crystals. (B) Magnetoelectric polarization (P_{yx}) of $\text{HoGa}_3(\text{BO}_3)_4$.

The value of the magnetoelectric effect in $\text{HoGa}_3(\text{BO}_3)_4$ depends not only on the size and electronic structure of Ga^{3+} ions, but also on the conditions of heat treatment of the grown crystals.

The study was supported by the Russian Foundation for Basic Research, project no. 13-02-12442.

[1]. A.M. Kadomtseva, Yu.F. Popov, G.P. Vorob'ev, et al., *Low Temp. Phys.* **36**, (2010) 511.

[2]. K.-C. Liang, R.P. Chaudhury, B.Lorenz, et al., *J. Phys.: Conf. Ser.* **400** (2012) 032046.

[3]. I.A. Gudim, E.V. Eremin, and V.L. Temerov, *J. Crystal Growth* **312** (2010) 2427.

30PO-M-15

SCALING BEHAVIOR OF LOOP AREA, MAGNETIC REMANENCE, AND COERCIVITY IN THERMAL DEPENDENCE OF DOUBLE PEROVSKITE

$\text{Ba}_{1.7}\text{La}_{0.3}\text{FeMoO}_6$

Handoko Djati¹, Thanh Tran Dang¹, Nanto Dwi¹, Yu Seong-Cho¹, Oh Suhk Kun¹, Kim Dong-Hyun^{1}, Demyanov S.E.², Kalanda N.A.², Yarmdich M.V.², Kovalev L.V.²*

¹ Department of Physics Chungbuk National University, Cheongju 361-763, South Korea

² Scientific-Practical Research Centre of NAS of Belarus, BY-220072 Minsk, Belarus

*donghyun@chungbuk.ac.kr

We have detailed investigated the scaling behavior of loop area with respect to temperature for $\text{Ba}_{1.7}\text{La}_{0.3}\text{FeMoO}_6$ double perovskite compound. The hysteresis loop was performed on a vibrating sample magnetometer (VSM-Lakeshore 331) from below to critical temperature with fixed range applied field (0 – 10 kOe). Base on field dependence of magnetization, we observed that the loop area remain constant within the range below to near critical temperature then decrease abruptly at around critical temperature, exhibits scaling behavior with respect to temperature as shown in Fig. 1. The scaling exponent of magnetic remanence and coercivity field with respect to temperature are analyzed together. The result indicates a coexistence of loop area, magnetic remanence and coercivity field in $\text{Ba}_{1.7}\text{La}_{0.3}\text{FeMoO}_6$ double perovskite compound.

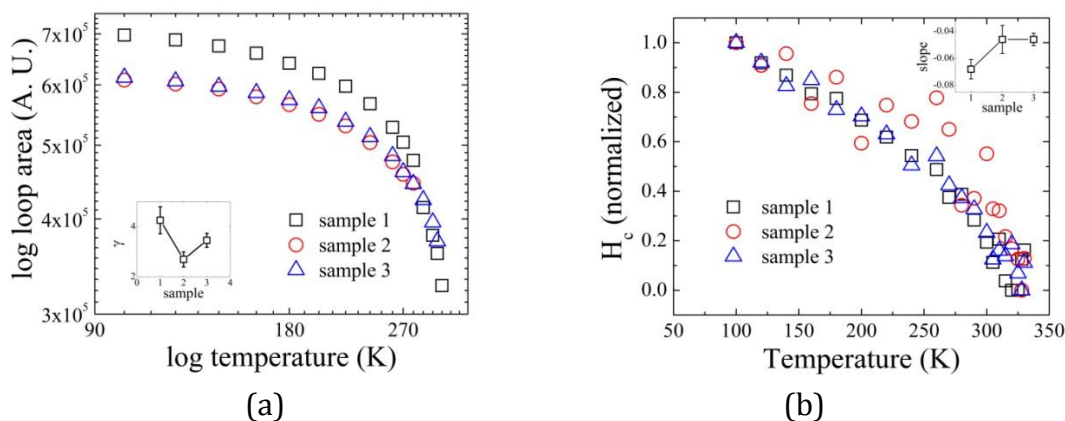


Fig. 1. Loop area (a) and coercivity (b) with respect to temperature for 3 different $\text{Ba}_{1.7}\text{La}_{0.3}\text{FeMoO}_6$ samples.

30PO-M-16

MAGNETIC PHASE TRANSITIONS IN Nd_{0.6}Dy_{0.4}Fe₃(BO₃)₄ FERROBORATE

*Zvyagina G.A.¹, Bilych I.V.¹, Zhekov K.R.¹, Zvyagin A.A.¹, Bludov A.N.¹, Pashchenko V.A.¹,
Gudim I.A.², Eremin E.V.²*

¹ B. Verkin Institute for Low Temperature Physics and Engineering, Kharkov, Ukraine

² L.V. Kirensky Institute for Physics, Siberian Branch of the Russian Academy of Sciences,
Krasnoyarsk, Russia
zvyagina@ilt.kharkov.ua

The rare-earth ferrobates RFe₃(BO₃)₄ (R=Y; La–Nd; Sm–Er) (space group R32) are of interest due to the coupling of the magnetic, electric and elastic subsystems that has been discovered there, specifically, multiferroic effects in some of them. The specific nature of their magnetic and magnetoelectric properties is due to the exchange interaction between the magnetic subsystems of the iron and rare-earth ions [1]. The magnetic structures realized in these crystals below Neel temperatures (T_N) are very diverse: depending on the type of R ion compounds can be easy-axis (Tb, Dy-ferrobates) or easy-plane (Nd, Sm-ferrobates) antiferromagnets, or spontaneously transferred from an easy-plane to an easy-axis state (Gd, Ho-ferrobates).

In binary compounds of the type Nd_{1-x}Dy_xFe₃(BO₃)₄ the contributions of the R ions to the magnetic anisotropy can be competitive with one another. Studies of the specific heat and magnetization [2] and our magnetoacoustic studies [3, 4] of Nd_{0.75}Dy_{0.25}Fe₃(BO₃)₄ crystal have shown that the restructuring of its magnetic structure does not reduce to a simple superposition of the features characteristic of the NdFe₃(BO₃)₄ and DyFe₃(BO₃)₄. In this compound we have detected new phase transitions with temperature and in an external magnetic field. To our mind, these magnetic phase transitions can be related to spin reorientation of the several magnetic sublattices of this magnetic material.

Low temperature studies of elastic and magnetic characteristics of the single crystal Nd_{0.6}Dy_{0.4}Fe₃(BO₃)₄ have been performed. A transition to the antiferromagnetically ordered state of the magnetic subsystem has been manifested in the temperature behavior of the velocity and attenuation of acoustic modes.

Two following each other spin-reorientation phase transitions which reveal themselves as anomalies in the behavior of elastic and magnetic characteristics of the crystal in the external magnetic field applied along the axis of the trigonal symmetry of the crystal have been discovered. The phase H-T diagram for H || C₃ has been constructed.

These results permitted to draw the conclusion that this compound, analogous to the Nd_{0.75}Dy_{0.25}Fe₃(BO₃)₄, exhibits several magnetic phases and, correspondingly, several phase-transition lines in the H-T phase diagram.

[1] A.M. Kadomtseva, Yu.F. Popov, G.P. Vorob'ev, et al, *Fiz. Nizk. Temp.* **36** (2010) 640 [*Low Temp. Phys.* **36** (2010) 511].

[2] I.A. Gudim, E.V. Eremin, and V.L. Temerov, *J. Cryst. Growth* **312** (2010) 2427.

[3] G.A. Zvyagina, K.R. Zhekov, A.A. Zvyagin, I.V. Bilych, L.N. Bezmaternykh, and I.A. Gudim, *Fiz. Nizk. Temp.* **36** (2010) 376 [*Low Temp. Phys.* **36** (2010) 296].

[4] G.A. Zvyagina, K.R. Zhekov, A.A. Zvyagin, I.A. Gudim, and I.V. Bilych, *Fiz. Nizk. Temp.* **38** (2012) 571 [*Low Temp. Phys.* **38** (2012) 446].

30PO-M-17

COMPLEX DOMAIN WALLS IN MULTIFERROICS

Gareeva Z.V.¹, Zvezdin A.K.², Iniguez J.³, Dieguez O.³

¹ Institute of Molecular and Crystal Physics, Ufa, Russia

² A.M. Prokhorov General Physics Institute, Moscow, Russia

³ Institut de Ciencia de Materials de Barcelona (ICMAB-CSIC), Bellaterra, Spain

gzv@anrb.ru

Domain engineering is intensively developing branch of the modern technology looking for the novel functional materials. The best candidates are multiferroics combining ferroelectricity and magnetism. In order to control and manipulate these properties is required to explore magnetic and ferroelectric configurations, understand the mechanisms responsible for order parameters interaction, and clarify the role of magnetoelectricity resulting in the clamping of ferroelectric and magnetic domains.

In the present work we pursue a goal of complex investigation of domain structures realizing in epitaxial thin BiFeO₃ films [1, 2]. As was shown in [3, 4] the cycloidal structure inherent to BiFeO₃ can be suppressed in thin BiFeO₃ films dependent on the growth conditions. Based on the atomistic and phenomenological approaches we explore the magnetization across the 180°, 109°, 71° ferroelectric domains. Fig.1 illustrates the distribution of magnetic moments across 180° ferroelectric wall. We show that magnetic domain walls in multiferroics are more complicated comparing to the walls in magnetic materials. The magnetization vector deviates from the spin rotational plane in a vicinity of ferroelectric domain walls due to the coupling between magnetic and ferroelectric parameters. It substantiates experiments revealing magnetization close to ferroelectric domain boundaries [1] and confirms the fact that ferroelectric walls in BiFeO₃ produce magnetization.

We show that the type of magnetic walls depends on ferroelectric domain patterning. 90° magnetic walls are realized nearby 109° and 71° ferroelectric walls, the distribution of magnetization vector through the wall in these two cases differ insignificantly. Magnetization vector conserves its position in the magnetic domains accompanying 180° ferroelectric domains but between them spins deviate from an equilibrium position due to the Dzyaloshinskii – Moriya interaction leading to the appearance of domain wall with non-trivial spin configuration.

Magnetism in multiferroics is a contentious subject.

Our findings indicate the novel mechanism of domain origin giving rise to magnetization in multiferroics.

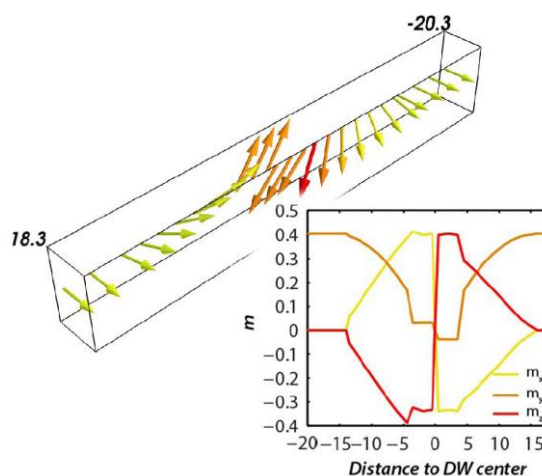


Fig. 1. Distribution of magnetization vector in 180° ferroelectric domain wall.

- [1] L.Martin et al. *Nanoletters*. **8** (2008) 2050 – 2055.
- [2] Q. He et al. *Nature Commun.* **2** (2011) 1 – 5.
- [3] J. Li et al. *Appl. Phys. Lett.* **84** (2004) 5261 – 5263.
- [4] D. Sando et al. *Nature Materials* **12** (2013) 641 – 646.

30PO-M-18

MAGNETIC AND MAGNETOELASTIC PROPERTIES OF $\text{TmAl}_3(\text{BO}_3)_4$ Begunov A.I.¹, Demidov A.A.¹, Volkov D.V.², Gudim I.A.³, Eremin E.V.³, Boldyrev K.N.⁴¹ Bryansk State Technical University, Bryansk, Russia² M.V. Lomonosov Moscow State University, Moscow, Russia³ Kirensky Institute of Physics SB RAS, Krasnoyarsk, Russia⁴ Institute of Spectroscopy RAS, Troitsk, Moscow region, Russia

demandr@yandex.ru

The borates with a single magnetic subsystem $\text{RAl}_3(\text{BO}_3)_4$ (alumoborates) exhibit a combination of good luminescent and clearly pronounced nonlinear optical properties as well as recently discovered strong multiferroicity. A giant magnetoelectric polarization in $\text{HoAl}_3(\text{BO}_3)_4$ achieves the value $\Delta P_{ba}(B_a) \approx -5240 \mu\text{C}/\text{m}^2$ [1]. In $\text{TmAl}_3(\text{BO}_3)_4$ a strong magnetoelectric effect comparable with that in isostructural ferrobates $\text{RFe}_3(\text{BO}_3)_4$ has been found [2]. Magnetostriction and thermal expansion of $\text{TmAl}_3(\text{BO}_3)_4$ were experimentally studied in [2] as well.

In this work the experimental and theoretical investigations of the field (up to 9 T) and temperature dependences of magnetization, magnetostriction and thermal expansion of $\text{TmAl}_3(\text{BO}_3)_4$ have been performed. The analysis of the measured transmission spectra allows us to identify the ground multiplet energy levels of the Tm^{3+} ion: 0, 27, 73, 104, 168, 202, 315, 390, and 460 cm^{-1} . In our calculations we used a theoretical approach which has been successfully applied to describe the magnetic and magnetoelastic properties of $\text{HoAl}_3(\text{BO}_3)_4$ [1, 3] and $\text{HoGa}_3(\text{BO}_3)_4$ [4]. Good agreement of experimental and calculated temperature dependences of the magnetic susceptibility $\chi_{c,\perp c}(T)$ and magnetization curves $M_{c,\perp c}(B)$ was achieved (Fig. 1). A difference between $\chi_c(T)$ which was measured by us and $\chi_c(T)$ from [2] has been found for $T < 50 \text{ K}$. Calculated field and temperature dependences of the multipole moments of the Tm^{3+} ion in $\text{TmAl}_3(\text{BO}_3)_4$ made it possible to describe the magnetostriction data from [2]. The low-temperature anomalies of thermal expansion caused by the change in the 4f electron shell of the rare-earth ion are described.

This work was supported by the RFBR (project no. 13-02-12442 ofi_m2) and the Grant of the President of the Russian Federation MK-1700.2013.2 (B.K.N.).

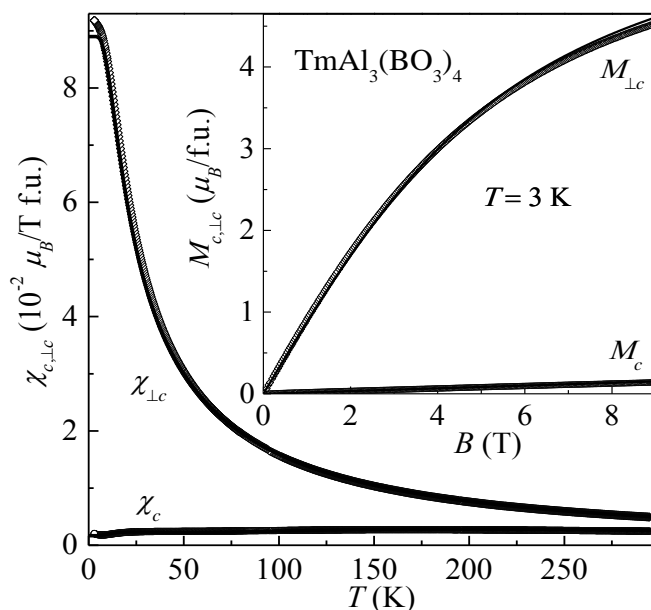


Fig. 1. The temperature dependences of the $\chi_{c,\perp c}(T)$ at $B = 0.1 \text{ T}$ and $M_{c,\perp c}(B)$ (inset).

- [1] A.I. Begunov, A.A. Demidov, I.A. Gudim et al., *JETP Lett.*, **97** (2013) 528-534.
 [2] R.P. Chaudhury, B. Lorenz, Y.Y. Sun, et al., *Phys. Rev. B*, **81** (2010) 220-402.
 [3] A.I. Begunov, D.V. Volkov, A.A. Demidov, *Phys. of the Sol. St.*, **56** (2014) 511-517.
 [4] N.V. Volkov, I.A. Gudim, E.V. Eremin et al., *JETP Lett.*, **99** (2014) 67-75.

30PO-M-19

MAGNETIC STRUCTURE OF MULTIFERROIC COMPOUNDS Ba₃AFe₃Si₂O₁₄ (A = Sb, Nb, Ta) AS SEEN BY NMR AND MOESSBAUER SPECTROSCOPY

Tkachev A.V.¹, Gippius A.A.¹, Lyubutin I.S.²

¹ Faculty of Physics, M.V. Lomonosov Moscow State University, 119991, Moscow, Russia

² A.V. Shubnikov Institute of Crystallography, 119333, Moscow, Russia

av.tkachev@physics.msu.ru

The langasite (La₃Ga₅SiO₁₄) family materials attract a great interest due to their piezoelectric properties with better electromechanical coupling and weaker impedance than quartz. A strong interest is attracted to the langasite-type compounds containing magnetic ions: coexistence of electric and magnetic order parameters in these materials would provide a new type of multiferroics. Recent neutron diffraction studies of Ba₃NbFe₃Si₂O₁₄ revealed the effect of spin rotation related to magnetic chirality in the helical magnetic structure in the magnetically ordered phase [1].

Initial study of the magnetic properties of iron-containing langasite compounds Ba₃AFe₃Si₂O₁₄ (A = Sb, Nb, Ta) was performed by the Mössbauer spectroscopy [2,3]. Temperature dependences of the hyperfine magnetic fields H_{hf} at iron nuclei and the T_N values have been obtained for these compounds. Two magnetically nonequivalent Fe sites were revealed in the compounds with A = Nb and Ta, and the Fe spins reorientation effect was found in the magnetically ordered state.

Here we present the further study of the Ba₃AFe₃Si₂O₁₄ samples by zero-field (ZF) NMR spectroscopy at ⁵⁷Fe nuclei and field-sweep NMR spectroscopy at ⁵⁷Fe and ¹²¹Sb nuclei. The line shape of ZF NMR provides an exact profile of the internal hyperfine field H_{hf} distribution at ⁵⁷Fe nuclei. Measurements at 4.2 K revealed complex structure of such distribution (Fig.1). In all compounds the magnetic field profile deviates from simple model of two independent peaks. Probably, this effect can be attributed to the spin-density wave in the helical magnetic structure. Field-sweep NMR spectroscopy data is in agreement with ZF NMR observations.

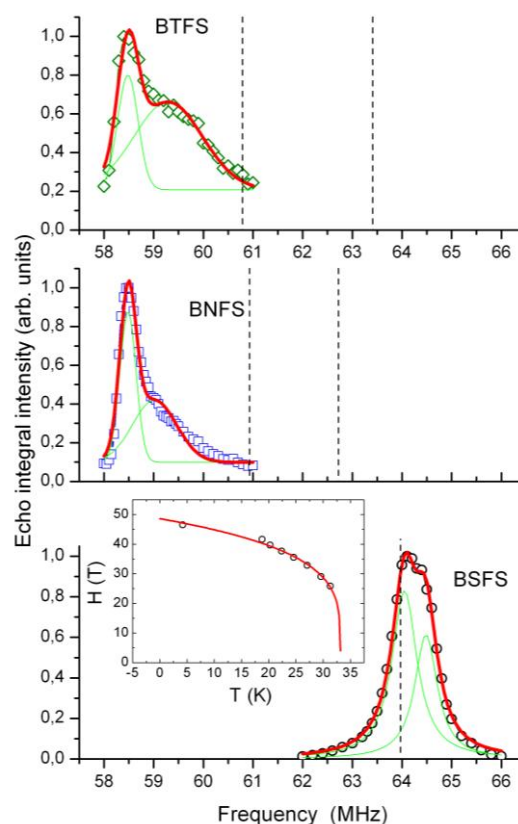


Fig. 1. Zero-field NMR spectra of ⁵⁷Fe in Ba₃AFe₃Si₂O₁₄ (BAFS) samples at 4.2 K. Vertical dashed lines correspond to the Mössbauer data [2]. Inset: temperature dependence of intrinsic field for BSFS.

data is in agreement with ZF NMR

Support by the Russian Foundation for Basic Researches (Grants #14-02-00483) is acknowledged.

[1] K. Marty *et al.*, *Phys. Rev. Lett.*, **101** (2008) 247201.

[2] I.S. Lyubutin *et al.*, *Phys. Rev. B*, **84** (2011) 214425.

[3] I.S. Lyubutin *et al.*, *Euro. Phys. Lett.*, **90** (2010) 67005.

30PO-M-20

INFRARED SPECTROSCOPY OF MULTIFERROIC o-DyMnO₃

Kashchenko M.A.^{1,2}, *Klimin S.A.*¹

¹ Institute of Spectroscopy, RAS, Moscow, Troitsk, Russia

² Moscow Institute of Physics and Technology (State University), Dolgoprudnyi, Russia
kacmisha@gmail.com

The rare-earth (RE) manganites $R\text{MnO}_3$ show a strong interplay between lattice, magnetic, and charge degrees of freedom. Numerous multiferroic features found in manganites, such as a flop of the direction of the spontaneous polarization in a magnetic field [1] and electromagnons, make these compounds very interesting and promising from the point of view of both fundamental investigation and applications. The present study focuses on the infrared spectra of the orthorhombic o-DyMnO₃, though there exists also another structural form, the hexagonal one, h-DyMnO₃. Energies of the crystal-field (CF) levels of Dy³⁺ ion in o-DyMnO₃ for ⁶H_{13/2} multiplet only and the splitting $\Delta_0 = 30 \text{ cm}^{-1}$ of the Dy³⁺ ground Kramers doublet were reported in Ref. [2]. In this study, we show that the f-f spectral transitions of Dy³⁺ are sensitive to phase transitions at $T_N^{\text{Mn}} = 39\text{K}$, $T_{\text{FE}} = 19\text{K}$, and $T_{\text{Dy}} = 6,5\text{K}$ and that the splitting Δ_0 does not exceed 10 cm^{-1} and is observed only below T_{Dy} .

Optical transmittance spectra of oriented single-crystalline samples of 100 and 600 μm thickness and of a polycrystalline sample of DyMnO₃ mixed with KBr and pressed into a tablet were investigated over a wide spectral ($1000\text{-}8000 \text{ cm}^{-1}$) and temperature (3.5-300 K) ranges. The absorption spectra show relatively narrow lines of transitions from the ground ⁶H_{15/2} to the excited ⁶H_{13/2}, ⁶H_{11/2}, ⁶H_{9/2}+⁶F_{11/2}, and ⁶H_{7/2}+⁶F_{9/2} multiplets of the Dy³⁺ ions and a broad absorption band originating from Mn³⁺ d-d transitions. Fig. 1 displays transmission spectra in the region of one of the spectral lines. Spectral position of this line demonstrates peculiarities at T_N^{Mn} and T_{Dy} . Similar peculiarities are seen in temperature dependences of positions and half widths of other spectral lines. The nature of phase transitions is discussed.

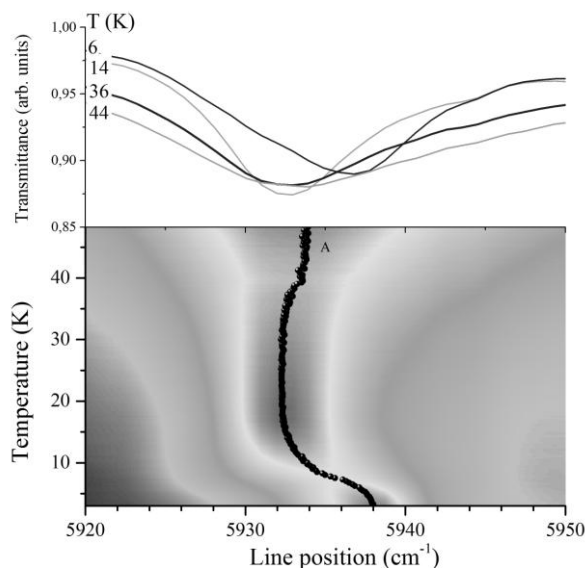


Fig. 1. Transmission spectra of DyMnO₃ in the region of one of the spectral lines of the ⁶H_{15/2}→⁶H_{11/2} transition at different temperatures and an intensity map for this line, together with the temperature dependence for the maximum position of the line.

Support by the Russian Academy of Sciences under the Program for Basic Research is acknowledged.

[1] T. Goto, T. Kimura, G. Lawes, A. P. Ramirez, Y. Tokura, *Phys. Rev. Lett.*, **92** (2004) 257201

[2] S. Jandl, S. Mansouri, A.A. Mukhin, V. Yu. Ivanov, A. Balbashov, M.M. Gospodino, V. Nekvasil, M. Orlita, *Journal of Magnetism and Magnetic Materials*, **323** (2011) 1104-1108.

30PO-M-21

NUCLEAR MAGNETIC RESONANCE IN HELIMAGNETS

Tankejev A.P., Borich M.A., Smagin V.V.

Institute of Metal Physics, Ural Division of RAS, Ekaterinburg, Russia

tankeyev@imp.uran.ru

Currently, considerable attention is paid to investigations of magnets with inhomogeneous ground state and, in particular, magnets with the chiral helimagnetic order of magnetic moments. The enhanced interest in this class of substances is due to their unusual fundamental properties, as well as due to the prospects of application of these properties in spintronics, magnetic memory, and sensorics. One specific feature of these substances is that they allow for the existence of the Dzyaloshinskii-Moriya (DM) interaction. The competition between the isotropic exchange interaction and DM interaction leads to the formation of the so-called long-period helical structure. A magnetic field applied perpendicular to the helical axis destabilizes the ground state helical ordering into a soliton lattice, which is called as chiral magnetic soliton lattice.

The structure and the stability of the ground state of such a magnet can be studied by analyzing the spectrum of spin excitations against its background, which can in turn be studied through the interaction of these excitations with the system of nuclear spins. The system of nuclear spins under the conditions of nuclear magnetic resonance (NMR) is a unique source of information on the local spatial distribution of electron and spin density in a magnet. The spectrum of elementary spin excitations of the system under study has two distinctly pronounced branches: besides with the usual spin-wave excitations (call them d magnons), there are excitations localized on solitons (call them w magnons) [1].

In this study specific features of nuclear magnetic resonance (NMR) of such systems have been studied. Within the spin-wave approximation, the following basic local characteristics of the NMR of such structure have been calculated: the NMR frequency, the frequency shift, the tensor of enhancement coefficients and the line broadening. In addition, the field and temperature dependences of these characteristics have been investigated. The magnetic resonance susceptibility of the electron-nucleus spin system has been calculated; the integral shape of the NMR absorption line has been analyzed. The problem of the evolution of the NMR absorption line upon the change in magnitude of the external magnetic field has been solved [2].

For the first time, the characteristic properties of the Suhl-Nakamura interaction (SNI) between nuclear spins via virtual spin waves in a chiral helimagnet are studied as a function of the external magnetic field. The calculations take into account the additive contributions of both branches of spin excitations in the SNI. It is shown that the amplitude of the SNI can oscillate and even grow depending on magnetic field values. The local NMR line width determined by the SNI was calculated.

The obtained results can be used in the study of the ground state of the new materials with modulated magnetic structure (in the case of cubic or uniaxial anisotropy), characteristic features of rearrangement of its structure in the vicinity of phase transitions and high-frequency magnetic properties [3-5].

- [1] A.P.Tankejev, M.A.Borich, V.V.Smagin et.al. *Fiz.Metallov i Metallovedenie*, **115**(2014), 248-259.
- [2] A.P.Tankejev, M.A.Borich, V.V.Smagin et.al. *Fiz.Metallov i Metallovedenie*, **115**,(2014), 455-466.
- [3] N.J. Ghimire, M.A., McGuire et.al. *Phys.Rev. B*, **87** (2013) 104403.
- [4] Y .Togava , T. Koyama et.al. *Phys. Rev.Lett.* **108** (2012) 107202.
- [5] F.B.Mushenok, *Eur.Phys.J.B*, **86** (2013) 342.

30PO-M-22

IMPROVING ONE'S UNDERSTANDING OF MAGNETIC PROPERTIES OF $\text{SmFe}_3(\text{BO}_3)_4$ BY MEANS OF SPECTROSCOPIC DATA

Chukalina E.P.¹, Erofeev D.A.^{1,2}, Malkin B.Z.³, Bezmaternykh L.N.⁴, Gudim I.A.⁴, Popova M.N.¹

¹ Institute of Spectroscopy, Russian Academy of Sciences, Troitsk, Moscow, Russia

² Moscow Institute of Physics and Technology (State University), Dolgoprudni, Moscow, Russia

³ Kazan (Privolzhsky) Federal University, Kazan, Russia

⁴ Kirenskii Institute of Physics, Siberian Branch of RAS, Krasnoyarsk, Russia

kinson@mail.ru

$\text{SmFe}_3(\text{BO}_3)_4$ crystallizes in the huntite-type non-centrosymmetric trigonal structure (S.G. R32). This compound is a member of the family of multiferroics $\text{RFe}_3(\text{BO}_3)_4$ ($\text{R} = \text{Y}, \text{La-Lu}$) which demonstrate a vast variety of dielectric, magnetic, magnetoelectric, and optical properties, depending on different R elements. That is why they are interesting from both application and fundamental points of view. According to the magnetic susceptibility, spectroscopic, and neutron diffraction data, $\text{SmFe}_3(\text{BO}_3)_4$ orders antiferromagnetically at $T_N \approx 33$ K into an easy-plane structure [1-3]. $\text{SmFe}_3(\text{BO}_3)_4$ and $\text{NdFe}_3(\text{BO}_3)_4$ are the only iron borates with a purely easy-plane magnetic structure. The colossal magnetodielectric effect and noticeable spontaneous electric polarization were observed in $\text{SmFe}_3(\text{BO}_3)_4$ [2]. To explain magnetic and magnetoelectric properties of $\text{SmFe}_3(\text{BO}_3)_4$, the crystal-field parameters for Sm^{3+} and parameters of the exchange interaction between samarium and iron ions are necessary. These can be obtained from an analysis of spectroscopic data. We have performed the optical absorption study of $f-f$ transitions in $\text{SmFe}_3(\text{BO}_3)_4$ and crystal-field calculations, based on optical data.

Single crystals of samarium iron borate were grown by the flux method. Polarized absorption spectra were measured in the temperature range from 5 to 300 K in the spectral region 1500-25000 cm^{-1} using a Fourier-transform spectrometer Bruker IFS 125HR. The energies, symmetry properties, and the exchange splittings of the crystal-field levels of the ground and 17 excited multiplets of the Sm^{3+} ion were determined from the spectra. The crystal-field parameters and the parameters of the $f-d$ exchange interaction between the nearest iron and samarium ions, and of the exchange interaction between the nearest iron ions were found. The obtained parameters were used to simulate the magnetic properties of $\text{SmFe}_3(\text{BO}_3)_4$ [4].

In addition, we investigated the transmission of a plane-parallel sample of $\text{SmFe}_3(\text{BO}_3)_4$ for the light polarized along the c -axis of the crystal and perpendicular to it. The temperature dependences of the positions of interference maxima in the middle and near infrared regions exhibit pronounced features at T_N and a strong shift below this temperature, which is in agreement with earlier observed colossal magnetodielectric effect.

Support by the Russian Foundation for Basic Research (Grant №13-02-00787) is acknowledged.

- [1] E.P. Chukalina, M. Popova, L.N. Bezmaternykh, I.A. Gudim, *Phys.Lett.A* **374** (2010) 1790.
 [2] A.A. Mukhin, G.P. Vorob'ev, V.Yu. Ivanov, A.M. Kadomtseva, A.S. Narizhnaya, A.M. Kuz'menko, Yu.F. Popov, L.N. Bezmaternykh, I.A. Gudim, *JETP Lett.*, **93** (2011) 275.
 [3] C. Ritter, A. Pankrats, I. Gudim, A. Vorotynov, *J. Phys.: Condens.Matter* **24** (2012) 386002.
 [4] M.N. Popova, E.P. Chukalina, B.Z. Malkin, D.A. Erofeev, L.N. Bezmaternykh, I.A. Gudim, *JETP* **118** (2014) 111.

30 June

Monday

17:30-19:00

poster session

30PO-P

**“Soft and Hard
Magnetic Materials”**

30PO-P-1

MICROSTRUCTURE AND MAGNETIC PROPERTIES OF Fe-Co-Ni-Al-Si-Nd MELT-SPUN RIBBONS

Menushenkov V.P.¹, Gorshenkov M.V.¹, Savchenko E.S.¹

¹ National University of Science and Technology “NITU MISiS”, Moscow, Russia
menushenkov@gmail.com

The Alnico 5 alloy is known as hard magnetic materials whose coercive force is $H_c \approx 800$ Oe. The magnetic hardness of as-cast Alnico magnets gain as results of supersaturated solid solution decomposition in two isomorphous cubic phases representing solid solutions based on Fe-Co (β_1 -phase) and Ni-Al (β_2 -phase). The optimal microstructure is formed when as-cast alloys are subjected to a special heat treatment. High H_c is related with the shape anisotropy of strongly magnetic β_1 -phase precipitates in weakly magnetic matrix β_2 -phase. Recently [1] the behavior of thin Alnico films produced by magnetron sputtering on Si substrates were studied. The heat treatment of Alnico films in the range of 600–900°C gave a room temperature coercivity of 6.5 kOe after annealing at 800-900°C. Such enormous coercivity was achieved due to Si diffusion into the films and a new magnetically hard Fe-Co-Si-based phase with BCT structure had been formed.

In the present work, we studied the structural, microstructural and magnetic properties of Fe-Co-Ni-Al-Si-Nd melt-spun ribbons. Microcrystalline Alnico 5-based alloy with the nominal composition $Fe_{43.2}Co_{19.7}Ni_{11.2}Al_{11.8}Cu_{2.3}Si_{11}Nd_{0.8}$ was prepared by melt-spinning. The thickness of the ribbons was 30–40 μm . X-ray diffraction analyses were performed using x-ray diffraction on a Rigaku X-ray diffractometer with Co $K\alpha$ radiation and graphite monochromator. The thin foils were examined by JEM-1400 TEM with high tension 120 kV. Detailed studies of the phase composition, microstructure and magnetic properties of the ribbons subjected to isothermal annealing at 600°C for 15 min were performed. Transmission electron microscopy investigations of as-quenched and annealed ribbons have revealed the presence of spherical precipitates of Nd-rich phase ($NdCo_4Al$ type) decorating grain boundaries and very fine Si-rich precipitates inside the grains with size of 0.5–3 μm . The annealing at 600°C led to the coarsening of both types of precipitates and decomposition of solid solution by formation of modulated microstructure inside the grains. The electron diffraction patterns with zone axis [001] of as-prepared rapidly solidified ribbons correspond to disordered A2 phase (Fe-based solid solution) and the coherent long-period phase precipitation. The dark-field image from a superlattice reflection 010 of the second phase showed a modulated microstructure composed of alternate precipitates of two phases which had been formed when annealing.

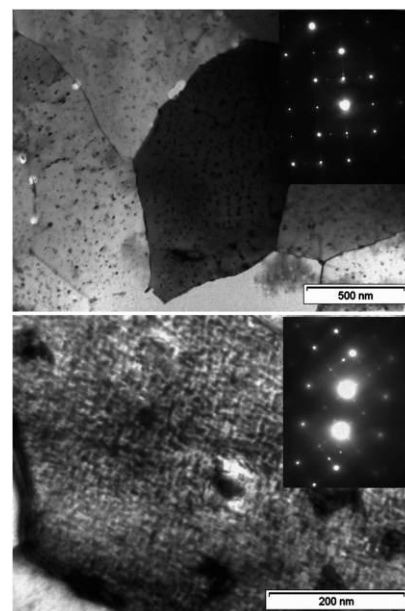


Fig. 1. TEM micrograph of as prepared ribbon upper and annealed at 600°C bottom

[1] O. Akdogan, G. C. Hadjipanayis. *Journal of Physics: Conference Series* **200** (2010) 072001.

30PO-P-2

MONTE CARLO SIMULATION OF MAGNETIC PHASE DIAGRAMS OF RARE-EARTH AMORPHOUS ALLOYS

Bondarev A.V., Ozherelyev V.V., Bataronov I.L., Barmin Yu.V.

Voronezh State Technical University, Voronezh, Russia

bondarev@vmail.ru

Using the Monte Carlo method in the frame of the Heisenberg model, the computer simulation of magnetic properties of Re-Tb and Re-Gd amorphous alloys was carried out. The temperature dependencies of spontaneous magnetization, Edwards–Anderson order parameter, magnetic susceptibility and specific heat were calculated.

The magnetic phase diagrams for pure amorphous Tb and for the Re-Tb amorphous alloys were constructed. The model Hamiltonian contained two terms responsible for nearest-neighbour exchange interaction between the Tb ions with the mean value J_0 and for random single-ion anisotropy D . For pure amorphous Tb the dependence of the temperature of the spin-glass-like transition T_f on the D/J_0 ratio was calculated. Thus, the magnetic phase diagram for an amorphous magnet with random anisotropy in the $D/J_0 - T$ coordinates was constructed which allows one to determine the phase state of the system in the dependence on temperature and the anisotropy constant D .

For the models of the Re-Tb amorphous alloys, the spin-glass-like phase transition was also observed. With increasing concentration of Tb atoms, the transition temperature linearly increases, which is in a good agreement with the experimental results. The spin-glass transition is observed only above the percolation threshold in this system, i.e. at $x > 13$ at. % Tb.

The magnetic phase diagrams for pure amorphous Gd and for the Re-Gd amorphous alloys were also constructed. The model Hamiltonian contained two terms responsible for ferromagnetic exchange interaction J_1 between the nearest-neighbour Gd ions and for antiferromagnetic exchange interaction J_2 between the Gd ions that were in the second coordination sphere. For pure amorphous Gd the dependence of the temperature of the spin-glass transition T_f on the J_1/J_2 ratio was calculated. Thus, the magnetic phase diagram for an amorphous magnet with competition of exchange interactions of different signs in the $J_1/J_2 - T$ coordinates was constructed which allows one to determine the phase state of the system in the dependence on temperature and the value of the exchange integral in the second coordination sphere J_2 .

For the models of the Re-Gd amorphous alloys, the spin-glass phase transition was also observed. With increasing concentration of Gd atoms, the spin-glass transition temperature linearly increases, which is in a good agreement with the experimental results.

For all the models studied above, the magnetization curves, hysteresis loops, remanent magnetization, coercive field, spin-spin correlation functions at different temperatures are also calculated. The magnetization relaxation after switching-off the external magnetic field was also studied. Our results qualitatively agree with the experimental results obtained for amorphous alloys based on rare-earth metals.

30PO-P-3

HIGH TEMPERATURE PROPERTIES OF CoFe/FeNi and Fe/FeNi BIPHASE MICROWIRES

Iglesias I.¹, Rodionova V.^{1,2}, Kammouni R.E.³, Vazquez M.³

¹ Immanuel Kant Baltic Federal University, Kaliningrad, Russia

² National University of Science and Technology "MIS&S", Moscow 119049, Russia

³ Materials Science Institute of Madrid, CSIC, Madrid, Spain

The magnetization process of biphasic microwires has been investigated along the last few years at room temperature. While most of devices are envisaged to work around room temperature, technological applications can in principle be extended to a much wider range of temperatures, particularly above room temperature [1]. In this regard, it is important to analyze in further detail the high temperature dependence of magnetic properties (saturation magnetization, hysteresis loops shape, susceptibility, coercivity) of biphasic magnetic microwires, which has been the objective of the present work. The ferromagnetic biphasic amorphous microwires were prepared by combined quenching & drawing and electroplating techniques [2]. Using first method we prepared the glass-coated microwires with compositions: $(\text{Co}_{0.94}\text{Fe}_{0.06})_{72.5}\text{Si}_{12.5}\text{B}_{15}$ ($\lambda_S \sim 0$, λ_S – saturation magnetostriction constant) and $\text{Fe}_{77.5}\text{Si}_{7.5}\text{B}_{15}$ ($\lambda_S > 0$). The diameters of the metallic core were $d=8\mu\text{m}$ and $d=12\mu\text{m}$, respectively. Then a second (external) magnetically soft FeNi phase was electroplated onto the single microwires. The thicknesses of the FeNi shell were $t_{\text{FeNi}}=1-4\mu\text{m}$ (t_{FeNi} was controlled by the electroplating time) [2]. The samples were 4 mm length. The magnetic properties for both types of microwires were analyzed as a function of temperature in the range from 295 K to 1200 K in a Vibrating Sample Magnetometer (Lake Shore) under argon atmosphere.

The biphasic microwires exhibit two-steps hysteresis loops at room temperature, each of them corresponds to respective remagnetization process of the phases: of the core (take place in small magnetic field) and of the shell (take place in higher magnetic field). When the temperature increase the steps became smaller and disappeared after the reaching of the Curie temperature of the core $T_c=700\text{K}$. The temperature dependence of magnetic moment under applied magnetic field of 100 Oe for Fe/FeNi microwire with the thicknesses of the shell of $1\mu\text{m}$ is depicted in the Figure. The magnetic moment decreases with temperature from 300 to 700K (that corresponds to the Curie temperature of the core), after $T=775\text{K}$ starts to increase again and after $T=800\text{K}$ decreases until $T=1200\text{K}$. Analysis of the magnetization process of each phase in each measuring temperature region has been performed.

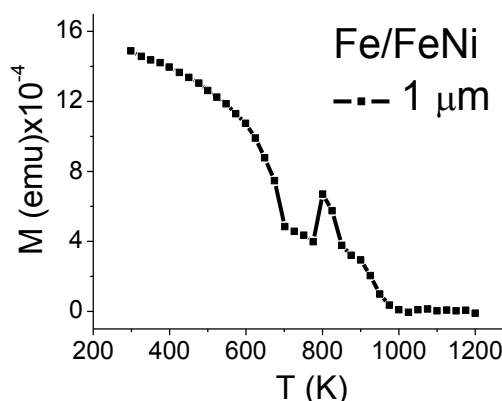


Figure. Temperature dependence for Fe/FeNi microwires with $t_{\text{FeNi}}=1\mu\text{m}$ in the temperature range from 295K to 1200K.

[1] M. Vazquez, H. Chiriac, A. Zhukov, L. Panina and T. Uchiyama, *Phys. Stat. Sol. A*, (2010) 1-9.

[2] K. Pirota, M. Hernandez-Velez, D. Navas, A. Zhukov, M. Vazquez, *Adv. Funct. Mater.* **14** (3) (2004) 266–268.

30PO-P-4

A NEW METHOD OF INTEGRAIN EXCHANGE INTERACTION ENERGY DETERMINATION IN NANOSTRUCTURED ALLOYS WITH SPONTANEOUS SPIN-REORIENTATION TRANSITION

Volegov A.S., Kudrevatykh N.V.
UrFU, Yekaterinburg, Russia
Nikolai.Kudrevatykh@usu.ru

The “nanocomposite” or “exchange-spring” magnets are composed of intimately combined nanoscaled hard and soft magnetic phases that are exchange coupled at the mutual interface. Such systems are considered as alternative for rare earth free magnets due to both a moderate cost and improved hard magnetic properties. Investigation of exchange interaction between neighbour nanograins is the first step toward to moderate the permanent magnet with high energy product. But there is too little information about intergrain exchange energy density (IEED) in the literature [1]. The aim of this work is development of an independent method for IEED estimation.

Despite of negative role of the spontaneous spin-reorientation transition in Nd-Fe-B nanostructured alloys in hysteresis loop squareness and maximal energy product at low temperatures this transition can be exploit for the quantitative estimation the IEED between neighbour grains in Nd-Fe-B type nanostructured alloys, such as MQP-B+ type. The idea is based on comparison of intergrain exchange interaction energy and the energy of magnetocrystalline anisotropy. At the first step previously magnetized isotropic nanostructured Nd-Fe-B type alloy is cooled in negative magnetic field. Magnetic field strength H is determined by the experimentally. It should be more than exchange field and smaller than coercivity value. Turning to zero the external magnetic field after the sample cooling provoke the change of magnetic moment disposition of each grain because of IEED. The example of this behaviour is shown on the Fig. 1.

The energy barrier between different directions determination can be calculated from the equation 1

$$E_A = K_1 \sin^2 \theta + (K_2 + K_2' \cos 4\varphi) \sin^4 \theta + (K_3 + K_3' \cos 4\varphi) \sin^6 \theta \quad (1)$$

Knowing the anisotropy constant K_i and H_{ex} values it was possible to determine the IEED for mentioned alloy. These results of will be presented in the report.

This work supported by the state order project 2582 and UrFU Young scientists competition grant.

[1] D. Ogawa, K. Koike, H. Kato, S. Mizukami, T. Miyazaki, M. Oogane, Y. Ando, *Journal of the Korean Physical Society*, **63/3** (2013) 489-492.

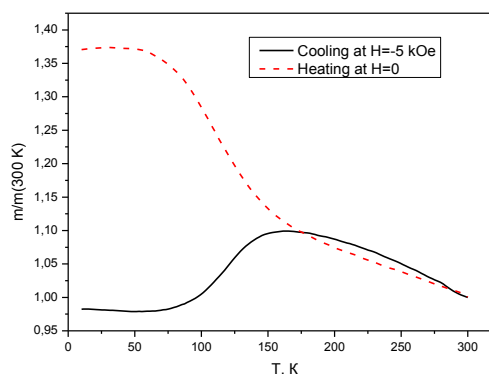


Fig. 1. Temperature dependencies of the relative magnetization in rapidly quenched alloy MQP-B+ brand

30PO-P-5

INVESTIGATION OF AMORPHOUS MICROWIRES WITH MAGNETO-OPTICAL METHOD

Nikitin L.V., Zotova O.V.

Moscow State University, Physical department, Moscow, 119899, Russia

Magneto-optical spectroscopy has been used successfully for the analysis of amorphous fine crystalline and other inhomogeneous states of the samples. Most efforts are aimed at studies of the magnetization processes in microwire and the distribution of local anisotropy axes.

In this paper we attempt to study amorphous microwires on the basis of alloys of iron and cobalt. The data obtained on amorphous ribbons and films have been used for the analysis of the results .

A method for the study of the dispersion curves of equatorial MOKE at the microwire in a wide range of photon energies of the incident light have $\hbar\omega = 1 - 5 \text{ eV}$ been developed. On the microwires of various compositions with different geometric parameters the dispersion, angular and field dependence of equatorial MOKE have been investigated. Found that x-ray amorphous microwires based on alloy, $\text{Co}_{81,73} \text{B}_{3,36} \text{Si}_{5,81} \text{Mn}_{9,9}$ according to the diameter of metal wires may be in the fine-crystalline, amorphous or inhomogeneous state.

In the study of x-ray amorphous microwires on the basis of iron alloys was observed the influence of structure on the conditions of amorphization of microwires metal core. In the angular dependence of the equatorial MOKE, the phenomenon of magneto optical interference was found.

Using a geometric model of the light was analyzed the influence of various geometrical parameters of the microwire and optical properties of glass on the nature of the interference. Comparison of these experimental results with theoretical calculations revealed changes in the optical properties of microwires glass cover. In the microwires based on a high iron content alloy in the metal-glass border a transition layer whose optical properties differ from those of metal wires and glass coating was detected. It is shown that such a transition layer changes the nature of magneto-optical interference during the transition into the ultraviolet spectrum.

30PO-P-6

TRANSFORMATION OF MAGNETIC STRUCTURES AS A RESULT OF THERMOMECHANICAL PROCESSING

Larin V.S.¹, Zaporozhan S.I.^{1,2}, Kalmykov I.A.^{1,2}, Chicu L.I.¹, Bucatco I.V.¹

¹Microfir Tehnologii Industriale, Chisinau, Republic of Moldova

²Technical University of Moldova, Chisinau, Republic of Moldova

mfti@company.md

The microwires, cast from liquid phase using method of Ulitovskii-Taylor originally present in the magnetic anisotropy. The most important is magnitostatic or shape anisotropy related to cylindric shape of microwire core, and also, magnetoelastic related to stresses caused by glass shell firmly connected to the metal core. Due to the difference in expansion coefficients (glass about 10 times less than metal) in a metal core appears in every direction tensile stresses and compressive stresses in the glass. Axial, radial and tangential stresses create a large variety of magnetic structures and magnetic properties.

Amorphous microwires with positive magnetostriction.

At positive magnetostriction the direction of the magnetostatic and magnetoelastic anisotropy, and therefore the direction of easy magnetization coincide with microwire axis. Microwire has the property of bistability. Remagnetization occur with one large Barkhausen jump.

At segment's length less than critical, it is possible reversal magnetization in two or more stages, and also possible existence of structures with two domains in absence of external field. The critical length of segment is determined by relation of length and diameter of wire, depends on value of magnetostriction and diameter of metal core. For segments of microwire with length less than critical it is possible existence of structure with two domains that leads to multilevel jumps of reversal magnetization.

Induced magnetic anisotropy in amorphous microwires.

During heat treatment of amorphous alloys occurs the relaxation of stresses and ordering of the short-range atoms, resulting the change of the volume (so-called effect of liberation the free volume). In the field of elastic stresses (inner and external), ordering flows toward maximum stress. Thermomechanical processing – processing of stretched microwires occurs to directed relaxation of the amorphous metal, namely along to microwire axis. Thus, in the stretched sample of microwire changes the dimension of metal core in direction of increasing the length. But is practically no change in dimensions of the glass shield. As a result changes the ratio of the radial, tangential and axial stresses. Axis stresses become smaller than tangential, which leads to new magnetic structures and changes of magnetic properties. As a result of thermomechanical processing (TMP) of microwires based on alloys with positive magnetostriction, changes the character of magnetization – rectangular hysteresis loop, characteristic for bistable microwires, becomes oblique. For alloys with positive magnetostriction transformation of inclined loop in rectangular one happens in several stages.

1. Stage – loop becomes oblique with a small value of H_k . Reversal magnetization happens at central layer, which is less 10% than whole volume of measured segment.

2. Stage – hysteresis loop becomes rectangular with small coercive force, with narrow pulse of reversal magnetization and small pulse amplitude. Coercive force can be with value of several A/m.

3. Stage – with increasing of external load H_c increase by law $H_c \propto \sigma^{1/2}$ till stresses value, when appear the second peak of reversal magnetization. With increasing the stress increases the value of H_c of first and second peak by law $H \propto \sigma^{1/2}$. If the stress continue to increase can appear the third, fourth and etc. peaks of reversal magnetization.

4. Stage – the peaks of reversal magnetization merge into one, with coercive force near to initial sample.

30PO-P-7

MAGNETIC PROPERTIES OF NiFe AND FeCuNbSiB THIN FILMS: EFFECT OF THICKNESS ON STATIC PERMEABILITY

Moulin J., Shahosseini I., Woytasik M., Nhung Dinh T.H., Garel O.

Institut d'Electronique Fondamentale, Univ. Paris Sud, 91405 Orsay, France

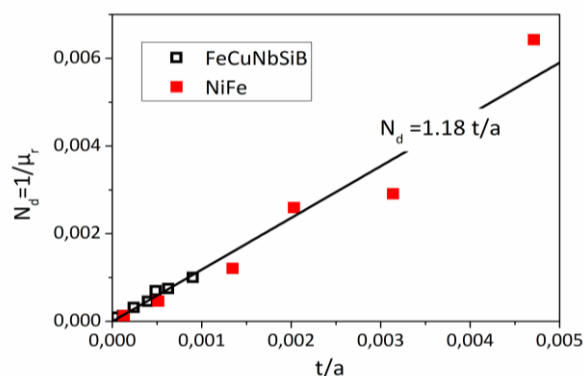
johan.moulin@u-psud.fr

This study presents magnetic properties of FeCuNbSiB and FeNi films with thicknesses varying from 50 nm to 9 μm . These materials are dedicated to be integrated in magnetic microdevices, as magnetic cores or functional materials for microsensors. Thus effective properties like permeability and coercivity of patterned structures have been studied.

Thin films of $\text{Fe}_{73.5}\text{Cu}_1\text{Nb}_3\text{Si}_{15.5}\text{B}_7$ films were deposited by RF sputtering in argon plasma with a deposition rate close to 14 nm min^{-1} . Samples were annealed in order to release stress induced by the deposition. The FeCuNbSiB films were patterned in 2 mm x 2 mm squares by shadow masking with a thickness varying from 60 nm to 1800 nm. NiFe thick films were electrodeposited on Si wafers covered by a Cu(100nm)/Ti(10nm) seed layer. The films were patterned in 1 mm x 1 mm squares using micromolding, i.e. electrodeposition in a thick mold realized by UV photolithography.

The magnetic properties of both FeCuNbSiB and NiFe patterns were extracted from the hysteresis loops. It is showed that both the coercivity and the effective magnetic permeability depend on the film thickness. However these two characteristics are not directly linked, as both coercivity and permeability decreases with the film thickness. Thus it is supposed that variations in the permeability are related to geometrical effect only and not to a modification of the magnetic anisotropy.

Despite calculus and MOKE observation assess that patterns should not be monodomain, the static permeability of both FeCuNbSiB and NiFe patterns has been measured inversely proportional to the films thickness (see figure) and more precisely to the ratio t/a (t and a the thickness and the pattern size respectively). This hypothesis allows introducing a demagnetizing-like coefficient N_d which, in case of soft films, can be related to the permeability: $N_d \approx 1/\mu$. From measurements has been extract $N_d \approx 1.18 t/a$. This coefficient 1.18 is consistent with the one of monodomain disk which is $\pi/2$. By correcting the hysteresis loops using this coefficient N_d , the loops for different film thicknesses become superposed.



Inverse of permeability as a function of the pattern thickness/size ratio for different materials

French Agence Nationale pour la Recherche is thanked.

30PO-P-8

CRYSTAL STRUCTURE AND MAGNETIC PROPERTIES OF $\text{Fe}_{7-y}\text{Ti}_y\text{X}_8$ ($\text{X} = \text{S}, \text{Se}$) COMPOUNDS INFLUENCED BY SUBSTITUTIONS

Baranov N.V.^{1,2}, Ibrahim P.N.G.², Selezneva N.V.², Volegov A.S.², Shishkin D.A.¹

¹ Institute of Metal Physics, RAS, Ekaterinburg, Russia

² Institute of Natural Sciences, Ural Federal University, Ekaterinburg, Russia

baranov@imp.uran.ru

The Fe_7S_8 compound belongs to a group of minerals pyrrhotite $\text{Fe}_{1-\delta}\text{S}$ ($0.05 < \delta \leq 0.125$), which are of interest from different points of view, such as geomagnetism, physics of the Earth's core, meteoritics, metallurgy, physics and chemistry of solids. For $\delta = 0.125$, the Fe_7S_8 compound (pyrrhotite) has a layered superstructure of the NiAs type with alternating layers of iron and sulfur. According to neutron diffraction the magnetic moments of iron atoms ($\mu_{\text{Fe}} \sim 3.2 \mu_{\text{B}}$) are arranged ferromagnetically inside each layer, but coupled antiferromagnetically between adjacent layers [1]. The presence of vacancies in every second iron layer leads to incomplete compensation of magnetic moments and hence to the appearance of ferrimagnetism in Fe_7S_8 with critical (Neel) temperatures of about 590 K. The iron selenide Fe_7Se_8 having also a NiAs-type structure exhibits a ferrimagnetic order below 480 K.

In the present work, we have synthesized the $\text{Fe}_{7-y}\text{Ti}_y\text{X}_8$ ($\text{X} = \text{S}, \text{Se}$) compounds in which the Fe atoms are partly replaced by Ti, and performed a study of their crystal structure and magnetic properties. The substitution of Ti for Fe in $\text{Fe}_{7-y}\text{Ti}_y\text{X}_8$ modifies its crystal structure from the initial monoclinic 4C superstructure of the NiAs-type to the hexagonal 3C superstructure at $y = 1$ and then to the 2C monoclinic superstructure at $y \geq 2$. The growth of the Ti content in $\text{Fe}_{7-x}\text{Ti}_x\text{S}_8$ is accompanied by a gradual decrease of the magnetic ordering temperature from ~ 590 K at $y = 0$ down to 145 K at $y = 4$, by a substantial increase of the low-temperature coercive field (up to 24 kOe) and reduction of the effective magnetic moment from $\sim 5.8 \mu_{\text{B}}$ to $4.3 \mu_{\text{B}}$. Unlike ferrimagnetic order in Fe_7S_8 , the compound $\text{Fe}_6\text{Ti}_1\text{S}_8$ shows an antiferromagnetic behavior, while further growth of the Ti concentration above $y = 2$ increases the resultant magnetization up to a value almost in twice higher than the value for non-substituted Fe_7S_8 (see Fig.1.) Such non-monotonous changes in magnetization behavior with increasing Ti concentration are associated with the preferential substitution of Ti for Fe in alternating metallic layers [2]. The non-monotonous behavior of the magnetization was also revealed at the Ti for Fe substitution in the $\text{Fe}_{1-y}\text{Ti}_y\text{Se}_8$ system.

This work was supported by RFBR (projects 13-02-00364 and 13-02-96038) and by the program of the Ural Branch of RAS (project No 12-T-2-1012).

[1] A.V. Powell et.al., *Phys. Rev. B* **70** (2004) 014415.

[3] P.N.G Ibrahim, N.V. Selezneva, A.F. Gubkin and N.V. Baranov, *Solid State Sciences* **24** (2013), 26.

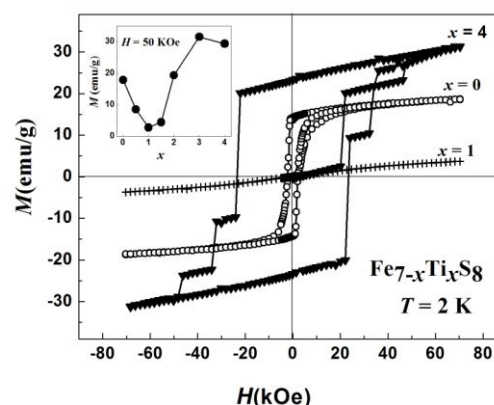


Fig.1. Field dependences of the magnetization for $\text{Fe}_{7-x}\text{Ti}_x\text{S}_8$ compounds with various Ti concentrations. Insert shows the concentration dependence of the magnetization measured at $T = 2$ K in magnetic field 50 kOe.

30PO-P-9

MAGNETIC PROPERTIES OF THE OFF-STOICHIOMETRIC GdNi_2Mn_x COMPOUNDS

Gerasimov E.G., Mushnikov N.V., Terentev P.B., Gaviko V.S., Inishev A.A.

Institute of Metal Physics UB RAS, Ekaterinburg, Russia

gerasimov@imp.uran.ru

The crystal structure, magnetic properties and magnetocaloric effect of novel off-stoichiometric GdNi_2Mn_x ($0 \leq x \leq 0.6$) compounds have been studied.

The alloys with $0 < x < 0.4$ crystallize in a cubic structure of the MgCu_2 -type, whereas, starting from the composition $x \geq 0.4$, in the samples there forms the PuNi_3 -type phase [1]. Increase in the Mn content is found to lead to a considerable growth of the Curie temperature from 80 K for the binary GdNi_2 up to 190 K for the $\text{GdNi}_2\text{Mn}_{0.4}$ compound (Fig 1). Magnetization at 4 K decreases with increasing x (Fig 1), which indicates the formation of a ferrimagnetic structure.

The magnetic entropy change has been determined from temperature dependences of the magnetization using the Maxwell equation. For $\text{GdNi}_2\text{Mn}_{0.4}$, upon changing the magnetic field from 0 to 9 T, the isothermal entropy change in the vicinity of the Curie temperature has been found to be $4.6 \text{ J kg}^{-1}\text{K}^{-1}$ (Fig 2). This value is somewhat lower than those determined earlier for the RNi_2Mn ($R = \text{Tb, Ho, Er}$) compounds [2]. However, in the compounds with Gd, the value of ΔS is rather high in a wide temperature range, which is important for practical applications in magnetothermal devices.

The results are discussed under assumption of growth of both the Ni magnetic moment and Gd-Mn and Ni-Mn exchange interactions with increasing the manganese content.

This work has been partially supported by RFBR grants 12-02-00864 and 13-02-96022 and by Program of UB RAS (project 12-T-2-1012).

[1] E.G. Gerasimov, N.V. Mushnikov, P.B. Terentev, V.S. Gaviko, A.A. Inishev, *Journal of Alloys and Compounds*, **571** (2013) 132-137.

[2] J.L. Wang, S.J. Campbell, S.J. Kennedy, R. Zeng, S.X. Dou, G.H. Wu, *J. Phys.: Condens. Matter*, **23** (2011) 216002.

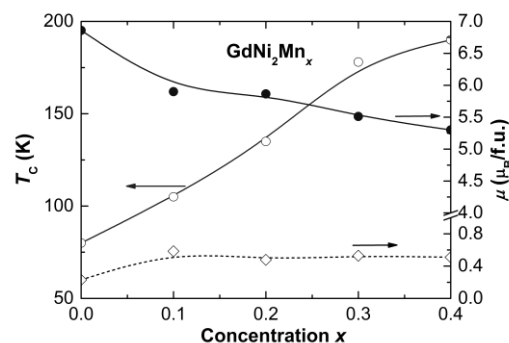


Fig. 1. Concentration dependences of the Curie temperature (o), molecular magnetic moment (•) and magnetic moment of nickel (◊) for the GdNi_2Mn_x compounds. Lines are guide for eyes.

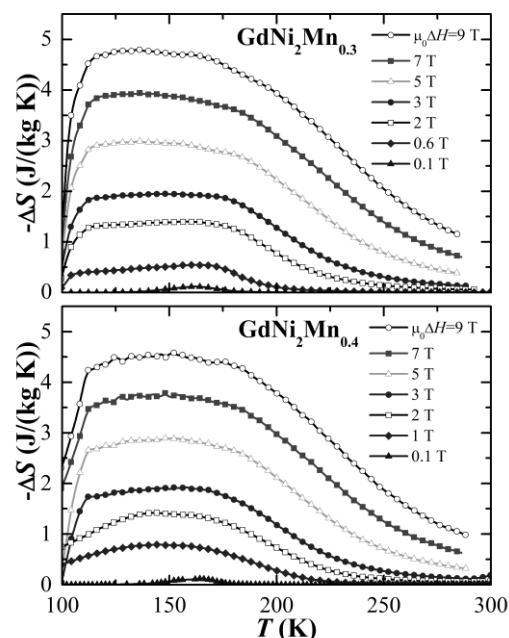


Fig. 2. Temperature dependences of the isothermal magnetic entropy change for the $\text{GdNi}_2\text{Mn}_{0.3}$ and $\text{GdNi}_2\text{Mn}_{0.4}$ compounds for various values of the magnetic field change.

30PO-P-10

MAGNETIC PROPERTIES OF MARAGING STEELS SUBJECTED TO PLASTIC DEFORMATION

Stashkov A.N., Somova V.M., Sazhina E.Yu., Stashkova L.A.

IMP, Ural Division of RAS, S. Kovalevskoy, 18, Ekaterinburg, Russia
stashkov@imp.uran.ru

Maraging steels are widely used in shipbuilding, the aircraft industry, and rocket production. The advantages of these steels are the high strength with sufficient plasticity and high corrosion resistance, good weldability, and ability for hot and cold plastic deformation; the disadvantage is that variation in the chemical composition in the limits of the steel grade properties, for example, by Carbon and Titanium, may substantially change the mechanical properties in the aged state. In addition, the mechanical properties are generally determined by the content of retained austenite (RA), its stability, and doping level. The aim of this work was to study the magnetic properties, hardness and phase composition maraging steels with different contents of RA subjected to plastic deformation by stretching for developing a method for non-destructive testing.

The magnetic properties, hardness and phase composition were measured on two groups of samples: maraging steels ChS-5VI (with 18%Ni and Cobalt-free) and ChS-4VI (with 18%Ni and 8%Co) in undeformed and plastically deformed conditions. To obtain various contents of retained austenite and hardness the samples were subjected to aging with different temperatures. Based on the magnetic-hysteresis loops, were determined coercive force H_c , the saturation induction B_s and the value N' , which correlates with the internal demagnetization coefficient [1]. A good correlation was obtained between the B_s and RA as well as between N' and RA in undeformed conditions. The maximum of retained austenite and minimum of B_s are in the sample with $T_{aging} = 600$ °C (for ChS-4VI steel) and $T_{aging} = 580$ °C (for cobalt-free ChS-5VI steel).

It has been established that strain elongation of the maraging steels samples leads to a reduction of the retained austenite that was confirmed by X-ray investigations and behaviour of the magnetic properties B_s and N' . For example, the reduction of amount of paramagnetic RA increases the saturation induction B_s and reduces N' . The greater the initial retained austenite content is in undeformed samples, the more its content disintegrates under deformation actions. The most intensive changes in the phase composition of samples are observed at elongations up to 4-5%. Correlation between N' and RA breaks down in deformed conditions due to the parameter N' is a structurally sensitive (additionally depends on stress-strain state). A two-parameter (with the use of B_s and N') technique may be used for non-destructive determination of the retained austenite containing and mechanical properties testing.

This work was supported by the Russian Foundation for Basic Research (project no. 12-08-33098 mol_a_ved), the Program of Oriented Fundamental Investigation (project no. 13-2-052-UVG), and the Presidium of the Russian Academy of Sciences (project no. 12-P-2-1031).

[1] A.N. Stashkov, V.M. Somova, E.Yu. Sazhina et.al., *Russian Journal of Nondestructive Testing*, **49** (2013) 705–714.

30PO-P-11

INVESTIGATION OF HYDROTHERMALLY SYNTHESIZED GREIGITE MAGNETIC PROPERTIES

Krivenkov M.S.¹, Gendler T.S.², Novakova A.A.¹

¹ Lomonosov Moscow State University, Moscow, Russia

² Schmidt Institute of Physics of the Earth RAS, Moscow, Russia

krivenkov@physics.msu.ru

Greigite (Fe_3S_4) is an iron sulfide with inverse spinel structure, same as the structure of magnetite. As well as magnetite, Greigite is ferrimagnetic. Half-metallic properties in combination with ferrimagnetic nature of greigite puts this mineral in a fairly narrow group of materials that are potentially suitable for spintronics [1].

However, greigite occurs in nature mainly in the form of small (tens of nanometers), often superparamagnetic particles. In addition, it is thermodynamically metastable and easily transforms to other sulfide phases, so it is hard to find pure natural greigite. In recent decades, by using hydrothermal method, a huge progress has been made in the area of greigite synthesis [2].

In this paper, we conducted a comparative study of magnetic properties of greigite crystals obtained by hydrothermal synthesis. Application of different surfactants and duration of synthesis yielded to formation of Fe_3S_4 particles of different sizes (from 0.5 microns up to 5 microns) and purity (single- or multi-phase).

Conducted Mossbauer spectroscopy study showed that these samples differ in the cation distribution of ferric and ferrous ions in the sublattices. Unusual temperature dependencies of effective magnetic fields for A and B-site iron atoms were obtained. It was found that coercive magnetic parameters and hysteresis loops shape as well as greigite stability depend on the synthesis procedure. Stepwise thermomagnetic analysis in saturating field allowed us to obtain the synthesized greigite critical temperatures of structural stability ($T \sim 240^\circ\text{C}$), after which the sequential process of greigite transformation to pyrite, metastable maghemite (or magnetite) and finally to hematite begins. All of the found greigite peculiarities not only expand the knowledge about this complicated ferrimagnetic phase but can be used as guidance for optimal synthesis conditions.

[1] S.A. Wolf, D.D. Awschalom et al., *Science*, **294** (2001) 1488-1495.

[2] L.R. Chang, A.P. Roberts et al., *J. Geophys. Res.*, **113** (2008) B06104.

30PO-P-12

MAGNETOSTATIC ENERGY OF THE DOMAIN WALLS IN UNIAXIAL FILMS OF FINITE DIMENSIONS

*Vetoshko P.M.*¹, *Skidanov V.A.*², *Vetoshko F.P.*²

¹ Institute of Radioengineering and Electronics, Moscow, Russia

² Institute for Design Problems in Microelectronics, Moscow, Russia
pvetoshko@mail.ru

The analytical expressions for the magnetostatic energy of the domain wall (DW) was obtained, taking into account the finite size of the sample. To calculate the magnetostatic energy, a method of equivalent currents has been used, which is in essence a uniformly magnetized magnetization representation with equivalent body surface current [1]. For sufficiently large uniaxial anisotropy, the distribution of magnetization within the domains can be taken as uniformly directed along the normal to the film. That's why this method is especially useful for magnetostatic calculations in uniaxial films. Thus, the calculation of the magnetostatic energy element with uniaxial anisotropy is reduced to the calculation of the mutual inductances of the circuits, limiting the area of uniform magnetization. In turn, the allowance for the finite length of the DW makes it possible to determine the magnetostatic energy in structures with arbitrary aspect ratio sides. Such element made as a bridge between two narrow strips is found to possess an indefinite DW equilibrium position which is highly sensitive to external field [2]. Fig. 1 shows the results of analytical calculations of the DW magnetostatic energy depending on the DW displacement with size of strips $W = 9$ mkm.

Thus, the formula in the computation can accelerate the magnetostatic potential and build a functional depending on the sizes of the element.

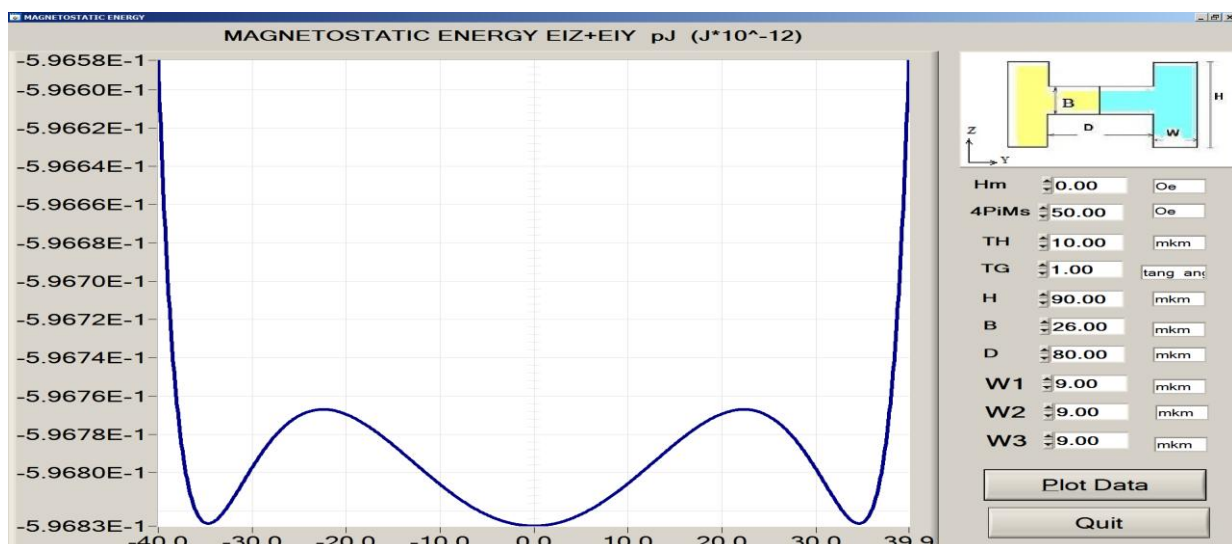


Fig. 1. Calculated magnetostatic energy schemes for uniaxial garnet film element with constant DW length during magnetization reversal in compensation point $W = 9$ mkm. The X axis – DW displacement in mkm, the Y axis – magnetostatic energy in pJ.

[1] O'Dell T.H. Magnetic bubbles. The Macmillan Press Ltd. Bristol (1974).

[2] V.Skidanov, P. Vetoshko, *Procedia Engineering*, **5** (2010), pp. 989-992.

30PO-P-13

MODELLING OF THE DISORDERED EXCHANGE-COUPLED NANOCOMPOSITE OF HARD AND SOFT MAGNETIC PHASES

Bolyachkin A.S., Volegov A.S.

Ural Federal University, Yekaterinburg, Russia
anton.bolyachkin@urfu.ru

Unfailing scientific interest is dedicated to nanostructured magnets consisted of hard and soft magnetic phases [1]. The idea behind these systems is that the comparatively low remanence of a hard phase (HP) can be improved by exchange coupling with a soft phase (SP). The drawback, however, is a reduced coercivity of the nanocomposite. Nevertheless, through competition of both facts in some concentration of the soft phase a significant increase of energy product for such systems can be achieved [2].

While nanocomposites with an ideal structure were investigated theoretically and by means of simulations in details, this work was concentrated on the case of disordered isotropic ensembles (fig. 1, a), which is close to the most experiments. The program for computer modelling of such systems was created in the MATLAB environment. Its algorithm for single-domain particles of ensemble performs iterative minimization of energy consisted of a magnetocrystalline anisotropy contribution, an intergrain exchange interaction ones and energy in an external magnetic field. In aims of experimental verification materials parameters for $\text{Nd}_2\text{Fe}_{14}\text{B}$ and $\alpha\text{-Fe}$ were used.

Magnetization processes (fig. 1, b) for a different volume ratio of the hard and the soft magnetic phases were investigated. For the isotropic disordered nanocomposite a dependency between the energy product and the volume ratio was established. The dependency evolution during grain size changing was received also.

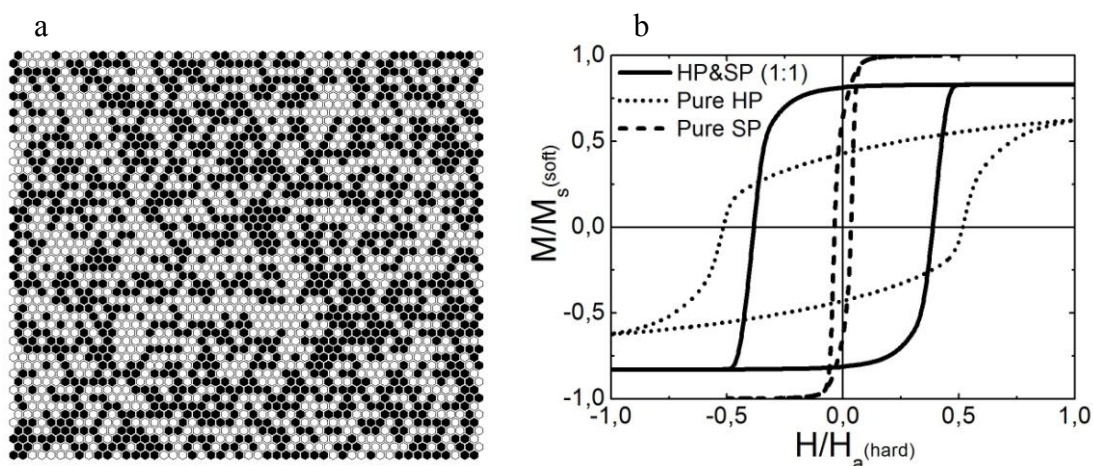


Fig. 1. Model of disordered nanocomposite (a); hysteresis loops for isotropic exchange-coupled ensemble (solid) and each magnetic phase separately (b).

Support by state order project 2582 and UrFU Young scientists competition grant is acknowledged.

- [1] B. Balamurugan, D.J. Sellmyer, G.C. Hadjipanayis et al., *Scripta Mater.*, **67** (2012) 542-547.
[2] H. Zeng, J. Li, P. Liu, Z.L. Wang, S. Sun, *Nature*, **420** (2002) 395-398.

30PO-P-14

INFLUENCE OF ANNEALING ON THE SURFACE TOPOGRAPHY AND MAGNETIC PROPERTIES OF THE THIN FILM FINEMET-TYPE ALLOY

Mikhailitsyna E.A.¹, Kataev V.A.¹, Lepalovsky V.N.¹, Geydt P.V.², Lähderanta E.²

¹ Ural Federal University, Yekaterinburg, Russia

² Lappeenranta University of Technology, Lappeenranta, Finland
evgenia.mihalitsyna@gmail.com

Nanocrystalline Finemet alloy is well known due to their outstanding soft magnetic properties conditioned by alloy microstructure. Interest to the thin film state of the Finemet alloy is connected with their possible of application in magnetic film sensors based one the giant magneto-impedance effect.

In this work, the films were obtained by RF sputtering technique of the $\text{Fe}_{72.5}\text{Cu}_{1.1}\text{Nb}_{1.9}\text{Mo}_{1.5}\text{Si}_{14.2}\text{B}_{8.7}$ (modified Finemet) alloy target and their microstructure and magnetic properties were studied. Films were sputtered in presence of uniform magnetic field 100 Oe. Thicknesses of the films were varied from 10 to 800 nm. Films were annealed at 450 °C and 540 °C. The magnetic properties at room temperature were measured using a vibrating sample magnetometer Lake Shore 7407, and topography was measured using atom force microscopy (AFM) Multimode 8.

AFM investigations were shown a grain structure formation on the surface of annealed samples that not observed for samples in as-prepared state (fig. 1 (a) and (b)). In accordance with previous studies, this structure could be corresponded to grains of bcc-Fe(Si) [1] uniformly dispersed in residual amorphous matrix. The appearance of the grain structure and changing of the surface roughness can affect on magnetic properties as reported in [2]. The average diameter of grains was 50 nm and their amount was about 450 for $2 \times 2 \mu\text{m}$ scan.

Fig. 1 (c) shows hysteresis loops of films with thickness 45 nm in as-prepared state and after annealing at 450 °C for 1 hour. Evidently, that annealing leads to a parameters changing of demagnetization process in particular to increase of the coercive force.

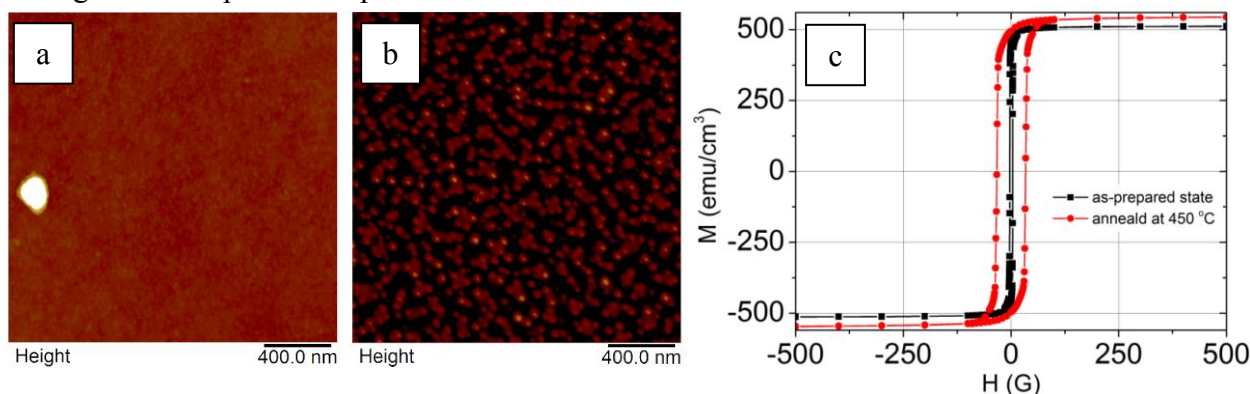


Fig. 1. AFM patterns of surface for the film thickness of 45 nm in as-prepared state (a) and ones annealed at 450 °C (b); hysteresis loops (c) for the same samples.

An investigation of the magnetic phase contrast of the studied films was carried by a magnetic force microscopy method. For as-prepared samples any magnetic contrast was not observed, while for the annealed samples magnetic contrast was revealed, and is did not correlate strongly with topography.

[1] J. Balcerski, R. Brzozowski, M. Wasiak, et al., *Vacuum*, **83** (2009) 5182-5185.

[2] Y. Cao, C. Zhou, *J. Magn. Magn. Mater.*, **333** (2013) 1-7.

30PO-P-15

MÖSSBAUER STUDY OF FERROMAGNETIC AND ANTIFERROMAGNETIC STATES IN $\text{Ce}(\text{Fe}_{1-x}\text{Si}_x)_2$ COMPOUNDS

*Vershinin A.V.*¹, *Serikov V.V.*¹, *Kleinerman N.M.*¹, *Mushnikov N.V.*¹, *Rusakov V.S.*²

¹ Institute of Metal Physics (IMP), Ekaterinburg, Russia

² Moscow State University (MSU), Moscow, Russia

vershinin@imp.uran.ru

$\text{Ce}(\text{Fe}_{1-x}\text{M}_x)_2$ ($M = \text{Co}, \text{Ru}, \text{Si}, \text{Al}, \text{Cu}$) compounds attract much attention due to a sophisticated magnetic phase diagram and anomalous magnetic properties. The binary compound CeFe_2 crystallizes in the cubic MgCu_2 -type Laves phase. It is a ferromagnet (FM) with a Curie temperature of 230 K. Upon partial substitution of Fe atoms by impurity atoms in the compounds $\text{Ce}(\text{Fe}_{1-x}\text{M}_x)_2$, antiferromagnetic (AF) ordering at low temperatures is observed [1]. The FM-AF phase transition is a first order transition. It is accompanied by a cubic to rhombohedral structural distortion and discontinuous change of the unit cell volume. Due to a competition between the FM and AF exchange interactions and strong magnetostructural coupling, this system is very sensitive to alloying, application of magnetic field and pressure. The aim of this work was a comparative study of the crystal structure, magnetic properties and hyperfine interactions for two compounds of $\text{Ce}(\text{Fe}_{1-x}\text{Si}_x)_2$ family: with ferromagnetic ($x = 0$) and antiferromagnetic ($x = 0.07$) ground states.

Figure 1 shows Mössbauer spectra of the compounds measured at 130 K. At this temperature, the binary CeFe_2 is in the FM state, while for the ternary $\text{Ce}(\text{Fe}_{0.93}\text{Si}_{0.07})_2$ the AF state is realized. In spite of a relatively simple cubic structure of the binary compound, its Mössbauer spectrum cannot be treated well in the model of distribution of hyperfine fields. The amount of magnetically nonequivalent positions of iron due to different orientations of the local symmetry axes and the second-order quadrupole coupling constants were taken into account to get best fitting of the spectrum in the direct problem (Fig. 1a).

With addition of silicon, the spectrum changes drastically (Fig. 1b). Because of the rhombohedral distortions, there are no reasons to consider high-order quadrupole coupling. Instead, different environment of resonant atoms depending on the number of impurity atoms in the first coordination sphere should be taken into account. Therefore, the spectrum was fitted with the distribution function of hyperfine fields. The obtained results are discussed in the model of competition of the FM and AF couplings between different pairs of the Ce and Fe spins [2].

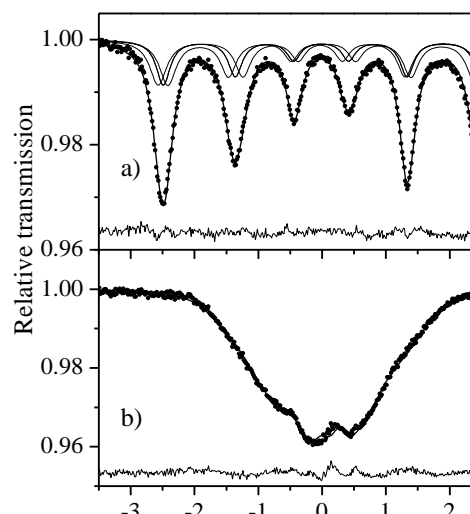


Fig. 1. Mössbauer spectra for $\text{Ce}(\text{Fe}_{1-x}\text{Si}_x)_2$ with $x = 0$ (a) and $x = 0.07$ (b) at 130 K.

This work has been partially supported by RFBR (project 12-02-00864) and by Program of UB RAS (project 12-T-2-1012).

[1] S.B. Roy, B.R. Colles, *J. Phys.: Condens. Matter*, **1** (1989) 419-430.

[2] J. Wang et al., *Phys. Rev. B*, **86** (2012) 014422-1-7.

30PO-P-16

MAGNETIC PROPERTIES OF THE $Tb_{1-x}Sm_xMn_6Sn_6$ COMPOUNDS

Terentev P.B., Mushnikov N.V., Gerasimov E.G., Gaviko V.S., Gubkin A.F.

Institute of Metal Physics, Ural Division of RAS, Ekaterinburg, Russia

terentev@imp.uran.ru

In this work we studied the magnetic properties and crystal structure of the quasi-ternary $Tb_{1-x}Sm_xMn_6Sn_6$ ($0 \leq x \leq 1$) compounds in which negative Tb-Mn and positive Sm-Mn competitive exchange interactions can be gradually change.

It was shown that the $Tb_{1-x}Sm_xMn_6Sn_6$ compounds crystallize in the $HfFe_6Ge_6$ -type structure at $0 \leq x \leq 0.6$ and in the $HoFe_6Sn_6$ -type structure at $x = 1$. In the compounds with $0 \leq x \leq 0.6$ a spontaneous spin-reorientation transition with increasing the temperature from easy axis to easy plane type of magnetic anisotropy at a critical temperature T_{sr} was observed. It was shown that the T_{sr} temperature decreases with increasing Sm concentration. The Curie temperature T_C of the compounds slightly increases with decreasing Sm concentration. The x - T magnetic phase diagram was constructed (see Fig.1) using measurements of temperature dependences of the AC susceptibility.

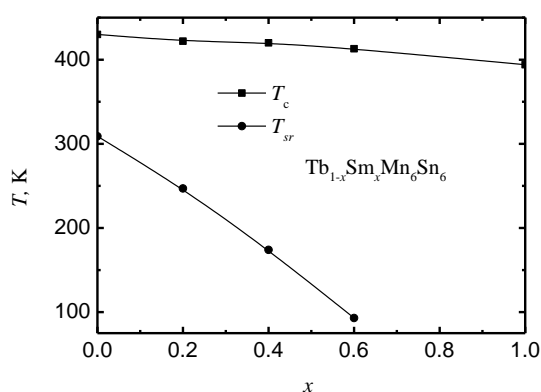


Fig. 1. x - T magnetic phase diagram of the $Tb_{1-x}Sm_xMn_6Sn_6$ compounds.

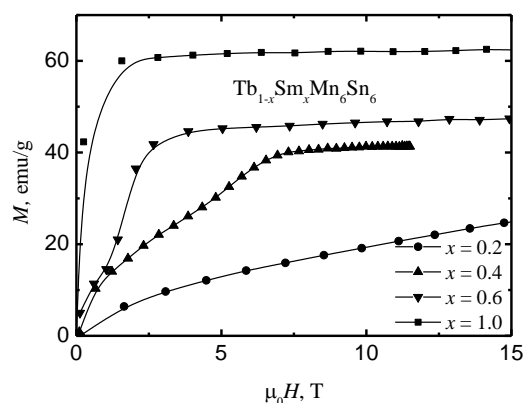


Fig. 2. Magnetization curves of the $Tb_{1-x}Sm_xMn_6Sn_6$ compounds measured for the oriented powder samples in magnetic field applied in the basal plane at $T = 77$ K.

The jumps of magnetization were observed in magnetic field applied along the hard direction for $Tb_{1-x}Sm_xMn_6Sn_6$ compounds (see Fig.2). These jumps of magnetization can be explained by FOMP (First Order Magnetization Process).

The obtained results were compared with results from work [1] for $Tb_{1-x}Sm_xMn_6Sn_6$ ($R = Gd, Y$) compounds. It was discussed a significant role of complicate Mn-Mn and Mn-R exchange interactions in formation of the magnetic structures of RMn_6Sn_6 compounds.

This work has been partially supported by RFBR grants 12-02-00864 and 13-02-96022 and by Program of UB RAS (project 12-T-2-1012).

[1] N.V. Mushnikov, P.B. Terent'ev, V.S. Gaviko, E.G. Gerasimov, E.V. Rosenfeld, L.A. Shreder, *Solid State Phenomena*, **152-153** (2009) 132-137.

30PO-P-17

DILATOMETRIC ANALYSIS OF PHASE TRANSFORMATIONS IN FE-CR-CO HARD MAGNETIC MATERIALS WITH LOW COBALT CONTENT

Vompe T.A., Milyaev I.M.

A.A. Baikov Institute of Metallurgy and Material Science, Moscow, Russia
tvompe@gmail.com

Fe-Cr-Co permanent magnets are widely used in production [1]. They have good permanent magnetic properties and good ductility. High coercive force of the alloys of Fe-Cr-Co system is associated with their modulated structures, consisting of two isomorphic phases: an iron-rich phase α_1 and chromium-rich phase α_2 produced as a result of spinodal reaction of decomposition of the high-temperature phase α from the solid solution during aging.

Cobalt is one of the expensive compounds of this magnet. To decrease cobalt content and to receive good magnetic properties on such magnets is an actual task [2].

The purpose of this work was to study the phase transformation in the hard magnetic Fe-Cr-(7-13wt.%)Co alloys with low cobalt content to make heat treatment more better to receive the best magnetic properties on these alloys.

The powder of iron, chromium, cobalt, molybdenum and silicon were used for preparation of the powder samples. The initial powders were mixed in the vertical mixer C 2.0, then they were pressed on the manual press in the detachable matrix with inner diameter 13,6 mm under the pressure of 600 MPa. Sintering was performed in a vacuum shaft furnace SSHV-1,25/24-I1 in a vacuum of 10^{-2} Pa. Samples had the density value 98-99 %.

The chemical composition of the samples after sintering and pressing were studied by X-ray fluorescence analysis method with a wave dispersive spectrometer ARL OPTIM'X firm Thermo Fisher Scientific (Switzerland).

The investigation of phase transformation in the hard magnetic Fe-Cr-(7-13wt.%)Co alloys were made under heating with the rate 10 °C/min in the temperature interval from 20 °C to 1300 °C on the dilatometer DIL 402 C7G produced by NETZSCH Gerätetechnik GmbH (Germany). The dilatometric curves were calculated and the temperatures of the phase transformation were found.

It was found that the Curie temperature T_c of the α -solid solution decreases with the increase in the chromium content.

The temperature of the spinodal decomposition in Fe-Cr-Co hard magnetic alloys with low cobalt content is lower than in Fe-Cr-Co with 15 % Co.

The found temperatures of phase transformation will help to change the mode of heat treatment to receive better magnetic properties in Fe-Cr-Co with low cobalt content.

This work was supported by the Russian Foundation for Basic Research.

[1] E.V. Artamonov, M.A. Liebman, *Steel*, **6** (2007) 65-68.

[2] T.A. Vompe, I.M. Milyaev, V.S. Yusupov, *Perspektivnye Materialy*, **4** (2013) 59 - 63.

30PO-P-18

PHYSICAL EXPERIMENT ON MAGNETISM IN GENERAL PHYSICAL PRACTICUM

Kozlov V.I.

Faculty of Physics, Moscow State University of M.V. Lomonosov

In the practicum of physical faculty, the magnetism was presented from the very beginning. Collection of works [1] of 1909 contains the laboratory works "Comparison of horizontal components of the Earth magnetic field at two spots by a Kohlrausch variometer", "Determination of the magnetic-needle inclination by inclinometers", "Determination of horizontal components of the Earth magnetism by the Gaussian method".

Nowadays, the number of subjects on magnetism in the general physical practicum is expanded. We can distinguish two sections of this topic. The first one - "Methods of generating a magnetic field and measuring its induction". In this laboratory work, the magnetic field of the solenoid is studied by measuring its induction along the axis by the ballistic method. The magnetic field generated by Helmholtz coils is measured with using the Hall effect. In this case, the field induction one coil is measured along its axis and that of two coils for different distances between coils. The magnetic field of the electromagnet is measured with using a Hall sensor and by means of the nuclear magnetic resonance. There is an experimental setup in which a pulsed magnetic field is generated and studied. The pulsed field is generated, when a capacitor is discharged through a solenoid. With the current pulse to 5 kA, the magnetic field in the solenoid attains a value of 0.2 T.

The second section - "Physical effects due to the magnetic field". This is, first of all, the magnetic induction in ferromagnets. We study the magnetization and magnetization reversal of a ferromagnet. The hysteresis loop is observed with an oscilloscope. The parameters of the loop are as follows: the saturation induction, the coercive force H_c and the residual induction B_{res} . True-magnetization curves and the ferromagnet hysteresis loops are measured by oscilloscope when increasing the reversal field amplitude. The curve of the true-magnetization and the hysteresis loop of a ferromagnet are measured by the dc ballistic method. In both cases, we plot the curve of the permeability of material as a function of the magnetizing field (curve of Stoletov). By observing the hysteresis loop of a ferromagnet at different temperatures (on heating), we study the temperature dependence of the magnetic field in the ferromagnet and determine its Curie temperature. In other laboratory works, we study the dependence of the Hall voltage on the magnetic field, determine the conductivity of the sample, the carrier concentration and some other parameters. The magnetization of ferromagnets, their domain structure, the students study in the work on the Faraday effect. Here the principal characteristics of the magnetic hysteresis loop should be also measured. We study one of the magnetomechanical phenomena – the ferromagnetic resonance. The performed measurements enable us to verify the Larmor theorem, detect the anisotropy of the magnetic properties of the under investigation and determine the nature of elementary carriers of the atomic magnetic moment.

[1] V.I. Kozlov, S.V. Galuso, V.V. Grishachev, E.N. Il'icheva, N.G. Kanavina, S.A. Kirov, T.M. Kozlova, I.E. Leksina, A.M. Saletskii, A.G. Shishkov. *Physical experiment on magnetism in general physical practicum*. Moscow (2008) 139.

30PO-P-18

SHORT-RANGE ORDER FORMATION AND MAGNETISM IN Fe-Si AND Fe-Ga ALLOYS

Kuznetsov A.R.^{1,3}, *Petrik M.V.*^{2,3}, *Gorbatov O.I.*^{3,4}, *Gornostyrev Yu.N.*^{1,3}

¹Institute of Metal Physics UB RAS, Yekaterinburg, Russia

²Ural Federal University, Yekaterinburg, Russia

³Institute of Quantum Materials Science, Yekaterinburg, Russia

⁴KTH Royal Institute of Technology, Stockholm, Sweden

a_kuznetsov@imp.uran.ru

Alloys Fe-X (X = Al, Si, Ga, Ge) with the concentration of the doping element near the boundary of two-phase region attracting attention as magnetic materials. Among them, Fe-Ga alloy has a large magnetostriction value, while in the Fe-Si shows a high value of the induced magnetic anisotropy that is formed during annealing under an external impact. The nature of these phenomena is related to the electronic and structural (short-range order (SRO)) features of the alloys and continues to be a subject of debates [1,2].

We investigated SRO formation in these alloys in ferro and paramagnetic state using Monte Carlo simulation with ab initio effective X-X interactions. It was shown that SRO depends on the state of the magnetic alloy: well-defined SRO D0₃-type is present at temperatures below Curie point, while at $T > T_C$ X-X pairs of the second neighbors (B2-type SRO) are formed in Fe-Si, and SRO is absent in Fe-Ga (Fig. 1). Electronic structure calculations showed that Si forms quasi-covalent bonds with Fe atoms due to hybridization of 3p Si 3d Fe states, unlike Ga in the vicinity of which Fe d states are unbounded; in Fe-Si alloy similar situation occurs for some Fe atoms neighboring with Si-Si second neighbor pairs. As a result, the phenomenon of induced anisotropy requires the formation of Si-Si pairs in Fe-Si, while magnetostriction of Fe-Ga is the property due to a change of the electronic structure of individual atoms near Ga.

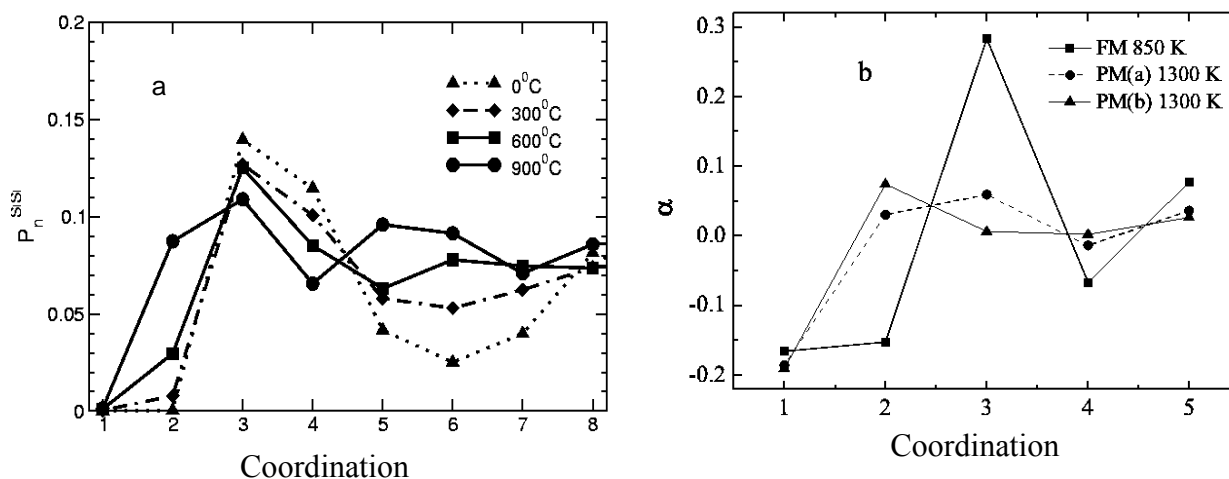


Fig. 1. The results of Monte Carlo simulation of SRO in Fe-Si (a) and Fe-Ga (b) alloys: P_n^{SiSi} - the probability of Si atom being in the n-th coordination shell; α - Warren-Cowley SRO parameter.

[1] H. Wang, Y.N. Zhang, R.Q. Wu et al., *Scientific Reports*, **3** (2013) 3521.

[2] O.I. Gorbatov, A.R. Kuznetsov, Yu.N. Gornostyrev et al., *JETP*, **139** (2011) 969.

1 July

Tuesday

09:30-11:00

plenary lectures
1PL-A

1PL-A-1

DEVELOPMENT OF MEDIA NANOSTRUCTURE FOR PERPENDICULAR MAGNETIC RECORDING

Futamoto M., Ohtake M.

Chuo University, Tokyo, Japan
futamoto@elect.chuo-u.ac.jp

Perpendicular magnetic recording (PMR) technology started to be introduced in commercial hard disk drives (HDDs) in 2005, and now all the high-end HDDs are based on this technology. The areal density has been increasing and it is expected to reach 10 Tb/in² around 2020, where the bit length is 4 – 6 nm. To cope with the increasing trend of areal density, key technologies including recording media, magnetic head, mechanical positioning, and interface technologies must be improved simultaneously. In the present talk, after a brief review on the PMR media technology, future possibilities will be discussed based on preliminary experiments.

PMR media employs double magnetic layer structure; semi-hard recording layer on soft-magnetic back-layer. The recording layer of current HDD is a granular type consisting of magnetic crystal grains with controlled diameter. One recorded bit includes multiple crystal grains. For the recording layer, several basic conditions must be satisfied. (a) The easy magnetization axis of magnetic crystal grain is perpendicular to the substrate surface. (b) Neighboring crystal grains are magnetically separated. (c) The grain diameter is well below the bit length. (d) The surface undulation of recording layer is below the physical spacing between head and medium. (e) The thickness of interlayer existing between the semi-hard and soft magnetic layers is small enough to keep a good writing efficiency of single-pole magnetic head. (f) And some other practical conditions exist considering mass-production of PMR media.

Tailoring the nanostructure of PMR media is based on the thin film growth physics which includes nucleation and growth of crystal, hetero-epitaxy, segregation of alloy elements or crystallographic phases, etc. The magnetic material for PMR recording layer has been chosen from Co-alloys ($K_u < 10^7$ erg/cm³) with hcp structure. Alignment of easy magnetization axis, *c*-axis, is realized through hetero-epitaxial growth on Ru (0001) textured polycrystalline film, which has been optimized after intensive investigations that lasted for many years [1]. Magnetic decoupling was initially tried by Cr segregation toward grain boundaries, and later it started to employ more effective phase segregation of SiO_x and CoPt-alloy materials [2]. In order to maintain the thermal stability of recorded information ($K_u V / k_B T > 60$) with magnetic crystal under a reduced volume condition, a high- K_u magnetic material such as FePt-alloy with $L1_0$ ordered structure ($K_u = 6.6 \times 10^7$ erg/cm³) is going to be introduced in commercial PMR media.

To further increase the areal density beyond 5 Tb/in², bit patterned media with isolated magnetic crystals will be employed. $L1_0$ -FePt-alloy has fct structure and involves disorder ($A1$) – order ($L1_0$) phase transformation during film growth process. Technologies in aligning the easy magnetization axis and in keeping flatness of $L1_0$ -FePt-alloy magnetic layer need to be developed. Preliminary experiments [3] suggest a possibility in tailoring the nanostructure of PMR media for 5 – 10 Tb/in² areal density.

[1] M. Futamoto, *ECS Transactions*, **50** (2013) 59–67.

[2] M. Futamoto, *J. Optoelectronics and Advanced Materials*, **11** (2009) 1567–1575.

[3] M. Ohtake, A. Itabashi, M. Futamoto, F. Kirino, N. Inaba, *Dig. Intermag 2014*, BB-09.

1PL-A-2

COEXISTENCE OF SUPERCONDUCTIVITY AND MAGNETISM AT THE NANOSCALE

Buzdin A.^{1,2}

¹ University of Bordeaux I, 33405, Bordeaux, France

² Institut Universitaire de France, Paris, France

a.bouzdine@loma.u-bordeaux1.fr

The main mechanisms of the interplay between magnetism and superconductivity and the coexistence between these two different long ranged orders in the bulk magnetic superconductors will be reviewed. The antagonism of ferromagnetism with a singlet superconductivity leads to spectacular effects such as a re-entrant superconductivity and the nanoscopic domain magnetic structure formation. In the triplet ferromagnetic superconductors, the competition between a self-induced vortex phase and a short-period domain structure may occur.

The very special character of the proximity effect in superconductor-ferromagnet heterostructures is revealed in the damped oscillatory behaviour of the Cooper pair wave function. And the formation of the special π -Josephson junctions is possible. Such " π -junction" incorporated in a superconducting circuit may generate a spontaneous current. The quantum oscillations and the " π "-states should also be present in multiply connected ferromagnet-superconductor hybrids, for example in a thin-walled superconducting shell surrounding a ferromagnetic cylinder.

The proximity effect in S/F structures is usually short-ranged though it can become long ranged when the magnetic structure is non-collinear. Recently it has been demonstrated that the Josephson junctions with a composite ferromagnetic interlayer indeed reveal the triplet long-ranged superconducting current. The triplet superconducting correlations provide the possibility to generate the magnetization in the Josephson junction. Such induced magnetization occurs at a relatively large distance, and is sensitive to the superconducting phase difference. By tuning the Josephson current, one may manipulate the long-range induced magnetic moment. The induced magnetic moment controlled by the Josephson current may therefore be used in spintronics devices instead of the spin-torque effect.

Moreover, Josephson junction with the weak link formed by a non-centrosymmetric ferromagnet possesses certain unusual properties. The ground state of this junction is characterized by the finite phase difference φ_0 , which is proportional to the strength of the spin-orbit interaction, and the exchange field in the normal metal. Such " φ_0 -junction" realises a direct coupling of the superconducting current with the magnetic moment. The superconducting current could flip the magnetic moment and, inversely, the ac Josephson effect should generate a magnetic precession providing then a feedback to the current.

Coupling between the superconducting current and magnetization opens the very interesting perspectives for emerging superconducting spintronics.

Support by European NanoSC COST Action MP1201, and French ANR "MASH" is acknowledged.

1 July

Tuesday

11:30-13:00

14:30-17:00

oral session

1TL-A

1RP-A

1OR-A

**“Spintronics and
Magnetotransport”**

1TL-A-1

THERMALLY ASSISTED SWITCHING-MRAM AND BEYOND

Alvarez-Herault J., Audinet P., Lombard L., Bandiera S., Ducruet C., Portemont C., Creuzet C., Conraux Y., Pereira J., Vidal J., Mackay K.
Crocus Technology, Grenoble, France
jherault@crocus-technology.com

Since 2006, Crocus Technology has been developing a new MRAM technology, the so-called Thermally Assisted Switching MRAM (TAS-MRAM) [1]. It is based on a storage layer made of a ferromagnet coupled to an antiferromagnet. When heated above the blocking temperature of the antiferromagnet, the ferromagnet becomes unpinned and can be switched. After cooling down the storage layer under a magnetic field, the ferromagnet is pinned in a new direction defined by the magnetic field orientation. In this technology, the heating process is done by applying a voltage to the magnetic bit that makes its temperature rise. This gives a very high selectivity with no chance of disturbing neighbors during a write process.

The stack used on our first generation memory consists in PtMn/SAF1/MgO/SAF2/FeMn. The FeMn layer ensures good data retention up to 85°C while having a low enough write temperature that yields a large gap between write voltage and MgO breakdown voltage. The PtMn layer is stable up to 300°C, far above the write temperature.

The first generation product is a 4Mb device (512KB) for Battery Backed-SRAM replacement, coming with 44-lead TSOP-II and 48-ball TFBGA packaging, powered with 3.3V. It has 8 banks of 512Kb, with field line drivers in the middle for each of them (see insert in Figure 1). Figure 1 shows the distributions of write and breakdown voltage in this TAS-MRAM product. The separation between the two distributions is essential to ensure good endurance. The write/read cycle can be as fast as 35ns, with a write heating pulse of about 10ns, which is in the order of magnitude of the thermal time constant [2].

A second generation of product is under development in Crocus named as Magnetic Logic Unit (MLUTM) [3]. The reference layer is replaced by a free ferromagnet: F / MgO / SAF / AF. Differential reading of the resistance under two successive magnetic field of opposite sign allow us to define the stored state in the bit cell without requiring any external reference. This self-referenced bitcell enable us to scale down the technology down to 45nm technology node.

Other features of this technology includes within cell logical XOR comparison for the development of Magnetic Logic Unit (MLUTM), fast and secure authentication system (Match-In-PlaceTM) as well as reliable high operating temperature memory, up to 250°C or higher.

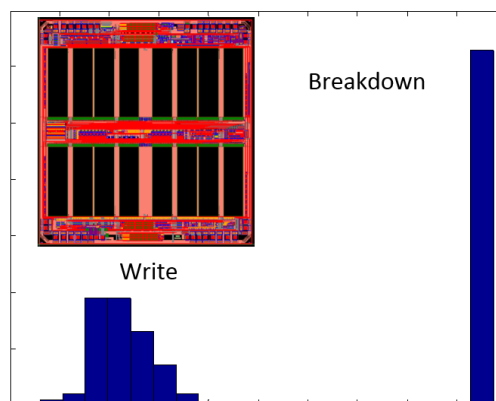


Figure 1: Distributions of write and breakdown voltages for the TAS-MRAM. Insert: top view of the 4Mb

[1] I.L. Prejbeanu et al, *J. Phys.: Condens. Matter*, **19** (2007).

[2] C. Papisoi et al, *New Journal of Physics*, **10** (2008).

[3] I.L. Prejbeanu et al, *J. Phys. D: Appl. Phys.* **46** (2013).

1OR-A-2

SPATIO-TEMPORALLY RESOLVED STUDY OF SPIN WAVE GENERATED BY LIGHT PULSES

Yoshimine I.¹, Satoh T.^{1,2}, Stupakiewicz A.³, Maziewski A.³, Shimura T.¹

¹ Institute of Industrial Science, the Univ. of Tokyo, Tokyo 153-8505, Japan

² PRESTO, Japan Science and Technology Agency, Tokyo 102-0076, Japan

³ Laboratory of Magnetism, Faculty of Physics, Univ. of Bialystok, Bialystok 15-424, Poland
yoshi3ne@iis.u-tokyo.ac.jp

Spin wave is propagating disturbance in magnetically ordered materials without Joule heating because net electron charges do not flow. It is expected that spin wave can be applied to information processing devices with low energy consumption.

Using polarized light pulses, spin wave can be generated via the inverse Faraday effect or the inverse Cotton-Mouton effect. This method does not need attaching electrodes for the excitation of the spin wave. Two techniques have been proposed to achieve direction control of the spin wave propagation; spatially-shaped light spot [1] and phased array [2].

In this study, we report the 3D-spatio-temporal (2D-spatial and 1D-temporal) waveform measurements of spin wave generated by light pulses with a pump-probe geometry using CCD camera. Circularly polarized pump pulses with 1300 nm wavelength and 150 fs time duration were focused on a $\text{Gd}_{3/4}\text{Yb}_{2/3}\text{BiFe}_5\text{O}_{12}$ single crystal to a spot diameter of 70 μm . In-plane external magnetic field $\mathbf{H} = 1$ kOe was applied to make the sample monodomain. Large area of the sample was illuminated with linearly polarized probe pulses and the probe pulses transmitted the sample and an analyzer were detected by CCD camera. The Faraday rotation of the probe pulse was calculated from multiple (about 20) images taken with changing the azimuth angle of the analyzer.

Measured map of the Faraday rotation of probe pulses at 1 ns after the generation of the spin wave is shown in Fig. 1(a). Good agreement between the experimental result and the calculated waveform of the spin wave is shown, assuming backward volume magnetostatic wave (Fig. 1(b)).

[1] T. Satoh, Y. Terui, R. Moriya, B. A. Ivanov, K. Ando, E. Saitoh, T. Shimura, K. Kuroda, *Nature Photon.*, **6** (2012) 662.

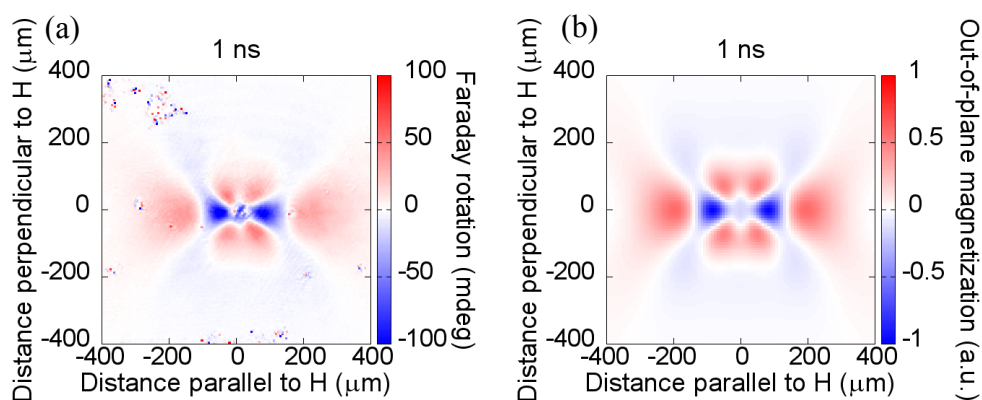


Fig. 1. (a) Measured map of the Faraday rotation of probe pulses.
(b) Calculated waveform of the spin wave.

1OR-A-3

NANOSIZED YTTRIUM-IRON GARNET FILMS ON Si: SYNTHESIS, MICROWAVE AND MAGNETOTRANSPORT PROPERTIES

*Stognij A.I.*¹, *Novitskii N.N.*¹, *Ketsko V.A.*², *Lutsev L.V.*³

¹ Scientific and Practical Materials Research Centre, National Academy of Sciences of Belarus, Minsk, Belarus

² Kurnakov Institute of General and Inorganic Chemistry, Russian Academy of Sciences, Moscow, Russia

³ Ioffe Physical-Technical Institute, Russian Academy of Sciences, St. Petersburg, Russia
l_lutsev@mail.ru

Nanosized magnetic films are of great interest due to their perspective applications in spin-wave and spintronic devices. Low relaxation of spin waves in thin magnetic films [1] and interaction between spin excitations in magnetic films and 2D electron interface layer in semiconductors in magnetic film / semiconductor heterostructures give us an opportunity to construct devices with new functional characteristics. In this paper we describe synthesis of garnet $\text{Y}_3\text{Fe}_5\text{O}_{12}$ (YIG) films sputtered on Si substrates and present results of the investigation of YIG / Si heterostructures – YIG film structure, interface layer characteristics, microwave and magnetotransport properties.

YIG films were deposited on Si substrates by ion-beam sputtering in Ar + O₂ atmosphere. In order to eliminate the lattice mismatch between YIG and Si, before sputtering process nanosized buffer amorphous AlO_x (SiO_x) layers were deposited on substrates. These layers with thicknesses lesser than 14 nm prevent diffusion of Si ions into YIG, stabilize YIG / Si interface during YIG crystallization and provide high adhesion properties of YIG films. After air annealing of YIG / Si heterostructures during 30 min at 800°C sputtered YIG films obtain polycrystal structure. Thicknesses of YIG films are in the range 20 – 100 nm.

Microwave properties of YIG / Si heterostructures were investigated in 2 – 4 and 9 – 10 GHz frequency bands. Magnetic and relaxation parameters of YIG films were found by the ferromagnetic resonance method. The effective magnetization of YIG films $4\pi M - H_a$, where $4\pi M$ is the magnetization and H_a is the anisotropy field, is in the range 1400 – 1600 Oe and is less than magnetization of the bulk YIG (1750 Oe). The FMR linewidth ΔH reaches 30 Oe.

Interaction between spin excitations in YIG films and electrons in 2D electron layers in Si at interfaces were studied on YIG / Si heterostructures with homogeneous YIG films and with periodic 1D structures performed on YIG (Fig. 1). This study is important for applications of magnon crystals for microwave modulations of current in semiconductors.

This work was supported (Lutsev) by the Government of Russia (project № 14.Z50.31.0021, leading scientist M. Bayer).

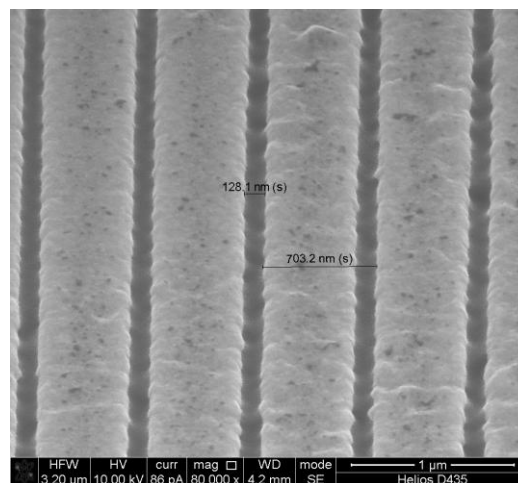


Fig. 1. Periodic structure performed on the YIG film with the thickness of 80 nm on the Si substrate. The width of YIG stripes is 575 nm, the period of the 1D structure is equal to 703 nm.

[1] L.V. Lutsev, *Physical Review B*, **85** (2012) 214413.

1OR-A-4

PECULIARITIES OF THE INTERFACE IN NANOSTRUCTURED Fe/Si AND Mn/Si FILMS

*Varnakov S.N.^{1,2}, Gomoyunova M.V.⁴, Grebenyuk G.S.⁴, Zabluda V.N.¹, Komogortsev S.V.^{1,3},
Platunov M.S.¹, Ovchinnikov S.G.¹, Pronin I.I.⁴*

¹ Kirensky Institute of Physics SB RAS, Krasnoyarsk, Russia

² Siberian State Aerospace University, Krasnoyarsk, Russia

³ Siberian State Technological University, Krasnoyarsk, Russia

⁴ Ioffe Physical Technical Institute RAS, St. Petersburg, Russia

vsn@iph.krasn.ru

Thin films of transition metal silicides are very promising for spintronics. Great attention is currently paid to iron and manganese silicides. Reports have shown the crystalline nature of the Fe layer, the amorphous nature of the Si layer, the interdiffusion of Fe and Si and the formation of different silicides, in Fe/Si thin films. Fe/Si bilayer and trilayer studies show the formation asymmetric silicide interlayers at Fe/Si and Si/Fe interfaces [1].

The formation of manganese-based magnetic structures also requires detailed knowledge of the interaction of Mn atoms with the silicon surface. Although manganese silicides either have a very low Curie temperature (TC) or are nonmagnetic in a bulk phase, they can possess high-temperature ferromagnetism in thin layers. Theoretical evaluations of TC performed for metastable MnSi layers with the structure of the B2 type stabilized by the Si(100) surface showed that this temperature for films one and two monolayers thickness can reach 241 and 328 K, respectively [2].

The objective of this work is to find the relative amount of magnetic and nonmagnetic phases, which are formed both during the synthetic procedure of Fe/Si and Si/Fe interfaces by X-ray magnetic circular dichroism (XMCD) study using its surface sensitivity. We present also (Fig 1) the results of the initial growth stages of the Mn films on Si(100)2×1 substrate investigation. Using high-energy-resolution photoelectron spectroscopy, we revealed the evolution of the variation in the phase composition of the film with the coverage growth.

Thickness of nonmagnetic FeSi and MnSi layers as well as magnetic silicides layer has been found for both Fe/Si and Mn/Si interfaces. All experiments were carried out using the Russian–German and UE46-PGM1 beamlines at the synchrotron radiation facility the HZB Bessy II electron storage ring.

Support by the Russian–German Laboratory at HZB BESSY, grant NSH-2886.2014.2 and the Russian Foundation for Basic Research (project nos. 13-02-00398 and 13-02-01265).

[1] S.R. Naik, S. Rai, M.K. Tiwari, G.S. Lodha, *J. Phys. D: Appl. Phys.*, **41** (2008) 115307.

[2] M. Hortamani, L. Sandratskii, P. Kratzer, I. Mertig, M. Scheffler, *Phys. Rev. B: Condens. Matter*, **78** (2008) 104402.

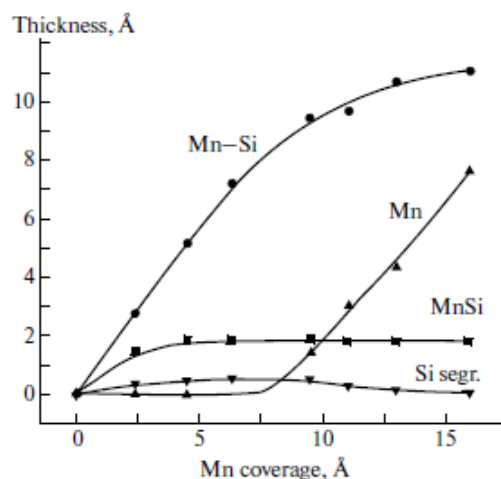


Fig. 1. Dependences of the average thickness of the layers of various chemical phases formed in the region of the Mn/Si interface on the coverage.

SPIN TRANSFER BY MOVING QUANTUM DOT

Kikoin K.

Tel Aviv University, Tel Aviv, Israel

konstk@post.tau.ac.il

Quantum dot (QD) under strong Coulomb blockade in a tunneling contact with metallic leads may be treated as an analog of magnetic impurity in Fermi liquid [1] where the tunneling rates in the former problem play the same part as the scattering rates in the latter problem. One can make tunneling rates time-dependent by means of variable gate voltage and/or external magnetic field. The dot itself can become movable being put on the tip of oscillating cantilever. In the latter case the QD works as a single electron shuttle transporting charge and spin between the leads [2,3].

We consider various shuttling mechanisms for a QD oscillating between the electrodes. The shuttling dot can contain both odd number of electrons with a local spin $\frac{1}{2}$ and even number of electrons in spin singlet ($S=0$) or triplet ($S=1$) state depending on the sign of exchange interaction. Electron cotunneling with spin flip results in many-electron Abrikosov–Suhl resonance at the Fermi level due to the Kondo effect for both odd and even occupation of QT [4]. Kondo screening gives substantial contribution in a resonance spin current. In case of moving Kondo shuttle the Kondo temperature is time dependent. As a result additional splashes in ac and dc current arise [5,6].

A Kondo shuttle in external magnetic field is a nano-electromechanical system (NEMS) [3], combining both classical elements (current carrying metallic cantilever moving in magnetic field) and quantum junction elements (tunneling contacts) [6]. We consider mechanisms of mechanical instabilities of NEMS due to Kondo screening effects and transitions from harmonic oscillations with weak damping to the self-sustained steady state with beatings [7]. The size of the Kondo screening cloud may be measured in such NEMS.

[1] L.I. Glazman, R.I. Shekhter, *J. Phys.: Condens. Mat.*, **1** (1989) 5811.

[2] Y. Azuma *et al.*, *Appl. Phys. Lett.*, **91** (2007) 053120.

[3] R.I. Shekhter *et al.*, *Nanoelectromech. Systems*, **1** (2013) 1-25.

[4] K. Kikoin *et al.*, (2012) *Dynamical Symmetries for Nanostructures*, Wien: Springer.

[5] M.N. Kiselev *et al.*, (2006) *Phys. Rev. B* **74**, 233403.

[6] M.N. Kiselev *et al.*, *Phys. Rev. Lett.*, **110**, 066804.

[7] T. Song *et al.*, *ArXiv*:1311.2317.

1TL-A-6

CORRELATIONS BETWEEN DIRECT AND CROSSED ANDREEV REFLECTIONS IN HYBRID NANOWIRES

*Bulka B.R.*¹, *Michalek G.*², *Domański T.*², *Wysokiński K.I.*²

¹ Institute of Molecular Physics, Polish Academy of Sciences, Poznań, Poland

² Institute of Physics, M. Curie-Skłodowska University, Lublin, Poland

bulka@ifmpan.poznan.pl

The hybrid multiterminal systems with normal, superconducting, and/or ferromagnetic electrodes attract a great interest for their rich physics and potential applications in spintronics [1]. Recently such systems have been proposed as effective sources of entangled electrons resulting from splitting of Cooper pairs. The entanglement can be detected via nonlocal conductances due to the Andreev reflections.

We consider the system [2] composed of an interacting quantum dot attached to three leads: two normal metallic and one superconducting. We study the interplay between various many-body effects in the electronic transport through this hybrid system. By the proximity effect the superconducting electrode induces pairing correlations on the quantum dot. The studies are focused on the subgap region where one can observe direct (DAR) and crossed (CAR) Andreev reflections, which compete with the usual electron transfer (ET) between normal electrodes. The interactions of electrons on the quantum dot lead to such phenomena as the Coulomb blockade and the Kondo effect. We show that these effects severely modify the currents flowing in the system.

The electronic transport is studied by means of the nonequilibrium Green function approach. Electron correlations are treated by approximate methods based on the equation of motion procedure and the iterative perturbation theory (applicable for the description of the Coulomb blockade and the Kondo correlations). The local and nonlocal differential conductances are calculated numerically for each conducting channel.

Our analysis shows that the Coulomb interactions generally suppress CAR processes in the large range of bias voltages. However, the CAR processes can dominate the transport in the vicinity of the Andreev bound states. The nonlocal conductance is then negative, what indicates entanglement of pairs of separated electrons: one of them entering to the left and the other one to the right normal electrode. The most interesting findings is that entanglement between electrons forming Cooper pair is not destroyed by the formation of the many particle collective singlet states (the Kondo cloud). We predict that in the Kondo regime the CAR processes dominate in the nonlocal transport channel at low voltages, leading to a large negative value of the total zero bias conductance.

Support by National Science Centre (under Contract DEC-2012/05/B/ST3/03208 and DEC-2011/01/B/ST3/04428) is acknowledged.

[1] S. D. Franceschi, et al., *Nat. Nanotechnol.*, **5** 703 (2010).

[2] G. Michalek, et al., *Phys. Rev. B* (2013).

1TL-A-7

ANATOMY OF PERPENDICULAR MAGNETIC ANISOTROPY IN MgO-BASED MAGNETIC TUNNEL JUNCTIONS FROM FIRST PRINCIPLES

Yang H. X., Hallal H., Dieny B., Chshiev M.

SPINTEC, UMR CEA/CNRS/UJF-Grenoble 1/Grenoble-INP, INAC, 38054 Grenoble, France
mair.chshiev@cea.fr

MgO-based magnetic tunnel junctions (MTJ) have been an object of overwhelming interest for spintronics due to Bloch states symmetry spin filtering leading to high tunnel magnetoresistance (TMR) for more than a decade [1]. Yet, the interest has been strongly reinforced and refocused by the discovery of large perpendicular magnetic anisotropy (PMA) at Co/AlO_x and FeCo(B)/MgO interfaces [2,3] due to the presence of large PMA values in perpendicular MTJs (pMTJ). This makes them ideally suitable for implementation as bit cells in spin transfer torque switching based magnetic random access memories (STT-MRAM) because they offer much better down-size scalability (increased density) and thermal stability than their in-plane counterparts [3].

Using first principles calculations, we unveil and elucidate microscopic mechanisms of PMA by anatomy of the orbital and atomic layer resolved contributions to magnetic anisotropy in Fe/MgO interfaces with different interfacial conditions [4,5]. First, very large perpendicular magnetocrystalline anisotropy values are found for Fe/MgO/Fe MTJs with pure interfaces and we demonstrate that oxidation conditions strongly affect the PMA which strongly correlates with TMR in agreement with experiments [2-7]. Second, it is demonstrated that the origin of the large PMA values is far beyond simply considering the hybridization between Fe-3d and O-2p orbitals at the interface between the metal and the insulator. Our on-site projected analysis show that the anisotropy energy is not localized at the interface but it rather propagates into the bulk showing an attenuating oscillatory behavior which depends on orbital character of contributing states and interfacial conditions [7]. Next, we show that states with $d_{yz(xz)}$ and d_{z^2} character tend always to maintain the PMA while those with d_{xy} and $d_{x^2-y^2}$ character tend to favor the in-plane anisotropy. It is also found that while MgO thickness has almost no influence on PMA, the calculated perpendicular magnetic anisotropy oscillates as a function of Fe thickness with a period of 2 atomic layers. Moreover, the behavior of effective anisotropy as a function of Fe thickness is demonstrated and analyzed. All these findings are in agreement with recent experiments reported by several groups (see Ref. [6] and references therein). Finally, we propose two ways to improve the effective out-of-plane anisotropy either by placing impurities in the ferromagnetic layer to decrease the demagnetizing fields or by introducing impurities at the insulating layer to increase interfacial PMA [8,9].

This work was supported by the Chair of Excellence Program of the Nanosciences Foundation in Grenoble, France, the ERC Advanced Grant Hymagine, and the KRCF DRC program.

- [1] W. H. Butler et al., *Phys. Rev. B* **63** (2001) 054416; *IEEE Trans. Magn.* **41** (2005) 2645.
- [2] S. Monso et al., *Appl. Phys. Lett.* **80** (2002) 4157; B. Rodmacq et al., *J. Appl. Phys.* **93** (2003) 7513; L. E. Nistor, B. Rodmacq, S. Auffret and B. Dieny, *Appl. Phys. Lett.* **94** (2009) 012512.
- [3] S. Ikeda et al., *Nature Mat.* **9** (2010) 271.
- [4] L. Nistor et al., *Phys. Rev. B* **81** (2010) 220407.
- [5] H.-X. Yang et al., *Phys. Rev. B* **84** (2011) 054401.
- [6] A. Hallal et al., *Phys. Rev. B* **88** (2013) 184423.
- [7] L. Nistor et al., *IEEE Trans. Magn.* **46** (2010)1412.
- [8] A. Hallal et al., submitted.
- [9] H. X. Yang et al., in prep.

1OR-A-8

MAGNETOTRANSPORT IN $\text{Ho}_x\text{Lu}_{1-x}\text{B}_{12}$: SEPARATING NEGATIVE AND POSITIVE MAGNETORESISTANCE IN METALS WITH MAGNETIC IONS

Sluchanko N.¹, Khoroshilov A.^{1,2}, Azarevich A.^{1,2}, Bogach A.¹, Glushkov V.^{1,2}, Demishev S.^{1,2},
Shitsevalova N.³, Filippov V.³, Levchenko A.³, Pristas G.⁴, Gabani S.⁴, Flachbart K.⁴

¹ Prokhorov General Physics Institute of RAS, Moscow, 119991 Russia

² Moscow Institute of Physics and Technology (State University), 141700, Dolgoprudnyi, Russia

³ Frantsevich Institute for Problems of Materials Science of NASU, Kiev, 03680 Ukraine

⁴ Institute of Experimental Physics of SAS, 040 01 Košice, Slovak Republic

nes@lt.gpi.ru

During last two decades a special attention was paid to compounds with a magnetic $d(f)$ -ions having “colossal” negative magnetoresistance (MR), where the MR is largest near ferro- or antiferromagnetic phase transitions¹. A various type imperfections (substitutional disorder, vacancies and other lattice defects, electronic, magnetic and structural inhomogeneities, non-stoichiometry, phase separation etc.) dominate these compounds with rare earth (RE) and transition metal (TM) ions to be discussing as possible common features responsible for the colossal MR effect. To shed more light on the origin of large negative MR observed in RE and TM systems in vicinity of Neel (T_N) and Curie temperatures it is promising to investigate model compounds with simple crystalline and magnetic structures in which both the different type of disorder and the dispersion of size and concentration of magnetic clusters can be controlled.

In this report we show that it is very effective to perform a study of negative MR effect in *fcc* metallic solid solutions $\text{Ho}_x\text{Lu}_{1-x}\text{B}_{12}$ with Ho^{3+} magnetic ions embedded in the rigid covalent boron cage. Recently the comprehensive measurements of LuB_{12} crystals enabled us to find a new disordered “cage-glass” phase at nitrogen temperatures². It was shown² that the combination of loosely bound state of the RE ions in the rigid boron sub-lattice of RB_{12} together with randomly arranged boron vacancies ($\sim 1\text{-}3\%$) initiate the development of a lattice instability at intermediate temperatures. As a results, below $T^* \sim 60$ K the RE-ions become frozen in randomly distributed off-center positions inside truncated B_{24} octahedrons. In $\text{Ho}_x\text{Lu}_{1-x}\text{B}_{12}$ with magnetic Ho^{3+} -ions there is in addition substitutional disorder which interferes with random displacements (static disorder) of RE-sites in the metallic cage glass phase.

Dealing with dilute ($x \leq 0.1$) paramagnetic and concentrated ($0.3 \leq x \leq 0.5$) antiferromagnetic $\text{Ho}_x\text{Lu}_{1-x}\text{B}_{12}$ borides we have observed both the appearance of negative MR (Fig. 1) simultaneously with emergence of Ho^{3+} nanosize clusters in the RB_{12} matrix and an enhancement of this effect in the vicinity of T_N . The analysis developed here, allowed us (i) to estimate from MR results the salient characteristics of magnetic clusters below (dimers, trimers etc) and above (a short range order AF domains) the percolation threshold x_C and (ii) to conclude in favor of an interference between local ($4f$) and itinerant ($5d$) components in the complex magnetic structure of these antiferromagnets.

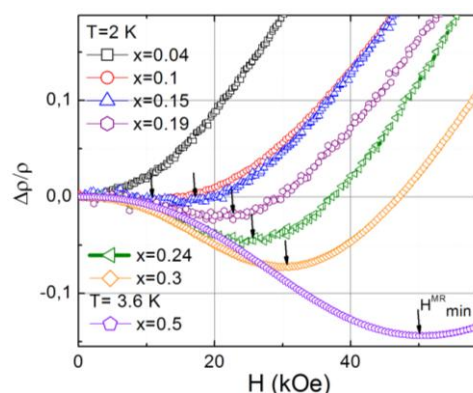


Fig. 1. Low temperature magnetoresistance in $\text{Ho}_x\text{Lu}_{1-x}\text{B}_{12}$.

[1] E.Dagotto, T.Hotta, A.Moreo, *Phys. Rep.* **344** (2001)1-153.

[2] N.E. Sluchanko, A.N. Azarevich, A.V. Bogach, et. al., *JETP* **113** (2011) 468.

1RP-A-9

TOPOLOGICALLY PROTECTED DYNAMICS OF SPIN TEXTURES*Tretiakov O.A.*Institute for Materials Research, Tohoku University, Sendai, Japan
olegt@imr.tohoku.ac.jp

Ferromagnets (FMs) and antiferromagnets (AFMs) can be used to store and manipulate spin information, and new developments have created opportunities to use them as active components in spintronic devices. We study current-induced domain-wall (DW) dynamics in thin FM and AFM nanowires. We derive effective equations of motion describing the dynamics of the DW soft modes associated with topological defects. Because the DWs are topological objects, these equations are rather universal and depend only on a few parameters. Similar equations describe the dynamics of skyrmions in FMs. We obtain spin spiral DW structure in FM wires with Dzyaloshinskii-Moriya interaction (DMI) and critical current dependence on the DMI [1]. We also find the most efficient way to move the DWs by resonant current pulses [2] and propose a procedure to determine the DW dynamics by measuring the voltage induced by moving DW [3]. Based on translationally non-invariant nanowires, we show how to make prospective magnetic memory nanodevices much more energy efficient [4]. In AFMs, the dynamics is more complex because of the coupling between the staggered field and magnetization. Nevertheless, using collective coordinate approach we are able to describe the AFM dynamics and show that it is equivalent to the motion of a massive particle subjected to friction and external forces. We find that in AFMs the currents induce DW motion by means of dissipative rather than reactive torques [5].

Support by MEXT, Japan is acknowledged.

- [1] O.A. Tretiakov, Ar. Abanov, *Phys. Rev. Lett.*, **105** (2010) 157201.
- [2] O.A. Tretiakov, Y. Liu, Ar. Abanov, *Phys. Rev. Lett.*, **105** (2010) 217203.
- [3] Y. Liu, O.A. Tretiakov, Ar. Abanov, *Phys. Rev. B*, **84** (2011) 052403.
- [4] O.A. Tretiakov, Y. Liu, Ar. Abanov, *Phys. Rev. Lett.*, **108** (2012) 247201.
- [5] E.G. Tveten, A. Qaiumzadeh, O.A. Tretiakov, A. Brataas, *Phys. Rev. Lett.*, **110** (2013) 127208.

1RP-A-10

BIAS-VOLTAGE-CONTROLLED AC AND DC MAGNETOTRANSPORT PHENOMENA IN HYBRID STRUCTURES

Volkov N.V.^{1,2}, Tarasov A.S.¹, Smolyakov D.A.¹, Varnakov S.N.^{1,2}, Ovchinnikov S.G.¹

¹ L.V. Kirensky Institute of Physics, Russian Academy of Sciences, Siberian Branch, Krasnoyarsk, Russia

² Institute of Space Technologies, Siberian State Aerospace University, Krasnoyarsk, Russia
volk@iph.krasn.ru

The systematic search for novel systems with the transport properties highly sensitive to an external magnetic field is a topical problem due to the high application potential of such systems. Here, we demonstrate that the metal/insulator/semiconductor hybrid structures (MIS structures) with the Schottky barrier exhibit a number of specific ac and dc magnetotransport phenomena [1–3]. We studied the Fe/SiO₂/p(n)-Si structures and simple devices based on them. It was found that the structures are characterized by a dc magnetoresistance (MR). The value of the MR ratio of the Fe/SiO₂/p-Si structure is not high (no more than 20% at 9 T); however, the value and sign of the MR ratio can be controlled by a bias voltage applied to the structure. It was established that a magnetic field affects stronger the ac transport properties of the structures. The gigantic change in the impedance in an applied magnetic field was observed in a MIS diode with the Schottky barrier fabricated on the basis of the Fe/SiO₂/n-Si structure. The maximum effect was observed at temperatures of 10–30 K in the frequency range 10 Hz – 1 MHz, where the ac magnetoresistance and magnetoreactance ratios exceed 300% and 600%, respectively, at 1 T. In the low-frequency region (< 1 kHz), the ratios can vary within a wide range by applying a bias voltage to the diode.

In addition, we observed a fundamentally new phenomenon: the dc MR effect that occurs under the action of optical radiation in a planar devices built on the Fe/SiO₂/p(n)-Si hybrid structures. The devices comprise two Schottky diodes connected by a silicon substrate. The photoinduced MR is positive and the MR ratio attains the values over 10⁵%. The main specific feature of the MR behavior is the strong dependence of MR on the value and sign of the bias current across the device and, which is the most surprising, on magnetic field polarity.

We established that all the observed magnetotransport properties are related to the existence of the states localized near the SiO₂/p(n)-Si interface. These centers affect the transport properties of the structures, participating in recharging. The processes of electron capture and emission couple the interface levels and the conduction band. Moreover, electron tunneling through the SiO₂ barrier occurs and, under illumination, electrons participate also in the optical transitions. The application of a magnetic field changes mainly the energy structure of the interface states, thereby exerting the influence on the processes of center recharging. Under certain conditions, a magnetic field can directly affect the probability of electron tunneling between the interface states and the ferromagnetic electrode of the structure. The asymmetry relative to the magnetic field sign observed for the photoinduced MR effect originates from the Lorentz forces that affect nonequilibrium carriers and from a specific topology of the device.

This study was supported by the Russian Foundation for Basic Research, project no. 14-02-00234-a; the Presidium of the Russian Academy of Sciences, program “Quantum Mesoscopic and Disordered Structures”, project no. 20.8.

[1] N.V. Volkov et al., *J. Appl. Phys.*, **109** (2011) 123924.

[2] N.V. Volkov et al., *J. Appl. Phys.*, **112** (2012) 123906.

[3] N.V. Volkov et al., *J. Appl. Phys.*, **114** (2013) 093903.

1OR-A-11

HALL EFFECT INDUCED BY SPIN-WAVE EXCITATION IN METAL/FERROMAGNETIC INSULATOR BILAYER.

Vedyayev A.V.¹, Zhuravlev M.Ye.², Titova M.S.¹, Ryzhanova N.V.¹, Guskova D.³

¹ Department of Physics, M. V. Lomonosov Moscow State University, 119991 Moscow, Russia

² Kurnakov Institute for General and Inorganic Chemistry, Russian Academy of Sciences, 119991 Moscow, Russia

³ INAC, UMR CEA CNRS UJF Grenoble Grenoble INP 1, SPINTEC, F-38045 Grenoble, France
myezhur@gmail.com

The Anomalous Hall Effect (AHE) has recently attracted significant interest due to its potential application in spintronics. AHE is caused by spin-orbit interactions of several types. In our theoretical investigation we consider two-layered system. Spin-orbit interaction of Rashba type takes place near metal/insulator interface. Magnetization of the ferromagnetic insulator rotates with some frequency ω by microwave radiation under ferromagnetic resonance condition.

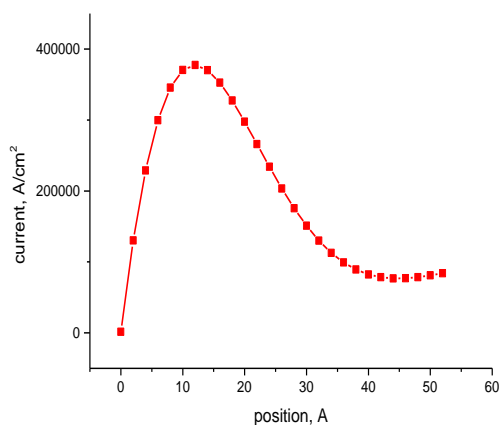


Fig. 1

Hall current as a function of the distance from the interface. Fermi energy $E_F = 2eV$, the barrier for up and down- electrons $U - E_F \pm J_{sd}$, $U = 3.5eV$, $J_{sd} = 1eV$, $\omega = 50 \text{ GHz}$.

This rotation together with spin-orbit interaction in non-magnetic metal layer induces Hall current along the interface. The Hall current appears under zero bias in the system. It disappears when exchange splitting of the insulator's bands tends to zero. We apply free-electron model to calculate the Hall current in the system and we adopt the approach which was used in several preceding works to investigate Hall Effect and Spin Hall Effect in disordered ferromagnetics and magnetic tunnel junctions [1-3]. The dependence of Hall current on the exchange splitting, the magnetization rotation frequency and the barrier height are calculated. Fig. 1 displays the dependence of Hall current in the metal on the distance from the interface. We analyze various contributions in Hall current and discuss the limit of small frequencies. Also we investigate time dependence of Hall current in the bilayer system.

The work was supported by the Russian Foundation for Fundamental Research, Grant No. 13-02-01452.

[1] P. Wölfle and K. A. Muttalib, *Ann. Phys.* **15**, 508 (2006).

[2] A. Vedyayev, N. Ryzhanova, N. Strelkov, B. Dieny, *Phys. Rev. Lett.* **110**, 247294 (2013).

[3] A.V. Vedyayev, M.S. Titova, N.V. Ryzhanova, M.Ye. Zhuravlev, E.Y. Tsymbal, *Appl. Phys. Lett.* **103**, 032406 (2013).

1 July

Tuesday

11:30-13:00

14:30-17:00

oral session

1TL-B

1TL-LT

1RP-LT

1OR-LT

**“Magnetism and
Superconductivity”**

1TL-B-1

PERSISTENT CURRENTS IN QUANTUM PHASE SLIP RINGS*Semenov A.G.¹, Zaikin A.D.^{1,2}*¹ I.E.Tamm Department of Theoretical Physics, P.N.Lebedev Physics Institute, Moscow, Russia² Institute of Nanotechnology, Karlsruhe Institute of Technology (KIT), Karlsruhe, Germany
andrei.zaikin@kit.edu

We investigate the effect of interacting quantum phase slips on persistent current and its fluctuations in ultrathin superconducting nanowires and nanorings pierced by the external magnetic flux. We derive the effective action for these systems and map the original problem onto an effective sine-Gordon theory on torus. We evaluate both the flux dependent persistent current and the critical radius of the ring beyond which this current gets exponentially suppressed by quantum fluctuations. We also analyze fluctuations of persistent current caused by quantum phase slips. At low temperatures the supercurrent noise spectrum has the form of coherent peaks which can be tuned by the magnetic flux [1]. Experimental observation of these peaks can directly demonstrate the existence of plasma modes in superconducting nanorings.

[1] A.G. Semenov, A.D. Zaikin, *Phys. Rev. B*, **88** (2013) 054505.

1TL-B-2

TRANSPORT IN PROXIMITY-COUPLED SUPERCONDUCTOR-FERROMAGNET DEVICES*Eschrig M.*SEPnet and Hubbard Theory Consortium, Department of Physics, Royal Holloway,
University of London, Egham, Surrey TW20 0EX, United Kingdom
matthias.eschrig@rhul.ac.uk

Superconducting spintronics is an emerging field that combines the two highly successful areas of spintronics and superconductivity. Whereas in spintronics the manipulation and control of the spin of quasiparticles is the focus, superconductivity deals predominantly with macroscopic quantum interference. The combination of both fields is promising for applications as well as for fundamental science.

We discuss phenomena that are based on induced spin-triplet Cooper pairs in devices composed of superconducting and ferromagnetic parts. Such phenomena include for example equal-spin triplet super currents in Josephson devices, thermoelectric phenomena, as well as non-local transport phenomena in multi-terminal superconductor-ferromagnet devices.

We elucidate the crucial role of spin-dependent scattering phases at interfaces for the properties of ferromagnet-superconductor devices in both the diffusive and ballistic limit. Such scattering phases lead to spin-polarised sub-gap Andreev states which dominate transport phenomena in a characteristic way. We show examples for energy and charge transport in three-terminal junctions composed of two ferromagnets and a spin-singlet superconductor.

This work is supported by the EPSRC under grant reference EP/J010618/1.

1TL-B-3

GIANT THERMOELECTRIC EFFECTS IN A PROXIMITY-COUPLED SUPERCONDUCTOR-FERROMAGNET DEVICE

Belzig W.¹, Machon P.¹, Eschrig M.²

¹ Department of Physics, University of Konstanz, D-78457 Konstanz, Germany

² SEPnet and Hubbard Theory Consortium, Department of Physics, Royal Holloway, University of London, Egham, Surrey TW20 0EX, United Kingdom

Wolfgang.Belzig@uni-konstanz.de

We study thermal and charge transport in a three-terminal setup consisting of one superconducting and two ferromagnetic contacts. We predict that the simultaneous presence of spin filtering and of spin-dependent scattering phase shifts at each of the two interfaces will lead to very large nonlocal thermoelectric effects both in clean and in disordered systems. The symmetries of thermal and electric transport coefficients are related to fundamental thermodynamic principles by the Onsager reciprocity. Our results show that a nonlocal version of the Onsager relations for thermoelectric currents holds in a three-terminal quantum coherent ferromagnet-superconductor heterostructure including a spin-dependent crossed Andreev reflection and coherent electron transfer processes [1].

As a result, the usually negligibly small thermoelectric effects in superconducting heterostructures can be boosted dramatically due to the simultaneous effect of spin splitting and spin filtering [1]. Building on that observation, we propose realistic mesoscopic setups to observe thermoelectric effects in superconductor heterostructures [2]. We focus on the Seebeck effect being a direct measure of the local thermoelectric response and find that a thermopower of the order of $200\mu\text{V/K}$ can be achieved in a transistor-like structure with normal source and drain, in which the third superconducting terminal induces a strongly modified spin-polarized density of states in the active region. A measurement of the thermopower in such a setup can furthermore be used to determine quantitatively the spin-dependent interface parameters that induce the spin splitting. For applications in nanoscale cooling we discuss the figure of merit for which we find large values exceeding 1.5 for temperature about or less than 1K [2].

[1] P. Machon, M. Eschrig, and W. Belzig, *Phys. Rev. Lett.* **110**, 047002 (2013).

[2] P. Machon, M. Eschrig, and W. Belzig, *arXiv:1402.7373*.

1TL-LT-1

RESONANT INELASTIC X-RAY SCATTERING ON HIGH T_c CUPRATES AND MAGNETIC IRIDATES

van den Brink J.

Institute for Theoretical Solid State Physics, IFW Dresden, Helmholtzstr. 20, 01069 Dresden, Germany

j.van.den.brink@ifw-dresden.de

Resonant Inelastic X-ray Scattering (RIXS) provides direct access to elementary charge, spin and orbital excitations in complex oxides. As a technique it has made tremendous progress with the advent high-brilliance synchrotron X-ray sources. From the theoretical perspective the fundamental question is to precisely which low-energy correlation functions RIXS is sensitive. Depending on the experimental RIXS setup, the measured charge dynamics can include charge-transfer, phonon, d-d and orbital excitations [1]. The focus of this talk will be on RIXS as a probe of spin dynamics and superconducting gap of high- T_c cuprates [2–4] and the combined magnetic and orbital modes in strongly spin-orbit coupled iridium-oxides [5–10].

PACS numbers: PACS numbers: 71.27.+a, 71.70.-d, 71.70.Gm, 74.70.-b

- [1] L. J. P. Ament, M. van Veenendaal, T. P. Devereaux, J. P. Hill, J. van den Brink, *Rev. Mod. Phys.* **83**, 705 (2011).
- [2] L. Braicovich, et al., *Phys. Rev. Lett.* **104**, 077002 (2010).
- [3] M. P. M. Dean, et al., *Nature Materials* **11**, 850 (2012).
- [4] P. Marra, S. Sykora, K. Wohlfeld, J. van den Brink, *Phys. Rev. Lett.* **110**, 117005 (2013).
- [5] L. J. P. Ament, G. Khaliullin, J. van den Brink, *Phys. Rev. B* **84**, 020403 (2011).
- [6] V. M. Katukuri, H. Stoll, J. van den Brink, L. Hozoi, *Phys. Rev. B* **85**, 220402 (2012).
- [7] N. A. Bogdanov, V. M. Katukuri, H. Stoll, J. van den Brink, L. Hozoi, *Phys. Rev. B* **85**, 235147 (2012).
- [8] J. Kim, et al., *Phys. Rev. Lett.* **108**, 177003 (2012).
- [9] X. Liu, et al., *Phys. Rev. Lett.* **109**, 157401 (2012).
- [10] H. Gretarsson, et al., *Phys. Rev. Lett.* **110**, 076402 (2013).

1TL-LT-2

DIRECT OBSERVATION OF THE INDUCED Cu MAGNETIC ORDER IN LCMO/YBCO BILAYERS BY THE RESONANCE SOFT X-RAY MAGNETIC SCATTERING

Lin J.-Y.,^{1,2}, Huang Shih-Wen,^{1,3}, Wray A.L.¹, Jeng Horng-Tay^{4,5}, Lee J.M.⁶, Langer M.C.³,
Tra V. T.², Chen J.M.⁶, Chu Y.H.⁷, Schoenlein R.W.³, Chuang Yi-De¹

¹ Advanced Light Source, Lawrence Berkeley National Laboratory, Berkeley, CA 94720, USA

² Institute of Physics, National Chiao Tung University, Hsinchu 30010, Taiwan

³ Materials Sciences Division, Lawrence Berkeley National Laboratory, Berkeley, CA 94720, USA

⁴ Department of Physics, National Tsing Hua University, Hsinchu 30013, Taiwan

⁵ Institute of Physics, Academia Sinica, Taipei 11529, Taiwan

⁶ National Synchrotron Radiation Research Center, Hsinchu 30076, Taiwan

⁷ Department of Materials Science and Engineering, National Chiao Tung University, Hsinchu, 30010, Taiwan

JYL: jiunn-yuanlin@lbl.gov

“The interface is the device.” Novel phenomena emerging at the interface of two materials are possible routes to create new and multi-functionality devices, which are one of the focal points for nano-science and technology. Utilizing the resonance soft x-ray magnetic scattering (RXS), we investigated the magnetic proximity effect of ferromagnetic $\text{La}_{0.7}\text{Ca}_{0.3}\text{MnO}_7$ /superconducting $\text{YBa}_2\text{Cu}_3\text{O}_{7-x}$ bilayers with two distinct types of terminations (shown in the following figure). The temperature dependent RXS results indicate a long range magnetic order of CuO_2 planes, which develops in accord with the ferromagnetic ordering of Mn ions. Furthermore, by measuring the YBCO (0 0 1) lattice peak as a function of energy, we unexpectedly observed a coherently charge redistribution on CuO chains.

This work was supported by NSC, Taiwan and DOE, USA.

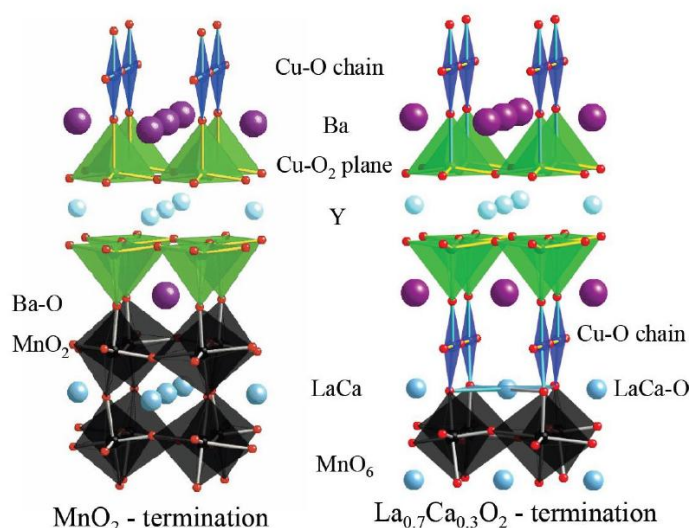


Figure. Schematics of the MnO_2 - and $\text{La}_{0.7}\text{Ca}_{0.3}$ -terminated interfaces.

1TL-LT-3

ELECTRONIC ANOMALIES IN THE SUPERCONDUCTING STATE OF HIGH- T_c CUPRATES AS FINGERPRINTS OF SPIN FLUCTUATION MEDIATED SUPERCONDUCTIVITY

Onufrieva F., Pfeuty P.

Laboratoire Leon Brillouin, CE-Saclay

The role of spin fluctuations (SFs) for electronic properties of high- T_c cuprates is still a subject for hot debates. It becomes clear now that the scenario of the superconductivity mediated by SFs can explain certain crucial electronic properties observed experimentally : the d-symmetry of pairing, the important details in the form of electron spectral functions observed near optimal doping, such as the nodal kink, peak-dip-hump form of spectral functions etc., see for example [1-3]. It is the underdoped regime that poses a problem.

In the talk I will present a theoretical study of the impact of spin fluctuations (SFs) on electronic properties when these fluctuations are soft and strong as in the low doped cuprates. We have shown [4] that above certain threshold the stronger spin fluctuations the more destructive role they play for superconducting pairing contrary to naïve expectations and especially contrary to the ordinary phonon induced superconductivity. This happens since simultaneously with effect to produce the attractive interaction, SFs destroy the electron coherence. On the other hand, the softening of SFs produces the same effect as their strengthening so that at low doping where SFs are soft and strong in approaching the AF instability, two effects mediated by SFs are in competition: the destruction of electron coherence and the attraction in the SC channel. The resulting SC state is quite interesting, it shows up the anomalous behaviour of electronic properties amusingly close to those observed experimentally in highly underdoped cuprates (ARPES, STM, Raman).

This scenario can also explain the form in dome of T_c versus doping. Indeed, as follows from our results, the higher the characteristic energy of SFs, ω_0 , with respect to the maximum electron gap, Δ_{\max} , the more effective SFs for SC pairing. Since ω_0 increases with increase the distance from AF instability, i.e. with increasing doping, while Δ_{\max} decreases with doping, the optimal doping occurs when $\omega_0 \sim \Delta_{\max}$.

- [1] P. Monthoux and D. Pines, *Phys.Rev.Lett.*, **69** (1992) 961.
- [2] M. Eschrig and M. Norman, *Phys.Rev.B*, **67** (2003)144503.
- [3] F.Onufrieva and P.Pfeuty, *Phys.Rev.Lett.*, **102** (2009) 207003.
- [4] F.Onufrieva and P.Pfeuty, *Phys.Rev.Lett.*, **109** (2012) 257001.

1TL-LT-4

SUPERCONDUCTING SPIN VALVES, CURRENT STATUS

*Kupriyanov M.Yu.^{1,4}, Bakurskiy S.V.^{2,4}, Golubov A.A.^{3,4}, Karminskaya T.Yu.¹, Klenov N.V.²,
Pugach N.G.¹, Prischepa S.L.⁵, Soloviev I.I.¹*

¹ Skobeltsyn Institute of Nuclear Physics Lomonosov Moscow State University, Moscow, Russian Federation

² Physics Department Lomonosov Moscow State University, Moscow, Russian Federation

³ Faculty of Science and Technology and MESA+ Institute for Nanotechnology, University of Twente, The Netherlands

⁴ Moscow Institute of Physics and Technology, State University, Dolgoprudniy, Moscow region, Russian Federation

⁵ Belarusian State University of Informatics and RadioElectronics, Minsk, Belarus

Corresponding author: mkupr@pn.sinp.msu.ru

We discuss the current status of theoretical understanding and experimental realizations of superconducting spin valves.

The interest to this problem is motivated by the recent developments, which clearly demonstrated that the achieved background in this field provides the opportunity for finding solutions for elaboration of superconducting memory cells, which can be integrated with RSFQ logic circuits. These cells are based on heterostructures, which consist of superconducting (S) materials, insulator (I), ferromagnetic (F) and normal (N) metals. Fabrication and study of such heterostructures is one of the components of the new U.S. program, providing for the next 4 years the establishment of production for the manufacture of working model of a prototype superconducting computer [1].

We start with the brief discussion of peculiarities of proximity effect in SF and SFF multilayers and their manifestation in spin valve devices controlling critical temperature of S film or conductance of one of the F layers.

The recent status of experimental and theoretical achievements in developing SISFS and SFFS Josephson devices, which are considered as the control unit of superconducting memory cell will be discussed. Special attention will be given to the effect of formation of domain walls and normal phase inclusions in the F films on the junction critical current.

Support by RFBR grants 14-02-90018, 14-02-31002_mol_a, Ministry of Education and Science of the Russian Federation, President grant MK-1841.2014.2, and BFBR grant F14R-020 is acknowledged.

[1] D. S. Holmes, A.L.Ripple, and M.A. Manheimer, *IEEE Trans. on Appl. Supercond.*, **23** (2013) 1701610.

http://www.iarpa.gov/Programs/sso/C3/solicitation_c3.html

1RP-LT-5

INTERFERENCE PHENOMENA AND LONG-RANGE PROXIMITY EFFECT IN CLEAN SUPERCONDUCTOR-FERROMAGNET SYSTEMS

Mel'nikov A.S.¹, Samokhvalov A.V.¹, Buzdin A.I.²

¹ Institute for Physics of Microstructures, Russian Academy of Sciences, Nizhny Novgorod, Russia

² Institut Universitaire de France and Universite Bordeaux I, Bordeaux, France

melnikov@ipm.sci-nnov.ru

We study peculiarities of the proximity effect in clean superconductor-ferromagnet structures caused by either the spatial or momentum dependence of the exchange field. Even a small modulation of the exchange field along the quasiparticle trajectories is shown to provide a long-range contribution to the supercurrent due to the specific interference of particle- and holelike wave functions. The momentum dependence of the exchange field caused by the spin-orbit interaction results in long-range superconducting correlations even in the absence of a ferromagnetic domain structure and can explain recent experiments on ferromagnetic nanowires.

The exchange field h in ferromagnetic (F) metals is well known to destroy Cooper pairs resulting, thus, in a strong decay of superconducting correlations in the F material and suppression of the Josephson current in superconductor-ferromagnet-superconductor (S-F-S) junctions. This destructive effect of the exchange field can be viewed as a consequence of the phase difference $\gamma = L/\xi_h = 2Lh/\hbar v_F$ gained between the electron- and holelike parts of the total wave function for a path of length L . The measurable quantities should be calculated as superpositions of fast oscillating contributions $e^{i\gamma}$ from different trajectories and, thus, rapidly vanish with increasing distance from the superconductor-ferromagnet boundary. This conclusion is in sharp contrast with a number of recent experiments which point to an anomalously large length of decay of superconducting correlations inside the F metal. In the dirty limit such a strong proximity effect can hardly be explained even taking into account long-range triplet correlations induced by the exchange field inhomogeneity. Naturally, the inhomogeneity of the field h caused by the ferromagnetic domain structure can improve the conditions of Cooper pair survival in the clean limit as well. To suppress the destructive trajectory interference mentioned above the domain structure should cancel the phase gain γ for a certain group of quasiparticle trajectories. On the other hand in the diffusive limit this compensation effect vanishes. Note that an exchange field inhomogeneity along the quasiclassical trajectory experiencing multiple reflections from the ferromagnet surface can appear even in the absence of the spatial domain structure. Indeed, the exchange field acting on band electrons in a solid with a finite spin-orbit interaction should obviously depend on the quasiparticle momentum: $\vec{h} = \vec{h}(\vec{k})$. The normal quasiparticle reflection is accompanied, of course, by a change in the momentum direction, and, thus, by a change in the exchange field. The momentum dependent h field can strongly affect the phase gain γ along the trajectories even in a F sample prepared in a single domain state. The goal of this talk is to show that this effect provides the possibility of cancelling the particle-hole phase difference for a large group of quasiclassical trajectories due to either the spatial or momentum dependence of the exchange field. Such a set of trajectories provides a long-range contribution to the Josephson current through a ferromagnetic system. We consider two generic examples which illustrate the above scenario of a long-range proximity effect: (i) Josephson transport through a pair of ferromagnetic layers with a stepwise exchange field distribution; (ii) Josephson transport through a nanowire with a specular electron reflection at the surface and an exchange field varying with the changing quasiparticle momentum.

1RP-LT-6

DETECTION OF SMALL EXCHANGE FIELDS IN S/F STRUCTURES*Vasenko A.S.*¹, *Kawabata S.*², *Ozaeta A.*³, *Golubov A.A.*⁴, *Bergeret F.S.*³, *Hekking F.W.J.*¹¹ LPMMC, Université Joseph Fourier and CNRS, 25 Avenue des Martyrs, Grenoble, France² Electronics and Photonics Research Institute (ESPRIT), National Institute of Advanced Industrial Science and Technology (AIST), Tsukuba, Ibaraki, 305-8568, Japan³ Donostia International Physics Center (DIPC), Manuel de Lardizabal 4, San Sebastian, Spain⁴ Faculty of Science and Technology and MESA+ Institute for Nanotechnology, University of Twente, 7500 AE Enschede, The Netherlands

andrey.vasenko@lpmmc.cnrs.fr

Ferromagnetic materials with exchange fields E_{ex} smaller or of the order of the superconducting gap Δ are important for applications of corresponding (s-wave) superconductor/ferromagnet/superconductor (SFS) junctions. Presently such materials are not known but there are several proposals how to create them. Small exchange fields are in principle difficult to detect. Based on our results we propose reliable detection methods of such small E_{ex} [1]. For exchange fields smaller than the superconducting gap the subgap differential conductance of the normal metal - ferromagnet - insulator - superconductor (NFIS) junction shows a peak at the voltage bias equal to the exchange field of the ferromagnetic layer, $eV = E_{ex}$ [2]. Thus measuring the subgap conductance one can reliably determine small $E_{ex} < \Delta$. In the opposite case $E_{ex} > \Delta$ one can determine the exchange field in scanning tunneling microscopy (STM) experiment. The density of states of the FS bilayer measured at the outer border of the ferromagnet shows a peak at the energy equal to the exchange field, $E = E_{ex}$ [3]. This peak can be only visible for small enough exchange fields of the order of few Δ .

[1] A. S. Vasenko, S. Kawabata, A. Ozaeta, A. A. Golubov, F. S. Bergeret, and F. W. J. Hekking, unpublished [arXiv:1401.0646].

[2] A. Ozaeta, A. S. Vasenko, F. W. J. Hekking, and F. S. Bergeret, *Phys. Rev. B*, **86** (2012) 060509(R).

[3] A. S. Vasenko, S. Kawabata, A. A. Golubov, M. Yu. Kupriyanov, C. Lacroix, F. S. Bergeret, and F. W. J. Hekking, *Phys. Rev. B*, **84** (2011) 024524.

1OR-LT-7

CURRENT PROPERTIES OF JOSEPHSON SISFS JUNCTIONS

Bakurskiy S.V.^{1,3}, *Klenov N.V.*¹, *Soloviev I.I.*², *Pugach N.G.*², *Golubov A.A.*^{3,4}, *Kupriyanov M.Yu.*^{2,3}

¹ Faculty of Physics, Lomonosov MSU, Moscow, Russia

² SINP, Lomonosov MSU, Moscow, Russia

³ Moscow Institute of Physics and Technology, Dolgoprudny, Moscow Region, Russia

⁴ Faculty of Science and Technology, University of Twente, The Netherlands

r4zz@mail.ru

In recent years Josephson junctions with ferromagnetic F layers became one of the most desirable and actively developed devices in superconductive electronics. The oscillating nature of superconductive proximity effect in the magnetics leads to appearance of π state and provides opportunities to develop a wide range of applications. Among them there are memory elements, improved RSFQ circuits and metamaterial elements.

Unfortunately, characteristic voltage, $I_C R_N$, of conventional SFS junctions is much smaller than that of tunnel SIS devices, which are widely used in superconductive electronics. This leads to deficient value of characteristic frequency and to difficulties in integration with other circuits.

As possible way to solve this task we considered Josephson SISFS structures with complex interlayer consisting of tunnel barrier 'T', ferromagnetic layer 'F' and thin superconductor layer 's' and we outlined operational modes of these junction. Due to superconductive support inside weak link this structure achieves both high frequency and has magnetic properties. Thus SISFS can be used as high-speed π junction or memory element [1-2].

However pairing in the thin middle superconductive film 's' suffers from proximity effect with ferromagnetic layer and stays in the critical regime. It means that state of that layer significantly depends from inhomogeneities in ferromagnetic layer. We study impact on current properties of different types of inhomogeneities including domains walls and normal phase inclusions.

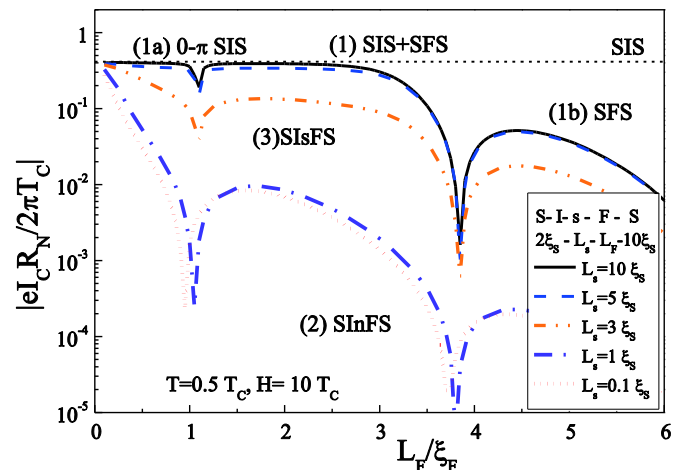


Fig. 1 Operational Modes of SISFS structure: Characteristic voltage $I_C R_N$ versus thickness of F-layer L_F for the set of different s-layer thickness L_s

This work was supported in part by the Ministry of Education and Science of the Russian Federation, President grant MK-1841.2014.2, President Scholarship and RFBR grants 14-02-90018, 14-02-31002_mol_a.

[1] T. I. Larkin, V. V. Bol'ginov, V. S. Stolyarov, V. V. Ryazanov, I. V. Vernik, S. K. Tolpygo, and O. A. Mukhanov, *Appl. Phys. Lett.* **100**, 222601 (2012).

[2] S. V. Bakurskiy, N. V. Klenov, I. I. Soloviev, M. Yu. Kupriyanov, A. A. Golubov, *Physical Review B*, **88** (14), 144519 (2013).

1RP-LT-8

INTERELECTRONIC INTERACTION IN DIRTY FS TRILAYERS: A MANIFESTATION OF "HIDDEN" SUPERCONDUCTIVITY

Proshin Y.N., Avdeev M.V.

Kazan Federal University, Kazan, Russia
yurii.proshin@kpfu.ru

An electron-electron interaction in a ferromagnet (F) was neglected in the standard approach to the proximity effect theories for the layered SF structures (see [1,2] and references therein), S is used for a superconductor. In other words a superconducting order parameter Δ_F and an interelectronic interaction constant λ_F were taken as zero for a ferromagnet. Actually this interaction exists, but it is suppressed by strong exchange field I and can be revealed if an exchange field disappears. So, in this case a ferromagnet is transformed to normal metal and that "unhidden" interelectronic interaction can lead to superconducting correlations and, therefore, a superconductivity onset with critical temperature T_{cf} , estimated by the BCS expression.

Previously we shown that a consideration of this interaction in the clean F/S structures limit [3,4] can explain a surprisingly high critical temperature T_c in the short-periodic Gd/La superlattice [5]. Now we analyse this problem for dirty case basing on solutions of the Usadel equations, changing different parameters of asymmetrical FSF' trilayer (thicknesses of layers, transparencies σ_s , external magnetic field and so on). Taking into account an interelectronic interaction leads to an appearance of "hidden" superconductivity of F layers which can be manifest itself in the proximity effect conditions. It will be especially expressed if exchange fields in both F layers have opposite signs. In Fig. 1 we show the dependence of critical temperature $t = T_c/T_{cs}$ on the "hidden" interelectronic interaction in F layers for case of ideal transparence ($\sigma_s=1000$). Here $l_s=0.7\xi_s$, $n_{sf}=3.5$, $l_f=0.5\xi_f$, $I/\pi T_{cs}=10$ (we use notations as in [1]). T_{cs} is critical temperature of S metal. The solid line in panel (b) corresponds to previous theoretical approaches with neglecting λ_F ($T_{cf}=0$). The solitary reentrant superconductivity predicted for different asymmetrical clean FS structures [3,4] is also discussed for *asymmetrical* case of the FSF' trilayer. So, we see that "hidden" electron-electron interaction in a ferromagnet can essentially change the phase diagrams of the FS systems.

The work is partially supported by the RF ME&S and the RFBR (13-02-01202).

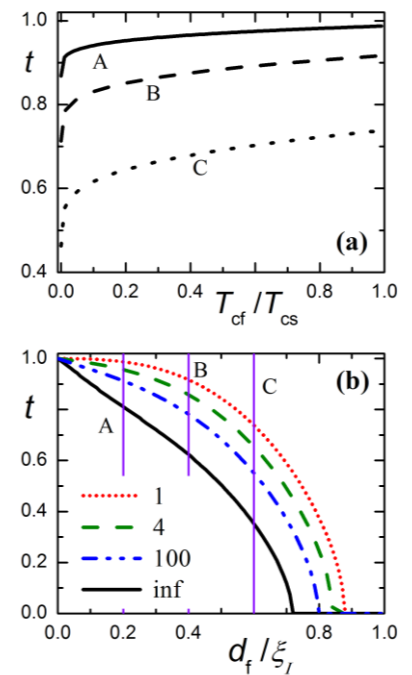


Fig. 1 The dependence of critical temperature $t = T_c/T_{cs}$ for FSF trilayer: (a) versus T_{cf}/T_{cs} (three lines correspond to different thicknesses of F layers noted in lower panel); (b) versus thicknesses of F layers (four different lines correspond to various values of T_{cf}/T_{cs} parameter).

- [1] Y.A. Izyumov, Y.N. Proshin, M.G. Khusainov, *Physics/Uspekhi*, **45** (2002) 109.
- [2] A.I. Buzdin, *Rev. Mod. Phys.*, **77** (2005) 935.
- [3] M.G. Khusainov, et al. *JETP Lett.* **89** (2009) 626.
- [4] Y.N. Proshin, M.M. Khusainov, A. Minnullin, *Phys. Stat.Sol. C* (2014) accepted.
- [5] J.P. Goff, et al. *JMMM* 240 (2002) 592; P.P. Deen, et al. *J. Phys.: Cond. Matt.* **17** (2005) 3305.

1OR-LT-9

PROXIMITY EFFECTS IN SUPERCONDUCTING TRIPLET SPIN-VALVE F2F1S STRUCTURES

Deminov R.G.¹, Tagirov L.R.¹, Gaifullin R.R.¹, Fominov Ya.V.², Karminskaya T.Yu.³, Kupriyanov M.Yu.³, Golubov A.A.⁴

¹ Institute of Physics, Kazan Federal University, 420008 Kazan, Russia

² L.D. Landau Institute for Theoretical Physics RAS, 119334 Moscow, Russia

³ Skobeltsyn Institute of Nuclear Physics, Moscow State University, 119992 Moscow, Russia

⁴ Faculty of Science and Technology and MESA+ Institute of Nanotechnology, University of Twente, P.O. Box 217, 7500 AE Enschede, The Netherlands

Raphael.Deminov@kpfu.ru

We investigate critical temperature T_c of F2F1S trilayers (S is a singlet superconductor, Fi is a ferromagnetic metal), where the long-range triplet superconducting pairing component is generated at noncollinear magnetizations of the F layers [1]. Earlier we demonstrated that T_c in such structures can be non-monotonic function of the angle α between magnetizations of the two F layers [2,3]. It was shown recently [4] that anomalous dependence of the spin-triplet correlations on the angle α in FFS structures can be realized.

We demonstrate that it is possible to realize different spin-valve effect modes - the standard switching effect, the triplet spin-valve effect, reentrant $T_c(\alpha)$ dependence or reentrant $T_c(\alpha)$ dependence with the inverse switching effect - by variation of the F2/F1 interface transparency or the exchange splitting energy.

Moreover, we show that position of the T_c minimum can be changed by joint variation of the F2/F1 interface transparency and the layer thicknesses.

Thereby we demonstrate that the realization of one of the spin-valve effect modes can be done not only by variation of the F layers thicknesses, but also by varying the F2/F1 interface transparency or the exchange field energy. It is explained by changes in the interference conditions for the condensate functions. This interference depends on the F layers thicknesses, the F2/F1 interface transparency, and the exchange splitting energy.

The support by RFBR (grants No. 14-02-00348-a and No. 14-02-00793-a) is gratefully acknowledged.

[1] F.S. Bergeret, A.F. Volkov, and K.B. Efetov, *Rev. Mod. Phys.*, **77** (2005) 1321-1373.

[2] Ya.V. Fominov, A.A. Golubov, T.Yu. Karminskaya, M.Yu. Kupriyanov, R.G. Deminov, and L.R. Tagirov, *JETP Lett.*, **91** (2010) 308-313.

[3] R.G. Deminov, L.R. Tagirov, T.Yu. Karminskaya, M.Yu. Kupriyanov, Ya.V. Fominov, and A.A. Golubov, *Phys. Rev. B* (to be submitted).

[4] T.Yu. Karminskaya, A.A. Golubov, M.Yu. Kupriyanov, *Phys. Rev. B*, **84** (064531) (2011) 1-5.

1RP-LT-10

SPIN-TRIPLET SUPERCONDUCTING CORRELATIONS IN THE OXIDE HETEROSTRUCTURE INDUCED BY A NON-COLLINEAR MAGNETIC STATE

Khaydukov Yu.N.^{1,4,6}, *Ovsyannikov G.A.*^{2,3}, *Sheyerman A.E.*², *Constantinian K.Y.*², *Mustafa L.*¹, *Keller T.*^{1,4}, *Uribe-Laverde M.A.*⁵, *Kislinskii Yu.V.*², *Shadrin A.V.*^{2,3}, *Kalabukhov A.*³, *Keimer B.*¹, *Winkler D.*³

¹ Max-Planck Institute for Solid State Research, 70569, Stuttgart, Germany

² Kotelnikov Institute of Radio Engineering and Electronics of RAS, 125009, Moscow, Russia

³ Chalmers University of Technology, Gothenburg, S-41296, Sweden

⁴ Max Planck Society Outstation at the FRM II D-85747 Garching, Germany

⁵ University of Fribourg, Chemin du Mus'ee 3, CH-1700 Fribourg, Switzerland

⁶ Skobeltsyn Institute of Nuclear Physics, MSU, Moscow, Russia

y.khaydukov@fkf.mpg.de

Triplet pairing in oxide superconducting/ferromagnetic (S/F) heterostructures with non-collinear magnetization state was experimentally studied [1,2]. Heterostructures of Au/La_{0.7}Sr_{0.3}MnO₃/SrRuO₃/YBa₂Cu₃O_{7- δ} composition have been prepared using the pulsed laser ablation. The high quality of the crystal and layers growth has been revealed by using X-ray diffraction and reflectometry techniques. In particular, the crystallographic lattice parameters of ferromagnetic interlayers (LSMO and SRO) differ by 1% from the one for the reference films deposited directly on the substrate. The non-collinear magnetic state of the heterostructure has been revealed by means of SQUID magnetometry and Polarized Neutron Reflectometry measurements. We have observed the superconducting current in mesa-structures fabricated by deposition of a superconducting Nb layer on top of the heterostructure, patterned by photolithography and ion-beam etching. The Josephson effect observed in the mesa-structures is explained by the penetration of the long-range triplet component of the superconducting order parameter into the magnetic interlayer. Additionally we have observed increase of the magnetic moment below T_C. Origin of the effect is discussed in the frame of inverse proximity effect [3] and paramagnetic Meissner response of the triplet condensate [4]

[1] G.A. Ovsyannikov, A.E. Sheierman, A.V. Shadrin, et al, *JETP Letters*, **97** (2013) 145.

[2] Yu. N. Khaydukov, G.A. Ovsyannikov, A.E. Sheyerman et al. In preparation.

[3] N.G. Pugach and A.I. Buzdin *Appl. Phys. Lett.*, **101** (2012) 242602.

[4] M. Alidoust, K. Halterman, J. Linder, *Phys. Rev. B*, **89** (2014) 054508.

1RP-LT-11

SUPERCONDUCTING PROXIMITY EFFECT IN QUANTUM WIRES WITHOUT TIME-REVERSAL SYMMETRY

Skvortsov M.A.^{1,2}, Ostrovsky P.M.^{1,3}, Ivanov D.A.^{4,5}, Fominov Ya.V.^{1,2}

¹ L.D. Landau Institute for Theoretical Physics, Chernogolovka, Russia

² Moscow Institute of Physics and Technology, Moscow, Russia

³ Max Planck Institute for Solid State Research, Stuttgart, Germany

⁴ Institute for Theoretical Physics, ETH Zürich, Switzerland

⁵ Institute for Theoretical Physics, University of Zürich, Switzerland
fominov@landau.ac.ru

We study the superconducting proximity effect in a quantum wire with broken time-reversal (TR) symmetry connected to a conventional superconductor. We consider the situation of a strong TR-symmetry breaking, so that Cooper pairs entering the wire from the superconductor are immediately destroyed. Nevertheless, some traces of the proximity effect survive: for example, the local electronic density of states (LDOS) is influenced by the proximity to the superconductor, provided that localization effects are taken into account. With the help of the supersymmetric sigma model, we calculate the average LDOS in such a system. The LDOS in the wire is strongly modified close to the interface with the superconductor at energies near the Fermi level. The relevant distances from the interface are of the order of the localization length, and the size of the energy window around the Fermi level is of the order of the mean level spacing at the localization length. Remarkably, the sign of the effect is sensitive to the way the TR symmetry is broken: In the spin-symmetric case (orbital magnetic field), the LDOS is depleted near the Fermi energy, whereas for the broken spin symmetry (magnetic impurities), the LDOS at the Fermi energy is enhanced.

The talk is based on the paper [1].

[1] M.A. Skvortsov, P.M. Ostrovsky, D.A. Ivanov, Ya.V. Fominov, Superconducting proximity effect in quantum wires without time-reversal symmetry, *Phys. Rev. B*, **87** 104502 (2013).

1 July

Tuesday

11:30-13:00

oral session

1OR-C

**“Materials &
Nanostructures”**

1OR-C-1

REMARKABLE CHANGE OF MAGNETIC ANISOTROPY INFLICTED BY HYDROGEN ABSORPTION IN R_2Fe_{17} (R=Tb, Dy) COMPOUNDS AT AMBIENT TEMPERATURES

Tereshina I.S.^{1,2}, Tereshina E.A.³, Pelevin I.A.², Drulis H.⁴, Telegina I.¹, Doerr M.⁵

¹ Lomonosov Moscow State University, Moscow, Russia

² Baikov Institute of Metallurgy and Materials Science RAS, Moscow, Russia

³ Institute of Physics ASCR, Prague, Czech Republic

⁴ Institute of Low Temperature and Structure Research, Wroclaw, Poland

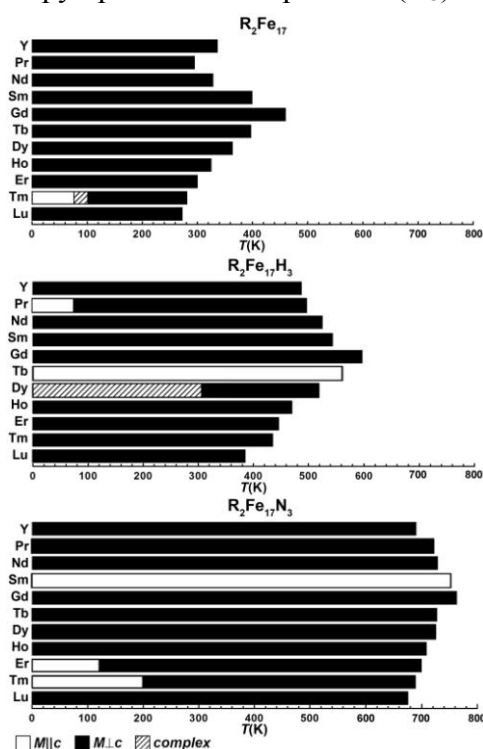
⁵ Technische Universität Dresden, Dresden, Germany

irina_tereshina@mail.ru

Binary R_2Fe_{17} alloys (R is a rare earth) are rather well studied due to special attention they have attracted in the past several decades. However, challenges remain. Primarily it concerns the “wrong”, easy-plane type of magnetocrystalline anisotropy (MCA) at all temperatures in R_2Fe_{17} compounds but one, Tm_2Fe_{17} (see Fig. 1). For the latter however, the easy-axis anisotropy ceases to exist above 80 K. R_2Fe_{17} with the light and heavy rare earths crystallize in the rhombohedral Th_2Zn_{17} and hexagonal Th_2Ni_{17} lattices, respectively. The compounds with Gd, Tb and Y can be found in both modifications or as a mixture of phases. Furthermore, one should bear in mind large effects of nonstoichiometry and, as a result, disordered structures in a number of hexagonal R_2Fe_{17} compounds. Attempts to change the magnetic anisotropy type to the desired easy axis at usable operating temperatures, i.e. covering the room-temperature interval, by using either substitution or interstitial doping were made for R_2Fe_{17} . The easy-axis anisotropy up to Curie temperature (T_C) was successfully stabilized in $Sm_2Fe_{17}N_{3-d}$ and $Sm_2Fe_{17}C_{3-d}$. As for the hydrides, there also exists one compound with the easy axis MCA at all temperatures up to T_C [1]. It is a trihydride $Tb_2Fe_{17}H_{3-d}$. The reported anisotropy field μ_0H_a in $Tb_2Fe_{17}H_3$ is reaching 16 T at 4.2 K and 2.5 T at 300 K. Further, the compound with dysprosium is not the least interesting. Giant easy-plane anisotropy of 35 T (at 4.2 K) of the parent Dy_2Fe_{17} is replaced by the easy-cone anisotropy in its trihydride $Dy_2Fe_{17}H_3$ (from the study performed on singlecrystalline samples with the use of special equipment – magnetic anisometer). In this work we show that the range of temperatures where the easycone MCA is observed is sensitive not only to the hydrogen content but also to the R/Fe ratio. In addition we find that $Dy_2Fe_{17}H_x$ hydrides demonstrate rather large values of high-field magnetostriction at ambient temperatures. In summary, hydrogen is proven to be an important tool in controlling the magnetic anisotropy of R_2Fe_{17} with Tb and Dy at ambient temperatures. This shows promise for the purpose-oriented use of the R_2Fe_{17} -H system.

Supported by RFBR, pr. No. 13-03-00744, 14-03-31395 and by the Czech Science Foundation under Grant No. P204/12/0150, by HLD at HZDR, member of the European Magnetic Field Laboratory (EMFL). Part of measurements has been performed in MLTL (<http://mltl.eu>), which is supported within the program of Czech Research Infrastructures (project no. LM2011025).

[1] E. A. Tereshina, H. Drulis, Y. Skourski, I. S. Tereshina, *Phys Rev B* **87**, 214425 (2013).



1OR-C-2

MAGNETIC DOMAIN STRUCTURE OF HARD MAGNETIC MATERIALS AND QUANTITATIVE ANALYSIS OF MAGNETIC REVERSAL PROCESSES

Pastushenkov Yu.G.¹, Pastushenkov A.G.¹, Skokov K.P.^{1,2}, Lahova M.B.¹, Semenova E.M.¹

¹ Tver state university, Tver, Russia

² TU Darmstadt, Darmstadt, Germany

yupast@mail.ru

A complex investigation was performed into the microstructure and magnetic domain structure (DS) of modern hard magnetic materials with different coercivity mechanisms and microstructures, in a thermally demagnetized state and during the magnetic reversal process [1,2].

Emphasis was given to observing features of DS reorganization on the magnets surfaces parallel to the texture axis, and to thermal and hysteresis properties of the investigated magnets. New data were obtained concerning the formation of fundamental structurally-sensitive characteristics of modern hard magnetic materials. These data are needed for developing valid descriptions of these permanent magnets, physically modeling them, and tuning them for special-purpose uses.

Several problems were discovered concerning quantitative estimations produced by varying methods of DS analysis of the basic micromagnetic parameters of hard magnetic phases of permanent magnets. These discoveries demonstrated the need to adapt traditional methods of quantitative analysis of DS [3] for modern permanent magnets. It was established that the ways of correcting methods of quantitative analysis of DS of permanent magnets should be different depending on the coercivity mechanism and structural condition of magnets. Possible schemes for calculations were suggested.

Nanostructured permanent magnets were also studied; this work demonstrated that traditional methods of quantitative analysis of DS are inapplicable to this group of materials.

On the basis of the gathered data, we suggested new schemes for the analysis of micromagnetic parameters of microcrystalline and microheterogeneous materials based on examination of their magnetic domain structure.

The foundations of a micromagnetic approach to the description of the fundamental and structurally-sensitive properties of pseudo-monocrystalline, microcrystalline, nanocrystalline and nanostructured magnetic materials were developed. These approaches make it possible to reduce errors by simulating the fundamental and structurally-sensitive properties of these materials.

The work was supported by the RFBR - grant 13-02-00856.

[1] Yu.G. Pastushenkov, K.P. Skokov, *Proc. of 19th International Workshop on Rare Earth Permanent Magnets and Their Applications*, (Beijing, 2006) 79-86.

[2] Yu.G.Pastushenkov, K.P.Skokov, E.M.Semenova, *etc. TSU-Bulletin*, **10** (2010) 13-19.

[3] A. Hubert, R. Schäfer, *Springer* (1998), 696 p.

1OR-C-3

SEARCH OF NEW MAGNETIC MATERIALS WITH EVOLUTIONARY ALGORITHM USPEX

Blinov I.¹, Oganov A.^{1,2}, Qian G.²

¹ Moscow Institute of Physics and Technology, Moscow, Russia

² Stonybrook University, Stonybrook, USA

blinov@phystech.edu, artem.oganov@stonybrook.edu, iqianguangrui@gmail.com

It's easy to understand why are magnetic materials so important. Usage of hard magnetic materials in technology is not the thing we can be surprised. For now there probably two types of hard magnetics: Nd-Fe-B, Ba-Fe-O.

The goal of our work was to predict new compound comparable with this well-known types by it's characteristics. The additional target was to make this material suitable for usage in technology.

Firstly we changed USPEX-algorithm [1] to work with strong-correlated system. We used DFT+U in Dudarev notation [2] as it implemented in VASP.

We tested our method on SmCo5 system and obtain satisfactory results for primitive unit cell and atomic positions (fig 1).

We made a search in systems consisting of three elements: heavy one, transition and the third to stabilize. Begin with most abundant ones, we made a computational search through about 8 full-systems and about 18³ different stoichiometry in every system.

Up to now, we found some interesting never-known before stable compounds in one of the systems we observed. As it was said, it consists of desirable type of atoms. Consisting of transition elements, it has big momentum per atom in unit cell and very anisotropic structure.

	<i>USPEX</i>	<i>Experiment, [3]</i>
<i>a</i>	<i>5,1</i>	<i>5,05</i>
<i>b</i>	<i>4,9</i>	<i>5,05</i>
<i>c</i>	<i>3,88</i>	<i>3,96</i>
<i>α</i>	<i>90</i>	<i>90</i>
<i>β</i>	<i>90</i>	<i>90</i>
<i>γ</i>	<i>116</i>	<i>120</i>

Supported by grant of the Government of the Russian Federation № 14.A12.31.0003.

[1] A.R. Oganov, C.W. Glass. *J. Chem. Phys.*, **124** (2006), art. 244704.

[2] S. L. Dudarev, G. A. Botton, S. Y. Savrasov, C. J. Humphreys and A. P. Sutton, *Phys. Rev. B* **57**, (1998) 1505.

[3] Marc de Graef, «*Structure of materials*», Cambridge 2007.

1OR-C-4

HIGH-FIELD MAGNETIZATION MEASUREMENTS: $\text{Ho}_2\text{Fe}_{14}\text{B}$ AS A CASE STUDY

Tereshina E.A.^{1,2}, *Law J.M.*³, *Tereshina I.S.*^{1,4,5}, *Pelevin I.A.*⁴, *Paukov M.*⁶, *Havela L.*⁶

¹Lomonosov Moscow State University, 119991 Moscow, Russia

²Institute of Physics ASCR, 18221 Prague, Czech Republic

³Dresden High Magnetic Field Laboratory (HLD), Helmholtz-Zentrum Dresden-Rossendorf, D-01314 Dresden, Germany

⁴Baikov Institute of Metallurgy and Material Science RAS, 119991 Moscow, Russia

⁵International Laboratory of High Magnetic Fields and Low Temperatures, Wroclaw, Poland

⁶Department of Condensed Matter Physics, Faculty of Mathematics and Physics, Charles University, 12116 Prague, Czech Republic
teresh@fzu.cz

The present report is concerned with the non-destructive high-field methodology in pulsed magnetic fields up to 60 T via induced voltages with the compensated coil technique. As a rule, the measurements are done with and without the sample in the coil set (magnetometer) with the difference leaving solely the sample signal. The experimental setup realised in the Dresden High-Field Laboratory is discussed. The magnetization study is presented for a rare-earth (R) intermetallic compound $\text{Ho}_2\text{Fe}_{14}\text{B}$, belonging to the family of permanent-magnet type materials, and a comparative investigation of the parent and hydrogenated samples is performed.

For this work, $\text{Ho}_2\text{Fe}_{14}\text{B}$ single crystals were hydrogenated to different hydrogen concentration. In addition, a polycrystalline specimen subjected to severe plastic deformation was investigated. (The atomic force microscopy showed that the grain size in the latter material varies from 30 to 100 nm.) Since $\text{Ho}_2\text{Fe}_{14}\text{B}$ undergoes a spin-reorientation transition of the “easy-axis”-“easy-cone” type at 55 K as the temperature is decreased [1], the magnetization curves of $\text{Ho}_2\text{Fe}_{14}\text{BH}_x$ were obtained along principal crystallographic directions at 4.2, 50 and 100 K in pulsed fields up to 60 T. Figure 1 compares the data for a single crystal measured along the [001] axis and a nanostructured specimen at 4.2 K. The structural state evidently influences both the saturation magnetization and the character of a field-induced magnetic spin-reorientation transition by smearing it out in the nano-crystalline material. Hydrogenation, on the other hand, strongly affects the value of the critical field of the transition. The strength of the R-Fe exchange interactions in the hydrogen-charged $\text{Ho}_2\text{Fe}_{14}\text{B}$ system is determined and the magnetic phase diagrams are constructed.

The work is supported by RFBR, pr. No. 13-03-00744 and by the Czech Science Foundation, P204/12/0150. The authors thank HLD at HZDR, a member of the European Magnetic Field Laboratory (EMFL) for the high-field measurements. Magnetic measurements in steady fields have been performed in MLTL (<http://mltl.eu>) supported within the program of the Czech Research Infrastructures (project no. LM2011025).

[1] J. F. Herbst, *Rev. Mod. Phys.* **63** (1991) 819-898.

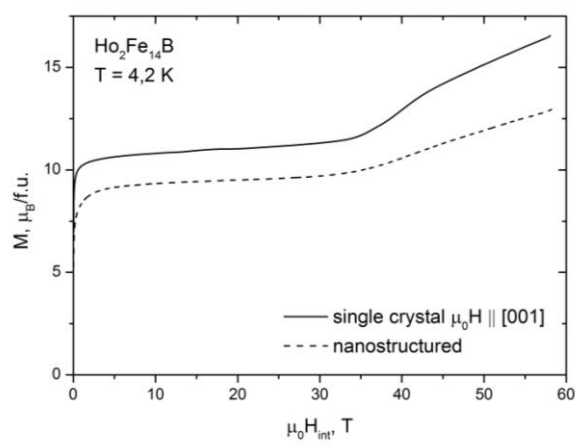


Fig. 1. High-field magnetization of single- and nano-crystalline $\text{Ho}_2\text{Fe}_{14}\text{B}$ at 4.2 K.

1OR-C-5

MAGNETIC PROPERTIES OF SEVERE PLASTIC DEFORMED Gd, Nd, Sm IN HIGH MAGNETIC FIELDS

*Taskaev S.V.¹, Skokov K.P.², Ulyanov M.N.¹, Bataev D.S.¹, Buchelnikov V.D.¹,
Khovaylo V.V.³, Pellenen A.P.⁴*

¹ Department of Physics, Chelyabinsk State University, Chelyabinsk, Russia

² Institut für Materialwissenschaft, TU Darmstadt, Darmstadt, Germany

³ National University of Science and Technology "MISIS", Moscow, Russia

⁴ National Research South Ural State University, Chelyabinsk, Russia

tsv@csu.ru

This work reports the magnetic properties of thin Gd ribbons obtained with the help of severe plastic deformation (SPD) technique. Severe plastic deformation procedures are very interesting for designing novel functional materials. Depending on the degree of deformation, magnetic, structural or thermodynamic properties could be varied in severely deformed materials, especially in thin ribbons of SPD-treated materials.

The interest in this matter is far from being purely academic. Since the discovery of the “giant” magnetocaloric effect [1], the development of magnetic refrigeration gained increased attention. A review on magnetic refrigerator and heat pump prototypes built before the 2010 shows different constructions of the magnetocaloric devices [2]. And one of the possible ways of engineering magnetocaloric (MCE) materials is tightly connected with preparing very thin (a few microns) ribbons of high value MCE alloys with good mechanical properties.

A significant depression of magnetic and thermodynamic properties occurs in severely deformed samples of Gd. The reason of such behavior is in a giant magnetic anisotropy induced by SPD. This unexpected phenomena drives to a new thermodynamic and magnetic properties of severely deformed Gd ribbons [3] which are inapplicable for magnetocaloric applications without additional heat treatment procedure. The heat treatment regimes are directly connected with the degree of plastic deformation.

In this work we continue our previous investigations of the SPD on the magnetic properties of 4-f elements, with special accent on magnetic anisotropy. In Figure 1 the high field dependences of magnetization of the Gd stripes are shown, it is clearly seen that saturation of the magnetization in both directions achieved only near 30T.

Authors appreciate RFBR grant 12-07-00676-a and RF President grant MD-770.2014.2 for financing this work.

[1] K. A. Jr. Gschneidner, V. K. Pecharsky, *Int. J. Refrig.*, **31** (2008) 945.

[2] Yu Bingfeng, M. Liu, P. W. Egolf, A. Kitanovski, *Int. J. Refrig.*, **33** (2010) 1029.

[3] S.V. Taskaev, M.D. Kuz'min, K.P. Skokov, D.Yu.Karpenkov, A.P.Pellenen, V.D. Buchelnikov, O. Gutfleisch, *JMMM*, **331** (2013) 33.

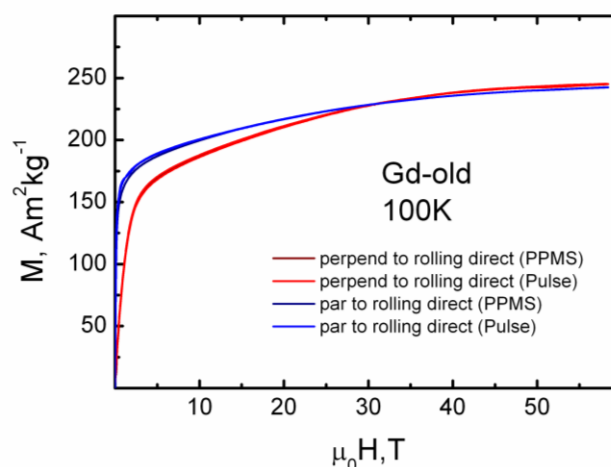


Figure 1. High field dependences of magnetization of the Gd stripes

1OR-C-6

ENERGY SPECTRUM, MAGNETIC DYNAMICS AND MACROSCOPIC QUANTUM EFFECTS OF AFM NANOPARTICLES IN MÖSSBAUER SPECTROSCOPY

Chuev M.A.

Institute of Physics and Technology, Russian Academy of Sciences, Moscow, Russia
chuev@ftian.ru

Wide applications of modern materials containing nano-sized magnetic particles or clusters in different branches of nanotechnology are based primarily on a number of specific structural, magnetic and thermodynamic properties of these materials found within long-term fundamental studies. However, the principle question of the effect of the magnetic nature of particles on their properties remains actually open to a large extent since the widely studied and obvious effect in the field is only superparamagnetism of ferromagnetic (FM) particles. The physical ideas for understanding magnetic properties of antiferromagnetic (AFM) nanoparticles on a phenomenological level have been suggested by Néel in terms of uncompensated magnetic moments on two magnetic sublattices and superantiferromagnetism [1]. Several models incorporating the uncompensated moment for describing magnetization curves of AFM particles have been developed, which are actually reduced, from the thermodynamic viewpoint, only to modifications of the Langevin function whereas the ground AFM state is treated in a rather simplified manner [2]. The same Néel's idea has been widely explored in studies of macroscopic quantum phenomena in small AFM particles [3], but again within a simplified treatment of the ground and lowest-lying states in the large spin approximation. Generally speaking, in spite of the right physical meaning of the Néel's idea [1], it has also played a negative role because the behavior of ideal (compensated) AFM nanoparticles has not been seriously considered so far, that in its turn has restricted the development of a general theory.

In the present contribution I will discuss first a quantum-mechanical model for describing thermodynamic properties of an ensemble of ideal and "uncompensated" AFM nanoparticles with axial magnetic anisotropy in the first approximation of slowly relaxing macrospins of magnetic sublattices [4]. This model clarifies principally the difference in thermodynamic behavior of FM and AFM particles revealed in spectroscopic measurements. In particular, one can now qualitatively describe specific (non-superparamagnetic) temperature evolution of the ^{57}Fe Mössbauer spectra of AFM nanoparticles, which has been often observed for almost half a century and looks like a quantum superposition of well-resolved magnetic hyperfine structure and single line (or quadrupolar doublet of lines) with the temperature-dependent partial spectral areas. Generalization of the approach in the macroscopic limit describing magnetic relaxation processes in AFM [5] and ferrimagnetic [6] nanoparticles would allow one to take directly into account the magnetic nature inherent to the particles in analyzing and re-evaluating a large amount of experimental data collected so far.

Support by RFBR is acknowledged.

- [1] L. Néel, *C. R. Acad. Sciences*, **253** (1961) 203-208.
- [2] C. Gilles, et al., *J. Magn. Magn. Mater.*, **241** (2002) 430-440.
- [3] Y.-H. Nie, et al., *Physica B*, **270** (1999) 95-103.
- [4] M.A. Chuev, *JETP Lett.*, **95** (2012) 295-301.
- [5] M.A. Chuev, *Pis'ma v ZhETF*, **99** (2014) 319-324.
- [6] M.A. Chuev, *JETP Lett.*, **98** (2013) 465-470.

1 July

Tuesday

11:30-13:00

14:30-17:00

oral session

1TL-D

1RP-D

1TL-Q

1RP-Q

1OR-Q

**“Magnetic Shape
Memory and
Magnetocaloric Effect”**

1TL-D-1

MAGNETIC PROPERTIES AND ELECTRONIC STATE OF Ni-Mn-Sn METAMAGNETIC SHAPE MEMORY ALLOYS

Umetsu R.Y.^{1,2}, Ito W.³, Kanomata T.^{1,4}, Kainuma R.¹

¹Tohoku University, Sendai, Japan

²JST- Precursory Research for Embryonic Science and Technology, Kawaguchi, Japan

³Sendai National College of Technology, Natori, Japan

⁴Tohoku Gakuin University, Tagajo, Japan

riume@imr.tohoku.ac.jp (R.Y. Umetsu)

Ferromagnetic shape memory alloys with Ni-Mn based Heusler-type structure exhibit both the ferromagnetic and martensitic transformations. Since the two phase transformations occur at the same time and they are induced by applied magnetic field [1,2], these materials show a rich variety of physical properties, such as large magnetoresistance, magnetic superelasticity and large inverse magnetocaloric effects, and drastic change of the thermal transport properties. In the present studies, low-temperature specific heat measurements were carried out in wide concentration region for Ni-Mn-Z ($Z = \text{Sn}$ and In) ferromagnetic shape memory alloys because the investigations for the electronic state will give important aspects for considering the mechanism of the martensitic transformation in these alloys.

The alloys were made by induction furnace melting in an argon atmosphere. Obtained ingots of Ni-Mn-Sn and Ni-Mn-In alloys were annealed at 1073 ~ 1273 K for 1 day, and subsequently quenched into water. Specific heat measurements were carried out by relaxation method with using physical property measurement system (PPMS) by Quantum Design Inc.

Figure 1 indicates $C_p/T-T^2$ (C_p : Specific heat, T : Temperature) plots for $\text{Ni}_{50}\text{Mn}_{50-x}\text{Sn}_x$ ($x = 2, 4, 6, 8$ and 10) alloys in the martensite phase. Here, electronic specific heat coefficient, γ (mJ/mol-K^2), and the Debye temperature, θ_D (K), are obtained from the values of ordinate intercept and slope of the straight line, respectively. It is shown that the intercept and the slope gradually increase with increasing Sn concentration. Inset shows concentration dependence of γ and θ_D obtained from the Fig. 1, together with that in the parent phase for $\text{Ni}_{50}\text{Mn}_{50-x}\text{Sn}_x$ alloys. Because the value of γ corresponds to total density of states at the Fermi energy, variation of γ suggests the change of the electronic states. The value of γ changes with changing the Sn concentration, especially in the parent phase region. As a result, it is expected that γ drastically changes when the martensitic transformation occurs around $x = 14$. From the variation of θ_D , it is said that θ_D in the parent phase is lower than that in the martensite phase, attributed to expansion of the lattice.

This work was partly supported by a Grant-in-Aid for Scientific Research from the Japan Society for the Promotion of Science

[1] Y. Sutou, *et al.*, *Appl. Phys. Lett.* **85**, 4358 (2004).

[2] R. Kainuma, *et al.*, *Nature*. **439**, 957 (2006).

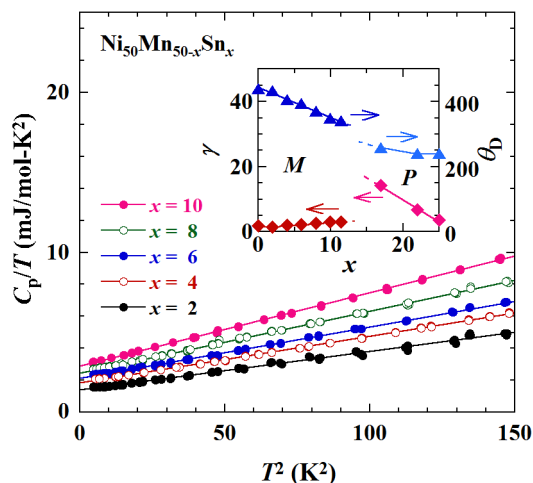


Fig. 1. $C_p/T-T^2$ (C_p : Specific heat, T : Temperature) plots for $\text{Ni}_{50}\text{Mn}_{50-x}\text{Sn}_x$ alloys in martensite phase (M). Concentration dependence of electronic specific heat coefficient, γ , and the Debye temperature, θ_D , (inset).

1RP-D-2

FIRST-PRINCIPLES STUDY OF THE STRUCTURAL AND MAGNETIC PROPERTIES OF Ni-Co-Mn-Sn HEUSLER ALLOYS

Buchelnikov V.D.¹, Sokolovskiy V.V.^{1,2}, Tufatullina M.A.¹, Zagrebin M.A.^{1,3}, Entel P.⁴

¹ Condensed Matter Physics Department, Chelyabinsk State University, 454001 Chelyabinsk, Russia

² National University of Science and Technology "MIS&S", 119049, Moscow, Russia

³ South Ural State University (National Research University), 454080 Chelyabinsk, Russia

⁴ Faculty of Physics, University Duisburg-Essen, 47048 Duisburg, Germany
buche@csu.ru

The functional properties of Ni-(Co)-Mn-Z (Z = Ga, In, Sn) Heusler alloys like the magnetic shape memory effect, exchange bias effect and the magnetocaloric effect (MCE) are promising for future technologies [1]. These effects are associated with the complex magnetic ordering in austenite and martensite [2]. The competing magnetic interactions lead the characteristic drops of magnetization curves across the magnetostructural transformation for the Ni-(Co)-Mn-Sn alloys [2, 3]. The strong antiferromagnetic correlations start to appear with the Mn excess atoms which mainly occupy sites of the Z sublattice, causing the nearest neighbor Mn-Mn distances to shrink.

In this work we study the structural and magnetic properties of Ni-Co-Mn-Sn alloys by the help of first-principles and Monte Carlo methods. Before the theoretical modelling of the MCE by the Monte Carlo method we are calculated the equilibrium properties of Ni-Co-Mn-Sn alloys from first principles. We used Quantum ESPRESSO package [4] to determine the optimized lattice parameters of the cubic L₂₁ phase and *c/a* relaxation. Calculations were carried out for Ni₇CoMn₆Sn₂ alloy. The excess of Mn atoms in L₂₁ structure was supposed to be at Sn-site and Co atom occupy the Ni site. We considered the ferromagnetic (FM) and ferrimagnetic (FRM) states. In FM state all magnetic moments of Ni and Mn atoms are parallel. In FRM state the magnetic moments of Mn excess are antiparallel to magnetic moments of Mn atoms on Mn-sites. The calculations were done with the cubic cell with 16 atoms. The results show that both magnetic states are stable. The FM state has lower energy than the FRM one. The FM and FRM states have the energy minima at *a*=5.958 and 5.937 Å, respectively. We have also calculated the equilibrium tetragonality (*c/a* relaxation). It was obtained that for Ni₇CoMn₆Sn₂ alloy there is only one minimum for FM (*c/a*=1) state and two minimum for FRM one at *c/a*=1.02 and *c/a*=1.26. Ni₇CoMn₆Sn₂ alloy in austenite state have to possess the FM arrangement, but in martensite phase it will transit to FRM state which has lower energy and magnetic moment. This may be the reason of the sharp decrease of magnetization in Ni-Co-Mn-In alloys at the martensitic transition. We also calculated the total moments and the exchange constants in austenite and martensite for the FM and FRM phases.

Support by RFBR Grant #14-02-01085 and the Creation and Development Program of NUST "MIS&S" is acknowledged.

- [1] A. Planes, L. Manosa, and M. Acet, *J. Phys.: Condens. Matter*, **21** (2009) 233201.
- [2] D.Y. Cong, S. Roth, and L. Schultz, *Acta Mater.*, **60** (2012) 5335.
- [3] P. Entel, M. Siewert, M.E. Gruner et al., *Eur. Phys. J. B*, **86** (2013) 65.
- [4] Quantum ESPRESSO package, Version 5.0. <http://www.pwscf.org>.

1RP-D-3

MAGNETIC AND MAGNETOCALORIC PROPERTIES OF Ni-Mn BASED HEUSLER ALLOYS

Nigam A.K.

Tata Institute of Fundamental Research, Homi Bhabha Road, Colaba, Mumbai 400005 India
aknm@tifr.res.in, aknm16@gmail.com

Although discovered more than a century ago (in 1903) the interest in the study of Heusler alloys has remained alive and gained renewed thrust during the last three decades, due to emergence of new materials with Heusler phase, having promising applications. For example, the discovery of giant magnetic field induced strain in Ni_2MnGa in 1996 has lead to great deal of interest in the Ni-Mn based full Heusler alloys. Some of these alloys exhibit multifunctional properties, such as shape-memory effect, large magneo-caloric effect, high magneto-resistance, exchange bias behavior etc. Many of these effects are manifestations of first order magneto-structural transition that provides the possibility of controlling the structural transformation by magnetic field. Among such materials, Ni-Mn based Ferromagnetic Shape Memory alloys (FSMA) have attracted significant interest due to observation of large magneto-caloric effect (MCE) in many of them. Detailed studies have been carried out in off-stoichiometric Ni-Mn-In and Ni-Mn-Sb based systems with other transition metal substitutions. The results show interesting magnetic behavior in the martensite phase. Also, a large magneto-caloric effect (MCE), high magnetoresistance, etc. is observed in some of these alloys. Most of these properties occur as a consequence of the existence of phase transition with strong magneto-structural coupling. A study has been carried out in *Fe* and *Pd* doped $\text{Ni}_{50}\text{Mn}_{35}\text{In}_{15}$ and Co-substituted $\text{Ni}_{50}\text{Mn}_{38}\text{Sb}_{12}$ alloys. The martensitic transition disappears even with a 2at% Fe substitution, whereas for 1 at% Fe-substitution, Martensitic behavior is observed along with enhancement of MCE. In Co-substituted Ni-Mn-Sb alloys, large tunable entropy changes up to a maximum of $80 \text{ Jkg}^{-1}\text{K}^{-1}$ are observed around room temperature for a given Ni/Co ratio. Another interesting feature of these alloys is the existence of complex magnetic order in the martensitic phase. Also a pronounced exchange-bias (EB) effect is seen in some of these alloys at low temperatures. From the detailed magnetization study, it appears that the origin of the anomalous magnetization behavior and the exotic properties associated with it could be due to competing ferro- and antiferro-magnetic interactions. The results of some of the results carried out on these alloys would be presented and discussed.

1TL-Q-6

**MAGNETOSTRUCTURAL PHASE TRANSITION IN $\text{Ni}_{45+X}\text{Mn}_{44-X-Y}\text{In}_{11+Y}$
($X=0,2,3$; $Y=0,1,2$) RIBBON-SHAPE HEUSLER ALLOYS**

González-Legarreta L.¹, González-Alonso D.², Rosa W.O.³, Suñol J.J.⁴, González J.⁵, Hernando B.¹

¹ Dept. de Física, Universidad de Oviedo, Calvo Sotelo s/n, 33007 Oviedo, Spain

² Facultat de Física, Departament d'Estructura i Constituents de la Matèria, Universitat de Barcelona, Diagonal 647, E-08028 Barcelona, Spain

³ Centro Brasileiro de Pesquisas Físicas, Rua Dr. Xavier Sigaud, 150 Urca., 22290-180 Rio de Janeiro, RJ, Brazil

⁴ Universidad de Girona, Montilivi edifici PII, Lluís Santaló s/n. 17003 Girona, Spain

⁵ Department of Materials Physics, Faculty of Chemistry, University of the Basque Country, 20018 San Sebastian, Spain

Corresponding author: grande@uniovi.es

We report the features of the martensitic transformation for three off-stoichiometric Ni-Mn-In Heusler ribbon-shape alloys. The $\text{Ni}_{45}\text{Mn}_{44}\text{In}_{11}$, $\text{Ni}_{47}\text{Mn}_{41}\text{In}_{12}$ and $\text{Ni}_{48}\text{Mn}_{39}\text{In}_{13}$ ribbon-nominal-compositions were selected for the $7.8 < e/a < 8.0$ range, being e/a the valence electron concentration per atom, due to its interesting functional properties near room-temperature [1,2]. Prior to the ribbon-flakes production by the melt-spinning technique, polycrystalline Ni-Mn-In alloy ingots were prepared by conventional arc-melting method with the subsequent annealing during 24h at 900°C to avoid inhomogeneities. Besides the morphology, the average composition for the as-quenched ribbons were performed by means of Scanning Electron Microscopy (SEMJEOL6100) equipped with an Energy Dispersive Xray microanalysis system (EDX-Inca Energy 200). The structural transformation was analysed by means of Differential Scanning Calorimetry (DSCQ2000), and the thermomagnetic behavior was studied in the range of 50 - 400 K and up to 30 kOe applied field by a Quantum Design VersaLab VSM. From thermomagnetic and calorimetric measurements the characteristic temperatures of the transformation are in good agreement. Direct and inverse magnetocaloric effects near the Curie-point of the parent-phase and martensitic transformation temperature, respectively, have been clearly revealed. The estimated MCE increases along with e/a as well as the martensitic transformation shifts toward high-temperatures as the e/a rises, which agree with previous works in bulk [2] and in ribbon [3] sample alloys of similar compositions.

[1] T. Krenke et al., *Phys. Rev. B* **73** (2006) 174413.

[2] A. Planes et al., *J. Phys.: Condens. Matter.*, **21** (2009) 233201.

[3] W.O. Rosa, et al., *Phys. Res. Int.*, **2012** 794171, Hindawi Publishing Corp., 2012.

1RP-Q-7

**MULTIFUNCTIONAL PROPERTIES RELATED TO
MAGNETOSTRUCTURAL TRANSITIONS IN TERNARY AND
QUATERNARY HEUSLER ALLOYS**

*Dubenko I.S.¹, Quetz A.¹, Pandey S.¹, Aryal A.¹, Eubank M.¹, Rodionov I.D.², Titov I.S.²,
Prudnikov V.N.², Granovsky A.B.², Samanta T.³, Saleheen A.³, Stadler S.³, Ali N.¹*

¹ Department of Physics, Southern Illinois University, Carbondale, USA

² Faculty of Physics, Lomonosov Moscow State University, Moscow, Russia

³ Department of Physics & Astronomy, Louisiana State University, Baton Rouge, LA, USA

igor_dubenko@yahoo.com

In spite of significant progress made in recent years in understanding multifunctional properties related to magnetostructural transitions (MST) in Ni-Mn-In based Heusler alloys, the detailed mechanisms responsible for the transitions are far from being well understood. Due to the delicate balance between electronic, ionic, vibrational, and magnetic energies in the vicinity of the MST, the properties of these alloys are extremely sensitive to any changes in intrinsic parameters, such as chemical composition, type of the crystal structure, as well as on extrinsic parameters, like fabrication techniques and conditions, annealing temperature, applied magnetic field, pressure, rate of heating and cooling, sequence of measurements, and cycling.

In this report, we summarize the results of our studies on the effects of compositional variations induced by the small changes in concentration of the parent component, and/or by the substitution of Ni, Mn, or In for an extra element Z on the phase transitions and phenomena related to the MSTs in off-stoichiometric Ni-Mn-In based Heusler alloys. The crystal structure, phase transitions temperatures, magnetic, magnetocaloric, electrical, and magnetotransport properties were studied for the following alloys systems (near of 15 at.% of indium concentration): Ni_{50-x}Cr_xMn₃₅In₁₅; Ni₅₀Mn₃₅In_{15-x}B_x; Ni₅₀Mn_{35-x}Cu_xIn₁₅; Ni₅₀Mn_{1-x}Cu_xIn₁₄B; Ni_{50-x}Mn_{35+x}In₁₅; Ni_{50-x}Mn_{34.5+x}In_{15.5}; Ni_{47-x}Fe₃Mn_{34.5+x}In_{15.5}; Ni_{40-x}Mn_{34.8+x}In₁₅Ag_{0.2}; Ni_{50-x}Mn_{34.5}In_{15.5+x}; Ni₅₀Mn_{34.8+x}In_{15.2+x} and Ni₅₀Mn₃₅In_{15-x}Al_x.

The influence of hydrostatic and “positive”/“negative” chemical pressures, and changes in conduction electron concentration on the magnetic properties, magnetocaloric parameters, magnetic entropy, asymmetric magnetoresistance, and ordinary and anomalous Hall coefficients are discussed.

This work was partly supported by the Russian Foundation for Basic Research (grant No. 12-02-00095a) and by the Office of Basic Energy Sciences, Material Science Division of the U.S. Department of Energy (DE-FG02-06ER46291 and DE-FG02-13ER46946).

1RP-Q-8

Co AND In DOPED Ni-Mn-Ga MAGNETIC SHAPE MEMORY ALLOYS: A STRUCTURAL, MAGNETIC AND MAGNETOCALORIC STUDY

Fabbrici S.^{1,2}, *Porcari G.*³, *Cugini F.*³, *Solzi M.*³, *Kamarad J.*⁴, *Arnold Z.*⁴, *Cabassi R.*², *Albertini F.*²

¹ MIST E-R Laboratory, Bologna, Italy

² IMEM-CNR, Parma, Italy

³ University of Parma, Physics and Earth Science dept., Parma, Italy

⁴ Institute of Physics AS CR, Prague, Czech Republic

fabbrici@imem.cnr.it

The vast family of Ni-Mn based Heusler alloys provides an extended playground of physical properties. The interplay between a reversible martensitic transformation (MT) and magnetically ordered states gives rise to a series of functional properties that can be exploited for developing innovative devices [1] which originate from the possibility to dramatically change the materials properties by an applied external stimulus, such as magnetic field, stress or pressure. During the last decade, significant achievements have been obtained by introducing Co to the ternary Ni-Mn-Z compounds. Such quaternary full Heusler alloys show a metamagnetic martensitic transformation between a low moment martensite and a strongly ferromagnetic austenite: high values of giant magneto- and baro-caloric effects, giant magnetoresistance and magnetic superelasticity have been observed. For instance, giant magnetocaloric effect (MCE) with very high ΔT_{ad} values have been observed in several compositions of Ni-Co-Mn-In [2].

Ga based quaternary Ni-Co-Mn-Ga Heuslers can be tuned to show both direct and inverse MCE by proper compositional adjustments [3]. In a well defined compositional range they display a reverse metamagnetic transition which is associated to remarkable values of positive magnetic entropy change (inverse MCE), to high sensitivity of the MT to applied magnetic field and pressure (dT_C/dH and dT_C/dp) as well as high structural and magnetic discontinuities [4].

In this contribution we will review our findings on the role of In in the MCE properties of Ni-Co-Mn-Ga alloys: partial substitution of Ga with In allows to independently tune the magnetic and magnetostructural critical temperatures, emphasizing the figures of interest for applications and ultimately achieving promising values of adiabatic temperature change (up to 3 K in a 1.8T field span). We will show the MCE characterization both from direct and indirect methods, and we will discuss the non straightforward relation between the measured ΔS_{iso} and ΔT_{ad} values [5].

Starting from a thorough measurement analysis on an array of samples with different compositions, comprising magnetic, calorimetric, structural and under pressure measurements, we will discuss which properties are supposed to play a key role in the improvement of MCE.

Finally, we will highlight the possible correlations that exist between the magnetic and structural features of interest to the MCE with the hysteretic figures of the martensitic transition, a detrimental property which actually prevents the cyclic MCE operation in Heusler alloys.

Support from the 2007-2013 FESR Operative program of the Emilia Romagna Region (Activity 1.1.1) is acknowledged.

[1] T. Graf, C. Felser, S. Parkin, *Prog. Solid State Chem.* **39**, 1-50 (2011).

[2] J. Liu et al., *Nature Mat.* **11**, 620 (2011).

[3] S. Fabbrici et al., *Acta Mater.* **59**, 412 (2011).

[4] F. Albertini et al., *Mat. Sci. Forum* **684**, 151 (2011).

[5] G. Porcari et al., *Phys. Rev. B* **85** 024414 (2012).

1OR-Q-9

EXCHANGE BIAS EFFECT IN POLYCRYSTALLINE RIBBONS OF HEUSLER ALLOY Ni-Mn-Al-Si

Singh R.¹, Ingale B.¹, Khovaylo V.V.², Varga L.K.³, Chatterjee R.¹

¹Magnetics and Advanced Ceramics Laboratory, Physics Department, Indian Institute of Technology Delhi, Hauz Khas, New Delhi-110016

²National University of Science and Technology MISiS, Moscow-119049, Russia

³Research Institute for Solid State Physics and Optics of the Hungarian Academy of Sciences, H-1525 Budapest, P.O.B. 49, Hungary
rmala@physics.iitd.ac.in

When the materials with antiferromagnetic-ferromagnetic (AFM-FM) interfaces are cooled through the Néel temperature (T_N) of AFM phase in presence of magnetic field, a unidirectional anisotropy is induced in the material which is called Exchange bias (EB) [1]. Over the six decades of its discovery [1], EB effect has been studied in various types of systems such as nanoparticle oxides, the inhomogeneous magnetic materials, for example, spin-glasses, magnetic complex oxides, Heusler alloys systems and layered magnetic thin film systems. The main indication of presence of EB are normally identified as: (1) horizontal shift of the field-cooled (FC) magnetic hysteresis (M - H) loop, (2) enhancement of coercivity (H_C) as compared to the zero-field-cooled (ZFC) case, and (3) the existence of the magnetic training effect (TE), i.e., the gradual decrease of EB field (H_{EB}) with increasing number of M - H loop cycles (n) at a particular temperature. Till date the highest value of H_{EB} of ~ 2.23 kOe has been reported for the Ni-Mn-Sn alloys by Wang *et al.*[2] at 10 K.

In this work we present detailed studies of structural, magnetic and EB behavior of polycrystalline ribbons of Ni₅₆Mn₂₁Al₂₂Si₁ Heusler alloy. Room temperature structure was noted as orthorhombic 14M (martensite). Spin-glass behavior in the samples below 68 K can be seen as a bifurcation of the ZFC and FC data which have been further investigated by a memory effect in stop and wait protocol from magnetization verses temperature (M - T) data. The sample shows superparamagnetic behavior in temperature range of $70 \leq T \leq 250$ K. We report the $H_{EB} \sim 2.60$ kOe at 2 K for Ni₅₆Mn₂₁Al₂₂Si₁ polycrystalline ribbon in cooling field (H_{CF}) of 20 kOe, which is the highest value reported till date in any metallic alloys [2].

SQUID facility at IITD is acknowledged.

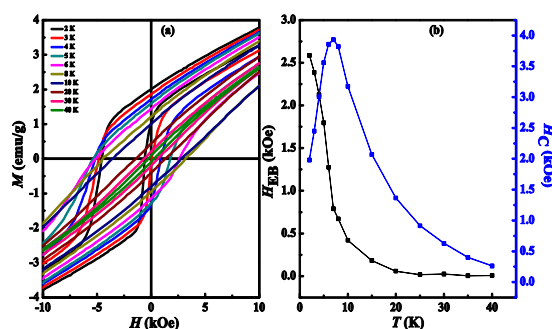


Fig. 1. (a) M - H loops at various temperatures and (b) Temperature dependence of H_{EB} and H_C for Ni₅₆Mn₂₁Al₂₂Si₁ polycrystalline ribbon in cooling field $H_{CF} = 20$ kOe.

[1]. W. H. Meiklejohn and C. P. Bean, *Phys. Rev.*, **102** (1956) 1413.

[2]. B. M. Wang, Y. Liu, B. Xia, P. Ren, and L. Wang, *J. Appl. Phys.*, **111** (2012) 043912.

1OR-Q-10

**ANNEALING INFLUENCE ON THE EXCHANGE-BIAS AND
MAGNETOSTRUCTURAL PROPERTIES IN THE Ni_{50.0}Mn_{36.5}Sn_{13.5}
RIBBON-SHAPE ALLOY**

*González-Legarreta L.¹, Ipatov M.², González-Alonso D.³, Kamantsev A.⁴, Koledov V.V.⁴,
Shavrov V.G.⁴, Hernando B.¹*

¹ Dept. de Física, Universidad de Oviedo, Calvo Sotelo s/n, 33007 Oviedo, Spain

² Department of Materials Physics, Faculty of Chemistry, University of the Basque Country, San Sebastian 20018, Spain

³ Facultat de Física, Departament d'Estructura i Constituents de la Matèria, Universitat de Barcelona, Diagonal 647, E-08028 Barcelona, Spain

⁴ Kotelnikov Institute of Radio Engineering and Electronics, RAS, Moscow 125009, Russia
lorena.glegarreta@gmail.com

An off-stoichiometric Ni_{50.0}Mn_{36.5}Sn_{13.5} Heusler ribbon alloy has been prepared in order to study the annealing influence on the martensitic transformation, exchange-bias effect and magnetic behaviour of both austenitic and martensitic phases. The master alloy was performed by arc-melting technique and produced in ribbon-shape by rapid solidification using the melt-spinning method. Some ribbon-flake samples were annealed during 10 min at 923 K and 1073 K. The morphology and the average composition for all the ribbon samples were performed by means of Scanning Electron Microscopy (SEM-JEOL6100) equipped with an Energy Dispersive X-ray microanalysis system (EDX-Inca Energy 200). The magnetic measurements were done under Zero-Field-Cooling (ZFC) Field-Cooling (FC) and Field-Heating (FH) protocols by Vibrating Sample Magnetometer (VSM, VersaLab QD) in the range of 5 – 400 K and at an applied magnetic field ranging from 50 Oe up to 30 kOe. Hysteresis loops $M(H)$ and AC susceptibility with 10 Oe exciting magnetic field at different frequencies were measured within the temperatures range from 5 K to 300 K by a Physical Property Measurement System (PPMS-9, QD). Isofield curves show a shift toward high temperatures stabilising the martensitic phase at the expense of the parent one, as well as a reduction in the inverse magnetocaloric effect is observed as increasing the temperature of the thermal treatment, that is in agreement with the grain size increment as a result of the annealing. Isothermal $M(H)$ curves show an exchange bias effect below 100 K for all samples. Furthermore, a spontaneous exchange bias after ZFC protocol has also been revealed for the three samples, being more significant in the ribbon annealed at 1023 K, which indicates the existence of antiferromagnetic interactions at low temperature [1-3].

[1] B.M. Wang, Y. Liu, P. Ren, B. Xia, K.B. Ruan, J.B. Yi, J. Ding, X.G. Li, L. Wang, *Phys. Rev. Lett.* **106** (2011) 077203.

[2] S. Giri, M. Patra y S. Majumdar, *J. Phys.: Condens. Matter.*, **23** (2011) 073201.

[3] A. K. Nayak, M. Nicklas, S. Chadov, C. Shekhar, Y. Skourski, J. Winterlik, C. Felser, *Phys. Rev. Lett.*, **110** (2013) 127204.

1OR-Q-11

EFFECT OF HEAT TREATMENT ON THE MAGNETIC PROPERTIES OF Ni-Mn-In-Co HEUSLER ALLOYS

Dilmieva E.T.¹, Kamantsev A.P.¹, Koledov V.V.¹, Mashirov A.V.¹, Shavrov V.G.¹, Khovaylo V.V.², González-Legarreta L.³, Hernando B.³, Kokorin V.V.⁴, Konoplyuk S.M.⁴

¹ Kotel'nikov Institute of Radio Engineering and Electronics of RAS, Moscow, Russia

² National science technological university "MISiS", Moscow, Russia

³ Dept. de Física, Universidad de Oviedo, Calvo Sotelo s/n, 33007 Oviedo, Spain

⁴ Institute of Magnetism of NASU, Kiev, Ukraine

Kelvit@mail.ru

Recently many efforts are directed to application of shape memory alloys (SMAs) to MEMS-NEMS technology. As examples the nanotweezers on the basis of composite Ti_2NiCu/Pt controlled by the temperature $T=40-60$ °C and Ni_2MnGa/Pt controlled by magnetic field 0-8 T are demonstrated [1, 2]. The main obstacles on the way to their implementation are high working temperature in case of non-magnetic SMAs (in this case living objects: microbes, cages can die) or too strong magnetic fields for ferromagnetic SMAs. The purpose of the present work is the investigation of possibility to diminish magnetic fields demanded for control of shape memory effect in ferromagnetic SMA Ni-Mn-In-Co via proper heat treatment and consequent diminishing of metamagtostructural phase transition thermal hysteresis.

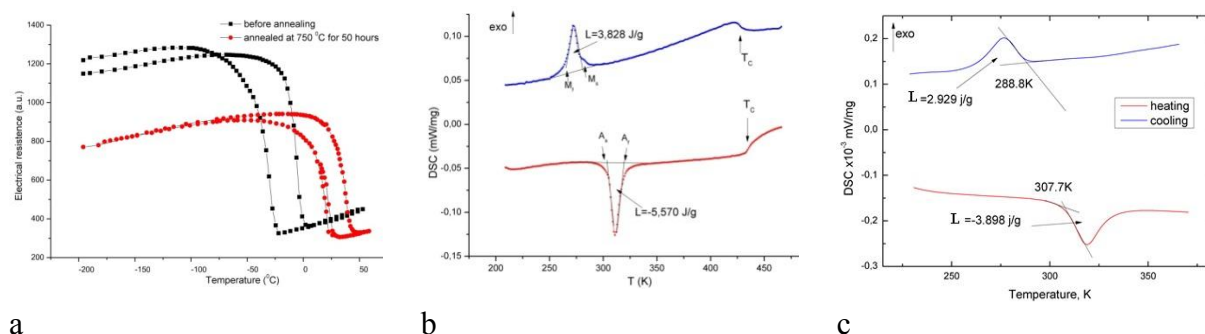


Fig. 1. (a) -dependences of resistance on Ni₄₃Mn_{37,8}In_{12,2}Co₇ sample temperature; (b) - DSC data sample after the first annealing; (c) - DSC data sample after the second annealing.

Samples of Ni₄₃Mn_{37,8}In_{12,2}Co₇ were prepared by arc melting in argon atmosphere. On the first stage the annealing for 48 hours at 1173K in vacuum was done. On the second stage the homogenizing annealing at 1023K for 50 hours was done. Both electrical resistivity and DSC measurements show that two stage annealing have led to diminishing of the width of temperature hysteresis of metamagnetostuctural transition about 1.5 - 2 times. This can show the way to improvement of the sensitivity of the Ni-Mn-In-Co alloy to magnetic field, with purpose being the permanent magnet field control of the SMA based micromechanical devices.

Support by RFBR 12-08-01043, 2-07-00811, 12-07-00676, 12-07-00656, 13-07-12130 and CRDF RUP1-7028-MO-11 is acknowledged.

[1] A.Irzhak et. al. *Journal of Alloys and Compounds*, **586**, S464–S468 (2014).

http://www.youtube.com/watch?v=pEGL_IcLxDs

[2] E. Kalimullina, A. Kamantsev, V. Koledov. *Nonlinear world*, **2**, 42-44 (2014).

10R-Q-12

THE UNIQUE MAGNETIC BEHAVIOR OF A GMCE ALLOY

*Ari-Gur P.¹, Felner I.², Tsindlekht M.I.², Shavrov V.³, Koledov V.³, Mashirov A.³,
Madiligama A.S.B.¹*

¹ Western Michigan University, Kalamazoo, Michigan, USA

² Racah Institute of Physics, The Hebrew University, Jerusalem, Israel

³ Kotelnikov Institute of Radio-engineering and Electronics, RAS, Moscow, Russia
pnina.ari-gur@wmich.edu

Heusler alloys NiMnX have been known to demonstrate strong ferromagnetic shape memory effect [1]. In recent years, some of them have also been explored, with great success, for “giant” magnetocaloric effect (MCE). This makes them highly promising in solid state magnetic cooling systems for alternative energy applications. The MCE some of these alloys demonstrate is “inverse”; i.e. when a field is applied, the material *absorbs* heat at the merged transitions. This results from the fact that cooling through the structural transformation results in *metamagnetic* transition from a ferromagnetic to a non-ferromagnetic state. The temperature is reduced under an applied field. The key for their performance is the co-occurrence of the magnetic and structural transitions, which is first order transition in nature. Until now, the nature of magnetic ordering in the martensitic phase (spin glass or antiferromagnetic), which is critical for giant MCE because of the very large difference of their entropies, has remained unknown.

The goal of this work was to determine the nature of the lower temperature phase and the shift in transformation temperature under magnetic field.

Isothermal magnetization measurements at elevated temperatures were performed by a SQUID magnetometer. The results are shown in Fig. 1. The ferromagnetic nature at 310 K is clearly seen, as well as the paramagnetic behavior at 330 K. At 285 K, the behavior is non-magnetic (almost zero moment). Based on this behavior, the possibilities for this phase are either anti-ferromagnetic or spin glass. AC-SQUID measurements were then conducted (Fig. 2) where the imaginary part of the susceptibility confirms the anti-ferromagnetic nature; the lack of frequency dependence excludes spin-glass behavior.

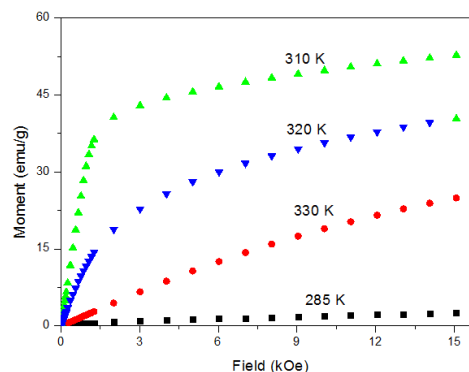


Fig. 1. \uparrow Temperature dependence of the magnetic moment, demonstrating ferromagnetic (310 K) paramagnetic (330 K) and anti-ferromagnetic (285 K) behaviors.

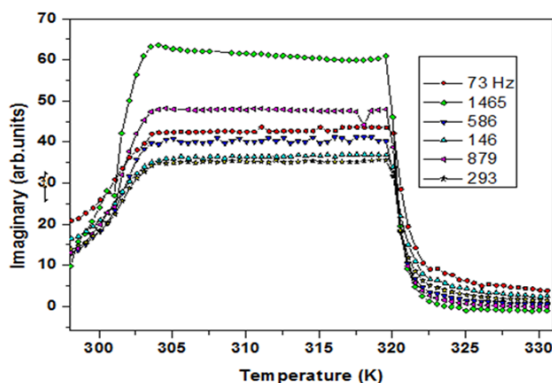


Fig. 2. \leftarrow The imaginary part of the AC-susceptibility as a function of frequency, showing no spin-glass behavior.

Support by Award No. RUP1-7028-MO-11 of the US CRDF Global is acknowledged.

1OR-Q-13

MAGNETOCALORIC AND MAGNETOELASTIC PROPERTIES OF COMPOUNDS BASED ON GADOLINIUM AND P-ELEMENTS

Nikitin S.A.¹, Bogdanov A.E.¹, Ovchenkova I.A.¹, Ovchenkov E.A.¹, Smirnov A.V.¹, Morozkin A.V.¹

¹Lomonosov Moscow State University, Moscow, Russia
andrey07_91@mail.ru

The purpose of this work was the complex investigation of magnetic, magnetocaloric and magnetoelastic properties of compounds based on $Gd_5Si_2Ge_2$ with small In substitutions in p-sublattice. Particular attention was given to the study of these compounds under the action of high magnetic fields, as well as the study of the thermomagnetic hysteresis. The magnetocaloric effect (MCE) was measured directly and calculated from the magnetization measurements both in pulsed and static magnetic fields.

The samples $Gd_5Si_{2-x}Ge_{2-x}In_{2x}$ ($2x = 0, 0.05, 0.07, 0.1, 0.15, 0.2$) were prepared by arc melting. They remelted three times, followed by annealing at 1070 K for 150 hours. According to X-ray analysis the main phase in all compounds is monoclinic $Gd_5Si_2Ge_2$ -type phase (space group $P112_1/b$). In addition to it, there is a small amount of impurity phase in the samples: either the orthorhombic $GdGe$ -type, or hexagonal Gd_5Si_3 -type.

For all investigated compounds the essential MCE ($\sim 1.6-1.8$ K for $\Delta H = 13.5$ kOe) was observed on the direct measurements upon cooling of the sample. The addition of In slightly increases both the Curie temperature and MCE value. The direct measurements of MCE upon the heating of the sample give the lower values of the MCE. Moreover the MCE significantly depends on the number of thermal cycles near T_C .

The calculation of the ΔT -effect from the measurements of the magnetization curves in high pulsed magnetic fields and the magnetic entropy change from the measurements in the static magnetic fields gives high MCE values in good accordance with literature data [1,2] ($\Delta T = 18$ K for $\Delta H = 80$ kOe). The high values of the MCE are due to the heat release by inducing the first order magnetic field-induced phase transitions. The presence of the magnetic phase transition, which is accompanied by a structural transformation leads to the fact that the temperature dependence of the ΔT -effect measured directly in moderate magnetic fields is not the same upon heating and cooling.

Volume magnetostriction of $Gd_5Si_2Ge_2$ reaches $900 \cdot 10^{-6}$ in the field of 11.8 kOe if sample is cooled from the paramagnetic to the ferromagnetic state. Upon heating the sample volume magnetostriction value reaches $250 \cdot 10^{-6}$. For the composition $Gd_5Si_{1.975}Ge_{1.975}In_{0.05}$ volume magnetostriction is approximately equal $400 \cdot 10^{-6}$ and $100 \cdot 10^{-6}$ upon cooling and heating of the sample, respectively.

The temperature dependences of MCE for compounds with In substitution have two maxima. That may arise due to different temperatures of structural and magnetic phase transitions. This effect increases the area where the MCE has a significant value, and correspondingly increases refrigerant capacity of the sample.

The work has been supported by RFBR grant № 13-02-00916A.

[1] V.K. Pecharsky, K. A. Gschneidner Jr., *Physical Review Letters*, **78** (1997) 4494–4497.

[2] A.O. Pecharsky, V. K. Pecharsky, K. A. Gschneidner Jr., *J. Appl. Phys.*, **93** (2003) 4722–4728.

1 July

Tuesday

11:30-13:30

14:30-17:15

oral session

1TL-E

1RP-E

1OR-E

**“Magnetism in Biology
and Medicine”**

1TL-E-1

NANOPARTICLES FOR BIOTECHNOLOGICAL AND BIOMEDICAL APPLICATIONS PREPARED BY A TOP-DOWN APPROACH

Joisten H.^{1,2}, *Leulmi S.*¹, *Iss C.*¹, *Morcrette M.*¹, *Dietsch T.*¹, *Ortiz G.*¹, *Hou Y.*³, *Livache T.*³,
*Calemczuk R.*³, *Carriere M.*⁴, *Sabon P.*¹, *Auffret S.*¹, *Dieny B.*¹

¹ SPINTEC, UMR-8191, CEA-INAC/CNRS/UJF-Grenoble 1/Grenoble-INP, Grenoble, France

² CEA, LETI, MINATEC Campus, 17 Avenue Martyrs, 38054 Grenoble, France

³ SPram, UMR 5819 (CEA-CNRS-UJF-Grenoble 1), Institut Nanosciences et Cryogénie, CEA-Grenoble 38054 Grenoble, France

⁴ SCIB/LAN, UMR E3 CEA-UJF Grenoble 1, Institut Nanosciences et Cryogénie, CEA-Grenoble 38054 Grenoble, France
helene.joisten@cea.fr

Magnetic nanoparticles are more and more used for various biotechnological and biomedical applications, due to their capability to exert actuation on targeted biological species, remotely controlled by external magnetic fields. In the past few years, a new generation of magnetic nanoparticles has appeared, elaborated by the techniques of micro/ nan conventional magnetic nanoparticles prepared by chemical routes. Interestingly, this top-down approach allows arbitrary choices of magnetic material composition as well as of particles shape, within the broad limits of the thin films nanostructuration. A first study presented here addressed the comparison of two types of magnetic nanoparticles made of i) synthetic antiferromagnetic multilayers (SAF) and ii) magnetic vortex mono layer, in terms of magnetic properties, actuation abilities, and agglomeration/ dispersion control when released in solution. The latter control previously established and modeled for SAF particles [1] has been likewise obtained for vortex particles, Fig.1. Our comparative study outlined, for both types of particles, their own advantages as well as their ability to produce large magnetic torques in weak magnetic field on biological species [2]. In this context, thanks to their capacity to be actuated in an external magnetic field, an innovative biomedical application has recently emerged, aiming at the destruction of targeted cancer cells [3]. Using our particles, we have launched an *in-vitro* biological study aiming at the destruction of renal carcinoma cancer cells. The nanoparticles are specifically functionalized for targeting the cancer cells membranes. Once the particles are attached to the membrane, they are submitted to an alternating field of moderate amplitude and frequency (20mT at 20Hz). Thanks to the stress exerted on the cell membrane and the associated change in ionic transport through the membrane, this excitation triggers the spontaneous death of the cells (apoptosis). A second investigation presented here is focused on the design and realization of particles of more complex shapes and new functionalities such as magnetic nano-tweezers or magnetic nanoswimmers.

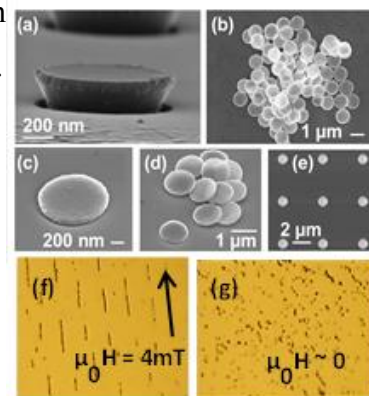


Fig.1. (a–e) SEM photos of vortex particles; (f–g) Optical microscopy in solution, in 4 mT: chains formation, followed by a dispersion in $H \sim 0$.

Support by ANR (Agence Nationale de la Recherche) via the P2N grant Nano-shark ref ANR-11-NANO-001, and by a grant CIBLE 2012 from La Région Rhône-Alpes is acknowledged.

[1] H. Joisten et al., *Appl. Phys. Lett.* **97**, (2010) 253112.

[2] S. Leulmi et al., *Appl. Phys. Lett.* **103** (2013) 132412.

[3] D.-H. Kim et al., *Nature Mater.* **9**, (2010) 165.

1TL-E-2

MAGNETIC NANOPARTICLES FOR BIOPHYSICAL APPLICATIONS SYNTHESIZED BY HIGH-POWER PHYSICAL DISPERSION

Safronov A.P.¹, Beketov I.V.^{1,2}, Tyukova I.S.¹, Medvedev A.I.^{1,2}, Samatov O.M.², Murzakaev A.M.²

¹ Ural Federal University, Ekaterinburg, Russia

² Institute of Electrophysics, Ural branch of RAS, Ekaterinburg, Russia

Safronov@iep.uran.ru

The biomedical application of magnetic nanoparticles (MNPs) is at the leading edge of the developing field of nanotechnology. A variety of promising schemes for the application MNPs include magnetically induced drug delivery, magnetic resonance imaging, cancer diagnostics and therapy by hyperthermia, cell markers, magnetically driven actuators etc [1]. Magnetically active iron oxides – magnetite and maghemite take the leading role among other MNPs potentially suitable for the biomedical applications. The most common route to biomedical magnetite MNPs now is the chemical precipitation from the mixture of ferrous and ferric chlorides. It gives the chemically stable but irregularly shaped monocrystalline MNPs with different particle size depended on the

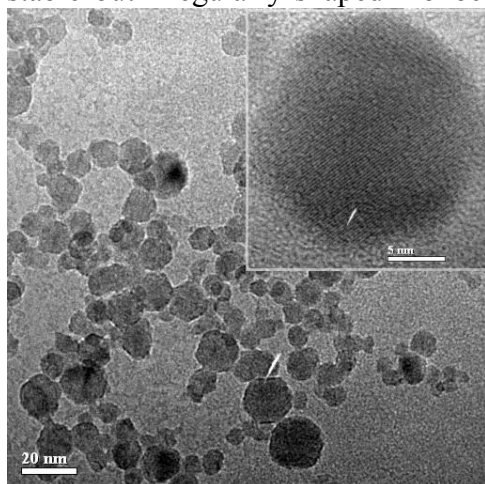


Fig.1 TEM and HTEM (inset) images of LTE iron oxide

synthesis conditions. However, the downside of the chemical synthesis is the strong batch to batch variability, which results in the low reproducibility of the properties of MNPs and the compositions based on them. Therefore, there is a demand for the alternative low cost and high output methods for the production of MNPs with controlled dispersion parameters and highly reproducible functional properties. The methods of high-power physical dispersion: electrical explosion of wire (EEW) and laser target evaporation (LTE) developed in the Institute of electrophysics of UB RAS meet these requirements. The synthesized MNPs are spherical in shape with mean diameter 15 – 30 nm and narrow particle size distribution (Fig.1). The phase composition, shape, particle size and functional properties of MNPs are cross-examined by a variety of contemporary experimental techniques. Due to the non-equilibrium conditions of the

dispersion the phase structure of MNPs corresponds to maghemite rather than magnetite. Meanwhile, their magnetic properties are reproducible and very close to the single domain superparamagnetic behavior [2,3]. Although the as-prepared MNPs are initially aggregated in the air-dry state their de-aggregation in liquid suspension as well as their modification can be successfully performed. The applicability of these MNPs in the biophysical purposes such as cell markers and hyperthermia has been demonstrated.

[1] S.Mournet, S.Vasseur, F.Grasset, E.Duguet *J. Mater. Chem.*, **14** (2004) 2161-2175.

[2] I.V. Beketov, A.P. Safronov, A.I. Medvedev, J. Alonso, G.V. Kurlyandskaya, S.M. Bhagat. *AIP Adv.*, **2** (2012) 022154.

[3] A.P. Safronov, I.V. Beketov, S.V. Komogortsev, G.V. Kurlyandskaya, A.I. Medvedev, D.V. Leiman, A. Larranaga, S.M. Bhagat *AIP Adv.*, **3** (2013) 052135.

1TL-E-3

MAGNETICALLY BARCODED MICROCARRIERS AND FABRICATION OF MAGNETIC NANOSTRUCTURES THROUGH SELF-ASSEMBLY

Llandro J., Love D.M., Cimorra C., Ionescu A., Barnes C.H.W.

Cavendish Laboratory, University of Cambridge, Cambridge CB3 0HE, UK
jl286@cam.ac.uk

We are working towards a novel lab-on-a-chip technology based on suspended magnetically encoded microcarriers [1,2]. Our newest generation of microcarriers consist of up to fourteen individual magnetic elements encapsulated within a SU8 polymer and gold layer (Fig. 1(b)), which both provide routes to bio-functionalization through surface epoxide groups and thiol chemistry [3]. The writing/reading of the digital magnetic codes is obtained through coercivity engineered magnetic elements (Fig. 1(a)). The global addressability of these bits is achieved by utilizing magnetic shape anisotropy. The possibility of attaching different fluorescent labels to each side of the microcarriers enables a positive control in binding assays. Potential applications for this platform range from DNA/protein analysis for genotyping and point-of-care diagnostics to drug development and combinatorial chemistry.

The use of self-assembly and bottom-up techniques for the fabrication of highly periodic nanostructured films is becoming increasingly important in interface science. Here, we present our recent work on self-assembled diblock copolymers, polystyrene bead templates and Bosch processing techniques for the fabrication of concavities, stacked cantilever and gyroid nanostructures (Fig. 1 (c-e)). These structures can be used to enhance the detection sensitivities of various sensor platforms and are often inspired by naturally occurring photonic crystals.

Finally, we will discuss how permanent magnetic structures with controlled dimension and architecture (labyrinthine, hexagonal, or dispersed columnar) are formed in a partially miscible ferrofluid-nonferrofluid mixture under the influence of a perpendicular magnetic field. The origin of the permanent structures, which have characteristic lateral dimensions ranging from 1 to 10 μm , is the repartitioning of the ferrofluid carrier solvent into the nonferrofluid polymeric phase. This polymer-solvent phase separation under a magnetic field leads to departures from the expected final dimension of the magnetically stabilized ferrofluid droplet sizes [4].

Support by the EPSRC is acknowledged.

[1] J. Llandro *et al.*, *Medical & Biological Engineering & Computing* **48**, 977 (2010).

[2] B. Hong *et al.*, in "Biomagnetism and Magnetic Biosystems Based on Molecular Recognition Processes", edited by J.A.C. Bland and A. Ionescu, *AIP Conf. Proc.* **1025** (2008).

[3] K.N. Vyas *et al.*, *Lab on a Chip* **12**, 5272 (2012).

[4] R. Rungsawang *et al.*, *Phys. Rev. Lett.* **104**, 255703 (2010).

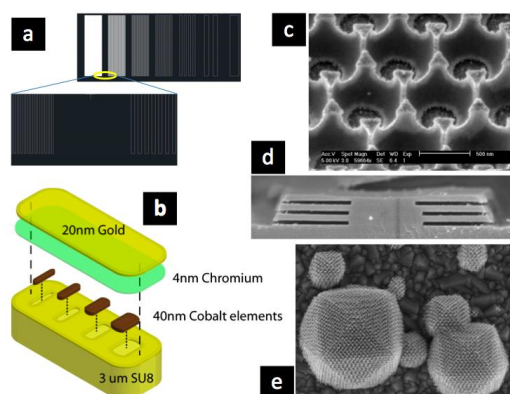


Figure 1: (a) Illustration of composite magnetic elements. (b) Constituents of bi-functional microcarriers. (c) SEM image of Au concavity nanostructures. (d) SEM image of TiO_x/AlO_x cantilever nanostructures. (e) SEM image of Pt gyroid crystallites.

1TL-E-4

MAGNETOPHORETIC CIRCUITS FOR DIGITAL CONTROL OF INDIVIDUAL LIVING CELLS

Lim Byeonghwa¹, Reddy Venu¹, Hu Xing Hao¹, Kim Kun Woo¹, Abedini-Nassab², Yellen Benjamin B.², Kim CheolGi¹

¹ Department of Emerging Materials Science, DGIST, Daegu, 711-873, Republic of Korea

² Department of Mechanical Engineering and Materials Science, Duke University, Box 90300 Hudson Hall, Durham, NC 27708, USA
cgkim@dgist.ac.kr

The ability to analyze the cellular contents of individual microorganisms would significantly benefit our understanding of many mechanisms in the minute world of cell biology. Compared with flow cytometry, single cell arrays are a promising multi-parameter tool for long term observation of biological processes by monitoring cells randomly deposited into micro-well arrays or locally trapped by hydrodynamic, electric or magnetic fields. However, these existing tools are frequently limited by either irreversibility in the placement of cells and/or lack of tools for efficient extraction of single cells, poor nutrient diffusion and temperature control, and the need for complex wiring and microfluidic patterns which prevent the highly parallel operations necessary for identifying extremely rare cells.

In this context, we develop lithographically patterned magnetophoretic pathways which transport single cells reversibly (conductor) or irreversibly (diode) and can locally store single cells in an array of apartments (capacitor). The active devices consist of current lines that can locally switch the trajectory of single cells (transistor) and when combined with the passive elements can produce highly scalable systems that have general multiplexing properties with dramatically reduced wiring constraints that allow for efficient implementation of digital circuitry for single cells. This work provides fundamental tools that enable breakthroughs in the analysis of cell heterogeneity and provide new routes for genomics/proteomics, human reproduction and cancer research.

1TL-E-5

MAGNETIC WIRELESS PUMPS AND THEIR APPLICATIONS

Ishiyama K.¹, Kim S.H.^{1,2}, Hashi S.¹

¹ Research Institute of Electrical Communication, Tohoku University, Sendai, Japan

² Frontier Research Institute for Interdisciplinary Science, Tohoku University, Sendai, Japan
ishiyama@riec.tohoku.ac.jp

The remarkable features of magnetic wireless pump are a wireless and battery-free operation. Because of these features, the pumps could have multi-scale and a variety of applications. In particular, we have developed two kinds of pump system: magnetic wireless artificial heart assist blood devices and micropump, as shown in Fig. 1. For the magnetic wireless operation, we utilized the electromagnetic and permanent magnet systems. The first approach is the magnetic torque control using two coils. The two coils generate a rotating magnetic field. Under application of a rotating magnetic field to the pump, the magnetic rotor is synchronized by the rotating magnetic field because of the magnetic torque [1]. The second method is magnetic force control using an external magnet with a DC motor. The combination of two magnets creates a magnetic interaction force at synchronous radial or axial couplings [2]. Using the wireless manipulation systems, we have developed the magnetic wireless pumps and conducted performance evaluations. First, our application was a wireless blood pump, as shown in Fig. 1 (a). To have both a compact size and sufficient pumping capability, the fully magnetic impeller has five stages and each stage includes 4-backward-curved blades. The pump has total and inner volumes of 20 cc and 9.8 cc, respectively, and weighs 52 g. The pump produces a flow rate of approximately 8 L/min at 80 mmHg. In addition, The pump also produces a minimum flow rate of 1.5 L/min and a pressure of 30 mmHg for circulation at a maximum distance of 7.5 cm. The other application is a micropump. In this case, we utilized spiral-type magnetic machine as an axial flow. The machine was composed of a NdFeB magnet and tungsten wire, as shown in Fig. 1 (b). The machine can perform multiple functions for micrototal analysis system, such as a micropump, microvalve, and micromixer. The fabricated machine was driven by a rotating magnetic field and conducted as a micropump. The micropump created a flow rate of approximately $8 \times 10^{-9} \text{ m}^3/\text{s}$ at 150 Hz with 1.6kA/m.

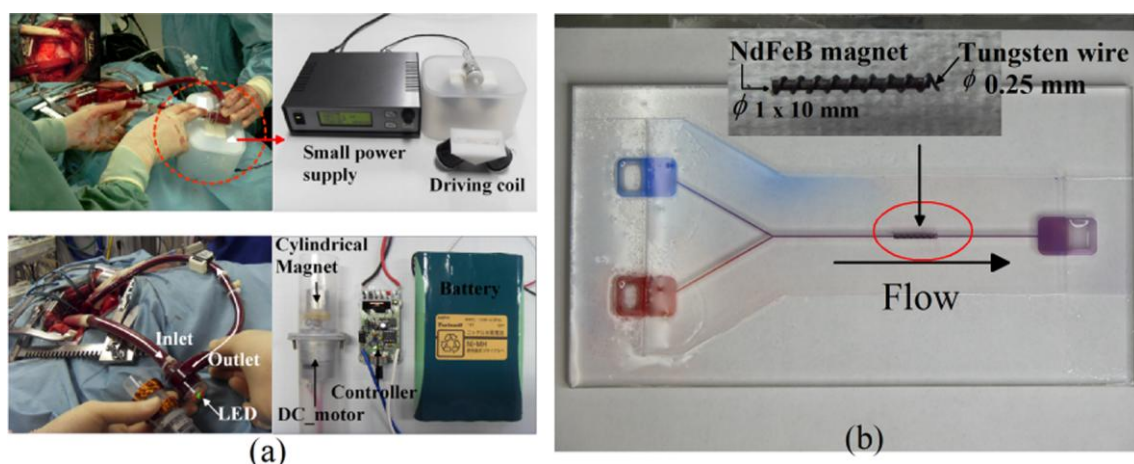


Fig. 1. Magnetic wireless pumps and their applications: (a) magnetic wireless blood pump and (b) magnetic wireless micropump.

[1] S.H. Kim, S.Hashi, K.Ishiyama, *IEEE Trans. Magnetics*, **48** (2012), pp.1869-74.

[2] S.H. Kim, J.W.S. Shin, S. Hashi, K. Ishiyama, *Smart Mater.Struct*, **50** (2011) 035014.

1TL-E-6

Fe-OXIDE NANOPARTICLES FOR BIOMEDICAL APPLICATIONS: ROLE OF SURFACE, AGGREGATION STATE, ENVIRONMENT ON THEIR MAGNETIC PROPERTIES

Allia P.¹, Tiberto P.², Barrera G.^{2,3}, Coïsson M.²

¹ DISAT, Politecnico di Torino, Torino, Italy

² INRIM, Torino, Italy

³ Università di Torino, Torino, Italy

m.coïsson@inrim.it

In recent years, Fe-oxide nanoparticles (NPs) have become one of the best study cases for testing models and concepts addressed to magnetic nanomaterials of relevance for biomedical applications. The current chemical routes to ferromagnetic Fe-oxide NP production have notable advantages, such as a quite reproducible output, a well-defined chemical composition and structure, a narrow spread of sizes/shapes. The synthesized NPs are often covered with a non-magnetic organic shell somewhat hindering NP aggregation by magnetic or electrostatic forces. A reduced interparticle contact interaction brings about, in turn, an individual rather than collective response to magnetic field.

Magnetite (Fe_3O_4) and maghemite ($\gamma\text{-Fe}_2\text{O}_3$) are the commonest magnetic oxide constituents of magnetic NPs. Both are cheap materials with a lower degree of toxicity than metallic ferromagnets and can be easily synthesized through a variety of low-cost techniques, such as the thermo-chemical route. Fe-oxide NPs can occur in a wide variety of forms: as dried powders, dispersed in a liquid (as in ejectable ferrofluids), or embedded in solid-state diamagnetic hosts such as polymers. In the latter case, magnetic NPs are first dispersed by stirring in a fluid containing the polymer precursor(s); the dispersion is finally solidified either by thermal treatment or by UV curing. A uniform dispersion of magnetic NPs in the host is a relevant issue, a bad (uneven) dispersion bringing about non-optimal magnetic properties along with worsened mechanical properties. In all systems where magnetic contact interaction can safely be excluded, dipolar interaction plays a central role. Systematic measurements indicate that the influence of dipolar interaction is not confined to the low-temperature domain, significant effects being measured even at much higher temperatures in systems of Fe-oxide NPs with a ferrimagnetic alignment of spins. These effects manifest themselves in the form of departures from both the SP magnetization law and the SP scaling; they can be accounted for either by simulations or by models, such as the ISP model [1], which can be applied to temperatures where dipolar interaction energy, although no longer being dominant as at very low Ts, is nevertheless comparable in magnitude to the thermal energy $k_B T$. In this case, it is possible to introduce an effective temperature T^* describing the degree of interparticle interaction of dipolar nature. The region where this approach is applicable extends over hundreds of kelvin in actual NP systems, in many cases reaching room temperature as well.

The interplay among nanoparticle coating, environment, dispersibility, and magnetic interaction, giving rise to different magnetic responses to an applied magnetic field will be elucidated by making reference to several examples taken from recent research activity in this area and referring to Fe-oxide NPs in different solid and liquid systems.

[1] P. Allia, M. Coïsson, P. Tiberto, F. Vinai, M. Knobel, M.A. Novak, W.C. Nunes, *Phys. Rev. B* **64** (2001) 144420.

1TL-E-7

DNA AS MOLECULAR LOCAL THERMAL PROBE FOR MAGNETIC HYPERTHERMIA ANALYSIS

Dias T.J.¹, Moros M.¹, del Pino P.^{1,2}, Rivera S.¹, Grazú V.^{1}, de la Fuente M. J.^{1,2*}*

¹ Instituto de Nanociencia de Aragon, Universidad de Zaragoza, C/ Mariano Esquillor s/n, Spain

² Fundación ARAID, 50004-Zaragoza, Spain

jmfuente@unizar.es, vgrazu@unizar.es

Magnetic nanoparticles when coupled to an alternating magnetic field are capable of energy absorption and then release it in form of heat.[1] Thus, enabling the heating of the surroundings of the excited nanoparticles which can be used as a tool in many bioapplications.[2,3] The determination of temperature increments around excited nanoparticles represent however an experimental challenge and existing reports tend to show simple and limited assessments.[4,5] We demonstrate experimentally these temperature increments, when 12 nm magnetic nanoparticles are exposed to a radiofrequency radiation. Moreover, by functionalizing the surface of the nanoparticles with DNA molecules and further hybridizing with different length fluorophore-modified DNA an accurate temperature spatial mapping could be determined. Due to the design of these DNAs, different denaturalization temperatures (melting temperature, T_m) could be achieved. The quantification of the denaturalized fluorophore-modified DNA, and by interpolation onto a Boltzmann fitting model, it has been possible to calculate the local temperature increments at different distances, corresponding to the length of each modified DNA, from the surface of the nanoparticles. The local increments achieved were up to 15°C, and the rigidity conferred by the double strand DNA allowed to evaluate the temperature at distances up to 5.6 nm from the nanoparticle surface.

[1] M. Colombo, S. Carregal-Romero, M. F. Casula, L. Gutierrez, M. P. Morales, I. B. Bohm, J.T. Heverhagen, D. Prospero, W. J. Parak, *Chem. Soc. Rev.* **41**, (2012) 4306-4334.

[2] S. Laurent, S. Dutz, U. O. Häfeli, M. Mahmoudi, *Adv. Colloid Interface Sci.* **166** (2011), 8.

[3] M. Creixell, A. C. Bohórquez, M. Torres-Lugo, C. Rinaldi, *ACS Nano* **5** (2011), 7124-7129.

[4] L. Polo-Corrales, C. Rinaldi, *J. Appl. Phys.* **111** (2012) 07B 334-333.

[5] A.M. Derfus, G. von Maltzahn, T. J. Harris, T. Duza, K. S. Vecchio, E. Ruoslahti, S. N. Bhatia, *Adv. Mater.* **19** (2007) 3932-3936.

1TL-E-8

FUNDAMENTAL MODE ORTHOGONAL FLUXGATE: A PLATFORM OF THE MAGNETOMETER AND THE GRADIOMETER

Sasada I., Karo H., Harada S., Farag L.A.

Kyushu University, Kasuga, Japan

sasada@ence.kyushu-u.ac.jp

Fundamental mode orthogonal fluxgate (FM-OFG) was proposed by one of the present authors in 2001. The basic configuration and the operating principle can be found in ref [1]. In this talk, recent developments of the fundamental mode orthogonal fluxgate will be presented encompassing ultrahigh resolution magnetometers, wide band FG-induction coil hybrid magnetometer and gradiometers. Some applications of the magnetometer include magneto-cardiography (MCG) measurement and also monitoring magnetometers are used as sensing element for the active magnetic shielding system. The gradiometer built on the FM-OFG is the most recent sensor that we have developed. It has a unique feature to suppress the sensitivity to the uniform magnetic field that can be tuned by adjusting a dc bias current to the magnetic wire core of the sensor head.

As one of the promising results obtained by the magnetometer, we will show 36-ch MCG, and also to be presented, is the performance of the gradiometer whose (uniform magnetic field sensitivity)/(gradient magnetic field sensitivity) ratio is in the range of 10,000~40,000.

This work is partially support by JST through A-Step program.

Acknowledgement: 36 ch MCG measurements could not be performed without helps of Drs. K. Kazami and H. Kubota of Yokogawa Electric Corporation, Japan.

[1] I. Sasada, *J. Appl. Phys.*, **91** (2002) 7789-7791.

1RP-E-9

TWO DIMENSION CELL STRUCTURE: FROM DIGITIZING TO ANALYSIS*Ivanov O.V.¹, Ignatov M.S.²*¹ Lebedev Physical Institute, RAS, Moscow, Russia² Main Botanical Garden, RAS, Moscow, Russia

ivanov@lpi.ru

Multicellular structure of different living beings is highly specific as well as diagnostic for species and their individual parts. Cells of complex organisms, including humans, are studied anatomically using series of cross sections of one cell thick. Some groups of higher plants, namely mosses and hepatics, have normally unistratose (one cell thick) leaves themselves, their essential structure can therefore be approximated by a two-dimensional slab. Full information on geometry of cellular network is essential for understanding both the plant taxonomy and ontogeny.

A graph on the surface is a natural language for formal description of such objects. This language makes such biological objects similar to a lot of physical objects due to the presence of the domain structure. To translate the cellular network into the graph form, we need to obtain a digital image with a sufficiently high contrast in the investigated structure. In the case of moss leaf (for study of which these algorithms were initially developed), the polarized light microscopy proved to be the best choice. The limitations of objective resolution and focus depth require creating a set of multiple images, which are used as the initial data set. This makes it necessary to use gluing algorithms, which unify data from all images in a unique graph. The algorithms can be constructed in two ways: first, to make glue images and then transform the whole image to a graph, or, alternatively, transform each image to a graph form to unite individual graphs in the unique graph thereafter. The second way is preferable, as it allows to work with images of different magnifications or partially focused images. In practice the same object area may be recognized as different graphs. To exclude this inconsistency, special algorithms were developed and successfully applied. The key underlying idea is the requirement of independence of results from a sequence of graph gluing. This leads to a well defined matching procedure which solves inconsistencies in a most robust way, and shows difficult places on original images to a researcher so that it could be corrected manually. The basic idea under the graph recognizing algorithm is to search for homogeneous domains, mark them, and inflate them further to full space filling. The border on this inflated area is presented as a graph.

This graph technique allows solving many biological problems simply by calculating its statistical characteristics and subsequent statistical analysis. In particular, the species identification and classifying is based on simple properties of the graph and quadratic programming. More sophisticated way is based on the graph transformation into a special tree graph. This tree restores the leaf development down to the level of each individual cell division under ontogeny. It opens up great opportunities for research of the ontogenesis regulation mechanisms and, particularly, of changes in evolution caused by various factors (chemical, changes in the genome, *etc.*). The method has been successfully used in the studies of both modern species and fossil specimens.

All the algorithms are realized as a set of programs with web interface. This set of algorithms has a much wider application area, for example, it can be used for structure recognition of magnetic domains.

Support by RFBR is acknowledged.

1OR-E-10

BIOSENSORS BASED ON ELECTRONIC AND OPTICAL DETECTION OF MAGNETIC NANOPARTICLES

Orlov A.V., Nikitin M.P., Bragina V.A., Znoyko S.L., Ksenevich T.I., Gorshkov B.G., Nikitin P.I.

A.M. Prokhorov General Physics Institute, Russian Academy of Sciences, Moscow, Russia
alexey.orlow@gmail.com

Highly sensitive electronic methods and compact devices have been developed for detection of magnetic nanoparticles (MNPs) employed as nanolabels of biochemical reactions in 3D structures that serve as a solid phase of bioassays. MNPs are counted by their non-linear magnetization and frequency mixing [1]. A sample is exposed to an *ac* magnetic field at two frequencies f_0 and f_i with recording the signal, which is proportional to the MNP quantity, at the combinatorial frequency $f_i \pm 2f_0$. The detection method is robust, features high signal-to-noise ratio and remarkably wide linear dynamic range of almost 5 orders of magnitude.

Optimization of MNP properties and bioassay conditions has been carried out by a novel method for quantitative study of affinity constants of antibodies (AB) on MNP. The method is based on the spectral correlation interferometry (SCI) [2]. The SCI allows recording of thickness changes of a layer of molecules or nanoparticles on a cover slip surface with picometer resolution averaged over the sensing area. The values of kinetic association constants of AB coupled with MNP are 2–3 orders of magnitude higher than those of molecular AB association with antigen. Such good kinetic characteristics of AB coupled with MNP are due to polyvalence of MNP that possess several AB simultaneously on the surface of nanoparticles. This optical method offers practical prospects for development of optomagnetic biosensors based on the SCI with MNP, which demonstrate high sensitivity and wide dynamic range for detection of antigens. The 50-nm MNP employed as labels yield 100-fold amplification of the SCI signals. The achieved detection limit for cTnI was 0.1 ng/ml, which is relevant to diagnostics of myocardial infarction. These optomagnetic biosensors with inexpensive cover slips employed as disposable sensor chips and MNP are an economically sound alternative for magnetoresistive biosensors.

The protocols of bioreactions optimized with SCI were also used for development of the second type of a biosensor based on counting of bound MNP by the electronic frequency mixing method. The MNP are registered from the entire volume of 3D membrane structures rather than from surface only while using of flat biochips (including GMR) or traditional optical labels. The advantages of the electronic biosensors were demonstrated by quantification of oncology markers in human serum. The detection limit of prostate-specific antigen was as low as 25 pg/mL in a wide dynamic range that exceeded 3 orders of magnitude (Fig. 1). These results are better than those obtained by the standard much more labor- and time-consuming ELISA. As the bioassay is based on dry chemistry, it is stable during long-term storage, easy to use and does not require skilled personnel. The developed biosensors are promising for highly sensitive detection of protein markers of various diseases, as well as of bioactive agents in complex biological fluids.

Support by RFBR grants is acknowledged.

[1]. P.I. Nikitin, P.M. Vetoshko. *Patents RU 2166751 & 2177611* (2000), *EP 1262766* (2001).

[2]. P.I. Nikitin, B.G. Gorshkov, E.P. Nikitin, T.I. Ksenevich. *Sens. & Act. B*, **111–112** (2005) 500.

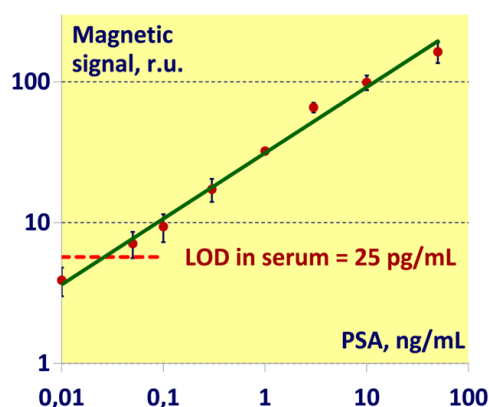


Fig.1. Calibration curve for PSA in human serum

1OR-E-11

MONOGRAPH: MAGNETIC NANOPARTICLES IN BIOSENSING AND MEDICINE*Llandro J.¹, Ionescu A.¹, Darton N.J.²*¹ Cavendish Laboratory, University of Cambridge, Cambridge CB3 0HE, UK² Arecor Ltd., CB4 0FE, Cambridge, U.K.
jl286@cam.ac.uk

The last decade has seen a surge of work being carried out on magnetic nanoparticles in biosensing and medicine [1]. Recent reviews focusing on applications of magnetic nanoparticles in biomedicine, their synthesis, detection and functionalisation reflect these efforts [2]. New avenues of research and clinical methods have been developed, such as magnetic actuation and the use of magnetic particles for MRI drug delivery [3]. However, there is currently no concise account of methods and techniques, which draws together the various interdisciplinary threads of this emerging research area. Hence, there is a need for a monograph to provide a common lexicon for researchers in this field. Furthermore, this monograph will aim also provide a guide to instruct a new generation of students embarking on research in biomagnetism and/or on diverse magnetic biosensors. Due to the interdisciplinary nature of the field, this book targets a readership of graduate students, post-doctoral researchers and faculty within the life sciences, physical sciences and engineering communities.

In this talk, the individual co-authors to this contributed monograph will be acknowledged and the subject matter of their chapters outlined.

Support by Cambridge University Press is acknowledged.

[1] A. Ionescu and J.A.C. Bland, AIP Press, New York, U.S., AIP Conference Proceedings **1025** (2008), ISBN: 978-0-7354-0547-9.

[2] J. Llandro, J.J. Palfreyman, A. Ionescu and C.H.W. Barnes, *Medical & Biological Engineering & Computing* **48**, (2010) 997.

[3] N.J. Darton, A.J. Sederman, A. Ionescu, C. Ducati, R.C. Darton, L.F. Gladden and N.K.H. Slater, *Nanotechnology* **19** (2008) 395102.

1 July

Tuesday

11:30-13:00

oral session

1TL-F

1RP-F

1OR-F

**“Diluted Magnetic
Semiconductors”**

1TL-F-1

ION BEAM SYNTHESIS OF THE FULL SPECTRUM OF III-V: Mn FERROMAGNETIC SEMICONDUCTORS

Zhou Sh.

Helmholtz - Zentrum Dresden – Rossendorf, Institute of Ion Beam Physics and Materials Research,
Bautzner Landstr. 400, 01328 Dresden, Germany
s.zhou@hzdr.de

Ferromagnetic semiconductors have been under intensive investigation during the last decade. Until now, III-Mn-V based compound semiconductors are the only well accepted class of materials. The prototype ferromagnetic semiconductor GaMnAs has revealed a variety of unique features induced by the combination of its magnetic and semiconducting properties. To prepare ferromagnetic semiconductors, one needs to dope the host with up to 5-10% Mn, which is far beyond the solid solubility of Mn in III-V compounds. As a non-equilibrium process, ion implantation can introduce enough dopants as required. However, the activation of dopants remains challenging due to the clustering of implanted ions during post-annealing. The solubility limit is a fundamental barrier for dopants incorporated into a specific semiconductor. On the other hand, one notes that the solubility limit in the liquid phase is generally much larger than that in the solid phase. Short-time annealing in the millisecond or nanosecond regime allows the epitaxial growth from a liquid phase. The mature development and commercialization of ion implantation promise the versatility. The approach combining ion implantation and pulsed laser melting allows us to prepare ferromagnetic semiconductors covering the full spectrum of III-V compound semiconductors.

We have successfully synthesized ferromagnetic Mn doped III-V from InAs and GaAs to InP and GaP with different bandgaps. The results of magnetization, magnetic anisotropy, resistivity, anomalous Hall effect, magnetoresistance and x-ray magnetic circular dichroism obtained from the synthesized samples confirm the intrinsic origin and the carrier-mediated nature of the ferromagnetism. Moreover, in different III-V hosts we observe distinct differences regarding the magnetic anisotropy and conduction mechanism which are related with the intrinsic parameters such as the lattice mismatch, energy gap and the acceptor level of Mn. These results could allow a panorama-like understanding of III-V:Mn based ferromagnetic semiconductors.

Support by HGF (NG-713) is acknowledged.

- [1] D. Bürger, S. Zhou, et al., *Phys. Rev. B* **81**, 115202 (2010).
- [2] S. Zhou, et al., *Appl. Phys. Lett.* **96**, 202105 (2010).
- [3] S. Zhou, et al., *Appl. Phys. Express* **5**, 093007 (2012).
- [4] M. Khalid et al., *Phys. Rev. B* **89**, 121301(R) (2014).
- [5] Y. Yuan, et al, *IEEE Magnetic Trans.*, submitted (2014).

1RP-F-2

HIGH-TEMPERATURE FERROMAGNETISM OF $\text{Si}_{1-x}\text{Mn}_x$ ($x \approx 0.5$) NONSTOICHIOMETRIC ALLOYS

Rylkov V.V.^{1,2,3}, *Bugaev A.S.*^{2,4}, *Novodvorskii O.A.*⁵, *Tugushev V.V.*^{1,6}, *Kulatov E.T.*⁶,
Zenkevich A.V.^{1,4}, *Semisalova A.S.*⁷, *Nikolaev S.N.*¹, *Vedeneev A.S.*², *Shorokhova A.V.*⁵,
*Aver'yanov D.V.*¹, *Chernoglazov K.Yu.*¹, *Gan'shina E.A.*⁷, *Perov N.S.*⁷, *Granovsky A.B.*^{3,7},
*Panchenko V.Ya.*⁵, *Zhou S.*⁸

¹ NRC "Kurchatov Institute", 123182 Moscow, Russia

² Kotel'nikov Institute of Radio Engineering and Electronics RAS, 141190 Fryazino, Russia

³ Institute of Theoretical and Applied Electromagnetics RAS, 125412 Moscow, Russia

⁴ Moscow Institute of Physics and Technology, 141700 Dolgoprudny, Moscow Region, Russia

⁵ Institute on Laser and Information Technologies RAS, 140700 Shatura, Moscow region, Russia

⁶ Prokhorov General Physics Institute RAS, 119991 Moscow, Russia

⁷ Faculty of physics, M.V. Lomonosov MSU, 119991 Moscow, Russia

⁸ Helmholtz-Zentrum Dresden-Rossendorf, Institute of Ion Beam Physics and Materials Research,

D-01314 Dresden, Germany

vvrylkov@mail.ru

Si-Mn alloys attract increasing interest due to their potential application in spintronics and magnetic storage devices [1]. In addition, these alloys exhibit unusual magnetic characteristics which cannot be adequately interpreted within the framework of available theoretical models (see [2,3] and references therein).

Recently we found that the Curie temperature ($T_C \geq 300$ K) in nonstoichiometric $\text{Si}_{1-x}\text{Mn}_x$ alloys slightly enriched in Mn ($x \approx 0.52-0.55$) in comparison to the stoichiometric monosilicide MnSi becomes about an order of magnitude higher than that in MnSi ($T_C \approx 30$ K). Deviations from the stoichiometry lead to a drastic decrease in the density of charge carriers (holes), whereas their mobility at about 100 K becomes an order of magnitude higher than the holes mobility in MnSi. The high-temperature ferromagnetism was explained by the formation of defects with localized magnetic moments coupled via spin fluctuations of itinerant electrons in the host [4].

$\text{Si}_{1-x}\text{Mn}_x$ films 60–70 nm thick with various Mn ($x \approx 0.52-0.55$) content were produced by the pulsed laser deposition (PLD) method onto the Al_2O_3 (0001) substrates at 340°C [4]. Here we present a comparative study of the anomalous Hall effect (AHE) and of the transverse Kerr effect (TKE) in these films. The data on AHE and TKE are consistent with each other and prove a global character of the ferromagnetic order as well as an absence of ferromagnetic clusters [5]. Magnetization data demonstrate good homogeneity of the film magnetization: variation of the saturation magnetization M_s in the samples with $T_C \approx 310$ K does not exceed 6 % in the temperature range $T = 10-100$ K and is well described by the Bloch law. It is also established that the qualitative textured $\text{Si}_{1-x}\text{Mn}_x$ films with $x \approx 0.51-0.52$ and $T_C \sim 300$ K could be formed by PLD method from the stoichiometric MnSi target in shadow geometry (at low energy of deposited atoms).

This work was partly supported by the RFBR (grant No. 13-07-12087, 13-07-00477, 14-07-00688) and DFG grant for initializing an international cooperation (ZH 225/4-1).

[1] S. Zhou and H. Schmidt, *Materials*, **3** (2010) 5054.

[2] A.F. Orlov, A.B. Granovsky, L.A. Balagurov et al., *J. Exp. Theor. Phys.*, **109** (2009) 602.

[3] V.N. Men'shov, V.V. Tugushev, S. Caprara, *Phys. Rev. B*, **83** (2011), 035201.

[4] V.V. Rylkov, S.N. Nikolaev, K.Yu. Chernoglazov et al., *JETP Lett.*, **96** (2012) 255.

[5] V.V. Rylkov, E.A. Gan'shina, O.A. Novodvorskii et al., *Europhys. Lett.* **103** (2013) 57014.

1RP-F-3

MAGNETISM AND MICROSTRUCTURE OF HIGH TEMPERATURE FERROMAGNETIC ALLOY $\text{Si}_{1-x}\text{Mn}_x$

Aronzon B.A.^{1,2}, Vasiliev A.L.¹, Semisalova A.S.^{3,6}, Perov N.S.³, Morgunov R.B.⁴,
Novodvorskii O.A.⁵, Lahderanta E.⁶

¹ NRC “Kurchatov institute”, Moscow, Russia

² P.N. Lebedev Physical Institute RAS, Moscow, Russia

³ M.V. Lomonosov MSU, Moscow, Russia

⁴ IPCP RAS, Chernogolovka, Russia

⁵ Institute of Laser and Information Technologies RAS, Shatura, Russia

⁶ Lappeenranta University of Technology, Lappeenranta, Finland

aronzon@mail.ru

Recently it was found that $\text{Si}_{1-x}\text{Mn}_x$, alloys with high Mn content show high temperature ferromagnetic state with Curie temperature T_c above 300 K [1,2,3]. These structures were grown by pulsed laser deposition (PLD). The ferromagnetic state at room temperature in these structures was detected by magnetometry measurements and was accompanied by observation of the anomalous Hall effect (AHE), indicating the existence of carrier spin polarization. After first publication the main attention was concentrated on structures with $x \approx 0.5$. It was suggested that the high temperature ferromagnetism is related to small deviation from the stoichiometrical composition, also it was suggested that composition of the sample is uniform.

In this report we present results of electron microscopy studies combined with magnetometry measurements. It is shown that samples obtained by PLD contain 3 different magnetic phases. Which are related to $\text{Si}_{0.5}\text{Mn}_{0.5}$ with $T_c \approx 30\text{K}$, high temperature ferromagnetic phase and superparamagnetic inclusions. This statement is based on the temperature dependence of saturated magnetization M_s , ZFC and FC curves and on results of the electron microscopy measurements with atomic resolution. Fitting of $M_s(T)$ curve by the well known simplified Brillouin function demonstrated that it could be approximated by the three term equation $M_s(T) = M_{s1}(0)[1 - (T/T_{C1})^{n1}] + M_{s2}(0)[1 - (T/T_{C2})^{n2}] + M_{s3}(0)[1 - (T/T_{C3})^{n3}]$. These terms are describing the $M_s(T)$ curve in the three different temperature ranges. The third term is related mainly to temperatures above the room that and for best samples could be neglected playing very small role and could be treated as superparamagnetic state contribution. First term with T_C about 30 K represents $\text{Si}_{0.5}\text{Mn}_{0.5}$ phase, while the second term with T_C about 300 K is of the most interest. From the results of the electron microscopy we conclude that sample structure could be treated as $\text{Mn}_{1.5}\text{Si}_{0.5}$ with structure parameter $a \approx 0.29$ nm while Mn1 position ($x=0, y=0, z=0$) are fully occupied while positions Mn2: $x=0.5, y=0.5, z=0.5$ and Si: $x=0.5, y=0.5, z=0.5$ are not fully occupied. That could be treated as sample consists from two phases $\text{Si}_{0.5}\text{Mn}_{0.5}$ and manganese silicide oversaturated with Mn. The last phase could be responsible for high temperature ferromagnetic state. Furthermore the above phases distributed over sample thickness not uniformly and we guess the relation between them could be the reason for the diversity of magnetic parameters for different samples.

[1] B.A. Aronzon, V.V. Rylkov, S.N. Nikolaev, et al., *PRB* **84**, 075209 (2011).

[2] S.N. Nikolaev, V.V. Rylkov, B.A. Aronzon, et al., *Semiconductors* **48**, 1510 (2012).

[3] V. V. Rylkov, E. A. Gan'shina, O. A. Novodvorskii, *Europhys. Letts* **103**, 57014 (2013).

1OR-F-4

MAGNETO-OPTICAL EVIDENCE FOR INTRINSIC FERROMAGNETISM IN (Ga,Mn)As LAYERS GROWN BY PULSED-LASER DEPOSITION

Gan'shina E.A.¹, Golik L.L.², Kovalev V.I.², Kun'kova Z.E.², Markin Yu.V.², Novikov A.I.¹, Zikov G.S.¹, Danilov Yu.A.³, Kudrin A.V.³, Vikhrova O.V.³, Zvonkov B.N.³

¹ Department of Physics, Moscow State University, Moscow, Russia

² Institute of Radioengineering and Electronics, RAS, Fryazino, Russia

³ Nizhny Novgorod State University, Nizhny Novgorod, Russia

zek@ms.ire.rssi.ru

Diluted magnetic semiconductors (DMS), (Ga,Mn)As in particular, attracted much interest owing to their potential for spintronics and novel magneto-optical device functionalities. Low-temperature molecular beam epitaxy (MBE) is commonly applied for growth of (Ga,Mn)As layers. Pulsed laser deposition (PLD) [1] is also used, but the layers grown with employing this technique usually contain ferromagnetic MnAs ($T_C=320$ K) inclusions, which significantly determine the properties of the layers [2]. In this work peculiarities in magneto-optical spectra of (Ga,Mn)As layers grown with PLD technique, which were conditioned by intrinsic ferromagnetism in (Ga,Mn)As, were studied. Quantity of Mn in the layers under study was controlled by the sputtering time ratio of Mn and GaAs ($Y_{Mn} = t_{Mn}/t_{Mn} + t_{GaAs}$) and substrate temperature (T_g). The layers approximately 100 nm thick were grown on GaAs(001) substrates at the process parameters of $Y_{Mn}=0.13$; $T_g, ^\circ\text{C}$: 300 (#1); 330 (#2) and 350 (#3).

Magneto-optical signal received from the samples was measured in the configuration of the transversal Kerr effect (TKE). TKE spectra, $\delta(E)$, were recorded in the energy range of $E = 0.5 - 4.0$ eV in alternating magnetic fields of $H \leq 3$ kOe at $T = 20 - 295$ K. Temperature dependences, $\delta(T)$, and magnetic field those, $\delta(H)$, were measured at several fixed energies. We also measured spectra of the ellipsometry parameters, $\tan\psi(E)$ and $\cos\Delta(E)$, $E = 1.24 - 4.5$ eV, $T = 295$ K.

Behavior of the $\delta(E)$ spectra strongly depends on the process parameter T_g . In the spectra of samples # 2 and # 3 measured at the room temperature one can observe the TKE bands caused by transitions in MnAs [2]. As the temperature decreases, the TKE signal increases and in addition a number of new peculiarities arises in the low-temperature $\delta(E)$ spectra (at $T=25$ K) of samples #2 and #3. Sample #1 grown at $T_g = 300^\circ\text{C}$ is of the greatest interest. At the temperature range of 295 - 85 K the TKE signal is very weak (it is close to the noise level). This signal is likely to be conditioned by the presence of MnAs traces. On cooling below 80 K, the TKE signal significantly increases, shape of the TKE spectrum being strongly different from that observed for the samples with MnAs inclusions. At $T < 80$ K the $\delta(H)$ dependences for sample # 1 display ferromagnetic behavior.

Using the experimental data we calculated spectral dependences of the real (ε'_1) and imaginary (ε'_2) parts of the off-diagonal components ($\varepsilon' = \varepsilon'_1 - i\varepsilon'_2$) of the dielectric permittivity tensor as well as spectra of the magnetic circular dichroism for the layers under study. The obtained dependences were compared with the published magneto-optical spectra of (Ga,Mn)As layers grown by MBE. It was concluded that intrinsic ferromagnetic ordering ($T_C \approx 80$ K) took place in the (Ga,Mn)As sample (#1) grown by pulse laser deposition. The peculiarities in the low-temperature $\delta(E)$ spectra of samples #2 and #3 were also caused by the ferromagnetic ordering of semiconducting host of these (Ga,Mn)As:MnAs layers.

[1] B.N. Zvonkov, O.V. Vikhrova, Yu.A. Danilov, et al., *J. Opt. Technol.*, **75** (2008) 389-393.

[2] E.A. Gan'shina, L.L. Golik, et al., *J. Magn. Magn. Mater.*, **321** (2009) 829-832.

1 July

Tuesday

11:30-13:00

14:30-17:00

oral session

1TL-G

1OR-G

1TL-B

1RP-B

1OR-B

**“Magnetism of
Nanostructures”**

1TL-G-1

ROLE OF Cu IN INTRINSIC EXCHANGE BIAS IN FeMn

Lapa P.N.¹, Kaya D.¹, Ambaye H.², Glavic A.², Lauter V.², Belliveau H.³, Eggers T.³, Miller C.W.³, Skoropata E.⁴, van Lierop J.⁴, Park S.⁵, Roshchin I.V.^{1,6}

¹ Department of Physics and Astronomy, Texas A&M University, College Station, TX, USA

² Neutron Sciences Directorate, Oak Ridge National Laboratory, Oak Ridge, TN, USA

³ Department of Physics, University of South Florida, Tampa, FL, USA

⁴ Department of Physics and Astronomy, University of Manitoba, Winnipeg, Canada

⁵ Department of Physics, Pusan National University, Busan, South Korea

⁶ Dept. of Materials Science and Engineering, Texas A&M Univ., College Station, TX, USA

roshchin@physics.tamu.edu

We report an unusual observation: a non-magnetic material, copper, can modify magnetic properties of the magnetic material in close proximity (antiferromagnetic FeMn). In FeMn thin films, we observe an “intrinsic exchange bias”. In this effect, the hysteresis loops are shifted as in the traditional exchange bias, but here, this shift is observed in only one magnetic layer, instead of two. The most unusual in this behavior is that it only occurs when a copper layer is present in contact with FeMn.

This “intrinsic” exchange bias (EB) is observed in a film system without a distinct, separate ferromagnetic (FM) layer; Ta(50 Å)/[FeMn(50–450 Å)/Cu(50 Å)]₁₀/Ta(50 Å) multilayers [1]. It occurs between pinned and unpinned uncompensated magnetization (UM) in the FeMn layers. The analysis of the remanent magnetization (M_R) shows that the unpinned (ferromagnet-like) UM is distributed uniformly throughout FeMn [1]. Since the magnitude of the EB loop shift (H_E) scales with the inverse thickness of the FeMn layer (Fig. 1), the EB is clearly an interfacial phenomena. This behavior is similar to that described by Malozemoff’s model for the bilayer (antiferromagnet-ferromagnet) EB systems [2]. So, the pinned UM should be located near the FeMn interfaces. This is consistent with the requirement of the Cu layer for the EB to occur.

To test the hypothesis that Cu might be diffusing into FeMn [1], Mössbauer spectroscopy was performed using the naturally occurring ⁵⁷Fe in FeMn. The spectra of the samples of one FeMn layer (50 and 150 Å) with and without Cu show two components: One corresponds to the stoichiometric FeMn, while the other is attributed to Fe-rich areas of FeMn. This indicates that Fe forms small clusters in disordered areas of FeMn, in agreement with the Mössbauer spectral lineshapes. These areas of the sample with clustered Fe are likely to be the source of the unpinned UM. No measurable difference in these spectra for the samples with and without Cu suggests that Cu is unlikely to diffuse into FeMn, contrary to the previously proposed hypothesis [1]. Results of polarized neutron reflectometry on these films that further describe the differences between the structures in the FeMn/Cu multilayers responsible for the unusual magnetism will be presented.

Work is supported by Texas A&M University, TAMU-CONACYT Collaborative Research Program, US DOE BES Scientific User Facilities Division (ORNL SNS), NSERC (University of Manitoba), NSF-CAREER (USF), NRF Korea – 2013-R1A4A1069587, 2011-0031933 (Pusan National University).

[1] D. Kaya *et al.*, *J. Appl. Phys.*, **113**, 17D717 (2013).

[2] A. P. Malozemoff, *Phys. Rev. B* **35**, 3679 (1987), *ibid.*, **37**, 7673 (1988).

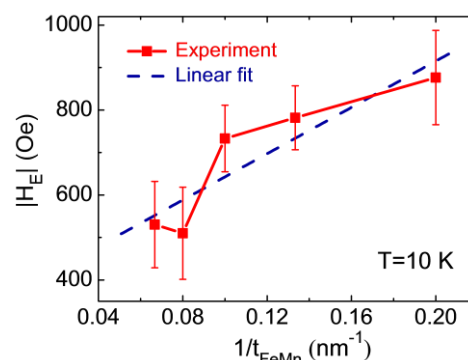


Fig. 1: Dependence of $|H_E|$ on the thickness of FeMn in FeMn/Cu superlattices.

1TL-G-2

SELF-ASSEMBLED ARRAYS OF FERROMAGNETIC NANO-WIRES: MAGNONIC, PHOTONIC AND MAGNETO-OPTIC PROPERTIES

Stashkevich A.¹, Roussigné Y.¹, Chérif S.-M.¹, Veniaminova Y.¹, Gueye M.¹, Poddubny A.²,
Murphy A.P.³, Atkinson R.³, Pollard R.J.³, Toal B.³, McMillen M.³, Zayats A.⁴

¹ LSPM CNRS (UPR 3407), Université Paris 13, 93430 Villetaneuse, France

² National Research University ITMO, St. Petersburg 197101, Russia

³ Centre for Nanostructured Media, Queen's University of Belfast, Belfast BT7 1NN, UK

⁴ Department of Physics, King's College London, Strand, London WC2R 2LS, UK

Magnetic properties of arrays of metal (Co, Ni, permalloy) nanowires in a dielectric substrate have been intensively studied during the last decades both theoretically and experimentally. Their unique properties make them potential candidates for numerous applications in such major fields as spintronics, microwave devices, photonics and even plasmonics.

The techniques of their elaboration relying on electro-deposition of metals in an anodized aluminum oxide self-assembled template, being both fast and inexpensive, are of high technological importance in their own right [1]. Major physical properties, including magnetic, optical and magneto-optical (MO) behavior can be varied over a very wide range by independently modifying the wire sizes and aspect ratio, their separation and composition.

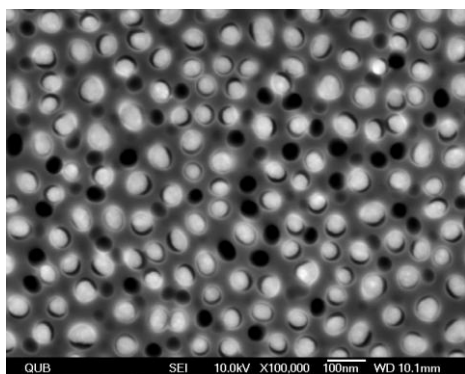


Fig.1a. SEM image of a typical diluted sample.

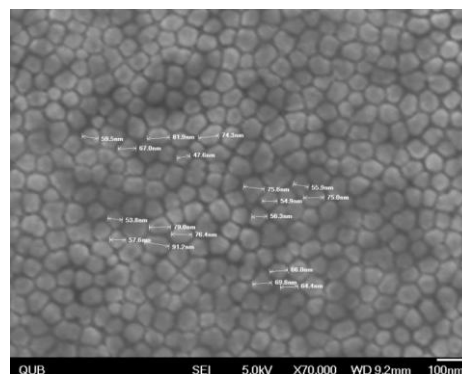


Fig.1b. SEM image of a typical dense sample.

More specifically, in this talk, based on the results obtained by means of Brillouin Light Scattering (BLS), we will address the following important features. First, magnonic behavior in general and the transition from magnetic oscillations localized on individual wires in dilute samples (Fig.1a) to collective modes in concentrated ones (Fig.1b) will be considered.

BLS spectroscopy is universally considered as a technique of MO characterization of magnetic properties of different materials. Our previous BLS studies have, however, revealed that this conventional logic can be inverted. In other words, through BLS one can gain access to crucial information, otherwise unattainable, on MO and optical properties of the studied structures. More specifically, this will discuss the cross-section of MO interactions between magnons and light, fine structure of BLS spectral lines as well as the Stokes/Anti-Stokes asymmetry.

[1] U. Ebels et al., *Phys. Rev. B* **64**, (2001) 144421.

[2] A.A. Stashkevich et al., *Phys. Rev. B* **80**, (2009) 144406 - 144419.

[3] Y. Veniaminova et al. *Optical Materials Express* **2**, (2012) 1260.

1OR-G-3

MAGNETIC AND ANISOTROPY OF MASS SELECTED FeCo NANOPARTICLES

Khadra G.¹, Tamion A.¹, Tournus F.¹, Aguilera-Granja J.F.², Montejano-Carrizales J.M.², Dupuis V.¹

¹ Institut Lumière Matière, UMR 5306 CNRS & Université Lyon 1, 69622 Villeurbanne, France

² Instituto de Física, Universidad Autónoma de San Luis Potosí, 78000 San Luis Potosí, México
Ghassan.khadra@univ-lyon1.fr

Over the last few decades, the recording media industry, mainly hard disk drives, have witnessed a remarkable increase in their capacity. This significant increase in the amount of information stored per unit area has been mainly achieved through the scaling of the recorded bits dimensions in the storage area [1]. The challenge is to overcome the superparamagnetic limit by using a material with a large magnetic anisotropy energy (MAE) and saturation magnetization (M_s). In the bulk phase, Iron-Cobalt alloys are known to have the highest magnetic moment but remain a soft magnetic material. At the nanoscale, this shortcoming must be overcome by increasing its MAE. Theoretical advances predicted that structural distortion of FeCo alloys in chemically ordered B2 phase leads to a giant MAE and large M_s [2].

For this study, FeCo nanoparticles (NPs) samples were prepared by mass-selected low energy cluster beam deposition (MS-LECBD) technique using a laser vaporization source that permits to have the same stoichiometry as the target source. In order to experimentally study the size effects on element specific relaxation in our FeCo NPs, we prepared a series of samples of diluted NPs of varying sizes (2-6 nm) embedded in an inert carbon matrix [3]. The magnetic properties of the samples were investigated by SQUID magnetometry and x-ray magnetic circular dichroism (XMCD) measurements under various thermal treatments. SQUID data was fitted using the “Triple-Fit” protocol [4]. For all sizes, annealing leads to a crystalline order as seen from high-resolution transmission electron microscopy (HRTEM) and an increase in the magnetic anisotropy and moment per atom (see Figure). From extended x-ray absorption fine structure measurements (EXAFS) at both Fe and Co edges, a chemically disordered A2 phase was found for the as-prepared FeCo NPs while the annealed NPs showed a chemically ordered B2 phase with a ratio $c/a > 1$ (tetragonal distortion). To relate structure and magnetic behaviour, density-functional ab-initio calculations were carried on using the SIESTA code [5] to perform first principles electronic, magnetic and structural calculations for FeCo NPs as a function of size.

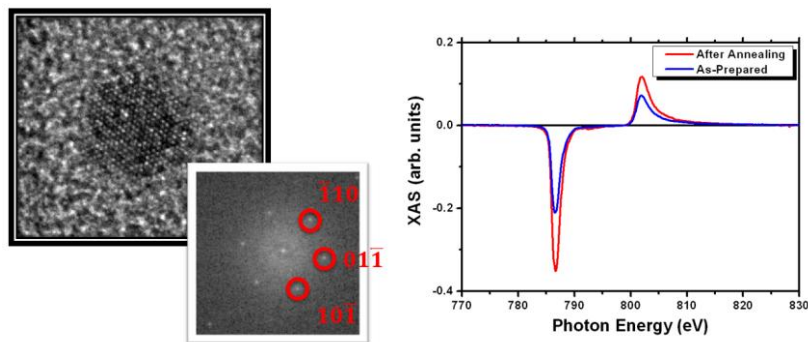


Figure - (Left) HRTEM image of an annealed FeCo NP well crystallized and its Fourier Transform showing a BCC structure in the 111 direction. (Right) XMCD signal of As-prepared and after annealing, at the Co edge, of the NP sample showing an enhancement of the magnetic moment.

[1] D. A. Thompson and J. S. Best, *IBM J. Res. Dev.* **44**, (2000) 311-322.

[2] T. Burkert, L. Nordstorm, O. Eriksson and O. Heinonen, *Phys. Rev. Lett.* **93**, (2004) 027203.

[3] A. Hillion, A. Cavallin, S. Vlaic, A. Tamion, et al., *Phys. Rev. Lett.* **110**, (2013) 087207.

[4] A. Tamion, M. Hillenkamp, F. Tournus, et al., *App. Phys. Lett.* **95**, (2009) 062503.

[5] J. M. Soler, E. Artacho, J. D. Gale, et al., *J. Phys.: Condens. Matter* **14**, (2002) 2745- 2779.

1OR-G-4

CHARGE DOPING AND ELECTRIC FIELDS AS A ROUTE TO TAILOR MAGNETIC PROPERTIES OF METALLIC SURFACES

Ruiz-Diaz P., Brovko O.O., Dasa T.R. , Stepanyuk V.S.

Max-Planck Institut für Mikrostrukturphysik, Halle, Germany

pruiz@mpi-halle.mpg.de

In the emerging field of spintronics local manipulation and control of magnetic properties of nano-sized systems is fundamental for the new generation of the high-density magnetic storage media. Several mechanisms to tailor the magnetic properties of atomic-scale magnetic structures such as exchange interactions and magnetic anisotropy have been explored [1].

The most conventional manner to do so is through the external magnetic field application.

Nevertheless, in the very recent years, external electric fields[2-4] and charge doping[5,6] have arisen as alternative promising techniques to alter the magnetic properties of atomic nano-systems, such as magnetic clusters on non-magnetic metallic surfaces[2] and thin films[1,4]. We present a first-principles study regarding the influence of external electric fields and charge doping on the magnetic properties of metallic surfaces with focus on 3d-5d-based compounds. Furthermore, through system-specific examples we show that these routes can be used to tailor magnetic anisotropy and direction of magnetization at the same time. We have found that magnetic anisotropy in metal-alloyed surfaces is strongly sensitive to electric field exposure and surface charge doping. The latter showing even a more profound effect on the magnetism of layered-systems[5,6].

- [1] O.O.Brovko,P.Ruiz-Díaz, T.R.Dasa, V.S.Stepanyuk, *J. Phys.:Condens.Matter* **26**(2014) 093001.
- [2] N N. Negulyaev, V.S. Stepanyuk, W.Hergert, J.Kirschner, *Phys. Rev. Lett.* **106**, (2011) 037202 .
- [3] T. R. Dasa, P. A. Ignatiev, V. S. Stepanyuk, *Phys. Rev. B* **85**, (2012), 205447.
- [4] T. R Dasa, P. Ruiz-Díaz, O. O Brovko, V, S Stepanyuk, *Phys. Rev. B* **88**, (2013) 104409.
- [5] P. Ruiz-Díaz, T. R. Dasa, V. S. Stepanyuk, *Phys. Rev. Lett.* **110** (2013) 267203.
- [6] P. Ruiz-Díaz and V. S. Stepanyuk, *J. Phys. D: Applied Phys.* **47** (2014) 105006.

1TL-B-4

FREE PRECESSIONAL DYNAMICS IN MAGNETIC HETEROSTRUCTURES

Salikhov R.^{1,3}, Buschhorn S.¹, Abrudan R.^{1,4}, Brüßing F.¹, Radu F.⁴, Zabel H.^{1,2}

¹ Ruhr-Universität Bochum, 44780 Bochum Germany

² Johannes Gutenberg Universität Mainz, 55099 Mainz, Germany

³ Universität Duisburg-Essen, 47057 Duisburg, Germany

⁴ Helmholtz-Zentrum Berlin, BESSY II, 12489 Berlin, Germany

hartmut.zabel@rub

Element specific free precessional dynamics of magnetic moments can be studied by time resolved x-ray resonant magnetic scattering (tr-XRMS) using magnetic field pulse – x-ray probe techniques with variable delay between pulse and probe [1,2]. With this technique we have investigated the precessional dynamics of ferromagnetically coupled Fe and Ni moments in Py [2] and antiferromagnetically coupled Fe (Ni) and Gd magnetic moments in Py_{1-x}Gd_x systems [3]. For pure Py we find that the Fe and Ni moments precess coherently at all times and exhibit the same damping parameter. Doping with Gd causes an increase of the intrinsic damping parameter, while the relaxation rate decreases, i.e. the magnetization after field pulse excitation relaxes more slowly to the new equilibrium position with increasing Gd concentration. Furthermore, we find that at room temperature the 3d and 4f sublattices preserve their collinear antiparallel alignment during their precession, whereas at lower temperatures the 3d and 4f moments precess with the same (but enhanced) frequency but at different precessional angles, i.e. the 3d and 4f moments are no longer collinear. – We have also investigated spin-pumping effects in trilayers consisting of F1/Cu/F2 [4], where F1=Py again serves as the probing layer for tr-XRMS experiments, and F2=Co is a different ferromagnetic layer. As Py and Co layers have very different coercive fields, the trilayer has spin-valve properties. The dynamical properties can thus be probed for parallel and antiparallel configuration of the spin valve. For antiparallel configuration we find an enhanced damping parameter, which we take as a clear indication for effective spin-pumping process acting between both magnetic layers [5]. We have also investigated potential other reasons for the configurational dependence of the damping parameter, such as domain wall induced coupling or magnetic dipole coupling [6]. We find that stray fields from magnetic inhomogeneities in layer F2, such as a domain state in Heusler layers, may cause a de-phasing during the precession of F1 magnetization that can be interpreted as a result of a two-magnon scattering process [7].

This work was supported by DFG-SFB 491 and BMBF contracts 05K13PC1 and 05ES3xBA/5.

- [1] W. E. Bailey, L. Cheng, D. J. Keavney, C.-C. Kao, E. Vescovo, D. A. Arena, *Phys. Rev. B* **70**, (2004) 172403.
- [2] S. Buschhorn, F. Brüßing, R. Abrudan, H. Zabel, *J. Phys. D: Appl. Phys.* **44**, (2011) 165001.
- [3] R. Salikhov, R. Abrudan, F. Römer, R. Meckenstock, K. Westerholt, F. Radu, M. Farle and H. Zabel, *to be published*.
- [4] J.-V. Kim, C. Chappert, *J Magn. Magn. Mat.* **286**, (2005) 56.
- [5] R. Salikhov, R. Abrudan, F. Brüßing, St. Buschhorn, M. Ewerlin, D. Mishra, F. Radu, I.A. Garifullin, and H. Zabel, *Appl. Phys. Lett.* **99**, (2011) 092509.
- [6] R. Salikhov, R. Abrudan, F. Brüßing, K. Gross, C. Luo, K. Westerholt, H. Zabel, F. Radu, I.A. Garifullin, *Phys. Rev. B* **86**, (2012) 144422.
- [7] R. Salikhov, F. Brüßing, K. Gross, K. Westerholt, R. Abrudan, H. Zabel, F. Radu, *submitted*.

1TL-B-5

STRUCTURE, ELECTRONIC SPECTRUM AND SPIN PROPERTIES OF SEMICONDUCTOR NANOOBJECTS

*Uspenskii Yu.A.*¹, *Tikhonov E.V.*², *Matsko N.L.*¹

¹ P.N. Lebedev Physical Institute, Russian Academy of Sciences, Moscow, Russia

² M.V. Lomonosov Moscow State University, Physics Department, Moscow, Russia
uspenski@lpi.ru

Structural, spectral and spin properties of nanoclusters drastically differ from characteristics of corresponding bulk materials. Although these three properties are closely interrelated, for each of them the difference between nano- and bulk characteristics has its own origin. In our presentation these differences are considered with emphasis on the criterion of ferromagnetism in nanoobjects. The spatial arrangement of atoms greatly affects the properties of solids. To understand trends relevant to clusters, we calculated the ground-state structure of silicon clusters using the evolutionary algorithm and density functional theory (DFT). Calculations showed that among twelve considered bare or hydrogen-passivated clusters only Si₁₀H₁₆ has the diamond structure of bulk silicon. Other ground-state and isomer structures have distinct symmetry elements or are non-symmetric. Our consideration of an ensemble of Si₁₀H_{2m} ($m = 0 - 11$) clusters at arbitrary H₂ concentration revealed that the ensemble is not uniform, but presents a mixture of different clusters and isomers. This result points to difficulties in measurement of cluster properties. We note that the electronic spectrum of clusters varies widely with cluster structure, size, and composition and correlates, by and large, with cluster stability.

Optical, especially luminescent, properties of semiconductor nanoclusters are of great promise for optoelectronic and other applications. The tunability of optical spectra, that is their dependence on cluster size and shape, is related to changes in the electronic spectrum. Our calculations of the electron quasiparticle spectrum were made using the DFT, hybrid functional and *GW* approaches. The obtained results were verified by comparison with measured photoemission spectra of organic molecules. The DFT spectrum is not adequate: the valence band is shrunk by 15%, the HOMO-LUMO gap is too narrow (by a factor of 2 to 3), and only the description of the conduction band is satisfactory. Within the hybrid functional method, the valence and conduction bands are correctly reproduced, however the gap is 1.5 to 2 times narrower than in experiment. The best spectrum was obtained with the *GW* approximation, but its computational cost is 1000 times higher than in DFT. We also made precise and less laborious calculations of the gap with Lehman's approach, which uses the total energies of DFT in the states with $N-1$, N , and $N+1$ electrons. As for magnetic nanoobjects, a spin splitting of their spectrum is too small in DFT, but is reproduced well by the hybrid functional and *GW* methods.

The Stoner criterion is known as a useful tool predicting the ferromagnetic (FM) state in metals. This criterion is not applied to nanoobjects, because of their discrete electron spectrum. In our presentation we consider a generalization of this criterion, which can be applied to magnetism in nanoobjects. To derive it, we compare total energies of the FM and non-magnetic states using many-body perturbation theory. The derived criterion has compact form and may be useful for prediction of ferromagnetism in nanoobjects. To check its precision, we performed first-principle calculations of several nanoobjects (doped nanoclusters and organic molecules) in the FM and non-magnetic states and compared their results with predicted ones.

This research was supported in part by the RFBR (grant 13-02-00655a) and Programs of RAS.

1TL-B-6

NEW INSIGHTS INTO NANOMAGNETISM BY SPIN-POLARIZED SCANNING TUNNELING MICROSCOPY AND SPECTROSCOPY

Sander D., Oka H., Ouazi S., Corbetta M., Brovko O., Rodary G., Ignatiev P., Niebergall L.,
Stepanyuk V., Kirschner J.

Max Planck Institute of Microstructure Physics, Weinberg 2, D-06120 Halle, Germany
sander@mpi-halle.de

An outstanding question in nanomagnetism is the quantitative understanding of magnetization reversal of nanoparticles. A priori it is not clear which reversal mechanism applies for a given nanostructure. Coherent rotation, domain nucleation and growth and other reversal mechanisms are conceivable. We use spin-STM at 8 K and in external magnetic fields of up to 6 T to elucidate the physics of the reversal. We extract its energy barrier from a quantitative analysis of the switching field of individual, nanometer small bilayer Co islands with several hundred to thousands of atoms on Cu(111). Our quantitative analysis reveals a crossover of the magnetization reversal with increasing island size from an exchange-spring behaviour with vanishing magnetic anisotropy of rim atoms to reversal by domain wall nucleation and growth for larger islands at an Co islands size of around 7500 atoms (base length of islands: 12 nm) [1].

We exploit the high spatial resolution and the spin-dependent differential conductance of spin-STM to obtain maps of the spin polarization [2] and of the tunnel magneto resistance ratio (TMR) of the Co islands [3]. These maps reveal a pronounced spatial modulation of these properties of up to 20% on a nm scale. In conjunction with density functional theory we ascribe this to a spatially modulated spin-polarization, which is induced by spin-dependent electron confinement within the nanoscale Co islands [3].

We elucidate the role of the well-established electronic rim state [4] for the spin-polarization and magnetic anisotropy of single Co islands. We present first results on Co island edge decoration by Fe. Its impact on the electronic properties of the Co core is twofold. It leads (a) to the disappearance of the rim state of the Co core and (b) the energy position of the Co 3d minority state is almost constant over the Co core in contrast to its pronounced spatial variation reported on pure Co islands [5]. The discussion of our results suggests novel insights into the origin of the inhomogeneous magnetic properties within individual Co islands by identifying pronounced spatial variations of the spin-dependent electronic structure. We discuss the consequence for spin-polarization, magnetic anisotropy and magnetization reversal of the islands.

[1] Ouazi, Wedekind, Rodary, Oka, Sander, Kirschner, *Phys. Rev. Lett.* **108** (2012) 107206.

[2] Oka, Ignatiev, Wedekind, Rodary, Niebergall, Stepanyuk, Sander, Kirschner, *Science* **327** (2010) 843.

[3] Oka, Tao, Wedekind, Rodary, Stepanyuk, Sander, Kirschner, *Phys. Rev. Lett.* **107** (2011) 187201.

[4] Pietzsch, Okatov, Kubetzka, Bode, Heinze, Lichtenstein, Wiesendanger, *Phys. Rev. Lett.* **96** (2006) 237203.

[5] Rastei, Heinrich, Limot, Ignatiev, Stepanyuk, Bruno, Bucher, *Phys. Rev. Lett.* **99** (2007) 246102.

IRP-B-7

MAGNETISM ON ATOMIC SCALE: TRANSITION METALS COMPARED TO LANTHANIDES

*Peters L.¹, Jalink J.¹, Dieleman D.¹, Sanyal B.², Eriksson O.², Niedner-Schatteburg G.³,
Katsnelson M.I.¹, Rasing Th.¹, Kirilyuk A.¹*

¹ Radboud University Nijmegen, IMM, NL-6525 AJ Nijmegen, The Netherlands

² Uppsala University, S-75121 Uppsala, Sweden

³ TU Kaiserslautern, D-67663 Kaiserslautern, Germany

A.Kirilyuk@science.ru.nl

Magnetism is a macroscopic phenomenon that occurs because of short-range exchange interactions. However, what happens if the size of the whole system becomes comparable to the length scale of the exchange? Furthermore, how the accompanying discretization of the electronic structure will affect the magnetism?

This work studies the magnetism of gas-phase atomic clusters of transition metals and lanthanides. First we follow, both experimentally and theoretically, the development of structure [1] and magnetism [2] in Tb clusters, starting from the diatomic limit and adding one atom at a time. The exchange is shown to drastically increase as compared to the bulk, and to oscillate as a function of the interatomic distance, qualitatively similar to the bulk-like RKKY interaction, even though the notion of Fermi surface is not applicable. As a consequence the magnetic moment oscillates with the cluster size, with the oscillations being universal for several lanthanides. The absence of bulk periodicity also leads to a huge, 5–10 meV/atom, magnetocrystalline anisotropy.

Magnetic properties of the most common transition metals, such as Co and Fe, have been studied in cluster form repeatedly. Nevertheless, the understanding of microscopic mechanisms is far from being complete. Here we carry out a comprehensive study of geometry [3], electronic structure [4] and magnetism of Co clusters. Geometrical conformation is deduced from the vibrational spectra measured at the intra-cavity free electron laser. Channeling the vibrational energy into the electronic system and measuring the ionization spectra provides the information on the electronic density of states in the vicinity of the Fermi energy [4]. On top of this, magnetic moment is shown to increase drastically when the cluster size is reduced towards the atomic limit, considerably more than the spin contribution alone can provide. Unlike in Tb, these changes are not due to the arrangement of the local atomic moments, but due to the value of the moments themselves. Therefore, strong unquenching of the orbital moments is taking place.

The orbital moments are usually strongly affected by the local atomic surroundings. To verify this, we doped Co clusters with Au and Rh dopants. We used X-Ray Magnetic Circular Dichroism (XMCD) at the BESSY II Synchrotron in Berlin in order to resolve the spin and orbital contributions to the total magnetic moment (see [5] for the details). We show that adding or replacing one atom in a cobalt cluster with just one dopant atom of gold or rhodium can significantly enhance or quench the magnetism, mainly due to the strong orbital moment of the dopant.

[1] J. Bowlan, D.J. Harding, J. Jalink, A. Kirilyuk, G. Meijer, and A. Fielicke, *J. Chem Phys.* **138** (2013) 031102.

[2] S. Ghosh, B. Sanyal, L. Peters, et al., *submitted*.

[3] J. Jalink, J.M. Bakker, D. Kiawi, D. Dieleman, Th. Rasing, and A. Kirilyuk, *submitted*.

[4] J. Jalink, J.M. Bakker, Th. Rasing, and A. Kirilyuk, *submitted*.

[5] S. Peredkov et al, *Phys. Rev. Lett.*, **107**, (2011) 233401.

1OR-B-8

FEMTOSECOND LASER-INDUCED MAGNETISATION DYNAMICS IN LSMO/SRO SUPERLATTICES

Razdolski I.¹, Subkhangulov R.R.¹, Gheorghe D.G.¹, Vrejoiu I.², Bern F.³, Kimel A.V.¹, Kirilyuk A.¹, Ziese M.³, Rasing Th.¹

¹ Institute for Molecules and Materials, Radboud University Nijmegen, The Netherlands

² Max-Planck-Institute of Microstructure Physics, Halle, Germany

³ Division of Superconductivity and Magnetism, University of Leipzig, Germany

i.razdolski@science.ru.nl

Superlattices of strongly correlated manganite oxides were demonstrated to exhibit intriguing electronic and magnetic properties, including antiferromagnetic coupling and confinement of free carriers at the interfaces [1,2]. In this work, magnetisation dynamics of a superlattice of 15 alternating $\text{La}_{0.7}\text{Sr}_{0.3}\text{MnO}_3$ and SrRuO_3 layers of 2.3 and 3.4 nm thickness, respectively, is studied by means of the pump-probe technique in the vicinity of the ferro/paramagnetic transition of SrRuO_3 . Below the transition temperature $T_C = 145$ K, laser-induced ultrafast demagnetisation is found to trigger a uniform precession of magnetisation around its equilibrium. Simulations based on the Landau-Lifshitz equation provided good fits for both amplitude and frequency of the oscillations of magnetisation.

As the initial temperature approaches T_C , the oscillations get suppressed and eventually vanish, as the magnetic properties of the superlattice are now dominated by the $\text{La}_{0.7}\text{Sr}_{0.3}\text{MnO}_3$ layers. New contributions to the magnetisation dynamics arise, with their characteristic times noticeably longer than those observed at lower temperatures. Substantial difference in magnetisation dynamics is shown for the cases of various external magnetic fields, when the ferromagnetically- or antiferromagnetically-coupled superlattice is subjected to the femtosecond laser pulse.

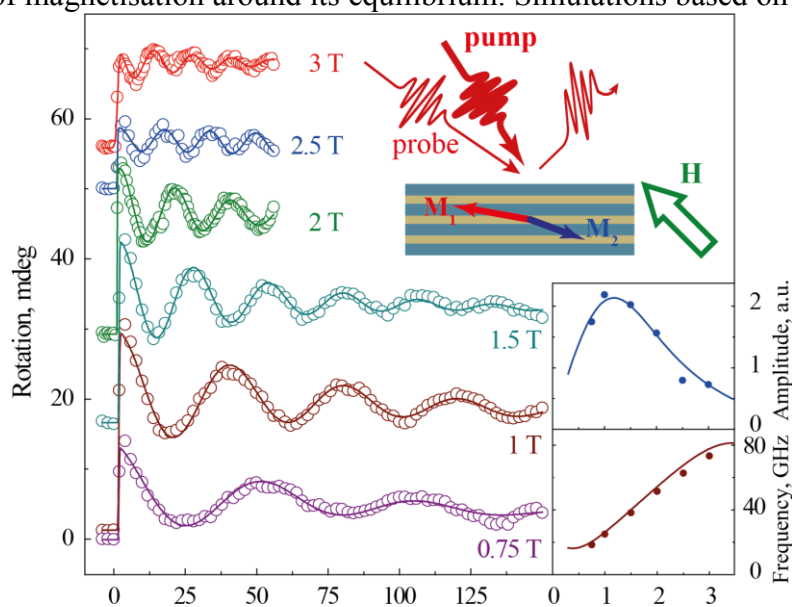


Fig.1. Dynamics of the Kerr rotation at 80 K in various magnetic fields. Insets: (top) experimental setup; (right) amplitude and frequency of the oscillations extracted from the fits (dots) and obtained from the Landau-Lifshitz equation (lines).

Support by EU's 7th Framework Program IFOX (NMP3-LA-2010 246102) and the European Research Council ERC Grant agreement No. 257280 (Femtomagnetism) is acknowledged.

[1] M. Ziese *et al.*, *Nano Lett.* **12** (2012).

[2] H.B. Zhao *et al.*, *Phys. Rev. Lett.* **100** (2008).

1OR-B-9

SKYRMION-LIKE MAGNETIZATION DISTRIBUTIONS IN FILMS WITH PERPENDICULAR ANISOTROPY

Vdovichev S.N.^{1,2}, Gribkov B.A.¹, Demidov E.S.², Ermolaeva O.L.¹, Gusev N.S.¹, Gusev S.A.¹, Skorohodov E.V.¹, Klimov A.Yu.¹, Mironov V.L.^{1,2}, Pestov A.E.¹, Rogov V.V.¹, Fraerman A.A.^{1,2}

¹ Institute for physics of microstructures RAS, Nizhniy Novgorod, Russia

² Lobachevsky State University, Nizhniy Novgorod, Russia

ermolaeva@ipmras.ru

The interest to a skyrmion distribution of magnetization has risen in the last few years. First of all it was caused by possibility of reducing the threshold currents inducing the skyrmion domain walls motion. In particular, the skyrmion lattice motion under the influence of current 10^2 A/cm² at the temperature 20 K was observed in MnSi crystals without inversion center [1]. However one of the substantial problems of further technological progress is the creation of skyrmion distributions at room temperature.

Recently the alternative way to create a skyrmion lattice in a ferromagnetic film with "perpendicular" anisotropy without attracting the Dzyaloshitsky – Moria interaction was proposed in [2]. The authors have demonstrated through micromagnetic simulation that skyrmion can be stabilized in a uniaxial magnetic film by exchange coupling with the vortex magnetic particle placed on the film surface. In our work we investigated experimentally the formation of skyrmion-like states in the system consisting of CoPt multilayer structure and Co nanodisks with vortex magnetization.

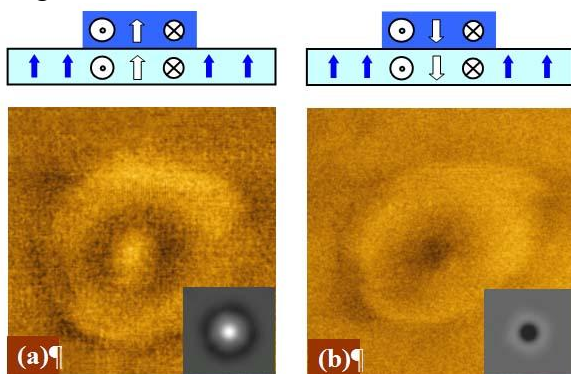


Fig. 1. Schematic drawing and corresponding experimental and model MFM images for vortex-uniform (a) and skyrmion (b) states in CoPt film / Co disk system.

The initial multilayer structures Co(0.5 nm)Pt(1 nm)×5, were fabricated on Si substrate with Ta (10 nm) buffer layer by magnetron sputtering. The additional Co film (20 nm) has been grown on top in one cycle. After that the array of circular disks with a diameter of 200 nm were fabricated from Co film by electron-beam lithography and ion etching techniques. The magnetic states were investigated by magnetic force microscopy. The micromagnetic modeling was performed with standard OOMMF code.

The investigation of ferromagnetic resonance in the CoPt / Co film structure showed the presence of a strong exchange coupling between CoPt multilayer system with the anisotropy of "easy axis" and the Co film with the anisotropy of "easy plane". In particular, it has been shown that the coating with thick Co film leads to a suppression of the perpendicular anisotropy in CoPt so the residual magnetization of CoPt/Co system lies in the plane of the sample. The MFM studies showed that the remanent state of the system CoPt film / Co disk after the magnetizing in strong (> 20 kOe) external field is the combined vortex – uniform state with the density of the topological charge equal to zero (see Fig. 1a). After applying the inverse magnetic field ~ 300 Oe we observed the formation of Skyrmion state (Fig. 1b). The corresponding experimental and model MFM images are presented in Fig. 1a,b. The peculiarities of domain structure in CoPt/Co systems are also discussed.

This work was supported by the Russian Foundation for Basic Research.

[1] N. Nagaosa, Y. Tokura, *Nature nanotechnology*, **8** (2013) 899.

[2] L. Sun, R.X. Cao, B.F. Miao et al., *Phys. Rev. Lett.*, **110** (2013) 167201.

1OR-B-10

MAGNETIC PROPERTIES OF Co-B NANOTUBES PREPARED VIA ELECTROLESS DEPOSITION

Richardson D., Rhen F.M.F.

Department of Physics and Energy, University of Limerick, Limerick, Ireland
Materials and Surface Science Institute (MSSI), University of Limerick, Limerick, Ireland
david.richardson@ul.ie, fernando.rhen@ul.ie

Recently many different methods have been used for the fabrication of a variety of nanostructures including nanowires and nanotubes. In many of these methods the nanotubes or nanowires are deposited onto a pre-existing template usually, a polycarbonate [1] or anodic aluminum oxide (AAO) [2] membrane. Previously electroless deposition has been used to deposit NiFeCo-B nanotubes [1], Co-P nanotubes [2] and Co-P nanowires [3]. The external diameter and length of the deposited nanotubes depend on the size of the membrane pores.

In this study Co-B nanotubes have been prepared via an electroless deposition method on a porous polycarbonate membrane. The pores had an outer diameter of 400 nm and length of 20 μm . The use of dimethylamineborane (DMAB) in the deposition bath resulted in the simultaneous deposition of boron to form a Co-B alloy. By varying the deposition time the thickness of the nanotubes was controlled.

The magnetic properties of the nanotubes were investigated using a vibrating sample magnetometer (VSM) up to a maximum applied field of 1.5 T. Magnetic properties were measured parallel and perpendicular to the nanotube growth. The nanotubes displayed an easy axis associated with measurements made perpendicular to the

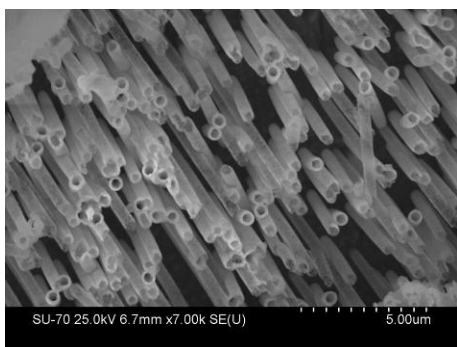


Fig. 2. SEM image of electroless plated Co-B nanotube array

nanotube growth. The perpendicular and parallel coercivities for a sample after 5 minutes of deposition were approximately 24 Oe and 61 Oe respectively as shown in Fig. 1.

X-Ray Diffraction (XRD) was used to determine that the Co-B deposit was an amorphous structure. The nanotubes were imaged using a scanning electron microscope (SEM). A nanotube array is shown in Fig. 2. The width of the nanotube opening and the associated wall thickness were measured using these images. In this study we examine the effects of tube thickness and pore diameter on the associated magnetic properties.

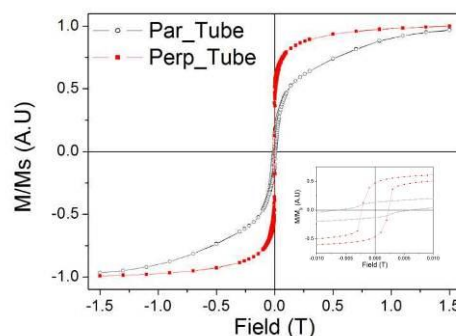


Fig. 1. Hysteresis measurement parallel (open black circles) and perpendicular (closed red squares) to Co-B nanotube arrays after 5 min electroless deposition.

This work is supported in part by the Irish Research Council (RS/2011/270), Science Foundation Ireland (12/IP/1692) and the Irish Research Council New Foundations grant.

- [1] J.F. Rohan, D.P. Casey, B.M. Ahern et al., *Electrochem. Commun.* **10**, (2008) 1419.
- [2] W. Wang, N. Li, X. Li, W. Geng, S. Qiu, *Mater. Res. Bull.* **41**, (2006) 1417.
- [3] X.Y. Yuan, G.S. Wu, T. Xie, Y. Lin, L.D. Zhang, *Nanotechnology.* **15**, (2004) 59.

1 July

Tuesday

11:30-13:00

oral session

1TL-H

1TL-D

1RP-D

1OR-D

“Magnetophotonics”

1TTL-H-1

NON-LOCALITY OF ULTRAFAST SPIN DYNAMICS IN Au/Fe/MgO(001) BI-LAYERS DUE TO SPIN-DEPENDENT HOT CARRIER TRANSPORT

Alekhin A.¹, Bürstel D.², Diesing D.², Wehling T.³, Rungger I.⁴, Stamenova M.⁴, Sanvito S.⁴, Münzenberg M.⁵, Bovensiepen U.⁶, Melnikov A.¹

¹ Fritz-Haber-Institut der MPG, Phys. Chemie, Faradayweg 4-6, 14195 Berlin, Germany

² Universität Duisburg-Essen, Fakultät für Chemie, Universitätsstr. 5, 45117 Essen, Germany

³ Universität Bremen, Theor. Physik, Otto-Hahn-Allee 1 (NW1), 28359 Bremen, Germany

⁴ School of Physics and CRANN, Trinity College Dublin, Dublin 2, Ireland

⁵ Universität Göttingen, I. Phys. Institut, Friedrich-Hund-Platz 1, 37077 Göttingen, Germany

⁶ Universität Duisburg-Essen, Fakultät für Physik, Lotharstraße 1, 47048 Duisburg, Germany
melnikov@fhi-berlin.mpg.de

The ultrafast spin dynamics induced by a transport of spin polarized carriers, is a hot topic, which is motivated by the fundamental interest in magnetic excitations and applications like spintronics and data storage. With this contribution, we make a step towards the understanding of ultrafast spin dynamics in metallic multi-layers, which is (i) spatially non-uniform due to interfaces and strong absorption of the pump pulse and (ii) non-local due to highly mobile hot carriers (HC) that are spin-polarized if excited in a ferromagnet. Combining the time-resolved bulk-sensitive magneto-optical Kerr effect (MOKE) and interface-sensitive magneto-induced second harmonic generation (mSHG) with *ab initio* calculations, we investigate the optically-induced response of Au/Fe/MgO(001) stacks. With 20 fs resolution which approaches characteristic timescales of underlying elementary processes, we show that in epitaxial multi-layers, the ultrafast spin dynamics is initially dominated by the transport of laser-excited spin-polarized HC.

Earlier [1], we have demonstrated spin-polarized HC transport through the Au/Fe/MgO(001): the excitation of Fe layer by femtosecond pulses leads to the injection of HC into Au and their consequent superdiffusive transport towards the Au surface which was probed by mSHG. Here we investigate the process of HC injection probing the Fe side of the stack and focus on the *ballistic* HC transport which dominates the spin dynamics during the first 50 fs. This transport leads to the transfer of magnetization from Fe to Au, which is rather efficient even at moderate pump fluences ($< 10 \text{ mJ/cm}^2$). We estimate thus achieved demagnetization of Fe to 20-30% of the equilibrium magnetization M_{Fe} for the Fe thickness $d_{\text{Fe}}=5 \text{ nm}$ and the transient magnetization of Au behind the Fe/Au interface to $\sim 0.1 M_{\text{Fe}}$. We reveal significant contribution of magnetized Au to the MOKE signal and estimate the magneto-optical constant of Au to be about twice larger than that of Fe. Probing the Au side for $d_{\text{Au}} < 150 \text{ nm}$, we detect a sizable transient MOKE signal attributed to the superdiffusive transport of majority HC across the Au layer, which also gives a signature in mSHG. However, in contrast to mSHG, MOKE lacks the depth resolution and is blind to the ballistic transport of minority HC. Basing on these results, we conclude that the ballistic transport of spin-polarized HC is responsible for initial stage of ultrafast demagnetization and establish a new technique for (i) strong ultrafast demagnetization of ferromagnets, (ii) strong ultrafast magnetization of non-magnetic (host) materials, and (iii) measurement of magneto-optical constants of non-magnetic materials in the presence of strong transient magnetization.

The authors thank A.I. Lichtenstein and P.M. Oppeneer for fruitful discussions. Funding by the DFG (ME 3570/1, Sfb 616) and EU 7-th framework program (CRONOS) is acknowledged.

[1] A. Melnikov, I. Razdolski, T. Wehling, E. Papaioannou, V. Roddatis, P. Fumagalli, O.A. Aktsipetrov, A. Lichtenstein, U. Bovensiepen, *Phys. Rev. Lett.*, **107** (2011) 076601.

1TL-H-2

THEORY OF ULTRAFAST MAGNETIZATION DYNAMICS

Carva K.¹, Battiato M.², Oppeneer P.M.³

¹ Charles University in Prague, DCMP, Prague, Czech Republic

² Institute of Solid State Physics, Vienna University of Technology, Vienna, Austria

³ Uppsala University, Uppsala, Sweden

karel.carva@mff.cuni.cz

Magnetization can be changed by means of a very strong laser light on the femtosecond timescale. This effect has a high application potential but it is also very interesting from the theoretical point of view due to reaching a previously unexplored nonequilibrium states of magnetic materials. We discuss here possible microscopic mechanisms proposed to explain the observed ultrafast demagnetization.

A special attention is paid to the Elliott-Yafet electron-phonon spin-flip (EY-SF) scattering [1]. We have calculated the spin-flip Eliashberg function for three ferromagnetic metals Fe, Co and Ni [2]. We consider both thermalized very hot electron distributions, as well as highly non-equilibrium electron distributions that are expected to be present immediately after the fs laser excitation. Based on this we evaluate the contribution of this process to the demagnetization [3] and discuss the physical relevance of the usually employed approximations.

Another proposed explanation is based on spin dependent electron diffusion [4]. A number of experimental findings support this explanation, including an ultrafast increase of magnetization or THz emission.

Recently an interesting magnetization dynamics has been observed in systems with 2 ferrimagnetically ordered sublattices. A complete reversal of magnetization in GdFeCo alloy can be achieved with a linearly-polarized laser pulse, without the help of external field, circular polarization of the laser pulse or any other direct source of angular momentum – similarly to the ultrafast demagnetization process. We calculate exchange interaction between the components of the compound as well as the intraatomic exchange between Gd 4f and 5d orbitals to allow mapping the problem to an effective orbital-resolved Heisenberg Hamiltonian. A subsequent simulation based on the Landau-Lifschitz-Gilbert equation has reproduced the switching behavior [5].

[1] B. Koopmans et al., *Nature Mater.* **9**, 259 (2010).

[2] K. Carva et al., *Phys. Rev. B* **87**, 184425 (2013).

[3] K. Carva, M. Battiato, P. M. Oppeneer, *Phys. Rev. Lett.*, **107**, 207201 (2011).

[4] M. Battiato, K. Carva, P.M. Oppeneer, *Phys Rev. Lett.* **105**, 027203 (2010).

[5] S. Wienholdt, D. Hinzke, K. Carva, P. M. Oppeneer, and U. Nowak, *Phys. Rev. B* **88**, 020406(R) (2013).

LASER-INDUCED LONGITUDINAL SPIN AND ORBITAL DYNAMICS IN MAGNETIC MATERIALS

Ivanov B.A.^{1,2}, *Butrim V.I.*³, *Yastremskii I.A.*² *Oppeneer P.M.*⁴

¹ Institute of Magnetism NASU, Kiev, Ukraine

² Shevchenko National University of Kiev, Kiev, Ukraine

³ Taurida National Vernadsky University, Simferopol, Crimea, Ukraine

⁴ Department of Physics and Astronomy, Uppsala University, Uppsala, Sweden
bor.a.ivanov@gmail.com

The possibility of the manipulating by the magnetization of magnets using femtosecond laser pulses has attracted significant interest, both fundamental and practical, see for review [1]. Beyond a few hundreds of femtoseconds, the dynamics of the magnetization \mathbf{M} (or sublattice magnetizations \mathbf{M}_α) can be described on the ground of the generalized dynamical equation for the magnetization alone, which include the ultrafast evolution of both direction and the modulus of magnetic moment (magnetization) $M = |\mathbf{M}|$. The description of such an evolution could be done on the ground of the concept of exchange relaxation applied to Landau-Lifshitz equation with the relaxation term proposed by Bar'yakhtar [2]. The modulus of the magnetization is determined by the exchange interaction, and consequently the time of longitudinal spin evolution could be quite fast. For a single-element ferromagnet, the exchange evolution produces non-linear diffusion of the modulus of spin density for non-uniform states, whereas one uniform exchange constant is allowed for two-sublattice ferrimagnet, leading to reversal of the total magnetic moment of ferrimagnets [3] and to transfer of energy to high-amplitude transversal oscillations of antiferromagnetic vector [4]

For the non-uniform evolution of the magnetization, the above mentioned phenomenological approach [2] have no alternative. Non-uniform initial perturbations appear naturally for the superdiffusive description of a laser excitation of magnetic heterostructures [5], leading to effects of spin current flowing between different elements. Within this approach, the non-local character of the recovery of magnetization for Ni-Ru-Fe heterostructures is explained [6]. The evolution of non-uniform profile of the magnetization is going through the creation of a wave front that can significantly increase the relaxation rate of the total magnetization of a microparticle [7]. The observed behavior reminds the classical Kolmogorov, Petrovsky and Piskunov (KPP) result of the formation of some diffusive front moving into the region with transient non-equilibrium magnetization created by the laser pulse. If the exchange relaxation dominates, the picosecond space-time oscillations appear during the evolution that is absent for traditional KPP problem.

For the picosecond longitudinal evolution of magnetization, spin dynamics can be essentially coupled with dynamically-unfrozen orbital degrees of freedom [8].

- [1] A. Kirilyuk, A. V. Kimel, and Th. Rasing, *Rep. Prog. Phys.*, **76** (2013) 026501.
- [2] V.G. Bar'yakhtar, *Zh. Eksp. Teor. Fiz.*, **87** (1984) 1501-1508; *ibid.* **94** (1988) 196-206.
- [3] J.H. Mentink, J. Hellsvik, D.V. Afanasiev, B.A. Ivanov, A. Kirilyuk, A.V. Kimel, O. Eriksson, M.I. Katsnelson, and Th. Rasing, *Phys. Rev. Lett.*, **108** (2012) 057202.
- [4] V.G. Bar'yakhtar, V.I. Butrim, and B.A. Ivanov, *JETP Letters*, **98**, (2013) 289–293.
- [5] M. Battiato, K. Carva, and P. M. Oppeneer, *Phys. Rev. B* **86** (2012) 024404.
- [6] I.A. Yastremskii, P. M. Oppeneer and B.A. Ivanov, *in preparation*.
- [7] I.A. Yastremskii, *Sol. State Phys.*, **56** (2014) accepted to the issue 6.
- [8] V.I. Butrim, *Low Temp. Physics (Kharkov)*, **40** (2014) accepted to the issue 6.

1TL-D-4

MERGING ACOUSTIC AND MAGNETIC EXCITATIONS IN NANOMETER FERROMAGNETIC FILMS

Scherbakov A.V.

Ioffe Physical-Technical Institute of the Russian Academy of Science, St. Petersburg, Russia
scherbakov@mail.ioffe.ru

The talk reports the magneto-acoustics studies, in which we utilize high-frequency acoustic excitations to manipulate magnetization of ferromagnetic thin films at gigahertz frequencies [1-4]. In our experiments, the dynamic strain modifies the magneto-crystalline anisotropy and launches the coherent magnetization precession. This recently developed technique was successfully used in experiments with ferromagnetic semiconductors [1-3] and metals [4,5]. In our recent experiments, we extend the ability of high-frequency magneto-acoustics by exploiting the peculiar acoustic properties of the studied ferromagnetic structures. We demonstrate resonance effects, which originate from the frequency and spatial matching of the Eigen magnon and acoustic modes of an excited ferromagnetic film.

The structures studied are films of ferromagnetic (Ga,Mn)As or Gallenol (an alloy of Fe and Ga) of $20 \div 200$ nm thickness grown on GaAs substrates. We study structures with a single ferromagnetic film as well as complex magneto-acoustic structures, in which a ferromagnetic layer is grown on the top of an acoustic Bragg mirror and plays a role of an acoustic nanocavity with resonance acoustic mode at tens GHz. At experiment, we realize acoustic excitation of a ferromagnetic film by injecting the optically generated picosecond acoustic pulse with broad spectrum from substrate. As an alternative approach, we use the direct optical excitation of a ferromagnetic layer in order to excite simultaneously the coherent magnetization precession and resonance acoustic modes. In both cases the pump optical pulse is provided by an amplified Ti:Sapphire laser (800 nm, 150 fs, 5 μ J per pulse and 100 kHz repetition rate). By monitoring the transient magneto-optical Kerr rotation of the probe pulse split from the same laser source, we detect the magnetization kinetics with femtosecond time resolution.

The typical response of magnetization on the pulse excitation (acoustic or optical) is coherent magnetization precession at the ferromagnetic resonance frequency. In this talk, we discuss how the properties of a ferromagnetic film (thickness, magnetic anisotropy, magneto-elastic coefficients), the parameters of acoustic excitation (e.g. its polarization) as well as strength and direction of external magnetic field determine amplitude and spectral content of the coherent magnetization response. The main part of the talk, however, focuses on the effects reflecting merging of acoustic and magnetic excitations inside a ferromagnetic structure. We demonstrate that the boundary conditions, which strictly determine the spatial distribution of the magnon and acoustic modes in a ferromagnetic layer, may result in selective excitation of a single standing spin wave among the broad magnon spectra [2]. In ferromagnetic acoustic nanocavity the magneto-acoustic coupling results in long-living magnetization precession unachievable in a single ferromagnetic film. A theoretical modelling supports the obtained experimental results.

The work is supported by the Government of Russia (14.B25.31.0025) and DFG (BA1549/14-1).

- [1] A.V. Scherbakov et al., *Phys. Rev. Lett.*, **105** (2010) 117204.
- [2] M. Bombeck et al., *Phys. Rev. B*, **85** (2012) 195324.
- [3] M. Bombeck et al., *Phys. Rev. B*, **87** (2013) 060302(R).
- [4] J. Jäger et al., *Appl. Phys. Lett.*, **103** (2013) 032409.
- [5] J.W. Kim, M. Vomir, and J.-Y. Bigot, *Phys. Rev. Lett.*, **109** (2012) 166601.

1TL-D-5

**OPTICAL CONTROL OF THE SUPER_EXCHANGE INTERACTION ON A
SUB-PICOSECOND TIMESCALE**

*Mikhaylovskiy R.V.¹, Hendry E.², Secchi A.², Mentink J.H.³, Eckstein M.³, Pisarev R.V.⁵,
Kruglyak V.V.², Katsnelson M.I.², Rasing Th.², Kimel A.V.¹*

¹ Radboud University, Nijmegen, Netherlands

² University of Exeter, Exeter, United Kingdom

³ University of Hamburg, Hamburg, Germany

⁴ Ioffe Physical-Technical Institute, St. Petersburg, Russia

R.Mikhaylovskiy@science.ru.nl

Magnetically ordered materials are the macroscopic manifestation of one of the strongest quantum effects – the exchange interaction - the strength of which can reach 10^3 Tesla. The symmetric part of the exchange is responsible for the very existence of magnetic order. The antisymmetric part, called Dzyaloshinskii-Moriya interaction, gives rise to canted antiferromagnetism - , magneto-electricity - , chiral magnetic structures and skyrmions. Here we demonstrate both experimentally and theoretically that the ratio between the antisymmetric and symmetric exchange components can be manipulated via ultrafast, sub-picosecond laser excitation of iron oxides which represent a very broad class of magnetic insulators. The resulting coherent spin oscillations lead to THz emission and from its strength we estimate that a sub-picosecond laser pulse with a moderate fluence of ~ 1 mJ/cm² acts as a pulsed magnetic field of 0.01 Tesla that corresponds to the change of the exchange energy of over 10 nJ. To support these findings we have developed a low-energy theory for the magnetic interactions between non-equilibrium electrons subjected to an external time-dependent electric field which reveals the possibility to modify the exchange interactions by light over 1 %.

1TL-D-6

NON-EQUILIBRIUM MAGNETIC INTERACTIONS IN STRONGLY CORRELATED SYSTEMS: A GREEN'S FUNCTION APPROACH

*Secchi A.*¹, *Brener S.*¹, *Lichtenstein A.I.*², *Katsnelson M.I.*¹

¹ Institute for Molecules and Materials, Radboud University, Nijmegen, The Netherlands

² Institut für Theoretische Physik, Universität Hamburg, Hamburg, Germany
a.secchi@science.ru.nl

Manipulating the magnetic order of materials via electromagnetic fields on increasingly fast time scales is one of the most intriguing and challenging issues of modern magnetism [1], being both a stimulus for the investigation of fundamental problems related to light-matter interactions in strongly correlated systems and a source of possible applications in the realization of ultrarapid memories. In this respect, optical pulses with characteristic durations of 60/70 fs can induce magnetization dynamics on sub-picosecond time scales [2, 3, 1], allowing us to enter the era of *ultrafast* magnetism.

The formulation of a realistic theory of ultrafast magnetism is a challenging problem. In equilibrium, magnetic interactions in magnetic metals and semiconductors are non-Heisenberg [4, 5], i.e., the lengths of magnetic moments and values of exchange parameters depend on the magnetic configuration for which they are computed, which calls for an accurate *ab initio* formulation even to compute equilibrium properties. The expressions for the parameters accounting for exchange interaction were given [6, 7] in terms of equilibrium electronic Green's functions of the Hubbard model, and they can be used within a classical Heisenberg model to simulate spin dynamics. However, this treatment is not expected to be appropriate for ultrafast dynamics [1], since the time scale of the laser excitation is faster than the precession time of a spin in the field of equilibrium exchange interactions in typical magnetic materials (10÷100 fs). Exchange parameters are thus time-dependent. We have derived their expressions in a general non-equilibrium framework, including an arbitrary external time-dependent optical field [8]. The resulting formulas are valid for any time scale, being thus applicable to ultrafast spin dynamics.

In my talk I will present our theory [8] as well as some of our theoretical and experimental results related to the optical manipulation of the superexchange interaction in iron oxides on a sub-picosecond timescale [9].

Support from EU Seventh Framework Program grant agreement No. 281043 (FEMTOSPIN) is acknowledged.

- [1] A. Kirilyuk, A. V. Kimel, and Th. Rasing, *Rev. Mod. Phys.*, **82** (2010) 2731-2784.
- [2] E. Beaupaire, J.-C. Merle, A. Daunois, and J.-Y. Bigot, *Phys. Rev. Lett.*, **76** (1996) 4250.
- [3] B. Koopmans, M. van Kampen, J. T. Kohlhepp, and W. J. M. de Jonge, *Phys. Rev. Lett.*, **85** (2000) 844.
- [4] E. L. Nagaev, *Physics of Magnetic Semiconductors* (Mir Publishers, Moscow, 1983).
- [5] M. I. Auslender, M. I. Katsnelson, *Solid State Comm.*, **44** (1982) 387-389.
- [6] A. I. Lichtenstein, M. I. Katsnelson, V. P. Antropov, V. A. Gubanov, *J. Magn. Magn. Mater.*, **67** (1987) 65-74.
- [7] M. I. Katsnelson, A. I. Lichtenstein, *Phys. Rev. B*, **61** (2000) 8906-8912.
- [8] A. Secchi, S. Brener, A. I. Lichtenstein, M. I. Katsnelson, *Ann. Phys.*, **333** (2013) 221-271.
- [9] R. Mikhaylovskiy, E. Hendry, A. Secchi, J. Mentink, M. Eckstein, A. Wu, R. V. Pisarev, V. V. Kruglyak, M. I. Katsnelson, Th. Rasing, and A. V. Kimel, submitted (2014).

1RP-D-7

ULTRAFAST PHOTOMAGNETIC EFFECT IN GARNETS*Stupakiewicz A., Maziewski A.*Laboratory of Magnetism, Faculty of Physics, University of Bialystok, Bialystok, Poland
and@uwb.edu.pl

The functionality of ferrimagnetic garnets has been shown to be very broad, with examples such as the excitation of surface plasmons, the propagation of nonlinear spin-waves, photomagnetism, the observation of the inverse Faraday effect induced by an ultrafast laser pulse and many others. In such material the magnetic state depends on the polarization of the induced light that defines are observed effect as not-thermal light interaction.

We observed in Co-substitute garnet films of the large-angle magnetization precession [1] with an amplitude, phase, and frequency determined by the characteristics of femtosecond laser pulses. The physical nature of this effect is related to light-induced charge redistribution between Co^{2+} and Co^{3+} ions in the ferrimagnetic garnet lattice, which are responsible for the magnetic anisotropy.

Ultrafast magnetization dynamics studies were performed on thin garnet films with and without ultrathin Co cover layer using time-resolved magneto-optical tools. These studies show the possibility of non-thermally exciting the magnetization using femtosecond laser pulses by the ultrafast photomagnetic effect in a bare garnet film. The mechanism that triggers the precession is a photo-induced change of the magnetic anisotropy in a garnet film. Optical excitation of a bare garnet leads to magnetization precession, with phase strongly dependent on the polarization of the pump light. Ultrathin Co layer deposited on top of the garnet film leads to substantial changes of the laser-induced dynamics. The modulation of the spin precession in a Co/garnet bilayer by femtosecond laser excitation has been observed [2]. The light triggers polarization independent precession in both the Co and garnet layers via the magnetostatic coupling between these layers, at two distinct frequencies typical for an ultrathin Co layer and a garnet film, respectively [3]. The results reveal the existence of ultrafast correlations between the spins of the magnetic layers.

Support by the National Science Centre Poland for project DEC-2013/09/B/ST3/02669 and SYMPHONY project operated within the Foundation for Polish Science Team Programme co-financed by the EU European Regional Development Fund, OPIE2007–2013.

[1] F. Atoneche et al, *Phys. Rev. B*, **81** (2010) 214440.

[2] A. Stupakiewicz et al, *Appl. Phys. Lett.*, **101** (2012) 262406.

[3] M. Pashkevich et al, *Europhys. Lett.*, **105** (2014) 27006.

1TL-D-8

THERMALLY ASSISTED MAGNETIC RECORDING APPLYING SURFACE PLASMON

Nakagawa K., Ashizawa Y.
Nihon University, Chiba, Japan
nakagawa.katsuji@nihon-u.ac.jp

Super high-density magnetic recording (Hard Disk Drive: HDD) beyond 10 Tbits per square inch is highly demanded. One of the promising technologies for the future HDD is Thermally Assisted Magnetic Recording (TAMR) [1] applying surface plasmon to the magnetic recording head combined with high stable magnetic recording disks.

Localized surface plasmon in a gold antenna, as shown in Fig. 1 for example, effectively enables light spot to be confined into less than 10 nm in diameter. Such a nm-size light spot can assist recording in the high-stable and high-density memory disk. The estimated light spot size was calculated by the Finite-Difference Time-Domain (FDTD) method.

The magnetic head embedded with laser light, however, is not easily fabricated, because the confined light spot must be located close to a magnetic pole in the head, as schematically shown in Fig. 2. The efficiency of the optical transfer energy from light source to the confined light spot is around 4%, when the surface plasmon antenna shown in Fig. 1 is directly exposed by laser light. The higher optical efficiency is extremely demanded, because the energy loss must compel the sharp temperature rise of the head.

It is found that the waveguide applying the surface plasmon polaritons (SPPs), let's say plasmonic waveguide [2], can effectively increase the optical efficiency. First, the SPPs energy and propagation ratio are calculated by the FDTD for the gold thin film located on the surface of a planer dielectric films. After choosing the optimal condition for high optical efficiency, the surface plasmon antenna, shown in Fig. 1, is placed at the end of the plasmonic waveguide. This plasmonic waveguide structure with a plasmon antenna shows the high optical efficiency up to 20%. The proposed system contributes less energy consumption and less temperature rise to the head.

This work was partially supported by a Grant-in-Aid for Scientific Research (C), No. 23560413, a Grant by Nihon University Strategic Projects for Academic Research, a MEXT-Supported Program for the Strategic Research Foundation at Private Universities, 2013-2017, and a Grant by the Storage Research Consortium.

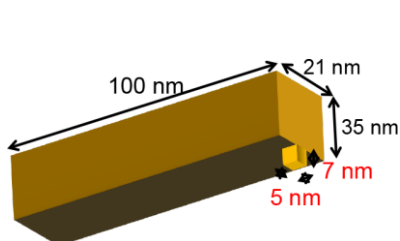


Fig. 1. One of designed surface plasmon antenna.

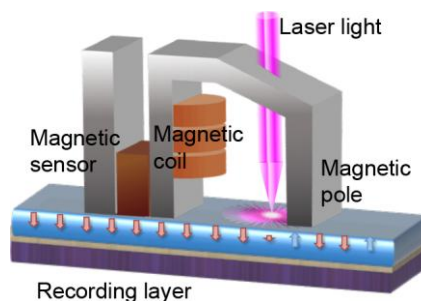


Fig. 2. Schematic diagram of magnetic recording head with laser light.

[1] M. H. Kryder, E. C. Gage, T. W. McDaniel, W. A. Challener, R. E. Rottmayer, G. Ju, Y.-T. Hsia, M. F. Erden: *Proc. of the IEEE*, **96** (2008) 1810.

[2] Y. Ashizawa, T. Ota, K. Tamura, K. Nakagawa: *J. Magn. Soc. Jpn.*, **37** (2013) 111 .

1OR-D-9

MODE-CROSSING IN CoFeB ANTIDOT LATTICE

Mansurova M.¹, Behrenz S.¹, Muenzenberg M.²

¹ I. Physics Institute, Georg-August University, Goettingen, Germany

² Institute for Physics, Ernst-Moritz-Arndt University, Greifswald, Germany
mmansur@gwdg.de

Magnonic crystals are a novel kind of material where spin-wave properties can be tuned by the antidot lattice constant, beside the film thickness. In this work we investigate spin wave modes in a 82.5nm-thick CoFeB, where an antidot lattice (magnonic crystal) was produced using Focused Ion Beam (FIB) technique. The lattice consists of a rectangular array of 1 μ m diameter antidots with 3.5 μ m lattice constant.

The thickness of the film determines the frequency of perpendicular standing spin wave (PSSW) mode in CoFeB. On the other hand, the frequency of Damon-Eshbach (DE) mode in CoFeB is determined by magnonic crystal's lattice constant [1]. As its name indicates PSSW is a spin wave mode between the two surfaces of the thin film, while the amplitude of DE surface mode decays exponentially into the film's thickness. This way, it is interesting to tune film's parameters in such a way that both PSSW and DE modes have the same frequency for some values of external magnetic field. Parameters used in this work allow this to happen at 100 mT.

Spin-wave modes have been excited and observed optically by a double-modulated pump-probe technique using a pulsed (40 fs) 800nm laser. Magnetization oscillations are detected using time resolved magneto-optical effect (TRMOKE) and the fundamental frequencies are determined performing fast Fourier transform of the signal.

We have successfully observed magnetization oscillation frequencies that match PSSW and DE modes varying external magnetic field 0-130 mT and as expected, both modes have the same frequency at approximately 100 mT, as shown in Fig.1. The PSSW mode is not observed after crossing and only DE mode mode remains at fields higher than 100 mT. Moreover, DE mode amplitude increases as compared to Kittel mode Fourier-amplitude (not shown).

Support by DFG MU 1780/ 6-1 Photo-Magnonics project is acknowledged.

[1] B. Lenk, N. Abeling, J. Panke, M. Muenzenberg, *J. Appl. Phys.* **112**, (2012) 083921.

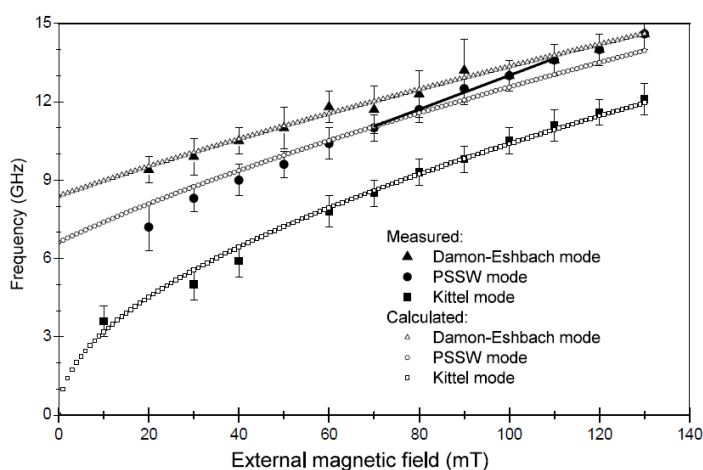


Fig.1 Measured and calculated frequencies of magnetization oscillation modes.

1 July

Tuesday

11:30-13:00

oral session

1TL-O

1RP-O

“Multiferroics”

1TL-O-1

HIGH FIELD STUDIES ON BiFeO₃ SINGLE CRYSTALS GROWN BY THE LASER-DIODE HEATING FLOATING ZONE METHOD

Tokunaga M.¹, Akaki M.¹, Miyake A.¹, Ito T.², Kuwahara H.³

¹ ISSP, The University of Tokyo, Kashiwa, Japan

² AIST, Tsukuba, Japan

³ Sophia University, Tokyo, Japan

tokunaga@issp.u-tokyo.ac.jp

BiFeO₃ has attracted considerable attention owing to the unique multiferroic nature beyond room temperature. The crystal has a hexagonal structure, in which ions in the perovskite-type structure shift and rotate along and/or around the $\langle 111 \rangle$ direction of the pseudo-cubic lattice. Since there are four, or eight including its orientation, equivalent $\langle 111 \rangle$ directions, the actual crystals usually contain multiple crystallographic domains having the different c -axis directions of the hexagonal lattice. This multi-domain nature has hindered the accurate determination of the basic physical properties of this material. Recent development of the growth of mono-domain crystals stimulated in-depth studies on BiFeO₃. In the previous study, we studied high-field magnetic and dielectric properties in mono-domain crystals of BiFeO₃ synthesized by the flux method [1]. Although the results revealed significant changes in magnetization and electric polarization at the field-induced magnetic transition, we could not proceed with further argument because the fragile dendritic crystals restricted the possible experimental configurations.

In this study, we measured magnetization and electric polarization in mono-domain crystals grown by the laser-diode heating floating zone method [2] in pulsed high magnetic fields up to 55 T. Since the crystals grown by this method are large and robust, we can study magnetization with higher accuracy and electric polarization in various directions. In magnetic fields parallel to the c -axis of the hexagonal lattice c_h , magnetization curves at 4.2 K shows steep increase at around 25 T, which corresponds to the magnetic transition from the cycloidal to the canted-antiferromagnetic phase (Fig. 1). Application of in-plane field causes transition at lower field. The magnetization curves are almost identical for $H \parallel a_h$ and $H \parallel b_h^*$ (normal to both a_h and c_h). Electric polarization also shows anomaly at the transition field (Fig. 2). In addition to these steep changes, we clearly observed linear and/or quadratic ME effects above the transition field. Comprehensive results at various temperatures and configurations will be presented.

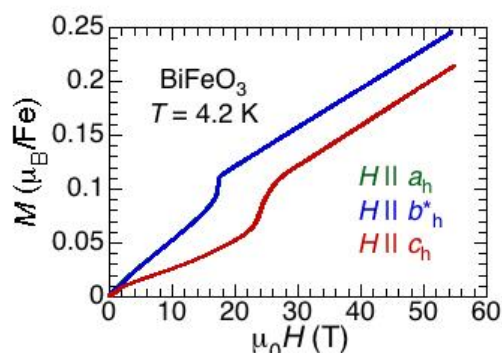


Fig. 1. High field magnetization curves at 4.2 K for $H \parallel a_h$, b_h^* , and c_h directions.

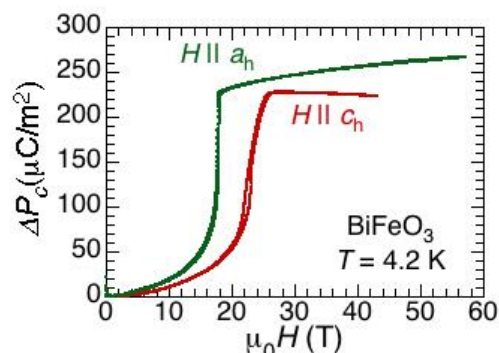


Fig. 2. Field-induced change in electric polarization along the c_h -axis in the fields along the a_h - and c_h -axes.

- [1] M. Tokunaga, M. Azuma, and Y. Shimakawa, *J. Phys. Soc. Jpn.* **76** (2010) 064713/1-5.
 [2] T. Ito *et al.*, *Cryst. Growth Des.* **11** (2011) 5139-5143.

1TL-O-2

SPECTRAL SIGNATURES OF SPIN-PHONON AND ELECTRON-PHONON INTERACTIONS IN MULTIFERROIC IRON BORATES

Popova M.N.

Institute of Spectroscopy, Russian Academy of Sciences, Moscow, Troitsk, Russia
popova@isan.troitsk.ru

This talk summarizes recent results of my group. A part of them can be found in the arXive [1].

The $R\text{Fe}_3(\text{BO}_3)_4$ compounds possess a huntite-type noncentrosymmetric trigonal structure that consists of helical chains of edge-sharing FeO_6 octahedra running along the c -axis of the crystal, interconnected by two kinds of BO_3 triangles and RO_6 distorted prisms. In the case of $R = \text{Pr}$, Nd , and Sm , the structure is described by the SG $R32$ at all the temperatures. The rest compounds of the family undergo a structural phase transition $R32 - P3_121$. All the iron borates antiferromagnetically order at $T_N \sim 30 - 40$ K, they demonstrate pronounced magnetoelectric, magnetodielectric, magnetoelastic phenomena and belong to a new class of multiferroics.

We have studied far infrared polarized transmission and reflection spectra of the Pr , Nd , Sm , and Eu iron borates in the spectral range $20 - 300 \text{ cm}^{-1}$ ($0.6 - 9 \text{ THz}$), at temperatures between 4 and 300 K. Peculiarities at T_N in the phonon frequency vs temperature curves were observed for all the compounds studied thus pointing to the spin – phonon interaction in them. Mechanisms of this interaction are discussed. Manifestations of an interaction between lattice phonons and crystal-field (CF) excitations of RE ions were observed in Nd and Pr iron borates. In $\text{NdFe}_3(\text{BO}_3)_4$, the electron-phonon coupling mediates an interaction between lattice modes via a CF level of Nd^{3+} . In $\text{PrFe}_3(\text{BO}_3)_4$, a coupled electron-phonon mode is formed at lowering the temperature, due to the interaction between the lowest-frequency A_2 phonon (near 50 cm^{-1}) and the $\Gamma_2 - \Gamma_1$ electronic excitation with nearly the same energy. A splitting of the reststrahlen band and a redistribution of intensities between a quasi-phonon mode and a quasi-electronic one were observed in the FIR spectra [1]. Magnetic ordering leads to dramatic spectral changes in the region of the coupled electron-phonon excitations. Frequencies of the latter were modeled by solving the following equation:

$$\omega^2 - \omega_0^2 + \frac{2\omega_0\omega_{12}(n_1 - n_2)|W|^2}{\omega^2 - \omega_{12}^2} = 0$$

Here ω_0 and ω_{12} are the frequencies (in cm^{-1}) of the vibrational and electronic excitations, respectively, in the absence of interaction; n_1 and n_2 are relative populations of the excited $|\Gamma_1\rangle$ and ground $|\Gamma_2\rangle$ CF states of Pr^{3+} , respectively; W is the interaction constant between the electronic excitation ω_{12} and the Γ -point A_2^1 optical phonon. Fitting of the TO frequency vs temperature experimental plots by theoretical curves revealed a rather large value of 14.8 cm^{-1} for the electron-phonon coupling constant, which points to an essential role played by the electron-phonon interaction in physics of multiferroics.

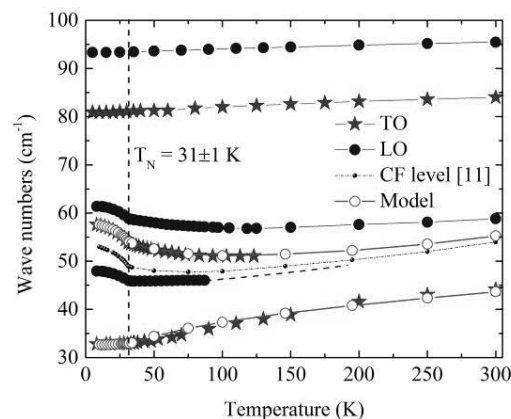


Fig. 1. Experimental and calculated temperature dependences of the coupled electron-phonon mode frequencies in $\text{PrFe}_3(\text{BO}_3)_4$.

[1] K. N. Boldyrev, T. N. Stanislavchuk, A. A. Sirenko, L. N. Bezmaternykh, M. N. Popova. *arXiv:1402.0434* [cond-mat.mtrl-sci].

1RP-O-3

GIANT OPTICAL ACTIVITY NEAR ELECTROMAGNONS IN MULTIFERROIC FERROBORITES: $\text{SmFe}_3(\text{BO}_3)_4$

*Mukhin A.A.¹, Kuzmenko A.M.¹, Ivanov V.Yu.¹, Shuvaev A.², Dziom V.², Pimenov A.²,
Bezmaternykh L.N.³, Gudim I.A.³*

¹ A.M. Prokhorov General Physics Institute of RAS, 119991 Moscow, Russia

² Institute of Solid State Physics, Vienna University of Technology, A-1040 Vienna, Austria

³ Institute of Physics SB RAS, 660036 Krasnoyarsk, Russia

mukhin@ran.gpi.ru

Rare-earth ferrobates $\text{RFe}_3(\text{BO}_3)_4$ have attracted recently a considerable attention due to observation of magnetoelectric effects as well as other interesting properties (magnetic, optical ..) which strongly depend on type of the rare-earth (R) ions and their interaction with antiferromagnetically ordered Fe-subsystem ($T_N = 30\text{-}40$ K). Various crystal-field transitions in R-ions and collective magnetic excitations in Fe-subsystem should be responsible for the static magnetic and magnetoelectric properties of the ferrobates. A symmetry of the ferrobates (space group R32) allows not only magnetically active excitations (see, for example, [1]) but also electrically active ones (electromagnons), which, however, were not observed so far.

In the present work we have observed such electromagnon in $\text{SmFe}_3(\text{BO}_3)_4$ ferrobate having easy-plane magnetic structure below $T_N=34$ K. Transmission spectra of the single crystalline $\text{SmFe}_3(\text{BO}_3)_4$ plates were measured in the frequency range 40-200 GHz by means of quasioptical backward-wave-oscillator technique in the magnetic fields up 7 T. The low frequency mode was observed below T_N with a linear dependence of the resonance frequency on magnetic field $H \perp c$ and specific polarization conditions indicating on the electric and magnetic activity of the mode. In particular, the mode can be excited either by an ac electric field with $e \perp P$ or by an ac magnetic field $h \perp M \parallel H$, where P is the static electric polarization and M is a magnetization induced by the external magnetic field H . We have identified this mode as the electromagnon originating from the in-plane antiferromagnetic resonance mode of the Fe-subsystem coupled with Sm ions. The extracted dielectric contribution of the electromagnon ($\Delta\epsilon \sim 30$) is in a good agreement with corresponding static permittivity and determines the origin of the giant magnetodielectric effect in $\text{SmFe}_3(\text{BO}_3)_4$ [2]. The significant dielectric contribution implies also large dynamic magnetoelectric susceptibility which can result in additional electrodynamic effects, in particular, optical activity near the electromagnon. To search for these phenomena we have measured the polarization state of the transmitted radiation for the analyzer rotated by the angle $0, \pm 45^\circ$ and 90° with respect to polarizer which have revealed a noticeable rotation of the polarization plane. The spectra of the angle of the polarization as well as the ellipticity have been extracted by processing of the transmission spectra. A remarkable result of these measurements is that a polarization rotation angle exceeds 120° for a sample thickness of 1.7 mm only. We note that this rotation arises purely from dynamic magnetoelectric susceptibility which is intrinsic for electromagnons in $\text{SmFe}_3(\text{BO}_3)_4$. Detail theoretical analysis and simulation of the observed dynamic phenomena have been performed and corresponding parameters of magnetic and magnetoelectric interaction have been extracted.

The work is partially supported by RFBR (12-02-01261).

[1] A.M. Kuz'menko, A.A. Mukhin, V. Yu. Ivanov, et al., *JETP Lett*, **94** (2011) 294.

[2] A.A. Mukhin, G.P. Vorob'ev, V.Yu. Ivanov, et al., *JETP Lett*, **93** (2011) 275.

1RP-O-4

LONGITUDINAL MAGNETOTELECTRIC EFFECT IN THE HIGH TEMPERATURE $\text{Ba}_{0.52}\text{Sr}_{2.48}\text{Co}_2\text{Fe}_{24}\text{O}_{41}$ HEXAFERRITE

Popov Yu.F.¹, Vorob'ev G.P.¹, Ivanov V.Yu.², Zverev V.I.¹, Mukhin A.A.², Pyatakov A.P.^{1,2}, Zvezdin A.K.², Shin Kwang Woo³, Kim Kee Hoon³

¹ Faculty of Physics, M.V. Lomonosov Moscow State University, 119992 Moscow, Russia

² Prokhorov General Physics Institute of the Russian Acad. Sci., 119991, Moscow, Russia

³ CeNSCMR Dept., of Phys. and Astron., Seoul National University, Seoul 151-747, South Korea

The last decade has witnessed a significant growth of research into materials with coupled magnetic and electric properties. [1] At the moment special attention is given to potentially practical materials that display magnetoelectric properties at room temperature which can be employed in information and energy saving technologies applications. After the recent discovery of the room-temperature effect in polycrystalline $\text{Sr}_3\text{Co}_2\text{Fe}_{24}\text{O}_{41}$ [2] hexaferrite ferroelectrics attract the increased attention of researchers.

In this work we present the results of magnetoelectric effect (ME) study of single crystalline $\text{Ba}_{0.52}\text{Sr}_{0.48}\text{Co}_2\text{Fe}_{24}\text{O}_{41}$ hexaferrite in pulsed/steady magnetic fields H up to 60 kOe. The electric polarization P was measured perpendicular to the c -axis versus H oriented also in the basis plane for two geometries: $P \perp H$ and $P \parallel H$. In addition to the already observed 'transverse' ($P \perp H$) ME [3] here we first report the 'longitudinal' ($P \parallel H$) ME [see Fig. 1]). We note the opposite sign of the field-induced polarization in both geometries which was confirmed by the measurements in the steady rotating magnetic field. Although the 'transverse' ME can be related to the spin cycloid structure formation [4] the existence of 'longitudinal' ME is not straightforward in the frames of this model. Both effects depend on the poling (annealing in magnetic and electric fields) and the prehistory.

This work was partially supported by RFBR (project 13-02-01093).

[1] A.P. Pyatakov, A.K. Zvezdin, *Phys. Usp.* **55**, 6 (2012).

[2] Y. Kitagawa, et al, *Nature Mater.* **9**, 797 (2010).

[3] Sae Hwan Chun, et al, *Phys. Rev. Lett.* **108**, 177201 (2012).

[4] M. Mostovoy, *Phys. Rev. Lett.* **96**, 067601 (2006).

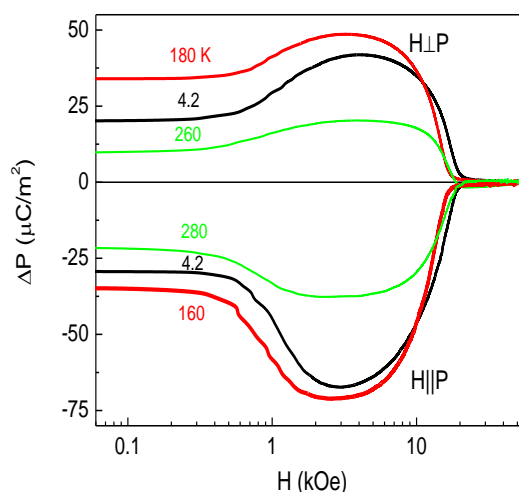


Fig. 1. Transverse ($P \perp H$) and longitudinal ($P \parallel H$) electric polarization of $\text{Ba}_{0.52}\text{Sr}_{0.48}\text{Co}_2\text{Fe}_{24}\text{O}_{41}$ at different T after ME poling with $E=300$ kV/m and $H=6$ T.

1 July

Tuesday

11:30-13:00

oral session

1TL-Q

1RP-Q

1OR-Q

**“Low Dimensional
Magnetism”**

1TL-Q-1

AB-INITIO STUDY OF LOW-DIMENSIONAL QUANTUM SPIN SYSTEMS*Saha-Dasgupta T.*

S.N.Bose National Centre for Basic Sciences, India

Low-dimensional quantum spin systems, characterized by their unconventional magnetic properties, have attracted much attention in recent years. Interest in quantum spin systems has been driven by the importance for understanding the mechanism of high-T_c superconductivity as well as for their potential applications in quantum computers. Synthesis of materials appropriate to various classes within these systems has made this field very attractive and a site of many activities. The experimental results like susceptibility data are fitted with the theoretical models to derive the underlying spin Hamiltonian. However, often such a fitting procedure which requires solution of the assumed spin Hamiltonian leads to ambiguity in deciding the representative model. V₂P₂O₇ forms a classic example in this regard which turned out to be an alternating chain compound while it was originally considered to be an example of ladder compound. Therefore, microscopic understanding is required for the sake of uniqueness. We have applied the NMTO-Wannier function technique to identify the underlying spin model, often coupled with the Quantum Monte Carlo technique for the investigation of magnetic properties in number of these compounds. In the present talk, we will focus on Zn₂VO(PO₄)₂, which is found to show [1] spin-gapped behaviour upon substitution. We will also touch upon metalorganic Fe-Nb compound which is found to be a spin cross-over compound [2].

[1] S.Kanungo, S.Kar, T. Saha-Dasgupta, *Phys. Rev. B* **87** (2013), 054431.

[2] K. Tarafder, S. Kanungo, P. M. Oppeneer, T. Saha-Dasgupta, *Phys. Rev. Lett.* **109** (2012), 077203.

1RP-Q-2

STRONGLY CORRELATED SYSTEMS ON FRUSTRATED LATTICES: THE FLAT-BAND SCENARIO AND BEYOND

Richter J.

Institut für Theoretische Physik, Universität Magdeburg, Germany
Johannes.Richter@Physik.Uni-Magdeburg.DE

Frustration in magnetic and electronic systems may lead to dispersionless (flat) one-particle bands which have a strong influence on the many-body physics of strongly correlated quantum systems. Thus, flat-band systems are receiving a great deal of attention right now, in particular with view of realizing new many-body phases there. In my talk I will give an overview on the low-temperature physics of flat-band Heisenberg spin systems and Hubbard electrons.

Interestingly for a large variety of such strongly correlated quantum systems a class of exact many-body eigenstates can be constructed [1,2]. Examples are the 1D sawtooth and kagome chains, the 2D kagome and checkerboard lattices, and the 3D pyrochlore lattice. The exact many-particle eigenstates consist of independent magnons (electrons) localized on finite areas of the lattice and become ground states for certain values of total magnetization (electron concentrations).

The correlated quantum systems having localized eigenstates exhibit a highly degenerate ground-state manifold at the saturation field H_{sat} (at a characteristic value of the chemical potential μ_0 for magnons (electrons)). The degeneracy grows exponentially with the system size and leads to a finite residual entropy. By mapping the localized magnon (electron) degrees of freedom onto a classical hard-core lattice gas one may find explicit analytical expressions for the low-temperature thermodynamics in the vicinity of H_{sat} (μ_0). Though the scenario of localized eigenstates is similar for spin and electron systems, the different statistics of spins and electrons leads to different construction rules for the localized eigenstates and, as a result, to different hard-core lattice gas descriptions.

For electrons the scenario of localized eigenstates is related to the so-called flat-band ferromagnetism [2]. For spin systems the localized many-body states lead to some spectacular features in strong magnetic fields, such as zero-temperature magnetization plateaus and jumps, magnetic-field driven spin-Peierls lattice instabilities, an extra peak in the specific heat at low temperatures as well as to an enhanced magnetocaloric effect [3].

In real systems typically the ideal flat-band geometry is distorted and the above illustrated features are modified. However, for small distortions the basic low-temperature features are still present which is relevant for the experimental access to the physical properties related to the flat band [4].

- [1] J. Schulenburg et al, *Phys. Rev. Lett.* **88**, 167207 (2002).
- [2] A. Mielke, *J. Phys. A* **24**, L73 (1991), O. Derzhko et al., *Phys. Rev. B* **76**, 220402(R) (2007); *ibid.* **81**, 014421 (2010); M. Maksymenko et al., *Phys. Rev. Lett.* **109**, 096404 (2012).
- [3] M.E.Zhitomirsky and H.Tsunetsugu, *Phys. Rev. B* **70**, 100403(R) (2004); O. Derzhko and J.Richter, *Phys. Rev. B* **70**, 104415 (2004); J. Richter et al., *Phys. Rev. Lett.* **93**, 107206 (2004); M.E.Zhitomirsky and H.Tsunetsugu, *Phys. Rev. B* **75**, 224416 (2007); M. Maksymenko et al., *Eur. Phys. J. B* **84**, 397 (2011); S. Capponi et al., *Phys. Rev. B* **88**, 144416 (2013).
- [4] O.Derzhko et al., *Phys. Rev. B* **88**, 094426 (2013).

1OR-Q-3

ELECTRON SPIN-RESONANCE STUDY OF THE STRONG-LEG SPIN LADDER

Glazkov V.N.^{1,2,*}, *Krasnikova Yu.V.*², *Schmidiger D.*³, *Zheludev A.I.*³

¹ P.Kapitza Institute for Physical Problems RAS, 119334 Moscow, Russia

² Moscow Institute of Physics and Technology, 141700 Dolgoprudny, Russia

³ Neutron Scattering and Magnetism, ETH Zurich, 8006 Zurich, Switzerland

* glazkov@kapitza.ras.ru

Spin ladder, a system of two coupled spin chains, is an interesting object in magnetism. While, naively, it could be considered as a first step from 1D to 2D magnet, its physical properties are remarkably different from both single spin-chain and a 2D system. In particular, for any ratio of the in-chain (or “leg”) J_{leg} and inter-chain (or “rung”) J_{rung} exchange couplings the excitations spectrum of the $S=1/2$ spin ladder is gapped. By varying strength of the rung coupling one can continuously move from the weakly coupled dimers limit ($J_{\text{rung}} \gg J_{\text{leg}}$) to the weakly coupled chains limit ($J_{\text{leg}} \gg J_{\text{rung}}$). The excitations spectrum continuously transforms from the well defined magnon branch in dimer limit to a spinon continuum in spin-chain limit. Most of the known spin-ladder systems are of a “strong-rung” type, with interchain exchange dominating. Recently found spin-ladder compound $(\text{C}_7\text{H}_{10}\text{N}_2)_2\text{CuBr}_4$, abbreviated DIMPY for short, is a rare example of “strong-leg” spin ladder with $J_{\text{leg}}=1.42\text{meV}$ and $J_{\text{rung}}=0.82\text{meV}$. [1]

We present results of the electron spin-resonance study of DIMPY. We have found that ESR signals from the two magnetically inequivalent spin ladders (these ladders are related by a C_2 rotation) can be resolved, which indicates absence of the inter-ladder couplings. ESR linewidth at low temperatures is found to be as low as 10 Oe in certain field orientations. Small linewidth and absence of the detectable splitting of the triplet states shows that DIMPY is really close to the model $S=1/2$ Heisenberg spin-ladder. Temperature dependence of the ESR linewidth is strongly non-monotonous, which is indicative of switching between different relaxation mechanisms.

The work was supported by RFBR.

[1] D.Schmidiger et al. *Phys. Rev. Lett.* **108**, 167201 (2012).

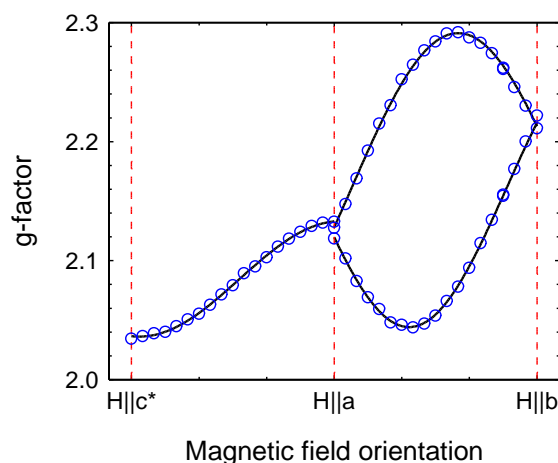


Figure 2 G-factor angular dependency at 77K.

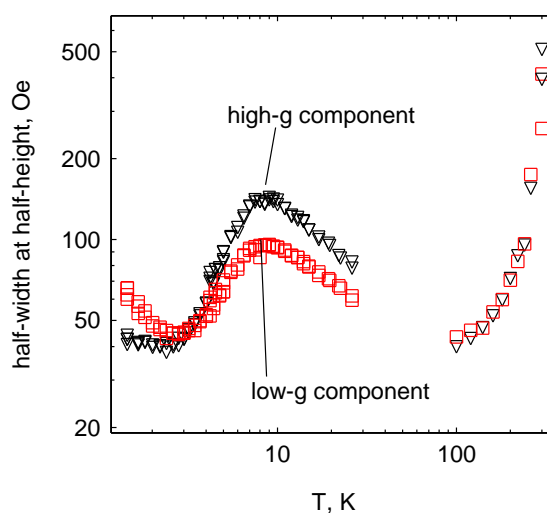


Figure 3 Temperature dependency of the ESR linewidth at the field applied at 45° from b-axis towards a-axis. $f=17.5$ GHz.

1OR-Q-4

**HIGH-FIELD MAGNETIC RESONANCE STUDY OF THE CHAIN
QUANTUM MAGNET BaAg₂Cu[VO₄]₂**

Vavilova E.^{1*}, *Kataev V.*^{1,2}, *Schäpers M.*², *Krupskaya Y.*², *Wolter-Giraud A.U.B.*², *Grafe H.-J.*²,
*Möller A.*³, *Büchner B.*²

¹ Zavoisky Physical Technical Institute of the RAS, Kazan, Russia

² IFW-Dresden, Dresden, Germany

³ University of Houston, Houston, United States

*jenia.vavilova@gmail.com

Here we report the results of the NMR and high-field ESR study of the local magnetic properties of a novel transition-metal (TM) oxide low-dimensional quantum magnet BaAg₂TM[VO₄]₂. Depending on the type of the TM ion, either frustrated triangular 2D spin lattices or a network of 1D spin chains can be realized in these materials [1]. A superposition of ferromagnetic ($J_{\text{FM}} = -19\text{K}$) and antiferromagnetic ($J_{\text{AFM}} = 9.5\text{K}$) uniform spin-1/2 chains supposed to play a major role in the physics of the Cu-based compound. A comparative analysis of the ⁵¹V NMR and Cu(II) ESR spectra enables to identify non-equivalent vanadium positions. The temperature dependence of the ⁵¹V Knight shifts and the relaxation rates as well as frequency-, magnetic field- and temperature dependence of the Cu(II) ESR signals suggest that non-equivalency of the VO₄ structural fragments affects the superexchange between the Cu ions in the chains. Our results support the scenario of the tunable ferro- and antiferromagnetic coupling in the Cu spin-1/2 chains driven by the specific tilting of the VO₄ exchange mediators.

[1] N. E. Amuneke et al., *Inorg. Chem.* **50**, (2011) 2207.

[2] A.A. Tsirlin et al., *Phys. Rev. B* **85**, (2012) 014401.

1OR-Q-5

COPPER NMR STUDY OF CuCrO₂Sakhratov Yu.A.^{1,2}, Svistov L.E.³, Reyes A.P.¹, Kuhns P.L.¹, Zhou H.D.^{1,4}, Matukhin V.L.²¹ National High Magnetic Field Laboratory, Tallahassee, Florida 32310, USA² Kazan State Power Engineering University, 420066 Kazan, Russia³ P. L. Kapitza Institute for Physical Problems RAS, 119334 Moscow, Russia⁴ Department of Physics and Astronomy, University of Tennessee, Knoxville, Tennessee 37996, USA
sakhratov@gmail.com

We have carried out Cu NMR spectra measurements in magnetic field up to about 15.5 T on single crystal of a triangular-lattice antiferromagnet CuCrO₂. The measurements were performed for perpendicular and parallel orientation of the magnetic field with respect to the *c*-axis of the crystal, and the detailed angle dependence of the spectra on the magnetic field direction within *ab*-plane was studied. The shape of the spectra below the ordering temperature $T_N \approx 24$ K can be well described in the model of spiral spin structure proposed by recent neutron diffraction experiments [1]. The earlier reported domain structure of CuCrO₂ controlled by annealing the sample in magnetic field [2] is well manifested through Cu NMR. The data for perpendicular orientation assume remarkable reorientation of spin plane simultaneous with rotation of the incommensurate wavevector influenced by the external magnetic field. These results are consistent with ESR experiments [3]. Parallel field data for the fields higher ~ 12 T indicate field evolution of the magnetic structure. We suggest two possible scenarios. The first one is the incommensurate spiral magnetic structure within every *ab*-plane with disorder in the *c* direction. And the second scenario is the commensurate magnetic structure. The observed feature possibly corresponds to a phase transition also seen by very recent electric polarization experiments [4].

Support by IIE FP (Grant 68435029), RFBR (Grant 13-02-00637), and NSF (Agreement DMR-0654118) is acknowledged.

[1] M. Frontzek, G. Ehlers, A. Podlesnyak, H. Cao, M. Matsuda, O. Zaharko, N. Aliouane, S. Barilo, S. V. Shiryayev, *J. Phys.: Condens. Matter* **24**, 016004 (2012).

[2] K. Kimura, H. Nakamura, S. Kimura, M. Hagiwara, and T. Kimura, *Phys. Rev. Lett.* **103**, 107201 (2009).

[3] A. M. Vasiliev, L. A. Prozorova, L. E. Svistov, V. Tsurkan, V. Dziom, A. Shuvaev, Anna Pimenov, and A. Pimenov, *Phys. Rev. B* **88**, 144403 (2013).

[4] Eundeok Mun, M. Frontzek, A. Podlesnyak, G. Ehlers, S. Barilo, S.V. Shiryayev, and Vivien S. Zapf, *Phys. Rev. B* **89**, 054411 (2014).

1 July

Tuesday

14:30-17:15

oral session

1TL-C

1RP-C

1OR-C

**“Soft and Hard
Magnetic Materials”**

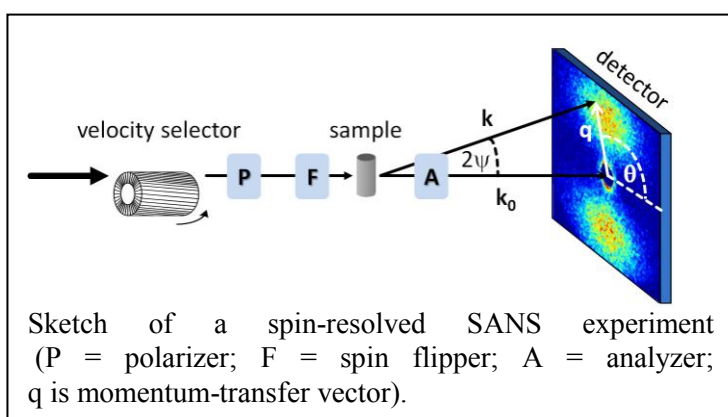
1TL-C-7

SANS ON MAGNETIC NANOSTRUCTURES

Michels A.

Physics and Materials Science Research Unit, University of Luxembourg
andreas.michels@uni.lu

Magnetic small-angle neutron scattering (SANS) measures the diffuse scattering along the forward direction (scattering angle $2\psi \delta 10^\circ$), which arises from both nanoscale variations of the magnitude $M_s(\mathbf{r})$ and of the orientation of the magnetization vector field $\mathbf{M}(\mathbf{r})$. SANS is probably the only technique which provides information from within the *bulk* of a material and on a length scale between a few nanometers and a few hundred of nanometers ($\sim 1\text{-}300$ nm) [1]. However, up



to now, SANS was almost exclusively utilized with an unpolarized or a polarized incident neutron beam (denoted as SANSPOL), and an analysis of the spin state of the neutron after the scattering process is frequently not performed. Due to recent progress in the development of efficient ^3He spin filters/analyzers, it has only now become possible to perform routinely longitudinal (also called uniaxial or one-dimensional) neutron-polarization

analysis (so-called POLARIS), e.g., at the instruments D22 and D33 at the Institut Laue-Langevin. In the first part of the talk, we discuss recent POLARIS results on several nanocrystalline ferromagnets; in particular, we report on the observation of a cross-shaped angular anisotropy in the non-spin-flip SANS cross section, only observable by means of POLARIS [2]. In a second example, we present unpolarized magnetic SANS data of a Nd-Fe-B nanocomposite permanent magnet [3]. Here, we have studied the magnetization-reversal process by computing the autocorrelation function of the spin misalignment, which provides information on the characteristic size and field dependence of spin inhomogeneities in the material. In the last part, we briefly introduce our recent analytical micromagnetic theory of magnetic SANS [4] and test it against experimental data [5]. This approach yields values for the mean exchange-stiffness constant and it provides the strength and spatial structure of the magnetic anisotropy and magnetostatic field.

[1] A. Michels and J. Weissmüller, *Rep. Prog. Phys.* **71**, 066501 (2008).

[2] A. Michels *et al.*, *Phys. Rev. B* **85**, 184417 (2012).

[3] J.-P. Bick *et al.*, *Appl. Phys. Lett.* **102**, 022415 (2013).

[4] D. Honecker and A. Michels, *Phys. Rev. B* **87**, 224426 (2013).

[5] D. Honecker *et al.*, *Phys. Rev. B* **88**, 094428 (2013).

1TL-C-8

ISOTROPIC Nd-Fe-B/ α -Fe NANO-COMPOSITE THICK FILM MAGNETS

Nakano M., Motomura K., Fujiyama K., Yanai T., Fukunaga H.

Nagasaki University, Nagasaki, Japan

mnakano@nagasaki-u.ac.jp

The preparation of a multi-polarly magnetized rotor comprising isotropic Nd-Fe-B thick-film magnets is effective to obtain a cylindrical motor[1], and the required values of coercivity, remanence and $(BH)_{\max}$ for the films are higher than 0.9 T, 400 kA/m, and 90 kJ/m³, respectively. Although we have reported a PLD(Pulsed Laser Deposition)-fabricated isotropic Nd-Fe-B/ α -Fe nano-composite thick film magnet as a good candidate for the magnet by using the laser energy density lower than 1 J/cm² because of a high deposition rate higher than 40 μ m/h together with a good transfer composition from a target to a film, the segregation of α -Fe grains around a Nd-Fe-B grain was observed and it was difficult to exceed the remanence value of 0.8 T[2]. The present investigation, therefore, focused on the above PLD-made nano-composite thick films by taking advantage of high energy density. It was clarified that a Nd-Fe-B/ α -Fe nano-composite thick film magnet usable for the above cylindrical motor could be obtained by using high energy density of above 10 J/cm².

The targets with various compositions of Nd_xFe₁₄B (x=1.8-2.8) were ablated by an Nd-YAG pulse laser (wave length = 355 nm). The range of laser energy density together with the distance between a target and a Ta substrate were fixed at above 10 J/cm² and 10 mm, respectively. The deposition rate range became from 20 to 40 μ m/h. All the as-deposited films thicker than 10 μ m had amorphous structure, and therefore they were crystallized by a pulse annealing (PA) method.

It was confirmed that the Nd contents of all the films decreased by approximately 6.0 at.% compared to the corresponding targets. The result is considered to be attributed that Fe atoms tend to move straightly to a substrate and Nd atoms are widely emitted under the high energy density. As show in the figure, the films prepared by using a Nd_{2.4}Fe₁₄B target indicated a promising potential for an isotropic thick films usable for the above cylindrical motor. For example, a 16 μ m-thick nano-composite film with remanence, coercivity and $(BH)_{\max}$ values of 1.04 T, 426 kA/m and 108 kJ/m³, respectively, could be obtained.

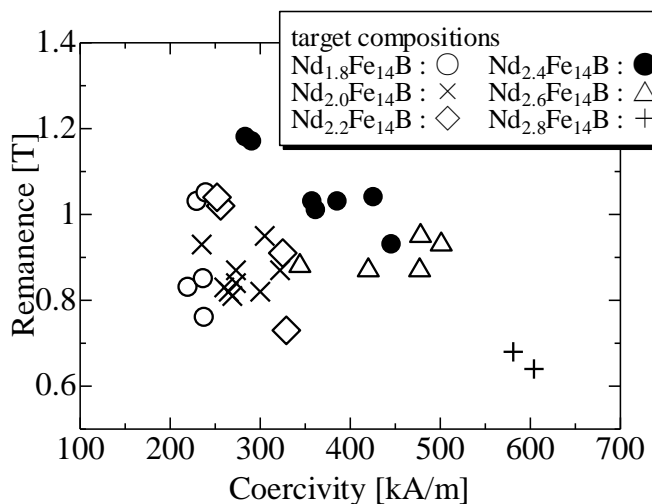


Fig. 1 Remanence and coercivity values of films prepared by various targets.

[1] F. Yamashita *et al.*, *J. Appl. Phys.* **109** (2011) 07A712-1-3.

[2] M. Nakano *et al.*, *IEEJ. Trans. on Fundamentals and Materials.* **132**,(2012) 844-847. (in Japanese).

1TL-C-9

MAGNETIC DOMAIN OBSERVATION OF Nd-Fe-B SINTERED MAGNETS WITH A KERR MICROSCOPE

Takezawa M., Ogimoto H., Morimoto Y.

Kyushu Institute of Technology, Kitakyushu, Japan
take@ele.kyutech.ac.jp

Electrical vehicles require heat-resistant Nd-Fe-B high-coercivity magnets. Through domain observation using an *in-situ* Kerr microscope, we report that the extent of the simultaneous magnetization-reversal area is related to the coercivity of Nd-Fe-B sintered magnets [1]. Moreover, we have examined the magnetization process at elevated temperatures by an image-processing technique using a Kerr microscope. We aim to clarify the reason for the decrease in the coercivity of sintered Nd-Fe-B magnets at elevated temperatures through domain observation.

The magnetic domain of a Nd-Fe-B sintered magnet was observed using a Kerr microscope. The demagnetization process of a previously magnetized magnet, with a pulse field of +50 kOe, was observed by applying a dc field from +14.2 to -14.2 kOe in the easy axis direction of the magnet. The sample temperatures were set to 21 - 150°C.

Figure 1 shows the domain images indicating the magnetization-reversal area for each magnetic field strength at temperatures of 21, 60, and 150°C. The simultaneous magnetization reversal occurred in a dc field from 0 to -4.0 kOe at 21°C, and from 0 to -1.0 kOe at 60°C, and from +1.5 to 0 kOe at 150°C. These data show that magnetization reversal is more likely to occur at elevated temperatures and that the negative magnetic field that causes saturation decreases with increasing temperature.

Note that the extent of simultaneous magnetization reversal increases with temperature. Although the extent of simultaneous magnetization reversal is a few grains at room temperature, reversal involves several grains at 60 °C and 150 °C. The magnetization reversal beyond the grain boundaries was found to easily occur with increasing temperature because the crystal magnetic anisotropy of Nd-Fe-B decreases and the hard magnetic properties deteriorate. Furthermore, one of the reasons for the increase in the extent of simultaneous magnetization reversal is the decrease in the pinning force of domain wall motion at the grain boundaries at elevated temperatures. Therefore, maintaining a high pinning force at grain boundaries at elevated temperatures is important to realize heat-resistant sintered Nd-Fe-B magnets.

[1] M. Takezawa, *et al.*, *IEEE Trans. Magn.*, **49**, (2013) 3262-3264.

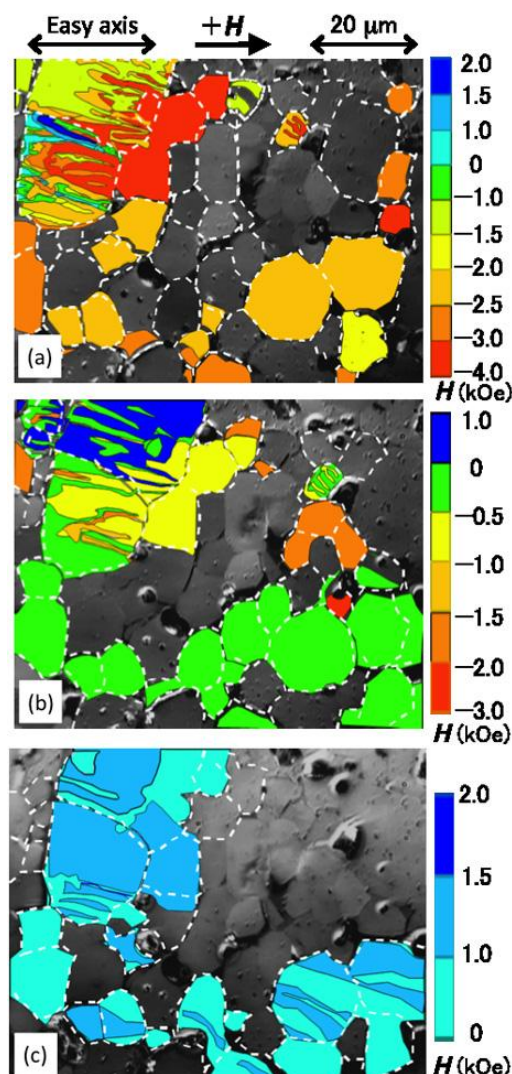


Fig. 1. Domain images indicating the magnetization-reversal area at: (a) 25 °C, (b) 60 °C, and (c) 150 °C.

1RP-C-10

SPONTANEOUS AND FIELD-INDUCED TRANSITIONS IN TmFe_5Al_7 *Gorbunov D.I.^{1,2}, Yasin S.³, Andreev A.V.¹, Mushnikov N.V.⁴, Rosenfeld Ye.V.⁴, Skourski Y.³, Zherlitsyn S.³, Wosnitza J.³*¹ Institute of Physics, Na Slovance 2, 182 21 Prague, Czech Republic² Charles University, DCMP, Ke Karlovu 5, 121 16 Prague, Czech Republic³ Dresden High Magnetic Field Laboratory, Helmholtz-Zentrum Dresden-Rossendorf, D-01314 Dresden, Germany⁴ Institute of Metal Physics, Kovalevskaya 18, 620990 Ekaterinburg, Russia
gorbunov@fzu.cz

In the framework of our systematic study of RFe_5Al_7 intermetallic compounds (tetragonal crystal structure of the ThMn_{12} type) where R is a heavy rare-earth metal, magnetization and sound propagation of a TmFe_5Al_7 single crystal have been measured in magnetic fields up to 60 T. The compound is a ferrimagnet with Curie temperature $T_C = 193$ K. In contrast to previously studied RFe_5Al_7 with R = Gd, Tb, Dy, Ho and Er with easy-plane anisotropy, at low temperatures the magnetic moments in TmFe_5Al_7 lie along the c axis as the magnetic anisotropy is dominated by the uniaxial Tm sublattice. The competition between the uniaxial Tm anisotropy and the planar Fe anisotropy results in a first-order spin-reorientation transition at 64 K when the magnetic moments rotate from the c axis to the basal plane. The transition affects exchange interactions in TmFe_5Al_7 that becomes antiferromagnetic (Fig. 1). The changes in the magnetic state at 64 K are reflected in the sound velocity and specific heat as well (insets in Fig. 1). Ferrimagnetism is restored at 82 K via another first-order phase transition. Such a set of the magnetic transitions may be due to a relatively weak Tm-Fe exchange interaction. At low temperatures TmFe_5Al_7 exhibits a field-induced magnetic transition along the easy c axis (Fig. 2). The spin-phonon coupling is affected by the jump, which is manifested by a decrease in the sound velocity.

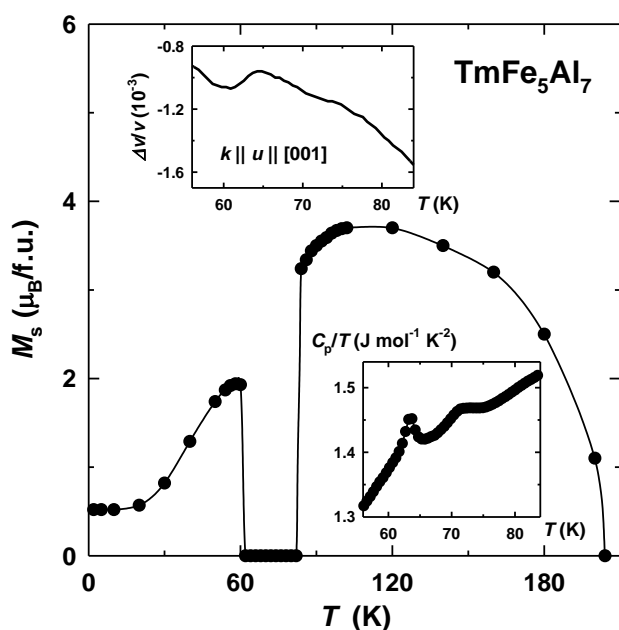


Fig. 1. Temperature dependence of the spontaneous magnetic moment M_s of TmFe_5Al_7 . The upper inset shows the relative change of sound velocity $\Delta v/v$ of a longitudinal acoustic wave propagating along the [001] axis and the lower inset the specific heat over temperature ratio C_p/T in the range $T = 56$ -84 K.

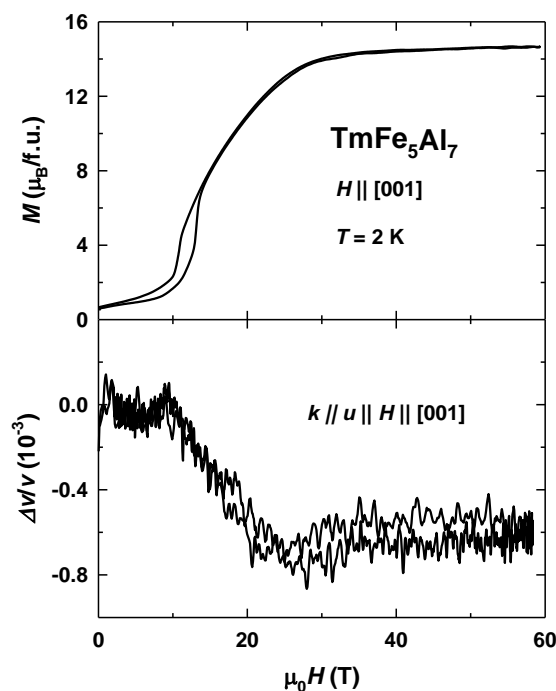


Fig. 2. Magnetization M and relative change of sound velocity $\Delta v/v$ measured along the [001] axis of TmFe_5Al_7 in pulsed magnetic fields at $T = 2$ K.

1RP-C-11

PRESSLESS PROCESS IN ROUTE OF OBTAINING SINTERED Nd-Fe-B MAGNETS

Popov A.G.

Institute of Metal Physics, UB RAS, 18, S. Kovalevskoy, Str., 620990, Ekaterinburg, Russia
apopov@imp.uran.ru

Production of the sintered Nd-Fe-B magnets by means of powder metallurgy includes many steps; among them the processes of alignment and pressing of the powders are the most complex. Recently, the extended application of the sintered Nd-Fe-B magnets sets essential task of production of magnets with higher performance at lower cost. To solve this problem, a new process, which is characterized by the absence of the stage of pressing Nd-Fe-B powders, was offered by Sagawa and Une [1]. This process is called pressless process, or PLP. The advantage of PLP is the complete exclusion of large and heavy press machines and DC electric magnets from technology process allowing to handle fine and reactive powders within a low oxygen environments. This opens a way toward high coercivity Dy-free Nd-Fe-B sintered magnets.

In order to increase the values of remanence B_r and maximum energy product $(BH)_{\max}$ of the PLP magnets we used internal lubricants, which improved magnetic alignment of powders. The strip casting alloy, which consists of 31.5 Nd, 1 B, bal. Fe (mass %), after hydrogen decrepitation and coarse grinding was milled in a vibratory mill in toluene. Lubricant additives - zinc stearate powder or esters of carboxylic acids - were put into the mill vessel together with the alloy powder. After milling to an average particle size of 3 - 5 μm , the dry or wet powder was loaded into molybdenum containers with a loading density of 3.0 to 3.5 g/cm^3 . Alignment of powders was performed by a pulsed magnetic field of 46 kOe; after PLP the magnets were sintered in vacuum at 1090 $^{\circ}\text{C}$. The low evaporation temperatures of the lubricants allowed for their removal from the powder particles surface by slow heating under vacuum at a temperature no higher than 500 $^{\circ}\text{C}$.

It is shown that addition of the internal lubricants in toluene upon milling of the Nd-Fe-B alloy increases the remanence of the sintered magnets by 5 - 7%. The maximum concentration of the zinc stearate and esters of carboxylic acids should not exceed 0.2 and 1.5%, respectively, of the mass of Nd-Fe-B powder. The higher lubricant concentrations led to interaction of the lubricant with the Nd-rich phase during sintering of the magnets resulting in a sharp decrease of the magnetic hysteresis properties. The PLP magnets prepared using lubricant additives exhibited the density of 7.5 g/cm^3 , $B_r \geq 14$ kG, $H_c \geq 8$ kOe and $(BH)_{\max} \geq 46$ MGOe.

The work is supported by GLOBAL CRDF – UB RAS (project RUP2-7104-EK-13) and UB RAS (project № 12-M-23-2066).

[1] M. Sagawa, Y. Une, Proc. 20th Int. *Workshop on Rare Earth Permanent Magnets and Their Applications (Knossos-Crete, 2008)*, pp.103-105.

1RP-C-12

MOLECULAR MAGNETISM AND CRYSTAL FIELD EFFECTS IN THE KONDO SYSTEM $\text{Ce}_3\text{Pd}_{20}(\text{Si},\text{Ge})_6$ WITH TWO Ce SUBLATTICES

Nikiforov V.N.^{1*}, Koksharov Yu.A.¹, Griбанov A.V.¹, Baran M.², Irkhin V.Yu.³

¹ Moscow State University, 117234 Moscow, Russia

² Institute of Physics, Polish Academy of Science, Warsaw, Poland

³ Institute of Metal Physics, 620990 Ekaterinburg, Russia

*pppnvn@yandex.ru

The Kondo systems $\text{Ce}_3\text{Pd}_{20}\text{T}_6$ ($\text{T} = \text{Ge}, \text{Si}$) with two characteristic temperatures Kondo demonstrates unusual magnetic and transport properties first discussed in [1]. The feature of this cubic system is two nested cubes composed of cerium ions, Ce1 and Ce2, in two non-equivalent positions. These systems demonstrate high electron heat capacity: estimations above $T = 6$ K give the value of $\gamma=0.3$ and 0.21 J/mol K^2 for $\text{T} = \text{Si}$ and Ge . $\text{Ce}_3\text{Pd}_{20}\text{Si}_6$ has at ultralow temperatures $T = 0.3\div 2$ K anomalous heat capacity which is almost constant, and formally calculated γ grows up to 10^4 J/mol K^2 .

The logarithmic growth of resistance for both systems (Fig.1) confirms the presence of the Kondo effect in the two respective temperature ranges. The two-scale behavior is explained by consecutive splitting of Ce ion levels in the crystal field [2]. The calculation of the crystal field parameters is performed basing on experimental data on magnetic susceptibility. The effects of the frustration caused by the coexistence of the different positions of cerium may also significantly enhance the observed values of specific heat. Replacing of Ce by U and Sm leads to dramatic disappearance of anomalies discussed.

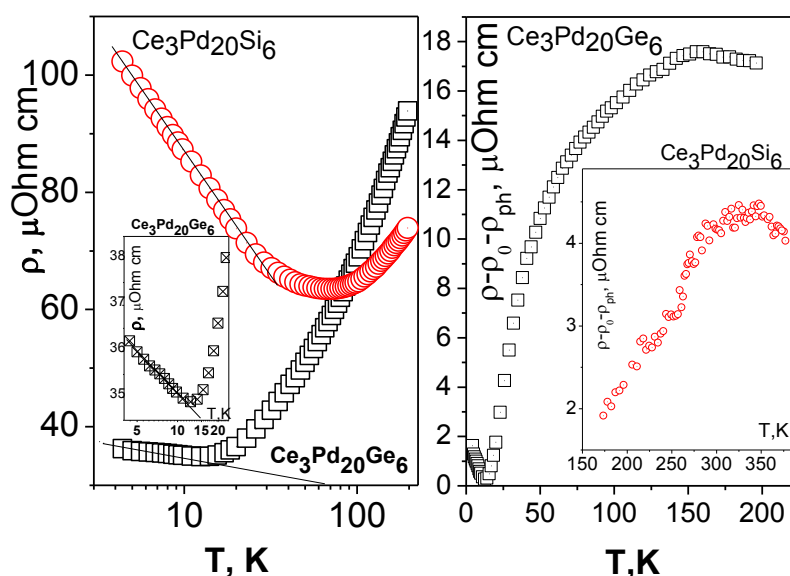


Fig.1. Temperature dependences of resistivity at low temperature (left) and at more high temperatures (right; phonon contribution is subtracted)

[1] V.N. Nikiforov et al, *Int. Conf. on Solid Compound of Transition Elements*, Wroclaw, 1994, pp.79-90; Yu P. Gajdukov et al, *JETP Letters*, **61**, 391 (1995).

[2] S. Kashiba et al, *J. Phys. Soc. Jpn* **55**; 1341 (1986).

1OR-C-13

TOPOLOGICAL PECULIARITIES AND STABILITY OF MAGNETIC INHOMOGENEITIES WHICH ORIGINATE UPON DEFECTS

Vakhitov R.M.¹, Solonetskiy R.V.¹, Yumaguzin A.R.¹

¹ Institute of Physics and Technology, Federal State Budget-funded Educational Institution of
Higher Professional Education Bashkir State University, Ufa, Russia
VakhitovRM@yahoo.com

The presence of defects in magnetic materials is known to considerably modify the properties of such materials [1]. Magnetic inhomogeneities originate upon defects under certain conditions, these inhomogeneities significantly influencing the processes of magnetization and magnetization reversal of magnets, specifically, the magnitude of coercive force [2]. In view of this, a research into the structure and properties of magnetic inhomogeneities which originate in the defects area acquires topicality. The recent paper [3] demonstrated that on defects in a uniaxial ferromagnet under the same values of material parameters there can form two types of magnetic inhomogeneities which correspond to the 0-degree domain wall (0°-DW) and which differ in terms of energy E , amplitude θ_m (maximum angle of deviation of magnetization vector \mathbf{M} from the homogeneous state) and width Δ . Notably, the characteristics of the low-amplitude inhomogeneity (0°-DW(I)) turned out to be smaller in magnitude than those of the high-amplitude inhomogeneity (0°-DW(II)). To determine the contribution made by 0°-DW(II) to the magnetization reversal processes of real magnets one has to identify the conditions (or to take additional factors into consideration) at which they become an energetically advantageous formation. Taking account of the demagnetizing fields from the surface charges conditioned by finiteness of the sample (slab) is apparently one of such factors. This is connected with the fact that there is a region $(\frac{\pi}{2} < \theta$, where θ is the angle between the magnet's symmetry axis and magnetization \mathbf{M}) in magnetization distribution in the 0°-DW(II), at the expense of which magnetostatic energy of the 0°-DW (II) becomes smaller than that for the 0°-DW (I).

The paper investigates the stable states of 0°-DWs of both types, localized upon the defect, in a finite-thickness uniaxial ferromagnet slab. In this case, the Euler-Lagrange equation which describes the structure of a 0°-DW [4] represents non-linear integro-differential second-order equation with non-constant coefficients. The two approaches were employed for solving such problems: the variational one (which proved to be efficient when studying the spin-reorientational processes in real crystals [4]), and numerical integration of the original equations. In the latter case, the sweep method was used employing Newton's iterative procedure. It follows from the results obtained that in both cases the 0°-DW (II) can be a stable formation and energetically more advantageous compared to the 0°-DW (I). A diagram of the stable states of the 0°-DWs of both types was constructed and a parameter region of magnets was defined in which magnetic inhomogeneities of the second type can play a leading part in the material magnetization and magnetization reversal processes.

References

- [1] D.D. Mishin. *Magnetic Materials. M.: Vysshaya Shkola*, 1991. - 384 p.
- [2] G.S. Kandaurova. *Soros Educational Journal*. **1** (1997) 100 – 106.
- [3] Ye.B. Magadeev, R.M. Vakhitov // *Abstracts of International Conference "Functional Materials" ICFM'2013*. September 29 – October 5 (2013), 502 p.
- [4] R.M. Vakhitov, Ye.R. Gareyeva, M.M. Vakhitova, A.R. Yumaguzin. *ZhTF* **79**, 8 (2009), 50-55.

1OR-C-14

NANOFABRICATION AND CHARACTERIZATION OF MAGNESIUM DOPED CADMIUM FERRITES

Gupta M.^{1,2}, Randhawa B.S.^{1}*

¹ Department of Chemistry, Guru Nanak Dev University, Amritsar, Punjab-143005, India

² Department of Chemistry, DAV College, Amritsar, Punjab-143001, India
manuchemistry@gmail.com

Influence of Mg²⁺ doping on the synthesis and properties of cadmium ferrite nanoparticles (Fig. 1) of basic composition CdFe_{2-x}Mg_{1.5x}O₄ (x = 0.0 – 1.0) prepared through simple citrate - metal nitrate solution combustion route is reported. Structural, chemical, magnetic and electrical properties of the prepared samples were analyzed by using various spectroscopic techniques. FT-IR study shows the presence of two prominent absorption bands in the regions 600 cm⁻¹ and 400 cm⁻¹ corresponding to tetrahedral and octahedral sites respectively [1]. X-Ray Diffraction (Powder) results (Fig. 2) confirm that all the samples are single-phase cubic spinel in structure excluding the presence of any secondary phase and maximum substitution is attained at x = 1.0. The purity and stoichiometry of the compositions after final sintering were confirmed by Energy Dispersive X-ray (EDX) analysis. The increase in Mg-substitution leads to an increase in the lattice parameter as well as BET surface area of the prepared ferrites. The dielectric constant (ϵ') and loss tangent ($\tan \delta$) measured at room temperature as a function of frequency (42 Hz to 5 MHz) decreases with increase of frequency, indicating decrease in polarization. Magnetic and Mössbauer studies suggest that both the nature and concentration of dopant controls the site preferences in the crystal lattices. The saturation magnetization and magnetic moments of the ferrite samples estimated from VSM analysis (Fig. 3) were found to increase with Mg content and confirms the inverted spinel structure of cadmium ferrites.

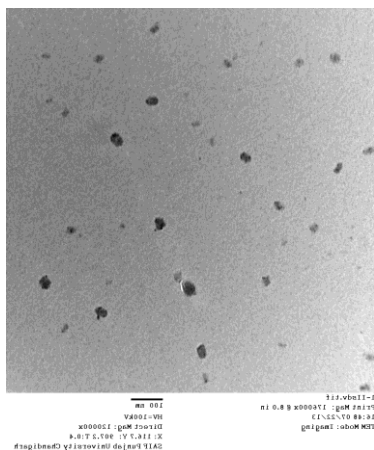


Fig. 1. TEM Micrograph for Cadmium ferrites

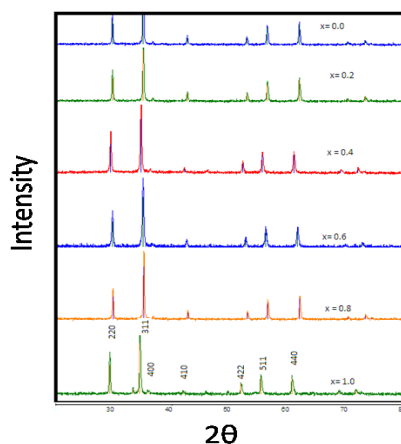


Fig. 2. XRD pattern for Cadmium ferrites

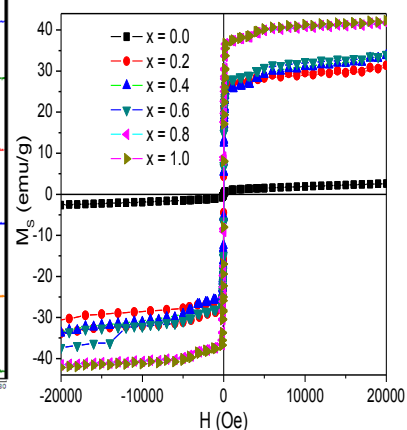


Fig. 3 VSM Analysis of Cadmium ferrites

Presenting author is thankful to UGC, New Delhi, India for providing financial assistance and leave for research work under FIP scheme.

Services of SAIF centre, Punjab University, Chandigarh, India for TEM studies is also highly acknowledged.

[1] M. Gupta, M. Gupta, V. S. Jaswal, B.S. Randhawa, *J. Analytical and Applied Pyrolysis*, **104** (2013) 73-76.

1 July

Tuesday

14:30-17:00

oral session

1TL-F

1RP-F

1OR-F

**“Magnetic Soft Matter
(magnetic polymers,
fluids and
suspensions)”**

1TL-F-5

RHEOLOGICAL PROBING OF SOFT MAGNETIC MATERIALS

Galindo-Gonzalez C.¹, Bee A.², Chevalet J.², Dubois E.², Perzynski R.², Ponton A.¹, Talbot D.²

¹ MSC - Univ. Paris Diderot, Paris, France

² PHENIX - Univ. P. et M. Curie - Paris 6, Paris, France

regine.perzynski@upmc.fr

Macroscopic rheological properties of soft materials are very sensitive to their local structure. As an example Fig. 1 shows how different can be such properties, probed under-field, in a magnetic fluid depending on the local organization of their 10 nm sized nanoparticles (NPs).

A regular ferrofluid with individually dispersed NPs is Newtonian under-field and presents an under field viscosity (with applied field normal to the local vorticity of the flow) well described by M.I. Shliomis formalism [1] (see Fig.1a). If now the NPs form clusters or associate together in a thixotropic gel [2], a yield stress is now observed in zero field, of the order of 10 mPa for sols of clusters and of 200 mPa for thixotropic gels. Under a field $H = 32$ kA/m, this yield stress may increase by a factor of the order of 400 as illustrated in Fig. 1b [3].

Another situation may be encountered with magnetic fluids: a phase-separated sample containing droplets of concentrated phase, easily deformable under-field, of typical size 10 μm , which are dispersed in a more dilute phase (see insets of Fig. 1c). This situation is here illustrated with a heterogeneous aqueous mixture of a ferrofluid and poly-alginate chains, rheologically probed under 1 Hz oscillations as a function of strain. Fig. 1c shows mean values of its elastic G' and viscous G'' moduli in the linear viscoelastic domain. Its under-field rheological behavior is dominated by the droplets' elongation and their merging together.

In soft magnetic materials, rheological properties may also be studied at a more local scale through magneto-optical birefringence, which probes the rotational diffusion of the NPs. This is a very powerful technique to study sol-gel transitions or local NPs rotational abilities in a gel [4].

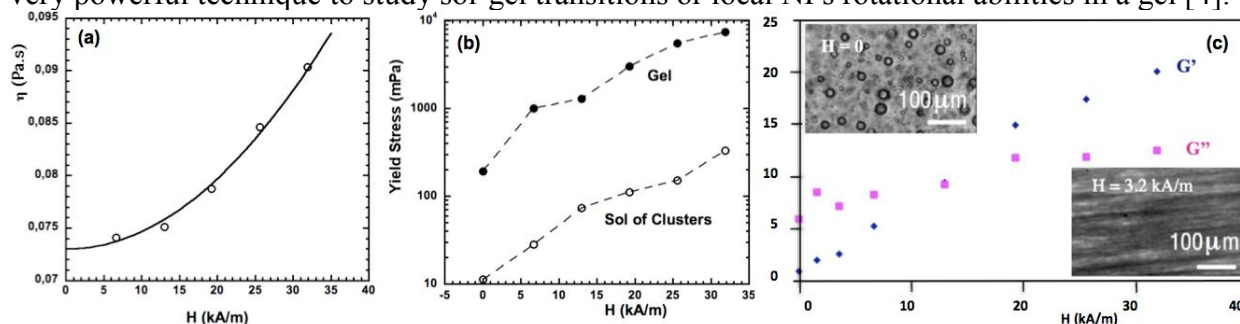


Fig 1 Field dependences of : (a) the viscosity of a ferrofluid based on individual NPs dispersed in dibutyl phtalate, full line is a fit by M.I. Shliomis's formalism; (b) the yield stress of aqueous ferrofluids being either a Sol of NPs Clusters or a thixotropic Gel - dashed lines are guides for the eye; (c) the shear modulus G' and the loss modulus G'' of a heterogeneous aqueous mixture of a ferrofluid and poly-alginate chains with magnetic liquid droplets elongating along the applied field thus transforming the system from a viscoelastic liquid to a viscoelastic solid.

This work was supported by E.U. under grant from Intra European Fellowship Seventh Framework Program (Marie Curie Actions) and ANR-THERMELEC.

[1] M.I. Shliomis, *Soviet Phys. J.E.T.P.*, **34** (1972) 1291-1294.

[2] B.Frka-Petesic et al, *Magnetohydrodyn.* **49** (2013) 328-338.

[3] C. Galindo-Gonzalez et al, to be published.

[4] A. Galicia et al, *Soft Matter* **5** (2009) 2614-2624.

1TL-F-6

MAGNETO-SENSITIVE ELASTOMERS AND THEIR MODELING

Ivaneyko D., Toshchevnikov V., Saphiannikova M., Heinrich G.

Leibniz-Institut für Polymerforschung Dresden, Germany

grenzer@ipfdd.de

Magneto-sensitive elastomers (MSEs) belong to a class of smart materials whose mechanical behavior can be controlled by an external magnetic field. This makes MSEs especially attractive for diverse actuator applications. Typically, MSEs represent a two-component system, in which micron-sized magnetizable particles are embedded in a polymer network. The spatial distribution of particles can be either isotropic or anisotropic depending on whether they have been aligned before the cross-linking of a polymer. Magnetically induced deformations (magnetostriction) and the change of the mechanical moduli under the magnetic field (magneto-rheological (MR) effect) are the most significant features of MSEs. Only a few works including ours [1] were proposed to study the MR effect depending on spatial distribution of magnetic particles. These works consider infinite MSE samples and thus neglect the effects of shape change for finite samples.

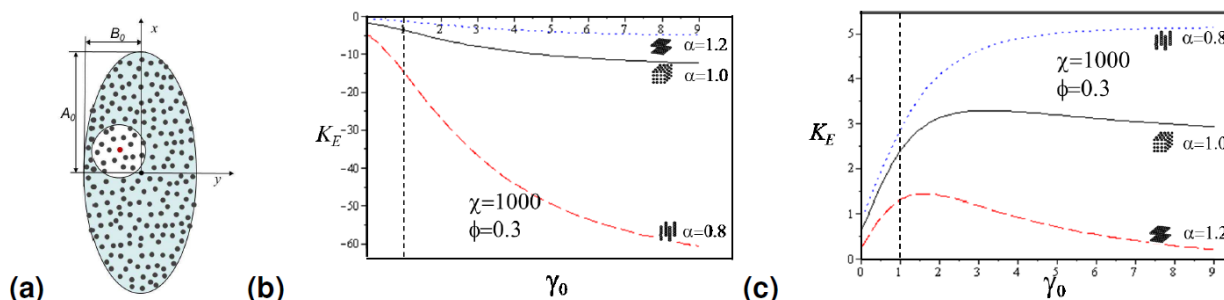


Fig.1. Microscopic model of an ellipsoidal MSE sample (a). The coefficient K_E which determines the sign of MR effect calculated for different particle distributions on the tetragonal (b) and HCP (c) lattices.

Recently we proposed a new theoretical formalism which predicts the mechanical properties of the MSEs with different shapes and with different particle distributions [2]. It is assumed that a finite MSE sample has the shape of an ellipsoid of revolution with the aspect ratio $\gamma_0 = A_0 / B_0$ (Fig. 1a). The field inside the MSE can be separated into two contributions: one which depends on the initial shape of the sample γ_0 and the other, which depends on the local particle distribution. In the magnetic field \mathbf{H}_0 both the shape of a sample and the particle distribution are changed. This leads to the change of the elastic modulus, ΔE , which is found to be proportional to H_0^2 . The proportionality coefficient K_E depends on the volume fraction of magnetic particles, their magnetic susceptibility and the art of coupling between the particle distribution and the magnetically induced deformation of the sample. We found that the affine coupling, which takes place for highly cross-linked MSEs, results in diverse macroscopic responses: the magnetostriction and MR effects can be both negative (Fig. 1b) and positive (Fig. 1c), depending on the initial particle distribution and the initial sample shape.

Support by DFG grant GR 3725/6-1 is gratefully acknowledged.

[1] D. Ivaneyko, V. Toshchevnikov, M. Saphiannikova, G. Heinrich, *Macromol. Theory Simul.* **20** (2011) 411-424; *Condensed Matter Physics* **15** (2012) 33601.

[2] D.Ivaneyko, V.Toshchevnikov, M.Saphiannikova, G.Heinrich, *Soft Matter* **10** (2014) 2213-2225.

1OR-F-7

FIELD CONTROL OVER MONOLAYER FILMS OF SOFT MAGNETIC ELASTOMERS

*Stolbov O.V.*¹, *Raikher Yu.L.*^{1,2}, *Balasoiu M.*^{3,4}

¹ Institute of Continuous Media Mechanics, UrB RAS, Perm, Russia

² Perm National Research Polytechnic University, Perm, Russia

³ Frank Neutron Physics Laboratory, Joint Institute for Nuclear Research, Dubna, Russia

⁴ Horia Hulubei National Institute for Physics and Nuclear Engineering, Bucharest, Romania

Corresponding author: stolbov@icmm.ru

Elastomeric matrices filled with magnetic nano- or microparticles are known under several names: *magnetorheological elastomers*, *soft magnetic elastomers* (SME), *magnetoactive elastomers*, etc. None of them is exhaustively indicative, since there are always a number of essential characteristics to be added. Those are: the order of magnitude of the matrix elastic modulus, the reference size of the particles, and their material because, depending of the latter, the magnetic grains behave either as field-polarizable objects or as tiny permanent magnets.

Nowadays, as the most technologically prospective composites, are considered weakly-linked rubber-like systems filled with micron-size iron grains. These SMEs are sufficiently soft rheologically and sufficiently loaded magnetically as to display considerable magnetomechanical effects like large field-induced strains, notable field-tuning of the effective elastic modulus, certain type of shape-memory behavior and some other unique properties.

The most worked-on applications of SMEs' are field-controlled adaptable dampers and bearings. For that purposes the bulk samples, whose all linear dimensions are comparable: slabs, cubes, etc. are used. Our study is aimed at different case: we focus on SME films. These quasi-two dimensional samples are more flexible mechanically and, thus, more sensitive to the applied field than the bulk ones. However, the macroscopic behavior of a SME film is, in fact, the net result of the particle-matrix interactions, both of which are 3D on the mesoscopic scale. Due to that, to get a correct description, a SME film is to be always treated as 3-dimensional.

To reveal the specifics of films, we study the magnetomechanical effects occurring in monolayer structures, i.e., polymer slabs with the thickness of the order of the particle diameter. In such a sample the particle displacements and, thus, the film response crucially depends on the direction of the applied field. The in-plane one produces the deformation similar to that in a bulk sample except for the reduced number of neighbors. The deformation under a field normal to the film is a new mode always making the particles to move away from one another.

In numerical modeling, instead of a plain magnetic dipole-dipole energy, we use the effective interparticle potential, which accounts for the magnetic softness of the particles and, thus, for their non-uniform magnetization. The field-induced response of SME films is discussed and the crucial role of their internal structure—the shape of the particles and the type of the short-range arrangements—is demonstrated with a number of examples.

Support by RFBR grants # 13-01-96056 and 14-02-96003), Ural Branch of RAS Programme #10 (12-P-01-108) and project MIG S26/617 from Ministry of Education and Science of Perm Region is acknowledged.

1OR-F-8

INTERACTION OF MAGNETICALLY SOFT MICROPARTICLES EMBEDDED IN AN ELASTOMER MATRIX

Biller A.M.¹, Stolbov O.V.¹, Raikher Yu.L.^{1,2}

¹ Institute of Continuous Media Mechanics, UrB RAS, Perm, Russia

² Perm National Research Polytechnic University, Perm, Russia
kam@icmm.ru

The magnetostatic forces between two micron size spherical particles made of an isotropic linearly polarizable magnetic substance and subjected to a uniform external field are studied. Under these conditions, the magnetization distribution within a given particle depends on the position and magnetization of the neighboring one.

The solution for the magnetic energy U of the pair has the form of power series with respect to the ratio of the particle radius to the particle center-to-center distance. The coefficients of this series are found numerically taking in about hundred terms. Evaluation of the interparticle forces, which requires differentiation of the energy over coordinates, is facilitated by proposing an approximate formula for U , which enables one to avoid the laborious numeric procedure. In such a way, the distribution of interparticle forces is obtained and compared to that provided by the point magnetic moment model. It is shown that at close neighboring of the particles, the magnetic force differs substantially from that predicted by the dipole model.

When analyzing the sign of the force, it is found that the angular interval between the field and the particle center-to-center vector, which corresponds to repulsion, is much more narrow than that for point dipoles. This means that in a system of magnetizable particles attraction is the dominating type of interaction.

The problem is extended to magnetomechanics by considering the same pair of particles in an elastic matrix. There, the state of the system, when magnetized, is determined by interplay of magnetic and elastic forces. It is shown that in the field applied along the center-to-center direction, the configuration of the pair essentially depends on the field strength. In a low field the equilibrium interparticle gap changes but slightly since weak magnetic attraction induces weak restoring elastic forces. However, in stronger fields the system becomes bistable: besides the energy minimum located close to the initial interparticle gap, another minimum emerges, which corresponds to a close approach (clustering) of the particles. In the latter state both the magnetic and elastic forces are strong. Yet higher field eliminates the equilibrium at small deformation and the only stationary state of the particle pair is that of a cluster. Being not sensitive to thermal fluctuations, within the field strength interval of its bistability the system behaves in a distinctively hysteric way.

This effect has important implications in mechanics of soft magnetic elastomers. In particular, it explains the occurrence of “magnetic stapling” phenomenon, strong indications of which follow from experimental evidence.

Support by RFBR grants # 13-01-96056 and 14-02-96003), Ural Branch of RAS Programme #10 (12-P-01-1018) and project MIG S26/617 from Ministry of Education and Science of Perm Region is acknowledged.

1RP-F-9

ON THE MAGNETIC STRUCTURE OF POLYDIMETYLSELOXANE BASED ELASTOMERS POLYMERIZED WITH Fe₂O₄ FERROFLUID*Balasoiu M.^{1,2}, Loginova L.A.³, Almasy L.⁴, Bica I.⁵, Raikher Yu.L.⁶*¹ Joint Institute for Nuclear Research, Dubna, Russia² Horia Hulubei National Institute for Physics and Nuclear Engineering, Bucharest, Romania³ Faculty of Physics, Moscow State University, Moscow, Russia⁴ Research Institute for Solid State Physics and Optics, Budapest, Hungary⁵ West University of Timisoara, Department of Physics, Timisoara, Romania⁶ Institute of Continuous Media Mechanics, Ural Branch of RAS, Perm, Russia

balas@jinr.ru

The synthesis and the study of structure and physical properties of ferroelastomers materials combining the functional properties of highly elastic polymers and ferromagnetic substances should be considered as a perspective way to provide the understanding of construction principles of a wide class of materials for electronics, electrical engineering, medicine, aero- and cosmic industries. Also from the fundamental point of view it is needed a comprehensive analysis of the relationship between the macroscopic and microscopic properties of the disperse magnetic phase structures behaviors.

In the present paper structure and magnetic properties of ferroelastomers composed of polydimethylsiloxane with Fe₃O₄ ferrofluid [1] embedded during polymerization are studied by small-angle neutron scattering and magnetization measurements with the variation of magnetic component content.

[1] M. BalasoIU, V.T. Lebedev, D.N. Orlova, I. Bica and Yu.L.Raikher, *Journal of Physics: Conference Series*, **351** (1) (2012) 012014(9).

1OR-F-10

RHEOLOGY OF MAGNETIC ELASTOMERS BASED ON SOFT AND HARD MAGNETIC FILLER

*Sorokin V.V.*¹, *Stepanov G.V.*², *Vasiliev V.G.*³, *Kramarenko E.Yu.*^{1,3}, *Mayer M.*⁴, *Shamonine M.*⁴,
*Monkman G.*⁴

¹ Physics Department, Moscow State University, Moscow, Russia

² State Institute for Chemistry and Technology of Organoelement Compounds, Moscow, Russia

³ A.N. Nesmeyanov Institute for Organoelement Compounds RAS, Moscow, Russia

⁴ Ostbayerische Technische Hochschule Regensburg, Regensburg, Germany

v_sorokin@polly.phys.msu.ru

Nowadays much attention is paid to a development of a new type of magnetic elastomers (ME) demonstrating high responsiveness to external magnetic fields. They are based on rather soft polymer matrices filled with magnetic particles of nano- and/or micrometer size. Due to a coupling between polymer elasticity and magnetic forces acting between magnetic particles in a magnetic field these materials acquire a number of striking properties controlled by magnetic field. Particularly, ME are able to significantly change their rheological characteristics in presence of a homogeneous magnetic field of rather small density ($0-600\text{ mT}$).

In this work we study and compare rheological characteristics of ME based on magnetically soft (carbonyl iron) and magnetically hard (NdFeB) fillers. Silicone rubber is used as a matrix. Two types of matrices were synthesized differing in the Young modulus (soft and hard matrices). The filler content was varied in the range of 70 – 82 mass %. Isotropic and anisotropic samples were synthesized. After curing, the samples based of NdFeB were magnetized in the homogeneous magnetic field of different strengths ($0, 3, 6, 9, 12, 15\text{ kOe}$).

Rheological measurements were made using the commercial rheometer Anton Paar, model Physica MCR 301, with measuring “plate-plate” unit and a magnetic cell.

Dependencies of the storage modulus G' and the loss modulus G'' on the oscillation frequency f at a constant strain amplitude as well as on the strain amplitude at a constant frequency were obtained in the absence and presence of magnetic field B . Moduli of magnetically soft ME become strain-dependent in the magnetic field. The maximum increase of the moduli (2-3 orders of magnitude for G' and 2-3 orders of magnitude for G'') is observed at small strains. Normal force significantly increases in the presence of magnetic field as well. These phenomena could be explained by the process of structuring of magnetic particles within the matrix. Particles form chains aligned to the direction of magnetic field and these chains form some kind of a net structure that makes sample stiffer.

Magnetization of magnetically hard ME causes a change of their rheological behavior already without any additional magnetic field. In particular, their moduli increase with magnetization field and acquire well-pronounced strain dependence. Normal force in this case decreases with time, demonstrating a shape memory effect of ME induced by magnetic interactions.

Financial support of the Russian Foundation for Basic Research (project 13-03-12147) and the International Bureau of the BMBF (grant Nr. 01DJ13006) is gratefully acknowledged.

1OR-F-11

VISCOELASTIC PROPERTIES OF MAGNETIC FLUIDS WITH NANOFIBERS

Zubarev A.Yu¹, Chirikov D.N.^{1,2}

¹ Ural Federal University, Lenina Ave 51, 620083, Yekaterinburg, Russia

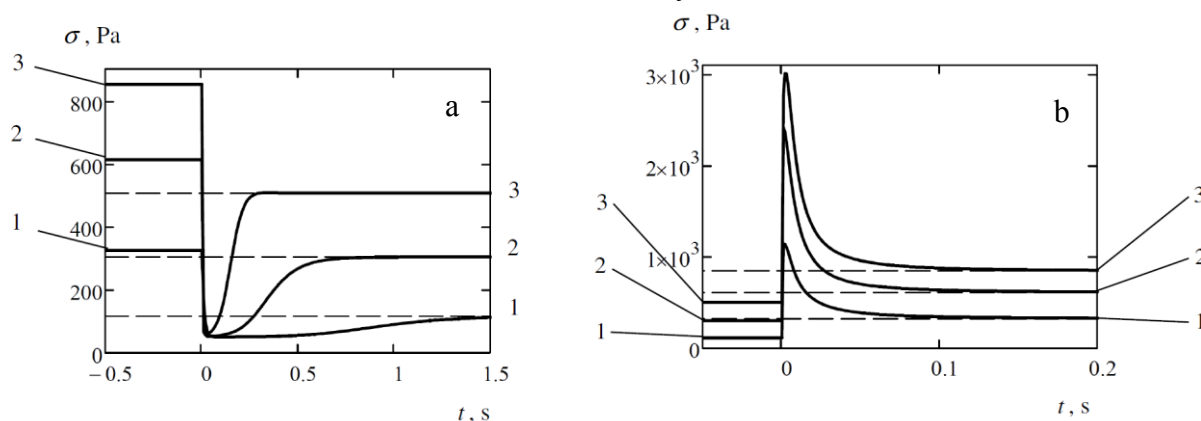
² Ozyorsk Engineering Institute an affiliate of Moscow Engineering-Physical State University, Ozyorsk, Russia

Andrey.Zubarev@usu.ru, cloud28021985@gmail.com

Rheological properties of magnetic suspensions with the fiber nanoparticles considerably differ from those of the suspensions with the spherical particles. In part they demonstrate the N-like dependence of the macroscopical shear stress on the shear rate of the suspension flow [1]. This feature of the rheogram is explained in ref. [2] on the basis of the suggestion, that the nanofibers form two types of the bulk strongly elongated aggregates with the net-like structures. This model is a simplification of the real situation in which a more or less continuous distribution of the aggregates over the friction forces is expected. In spite of this simplification, the model predictions of the stationary magnetoviscous effects and the shape of the stationary rheograms are in quantitative agreement with the experimental results.

Nonstationary viscoelastic effects in ferrofluids with nanofibers are of interest both in terms of the fundamental research and applied perspective. We propose a model of the viscoelastic behavior of these ferrofluids, based on the same ideas as in [2] on the microscopic structure of the suspension with the discussed types of the aggregates.

The figures show the results of calculations of the macroscopical shear stress as functions of the time after instant change of the shear rate (a) – from 200 s⁻¹ to the 10 s⁻¹; (b) – from 10 s⁻¹ to the 200 s⁻¹. Applied magnetic field (1) – 200 kA/m; (2) – 300 kA/m; (3) – 400 kA/m. The physical parameters of the systems are the same as in [1,2]. The viscoelastic effects with strong overshoots and the relaxation time about 0.1 sec can play important role in the work of various dampers, shock and vibration absorbers, as well as in the work of many other devices.



This work has been done under support of Russian Fund of Fundamental Investigations, grants 12-01-00132, 13-02-91052, 13-01-96047 and 14-08-00283; by the Act 211 Government of the Russian Federation № 02.A03.21.0006. One of us (D.Ch.) is grateful to the Development Program for the young scientists of the Ural Federal University

[1] M.T. Lopez-Lopez, A. Gomez-Ramirez, L. Rodriguez-Arco, J. D. G. Duran, L. Iskakova and A. Zubarev, *Langmuir*, **28**, (2012) 6232.

[2] A.Zubarev, M.T.Lopez-Lopez, L.Iskakova, F.Gonzalez-Caballero, *Soft Matter*, **9** (2013) 1902.

1 July

Tuesday

14:30-17:00

oral session

1TL-G

1OR-G

“Magnetic Oxides”

1TL-G-5

STRONG COVALENCY AND LIGAND HOLES, OR HOW TO MAKE MAGNETIC GOLD?

Khomskii D.I.

II. Physikalisches Institut, Universität zu Köln, Köln, Germany
khomskii@ph2.uni-koeln.de

In this talk, I will discuss some effects occurring in transition metal compounds with small or negative charge transfer gap and with large contribution of ligand (e.g. oxygen) holes. Special attention will be paid to the compounds of $4d$ and $5d$ elements. The apparent inversion of crystal field levels, as well as the tendency to spontaneous charge disproportionation will be discussed. Specifically, some systems containing gold, such as $\text{Cs}_2\text{Au}_2\text{Cl}_6$ and AuTe_2 will be discussed, and the question formulated in the title will be addressed.

1TL-G-6

LOW-ENERGY SPIN DYNAMICS OF THE SPIN-ORBITAL MOTT INSULATOR Sr_2IrO_4

Kataev V.

Leibniz Institute of Solid State and Materials Research IFW Dresden, D-01069 Dresden, Germany
Corresponding author e-mail address: v.kataev@ifw-dresden.de

The $5d$ layered metal oxide Sr_2IrO_4 has been recently proposed to be a novel kind of insulator where the Mott insulating state arises due to electron correlation effects combined with strong relativistic spin-orbit coupling. Owing to a complex spin-orbital character of the effective spin $J_{\text{eff}} = 1/2$ ground state of Ir^{4+} ions a rich variety of magnetically ordered phases in iridium oxides ranging from a Heisenberg to exotic quantum compass and Kitaev models have been predicted theoretically.

Experimentally one observes in Sr_2IrO_4 below $T_N = 230$ K a canted antiferromagnetically (AFM) “easy-plane” ordered spin structure with an anomalously large “hidden” ferromagnetic (FM) moment.

We have studied low-energy magnetic excitations at the AFM zone center in a single crystal of Sr_2IrO_4 by high field ESR spectroscopy in the sub-THz frequency domain. We can identify both the “low” frequency mode due to the precession of the FM moments and the “high” frequency modes due to the precession of the AFM sublattices.

Surprisingly, despite the spin-orbital entanglement in the ground state, the energy gap for the out-of-plane AFM excitations appears to be very small, amounting to 0.83 meV only. This suggests a rather isotropic Heisenberg dynamics of Ir spins in the AFM ordered state. We compare our ESR data with recent inelastic x-ray scattering and inelastic neutron scattering results on iridium oxides and discuss possible reasons for the smallness of the magnon gap in Sr_2IrO_4 .

This work has been done in cooperation with S. Bahr, A. Alfonsov, B. Büchner (IFW Dresden), G. Jackeli, G. Khaliullin, T. Takayama (Max Planck Institute for Solid State Research, Stuttgart), A. Matsumoto (Department of Physics and Department of Advanced Materials, University of Tokyo) and H. Takagi (Max Planck Institute for Solid State Research, Stuttgart and Department of Physics and Department of Advanced Materials, University of Tokyo).

1TL-G-7

DESCRIPTION OF THE MAGNETIC PROPERTIES OF STRONGLY CORRELATED DISORDERED SOLID SOLUTIONS IN THE COHERENT POTENTIAL APPROXIMATION

Korotin M.A.

Institute of Metal Physics, Ekaterinburg, Russia
michael.korotin@imp.uran.ru

Recently we have proposed both the new version of the coherent potential approximation (CPA), and the original computer codes complex, which realizes this approach, for calculation and prediction of the physical properties of real disorder materials, including those containing impurities [1]. The CPA which is being developed is formulated and realized in the spirit of modern ideas of the dynamical mean-field theory. It does not depend on the methods of calculation of the electronic properties of ideal crystals, since it is designed in the flexible basis of the localized Wannier functions. In new CPA the possibility of simultaneous consideration of several impurities is realized; moreover, both atom of other sort and vacancy can act as an impurity. Strong electronic correlations in the static limit are considered in this CPA also.

In my talk I will focus on the CPA results of the evolution of electronic spectra and magnetic properties for $3d$ metal compounds such as NiO–ZnO solid solution where the content of $3d$ metal sublattice is varied [2], perovskite systems in dependence on oxygen deficiency LaMnO_{3-x} and SrFeO_{3-x} , and for rare-earth intermetallic compound GdNi_2Mn_x with manganese impurity both in gadolinium and nickel sites doped simultaneously.

In particular, the total density of states of $\text{LaMnO}_{2.95}$ obtained in the CPA is presented in Figure. The spectrum of $\text{LaMnO}_{2.95}$ has insulating character. Two new features inside the band gap of stoichiometric LaMnO_3 appear: above the top of valence band (**A**) and below the bottom of conduction band (**B**). As a result of oxygen nonstoichiometry, the value of the calculated band gap is decreased from 1.7 eV to 1.2 eV, the value of d -Mn spin magnetic moment is decreased insignificantly from $3.57 \mu_B$ to $3.56 \mu_B$. The energy dependence of calculated coherent potentials clarifies the nature of the occurrence of these peaks. Peak **A** is originated from the coherent potential of majority states of s -symmetry. Peak **B** is originated from the coherent potential of minority states of p -symmetry.

Support by the basic research program of UB RAS, project 12-P-2-1021 is acknowledged.

[1] M.A. Korotin et al., *JETP Lett.*, **94** (2012) 806-810.

[2] M.A. Korotin et al., *J. Phys.: Condens. Matter*, **26** (2014) 115501 (6 pp).

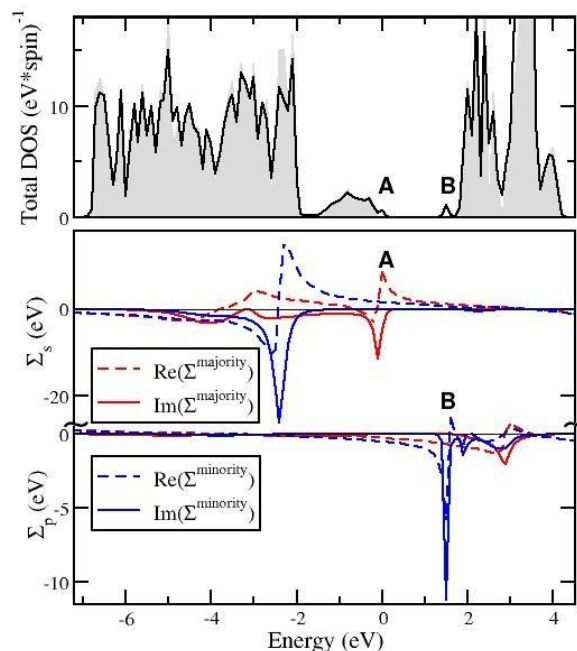


Fig. *Top panel*: Total density of states for $\text{LaMnO}_{2.95}$ (full line) in comparison with that for LaMnO_3 (gray area). Coherent potentials on real energy axis of s - (*middle panel*) and p - (*bottom panel*) symmetry.

1OR-G-8

MAGNETO-ELECTRONIC PHASE SEPARATION IN $\text{La}_{0.7}\text{Sr}_{0.3}\text{MnO}_3$ WITH METALLIC BEHAVIOUR IN PARAMAGNETIC REGION

Ryzhov V.A.¹, Khavronin V.P.¹, || Mukovskii Ya.M.² ||, Chichkov V.I.²

¹ Petersburg Nuclear Physics Institute, NRC ‘Kurchatov Institute’, Gatchina 188300, Russia

² National Research and Technology University ‘MISiS’, Moscow 119049, Russia

ryzhov@omrb.pnpi.spb.ru

The important role in forming magnetic and transport properties of the hole doped manganites belongs to one of the forms of microscopic magneto-electronic phase separation (MEPS) that occurs below some temperature T^* above T_C and consists in the origination of the ferromagnetic (FM) metal (M) clusters (via double exchange) in the paramagnetic (PM) insulator (I) phase [1]. It was recently found that cluster subsystem is formed in two stages [2]. Initially the FM clusters originate in the preferable sites associated with the chemical inhomogeneities which are related to doping and oxygen nonstoichiometry. On further cooling, below some temperature $T^\# > T_C$ fast growth of the isolated clusters density (homogeneous nucleation) starts, which continues down to T_C where FM ordering of the matrix develops. This stage can be accompanied by percolating insulator-metal (I-M) transition above or below T_C at appropriate level of doping [2]. To elucidate whether this MEPS has a universal character and originates as well in manganites with a metallic character of resistivity in PM region, the single crystalline $\text{La}_{1-x}\text{Sr}_x\text{MnO}_3$ $x = 0.3$ was studied. The data on its magnetic properties (the ac linear, χ'' , and nonlinear (second M_2 and third order M_3) susceptibilities) as well as on resistance are presented here.

This metallic compound reveals the rhombohedral $R3c$ space group. Resistance of the sample exhibits a kink to faster decreasing at cooling below T_C . $M_2(H, T)$ measurements, allowing to observe specific signal from FM clusters, indicate their nucleation in $\text{La}_{0.7}\text{Sr}_{0.3}\text{MnO}_3$ by two stage similar to that in insulating compounds [3]. *The second stage of homogeneous nucleation occurs below $T^\# \approx 366$ K ($T^* > 430$ K), which is unusually close to $T_C \approx 363$ K of matrix.* Cluster presence is evidenced by the appearance of region with larger slope in weak H in $\text{Re}M_2(H)$ (H is steady magnetic field) and of a weak signal of opposite sign against the matrix signal in $\text{Im}M_2(H)$ at $T \leq T^\#$, see Fig.1, $T = 364$ K. Fig.1 displays also $M_2(H)$ response of $\text{La}_{0.83}\text{Sr}_{0.17}\text{MnO}_3$ at $T = 295$ K $> T_C \approx 263$ K $> T_{IM} \approx 252$ K with I state in PM region, which exhibits MEPS below $T^* = 313$ K [2]. In its $\text{Im}M_2$ component a like cluster signal can be seen.

As Fig.1 displays, cluster signal is more hysteretic at less doping $x = 0.17$. It is better observed in $\text{Re}M_2$ of this compound since matrix contribution is smaller there (the response is obtained at larger $\tau = (T - T_C)/T_C$) than in $\text{La}_{0.7}\text{Sr}_{0.3}\text{MnO}_3$. The arising of FM cluster subsystem in the latter is confirmed by a deviation of $1/4\pi\chi'(T)$ from the Curie-Weiss law to T axis below $T^\# > T_C$ (this used usually for detection of FM cluster origination [4]). The obtained results indicate a universality of EMPS above T_C for a class of hole doped manganites, exhibiting metallic behavior in this T -region.

[1] E. Dagotto, *New J. Phys.*, **7** (2005) 1–28.

[2] V.A. Ryzhov, A.V. Lazuta, P.L. Molkanov et al., *J. Magn. Magn. Mater.*, **324** (2012) 3432–6.

[3] V.A. Ryzhov, A.V. Lazuta et al., *J. Phys.: Cond. Matt.*, **26** (2014) 076001–10.

[4] M.B. Salamon, P. Lin, S.H. Chun, *Phys. Rev. Lett.*, **88** (2002) 197203-4.

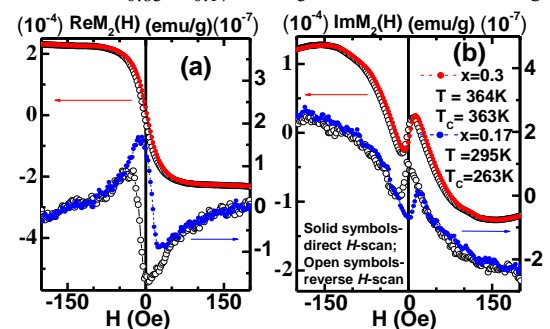


Fig.1. Phase components of M_2 vs. steady field H at some T above T_C for $\text{La}_{1-x}\text{Sr}_x\text{MnO}_3$ $x = 0.17, 0.3$ ($T^* = 313$ K [2], and > 430 K respectively) single crystals.

1TL-G-9

SPIN DENSITY WAVE STATES AND PHASE SEPARATION IN DOPED IRON PnictIDES

Kugel K.I.¹, Rakhmanov A.L.¹, Rozhkov A.V.¹, Sboychakov A.O.¹, Nori F.²

¹ Institute for Theoretical and Applied Electrodynamics, Russian Acad. Sci., Moscow, Russia

² Center for Emergent Matter Science, RIKEN, Saitama, Japan

kugel@orc.ru

A possible mechanism of electronic phase separation in the normal state of iron-based superconducting materials is proposed. It is based on the imperfect nesting of different portions of the Fermi surface in doped iron pnictides and chalcogenides. Similar approach [1] can be applied also to other materials with imperfect nesting, such as AA stacked graphene bilayer [2], chromium alloys, etc. We model the Fermi surface by two elliptical electron pockets and three nearly circular hole pockets.

The ellipticity of the electron bands is characterized by parameter α , where $\alpha = 0$ describes the circle and $\alpha \rightarrow \infty$ corresponds to the limit of infinitely thin ellipse. The coupling of charge carriers belonging to one electron and one hole bands by a weak electron-electron interactions leads to the formation of the commensurate spin-density wave (SDW) order. The commensurate SDW in the parent compound transforms to the incommensurate phase when doping is introduced. We show that, for certain values of the ellipticity and doping level x , the uniform state is unstable with respect to the phase separation. The resulting inhomogeneous state consists of regions of commensurate and incommensurate SDW phases with different charge carrier densities [3]. The phase diagram in the doping-ellipticity plane is illustrated in Fig. 1. Our results are in qualitative agreement with recent observations of incommensurate spin density waves and electronic inhomogeneity in iron pnictides.

The work was supported by the Russian Foundation for Basic Research (projects 11-02-00708, 12-02-92100_Jap, and 14-02-00276). A.O.S. acknowledges support from the RFBR project 12-02-31400 and the Dynasty Foundation.

[1] A.L. Rakhmanov, A.V. Rozhkov, A.O. Sboychakov, F. Nori, *Phys. Rev. B*, **87** (2013) 075128.

[2] A.L. Rakhmanov, A.V. Rozhkov, A.O. Sboychakov, F. Nori, *Phys. Rev. Lett.*, **109** (2012) 206801; *Phys. Rev. B*, **87** (2013) 121401.

[3] A.O. Sboychakov, A.V. Rozhkov, K.I. Kugel, A.L. Rakhmanov, F. Nori, *Phys. Rev. B*, **88** (2013) 195142.

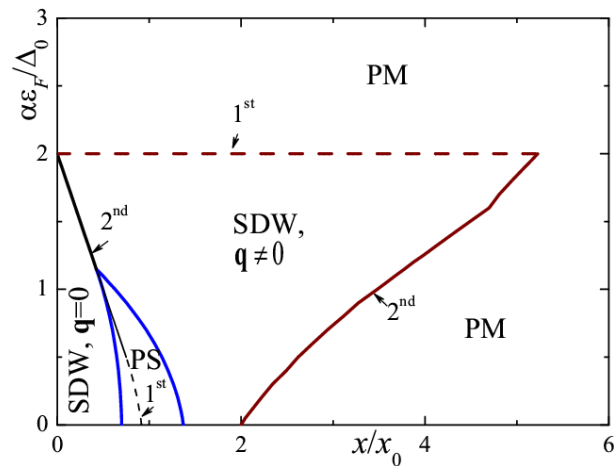


Fig. 1. Phase diagram in the normalized doping-ellipticity plane. Dashed and solid lines denote 1st and 2nd order phase transitions, respectively; PM is the paramagnetic phase. The region of phase separation (PS) is also bordered by solid lines; the line within the PS region illustrates the phase boundary between homogeneous states in the absence of PS.

1 July

Tuesday

14:30-17:00

oral session

1TL-H

1OR-H

**“Topological
Insulators”**

1TL-H-4

THEORETICAL ENGINEERING OF TOPOLOGICAL INSULATOR SYSTEMS: ELECTRONIC STRUCTURE AND MAGNETIC EFFECTS

Chulkov E.V.^{1,2,3}, Ereemeev S.V.^{4,5}, Ernst A.⁶, Koroteev Yu.M.^{4,5}, Meshchikova T.V.⁴, Menshov V.N.⁷, Nechaev I.A.^{1,4}, Otrokov M.M.^{1,4}, Tsirkin S.S.^{1,4}, Tugushev V.V.⁷, Vergniory M.^{1,6}

¹ Donostia International Physics Center (DIPC), 20018 San Sebastián, Basque Country, Spain

² Departamento de Física de Materiales, UPV/EHU, Apdo. 1072, 20080 San-Sebastián, Spain

³ CFM - MPC, Centro Mixto CSIC - UPV/EHU, 20018 San Sebastián, Spain

⁴ Tomsk State University, pr. Lenina 36, 634050, Tomsk, Russian Federation

⁵ Institute of Strength Physics and Materials Science, pr. Akademicheskii 2/4, 634021, Tomsk, Russian Federation

⁶ Max-Planck-Institut für Mikrostrukturphysik, Weinberg 2, D-06120, Halle, Germany

⁷ National Research Centre “Kurchatov Institute”, 123182, Moscow, Russian Federation
evguenivladimirovich.tchoulkov@ehu.es

Spin-orbit interaction underlies many bulk and surface phenomena with intriguing potential applications. It plays especially important role in the surface electronic structure leading to massless states on a surface of many narrow gap semiconductors (topological insulators) [1-10]. Topological insulators (TIs) exhibit robust Dirac-like surface states protected by time-reversal symmetry. Breaking time-reversal symmetry causes splitting of the topological surface state at the Dirac point thus making the surface insulating. Here we present and discuss recent results for complex topological insulator systems that include pristine TIs, topological insulators with overlayers, topological insulator alloys, and TIs under external electric field. Magnetic and nonmagnetic impurities [11] and magnetic proximity [12,13] effects on electronic structure of these materials and splitting of the topological surface state are also discussed in detail.

- [1] M.Z. Hasan, C. L. Kane, *Rev. Mod. Phys.* **82** (2010) 3045-3067.
- [2] K. Kuroda et al., *Phys. Rev. Lett.* **105** (2010) 076802.
- [3] S.V. Ereemeev et al., *Phys. Rev. B* **83** (2011) 205129.
- [4] T.V. Meshchikova et al., *JETP Lett.* **93** (2011) 15-20.
- [5] S.V. Ereemeev et al., *Nature Commun.* **3** (2012) 635.
- [6] K. Miyamoto et al., *Phys. Rev. Lett.* **109** (2012) 166802.
- [7] D. Niesner et al., *Phys. Rev. B* **86** (2012) 205403.
- [8] T. Okuda et al., *Phys. Rev. Lett.* **111** (2013) 206803.
- [9] T.V. Meshchikova et al., *Nano Lett.* **13** (2013) 6064-6069.
- [10] G. Landolt et al., *Phys. Rev. Lett.* **112** (2014) 057601.
- [11] J. Henk et al., *Phys. Rev. Lett.* **109** (2012) 076801.
- [12] S. V. Ereemeev et al., *Phys. Rev. B* **88** (2013) 144430.
- [13] V. N. Menshov et al., *Phys. Rev. B* **88** (2013) 224401.

1TL-H-5

MAGNETOOPTICS IN TOPOLOGICAL INSULATORS*Lozovik Yu.E.*^{1,2}¹ ISAN, Troitsk, Moscow, Russia² Moscow Institute of Physics and Technology, Dolgoprudnii, Russia
lozovik@isan.troitsk.ru

Topological insulators (TI) is the new state of matter that is intensively studied now both theoretically and experimentally. Properties of topological insulators will be shortly reviewed and new results on magneto-optics and collective phenomena in TI will be discussed. 3D topological insulators have insulating bulk and topologically protected helical states on the surface that can be described by Dirac-like equation for massless particles analogously to electrons in graphene. Similarity and distinctions between chiral Dirac electrons in graphene and on the surface of topological insulator will be discussed. Collective excitations and different phases in Dirac electrons in topological insulator, graphene and graphene based structures are considered.

Properties of new quasiparticles, dyons - coupled electrons and magnetic monopole-like polarization originated from magnetoelectric effect in topological insulators will be discussed.

The collective excitations on a surface of three-dimensional topological insulator are discussed. Electrons on surface of topological insulator obeys Dirac-like equation for massless particles and direction of its spin is strictly determined by its momentum. Due to this spin-momentum locking, collective excitations in the system manifest themselves as coupled charge- and spin-density waves.

Quantized magnetoelectric effect and its manifestation in Quantized Faraday and Kerr effects in chiral 2D Dirac electron layer on the surface of topological insulator will be discussed. Resonance enhancement of Faraday effect by chiral excitons is considered.

[1] Yu.E.Loosovik , *Physics: Uspekhi*, **55** (2012), No.10, 1035-1039.

[2] D. K. Efimkin, Yu. E. Loosovik, A. A. Sokolik, *Phys. Rev. B* **86** (2012), 115436.

[3] Efimkin D.K., Loosovik Yu.E., Sokolik A.A., *Nanoscale Research Letters*, **7** (2012)163.

[4] D. K. Efimkin and Yu. E. Loosovik, *Phys.Rev.B* **87** (2013), 245416.

[5] D. K. Efimkin and Yu. E. Loosovik, *Phys. Rev. B* **88** (2013), 085414.

[6] Yu.E.Loosovik (to be publ.).

1TL-H-6

INTERACTION AND DISORDER EFFECTS IN 3D TOPOLOGICAL INSULATOR THIN FILMS

Konig E.J.^{1,2}, Ostrovsky P.M.^{3,4}, Protopopov I.V.^{5,4}, Gornyi I.V.^{5,6}, Burmistrov I.S.⁴, Mirlin A.D.^{5,1,2,7}

¹ Inst. für Theorie der kondensierten Materie, Karlsruhe Institute of Technology, 76128 Karlsruhe, Germany

² DFG Center for Functional Nanostructures, Karlsruhe Institute of Technology, 76128 Karlsruhe, Germany

³ Max-Planck-Institute for Solid State Research, D-70569 Stuttgart, Germany

⁴ L.D. Landau Institute for Theoretical Physics RAS, 119334 Moscow, Russia

⁵ Institute of Nanotechnology, Karlsruhe Institute of Technology, 76021 Karlsruhe, Germany

⁶ A.F. Ioffe Physico-Technical Institute, 194021 St. Petersburg, Russia

⁷ Petersburg Nuclear Physics Institute, 188300 St. Petersburg, Russia
burmi@itp.ac.ru

A theory of combined interference and interaction effects on the diffusive transport properties of 3D topological insulator surface states is developed. We focus on a slab geometry (characteristic for most experiments) and show that interactions between the top and bottom surfaces are important at not too high temperatures. We treat the general case of different surfaces (different carrier densities, uncorrelated disorder, arbitrary dielectric environment, etc.). In order to access the low-energy behavior of the system we renormalize the interacting diffusive sigma model in the one loop approximation. It is shown that intersurface interaction is relevant in the renormalization group (RG) sense and the case of decoupled surfaces is therefore unstable. An analysis of the emerging RG flow yields a rather rich behavior. We discuss realistic experimental scenarios and predict a characteristic non-monotonic temperature dependence of the conductivity. In the infrared (low-temperature) limit, the systems flows into a metallic fixed point. At this point, even initially different surfaces have the same transport properties. Investigating topological effects, we present a local expression of the \mathbb{Z}_2 theta term in the sigma model by first deriving the Wess-Zumino-Witten theory for class DIII by means of non-abelian bosonization and then breaking the symmetry down to AII. This allows us to study a response of the system to an external electromagnetic field. Further, we discuss the difference between the system of Dirac fermions on the top and bottom surfaces of a topological insulator slab and its non-topological counterpart in a double-well structure with strong spin-orbit interaction. The result are published in [1].

Support by BMBF, DAAD, DFG, RAS, Russian Ministry of Science and Education, RFBR is acknowledged.

[1] E.J. Konig, P.M. Ostrovsky, I.V. Protopopov, I.V. Gornyi, I.S. Burmistrov, A.D. Mirlin, *Phys. Rev. B*, **88** (2013) 035106.

1TL-H-7

TOPOLOGICAL INSULATOR IN JUNCTION WITH FERROMAGNETS: QUANTUM HALL EFFECTS

Kagalovsky V.¹, Chudnovskiy A.L.²

¹ Shamoon College of Engineering, Beer-Sheva, Israel

² Institut für Theoretische Physik, Universität Hamburg, Germany
victork@sce.ac.il

The ferromagnet-topological insulator-ferromagnet (FM-TI-FM) junction exhibits thermal and electrical quantum Hall effects. The generated Hall voltage and transverse temperature gradient can be controlled by the directions of magnetizations in the FM leads, which inspires the use of FM-TI-FM junctions as electrical and as heat switches in spintronic devices. Thermal and electrical Hall coefficients are calculated as functions of the magnetization directions in ferromagnets and the spin-scattering time in TI. Both the Hall voltage and the transverse temperature gradient decrease but are not completely suppressed even at very short spin-scattering times. The Hall coefficients turn out to be independent of the spin-scattering time for symmetric configuration of FM leads.

The discovery and experimental realization of topological insulators opened a new and vividly developing field of theoretical and experimental investigations [1,2]. Two-dimensional TI belong to the class of quantum spin Hall systems [1,2], that are distinguished by the existence of chiral spin-polarized edge states. There are two chiral states with opposite spin-projections at each edge that propagate in the opposite directions. The existence of the edge states implies strong similarity between the properties of TI and of a quantum Hall system, although no external magnetic field is applied. It has been suggested in the early papers on quantum spin Hall effect that the properties of spin-polarized edge states can be probed by injecting spin-polarized currents in TI [1,2].

In this paper we show, that the quantum Hall conductance and the thermal Hall coefficient can be revealed in the experimental measurements on a two-dimensional TI sandwiched between the two ferromagnets in a FM-TI-FM junction. The use of ferromagnets allows spin-selective contacting of the edge states in TI. Thus, it provides the way to break the generic symmetry between the spin-up and spin-down states, recovering the electrical and thermal quantum Hall effects hidden in the isolated TI. In the ideal situation of completely polarized ferromagnets it is possible to contact a single chiral spin-polarized edge state. Thus one would measure quantized values of electrical and thermal Hall coefficients proper to the lowest Landau level of the integer quantum Hall effect

$$G_q = \frac{dI}{dV_H} = \frac{e^2}{h}, \quad K_q = \frac{dQ}{dT_\perp} = \frac{\pi^2 k_B^2 T}{3h}.$$

[1] C. L. Kane, E. J. Mele, *Phys. Rev. Lett.* **95**, (2005) 146802; C. L. Kane, E. J. Mele, *ibid.*, **95** (2005) 226801.

[2] B. Andrei Bernevig and Shou-Cheng Zhang, *Phys. Rev. Lett.*, **96** (2006) 106802.

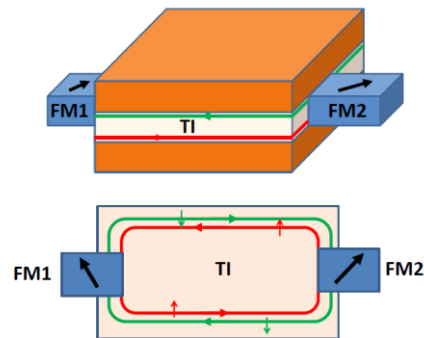


Fig. 1. Proposed experimental setup of FM-TI-FM junction. Spin- \uparrow and spin- \downarrow edge states have opposite chirality.

10R-H-8

ATOMIC STRUCTURE AND PROPERTIES OF MAGNETIC ADSORBATES ON THE TOPOLOGICAL INSULATOR Bi_2Se_3

*Meyerheim H.L.*¹, *Ernst A.*^{1,2}, *Roy S.*¹, *Maznichenko I.V.*³, *Mohseni K.*¹, *Tusche C.*¹, *Manna S.*¹, *Shokri R.*¹, *Vergniory M.G.*¹, *Chulkov E.*⁴, *Mertig I.*^{1,3}, *Kirschner J.*^{1,3}

¹ MPI f. Mikrostrukturphysik, 06120 Halle, Germany

² Wilhelm-Ostwald-Institut f. Phys.& Th. Chemie, Univ. Leipzig, 04103 Leipzig, Germany

³ Institut f. Physik, Martin-Luther-Univ., D-06099 Halle, Germany

⁴ DIPC, PaseoManuel de Lardizabal 4, 20080 San Sebastian, Spain

hmeyerhm@mpi-halle.mpg.de

Topological insulators (TI) represent an unusual state of matter. While they are insulators in the bulk they are metals at the surface. Tremendous interest has arisen in the recent past primarily focused on the study of the electronic and transport properties of uncovered and adsorbate covered TIs. The latter is motivated by the question whether the topological state is robust against adsorption of magnetic and non-magnetic adsorbates [1,2]. By contrast, atomically resolved structure studies relating electronic properties to the geometric structure are hardly available.

We have carried out combined experimental and theoretical studies on uncovered and adsorbate covered $\text{Bi}_2\text{Se}_3(0001)$ after *in-situ* deposition of ultra-thin films of Fe and Cr. We have analyzed the atomic structure by surface-x-ray diffraction, in combination with scanning tunneling microscopy/spectroscopy (STM/STS), and angular resolved photoemission (ARUPS). Experiments were complemented by *ab-initio* calculations. Our investigations have revealed many unexpected results. This presentation gives an overview over some of them. For instance:

(i): The top layer spacing (Se/Bi) of bare bulk $\text{Bi}_2\text{Se}_3(0001)$ shows an expansion in the 2-10 percent range relative to the bulk. This depends on the (very small) amount of carbon contamination always present in bulk samples. ARUPS and theory confirm the concomitant shift of the bulk states relative to the (intact) Dirac cone. (ii): Adsorbed Cr-atoms reside in threefold hollow sites next to surface Se atoms (Fig.1) and form a distorted hexagonal overlayer which is ferrimagnetic ($T_C \approx 50$ K) with an in-plane easy axis magnetization as confirmed by Magneto-optic Kerr effect (MOKE) experiments and theory. (iii): Fe adsorption at room temperature in the monolayer range induces an approx 20-30% Fe/Bi substitution within the first quintuple layer. At elevated temperatures ($T > 140^\circ\text{C}$) the formation of a ≈ 15 Å thick orthorhombically distorted FeSe film sets in. Its lattice parameter is compressed by 5% relative to the tetragonal bulk structure (3.56 Å vs. 3.77 Å) along one in-plane axis. STS shows signatures linked to superconductivity up to $T = 30$ K at least. In all studies no substantial fraction of intercalated atoms within the first van-der-Waals gap is found.

Support by DFG through SPP1666 is acknowledged.
[1] L. A. Wray, S.Y. Xu, Y. Xia, et al. *Nature Phys.*, **7** (2010) 32.
[2] T. Valla, Z.-H. Pan, D. Gardner, Y.S. Lee, and S. Chu, *Phys. Rev. Lett.* **108** (2012) 117601.

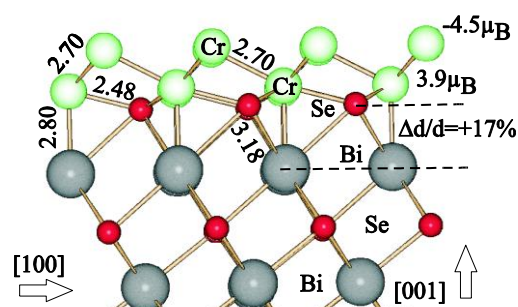


Fig. 1. Model of the structure of Cr on $\text{Bi}_2\text{Se}_3(0001)$. Distances in Å, magnetic moments in μ_B .

1OR-H-9

SPIN-POLARIZED BOUND ELECTRON STATES AT THE 3D TOPOLOGICAL INSULATOR/FERROMAGNETIC INSULATOR INTERFACE

Eremeev S.V.^{1,3,5}, Menshov V.N.^{1,2,3}, Tugushev V.V.^{1,2,3,4}, Chulkov E.V.^{1,3}

¹ Donostia International Physics Center, P.de Manuel Lardizabal,4, Donostia/San Sebastian, 20018, Basque Country, Spain

² National Research Centre Kurchatov Institute, Kurchatov Sqr. 1, 123182, Moscow, Russia

³ Tomsk State University, pr. Lenina 36, 634050, Tomsk, Russia

⁴ Prokhorov General Physics Institute, Vavilov st. 38, 119991, Moscow, Russia

⁵ Institute of Strength Physics and Materials Science, 634021, Tomsk, Russia
tuvictor@mail.ru

The electronic rearrangement at the interface, accompanied by appearance of spin-polarized bound states at the boundary, is inherent in heterostructures composed of a conventional semiconductor and a magnetic material. This feature underlies the magnetic proximity effect (MPE) when spin ordering penetrates inside semiconductor over the interface. The question then arises as to what kind of the MPE peculiarities can be caused by the replacement of the conventional band semiconductor by a time-reversal-invariant semiconductor with inverted band gap, which is known as a three dimensional topological insulator (3D TI) [1]. The basic feature of the heterostructures containing the 3D TI layers is the topologically protected electron helical states with the linear Dirac-cone-like energy-momentum dispersion living at a boundary between topologically nonequivalent regions. When a TI is in the contact with a ferromagnetic insulator (FMI), these states are influenced by a presence of magnetic ordering via time-reversal symmetry breaking and are described within a simple phenomenological Hamiltonian of the 2D Dirac-like states with spin-momentum locking for helical electrons in an homogeneous exchange field, which is simply postulated without a serious analysis of its microscopic origin (see, for example [2]).

In this work we theoretically study MPE at the 3D TI/FMI interface. Within the continual approach based on the KP Hamiltonian we predict that two types of bound electron states (referred as the topological and ordinary state, respectively) appear at the TI side of the interface. These states have different physical origins, spatial distributions and energy spectra. Namely, the bound topological state stems from a breaking of the Z_2 invariant of TI at the boundary with FMI. This state is located relatively distant from the interface and is weakly spin polarized; its spectrum is almost gapless and lies inside the bulk energy gap of TI. In contrast, the bound ordinary state results from the crystal symmetry breaking at the TI/MI interface. This state is located nearby the interface and is strongly spin polarized; its spectrum is gapped and lies far below the bulk energy gap of TI due to the band bending at the TI side of the interface. Effective Hamiltonian of bound states contains two coupled 2D electron bands (metallic band with strong exchange splitting and Dirac-like band with small exchange splitting) having different magnetic and transport characteristics. To elucidate analytical results, we perform numerical density functional theory calculations and discuss recently reported magnetic [3] and transport [4] measurements for the $\text{Bi}_2\text{Se}_3/\text{EuS}$ structures.

[1] M.Z. Hasan and C.L. Kane, *Rev.Mod. Phys.*, **82** (2010) 3045.

[2] I.Garate and M. Franz, *Phys.Rev.Lett.*, **104** (2010) 146802.

[3] P.Wei et al., *Phys.Rev.Lett.*, **110** (2013) 186807.

[4] Q.I.Yang et al., *Phys. Rev.B*, **88** (2013) 081407(R).

1 July

Tuesday

17:30-19:00

poster session

1PO-I1

**“Magnetic
Nanostructures and
Low Dimensional
Magnetism”**

1PO-11-1

EFFECT OF THE INTERDISKS DISTANCE ON CONFIGURATIONAL ANISOTROPY IN ARRAYS OF MAGNETIC NANOSTRUCTURES

Stebliy M.E., Ognev A.V., Samardak A.S., Kolesnikov A.G., Chebotkevich L.A.

Laboratory of Thin Film Technologies, School of Natural Sciences, Far Eastern Federal University, Vladivostok 690950, Russia
ognevav@gmail.com

In this abstract an influence of the lattice symmetry of arrays and distance between nanodisk on the anisotropy of magnetization processes is shown. The arrays were patterning by means of electron-beam lithography. Polycrystalline Py disks with thickness 30 nm and diameter 600 nm were fabricated by magnetron sputtering in UHV. Magnetic properties were investigated by the magneto-optical Kerr effect magnetometer. Disks were arranged into different two-dimensional lattices: square, rectangular, oblique with an angle at the base $\theta = 100^\circ$ and 115° , and hexagonal. Schemes and SEM images of arrays are shown in Fig.1. The distance between the disks' centres (a and b) was varied in dependence on the lattice type, and it was not more than 900 nm.

Using micromagnetic simulation and analytical calculation we demonstrated that oscillations of the critical field caused by the symmetry of dipole-dipole interaction.

We found that the anisotropy of magnetization processes was determined by the lattice symmetry. If the difference between a and b more than 7%, then an array can be considered in view of chains consisting of independent disks. In this case the uniaxial anisotropy of magnetization processes was observed. In arrays with square and hexagonal lattices the bi- and tri-axial configurational anisotropy of the magnetisation process were found.

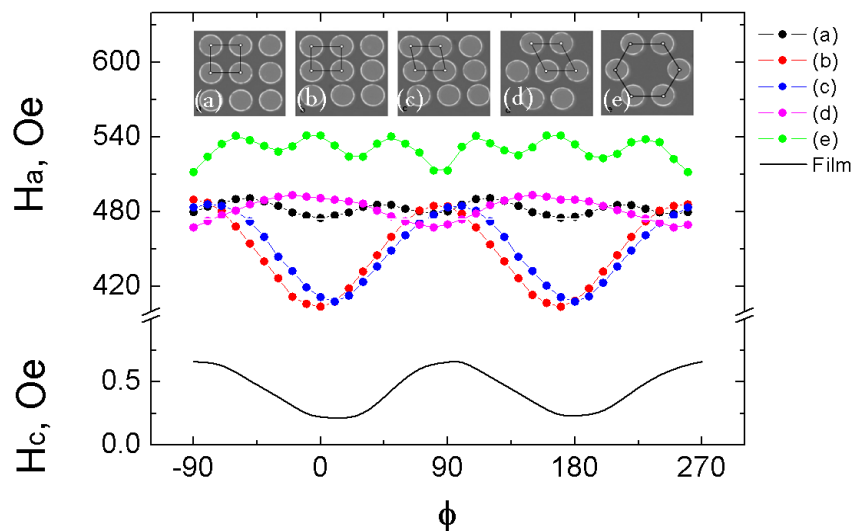


Fig. 1. Coercive force H_c for Py film versus orientation of magnetic field applied in samples plane and values of the vortex annihilation field H_a for different lattice types: (a) square, (b) rectangular, (c) oblique with $\theta = 100^\circ$, (d) oblique with $\theta = 115^\circ$, (e) hexagonal.

This work was supported in part by the Russian Ministry of Education and Science and the Scientific Fund of Far Eastern Federal University.

1PO-I1-2

FM/AFM BILAYER WITH EXCHANGE BIAS*Kovalev A.S.^{1,2}, Pankratova M.L.¹*¹ B.Verkin Institute for Low Temperature Physics and Engineering of NAS of Ukraine,
47 Lenin Ave., 61103 Kharkov, Ukraine² V.N. Karazin Kharkov National University 4 Svobodi sq., 61107 Kharkov, Ukraine
e-mail: pankratova@ilt.kharkov.ua

The magnetization of ferromagnetic (FM) film in contact with antiferromagnet (AFM) may demonstrate the field-shifted dependence [1,2]. In addition, the hysteresis loop may be asymmetric in field with the horizontal plateau of magnetization on the curve $M = M(H)$. We assume that these phenomena are related to the roughness of the FM/AFM interface [3]. The atomic steps on the interface are considered which initiate the appearance of the domain walls in the FM subsystem. The AFM is assumed to be a hard magnetic material with fixed magnetic moments while changing of magnetic field. The exchange interaction in the FM film is defined by the parameter J , and exchange interaction through the FM/AFM interface is J_0 . The strong easy plane anisotropy and small additional anisotropy β in this plane are assumed. The orientation of the FM magnetic moments in easy plane is defined by the angle φ . The equation for the magnetization distribution reads:

$$-Ja^2\varphi'' + (H + J_0f(x))\sin\varphi + \beta\sin\varphi\cos\varphi = 0, \quad (1)$$

where the periodic function

$$f(x) = 2\sum_n \left(\mathcal{G}(x + 2nL) - \mathcal{G}(x + (2n+1)L) \right) - 1 \quad (2)$$

simulates the roughness of the FM/AFM interface, \mathcal{G} is Heaviside function, H is an external magnetic field, L - the period of the surface structure and a - interatomic distance.

The solutions of Eq. (1) represent the collinear structures with $\varphi = 0$ or $\varphi = \pi$, antiparallel one with alternating $\varphi = 0, \pi$, and canted structures which correspond to the inclined part of the magnetization curve. We got the expressions for the area of the stability for these structures analytically. The magnetization of the system was obtained numerically. The magnetization curve for the FM/AFM bilayer with periodically distributed atomic steps on the interface isn't shifted along the field axis. However, for some value of the exchange interaction in the FM film and through the FM/AFM interface the hysteresis loop splits into two loops with the horizontal plateau with $M=0$ or the inclined part of the curve between two loops. The hysteresis loop is symmetric with respect to the point $H=0$. The case with two-periodical atomic steps on the FM/AFM interface and

$$f(x) = 2\sum_n \left(\mathcal{G}(x + 2nL_1) - \mathcal{G}(x + (2n+1)L_2) \right) - 1 \quad (3)$$

was considered as well. In this case the hysteresis loop shifts from the point $H=0$ and becomes asymmetric. The horizontal plateau appears with $M = const \neq 0$.

[1] Maklejohn W.H., Bean C.P., *Phys. Rev.*, **102** (1956) 1413.

[2] A.G. Grechnev, A.S. Kovalev, M.L. Pankratova, *Low. Temp. Phys.*, **39** (2013) 1060.

[3] A.S. Kovalev, M.L. Pankratova, *Low. Temp. Phys.*, **37** (2011) 866.

1PO-I1-3

FERROMAGNETIC AND SPIN-WAVE RESONANCE IN $\text{Fe}_x\text{Ni}_{1-x}$ ($0 < X < 1$) FILMS

Iskhakov R.S.¹, Stolyar S.V.^{1,2}, Yakovchuk V.Yu.¹, Chekanova L.A.¹, Vazhenina I.G.³

¹ Kirensky Institute of Physics, Krasnoyarsk, Russia

² Siberian Federal University, Krasnoyarsk, Russia

³ Krasnoyarsk Institute of rail transport, Krasnoyarsk, Russia

rauf@iph.krasn.ru

To date available models explaining physical properties of FeNi invar alloys are reduced in the final analysis to availability in alloys of magnetic heterogeneity that can be caused heterophaseness, chemical inhomogeneity or unlike signs (magnitude) of exchange interaction carried out in alloy different regions [1]. In this article magnetic heterogeneity of the metastable $\text{Fe}_x\text{Ni}_{1-x}$ films obtained by two different methods (both thermal spraying and chemical deposition) was researched the in all concentration range. The ferromagnetic resonance curve, spin-wave resonance spectrum were measured by pumping frequency 9,2 GHz in the field up to 20 kOe for studying of this films by spin-wave spectroscopy method [2]. This method is based on experimental of dispersion law for spin waves $\varepsilon \sim \eta \kappa^2$ (where ε is magnon energy, η - ferromagnetic exchange hardness, κ - wave vector) and allows to identify type and extent of magnetic heterogeneity.

The dispersion curves $H(n^2)$ for films obtained chemical deposition method is shown an figure 1.

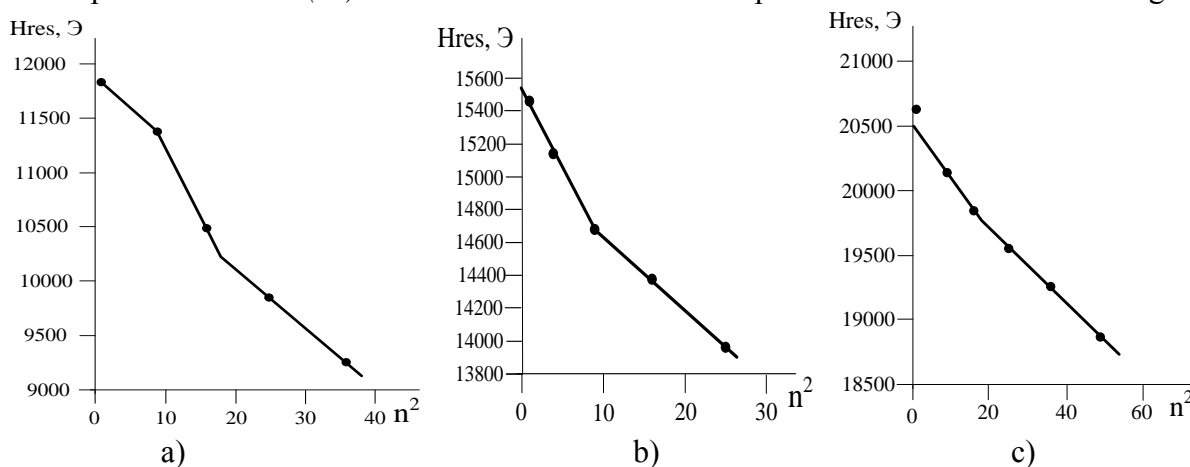


Fig.1. The dependences of the resonance field H_n on square number of the spin-wave mode n^2 are plotted from SWR spectrums of the films a) $(\text{Fe}_{25}\text{Ni}_{75})_{98}\text{-P}_2$, b) $(\text{Fe}_{55}\text{Ni}_{45})_{98}\text{-P}_2$, c) $(\text{Fe}_{66}\text{Ni}_{34})_{98}\text{-P}_2$.

It was found that the $\text{Fe}_x\text{Ni}_{1-x}$ films of the alloy with invar composition having metastable bcc structure are most dispersed in respect of magnetic property.

Support by the Ministry of education and science of the Russian Federation in the network with the state task is acknowledged.

[1] V.L. Sedov, *M: Science*. (1987) 288.

[2] V.A. Ignatchenko, R.S. Iskhakov, *Novosibirsk Science* (1989).

1PO-I1-4

INFLUENCE OF STRUCTURAL FACTORS ON FERROMAGNETIC RESONANCE LINEWIDTH IN SYSTEMS WITH EXCHANGE BIAS

Shanova E.I.¹, Dzhun I.O.¹, Chechenin N.G.^{1,2}

¹ Skobeltsyn Institute of Nuclear Physics, Lomonosov Moscow State University, Moscow, Russian Federation,

² Faculty of Physics, Lomonosov Moscow State University, Moscow, Russian Federation
shanova@physics.msu.ru

Extrinsic factors contributing to the ferromagnetic resonance (FMR) linewidth are investigated in ferromagnetic/antiferromagnetic (F/AF) exchanged biased systems with different deposition order of layers.

The FMR was measured for a set of angles between the directions of the external field and anisotropy axis in the sample induced by the magnetic field, applied to the samples during the layers deposition, thus 0° and 90° correspond to the measurements along the easy (EA) and hard (HA) axis, respectively. In spite of large variations with the thickness of the AF layer, line widths were found very close for the EA and HA in top systems (F below AF layer) (TS). For bottom systems (AF below F layer) (BS), close linewidths for EA and HA were found for smaller AF layer thickness (up to 20 nm), while for thickness larger than 20 nm the linewidths alternately diverge.

The exchange bias field is supposed to be aligned along EA. Then, the unidirectional anisotropy H_{EB} contribution to the FMR field H_r can be essential for measurements along the EA and should be absent along the HA. Similar effect one could expect for FMR linewidth. The evidence that linewidths are about the same for EA and HA for TS samples promotes a conclusion that either there is no exchange biasing, or the effect of biasing is negligible compared to other factors of influence. Since the former assumption is disproved by our measurements [1], one have to admit the latter one is valid for TS samples. This is a strong conclusion since it contradicts with conclusions in some other publications.

In the TS samples FMR linewidth increases proportionally to the average size of the surface roughness. In BS samples the uniaxial anisotropy provides a significant contribution to the line width. The FMR line width is in a squared relationship (1) with the uniaxial anisotropy and in an inverse relationship (2) with the antiferromagnetic layer thickness which referred to a microstructural variation with the thickness as an extrinsic factor of the FMR damping.

$$\Delta H_{BS}^{HA} - \Delta H_{BS}^{EA} = AH_K^2 + B \quad (1)$$

Where fitting parameters are $A=0,15\pm0,02$, $B=4,83\pm2,37$

$$\Delta H_{BS}^{EA}(t_{AF}) - \Delta H_{BS}^{EA}(t_{AF} = \infty) \propto \frac{1}{t_{AF}^\beta} \quad (2)$$

The exponent $\beta = 1, 2$ and 3 and $\Delta H_{BS}^{EA}(t_{AF}=\infty)_{\beta=1,2,3} = 139,51\pm19,17, 158,08\pm9,96, 163,09\pm7,25$ - the linewidth for large thickness of the AF film, respectively. The exponent value is in the range of similar coefficient for ferromagnet thickness dependence discussed in other publications. This observation points to a common reason for such dependence in both, F and AF thickness variation, as due to a microstructure change (grain size growth) with the layer thickness.

[1] Shanova E. I., Dzhun I. O., Chechenin N. G. *Perspectivnye Materialy (in Russian) (Inorganic Materials: Applied Research)* **11** (2013) 5-11.

1PO-I1-5

3D GLAUBER DYNAMICS OF FRUSTRATED SYSTEM: INFLUENCE OF SPIN FLIP PROBABILITY

Korshunov A.S.^{1,2}, Kudasov Yu.B.^{1,2}, Maslov D.A.^{1,2}, Pavlov V.N.¹

¹ Russian Federal Nuclear Center – VNIIEF, Sarov, Russian Federation

² SarFTI, National Research Nuclear University “MEPhI”, Sarov, Russian Federation
al.korshunof@gmail.com

During the last decade a compound $\text{Ca}_3\text{Co}_2\text{O}_6$ is very attractive. A magnetization curve at low temperatures is one of the unique results obtained in $\text{Ca}_3\text{Co}_2\text{O}_6$. A sequence of equidistant steps on the magnetic field was found on this curve. Though their quantity depends both on temperature and rate of the external magnetic field change [1].

The majority of regularities, which appear at magnetization of the compound, were explained by means of numerical simulation of magnetic dynamics in the frameworks of the main kinetic equation [2-4]. However, the investigation shows that probability of a spin turnover could be selected ambiguously, through it must meet the principle of detailed equilibrium [4]. Selection of the turnover probability influences significantly on dynamic properties of the system. Thus, for example, special terms, such as “soft” and “rigid” dynamics, formed depending on the magnetic field influence selection method [5].

In this paper the authors discuss Glauber dynamics of three-dimensional frustrated lattice of Ising chains in the external magnetic field. Also, forms of the spin turnover probability, which lead the system to equilibrium distribution, but different by the external magnetic field and neighbors influence degree, are considered. Results of numerical simulation of the spins dynamics at different probabilities and temperatures are presented. Magnetization curve shape and spins system state at evenly increasing and decreasing magnetic field is discussed. The research results are used to explain the magnetic dynamics of $\text{Ca}_3\text{Co}_2\text{O}_6$ compound.

The work was supported by the Russian Foundation for Basic Research (Project No. 13-02-01194) and the Russian Federal Education Agency.

[1] V. Hardy, D. Flahaut, M. R. Lees, and O. A. Petrenko, *Phys. Rev. B* **70**, 214439 (2004).

[2] Yu. B. Kudasov, A. S. Korshunov, V. N. Pavlov, D. A. Maslov, *Phys. Rev. B* **78**, 132407 (2008).

[3] Yu.B. Kudasov, A.S. Korshunov, V.N. Pavlov, D.A. Maslov, *Phys. Rev. B*, **83** (2011) 092404.

[4] Yu.B. Kudasov, A.S. Korshunov, V.N. Pavlov, D.A. Maslov, *Phys. Usp.*, **55** (2012) 1169.

[5] K. Park et al. *Phys. Rev. Lett.* **92** (2004) 015701.

1PO-11-6

SHAPE EFFECT ON THE NANO-TRIANGLE MAGNETIZATION STATES

Vasil'evskii I.S.¹, Eremin I.S.¹, Kolentcova O.S.¹, Kargin N.I.¹, Strikhanov M.N.¹, Fisher T.², Kozhanov A.²

¹ National Research Nuclear University MEPhI, Moscow, Russia

² Center for Nano-Optics, Department of Physics and Astronomy,
Georgia State University, Atlanta, GA, USA
ivasilevskii@mail.ru

Rapid evolution of the modern electronics requires both the novel materials and the operational principles combined together with apparent 3D scaling to nano-dimensions. The other technological trend aims at the device multifunctioning. Single domain magnetic nanostructures demonstrate the potential for combination of non-volatile magnetic memory and logic applications. Recently a non-volatile logic device based on the NiFe soft magnetic nano-triangle was proposed [1]. Specific symmetry of triangle leads to the two “Y” or “Λ” ground states that are defined by triangle shape configurational anisotropy and by dimensions. Energy barrier between the states defines the stability of “state storage”. In the “Y” ground state the local magnetization is aligned to point either towards or away from the triangle vertices. The magnetization of the third triangle vertex is dependent on that at the two other vertices. Thus switching between different ground states performs logic operations. Triangle shape distortions such as corner rounding (typical for fabrication) result in preferable “Λ” ground state not favourable for non-volatile logic applications [2].

In this work we investigate the effect of the triangle dimensions and shape on the configurational anisotropy and magnetization ground state profile.

Energy and magnetization profile of the magnetic ground states and switching dynamics in the external magnetic field was numerically simulated by solving of Landau-Lifshitz-Gilbert equation. We demonstrate that triangle shape variations can be used to effectively manipulate its anisotropy profile, ground state stability and switching times. We calculate the “Y” and “Λ” triangle ground state diagram in the dimension-concavity-corner rounding parameter space (Fig 1). For the shapes demonstrating the “Y” magnetization state we correlate the triangle geometry with the ground state energy profile and ground state switching dynamics.

Experimental samples of 100 to 500 nm aside Ni₈₀Fe₂₀ triangles capped with 3nm Al layer were fabricated in 200 μm×200 μm arrays by the electron beam nanolithography and lift-off process.

Results of the FMR, MOKE and MFM measurements are compared to the results of numeric simulations.

The investigated triangle shapes are assessed for the non-volatile logic and magnetic memory applications.

[1] A. Kozhanov, S. J. Allen, and C. Palmstrom. *U.S. Patent*, **8** (2012) 198,919.

[2] D.K. Koltsov et al., *J.Appl.Phys.* **88**, (2000)5315; R.P.Cowburn, *J.Phys.D:Appl.Phys.*, **33** (2000) R1–R16.

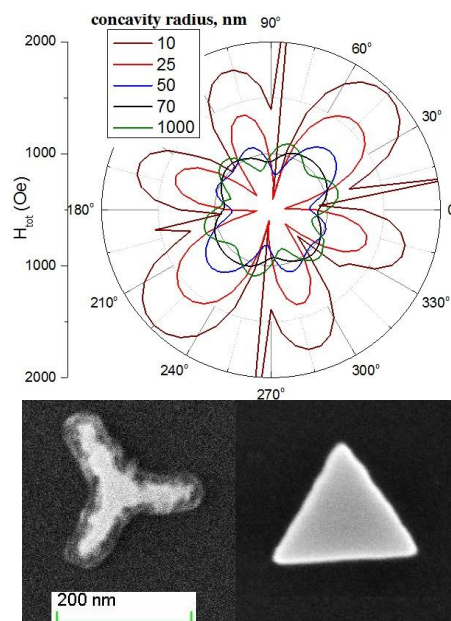


Fig. 1. Angular field anisotropy of NiFe nanostructures with the different concavity. SEM scans of the fabricated structures.

1PO-11-7

PECULIARITIES OF ELASTIC PROPERTIES OF RE COBALTITES R_{Ba}Co₄O₇ (R = Dy - Er, Y) AT MAGNETIC PHASE TRANSITIONS

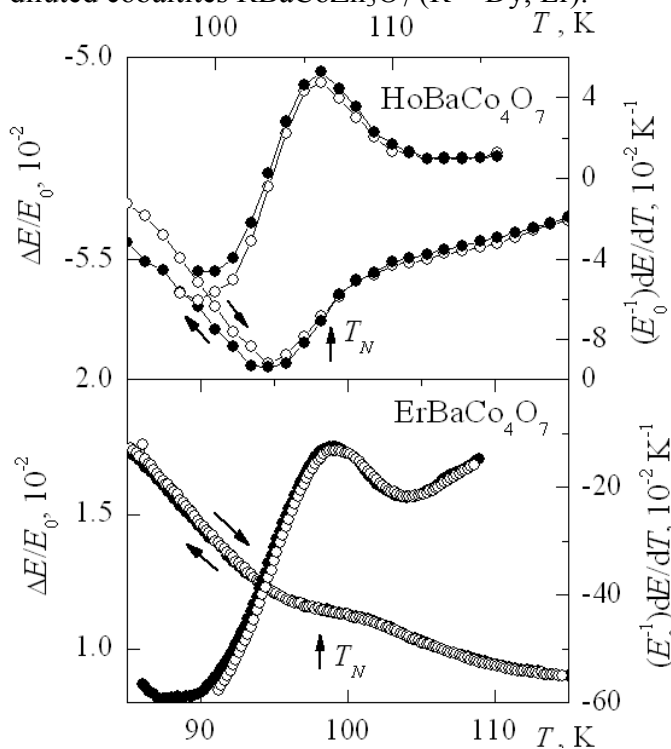
Kazei Z.A., Snegirev V.V., Andreenko A.S., Kozeeva L.P., Kameneva M. Yu.

Moscow State University, 119992 Moscow, Russia

The family of rare-earth (RE) cobaltites R_{Ba}Co₄O_{7+δ} (R is the RE ion or Y) exhibits an unusual magnetic behavior due to the frustration of exchange interactions and the mixed valence in the 3d subsystem. The distortion of the structure due to the phase transition changes the geometry of exchange bonds and, primarily, relieves their frustration, which should affect the magnetic phase transitions in the Co subsystem at temperatures $T_N < T_s$. We revealed specific features of anomalies in elastic properties of RE cobaltites in the temperature range of structural phase transitions (PT) when moving in the RE series from Lu to Er. This work is devoted to the experimental investigation of the elastic properties of R_{Ba}Co₄O₇ in the range of magnetic PT.

Young's modulus $\Delta E/E_0 = [E(T)/E_0(280 \text{ K}) - 1]$ and internal friction coefficient q^{-1} were measured by the composite resonator method at frequency $\sim (110 - 200)$ kHz in the temperature range (4.2 - 300) K on polycrystalline samples R_{Ba}Co₄O₇ (R = Dy - Er, Y).

For RE cobaltites with R = Dy - Er, Y, having temperatures T_N above 80 K, qualitatively similar behaviour of elastic characteristics is observed in the temperature range of magnetic ordering. The internal friction coefficient $q^{-1}(T)$ begins to sharply increase below $T \sim 110$ K, which is close to the temperature of the magnetic PT, and exhibits the strong maximum of about 10^{-2} in the range $T \sim 80 - 100$ K. This maximum seems to correlate to magnetic PT since it is not observed in the diluted cobaltites R_{Ba}CoZn₃O₇ (R = Dy, Er).



At $T_N < T_s$, the jump-like anomaly of Young's modulus $\Delta E/E_0$ is observed in the studied RE cobaltites, which corresponds to a maximum in a derivative $(E_0^{-1})dE/dT$ (fig.). The jump has the largest value $\Delta E(T)/E_0 \approx 3 \cdot 10^{-3}$ for Ho-cobaltite (fig.) and is of the same character as that observed earlier for Lu-cobaltite. For Er-, Dy-, and Y-cobaltites magnetoelastic anomaly due to magnetic ordering gradually decreases, however remains reliably observed in the derivative $(E_0^{-1})dE/dT$, calculated from the measured experimental curves $\Delta E(T)/E_0$. Dependence of the value of the magnetoelastic anomaly on the type of RE ion, experimental conditions and thermo cycling is found out and investigated. Various factors effected the value of magnetoelastic anomaly are discussed: a structure-domain state, magnetic state, character of magnetic anisotropy, etc.

1PO-11-8

EFFECT OF OXIGEN ON ANISOTROPIC MAGNETIC PROPERTIES OF Co NANOWIERS ON Cu(210) SURFACE – *ab initio* STUDY.

Korobova J.G.¹, Bazhanov D.I.¹, Kamynina I.A.¹

Moscow State University, Physical Department, GSP-1, Lenin Hills, 119991, Moscow, Russia
korobovajg@yandex.ru

The development of magnetic memory devices with high density recording is one of the main goals of modern nanoelectronics. For this purpose materials with high magnetic anisotropy are needed. Therefore, such materials (ultrathin films, nanowires (NW), atomic chains) attract a great interest of experimental and theoretical studies in past decade [1]. In this work an *ab initio* study of anisotropic magnetic properties of Co monatomic NWs on clean and oxygen reconstructed Cu(210) surface was carried out in order to find out the effect of gas impurity on magnetic properties of Co monatomic NWs. This study was motivated by recent experimental investigation of selforganized growth of Co NWs on nitrogen activated Cu(210) surface [2], where the enhancement of magnetic anisotropy energy (MAE) and the changing of magnetization direction were observed on nitridized Cu(210) surface in comparison to clean Cu(210). In our study we used experimentally obtained reconstructed Cu(210) surface,

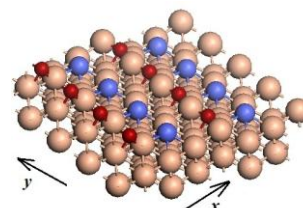


Figure 4. Co atoms (blue) in *fcc* positions in the bottom of trenches on oxygen (red) reconstructed Cu(210)

Co position	MAE, meV	ϕ_{easy} , degrees	ϕ_{hard} , degrees	M_s , μ_B
pure Cu(210)				
«fcc»	~0.75	~45	~-45	1.79
Cu(210) with 0.5ML of O				
«fcc»	~1.24	~75	~-30	1.74
«br»	~0.95	~70	~-30	1.81

Table 1. Magnetic properties of Co NW on clean and oxygen reconstructed Cu(210)

which is formed by adsorption of 0.5 ML oxygen (Cu(210)-(2×1)O structure) [3]. Deep trenches are observed on such reconstructed surface, thus this surface can be considered as a template for growth of Co NWs in [001] direction. We performed the calculations in the framework of density functional theory as implemented in VASP code [4]. Total energy calculations with ionic relaxations showed that *fcc* position of substrate is the most energetically preferable for Co adsorption on clean Cu(210). After oxygen induced reconstruction this position (Fig.1) is only in 0.08 eV less preferable than *fcc* position in the bottom of the trenches. The calculated values of local magnetic moments, MAE and direction of magnetization are summarized in Table1. As one can see the presence of oxygen atoms on template surface leads to the enhancement of MAE and to the changing of magnetization easy axis direction, while magnetic moment is practically unchanged. The values of calculated orbital moment (M_L) projections on easy and hard axis agree with experimental data [5]. In order to understand the enhancement of MAE we used Bruno formula and partial density of states analysis.

Support by the Russian Foundation for Basic Research (Grant № 13-02-01322-a).

[1]. V. Repain, et al., *Surf. Sci.* **447**, L152 (2000); S. Shiraki, H. Fujisawa, et al., *Phys. Rev. Lett.* **92**, 096102 (2004); P. Gambardella, A. Dallmeyer, et al., *Nature(London)* **416**, 301 (2002); P. Gambardella, et al. *Phys. Rev. Lett.* **93** (2004) 077203.

[2]. H. Xu et al, *Japanese Journ. Of Appl. Phys.*, **45** (2006) 2106.

[3]. Y.P. Guo et al., *Phys. Rev. B*, **66** (2002) 165410.

[4]. G. Kresse, J. Furthmuller, *Phys. Rev. B*, **54** (1996) 11169; Y.P. Guo et al., *Phys. Rev. B*, **66** (2002) 165410.

[5]. T. Nakagawa, Y. Takagi et al., *Japanese Journal of Applied Physics*, **47(4)** (2008) 2132.

1PO-11-9

PECULIARITIES OF THE INTERFACE FORMING IN THE «NANOCOMPOSITE-BISMUTH TELLURIDE» MULTILAYER SYSTEM

Zykov G.S.¹, Gan'shina E.A.¹, Novikov A.I.¹, Kalinin Yu.E.², Sitnikov A.V.²

¹ Faculty of Physics, Lomonosov Moscow State University, Moscow, Russian Federation

² Voronezh State Technical University, Russian Federation

V0tum-Separatum@yandex.ru

The multilayer systems based on ferromagnetic (FM) metals and semiconductors are being actively investigated. In previous works [1-3] it had been shown that the adding of a semiconducting layer to a composite multilayer system had led to an anomalous behavior of electric, magnetic and magneto-optical properties of the «nanocomposite – semiconductor» (CoFeZr-Al₂O₃/Si) multilayer systems in the range of small thicknesses of silicon. That kind of behavior had been connected with the interface forming peculiarity at the «FM-granule-semiconductor». It was interesting to investigate, how the properties would change, when the composite and semiconductor compounds were different.

Current multilayered nanostructures [(Co₄₀Fe₄₀B₂₀)_{33.9}(SiO₂)_{66.1}]/[Te₃Bi₂] had been prepared by ion-beam sputtering. Nominal thicknesses of the studied samples ranged from 2.70 to 5.52 nm for composite layers and from 0.12 to 1.03 nm for semiconductor spacer, number of bilayers was 101. Concentrations of metal in the composite layers were below the percolation threshold in the bulk samples with the same compositions. The characteristic granule size in bulk composites at given concentrations was 2-3 nm.

Magneto-optical properties of samples have been measured in the TKE (Transversal Kerr Effect) geometry. TKE measurements have been performed in the energy range of 0.5 ч 4.0 eV, at the light incidence angle of 68° and in magnetic fields up to 3.0 kOe. The sensitivity of the experimental set-up was 10⁻⁵.

Magneto-optical properties have been studied in the wide range of thicknesses of the magnetic and semiconductor layers for {[(Co₄₀Fe₄₀B₂₀)_{33.9}(SiO₂)_{66.1}]/[Te₃Bi₂]}₁₀₁ and [(Co₄₀Fe₄₀B₂₀)_{33.9}(SiO₂)_{66.1}]₁₀₁ multilayer structures. It has been established that the shapes of TKE spectra as well as magnitude of the effect depend on composite and spacer thicknesses.

The amplification of MO response has been revealed in the range of a small spacer thicknesses for {[(Co₄₀Fe₄₀B₂₀)_{33.9}(SiO₂)_{66.1}]/[Te₃Bi₂]}₁₀₁ multilayer system. This amplification is the biggest among the other spacers (Cu, SiC, Si). The shapes of spectra, which were obtained from layer-by-layer deposited composites and multilayer system with the same composite thicknesses, are almost alike, however adding the Te₃Bi₂ to a composite system increased the magnitude TKE considerably.

The good correlation between thickness dependencies of magneto-optical and magnetotransport properties has been found. This correlation is related to peculiarities of interface forming at the «FM-granule - semiconductor» interface, which may presumably be connected with the big value of bismuths spin-orbital constant, and to percolation process in multilayer structures.

This research was supported by the Russian Foundation for Basic Researches (grant No 13-02-90491).

[1] A. V. Ivanov, Yu. E. Kalinin, et. al. *Physics of the Solid State*, **5** (2009) 2474.

[2] E. A. Gan'shina, N. S. Perov, et al. *Bulletin of RAS: Physics*, **72** (2008) 1455.

[3] V. Buravtsova, E. Gan'shina, et al. *Solid State Phenomena*, **168–169** (2011) 533.

1PO-I1-10

LOW-ENERGY DYNAMICS OF SPIN-1/2 SQUARE J_1 - J_2 HEISENBERG ANTIFERROMAGNET

Akterskiy A. Yu.¹, Syromyatnikov A. V.^{1,2}

¹ Petersburg Nuclear Physics Institute NRC "Kurchatov Institute", Gatchina, St. Petersburg, Russia

² Department of Physics, Saint Petersburg State University, St. Petersburg, Russia

aktersky@gmail.com

It has been found recently numerically [1] that spin-1/2 J_1 - J_2 Heisenberg antiferromagnet on a square lattice has a singlet ground state in the range $0.41J_1 < J_2 < 0.62J_1$ that is separated from the first excited (singlet) level by a gap. It is argued in [1] that a topological quantum spin liquid phase (QSLP) is realized in the range $0.41J_1 < J_2 < 0.62J_1$. Values of the ground state energy and the gap are found numerically in [1] but the problem remains open of the low-energy sector quantitative description in QSLP.

We give a physical picture of the low-energy sector in QSLP. Using a series expansion, we find an effective Hamiltonian describing an anisotropic spin-1/2 ferromagnet on the square lattice in magnetic field, which low-energy sector is fully equivalent to that of J_1 - J_2 model in QSLP. Remarkably, this effective model possesses a long-range magnetic order. Thus, we show that QSLP in J_1 - J_2 antiferromagnet is equivalent to the magnet with the local order parameter. This situation is similar to that found in [2] for topological phases in Kitaev model. We discuss the effective model numerically and using the standard $1/S$ expansion and find the value of the order parameter and the elementary excitation spectrum. In particular, our results for the ground state energy and the gap values are in quantitative agreement with previous numerical findings [1].

Support by the Dynasty foundation and RFBR grant 12-02-01234 is acknowledged.

[1] H.-C. Jiang, H. Yao, and L. Balents, *Phys. Rev. B*, **86** (2012) 024424.

[2] Xiao-Yong Feng et al., "Topological Characterization of Quantum Phase Transitions in a Spin-1/2 Model", *Phys. Rev. Lett.*, **98** (2007) 087204.

1PO-11-11

TWO DIMENSIONAL MAGNETIZATION RIPPLE AND STOCHASTIC MAGNETIC DOMAINS IN THREE DIMENSIONAL RIBBONS OF RAPIDLY QUENCHED FECOB

Iskhakov R.S.¹, Komogortsev S.V.¹, Balaev A.D.¹, Gavriiliuk A.A.²

¹ Institute of Physics, SB Russian Academy of Sciences, Krasnoyarsk, 660036 Russia

² Irkutsk State University, Irkutsk, 664003 Russia

komogor@iph.krasn.ru

Magnetic microstructure and, as a consequence, the parameters of the magnetization curves of amorphous and nanocrystalline soft magnetic alloys in addition to the classical elements (magnetic domain, domain wall), is characterized and determined by the new unit of magnetic microstructure - stochastic magnetic domain. The size and the anisotropy of these domains are determined by the exchange interaction constant, the saturation magnetization, the local magnetic anisotropy energy localized at the scale about the grain size and by the dimension of the grains package inside stochastic domain.

We report about the surprising results of our studies of the structure and magnetic properties of the alloy ribbons $\text{Fe}_{64}\text{Co}_{21}\text{B}_{15}$ that reveal unexpected features of stochastic magnetic domains in this material.

Experimental dependences of the magnetic characteristics of amorphous and nanocrystalline ribbons of ferromagnetic alloys FeCoB - dependence of the coercivity from the grain size, approach magnetization to saturation indicate the formation of two-dimensional stochastic magnetic domains in these materials. This is discussed as the effect from different correlation radii in atomic microstructure of the alloys. The inequality defining non spherical shape of such inhomogeneities is proposed.

1PO-I1-12

MAGNETIC STRUCTURE OF CoFeBO_4 WARWICKITE IN TERMS OF SUPEREXCHANGE INTERACTIONS

Knyazev Yu.V.¹, Bayukov O.A.², Ivanova N.B.¹, Kazak N.V.², Bezmaternykh L.N.², Platonov M.S.², Arauzo A.³, Bartolomé J.³, Ovchinnikov S.G.²

¹ Siberian Federal University, Krasnoyarsk, Russia

² Kirensky Institute of Physics SB of RAS, Krasnoyarsk, Russia

³ Universidad de Zaragoza, Zaragoza, Spain

yuvknyazev@mail.ru

CoFeBO_4 is mixed warwickite, with orthorhombic structure ($Pnam$ space group). The crystal structure refinement has been carried out in work [1]. There are two crystallographically inequivalent metal positions M1 and M2 which occupied by the divalent Co and trivalent Fe ions. Crystal structure can be presented by assembly of the *ribbons*, consisting of the oxygen octahedral extending along c -axis. The transition to the spin-glass state at rather low temperature ($T_{SG} = 22$ K) and uniaxial anisotropy, where b -axis is the easy axis of magnetization were found from magnetic study [1].

In the base of X-Ray and Mössbauer data and using simple model of superexchange interactions [2] we have tried to describe magnetic structure of CoFeBO_4 . The calculated magnetic structure was obtained not taking into account of other types of magnetic interactions (Direct and Double Exchange) and anisotropy. The interactions between nearest neighbors is taking into consideration only.

The total integral of cation-cation exchange interaction J was calculated as a sum of individual orbits exchange integrals.

In the frame of this model, the magnetic structure of CoFeBO_4 can be satisfactorily described by nine exchange integrals (EI) $J1 - J9$. The $J1-J6$ integrals (Fig. 1) describes the intra-ribbon interactions while $J7 - J9$ are inter-ribbon ones. The main contribution is antiferromagnetic (AF) excluding ferromagnetic (FM) $J4, J5$ interactions. The strongest interactions are ones inside the rows 2-1-1-2 ($J1, J2$). The rather weak interribbon interactions ($J7 = -2,26$ K, $J8 = -1,96$ K) are frustrating while $J9 = -2,83$ K is ordering.

The crystal structure features consisting of the isosceles triangles ($d = 2,9-3,2$ Å) existing and strong AF interactions leads to high level of magnetic frustrations and as a consequence to the spin glass behavior observed from magnetic experiment.

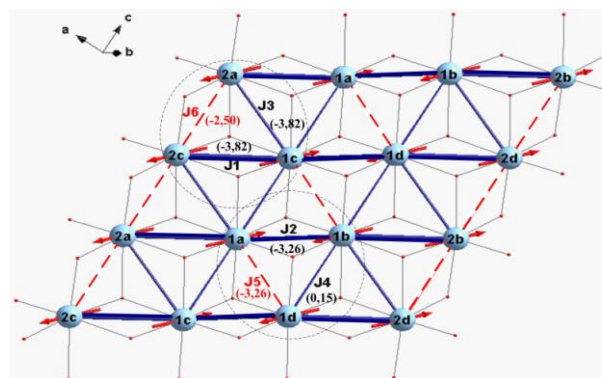


Fig. 1. The magnetic moments orientation (arrows) obtained from the exchange interaction model. The values of EI are shown in Kelvin. Frustrating interactions highlights dashed lines, the strongest bonds are shown by bold. Circles indicates two types of triangles with frustrating bonds.

Support by RFBR № 12-02-00175, 14-02-31051-mol-a, 13-02-00958, 13-02-00358-a. the programs Leading Scientific Schools NSch 2886.2014.2

[1] A. Arauzo, N.V. Kazak, N.B. Ivanova, et al., Be published in 2014.

[2] O.A. Bayukov, A.F. Savitskii. *Phys. stat. sol. (b)*, **155** (1989) 2, 249-255.

1PO-I1-13

CANTED SPIRAL MAGNETIC ORDER IN LAYERED SYSTEMS*Timirgazin M.A.*¹, *Gilmutdinov V.F.*², *Arzhnikov A.K.*¹¹ Physical-Technical Institute of Ural Branch of RAS, Izhevsk, Russia² Udmurt State University, Izhevsk, Russia

timirgazin@gmail.com

The magnetic structure of high-temperature superconductor $\text{La}_{2-x}\text{Sr}_x\text{CuO}_4$ is fairly nontrivial and remains a subject of theoretical and experimental studies. $\text{La}_{2-x}\text{Sr}_x\text{CuO}_4$ has a layered structure, and the electron conductivity is provided mostly by cuprate layers. Exchange interaction between the nearest copper-oxygen layers in $\text{La}_{2-x}\text{Sr}_x\text{CuO}_4$ is negligible and is about 10^{-5} of the intralayer exchange interaction [1]. This allows to consider $\text{La}_{2-x}\text{Sr}_x\text{CuO}_4$ as quasi-2D compound and its theoretical study is carried out using two-dimensional models, which is reasonable in most cases. Nevertheless, despite its smallness, the interlayer interaction may play a role in the formation of the magnetic order. In the experiments [2,3], it was found that the magnetic moments in neighboring copper-oxygen layers are weakly antiferromagnetically ordered with respect to each other in the direction perpendicular to the plane. With account of intralayer spiral ordering it is so-called canted structure, in which the angle of canting with respect to the copper-oxygen plane layer is 0.17 degrees. In the literature it is assumed, that the reason for the formation of the canted structure in $\text{La}_{2-x}\text{Sr}_x\text{CuO}_4$ is Dzyaloshinskii-Moriya interaction.

We have shown that the canted magnetic structure can be explained in the framework of the simple Hartree-Fock approximation for the Hubbard model, if we take into consideration the small interlayer electron hopping integral. Thus, an alternative mechanism of the $\text{La}_{2-x}\text{Sr}_x\text{CuO}_4$ magnetic structure formation is proposed, which is based on the band approach and do not require the presence in the system of the spin-orbit interaction.

Support by RFBR #14-02-31603 and UrBrRAS #14-2-NP-273 is acknowledged.

[1] S-W. Cheong et al., *Solid State Comm.*, **65** (1988) 111-114.

[2] T. Thio et al., *Phys. Rev. B*, **38** (1988) 905-908.

[3] A.N. Lavrov et al., *Phys. Rev. Lett.*, **87** (2001) 017007.

1PO-II-14

SYNTHESIS, STRUCTURE AND PROPERTIES OF MAGNETICALLY ACTIVE COMPOUNDS Cu(II) WITH 3-AMINO-5-(4-METHYLPHENYL) ISOXAZOLE

Protsenko A.N.¹, Shakirova O.G.¹, Kuratieva N.V.², Lavrenova L.G.², Tkachenko I.A.³

¹ Komsomolsk-on-Amur State Technical University, Komsomolsk-on-Amur, Russia

² Nikolaev Institute of Inorganic Chemistry of SB RAS, Novosibirsk, Russia

³ Institute of Chemistry of FEB RAS, Vladivostok, Russia

Protsenko.chem@gmail.com

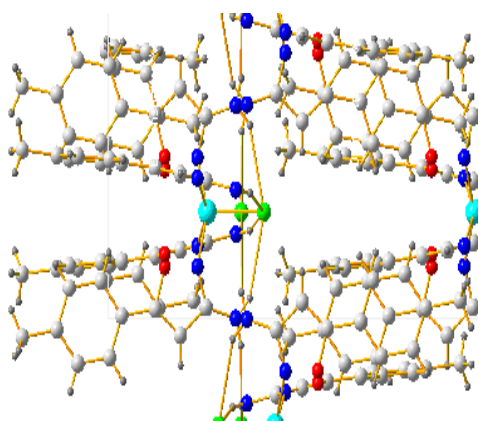


Fig. 1. [CuL4Cl(μ-Cl)]

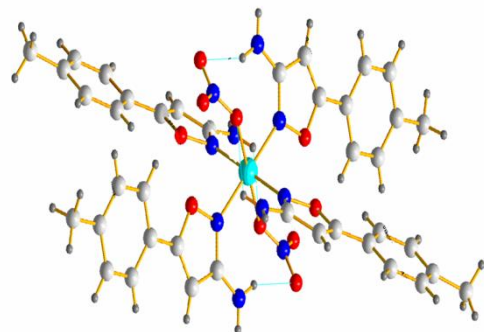


Fig. 2. [CuL4(NO3)2]

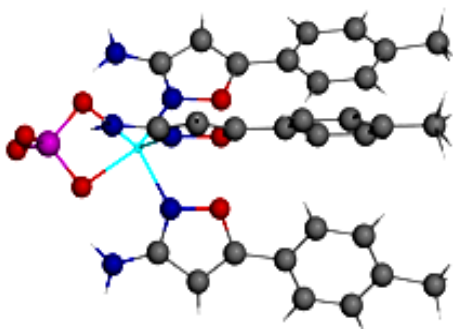


Fig. 3. [CuL3SO4]

Substituted isoxazoles are promising ligands for the synthesis of biological and magnetically active coordination compounds [1]. The syntheses of new complex compounds of copper(II) with 3-amino-5-(4-methylphenyl)isoxazole have been developed. Complexes have been investigated by XRD, electronic, IR spectroscopy, static magnetic susceptibility measurements. Composition and structure of the complexes depend upon the nature of the anion included in the inner coordination sphere (fig. 1-3). Exchange interactions between the unpaired electrons of Cu(II) have a different character depending on the composition of the complex (fig. 4).

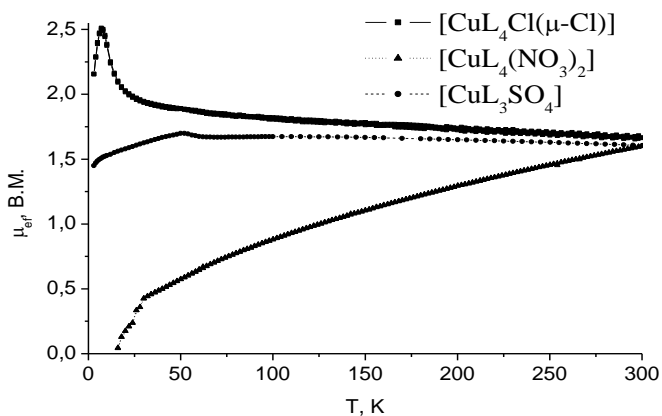


Fig. 4. Curve for the dependence $\mu_{\text{eff}}(T)$.

[1] O.G. Shakirova, N.V. Kuratieva, L.G. Lavrenova, A.S. Bogomyakov, S.K. Petkevich, V.I. Potkin, *Journal of Structural Chemistry*, **51** (2010) 703-708.

1PO-11-15

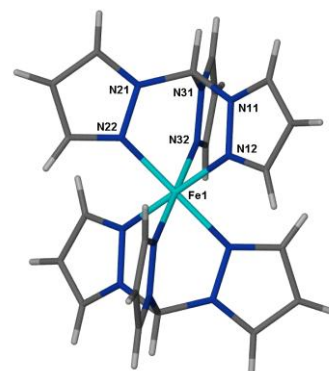
NEW IRON(II) COMPLEXES $[\text{Fe}(\text{HC}(\text{Pz})_3)_2]\text{A}_2$ WITH SPIN-CROSSOVER

Shakirova O.G.¹, Kuratieva N.V.², Korotaev E.V.², Lavrenova L.G.²

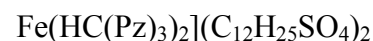
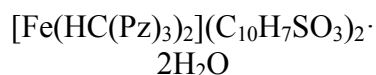
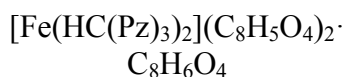
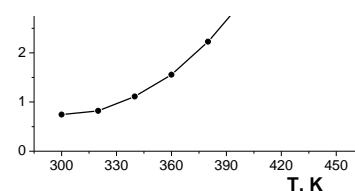
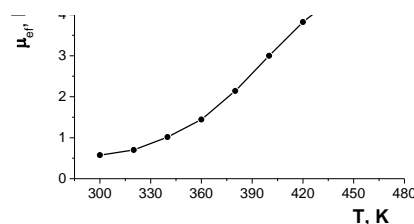
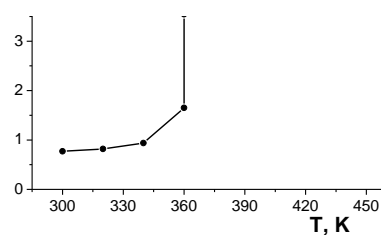
¹ Komsomolsk-on-Amur State Technical University, Komsomolsk-on-Amur, Russia

² Nikolaev Institute of Inorganic Chemistry of SB RAS, Novosibirsk, Russia
Shakirova_Olga@mail.ru

Actual direction of the chemistry of coordination compounds is the synthesis and study of complexes with the ability to spin crossover from low (LS) to the high (HS) state under the influence of external factors - temperature, pressure, or light of a specific wavelength. One class of compounds having such properties are complexes of iron(II) with tris(pyrazol-1-yl)methane ($\text{HC}(\text{Pz})_3$). In these compounds of the common composition $[\text{FeL}_2]\text{Am}\cdot n\text{H}_2\text{O}$ (where A = one- or two-charged anions; n = 0-7) a spin transition $1\text{A}_1 \leftrightarrow 5\text{T}_2$, which accompanied by thermochromism (colour change from pink (HS phase) to white (LS phase)) is observed [1-3]. This potentially allows us to use these complexes in molecular electronics and use them as thermochromic materials. In addition, metal complexes with substituted pyrazoles are biomimetic of some metal-protein, as well as of practical interest in connection with their biological activity (antioxidant, herbicide, fungicide).



We have developed methods of synthesis of several mononuclear compounds of $[\text{Fe}(\text{HC}(\text{Pz})_3)_2]^{2+}$ with phthalate, naphthalenesulfonate and lauryl anions. The complexes were studied by static magnetic susceptibility measurements (Fig. 2), UV/Vis and IR-spectroscopy. Study the dependence of the effective magnetic moment (μ_{eff}) of temperature showed that in complexes observed high-temperature spin-crossover (SCO) $1\text{A}_1 \leftrightarrow 5\text{T}_2$, which accompanied by thermochromism (color changes pink \leftrightarrow white).



The investigations were carried out under the RFBR Grant № 12-03-98502-r_FarEast_a.

- [1] O.G.Shakirova, L.G.Lavrenova, V.A.Daletsky et al., *Inorg. Chim.Acta*, **363** (2010) 4059-4064.
 [2] O.G.Shakirova, V.A.Daletskii, L.G.Lavrenova et al., *Russ. J. Coord. Chem.*, **37** (2011) 511-516.
 [3] O.G.Shakirova, V.A.Daletskii et al., *Russian Journal of Inorganic Chemistry*, **58** (2013) 650-656.

IPO-11-16

UNIDIRECTIONAL ANISOTROPY IN NANOSTRUCTURES WITH ANTIFERROMAGNETIC NiFeMn LAYER

Blinov I.V.¹, Krinitsina T.P., Milyaev M.A., Popov V.V., Ustinov V.V.

IMP Ural Branch of RAS, Ekaterinburg, Russian Federation

¹ blinoviv@mail.ru

Magnetic properties of nanostructures including antiferromagnetic $(\text{Ni}_{80}\text{Fe}_{20})_{1-x}\text{Mn}_x$ alloy have been studied depending on the mode of this antiferromagnetic layer preparation. A possibility of application of the $(\text{Ni}_{80}\text{Fe}_{20})_{1-x}\text{Mn}_x$ alloy as a material for a pinning layer in spin valves is considered.

Nanostructures including a disordered AFM alloy $(\text{Ni}_{80}\text{Fe}_{20})_{1-x}\text{Mn}_x$ have been prepared by DC magnetron sputtering in an evaporation device MPS-4000-C6 (Ulvac) on substrates made of single crystal sapphire $(10\bar{1}2)$ Al_2O_3 and glass (Corning). To obtain unidirectional anisotropy in the sputtered nanostructures a magnetic field of 110 Oe formed by constant magnets was applied.

The as-prepared specimens are characterized by a hysteresis loop shifted relative to the applied magnetic field axis. The surface density of exchange interaction energy at a FM/AFM interface, $J_{\text{ex}} = M_{\text{FM}} \cdot t_{\text{FM}} \cdot H_{\text{ex}}$ (where M_{FM} is a saturation magnetization of a ferromagnetic and t_{FM} is its thickness), equals to 0.05 erg/cm^2 . The measured blocking temperature of the $\text{Ni}_{80}\text{Fe}_{20}(20\text{nm})/(\text{Ni}_{80}\text{Fe}_{20})_{1-x}\text{Mn}_x$ (50 nm) system is $T_b \cong 150^\circ\text{C}$.

A higher blocking temperature, $T_b \cong 270^\circ\text{C}$, has been obtained for the $\text{Al}_2\text{O}_3/\text{Ni}_{77}\text{Fe}_{23}(5\text{nm})/\text{Mn}(50\text{nm})/\text{Ni}_{77}\text{Fe}_{23}(30\text{nm})/\text{Ta}(5\text{nm})$ system, prepared by electron-beam evaporation in Varian device, after the thermomagnetic treatment at 260°C , 4 h. In this case an ordered AFM phase NiFeMn is formed, which is indicated by an appearance of superstructure rings in electron diffraction patterns. The surface density of the exchange interaction energy at a FM/AFM interface is $J_{\text{ex}} = 0.27 \text{ erg/cm}^2$. The values obtained are considerably higher than T_b and J_{ex} for the $\text{Ni}_{80}\text{Fe}_{20}/(\text{Ni}_{80}\text{Fe}_{20})_{1-x}\text{Mn}_x$ system and are comparable with T_b and J_{ex} for a system with an AFM layer IrMn ($240 - 290^\circ\text{C}$), which is widely used in working out elements of magnetic memory (MRAM). An opportunity to use the antiferromagnetic $(\text{Ni}_{80}\text{Fe}_{20})_{1-x}\text{Mn}_x$ for the spin valve devices has been tested on a specimen of the following composition: glass/ $\text{Ta}(5\text{nm})/\text{Ni}_{80}\text{Fe}_{20}(2\text{nm})/\text{Co}_{90}\text{Fe}_{10}(5.5\text{nm})/\text{Cu}(3.6\text{nm})/\text{Co}_{90}\text{Fe}_{10}(5.5\text{nm})/(\text{Ni}_{80}\text{Fe}_{20})_{17}\text{Mn}_{83}(25\text{nm})/\text{Ta}(2\text{nm})$. The measured magnetoresistance value is 6.7 %.

Thus, the results obtained demonstrate an opportunity of using antiferromagnetic alloys $(\text{Ni}_{80}\text{Fe}_{20})_{1-x}\text{Mn}_x$ in spin valves for the ferromagnetic layer pinning.

The work has been done under the support of the Ural Branch of RAS, project No. 12-P-2-1051.

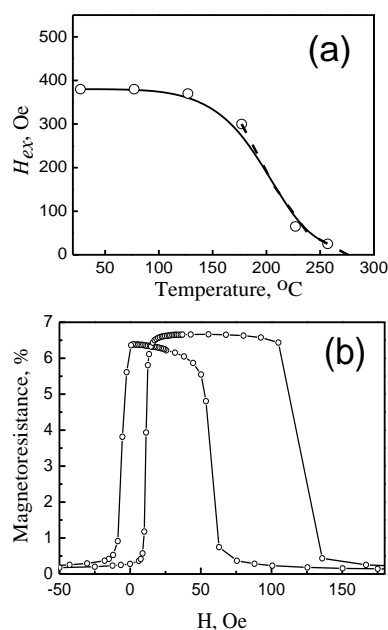


Fig. 1. (a) Temperature dependence of exchange bias field of $\text{Al}_2\text{O}_3/\text{Ni}_{77}\text{Fe}_{23}(5\text{nm})/\text{Mn}(50\text{nm})/\text{Ni}_{77}\text{Fe}_{23}(30\text{nm})/\text{Ta}(5\text{nm})$ specimen annealed at 260°C . (b) Field dependence of magnetoresistance of a spin valve glass/ $\text{Ta}(5\text{nm})/\text{Ni}_{80}\text{Fe}_{20}(2\text{nm})/\text{Co}_{90}\text{Fe}_{10}(5.5\text{nm})/\text{Cu}(3.6\text{nm})/\text{Co}_{90}\text{Fe}_{10}(5.5\text{nm})/(\text{Ni}_{80}\text{Fe}_{20})_{17}\text{Mn}_{83}(25\text{nm})/\text{Ta}(2\text{nm})$.

1PO-11-17

MICRO GRID FRAME OF ELECTROLESS DEPOSITED Co-P MAGNETIC TUBES

Chekanova L.A.¹, Denisova E.A.¹, Komogortsev S.V.¹, Velikanov D.A.¹, Zhizhaev A.M.¹, Iskhakov R.S.¹, Yaroslavtsev R.N.²

¹ Institute of Physics, SB Russian Academy of Sciences, Krasnoyarsk, 660036 Russia

² Siberian Federal University, Krasnoyarsk, 660036 Russia
rauf@iph.krasn.ru

Regular structures on the basis of magnetic elements with sizes ranging from a fraction to several micrometers increasing attention due to their applications in microwave electronics as so-called magnon crystals [1], [2]. A method for preparing such structures is the electroless deposition of metal salts on the template in the form of ordered lattices.

We report about the synthesis and primary magnetic characterization of the Co-P coating chemically deposited on the surface of a square copper grid with a mesh size of 50 microns. The advantage of the chemical vapor deposition method in comparison with the gas phase deposition and electrolytic deposition of on the copper basis of such morphology is the better uniformity of coating thickness. According the grid images (fig.1) obtained by electron microscope the obtained Co-P coating is sufficiently homogeneous with the thickness of about 1 micron. Since the copper fibers constituting the grid that are the substrate, the coating have the shape of a cylinder with inner diameter of 10 microns, then the resulting shape of the coating is the regular frame of the micro-tubes Co-P with the inner diameter equal to the diameter of the copper fibers, wherein the axis of the micro-tubes lie in the same plane. There is well pronounced biaxial magnetic anisotropy in the plane with orthogonal easy magnetization axes oriented along the diagonal of a square grid cell (fig.2). The features of the magnetization curves and ferromagnetic resonance spectra of prepared grids, and their properties in comparison with micro-grid fibers are discusses in the report.

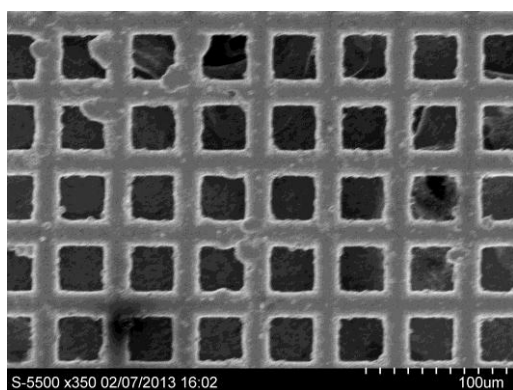


Fig.1. SEM image of Co-P coating deposited on the copper micro-grid.

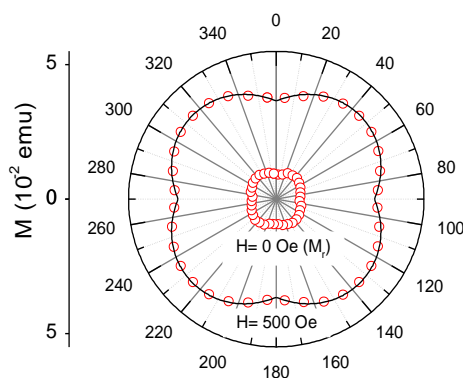


Fig.2. Polar plot of magnetization in Co-P coating deposited on the copper micro-grid.

This work was partially supported by Russian Foundation of Basic Research 13-03-00476-a.

[1] S.A. Nikitov, P. Tailhades, C.S. Tsai, *J. Magn. Magn. Mater.* **236** (2001) 320–330.

[2] M. Darques, J. Spiegel, J. De la Torre Medina, I. Huynen, L. Piraux, *J. Magn. Magn. Mater.* **321** (2009) 2055–2065.

1PO-11-18

EFFECT OF MAGNETIC ANISOTROPY IN ION-BEAM-SYNTHESIZED IRON SILICIDE FILMS ON FMR SPECTRA

Gumarov G. G.¹, Alekseev A. V.¹, Bakirov M. M.¹, Petukhov V. Yu.^{1,2}, Valeev V. F.¹

¹ Zavoisky Physical Technical Institute, RAS, Kazan, Russia

² Kazan Federal University, Kazan, Russia

gumarov@kfti.knc.ru

Earlier we used magnetic-field-assisted ion-beam synthesis to produce thin films of ferromagnetic silicide Fe₃Si in single-crystal silicon substrates [1]. It was shown that application of the magnetic field during the high-dose Fe ion implantation led to the pronounced in-plane magnetic anisotropy in the synthesized films. The goal of the present work is to investigate the magnetic properties of ion-beam synthesized thin iron silicide films using the method of ferromagnetic resonance.

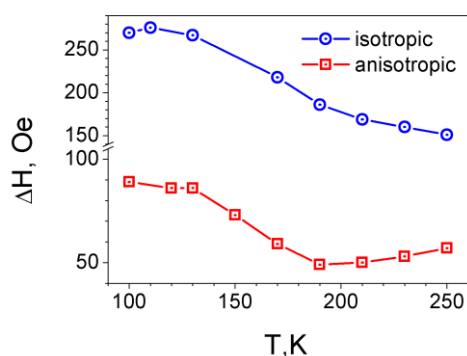


Fig. 1. Temperature dependence of FMR linewidth for isotropic and anisotropic samples.

Isotropic as well as anisotropic thin film samples of iron silicides were ion-beam synthesized with doses in a wide range. Magneto-optical Kerr effect have revealed the curves of magnetization being characteristic for single-domain particles. FMR experiments showed that the linewidth for anisotropic samples considerably narrower than that for isotropic ones. Moreover the nonmonotonic temperature dependence of FMR linewidth was observed both for isotropic and anisotropic samples (Fig.1). Such dependence can be explained on the basis of model of magnetic resonance in an assembly of single-domain uniaxially anisotropic particles. As the temperature rises, the orientational fluctuations of the magnetic moment weaken the inhomogeneous

broadening of the FMR line arising from the distribution in the directions of anisotropy axes of the particles. It should be noted that FMR linewidth for anisotropic samples is nearly constant with temperature variation.

This behavior is in a good agreement with Raikher and Stepanov model [2]. When the dispersion in the directions of anisotropy axes of the particles is absent the contribution of inhomogeneous broadening to linewidth is negligible at low temperatures. Superparamagnetic broadening in this region is also insignificant. As a consequence the linewidth is practically temperature independent, at least in scale of relative variations. In summary our FMR results show that isotropic samples consist of particles with randomly ori-ented easy magnetization axes whereas anisotropic samples – nearly unidirectional easy magnetization axis.

The work was supported by grant of Nanotechnology and Information Technology Division of RAS №3, project №1.12 and grant of Physical Sciences Department of RAS II.5, project B24.

[1] G.G. Gumarov et al. *Nucl. Instr. Meth. Phys. Res. B* **267** (2009) 1600.

[2] Yu. L. Raikher and V. I. Stepanov, *Sov. Phys. JETP* **75** (1992) 764.

1PO-11-19

ZIGZAG MAGNETIC CHAINS WITH SPIN $S = 1/2$ IN BaV_3O_8 Gippius A.A.^{1,2}, Tkachev A.V.¹, Ignatiev M.S.¹, Chakrabarty T.³, Mahajan A.V.³, Buttgen N.⁴,
Kraetschmer W.⁴¹ Faculty of Physics, Moscow State University, 119991, Moscow, Russia² A.V. Shubnikov Institute of Crystallography, 119333, Moscow, Russia³ Department of Physics, IIT Bombay, 400076, Powai, Mumbai, India⁴ Institute of Physics, University of Augsburg, D-86135, Augsburg, Germany
av.tkachev@physics.msu.ru

In present time the investigation of low-dimensional and geometrically frustrated magnetic systems is an area of active researches in the solid state physics. Especial interest is focused on one-dimensional (1D) antiferromagnetic chains in which besides the nearest neighbor (nn) interaction the frustrating next nearest neighbor (nnn) interaction is also present. Depending on different values of the ratio of these interactions ($J_{\text{nnn}}/J_{\text{nn}}$) different phases may be realized.

BaV_3O_8 is an example of such a system with $J_{\text{nnn}}/J_{\text{nn}} \sim 2$. One of the V sites (V^{4+}) is magnetic and forms 1D chains with significant interactions both nn and nnn. So the idea of the present work was to perform complex investigation of BaV_3O_8 using both the measurements of the macroscopic sample properties and the microscopic methods in particular extensive ^{51}V NMR measurements.

The forming of the long range order (LRO) is observed at $T_N \sim 6$ K by both magnetic susceptibility and specific heat data. The results of these measurements also matches well with the coupled $J_{\text{nn}} - J_{\text{nnn}}$ Heisenberg chain model [1]. The value of the “frustration parameter” ($f = |\theta/T_N| \sim 5$) suggests that the system is moderately frustrated [2].

The complex ^{51}V NMR study was performed on the nonmagnetic vanadium ions V^{5+} . Unfortunately we were unable to detect the NMR signal associated with the magnetic V^{4+} nuclei probably due to a strong on-site local moment, which naturally couples strongly with its own nucleus. The fluctuations of this moment are very effective in causing a fast relaxation of the nuclear magnetization. This makes the detection of the NMR signal difficult like in Cs_2CuCl_4 [3]. Anomalies at 6 K were observed in the variation with temperature of the ^{51}V NMR linewidth (field-sweep spectra at different frequencies) and the spin-lattice relaxation rate $1/T_1$ indicating that they are sensitive to the LRO onset and fluctuations at the magnetic vanadium sites. The coexistence of two components (one fast relaxing and another one slowly relaxing) is observed in the spin-spin relaxation rate $1/T_2$ data in the vicinity of T_N . The shorter component seems to be intimately connected with the magnetically ordered state. We suggest that both LRO and non-LRO regions coexist in this compound below the long-range-ordering temperature.

Support by the joint RFBR-DST grant № 11-02-92707-IND is acknowledged.

[1] A.V. Tkachev, A.A. Gippius, T. Chakrabarty, A.V. Mahajan, N. Buttgen, and W. Kraetschmer, *Phys. Rev. B*, **88** (2013) 014433.

[2] S. Derakhshan, J. E. Greedan, and L. M. D. Cranswick, *Phys. Rev. B*, **77** (2008) 014408.

[3] M.A. Vachon, W. Kundhikanjana, A. Straub, V.F. Mitrovic, A.P. Reyes, P. Kuhns, R. Coldea, Z. Tylczynski, *New J. Phys.*, **8** (2006) 222.

1PO-11-20

SCALING AND THE LAW OF APPROACH OF THE MAGNETIZATION TO SATURATION IN NANOSTRUCTURED MAGNETIC MATERIALS

Komogortsev S.V., Iskhakov R.S.

Institute of Physics, SB Russian Academy of Sciences, Krasnoyarsk, 660036 Russia
komogor@iph.krasn.ru

In nanomaterials consisting of particles with randomly oriented easy magnetization axis approach magnetization to saturation technique (AMS) allow one to determine magnetic anisotropy energy that is localized on a small scale of the order of particle, grain or crystallite size. Such materials include poly-nano crystalline, amorphous ferromagnetic materials, granular materials, powder, etc. This makes AMS stand out in comparison with the widespread and well-developed technique of magnetic anisotropy study on the scale of the sample size such as ferromagnetic resonance, magnetic torque measurement, measurement magnetization curves along the principal axes, etc.. At the same time, unlike the local magnetometric techniques, for example XMCD (Kerr effect) AMS gives information on the magnetic anisotropy averaged over the entire sample volume and can thus be used for integral material characterization. In the last decade it has been shown that the AMS study in nanostructured magnetic materials provide information not only on the local magnetic anisotropy and the size of its localization, but also on the magnetic anisotropy, averaged on the magnetic correlation length, and allow to evaluate the magnetic correlation length. It was found that as the magnetic correlation length decreases with increasing applied magnetic field. As the result AMS curve investigation gives the information on the anisotropy of the material in a wide range of scales, and therefore information about the dimensionality of anisotropy inhomogeneity or the dimensionality of magnetization correlations.

The examples of using the AMS technique in the study and characterization of the well-known alloys such as $\text{Fe}_{73.5}\text{CuNb}_3\text{Si}_{13.5}\text{B}_9$, $\text{Fe}_{73}\text{CuNb}_3\text{Si}_{16}\text{B}_7$, $\text{Fe}_{64}\text{Co}_{21}\text{B}_{15}$ are presented in the report. In the course of recent experimental studies new unexpected data have been obtained.

The method consists in fitting the experimental approach magnetization to saturation curve by theoretical expressions obtained in the framework of the random magnetic anisotropy model and identification of intermediate power asymptotic in these dependencies. To improve the reliability of the information obtained by AMS technique new ways of processing the experimental magnetization curve are developed. The example is the analysis aimed at finding of regions with power behavior in experimental curve $M(H)$. The small parts of $M(H)$ in the range $(H-\Delta H, H+\Delta H)$ are fit by power law $M(H) = H^\alpha$ and then α is plotted vs applied field H . The power asymptotic is revealed as horizontal section in $\alpha(H)$ plot. The experimental $\alpha(H)$ plots showed that the switching between different power modes is much faster than predicted by the perturbation theory. The new theoretical expressions for AMS based on the scaling approach are proposed to eliminate this inconsistency. There is surprisingly good consistence of this new expression with experimental data. This makes it useful to fitting experimental approach to saturation curves.

1PO-11-21

INVESTIGATION OF THE INFLUENCE OF MICROWAVE MAGNETIC PROPERTIES OF COOLING TO LIQUID NITROGEN TEMPERATURES FOR COMPOSITE FILMS

Turkov V.K.¹, Kotov L.N.¹, Kalinin Yu.E.², Sitnikov A.V.²

¹ Syktyvkar State University (*SyktSU*), Syktyvkar, Russia

² Voronez State Technical University (*VorSTU*), Voronez, Russia

turkov_1956@yandex.ru

Multiphase nanocomposites based on amorphous ferromagnetic alloys obtained by spraying are not adequately studied. Many of the properties of composite films near the "metal-insulator" are not entirely clear.

In this work the microwave magnetic properties of monolayer composite films and multilayer composite films were compared at room temperature and liquid nitrogen temperature. Concentration dependence of the resonance field and the width of resonance line of FMR spectra were investigated. Samples with a concentration of the metal phase before and after percolation transition were measured.

Composition of monolayer composite films:

(FeCoZr)_x(Al₂O₃)_{100-x} two series sputtered in an argon atmosphere with the addition of oxygen (Series B) and without addition of oxygen (Series A), (FeCoZr)_x(CaF)_{100-x} (Series F), (CoTaNb)_x-(SiO₂)_y (Series L).

Composition of multilayer composite films:

[(CoFeZr)_x(Al₂O₃)_{100-x}]-[Si] (series D), [(CoFeZr)_x(Al₂O₃)_{100-x}]-[Si] with the addition of hydrogen (series E), {(CoTaNb)_x-(SiO₂)_y}-[SiO₂]₅₆ (series M).

The samples was on the substrate of glassceramics (polycrystalline glass) substrate and on the lavesan (polyester). Thickness of the samples was 0.15 - 6.5.

The principal difference between temperature dependences of linewidth of the homogeneous magnetization precession ΔH was found for the samples before and after the percolation threshold in nanocomposite films of series A, F, L and D. In the first case there is a sharp increase of resonance linewidth in the result its shape deform. In the second case (above the percolation threshold) line shape does not change, but there is a slight increase the width of the line and its shift toward lower resonance fields. Dependences of the linewidth of uniform precession of the magnetization and the resonance fields of the angle of incidence of a constant magnetic field for films of series A were obtained. g-factor was calculated for the sample with a concentration of 51.2% of the metallic phase at ambient temperature and liquid nitrogen temperatures from the experimental curves. Experimental dependence of the resonance field (H_{rez}) and linewidth (H) of metallic phase concentration for the films deposited in argon and oxygen (series B) at temperatures of liquid nitrogen and room practically coincide. It was found with the temperature measurements that exchange interaction between the composite nanolayers influences on the linewidth in multilayer structures and the value of the resonance field has the.

The work was supported by RFBR (№ 13-02-01401).

[1] L.N. Kotov et al., *Material Science and Engineering*, **442** (2006) 352.

1PO-11-22

MAGNETIC AND ELECTRONIC PROPERTIES OF IRON SELENIDE Fe₆₋₇Se₈ NANOCOMPOSITES WITH HEXAGONAL AND MONOCLINIC CRYSTAL STRUCTURE

Funtov K.O.¹, Lin Chun-Rong², Lyubutin I.S.¹, Dmitrieva T.V.¹, Starchikov S.S.¹

¹ Shubnikov Institute of Crystallography, Russian Academy of Sciences, Moscow 119333, Russia

² Department of Applied Physics, National Pingtung University of Education, Pingtung County
90003, Taiwan

funtov.ko@gmail.com

Iron selenide nanocomposites Fe₆₋₇Se₈ were synthesized by thermal decomposition of iron chloride and selenium powder in high-temperature organic solvent. Depending on the time of the compound processing at 340⁰C, the nanocrystals with monoclinic (M) - Fe₃Se₄ or hexagonal (H) - Fe₇Se₈ structures as well as a mixture of these two phases can be obtained.

The magnetic behavior of monoclinic and hexagonal phases is very different. The applied-field and temperature dependences of magnetization reveal a complicated transformation between ferrimagnetic (FRM) and antiferromagnetic (AFM) structures which can be related to the spin rotation process connected with the redistribution of cation vacancies. The 3c type superstructure of the vacancy ordering was found in the hexagonal Fe₇Se₈. The vacancies redistribution in Fe₇Se₈ from random to ordered leads to transformation of the magnetic structure from FRM to AFM. The hysteresis loops in both the hexagonal Fe₇Se₈ and monoclinic Fe₃Se₄ nanocrystals indicate the unusually high coercive force H_c which value is highest (“giant”) in Fe₃Se₄ (of about 25 kOe), and it is almost constant in the temperature range from 5 to 100 K. This can be explained by the surface magnetic anisotropy of the Fe₃Se₄ nanoparticles which is essentially larger than the bulk (core) anisotropy. Such a large coercivity is rare for materials without rare earth or noble metal elements, and Fe₃Se₄-based compounds can be a low-cost, nontoxic alternative materials for advanced magnets.

Besides the Neel temperature at 340 and 450 K in (M) and (H) samples, respectively, the magnetic transitions were found at 180 and 130 K related to the spin rotation due to the vacancies redistribution.

The ⁵⁷Fe-Mössbauer spectroscopy data reveal several nonequivalent positions of iron ions in the monoclinic Fe₃Se₄ which explains by presence of cationic vacancies in the nearest environment of Fe ions. It was shown that the ferric ions are more sensitive to the vacancies redistribution than the ferrous ions. This implies that more vacancies appear near the Fe³⁺ ions at this transition which stimulates the rotation of the Fe³⁺ magnetic moments.

Support by the Russian Scientific Foundation (Grants #14-12-00848) is acknowledged.

1PO-11-23

STRUCTURE AND STABILITY OF NANOCCLUSERS FROM EVOLUTIONARY ALGORITHM STUDY

Baturin V.S., Lepeshkin S.V., Matsko N.L., Uspenskii Yu.A.

Lebedev Physical Institute, Russian Academy of Sciences - 119991 Leninskii prosp. 53, Moscow,
Russia

Efficient computational method for structure and stability prediction is highly important for the design of new magnetic materials, especially nanomaterials. The structure of nanomaterials has features of their own. They arise from the fact that most atoms in nanoclusters are situated at the surface, where they have a smaller number of neighbors and reduced atomic binding. This fact determines the arrangements of atoms in clusters, which widely deviates from the crystal structure of bulk material. The direct measurements of cluster structure are difficult and few in number, so the first-principles calculations are valuable origins of structural information. In this presentation we consider the calculation of structure in silicon nanoclusters, which touches on many problems typical for such structural studies.

Our searching for the structure of silicon clusters Si_n ($n = 7 - 10$) and $\text{Si}_{10}\text{H}_{2m}$ ($m = 0 - 11$) was performed with the evolutionary algorithm implemented in USPEX code and density functional theory (DFT). The evolutionary algorithm is inspired by the biological process of natural selection. The corresponding code operates with sets of structures called generations. Every generation is produced from the previous one through the evolutionary operators. Each newly-produced candidate structure is then locally optimized to create next generation, etc. The local optimization is done by external facilities and we chose a DFT code as the most reliable and accurate tool.

As it takes about 1000 ab-initio local optimizations to perform one evolutionary search, the relaxation is the most computationally demanding part of the global optimization. So it is very important to eliminate the replicating candidate structures. For this purpose we used a classification scheme based on graph theory. It allowed to reduce the computational time and to extract the information concerning the low lying isomer structures.

The structures are found to be mostly of low symmetry with the exceptions of Si_7 (C_{5h} -symmetry), Si_{10} (C_{3v} -symmetry) and $\text{Si}_{10}\text{H}_{16}$ (T_d -symmetry). We explain this through the observed correlations between passivation degree and electronic spectra details. When all Si atoms have four-fold coordination ($m > 5$) the spectra exhibits gap widening, which favors the structure stability and is compatible with high symmetry only in few cases.

In most cases nanoparticles are synthesized in large numbers, as an ensemble. The ensemble is not necessarily uniform (which is desirable for many applications) and has the degree of freedom corresponding to relative concentrations of different constituents. Knowing cluster energies opens up the possibility to derive the phase composition of ensemble of clusters at zero and finite temperatures and at different concentration of passivating gas. We found that at zero temperature, depending on H_2 concentration, the ensemble of $\text{Si}_{10}\text{H}_{2m}$ clusters either uniform or represents binary mixture of clusters with two neighbouring m 's. The elevated temperature distorts this picture: isomers appear in ensemble as well as clusters with energetically unfavorable chemical compositions at $T=0$ K.

This research was supported in part by by programmes of Russian Academy of Sciences, and Russian Foundation for Basic Research (projects 14-02-00583, 14-02-00655).

1PO-11-24

STRUCTURES, SURFACE MAGNETIC FIELDS AND FMR PARAMETERS OF COMPOSITE FILMS

Kotov L.N.¹, Vlasov V.S.¹, Turkov V.K.¹, Lasek M.P.¹, Kalinin Yu. E.², Sitnikov A.V.², Golubev E.A.³

¹ Department of Radiophysics and Electronics, Syktyvkar State University, Syktyvkar, Russia

² Department of Solid State Physics, Voronezh State Technical University, Voronezh, Russia

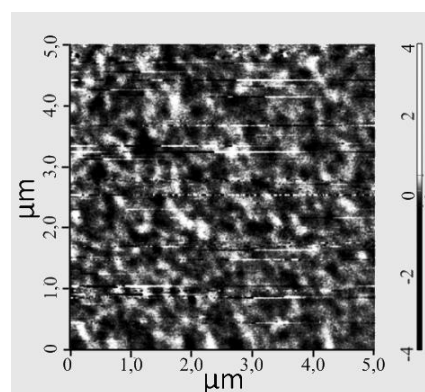
³ Institute of Geology, Komi Scientific Center of UB RAS, Syktyvkar, Russia

kolovln@mail.ru

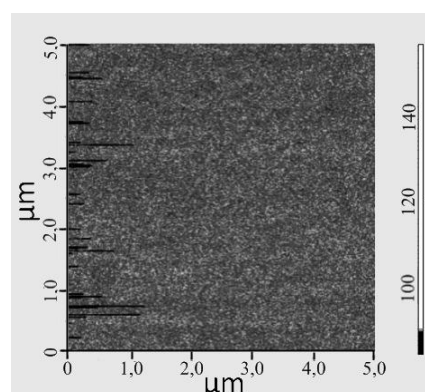
The research is devoted to the studying the micro- and nano- structures, the surface magnetic fields of the composite films. Based on the results of these studies the behavior characteristics of ferromagnetic resonance (FMR) (line width and resonance field values) for the composite films as a function of the concentration of magnetic alloy x before and after annealing were explained.

The composite films were obtained by the ion beam sputtering in the argon atmosphere with the following compositions $\{(Co_{1-x}Nb_{0.2}Ta_{0.05})_x(SiO_2)_{1-x}\}$, $0.2 < x < 0.7$. The chemical composition and thickness of the films with a scanning electron microscope JSM- 6400 are determined. To study the spatial distribution of magnetic field strength and the film surface with a lateral

resolution of 50 nm the magnetic force microscopy (MFM) was used. The study was conducted using an atomic force microscope ARIS-3500. Mode dynamic magnetic force microscopy Integra Prima (NT-MDT) was used. MFM is surface and the image of the magnetic forces a two-pass method. Topographic image of the interaction of the probe with the surface are thickness of the magnetic coating of the tip of was 30-50 nm, radius - about 30 nm. After topography measurements and magnetic fields near the surface of the films at room temperature, the films were annealed at 820 K. Annealing of the composite film reduces the surface roughness due to the merging of small metal granules and structure relaxation of the insulating phase. These processes led to the appearance of larger homogeneous areas. After annealing, even in the presence of heterogeneous areas, demagnetizing fields throughout the film are homogeneous (Fig. 1 a, b). There are the tone scales right from the Fig. 1. This are corresponded to values of the magnetic surface fields in Oersteds. Homogeneous field demagnetization occurs when a small distance between the large magnetic areas, the appropriate concentrations of the metal alloy $x > 0.52$.



a



b

Fig. 1. The magnetic fields of the films at $x = 0.52$ up to (a) and after annealing (b).

Support by RFBR (grant №13-02-01401-a).

1PO-11-25

INFLUENCE OF THE HEAT TREATMENT ON MAGNETIC PROPERTIES OF TbCo/FeNi FILMS WITH MODIFIED INTERLAYER INTERFACE

Balymov K.G., Kulesh N.A., Adanakova O.A.
Ural Federal University, Ekaterinburg, Russia
k.g.balymov@urfu.ru

Amorphous films containing rare earth and 3d transition metals demonstrate great potential for practical applications due to the vast variety of properties and possibility for its adjustment. In particular, ferrimagnetic system Tb-Co [1] can be considered as an effective source of the exchange bias in layered films with magnetoresistive effect such as Tb-Co/Fe₂₀Ni₈₀ [2]. In the last case magnetic properties of the permalloy layer depends strongly on the state of the interlayer interface. This work is devoted to the study of interlayer exchange interaction in layered films based on Tb-Co/Fe₂₀Ni₈₀ system with modified interface subjected to the stepped annealing.

The experiment was performed on four types of film samples: 1 – Fe₂₀Ni₈₀(50nm)/Tb-Co(110nm), 2 – Fe₂₀Ni₈₀(50nm) / Ti(0.7nm) / Tb-Co(110nm), 3 – Tb-Co(110nm) / Co(0.8nm) / Fe₂₀Ni₈₀(50nm), 4 - Fe₂₀Ni₈₀(50nm)/Tb-Co(110nm) with permalloy layer selectively annealed at 400°C for one hour. All samples were obtained by high-frequency ion sputtering of Ti, Co, alloyed Fe₂₀Ni₈₀, and mosaic Tb-Co targets. Composition of the mosaic target was adjusted to obtain Tb-Co layer with terbium concentration of 24-27 at.%. Films were deposited on Corning glass substrates in the argon medium with 2 mTorr pressure in presence of the uniform magnetic field of 150 Oe applied parallel to the substrate plane. In order to avoid oxidation of the samples, protective 15 nm Ti layer was used.

Each step of the cumulative annealing of the samples was performed in vacuumed chamber during one hour.

According to the results of x-ray structural analysis, Tb-Co layers were in amorphous state, permalloy and Ti layers were nanocrystalline. Heat treatment did not lead to any substantial structural changes.

For all types of samples in the initial state, hysteresis loop of the permalloy layer was shifted along the magnetic field axis, which was caused by the exchange coupling with adjoining Tb-Co layer. As a result, we obtained dependencies of the exchange bias field H_e and coercivity H_c of the permalloy layers on the annealing temperature T_a . It was shown, that the character of $H_e(T_a)$ and $H_c(T_a)$ dependencies varies for different types of samples. The obtained results were analyzed in terms of the model of interlayer diffusion, which can be blocked by introduction of the Ti spacer. The last modification was shown to provide improved thermal stability of the exchange bias in Fe₂₀Ni₈₀/Ti/Tb-Co samples.

This work was supported by The Ministry of Education and Science of the Russian Federation (contract 02.G36.31.0004), RFBR and Government of the Sverdlovsk region (grant 13-02-96027), UrFU under the Framework Program of development of UrFU through the «Young scientists UrFU» competition.

- [1] V.O. Vaskovskiy, K.G. Balymov *et al. Phys. Solid St.*, **53** (2011) 2275–2283.
[2] V.O. Vas'kovskii, K.G. Balymov *et al. Technical Physics*, **56** (2011) 981-985.

1PO-11-26

SPECIFIC FEATURES OF UNIDIRECTIONAL ANISOTROPY IN FeNi/FeMn AND FeNi/FeMn/FeNi FILMS

Gorkovenko A.N., Lepalovskij V.N., Stepanova E.A., Savin P.A.

Dept. Magnetism and Magnetic Nanomaterials, Ural Federal University, Ekaterinburg, Russia
angorkovenko@gmail.com

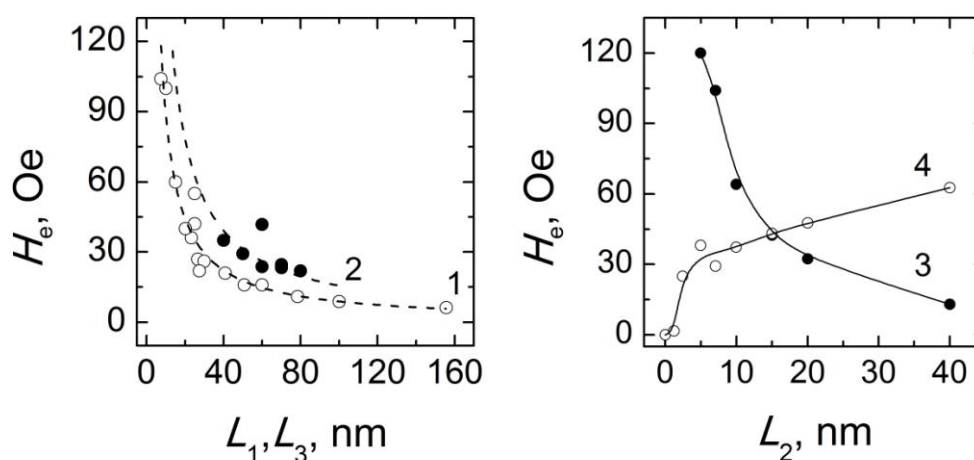
In this work basic laws of the formation of unidirectional anisotropy in films containing exchange coupled ferromagnetic ($\text{Fe}_{20}\text{Ni}_{80}$) and antiferromagnetic ($\text{Fe}_{50}\text{Mn}_{50}$) layers have been studied. Such film structures have been actively investigated, in particular with focus on their application in spin valves [1]. Previously [2] we have found that films with one ($\text{Fe}_{20}\text{Ni}_{80}/\text{FeMn}$) or two ($\text{Fe}_{20}\text{Ni}_{80}/\text{FeMn}/\text{Fe}_{20}\text{Ni}_{80}$) ferromagnetic layers differ significantly in the intensity of the interlayer exchange coupling. This work focuses on the comparison of properties of the films containing permalloy layers of increased thicknesses (≥ 40 nm).

Multilayer films were prepared by magnetron sputtering in the presence of a homogeneous magnetic field on the substrate. Three types of samples have been investigated:

A – $\text{SiO}_2/\text{Ta}(5)/\text{Fe}_{20}\text{Ni}_{80}(L_1)/\text{Fe}_{50}\text{Mn}_{50}(20)$;

B – $\text{SiO}_2/\text{Ta}(5)/\text{Fe}_{20}\text{Ni}_{80}(L_2)/\text{Fe}_{50}\text{Mn}_{50}(20)/\text{Fe}_{20}\text{Ni}_{80}(40)/\text{Ta}(5)$;

C – $\text{SiO}_2/\text{Ta}(5)/\text{Fe}_{20}\text{Ni}_{80}(5)/\text{Fe}_{50}\text{Mn}_{50}(20)/\text{Fe}_{20}\text{Ni}_{80}(L_3)/\text{Ta}(5)$. Values of fixed or variable (L_1, L_2, L_3) thicknesses of the layers are indicated in nm. Influence of these thicknesses and temperature on parameters of the hysteresis loops have been determined. Hysteresis loops were measured by MOKE magnetometer and MPMS-XL7 EC device.



Figures demonstrate dependencies of unidirectional anisotropy field on thickness of the permalloy layer in samples of series A (curve 1), the outer permalloy layer in samples of series C (curve 2), internal (curve 3) and external (curve 4) permalloy layers in samples of series B. Since using the data of temperature measurement of the magnetic properties, held in the range of 5-350 K, the analysis have been performed.

This research project has been supported by UrFU under the Framework Programme of development of UrFU through the «Young scientists UrFU» competition

[1] V. Kuncser, M. Valeanu, G. Schinteie, G. Filoti, *JMMM*, **320**, (2008) e226-e230.

[2] A.N. Gorkovenko, V.N. Lepalovskij, V.O. Vas'kovskiy, P.A. Savin, N.N. Shchegoleva, *Solid State Phenomena*, (2014). In print.

1PO-11-27

MAGNETIC PROPERTIES OF NANOSTRUCTURED $\text{Al}_2\text{O}_3/\text{Co-P}$ COMPOSITE PARTICLES PREPARED BY BALL MILLING

Denisova E.A.¹, Kuzovnikova L.A.^{1,2}, Iskhakov R.F.¹, Eremin E.V.¹

¹ Kirensky Institute of Physics SB RAS, Krasnoyarsk, Russian Federation

² Krasnoyarsk Institute of Railways Transport, Krasnoyarsk, Russian Federation
lund@mail.ru

The structural and magnetic properties of $\text{Al}_2\text{O}_3/\text{Co}_{95}\text{P}_5$ composite powders during ball milling and dynamic compaction processes have been investigated. The composite magnetic $\text{Al}_2\text{O}_3/\text{Co}_{100-X}\text{P}_X$ ($4 < X < 15$) particles were produced by coating of submicrometer-sized Al_2O_3 particles with Co-P alloy nanoparticle layers by electroless plating. The initial $\text{Al}_2\text{O}_3/\text{Co}_{100-X}\text{P}_X$ particles were treated by ball milling. The bulk composite samples were prepared by dynamic compaction (samples size is $7 \times 12 \times 1.5$ mm).

The morphology and the composition of the powders were analyzed using a scanning electron microscope and an energy-dispersive spectrometer. The crystalline structure of the composite powders was determined using a DRON-4 X-ray diffractometer.

After milling the particles were plastically deformed, average particle size increased, while we observe a wider particle size distribution. The XRD analysis were indicated transformations of Co hcp phase to Co fcc phase during milling.

Also after milling the coercivity values monotonically growth from 230 Oe for initial powder to 320 Oe for 75 minutes milled powder. It is likely that the reduction of the particle size during milling toward the size region of single domain results in the increase of H_c .

It is found that the volume fraction of superparamagnetic particles is significantly increased in the course of milling process. This is consistent with the decreasing of value magnetization of $\text{Al}_2\text{O}_3/\text{Co(P)}$ powders during milling process.

The regimes of dynamic compaction were selected so that the basic magnetic characteristics (saturation magnetization, M_0 , local magnetic anisotropy field, H_a , FMR linewidth, ΔH , coercive field, H_c) remain unchanged.

This work is supported by the Russian Foundation for Basic Research, project no. 13-03-00476-a.

1PO-11-28

OPERATION OF DEMAGNETIZING FIELD EFFECT IN MAGNETIC STUDIES OF FERROMAGNETIC POWDERS

*Yaroslavtsev R.N.¹, Komogortsev S.V.², Chekanova L.A.², Kuzovnikova L.A.³, Denisova E.A.²,
Li O.A.¹, Iskhakov R.S.²*

¹ Siberian Federal University, Krasnoyarsk, Russia

² Institute of Physics, SB Russian Academy of Sciences, Krasnoyarsk, Russia

³ Krasnoyarsk Institute of Railways Transport, Krasnoyarsk, Russia

rauf@iph.krasn.ru

Control of demagnetizing fields is necessary for appropriate interpretation of the magnetic properties in powders of ferromagnetic particles. The matter is that the dipole-dipole interaction between neighboring particles significantly influences both the orientation of the magnetization vector and the amount of work for magnetizing single particle. Due to the fact that the particles in the powder tend to form agglomerates of various size and shape, the demagnetizing field can vary dramatically from particle to particle, resulting in a strongly pronounced heterogeneity of the magnetic properties. In general account for these heterogeneities is too complicated. Therefore pretreatment of the powder sample is needed, that allow one to account of demagnetizing fields within the known micromagnetic models [1]. This report focuses on the discussion of the authors experience on modifying the demagnetizing fields of ferromagnetic powder in accordance with that task.

We discuss two approaches to the control of the demagnetizing fields. The first approach is interaction reduction between the particles, achieved through the separation of the particles by a layer of nonmagnetic phase. The second approach, on the contrary, is increasing the interaction between the particles enough to reach the applicability of the mean field theory.

Within the first approach the each particle of the powder is coated by the layer of nonmagnetic phase with different thickness by electroless deposition. The powders prepared by the electroless deposition method, consists of particles with ferromagnetic core Co-Ni and nonmagnetic shell of amorphous alloy Ni-P. Powders with different thickness of nonmagnetic shell have been synthesized. With increasing the thickness of nonmagnetic shell, the curve of the ferromagnetic resonance of the powder is considerably narrowed, the linewidth decreases almost an order of magnitude, and the magnitude of resonance field decreases also.

In second scenario the pressing of powders in tablets with the large aspect ratio is carried out. Pressing of powders Co-P and Co-P/Cu also leads to significant modification of the ferromagnetic resonance curves. Compacting is result in FMR linewidth decrease and the resonance field is displaced to the resonance field typical for continuous ferromagnetic plate.

In the report the magnetic properties, in particular features of FMR spectra and their modification in the samples are discussed. The purpose is estimation of magnetic parameters for the powder material that are not related with internal demagnetizing fields by the simple micro-magnetic models.

Work performed as part of the State job of the Ministry of Education and Science and by the Russian Foundation for Basic Research, project no. 13-03-00476-a.

[1] G. V. Kurlyandskaya, S.M. Bhagat, A.P. Safronov, I. V. Beketov, A. Larranbaga, *AIP Adv.*, **1** (2011) 042122.

1PO-11-29

MAGNETIC ANISOTROPY OF Co-NANOSTRUCTURES EMBEDDED IN MATRICES WITH DIFFERENT PORE SIZE AND MORPHOLOGY

Denisova E.A.^{1,2}, Chekanova L.A.¹, Komogortsev S.V.¹, Iskhakov R.S.¹, Nemtsev I.V.³

¹Kirensky Institute of Physics SB RAS, Krasnoyarsk, Russian Federation

²Krasnoyarsk Institute of Railways Transport, Krasnoyarsk, Russian Federation

³Krasnoyarsk Scientific Center SB RAS, Krasnoyarsk, 660036, Russian Federation
len-den@iph.krasn.ru

The incorporation of Co-nanostructures into a porous membrane allows to fabricate nanocomposites with different magnetic properties. The incorporation of metal nanostructures into the pores of non-magnetic silicon or polycarbonate track etched (PCTE) matrices leads to different magnetic properties depending on the pores morphology as well as the shape and distribution of the metal precipitations. Coercivity, squareness, and anisotropy can be tailored in varying the geometry and/or spatial distribution of the metal structures. In this work, we describe experimental results concerning the precipitation of Co(P) particles in porous of silica and (PCTE) membranes and the comparison of their structural and magnetic properties.

The precipitation of cobalt into the pores is carried out by electroless reduction of metal-salt solution with sodium hypophosphite as reducing agent. Several types of PCTE membranes with nominal pore sizes of 100, 200, 400 and 4.8 μ m have been selected to study the effect of pore size on magnetic properties of composite material. The possible porous silicon morphologies vary between meso (5– 50 nm) and macropores (up to a few ten micrometers) with linear or dendrite shape. The dependence of magnetic properties of the samples on the P content in the Co(P) alloys and on the column diameter are discussed. The macroscopic and local magnetic anisotropy of the Co(P) alloy embedded in the pores of the different matrices is studied. Typical magnetic hysteresis loops of Co(P) rods for fields applied parallel and perpendicular to the membrane surface are shown in figure 1 a. It can be seen that the easy axis of the all samples with linear pores is along the rods. Hence, the shape anisotropy dominates over the intrinsic magneto crystalline anisotropy. Finally, the sample with dendritic pores is almost magnetically isotropic (fig.1b). Information on local anisotropy field and the grain size was obtained from investigation of approach magnetization to saturation law. The local anisotropy field for all samples depends on P content. The H_a value increases with a decrease in P content. For Co(P) rods the H_a value is also determined by nominal pore sizes. For samples with linear pores the increasing of pore size causes a reduction in H_a value. Approach magnetization to saturation indicates that the investigated Co(P) rods is nanocrystalline.

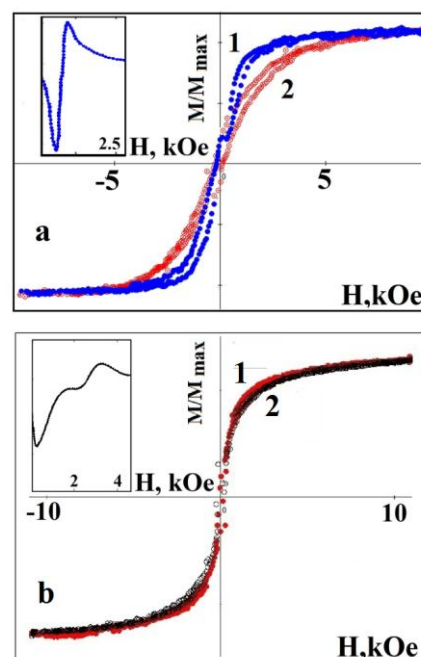


Fig.1. Hysteresis loops for the $\text{Co}_{86}\text{P}_{14}$ particles embedded in PCTE (a) and dendritic silica pores (b) for fields applied parallel (2) and perpendicular (1) to the membrane surface. Insets show FMR spectrum of composite materials

Support by RFBR 13-03-00476-a is acknowledged.

1PO-I1-30

INTERPLAY OF FERROMAGNETIC AND ANTIFERROMAGNETIC EXCHANGE INTEGRALS IN THE LOW-DIMENSIONAL NaCu_2O_2 COMPOUND

Dorgiev V.V., Vasiliev A.N., Volkov D.V.

M.V. Lomonosov Moscow State University, 119992 Moscow, Russia
denini.denini@gmail.com

Copper oxides with low-dimensional electronic structure have attracted much attention because of their unusual magnetic properties and a large variety of ground states. The NaCu_2O_2 compound is a mixed-valent Mott insulator composed of chains of edge-sharing Cu^{2+}O_4 plaquettes and $\text{O-Cu}^{1+}\text{-O}$ dumbbells. Its crystal structure belongs to the Pnma space group. The interplay between short- and long-range couplings generates spiral magnetism in the compound. Detailed and thorough experimental studies of magnetic and related characteristics, NMR spectra and LDA-based estimates of exchange integrals were performed in [1, 2]. We have continued a theoretical analysis of the electronic structure and have determined main ferromagnetic and antiferromagnetic couplings. For this purpose the full-potential local-orbital scheme FPLO (fplo 9.00-34) within the local (spin) density approximation LSDA+U [3] was used.

To begin with, we have repeated the LDA calculations and tight-binding model analysis and have got the same electronic structure and more accurate description of band structure than in [1] because of the usage of greater number of transfer integrals. Extended and tedious LSDA+U calculations for adequately chosen sets of supercells gave values of total exchange integrals and ferromagnetic contributions. The calculations confirmed the known statement that the nearest neighbor in-chain coupling is ferromagnetic J_{nn}^{FM} and the next-to-nearest neighbor in-chain one is antiferromagnetic J_{nnn}^{AFM} . Closeness of results of LSDA+U and tight-binding model calculations for all the other couplings gives evidence that the main contributions are antiferromagnetic. The obtained relation $|J_{nnn}^{AFM} / J_{nn}^{FM}| \approx 0.75$ is rather close to the experimental value of 0.55 determined from the neutron diffraction data [4]. We note that this relation was estimated as ≈ 2 in [1], where the ferromagnetic coupling was estimated (but not calculated). The band structure calculated with regard to electronic correlations in the mean field approximation is presented in Fig. 1.

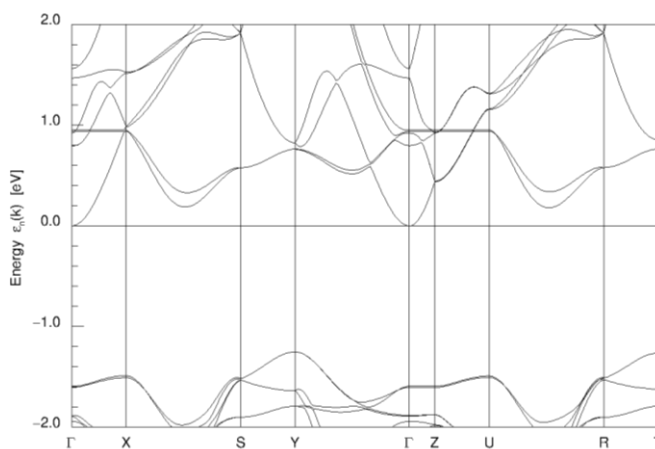


Fig. 1. Band structure of NaCu_2O_2 near Fermi level with $U_d=5.5$ eV.

We thank the SKIF MSU cluster Chebyshev for the use of their computational facilities. Support by RFBR (projects 13-02-00174, 14-02-92002) is acknowledged.

- [1] S.-L. Drechsler, J. Richter, A. A. Gippius et al., *Europhys. Lett.*, **73** (2006) 83-89.
- [2] A. A. Gippius, A. S. Moskvina, E. N. Morozova et al., *JETP*, **105** (2007) 86-89.
- [3] K. Koepnik, *FPLO MBBS. User's manual. Dresden* (2009) 43.
- [4] L. Capogna, M. Mayr, P. Horsch et al., *Phys. Rev. B* **71** (2005) 140402(R).

1PO-I1-31

MAGNETIC PROPERTIES OF NICKEL (II) AND COPPER (II) NITRATE COMPLEXES WITH EXTENDED STRUCTURE

Deeva E.B.¹, Merkulova A.M.¹, Morozov I.V.¹, Volkova O.S.², Balz C.³, Lake B.³, Troyanov S.I.¹, Zakharov M.A.¹, Tafeenko V.A.¹, Vasiliev A.N.²

¹ Department of Chemistry, Lomonosov Moscow State University, Moscow, Russian Federation

² Department of Physics, Lomonosov Moscow State University, Moscow, Russian Federation

³ Helmholtz-Zentrum Berlin, Berlin, Germany

deeva.e.b@gmail.com

Nitrate complexes of d-metals are able to form extended structures such as chains, layers, networks due to participation of bridge-nitrate groups. The fundamental motivation of these compounds investigation is based on the occurrence of low-dimensional magnetic properties under low temperatures due to a phenomenon of spin exchange coupling. Since nitrate group does not incline to exhibit bridging function, the nitrate complexes with extended structure are not very common; such substances are usually extremely hygroscopic, it makes the investigation of magnetic properties significantly complicated.

In our work we synthesized nitrosonium nitrato-metalates: NO[Cu(NO₃)₃] (**I**), α - and β -NO[Ni(NO₃)₃] (**II**, **III**), NO[Co(NO₃)₃] (**IV**). Anhydrous nitrates: γ -Cu(NO₃)₂ (**V**), Ni(NO₃)₂ (**VI**), Co(NO₃)₂ (**VII**) were obtained by vacuum thermal decomposition of corresponding nitrosonium salts. Crystal structures for **II-V** were first defined in our work. All of the compounds form extended structures; it allows us to expect the appearance of spin exchange interaction between metal atoms.

In the structure of nitrosonium nitrato-cuprate **I** the spin $\frac{1}{2}$ Cu²⁺ ions are coupled in antiferromagnetic chains along the crystallographic *b*-axis. This compound probably realises the theoretical Nersesyan-Tsvelik model [1] (fig. 1(a)): such geometry suggests a lack of long-range magnetic order up to 0 K. High-quality single crystals **I** were obtained to continue this research. Temperature of formation of the long-range antiferromagnetic order was determined by μ SR-spectroscopy and turned out was found to be $T = 0.585(2)$ K. Exchange coupling value along the crystallographic *b*-axis calculation was based on results of neutron inelastic scattering and turned out to be $J = 142(3)$ K.

The nickel (II) nitrate (**VI**) crystallizes in a rhombohedral $R\bar{3}$ space group with two non-equivalent positions for Ni²⁺ ions being in the ratio Ni(1):Ni(2) = 3:1 (figure 1(b)). In the *ab*-plane, the Ni(1) ions linked through N(1)O₃ groups forming structurally perfect kagomé layers with Ni(2) ions occupying the hexagons. The measurements showed that **VI**-Ni(NO₃)₂ appeared to be the low temperature noncollinear ferrimagnet. Its specific ground state is formed due to the kagomé-type arrangement of one species of nickel ions coupled antiferromagnetically with another species of nickel ions.

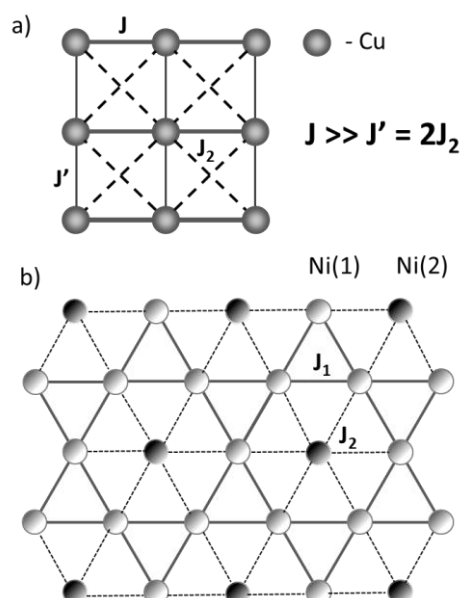


Fig. 1. Schematic representation of the structures **I** (a) and **VI** (b). Only the metal atoms and the path of the exchange interaction are shown.

[1] O. Volkova, I. Morozov, V. Shutov, E. Lapsheva, P. Sindzingre, O. Cépas, M. Yehia, V. Kataev, R. Klingeler, B. Büchner, and A. Vasiliev. *Phys. Rev. B*, **82** (2010) 054413.

1PO-11-32

MAGNETIC ANISOTROPY OF INTERACTING UNIAXIAL SINGLE DOMAIN PARTICLE ARRAYS: SIMULATION AND EXPERIMENT

Baranov D.A., Krichevstov B.B., Fedorov V.V., Sokolov N.S.

Ioffe Physical Technical Institute, St. Petersburg, Russia

dbaranov@mail.ioffe.ru

Two dimension arrays of closely spaced monodomain cobalt nanoparticles were grown by Molecular Beam Epitaxy on CaF₂ buffer layer. Due to specific growth conditions the fluoride buffer layer grown on Si(001) substrate exhibit a grooved and ridged surface morphology faceted by {111}-type surface planes oriented along [1-10] direction of Si substrate [1]. Presence of this preferred direction of corrugation determines the easy axis of magnetisation. Angular dependencies of hysteresis loop of the samples described were investigated by magneto-optical Kerr effect method (MOKE) and showed close to Stoner-Wolfarth system behaviour with the additional coercivity peak near a hard axis direction. Recently it was shown that the appearance of this unusual peak may be related with weak exchange-type interaction between particles and misorientations between their easy axes [2]. Modelling of hysteresis loops was provided on the basis of Stoner-Wohlfarth theory modified to describe this interaction. The Hamiltonian used for the calculations is written below:

$$E = -J \cos(\theta_1 - \theta_2) - K \left(\cos\left(\theta_1 - \frac{\omega}{2}\right)^2 + \cos\left(\theta_2 - \frac{\omega}{2}\right)^2 \right) - HM(\cos(\theta_1 - \beta) + \cos(\theta_2 - \beta)),$$

where J is the exchange interaction constant, K anisotropy constant, θ_1 , θ_2 azimuths of particle magnetisation, β azimuth of applied magnetic field, ω is the misorientation of easy axes directions of particles.

Using steepest descent method the hysteresis loops were calculated for a varied values of easy axes misorientations (ω) and exchange constants J . A peak near a hard axis is present and its parameters depend on a J and ω . Combining the results of modeling for Gaussian distributed J and ω values one can obtain the $H_c(\beta)$ dependences qualitatively agreed with the experimental ones.

Taking into account an easy axis could explain the presence of coercivity peak at hard axis in Co/CaF₂/Si(001) and analogous structures. Magnetic behavior can be described approximately by a weakly interacting nanoparticles with distribution of their easy axis orientations. The interaction energy should be of the order of magnetic anisotropy energy K and probably can arise due to tunneling of electrons between particles.

[1] Sokolov N. S. et al., *Applied Surface Science*, **234** (2004) 480–486.

[2] Idigoras O. et. al., *Physical Review B*, **84**(13) (2011) 132403.

1PO-11-33

THE PECULIARITIES OF MAGNETIZATION REVERSAL PROCESS IN FERROMAGNETIC NANOTUBE WITH HELICAL ANISOTROPY

Serebryakova O.N., Usov N.A.

Pushkov Institute of Terrestrial Magnetism, Ionosphere and Radio Wave Propagation RAS Troitsk,
Moscow, Russia
silver@izmiran.ru

It has been shown recently [1], that the presence of a small off-diagonal component $\sigma_{\varphi z}$ of the residual quenching stress in amorphous ferromagnetic microwire leads to a helical magnetic anisotropy. As a result, the behavior of the longitudinal α_z and circular α_φ components of the unit magnetization vector of the microwire turns out to be significantly correlated. Namely, the change of the sign of the α_z component under the influence of the axial magnetic field H_{0z} leads to a subsequent jump of the α_φ component at some critical value of the external magnetic field H_{0z}^* . The jump of the circular magnetization component can be eliminated by a circular magnetic field of a weak dc bias current flowing along the wire. In the present work this phenomenon is observed also in a soft magnetic nanotube with helical magnetic anisotropy. Using 2D micromagnetic simulation the critical field H_{0z}^* is calculated for a uniform tube as a function of the tube geometrical and magnetic parameters. It is found that the critical field H_{0z}^* only slightly depend on the value of the off-diagonal residual component $\sigma_{\varphi z}$, but it increases significantly as a function of the effective tube anisotropy constant, K_e . The 2D numerical simulation was used also to study the behavior of a tube having a defect in its middle part with different value of the $\sigma_{\varphi z}$ component. It is shown, that the jump of the circular magnetization component starts at the defect. As a result, two bamboo domain walls appear near the defect ends. The bamboo domain walls propagate to the tube ends if the longitudinal external magnetic field decreases further. Similar effect may explain the appearance of the bamboo domain walls in a slightly non uniform amorphous ferromagnetic microwire during magnetization reversal process.

[1] N.A. Usov, S.A. Gudoshnikov, *J. Appl. Phys.*, **113** (2013) 243902.

1PO-I1-34

TEMPERATURE BEHAVIOR OF MAGNETIZATION IN MULTIPHASE Co-P POWDERS IN UNSATURATED REGIME

Li O.A.¹, Komogortsev S.V.², Iskhakov R.S.², Chekanova L.A.², Eremin E.V.²

¹ Siberian Federal University, Krasnoyarsk, Russia

² Institute of Physics, SB RAS, Krasnoyarsk, Russia

rauf@iph.krasn.ru

The measurement of temperature behavior of magnetization is important for the magnetic characterization of material. In ferromagnetic sample at low temperatures this dependence should follow the Bloch $T^{3/2}$ law. Observation of this dependence indicates the dispersion relation $\omega \sim k^2$ for thermal magnons, i.e. proves the ferromagnetic nature of the material. Fitting the experimental data by the Bloch $T^{3/2}$ law allows one to calculate the exchange interaction constant of the material. For such measurements the careful choosing of the applied field is necessary. Small fields are unsuitable, since if the sample is in an unsaturated state the measured temperature dependence of the magnetic moment is largely determined by the dependence of the anisotropy on the temperature. At high fields formation of thermal magnons is suppressed by external magnetic field and there is also a deviation from the Bloch $T^{3/2}$ law. Therefore, it is necessary to select a range of the external magnetic field carefully to measure the temperature dependence of magnetization, wherein the mentioned mechanisms provide negligible contributions to the magnetization gradient in comparison with the Bloch $T^{3/2}$ law, or take into account all these contributions.

In this work we have taken into account these contributions to fit the temperature dependence of the magnetization of Co-P powders with nanocorundum and nanodiamond precipitates. The necessity of such consideration became clear when we primarily fitted $M(T)$ only by the Bloch $T^{3/2}$ law. We found the values of Bloch constant out of physical meaning. To improve the fitting expression we have taken into account both the contribution of the temperature dependence of the anisotropy and the Bose-Einstein function that allows us to describe the effect of the external magnetic field on the excitation of thermal magnons. Temperature dependence of the anisotropy constant is considered in accordance with the Akulov-Zener law $K_n \sim M^{n(2n+1)}$ [1], where n – is the order of magnetic anisotropy constant. Finally fitting expression contains three fitting parameters: magnetization at zero temperature, Bloch constant and the order of the magnetic anisotropy constant. As the result of fitting by these expressions, we find the values of Bloch constants consistent with published data, as well as the value of $n \approx 3$. Such order of magnetic anisotropy constant is possibly related to cubic symmetry of the local magnetic anisotropy in the Co-P alloy.

Work performed within the public task of the Ministry of Education and Science of the Russian Federation to Siberian Federal University in 2014. The support by RFBR Grant 13-03-00476-a is acknowledged.

[1] C. Zener, *Phys. Rev.*, **96** (1954) 1335–1337.

1 July

Tuesday

17:30-19:00

poster session

1PO-I2

**“Magnetic Shape
Memory and
Magnetocaloric Effect”**

1PO-I2-1

STRUCTURAL MARTENSITIC TRANSITION IN POLYCRYSTALLINE Ni-Mn-In HEUSLER ALLOY THIN FILMS

Grunin A.¹, Goikhman A.¹, Rodionova V.^{1,2}

¹ Immanuel Kant Baltic Federal University, 236041 Kaliningrad, Russia

² National University of Science and Technology "MIS&S", Moscow 119049, Russia
agrunin@innopark.kantiana.ru

Heusler alloys attract a lot of attention last decades because of many interesting properties, inherent them. Ni-Mn-In is one of the most studied Heusler alloys, because of the many interesting properties, important for different applications. First of all it is the giant magnetocaloric effect [1], which can be used to create magnetic refrigerator.

Obtaining of the new application opportunities of this exceptional material is possible due to the using of thin films. Therefore, it is very important to know structural and magnetic properties changing upon the decreasing z-dimension of the material from bulk to thin film.

We report here on the results of formation and investigation of polycrystalline thin films on MgO and Si substrates by pulsed laser deposition and two-lasers co-deposition. Structural and magnetic properties of these samples were investigated.

It was shown, that at same composition ($\text{Ni}_{52}\text{Mn}_{36}\text{In}_{12}$) polycrystalline samples on oxidized Si and MgO substrates are formed in different structural phases: B2 phase for MgO substrate and L2₁ for Si/SiO₂.

For both type of samples the structural dynamics of the martensitic transition and magnetic properties, depending on the composition, thickness and deposition parameters were investigated. For several samples near-room temperature or low temperature martensitic transition has been found (fig. 1).

For most of these samples magnetization data depending on temperature in the interval of martensitic transition are strongly differ from bulk samples with similar concentrations.

The work is supported by Ministry of Education and Science of the Russian Federation (Contracts № 14.Y26.31.0002 and 02.G25.31.0086)

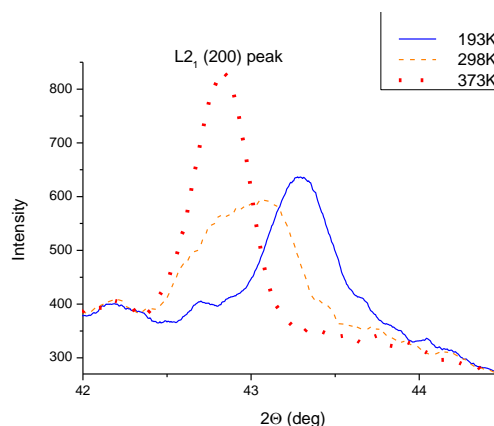


Fig. 1 XRD patterns for Si/SiO₂//Ni₅₁Mn₃₃In₁₆ sample observed at different temperatures

[1] J.Liu, T. Gottschall, K.P.Skokov// *Nature Materials.*, **11** (2012)620–626.

1PO-I2-2

MAGNETOCALORIC EFFECT OF CAST AND RAPIDLY QUENCHED Y₂Fe₁₇ SAMPLES

Karpenkov D.Yu., Skokov K.P., Semenova E.M., Karpenkov A.Yu., Smirnov I.A., Airiyan E.L.
Tver State University, Tver, Russia
karpenkov_d_y@mail.ru

Effect of grain size influence on the magnetocaloric effect (MCE) of the rapidly quenched Y₂Fe₁₇ ribbons was reported before [1], but all of the published MCE data are limited by the temperature dependences of magnetic entropy change $\Delta S_m(T)$, obtained from isothermal magnetization measurements with subsequent recalculation using Maxwell relations. On the other hand, for application in magnetic cooling, adiabatic temperature change ΔT_{ad} is the critical quantity which should be maximized. In this work we address the ΔT_{ad} in polycrystalline and nanocrystalline Y₂Fe₁₇ samples and present the comparable analysis of their magnetic properties.

Rapidly quenched samples were prepared by means of melt-spinning technique at different rotation speeds of copper wheel. Direct measurements of adiabatic temperature change ΔT_{ad} were carried out using the apparatus described in detail elsewhere [2].

Rietveld's analysis of the phase composition of the samples shows the presence of only one phase, which has a hexagonal Th₂Ni₁₇-type crystal structure, however, it should be noted that the lattice parameters for samples obtained at various quenching speed differ from each other. Dependence of the ΔT_{ad} and Curie temperatures on lattice parameters is presented in Table 1.

Table 1. Grain size, lattice parameters, unit volume, Curie temperature and maximum adiabatic temperatures changes of cast and rapidly quenched Y₂Fe₁₇ samples prepared at various copper wheel rotation speed.

Quenching rate, m/s	Grain size, nm	a, Å	c, Å	V, Å ³	T _C , K	ΔT _{ad} , K
cast	5×10 ⁴	8,45	8,30	513,23	335	1,21
10	400	8,44	8,32	513,25	340	1,29
20	200	8,45	8,32	514,46	340	1,29
30	100	8,46	8,30	514,44	332	1,41
35	40	8,44	8,35	515,10	368	1,16
40	20	8,44	8,35	515,10	368	1,07

As it is shown in spite of decreasing grain size a maximum of MCE is observed in the sample obtained at 30 m/s and reaches $\Delta T_{ad} = 1,41$ K. It was found the direct correlation between the lattice parameters and value of MCE in rapidly quenched Y₂Fe₁₇ samples. The variation of unit cell volume leads to shift of Curie temperatures. The last is in a good agreement with the previous investigations of Y₂Fe₁₇ under the pressure [3,4].

Support by grant of RFBR 13-02-00916 A.

- [1] Y. K. Fang, C. W. Chang, C. C. Yeh, et al., *Journal of Appl. Phys.* **103** (2008) 07B302.
 [2] J. Liu, M. Krautz, K.P. Skokov, T.G. Woodcock et al., *Acta Materialia* **59** (2011) 3602–3611.
 [3] S.A. Nikitin, A.M. Tishin, M.D. Kuz'min et al., *Physics Letters A* **153** №2,3 (1990) 155-161.
 [4] Z. Arnold et al., *Journal of Magn. and Mag. Mater.* **272–276** (2004) e1589–e1590.

IPO-I2-3

THE INFLUENCE OF RAPIDLY QUENCHING ON MAGNETOCALORIC EFFECT IN $R\text{Co}_2$ COMPOUNDS

Karpenkov D.Yu.¹, Nikitin S.A.², Karpenkov A.Yu.¹, Skokov K.P.¹, Semenova E.M.¹, Airiyan E.L.¹, Pastushenkov Yu.G.¹

¹ Tver State University, Tver, Russia

² Moscow State University, Moscow, Russia

karpenkov_d_y@mail.ru

The $R\text{Co}_2$ compounds are a one of the most promising candidates for using as refrigerants in magnetic cooling systems in temperature range of 30-150 K [1].

This paper presents the results of investigation of the MCE by means of indirect and direct methods in micro- and nanocrystalline samples of $R\text{Co}_2$ compounds ($R = \text{Er}, \text{Ho}, \text{Tb}, \text{Gd}$).

It was found that in compounds $R\text{Co}_2$ ($R = \text{Er}, \text{Ho}$), in which in cast state the first order phase transition is observed, rapidly quenching leads to a sharp decline of the MCE and the Curie temperature shift toward to higher temperatures (Figure 1).

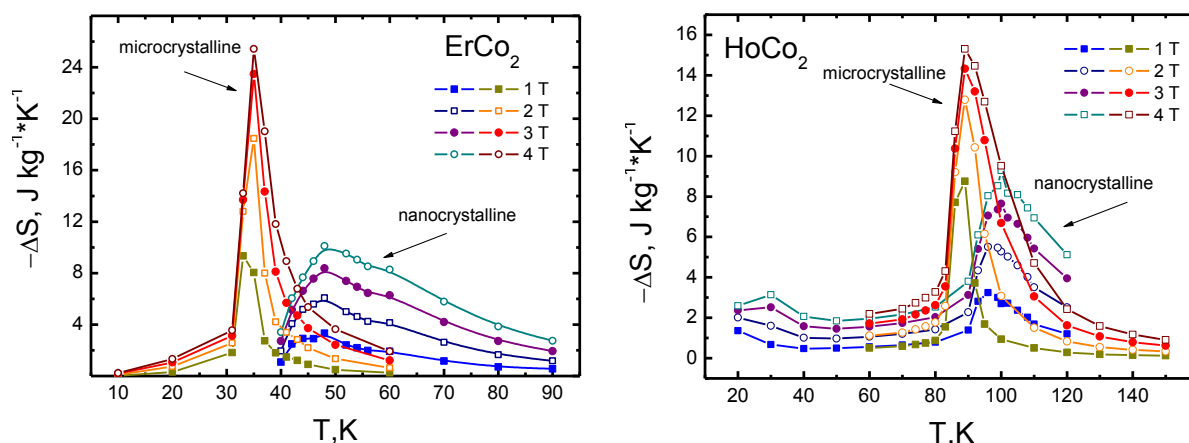


Figure 1. Temperature dependences of the magnetic entropy change for cast and rapidly quenched ErCo_2 HoCo_2 samples.

It is explained by the change of order of phase transition due to the decrease of the lattice parameter in nanocrystalline samples from 7,1555 Å to 7,1476 Å for ErCo_2 and from 7,1750 Å to 7,1698 Å for HoCo_2 in compare with cast samples. The evidence of this fact is the change of the form of Belov's curves. The $\Delta S_M(T)$ peak broadening for rapidly quenched tapes can be partly attributed to the Curie temperature distribution in the grains, which is induced by their size.

Direct measurement of MCE in micro- and nanocrystalline samples of GdCo_2 and TbCo_2 shown that the formation of nanostructures in rapidly quenched samples leads to decreasing of the values of Curie temperature. The magnitude of the magnetocaloric effect in nanocrystalline GdCo_2 sample is less in compare with cast sample. However, in a rapidly quenched TbCo_2 sample it was observed the increasing of MCE.

Support by grant of RFBR 13-02-00916 A.

[1] A.S. Andreenko, K.P. Belov, S.A. Nikitin, A.M. Tishin, *Physics-Uspekhi*, **158** (1989) 553–579.

1PO-I2-4

ELECTROMAGNETIC WAVES RADIATION IN MAGNETIC ALLOYS AT STRUCTURAL PHASE TRANSITIONS

*Kuzmin D.A.¹, Bychkov I.V.¹, Koledov V.V.², Kamantsev A.P.², Kalenov D.V.², Kuchin D.S.²,
Shavrov V.G.²*

¹ Chelyabinsk State University, Chelyabinsk, Russia

² Kotelnikov Institute of Radio-engineering and Electronics of RAS, Moscow, Russia
kuzminda89@gmail.com

In recent years theoreticians and experimentalists physicists have heightened interest in new effects of electromagnetic waves generation under nonequilibrium processes in condensed media. Phase transitions (PT) of 1st and 2nd orders are progressing at significant deviation from equilibrium state, and in this case the medium is active, i.e. it is capable to emit energy as electromagnetic and acoustic waves. So, there is a jump of magnetization ΔM or polarization ΔP of a sample at PT in the magnetic or electro-dipole subsystem respectively, which lead to generation of electromagnetic and acoustic fields pulses [1, 2]. Structural phase transitions of 1st order have a more complex nature of the radiation. Structural PT goes during a certain time when nuclei of a new phase, phase boundaries, various defects, dislocations and fractures may form in the sample, what lead to the generation of electromagnetic and acoustic pulses [3]. All these defects are accompanied by the formation of inhomogeneous elastic deformations.

There is a change of the magnetization of the sample ΔM at magnetic PT of 2nd order, and, as a consequence there is the change in magnetic induction $\Delta B = 4\pi\Delta M$. From Maxwell's equations one can estimate the amplitude of the electric field induced by this change: $E \sim 4\pi\lambda\Delta M (c\tau)^{-1}$. Here λ is a wavelength of radiation, τ is a characteristic time of PT.

The presence of inhomogeneous deformation leads to a redistribution of the electron density at the defect $\Delta n(z)$, and as a consequence to appearance of a dipole moment per unit area of the defect:

$$p_z = -e \int z \Delta n(z) dz.$$

We can represent the motion of a boundary as a moving dipole moment by limiting ourselves only generation of electromagnetic waves, and assuming that it occurs only due to the motion of the phase boundary. The intensity of radiation at a given frequency in the direction specified by an angle θ with z -axis, along which the border moves, has a form:

$$I_{\theta\omega} = \frac{\omega^4}{8\pi^2 c^3} p_{z\omega}^2 \sin^2 \theta$$

It can be seen that the greatest intensity of the radiation goes perpendicular to the direction of the phase boundary motion. When considering the structural PT in conducting materials, the main amount of the electromagnetic energy will emit border that moves on or near the surface of the sample.

[1]. A.M. Kosevich, *Pis'ma JETP*, **11** (1970) 537 (in russian).

[2]. Yu.I. Balkarey, E.V. Chenskii, *Pis'ma JETP*, **13** (1971) 266 (in russian).

[3]. A. Misra et al., *Int. J. Fract.*, **145** (2007) 99.

1PO-I2-5

THE MAGNETOCALORIC EFFECT AND MAGNETIC TRANSITIONS IN HYDRIDE COMPOUNDS: GdNiH_{3,2} AND TbNiH_{3,4}

Smarzhevskaya A.I.¹, Nikitin S.A.¹, Verbetsky V.N.¹, Iwasieczko W.², Golovanov A.N.¹

¹M.V. Lomonosov Moscow State University, Moscow, Russia

² Trzebiatowski Institute of Low Temperature and Structure Research, Polish Academy of Sciences,
Wroclaw, Poland
smarzhevskaya@physics.msu.ru

Rare earth-Ni-based compounds are of huge attention for investigations, as they perform a large magnetocaloric effect (MCE) at low temperature range. The interest for this research is due to the perspectives for mentioned compounds application in cryogenic systems.

Our work was dedicated to the study of transition temperatures and magnetocaloric properties of GdNiH_{3,2} and TbNiH_{3,4} hydride compounds, and their comparison with initial GdNi and TbNi. The possibility of their practical application is also discussed.

The magnetic properties of GdNi and TbNi are well-studied and were reported previously [1]. GdNi is a ferromagnet with collinear magnetic structure and Curie temperature $T_C \sim 70$ K. TbNi has a ferromagnetic state below $T_C \sim 60$ K, and complicated magnetic order (with antiferromagnetic component) at lowest temperatures (< 10 K).

It was shown earlier, that hydrogenation is a method performing a strong influence on crystal structure and magnetic properties of R-Ni compounds [2,3].

The initial GdNi and TbNi alloys were prepared by arc melting. The GdNiH_{3,2} and TbNiH_{3,4} samples were obtained by hydrogenation of initial materials using a Sieverts-type apparatus. The phase composition was examined by X-ray diffraction method.

The magnetization data for GdNi and GdNiH_{3,2} was obtained by SQUID-magnetometer, and for TbNi and TbNiH_{3,2} by PPMS, in the 2–200 K temperature range in 0.1 T field. The M-H isotherms were measured in fields up to 5 T in temperature region around the magnetic transition.

The determination of the isothermal magnetic entropy change ΔS_M in the region of transition temperatures was performed using the appropriate Maxwell thermodynamic relation. The $\Delta S_M(T)$ dependencies are calculated from the M-H isotherms, by numerical integration.

The defined value of transition temperature in GdNiH_{3,2} according to magnetization data in 0.1 T field is ~ 10 K. The corresponding value in TbNiH_{3,4} is ~ 8 K.

The $\Delta S_M(T)$ curves show that ΔS_M in GdNiH_{3,2} reaches its maximum value of $\sim 14 \text{ J kg}^{-1} \text{ K}^{-1}$ at ~ 11 K and ΔS_M in TbNiH_{3,4} reaches its maximum value of $\sim 10 \text{ J kg}^{-1} \text{ K}^{-1}$ at ~ 9 K in a field of 5 T. The maximum values of ΔS_M in hydride compounds are extremely large and obtained at much lower temperatures compared to initial compounds.

The work is supported by RFBR grant #13-02-00916

[1] R.E. Walline, W.E. Wallace, *J. Chem. Phys.*, **41** (1964) 1587.

[2] Yu.L. Yaropolov, V.N. Verbetsky, A.S. Andreenko, K.O. Berdyshev, S.A. Nikitin, *Inorg. Mater.*, **46** (2010) 364.

[3] W. Iwasieczko, H. Drulis, Yu.L. Yaropolov, S.A. Nikitin, V.N. Verbetsky, *J.All.Com.*, **509S** (2011) S827.

1PO-I2-6

STRUCTURAL AND MAGNETIC PROPERTIES OF Ni₂MnIn THIN FILMS*Gaidukova I.Yu.¹, Granovsky S.A.^{1,2}, Sokolov A.³, Devishvili A.⁴, Snegirev V.V.¹*¹ Faculty of Physics, M.V.Lomonosov Moscow State University, Moscow, Russia² Institut für Festkörperphysik, TU Dresden, Dresden, Germany³ UNL Department of Physics and Astronomy, Nebraska, USA⁴ Institut Laue-Langevin, Grenoble, France

ser@plms.ru

Coexistence of magnetism and the martensitic structural transition is reported for off-stoichiometric Mn-rich Heusler alloys Ni₅₀Mn_{50-x}In_x. A variety of magnetic effects in the room-temperature range among their advantages as relative low cost, productibility and harmless makes these materials suitable for practical applications.

Alloys with compositions close to Ni₅₀Mn₃₅In₁₅ are also interesting due to unusual magnetisation temperature dependence. With decreasing temperature these materials transform to ferromagnetic state. Afterwards, the martensitic transition corresponds to drastical decrease of magnetization. Below some characteristic temperature magnetization starts again to increase and a peak appears at $\chi_{ac}(T)$ dependence. Magnetic state in the martensitic phase above and below this transition is not unambiguously proved by microscopic measurements so far. To understand better the unusual properties of these practically applicable materials there is a need for the high-quality macroscopic and microscopic experimental data.

In this contribution we report and discuss the results of macroscopic (magnetisation, ac-susceptibility, magnetoresistance) measurements, X-ray diffraction and neutron reflectivity experiments on ≈ 25 nm thin films of Ni₅₀Mn₃₅In₁₅ grown using Pulsed laser deposition technique on MgO and SrTiO₃ (STO) single-crystalline substrates. These results compared with those, obtained from our measurements of the bulk samples of Ni₅₀Mn_{50-x}In_x.

IPO-I2-7

UNUSUAL TEMPERATURE DEPENDENCE OF THE MAGNETOCALORIC EFFECT IN THE $\text{Dy}(\text{Co}_{1-x}\text{Fe}_x)_2$, ($x = 0.10; 0.15$) COMPOUNDS.

Anikin M.S., Tarasov E.N., Osadchenko V.H., Zinin A.V., Kudrevatykh N.V.

Ural Federal University, Ekaterinburg, Russia

Maksim.Anikin@urfu.ru

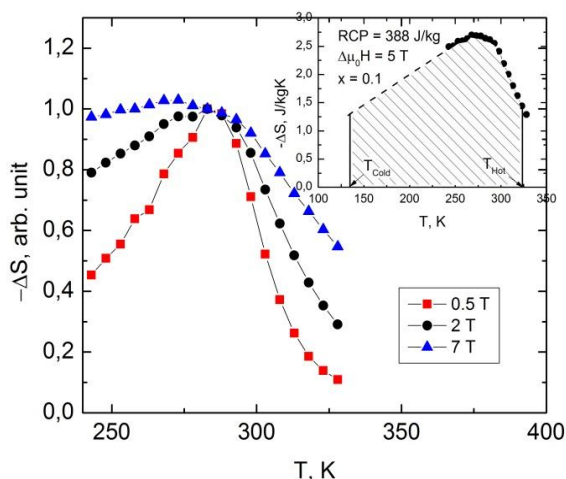


Fig. 1. Reduced value of the magnetic entropy change $-\Delta S_M$ vs temperature for $\text{Dy}(\text{Co}_{0.9}\text{Fe}_{0.1})_2$, sample at different external magnetic fields. The inset shows the $-\Delta S_M$ vs T curve for $\mu_0 H = 5$ T. The shaded area corresponds to the relative cooling power.

Structure, magnetic and thermomagnetic properties of the $\text{Dy}(\text{Co}_{1-x}\text{Fe}_x)_2$ alloys ($x = 0.10, 0.15$) as a perspective material for thermomagnetic machine have been investigated. The alloys were melted in an induction furnace in an argon atmosphere, followed by homogenizing annealing. The room temperature X-ray diffraction data analysis has shown that all samples under the study are nearly single-phase. The 1:2 composition phase has cubic structure of MgCu_2 type with $Fd\bar{3}m$ space group. The lattice parameter a is equal to 7.200 \AA and 7.225 \AA for $x = 0.10$ and 0.15 respectively. Magnetic properties were measured by MPMS XL7 Quantum Design under the field up to 7 T at temperature varied from 4.2 to 390 K. At the Curie temperature (corresponding values are 288 and 350 K respectively) the second-order ferromagnetic-paramagnetic phase transition was observed for all compositions. Temperature dependencies of the magnetic part entropy $-\Delta S(T)$, which were obtained from magnetization isotherms, demonstrated the maximum broadening at temperatures below Curie temperature under magnetic field increasing (Fig. 1.). The similar peak broadenings were observed in the $\text{R}(\text{Ni}_{1-x}\text{Fe}_x)_2$ and $\text{Tb}(\text{Co}_{1-x}\text{Fe}_x)_2$ compounds [1, 2]. In the first case the authors explained the ΔS maximum broadening by rare-earth ion magnetic moment orientations randomization at low temperatures, whereas for the second system authors [2] found the correlation between the width of magnetostructural transition with the maximum of ΔS width. Our results are discussed taking into account the magnetoelastic contribution to the entropy during this compound magnetizing. In paper [3] it was found that in this class of compounds, the contribution of the magnetoelastic energy in the MCE energy released the can be more than 30%.

The relative cooling capacity (RCP) [2] for $\text{Tb}(\text{Co}_{0.7}\text{Fe}_{0.3})_2$ in magnetic field of 5 T, equals to 299 J / kg. For $\text{Dy}(\text{Co}_{0.9}\text{Fe}_{0.1})_2$ the RCP has been calculated by the $\Delta S(T)$ data extrapolating to low temperatures region in a magnetic field of 5 T (inset in Fig. 1). It was found that its value equals to 388 J / kg, which is of practical interest.

- [1] Niraj K. Singh, K. G. Suresh, D. S. Rana, et al., *J. Phys.: Condens. Matter*, **18** (2006) 10775.
 [2] Madhumita Halder, S. M. Yusuf, M. D. Mukadam, et al., *Phys. Rev. B*, **81** (2010) 174402.
 [3] G.A. Politova, I.S. Tereshina, S.A. Nikitin, et al, *Adv. Mater. Special Issue on "Functional nanomaterials and high-purity substances"* (ed. By Acad. K.A. Solntsev) (2008) 405.

IPO-I2-8

STRUCTURAL AND MAGNETIC PROPERTIES OF Mn_2NiX ($X = Ga, In, Sn, Sb$) HEUSLER ALLOYS FROM *AB INITIO* CALCULATIONS

Sokolovskiy V.V.^{1,2}, Zagrebin M.A.^{1,3}, Sokolovskaya Y.A.¹, Buchelnikov V.D.¹

¹ Chelyabinsk State University, Chelyabinsk, Russia

² National University of Science and Technology "MIS&S", Moscow, Russia

³ National Research South Ural State University, Chelyabinsk, Russia

vsokolovsky84@mail.ru

As it is well known, the ferromagnetic Heusler compounds are multifunctional materials, which have been intensive investigated for several years. The interest in view of the research of Heusler alloys is related with unique properties of them and potential applications in the fields of magnetic refrigeration, actuators and spintronic devices. Most of functional properties (magnetic shape memory effect, magnetocaloric effect, magnetoresistance etc.) are coupled with interrelation between structure and magnetism. Typical examples of FSMA are Ni_2MnX ($X = Ga, In, Sn, Sb$), which has been explored extensively [1-3]. Recently, the novel Mn-based Heusler alloys have been proposed as new FSMA with improved functionalities, such as a higher martensitic transition temperature, T_m , and a higher Curie temperature, T_C . For example, T_m and T_C are of single crystalline Mn_2NiGa were found to be 270 and 588 K [4] in comparison with Ni_2MnGa ($T_m \approx 220$ and $T_C \approx 370$ K), respectively [5].

In this work we present first principles investigations structural and magnetic properties of Mn_2NiX Heusler alloys. The *ab initio* calculations have been carried out in the framework of the density functional theory using the SPR-KKR and QUANTUM ESPRESSO packages [6,7]. Our calculations have shown that in all series of Mn_2NiX the ferrimagnetic spin configuration between Mn atoms occupied different sublattices is favor in comparison with ferromagnetic one. In Fig. 1 we show the energy functions versus tetragonal distortion (c/a) for Mn_2NiX . It can be observed that the martensitic phase can be realized in Mn_2NiGa and Mn_2NiSn alloys with the tetragonality distortion of 1.28 and 1.16, respectively. The magnetic moments and exchange couplings in dependent on the lattice parameter, tetragonality and magnetic configuration were also calculated. The critical magnetic temperatures were obtained by means of the mean field approximation.

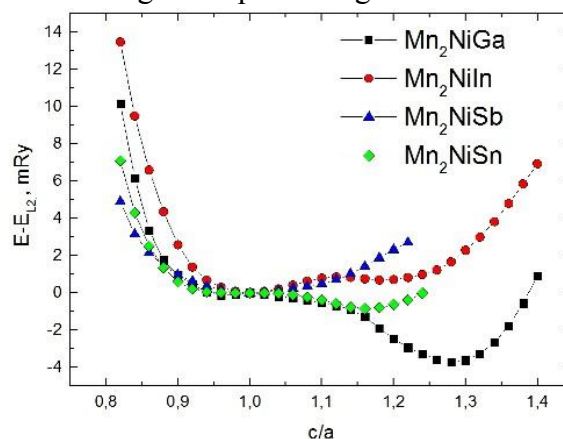


Fig. 1. Variation of the total energy with tetragonal distortion of Mn_2NiX alloys

Support by RFBR Grant # 14-02-01085 and the Creation and Development Program of NUST "MIS&S" are acknowledged.

- [1] A.N. Vasilev et al., *Phys.-Usp.*, **46** (2003) 559-588.
- [2] A. Planes et al., *J. Phys.: Condens. Matter.*, **21** (2009) 233201-29.
- [3] V.D. Buchelnikov and V.V. Sokolovskiy, *Phys. Met. Metallogr.*, **112** (2011), 633-655.
- [4] G. Liu et al., *Appl. Phys. Lett.*, **87** (2005) 262504-3.
- [5] P.J. Webster et al., *Philos. Mag. B*, **49** (1984) 295-310.
- [6] H. Ebert, SPR-KKR package Version 6.3 on. <http://ebert.cup.unimuenchen.de>.
- [7] Quantum ESPRESSO package Version 5.0. <http://www.pwscf.org>.

1PO-I2-9

MAGNETIC AND MAGNETOCALORIC PROPERTIES OF COLD ROLLED Gd_{100-x}Zr_x (x = 0..3) INTERMETALLIC ALLOYS

*Taskaev S.V.¹, Skokov K.P.², Ulyanov M.N.¹, Bataev D.S.¹, Buchelnikov V.D.¹,
Drobosyuk M.O.¹, Khovaylo V.V.³, Pellenen A.P.⁴*

¹ Department of Physics, Chelyabinsk State University, Chelyabinsk, Russia

² Institut für Materialwissenschaft, TU Darmstadt, Darmstadt, Germany

³ National University of Science and Technology "MISIS", Moscow, Russia

⁴ National Research South Ural State University, Chelyabinsk, Russia

tsv@csu.ru

In this work we report the magnetic and magnetocaloric properties of the series of intermetallic alloys Gd_{100-x}Zr_x (x = 0, 0.5, 1, 1.5, 2, 2.5, 3) treated with the help of severe plastic deformation (SPD) technique. Such set of the samples was select with the following reason that a solid solubility limit of Zr in Gd is around x = 3. Subsequent increase of x leads to appear multiphase state.

Such technique is very convenient for designing new functional materials. According the degree of plastic deformation magnetic, structural or thermodynamic properties of the media could be modified and that's the point not only of academic interest, but also of practical application. Since the discovery in 1997 of the «giant magnetocaloric effect» [1] the development of magnetic refrigeration has been growing exponentially. For instance, one of the possible ways for designing materials for magnetic refrigeration is tightly connected with preparation very thin (up to several micrometers) foils with high magnetocaloric effect and good mechanical properties. But as it is shown in our previous works, SPD leads to significant depression of the magnetocaloric effect in severe plastic deformed Gd foils. The reason of such behavior is in magnetic anisotropy induced during SPD treatment. So unusual phenomena drives to new thermodynamic and magnetic properties of deformed Gd foils [2] and make inapplicable them for magnetocaloric application without special high-temperature heat treatment. The heat treatment regimes are directly connected with the degree of deformation.

Here we expand our investigation to other intermetallic compounds Gd_{100-x}Zr_x (x = 0..3) with tunable Curie temperature. These are very simple and convenient materials for room-temperature magnetic refrigeration. Curie temperature linearly decrease with increasing x concentration interval from 291 K to 282 K and show almost the same magnetocaloric effect as observed on pure Gd. The slight decrease of the Curie temperature is observed due to reduction exchange interaction with increasing nonmagnetic Zr atoms concentration. The residual MCE observed in Gd₉₇Zr₃ is about 50% of MCE on pure Gd.

As in the case of pure Gd in the SPD treated Gd_{100-x}Zr_x (x = 0..3) alloys the magnetocaloric effect could be recovered by high-temperature annealing. That temperatures lay within the interval 1235-1300 C which is correspond to reversible structural phase transition from αGd to βGd.

Authors appreciate the RFBR 12-07-00676-a and RF President MD-770.2014.2 grants for financing this work.

[1] K. A. Jr. Gschneidner, V. K. Pecharsky, *Int. J. Refrig.*, **31** (2008) 945

[2] S.V. Taskaev, M.D. Kuz'min, K.P. Skokov, D.Yu. Karpenkov, A.P.Pellenen, V.D. Buchelnikov and O. Gutfleisch, *JMMM*, **331** (2013) 33.

1PO-I2-10

MAGNETIC AND MAGNETOCALORIC PROPERTIES OF COLD ROLLED $\text{Gd}_{100-x}\text{Y}_x$ ($x = 0..30$) INTERMETALLIC ALLOYS

*Taskaev S.V.¹, Skokov K.P.², Ulyanov M.N.¹, Bataev D.S.¹, Buchelnikov V.D.¹, Drobosyuk M.O.¹,
Khovaylo V.V.³, Pellenen A.P.⁴*

¹ Department of Physics, Chelyabinsk State University, Chelyabinsk, Russia

² Institut für Materialwissenschaft, TU Darmstadt, Darmstadt, Germany

³ National University of Science and Technology "MISIS", Moscow, Russia

⁴ National Research South Ural State University, Chelyabinsk, Russia

tsv@csu.ru

Gadolinium is a benchmark material in the magnetic refrigeration technology. As a rule, all magnetic and thermodynamical properties for a new magnetocaloric (MCE) materials are compared with the properties of pure Gd metal. Since the discovery in 1997 of the «giant magnetocaloric effect» [1] the development of magnetic refrigeration has been growing exponentially. Since that event numerous different families of alloys have been found and investigated, see for instance [2]. Some of them are used in known prototypes of magnetic refrigerators and heat pumps, a review of the machines built before the year 2010 can be found in [3]. Nevertheless, up to now Gd still one of the best materials for prototyping magnetic refrigerators.

One of the possible ways of producing MCE materials is connected with preparing very thin (a few microns) ribbons with a high value of MCE and good mechanical properties. At present rapid solidification [4] is the main technique for producing this kind of materials. But one finds little information in the literature about other techniques applied to thinning MCE materials, such as cold rolling. The reasons for thinning MCE materials have been explained by Kuz'min [5]. Apparently the required rapid heat transfer over distances of several centimeters can only be achieved in a two-stage process combining thermal conduction and forced convection. The former is a slow process and a bottle-neck of the whole scheme; it necessitates a close contact between the solid refrigerant and the heat exchange fluid. For an optimal performance at higher frequency, the dimensions should be reduced more significantly, down to 0.1 mm [5]. Examples are known of cooling devices [3] using foils as thin as 0.076 mm.

In this work we report the magnetic and magnetocaloric properties of the series of intermetallic alloys $\text{Gd}_{100-x}\text{Y}_x$ ($x = 0, 2.5, 5, 7.5, 10, 15, 20, 25, 30$) treated with the help of cold rolling. Both room-temperature *hcp* and high-temperature *bcc* forms exhibit complete solid solubility. During cold rolling we observe the same Curie temperatures for appropriate compounds, but the magnetocaloric effect significantly decreased. The as-cast samples cover the Curie temperature interval $\Delta T_C \approx 30$ K (that was the reason of selection x limit). The value of reduction magnetocaloric effect as in pure Gd case depends on the degree of plastic deformation.

As in the case of pure Gd in the cold rolled $\text{Gd}_{100-x}\text{Y}_x$ ($x = 0..30$) alloys magnetocaloric effect could be recovered by high-temperature annealing. Apart $\text{Gd}_{100-x}\text{Zr}_x$ ($x = 0..3$) the annealing temperatures increase with the concentration of yttrium and lay within the interval 1235-1300 C which is correspond to reversible structural phase transition from *hcp* phase to *bcc* phase.

Authors appreciate the RFBR and RF President grants: 12-07-00676-a, MD-770.2014.2.

[1] K. A. Jr. Gschneidner, V. K. Pecharsky, *Int. J. Refrig.*, **31** (2008) 945.

[2] K.A.Gschneidner Jr., V.K. Pecharsky and A.O. Tsokol, *Rep. Prog. Phys.*, **68** (2005) 1479.

[3] Bingfeng Yu, Min Liu, Peter W Egolf, Andrej Kitanovski, *Int. J. Refrig.*, **33** (2010) 1029.

[4] P. M. Shan, J. G. Bohnet, Jeffrey E. Shield, D. Schmitter et al., *Phys. Rev. B.*, **77** (2008) 184415.

[5] M.D. Kuz'min, *Appl. Phys. Lett.*, **90** (2007) 251916.

1PO-I2-11

THE INFLUENCE OF THE IONIC RADUIS OF A-CATIONS ON THE MAGNETOCALORIC PROPERTIES OF $\text{La}_{0.5}\text{Ca}_{0.5-x}\text{Sr}_x\text{MnO}_3$

Batdalov A.B.¹, Gamzatov A.G.¹, Aiev A.M.¹, Amirzadeh P.², Kameli P.², Ahmadvand H.², Salamati H.²

¹ Amirkhanov Institute of Physics of DSC RAS, Makhachkala, Russia

² Department of Physics, Isfahan University of Technology, Isfahan, Iran
Gamzatov_adler@mail.ru

This report presents the experimental data on influence of substitution of Ca^{2+} ions by Sr^{2+} ions of large radius on the heat capacity, susceptibility, and magnetocaloric effect in charge-ordered manganite $\text{La}_{0.5}\text{Ca}_{0.5-x}\text{Sr}_x\text{MnO}_3$ ($x=0, 0.1, 0.2, 0.3, 0.4$).

It is known that the properties of manganites depend on many factors such as a $\text{Mn}^{3+}/\text{Mn}^{4+}$ correlation value, mean ionic radius of A-cations $\langle r_A \rangle$, and a disorder caused by a difference in ionic radius of A-cations σ^2 defined as follows: $\langle r_A \rangle = 0.5r_{\text{La}} + (0.5-x)r_{\text{Ca}} + xr_{\text{Sr}}$ and $\sigma^2 = \sum x_i r_i^2 - \langle r_A \rangle^2$, where x_i and r_i denote a concentration and an ionic radius of i-cation. According to our data the increase of $\langle r_A \rangle$ and σ^2 is attended by the increase in T_C what agrees with the existing concept that a mean radius growth is attended by an increase in Mn-O-Mn bond angle and the amplification of exchange interactions between Mn atoms of different valence.

Direct and precise measurements of MCE allow to estimate the magnetocaloric prospects of materials as well as to determine their phase composition and the dynamics of its change. This follows from that the MCE for ferromagnets is positive and for antiferromagnets is negative, and in a region of the co-existence of both phases there is the different effect what must display in the shape of $\Delta T(T)$ curve.

A Figure depicts that for all samples the MCE is observed. A MCE value increases with rising of x , i. e. when growing the mean ionic radius $\langle r_A \rangle$. For weakly doped compounds the bend-shape anomalies are observed to leftward of maximum which, in our opinion, are connected with co-existence of charge-ordered antiferromagnetic phase with ferromagnetic one. In the pure state, the antiferromagnetic phase is observed for $x=0.3$ only as an inverse magnetocaloric effect. Our results showing the suppression of charge-ordered phase at increase in $\langle r_A \rangle$ correlate with the data of measurements of the heat capacity and susceptibility, and agree with data on researches of magnetic and structural properties of $\text{La}_{0.5}\text{Ca}_{0.5-x}\text{Sr}_x\text{MnO}_3$ reported in [1,2].

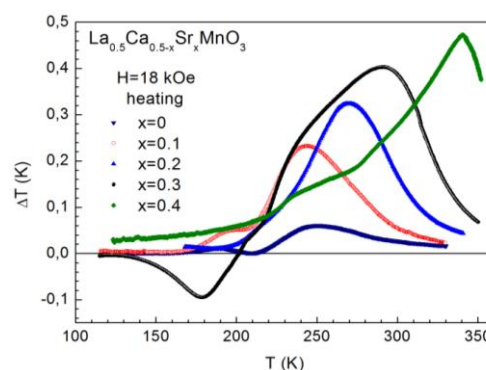


Fig. 1. Temperature dependence of the MCE for $\text{La}_{0.5}\text{Ca}_{0.5-x}\text{Sr}_x\text{MnO}_3$.

This work was supported by the Branch of Physical Sciences of the Russian Academy of Sciences within the framework of the program “Strongly Correlated Electrons in Solids and Structures,” RFBR (Grant Nos. 14-02-01177, 12-02-96506).

[1] M. Bejar et al. *Journal of Alloys and Compounds*, **414** (2006) 31-35.

[2] A. Sundaresan et al. *Phys. Rev. B*, **57** (1998) 2690.

1PO-I2-12

EFFECT OF MAGNETIC FIELD ON THE DILATATION Ni-Mn-Ga ALLOY DURING THE MARTENSITIC TRANSFORMATION

Musabirov I.I.¹, Mulyukov R.R.¹, Koledov V.V.²

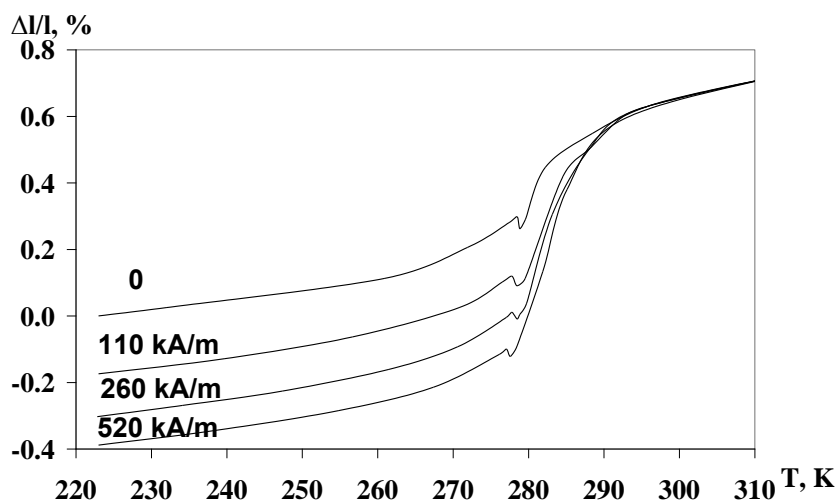
¹ Institute for Metals Superplasticity Problems of RAS, Ufa, Russia

² Institute of Radio Engineering and Electronics of RAS, 125009, Moscow, Russia

irekmusabirov@imsp.ru

Ferromagnetic Heusler alloys of Ni-Mn-Ga belong to the class of promising functional materials. The martensitic phase transformation at the room temperature is observed. Due to this effect the magnetic induced deformation is observed. In the single crystal samples of alloys the reversible deformation of the material under the action reaches 6% in magnetic fields up to 1 T. In the polycrystalline alloys of the value does not exceed one percent. As the polycrystalline materials are cheaper to produce, it is very promising to get the values of the magnetic field induced deformation close to 1% or more. This requires a deep study of the influence of magnetic field on the structure and dimensions of this alloy system.

The results of the magnetic field influence on the geometry of the polycrystalline $\text{Ni}_{2.08}\text{Mn}_{0.96}\text{Ga}_{0.96}$ alloy in the region of the martensitic transformation are presented in this work. The alloy has the following transformation temperature in and around room temperatures: $M_S = 294$ K (21°C); $M_F = 267$ K (-60°C); $A_S = 287$ K (14°C); $A_F = 304$ K (31°C); $T_C = 375$ K (102°C). The size of the sample is 1 mm × 1 mm × 6 mm. It was cut along the



long axis of the alloy ingot. The record of the temperature dependence of thermal expansion of the alloy was carried out in a magnetic field strength of 110 kA/m, 260 kA/m and 520 kA/m when the sample is cooled in the temperature range 310K - 223K. Corresponding results are shown in Fig. As it can be seen, the sample is cooled in the absence of the magnetic field during the martensitic transformation it undergoes an abrupt reduction in the length of 0.35%. The rest of the temperature decrease in the length of the sample cooling is due to anharmonicity. While applying a magnetic field to the sample during its cooling abrupt change of its length during the martensitic transformation increases with the magnetic field increasing. In a magnetic field of 520 kA/m, it reaches 0.75%. Thus, on a polycrystalline $\text{Ni}_{2.08}\text{Mn}_{0.96}\text{Ga}_{0.96}$ alloy it is possible to obtain quantities magnetic field induced deformation close to 1%.

Application or removal of the magnetic field to the sample in the martensitic state does not lead to the change of its geometry. That means that the magnetic field up to 520 kA/m has an impact on the geometry of the polycrystalline $\text{Ni}_{2.08}\text{Mn}_{0.96}\text{Ga}_{0.96}$ alloy sample only during the martensitic transformation.

The work was supported by grant RFBI 14-02-31699 mol_a.

1PO-I2-13

EFFECTS OF COBALT ON THE CRYSTALLINE STRUCTURE AND MAGNETIC ORDERING OF THE Ni-Mn-In GMCE HEUSLER ALLOYS

Madiligama A.S.B.¹, Ari-Gur P.¹, Shavrov V.², Koledov V.²

¹ Western Michigan University, Kalamazoo, MI 49008, USA

² Kotelnikov Institute of Radio-engineering and Electronics of the Russian Academy of Sciences,
Moscow, Russia
amila.bandara@wmich.edu

The giant inverse magnetocaloric effect driven by the merged structural and magnetic transformations in Ni-Mn-X (X-In, Sn, Sb) Heusler alloys, makes them highly promising as solid state refrigerants in magnetic cooling systems operating in near room temperatures [1]. The substitution of small percentage of cobalt with nickel in these alloys intensifies their magnetocaloric performances significantly and results in higher adiabatic temperature changes than other Ni-Mn-X based Heusler alloys even under the moderate magnetic field of 2 T [2]. The governing role of the large cooling effect observed under the application of a magnetic field, plays by the structural transition. Yet, the magnetic spin alignment contribution is equally important as the driving force of the metamagnetic transformations [2]. Investigation of the effects of the Co substitution on the crystalline structure of the martensitic phase is very important to understand the effect of Co substitution on the magnetocaloric effect. The main objectives of this study were to determine the crystalline structure and magnetic ordering of Ni-Mn-In-Co alloys. Constant wavelength neutron diffraction data of the Ni-Mn-In-Co alloy were collected at Oak-Ridge National Laboratory (ORNL) at different temperatures in the range between 50 K and 600 K (Fig. 1). Crystalline structures and magnetic ordering of the martensitic phase were determined by Rietveld refinements of the neutron data. The chemical composition of the sample was determined by the Rutherford Backscattering Spectroscopy and Rietveld refinement of synchrotron and neutron data.

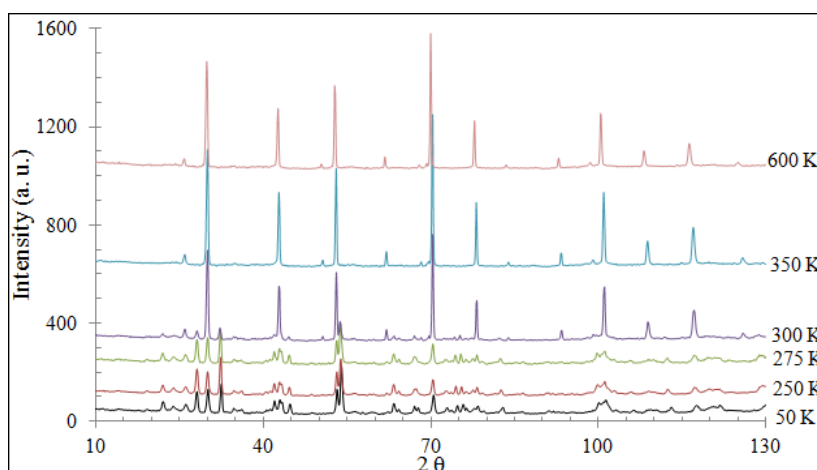


Fig. 1: Temperature variation of the neutron diffraction patterns of Ni-Mn-In-Co showing the transformation from austenite to martensite (below 300K).

Support by Award No. RUP1-7028-MO-11 of the US CRDF Global is acknowledged.

[1] T. Krenke, E. Duman, M. Acet, E. F. Wassermann, X. Moya, L. Mañosa, A. Planes, *Nature*, **4** (2005) 450-454.

[2] J. Liu, T. Gottschall, K. P. Skokov, J. D. Moore and O. Gutfleisch, *nature materials*, **11** (2012) 620-626.

IPO-I2-14

GLASSINES AND MAGNETOCALORIC EFFECT IN Er_5Pd_2

Gubkin A.F.¹, Sherstobitova E.A.², Baranov N.V.^{1,2}

¹ Institute of Metal Physics, RAS, Yekaterinburg, Russia

² Institute of Natural Science, Ural Federal University, Yekaterinburg, Russia
agubkin@imp.uran.ru

The rare-earth intermetallic compounds R_5Pd_2 ($\text{R} = \text{Tb}, \text{Dy}, \text{Ho}, \text{Er}$) possess the highest content of the R-element within the R-Pd series. All these compounds crystallize in a cubic crystal structure which can be described by the space group $Fd\bar{3}m$ [1]. It has recently been shown that the magnetic state of Tb_5Pd_2 and Ho_5Pd_2 compounds exhibit a complicated cluster-glass-like magnetic state [2]. In order to study the magnetic state and magnetocaloric properties of Er_5Pd_2 we have performed the DC and AC magnetic susceptibility measurements by using a MPMS Quantum Design SQUID magnetometer. The AC-susceptibility was measured using driven field amplitude $H_a = 4$ Oe in the frequency range 0.9-997 Hz. It has been found that both the real (see fig. 1) and imaginary components of the AC-susceptibility reveal drastic frequency dependence below the cusp temperature. Moreover, the cusp shifting towards higher temperature with frequency rise implies a cluster-glass-like transition at $T_f \approx 13.5$ K. The DC magnetic measurements on a polycrystalline Er_5Pd_2 sample on ZFC-FC procedure have revealed a highly irreversible behaviour below 13.5 K (see inset in the fig.1). The results obtained allow us to suggest that the Er_5Pd_2 compound exhibits a complex non-ergodic magnetic state of a cluster-glass type associated with frustrations in the RKKY-type exchange interaction. An estimation of the isothermal entropy change ($-\text{dS}_m$) for magnetic fields up to 50 kOe (fig. 2) shows that the maximal values of ($-\text{dS}_m$) observed for Er_5Pd_2 are of the same order as for other well known magnetocaloric materials. This work was supported in part by the by the program of the Ural Branch of RAS (project No 12-T-2-1012).

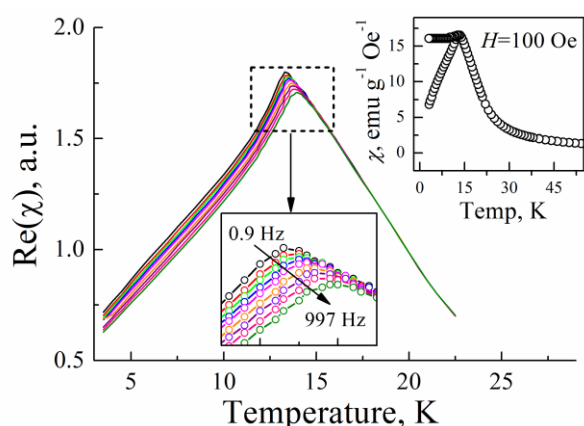


Fig. 1 Real component of the AC-susceptibility as a function of temperature for Er_5Pd_2 . (Inset) ZFC-FC curves of the DC susceptibility measured in a field of 100 Oe.

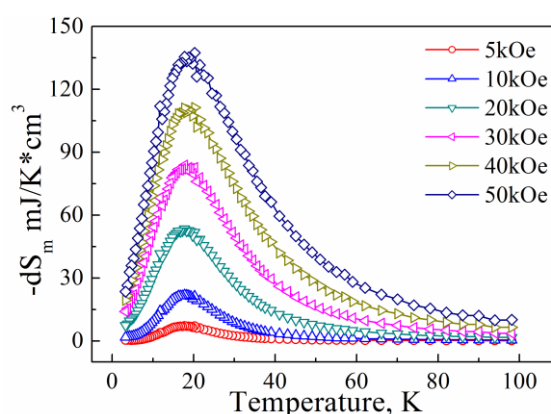


Fig. 2 Isothermal entropy change ($-\text{dS}_m$) for Er_5Pd_2 as a function of temperature.

[1] M. L. Fornasini and A. Palenzona, *J. Less-Common Met.*, **38** (1974) 77–82.

[2] A. F. Gubkin, E. A. Sherstobitova, P. B. Terentyev, A. Hoser and N. V. Baranov *J. Phys.: Condens. Matter* **25** (2013) 236003.

1PO-I2-15

HEAT PUMPING SCHEME BASED ON INDUCEMENT OF THE F-AF TRANSITION IN FeRh BY PRESSURE

Rodionov V.V.¹, Rodionova V.V.^{1,2}, Annaorazov M.P.¹

¹ Immanuel Kant Baltic Federal University, Innovation park, Kaliningrad 236000, Russia

² National University of Science and Technology "MIS&S", Moscow 119049, Russia

rodionov_vlad@mail.ru

The heat pump cycles based on inducement of the AF-F transition in FeRh alloys by tensile stress and magnetic field, were recently discussed [1, 2]. Since this transition can be induced by pressure as well [3], it may be used for construction of combined heat pump cycles with sign-changing mechanical load of the alloy, which may be useful, for example, for broadening of the cycles' temperature range. Present work is devoted to estimation of the efficiency of the heat pump cycles based on the pressure induced F-AF transition in FeRh alloy.

The efficiency of a heat-pump cycle is expressed in terms of the coefficient of performance, φ , which is defined as the ratio of the amount of heat given by the system undergoing the cycle to the heat receiver, Q_{HR} , to the work transfer of energy into the system to accomplish this effect.

On the base of the model $S-T$ projection of $S-T-P$ surface for FeRh alloy [4] the 3 types of heat pump cycles are drawn up:

- (1) with acquisition by the alloy the heat from external heat source;
- (2) partial acquisition by the alloy the heat from external heat source;
- (3) and the cycles based on the adiabatic inducement the F-AF transition by pressure.

Corresponding efficiencies φ_1 , φ_2 , and φ_3 of these cycles as functions of temperature at various differences between initial and final temperatures (permanent thermal load ΔT) and as a function of pressure at various differences between initial and final temperatures are analyzed using the certain set of the experimental data [4].

It is found, particularly (Fig. 1), that within the temperature range (320 – 370) K and pressure range $(0.4 - 1.0) \cdot 10^9$ Pa efficiency of the heat-pump cycles takes the values from the interval from 30 to 35. These values are comparable to those found in [1] with using the tensile stress up to $\psi = 1 \cdot 10^9$ Pa and in [2] with using the magnetic field up to $H = 2 \cdot 10^6$ A/m.

[1] M.P. Annaorazov *et al.*, *Int. J. Refrigeration*, **25** (2002) 1034-1042.

[2] M.P. Annaorazov *et al.*, *J. Magn. Magn. Mater.*, **251** (2002) 61-73.

[3] L.I. Vinokurova *et al.*, *phys. stat. sol. (b)*, **78** (1976) 353-357.

[4] M.P. Annaorazov, *J. Alloys Compd.* **354** (2003) 1-5.

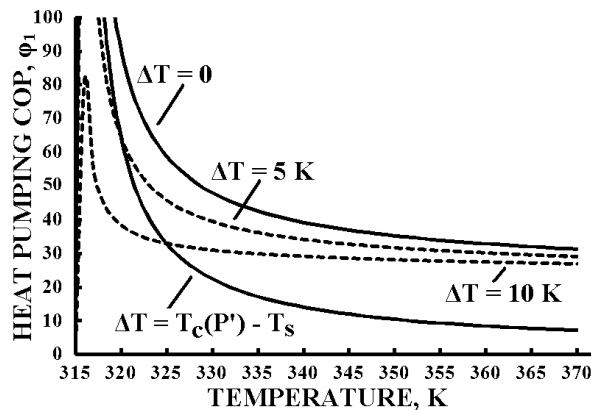


Fig. 1. Efficiency φ_1 of a heat-pump cycles based on inducement of the F-AF transition in FeRh by pressure. $T_c(P')$ – the critical temperature of the F-AF transition at pressure P' , T_s – the temperature of the surroundings.

1PO-I2-16

MAGNETIC PHASE TRANSITIONS AND MAGNETOCALORIC EFFECT IN R₂Fe₁₇ (R = Y, Tb, Er) COMPOUNDS

Nikitin S.A.¹, Ovchenkova I.A.¹, Tskhadadze G.A.¹, Skokov K.P.²

¹ M.V.Lomonosov Moscow State University, Physics Dept., Moscow, Russia

² Physical-Technical Dept, Tver State University, Tver, Russia
ovtchenkova@mail.ru

The direct measurements of the magnetocaloric effect (MCE) and the magnetization have been conducted for R₂Fe₁₇ (R = Y, Tb, Dy) compounds.

The R₂Fe₁₇ compounds are the two sublattice magnetics with a high concentration of 3d-metal. The ferrimagnetic ordering with the opposite orientation of R and Fe sublattices realizes in R₂Fe₁₇ compounds with the heavy rare earth elements (R = Gd – Tm), while the compounds with light rare earth elements and Y are ferromagnetics. The moderate magnetic ordering temperatures (around the room temperature) make these compounds promising for magnetic refrigeration.

The wide maximum of the MCE is observed around the Curie temperature T_C for all the investigated compounds. The maximal value of the MCE is almost the same and is equal to 0.8 – 0.85 K at $\Delta H = 13.5$ kOe near T_C .

The magnetization and the MCE measurements reveal the following peculiarities in R₂Fe₁₇ compounds:

1. The wide region of the magnetic phase transition.

2. In contrast to the majority of previously investigated compounds [1], to analyze the dependence of ΔT on magnetization of the sample I , it is necessary to include not only the second power of the magnetization, but also its forth power. At the Curie temperature where the spontaneous magnetization $I_s = 0$, this dependence can be recorded as

$$\frac{\Delta T}{I^2} = \frac{T}{C_{V,I}} \frac{\alpha}{2} + \frac{T}{C_{V,I}} \frac{1}{4} \beta I^2,$$

where α , β – are the temperature coefficients, $C_{V,I}$ – the heat capacity.

3. The thermodynamic Arrot-Belov plots (H/I on I^2) are not linear, while the H/I on I^4 plots are the straight lines.

An exceedingly low in comparison with pure iron magnetic ordering temperatures, and a strong dependence of magnetic properties on the hydrostatic pressure or the injection of the interstitial atoms [2, 3] indicate to the presents of the atomic positions with interatomic distances close to the critical. That leads to the occurrence of the mixed exchange interaction (both ferro- and antiferromagnetic).

Thus the magnetic phase transition to magnetically ordered state in R₂Fe₁₇ compounds has a complex character. To describe this transition it is essential to consider not only the thermal fluctuations but also the local fluctuations of the exchange integrals. This leads to the modifications of dependences of $\Delta T(I)$ and $I(H)$ in comparison with the classical ferromagnetics. The contributions of fluctuations proportional to the forth power of magnetization play an important role.

The work has been supported by RFBR grant 13-02-00916A.

[1] S.A. Nikitin, G.A. Tskhadadze, I.A. Ovchenkova, D.A. Zhukova, T.I. Ivanova, *Solid State Phenomena*, **168** (2011) 119-121.

[2] S.A. Nikitin, A.M. Tishin, M.D. Kuzmin, Yu.I. Spichkin, *Phys.Let.A.*, **153** (1991) 155-161.

[3] S.A. Nikitin, *Moscow University Physics Bulletin*, **66**(6) 519-533.

1PO-I2-17

OSCILLATING MAGNETOCALORIC EFFECT IN GRAPHENE

Alisultanov Z.Z.^{1,2}

¹ Amirkhanov Institute of Physics, Dagestan Science Centre, RAS, Makhachkala, Russia

² Dagestan State University, Makhachkala, Russia
zaur0102@gmail.com

Recently, oscillating MCE in diamagnetic materials was investigated [1-3]. This new effect was studied in 3D, 2D non-relativistic materials [1], graphene monolayer [2] and in size-quantized diamagnetic film [3]. The magnetic part of the entropy has a maximal value at some temperature. Such behavior of the entropy is not observed in magneto-ordered materials. Other interesting results have been obtained: the temperature, at which peak entropy is observed in graphene, is almost 100 times more than in the non-relativistic materials. The study of oscillating MCE provides additional information about the system, in particular, the energy spectrum of media, information about the fundamental physical constants etc.

In this paper we study the oscillating magnetocaloric effect in biased and unbiased bilayer graphene. We obtained the general expression for thermodynamic potential. We investigated the entropy and adiabatic temperature change as functions of magnetic field and gate voltage. We compare our results with case of monolayer graphene and we give a qualitative explanation of effects. We proposed a new electrocaloric effect in bilayer graphene.

Oscillations of adiabatic temperature change in monolayer are shown in Fig. 1. As we see from Fig. 1, the temperature change in monolayer is more than in BG. A large change of the electron temperature in this case is apparently can be explained as follows. Temperature of system is determined by entropy. The entropy, for given energy, is determined by concentration of energy states in the vicinity of this energy (in Boltzmann

thermodynamics) or by total number of states with energy less than this energy (in Gibbs thermodynamics). Change of these energy states determines the temperature change. In magnetic field, the number of states changes, that is due to the appearance of the Landau levels. Obviously, that the greater the distance between these levels, the lower the number of the levels, and therefore the greater the change in entropy. Taking into account that distance between Landau levels in graphene is much larger, than in non-relativistic materials, our result becomes clear.

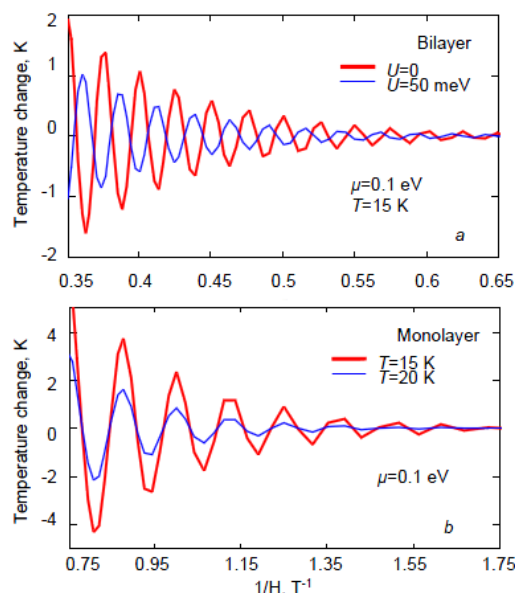


Fig. 1. Adiabatic temperature change as function of a reverse magnetic field for bilayer (a) and monolayer (b).

- [1] M.S. Reis, *Appl. Phys. Lett.* **99** (2011) 052511.
 [2] M.S. Reis, *Appl. Phys. Lett.* **101** (2012) 222405.
 [3] Z.Z. Alisultanov, *J. of Appl. Phys.* **115** (2014) 113913.
 [4] Z.Z. Alisultanov, *JETP* **119** (2014) (in press).

1PO-I2-18

UHF RADIATION AT MARTENSITIC TRANSITION OF $\text{Ni}_{2,14}\text{Mn}_{0,81}\text{GaFe}_{0,05}$ FERROMAGNETIC HEUSLER ALLOY

Kuzmin D.A.¹, Bychkov I.V.¹, Kalenov D.V.², Kamancev A.P.², Koledov V.V.², Kuchin D.S.², von Gratowski S.V.², Meriakri V.V.², Parkhomenko M.P.², Shavrov V.G.²

¹Chelyabinsk State University Russia

²Kotelnikov Institute of Radioengineering and Electronics of RAS, Moscow, Russia
victor_koledov@mail.ru

In this paper we investigate experimentally the electromagnetic response and the ability to self-radiation of electromagnetic wave (EMW) at the free surface of the sample Heusler alloy $\text{Ni}_{2,14}\text{Mn}_{0,81}\text{GaFe}_{0,05}$ in the UHF wavelength range of 8 mm. The phase transitions (PTs) in this alloy are known to occur: magnetic PT of 2nd order paramagnet - ferromagnet ($T_c = 90^\circ\text{C}$) and a structural thermoelastic PT of the 1st order from austenite to martensite ($A_s = 54^\circ\text{C}$, $A_f = 63^\circ\text{C}$, $M_s = 58^\circ\text{C}$, $M_f = 45^\circ\text{C}$) [1].

To investigate the radiation of the sample and to separate the contributions from radiation caused by the sample at PT, and the contribution of changes in the reflection coefficients of thermal radiation environment in the range 24 - 30 GHz, an original experimental setup was constructed. It includes test sample Heusler alloy in the form of a plate with dimensions 10x10x0.5 mm with a temperature control system in the range from 0 to 120 °C, and magnetometer for registration of magnetic susceptibility of the sample *in situ*, the radiometer with the waveguide in direct contact with the sample, circulator and radiating load whose temperature can vary from room temperature to liquid nitrogen. Miniature temperature sensor is installed directly on the sample surface in order to prove monotonic temperature evolution of the sample at PTs. Radiometer output data (U) are shown in Fig. 1 (depending on time). Analysis of typical dependencies of radiometer signal shows that the radiation output of the alloy sample is the nonmonotonic function of temperature, and has pronounced anomalies near the PTs (Fig. 1).

The peaks of the radiation do not disappear when the load temperature increases from liquid nitrogen temperature to room temperature. This proves that the external radiation reflected from the sample surface with different coefficients in different structural phases does not explain the registered by radiometer peaks.

Theoretical model is also proposed in order to explain the experimental evidence of specific radiation at martensitic PT. The model is based on the assumption that electronic structure and electron concentration on the boundaries of different structural phases in the Heusler alloy can lead to EMW generation when these boundaries are caused to move at PT.

Support by RFBR 12-08-01043, 2-07-00811, 12-07-00676, 12-07-00656, 13-07-12130 and CRDF RUP1-7028-MO-11 is acknowledged.

[1] A.A. Cherechukin et al. *Physics Letters A*, **291** (2001) 175–183.

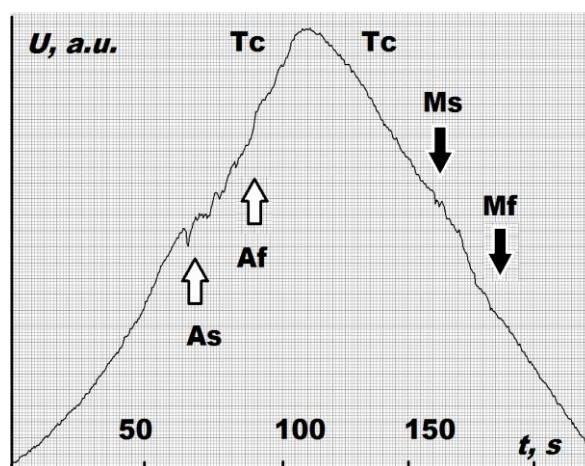


Fig. 1. UHF radiation at 8 mm wave length measured *in situ* at phase transitions from NiMnGaFe Heusler alloy.

1PO-I2-19

THE INFLUENCE OF Fe-DOPING ON THE MAGNETOCALORIC EFFECT OF (Tb,Dy,Ho) Co₂ COMPOUND

Chzhan V.B.^{1,2}, Politova G.A.^{1,2}, Tereshina I.S.^{1,2,3}, Burkhanov G.S.¹, Tereshina E.A.^{3,4}, Chistyakov O.D.¹, Il'yushin A.S.³

¹ Baikov Institute of Metallurgy and Material Sciences RAS, Moscow 119991, Russia

² International Laboratory of High Magnetic Fields and Low Temperatures, Wroclaw 53-421, Poland

³ M.V. Lomonosov Moscow State University, Faculty of Physics, Moscow 119991, Russia

⁴ Institute of Physics ASCR, Prague 18221, Czech Republic

lemuriform@gmail.com

The alloys of rare earths (R) and transition metals (T) form a large class of materials important from both the fundamental point of view and technological application. Among them, special attention is attracted to the cubic Laves phases compounds RT₂ (T = Fe, Co). Relatively simple crystallographic and magnetic structures make these compounds suitable model objects. High magnetostriction of Co-based materials in the vicinity of the Curie temperature is at the same time accompanied by a significant magnetocaloric effect (MCE). In recent years, the latter created a continuous growing interest due to its possible practical application in magnetic refrigerants.

The present work focuses on the study of a multicomponent (Tb_xHo_{0.75-x}Dy_{0.25})Co₂ and (Tb_xHo_{0.75-x}Dy_{0.25})Co_{1.75}Fe_{0.25} (x=0.25 and 0.5) compounds synthesized with the use of high-purity rare-earth metals. The MCE measurements were performed by a direct method in the fields up to 1.8 T. In Fig.1 performed adiabatic temperature change (ΔT_{ad}) of Tb_{0.5}Dy_{0.25}Ho_{0.25}Co₂ compound. It is seen that a rather sharp maximum of the adiabatic variation in temperature is observed at the temperature of the magnetic phase transition ($T_C=173$ K). It should be noted that the value of the MCE reaches saturation in the field 1.5 T (see inset in Fig.1).

For a practical applications, it is important to shift the transition temperature to climatic temperatures region. For this purpose we have been done on substitution of cobalt for iron atoms. As a result, small dope of iron was able to raise the transition temperature to room temperature, whereas the value of the MCE is significantly reduced.

The increase in the Curie temperature and distinct broadening the paramagnetic-ferromagnetic phase transition, which were found upon Fe-doping of this compounds give an opportunity to use such materials in practice.

The work is supported by RFBR, pr. No. 13-03-00744, pr. No. 14-03-31342 and by the Czech Science Foundation, P204/12/0150. Magnetic measurements in steady fields have been performed in MLTL (<http://mltl.eu>) supported within the program of the Czech Research Infrastructures (project no. LM2011025).

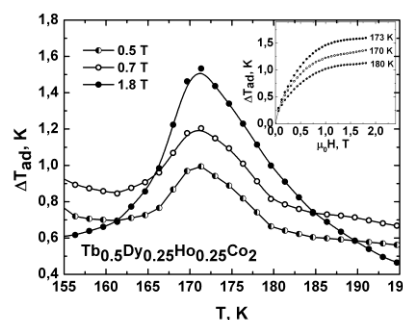


Fig. 1. Adiabatic temperature change ΔT_{ad} vs. temperature for Tb_{0.5}Dy_{0.25}Ho_{0.25}Co₂ (On inset: ΔT_{ad} vs. magnetic field)

1PO-I2-20

STRUCTURE, ELECTRICAL AND MAGNETIC PROPERTIES OF Ni-Mn-In BASED HEUSLER ALLOYS

*Emelyanova S.M.¹, Marchenkov V.V.¹, Platonov E.P.¹, Belozerova K.A.¹, Patrakov E.I.¹,
Wang R.L.², Yang C.P.², Weber H.W.³, Eisterer M.³, Kaletina Yu.V.¹*

¹ Institute of Metal Physics Ural Branch of the Russian Academy of Sciences, 620990 Ekaterinburg, Russia

² Faculty of Physics and Electronic Technology, Hubei University, 430062 Wuhan, People's Republic of China

³ Atominstitut, Vienna University of Technology, 1020 Vienna, Austria
890_sm@mail.ru

Magnetic materials with a giant magnetocaloric effect (MCE) are of great scientific and practical interest due to their potential application in magnetic refrigeration [1, 2]. This technology [3] is environmentally friendly and energy saving. A significant magnetocaloric effect had been already observed in ferromagnetic Heusler alloys with shape memory based on Ni-Mn-Z (Z = Sn, Ga, In) [4].

In this study we investigated structure, magnetic and electrical properties of the Heusler alloys $\text{Ni}_{47-x}\text{Mn}_{42+x}\text{In}_{11}$ ($x = 0, 1, 2$). An elemental analysis demonstrated that the alloy composition corresponded to the nominal composition. XRD investigations confirmed the presence of the $L2_1$ structure in all samples. Fig. 1 shows the temperature dependence of the magnetic entropy change ΔS , obtained similarly to Ref. [5] in a field of 7 T.

In the $\text{Ni}_{47}\text{Mn}_{42}\text{In}_{11}$ alloy (Curie temperature $T_C = 338$ K) there is a peak of ΔS at $T = 310$ K with a maximum value of $\Delta S_{\text{max}} = 14.2$ J/(kg·K). Substitution of Ni atoms by Mn atoms leads to a decrease of the ΔS value and to a peak shift to the low temperature region, i.e. to 8.5 J/(kg·K) at 270 K for the $\text{Ni}_{46}\text{Mn}_{43}\text{In}_{11}$ alloy ($T_C = 328$ K) and to 3.6 J/(kg·K) at 220 K for the $\text{Ni}_{45}\text{Mn}_{44}\text{In}_{11}$ alloy ($T_C = 330$ K), respectively. The results are discussed in the frame of modern concepts and can be used for practical applications.

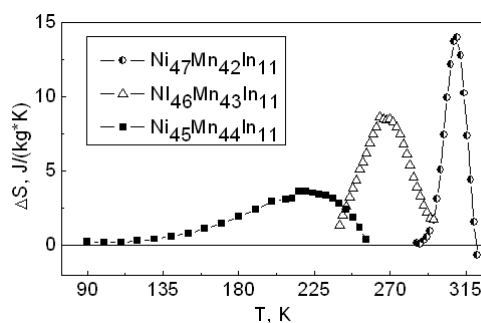


Fig. 1. Temperature dependence of the magnetic entropy change ΔS in a field of 7 T.

This work was partially supported by the Program of UB RAS (project No 12-U-2-1036) and by RFBR (grant No 12-03-00050).

- [1] V.K. Pecharsky, K.A. Gschneider, *Phys. Rev. Lett.*, **78** (1997) 4494.
 [2] O. Tegus et. al., *Nature* (London), **415** (2002) 150.
 [3] K.A. Gschneider et. al., *Rep. Prog. Phys.*, **68** (2005) 1479.
 [4] J. Du et. al., *J. Appl. Phys.*, **40** (2007) 5523.
 [5] R.L. Wang et. al., *Solid State Commun.*, **151**, (2011) 1196–1199.

1PO-I2-21

MAGNETOCALORIC EFFECT AND FRUSTRATIONS IN ONE-DIMENSIONAL MAGNETS

Zarubin A.V.¹, Kassan-Ogly F.A.¹, Medvedev M.V.², Proshkin A.I.¹

¹ Institute of Metal Physics, Ural Division, RAS, Ekaterinburg, Russia

² Institute of Electrophysics, Ural Division, RAS, Ekaterinburg, Russia

alexander.zarubin@imp.uran.ru

We investigated magnetocaloric effect [1] in different 1D ferro- and antiferromagnetic models: Ising, Heisenberg, XY-model, standard, planar, and modified Potts models on the base of exact solutions in the framework of Kramers-Wannier transfer matrix method. The Ising model was solved for arbitrary spin value. We also obtained a general solution for magnetocaloric effect in paramagnets for any model, in any lattice of arbitrary dimension. The magnetocaloric effect (MCE)

$$\left(\frac{\partial T}{\partial H}\right)_S = -\frac{T}{C}\left(\frac{\partial S}{\partial H}\right)_T.$$

is expressed through the maximum eigenvalue of the transfer matrix in such a way:

$$MCE = \frac{\lambda \frac{\partial \lambda}{\partial H} + T\lambda \frac{\partial}{\partial T} \frac{\partial \lambda}{\partial H} - T \frac{\partial \lambda}{\partial H} \frac{\partial \lambda}{\partial T}}{2\lambda \frac{\partial \lambda}{\partial T} - T\left(\frac{\partial \lambda}{\partial T}\right)^2 + T\lambda \frac{\partial^2 \lambda}{\partial T^2}},$$

Main conclusions.

The magnetocaloric effect in a ferromagnet (without competing interactions) is always positive and achieves maximum values in a field $H \rightarrow 0$, and in 1D case, it takes place at $T \rightarrow 0$.

In antiferromagnets, there always exist the frustration fields [2] even with only nearest-neighbor interaction J taken into account. For example, the frustration field in the Ising model with arbitrary spin s is equal to $-2sJ$ and the entropy in the frustration field at $T=0$ is equal to $\ln[(1+\sqrt{1+8s})/2]$. In an antiferromagnet MCE can be both positive and negative (Fig. 1). It achieves arbitrary great values in a field tending to the critical field that coincides with the frustration field at $T=0$. The critical field decreases with T increasing, vanishing at some temperature. Depending on a model (with next-nearest-neighbor interactions), the frustration fields may be several. The MCE changes sign when crossing the critical fields corresponding to every frustration field.

In paramagnets, the magnetocaloric effect is always equal to T/H irrespective of a model, type of lattice, a dimension, and field direction.

Support by project of Integrated Fundamental Research of UD RAS no.12-I-2-2020 is acknowledged.

[1] M.E. Zhitomirsky and A. Honecker. *J. Stat. Mech.* (2004) P07012.

[2] F.A. Kassan-Ogly, B.N. Filippov, A.K. Murtazaev, M.K. Ramazanov, M.K. Badiev. *JMMM*, **324** (2012) 3418-3421.

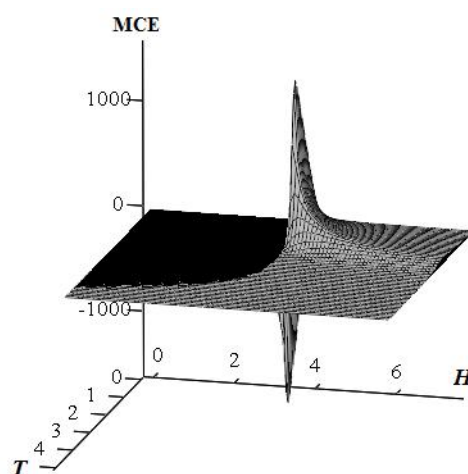


Fig. 1. Magnetocaloric effect nearby the critical field in antiferromagnet.

1PO-I2-22

MAGNETOCALORIC EFFECT IN Ni-Mn-In BASED HEUSLER ALLOYS*Rodionov I.D.¹, Prudnikov V.N.¹, Pavlochev S.Y.¹, Dubenko I.S.², Ali N.², Granovsky A.B.¹*¹ Faculty of Physics, Lomonosov Moscow State University, Moscow, Russia² Department of Physics, Southern Illinois University, Carbondale, USA

rodionovID@yandex.ru

It has been found that off-stoichiometric Ni₅₀Mn_{50-x}In_x Heusler alloys exhibit field and temperature induced magnetostructural transitions, exchange bias, giant deformations, kinetic arrest, direct and inverse magnetocaloric effect (MCE) [1,2], large magnetoresistance, giant anomalous Hall effect [3] and other interesting properties from the point of view of potential technological applications. These alloys are considered among most promising materials for magnetic refrigerators based on MCE [2]. Since disorder in these alloys plays a key role, even a small change in composition or an addition of fourth element Z to Ni-Mn-In alloys can drastically change all their properties that allow tuning their MCE parameters.

We present our last experimental results on MCE in ternary Ni₅₀Mn_{50-x}In_x alloys with the ratio e/a between 7.8 and 7.9 and in different quaternary Ni-Mn-In-Z (Z =Co, Ag, Al, B, Si) bulk Heusler alloys focusing on direct measurements of the adiabatic change of temperature $\Delta T_{ad}(H)$ under an applied magnetic field H up to 18 kOe in the vicinity of the first-order magnetostructural phase transition and second-order magnetic phase transition. Direct measurements of $\Delta T_{ad}(H)$ were done using an adiabatic magnetocalorimeter (MagEq MMS 801 set up) at heating and cooling the samples in a temperature range of 250-350 K. To compare with indirect estimations of the MCE parameters we also found the change of magnetic entropy $\Delta S_{mag}(H)$ using magnetic measurements and Maxwell equation.

As a rule results of direct and indirect determination of the MCE parameters are consistent with each other but we found that some features found by direct measurements are not seen in indirect measurements. For example, we observed that $\Delta T_{ad}(H)$ is always smaller at cooling than at heating in the vicinity of the first-order phase transition. We also observed besides large MCE near first- and second-order phase transitions an additional small peak in $\Delta T_{ad}(H)$ for Ni-Mn-In-Al, which could not be resolved using magnetic measurements. The value of $\Delta T_{ad}(H)$ varies between 1.0 and 3.0 K depending on type of doping element Z and characteristic temperature of the phase transition. It is also shown that simple considerations on phase transitions and MCE parameters based on the ratio e/a are not appropriated to Ni-Mn-In based alloys.

This work was partly supported by the Russian Foundation for Basic Research (grant No. 12-02-00095a) and by the Office of Basic Energy Sciences, Material Science Division of the U.S. Department of Energy (Grant No. DE-FG02-06ER46291).

[1] I. Dubenko et al., *J. Magn.Magn.Mat.* **324**, 3530-3534 (2012).

[2] J. Liu et al., *Nature Materials* **11**, 620-626 (2012).

[3] A. Granovsky et al., *JETP* **115**, 805-814 (2012).

1PO-I2-23

TOWARDS THE DEFINITION OF REFRIGERANT CAPACITY OF MAGNETOCALORIC MATERIALS

*Karpenkov A.Yu., Skokov K.P., Karpenkov D.Yu., Balbikhina O.V., Airiyan E.L.,
Pastushenkov Yu.G.*

Tver State University, Tver, Russia
karpenkov_alex@mail.ru

Currently, there is the question about evaluating the effectiveness of using the magnetocaloric material as a working body of magnetic refrigerators. On the one part, in the terminology of refrigeration engineering the refrigerant capacity is defined as an amount of heat absorbing from the cooled object per refrigeration cycle Q_c (per mass/volume unit of refrigerant), i.e. for conventional refrigerators the refrigerant capacity is the latent heat of vaporization of liquid refrigerant.

Despite of this, in the majority of publications devoted to the research of magnetocaloric materials, authors use parameter q also called the refrigerant capacity [1, 2]:

$$q = - \int_{T_2}^{T_1} \Delta S_M(T) dT \quad (1)$$

However, using S-T diagram for rare-earth gadolinium (Fig 1), it is easy to show, that so called refrigerant capacity q describes not the amount of heat absorbing from the cooled object per cycle, but the work consuming in the Ericsson cycle operating between cold and hot reservoirs of infinite heat capacity with temperatures T_1 and T_2 ($ABCD$ area) [3].

On the other side the $EADF$ area in Fig. 1 (product of magnetic entropy change ΔS_M and temperature T) exactly corresponds to Q_c and we suggest to use the Q_c , calculated by our route as figures of merit for evaluation of magnetocaloric materials instead of the conventional usage for these purposes refrigerator capacity (RC).

Using our magnetic entropy change $\Delta S_m(T)$ data for $\text{La}(\text{FeSi})_{13}$, $\text{La}(\text{FeCoSi})_{13}$, $\text{La}(\text{FeSi})_{13}\text{H}$ alloys and Gd-metal, we compare the parameter $Q_c = T \cdot \Delta S_m(T)$ with the parameter q . Also by using on our data of adiabatic temperature change $\Delta T_{ad}(T)$ we are showing a principal restriction on temperatures T_1 and T_2 in eq. (1), which is usually ignored by the authors who use parameter q instead of Q_c .

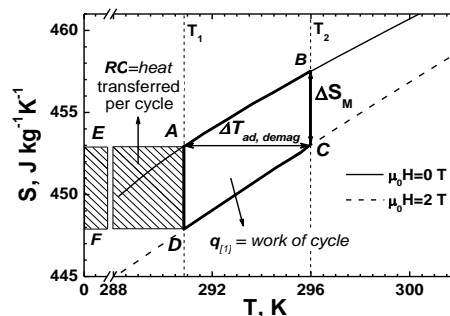


Fig. 1. Fragment of S-T diagram of rare-earth gadolinium

Support by grant of the President of the Russian Federation for young scientists and graduate students.

- [1] K.A. Gschneidner Jr., V.K. Pecharsky, *Annual Review of Materials Science*, **30** (2000) 387.
 [2] M.E. Wood, W.H. Potter, *Cryogenics*, **25** (1985) 667.
 [3] K. P. Skokov, A. Yu. Karpenkov, D. Yu. Karpenkov, O. Gutfleisch, *Journal of Applied Physics*, **113** (2013) 17A945.

1PO-I2-24

MAGNETO-OPTICAL STUDY OF MARTENSITIC TRANSITION IN Ni-Mn-In-Co SINGLE CRYSTALS

Gan'shina E.A.¹, Novikov A.I.¹, Chernenko V.A.^{2,3}, Barandiaran J.M.², Cesari E.⁴, Rodionov I.D.¹,
Titov I.S.¹, Prudnikov V.N.¹, Granovsky A.B.¹

¹ Faculty of Physics, Lomonosov Moscow State University, Moscow, Russia

² BCMaterials & University of Basque Country (UPV/EHU), Bilbao, Spain

³ Ikerbasque, Basque Foundation for Science, Bilbao, Spain

⁴ Dept. de Física, Universitat de les Illes Balears, Palma de Mallorca, Spain

eagan@mail.ru

The Mn-rich Ni-Mn-(In,Sn,Ga) Heusler alloys exhibit martensitic transformation (MT) accompanied by a huge drop of saturating magnetization. The origin of MT is commonly related to the electronic instabilities and band Jahn-Teller effect, although this mechanism is questioned in view of recent experimental data on Hall effect [1]. It is well known that magneto-optical (MO) spectroscopy can give information on the behavior of electronic structure and also on magnetic properties of surface layers. In the present work, we applied MO technique in the geometry of the transverse Kerr effect (TKE) at visible wavelengths to study MO spectra of weakly magnetic martensitic state and ferromagnetic austenitic state of Ni₄₅Mn_{36.7}In_{13.3}Co₅ (at.%) single crystals.

The single crystalline ingot was grown by the Czochralski method. After 24 h of homogenization at 1170 K under vacuum, one series of samples was quenched into cold water, the other series after quenching was heated at 770K for 20 min and slowly cooled to assure a complete atomic order (see details in [2]). Bulk magnetic properties were studied by SQUID and VSM magnetometers.

In two of the three samples, which do not have full atomic ordering, we observed martensitic transformation. Third sample (with full atomic ordering) did not demonstrate any symptoms of this transformation. Martensitic transformation from ferromagnetic austenite to weakly magnetic martensite starts at 258 K, according to DSC measurements. We observed the following features by measuring the TKE response from the surface layers in the applied field up to 3.0 kOe: (i) MO signal decreases in martensitic phase compared to austenitic as well as magnetization; (ii) but the characteristic temperatures of martensitic transition differ from those for the bulk and depend on annealing conditions; (iii) spectral positions of MO spectra positive and negative peaks do not change significantly during MT; (iv) MO spectra profile of single crystals is similar but not identical with that for Ni₂MnIn thin films [3]; (v) MO signal is weakly anisotropic.

The observed peculiarities are discussed in the framework of the theory of MO spectra of Heusler alloys [3,4].

This work was partly supported by the Russian Foundation for Basic Research (grant No. 14-02-31714-mol_a).

[1] A. B. Granovskii, V. N. Prudnikov, A. P. Kazakov et al., *JETP*, **115** (5) (2012) 805-814.

[2] J. I. Perez-Landazabal, V. Recarte, et al., *J. Alloys and Compounds*, **536S** (2012) S277.

[3] Y. V. Kudryavtsev, Y. P. Lee, J. Y. Rhee, *Phys. Rev. B*, **69** (2004) 195104.

[4] S. Picozzi, A. Continenza, A. J. Freeman, *J. Phys. D: Appl. Phys.*, **39** (2006) 851.

1PO-I2-25

FIRST PRINCIPLES INVESTIGATIONS OF STRUCTURAL AND MAGNETIC PROPERTIES OF Fe-Ni-Mn-Al HEUSLER ALLOYS

Buchelnikov V.D.¹, Zagrebin M.A.^{1,2}, Klyuchnikova M.A.¹, Sokolovskiy V.V.^{1,3}

¹ Chelyabinsk State University, Chelyabinsk, Russia

² National Research South Ural State University, Chelyabinsk, Russia

³ National University of Science and Technology "MIS&S", Moscow, Russia
miczag@mail.ru

Heusler alloys containing Ni and Mn atoms have attracted a lot of attention due to the possibility of observing shape memory effect, the giant magnetoresistance, magnetocaloric effect etc. [1-3]. In the last years, novel Fe-Mn-Al and Fe-Ni-Mn-Al Heusler compounds have been intensively investigated by experimentalists and theoreticians [4-6]. These interesting magnetic materials are considered to be very promising for technological applications utilizing their properties such as anomalous behaviours of optical, magnetic and transport properties. Especially interesting behaviour of these compounds is related to the competing ferromagnetic (FM) – antiferromagnetic (AF) exchange interactions between Fe atoms at the order-disorder structural transition from A2 to B2 structure [5, 6].

In this work we theoretically investigate the equilibrium lattice properties and exchange interactions of $\text{Fe}_{2-x}\text{Ni}_x\text{MnAl}$ alloys with the help of ab initio calculations. To perform this study we used Quantum ESPRESSO [7,8] and the spin-polarized Korringa-Kohn-Rostoker Munich [9,10] packages.

The lattice relaxation for cubic phase was calculated and equilibrium lattice parameters were found. Results of lattice relaxation show that different types of ferromagnetic state has lower energy than antiferromagnetic state. The least energy has state where Ni atoms are placed on Fe positions and ferromagnetic. We also carried out the calculations of the lattice energy dependence from c/a ratio for tetragonal lattice. Obtained values of equilibrium lattice parameters and c/a ratio we used for calculations of the magnetic exchange parameters for austenite and martensite states of Fe-Ni-Mn-Al for different magnetic states.

It is follow from our calculations that Fe-Ni-Mn-Al alloys are very interesting compounds and theoretical study of them allows to predict the new features of Heusler alloys.

Support by RFBR (grants No. 14-02-01085 and 14-02-31189) is acknowledged.

- [1] A.N. Vasil'ev, V.D. Buchel'nikov, T. Takagi et al., *Physics–Uspekhi*, **46** (2003) 559.
- [2] A. Planes, L. Mañosa and M. Acet, *J. Phys.: Condens. Matter*, **21** (2009) 233201.
- [3] V.D. Buchelnikov, V.V. Sokolovskiy, *The Physics of Metals and Metallography*, **112** (2011) 633.
- [4] G.A. Perez Alcazar, J.A. Plascak, E.G. da Silva, *Phys. Rev. B*, **38(4)** (1988) 2816.
- [5] H. Bremers, J. Hesse, H. Ahlers, J. Sievert et al., *J. of Alloys and Compounds*, **366** (2004) 67.
- [6] Z. Liu, X. Ma, F. Meng, G. Wu, *J. of Alloys and Compounds*, **509** (2011) 3219.
- [7] Quantum ESPRESSO package, Version 5.0. <http://www.pwscf.org>.
- [8] P. Giannozzi, S. Baroni, N. Bonini et al., *J. Phys.: Condens. Matter.*, **21** (2009) 395502.
- [9] H. Ebert, D. Ködderitzsch, J. Minár, *Reports on Progress in Physics*, **74** (2011) 096501.
- [10] SPR-KKR package Version 6.3, <http://ebert.cup.unimuenchen.de>.

1PO-I2-26

MAGNETOCALORIC EFFECT OF GADOLINIUM AT ADIABATIC AND QUASI-ISOTHERMAL CONDITIONS IN MAGNETIC FIELDS UP TO 14 T

Kamantsev A.P.^{1,2}, Koledov V.V.^{1,2}, Mashirov A.V.^{1,2}, Dilmieva E.T.¹, Shavrov V.G.¹, Cwik J.², Tereshina I.S.^{2,3}

¹ Kotelnikov Institute of Radio-engineering and Electronics of RAS, Moscow, Russia

² International Laboratory of High Magnetic Fields and Low Temperatures, Wroclaw, Poland

³ Baikov Institute of Metallurgy and Material Science of RAS, Moscow, Russia

kama@cplire.ru

Recently, big interest is attached to application of materials with a giant magnetocaloric effect (MCE) at phase transformation (PT) for creation of household and industrial refrigerators, operating at room temperature [1]. High power of such devices can be achieved only at large adiabatic temperature change ΔT and high amounts of heat, which can transferred in one cycle from cold end to hot end ΔQ in a magnetic field. The amount of the heat transferred per one cycle ΔQ is the MCE of the material at quasi-isothermal conditions.

If a sample of material with MCE is connected to the surroundings – to a massive nonmagnetic block with definite heat capacity and good heat diffusivity, then one can experimentally estimate ΔQ of a sample at quasi-isothermal conditions. We can neglect the heat which connected with temperature change of a sample, because its mass should be in 10-20 times less than the mass of a block. One can estimate ΔQ by means of measuring the temperature change of massive block (Fig.1) at magnetic field change:

$$\Delta Q \cdot m = M \cdot C \cdot \Delta t + m \cdot c \cdot \Delta t, \quad M \gg m \text{ and following } \Delta Q \approx M/m \cdot C \cdot \Delta t,$$

where M – the mass of a block, C – the specific heat capacity of a block, m – the mass of a sample, c – the specific heat capacity of a sample and Δt – the temperature change of a block with a sample at magnetic field change.

The maximal values of MCE of pure Gadolinium [2] obtained by our direct experiments are: $\Delta T = +17,5$ K and $\Delta Q = +6000$ J/kg in a magnetic field change of 140 kOe at an initial temperature $T_0 = 293$ K (Fig.2).

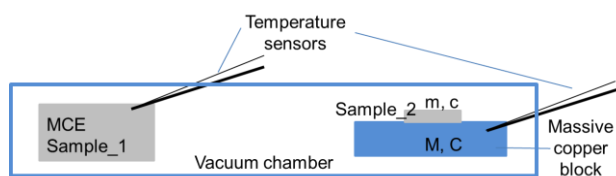


Fig.1 The diagram of the experimental setup for simultaneous direct measuring of ΔT and ΔQ in Bitter coil magnet.

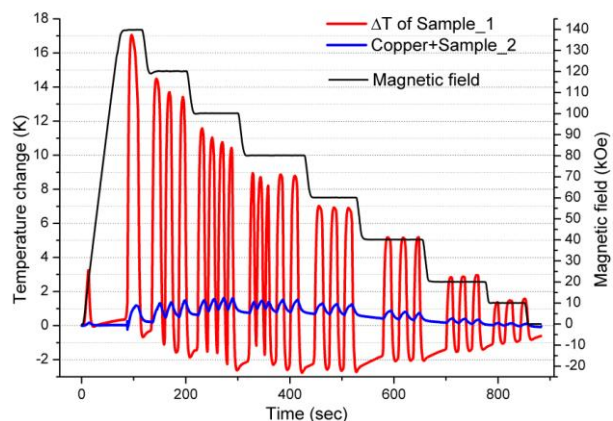


Fig.2 The time dependence of magnetic field change, corresponding ΔT of Gd sample and temperature change of copper block. $T_0 = 293$ K.

Support by RFBR is acknowledged, grants No. 12-07-00656, 12-08-01043, 13-07-12130.

[1] K.A. Gschneidner Jr., V.K. Pecharsky, *Int. J. Refrig.*, **31** (2008) 945-961.

[2] S.Yu. Dan'kov, A. M. Tishin, V. K. Pecharsky, et al., *Phys. Rev. B*, **57** (1998) 3478-3490.

1PO-I2-27

STRUCTURAL AND MAGNETIC PROPERTIES OF Ni₄₅Mn₄₀In₁₅ THIN FILMS

Lyange M.V.¹, Khovaylo V.V.¹, Miki H.², Otsuka M.², Takagi T.²

¹ National University of Science and Technology "MISiS", Moscow 119049, Russia

² Tohoku University, Sendai 980-8577, Japan

maria.lyange@gmail.com

Heusler alloys are receiving increasing attention from both the magnetism and material science spheres due to their large variety of magneto-responsive effects, such as magnetic shape memory, large magnetoresistance, anomalous Hall, and magnetocaloric effects. The broad spectrum of properties of these materials is mainly attributed to the specific type of structural instability known as a martensitic transformation observed in these compounds. The study of Ni-Mn-In system is mainly concern bulk alloys, but it is extremely desirable to synthesize these alloys in form of thin films.

In the present work we study the influence of heat treatment on the structure and magnetic properties of Ni₄₅Mn₄₀In₁₅ thin films. The films of 1 μm thickness were deposited on aluminum oxide by a magnetron sputtering technique. The heat treatment of the as-prepared films was performed at 1073 K.

The room temperature x-ray analysis clearly indicates the presence of single B2 phase in as-deposited film. The heat treatment provokes appearance of additional peak at 2θ=40° and splitting of the peaks at 2θ=43° and 2θ=53° which imply that martensitic phase is formed upon thermal treatment.

The temperature dependence of magnetization was measured in a magnetic field 500 Oe for both as-deposited and the heat treated films. The sharp decrease of magnetization is observed at Curie temperatures indicating the second order phase transition. The splitting of the magnetization seen at low temperatures is associated with the spin-glass state. Heat treatment increases Curie temperature T_C which reaches T_C=322 K in the heat treated sample. The field dependence of magnetization measured at 4.2 K shows that the saturation magnetization is lower in the heat treated sample (M_s = 35 emu/g) as compared to the as-prepared one.

We can make a conclusion that heat treatment converts room-temperature structural state of the film from austenitic (in the as-prepared sample) to martensitic (in the heat treated sample). The martensitic phase has a lower saturation magnetization and a higher Curie temperature. Obtained results agree fairly well with those reported for bulk samples [1] and Ni₅₀Mn₃₅In₁₅ films [2]

[1] A. Sokolov et al., *Appl. Phys. Lett.*, **102** (2013) 072407.

[2] A. K. Pathak et al., *Appl. Phys. Lett.*, **90** (2007) 262504.

1PO-I2-28

COMPARISON OF MAGNETIC AND STRUCTURAL PROPERTIES OF RAPIDLY QUENCHED BULK AND RIBBON $\text{Ni}_{50}\text{Mn}_{25+x}\text{Ga}_{25-x}$ HEUSLER ALLOYS

Ryba T.¹, Vargova Z.², Ilkovic S.³, Reiffers M.³, Gyepes R.⁴, Varga R.¹

¹ Institute of Physics, UPJS, Kosice, 041 54, Slovakia

² Institute of Chemistry, UPJS, Kosice, 041 54, Slovakia

³ Univ. of Presov, Fac. Hum. and Nat. Sci., SK-08078 Presov, Slovakia

⁴ Dept. of Chemistry, Faculty of Education, J. Selye University, Komarno, Slovakia
zuzana.vargova@upjs.sk

Heusler alloys are new perspective materials for various applications [1-2]. The X_2YZ full Heusler alloys show interesting properties as magnetocaloric effect, shape memory effect etc. The ideal materials for shape memory application must show the structural transition near room temperature [3]. The typical full Heusler alloy with shape memory effects is $\text{Ni}_{50}\text{Mn}_{25}\text{Ga}_{25}$.

The new rapid quenching method has been recently successfully introduced to prepare the full Heusler alloy [4]. It allows a fast production of relatively large amount of alloy by arc melting (bulk, rod) and later by melt spinning methods (ribbon).

In the given contribution, we are dealing with Heusler alloys produced by rapid quenching. Heusler alloys with composition $\text{Ni}_{50}\text{Mn}_{25+x}\text{Ga}_{25-x}$ have been prepared in the form of ribbon (by melt-spinning) and rod (by suction casting). Magnetic properties like temperature dependence of magnetization and hysteresis loops have been studied by VSM. The SEM and X-ray characterizations were used to estimate their composition and structure determination.

This study was supported by the project NanoCEXmat Nr. ITMS 26220120019, Slovak VEGA grant. No. 1/0060/13, APVV-0027-11 and APVV-0266-10.

- [1] A. Hirohata, M. Kikuchi, N. Tezuka, K. Inomata, J.S. Claydon, Y.B. Xu, G. van der Laan, *Curr. Opin. Sol. State Mat. Sci.*, **10** (2006) 93.
- [2] T. Graf, C. Felser, S.S.P. Parkin, *Prog. Solid State Chem.*, **39** (2011) 1.
- [3] J.D.Santos, R.Varga, B.Hernando, A.Zhukov, *J. Magn. Magn. Mater.*, **321** (2009) 3875.
- [4] B.Hernando, J.LSanchez Liamazares, J.D.Santos, V.M.Prida, D.Baldomir, D.Sarentes, R.Varga, J.Gonzales, *Appl. Phys. Lett.*, **92** (2008) 132507.

1PO-I2-29

MAGNETO-OPTICAL SPECTROSCOPY OF Ni₄₇Mn₄₁In₁₂ RIBBONS

Novikov A.I.¹, Gan'shina E.A.¹, Gonzalez-Legarreta L.², Prida V.M.², Hernando B.², Granovsky A.B.¹

¹ Faculty of Physics, Lomonosov Moscow State University, Moscow, Russia

² Dept. de Física, Universidad de Oviedo, Oviedo, Spain

eagan@mail.ru

We present our experimental results on magneto-optical (MO) spectra of Ni₄₇Mn₄₁In₁₂ ribbon. The samples were produced by rapid solidification using melt spinning technique and their structural and magnetic parameters are similar to those found in bulk samples of this composition. Quite large magnetization in both austenitic and martensitic states in comparison with that for other Ni-Mn-In ribbons as well as a high optical quality of the as-cast ribbon surface allow us to investigate magnetization of the surface layers (Fig.1) and MO spectra in both martensitic and austenitic phases (Fig.2). We used the MO transversal Kerr effect (TKE) in the energy range of 0.5 ÷ 3.5 eV under the external magnetic fields up to 3.0 kOe. It was shown that surface layers exhibit a well-defined martensitic transition but the characteristic temperatures of this transition as well as the Curie temperature of austenitic phase are not exactly the same as those for the samples measured by VSM. It means that the chemical composition and/or microstructure are not identical in the bulk and surface of the ribbon. The MO spectra profile does not change during the magnetostructural transition. The amplitude of the MO response is approximately linear to magnetization and therefore decreases during the martensitic transition. We discuss the observed behavior of the MO spectra in comparison with available experimental data for MO spectra for other compositions of Heusler alloys in the form of bulk and thin films samples.

This work was partly supported by the Russian Foundation for Basic Research (grant No. 14-02-31714-mol_a).

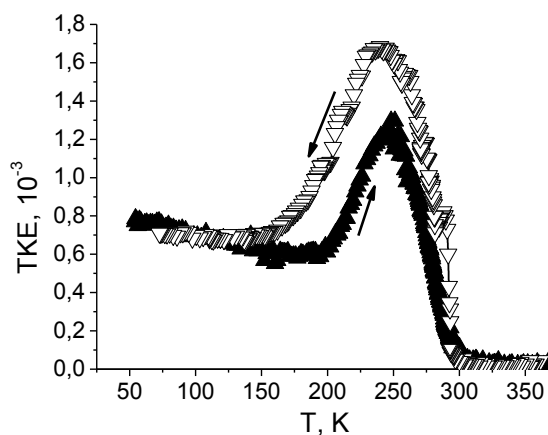


Fig. 1. Temperature dependence of TKE at 3 kOe for Ni₄₇Mn₄₁In₁₂ alloy ribbon.

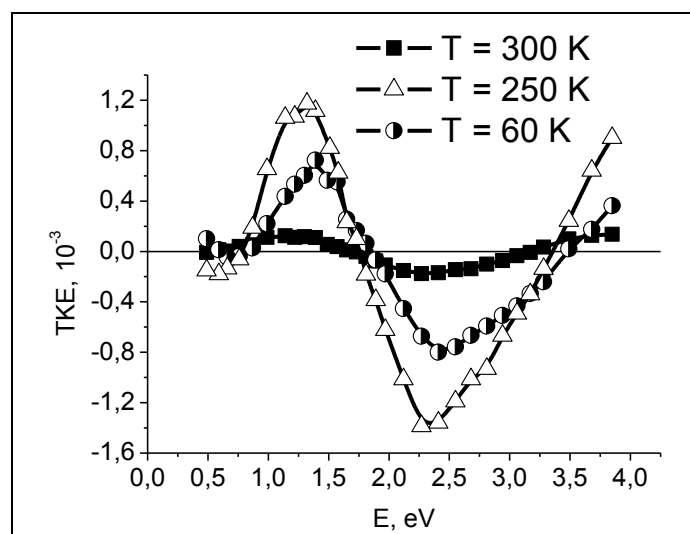


Fig. 2. TKE spectra for Ni₄₇Mn₄₁In₁₂ alloy ribbon.

1PO-I2-30

MAGNETOCALORIC EFFECT DRIVEN BY MAGNETIC AND STRUCTURAL TRANSITIONS IN $\text{Ni}_{45.37}\text{Mn}_{40.91}\text{In}_{13.72}$ HEUSLER ALLOYS

Fayzullin R.R.¹, Buchelnikov V.D.¹, Zhukov M.V.², Kamantsev A.P.³, Mashirov A.V.³

¹ Chelyabinsk State University, Chelyabinsk, Russia

² Russian Research Institute of the Tube & Pipe Industries, Chelyabinsk, Russia

³ Kotelnikov Institute of Radioengineering and Electronics of RAS, Moscow, Russia
fayzullinrr@gmail.com

The magnetocaloric effect (MCE) is the ability of magnetic materials to heat up or cool down when placed in or removed from an external magnetic field. It has great importance in the technology of magnetic refrigeration. The magnetic materials with large values of MCE can be applied in the magnetic refrigeration technique [1]. Recent experimental studies have shown that Ni-Mn-In Heusler alloys are also attractive for the application in magnetic refrigeration [2].

In this work we study experimentally phase transitions and magnetocaloric effect (MCE) in $\text{Ni}_{45.37}\text{Mn}_{40.91}\text{In}_{13.72}$ Heusler alloys. Polycrystalline ingots with nominal compositions were prepared by an arc-melting method. WDX spectrometry showed that the real compositions correspond to the nominal ones. The ingots were annealed at 1100 K for 9 days quenched in ice water. Samples for MCE measurements were cut from the middle part of the ingots.

The MCE measurements were performed by the setup produced by AMT&C [3]. In this setup, the adiabatic temperature change ΔT_{ad} was measured by a direct method with help of a thermocouple. Magnetic field up to 2 T was created by Halbach permanent magnet. The magnetic field strength was measured by Hall probe. Signals from the thermocouple and Hall probe were recorded simultaneously what allowed us to measure ΔT_{ad} as a function of magnetic field H . The phase transitions temperatures were determined from measuring differential scanning calorimetry and field magnetization curves of the temperature.

The temperature dependencies of ΔT_{ad} for $\text{Ni}_{45.37}\text{Mn}_{40.91}\text{In}_{13.72}$ Heusler alloys for the magnetic field change $\Delta H = 2$ T was measured (fig.1). It is shown that maximal positive MCE takes place near the magnetic phase transition and its value is 2K. The maximal negative MCE takes place near the martensitic phase transition and its value is -2K. So, we can conclude that investigated alloy is perspective for magnetic refrigeration.

[1] K. Gschneidner, Jr. and V.K. Pecharsky, *Int. J. Refrig.*, **31** (2008) 945.

[2] X. Moya, L. Manosa, A. Planes, et al., *Phys. Rev. B.*, **75** (2007) 184412-5.

[3] Y.I. Spichkin., et al, *Proc. 3rd IIF-IIR Intern. Conf. Magnetic Refrigeration at Room Temperature*, IIF/IIR (2009) 173.

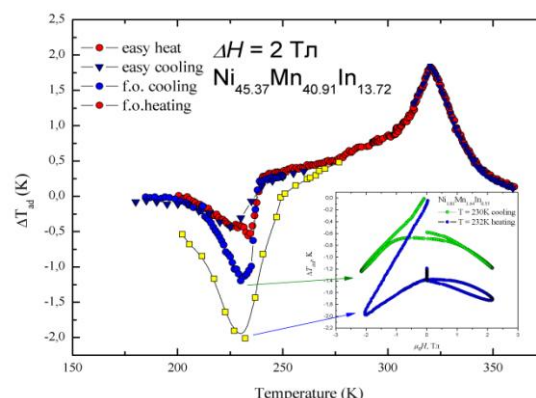


Fig. 1. Adiabatic temperature change in $\text{Ni}_{45.37}\text{Mn}_{40.91}\text{In}_{13.72}$

1PO-I2-31

ANOMALOUS PEAK OF INVERSE MAGNETOCALORIC EFFECT IN HEUSLER ALLOY $\text{Ni}_{50}\text{Mn}_{35}\text{In}_{13.5}\text{Al}_{1.5}$

Pavlochev S.Y.¹, Rodionov I.D.¹, Dubenko I.S.², Granovsky A.B.¹

¹ Faculty of Physics, Lomonosov Moscow State University, Moscow, Russia

² Department of Physics, Southern Illinois University, Carbondale, USA

Magnetocaloric effect (MCE) means that temperature of the sample will change when external magnetic field will be applied or removed. Usually MCE reaches its highest value in area of phase transition with sharp change of magnetic structure.

Non-stoichiometric Mn-based Heusler alloys undergoes martensitic transformation. This is first order phase transition in which a high-temperature austenite phase with cubic L21 structure goes to low-temperature martensite phase with tetragonal L10 structure. Martensitic transformation in non-stoichiometric Heusler alloys based on Ni-Mn-In is accompanied by transition from weak magnetic martensite phase in ferromagnetic austenite phase. Commonly this magnetization change leads to negative peak of MCE in pretty narrow range of temperature.

In this work ternary Heusler alloy $\text{Ni}_{50}\text{Mn}_{35}\text{In}_{13.5}\text{Al}_{1.5}$ is considered. The sample was prepared by arc melting in argon atmosphere. Then it was annealed at 850 K for 24 hours and slowly cooled to 300 K. Magnetic and magnetocaloric properties were investigated using vibrating magnetometer VSM Lake Shore 7407 and magnetocaloric measuring set MagEq MMS 801.

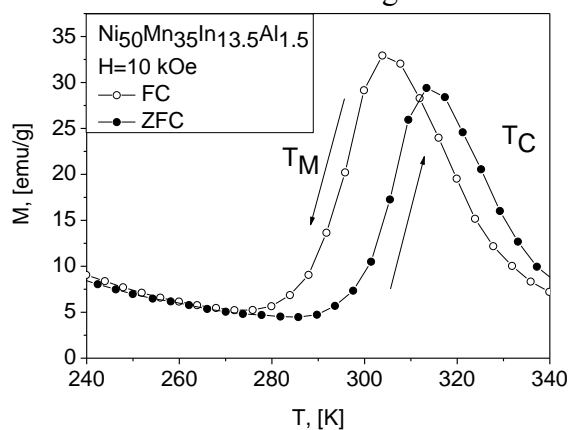


Figure 1. Temperature dependence of the magnetization

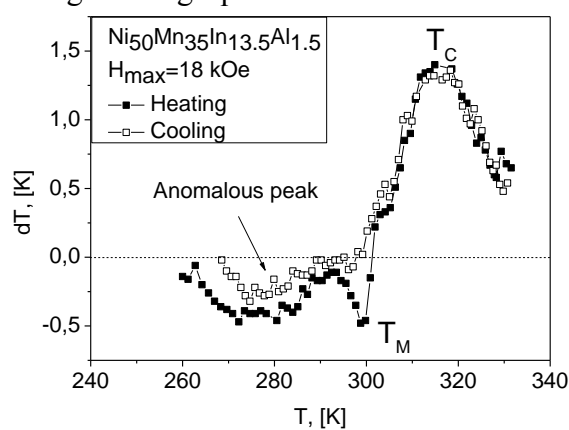


Figure 2. Temperature dependence of the MCE

Temperature dependence of magnetization and MCE are shown at figures 1 and 2. At area of high temperatures austenite phase undergoes second order phase transition from paramagnetic to ferromagnetic state. At low temperatures austenite phase transforms to martensite. These transitions are accompanied by the conventional and inverse peaks of MCE. But at figure 2 below temperature of martensite transition peak of anomalous inverse MCE exists. It is observed in a wide range of temperatures not typical to martensitic transformation and existence of this peak was not confirmed by magnetic measurements.

1PO-I2-32

EFFECT OF STOICHIOMETRY ON MAGNETIC INTERACTIONS In Ni-Mn-Ga AND Ni-Mn-Sn ALLOYS

Titov I.^{1,2}, Acet M.², Su Y.³

¹ Faculty of Physics, Lomonosov Moscow State University, Moscow, Russia

² Fakultät für Physik, Universität Duisburg-Essen, Duisburg, Germany

³ Heinz Maier-Leibnitz Zentrum Neutrons for Research
iohann.s.titov@gmail.com

The problem of magnetic interactions in NiMn-based Heusler alloys doped with Ga, In and Sn was setup quite a long time ago. The phenomena exhibited by these Heusler alloys in martensitic state (like exchange bias effect, splitting between ZFC and FC magnetization curves, smeared out magnetic transition in martensitic state) can be explained with hypothesis that Mn atoms, bearing the major magnetic moment in the cell, in short range couple together antiferromagnetically in addition to ferromagnetic coupling. For example, AFM interactions are observed in similar alloys: stoichiometric Ni₂MnAl features cone spiral AFM magnetic ordering of Mn moments, while NiMn is collinear antiferromagnet. There are series of the experiments on NiMn-based Heusler alloys doped with In, Sb and Sn giving the direct evidence this hypothesis, using FMR techniques and polarized neutron scattering [1,2].

Here we present our temperature-dependent studies of the Ni-Mn-Ga and Ni-Mn-Sn alloys with varying concentrations of Sn and Ga using FMR techniques and polarized neutron scattering. For these studies we prepared two series of samples with Mn-rich and Mn-poor compositions (comparing to stoichiometric Ni₂MnZ alloy, where Z = Ga and Sn). These series contain samples both undergoing martensitic transition and residing in austenite phase.

The discussion of the results is given in relation to lattice and magnetic properties of the samples studied.

This work was supported by the Deutsche Forschungs-gemeinschaft, Project SPP 1239.

[1] S. Aksoy, M. Acet, P. P. Deen, L. Manosa, and A. Planes. *Phys. Rev. B*, **79** (2009) 212401.

[2] Aksoy S, Posth O et al. *Journal of Physics: Conference Series*, **200**(9) (2010) 092001.

1PO-I2-33

INFLUENCE OF RAPID QUENCHING ON MAGNETOCALORIC EFFECT OF $Y_2(Fe,Mn)_{17}$ INTERMETALLIC COMPOUNDS

Zvonov A.I.¹, Pankratov N.Yu.¹, Karpenkov D.Yu.², Karpenkov A.Yu.², Nikitin S.A.¹

¹ Lomonosov Moscow State University, Moscow, Russia

² Tver State University, Tver, Russia

zvonov@physics.msu.ru

The scientific and industrial interest in magnetocaloric materials is caused by the perspectives of their use in variety of devices, for example, in refrigerating systems. It is necessary to make such material not only having a big value of magnetocaloric effect (MCE), but also make them relatively cheap, to provide their use in technical applications. So, alloys, containing a very small amount of rare earth elements, for example $Y_2Fe_{17-x}Mn_x$, fits this criterion.

The $Y_2(Fe,Mn)_{17}$ compounds have a Th_2Zn_{17} type crystal structure. Magnetic properties of $Y_2Fe_{17-x}Mn_x$ compounds were investigated previously in pure [1,2], and also in hydrogenated state [3]. But no attention was paid to influence of rapid quenching on their magnetocaloric properties.

The main purpose of this work was to investigate the influence of rapid quenching from the melt on MCE in $Y_2Fe_{17-x}Mn_x$ ($x = 0-4$) alloys, using the direct method of MCE measurement.

The detailed description of the preparation method of the initial compounds $Y_2(Fe,Mn)_{17}$, used in this work has been given earlier [3]. Initial elements have been put to closed alundum container for the purpose of Mn retaining. By this method the loss of Mn has been less than 0.05%.

The rapidly quenched alloys were obtained by melt spinning method. The melted initial compounds were crystallized by rapid quenching on fast rotating copper disk.

The MCE measurements were carried out by the direct method in the temperature range 100-300 K. The sample was placed in a container with thermo-insulation and high vacuum $\sim 10^{-4}$ mmHg to achieve adiabatic conditions.

Comparison of MCE temperature dependences for rapidly quenched (RQ) and non RQ compounds clearly shows that in RQ $Y_2Fe_{14}Mn_3$ compound the maximum magnitude of MCE is 60% higher than in non RQ compound.

Rapid quenching leads to the decreasing of the sample's crystallites sizes, which leads to increasing the number of atoms on the crystallite's surface. The large amount of interface atoms in RQ material leads to existence of atoms with a lower number of the nearest-neighbor atoms, which can cause the magnetic phase transition temperature and maximum value of MCE change in comparison with the similar non RQ material.

This work is supported by RFBR grant # 12-02-31516.

[1] N.M. Hong, N.P. Thuy, J.J.M. Franse, *Phys. B: Condens. Matter*, **153** (1-3) (1988) 53–60.

[2] Y.-g.Wang, F.Yang, C.Chen, N.Tang, H.Pan, Q.Wang, *J.Alloys Comp.*, **242** (1-2) (1996) 66–69.

[3] W. Iwasieczko, N.Yu. Pankratov E.A. Tereshina, S.A. Nikitin, I.S. Tereshina, K.P. Skokov, A.Yu. Karpenkov, R.M. Grechishkin, H. Drulis, *J. Alloys Comp.*, **587** (2014) 739–746.

1PO-I2-34

TRANSFORMATION OF MAGNETOCALORIC EFFECT AND MAGNETIC PROPERTIES OF RAPIDLY QUENCHED RARE EARTH METALS

Pankratov N.Yu.^{1,2}, Zvonov A.I.¹, Cwik J.², Karpenkov D.Yu.³, Nikitin S.A.¹

¹ Faculty of Physics, M. V. Lomonosov Moscow State University, Moscow, Russia

² Department of Physics, Tver State University, Tver, Russia

³ International Laboratory of High Magnetic Fields and Low Temperatures, Wroclaw, Poland
pankratov@phys.msu.ru

The rare-earth metals (REM) are drawn attention due to their magnetic characteristics and the potential enhancement of these properties [1]. Terbium, dysprosium and gadolinium have been extensively investigated on both single crystal and polycrystalline over the last few decades due to its interesting magnetism, which includes high magnetocrystalline anisotropy, complex magnetic structure, and magnetostriction [1-2]. Stoichiometric they crystallises in a hexagonal closepacked crystal structure with $P6_3/mmc$ space group. In magnetic field less than critical value $H_{cr} = 180$ Oe in temperature range between $\Theta_1 = 225$ K and $\Theta_2 = 235$ K [1], Tb possess a helicoidal antiferromagnetic (HAFM) state. Below Θ_1 it has a ferromagnetic state and above Θ_2 it has a paramagnetic one. The HAFM state is suppressed by critical field H_{cr} and transforms to ferromagnetic one. Thus, in fields above H_{cr} a single magnetic phase transition from ferromagnetic to paramagnetic state is observed at Curie temperature (T_C) [1-2]. Similar behaviour of magnetic properties is demonstrated by Dy, however, the its critical filed is above 12 kOe and HAFM state exists in temperature range 86-179 K. For nanoscale REM curiously optical, electronic, magnetic, and catalytic properties can be expected because of significant increasing of surface area or crystallite boundary area. Because the Ruderman-Kittel- Kasuya-Yosida (RKKY) coupling is very sensitive to interatomic spacing, which varies drastically at the particle surface, deep effects are also expected in the magnetic properties of nanoscaled REM [1]. The aim of our work was to investigate magnetic properties and magnetocaloric effect (MCE) of rapidly terbium quenched (RQ) terbium and dysprosium.

It was estimated by analysing the powder XRD patterns by employing Rietveld refinement technique, that both polycrystalline and rapid quenching metals have hexagonal close-packed crystal structure and the lattice parameters are equal to each other. It was established by analysis of the AFM images, that average crystallite size is 108 nm for Tb-RQ and 110 nm for Dy-RQ and that there are a lot of crystallites with linear size less 100 nm. The results of structural investigations allow to conclude that the rapid quenching preserves crystal structure and drastically decrease the crystallite size.

It was found that spontaneous magnetisation and coercive force at $T = 4.2$ K decrease in both Tb-RQ and Dy-RQ. The maximum values of MCE in field 10 kOe are equal to 2.2 and 1.5 K for Tb and Tb-RQ, respectively. Compare to microcrystalline, Tb-RQ shows the decrease of T_C by 2 K and decrease of MCE maximum by 0.7 K. A significant decrease of phase transition temperature in RQ metals is associated with increase of the number of atoms at the surface of the crystallites having a smaller number of neighbours in the first coordination spheres. Increasing the number of surface atoms reduces the exchange interaction energy and thus to reduce the energy required for destruction of the magnetic order.

This work is supported by RFBR grants # 13-02-00916 and 12-02-31516.

- [1] K.N.R. Taylor, M.I. Darby. *Physics of Rare Earth Solids*. Chapman and Hall., London, 1972.
[2] A. S. Andreenko, K. P. Belov, S. A. Nikitin, et.al. *Sov. Phys. Usp.* **32** (1989) 649.

1 July

Tuesday

17:30-19:00

poster session
1PO-J1

**“Diluted Magnetic
Semiconductors and
Oxides”**

1PO-J1-1

EFFECT OF Co DOPING ON THE STRUCTURE, MAGNETIC AND GALVANOMAGNETIC PROPERTIES OF ZnO THIN FILMS

Kytin V.G., Reukova O.V., Melnik D.D., Burova L.I., Kaul A.R., Kulbachinskii V.A.

M.V Lomonosov MSU, Moscow, Russia

kytin@mig.phys.msu.ru

The effect of Co doping on the properties of zinc oxide films was investigated. The films were grown by oxygen and water assisted MOCVD. According to X-ray diffraction the films deposited by oxygen assisted MOCVD were nearly epitaxial while the films deposited by water assisted MOCVD were polycrystalline with chaotic orientation of crystallites or partially amorphous. The EXAFS data shows that Co substitutes Zn in a crystalline lattice. This fact is confirmed by nearly linear increase of the lattice constant with Co content up to 33at.% obtained from X-ray diffraction data. Magnetization data exhibit a ferromagnetic behavior for Co containing films (fig. 1).

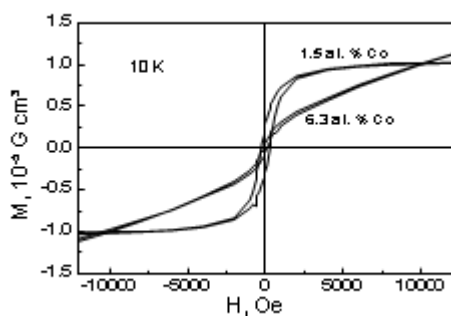


Fig. 1 Magnetization of ZnCoO films

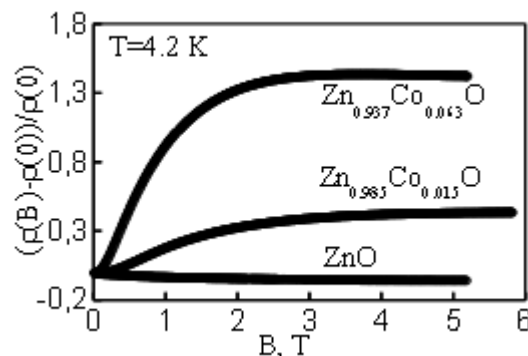


Fig. 2 Magnetoresistance of ZnCoO films

The magnetization at a saturation and the coercive force does not depend on the Co content. This is consistent with the result of Ref. [1]. The paramagnetic susceptibility in high magnetic field increases with the Co content. Cobalt doping affects strongly magnetoresistance and Hall effect at low temperatures. The large positive magnetoresistance (Fig. 2) and non-linear Hall effect was observed in Co doped films at low temperatures while the negative magnetoresistance and linear Hall effect were observed in undoped ZnO films. The value of positive magnetoresistance increases with an increase of the Co content. Galvanomagnetic properties of the films were interpreted in a frame of the spin dependent hopping conductivity [2].

[1] M. Kapilashrami, et. al. *Appl. Phys. Lett.* **95** (2009) 033104-1-3.

[2] Y. Meir., *Europhys. Lett.*, **33** (1996), 471-476.

1PO-J1-2

LOCAL MAGNETIC PROPERTIES AND ORBITAL ORDERING IN $R_2V_2O_7$ SYSTEMS ($R^{3+} = \text{Lu, Y}$)

Agzamova P.A.^{1,2}, Petrov V.P.², Chernyshev V.A.², Leskova Yu.V.², Nikiforov A.E.²

¹ Institute of Metal Physics UB RAS, Yekaterinburg, Russia

² Ural Federal University, Yekaterinburg, Russia

polly@imp.uran.ru

The vanadium pyrochlores $R_2V_2O_7$ ($R = \text{rare earth or Y}$) being the geometrically frustrated magnetic systems are attractive for both theoretical and experimental investigations due intriguing electronic and magnetic properties. Among these systems $\text{Lu}_2\text{V}_2\text{O}_7$ and $\text{Y}_2\text{V}_2\text{O}_7$ are most simple objects for studying since Lu^{3+} and Y^{3+} ions are nonmagnetic at R -site and their electronic and magnetic properties formed by the sublattice of V^{3+} magnetic ions. In addition, $\text{Y}_2\text{V}_2\text{O}_7$ and $\text{Lu}_2\text{V}_2\text{O}_7$ are ferromagnets with $T_C = 68$ K and 70 K, respectively, and at the same time Mott insulators contrary to the common belief that ferromagnetism leads usually to metallic conductivity [1]. Many investigators suppose that the orbital moment of $3d$ ions (V^{4+}) affects on such magnetic properties of vanadium pyrochlores as magnetic susceptibility, the Curie temperature etc. The orbital ordering pattern of $R_2V_2O_7$ pyrochlores was determined by the neutron diffraction measurements [2], which showed that each orbital extended along the four local $\langle 111 \rangle$ directions towards the center-of-mass of the elementary V_4 -tetrahedron. On the other hand, recently the presence of the orbital fluctuations and the orbital liquid state in the Mott insulators became the subject under hot discussions. There are many experimental techniques for orbital physics investigations. Among them the NMR technique has an advantage in observing each orbital state directly with a quantitative evaluation of $3d$ quadrupole moment which is the order parameter for the orbital degree of freedom. Thereby, the NMR method can give additional information about the presence or absence of orbital fluctuations in $3d$ -ions sublattice. In paper [3] ^{51}V NMR measurements in $\text{Lu}_2\text{V}_2\text{O}_7$ have been performed to investigate the orbital ordering of this compound. With rotation of $\text{Lu}_2\text{V}_2\text{O}_7$ single crystal in an external magnetic field, NMR spectra showed a characteristic angle dependence, which reproduced V $3d$ orbital states and clearly identified the orbital ordering of $\text{Lu}_2\text{V}_2\text{O}_7$. Unfortunately there are not any known experimental NMR data for $\text{Y}_2\text{V}_2\text{O}_7$ system.

In this work we try to explain theoretically the available experimental NMR data in $\text{Lu}_2\text{V}_2\text{O}_7$ pyrochlore and extend our theoretical model to $\text{Y}_2\text{V}_2\text{O}_7$ compound. We have proposed the theoretical model of magnetic hyperfine interactions formation on $3d^1$ -ion (V^{4+}) nuclei in vanadium pyrochlores. Our model includes the isotropic (Fermi-contact) and anisotropic (electron-dipole-nuclear-dipole) hyperfine interaction, where the last of them contains $3d$ quadrupole moment of V, for quantitative explaining of the orbital ordering pattern in these compounds. Moreover, we have performed the ab initio calculations of NMR spectra parameters in the molecular orbital method approximation in CRYSTAL09 package [5], dedicated to the periodical system, by the unrestricted Hartree-Fock method and the density functional theory (DFT B3LYP) with using of all-electron basis sets to evaluate the isotropic and anisotropic magnetic hyperfine interactions parameters and the electric field gradient tensor on ^{51}V nuclei.

Support by RFBR (# 14-02-00260) is acknowledged.

- [1] J.S. Gardner, M.J.P. Gingras, J.E. Greedan, *Rev. Mod. Phys.*, **82** (2010) 53.
- [2] H. Ichikawa, L. Kano, M. Saitoh et al, *JPSJ*, **74** (2005) 1020.
- [3] T. Kiyama, T. Shiraoka, M. Itoh et al, *Phys. Rev. B*, **73** (2006) 184422.
- [4] R. Dovesi, V.R. Saunders, C. Roetti et al, *CRYSTAL09 User's Manual* (2009).

1PO-J1-3

HETEROGENOUS PARAMAGNETIC STATE AND THE METHOD FOR DETERMINING THE CURIE TEMPERATURE IN $\text{La}_{1-x}\text{A}_x\text{MnO}_{3+\delta}$

Arbuzova T.I.¹, Naumov S.V.¹

¹ Institute of Metal Physics, Ural Branch of RAS, 620990 Ekaterinburg, Russia
naumov@imp.uran.ru

In lanthanum manganites the correlations between magnetic, electronic and lattice subsystems lead to the appearance of nanoscale inhomogeneities of various types. In $\text{La}_{1-x}\text{A}_x\text{MnO}_{3+\delta}$ (A= Ca, Ba, Sr) ferromagnetic order takes place due to superexchange between Mn^{3+} ($S = 2$) and Mn^{4+} ($S = 3/2$) ions and the double exchange at transfer of e_g electrons. In the region $T > T_C$ it is possible the presence of magnetic polarons with a large magnetic moment, which can remain up to high temperatures. The Curie-Weiss law $\chi = N\mu_{\text{eff}}^2 / 3k_B(T - \Theta)$ does not hold due to spin correlations (Θ -paramagnetic Curie temperature). It was shown [1] that for $\text{LaMnO}_{3+\delta}$ with different content of Mn^{4+} ions the temperature dependences of the paramagnetic susceptibility can be described by the formula

$$\chi = \frac{C_\infty + P_1/T}{T - T_C} \quad (1)$$

Here T_C is ferromagnetic Curie temperature, the term C_∞ is connected to the effective magnetic moment μ_{eff} $\mu_{\text{eff}} = g\sqrt{S(S+1)}\mu_B$ for isolated ions and the member P_1/T reflects the change in the magnetic moment of polarons at increasing of T . We used the formula (1) in order to describe the experimental dependencies $1/\chi(T)$ and to determine the values of T_C for compounds $\text{LaMnO}_{3+\delta}$, $\text{La}_{0.7}\text{Ca}_{0.3}\text{MnO}_3$, $\text{La}_{0.7}\text{Ba}_{0.3}\text{MnO}_3$, and $\text{La}_{0.7}\text{Sr}_{0.3}\text{MnO}_3$, which contain 30 % of the Mn^{4+} ions. Close values of the experimental T_C and calculated one point out the possibility for the determination of the ferromagnetic Curie temperature in the manganites (Table 1).

Table 1

	$\text{LaMnO}_{3+\delta}$	$\text{La}_{0.7}\text{Ca}_{0.3}\text{MnO}_3$	$\text{La}_{0.7}\text{Ba}_{0.3}\text{MnO}_3$	$\text{La}_{0.7}\text{Sr}_{0.3}\text{MnO}_3$
V/form.unit, \AA^3	58.69	57.73	59.83	58.42
T_C exp., K	162	259	340	360 [2]
T_C calc., K	157	252	346	368

It should be noted that the first three samples have a sharp magnetic transition near T_C and insulating behavior of the resistivity above T_C . In $\text{La}_{0.7}\text{Sr}_{0.3}\text{MnO}_3$ the resistivity is metallic at all temperatures. The temperature range of the transition from the ferromagnetic state to the polaron state is elongated because of the high transfer energy of holes in the e_g -zone. The presence of correlated polarons above T_C is confirmed by neutron scattering measurements [3].

Support by RFBR 12-02-00208, FEB-UB RAS 12-C-2-1026, the program of the Presidium RAS 12-P-2-1034 is acknowledged.

[1] T. I. Arbuzova, S. V. Naumov, N. G. Bebenin, *JETP Letters*, **98** (2013) 80-83.

[2] M.C. Martin, G. Shirane, Y. Endoh, et.al., *Phys. Rev. B*, **53** (1996) 14285.

[3] M.B. Salamon, S.H. Chun, *Phys. Rev. B*, **68** (2003) 014411.

1PO-J1-4

MAGNETIC PROPERTIES OF THE COBALT-DEFICIENT SINGLE CRYSTAL $\text{GdBaCo}_{1.86}\text{O}_{5.32}$

Naumov S.V.¹, Arbuzova T.I.¹, Telegin S.V.¹, Korolev A.V.¹

¹ Institute of Metal Physics, Ural Branch of RAS, 620990 Ekaterinburg, Russia
naumov@imp.uran.ru

The layered cobaltites with the general formula $\text{LnBaCo}_2\text{O}_{5+\delta}$ (Ln = rare earth) have the rich phase diagram. These compounds are suitable for study of influence of spin state of Co^{3+} ions on phase transitions [1]. The evolutions of the physical properties with the oxygen content have been studied in detail for layered cobaltites [2]. We report the data on the magnetic properties of cobalt-deficient $\text{GdBaCo}_{2-x}\text{O}_{5+\delta}$ single crystal in a wide range of temperatures.

The single crystal was grown by zone melting method. We carried out X-ray experiments, elemental analysis and defined the oxygen content in the sample. It was established that the sample is the single crystal, which has the composition $\text{GdBaCo}_{1.86}\text{O}_{5.32}$. In our sample the ratio $\text{Co}^{3+}/\text{Co}^{4+}$ is close to that for $\text{GdBaCo}_2\text{O}_{5.53}$. The crystal with cobalt deficiency has a number of features in the magnetic properties. We associate these features with the disorder in the cation sublattices. Above 200 K the sample demonstrates ferrimagnetic state with the Curie temperature of 262 K and the Neel temperature of 370 K (Fig.1 a, b). In spite of the deficit of cobalt ions the Curie temperature is close to T_C for the stoichiometric composition of $\text{GdBaCo}_2\text{O}_{5.5}$. This can be explained by assuming that all cobalt vacancies are concentrated in the octahedral sites, where Co^{3+} ions have the low-spin state ($S = 0$) [3]. It is possible to see two anomalies in temperature dependence of the magnetic susceptibility $\chi(T)$ at 180 K and 50 K. The maximum of magnetization at 180 K shifts towards low temperatures and the second one at 50 K becomes smoothed at increase of the field up to 50 kOe. Such behavior of the magnetization $M(T)$ can be connected with the formation of magnetic glass state in region $T=50-180$ K [4].

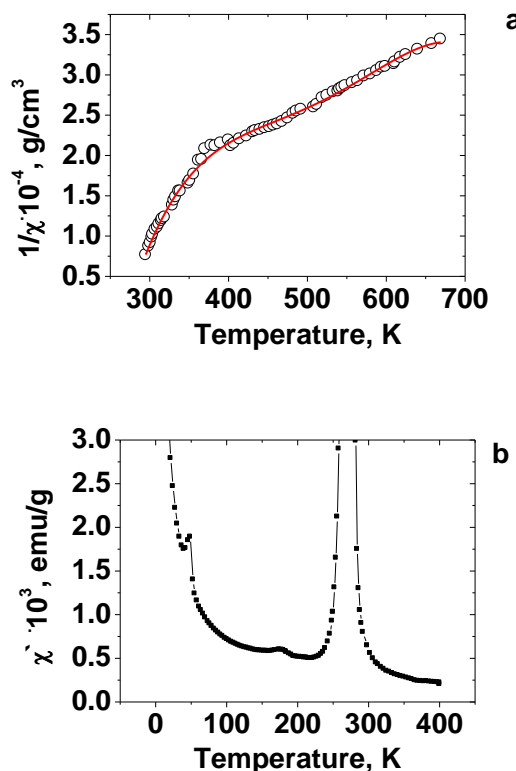


Fig. 1. Temperature dependences of the inverse magnetic susceptibility in magnetic field $H = 2.65$ kOe (a) and ac -susceptibility χ' for $H \perp c$ (b).

Support by RFBR 14-02-00432a, Presidium UB RAS 14-2-SP-247, FEB-UB RAS 12-C-2-1026, and program of the BPS RAS 12-T-2-1005 is acknowledged.

- [1] M.A. Korotin, S.Yu. Ezhov, I.V. Solovyev, et.al., *Phys. Rev. B*, **54** (1996) 5309.
 [2] A. A. Taskin, A. N. Lavrov, and Yoichi Ando, *Phys. Rev. B*, **71** (2005) 134414.
 [3] C. Frontera, J. L. Garcí'a-Muñoz, A. Llobet, et.al., *Phys. Rev. B*, **65** (2002) 180405.
 [4] T. Sarkar, V. Pralong, B. Raveau, *Phys. Rev. B*, **83** (2011) 214428.

1PO-J1-5

OPTICAL STUDY OF ELECTRONIC STRUCTURE OF COBALT DEFICIENCY SINGLE CRYSTAL $\text{GdBaCo}_{2-x}\text{O}_{5+\delta}$

Nomerovannaya L.V., Makhnev A.A., Naumov S.V., Telegin S.V.

¹ Institute of Metal Physics, UD RAS, Ekaterinburg, 620990, Russia
almakhnev@imp.uran.ru

Optical spectroscopy is one of the most informative tools for studying of the electronic structure of 3d-metal oxides. The layered cobaltite $\text{GdBaCo}_2\text{O}_{5.5}$ is compound with an interesting combination of electronic and magnetic properties. Recently it has been shown that in cobalt-deficiency single crystal $\text{GdBaCo}_{1.86}\text{O}_{5.32}$ the AF and FM orders are different from magnetic order in the $\text{GdBaCo}_2\text{O}_{5.5}$ [1].

In this work we present the results of the optical spectroscopy experiment. The complex permittivity $\varepsilon = \varepsilon_1 + i\varepsilon_2$ of $\text{GdBaCo}_{1.86}\text{O}_{5+\delta}$ ($\delta = 0.32$ and 0.07) was studied in the spectral range $E = 0.15 - 4.8$ eV by the ellipsometry method. Our research is aimed to elucidate of electronic structure's change of the cobalt-deficiency samples with various contents of oxygen.

The single crystal was grown by floating zone method. It was established that the samples are single crystal and its composition corresponds to the formula $\text{GdBaCo}_{1.86}\text{O}_{5.32}$. The sample $\text{GdBaCo}_{1.86}\text{O}_{5.07}$ was obtained from initial single crystal by means of annealing in flow Ar at 700°C .

The real part of optical conductivity spectra $\sigma_1(E)$ are characterized by the intensive broad absorption band at 1.8-4.0 eV and the band centred at ~ 1.2 eV (Fig. 1). The inset is shown the behavior $\sigma_1(E)$ at low-energy of absorption edge. The energy positions of interband transitions peaks at range 1.8-4.0 eV are almost insensitive for study samples in comparison with stoichiometric $\text{GdBaCo}_2\text{O}_{5.5}$ [2]. The principal difference between $\text{GdBaCo}_2\text{O}_{5.5}$ and cobalt-deficiency samples are the parity blockade of electronic transitions near absorption edge at 0.5-0.9 eV. Moreover, electronic states appears in insulator gap (Fig. 1, inset). Such change can be explained by increasing a number of defects in the samples and cobalt vacancies.

The influence of the oxygen content on the optical response is studied also. The $\sigma_1(E)$ spectra are smoothed, the intensity of interband absorption decreases and the relatively weak band appears near ~ 3.7 eV for single $\text{GdBaCo}_{1.86}\text{O}_{5.07}$.

The difference of nature $\sigma_1(E)$ spectra was analyzed taking into account of the electronic structure calculation $\text{GdBaCo}_2\text{O}_{5.5}$ [2].

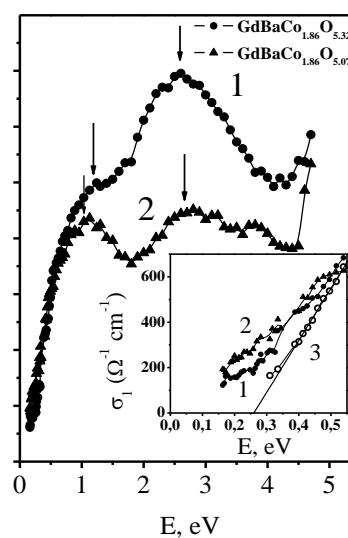


Fig. 1. $\sigma_1(E)$ spectra $\text{GdBaCo}_{1.86}\text{O}_{5.32}$ (1), $\text{GdBaCo}_{1.86}\text{O}_{5.07}$ (2) and $\text{GdBaCo}_2\text{O}_{5.5}$ (3) [2].

Support by RFBR 14-02-00432a, Presidium UB RAS 14-2-SP-247 is acknowledged.

[1] T.I. Arbutova, S.V. Telegin, S.V. Naumov et al., *Abstracts EASTMAG-2013*, (2013) 122.

[2] A.A. Makhnev, L.V. Nomerovannaya, S.V. Strel'tsov et al., *Physics of the Solid State*, **51** (2009) 525-531.

1PO-J1-6

EFFECT OF Mn DOPING ON MAGNETIC AND DIELECTRIC PROPERTIES OF $\text{Bi}_2\text{Sn}_2\text{O}_7$

Udod L.V.^{1,2}, *Aplesnin S.S.*^{1,2}, *Eremin E.V.*¹, *Sitnikov M.N.*², *Molokeev M.S.*¹

¹L.V. Kirensky Institute of Physics, Krasnoyarsk, Russia

²M. F. Reshetneva Aerocosmic Siberian State University, Krasnoyarsk, Russia
luba@iph.krasn.ru

Bismuth oxides, for example bismuth stannate $\text{Bi}_2\text{Sn}_2\text{O}_7$, are of considerable importance as heterogeneous catalysts for a variety of processes including the oxidative coupling of methane, of propylene, and the oxidation of hydrocarbons. They are also used as sensors and as electrode materials in the reduction of oxygen [1,2]. The substitution of Sn^{4+} ions by paramagnetic Mn^{4+} ions can lead to change of the magnetic properties and magnetic state of the $\text{Bi}_2\text{Sn}_2\text{O}_7$. The aim of this work is to study the effect of Mn substitution on the magnetic and dielectric properties of $\text{Bi}_2\text{Sn}_2\text{O}_7$.

The sample $\text{Bi}_2\text{Sn}_{1.95}\text{Mn}_{0.05}\text{O}_7$ has been synthesized by conventional solid-state reaction method. According to the X-ray powder diffraction research, our samples include of two co-existing polymorphic phase cubic and rhombic, that similar to the pure $\text{Bi}_2\text{Sn}_2\text{O}_7$. The magnetic moment has been measured in the temperature range 4.2-300 K and in magnetic field up to ± 6 T. The temperature dependence of the inverse magnetic susceptibility $\text{Bi}_2\text{Sn}_{1.95}\text{Mn}_{0.05}\text{O}_7$ has anomaly at 150 K which may be due change in the exchange interactions as a result of phase transition from rhombic to cubic. In the lower temperature region the inverse susceptibility is described by the Curie-Weiss law with the negative paramagnetic Curie temperature (Fig 1). The magnetization field dependence is not linear at temperature $T = 4.2$ K and fitted by linear function at $T = 50$ K.

The dielectric permeability investigation $\text{Bi}_2\text{Sn}_{1.95}\text{Mn}_{0.05}\text{O}_7$ was carried out in the temperature range 300-650 K and at the frequency 100 kHz. The dielectric permeability is monotonic increased with growth of temperature. Both temperature dependences of the real dielectric permeability $\text{Re}(\epsilon)$ and imaginary dielectric permeability $\text{Im}(\epsilon)$ have small maxima at $T=350$ K that correlated with the pure $\text{Bi}_2\text{Sn}_2\text{O}_7$ and it is interpreted by polymorphs transition.

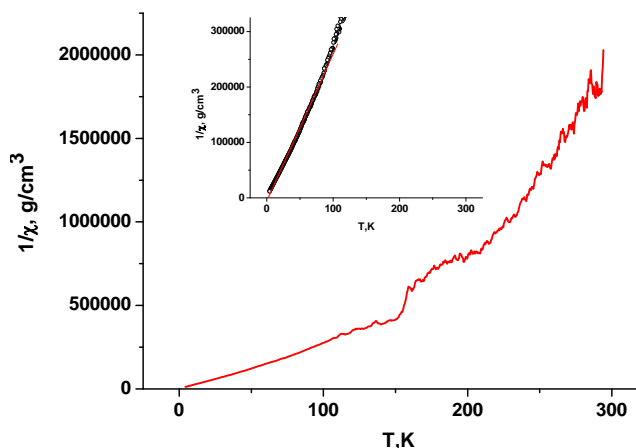


Fig. 1 The temperature dependences of the inverse magnetic susceptibility $\text{Bi}_2\text{Sn}_{1.95}\text{Mn}_{0.05}\text{O}_7$

Support by the Russian Foundation for Basic Research project № 12-02-00125-a; 14-12-00124.

[1] G. S. Devi, S. V. Manorama, V. J. Rao, *J. Electrochemical Soc.* **145** (1998) 1039.

[2] M. Besson, F. Lahmer, P. Gallezot, P. Fuertes, and G. Fleche, *J. Catal.* **152**, (1995) 116.

1PO-J1-7

ANOMALOUS HALL EFFECT IN 2D DMS

Oveshnikov L.N.¹, Kulbachinskii V.A.³, Davydov A.B.², Aronzon B.A.^{2,1}

¹ National Research Center, Kurchatov Institute, Moscow 123182, Russia

² P.N. Lebedev Physical Institute RAS, Moscow 119991, Russia

³ MSU M.V. Lomonosov, Low Temperature Physics Department, Moscow 119991, Russia
Ragnos@list.ru

Anomalous Hall Effect (AHE) has a significant fundamental role, because it allows to study the unique parameters of a system, which do not appear in other transport effects, but they are crucial for the formulating appropriate theory approach in condensed matter physics. As for the applied science, AHE is indispensable for spintronics. In the present work we studied diluted magnetic semiconductor (DMS) heterostructures with a quantum well (QW) GaAs/InGaAs/GaAs, doped by Mn δ -layer via spacer. There are 3 basic mechanisms responsible for AHE (skew scattering, side-jump, intrinsic). According to the experimental data, the skew scattering did not contribute to the AHE in our case, only side-jump and intrinsic mechanisms could be essential. This conclusion is based on the dependence of the anomalous Hall resistivity R_{xy}^a on the magnetoresistivity, which appeared to be quadratic ($R_{xy}^a \sim R_{xx}^2$) [1] (Fig.1). The sign for the each contribution can be both “+” or “-“, regardless of the carrier type in the system. In the experiment we observed the change of the AHE sign with decreasing the temperature (Fig.2). We suppose, that the change of the sign is caused by change of the dominant AHE mechanism: the scattering rate increases while temperature increases. The side-jump contribution is affected by a scattering, while the magnitude of the dissipationless intrinsic contribution, related to the Berry phase, is a scattering-independent. The change of the AHE sign in 2D DMS system also have been reported in [2]. It is worth to note, that observed temperature of the sign change in the AHE is close to temperature of the magnetic percolation. This fact allows us to consider that the percolation cluster can be responsible for the AHE. Thus our results are the experimental confirmation of the intrinsic mechanism for the AHE in Mn-doped QW GaAs/InGaAs/GaAs.

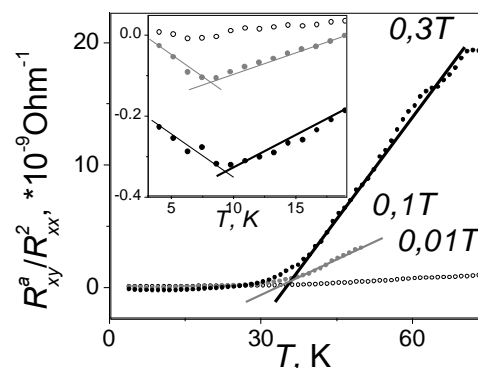


Fig. 1. Temperature dependence of the R_{xy}^a / R_{xx}^2 ratio in different magnetic field. Inset shows the low temperature data

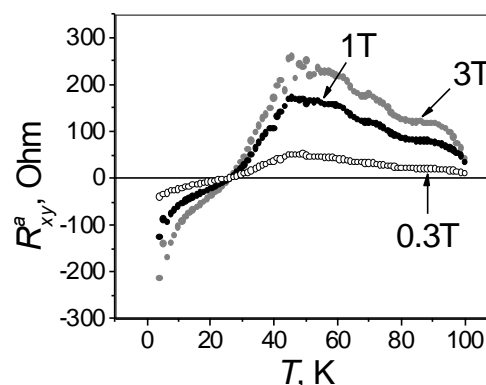


Fig. 2 Temperature dependence of the R_{xy}^a value in different magnetic fields

Acknowledgments: The work was supported by RFBR grant № 14-02-00586.

[1] N. Nagaosa *et al.*, *Reviews of Modern Physics*, **82** (2010) 1539-1592.

[2] D. Chiba *et al.*, *Physical Review Letters*, **104** (2010) 106601.

1PO-J1-8

ROLE OF OXYGEN VACANCIES IN Fe-DOPED In_2O_3 THIN FILMS

Alshammari M.^{1,2}, *Al-Qahtani M.*², *Score D.S.*², *Alshetwi Y.A.*¹, *Alfehaid S.*¹, *Fox A.M.*²,
*Gehring G.A.*²

¹ The National Centre of Nanotechnology, KACST, P.O Box 6086, Riyadh 11442, Saudi Arabia

² Dept. of Physics and Astronomy, University of Sheffield, Sheffield S3 7RH, UK

alshammari@kacst.edu.sa

In_2O_3 doped with a transition metal (Co, Fe, Mn and Cr) is considered to be a promising material for future spintronics devices because it is already established that these films may be magnetic when grown strongly n type [1, 2]. Recently, there has been an exciting prediction that films which are co-doped with an acceptor and a higher concentration of a donor will have a fully polarised impurity band in the gap that will enhance magnetism [3], this is achieved in In_2O_3 via the donor band associated with oxygen deficiency and the addition of divalent TM ions. Fe-doped In_2O_3 [4,5] has a high solubility of Fe in the In_2O_3 matrix, which is desirable for spintronic device applications.

The magnetic and optical properties of films of In_2O_3 doped with Fe at a variety of impurity concentrations were investigated at an applied magnetic field of 1.8 Tesla. These films were grown on sapphire substrates using pulsed laser deposition system at low oxygen pressure in the PLD chamber in order to increase the concentration of donor levels associated with oxygen deficiency and their magnetic moment was measured in a SQUID magnetometer.

Room temperature ferromagnetism has been observed, and it depends sensitively on Fe concentration. However, we found from the low temperature susceptibility that Fe^{2+} is paramagnetic and the magnetization is due to the oxygen vacancies. The magnetic circular dichroism spectra at room temperature due to mid-gap states is visible at energies below the band edge, $3 < E < 4$ eV, when measured at field and at remanence.

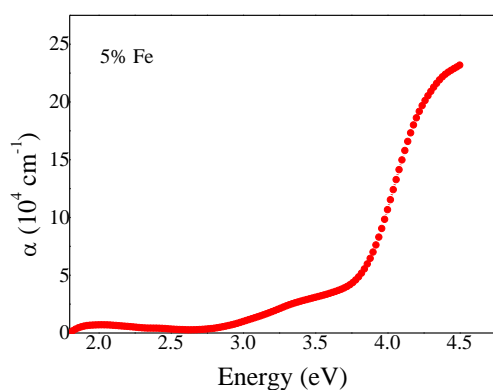


Fig. 1. The absorption spectra of 5% Fe doped In_2O_3 .

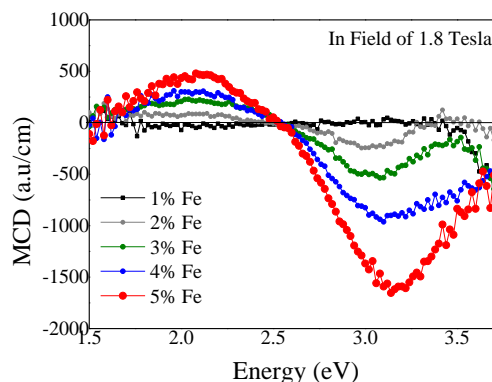


Fig. 2. The MCD spectra at RT and 1.8 Tesla.

- [1] Xiao-Hong Xu, et al, *Appl. Phys. Let.*, **94** (2009) 212510.
- [2] Feng-Xian Jiang et al, *Appl. Phys. Let.*, **96** (2010) 052503.
- [3] Wenguang Zhu et al, *PRL*, **103** (2009) 226401.
- [4] T. Ohno et al, *Jpn. J. Appl. Phys.*, Part 1 **45** (2005) L957.
- [5] H. W. Ho, et al, *J. Phys.: Condens. Matter*, **20** (2008) 475204.

1PO-J1-9

MAGNETIC PHASE TRANSITIONS AND STRUCTURE OF NEW Cu-Mn OXYBORATES

Kolesnikova E.M.^{1*}, *Bezmaternykh L.N.*¹, *Eremin E.V.*¹, *Seryotkin Yu.V.*²

¹L.V. Kirensky Institute of Physics, SB RAS, Russia

²V.S. Sobolev Institute of Geology and Mineralogy, SB RAS, Russia
ekoles@iph.krasn.ru

The magnetic phase transitions in single crystals of Mn – heterovalent oxyborates with warvikite structure $Mn_{1-x}^{2+}Cu_xMn^{3+}BO_4$ and ludwigite structure $Mn_{2-x}^{2+}Cu_xMn^{3+}BO_5$ are discussed based on the measured field-temperature and orientational dependencies. The relationship of its features and crystallochemical parameters is analyzed.

Single crystals were grown by flux method. Its crystallochemical characterization is based on the X-ray data. Magnetic measurements were carried out in the temperature range $T=2\div 300$ K and in the magnetic fields $H=0.2\div 80$ kOe, oriented either parallel or perpendicular to crystallographic axis c , coinciding with direction of dense packing.

As a result of experiment, it was found that all synthesized warvikites ($0\leq x\leq 0.65$), as the temperature decreases, pass from the paramagnetic state to antiferromagnetic state with ordering of magnetic moments in plane $\perp c$. And the Neel temperature, depending on Cu concentration, varies in the range $T_N=27\div 13$ K. Small magnetizations and low paramagnetic Curie temperatures denote strong antiferromagnetic interaction. Temperature dependencies of magnetization (Fig.1) also denote the existence of one more phase transition at $T=6$ K in all samples. This feature is associated with reorientation of magnetic moments in plane $\perp c$.

The nontrivial combination of magnetic phase transitions (Fig.2) was found in the ludwigite with minimum reached copper concentration ($x=1.5$). Firstly, in the regime FC ($H=0.2$ kOe), the transition with temperature hysteresis is present. Secondly, in the regime ZFC, as the magnetic field of the same magnitude switches on, this crystal passes to the state with negative susceptibility. As the temperature increases, the susceptibility changes the sign, and at some temperature $T_{cr}<T_N$ the states ZFC and FC are the same. As the magnetic field increases, the effects subside, and at $H\geq 1$ kOe disappear.

To clarify the role of the spin-lattice interactions, these effects are compared with the previously observed transitions in antiferromagnetic ludwigite $Mn_{1.5}^{2+}Ni_{0.5}Mn^{3+}BO_5$ with a strong spin-lattice coupling [1].

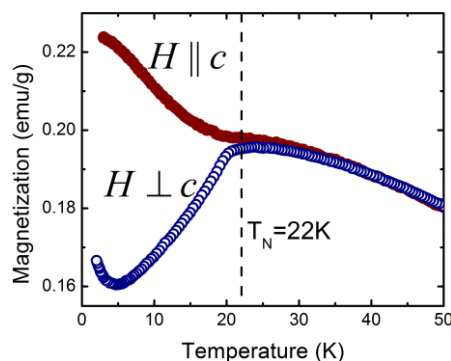


Fig. 1 Magnetization of warvikite $Mn_{1.65}Cu_{0.35}BO_4$ ($H=1$ kOe)

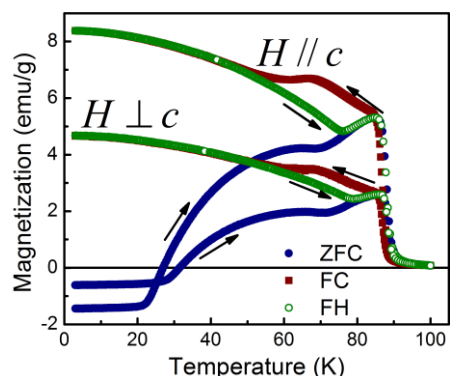


Fig. 2 Magnetization of ludwigite $Mn_{1.5}Cu_{1.5}BO_5$ ($H=0.2$ kOe)

[1] L. N. Bezmaternykh, E. M. Kolesnikova et.al. // <http://arxiv.org/abs/1401.2351>.

1PO-J1-10

ROLE OF MAGNETIC SUBSYSTEMS TO FORM A COMPLEX MAGNETIC STRUCTURE Mn_2GeO_4 SINGLE CRYSTALS

Volkov N.V.^{1,2}, Mikhashenok N.V.¹, Sablina K.A.¹, Pankrats A.I.^{1,2}, Balaev A.D.¹, Gorev M.V.^{1,2}

¹ Kirensky Institute of Physics SB RAS, Krasnoyarsk, Russia

² Siberian Federal University, Krasnoyarsk, Russia

stasha-83@yandex.ru

Magnetic materials with paramagnetic ions of the same type in two different crystallographic positions are of considerable interest due to great opportunities in forming their complex magnetic structures and rich phase diagrams. Examples of such compounds include copper metaborate CuB_2O_4 [1] and rare-earth ferrobates with huntite structure [3] which received much research attention.

The single crystals Mn_2GeO_4 have been grown by the flux method using the original technique described in our work [3]. The crystal structure, magnetic, resonance and thermodynamic properties of single crystals were studied within the framework of our research. Based on these data the magnetic phase diagram was constructed (fig.1). The clearly marked sequence of magnetic phase transitions is observed at $T_1=47$ K, $T_2=17$ K and $T_3=5.5$ K. All three magnetic anomalies exactly correlate with anomalies in the specific heat $C_p(T)$. Also neutron diffraction measurements reported in [4] confirm these phase transitions.

Analysis of thermodynamic data allows us to conclude that at $T_1=T_N$ only one of the subsystems (Mn2) completely antiferromagnetically ordered while the magnetic moments of another subsystem (Mn1) are canted from the c axis of the orthorhombic structure P_{nma} .

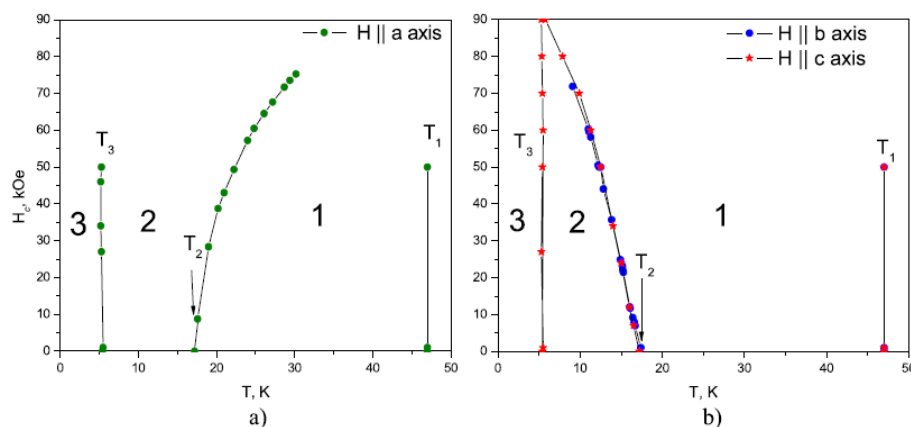


Fig. 1. Magnetic phase diagrams for (a) $H \parallel$ the a axis and (b) $H \parallel$ the b ; c axes built on the basis of the magnetic and specific heat data for Mn_2GeO_4 .

[1] M. Boehm, B. Roessli, J. Schefer, A.S. Wills, U. Staub, G.A. Petrakovskii *Phys. Rev. B*, **68** (2003) 024405.

[2] A. Pankrats, G. Petrakovskii, A. Kartashev, E. Eremin, V. Temerov, *J. Phys.: Condens. Matter*, **21** (2009) 436001.

[3] N.V. Saponova, N.V. Volkov, K.A. Sablina, G.A. Petrakovskii, O.A. Bayukov, A.M. Vorotynov, D.N. Velikanov, A.F. Bovina, A.D. Vasilyev, G.V. Bondarenko, *Phys. Stat. Sol. B.*, **246** (2009) 206.

1PO-J1-11

MAGNETIC FIELD AND MAGNETIC ISOTOPE EFFECTS ON THE SILICON OXIDATION

Koplak O., Morgunov R.
 IPCP RAS, Chernogolovka, Russia
 o.koplak@gmail.com

Silicon oxidation is shown to be accelerated by permanent magnetic field and by presence of silicon atoms ^{29}Si with nuclear magnetic moment [1] (fig.1). The latter are oxidized by almost twice as fast as atoms with spinless, nonmagnetic nuclei ^{28}Si and ^{30}Si . This is unambiguous indication that the silicon oxidation is a spin selective process.

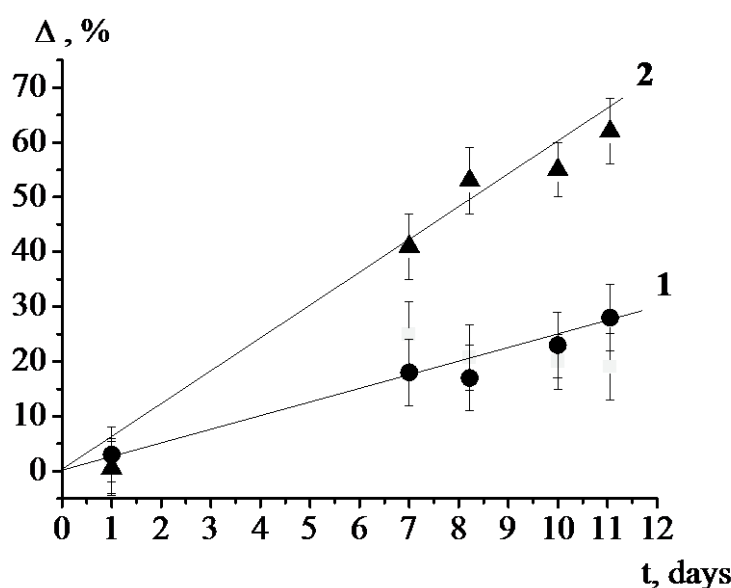


Fig.1. Relative changes of the secondary ion mass-spectroscopy signals $\Delta = (I_0 - I_t)/I_0$ as a function of time for ^{28}Si (circles) and ^{30}Si (squares) (1), and for ^{29}Si (triangles) (2).

A dominating role in chemical mechanism of oxidation is concluded to belong to the oxidizing species (preferably, O_2 molecules) in triplet spin state. The insertion of oxygen molecule into the chemical Si-Si bond as a key primary reaction of silicon oxidation is reversible, i.e. radical $\text{SiO}_2\cdot$ may eliminate oxygen molecule regenerating starting reactants; the rate of this reaction is comparable with that of triplet-singlet spin conversion in the radical pair $[\text{Si}\cdot \cdot \text{O}_2\text{Si}]$.

The observation of ^{29}Si MIE unambiguously supports the insertion of oxygen molecule into the Si-Si bond as a primary reaction of silicon oxidation. It is also in a perfect agreement with conclusion derived from the absolutely different and independent arguments based on the molecular dynamics calculations [2].

Supported by Russian Fund for Basic Researches (grant 14-03-31004 mol_a).

[1] O Koplak, R Morgunov, A Buchachenko, *Chemical Physics Letters* **560** (2013) 29-31.

[2] A. Bongiorno, A. Pasquarello, *Phys. Rev. Lett.* **93** (2004) 086102.

IPO-J1-12

RELAXATION ATTENUATION OF ULTRASOUND BY THE JAHN-TELLER CENTERS IN ZnSe:Cr IN STRONG MAGNETIC FIELD

Averkiev N.S.¹, Bersuker I.B.², Gudkov V.V.³, Zherlitsyn S.⁴, Yasin S.⁴, Zhevstovskikh I.V.^{3,5},
Baryshnikov K.A.¹, Monakhov A.M.¹, Sarychev M.N.³, Korostelin Yu.V.⁶, Landman A.I.⁶

¹ A.F. Ioffe Physical Technical Institute, RAS, 194042 St.-Petersburg, Russia

² Institute for Theoretical Chemistry, The University of Texas at Austin, TX 78712 Austin, USA

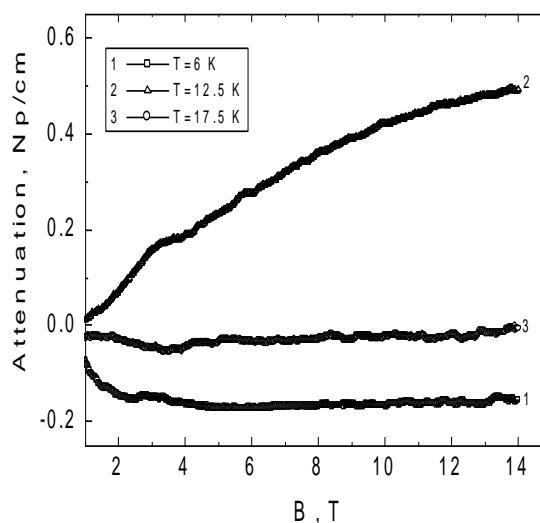
³ Ural Federal University, 620002, Ekaterinburg, Russia

⁴ Dresden High Magnetic Field Laboratory, Helmholtz-Zentrum Dresden-Rossendorf, D-01314 Dresden, Germany

⁵ Institute for Metal Physics, UD RAS, 620990 Ekaterinburg, Russia

⁶ P.N. Lebedev Physical Institute, RAS, 119991 Moscow, Russia

In our former investigations [1], we have found the peak of ultrasonic attenuation $\alpha(T)$ in ZnSe:Cr²⁺ crystal. We have interpreted it as due to relaxation in the system of Jahn-Teller centers Cr4Se. Later, magnetoacoustic investigations [2] have revealed resonant-like curve of the attenuation field dependence at considerably low magnetic fields. Here we report the results of our recent measurements in strong fields at a number of fixed temperatures: 1.4, 2, 4.2, 6, 8, 9, 10, 12.5, 15, 17.5, 20 K. We have observed a monotonous increase of attenuation which was proportional to the magnitude of relaxation attenuation at given temperature. In the figure, one can see the most typical dependences obtained at 29.5 MHz for the slow shear mode propagating along the $\langle 110 \rangle$ crystallographic axis. Peak of relaxation attenuation at this frequency is observed at 11.7 K, so, the most pronounced magnetic field variation of attenuation is seen at 12.5 K (if to discuss the measured row of temperatures). Theoretical consideration of the Jahn-Teller effect and spin-orbit Hamiltonian for the impurity complex shows that sixfold degenerate (with spin states) ground state at $B=0$ splits in strong magnetic field and the lowest energy states represent 2 degenerate levels. Calculation shows that variation in population distribution of the centers among these levels should lead to increase of attenuation by the factor of 1/3 that is in good agreement with the experimental data.



Support by RFBR grant № 12-02-00476-a is acknowledged. K.A. Baryshnikov is grateful for the financial support of the Dynasty Foundation.

[1] V.V.Gudkov, A.T.Lonchakov, V.I.Sokolov, I.V.Zhevstovskikh, *Phys.Rev.B*, **73** (2006) 035213.

[2] V.V. Gudkov, I.B. Bersuker, S. Yasin, S. Zherlitsyn, I.V. Zhevstovskikh, V.Yu. Mayakin, M.N.Sarychev, A.A.Suvorov, *Sol. State Phen.*, **190** (2012) 707.

1PO-J1-13

MAGNETOTRANSPORT PROPERTIES OF THIN FILMS OF DILUTED MAGNETIC OXIDES $Zn_{1-x}Co_xO$ ($x \sim 0.2$)

*Pankov M.A.*¹, *Lotin A.A.*², *Semisalova A.S.*³, *Parshina L.S.*², *Chernoglazov K.Yu.*⁴

¹ P.N. Lebedev Research Center in Physics, 119991 Moscow, Russia

² Institute on Laser and Information Technologies of RAS, 140700 Shatura, Russia

³ Faculty of Physics, Lomonosov Moscow State University, 119991 Moscow, Russia

⁴ NRC "Kurchatov Institute", 123182 Moscow, Russia

mpa.off@gmail.com

The wide band gap semiconductors with magnetic impurities are attractive for fabrication of the ferromagnetic semiconductor nanostructures with high values of Curie temperature. One of such materials is a zinc oxide doped with the transition 3d-metals which can be ferromagnetic at room temperature and higher which accordingly to the theoretical estimates [1]. It is known that among 3d-metals Co has the highest solubility limit in the $Zn_{1-x}Co_xO$ solid solution [2]. This report represents the investigation results of magnetic and transport properties of $Zn_{1-x}Co_xO$ films 60-300 nm thick with various Co content ($x=0.05-0.45$) which were produced by a pulsed laser deposition method using the time-of-flight separation of the deposited particles.

The sign of the anomalous Hall effect is found to be positive and opposite to the sign of the normal Hall effect, as occurs in Co metal layers. This is indicative of the cluster nature of ferromagnetism in the $Zn_{1-x}Co_xO$ [3]. It is found that the transport properties of thin $Zn_{1-x}Co_xO$ films with $x=0.2$ and thickness $d = 60$ nm exhibit unexpected behavior. In these films, we observe negative magnetoresistance with well-pronounced hysteresis in magnetic field dependence of the $R_{xx}(B)$ when field is oriented perpendicularly to the film plane (Fig. 1a). The hysteresis in the dependence $R_{xx}(B)$ is practically lacking for the samples with a thickness of $d > 100$ nm.

For comparison on Fig. 1b the field dependence of the magnetic moment $M_{\Sigma}(B)$ is shown for the field in the film plane. It can be seen that the coercive field in the hysteresis of $R_{xx}(B)$ reaches 2.4 kOe, whereas the value of H_C in the magnetization does not exceed 100 Oe. This observation evidences of the out-of-plane easy axis of magnetization probably caused by the columnar film structure (elongation of clusters along the axis of film growth).

Supported by RFBR (14-07-31084).

[1] T. Dietl, H. Ohno, F. Matsukura, J. Cibert, and D. Ferrnd, *Science*, **287** (2000) p. 1019.

[2] Kenji Ueda, Hitoshi Tabata, and Tomoji Kawai, *Appl. Phys. Lett.*, **79** (2001) p. 988.

[3] A.A. Lotin, O.A. Novodvorsky, V.V. Rylkov, D.A. Zuev, O.D. Khramova, M.A. Pankov, B.A. Aronzon, A.S. Semisalova, N.S. Perov, A. Lashkul, E. Lahderanta, V.Ya. Panchenko. *Semiconductors*, **48** (2014) 556.

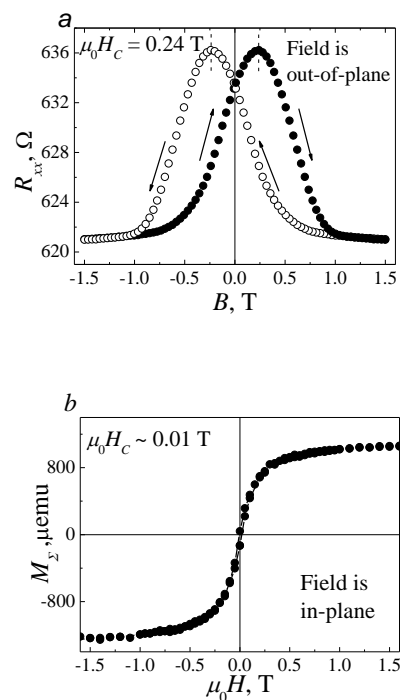


Fig. 1. Magnetic-field dependences $R_{xx}(B)$ (a) in the field perpendicular to the film and (b) $M_{\Sigma}(B)$ in the field parallel to the film for the $Zn_{1-x}Co_xO$ sample with a thickness $d=60$ nm ($T = 40$ K).

1PO-J1-14

SYNTHESIS AND MAGNETIC PROPERTIES OF $\text{Cu}_3\text{Fe}_4(\text{VO}_4)_6$ SINGLE CRYSTALS

Bayukov O.A.¹, Eremin E.V.¹, Molokeev M.S.¹, Pankrats A.I.^{1,2}, Sablina K.A.¹, Velikanov D.A.^{1,2*}, Vorotynev A.M.¹

¹ L.V. Kirensky Institute of Physics, SB RAS, 50/38 Akademgorodok, Krasnoyarsk, Russia

² Siberian Federal University, 79 Svobodny prosp., Krasnoyarsk, Russia

* dpona@rambler.ru

A $\text{Cu}_3\text{Fe}_4(\text{VO}_4)_6$ compound belongs to the crystals group with the lyonsite structure [1]. The interest to such multicomponent compounds caused by a high frustration of exchange interactions which gives rise to complex magnetic structures. Despite a strong antiferromagnetic coupling between the Fe^{3+} ions, the competition of exchange interactions prevents the formation of a magnetically ordered state even at liquid helium temperatures. A geometrically complex crystal structure determines the existence of various frustrated exchange interactions in these compounds that may ultimately be the dominant factor for the occurrence of a spin-glass state.

The $\text{Cu}_3\text{Fe}_4(\text{VO}_4)_6$ single crystals were grown for the first time using the method of spontaneous crystallization from solution-melt. To prevent the contamination of these crystals by extraneous elements, the $\text{V}_2\text{O}_5:\text{PbO} = 1:1$ mixture was used as solvent. The mixture was placed in a platinum crucible, heated to a temperature of 920 °C and held for several hours, and then cooled at a rate of 5 °C/h to 700 °C. The crystals with typical dimensions of ~3 mm were extracted from the crucible by mechanical means.

X-ray analysis confirmed the triclinic symmetry $P\bar{1}$. An interesting feature of this compound is dimeric grid of two types: $\text{Fe}_2\text{O} - 10$ octahedral dimers and $\text{Fe}_2\text{V}_2 - 2$ octahedral dimers. Copper Cu^{2+} ions are in two positions: trigonal bipyramid and square plane which is typical for oxokuprates with Jahn-Teller distortion of the oxygen environment of Cu^{2+} .

Static magnetic properties of monocrystalline $\text{Cu}_3\text{Fe}_4(\text{VO}_4)_6$ were measured in the temperature range 2÷300 K in fields up to 90 kOe using SQUID and vibrating sample magnetometers at the magnetic field oriented along different crystallographic axes. Mössbauer spectra were obtained at room temperature using MS1104Em spectrometer with Co^{57} (Cr) source. EPR spectra were registered with Bruker Elexsys E-580 spectrometer in the temperature range 110÷300 K. Angular and temperature dependences of the resonance linewidth, resonance field and absorption amplitude were studied.

Fig. 1 shows a fragments of the temperature dependences of magnetization obtained for ZFC and FC cooling modes. Such dependences closely resemble a spin-glass behavior. It is seen that the temperatures of magnetization maximum depend essentially on the orientation of the magnetic field relative to the crystal axes. At the same time the magnetic properties of $\text{Cu}_3\text{Fe}_4(\text{VO}_4)_6$ above 10 K do not show noticeable anisotropy.

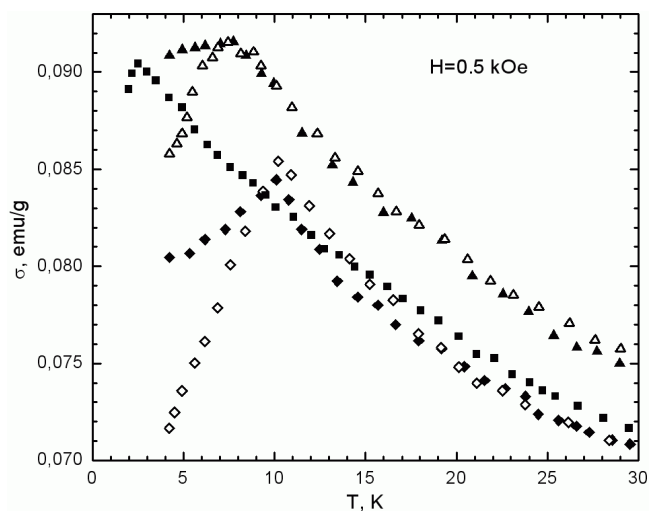


Fig. 1. Temperature dependences of magnetization for a single-crystal $\text{Cu}_3\text{Fe}_4(\text{VO}_4)_6$ samples, measured in a magnetic field of 0.5 kOe along three mutually perpendicular directions. Open and close points correspond to ZFC and FC measurements, respectively.

[1] M.A. Lafontaine, J.M. Grenéche, Y. Lalignant, G. Férey, *J. Sol. St. Chem.*, **108** (1994) 1–10.

1PO-J1-15

MAGNETIC AND ELASTIC PROPERTIES OF $\text{La}_{0.7-y}\text{Pr}_y\text{Ca}_{0.3}\text{MnO}_3$ SINGLE CRYSTALS

Zainullina R.I.¹, Bebenin N.G.¹, Ustinov V.V.¹, Mukovskii Ya.M.²

¹ Institute of Metal Physics UB RAS, Ekaterinburg, Russia

² National Science and Technology University "MISiS", Moscow, Russia

Zainul@imp.uran.ru

The lanthanum manganites $\text{La}_{1-x}\text{D}_x\text{MnO}_3$ (D=Ca, Sr, or Ba) attract attention due to colossal magnetoresistance (CMR) that is observed near Curie temperature T_C . A characteristic feature of the manganites is the strong interaction between the charge carriers, localized spins, and crystal lattice. In the greatest extent, this interaction manifests itself when a first-order phase transition takes place at T_C . The manganites $\text{La}_{1-x}\text{Ca}_x\text{MnO}_3$ with $x \approx 1/3$ belong to such compounds. The properties of these manganites can be changed by substitution of Pr for La because the ionic radius of Pr^{3+} (1.29 Å) is less than that of La^{3+} (1.36 Å) and the magnetic moment of the Pr^{3+} is nonzero. The presence in the A-position of the perovskite unit cell of ions with different radii and different magnetic moments should lead to inhomogeneity of both lattice and magnetic subsystems of the crystals.

This work aims at studying the effect of substitution of Pr for La in $\text{La}_{0.7}\text{Ca}_{0.3}\text{MnO}_3$ on the magnetic and elastic properties. The single crystals of $\text{La}_{0.7-y}\text{Pr}_y\text{Ca}_{0.3}\text{MnO}_3$ with $y=0, 0.1, 0.2,$ and 0.3 were grown by the floating-zone method. The temperature and magnetic field dependences of magnetization were measured using a vibrating sample magnetometer. The ultrasound velocity and internal friction were measured by the composite vibrator method.

It is shown that Curie temperature increases with increasing magnetic field, which is typical of first order magnetic phase transition: $T_C(H) = T_C(0) + BH$, B being about 0.8K/kOe for y from 0 to 0.2 and ≈ 1.2 K/kOe for $y = 0.3$. The value of T_C is linear function of Pr concentration: $T_C \approx (229 - 270y)$ K, which agrees with [1]. The magnetic moments of Pr and Mn are parallel to each other. In addition to the decrease of T_C the effect of Pr doping results in a broadening of transition region, which indicates enhancement of the magnetic inhomogeneity.

The substitution of Pr for La leads to significant decrease of the velocity of ultrasound waves. A sharp change in the sound velocity occurs in the range that almost coincides with the transition region determined from the magnetization data. It follows that the phase transition at T_C in $\text{La}_{0.7-y}\text{Pr}_y\text{Ca}_{0.3}\text{MnO}_3$ is magnetostructural transition rather than purely magnetic one. The surprisingly strong hysteresis in the temperature dependence of ultrasound velocity is observed in paramagnetic state, the width of the hysteresis loop being increased with Pr content. Slow relaxation of the sound velocity is revealed.

The work was supported in part by grants 12-T-2-1005, 12-P-2-1034, and RFBR 12-02-00208.

[1] A. M. Balagurov, V. Yu. Pomjakushin, D. V. Sheptyakov, V. L. Aksenov, P. Fischer, L. Keller, O.Yu. Gorbenko, A.R. Kaul, N. A. Babushkina, *Phys. Rev. B*, **64** (2001) 024420(1-10).

1PO-J1-16

GRANULAR FERROMAGNETIC-SEMICONDUCTOR STRUCTURES BASED ON $A^{II}B^{IV}C^V_2$

Fedorchenko I.V.¹, Aronov A.V.¹, Marenkin S.F.¹, Kilanski L.², Dobrowolski W.², Lahderanta E.³

¹Kurnakov Institute of General and Inorganic Chemistry, RAS, Moscow, Russia

²Institute of Physics PAN, Warsaw, Poland

³Lappeenranta University of Technology, Lappeenranta, Finland

fedorkin-san@rambler.ru

Nanogranular structures based on semiconductor host and ferromagnetic nanoinclusions are promising materials for spintronics. It has the advantages of both “non magnetic metal-ferromagnetic” and “dielectric-ferromagnets” granular structures. The most valuable benefits of such structures are compatible with semiconductor technology and eutectic type of interaction in the system semiconductor-ferromagnetic, which provides the stable interface between phases in the structure. The magnetic properties of granular structures are determined by ferromagnetic nanoclusters. The nanogranular structures based on $ZnGeAs_2$, $CdGeAs_2$ and other isostructural semiconductors with MnAs ferromagnetic inclusions were synthesized [1]. In these structures positive and negative magnetoresistance (MR) was observed [2, 3]. MR character depends on the phase interaction in the systems. The structures where eutectic point shifted to the semiconductor has negative MR, but structures where eutectic point shifted to the middle part of the phase diagram chalcopyrite – ferromagnet has positive MR. If the eutectic point is situated in the middle part of the diagram, the needles eutectic will be formed in the structure. Such type of eutectic causes the formation of percolation cluster.

This work supports by Grant of President of Russian Federation for young researcher MK-1454.2014.3.

[1] I.V. Fedorchenko, A. Kochura and et.al, *IEEE trans. magn.*, **48**, 4 (2012) 1581-1584.

[2] L.Kilanski, M.Gorska, W. Dobrowolski and et., *J. Appl. Phys.* **108**, (2010) 073925.

[3] L. Kilanski, W. Dobrowolski, E. Dyniwska and et.all, *Solid State Comm.* **151**, (2011) 870-873.

1PO-J1-17

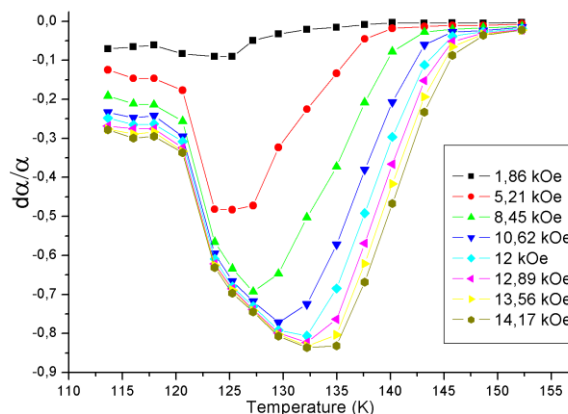
GIANT MAGNETOTHERMOPOWER IN $\text{Sm}_{0.55}\text{Sr}_{0.45}\text{MnO}_3$ MANGANITE

Koroleva L.I.¹, Morozov A.S., Jakina E.S.
 Moscow State University, Moscow, Russia
¹ koroleva@phys.msu.ru

Currently, practical use of thermoelectricity is mostly limited to thermocouples for temperature measurement. It's not applicable in other devices such as thermoelectric generator, refrigerator and heaters due to the low efficiency. It will be shown that the usage for this purposes the heterogeneous magnetic semiconductors can significantly increase the efficiency of devices based on them. Consider a semiconductor inside which is located a one nanocluster with charge carrier concentration and the crystal structure different than in the matrix. Electric current, flowing in the sample during the measurement of thermopower α , causes the Peltier effect at a boundaries of the cluster, i.e. a temperature difference ΔT , which, in turn, produces thermopower α_1 on it. This cluster contribute $(\alpha_1 - \alpha_2)\Delta T$ in thermopower of the whole sample. Here α_2 is thermopower of a sample in the absence of nanoclusters. That contribution from nanoclusters affects to the effective value α of the entire sample. Obviously when the sample has a large number of nanoclusters, α value may be considerable. The researching of neutron and electron diffraction and magnetic properties of $\text{Sm}_{0.55}\text{Sr}_{0.45}\text{MnO}_3$ have shown that there is a magnetic inhomogeneous state in it consisting of ferromagnetic (F) clusters with Curie point $T_C = 134$ K, A-type antiferromagnetic (AF) clusters with Neel temperature $T_{NA} \sim T_C$ and CE-type AF clusters with $T_{NCE} = 240$ K.

We have investigated the thermopower α and longitudinal magnetothermopower $\Delta\alpha/\alpha = (\alpha_{H=0} - \alpha_H)/\alpha_{H=0}$ of the monocrystalline and polycrystalline $\text{Sm}_{0.55}\text{Sr}_{0.45}\text{MnO}_3$ in magnetic field up to 13.2 kOe. The broad maximum on temperature dependence of absolute value $\alpha(T)$ includes T_C , but near T_C is also the sharp giant minimum on the $\{\Delta\alpha/\alpha\}(T)$ curves as it shown at Fig.1. Sharp decrease of α in T_C under the action of magnetic field is connected with destruction of the F nanoclusters in which the crystalline lattice is pressed by strong s-d exchange. Negative magnetothermopower in its minimum achieves the giant value of 90% in magnetic field $H = 14,2$ kOe. The changed crystalline lattice in these clusters excites the change of thermopower in them. This cluster's thermopower influences on the voltage drop of whole sample during the measurement of thermopower and, consequently, on the effective value α of the whole sample. This means that F clusters make the basic contribution in the total thermopower.

Recently we have shown that in $\text{Sm}_{0.55}\text{Sr}_{0.45}\text{MnO}_3$ single crystal annealed in oxygen, in which broken connections Mn-V-Mn (V is vacancy) are closed, CE-type AF phase becomes dominant in the sample. In this case the giant minimum on $\{\Delta\alpha/\alpha\}(T)$ curves is sharp and located near the T_{NCE} . Sharp decrease of α in T_{NCE} under the action of magnetic field is connected with destruction of CE-type AF phase and, consequently, destruction of charge ordering, displacing the oxygen ions [1].



[1] L.I. Koroleva, A.S. Morozov, E.S. Jakina. *Physics of Solid State*, **56** (2014) 1069-1072.

Fig. 1. Magnetothermopower of $\text{Sm}_{0.55}\text{Sr}_{0.45}\text{MnO}_3$ near $T_C = 134$ K in different magnetic fields.

1PO-J1-18

FMR STUDY OF MAGNETIC ANISOTROPY IN $\text{Mn}_{52}\text{Si}_{48}$ HIGH- T_c THIN FILM

Drovosekov A.B.¹, Kapelnitsky S.V.², Kreines N.M.¹, Rylkov V.V.², Tugushev V.V.², Zhou S.³

¹ P.L.Kapitza Institute for Physical Problems RAS, 117334 Moscow, Russia

² NRC “Kurchatov institute”, 123182, Moscow, Russia

³ Helmholtz-Zentrum Dresden-Rossendorf, Institute of Ion Beam Physics and Materials Research, D-01314 Dresden, Germany
kapelnitski@gmail.com

Recently, above-room Curie temperature $T_c \approx 330$ K which exceeds by an order of magnitude the value ($T_c \approx 30$ K) for the bulk MnSi material, was observed in the non-stoichiometric $\text{Mn}_{1-x}\text{Si}_x$ ($x \approx 0.5$) thin films [1,2] using static magnetic field, magneto-transport and magneto-optic measurements. Below, ferromagnetic resonance (FMR) method in the frequency range from 7.65 to 54.34 GHz is used to study 70 nm thick $\text{Mn}_{52}\text{Si}_{48}$ films prepared by pulse laser plasma deposition on Al_2O_3 (0001) substrate at 340 °C.

The FMR resonance line has the nearly Lorenz form, the resonance field is isotropic when the external field lies in the film plane. In order to explain the orientation dependence of FMR vs angle between the external field and the direction normal to the film plane, both the 2-nd and 4-th order effective magnetic anisotropy fields should be taken into account:

$$E = -\mathbf{HM} + (1/2)K_2M_z^2 - (1/4)K_4M_z^4/M_S^2 \quad (1a), \quad \mathbf{H}_{eff} = \mathbf{H} - K_2M_z \mathbf{z} + K_4M_z^3/M_S^2 \mathbf{z}, \quad (1b)$$

where \mathbf{M} is magnetisation vector, K_2 and K_4 are coefficients ($K_2 = 4\pi$ for the shape anisotropy).

The best fit of experimental data for the ‘in plane’ and ‘normal to plane’ orientations of the external field is achieved for the *second order easy plane* and *fourth order easy axis* anisotropy fields. The values of parameters are $K_2 = 20.9$ and $K_4 = 6.1$ at $T = 40$ K (magnetization $M_S = 440$ Gs was taken from the static measurements data). The matching of the ‘in plane’ and ‘normal to plane’ magnetization curves, gives respectively $K_2 = 18$ and $K_4 = 5.5$ assuming the (1b) expression for the net anisotropy. That is in good agreement with K_2 , K_4 obtained from the FMR data.

The temperature dependence of anisotropy fields in the temperature range 4.2-350 K was calculated from FMR data using the following expression for magnetization obtained in [2] within the spin-fluctuation model for weak itinerant ferromagnets with embedded defect-induced local moments:

$$M_s(T) \approx M_s(0) \{1 - [T(T - T_c^0)/T_c(T_c - T_c^0)]^{1.4}\}, \quad (2)$$

where $T_c^0 \approx 30$ K is ‘intrinsic’ Curie temperature for itinerant ferromagnetic MnSi.

Angular dependence of magnetic anisotropy in Eqs. (1a, b) might be attributed to the magneto-elastic deformation effects and complex texture of the film induced by the film-substrate interface. Both phenomena lead to the random in-plane orientation of deformed nanometer size $\text{Mn}_{52}\text{Si}_{48}$ crystallites with the texture axis normal to the interface. Eqs. (1a,b) may be obtained in frame of the model [2] in the fourth-order approximation over the spin-orbit interaction between itinerant electrons and defect-induced local moments, taking into account the perturbation of crystal potential of the film by the deformation and texture effects near the film-substrate interface.

The work is partially supported by RFBR (grants 13-07-12087, 13-07-00477).

[1] V.V. Rylkov, S.N. Nikolaev, K.Yu. Chernoglazov et al, *JETP Lett.*, **96** (2012) 272–280.

[2] V. V. Rylkov, E. A. Gan’shina, O. A. Novodvorskii et al, *Eur. Phys.Lett.*, **103** (2013) 57014.

[3] V.N. Men’shov, V.V. Tugushev, S. Caprara, *Phys. Rev. B*, **83** (2011) 035201.

1 July

17:30-19:00

Tuesday

poster session

1PO-J2

“Theory”

1PO-J2-1

CALCULATION OF THE MAGNETIC PROPERTIES OF THE DISORDERED FERRIMAGNETIC Fe-Si, Fe-Sn ALLOYS TAKING INTO ACCOUNT THE SPIN FLUCTUATIONS

Radzivonchik D.I.¹, Grebennikov V.I.¹

¹ Institute of Metal Physics UD RAS, Yekaterinburg, Russia
radzivonchik@imp.uran.ru

In this work we investigate the magnetic and thermodynamic properties of the disordered ferrimagnetic *Fe-Si* and *Fe-Sn* alloys. One possible approach for describing the magnetism of the disordered transition metal alloys with *sp*-elements is based on the dynamic spin-fluctuation theory [1]. The Stratonovich-Hubbard transformation replaces the system of pair electron interaction by the system of electrons interacting with exchange fluctuating field in space and «thermodynamic time». Fluctuations of the electron spin density play an important role in the system because they provide the basic mechanism disorientating the local magnetic moments with increasing temperature, since the excitation energy of spin fluctuations is less than energy of the thermal electron excitations.

Novelty of this work compared with the standard spin-fluctuation theory is the dependence of the intra-atomic coupling constant u_j of the interaction *3d*-electrons on the *j* type of site. Such consideration allows more realistic to describe a ferrimagnetic system and take into account various concentrations of *sp*-elements.

A system of nonlinear equations for the average of the exchange field, the mean square of fluctuating exchange field and the average spin moment at the sites was obtained. A self-consistent solution of the system of equations allows to define a magnetic characteristics at the different temperatures. The magnetization-temperature dependence, the Curie temperature, the values of local spin moments, the temperature dependence of susceptibility, heat capacity and entropy for metallic *Fe-Si* and *Fe-Sn* alloys with different concentrations *Si*, *Sn* were calculated.

Support by RFBR (grant 14-02-00080) and UD RAS (grant 12-Y-2-1002) is acknowledged.
[1] N.B. Melnikov, B.I. Reser, V.I. Grebennikov, *J. Phys.: Conden. Matt.*, **23** (2011) 276003.

1PO-J2-2

ANALYTICAL AVERAGING OVER DISORDER IN MONTE CARLO METHODS

Sizanov A.V.^{1,2}, Syromyatnikov A.V.^{2,1}

¹ Physical Faculty of Saint Petersburg State University, Saint Petersburg, Russia
² Petersburg Nuclear Physics Institute, Gatchina, Leningrad district, Russia
alexey.sizanov@gmail.com

We present a common approach to the simulation of disordered systems with Monte Carlo methods (both classical and quantum) and illustrate it with applications. By changing the definition of statistical weight in Monte Carlo process we obtain analytical averaging over a disorder at every stochastic step. This change of statistical weight can be done for a wide range of models (however not for all). So we get faster result because of reduction of number of calculation steps. To illustrate the approach we consider disordered classical and quantum Heisenberg models and disorder-driven phase transitions in these systems.

1PO-J2-3

NON-EQUILIBRIUM CRITICAL BEHAVIOUR OF STRONG-DILUTED MAGNETS WITH LONG-RANGE CORRELATED DISORDER

Medvedeva M.A.¹, Prudnikov P.V.¹

¹ Omsk State University, Mira 55A, Omsk, Russia
mmed@mail.ru, prudnikp@univer.omsk.su

In this paper one present a Monte-Carlo study of the influence of structural long-range (LR) correlated defects on the non-equilibrium critical behavior of strong-diluted magnets described by the Heisenberg model, with Hamiltonian $H = -J \sum_{i,j} p_i p_j \bar{S}_i \bar{S}_j$. A special type of such a disorder has been considered at first by Weinrib and Halperin [1]. They showed that the disorder with power law correlation $g(x) \sim x^{-a}$ for large separations x is relevant $a < d$. As a result, the existence of LR correlations in the disorder gives significant effect and wider class of disordered systems can be characterized by a new universality class of critical behavior.

The method for calculation the critical temperature using the Binder cumulant and the intersection ξ/L was applied in work [2] for weakly disordered Heisenberg model with spin concentration $p = 0.80$ and was showed a good and reliable results. Therefore, in this paper, we use the same method to calculate the critical temperature $T_c = 0.888(5)$ for strong-diluted Heisenberg model with total spin concentration $p=0.60$. But the cluster algorithm should be modified by Swendsen-Wang algorithm for the simulation of system low-temperature behavior.

In the vicinity of criticality cumulant U_4 characterized by scaling form $dU_4/dT \sim L^{1/\nu}$. The critical exponent of the correlation length $\nu = 0.821(14)$ was obtained for strong-diluted Heisenberg model. The value of $\nu = 0.7048(30)$ for pure Heisenberg model was obtained in [3] and $\nu = 0.758(10)$ for weakly disordered Heisenberg model was obtained in [2].

We have used a short-time dynamics (STD) approach to obtain the values of dynamic and static critical exponents. The completely ordered state has been chosen as the initial configuration. In this case, the initial state corresponds to $T = 0$ (when all the spins are oriented in one direction). Scaling analysis for STD shows that, for an ordered initial state quenched to T_c , the order parameter behaves as $m(t) \sim t^{-\beta/z\nu}$ and cumulant behaves as $U_2(t) \sim t^{d/z}$. We have used cubic lattice of linear size $L=64$ at the critical temperature $T_c = 0.888(5)$ to carried out simulation.

The influence of a leading correction to the scaling on asymptotic values of exponents were considered to obtain accurate values of the critical exponents. We have found dynamic and static critical exponents $z = 3.529(125)$, $\beta/\nu = 0.946(48)$. It is shown that weakly and strongly disordered Heisenberg model with long-range correlated disorder belong to different universality classes. It is found that increasing the concentration of structural defects with long-range correlations lead to a significant slowdown of the critical relaxation processes in comparison with pure[3] and weakly disordered systems[2,4]. The aging effects are observed in the non-equilibrium behavior of the Heisenberg model with linear defects. The aging effects are the slowing of relaxation processes in system with increasing waiting time.

This work was supported in part by Ministry of Education and Science of Russia Federation through project no. 1627. Studies were performed using the supercomputer system resources of the Moscow State University.

[1] A. Weinrib, B.I. Halperin, *Phys. Rev. B.*, **27** (1983) 413.

[2] P.V. Prudnikov, M.A. Medvedeva, *Prog. Theor. Phys.*, **127** (2012) 369.

[3] H.A. Fernandes, Roberto da Silva, J.R. Drugowich de Felício, *J. Stat. Mech.*, **10** (2006) 10002.

[4] V.V. Prudnikov, P.V. Prudnikov, A.A. Fedorenko, *Phys. Rev. B.*, **62** (2000) 8777.

1PO-J2-4

EFFECTS OF AGING AND COARSENING IN CRITICAL DYNAMICS OF 2D XY-MODEL

Popov I.S.¹, Prudnikov P.V.²

^{1,2} Omsk State University, Omsk, Russia

¹diphosgen@mail.ru, ²prudnikp@univer.omsk.su

In the past few years, systems with slow dynamics have attracted considerable theoretical and experimental interest [1]. Aging phenomena are observed during this everlasting non-equilibrium evolution. This is due to the predicted and observed ageing at a slow evolution of non-equilibrium systems and violations of the fluctuation-dissipation theorem. However, these features of the non-equilibrium behaviour, as it have been shown by analytical and numerical studies [2], can also be observed in systems near the critical temperature because the critical dynamics of such systems is characterized by extremely large relaxation times. Ageing is a phenomenon of growth of the relaxation time with the increase of the system *age* i.e. older samples correspond to more slow dynamics. Systems with slow dynamics characterized by coarsening effects. Coarsening are the effects, which consist in the growth regions of order and quasi-long domain structures. The two-dimensional XY – model demonstrates abnormal slow dynamics, but the main distinguishing feature of the 2D XY – model is that it shows an anomalous behavior is not only in vicinity of the temperature phase transition *Berezinskii-Kosterlitz-Thouless* T_{BKT} , but also for $T < T_{\text{BKT}}$ [3,4].

Relevance of the study of two-dimensional XY -model due to the extensive a number of physical systems whose behaviour can be described by this model [5].

In this reaserch the non-equilibrium critical dynamics, particularly, ageing and coarseing of pure and diluted 2D XY-model were investigated by Monte-Carlo methods in whole Bereziskii-phase. To study coarsening developed a special numerical algorithm for allocating vortex and antivortex excitations and calculating the parameters of quasi-long domain structures (Fig.1).

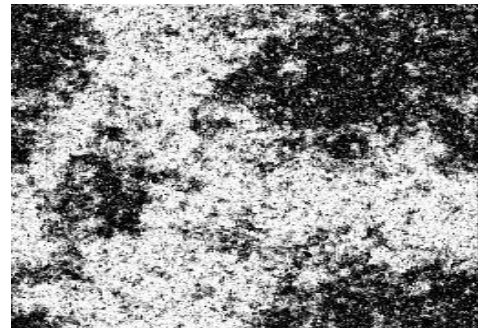


Fig. 1. Visualization of system state $L=256$ and $p=1.0$ with $T=0.1$ at time $t=1000$ MCS/s. The color intensity is proportional to the $\cos(\varphi_i/2)$, where φ_i – phase.

The non-equilibrium effects in critical behaviour of pure and structural disordered 2D XY – model have been investigated. It has revealed significant differences in the non-equilibrium evolution from the different initial states. These differences can be explained by role of vortices interaction. It was shown that the presence of structural disorder lead to significant slowing-down of the system dynamics.

This work was supported in part by Ministry of Education and Science of Russia Federation through project no. 1627. Studies were performed using the supercomputer resources of the Moscow State University and Joint Supercomputer Center of the Russian Academy of Sciences.

- [1] N. Afzal., M. Pleimling, *Phys. Rev. B*, **87** (2013) 012114.
- [2] M. Pleming, A. Gambassi, *Phys. Rev. B*, **71** (2005) 180401.
- [3] V. Berezinskii, *JETP*, **59** (1970) 907; J. Kosterlitz., D. Thouless, *J. Phys. C*, **6** (1973) 1181.
- [4] S. Korshunov, *Physics-Uspokhi*, **176** (2006) 233.
- [5] C.A.F. Vaz, J.A.C. Bland, G. Lauhoff, *Rep. Prog. Phys.*, **71** (2008) 056501.

1PO-J2-5

ANOMALOUS TEMPERATURE BEHAVIOR OF MAGNETIZATION IN CUBIC LATTICE FRUSTRATED FERROMAGNETS

Ignatenko A.N., Katanin A.A., Irkhin V.Yu.

Institute of Metal Physics, 620990 Ekaterinburg, Russia

Ignatenko@imp.uran.ru

Recently the existence of a quantum disordered ground state in *two-dimensional* magnets with predominantly *ferromagnetic* interactions was demonstrated [1]. Since in the ferromagnetic ground state quantum fluctuations are completely absent, the physics of such “frustrated ferromagnets” differs substantially from the physics of antiferromagnets with competing exchange interactions. Magnetic frustrations can also significantly influence the thermodynamic properties of three-dimensional ferromagnetic systems. Anomalous temperature dependences of magnetization are indeed observed experimentally, e.g., in the overdoped europium chalcogenides. We show that these anomalies can be naturally obtained in the framework of the Heisenberg model by taking into account the frustration.

We have considered thermodynamic properties of cubic Heisenberg ferromagnets with competing exchange interactions near the frustration point where the coefficient D_0 in the spin-wave spectrum $E_k \sim D_0 k^2$ vanishes [2]. Within the Dyson-Maleev formalism it is found that at low temperatures thermal fluctuations stabilize ferromagnetism by increasing the value of D with T . For not too strong frustration, this leads to an unusual “concave” shape of the temperature dependence of magnetization. The short-range magnetic order is retained well above the Curie temperature, which is usual for frustrated magnetic systems [3].

The phase diagram is constructed by means of Monte Carlo simulation, and suppression of magnetization and Curie temperature is found in comparison with the results of the self consistent spin-wave theory (SSWT). This effect is explained by the presence of non-analytical corrections to the spin-wave spectrum which are represented in the lowest order by the term $\sim (T/S)^2 k^2 \ln k$.

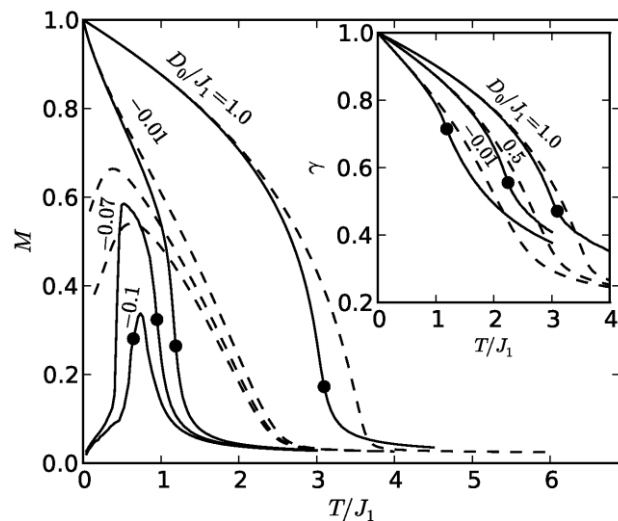


Fig. 1. Temperature dependence of the magnetization for the classical Heisenberg model on the fcc cubic lattice of finite size $14 \times 14 \times 14$ with the interaction of the first, second, and third neighbors, $J_2 = -0.3 J_1$, $J_3 = (D_0 - J_1 - J_2)/6$. The inset shows temperature dependences of the short-range order parameter $\gamma = (\langle \mathbf{S}_i \cdot \mathbf{S}_j \rangle)^{1/2}$ (i and j are nearest neighbors). Solid lines are the results of Monte Carlo simulation. Dashed lines are the result of SSWT. The filled circles indicate the Curie temperatures determined by the maximums of the susceptibility.

[1] N. Shannon, T. Momoi, and P. Sindzingre, *Phys. Rev. Lett.*, **96** (2006) 027213.

[2] A.N. Ignatenko, A.A. Katanin, V.Yu. Irkhin, *Pis'ma ZhETF*, **97** (2013) 235.

[3] A.N. Ignatenko, A.A. Katanin, V.Yu. Irkhin, *Pis'ma ZhETF*, **87** (2008) 642.

1PO-J2-6

AGING AND NON-EQUILIBRIUM PHENOMENA IN MONTE CARLO SIMULATIONS OF THE BULK AND LOW-DIMENSIONAL FERROMAGNETS

Prudnikov V.V.¹, Prudnikov P.V.¹, Pospelov E.A.¹

¹Omsk State University, Omsk, Russia

prudnikov@univer.omsk.su, prudnikp@univer.omsk.su, posevg@yandex.ru

It is considered the non-equilibrium critical evolution of spin systems with slow dynamics which displays some features, such as aging and violation of the fluctuation-dissipation theorem. We review some results of computations that have been obtained in recent years for such quantities, as the exponents determining the scaling behavior of dynamic response and correlation functions and the fluctuation-dissipation ratio, associated with the non-equilibrium critical dynamics, with particular focus on our original Monte Carlo simulation results for the 3D pure, diluted and low-dimensional Ising-like ferromagnets. Recently, non-ergodic behavior with dependence of sample magnetization on his magnetic prehistory is discovered in multilayer structure on the base of Fe/Cr [1].

We analyse an influence of different non-equilibrium initial states, presence of nonmagnetic impurities and dimensionality effects on two-time dependence of correlation and response functions on characteristic time variables as waiting time t_w and time of observation $t - t_w$ ($t > t_w$). The curves for autocorrelation $C(t, t_w)$ and response $R(t, t_w)$ functions are plotted in Fig. 1, which demonstrate that the ageing effects are increased with growth of defect concentrations.

We discuss the obtained values of non-equilibrium exponents for autocorrelation and response functions and values of the universal long-time limit of the fluctuation-dissipation ratio X^∞ as a new characteristics of non-ergodic behavior of ferromagnets near critical point. Our simulation results demonstrate for the first time that the insertion of disorder leads to new values of X^∞ with $X^\infty_{diluted}(p=0.6) = 0.443(10) > X^\infty_{diluted}(p=0.8) = 0.419(11) > X^\infty_{pure}(p=1.0) = 0.391(12)$ and with $X^\infty_{bulk} > X^\infty_{low-dimensional}$.

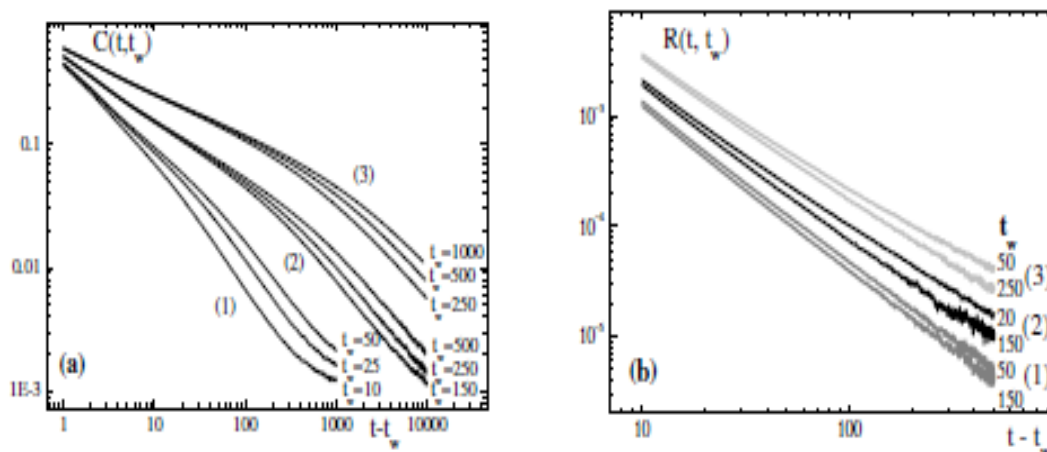


Fig. 1. Time dependence of correlation $C(t, t_w)$ (a) and response $R(t, t_w)$ (b) functions from $t - t_w$ for different values of waiting time t_w and spin concentrations p : (1) – $p=1.0$; (2) – $p=0.8$; (3) – $p=0.6$.

Support by Ministry of Education and Science of Russia through project no. 1627 is acknowledged.

[1] A.B. Drovosekov, N.M. Kreines, et.al., *JETP Letters*, **88** (2008) 118-122.

1 July

Tuesday

17:30-19:00

poster session
1PO-K

**“Spintronics and
Magnetotransport”**

1PO-K-1

FERROMAGNETIC STATE OF THE LaMnO_3 INTERLAYER IN $\text{La}_{0.7}\text{Sr}_{0.3}\text{MnO}_3/\text{LaMnO}_3/\text{SrRuO}_3$ HETEROSTRUCTURES

Petrzhik A.M.¹, Khaidukov Y.², Ovsyannikov G.A.^{1,3}, Shadrin A.V.^{1,3}, Mustafa L.²

¹ Kotel'nikov IRE of RAS, Moscow, Russia

² Max Planck Institute for Solid State Research, Stuttgart, Germany

³ MC2, Chalmers University of Technology, Gothenburg, Sweden

petrzhik@hitech.cplire.ru

The epitaxial heterostructures $\text{La}_{0.7}\text{Sr}_{0.3}\text{MnO}_3/\text{LaMnO}_3/\text{SrRuO}_3$ (LSMO/LMO/SRO) were grown by pulse laser deposition at high temperature. The heterostructures with two FM layers and insulator layer (MgO, SrTiO_3 et al) between them can be used as magnetic tunnel junctions. LaMnO_3 layer with the thickness 0 to 35nm was selected in our case. X-ray diffraction studies and transmission electron microscopy data showed sharp interface between layers and epitaxial growth of LSMO, LMO and SRO layers.

Magnetic state was studied by SQUID and by polarized neutron scattering techniques. The fit of neutron experiment data give us the magnetization of each layer, while the SQUID gives the total magnetization of our structure (see Fig.1). The magnetic moment of the LMO layer with $T_{\text{cu}}=150\text{K}$ has magnetization $M = 4.2 \text{ kG}$ (2.4 mB/Mn) at $T=10\text{K}$. Magnetic tunnel junctions (MTJ) LSMO/LMO/SRO in form of mesa-structure were fabricated from the heterostructure by photolithography and ion milling. The magnitude of the magnetoresistance of MTJ decreases with increasing thickness of the interlayer LMO. Without LMO layer the negative magnetoresistance is observed that probably caused by the negative magnetization of SRO layer.

This work was supported by RAS, RFBR 14-07-00258 and by Scientific School 4871.2014.2.

[1] S. Yunoki, E. Dagotto, S. Costamagna and J.A. Riera *Phys. Rev. B* **78** (2008) 024405.

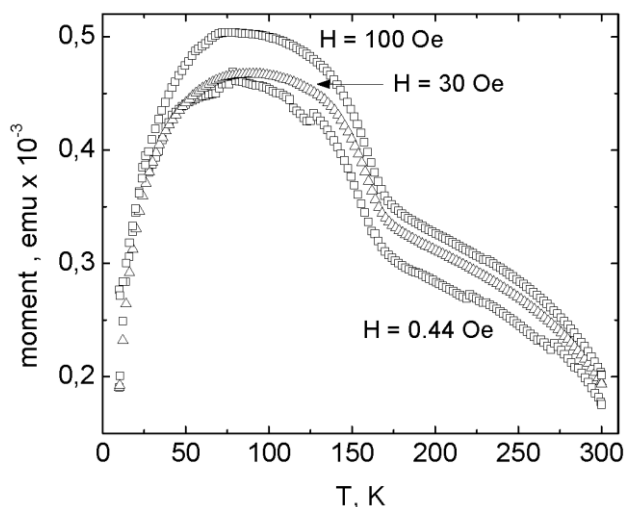


Fig. 1. Temperature dependence of magnetization. SQUID data.

1PO-K-2

SIMULATION OF VORTEX CORES SWITCHING IN NANOCOLUMNAR CONDUCTING TRIPLEX STRUCTURE

Ekomasov A.E.¹, Stepanov S.V.¹, Khvalkovskiy A.V.², Zvezdin K.A.², Ekomasov E.G.¹

¹ Bashkir State University, Ufa, Russia

² Prokhorov General Physics Institute, Russian Academy of Sciences, Moscow, Russia
ekomasovae@gmail.com

One of the actual physical issues is the development of a new generation of high-speed and ergonomic electronic devices. The phenomenon of the magnetization oscillations switching and excitation in magnetic nanostructures, using the spin-polarized current of high enough density [1], will increase the speed of the hard disks and magnetic memory devices up to terahertz level. Magnetization oscillations frequency, excited using spin transfer torque, in magnetic nanostructures can be reconfigured by application of external magnetic fields and currents and used for the development of advanced radio applications. Currently great interest represents a spin-transfer nanogenerator (STNG) microwave, which significantly differs in its power output, small width and relatively large frequencies range, even without the application of external magnetic field. Most of these structures have two magnetic layers separated by a nonmagnetic interlayer.

In this paper we study the STNG, consisting of three layers (permalloy (Py) 4 nm/Cu - 10 nm/Py – 15 nm) of circular section and different diameters. The magnetizations of both magnetic layers are in the vortex state. The reference case is when two magnetic layers interact through the demagnetization fields and spin-polarized current and, thus, the system is in an external magnetic field, perpendicular to the layers plane. With the help of a software package SpinPM we conducted a numerical simulation of a bound vortex dynamics. Such dynamics various modes (damped bound oscillations of the vortex cores and their stationary dynamics) were investigated. The processes of magnetic vortexes dynamic transformation (vortex core polarity switching) are studied for currents various in size and polarization. The simulation showed that both the dynamic [3] and static [4] switching scenario are observed under various fields/currents. The switching time for the static scenario may be less than 1 ns and it can be an order of magnitude bigger for a dynamic scenario. Also a comparison of the known experimental [3,5] and numerical results was conducted.

[1] A.K. Zvezdin, K.A. Zvezdin, A.V. Khvalkovskiy, *Physics-Uspokhi*, **178**, 4 (2008) 436-442.

[2] N. Locatelli et al, *Appl. Phys. Lett.*, **98** (2011) 062501.

[3] A. V. Khvalkovskiy, A. N. Slavin, J. Grollier, et al., *Appl. Phys.Lett.*, **96** (2010) 022504.

[4] A. Thiaville, J. M. Garcia, R. Dittrich, et al., *Phys. Rev. B*, **67** (2003) 094410.

[5] N. Locatelli et al, *Appl. Phys. Lett.*, **102** (2013) 062401.

IPO-K-3

IMPEDANCE AND MAGNETOIMPEDANCE IN Mn/SiO₂/P-Si HYBRID STRUCTURES

Dorofeev N.V.^{1,2}, Bondarev I.A.^{1,2}, Tarasov A.S.¹, Volkov N.V.^{1,2}

¹ Kirensky Institute of Physics, Russian Academy of Sciences, Siberian Branch, Krasnoyarsk, 660036 Russia

² Siberian Federal University, Krasnoyarsk, 660041 Russia
bumer254@yandex.ru

At present, study of hybrid nanostructures is one of the most attractive and rapidly developed directions in spintronics. These structures represent different combinations of ferromagnetic (FM) elements and nonmagnetic semiconductors [1] and combine a huge potential of traditional semiconductor electronics with the important properties of magnetic materials that allow controlling electronic transport, manipulating an electron spin state, and using spin transport.

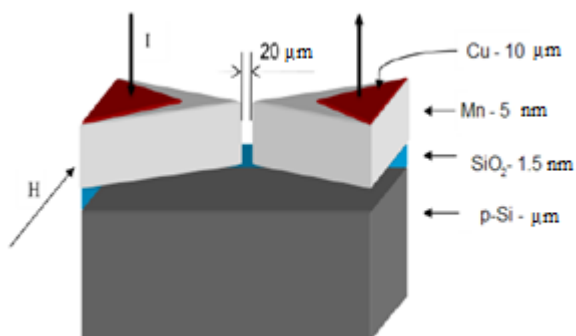


Fig. 1. Mn/SiO₂/p-Si sample structure.

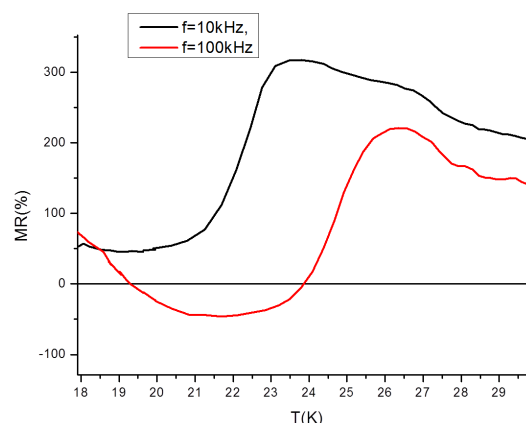


Fig. 2. Temperature dependence of magnetoresistance for the structure with the gap.

In this work, we investigate the ac transport and magnetic properties of the Mn/SiO₂/p-Si hybrid structure with the gap. The structure consists of two metal/insulator/semiconductor diodes formed by nanolithography. A 20- μ m gap was etched on the Mn film surface (Fig. 1). We measured the real and imaginary parts of the impedance in zero magnetic field and in a field of 1 T. Figure 2 shows the temperature dependence of the relative change in the real part of the impedance of the structure in a magnetic field with a frequency of 100 and 10 kHz. As the temperature is increased, magnetoresistance grows and attains its maximum value at 23 K for $f=10$ kHz and 26 K for $f=100$ kHz, and then decrease. The maximum values of magnetoresistance at frequency 10 kHz attain 300% and 200% for 100 kHz. Similar dependences were observed previously for the Al/SiO₂/p-Si and Fe/SiO₂/p-Si structures [2, 3]. We attribute the existence of the MR effect and its behavior to surface impurity centers located near the insulator/semiconductor interface.

[1] A. Fert, *Thin Solid Films*, **2-5** (2008) 517.

[2] J. J. H. M. Schoonus, et al. *PRL*, **100** (2008) 127202.

[3] N.V. Volkov, A.S. Tarasov, E.V. Eremin, et al., *J. Appl. Phys.*, **112** (2012) 123906.

IPO-K-4

OPTICALLY INDUCED MAGNETOTRANSPORT PROPERTIES OF Fe/SiO₂/P-Si AND Fe/SiO₂/N-Si HYBRID STRUCTURES

Bondarev I.A.^{1,2}, Dorofeev N.V.^{1,2}, Tarasov A.S.¹, Volkov N.V.^{1,2}

¹ Kirensky Institute of Physics, Russian Academy of Sciences, Siberian Branch, Krasnoyarsk, 660036 Russia

² Siberian Federal University, Krasnoyarsk, 660041 Russia
fbi1993@mail.ru

Hybrid nanostructures that allow manipulating the spin transport attract much attention of researchers. Application of hybrid nanostructures requires understanding such phenomena as spin injection in a semiconductor, spin diffusion, spin accumulation, etc.

One of the most interesting effects in hybrid nanostructures is the giant magnetoresistive effect (GMR). Resistivity of such structures varies with the change in the respective directions of magnetizations of the neighboring layers.

In this work, we investigate the optically induced magnetic properties of the Fe/SiO₂/p-Si and Fe/SiO₂/n-Si structures [1, 2]. In the Fe/SiO₂/p-Si structure under optical irradiation with the wavelength $\lambda = 0.98$ nm, the optically induced magnetoresistance is observed, which attains the giant values of about 10⁵% in magnetic fields of no higher than 2 kOe and the temperature $T = 15$ K. This effect is also observed in Fe/SiO₂/n-Si under the similar external factors and close temperatures; however, its maximum value is not so high (10³%). It should be noticed that the value and sign of the optically induced magnetoresistance strongly depend on bias on the device and the applied magnetic field direction (Fig. 1).

We attribute the optically induced magnetoresistance to the surface centers located near the insulator/semiconductor interface, which were previously observed by us using impedance spectroscopy [3]. The alternative explanation is the Rashba spin splitting. As was demonstrated in our previous studies, the investigated effect observed in the near-interface region can reach significant values.

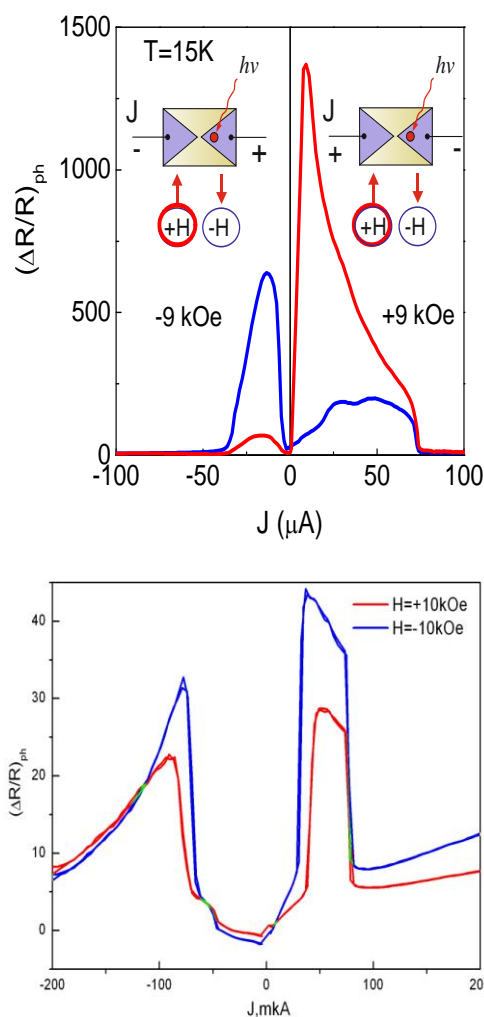


Fig. 1. Bias dependence of magnetoresistance at different magnetic field directions in (a) Fe/SiO₂/p-Si and (b) Fe/SiO₂/n-Si

[1] N.V. Volkov, R.M. Fedorishchev, A.O. Gustaitsev, I.A. Bondarev, S.N. Varnakov et al., *Book of Abstracts, EASTMAG-2013*, 15 - 21 September 2013, Russky Island, Vladivostok, Russia, p.288.

[2] N.V. Volkov, A.S. Tarasov, E.V. Eremin, F.A. Baron et al. *J.Appl.Phys.*, **114** (2013) 093903.

[3] N.V. Volkov, A.S.Tarasov, E.V.Eremin, A.V. Eremin et al. *J.Appl. Phys.*, **112** (2012) 123906.

1PO-K-5

IMPEDANCE OF THE Fe/SiO₂/N-SI HYBRID STRUCTURE IN A HIGH MAGNETIC FIELD

Gustaitsev A.O.^{1,2}, Smolyakov D.A.¹, Volkov N.V.^{1,2}

¹ Kirensky Institute of Physics, Krasnoyarsk, 660036 Russia

² Siberian Federal University, Krasnoyarsk, 660041 Russia

arthur4ik_72@mail.ru

The analysis of hybrid structures with the giant magnetoimpedance is of great importance due to their potential for application in magnetic devices.

In this work, we investigate the effect of a magnetic field on the impedance in the Fe/SiO₂/n-Si hybrid structure in the geometries with an external magnetic field perpendicular and parallel to the sample plane.

The structure was fabricated on a single-crystal Si substrate. The substrate surface was pre-cleaned by the Shiraki method. A SiO₂ layer with a thickness of 1 nm was formed on the substrate surface by chemical oxidation; on the top of this layer, a Fe layer with a thickness of 10 nm was deposited by thermal evaporation. The investigations were performed by a two-contact method. On the iron surface, strip-shaped conductive adhesive contacts were formed; on the opposite side of n-Si, an ohmic contact was formed, which was confirmed by the current-voltage characteristic. Experiments were conducted on a Physical Property Measurement System (PPMS-9) in external magnetic fields up to 9 T. The impedance was measured on an Agilent E4980A LCR meter.

The largest effect of a magnetic field on the impedance is observed in the narrow temperature range 15–30 K, where there is a peak in the temperature dependence of the real part of the impedance (Fig. 1). Under the action of an external magnetic field, this feature shifts toward higher temperatures and its amplitude increases. For the imaginary part of the impedance, the step dependence is observed, which also shifts toward higher temperatures. Similar dependences were observed for the Fe/SiO₂/p-Si structure [1–2]. Analogously to our previous studies, we attribute the magnetoimpedance effect and its behavior to surface impurity centers located near the insulator/semiconductor interface.

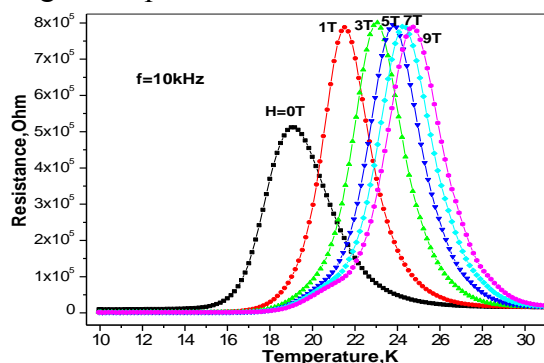


Fig. 1. Temperature dependence of the real parts of the impedance in an external magnetic field.

In magnetic fields from 1 to 9 T, the saturation is observed (Fig. 1), i.e., the peak amplitude of the real part of the impedance does not increase any more and the impedance shift slows down with increasing external magnetic field. In addition, there is a strong anisotropy of the magnetic impedance. The effect of the magnetic field directed perpendicular to the structure plane is much weaker as compared with the geometry when the field lies in the sample plane. To clarify the origin of this behavior, we need to determine the nature of the surface states and identify the mechanisms of the magnetic field effect on the energy structure. To date, these issues remain unclear.

[1] N.V. Volkov, A.S. Tarasov, E.V. Eremin, A.V. Eremin, S.N. Varnakov, S.G. Ovchinnikov, *J. Appl. Phys.*, **112** (2012).

[2] N.V. Volkov, A.S. Tarasov, E.V. Eremin, S.N. Varnakov, S.G. Ovchinnikov, S. M. Zharkov, *J. Appl. Phys.*, **109** (2011).

1PO-K-6

INFLUENCE OF STRUCTURE ON MAGNETORESISTIVITY OF (Cu+Co₄₁Fe₃₉B₂₀)_x(Cu_nO)_{100-x} COMPOSITES

Kalinin Yu.E., Kashirin M.A., Makagonov V.A., Sitnikov A.V.
Voronezh State Technical University, Voronezh, 394026, Russia
vlad_makagonov@mail.ru

The results of structure investigation and magnetoresistivity (MR) of granular nanocomposites (Cu+Co₄₁Fe₃₉B₂₀)_x(Cu_nO)_{100-x} are presented. The granular nanoclusters of pure metal or metal alloy (Cu, Co₄₁Fe₃₉B₂₀) which it is randomly distributed in a dielectric amorphous matrix Cu_nO have been obtained by ion-beam sputtering of composite targets and depositing of the material to ceramic substrates. The nanocomposites with wide and continuous concentration were formed during simultaneous deposition of metal and dielectric phases by using complicated targets.

The transmission electron microscopy (TEM) investigations of (Cu + Co₄₁Fe₃₉B₂₀)_x(Cu_nO)_{100-x} composites showed, that there is a significant change in structure with content of metallic phase. For all studied compositions the structure was granular, where the granules are crystalline copper nanoparticles (size 3-5 nm) and granules of amorphous ferromagnetic alloy Co₄₁Fe₃₉B₂₀, size and shape which depend on composition. At low concentrations of amorphous conductive phase Co₄₁Fe₃₉B₂₀ the complex heterogeneous is prevails system, where crystalline phase Cu₂O dominated as 20-50 nm clusters. At increasing of concentration Co₄₁Fe₃₉B₂₀ the grain size is increasing slightly and at the concentration of Co₄₁Fe₃₉B₂₀ about 16-20 at. % the electron diffraction reflexes from the lattice of crystalline copper are starting to appear. With further increasing of concentration ferromagnetic phase (40-55 at.% Co₄₁Fe₃₉B₂₀) TEM micrographs appears labyrinth structure from amorphous ferromagnetic particles, consisting of several (5-8) contacting granules which formed continuous conductive network within Cu_nO matrix at high concentrations.

The changing of the phase composition and the shape of ferromagnetic inclusions of investigated composites have a significant impact on the character of changes in electrical resistance at external magnetic fields. At low concentrations of amorphous ferromagnetic phase Co₄₁Fe₃₉B₂₀, when round shape granules were isolated in matrix, negative magnetoresistance due to spin-dependent tunneling of charge carriers between the grains was observed. At the concentration of amorphous ferromagnetic phase Co₄₁Fe₃₉B₂₀ more than 40 at. %, when the ferromagnetic granules formed a chain of contacting particles was appears positive component of the magnetoresistance at small magnetic field strength (E lower then 500-850 Oe), which was observed only for composites containing crystal cobalt grains. The positive component of the magnetoresistance is associated with quantitative differences in the value of the magnetic anisotropy energy of granules and clusters as well as presence of a strong dipole-dipole interaction between them.

This work was supported by the Russian Scientific Foundation (Grant N14-13-00403).

1PO-K-7

A COMPARATIVE STUDY OF CONDUCTION ELECTRON SCATTERING AT Fe/Cr AND Co/Cu INTERFACES

Lobov I.D., Kirillova M.M., Romashev L.N., Milyaev M.A., Ustinov V.V.

Institute of Metal Physics, UB RAS, 18 Kovalevskaya St., Ekaterinburg 620990, Russia
i_lobov@imp.uran.ru

The intensive study of magnetotransport properties of multilayer metal nanostructures with giant magnetoresistance (GMR) continues because of large prospects of these materials in modern electronic devices. Being an optical analogue of the giant magnetoresistance, the magnetorefractive effect (MRE) [1-3] is one of the sources of information on the magnetotransport characteristics of such nanostructures. In the present work we analyze the results of our investigation of magnetorefractive effect in two "classical" multilayer systems of Fe/Cr and Co/Cu. The similarity and differences between MRE and GMR characteristics of these nanostructures are discussed. We show that unlike the Fe/Cr system, in a Co/Cu multilayer structure we actually managed to approach the technological limit of magnetotransport characteristics underlying the GMR and MRE effects. Such a conclusion is based on the analysis of the spin-dependent scattering of conduction electrons at the Co/Cu interfaces. It is demonstrated that the parameter τ_i^{\uparrow} ($\tau_i^{\uparrow(\downarrow)}$ are the electron relaxation times) almost reaches the relaxation time of the conduction electrons in the bulk of the copper layer τ_{Cu} . The results are considered in the interrelation with the electronic structure of the ferromagnetic Co and nonmagnetic Cu. The reasons preventing obtaining similar results in the Fe/Cr system are discussed. [Fe/Cr(t_x , Å)] superlattices, $t_x=(10-23)$ Å, were grown by the method of molecular beam epitaxy using a Katun'-S ultrahigh vacuum setup. Monocrystal MgO and Al₂O₃ plates with a Cr buffer layer 80 Å thick served as substrates. The [Co/Cu(t_x , Å)] superlattices, $t_x=(8.25-27)$ Å, with a Fe buffer layer of 50 Å were obtained by magnetron sputtering onto glass in the Ulvac MPS 4000 C6 sputtering system. MRE reflection measurements were performed in *p*-polarized light using a Frontier Fourier spectrometer with a VeeMAX2 optical attachment in the wavelength range of 1.2-28 μm and the angle of incidence of light 70° in a constant magnetic field. Simulation of the spectra is carried out in the framework of [1] using a modified complex dielectric function of a multilayer structure in the intraband absorption region ε_{SAL} .

This work was supported by the RFBR, project No. 13-02-00749, the Program of the Presidium of Russian Academy of Sciences, project No. 12-P-2-1051, and the Grant of Scientific School No. 1540.2014.2.

- [1] J.C. Jacquet and T. Valet, in: E. Marinero (ed.), *Magnetic Ultrathin Films, Multilayers and Surfaces, MRS Symposia Proceedings, Pittsburgh*, **384** (1995) 477-490.
- [2] I.D. Lobov, M.M. Kirillova, A.A. Makhnev, L.N. Romashev, V.V. Ustinov, *Phys. Rev. B*, **81** (2010) 134436.
- [3] I.D. Lobov, M.M. Kirillova, L.N. Romashev, M.A. Milyaev, and V.V. Ustinov, *The Physics of Metals and Metallography*, **113** (2012) 1153–1161.

1PO-K-8

BIAS-CONTROLLED MAGNETOIMPEDANCE EFFECT IN A MIS STRUCTURE

Smolyakov D.A.¹, Gustaitsev A.O.¹, Volkov N.V.^{1,2}

¹ Kirensky Institute of Physics, Krasnoyarsk, 660036 Russia

² Siberian Federal University, Krasnoyarsk, 660041 Russia

berkut-breaker@rambler.ru

At present, it is urgent to search for the systems that exhibit the giant magnetoimpedance effect because of their potential for application in magnetoelectronic devices. Here, we demonstrate this effect on the Fe/SiO₂/n-Si hybrid structure.

The structure is a ferromagnetic metal/insulator/semiconductor (MIS) diode with the Schottky barrier. The sample was prepared on a single-crystal Si substrate. The substrate's surface was pre-cleaned by the Shiraki method. A SiO₂ layer with a thickness of 1 nm was formed on the substrate's surface by a chemical method. An iron film with a thickness of 10 nm was deposited by thermal evaporation. The investigations were performed by a two-probe method. Contacts were formed on the iron film and the bottom of the n-Si(100) substrate.

The strong effect of a magnetic field on the impedance of the structure was found in the temperature range 10–30 K, where an intense peak of the real part of the impedance (Fig. 1a) and a step in the behavior of its imaginary part (Fig. 1b) are observed in the temperature dependence. The effect of a magnetic field on the temperature dependences of the impedance manifests itself as a shift of the peak in the real part and the step of the imaginary part of the impedance. In addition, at an applied voltage of 5 V the peak in the real part and the step in the imaginary part of the impedance shift toward lower temperatures by the same value with and without magnetic field. When a voltage of –5 V is applied, no effect of the temperature dependence of the impedance is observed.

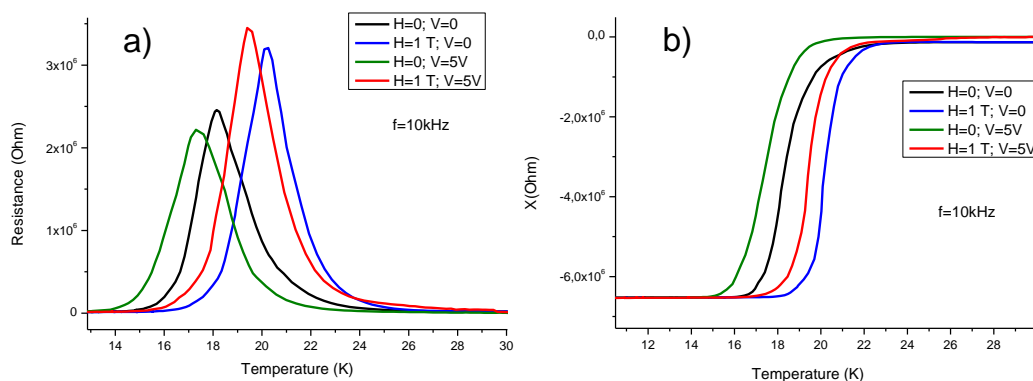


Fig. 1. Temperature dependence of the real and imaginary parts of the impedance

The magnetoimpedance effect is explained by the presence of surface states at the SiO₂/n-Si interface [1–3] that participate in recharging under the action of a varying voltage applied to the structure. The levels of the surface states are shifted by an applied magnetic field. However, a value of the bias can affect the probability of electron tunneling between the surface states and a ferromagnetic electrode.

[1] N.V. Volkov, A.S. Tarasov, E.V. Eremin, A.V. Eremin, et al. *J. Appl. Phys.*, **112** (2012).

[2] N.V. Volkov, A.S. Tarasov, E.V. Eremin, S.N. Varnakov, et al. *J. Appl. Phys.*, **109** (2011).

[3] N.V. Volkov, A.S. Tarasov, E.V. Eremin, F.A. Baron, et al., *J. Appl. Phys.*, **114** (2013).

1PO-K-9

PECULIARITIES OF TRANSPORT, RESONANCE AND OPTICAL PROPERTIES OF THE ANION-SUBSTITUTED CHALCOGENIDES MANGANESE

Romanova O.B.^{1,2}, *Aplesnin S.S.*^{1,2}, *Vorotynov A.M.*¹, *Makovetskii G.I.*³, *Demidenko O.F.*³, *Yanushkevich K.I.*³

¹ L.V. Kirensky Institute of Physics, Siberian Branch of the Russian Academy of Sciences, Krasnoyarsk, Russia

² Siberian State Aerospace University, Krasnoyarsk, Russia

³ GO NPTs Materials Science Center, National Academy of Sciences of Belarus, Minsk, Belarus
rob@iph.krasn.ru

Magnetic semiconductors, undergoes a phase transition metal-insulator (MIT) and possessing magnetoresistance effect are perspective materials for spintronics and microelectronics. Such compounds include anion - substituted solid solutions $\text{MnSe}_{1-x}\text{Te}_x$ with concentration of substitution ($0.1 \leq X \leq 0.4$) in the space group of the structure $Fm\bar{3}m(225)$ characteristic of manganese monoselenide [1]. Chalcogenides $\text{MnSe}_{1-x}\text{Te}_x$ is antiferromagnetic and have conductivity type semiconductor. From the temperature dependence of the resistivity is determined the activation energy $\Delta E \approx (0.07-0.09)$ eV, which is almost independent of the composition of these samples and the order of magnitude smaller band gap. The volume of hexagonal phase and magnitude of the electrical resistivity is decreased with increasing concentration of tellurium substitution. The effect of a magnetic field on magnetotransport properties get to a maximum value of 100% in the vicinity of the Neel temperature for $X = 0.1$. Two regions in the temperature dependence of the dielectric permittivity can be distinguished. A small maximum is observed in the magnetic phase transition at T_N and a sharp increase in the values of dielectric permittivity at ~ 260 K, which correlates with the measurements of the magnetic and structural properties. The inhomogeneity of the magnetic system and the mechanism of magnetic moment relaxation have been investigated by the electron paramagnetic resonance (EPR). For $X = 0.2$ g-factor is almost independent of temperature and takes a value of the order of $g \approx 2,03$ and for $X = 0,4$ g-factor increases from 1.95 to 2.05 in the temperature range of $120 \text{ K} < T < 220 \text{ K}$. EPR intensity go up an order of magnitude with increasing tellurium concentration. Influence of anionic substitution on the electronic structure was investigated by optical methods at room temperature in the range of energy $1000 \text{ cm}^{-1}-10\,000 \text{ cm}^{-1}$ as shown in fig.1. Energy corresponding to absorption maxima is attributed to the width of the forbidden band. Near the bottom of the conduction band are observed additional absorption maxima located at energies below the conduction band. Perhaps these lines correspond to the bound states of electrons and holes and form a exciton spectrum.

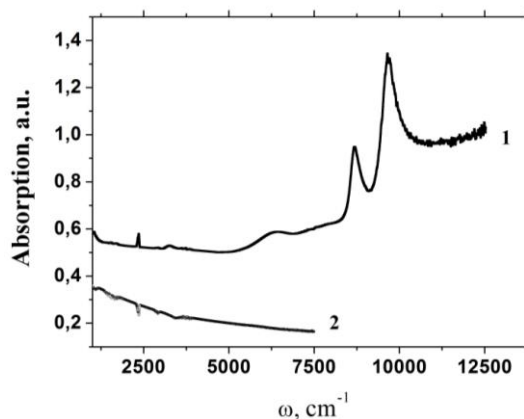


Fig.1. Absorption intensity for solid solutions $\text{MnSe}_{1-x}\text{Te}_x$ with $X = 0.4$ (1) 0.2 (2) depends on the frequency at $T = 300 \text{ K}$.

Support by RFBR projects 12-02-00125-a, 14-02-90010_Bel_a.

[1] S.S. Aplesnin, O.B. Romanova, M.V. Gorev et al., *FTT*, **54** (2012) 1296-1301.

IPO-K-10

STRUCTURAL, MAGNETIC AND ELECTRIC TRANSPORT PROPERTIES FOR $\text{Co}_2\text{FeAl}_{0.5}\text{Si}_{0.5}/\text{n-GaAs}$ JUNCTIONS

Tezuka N.¹, Saito T.¹, Matsuura M.¹, Sugimoto S.¹

¹ Dptm. of materials Science, Graduate School of Engineering, Tohoku University, Sendai, Japan
tezuka@material.tohoku.ac.jp

High efficient spin injection into semiconductor (SC) from ferromagnet (FM) is required to realize spintronics devices such as spin MOSFETs. High spin injection efficiency, however, has not been achieved because of conductivity mismatch[1]. To improve the spin injection efficiency, high spin-polarized spin injector and elimination of conductivity mismatch between FM and SC using tunnel barrier are effective[2]. $\text{Co}_2\text{FeAl}_{0.5}\text{Si}_{0.5}$ full-Heusler alloy (CFAS) is one of the attractive spin injector, because CFAS fabricated by MBE also showed high spin polarization by tunnel magnetoresistance measurement. In addition, Schottky tunnel barrier formed at the interface between CFAS and SC is expected to eliminate the conductivity mismatch. GaAs has close lattice constant to CFAS. Thus, CFAS deposited on GaAs substrates is expected to be a highly spin polarized injector or detector. In our previous results, spin signals from CFAS to n-GaAs were reported by three terminal Hanle, four terminal non-local, and two terminal local measurements[3]. It was found the dependence of spin signals on substrate temperature (T_{CFAS}) during deposition of CFAS on GaAs were different from these measurements, however, this origin was unclear. In this study, structural, magnetic and electrical properties for CFAS/n-GaAs were investigated and discuss the origin of spin signals in conjunction with these parameter.

The n-GaAs doped layer and CFAS thin films were deposited by MBE. The structure was analyzed by in situ RHEED, TEM and XRD after Ta sputtering. The magnetic properties were analyzed by VSM. The CFAS/GaAs junctions were fabricated by EB lithography and Ar ion milling. The electric transport properties were measured by four probe method.

From RHEED pattern and cross sectional TEM image of thin CFAS films, CFAS films found to be grown epitaxially on GaAs, and shown $L2_1$ -ordered structure for the films with $T_{\text{CFAS}} = 300^\circ\text{C}$ and 400°C . It is hard to find some additional phase around the interface between CFAS and GaAs. Magnetic moment (and magnetic anisotropy energy) of CFAS increased (and decreased) with increasing T_{CFAS} up to 300°C and decreased (and increased) at T_{CFAS} of 400°C , respectively. From the results of magnetic properties, the degree of ordering structure was increased with T_{CFAS} , however, the CFAS with T_{CFAS} of 400°C would have the contamination of Ga or As. In fig. 1, it was observed clear relationship between T_{CFAS} dependence of spin signal obtained by 4T non-local measurement and that of magnetic moment or magnetic anisotropy field.

This work was partly supported by the Asahi Glass Foundation, Grants-in-Aid for Scientific Research (B) and (S), and the Strategic Japanese-German Joint Research Program ASPIMATT from JST.

[1] G. Schmidt, D. Ferrand, L. Molenkamp, A. Filip, B. van Wees, *Phys. Rev. B*, **62** (2000) R4790.

[2] Fert and H. Jaffres, *Phys. Rev. B*, **64** (2001) 184420.

[3] T. Saito, N. Tezuka, M. Matsuura, S. Sugimoto, *IEEE Trans. Magn.*, **49** (2013) 4327; T. Saito, N. Tezuka, M. Matsuura, S. Sugimoto, *Jpn. J. Appl. Phys.*, **52** (2013) 063001.

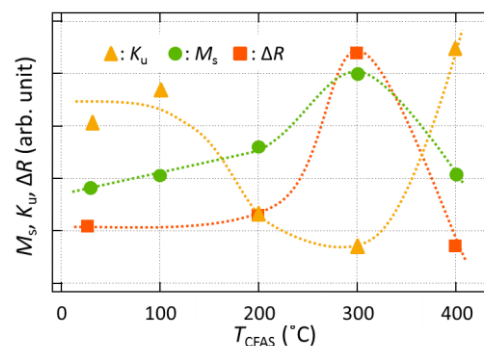


Fig. 1. T_{CFAS} dependence of spin signal, magnetic moment and magnetic anisotropy field for CFAS/n-GaAs.

IPO-K-11

MAGNETOTRANSPORT PROPERTIES OF CATION-SUBSTITUTED SULPHIDES $V_xMn_{1-x}S$

Ryabinkina L.I.¹, Romanova O.B.¹, Kisilev N.I.¹

¹ Kirensky Institute of Physics, Russian Academy of Sciences, Siberian Branch, 660036 Krasnoyarsk, Russia
rob@iph.krasn.ru

Reported the results of studies on the structural, electrical and magnetoelectric properties of cation-substituted sulphides $V_xMn_{1-x}S$ ($X = 0.45$), created on the basis of the antiferromagnetic semiconductor α -MnS. Investigations were carried out in the temperature interval 77-300K and magnetic fields up to 21 kOe to determine metal-insulator transition (MIT) and colossal magnetoresistance (CMR) in the new sulphide compounds and study the influence of magnetic field on the electronic structure [1]. Samples synthesized by ceramic technology and ampoule method of pure elements V, Mn, S and according to X-ray analysis is a solid solution of fcc α -MnS (structure of NaCl).

Compounds $V_{0.45}Mn_{0.55}S$ is an antiferromagnetic ($T_N = 130K$) and has a semiconductor-type conductivity with an activation energy $\Delta E = 0.02$ eV. In the area 180K a transition from semiconductor to semimetallic conductivity type, this is accompanied by changes in the magnetic properties and structure.

The study magnetoresistive properties sulfide $V_{0.45}Mn_{0.55}S$ found magnetoresistance ($\delta_H = (\rho_H - \rho_0)/\rho_0$) temperature dependence of magnitude and sign depend on the magnetic field. In a field $H = 5kOe$ magnetoresistance effect δ_H is positive at all temperatures. With increasing magnitude of the field, a change of sign to negative magnetoresistance δ_H in the 100-180K, and in a field $H = 10$ kOe ($\delta_H = -5\%$), decreasing with increasing field ($\delta_H = -2,5\%$ in the field $H = 21$ kOe). Below 100K and above 200K CMR effect is positive for all fields. Calculations of the magnetic phase diagram and magnetization measurements allow to make the assumption that one of the possible mechanisms of the observed effect CMR in magnetic semiconductors $V_xMn_{1-x}S$ can be magnetic and electronic phase separation [2] that is education system, the coexistence of ferromagnetic and antiferromagnetic semiconductor metal region (ferrons).

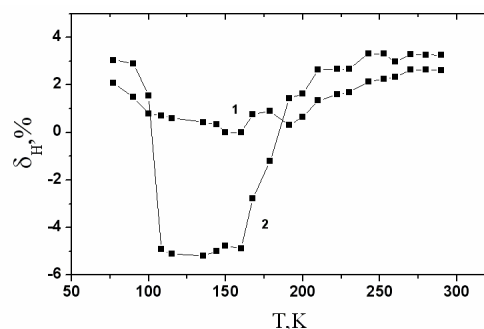


Fig. 1 Temperature dependence of the magnetoresistance δ_H fields 5 (1) и 10 (2) kOe for sample $V_{0.45}Mn_{0.55}S$

- [1] L.I. Ryabinkina, O.B. Romanova, S.S. Aplesnin, *Izvestiya RAN, Seriya Fiz.*, **8** (2008) 1115 – 1117.
[2] E. L. Nagaev, *UFN*, **166** (1996) 796-857.

IPO-K-12

TEMPERATURE DEPENDENCIES OF IMPEDANCE OF THE ELASTICALLY DEFORMED AMORPHOUS FERROMAGNETIC RIBBONS WITH POLIMER COVERING

Semirov A.V.^{1}, Derevyanko M.S.¹, Bukreev D.A.¹, Moiseev A.A.¹, Safronov A.P.², Kurlyandskaya G.V.^{2,3}*

¹ East-Siberian State Academy of Education, Irkutsk, Russia,

² Ural Federal University, Yekaterinburg, Russia

³ University of the Basque Country UPV-EHU, Campus of Leioa, Leioa, Spain

* semirov@igpu.ru

Recently, soft magnetic conductors with multifunctional polymer covering has been attracted much attention. Polymer films deposited onto the surface of magnetic sensitive element coverings can play protective or/and magnetoactive roles changing functional properties of magnetic component. In this work magnetic properties and an impedance of polymer /Fe₅Co₇₅Si₄B₁₆ amorphous ribbon based composites were studied in a wide range of the temperatures (165 – 390 K) and applied tensile forces (0 – 40 N). Fe₅Co₇₅Si₄B₁₆ samples having low magnetostriction $\lambda \sim 10^{-7}$ and saturation magnetization of 0.5 T had 3 cm × 2.7 mm × 33 μm dimensions. Two types of the samples were comparatively analyzed: with polymer covering and without it (Fig. 1.). Two selected types of polymer solutions were used for the formation of the surface top and bottom layers by casting at room temperature: BMR (copolymer solution of butyl methacrylate and methacrylic acid in isopropanol) and KO (solution of polymethylphenyl resin in toluene). All polymer films showed good adhesion. One of the basic aspects determining operational properties of magnetoimpedance transducers is response of their sensitive elements on external stresses. Tensile stress can significantly change the temperature dependence of an impedance relative change $(\Delta Z/Z)_T = 100\% \times (Z_T - Z_{Tmin})/Z_{Tmin}$, where Z_T – the ribbon's impedance at a temperature T , a Z_{Tmin} – the ribbon's impedance at the minimum temperature T_{min} . It can be seen that the impedance of the investigated ribbons monotonously increases with temperature increase with no tensile stress (Fig. 1. a). An application of the tensile stress leads to a change of the type of the impedance temperature dependence (Fig. 1. b). The features of this dependence are defined not only by a temperature dependence of magnetoelastic properties of the amorphous material but also by type of the polymer covering.

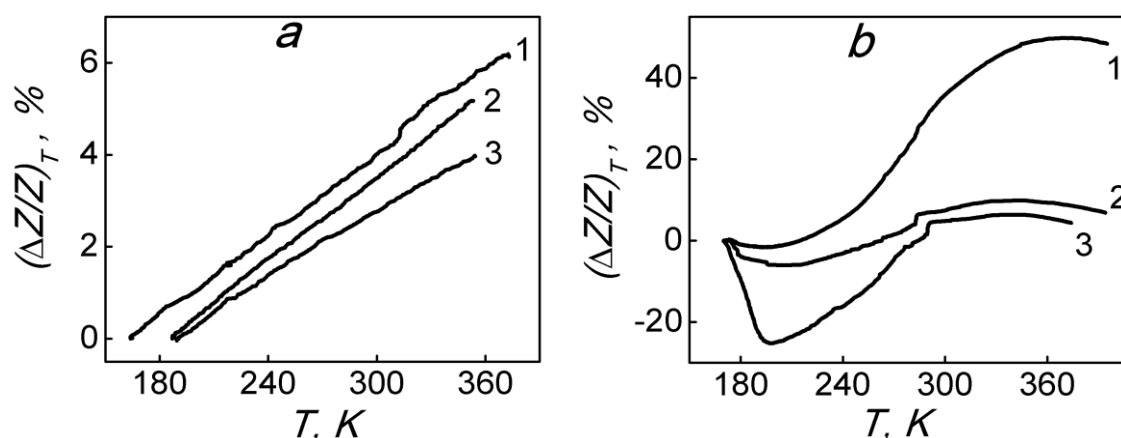


Fig. 1. Temperature dependencies of $(\Delta Z/Z)_T$ derived at the alternating current frequency of 10 MHz without (a) and with (b) applied tensile stress of 24 N. 1 – As-cast Fe₅Co₇₅Si₄B₁₆ ribbon, 2 – ribbon with BMR covering, 3 – ribbon with KO covering.

IPO-K-13

DOMAIN WALL DISPLACEMENT BY REMOTE SPIN-CURRENT INJECTION

Skirdkov P.N.^{1,2}, Zvezdin K.A.^{1,2}, Belanovsky A.D.^{1,2}, Grollier J.³, Cros V.³,
Ross C.A.⁴, Zvezdin A.K.^{1,2}

¹ A.M. Prokhorov General Physics Institute, Russian Academy of Sciences, Moscow, Russia

² Moscow Institute of Physics and Technology, Dolgoprudny, Russia

³ Unite Mixte de Physique CNRS/Thales and Universite Paris-Sud 11, Palaiseau, France

⁴ Massachusetts Institute of Technology, Cambridge, USA

petr.skirdkov@phystech.edu

Magnetic nano-constraints have attracted much attention in the last decade. The study of domain wall (DW) dynamics in magnetic nanostripes is especially interesting in this area because of both fundamental and applied motivations. Initially, it was proposed to control DW dynamics by magnetic field. However, this approach is hardly suitable for close-packed arrays of nanoscale devices due to significantly not local influence of the magnetic field. An alternative, that doesn't have this disadvantage, is to use current-induced domain wall motion that has been the subject of many experimental and theoretical researches. Most often the studied nanostructures are formed by a long and narrow magnetic film (nanostrip) containing the domain wall. For this geometry, there are two possible direction of the spin-polarized current: current-in-plane (CIP) and current perpendicular to the plane (CPP). Recent theoretical [1] and experimental [2] studies show that CPP configuration demonstrates the velocities of the domain wall up to two orders larger than those of the CIP case with the same applied current densities. The drawback of such configuration is very high electric currents required for efficient DW dynamic control, caused by the large cross-section of the CPP contact. Here we propose a new mechanism of remote CPP spin-current injection for DW dynamics excitation that can help to solve this issue.

We investigate numerically a long and narrow magnetic nanostripe with a single domain wall (DW). The spin-polarized current is injected perpendicular to the plane through a small contact which is located at certain distance from the domain wall initial position. We have demonstrated the possibility of spin current induced domain wall motion in this configuration [3]. DW dynamical characteristics are obtained using numerical solution of the LLG equation. We demonstrate that DW dynamics can be excited by very low remote CPP spin-polarized current (about 50 μ A), in contrast to the case when the current flows through the entire sample.

We have shown that the DW dynamics in this case is induced by indirect spin-torque, created by a remote spin-current injection, which is transferred then to the DW by the exchange-spring mechanism. The analytical description of this effect based on the soliton perturbation theory was proposed. Although this mechanism of DW dynamics excitation can be used by itself, it can also be effectively used to depin a DW, when magnetization dynamics is driven by less effective methods (e.g. in-plane current injection). On this basis, the remotely localized contact injection of CPP spin-polarized current becomes a very promising option for practical applications, such as racetrack memory, magnetic logic and neuromorphic devices.

Financial support by the RFBR Grants No. 12-02-01187 and No. 14-02-31781 and Skolkovo Inst. of Technology.

[1] A.V. Khvalkovskiy et al, *Phys. Rev. Lett.*, **102** (2009) 067206.

[2] A. Chanthbouala et al, *Nature Physics*, **7** (2011) 626–630.

[3] P.N. Skirdkov et al., arXiv:1311.0229 (2013).

IPO-K-14

HALL EFFECT IN $\text{Mn}_{1-x}\text{Fe}_x\text{Si}$ SOLID SOLUTIONS

Lobanova I.I.^{1,2}, *Demishev S.V.*², *Glushkov V.V.*^{1,2}, *Ivanov V.Yu.*², *Sluchanko N.E.*², *Chubova N.M.*³,
*Grigoriev S.V.*³

¹ Moscow Institute of Physics and Technology, Dolgoprudny, 141700, Russia

² Prokhorov General Physics Institute of RAS, Moscow, 119991, Russia

³ Konstantinov Petersburg Nuclear Physics Institute, Gatchina, 188300, Russia
innalobanova22@gmail.com

Strongly correlated chiral electron system MnSi recently attracted special attention due to the formation of magnetic nanovortices-skyrmions [1], observation of topological Hall effect in the vortex phase [2] and specific quantum critical scenario under high pressure [3]. In the case of $\text{Mn}_{1-x}\text{Fe}_x\text{Si}$ isostructural solid solutions it has been shown that substitution of Mn with Fe induces two quantum phase transitions, occurring at concentrations $x^* \sim 0.11$ and $x_c \sim 0.24$ and corresponding to suppression of the magnetic phases with long-range and short-range ordering, respectively [4]. In the present work we are aimed at the study of Hall effect in $\text{Mn}_{1-x}\text{Fe}_x\text{Si}$ ($x < 0.3$) system.

To understand the effect of doping we have probed the paramagnetic and spin-polarized phases [5] by resistivity ρ , Hall resistivity ρ_H and magnetization M measurements are carried out at 2-60 K in magnetic fields $B \leq 5$ T. The Hall resistivity ρ_H is shown to be determined by two contributions $\rho_H = R_H B + 4\pi M R_A$, where R_H and R_A denote ordinary and anomalous Hall coefficients [6]. The analysis of the experimental data (Fig.1) reveals that a good approximation could be obtained by assuming $R_A = S_1 \rho$, where S_1 is temperature-independent coefficient. At $T = 4.2$ K the parameter S_1 is found to increase almost linearly with x from $8 \cdot 10^{-7} \text{ G}^{-1}$ ($x=0$) to $5.3 \cdot 10^{-6} \text{ G}^{-1}$ ($x=0.29$). The observed behavior of R_A indicates the skew scattering of charge carriers [6] to be the main factor contributing to the anomalous Hall effect in $\text{Mn}_{1-x}\text{Fe}_x\text{Si}$ system.

Concerning the ordinary Hall coefficient, it is found that R_H is positive for all concentrations but two quantum critical points x^* and x_c . Interesting that absolute values of R_H and carriers mobility μ_H show weak dependence on the iron concentration for $x > 0.05$ staying at the average values $|R_H| \sim 1.03 \cdot 10^{-5} \text{ cm}^3 \cdot \text{C}^{-1}$ and $|\mu_H| \sim 0.5 \text{ cm}^2 \cdot \text{V}^{-1} \cdot \text{s}^{-1}$. The finding that R_H becomes negative only for critical concentrations x^* and x_c points to the non-trivial relation Hall effect anomalies and quantum criticality in $\text{Mn}_{1-x}\text{Fe}_x\text{Si}$ isostructural solid solutions.

This work was supported by The Programme of Russian Academy of Sciences “Strongly correlated electrons” and by RFBR grant 13-02-00160.

- [1] Tonomura et al., *Nano Lett.* **12** (2012) 1673.
 [2] Neubauer et al., *Phys. Rev. Lett.* **102** (2009) 186602.
 [3] D. Belitz et al., *Phys. Rev. Lett.* **94** (2005) 247205.
 [4] S.V. Demishev, et al., *JETP Letters*, **98** (2013) 933.
 [5] S.V. Demishev et al., *Phys. Rev. B* **85** (2012) 045131.
 [6] N. Nagaosa et al., *Rev. Mod. Phys.* **82** (2010) 2, 1539-1592.

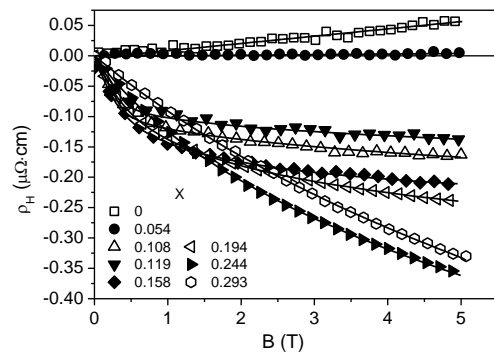


Fig.1 Hall resistivity $\rho_H(B)$ for $\text{Mn}_{1-x}\text{Fe}_x\text{Si}$ solid solutions at $T = 4.2$ K. Solid lines are the fits by the equation $\rho_H = R_H \cdot B + S_1 \cdot \rho \cdot M$ (see text)

1PO-K-15

MAGNETOIMPEDANCE OF THE Fe/SiO₂/N-Si HYBRID STRUCTURE UNDER OPTICAL IRRADIATION

Tarasov A.S.¹, Smolyakov D.A.¹, Bondarev I.A.¹, Volkov N.V.^{1,2}

¹ L.V. Kirensky Institute of Physics, Russian Academy of Sciences, Siberian Branch, Krasnoyarsk, 660036 Russia

² Siberian Federal University, Institute of Engineering Physics and Radio Electronics, Krasnoyarsk, 660041 Russia
taras@iph.krasn.ru

Hybrid nanostructures attract much attention of researches due to the combination of the magnetic and semiconductor properties. The use of the magnetic materials allows electron transport to be controlled via the spin state of electrons. At the same time, modern semiconductor technologies make it possible to control many parameters, such as concentration, mobility, and lifetime of charge carriers, and conductivity. An effective tool for governing the semiconductor properties is optical radiation.

Previously, we studied the dc effect of optically induced giant magnetoresistance [1] and magnetoimpedance in ferromagnetic metal/insulator/semiconductor hybrid structures [2]. Here, we explore the effect of optical irradiation on the magnetoimpedance of the Fe/SiO₂/n-Si hybrid structure.

A diode prepared in a special manner from the Fe/SiO₂/n-Si hybrid structure was irradiated by an IR semiconductor laser with the wavelength $\lambda = 0.98 \mu\text{m}$. The real and imaginary parts of the impedance were directly measured in zero magnetic field and in a field of $\pm 6 \text{ kOe}$. Figure 1 shows temperature dependences of the real part of the impedance $\text{Re}(Z)$ at different frequencies of an alternating current without magnetic field. Comparison with the previous results [1, 2] shows that dc and low frequencies ac the temperature dependences under irradiation are analogous, while at high frequencies there is an impedance peak similar to that observed without optical irradiation. Thus, we may conclude that the growth of the ac frequency reduces the optical irradiation effect on the transport properties of the hybrid structure. The same conclusion is valid for the optically induced magnetoresistance $\text{MRe}(Z)$ illustrated in Fig. 2.

This study was supported by the Russian Foundation for Basic Research, projects nos. 14-02-31156 and 14-02-00234.

[1] N.V. Volkov, A.S. Tarasov, E.V. Eremin, et al., *J. Appl. Phys.* **114** (2013) 093903.

[2] N.V. Volkov, A.S. Tarasov, E.V. Eremin, et al., *J. Appl. Phys.* **112** (2012) 123906.

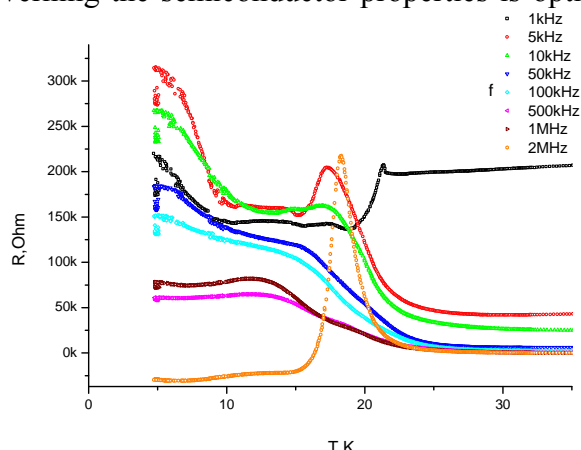


Fig. 1. Temperature dependences of $\text{Re}(Z)$ for set of frequencies

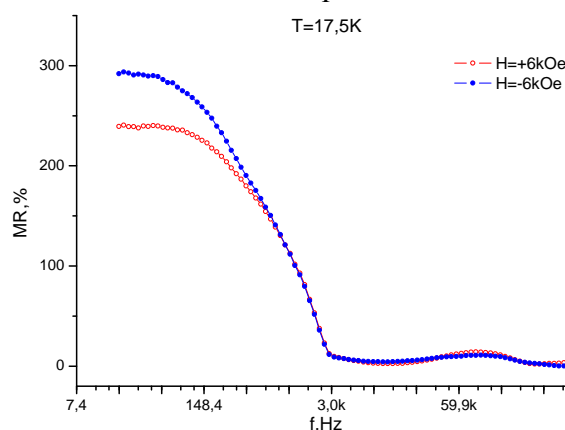


Fig. 2. Frequency dependences of $\text{MRe}(Z)$ for $H = \pm 6 \text{ kOe}$

1PO-K-16

THE RADIATION OF NEGATIVE SPIN-TEMPERATURE ELECTRONS INJECTED INTO MAGNETIC JUNCTION

Chigarev S.G.¹, Gulyaev Yu.V.¹, Mikhailov G.M.², Vilkov E.A.¹, Zilberman P.E.¹

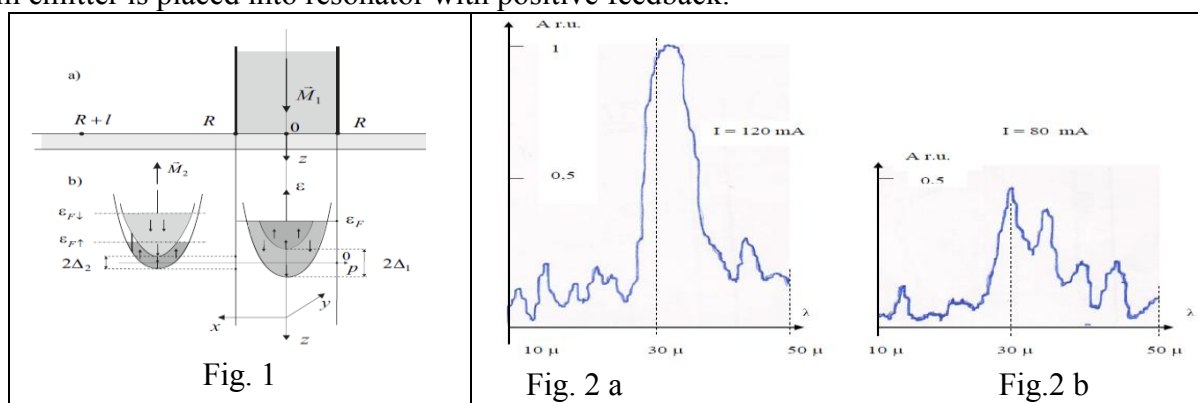
¹ Kotelnikov V.A. IRE RAS, Moscow – Fryazino, RF

² IPTM & High Purity Materials RAS, Chernogolovka, RF

Structures including ferromagnetic (FM), antiferromagnetic (AFM) and nonmagnetic metal layers may emit terahertz (THz) radiation through by spin-subband transitions of injected electrons with negative spin-temperature. We report here some new results concerning terahertz radiation recently revealed experimentally in magnetic nanojunctions [1].

Scheme of the experiment is presented in fig. 1a. Magnetically hard FM rod with diameter of few 10μ makes an electrical contact with a thin magnetic film of 10 nm thickness. Magnetic films may consist of soft FM (Py, Fe, magnetite and other) or AFM (FeMn, IrMn). Spin-polarized current flowing between the FM rod and magnetic film injects nonequilibrium electrons into the magnetic film and causes imbalance in spin-subbands electron population with different quasi-Fermi levels $\varepsilon_{F\downarrow}$ and $\varepsilon_{F\uparrow}$ (fig.1b). The spin relaxation is neglected in the vicinity of the rod on the distances equaled to a spin diffusion length ($\sim 20\text{-}30$ nm in FM), where quasi-Fermi level of more populated spin subzone is higher in energy. By this new mechanism, it establishes a negative spin temperature in this part of the magnetic film. The observed radiation is explained as quantum transitions between energy levels mainly laying between $\frac{2\Delta_1}{2}$ and $\varepsilon_{F\uparrow}$. One of these transitions is shown in fig. 1b by vertical solid line. We denote $2\Delta_{1,2} = 2\alpha\mu_B\mathbf{M}_{1,2} \cdot \hat{\mathbf{z}}$ as subzone separation for electrons inside and outside of the rod, $\alpha \sim 10^4$ is a dimensionless sd-exchange constant, μ_B is Bohr magneton and $|\hat{\mathbf{z}}|=1$.

The experimentally observed radiation spectra are shown in fig. 2a,b in case of the rod-magnetic film emitter is placed into resonator with positive feedback.



Under larger current (I), the single-mode radiation is observed that revealed as the dominant pick in Fig. 2a contrary to multi-modes radiation under lower current (Fig. 2b). We believe this result demonstrates the realization of terahertz wave stimulated radiation of the laser type. If so, such radiator acts as a quantum oscillator and may be analogously called “twaser”.

The work was supported by KIAS-RFBR grant # 13 - 02 - 12427.

[1] Yu. V. Gulyaev, P. E. Zilberman, I. V. Malikov, G. M. Mikhailov, A. I. Panas, S. G. Chigarev, E. M. Epshtein, *JETP Letters*, **93** (2011) 259-263.

1PO-K-17

THERMOELECTRIC POWER OF GRADIENT Fe-AL₂O_n COMPOSITE FILMS

Al-Maliki A.J.^{1,2}, Stognei O.V.², Sitnikov A.V.², Makagonov V.A.²

¹Basra University, Basra, Irak

²Voronezh State Technical University, Voronezh, Russia
sto@sci.vrn.ru

Composite concentration-gradient Fe-Al₂O_n films have been investigated. The studied samples were thin films deposited on the pyroceramics substrate. The samples size was 40 mm x 3 mm x 5 mkm. All samples were prepared by ion beam sputtering of a composite target in an argon atmosphere. The gradient of Fe concentration along the long axis of the samples was created by using of highly asymmetric configuration of the sputtering target [1]. Together with the gradient samples the homogeneous Fe-Al₂O_n composite samples with constant composition along the long axis were investigated (these samples were the referent ones). The electric and thermoelectric properties of the gradient and homogeneous composite samples have been investigated. The thermoelectric power was measured by the hot probe method. The temperature gradient was approximately 78 degrees (22 and 100 °C) over a distance of 40 mm. Totally 62 gradient samples were prepared and investigated. Each of the samples had a serial number, which was proportional to the average concentration of iron in the composite. Some gradient samples have the percolating threshold in their middle part (concentration of one end of these samples is before the threshold, concentration of another end lies behind the threshold).

The dependence of the thermoelectric power on the iron concentration in Fe-Al₂O_n composites, as well as the dependence of the thermo-power against the direction of the temperature gradient along the sample have been measured. For homogeneous samples the direction of the temperature gradient does not affect on the value of thermoelectric power, which is quite evident (fig. 1, a). Maximum values were observed in the pre-percolation region (32 - 36 at.% Fe). In gradient samples the thermo-power hysteresis was observed (fig. 1, b). In the case where the temperature gradient was oriented to the high resistance end of the sample (the region which is before the percolating threshold was heated) value of thermoelectric power was larger than in the opposite direction of the temperature gradient (fig. 1, b). The hysteresis is observed in the gradient samples which contain the percolation threshold.

Support by RSF (grant № 14-13-00403) is acknowledged.

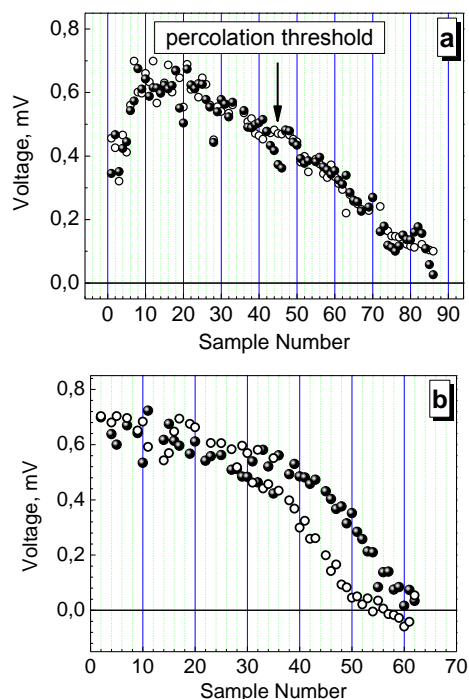


Fig. 1 Thermopower vs sample number and direction of temperature gradient for homogeneous and gradient Fe-Al₂O_n samples. Different symbols (○ and ●) indicate different gradient direction.

[1] O.V. Stognei et al. *Herald of Voronezh State Technical University* **10**, 1 (2014) 7-11.

IPO-K-18

BIFURCATIONS IN THE DYNAMICAL SYSTEM FOR THREE-LAYERED MAGNETIC VALVE

Ostrovskaya N.V.¹, Skidanov V.A.^{1,2}, Iusipova I.A.²

¹Institute for Design Problems in Microelectronics RAS, Sovetskaya street, 3, Zelenograd, Moscow, Russia, 124365

²National Research University of Electronic Technology, Solnechnaya Alleya 5, Zelenograd, Moscow, Russia, 124498
n.ost@russia.ru

Magnetization dynamics in a three-layered nanopillar Co/Cu/Co structure with one fixed and one free layer driven by external magnetic field H_{external} and spin-polarized electric current J_{inject} [1] was investigated using methods of the theory of bifurcations. Mathematical model is based on the Landau-Lifshits-Gilbert equations with the current term in the Slonczewski–Berger form. Orientation of applied magnetic field was considered to be parallel to the anisotropy axis. Physical model included the magnetocrystalline anisotropy field and the demagnetizing field. Because of small size of the structure the space dependence of magnetization usually is not taken into account in such a model, so the resulting system of equations has the form of the nonlinear dynamical system with the polynomial right sides. The phase space of the system is a unit sphere with two singular points $T_1 (+1,0,0)$, $T_2 (-1,0,0)$ that exist at any value of current and field. The bifurcation diagrams for these points are presented in Fig. 1, where h and j are dimensionless values of magnetic field and current density. In SI $h = H_{\text{external}}/M_s$ and $j = J_{\text{inject}} \hbar / (\mu_0 M_s^2 |e| d)$, where μ_0 is vacuum permeability, M_s is the saturation magnetization, e is the electron charge, \hbar is the Planck constant, d is the thickness of the free layer. Besides the points $T_1 (+1,0,0)$, $T_2 (-1,0,0)$, several additional singular points appear and disappear depending on the actual values of current and field. The corresponding bifurcation diagram was built.

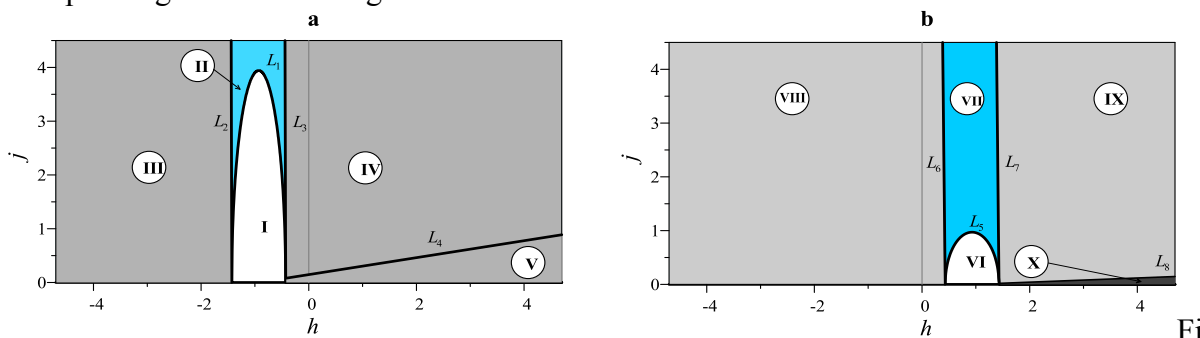


Fig. 1. Bifurcations of equilibrium points $T_1(+1,0,0)$ (a) and $T_2(-1,0,0)$ (b) depending on values of external field h and spin-polarized current j — a: region I — saddle, region II — unstable node, regions III and IV — unstable focus, region V — stable focus; b: region VI — saddle, VII — stable node, VIII and IX — stable focus, X — unstable focus. The calculations were made for cobalt with the parameter $d = 5$ nm.

Mathematical simulation of magnetization dynamics for several typical values of field and current was performed. The numerical experiments revealed the features of switching process in more detail.

[1] J.C. Slonczewski, *JMMM*, **159** (1996) L1.

IPO-K-19

TUNNEL MAGNETORESISTANCE IN ASYMMETRIC PLANAR DOUBLE-BARRIER MAGNETIC TUNNEL JUNCTIONS

Petukhov D.A., Useinov N.Kh., Tagirov L.R.

Kazan Federal University, Kazan, Russia

dapetukhov@mail.ru

Currently, layered magnetic nanostructures FM/I (ferromagnet/insulator) is one of the most exciting and rapidly developing areas of spintronics. Effects of tunneling magnetoresistance and magnetization switching in such structures are used in magnetic field sensors, nonvolatile magnetoresistive memory (MRAM, ST-MRAM), resonant tunneling diodes, spin transistors [1, 2]. In this report, we investigate theoretically the asymmetric double-barrier magnetic nanostructures $FM^L/I_1/FM^W/I_2/FM^R$. They consist of three ferromagnetic layers separated by dielectric layers. As the ferromagnetic layers material, Fe, Co, Ni and their alloys (CoFeB, FeNi) are considered. Insulating layers are usually AlO_x or MgO. Magnetization of the outer sheets (FM^L , FM^R) are co-directed and pinned by the exchange bias effect. Magnetization of the middle layer (FM^W) can be changed by an external magnetic field. One of such structures is shown in Fig. 1.

Usually, one considers two situations referring to relative orientations of the ferromagnetic layer magnetizations. P-orientation (parallel) is referred to the case when the magnetizations of all ferromagnetic layers are parallel, AP- orientation (anti-parallel), when the magnetization of the middle layer is directed opposite to the magnetizations of the side layers. If we apply a bias voltage to the external electrodes, a current flows across the structure. It is due to quantum mechanical tunneling of electrons through the barriers. Resistance of the structure depends on relative orientations of the ferromagnetic layers. The relative difference between resistances in the P and AP alignments may reach $\sim 1000\%$ at room temperature.

Analysis of the electron tunneling is based on the model of spin-conduction channels. Current calculation is performed using the quasiclassical theory [4]. The ferromagnetic layers are discussed in the framework of two-band model. Transmission coefficients of the structure are calculated quantum-mechanically in the effective-mass approximation for the conduction electrons [5]. As a result, we obtain the dependence of spin-polarized current and magnetoresistance on applied voltage.

The theory can be used for explanation of the experimental data, and searching for condition of softening the requirements to the magnitude of current necessary for switching of the tunnel magnetic structures between high and low resistance states.

Support of the RFBR grant № 1402-00348-a is gratefully acknowledged.

- [1] A. Fert, *Thin Solid Films*, **517** (2008) 2-5.
- [2] S. Ikeda *et al.*, *IEEE Trans. Electron Devices*, **54** (2007) 991–1002.
- [3] R.S. Liu *et al.*, *Phys. Rev. B*, **87** (2013) 024411.
- [4] L.R. Tagirov *et al.*, *Phys. Rev. B*, **63** (2001) 104468.
- [5] A.N. Useinov *et al.*, *Phys. Rev. B*, **84** (2011) 085424.

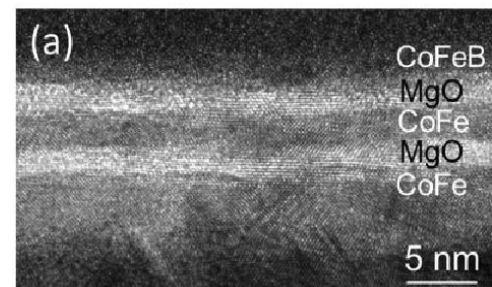


Fig. 1. Cross-sectional transmission electron microscopy image of the double-barrier magnetic tunnel junction (taken from Ref. [3]).

1PO-K-20

ANOMALOUS HALL EFFECT IN $(\text{Co}_{41}\text{Fe}_{39}\text{B}_{20})_x(\text{Al-O})_{100-x}$ NANOCOMPOSITES

*Mikhailovsky Yu.O.¹, Prudnikov V.N.¹, Chernoglazov K.Yu.², Rylkov V.V.², Sitnikov A.V.³,
Kalinin Yu.E.³, Bartov D.⁴, Gerber A.⁴, Granovsky A.B.¹*

¹ Faculty of Physics, Lomonosov Moscow State University, Moscow, Russia

² National Research Centre “Kurchatov Institute”, Moscow, Russia

³ Voronezh State Technical University, Voronezh, Russia

⁴ Tel Aviv University, Tel Aviv, Israel

mikhaylovskiy.yuriy@gmail.com

In spite of significant progress in understanding of the mechanisms underlying the anomalous Hall effect (AHE) in homogeneous metals and semiconductors [1], the developed theory of AHE fails to explain the experimental data on AHE in the systems with high electrical resistance [1,2]. Recently, it has been shown that neither intrinsic mechanism, nor skew scattering or side-jump mechanism [1], as well as other proposed specific mechanisms (see references in [2]) cannot explain both the large value and the concentration dependence of AHE resistivity in $(\text{Co}_{41}\text{Fe}_{39}\text{B}_{20})_x(\text{Al-O})_{100-x}$ nanocomposites at room temperature [2]. In this work we present our last results on magnetic properties, resistivity, magnetoresistance, Hall effect resistivity for these samples measured at 5-300 K focusing on the possible correlation between temperature dependence of AHE and resistivity.

It is shown that the temperature dependence of resistivity at $5\text{K} < T < T_k$ follows the well-known relation $\rho_{xx} = A(1 - \alpha \log T)$ [3], where the parameters A , α , T_k depend on x . For example for $x=56.6$, $T_k=34$ K, $A=0.0046$, $\alpha=0.06$, that taking into account an average grain size about 2.0 nm is in a good quantitative agreement with the theory [3]. For the same temperature range the correlation between AHE resistivity ρ_{xy} (T) and resistivity ρ_{xx} (T) can be described by the relation $\rho_{xy} \propto (\rho_{xx})^m$, where $m=0.55$, that is approximately the same as for concentration dependencies [2] and is quite typical for “bad” metals [1]. But at $T > T_k$ there are deviation from the relation $\rho_{xx} = A(1 - \alpha \ln T)$ and m increases up to $m \approx 1.0$.

The possible mechanisms of AHE in nanocomposites are discussed including influence of size-effect, correlated scattering by triangles, AHE enhancement due to Rashba spin-orbit coupling in tunnel junction [3], elastic and inelastic scattering by impurities located inside the tunnel barrier [4]. This work was partly supported by the Russian Foundation for Basic Research (grant No. 13-07-00477a, 14-02-31134)

[1] N.Nagaosa, J.Sinova, S.Onoda et al., *Rev. Mod. Phys.*, **82** (2010) 1539.

[2] Yu.O. Mikhailovsky, D.E. Metus, A.P. Kazakov et al., *JETP Lett.*, **97** (2013) 473.

[3] I.S. Beloborodov, A.V. Lopatin, V.M. Vinokur, K.B. Efetov, *Rev.Mod. Phys.*, **79** (2007) 469.

[4] A.V. Vedyayev, M.S. Titova, N.V. Ryzhanova et al., *Appl. Phys. Lett.*, **103** (2013) 032406.

[5] A.V. Vedyayev, N.V. Ryzhanova, N. Strelkov, B. Dieny, *Phys.Rev.Lett.*, **110** (2013) 247204.

1PO-K-21

TECHNOLOGICAL FEATURES INFLUENCE ON MAGNETIC SENSITIVITY OF FERROMAGNETIC NANOSTRUCTURES

Bespalov V.A.¹, Djuzhev N.A.¹, Yurov A.S.¹, Chinenkov M.Y.^{1,2}, Mazurkin N.S.¹

¹National Research University of Electronic Technology (MIET), Moscow, Russia

²SPINTEK, LLC, Moscow, Russia

chinenkov@inbox.ru

Effects associated with the magnetic properties of matter become actual as technology in the nanoscale. Magnetic materials provide a solution of many technical and technological problems in the world today. Electronic structures based on magnetic materials, in particular ferromagnets, have been used in computer science, electrical engineering, microwave technology, magnetic memory, bank cards, and many other areas. One of the effects, which provides a promising use of magnetic structures is the electrical resistance change in the magnetic field, i.e. magnetoresistive effect. The main urgent problems of the magnetic devices and primary converters development based on the magnetoresistive structures are the sensitivity improvement, thermal stability, as well as miniaturization [1].

In the course of this work it is shown that the sensor element based on the magnetoresistive nanostructures allows detecting the external magnetic field. Magnetoresistive nanostructures based on permalloy films in the sensory systems, the typical thickness of the permalloy layer in the magnetoresistor experimental samples is 20-30 nm. It is shown that the variation of the shape and size ratio of magnetoresistive elements [2] and barber-pole structures influence the characteristics of the magnetization and the dynamic range of the sensors, as well as their range of maximum magnetic field sensitivity. The obtained values of the sensor sensitivity provide an opportunity to develop a speed and angular position sensors based on the magnetoresistive nanostructures.

The influence of the initial imbalance of the magnetic system on the shape of the output signal is the particular interest. Increase of the initial imbalance of the magnetic system leads to a distortion of the output signal. For certain values of the imbalance the shift in the operating point of the sensor and a narrowing of the field of workability, and for sufficiently large values of its total loss take place. The value of the initial imbalance of the magnetic system is determined by two factors: the imbalance of technological magnetoresistive structures defined by resistors bridge precision fit; setting up of a permanent magnet. The latter fact is important in determining of performance region of the sensor as a whole. It should be noted that both components of the imbalance depend on the temperature. Thus, it is necessary to provide the minimum value of the initial imbalance of the magnetic system for the stable operation over a wide range of external influences, particularly temperature.

In the course of this work it is shown that the sensing element allows detecting changes in the external magnetic field. Reach sensitivity values obtained 9 mV / V / (kA / m) with sufficiently high thermal stability from -60 ° C to +150 ° C, which enables the development and speed sensor of the angular position based on magnetoresistive nanostructures.

Support by Minobrnauki RF (GK № 02.G25.31.0059) is acknowledged.

[1] Freitas P.P., Ferreira R. and Cardoso S. *J. Physics: Cond. Matt.*, **19** (2007) 165221.

[2] A.V. Goryachev, M.Yu. Chinenkov, N.A. Dyuzhev, A.M. Mednikov, A.F. Popkov, F.A. Pudonin. *Semiconductors*, **43** № **13** (2009) 1695-1699.

1PO-K-22

THE INFLUENCE OF THICKNESS OF THE INTERLAYER SEMICONDUCTOR ON ELECTRICAL AND MAGNETIC PROPERTIES OF MULTILAYER NANOSTRUCTURES

$\{[(\text{Co}_{41}\text{Fe}_{39}\text{B}_{20})_{33.9}(\text{SiO}_2)_{66.1}]/[\text{In}_{35.5}\text{Y}_{4.2}\text{O}_{60.3}]\}_{93}$

Babkina I.V., Gabriels K.S., Zhilova O.V., Kalinin Yu.E., Sitnikov A.V.

Voronezh State Technical University 14 Moskow ave, Voronezh. 394026, Russia

zhilova105@mail.ru

Development of structures comprising gazorezistivny, magnetoresistive and magnitogazovy effects simultaneously, is a unique challenge now days. Multilayer composite heterogeneous structures - semiconductor can combine all these properties simultaneously.

The aim of this work is to explore new multilayer structure of the composite - semiconductor. Composite layers ferromagnetic - insulator $(\text{Co}_{41}\text{Fe}_{39}\text{B}_{20})_{33.9}(\text{SiO}_2)_{66.1}$, are in a superparamagnetic state, and are semiconductor (dielectric) interlayer: $\text{In}_{35.5}\text{Y}_{4.2}\text{O}_{60.3}$.

Preparation of samples $\{[(\text{Co}_{41}\text{Fe}_{39}\text{B}_{20})_{33.9}(\text{SiO}_2)_{66.1}]/[\text{In}_{35.5}\text{Y}_{4.2}\text{O}_{60.3}]\}_{93}$ was carried out by ion-beam sputtering method on the original installation, designed on the basis of vacuum deposition post UVN-2M.

Investigations of the electrical properties of multilayer heterogeneous structures $\{[(\text{Co}_{40}\text{Fe}_{40}\text{B}_{20})_{33.9}(\text{SiO}_2)_{66.1}]/[\text{In}_{35.5}\text{Y}_{4.2}\text{O}_{60.3}]\}_{93}$ were done. The composition of the composite $\text{Co}_{40}\text{Fe}_{40}\text{B}_{20})_{33.9}(\text{SiO}_2)_{66.1}$ is to the percolation threshold. It is shown that the thickness of the semiconductor layer $\text{In}_{35.5}\text{Y}_{4.2}\text{O}_{60.3}$ has decisive importance for the mechanism of electromigration in the material. If h is less than 0.5 nm charge transfer process is determined by the composite $\text{Co}_{40}\text{Fe}_{40}\text{B}_{20})_{33.9}(\text{SiO}_2)_{66.1}$. For thickness of 0.5 to 1.2 nm we observe the redistribution on conduction, caused by to an transformation of metal – insulator – metal electron transfer to metal – semiconductor – metal transfer structure. When thickness is more 1.2 nm the distance between the metal granules increases and so the resistance grows.

Magnetoresistive properties were investigated multilayer heterogeneous structure $\{[(\text{Co}_{40}\text{Fe}_{40}\text{B}_{20})_{33.9}(\text{SiO}_2)_{66.1}]/[\text{In}_{35.5}\text{Y}_{4.2}\text{O}_{60.3}]\}_{93}$. In the initial samples magnetoresistive effect (MR) is absent. After the heat treatment on the magnetoresistance effect semiconductor layer thickness $\text{In}_{35.5}\text{Y}_{4.2}\text{O}_{60.3}$. When $h > 1.0$ nm the rise of the magnetoresistance, which correlates with an increase in the electrical conductivity of the samples (Fig. 1).

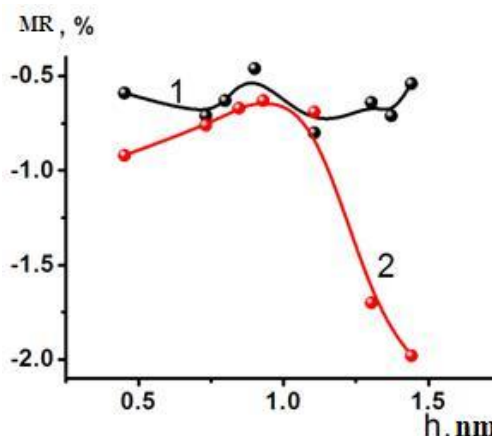


Fig. 1. The dependence of the thickness of the MR when the semiconductor layer $H = 0-8$ kOe

1 - the initial state of; 2 - after a thermal treatment at $T = 300$ °C for 30 minutes in a hydrogen atmosphere at a pressure of 7.8 Torr

Support by RFBR (grants №13-02-97512-r_centra).

1PO-K-23

EXCHANGE COUPLING AND SPIN-POLARISED SUPERCONDUCTIVITY IN Ni/Gd/DEVICES

Higgs T.D.C.¹, Banerjee N.¹, Wang X.², Bonetti S.³, Ohldag H.³, Blamire M.G.¹, Robinson J.W.A.¹

¹ Department of Materials Science and Metallurgy, University of Cambridge, Cambridge, UK

² Institute of Semiconductors, Chinese Academy of Science, Beijing, China

³ Stanford Synchrotron Radiation Laboratory, Menlo Park, California, USA

tdch4@cam.ac.uk

It has previously been shown that a long-range spin-triplet supercurrent can flow through a superconductor-ferromagnet (SF) system if suitable magnetic inhomogeneity is present at the SF interface [1-4]. Recently our group has demonstrated triplet supercurrents in sub-micron scale Josephson junctions with a Ni-Gd-Ni barrier [5] in which the triplet supercurrent densities were found to depend on the magnetic field history of the devices. In order to confirm this, the micromagnetic structure of Ni-Gd-Ni trilayers is being investigated by X-ray magnetic circular dichroism (XMCD) and vibrating sample magnetometry.

The thicknesses of the Ni-Gd-Ni layers in the structure chosen for further study range from 2-2-2 to 8-10-8 (in nanometres). So far, XMCD measurements have shown evidence for biquadratic coupling occurring between the Ni and Gd in a particular range of Gd thicknesses in unpatterned films. This is surprising since the existing theory predicts that at an interface between a rare-earth ferromagnet and a transition metal ferromagnet the moments align antiparallel. Other magnetic configurations are also thought to be possible; an in-plane domain wall can form in the Gd if the Ni layers have antiparallel magnetisations in order to lower the magnetic energy of the system.

A magnetisation rotation of more or less than 180 degrees (non-collinear coupling at Gd-Ni interfaces) in the Gd may depend on the thickness of the Gd layer. These magnetic configurations will be investigated for unpatterned films, but also for patterned mesas (~ 1 x 1 micro metre) in which the magnetostatics play a defining role in determining the micromagnetic structure.

The projected third phase of the experiment is to try to apply what we learn about the magnetic structure of devices to the generation and propagation of spin-triplet supercurrents in the nanopillar junctions.

[1] M. Eschrig, *Physics Today*, **64** (2011) 43.

[2] T. S. Khaire, M. A. Khasawneh, W. P. Pratt and N. O. Birge, *Phys. Rev. Lett.*, **104** (2010) 137002.

[3] C. Klose *et al*, *Phys. Rev. Lett.*, **108** (2012) 127002.

[4] J. W. A. Robinson, J. D. S. Witt and M. G. Blamire, *Science*, **329** (2010) 59.

[5] J.W.A. Robinson, F.Chiodi, M.Egilmex, G.B. Halasz and M. G. Blamire, *Sci. Rep.*, **2** (2012) 699.

IPO-K-24

MAGNETIC AND MAGNETORESISTANCE PROPERTIES OF (Co/Ge)_n FILMS

*Patrin G.S.^{1,2}, Turpanov I.A.¹, Maruschenko E.A.^{1,2}, Patrin K.G.^{1,2}, Kobyakov A.V.^{1,2}, Maltsev V.K.¹,
Yushkov V.I.^{1,2}*

¹ L.V. Kirensky Institute of Physics, Siberian Branch of Russian Academy of Sciences,
Krasnoyarsk, 660036, Russia

² Siberian Federal University, prospect Svobodny, 79, Krasnoyarsk, 660041, Russia
patrin@iph.krasn.ru

Considerable interest in heterostructures based on semiconductor and magnetic materials due to the fact that there is the possibility of integration of magnetism and semiconducting properties. Typically, the ultimate goal of creating a ferromagnet-semiconductor structures is the control of electrical properties by changing the magnetic parameters. In this case the fore the study of magnetic and interlayer interactions and the mechanisms responsible for their formation.

In order to elucidate the mechanism of the formation of the magnetic structure and the establishment of an interface we have synthesized two-layer films Ge/Co and examined the magnetic and resistive properties. The films were deposited on glass substrate by magnetron sputtering on ultra-high vacuum apparatus with four sources of the company «Omicron». Magnetic and electrical properties were made with the MPMS-XL. Investigations of two-layer film structures with a fixed thickness of germanium ($t_{\text{Ge}} = 8$ nm) with different thicknesses of the ferromagnetic layer of cobalt ($t_{\text{Co}} = 2 \div 11$ nm). Top and bottom of the investigated Co/Ge-structure of the protective layers were deposited copper thickness $t_{\text{Cu}} \sim 50$ nm, who performed the role of contact pads.

Electron microscopic examination of the cross sections of the films formed on the transmission electron microscope showed that films with thicknesses greater cobalt ($t_{\text{Co}} > 4$ nm) on the interface materials formed transition layer thickness of about 4 nm. At a smaller thickness of the cobalt layer is formed of mixed source elements. From the data obtained by e microdiffraction also that the cobalt layer is a hexagonal phase and a transition layer, apparently represents an alloy of Co-Ge.

At low temperatures for small thicknesses of cobalt (≤ 4 nm), where a large contribution from the intermediate layer, the loop is biased view. At large thicknesses of cobalt ($t_{\text{Co}}^* > 10$ nm) loops are symmetrical, and the dependence of the magnetic characteristics of the temperature stronger. It is established that the exchange field and the coercive forces correlated. Also found that there is a reduction in both the coercive force and the magnitude of the exchange bias field decreases the cobalt layer. Increasing the thickness of the magnetic layer to a value of t_{Co}^* increases as the coercive force and the exchange bias field.

The NMR studies of film structures in a cobalt–germanium system as a function of the cobalt layer thickness are made. Two phases of cobalt, one is a face-centered cubic phase and the other is presumably a Co–Ge alloy with a weakly ferromagnetic order, have been found to exist. A dependence of the temperature change in magnetization like the quadratic dependence, it is obtained in the Stoner model for weakly ferromagnetic systems of collective electrons. This suggests that a new cobalt–germanium compound with weakly ferromagnetic properties is formed at the interface. A “dead” layer no more than 2 nm in thickness is formed at the interface.

Also studied were synthesized electrical properties of the films. It was found that with increasing temperature resistivity decreases slightly at first, and at $T \geq 70$ K shows a metallic character. In this region, the temperature dependence of the resistivity is also observed feature, presumably related to the Schottky barrier type.

This study was supported by RFBR, № 14-02-00238-a.

IPO-K-25

LORENTZ ELECTRON MICROSCOPY OF THIN FILMS $\text{Fe}_{86}\text{Mn}_{13}\text{C}$ WITH FRUSTRATED MAGNETIC STRUCTURE

Kveglis L.I.^{1,2}, *Dzhes A.V.*³, *Volochaev M.N.*⁴, *Cherkov A.G.*⁵

¹ SFU, Krasnoyarsk, Russia

² EKSU, Ust-Kamenogorsk, Kazakhstan

³ EKSTU, Ust-Kamenogorsk, Kazakhstan

⁴ SibSAU, Krasnoyarsk, Russia

⁵ NSU, Novosibirsk, Russia

kveglis@iph.krasn.ru

In our earlier papers [1] the dependence of the thermoelectric effect (TE) on temperature in $\text{Fe}_{86}\text{Mn}_{13}\text{C}$ alloy was discussed. We seek to understand the reason for the change of the sign of TE depending on temperature in these films. It is shown that small changes in temperature and magnetic field lead to reorientation of the magnetic structure in thin $\text{Fe}_{86}\text{Mn}_{13}\text{C}$ films. Features of domain structure in thin films $\text{Fe}_{86}\text{Mn}_{13}\text{C}$ are investigated by methods of Lorentz's electron microscopy. In Fig. 1 the different types of magnetic contrast we observed. Various pictures of magnetic contrast show the magnetic heterogeneity of a film. The vector of magnetization has a changing component along the normal to the film plane due to formation of structural and magnetic irregularities (frustrates). The reason for the change of the sign of TE depending on temperature lies in the reversal of magnetization of deformation martensite, which creates a frustrated magnetic structure concentrated in shear bands. Correlation between the crystal structure and the unique magnetic and electrical properties of $\text{Fe}_{86}\text{Mn}_{13}\text{C}$ alloy can characterize it as a material for spintronics. Recently, it has been found that quantum-dot-like states also dominate the low-temperature TE behavior of nominally uniform InAs nanowires, but their behavior in the nonlinear TE regime is yet to be explored [2].

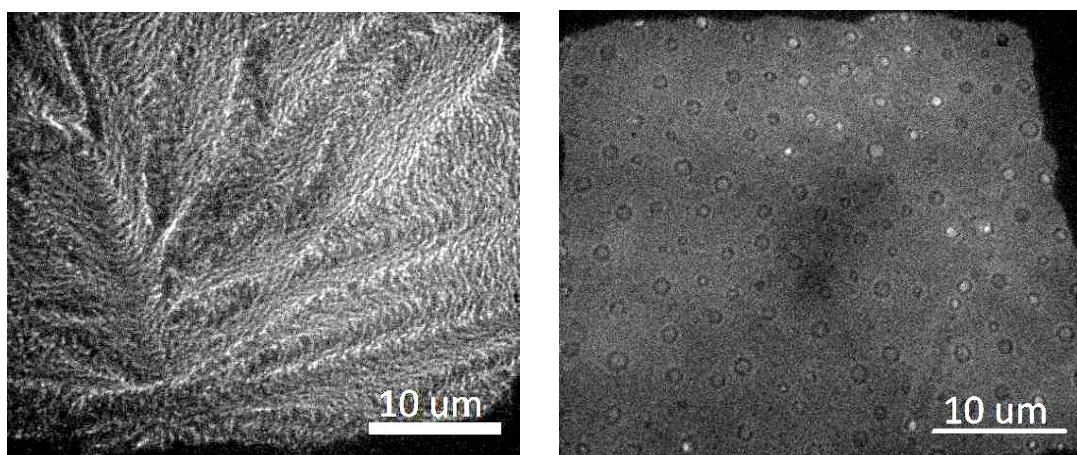


Fig. 1 The different types of magnetic contrast in thin films $\text{Fe}_{86}\text{Mn}_{13}\text{C}$: on the left with the objective lens switched off; on the right with the objective lens switched on.

This work was supported by Grant 278/2013 of the Ministry of Education and Science of the Republic of Kazakhstan

[1] U.V. Panichkin, R.B. Abylkalykova, L.I. Kveglis, V.V. Semchenko, *Scientific Israel - Technological Advantages*, **12** (2010) 30-35.

[2] P.M. Wu, J. Gooth, X. Zianni, S. Fahlvik Svensson, J.G. Gluschke, K.A. Dick, C. Thelander, K. Nielsch and H. Linke, *Nano Lett.*, **13** (2013) 4080.

1PO-K-26

PECULIARITIES OF SOLITARY DEFLECTION WAVES DYNAMICS ON THE DOMAIN WALLS OF YTTRIUM ORTHOFERRITE

Chetkin M.V., Kurbatova Yu.N., Shapaeva T.B.

Faculty of Physics M.V.Lomonosov Moscow State University, Moscow, Russia
shapaeva@mail.ru

It was shown experimentally that under sharp braking of a segment of the yttrium orthoferrite domain wall (DW) moving with supersonic velocity (12 km/s) a pair of solitary deflection waves appears. These waves have equal amplitudes and move with equal velocities in opposite directions along the DW. These solitary deflection waves accompany antiferromagnetic (AFM) vortices. These vortices are generated inside the DW and move along it. The existence of antiferromagnetic vortices in the yttrium orthoferrite DW was predicted theoretically by Farztdinov et al. [1].

The two-fold high-speed photography method with sub-nanosecond resolution was used to study these vortices dynamics. [2] From one photo of the dynamic DW with a fine structure this method allows to determine the DW velocity – v , the velocity of solitary deflection wave along the DW – u , the total velocity of this wave – w , its amplitude – a , tilt angle of the leading edge of this wave – φ and its existence time. According to experiment at fixed DW velocity the solitary deflection wave velocity along the DW, the wave amplitude and the tilt angle of the leading edge of this wave almost unchanged over time. The curve $w(v)$ demonstrates nonlinearly increase and saturation on the level 20 km/s. This value is a limiting DW velocity equals to the spin waves velocity on the linear part of their dispersion law. The increase of $w(v)$ dependence is sharper for solitary deflection waves with smaller amplitudes. At fixed DW velocity the solitary deflection wave with greater amplitude moves with smaller velocity along the DW. The dependence $\varphi(a)$ is nonlinear. For small amplitude values the angle φ linearly increases. For $a \approx 10 \mu\text{m}$ $\varphi \approx 30-35^\circ$, as amplitude increases to $18 \mu\text{m}$ angle φ doesn't change. Subsequent increasing of the wave amplitude leads to decreasing of φ .

Solitary deflection waves accompanying AFM vortices move along the supersonic part of the DW. The transition from sonic to supersonic motion of the orthoferrite DW happens very rapidly. [3] It can be seen experimentally as one part of the DW still moves with the sound velocity (4 km/s) another one moves with supersonic velocity (12 km/s). The solitary deflection waves accompanying AFM vortices move along the supersonic part of the DW. It was shown that angle φ decreases and tends to zero if the distance between solitary deflection wave and sound part of the DW decreases. This fact suggests that inside DW moving with velocity less or equal to sound velocity there are no AFM vortices.

In work [4] the theoretical simulation results of the AFM vortices dynamics in the DW of yttrium orthoferrite were compared with experimental data. Qualitative agreement between theory and experiment is observed only at the DW velocity greater than 12 km/s.

[1] M.M. Farztdinov, M.A. Shamsutdinov, A.A. Khalfina. *Fiz.Tverd. Tela*, **21** (1979) 1522-1527.

[2] M.V.Chetkin, Yu.N.Kurbatova, T.B.Shapaeva. *JMMM*, **321** (2009) 800-802.

[3] V.G. Bar'jakhtar, M.V. Chetkin, B.A. Ivanov, S.N. Gadetskiy, *Dynamics of Topological Magnetic Solitons* (Springer tracts in modern physics, Berlin), **129** (1994).

[4] M.V.Chetkin, Yu.N.Kurbatova, T.B.Shapaeva. *JMMM*, **324** (2012) 3576-3578.

1PO-K-27

CONTROL OF SPIN CONFIGURATIONS IN AN ASYMMETRIC DOUBLE DISK NANOSTRUCTURE BY PULSED MAGNETIC FIELD

Stebliy M.E.¹, Ognev A.V.¹, Samardak A.S.¹, Kolesnikov A.G.¹, Chebotkevich L.A.¹, Han X.²

¹ Laboratory of Thin Film Technologies, School of Natural Sciences, Far Eastern Federal University, Vladivostok 690950, Russia

² State Key Laboratory of Magnetism, Institute of Physics, Chinese Academy of Sciences, Beijing, China

ognevav@gmail.com

We propose a magnetoresistive memory cell on the basis of the three dimensional nanostructure “small disk on big disk” possessing the three stable configurations of magnetization. Magnetic behaviour of magnetostatically interacting nanodisks under an impact of the high frequency excitation has been studied by means of micromagnetic simulation. The movement of a vortex core in the big disk can induce a change in magnetization configuration in the small one. We prove that magnetic state variation in the double disk nanostructure can be registered by the transverse magnetoresistance measurement. Our calculation showed that the magnetoresistance ratio for all the three states is different and can be defined clearly (Fig. 1). This enables to use “small disk on big disk” system as a memory cell for information storage in base elements of ternary logic.

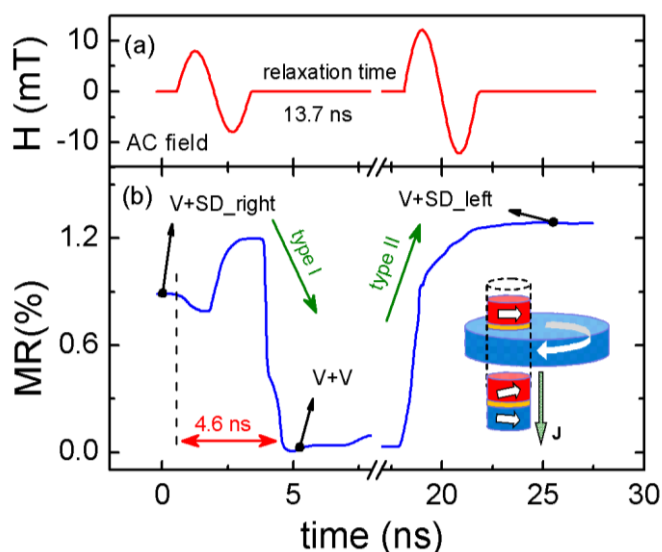


Fig. 1 - (a) Transition between magnetic states induced by the magnetic field variation. (b) Dependence of the magnetoresistance ratio of the “small disk on big disk” system on the combination of spin configurations in disks. The inset demonstrates visualization of the magnetoresistance calculation approach.

This work was supported in part by the Russian Ministry of Education and Science and the Scientific Fund of Far Eastern Federal University.

1 July

Tuesday

17:30-19:00

poster session

1PO-M

**“High Frequency
Properties and
Metamaterials”**

1PO-M-1

AC PROPERTIES OF FERRITE-DIELECTRIC COMPOSITE MATERIALS IN THE EFFECTIVE MEDIUM APPROXIMATION

Morchenko A.T.¹, Kostishyn V.G.¹, Panina L.V.¹, Podgornaya S.V.¹, Andreev V.G.², Bibikov S.B.³, Vergazov R.M.²

¹ National University of Science and Technology "MISIS" (MISIS), Moscow, Russia

² Kuznetsk Institute of Information and Management Technologies, Kuznetsk, Russia

³ Emanuel Institute of Biochemical Physics, Russian Academy of Sciences, Moscow, Russia
dratm@mail.ru

The development of ultra-wideband absorbers of electromagnetic waves depends largely on optimal combination of the medium characteristics that determine its absorption capacity. It is possible to achieve a higher absorption level in a wider frequency band by combining a variety of mechanisms enhancing the loss of electromagnetic field energy, for example, by combining specific constituents in a composite matrix.

The electromagnetic characteristics of heterogeneous systems can be represented in terms of the generalized parameters (e.g., electrical conductivity, permittivity, permeability, effective thickness, etc) which are derived from the individual characteristics of its constituents, matrix and structural morphology. If properly set, these parameters are useful to describe the overall electromagnetic response from the system. The structures of interest are multilayer nanostructures, island films, metal-polymer nanocomposites, bulk composite materials consisting of a dielectric matrix with metal or ferrite inclusions, etc., in the optical and microwave frequency ranges.

In the present work, the analysis of existing mixing models of meta-medium (metamaterial) in the effective medium approximation is carried out targeting ordered or disordered ferrite-dielectric composite materials. The modelling results are compared with the experimental data on the effective parameters of composites with conductive (semiconductive) and non-conductive ferrite fillers, which were deduced from refractive/transmission coefficients. The effects of both the individual filler properties and microstructure were demonstrated. The advantages and limitations of various mixing models were discussed.

Support by RFBR (grant 13-03-01316) is acknowledged.

1PO-M-2

OFF-DIAGONAL MAGNETOIMPEDANCE SENSOR IN MULTICORE CONFIGURATION

Yudanov N.A.¹, Rudenok A.A.¹, Morchenko A.T.¹, Panina L.V.^{1,2}

¹ National University of Science and Technology (MISIS), Moscow, Russia

² Institute for Design Problems in Microelectronics RAS, Moscow, Russia

kolyan2606@mail.ru

Magnetoimpedance (MI) sensor development has been driven by the need for improved sensitivity, smaller size, faster response and compatibility with electronic systems. The MI sensors utilize a very large change in the ac impedance, which reaches more than 100%/Oe in Co-rich amorphous wires for a driving current frequency of a few tens of MHz [1]. The sensing element can be as small as 10-30 micron in diameter and a few mm in length without compromising on sensitivity, which is in the range of **10 – 20 nT** for detecting an AC magnetic field [2]. The practical sensor design utilises off-diagonal MI when the MI element is excited by an or pulsed current and the output signal is taken from the coil [3]. To improve the signal-to-noise ratio, the number of the detection coil turns is relatively large, up to 600. However, this may not be desirable from the point of view of the complexity of sensor construction, size, and may also increase the electronic noise. In this work we investigate the off-diagonal impedance from a number of Co-based glass-coated amorphous wires connected in parallel and excited by harmonic or pulsed current. The detection pulse amplitude from two parallel wires spaced at 10 microns may increase a few times, which helps to decrease a number of detection coils. The peak field also increases improving the linearity range. The response drops if the distance between the wires is increased. This suggests a strong effect of the magnetostatic interaction between the wires. The maximum sensitivity for two wire sensor is about 300mV/Oe within the range of -1.5-1.5 Oe.

The work was partially supported by RFBS grant 13/08/01319

[1] D. P. Makhnovskiy, L. V. Panina, and D. J. Mapps, *Phys. Rev. B*, **63** (2001) 144424-23.

[2] T. Uchiyama, K. Mohri, Y. Honkura, and L.V. Panina, *IEEE Trans Magn*, **48** (2012) 3833-3839.

[3] S. Sandacci, D. Makhnovskiy, L. Panina, K. Mohri, and Y. Honkura, *IEEE Trans. Magn.*, **40** (2004) 3905-10.

1PO-M-3

PROBING MAGNETOELASTIC INTERACTION VIA SPIN WAVES IN YTTRIUM IRON GARNET FILMS AND MAGNONIC CRYSTALS USING MICRO-SIZED ANTENNAS

Khivintsev Y.V.^{1,2,}, Sakharov V.K.¹, Filimonov Y.A.^{1,2}, Nikitov S.A.^{2,3}*

¹ Kotelnikov IRE RAS, Saratov Branch, Saratov, Russia

² Chernyshevsky Saratov State University, Saratov, Russia

³ Kotelnikov IRE RAS, Moscow, Russia

* khivintsev@gmail.com

The resonant interaction of the spin waves (SW) and elastic waves (EW) leading to formation of so called magnetoelastic waves (MEW) experimentally can be probed via the SW or EW. Previously both these ways were extensively used to study MEW in yttrium iron garnet (YIG) thin film structures which have low damping for both SW and EW [1, 2]. However, so far, experiments with the SW in YIG films allowed observing formation of only so called fast MEW which have the phase velocities much higher than the sound speed and are result of the resonant interaction of the SW with the high order elastic waveguide modes. This is mainly due to the facts that antennas used for the SW excitation and detection are only effective for quite long waves (wave number $< 1000 \text{ cm}^{-1}$) and fundamental elastic modes are much shorter at the typical SW frequencies ($> 0.1 \text{ GHz}$). In this work we probed the magnetoelastic interaction via the SW using coplanar micro-sized antennas integrated with the YIG film. Such structures allowed us to excite and detect the SW with wave numbers in the range of $\sim 10^3 \div 3 \times 10^4 \text{ cm}^{-1}$ and test not only fast MEW but resonant interaction of the SW with the fundamental elastic mode as well.

Fabrication of the integrated structures YIG film - micro-sized coplanar antennas was done using photolithography and magnetron sputtering. Measurements were carried out using a vector network analyzer along with a microwave probe station. Scattering parameters were measured as a function of the frequency for various bias magnetic fields applied along the SW propagation direction. In addition to structures based on plain YIG film we fabricated and tested structures with YIG film based magnonic crystal (MC). The last was formed by focused ion beam milling of a periodical array of grooves in YIG film.

Resonant interaction of the SW with the transversal EW (TEW) modes was observed. It was showed up as oscillations in the SW transmission parameter at resonance frequencies for both plain YIG films and MC. In the last case the magnetoelastic oscillations remained inside the Bragg stop bands but some of them were changed from the absorption peaks to the transmission peaks in comparison to the plain film. Such behavior can be explained as a result of the strong change in the SW damping at Bragg resonances in the MC that did not affect much on the EW damping. The interaction of the SW with the fundamental TEW mode was observed for the structure based on Ga, Sc-doped YIG film that allows lowering the spin wave frequencies and getting the resonance at reasonable wave numbers. It was proved by the good agreement between theoretical dispersion for the fundamental TEW mode and obtained from the experimental data.

Support by Russian Foundation for Basic Research (grants # 13-07-00941, 13-07-12421 and 14-07-00896) and Grant of the Government of the Russian Federation for supporting scientific research projects supervised by leading scientists at Russian institutions of higher education (project # 11.G34.31.0030) is acknowledged.

[1] Yu.V. Gulyaev, P.E. Zil'berman, *Sov. Phys. J.*, **31**, 11 (1988) 860.

[2] G.T. Kazakov, et al., *J. Comm. Tech. El.*, **49**, 5 (2004) 568.

1PO-M-4

NONLINEAR EXCITATION OF ULTRASOUND IN BULK SAMPLES AND YIG FILMS IN INHOMOGENEOUS MAGNETIC FIELD

Kotov L.N.¹, Beznosikov D.S.¹, Vlasov V.S.¹, Ustygov V.A.¹, Shavrov V.G.², Shcheglov V.I.²,
Asadullin F.F.³, Poleshchikov S.M.³, Lutsev L.V.⁴

¹ Syktyvkar State University, Syktyvkar, Russia

² Institute of Radioengineering and Electronics of RAS, Moscow, Russia

³ St. Petersburg State Forest Technical University named after S.M. Kirov, St. Petersburg, Russia

⁴ Ioffe Physical-Technical Institute of RAS, St. Petersburg, Russia

uvn71p3@gmail.com

The problem of excitation of ultrasonic oscillations using magnetostrictive transducers has long attracted the attention of researchers [1]. The use of magnetostrictive transducers is promising in acoustoelectronics. The high Q values of ferrites allow to create new devices such as an acoustic maser, field sensors, filters of RF and microwave ranges.

Most experiments on the electromagnetic excitation of elastic oscillations were conducted at microwave frequencies [1, 2]. In the HF band 10^7 - 10^8 Hz a number of such researches is relatively small [3]. The magnetoacoustic interactions have a number of features in this frequency range [3]. Since the wavelength of the alternating field is much larger than the size of the sample the type of magnetic moment oscillations result in uniform precession. That is the realization of magnetoelastic transformation requires inhomogeneous magnetic field.

The work is devoted to the experiments on nonlinear excitation of ultrasound in bulk polycrystalline samples of yttrium iron garnet (YIG) $Y_3Fe_{5-x}Al_xO_{12}$ and epitaxial YIG films. The inhomogeneous internal magnetic field occurs due to the samples finite sizes, applying dc bias magnetic field directed perpendicular to the long side of the bulk samples. That is why, FMR conditions and excitation of elastic oscillations in the sample took place locally. For the sample with $x=0.3$ and $4.27 \times 4.90 \times 9.10$ mm³ sizes the maximum amplitudes of the fundamental harmonics due to natural FMR at zero external field were observed. The acoustic responses amplitudes (first harmonic) excited in different places of the sample with $x=1.5$ and $1.97 \times 4.80 \times 14.0$ mm³ sizes were measured.

The dependences of the amplitudes of the first, second and third harmonics of the external dc magnetic field for the sample with $x = 0.7$ and $3.45 \times 3.57 \times 14.75$ mm³ sizes were obtained. The amplitudes of all these harmonics have a maximum at the dc magnetic field value corresponding to the rotation of the magnetization vector processes followed by the single-domain sample.

To explain the experimental dependences the mathematical model of a multidimensional system of ordinary differential equations obtained by finite-difference approximation of the coordinate derivatives in the magnetoelastic equations was applied.

The dependences of the amplitudes of the elastic displacement from the frequency of the electromagnetic field and the strength of the dc magnetic field for the samples of different sizes and accordingly various irregularities of the demagnetization field were obtained.

The work is supported by the Russian Foundation of Basic Research (grant №12-02-01035-a).

[1] V.S.Vlasov, L.N. Kotov, V.G. Shavrov, V.I. Shcheglov, *J. Comm. Tech. El.*, **54** (2009) 821-832.

[2] Lemanov V., Pavlenko A., Grishmanovskii A., *Soviet physics JETP*, **32** (1971) 389-393.

[3] Belayeva O.Yu., Zarembo L.K., Karpachev S.N., *Usp. Fiz. Nauk*, **62** (1992) 107-138.

1PO-M-5

CONCENTRATION DEPENDENCES OF EXCHANGE FIELDS IN COMPOSITE AND MULTILAYER THIN FILMS

Golov A.V.¹, Kotov L.N.¹, Vlasov V.S.¹, Asadullin F.F.², Pilipets E.S.¹, Kalinin Yu.E.³, Sitnikov A.V.³

¹ Syktyvkar State University, Syktyvkar, Russia

² Saint-Petersburg State Forest Technical University named after S.M. Kirov, St-Petersburg, Russia

³ Voronezh State Technical University, Voronezh, Russia

antogolov@mail.ru

In recent decades researches show considerable interest to the study of new materials reflecting and absorbing HF and UHF electromagnetic radio waves. These materials are based on composites of various alloys of magnetic metals and dielectric and semiconductor substance.

Monolayer films of I series have composition Me_xD1_y (thickness: $3 \div 6$ microns) and multilayer films: II series - $\{(Me_xD1_y) - (Me_xD1_y)\}_{50}$ composite-composite layers (thickness: $0.2 \div 0.4$ microns), III series - $\{(Me_xD1_y)-Si\}_{120}$ - composite-semiconductor layers (thickness: $0.34 \div 0.9$ microns) and IV series- $\{(Me_xD1_y)-(Si: H)\}_{100}$ - composite-semiconductor with hydrogen layers (thickness: $0.34 \div 0.9$ microns) were investigated. Here $x = 0.3 \div 0.6$, $y = 30-30x$ and a metallic alloy $Me = Co_{45}-Fe_{45}-Zr_{10}$ and dielectric $D1 = Al_2O_3$. Numbers 50, 100 and 120 represent the amount of composite and the semiconductor layers in the films.

Dependences of the internal exchange fields from magnetic metal alloy concentration x in nanostructured single and multilayer films at room and liquid nitrogen temperatures were obtained. The calculation is made on the basis of the experimental data [1] and the relationship of the exchange interaction and the broadening of the FMR line [2].

The value of exchange field H_{EX} rises monotonously with the increase of metal alloy concentration x for films of I and II series at room temperature and $T=77 K$ with the transition to saturation (Fig. 1). Growth rate and magnitude of the exchange fields with increasing x for multilayer composite films of II series is much higher than for single-layer composite films of I series. That can be explained by significant differences in the thickness of these series of films. The influence of the demagnetizing factors in thin films is less than in thick ones. For multilayer films of III-IV series the magnitude of H_{EX} varies slightly with increasing x at temperatures of $T = 77 K, 300 K$ versus I-II series.

Similar results for films of different composition were obtained by other experimenters [3].

The work is supported by the Russian Foundation of Basic Research (grant №13-02-01401-a).

[1] L.N. Kotov et al., *Nanomateriali I nanostructure – XXI vek*, **4** (2011) 27-33.

[2] S.L. Yuan et al., *J. Phys.: Condens. Matter*, **12** (2000) 109-114.

[3] E.A. Denisova, R.S. Iskhakov et al., *Solid State Phenomena*, **168-169** (2001) 265-268.

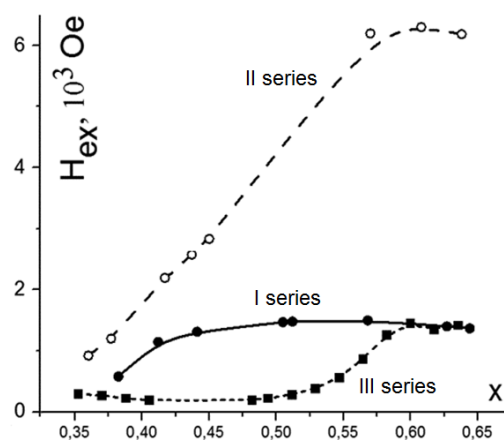


Fig. 1. Dependence of the exchange field of concentration x at $T=77K$.

1PO-M-6

MILLIMETER WAVE LATCHING PHASE SHIFTER UTILIZING PHASE-FREQUENCY BISTABILITY EFFECTS

Popov M.A.^{1,2}, Srinivasan G.², Zavislyak I.V.¹, Movchan N.N.¹

¹ Taras Shevchenko National University of Kyiv, Kyiv, Ukraine

² Oakland University, Rochester, Michigan, USA

zav@univ.kiev.ua

Highly anisotropic hexaferrites are well-known materials for millimeter wave and sub-THz ferromagnetic resonance-based frequency selective devices. The presence of the high uniaxial anisotropy field creates a unique situation when frequency of some magneto-dielectric resonances in hexaferrite samples can lie below ferromagnetic resonance (FMR) frequency for any magnitude of the bias magnetic field. Bistability, i.e., existence of the two stable states of a nonlinear resonance system, has been discovered for waves and oscillations of various physical natures. Frequency bistability in perpendicularly biased hexaferrite samples manifested itself in FMR frequency hysteresis dependence on magnetization pre-history [1].

In the current paper the phase-related aspects of bistability of magnetodynamic resonance in magnetodielectric resonator are investigated for the first time. This phase-frequency bistability consists of possibility of switching between two branches of hysteresis in frequency vs. field dependence for the lowest magnetodielectric $HE_{-11\delta}$ mode [2]. Hence, this mode can have two different resonant frequencies at the same H_0 , depending on current ferrite magnetization state. A discrete switchable mm-wave transmission-type waveguide phase shifter utilizing this phenomenon was suggested and its primary characteristics were measured and discussed.

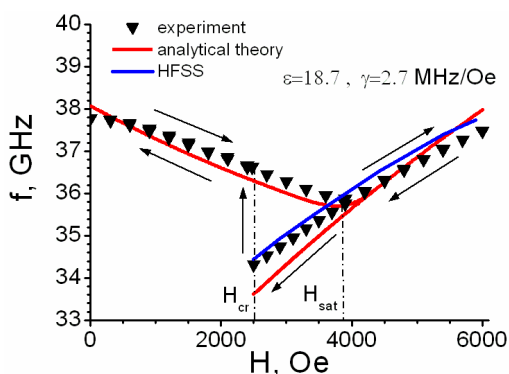


Fig. 1. Experimental (dots) and theoretical (lines) $HE_{-11\delta}$ frequency vs. field dependence

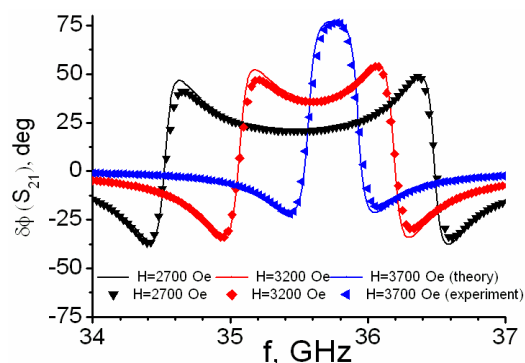


Fig. 2. Differential phase shift for different fields $H_{cr} < H_0 < H_{sat}$

It was found, that resonator bistability leads to noticeable phase shift $\delta\varphi = \varphi_{down} - \varphi_{up}$ of transmitted electromagnetic waves in frequency region between resonance frequencies, when ferrite resonator is switched amongst a two states on the hysteresis curve. From Fig. 2 one can see, that $\delta\varphi$ increase from 22° at 2700 Oe to 77° at 3700 Oe at middle frequency, but losses at the very same frequency also monotonically increase. Theoretical calculations, using HFSS and analytical theory [2] for frequency determination and equivalent circuit model for phase shift derivation, demonstrate rather satisfactory agreement with experimental data.

[1] I.V. Zavislyak, V.I. Kostenko, T.G. Chamor, L.V. Chevnyuk, *Techn. Phys.*, **50** (2005) 520-522.

[2] N.N. Movchan, I.V. Zavislyak, M.A. Popov, *Radioel. and Comm. Syst.*, **55** (2012) 549-558.

1PO-M-7

EFFECT OF MAGNETIC ANISOTROPY ON SPECTRAL COHERENCE OF SPIN WAVES

Kanazawa N.¹, Goto T.¹, Inoue M.^{1}*

¹ Toyohashi University of Technology, Toyohashi, Japan

*inoue@ee.tut.ac.jp

In the research field of magnonics, the flow control of spin waves is important for realization of the spin wave computation, which holds great promise to process information with high energy efficiency. Magnonic crystals (MCs) are analogous to the photonic crystals, which is essential technology for manipulating spin waves [1]. In this work, we investigated the effect of magnetic shape anisotropy on behavior of spin waves in the localized state.

The MCs can be realized with the periodic metal stripe of metallization width $L_M = 213 \mu\text{m}$ and gap $L_A = 193 \mu\text{m}$, which cover the surface of the spin wave waveguide, composed of the monocrystalline yttrium iron garnet film with $90 \mu\text{m}$ thick and 5mm width. This waveguide was located on the spin wave transducer comprising a couple of micro-strip antennas. The periodic metal stripe was sandwiched by the antennas. At the center of the stripe, a defect gap with $L_D = 386 \mu\text{m}$ was intentionally formed to provide localized state. This setup was placed under magnetic field $H_0 = 400 \text{Oe}$ so that magneto static surface wave was excited.

Transmission spectra were calculated by matrix approach. Shape magnetic anisotropy of the waveguide was calculated by finite element method. At the edge, the effective magnetic field H_{eff} and magnetization $4\pi M_S$ were strongly decreased by a diamagnetic field H_d . This anisotropy was taken into account to the matrix approach calculation. Owing to the magnetic field dependence of the spin wave dispersion relationship, transmission spectrum was shifted downward and the localized peak was broadened, Fig. 1 (a). At the localized frequency, amplitude profiles of the scalar potential following the spin wave was calculated, Fig. 1 (b). Increase of the amplitude by the Fabri-Perot resonance at the defect can be seen, but the anisotropic field strongly suppressed the amplitude. These results indicate that shape anisotropy depressed the spectral coherence of the spin wave in the MC due to the capability of propagation of the multiple spin wave modes. This behavior was also confirmed experimentally.

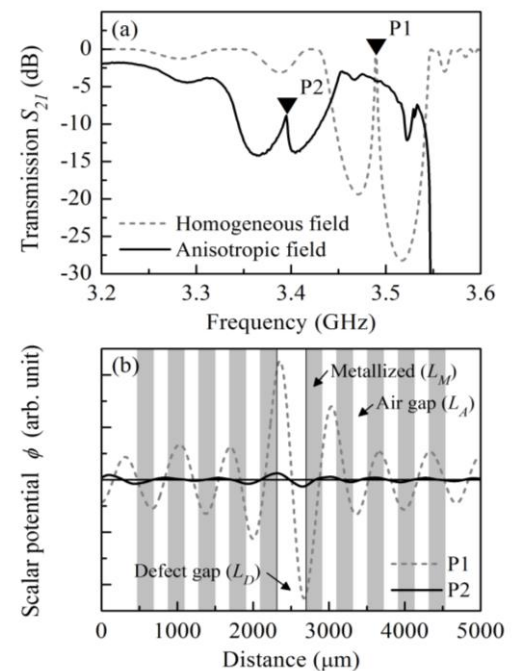


Fig. 1. (a) Transmission spectra and (b) scalar potential profile in the MCs. Gray area corresponds to the metallized regime and white area shows air. For both (a) and (b), solid lines show properties under the anisotropic field and dashed lines show that under homogeneous field.

This work was supported in part by the Grants-in-Aid for Scientific Research (A) 23246061.

[1] V. V Kruglyak, et. al., *J. Phys. D: Appl. Phys.*, **43** (2010) 264001.

1PO-M-8

TUNABLE ELECTROMAGNETIC WAVES ABSORPTION OF GRAPHENE – MAGNETIC SEMICONDUCTOR MULTILAYERED STRUCTURE IN MAGNETIC FIELD

Kuzmin D.A.¹, Bychkov I.V.¹, Shavrov V.G.²

¹ Chelyabinsk State University, Chelyabinsk, Russia

² Kotelnikov Institute of Radio-engineering and Electronics of RAS, Moscow, Russia

kuzminda89@gmail.com

Nowadays graphene attract researchers' attention with their special properties [1, 2], including electro-dynamical ones. So, for example, exciting of the surface plasmons in the graphene layers has been investigated theoretically [3] and experimentally [4]. These studies showed that both TE- and TM- polarized plasmons can exist in graphene. What is more, it is possible to control their dispersion characteristics by applying a voltage. Recently, the possibility of control of the hybrid surface waves in graphene placed between two dielectrics by applying an external magnetic field [5] has been studied. In work [6] the potential of creating of the hyperbolic metamaterial based on graphene – dielectric multilayer structure has been shown. Reflection and transmission of electromagnetic waves by the graphene layer and graphene superlattice have been well investigated in [7, 8]. Despite the large number of studies, the authors are usually limited by investigation of a non-magnetic dielectric medium, where graphene is placed.

This paper is devoted to investigation of the electromagnetic waves absorption by graphene – magnetic semiconductor multilayered structure placed in an external magnetic field \mathbf{H} , directed parallel to the structure surface, in vacuum.

Investigation showed that absorptance of electromagnetic waves by such a structure can be efficiently controlled. Fig. 1 shows frequency dependence of electromagnetic waves absorptance of the structure in magnetic field $H = 70$ kOe for different chemical potential values μ_{chem} . Absorptance also depends on number of the periods of the structure and magnetic field value.

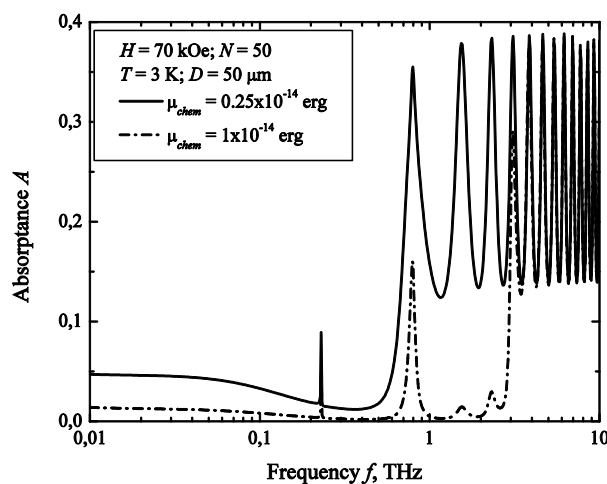


Fig. 1. Frequency dependence of electromagnetic waves absorptance of the structure in magnetic field $H = 70$ kOe for different chemical potential values μ_{chem} . Temperature $T = 3$ K, number of periods of the structure $N = 50$, thickness of the structure $D = 50$ μm .

- [1] R.R. Nair et al, *Science*, **320** (2008) 1308.
- [2] L.A. Falkovsky, *Phys. Usp.*, **55** (2012) 1140–1145.
- [3] S.A. Mikhailov, K. Ziegler, *Phys. Rev. Lett.*, **99** (2007) 016803.
- [4] Z. Fei et al, *Nature (London)*, **487** (2012) 82.
- [5] I. Iorsh et al, *JETP Lett.*, **97** (2013) 287.
- [6] I.V. Iorsh et al, *Phys. Rev. B*, **87** (2013) 075416.
- [7] L.A. Falkovsky, A.A. Varlamov, *Eur. Phys. J. B*, **56** (2007) 281.
- [8] L.A. Falkovsky, S.S. Pershoguba, *Phys. Rev. B*, **76** (2007) 153410.

1PO-M-9

COMBINED MAGNONIC CRYSTAL BASED ON YIG FILM

Filimonov Yu.A.^{1,2}, Khivintsev Yu.V.^{1,2}, Vysotsky S.L.¹, Nikitov S.A.², Shadrov V.G.³

¹ SB Kotel'nikov IRE RAS, Saratov, Russia

² Laboratory of Metamaterials of Chernyshevsky Saratov State University, Saratov, Russia

³ Scientific-practical materials research center of NAS of Belarus, Minsk, Belarus

vysotsl@gmail.com

In order to create magnonic crystal (MC) based on yttrium-iron garnet (YIG) film two simple ways are usually used: chemical etching of periodic structure on the surface of YIG film [1] and placing some periodic array of metal elements on the film's surface [2] (in both cases periodicity could be 1D or 2D). The period of the structure (or array) define the position of forbidden gaps in spectra of magnetostatic waves (MSW) propagating in the MC.

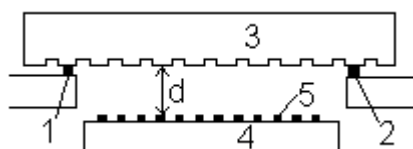


Fig. 1. Sketch of the studied structure:
1, 2 – input and output transducers, 3 – ferrite magnonic crystal, 4 – alumina plate with array of metal stripes 5.

We have studied the structure where both mentioned ways were used simultaneously – see Fig.1. YIG film with chemically etched 1D periodic structure of grooves (ferrite MC 3) was placed on input 1 and output 2 microstrip transducers, at the same time alumina plate 4 with 1D array of metal stripes 5 could be placed at distance $d=0 \div 1$ mm from the surface of ferrite MC 3. We have used 1D array of 270 μm wide metal stripes distanced by 120 μm from each other. Studied ferrite MCs were fabricated by etching of arrays of grooves with different width placed with a period of 0.3 mm, 0.2 mm and 0.15 mm in YIG film of

different thickness. In addition both ferrite MC and array of metal stripes with broken periodicity were made analogously [3].

We have studied propagation of surface MSW (SMSW) in the structure. SMSW transmission characteristics $S_{21}(f)$ were measured for different combinations of MC 3 and array of metal stripes 5 depending on distance d . A possibility to control of number and parameters of forbidden gaps in SWMS spectra was shown.

Support by the Russian Foundation for Basic Researches (Grants No. 14-07-90001-Bel-a, 13-07-00941-a, 14-07-00896-a, 13-07-12421-ofi_m) and by the Grant of the Government of the Russian Federation for supporting scientific research projects supervised by leading scientists at Russian institutions of higher education (Contract No. 11.G34.31.0030) is acknowledged.

[1] Nikitov S.A., Tailhades Ph., Tsai C.S., *JMMM* **236** (2001) 320-330.

[2] M.E. Dokukin, K. Togo and M. Inoue, *J. Magn. Soc. Jpn.*, **32** (2008) 103-105.

[3] Y. Filimonov, E. Pavlov, S. Vysotskii and S. Nikitov, *Appl.Phys.Lett*, **101** (2012) 242408.

1PO-M-10

SECOND ORDER PRECESSION IN THE PLATE WITH CUBIC ANISOTROPY AND MAGNETOELASTIC PROPERTIES

Kirushev M.S.¹, Vlasov V.S.¹, Pleshev D.A.², Kotov L.N.¹, Shavrov V.G.³, Shcheglov V.I.³

¹ Syktyvkar State University, Syktyvkar, Russia

² Saint-Petersburg state forest technical university named after S.M. Kirov, St-Petersburg, Russia

³ Institute of Radioengineering and Electronics of the Russian Academy of Sciences, Moscow, Russia

vlasovv78@mail.ru

In case of a normal magnetized ferrite plate the precession angles may be several tens degrees because parametrical excitation of exchange spin waves is excluded. The alternating circular polarized magnetic field causes the precession of magnetization vector equilibrium position (second order precession) when a bias magnetic field is less than a demagnetizing field [1]. The precession portrait of these oscillations is large regular circular ring filled in its generatrix with small regular rings.

We investigate the equilibrium position precession in a ferrite plate with the cubic anisotropy by cubic cell [001], [011] and [111] orientation from ferrite plate normal direction. On the precession portrait we find connection between small ring compositions and spatial positions of type [111] anisotropy axis. This connection was explained by the energy potential model. We found out a very high sensitivity of a second order precession to the anisotropy constant, bias dc and alternating field values and also to the cubic cell orientation. We suppose the possibility of use a very high sensitivity phenomenon in production of microwave devices, precise angle and magnetic field sensors and in material parameters investigations.

The amplitude-frequency characteristics of the second order precession were studied. The dependence of the alternating field amplitude of transition between regimes on frequency was defined. Changes in regimes of precession were found with changes of the anisotropy constant observed at low frequencies. It was found that regime number 3 of second order precession disappear at the critical values of the anisotropy constant.

The influence of the magnetoelastic properties of the plate to the second order precession was also considered. The biggest influence of the magnetoelastic interaction on the precession was observed in the condition of the elastic resonance. Elastic oscillations at five regimes of precession were investigated and described. It is found out that magnetoelastic oscillations occur at frequency of fast magnetic oscillations (small rings), and make double-modulated oscillations of the equilibrium position. It was found out that both modulations depend of the anisotropy constant and are possible only in the regimes number 2 and number 3 of the second order precession. It was also found out that the elastic interaction enhances the effect of anisotropy.

The work is supported by Russian Foundation of Basic Research (grant №12-02-01035-a).

[1] V.S. Vlasov, L.N. Kotov, V.G. Shavrov, V.I. Shcheglov, *J. Comm. Tech. El.*, **56** (2011) 73-84.

1PO-M-11

DYNAMIC AND STATIC MAGNETIC PROPERTIES OF CVD DEPOSITED Ni₉₀Pt₁₀ FILMS

Roussigné Y.¹, Stashkevich A.¹, Fetisov L.², Mercone S.¹, Karmous F.¹, Doppelt P.¹

¹ LSPM CNRS (UPR 3407), Université Paris 13, 93430 Villetaneuse, France

² Faculty of Physics, Moscow State University, Leninskie gori 1, 119991, Moscow, Russia
silvana.mercone@univ-paris13.fr

Multilayers of ferromagnetic metals, such as Co or Ni, and non-magnetic Platinum (Pt) are characterized by a pronounced perpendicular anisotropy, which makes them extremely attractive for a number of important applications, especially in data storage [1,2]. Typically, these are ultra-thin high-quality films deposited by means of sophisticated and thus costly techniques such as sputtering or molecular beam epitaxy. In this paper we report results of the investigation of magnetic properties, both static and dynamic, of films of the Ni_xPt_{1-x} alloy prepared by Chemical Vapour Deposition (CVD). This technology, being relatively inexpensive, is widely used in electronics in general and in microfabrication processes to deposit materials in various forms (nano-tubes, for example) in particular.

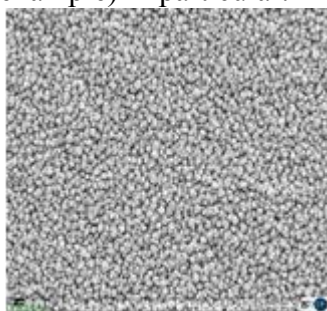


Fig.1. Typical FEG-SEM image of the sample.

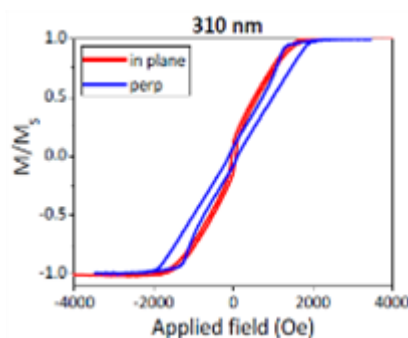


Fig.2. Typical hysteresis cycle for a thick sample.

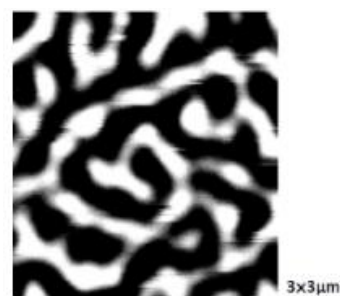


Fig.3. Typical domain pattern in the same film.

More specifically, we have studied CVD deposited Ni₉₀Pt₁₀ whose thickness varied from 140 nm to 310 nm. Our FEG-SEM and X-ray diffraction studies have revealed their nano-granular structure (grain size of several nm, see Fig.1). Static magnetic characterization relying on Vibrating Sample Magnetometer measurements (VSM) (Fig.2) and MFM imaging (Fig.3) suggests a transition from an in-plane magnetic anisotropy (thinner films) to an out-of-plane (thicker films), which means that the field of uniaxial magnetic anisotropy H_a varies from $4\pi M_s - \Delta H_a$ to $4\pi M_s + \Delta H_a$ with saturation magnetization approaching the conventional value of 6000 G and ΔH_a being on the order of a hundred Oe. Dynamic magnetic behavior was studied by means of Brillouin Light Scattering of thermal magnons. Interestingly, we have discovered an abnormally high level of microwave losses, corresponding to the equivalent FMR linewidth of $\Delta H_{FMR} \approx 2$ GHz.

ANR (Agence Nationale de la Recherche) and CGI (Commissariat à l'Investissement d'Avenir) are gratefully acknowledged for their financial support of this work through Labex SEAM (Science and Engineering for Advanced Materials and devices), as well as the Russian Fund for Fundamental Research.

[1] M. Robinson, Y. Au, J.W. Knepper, F.Y. Yang et al., *Phys. Rev.B*, **76**, (2006) 224422.

[2] P.J.Metaxas, J.P. Jamet, A. Mougín et al. *Phys. Rev. Lett.*, **99** (2007) 217208. Submitted to the *Moscow International Symposium on Magnetism*, June 29 – July 3, 2014, Moscow, RUSSIA.

IPO-M-12

NONLINEAR DAMPING OF MICROWAVE SPIN-ELECTROMAGNETIC WAVES IN INFINITE MULTIFERROICS

Ustinova I.A.¹, Cherkasskii M.A.¹

¹ St. Petersburg Electrotechnical University, St. Petersburg, Russia
ustinovairin@yahoo.com

In recent years a strong interest to new composite and structured magnetic materials has been renewed [1]. The one class of such materials is multiferroics which combine both electric and magnetic wave nonlinearities. The envelope solitons of spin-electromagnetic waves (SEWs) in infinite multiferroic medium had been studied in [2]. A nonlinear microwave phase shifter based on a planar multiferroic composite was described in [3]. In this work we report for the first time a theoretical investigation of nonlinear damping of the high power SEWs propagating in longitudinally magnetized infinite multiferroic medium. Features of the nonlinear damping of the SEWs, which were obtained in this work, could be used for creating of new microwave multiferroic devices. The study was carried out in several stages. In the first stage, the nonlinear dispersion characteristics were numerically simulated and analyzed employing nonlinear dispersion equation derived in the work [2]. In the second stage, the SEW propagation in a stable nonlinear regime was simulated numerically. The stable nonlinear regime is due to nonlinear four-wave process in which no enrichment of the spectrum of the microwave signal carried by SEWs takes place. Calculation of nonlinear damping and nonlinear phase shift was based on the nonlinear evolutionary Ginzburg-Landau equation similar to that reported in [4].

The calculation was carried out for the homogeneous multiferroic medium with parameters corresponding to two media: yttrium iron garnet (YIG) [5] and Al-substituted barium ferrite $\text{BaAl}_2\text{Fe}_{10}\text{O}_{19}$ [6]. Fig.1 shows typical simulation results for $\text{BaAl}_2\text{Fe}_{10}\text{O}_{19}$. They were calculated for bias magnetic field $H=1000$ Oe, dielectric permittivity $\varepsilon=19$, initial amplitude of SEW $|u|=0.5$, and wave number $k=7550$ m^{-1} . For these parameters SEW carrier frequency was 74.223 GHz. It is clear that the presence of nonlinear damping leads to a strong decrease in the amplitude and to the saturation of the nonlinear phase shift of SEW. It was found that the nonlinear effects become pronounced during SEW propagation if nonlinear damping coefficients exceed the following values: $\nu_1=10^8$ and $\nu_2=10^9$. For the described parameters the saturation value of nonlinear phase shift is -3.324 rad. The obtained values of the damping coefficients are found to be smaller than that for YIG films [4].

This work was supported in part by the Russian Foundation for Basic Research and the Ministry of Education and Science of Russia.

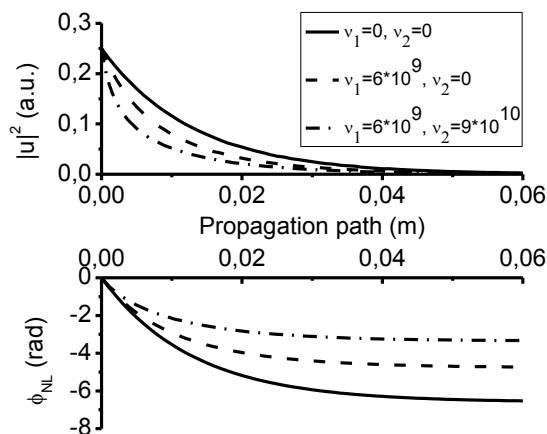


Fig. 1. Squared amplitude and nonlinear phase shift as a function of propagation path.

- [1] C.A.F. Vaz, *J. Phys.: Condens. Matter*, **24** (2012) 333201.
- [3] M.A. Cherkasskii, B.A. Kalinikos, *Tech. Phys. Lett.*, **39** (2013) 182.
- [4] A. B. Ustinov, B. A. Kalinikos, G. Srinivasan, *Appl. Phys. Lett.*, **104** (2014) 052911.
- [5] A.B.Ustinov, B.A. Kalinikos, *Appl. Phys. Lett.*, **93** (2008) 102504.
- [6] D. B. Nicholson, *Hewlett-Packard J.*, **41** (1990) 59.
- [7] A.B. Ustinov et. al., *J. Appl. Phys.*, **105** (2009) 023908.

IPO-M-13

THE ELECTROMAGNETIC TRANSPARENCY OF ANTIFERROMAGNET PLATE IN CROSSED DC MAGNETIC AND ELECTRIC FIELDS

Levchenko G.G.¹, Savchenko A.S.¹, Tarasenko A.S.¹, Tarasenko S.V.¹, Shavrov V.G.²

¹ Donetsk Institute for Physics & Engineering of the NAS of Ukraine, Donetsk, Ukraine

² Kotel'nikov Institute of Radio Engineering and Electronics of RAS, Moscow, Russia
a-savch@mail.ru

Recently, metasurfaces - electrodynamic structures, the input impedance of which depends in a specified way on the frequency, polarization, and propagation direction of the incident plane electromagnetic wave—have attracted a significant interest due to potential antenna applications[1]. However, for metasurfaces (as soon as for metamaterials), operating frequency are strictly defined and spatial dispersion effects quickly become significant with increasing frequency [2].

In this respect, of great interest would be to employ as a metasurface a spatially homogeneous medium the wave properties of which can be selectively adjusted by easily implementable external parameters (e.g., external dc magnetic \mathbf{H}_0 or electric \mathbf{E}_0 fields). Prominent among these media are antiferromagnetic (AFM) structures.

In this regard, the aim of this work is to analyze in the Voigt geometry the influence of the orientation of a constant external electric field \mathbf{E}_0 in the sagittal plane on the conditions of resonant transmission of bulk TM or TE electromagnetic (EM) waves incident on a transparent plate of a uniaxial centrosymmetric AFM in the “spin-flop” phase. In particular it was shown that for a bulk TM (TE) EM wave incident on the plate (\mathbf{q} is the normal to the plate surface) from outside the following conditions hold.

- 1) For a given wave frequency ω the half-wave transmission condition is non-reciprocal with respect to the sign inversion of the angle of incidence. In addition, for given ω and tangential wave number k_{\perp} , the absolute value of the phase of the transmission coefficient is non-reciprocal with respect to the sign inversion of $(\mathbf{E}_0\mathbf{q})$.
- 2) The sign change of the group velocity in the half-wave plate is determined by the points on the surface of wave vectors (SWV) of the layer for which, in the considered sagittal plane, the projection of the group velocity on the interface plane is zero. Such points might not exist in the cross-section of the SWV of the half-space by the sagittal plane. It is not one to one correspondence between this type points of SWV for case half-space medium and layer.
- 3) The condition of the half-wave transmission is equivalent to the dispersion relation for bulk polaritons in the considered AFM plate which has either zero surface wave impedance (for TM waves) or zero surface wave admittance (for TE waves). This condition is an electromagnetic analogue of the matching rule for an elastic wave incident from outside on a solid plate in liquid.
- 4) The condition for the half-wave transmission of a bulk TM (TE) wave through the plate is identical to the spectrum of a particular type of escaping bulk polaritons. For these values of the ω - k_{\perp} pair, when a bulk TM (TE) wave is incident on one surface of the plate embedded into symmetrical surrounding, there is no reflected wave, however, there exist a bulk wave of the same polarization emanating from another surface of the plate and carrying the energy into the lower half-space.

[1] A. Sihvola, S. Tretyakov, and A. de Baas, *J. Comm. Technol. Electron.*, **52** (2007) 986-990.

[2] A. N. Lagarkov, V. N. Kisel, A. K. Sarychev, and V. N. Semenenko, *High Temp.*, **48** (2010) 983-999.

IPO-M-14

GaBO₃: Ni SINGLE CRYSTALS STUDIED BY EPR*Seleznyova K.^{1,2}, Strugatsky M.¹, Yagupov S.¹, Kliava J.²*¹ Taurida National University, 4 Vernadsky Ave., 95007 Simferopol, Ukraine² LOMA, UMR 5798 Université Bordeaux 1-CNRS, 33405 Talence cedex, France

kira_seleznyova@mail.ru

Weak ferromagnetic iron borate, FeBO₃ is a unique crystal: one of few materials combining room temperature magnetism and high transparency up to near ultraviolet range. FeBO₃ has the rhombohedral calcite structure with the space group D_{3d}⁶. From the magnetic point of view, iron borate is a two-sublattice easy-plane antiferromagnetic with a weak in-plane moment and the Néel temperature $T_N = 348$ K. Its magnetic, optical, and magneto-optical properties have been reviewed by Diehl [1].

New materials with extraordinary physical characteristics are produced by isomorphous substitution of a part of iron in FeBO₃ crystals with various additives. In particular, Fedorov et al. have observed a photoinduced dynamical magnetic structure in Ni-containing iron borate [2]. A possible explanation of this phenomenon is the dynamical Jahn-Teller (JT) effect. In this relation, we have studied the behaviour of isolated nickel ions in gallium borate, GaBO₃, isomorphous to FeBO₃.

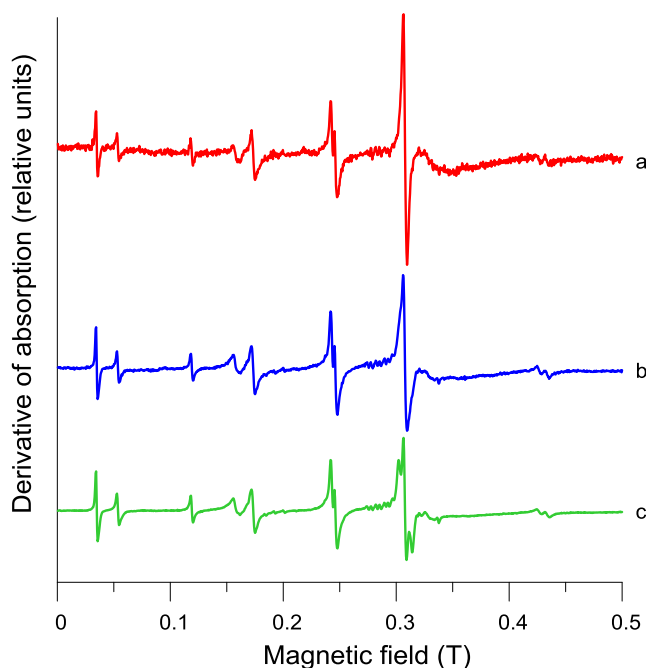


Fig. 1. EPR spectra of GaBO₃ containing 0.06 % of nickel at 36 (a), 12 (b) and 4 K (c). The spectra intensities are multiplied by the absolute temperature.

GaBO₃: Ni single crystals were studied by electron paramagnetic resonance (EPR) with a Bruker X-band (9.464 GHz) spectrometer in the temperature range from 4 to 290 K and static magnetic fields B up to 1 T. Figure 1 shows the EPR spectra of GaBO₃: Ni at different temperatures. One can observe a change in spectra shape for the feature located at ca. 0.3 T, tentatively ascribed to JT distortions. Computer simulations of the EPR spectra confirm this assumption.

Two different charge states of Ni ions have been identified by EPR. For Ni³⁺, full parametrization of the EPR spectra requires taking into account spin Hamiltonian terms cubic in the electron spin.

[1] R. Diehl, Jantz, B.I. Nolang and W. Wettling, in: Current Topics in Materials Science, E. Kaldis, ed., Elsevier, New-York, **11** (1984) 241.

[2] Yu.M. Fedorov, A.A. Leksikov and O.V. Vorotynova, *Journal of Magnetism and Magnetic Materials*, **68** (1987) 383.

1PO-M-15

AUTO-RESONANCE PARAMETRIC EXCITATION OF MAGNETIC BREATHER IN THREE-LAYERED FERROMAGNET

Ekomasov E.G.^{1,}, Nazarov V.N.^{2,1}, Murtazin R.R.¹, Shafeev R.R.¹*

¹ Bashkir State University, Ufa, Russia

² Institute of Molecule and Crystal Physics URC RAS, Ufa, Russia

EkomasovEG@gmail.com

At present sandwich-like magnetic structures are investigated extensively because there is the possibility of their practical application. Often they are periodically alternating layers of two materials with different physical properties. For the study of such new magnetic materials and processes taking place in them, are relevant investigations of the dynamic magnetization reversal, generation of homogeneous and heterogeneous structure of dynamical status under the action of high-frequency field [1, 2]. Of special interest is the study of controlled dynamic conditions, in which it is possible to achieve high angles of precession of the magnetization by fields sufficiently small amplitude [3].

This paper describes autoresonance parametric excitation of magnetic breather in three-layered ferromagnet with reduced value of the anisotropy in a thin layer by fields of variable frequency and small amplitude of a special form $h = h_1 \cos(\omega' \tau - \mu \tau^2 / 2)$. It is also believed that dissipation is weak and the frequency is the slow function of time. As it was shown [4], depending on the width of a thin layer of the magnetic reversal center with amplitude greater critical amplitude disappears, is fixed onto a thin layer, or exceeds the bounds of a thin layer, leading to formation of the domain of a new phase. In the case of an alternating external field, there is the probability of appearance of resonance effects that lead to more significant change of amplitude of breather A . With variable pump field frequency $\omega' - \mu \tau$, the time evolution of the square of the amplitude is determined from the resonance conditions $2\sqrt{1 - A^2} = \omega' - \mu \tau$. This ratio is interpreted as a capture system in parametric resonance and gives an approximate solution for the amplitude at long period of time. Near the starting point has a boundary layer, where the approximate solution is determined by the differential equations obtained by averaging. The main results of this work is concerned with the study of the averaged equations, which are called equations of main resonance. The analysis of these equations shows the existence of solutions with a growing and reduced amplitudes. Also, shown that is possibility of generation of magnetic breather with increasing amplitude in the field of thin layer from the equations of motion with the help of numerical methods.

[1] A.G. Gurevich and G.A. Melkov, *Nauka, Main Editorial for Literature on Physics and Mathematics*, Moscow, (1994) [in Russian].

[2] D.I. Sementsov and A.M. Shutyi, *Phys.Usp.*, **50** (2007) 793 [Usp. Fiz. Nauk **177** (2007) 831].

[3] M.A. Shamsutdinov, I.Yu. Lomakina, V.N. Nazarov, A.T. Kharisov and D.M. Shamsutdinov, *Nauka*, Moscow, (2009) [in Russian].

[4] V.N. Nazarov, R.R. Shafeev, M.A. Shamsutdinov, and I.Yu. Lomakina, *Physics of the Solid State*, **54** (2012) 298 (Fizika Tverdogo Tela **54** (2012) 282).

1 July

Tuesday

17:30-19:00

poster session

1PO-P

**“Soft and Hard
Magnetic Materials”**

1PO-P-1

INFLUENCE OF THE TEMPERATURE ON MAGNETIC PARAMETERS SENSITIVITY TO TENSILE STRESSES FOR AMORPHOUS FECOB RIBBONS

Gavriliuk A.A., Semenov A.L., Mokhovikov A.Yu., Morozova N.V.
Irkutsk State University, Irkutsk, Russia
zubr@api.isu.ru

Influence of the temperature on dynamic magnetic parameters sensitivity to tensile stresses for amorphous Fe₆₄Co₂₁B₁₅ ribbons was investigated. Samples of 0.05 m length and 0.8 mm width were pretreated by dc current in the density range of $j=(3,5\div 4,75) \cdot 10^7$ A/m². Dynamic magnetic properties were measured in the temperature range $T=20\div 310^\circ\text{C}$, and tensile stresses range of $\sigma=(0,5\div 9,5) \cdot 10^7$ Pa. It was figured out, maximal magnetic parameters changing has been observed at simultaneous applying of temperature and tensile stresses for pretreated samples by dc current density of $j=3,5 \cdot 10^7$ A/m².

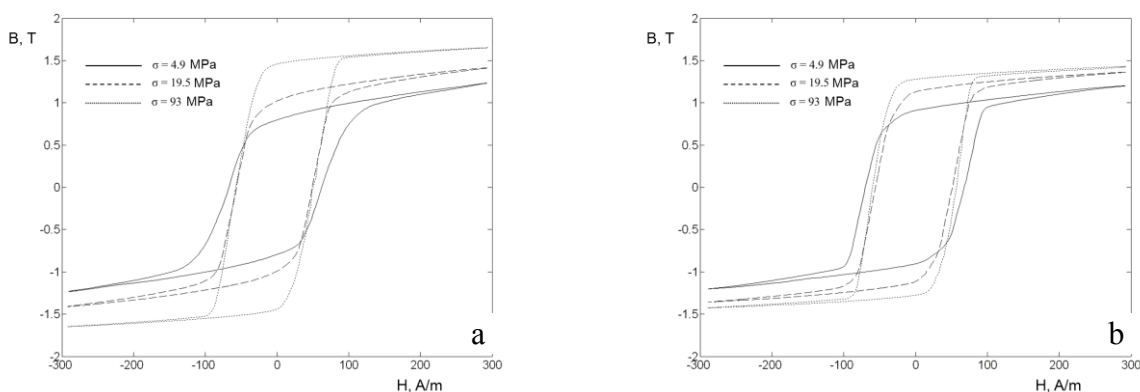


Fig.1. The hysteresis loops for amorphous Fe₆₄Co₂₁B₁₅ ribbons, pretreated by dc current density of $j=47.5$ MA/m². Heating temperature T: (a) – $T=20^\circ\text{C}$; (b) – $T=320^\circ\text{C}$.

The increase of j up to $4.75 \cdot 10^7$ A/m² led to the decrease of the temperature sensitivity of dynamic magnetic parameters versus σ . It has been shown, the remanence B_r changes strongly at increasing of T and σ . In addition, two characteristic regions have been observed on the dependence $B_r(\sigma)$ at all values of T . In the first region, there is a sharp B_r increase at small values of σ . Meanwhile, B_r increases less significantly at bigger values of σ (fig.1,2). Assuming that magnitude of B_r is determined by the induced anisotropy field for the coherent rotation magnetization process, and keeping in mind that the $B_r(T)$ dependence is like to $B_S(T)$ dependence, it has been concluded that magnetostriction behavior $\lambda_S(T)$ for ribbons is: $\lambda_S(T) \sim B_r^2(T) \sim B_S^2(T)$.

This research was held under the financial support of Russian Foundation for Basic Research (grant № 14-08-00339-a).

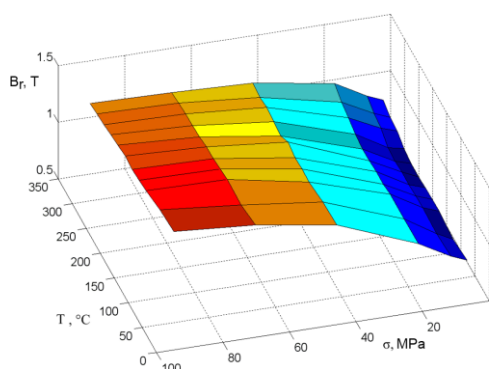


Fig.2. Remanence $B_r(T_{\text{heating}}, \sigma)$ dependencies for amorphous Fe₆₄Co₂₁B₁₅ ribbons, pretreated by dc current density of $j=47.5$ MA/m².

1PO-P-2

INFLUENCE OF THE CRYOGENIC PRETREATMENT ON DYNAMIC MAGNETIC PROPERTIES OF AMORPHOUS FeCoB RIBBONS.

Semenov A.L., Gavriiliuk A.A., Mokhovikov A.Yu., Bukreev D.A., Morozova N.V.

Irkutsk State University, Irkutsk, Russia

asem@api.isu.ru

In this work, it has been carried out the research of influence of the cryogenic pretreatment (in the liquid nitrogen with the simultaneous application of the impulse electric current) on the temperature stability of dynamic magnetic properties for amorphous Fe₆₄Co₂₁B₁₅ ribbons (0.05 m length, 0.1 mm width and 25 μm thickness). The initial instantaneous impulse electric current density range j was from 1.35 GA/m² up to 2.22 GA/m². Impulse electric current duration, corresponding to time of a current amplitude decrease in exponent times, was 0.78ms. Choice of the maximal initial instantaneous impulse electric current density and its duration were determined by the sample stability to destruction.

Influence of “heating-cooling” process on hysteresis loop behaviour, coercitivity H_c and remanence B_r have been observed by the means of the inductive method in the temperature range of $T = 20 \div 310^\circ\text{C}$ and frequency reversing field of 1 kHz. Linear heating velocity was 5°C/min. During measurements, magnetic field was applied along the sample length. Meanwhile, influence of the temperature on the sensitivity of dynamic magnetic properties to elastic tensile stresses was investigated in the range of $\sigma = (0.5 \div 9.5) \cdot 10^7$ Pa.

For all pretreated ribbons, $B_r(T, \sigma)$ and $H_c(T, \sigma)$ dependencies were obtained during “heating-cooling” cycle. Thus, on fig.1 it has been shown $B_r(T, \sigma)$ dependencies for pretreated samples at $j_0 = 2.22$ GA/m².

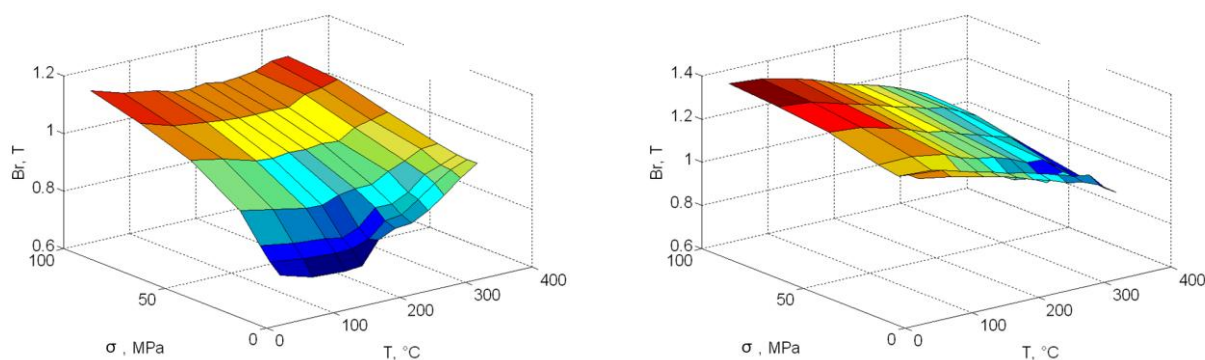


Fig.1. $B_r(T, \sigma)$ dependencies for cryogenic pretreated samples, stimulating simultaneously by impulse electric current density of $j_0 = 2.22$ GA/m² at thermocycling: a – heating, b – cooling.

It has been figured out the magnitude of the impulse electric current density during the cryogenic pretreatment has the significant influence on dynamic magnetic properties for investigated alloy. In addition, it has been carried out some features, corresponding to dynamic magnetic properties changes occurred at thermocycling for cryogenic pretreated ribbons. Thus, for instance, there are two regions on $B_r(T)$ dependence during the heating process for all pretreated samples. Decrease of B_r has been observed at the relative low heating temperature ($T = 20 \div 50^\circ\text{C}$). While B_r has increased at more high heating temperature ($T > 150 - 180^\circ\text{C}$).

This research was held under the financial support of Russian Foundation for Basic Research (grant № 14-08-00339-a).

1PO-P-3

GROWTH AND CHARACTERIZATION OF Al-SUBSTITUTED BARIUM HEXAFERRITE SINGLE CRYSTALS

Vinnik D.A.¹, Zherebtsov D.A.¹, Mashkovtseva L.S.¹, Nemrava S.², Bischoff M.², Niewa R.², Semisalova A.S.³, Krivtsov I.V.¹, Isayenko L.I.⁴, Mikhailov G.G.¹

¹ South Ural State University, Chelyabinsk, Russia

² University of Stuttgart, Stuttgart, Germany

³ Moscow State University, Moscow, Russia

⁴ Institute of Geology and Mineralogy SB RAS, Novosibirsk, Russia

denisvinnik@gmail.com

Barium ferrites are widely used in industry, e.g. in data storage and recording, transformers, communication devices, microelectronics due to high Curie temperatures, chemical stability, spontaneous magnetization and anisotropy of magnetic properties [1]. Modern developments lead to a continuous demand for materials with improved magnetic properties for science and technology applications.

Up to 2 mm large $\text{BaFe}_{12}\text{O}_{19}$ crystals doped with Al were grown from molten sodium carbonate flux on slow cooling from 1260 to 900 °C. The crystals were separated from the flux by leaching in hot nitric acid.

With iron substitution reaching up to 1.34 wt.% aluminum the unit cell parameters of the hexagonal magnetoplumbite structure change only slightly.

The volume decreases with the increasing of Al^{3+} concentration due to its smaller ionic radius in comparison with Fe^{3+} . Furthermore, a rise of aluminum level from 0.55 to 1.34 wt.% reduces the Curie temperature monotonously from 440 to 415 °C and saturation magnetization at room temperature from 68 to 46 emu/g.

Structure refinements of X-ray intensity data obtained from a single crystal with composition $\text{BaFe}_{10.8}\text{Al}_{1.2}\text{O}_{19}$ revealed Al to substitute all Fe sites except for the tetrahedrally coordinated Fe site. The highest accumulation of Al with 26 % is reached on one of the octahedrally coordinated sites, namely $M(1)$ (2a). A significant amount of aluminum is also observed on the other octahedrally coordinated sites and on the tetrahedrally coordinated position 4e, a split position between two face-sharing tetrahedral voids.

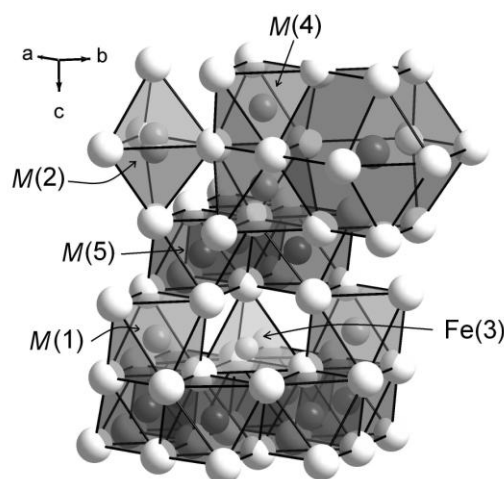


Fig. 1: Five sites of Fe in the crystal structure of $\text{BaFe}_{12}\text{O}_{19}$

[1] B. Halbedel, D.Hulsenberg, St.Belau, U.Schadewald, M. Jakob, *Cfi/Ber. DGK* **82** (2005) 10.

1PO-P-4

EFFECT OF SECONDARY DECOMPOSITION ON COERCIVITY OF Fe-Co-Cr ALLOYS WITH 15% Co

Menushenkov V.P., Shubakov V.S.

National Research Technological University "MISiS", 119049, Leninskij prospect 4, Moscow,
Russia.

menushenkov@gmail.com

Magnetically hard Fe-Co-Cr alloys remain attractive permanent-magnet materials because of the adequate combination of mechanical and magnetic properties. In general, Fe-Co-Cr alloys have the coercive force $H_{ci} = 45\text{-}52$ kA/m (560-650 Oe), which is lower than that of Alnico magnets. To widen the application of Fe-Co-Cr magnets, the increase of their coercivity is required. The magnetic properties of Fe-Co-Cr alloys are associated with a modulated microstructure, which results from the spinodal decomposition of the high-temperature bcc α -phase into α_1 and α_2 phases within the miscibility gap, which are iron- chromium-rich bcc phases, respectively. The magnetic properties are a function of the size and aspect ratio of the α_1 particles, the volume contribution of the phases and the chemical compositions of both phases.

Effect of secondary decomposition on coercivity of Fe-Co-Cr alloys with 15% Co has been studied by magnetic measurements and TEM. It was found that neither optimal regimes of step-aging nor continuous-cooling treatments followed by thermo-magnetic treatment result in secondary decomposition within both the matrix α_2 phase and the elongated α_1 particles. At higher treatment temperatures (630-600 °C), the secondary decomposition α_2 into α_1 and α_2 results in formation in the matrix surrounded the elongated α_1 particles with many fine α_1 precipitates, which increase in size, make worse the magnetic isolation of α_1 elongated particles and decrease coercive force. When the temperature of step-aging decreases in big steps, the secondary decomposition within the elongated α_1 particles takes place during treatment below 600°C. This decomposition causes the further α_1 phase separation into fine slightly elongated precipitates and decreases the coercive force.

1PO-P-5

INFLUENCE OF ARGON PRESSURE ON TEXTURE AND MICROSTRUCTURE FORMATION OF THIN Co FILMS PRODUCED BY DC-SPUTTERING

Nikulin Y.V., Dzhumaliev A.S., Filimonov Y.A.

Saratov Branch of Kotel'nikov IRE RAS, Saratov, Zelenaya 38, Russia

It is well known that in sputtering technique work gas pressure has a strong influence on thin films properties such crystallographic orientation and microstructure. Previously [1] formation of α -Co(002) textured films on SiO₂/Si substrates at high ($P \approx 0.4$ Pa) argon pressure when adatom mobility is suppressed was shown. But it wasn't until discussed what type of crystal structure and microstructure in Co films develops during sputtering at low (0.09-0.13Pa) argon pressures. In this work texture and microstructure of Co films with thicknesses $d \approx 200$ -400 nm produced by dc-sputtering at argon pressures

$P \approx 1.33$ -0.09Pa at room temperature (RT) and $T \approx 250^\circ\text{C}$ on SiO₂(300nm)/Si substrates were investigated. Target voltage was 480V. Postgrowth annealing was carried out in vacuum at 350°C during 30 minutes.

It is shown that sputtering at high ($P \approx 1.33$ Pa) argon pressures leads to formation of Co films with columnar microstructure and no sign of crystal structure (Fig.1,a,b1). Annealing of this film don't initiate crystallization process (Fig.1,a, squares line), so this films can be considered as amorphous. Decreasing of pressure to $P \approx 0.7$ -0.3Pa leads to formation Co films with columnar microstructure and crystallographic orientation (texture) of the lowest surface energy: α -Co(002) with hcp crystal structure. Annealing of these films greatly improves their crystallinity and texture (Fig.1,a, squares lines). Lowering of pressure to $P \approx 0.25$ Pa initiate formation of β -Co(200) crystal phase with fcc structure witch coexist with dominant α -Co(002) crystal phase. But, as argon pressure decreases to $P \approx 0.09$ Pa the dominant crystal phase changes from α -Co(002) to β -Co(200) (Fig.1,a,b1). Microstructure of these films is quasiuniform at thicknesses $d < d_{\text{crit}}$ (value of d_{crit} depends on deposition conditions). But as thickness d is increased ($d > d_{\text{crit}}$) microstructure changes to fibrous-grained (Fig.1,a,b2). Annealing of these films initiate α -Co(002) phase formation via crystallization of amorphous part of the film. Elevated substrate temperatures ($T \approx 250^\circ\text{C}$) at $P \approx 0.13$ -0.09Pa promotes formation of β -Co(200) crystal phase. Films deposited at $T \approx 250^\circ\text{C}$ show distinct change of microstructure from quasihomogenius for thicknesses $d < d_{\text{crit}}$ to grained at $d > d_{\text{crit}}$.

Work was supported by RFBR, grants № 14-0731107, 13-07-01023

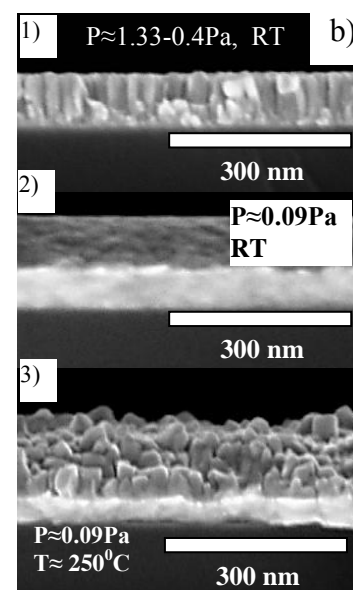
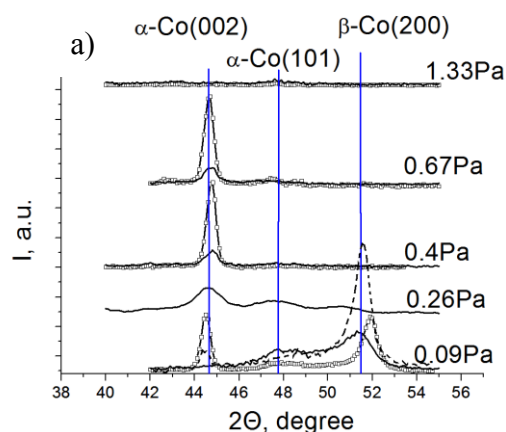


Figure 1 XRD (Cu-K α) patterns (a) and SEM cross-section view (b) of Co films deposited at different P and substrate temperature: (a) RT – straight line, $T \approx 250^\circ\text{C}$ – squares line. XRD patterns after annealing plotted as dashed line on Fig. (a).

[1] O. Kitakami, S. Okamoto, Y. Shimada. *J. Appl. Phys.*, **79** (1996) 6880.

1PO-P-6

MAGNETIC PROPERTIES OF RAPIDLY QUENCHED RIBBONS OF SOFT MAGNETIC IRON-BASED ALLOYS AFTER ANNEALING ON AIRE AND IN VACUUM

Skulkina N.A., Ivanov O.A., Stepanova E.A., Pavlova I.O.
Ural Federal University, Ekaterinburg, Russia
Elena.Stepanova@urfu.ru

The magnetic characteristics of the rapidly quenched ribbons of amorphous alloys are very low immediately upon receipt; therefore the problem of improvement of their magnetic properties is very important. The thermal processing that is carried out in different environments (e.g. annealing in vacuum, inert gas, air), is standard methods of improving of magnetic properties. Option annealing in air is the most economical. It should not lead to noticeable oxidation of the surface of the ribbon because of the relatively low temperature of isothermal shutter speed (350 - 400°C). In this work we investigated the physical cause of the influence of thermal treatment on the air and in vacuum on the magnetic properties of ribbons of amorphous soft magnetic iron-based alloys. The studies were performed on samples alloy $\text{Fe}_{81}\text{B}_{13}\text{Si}_4\text{C}_2$ with positive magnetostriction saturation. The samples had the form of strips dimensions 120 x 10 x 0,025 mm. The distribution of magnetization: relative volumes of domains with orthogonal (V_{ort}) and planar magnetization oriented along (V_{180}) and transversely (V_{90}) to axis of the ribbon was determined using the author's method [1] with an error of about 5 %. Errors in the determination of magnetic permeability and specific magnetic losses amounted to about 3% and 4% respectively. The thermal treatments were performed on samples with the same distribution of magnetization in the initial (as-quenched) state and a similar level of magnetic properties. Heat treatment in both cases was the same: the samples were heated up to 380 °C, holding at that temperature for 10 min and cooling with the speed of 10 K/min. Some results of the study are presented in the table.

State of the ribbon	μ_{max}	$V_{\text{ort}}, \%$	$V_{180}, \%$	$V_{90}, \%$	$P,$	$P_h,$	$P_{\text{dyn}},$
					W/kg	W/kg	W/kg
$B = 1,0 \text{ T}, f = 400 \text{ Hz}$							
Annealing on air	64000	14	62	24	1,48	0,64	0,84
Annealing in vacuum	92000	8	71	21	2,28	0,59	1,69

You can see that after heat treatment in vacuum samples have higher values of maximum magnetic permeability due to the formation of states with smaller relative volume domains with orthogonal magnetization and greater severity of magnetic texture in the plane of ribbon (V_{180}/V_{90}). However, after heat treatment in vacuum specific magnetic loss is higher. It is associated with high values of the dynamic component specific magnetic losses. The obtained results are explained in terms of the theory of directed regulation. The interaction of the ribbon with atmospheric water vapor at heat treatment in air leads to anisotropic oxidation and hydrogenisation of the surface. During annealing along the axis of the tape is formed increased concentration is introduced in the surface of ribbon atoms of hydrogen and oxygen. As a result, after annealing in the ribbon takes place tensile stresses along its axis, which lead to a reduction in the width of domains. The decrease of movement speed of domain walls in the process of magnetization reversal leads to decrease of dynamic component in specific magnetic losses.

[1] N.A. Skulkina, O.A. Ivanov, E.A. Stepanova, *Izvestiya Akademii Nauk. Ser. Fizicheskaya* **65**, 10 (2001) 1483-1486.

1PO-P-7

STUDIES OF THE DEFECTS INFLUENCE ON MAGNETIC PROPERTIES OF GLASS-COATED MICROWIRES

Zhukova V.¹, Churyukanova M.², Shuvaeva E.², Kaloshkin S.³, Kostitcyna E.², Talaat A.¹, Ipatov M.¹, Zhukov A.^{1,3}

¹Dpto. Física de Materiales, Fac. Químicas, UPV/EHU, 20009 San Sebastian, Spain

²National University of Science and Technology "MISIS", Moscow, 119049, Russia

³IKERBASQUE, Basque Foundation for Science, 48011 Bilbao, Spain

valentina.zhukova@ehu.es

Glass-coated amorphous microwires exhibiting soft magnetic properties attracted considerable technological interest owing to excellent magnetic properties, such as magnetic bistability, excellent magnetic softness and giant magneto-impedance, GMI, effect observed in amorphous microwires [1]. Until now most attention has been paid to the optimization of magnetic properties of amorphous microwires through the tailoring of the magnetoelastic anisotropy arising mostly from the different thermal expansion coefficients of metallic nucleus and glass coating during rapid solidification of the composite microwires [1].

Recently we reported that existence of the intrinsic defects related to the proper technological procedure of glass-coated microwires fabrication limits the domain wall velocity of the magnetization switching [2]. The origin of these defects in ferromagnetic amorphous microwires is unclear.

In fact fabrication involves complex metallurgical processes related with the melting of the metallic ingot by electromagnetic field of the inductor, the chemical interaction between the metallic alloy and the glass coating at elevated temperatures and simultaneous rapid solidification of metallic nucleus surrounded by the glass shell. These problems have been previously studied only for the non-magnetic (mostly Cu and Ag-rich) alloys produced by the same technology [1]. The character of interaction depends on chemical composition of the ingot as well as on properties and composition of the glass used for the casting process [1]. Consequently, in this paper we present our last results on studies of the inhomogeneities related with the fabrication process of amorphous ferromagnetic microwires.

We used the optical and scanning microscope for the studies of the composition and surface defects in Co- and Fe-rich glass-coated microwires.

Electron scanning allows obtaining images of the surface with high spatial resolution (a few nanometres), as well as to determine the composition, structure and properties of surface layers of materials.

We observed variation of Fe, Co and Si content along the microwires and oxygen presents in "defective" regions on the metallic nucleus surface. We observed the presence of oxygen not only in the glass, but in some parts of the metallic nucleus. Understanding of the origins of the defects is essential for enhancement of magnetic properties of glass-coated microwires.

Support by EU under FP7 "EM-safety" project, Spanish and the Basque Government is acknowledged.

[1] M. Vazquez, H. Chiriac, A. Zhukov, L. Panina, and T. Uchiyama, *Phys. Status Solidi A*, **208** (2011) 493–501.

[2] A. Zhukov, E. Kostitcyna, E. Shuvaeva, S. Kaloshkin, M. Churyukanova, V. Sudarchikova, A. Talaat, V. Zhukova, *Intermetallics*, **44** (2014) 88-93.

1PO-P-8

MONTE CARLO STUDY OF THE MAGNETIZATION BEHAVIOR IN SINGLE CRYSTAL AND POLYCRYSTALLINE Ni₂MnGa HEUSLER ALLOY

Pavluhina O.O.¹, Buchelnikov V.D.¹, Sokolovskiy V.V.^{1,2}

¹ Chelyabinsk State University, Chelyabinsk, Russian Federation

² National University of Science and Technology «MIS&S», Moscow, Russian Federation
pavluhinaoo@mail.ru

Magnetic shape memory alloys (MSMA) have attracted major interest due to large field-induced strains, rapid response rates and low energetic costs. The outstanding properties of these smart intermetallics are based on the interplay of structural and magnetic order. One of the famous prototype of MSMA is Heusler Ni₂MnGa alloy [1]. In spite of the large number theoretical works devoted to investigation of physical properties of Ni-Mn-Ga, at present there is no published evidences of the modeling of temperature dependencies of the magnetization curves in different magnetic fields for Ni₂MnGa alloy in the framework of microscopic statistical model using Monte Carlo technique.

This work is devoted to investigation the magnetization behavior in the single crystal and polycrystalline Ni₂MnGa in different magnetic fields. To discuss qualitatively physical properties associated with magnetic transitions and structural change of crystalline lattice in Heusler alloys it is necessary to employ a complex model with both magnetic and structural interactions. We improved our magnetostructural Potts-Blume-Emery-Griffiths Hamiltonian, which has been approved well for Heusler systems [2, 3]. It is significant that novel features of the proposed Hamiltonian are contained in account of long-range *ab initio* exchange interactions up to eight coordination shells and magnetic domains in which magnetic moments are interacted with the specific probability factor. In particular, the proposed microscopic approach with stochastic competition of the magnetic anisotropy field and external magnetic field is important in understanding the behavior of magnetic domains in a martensitic state, which is a key property for the magnetic shape memory effect.

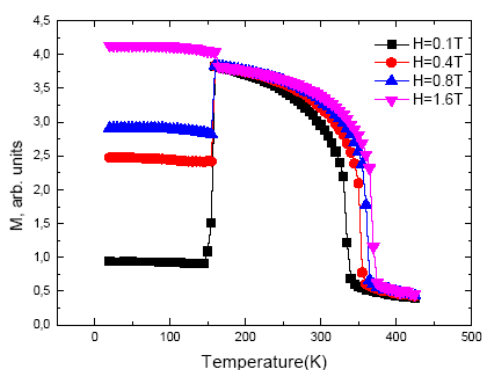


Fig. 1. Temperature dependence of the magnetization Ni₂MnGa.

For construction magnetic domain blocks, we are divided the model lattice into 16 and 32 sublattices (domain blocks) with random initial q-Potts variables (i.e. the spin directions of the domains are different from each other). Fig. 1 shows the calculated temperature dependence of the magnetization for 32 domain blocks in different magnetic field. We can see a good agreement of the magnetization curves for series of magnetic fields with experimental one [4].

This work is supported by RFBR Grants # 14-02-01085 and the Creation and Development Program of NUST “MIS&S”.

- [1] A.N. Vasil'ev et al., *Phys. Uspekhi*, **46** (2003) 559.
- [2] V.D. Buchelnikov et al., *Phys. Rev. B*, **81** (2010) 094411.
- [3] V.D. Buchelnikov et al., *J. Phys. D Appl. Phys.*, **44** (2011) 064012.
- [4] P.J. Webster et al., *Philos. Mag. B*, **49** (1984) 295.

1PO-P-9

TEMPERATURE-INDUCED TRANSFORMATION OF DOMAIN STRUCTURES IN MAGNETIC MICROWIRES

Chizhik A.¹, Zhukov A.^{1,2}, Gonzalez J.¹, Stupakiewicz A.³, Maziewski A.³, Zablotskii V.⁴

¹ Universidad del País Vasco UPV/EHU, San Sebastian, Spain

² IKERBASQUE, Basque Foundation for Science, Bilbao, Spain

³ University of Bialystok, Bialystok, Poland

⁴ Institute of Physics ASCR, Prague, Czech Republic

oleksandr.chyzyk@ehu.es

With the task of stable operation of the magnetic sensors using magnetic microwires as an active elements the investigation of the domain structure and magnetization reversal have been performed (glass-coated amorphous microwire with the nominal composition $\text{Fe}_{5,71}\text{Co}_{64,04}\text{B}_{15,88}\text{Si}_{10,94}\text{Cr}_{3,40}\text{Ni}_{0,03}$, metallic nucleus radius 50 μm , glass coating thickness 20 μm , ratio of metallic nucleus diameter to total microwire diameter $\rho = 0.7$). The investigations have been performed using the magneto-optical Kerr effect by means of polarizing microscopy at the temperature range 300-500 K. The microwire was mounted in the thermo-controlled stage.

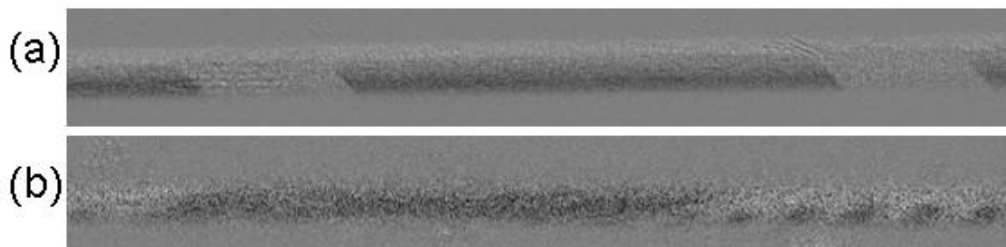


Fig. 1. Surface domain structure observed at 300K (a) and 350K (b).

It was found the heat induced change of the surface hysteresis loops and surface domain structure. At the temperature of about 350 K the regular domain structure (Fig. 1(a)) experiences the strong transformation. The different types of surface domains occur at this temperature (Fig. 1(b)). The domain structure is characterized by the unregularity and long distance distribution of the domain period.

The surface domain structure is determined basically by the magnetoelastic anisotropy. This magnetoelastic anisotropy is affected by internal stresses which in turn are originated by the difference in the thermal expansion coefficients between the glass coating and the ferromagnetic nucleus. The heating process changes the original stress distribution and in such a way produces the new distribution of surface anisotropy along the microwire. Namely this distribution is the most probable cause of the observed variety of surface domains and the hysteresis transformation.

[1] A. Chizhik, J. Gonzalez, *Pan Stanford Publishing, Singapore*, (2013).

1PO-P-10

SINGULAR POINTS IN VORTEX DOMAIN WALLS

Zverev V.V.¹, Filippov B.N.^{1,2}, Dubovik M.N.^{1,2}

¹ UrFU, Yekaterinburg, Russia

² IMP UB RAS, Yekaterinburg, Russia
dubovik@imp.uran.ru

The asymmetric domain walls in magnetically uniaxial films with in-plane anisotropy are found in several symmetrically equivalent forms [1]. A global domain wall in a real film usually consists of segments with specific orientation and chirality separated by transition structures (TS). Recently the existence of TS with a singular point (Bloch point) in the asymmetric Bloch wall (one-vortex wall) was demonstrated numerically [2]. Here we report the results of numerical simulations of a metastable configuration with two segments of the asymmetric Néel wall (two-vortex wall) and a TS with two singular points.

The conjugate gradient method was employed to minimize the energy (based on the Fletcher-Reeves algorithm). The calculations were performed using OOMMF solver [3]. We considered a rectangular shaped Permalloy film element with the sizes $L_x=100$ nm (film thickness), $L_y=400$ nm (inter-domain distance) and $L_z=750$ nm (along the domain wall and the easy axis; with periodic conditions).

We have used a procedure for visualisation of singular points and vortex cores [2]. The method is based on evaluations of topological charges by the way of calculating contour and surface integrals. The Bloch points are found to arise at the intersections of the vortex cores belonging to the domain wall segments with different orientations.

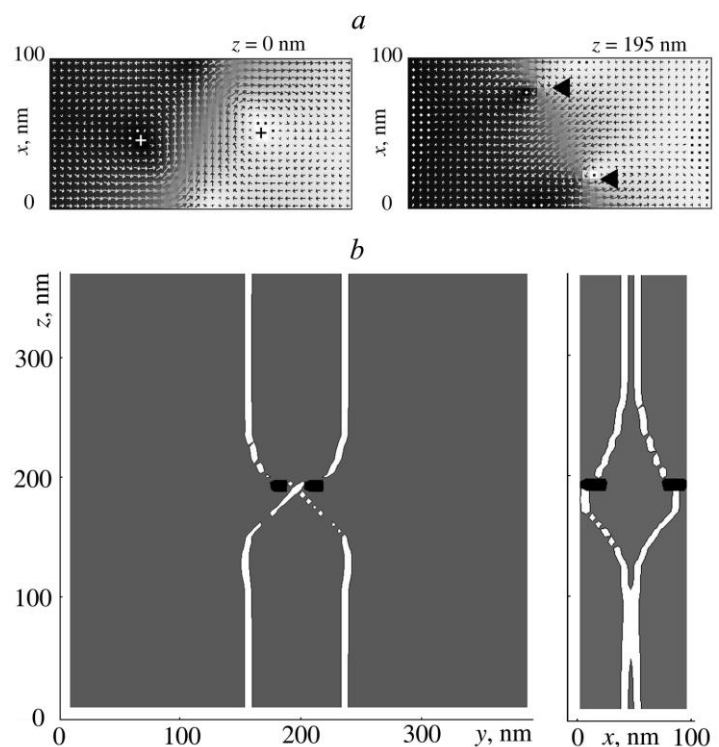


Fig. 1. (a) Asymmetric Néel domain wall sections. Singular points marked by the black triangles.

(b) Visualisation of the topological structure: the TS with two singular points in the asymmetric Néel wall. Light curves – yz (left) and xz (right) projections of the vortex cores; black bars – the singular points.

[1] R. Schäfer, W.K. Ho, J. Yamasaki, A. Hubert, F.B. Humphrey, *IEEE Trans. Magn.*, **27** (1991) 3678-3689.

[2] V.V. Zverev, B.N. Filippov, *JETP*, **117** (2013) 108-120.

[3] M.J. Donahue, D.G. Porter. *OOMMF User's Guide, Version 1.0* (NISTR, Gaithersburg, 1999).

1PO-P-11

THE EVIDENCE OF 3d-4f HYBRIDISATION IN MAGNETIC RARE-EARTH COBALT ARSENIDES RCo_2As_2

Menushenkov A.P.¹, Geondzhian A.Y.¹, Yaroslavtsev A.A.¹, Chernikov R.V.², Tan X.³, Shatruk M.³

¹National Research Nuclear University “MEPhI”, 115409, Moscow, Russia

²DESY Photon Science, D-22607, Hamburg, Germany

³Department of Chemistry and Biochemistry, Florida State University, FL 32306, Tallahassee, USA
areyougeonda@gmail.com

The recently prepared compounds RCo_2As_2 (R = La, Ce, Pr) of the ThCr_2Si_2 structure type are appealing from the magnetism point of view [1]. These compounds include two types of magnetic sublattices such as Co sublattice with delocalized 3d electrons and rare-earth sublattice with localized 4f-electrons, the interaction between which gives rise to a specific magnetic behavior. In present research the local electronic and atomic structure of phase-pure RCo_2As_2 compounds was studied by means of X-ray absorption spectroscopy. From the EXAFS data the interatomic R-Co, Co-Co and Co-As distances were obtained in 10-300 K temperature range. The XANES study of CeCo_2As_2 showed the cerium valence to be close to +3 but with small +4 contribution (Fig. 1), i.e. Ce is in the intermediate valence state. The decreasing of Ce-Co bond length with temperature correlates with Ce valence, which might indicate the strong 3d-4f hybridization in compound. Therefore, similar to related RCo_2P_2 materials [2, 3, 4], the magnetic properties of arsenides RCo_2As_2 might be influenced by the valence instability of rare-earth and behavior of other local parameters.

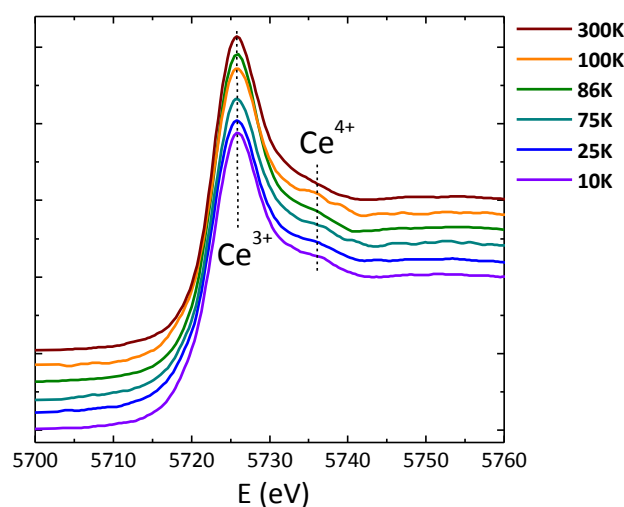


Fig. 1: L_3 -Ce XANES spectra of CeCo_2As_2 compound vs. temperature. Two contributions of cerium in different valence states Ce^{3+} and Ce^{4+} are marked.

- [1]. C.M. Thompson, K. Kovnir, S. Eveland, et al., *Chem. Commun.*, **47**(19) (2011) 5563.
 [2]. M. Chefki, M.M. Abd-Elmeguid, H. Micklitz, et al., *Phys. Rev. Lett.*, **80** (1998) 802.
 [3]. K. Kovnir, W.M. Reiff, A.P. Menushenkov, et al., *Chem. Mater.*, **23**(12) (2011) 3021.
 [4]. A.A. Yaroslavtsev, A.P. Menushenkov, et al., *JETP Letters*, **96**(1) (2012) 44

1PO-P-12

SUBSTITUTION AND PRESSURE EFFECTS ON MAGNETIC PROPERTIES OF $(\text{Fe}_{1-x}\text{Co}_x)_7\text{Se}_8$ COMPOUNDS

Ibrahim P.N.G.¹, Schottenhamel W.², Wolter A.U.B.², Büchner B.², Selezneva N.V.¹, Volegov A.S.¹, Baranov N.V.^{1,3}

¹ Institute of Natural Sciences, Ural Federal University, Ekaterinburg, Russia

² Leibniz Institute for Solid State and Materials Research, Dresden, Germany

³ Institute of Metal Physics, RAS, Ekaterinburg, Russia

Iron-selenide compounds with a composition around the equiatomic one have attracted great attention in recent years because of superconductivity observed in the FeSe compound having a small Fe excess and a tetragonal crystal structure of the PbO-type. Superconductivity and magnetic properties of this compound are strongly affected by substitutions and pressure. The aim of the present work is to study the influence of the Fe for Co substitution and hydrostatic pressure on magnetism of the iron-selenide compound Fe_7Se_8 with iron deficiency. The Fe_7Se_8 compound has a layered hexagonal superstructure of the NiAs type and shows soft ferrimagnetic properties below 455 K, while the isostructural compound Co_7Se_8 is a Pauli paramagnet [1]. The physical origin of the transition from ferri- to paramagnetism in the $(\text{Fe}_{1-x}\text{Co}_x)_7\text{Se}_8$ remains an open question.

In the present work a series of pseudobinary compounds $(\text{Fe}_{1-x}\text{Co}_x)_7\text{Se}_8$ has been synthesized by solid state reactions. The sample quality and changes in their crystal structure were examined by X-ray powder diffraction (Bruker D8 ADVANCE diffractometer with Cu K_α radiation), the magnetization measurements were made by means of a MPMS Quantum Design magnetometer equipped with a special cell at pressures up to 4.3 GPa.

All the obtained $(\text{Fe}_{1-x}\text{Co}_x)_7\text{Se}_8$ samples have a hexagonal superstructure of the NiAs type. The substitution of Co for Fe is accompanied by a substantial decrease of the c -parameter, spontaneous magnetization (M_s) and magnetic ordering temperature (T_N) (Fig. 1). The long-range ferrimagnetic order disappears at a critical concentration $x_c \sim 0.65$. The high-pressure measurements have revealed that an applied pressure of about 4 GPa leads to the collapse of the magnetic order in $(\text{Fe}_{0.6}\text{Co}_{0.4})_7\text{Se}_8$ (Fig.1). The results obtained allow us to suggest that the average interlayer distance is a key factor that governs the magnetism in these compounds.

This work was supported by RFBR (project 13-02-00364) and by the program of the Ural Branch of RAS (project No 12-T-2-1012).

[1] M. Sato, T. Kamimura, K. Iwata, *J. Appl. Phys.*, **57** (1985) 3244.

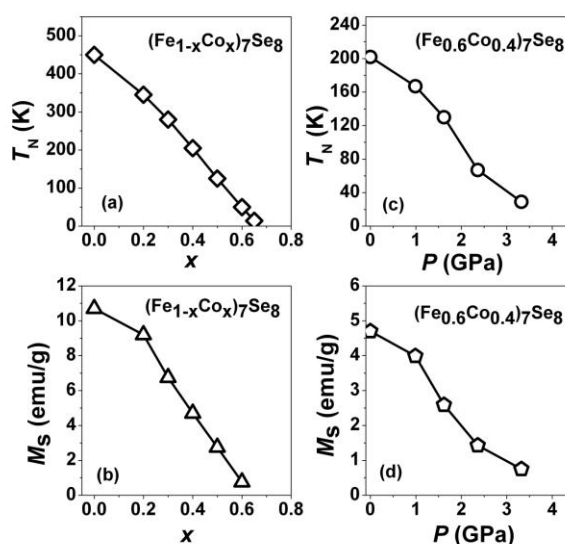


Fig. 1. Concentration dependence of the Neel temperature (a) and spontaneous magnetization (b) for the $(\text{Fe}_{1-x}\text{Co}_x)_7\text{Se}_8$ system; and the pressure dependence of T_N (c) and M_s (d) for $(\text{Fe}_{0.6}\text{Co}_{0.4})_7\text{Se}_8$.

1PO-P-13

PERIODIC VARIATION OF MAGNETIC ANISOTROPY IN MACROSTEPPED EPITAXIAL Co(111) FILMS

Davydenko A.V.¹, Kozlov A.G.¹, Chebotkevich L.A.^{1,2}

¹ Far Eastern Federal University, Vladivostok, Russia

² Institute of Automation and Control Processes, Vladivostok, Russia

avdavydenko@gmail.com

Magnetic anisotropy is one of the most important parameters of magnetic materials. Precise tuning of energy of magnetic anisotropy and geometrical dimensions of magnetic nanostructures allows obtaining desired magnetization reversal processes and domain patterns in magnetic nanostructures. Generally, magnetic anisotropy induced in magnetic nanostructures is uniform, however, searching for new artificial structures with novel magnetic properties causes applying new approach in modification of magnetic properties of nanostructures - spatial modulation of magnetic anisotropy [1]. We modulated magnetic anisotropy in Co films by modification of the topography of underlying Si(111) substrate.

We prepared Si(111) substrates with macrostep-bunches by curtain direct current annealing procedure. Single macrostep-bunch with height of 75-85 nm consisted of microstep-bunches with height of 4-6 nm divided by microterraces with the average width of 60 nm. Macrostep-bunches are divided by atomically flat macroterraces with the average width of 1.6 μm . The average sum width of macrostep-bunch and macroterrace is 2.3 μm . Periodic modulation of the topography of the Si(111) substrate induced spatial variation of the in-plane magnetic anisotropy in Co(111) film grown on macrostep-bunched Si(111) surface.

The easy axis of the magnetization of step-induced anisotropy was directed along the steps of the substrate both in the flat and stepped regions of the Co(111) film. The energy of the uniaxial magnetic anisotropy in the areas of the Co(111) film deposited on stepped surface was higher by the order of magnitude than the energy of the magnetic anisotropy in the areas grown on terraces. When magnetic field was applied along the easy axis of the magnetization, areas of the

Co(111) film located on terraces reversed in the lower negative fields than areas of the Co film located on the step-bunches. Hence we obtained quasi lateral spin-valve magnetic system characterized not by the alternating magnetic materials with different magnetic parameters, but by the alternating magnetic anisotropy in the same magnetic material. We showed the possibility to stabilize in the absent magnetic field magnetic state of the Co(111) film with high density of 180° Neel domain walls “artificially” created by anisotropy modulation.

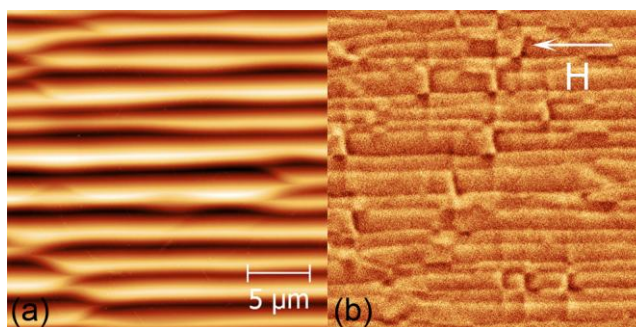


Fig.1. (a) Topography and (b) domain structure of the Co(111) film in the magnetic field $H = -70$ Oe.

[1] A. Aziz, S. J. Bending, H. G. Roberts, S. Crampin, P. J. Heard, and C. H. Marrows, *Phys. Rev. Lett.*, **97** (2006) 206602-1-4.

1PO-P-14

Fe-Zr-N FILMS: SYNTHESIS, PHASE AND STRUCTURAL STATES, AND MAGNETIC PROPERTIES

Sheftel E.N.¹, Kiryukhantsev-Korneev Ph.V.², Titova A.O.³, Harin E.V.¹, Tedzhetov V.A.¹, Semisalova A.S.³, Perov N.S.³, Trukhanov P.A.²

¹ A. A. Baikov Institute of Metallurgy and Material Science RAS, Moscow, Russia

² National University of Science and Technology "MISIS", Moscow, Russia

³ M.V. Lomonosov Moscow State University, Moscow, Russia
alextitova93@gmail.com

Nanocrystalline films of Fe-ZrN quasicutectic alloys are a novel class of soft magnetic materials possessing high saturation magnetization, low coercive force and thermal stability [1]. As such films' magnetic properties described by the random anisotropy model [2] are determined by their chemical composition and phase-structural state which in its turn is strongly dependent on magnetron sputtering conditions, the task of great importance is studying the correlation between these parameters.

To obtain Fe-Zr-N films with various Zr content we used FeZr_X targets (X = 2.4, 5.3, and 13.4 wt.%), being Fe disc with evenly distributed Zr pieces. In the magnetron chamber under exposure to plasma flame there occurred surface melting of Fe and Zr forming an alloy in the erosion zone. Deposition took place in gas atmosphere of Ar, Ar+5%N² or Ar+15%N² under total pressure of p_{Ar+N₂} 0,1-1 Pa. Glass plates were used as substrates. After sputtering the films were annealed in vacuum at 300, 400, 500, and 600°C during 1 hour to study thermal stability of their properties. The chemical composition and surface morphology of the films were studied by GDOES, EDS and SEM methods. Estimation of phase content was made using XRD. Magnetic properties were measured by VSM. The magnetic structure parameters of the films were evaluated by correlation magnetometry method [3].

Chemical composition of the films changes according to sputtering conditions within the range of 48-98 at.% Fe, 2-34 at.% Zr and 0-18 at.%. In the films there are different combinations of the following nanocrystalline phases: bcc solid solution on the base of α -Fe, γ -Fe₄N, ϵ -Fe₃N, and fcc-ZrN with grain size of 3-38 nm for the corresponding phases. On simultaneous Zr and N content increase the coercive force decrease in the films is observed (from 19 to 1 Oe due to grain size decrease) as well as the decrease of saturation magnetization (due to Zr and N content increase in solid solution on the base of bcc-Fe and Fe nitrides formation). Annealing at 400 and 500°C results in the lowest coercive force due to the decrease of effective local magnetic anisotropy owing to bcc-Fe grain release from solid solution without grain size growth. Annealing at 500 and 600°C results in quality change of hysteresis loop shapes due to microstructural alterations which cannot be defined by XRD method. All annealing processes result in increase of stochastic domain sizes which can result from increase of exchange stiffness owing to release of bcc-Fe grains from solid solution.

Support by RFBR (12-02-00116a) and by Presidential grant supporting leading scientific schools (NSh-6207.2014.3) is acknowledged.

[1] E. N. Sheftel, *Inorganic Materials: Applied Research*, **1** (2010) 17-24.

[2] G. Herzer, *Acta Materialia*, **61** (2013) 718-734.

[3] R.S. Iskhakov, S.V. Komogortsev, *Phys. Met. Metallogr.*, **112** (2011) 666-681.

1PO-P-15

MAGNETISM AND MAGNETOELASTICITY OF TbFe₅Al₇

Andreev A.V.¹, Gorbunov D.I.^{1,2}, Yasin S.³, Mushnikov N.V.⁴, Skourski Y.³, Zherlitsyn S.³,
Wosnitzer J.³

¹ Institute of Physics, Na Slovance 2, 182 21 Prague, Czech Republic

² Charles University, DCMP, Ke Karlovu 5, 121 16 Prague, Czech Republic

³ Dresden High Magnetic Field Laboratory, Helmholtz-Zentrum Dresden-Rossendorf, D-01314
Dresden, Germany

⁴ Institute of Metal Physics, Kovalevskaya 18, 620990 Ekaterinburg, Russia
a.andreev@seznam.cz

The TbFe₅Al₇ compound with a tetragonal crystal structure of the ThMn₁₂ type is a highly anisotropic ferrimagnet with Curie temperature $T_C = 242$ K and compensation point $T_{\text{comp}} = 84$ K [1]. In the present work magnetism and magnetoelasticity of a TbFe₅Al₇ single crystal have been studied in magnetic fields up to 60 T. TbFe₅Al₇ displays easy-plane anisotropy. In the vicinity of $T = T_{\text{comp}}$ the compound exhibits a spontaneous spin-reorientation transition from [100] to the [110] axis accompanied by pronounced anomalies in the relative sound-velocity change, $\Delta v/v$, and sound attenuation, $\Delta\alpha$ (Fig. 1). Field-induced magnetic transitions have been observed in TbFe₅Al₇ along the easy magnetization direction. Step-wise rotation of the magnetic moments with a wide hysteresis occurs for fields applied along the [100] axis at $T < T_{\text{comp}}$ and along the [110] axis at $T > T_{\text{comp}}$ (Fig. 2). The transitions affect sound propagation reflecting strong magnetoelastic interactions. The critical field of the transitions tends to zero near the compensation point and grows sharply away from it (inset in Fig. 2). From the obtained high-field data and using molecular-field theory the Tb-Fe inter-sublattice exchange constant has been determined to be $\lambda = 6.7$ T f.u./ μ_B (at $T = 2$ K).

[1] D.I. Gorbunov, A.V. Andreev, *J. Alloys Compd.* **577** (2013) 203-210.

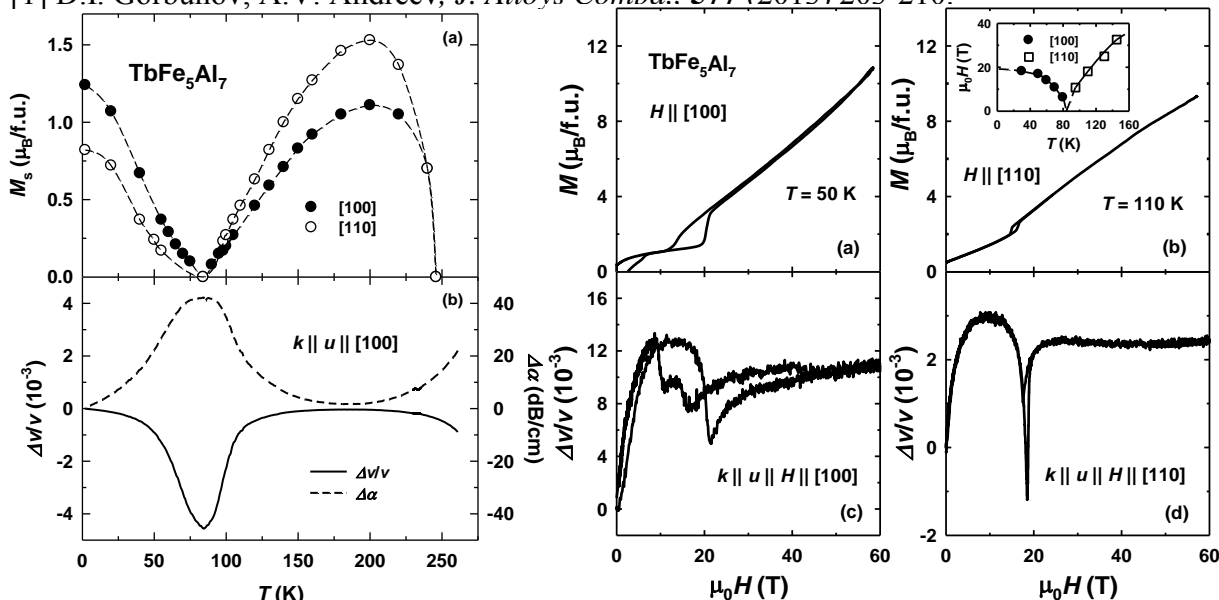


Fig. 1. Temperature dependence of (a) spontaneous magnetization along [100] and [110] and (b) of the relative change of the sound velocity and sound attenuation of a longitudinal acoustic wave propagating along the [100].

Fig. 2. Magnetization (a and b) and relative change of the sound velocity (c and d) measured for fields applied along the [100] axis of TbFe₅Al₇ in pulsed magnetic fields at 50 and 110 K. The inset shows the $T-H$ phase diagram.

1PO-P-16

PRESSURE EFFECTS ON TRANSPORT PROPERTIES OF $\text{La}_{0.85}\text{Sr}_{0.15}\text{MnO}_3$ SINGLE CRYSTALS

Shakin A.A.¹, Abashev D.M.¹, Shulyatev D.A.¹, Privezentsev R.V.¹, Andreev N.V.¹, Mukovskii Ya.M.¹

¹National University of Science and Technology "MISIS", Moscow, Russia

shakin-misis@yandex.ru

The transport properties of doped lanthanum manganites are strongly influenced by the subtle coupling of the spin, charge and lattice degrees of freedom. External hydrostatic pressure was chosen as method of exposure because it is “clean” method to change long range and local structure unlike chemical doping, which may change both the Mn valence and structure [1]. We have studied the system $\text{La}_{0.85}\text{Sr}_{0.15}\text{MnO}_3$ which has two transitions in temperature interval from 300 K to 70 K: insulator-metal transition at 245 K and charge ordering (transition from ferromagnetic metal to ferromagnetic insulator) at 204 K. We observed, that T_{IM} increases and T_{CO} decreases with the external hydrostatic pressure in the range of 0.1 MPa - 1.3 GPa. It is depicted in Fig 1. Growth of T_{IM} reveals that the application of pressure relaxes the lattice distortion and enhances the double-exchange interaction. Reduction of T_{CO} is related to destabilization of ordered Yahn Teller polarons and enhancing of electron hopping. According to phase diagrams of $\text{La}_{1-x}\text{Sr}_x\text{MnO}_3$ transition temperatures of $\text{La}_{0.85}\text{Sr}_{0.15}\text{MnO}_3$ change with amount of doped Sr (x) in the same way. Thus, the effects of hydrostatic pressure are equivalent to that of chemical doping.

This work was supported by RFBR 12-02-00717-a.

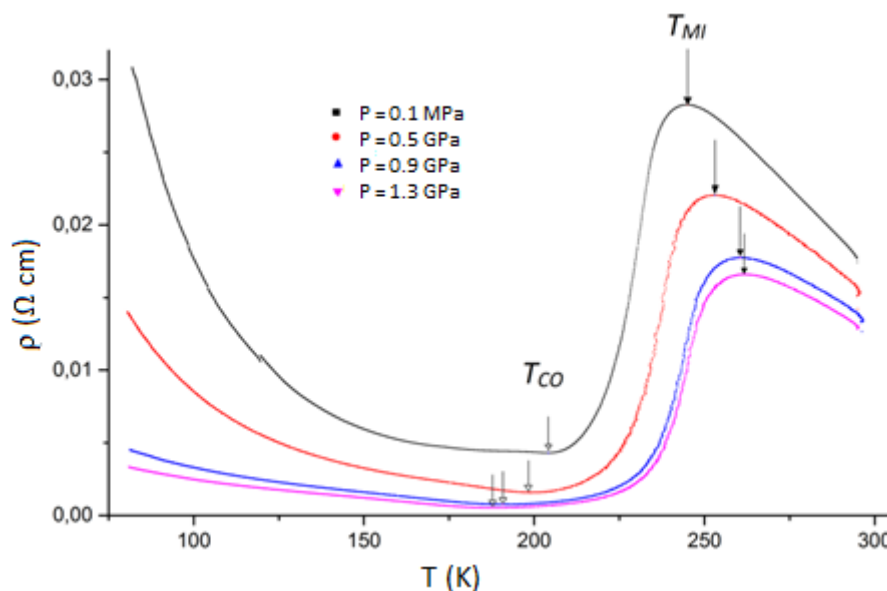


Fig 1. Temperature dependence of resistivity at various pressures for $\text{La}_{0.85}\text{Sr}_{0.15}\text{MnO}_3$ single crystal

[1] Congwu Cui, Trevor A. Tyson, Zhong Zhong, Jeremy P. Carlo and Yuhai Qin, *Physical Review B*, **67** (2003) 104107.

1PO-P-17

LAWS OF VOLUME ELASTICITY IN PHYSICAL PROCESSES OF FORMATION OF PHASE STATES AND PROPERTIES

Polyakov P.I.

Institute for Physics of Mining Processes, Donetsk, Ukraine
poljakov@mail.fti.ac.donetsk.ua

While studying a complex state of material, a researcher faces a great amount of information without proper treatment of the results. The empirical principles are not formulated correctly that does not contribute to the understanding of reality. A very complex task of a researcher is the control of intuition that allows one to distinguish sign of objective universality. Otherwise, it is impossible to suggest a real model of the studied physical process where any quantitative changes do not influence the basic physical principles forming the structure of a solid and cover a wide variety of macroand microscopic properties of the studied system.

Now we shall evaluate the levels of energy contribution in the course of consideration of critical phenomena and properties. This matter touches upon principal questions of the direct relation between thermodynamic parameters and structure evolution through the mechanisms of elastic stresses affecting the volume and other parameters controlling the structural phase transitions and the properties of phase states.

The most explicit demonstrations of this phenomenon are Kapitza's linear law and the statement of deforming effect of H-magnetic field [1], linear laws of elasticity under pressure in the works of Bridgman [2] and Vereschagin. The conception is also confirmed by linear regularities of conductivity in superconductors within a wide temperature range and structure parameters. Very important results of established analogies of P-T-H effect on the resistive, resonance properties and phase transitions are presented in [3]. They determine the causing role of transformed energies of elastic strains.

We shall estimate the energy of Coulomb interactions as $1 \div 10$ eV, the influence of the crystal field as $0.1 \div 1$ eV, spin-orbit relationship as $10^{-2} \div 10^{-1}$ eV, spin-spin (magnetic) bond as 10^{-4} eV, electron-nuclear bond as $10^{-4} \div 10^{-5}$ eV. According to our estimations, the energy of elastic stresses with taking into account the coefficient of compressibility is $1 \div 10$ eV. We should take into account that quantum mechanical forces forming the magnetism are of short range in fact, so deep understanding of the regularity if interaction is necessary for the estimation of this process. The elastic energy is an immediate energy of long range. These are elastic stresses in the structure that form the linearity of the magnetization regardless of important details of microscopic interactions. By definition, atoms and molecules have small magnetic moments of non-compensation. The structure is the totality of molecules and atoms brought into the sites of the structure (several atoms and molecules) and bound in the lattice by the compatibility of valent and free electrons. These are the approaches of the analysis that permit to define the causal role of the laws of bulk elasticity in the formation of the magnetism as well as their leading role in the first and second order structural phase transitions.

[1] P. Kapitza, *The strong magnetic fields* (Nauka, Moscow, 1988) [in Russian].

[2] P. Bridgman, *Physics of high pressure* (Nauka, Moscow, 1935) [in Russian].

[3] P.I. Polyakov, T.A. Ryumshina, *Magnetism and laws of bulk elasticity* (Transworld research network, Kerala, 2009).

1PO-P-18

EXPERIMENTAL SETUP FOR MAGNETOCALORIC MATERIALS STUDIES IN STRONG AND WEAK MAGNETIC FIELDS IN DYNAMIC MODE

Gimaev R.R.^{1,2}, Spichkin Y.I.¹, Tishin A.M.^{1,2}

¹ Advanced Magnetic Technologies and Consulting LLC, Troitsk, Moscow, Russia

² Faculty of Physics, M.V. Lomonosov Moscow State University, Moscow, Russia

gimaev@amtc.org

The experimental setup for direct adiabatic temperature change measurements is presented. The device allows to conduct the measurements at the following conditions: (i) in alternative periodic fields with amplitude up to 1.7 T and frequencies up to 1 Hz; (ii) in alternative periodic fields up to 0.15 T and frequencies up to 10 Hz; (iii) in pulsed magnetic fields up to 0.15 T. The experiments in (i) and (ii) cases are conducted in dynamic mode. The temperature region of the measurements is 78 K – 380 K. The adiabatic temperature change of polycrystalline Gd as the test sample was measured. The obtained results are important from the point of view high frequency operation of future magnetic refrigerators. Detailed comparison with a data obtained using other methods is done.

Work at Advanced Magnetic Technologies and Consulting LLC is supported by Skolkovo Foundation, Russia. Authors acknowledge support by the AMT&C Group Ltd., UK.

1PO-P-19

ANALYSIS AND OPTIMIZATION OF HIGH-ENERGY PERMANENT MAGNET ELECTROMAGNETIC DRIVE BY FINITE ELEMENT METHOD

Kopeliovich D.B.¹, Malyshev A.Y.¹, Melnikov Y.P.¹, Tishin A.M.^{1,2}, Spichkin Y.I.¹, Gimaev R.R.^{1,2}

¹ Advanced Magnetic Technologies and Consulting LLC, Moscow, Troitsk, Russia

² Faculty of Physics, M.V. Lomonosov Moscow State University, Moscow, Russia

spichkin@amtc.org

The high-energy permanent magnet electromagnetic drive is used as an executive device in a wide range of applications, including, in particular, gas and water valves, and is characterized by very low energy consumption at pulse switching. Its application allows to create nonvolatile controlled stop valves capable for operation for a long time (for several years) from one battery. The main part of the drive is the magnetic system including soft magnetic circuit and an anchor made on the basis of high-energy permanent magnet of complex configuration. The results on modeling and optimization of the hard-soft magnetic system the help of finite element method are presented. The optimization was performed on the basis of the criterion of minimal force on the movement of the anchor from one stable position to another by the magnetic field generated by a two-sectional solenoid. The preliminary permanent magnet configurations (Fig. 1a, b) are determined and magnetic field patterns inside the magnetic system (Fig. 1b) are calculated. The calculated anchor magnet configurations provide general match between the lines of magnetic field generated by solenoid and the magnetization inside the composite permanent magnet, which decreases the force required for the switching. According to the calculations the energy of the switching pulse is about 0,6 J.

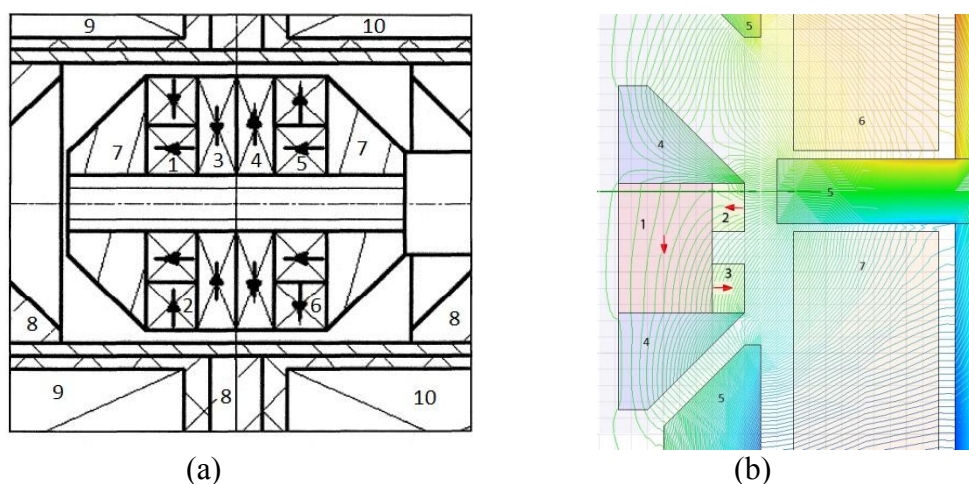


Fig. 1. Variants of the permanent magnet anchor configurations: (a) configuration with 6 rings (2 with axial magnetization (1 and 5) and 4 with radial magnetization (2, 3, 4 and 6), 7 – soft magnetic tips, 8 – soft magnetic circuit, 9 and 10 – solenoid coils); (b) configuration with 3 rings (1 with axial magnetization (1) and 2 with radial magnetization (2 and 3), 4 - soft magnetic tips, 5 - soft magnetic circuit, 6 and 7 - solenoid coils).

1PO-P-20

STUDY OF THE MAGNETIC PROPERTIES OF ROCKS (PYRITE, ARSENOPYRITE, CHALCOPYRITE AND MAGNETITE) AT HIGH TEMPERATURES

Kuvandikov O.K.¹, Shakarov H.O.¹, Shodiev Z.M.¹, Muzaffarov A.², Amonov B.U.¹, Nurimov U.E.¹, Karimov O.I.¹

¹ Samarkand State University, Samarkand, Uzbekistan

² Central research laboratory of Navoi mining-metallurgical combine, Navoi, Uzbekistan
kuvandikov@rambler.ru

To elucidate the origin and evolution of the magnetism of rocks and ores a study of the magnetic states of rocks and ores are of particular interest for the physics of magnetic phenomena, since, due to the complex crystal structure, magnetic structure of these minerals are essential for an understanding of some of their features. The aim of this work is to determine the main characteristics of magnetic iron-containing minerals pyrite (FeS₂), arsenopyrite (FeAsS), chalcopyrite (CuFeS₂) and magnetite (Fe₃O₄), which are members of the rocks of Uzbekistan, by measuring the temperature dependence of the magnetic susceptibility [$\chi(T)$] in the range of high 20-1200 °C temperatures. Magnetic susceptibility was measured by the Faraday method using high-temperature pendulum weights [1]. Maximum relative measurement error did not exceed 3%. Samples of rocks (minerals) were obtained in the Central Research Laboratory of Navoi Mining - Metallurgical Combine. Dependence $\chi(T)$ for pyrite and arsenopyrite were measured in the temperature range 20 - 800 °C, chalcopyrite - 500- 900 °C, and magnetite - 580- 1200 °C. Using the least squares method from the experimental curves of the samples we calculated their paramagnetic characteristics C , θ_p , the magnetic moment per chemical formula ($\mu_{\phi op}$), and the effective magnetic moment per iron atom ($\mu_{\phi \phi}$). Results of calculations are shown in the table. Data for pure iron were obtained from [3]. Analysis of the table shows that the values of the magnetic characteristics (θ_p and $\mu_{\phi \phi}$) of the studied compounds are lesser than the magnetic characteristics of pure iron. This can be explained by the increase of the distance between the magnetic ions of iron in the nodes of the sublattice of the studied compounds. This occurs by the presence of weakly magnetic elements in the crystal lattices of their compounds. Precisely because of this reason, there is a decrease of the magnetic exchange interaction of 3d-shell electrons of iron ions responsible for the occurrence of magnetic ordering of the studied compounds. θ_p is a measure of the energy of this interaction.

On the base of the obtained results we can make the following conclusion:

1. From experimental $\chi^{-1}(T)$ dependencies we identified main paramagnetic characteristics of the studied compounds. It was established that weakly-magnetic elements S, As, Cu, O reduces the magnetic characteristics of the iron.

- [1] Kuvandikov O.K., Shakarov H.O., Irgashev K.M. // In: Opto-acoustical, electrical, magnetic studies of condensed matter. – Samarkand. 1982. – pp. 122-130. [in Russian].
- [2] Nevzorova E.G., Gel'tekov B.P., Ravodsky I.Z., *Black metallurgy*, **9** (1972) 105-109. [in Russian].
- [3] O.K. Kuvandikov, H.O. Shakarov, D.A. Sayfullayeva, M.K. Salakhitdinova, *The Physics of Metals and Metallography*, **9** (2002) S48-S53.

1PO-P-21

EFFECT OF EXTREME CONDITIONS ON STRUCTURE AND MAGNETIC PROPERTIES OF ORDERING FePd ALLOY

Stashkova L.A., Vlasova N.I., Gaviko V.S., Popov A.G., Shchegoleva N.N., Kleinerman N.M., Serikov V.V.

IMP, Ural Division of RAS, S. Kovalevskoy, 18, Ekaterinburg, Russia
lshreder@imp.uran.ru

Among different materials for permanent magnets, the best corrosion resistance and good plasticity are exhibited by alloys of iron and cobalt with noble metals: CoPt, FePt, FePd. According to the modern first-principles based theory, high magnetocrystalline anisotropy of these alloys is mainly controlled by atomic ordering and depends on the degree of ordering. Results of experiments indicate that the magnitude of the effective magnetocrystalline-anisotropy constant and the level of magnetic hysteresis properties that are realized in these alloys after annealing for ordering depend on not only the degree of ordering but many other peculiarities of structural state such as phase composition, ratio of the volume fractions of disordered and ordered phases, way of contacting $L1_0$ -regions with a disordered matrix and with each other, size of magnetically independent elements of a complex multilevel hierarchy of crystalline nano-, micro-, and mesostructure.

The level of magnetic hysteresis properties gained in massive FePd samples after annealing for ordering turns out low and very far from the theoretical limit. The realization of high values of coercivity in FePd is a complicated problem, since it purports formation of a microstructure with high degree of ordering. Yet, the solution of this problem gives much promise, as it would allow application of cheaper FePd alloys both as corrosion-resistance permanent magnets and materials for high-density magnetic recording.

In the present work, comparative X-ray, TEM, thermomagnetic, and Mossbauer studies of the kinetics of phase transformation $A1 \rightarrow L1_0$ during isothermal annealing at 450 °C were performed on samples of the equiatomic FePd alloy in different initial states: 1) as-cast, 2) after severe plastic deformation by high-pressure torsion (HPT), and 3) after the rapid quenching onto the surface of a copper wheel.

The analysis of the combined research shows that the $A1 \rightarrow L1_0$ transition is a complex cascade-type transformation. Along with the $L1_0$ atomic ordering, such a transformation may include a shear- type transformation $A1$ (fcc) \rightarrow $A6$ (bct) and decomposition into cubic and tetragonal structural components with different composition and the degree of order depending on the initial state and annealing temperature. From the point of view of the symmetry and thermodynamics theories of structural phase transitions [1,2], the formation of intermediate phases is a natural stage of complex processes of phase transformations.

It is shown that in the states with the highest values of H_c , rapidly quenched and deformed samples are mainly tetragonal but highly inhomogeneous in the degree of long-range order. The $A6$ phase is sufficiently stable and is present in the samples even after 100 hours of annealing. The lack of long-range order due to its presence in the FePd alloy reduces the magnitude of the effective field of magnetocrystalline-anisotropy and may be one of the causes of low values of the maximum coercive force available.

Support by Ural Division of RAS, projects № 12-П-23-2005 and № 14-2-НП-75.

[1] N.I. Vlasova, et.al, *Acta Materialia*, **61** (2013) 2560-2570.

[2] Y. Ni, AG. Khachatryan, *Nature materials*, **8** (2009) 410-414.

1PO-P-22

NANOCRYSTALLINE SOFT MAGNETIC $(\text{Fe}_{0.7}\text{Co}_{0.3})_{88}\text{Hf}_2\text{W}_2\text{Mo}_2\text{Zr}_1\text{B}_4\text{Cu}_1$ ALLOY WITH ENHANCED THERMAL STABILITY OF MAGNETIC PROPERTIES

Lukshina V.A., Dmitrieva N.V., Volkova E.G., Potapov A.P., Filippov B.N., Shishkin D.A.
Institute of Metal Physics UD RAS, Ekaterinburg, Russia
lukshina@imp.uran.ru

It is important for high temperature applications of nanocrystalline alloys that they are to have, firstly, good soft magnetic properties at high temperatures, and secondly, the stability of magnetic properties and nanocrystalline structure at high temperatures for a long period of time (time of use of the material) [1]. In present work magnetic properties, thermal stability and structure of the $(\text{Fe}_{0.7}\text{Co}_{0.3})_{88}\text{Hf}_2\text{W}_2\text{Mo}_2\text{Zr}_1\text{B}_4\text{Cu}_1$ alloy obtained in the form of ribbons quenched from the melt were investigated after their nanocrystallization in the course of the thermal (TA) and stress- (SA) annealings (stretching stresses, $\sigma = 6\text{-}250$ MPa) in the air at temperatures $620\text{-}750^\circ\text{C}$. Magnetic state of specimens was determined from hysteresis loops measured by the ballistic method using galvanometric compensation microfluxmeter in the field of ± 4000 A/m applied along the axis of the ribbon. Thermal stability of magnetic properties was investigated after annealing of specimens without external influences ($\sigma = 0$) following the TA and SA. After each subsequent annealing the specimens were cooled to room temperature and hysteresis loops were measured. Thermal stability of the alloys was estimated from the change in magnetic properties (comparing to the magnetic properties at once after TA or SA) depending on temperature and duration of subsequent annealing. The structure of the alloys was studied by transmission electron microscopy (TEM).

It was shown that:

- SA at temperatures $620\text{-}750^\circ\text{C}$ resulted in the induction of magnetic anisotropy with an easy axis along the direction of the ribbon.

- After TA at 620°C for 20 min coercive force, H_c , was 250-300 A/m; after SA at 620°C for 20 min with $\sigma = 6\text{-}100$ MPa H_c decreased to 80-100 A/m; after SA with $\sigma > 100$ MPa H_c increased up to 250-300 A/m, as well. Nanocrystalline structure showed fine grains of about 4 nm with the main Fe- and Co-based bcc phase of solid solution. Part of the grains with the size more than 10 nm was about 6%.

- Thermal stability of the magnetic properties of the alloy after SA at 620°C for 20 min with $\sigma = 6\text{-}250$ MPa was determined by the thermal stability of induced magnetic anisotropy and depended on the value of σ . Magnetic properties of the alloy after SA at 620°C for 20 min with $\sigma = 170$ MPa were stable to the subsequent annealing at 570°C for 25 hours, and were not stable to annealing at 600°C and above.

- Structure of the alloy after TA at 620°C for 20 min was more stable in the course of heating from 20 to 820°C than after TA at 670 and 750°C .

- Thermal stability of magnetic properties of the alloy after TA in presence of stretching stresses (150-170 MPa) did not improve after increasing of TA temperature up to $670\text{-}720^\circ\text{C}$.

Thus, it is established that optimal conditions of the alloy nanocrystallization are: 620°C for 20 min, $\sigma = 150\text{-}170$ MPa. This kind of treatment provides stability of H_c , B_m and B_r/B_m to annealing at 570°C for 25 h.

Support of the UD RAS (project no. 12-T-2-1007) is acknowledged.

[1] T.Kulik, J.Ferenc, A.Kolano-Burian, X.B.Liang, M.Kowalczyk, *Journal of Alloys and Compounds*, **434–435** (2007) 623-627.

1PO-P-23

INFLUENCE OF WEAK OUTER MAGNETIC FIELD ON ELECTROCHEMICAL CORROSION RATE OF THIN Fe FILMS

Naboko A.S., Maklakov S.S., Maklakov S.A., Sedova M.V., Ryzhikov I.A., Osipov A.V.

Institute for Theoretical and Applied Electromagnetics
of the Russian Academy of Sciences, Moscow, Russia
nas.webwork@gmail.com

Ferromagnetic thin films are widely applied in magnetic field sensors and recording heads for magnetic storage devices; also, the films are perspective for microwave antennas and radar absorbing materials [1]. Working conditions of the devices suggest the presence of induced magnetic field of low strength ($H < 500$ Oe), which usually are not considered while estimating a corrosion resistance of ferromagnetic thin-film components. The contribution reports on a new phenomena, which shows that external magnetic field ($H =$ from 0 to 1000 Oe) influences significantly both on the corrosion rate and corrosion localization of thin Fe films [2].

A phenomenon of a micro-relief formation on a surface of thin Fe films under a short-term treatment by 30% CH_3COOH solution in an outer magnetic field was discovered [3]. Object under study was thin ($h = 150$ nm) Fe films obtained *via* electron-beam evaporation on glass and polyethylene terephthalate substrates. The relief formed reflects a magnetic domain structure of ferromagnetic film. The relief is formed of iron salts as a result of particular case of stress corrosion. Surface areas with micro-stresses act as corrosion localization areas; the stresses are caused by magnetostriction on magnetic domain boundaries in ferromagnetic film.

The relief is presented by prominences of 25 nm in height which divides surface onto areas of diverse shape (surface roughness within the areas is 5 nm, which does not exceed initial metal roughness); the shape depends on external magnetic field orientation. Magnetic field which induction is parallel to the film plane during oxidation causes oblong pattern; perpendicular orientation results in a pattern with circular elements. These transformations correlate well with magnetic domain conversion from stripe to circular structure.

Energy dispersive X-ray spectroscopy shows that the acid-treated film surface Fe consists primarily of O and Fe atoms; oxygen relative content is increased in prominences in comparison with other area (13.7 at.% *vs* 12.9 at.%). Raman spectra mapping additionally shows that iron oxides and salts form the prominences.

The dissolution rate of thin Fe films in 6% CH_3COOH in uniform external magnetic field ($H =$ from 0 to 1000 Oe) was investigated. The coulometry at a constant voltage was applied. The effect of influence of strength and orientation of the outer magnetic field on the rate of electrochemical corrosion of ferromagnetic thin Fe films was first discovered [3]. The influence of substrate stiffness on corrosion rate of thin Fe films was established.

The homogeneous outer magnetic field with weak strength $H < 1000$ Oe effects the corrosion of metal thin Fe films. The study of thin ferromagnetic film corrosion which is enhanced by weak external magnetic field is of fundamental and applied interest.

[1] I.T. Iakubov, A.N. Lagarkov, et.al., *JMMM*, **316** (2007) e813.

[2] A.S. Naboko, S.S. Maklakov, et.al., *Vestnik MITHT.*, **8** (2013) 92-95.

[3] A.V. Agaponova, I.V. Bykov, et.al., *Phys. Solid State.*, **53** (2011) 1013-1016.

1PO-P-24

MAGNETIC PROPERTIES AND ELECTRONIC STRUCTURE OF R_5Ge_3 ($R = Nd$ AND Er) INTERMETALLICS

Lukoyanov A.V.^{1,2}, *Knyazev Yu.V.*¹, *Kuz'min Yu.I.*¹

¹ Institute of Metal Physics, UrB RAS, 620990 Yekaterinburg, Russia

² Ural Federal University, 620002 Yekaterinburg, Russia

lukoyanov@imp.uran.ru

Intermetallic compounds Nd_5Ge_3 and Er_5Ge_3 have a variety of anomalies in magnetic and magnetotransport properties near Neel temperature $T_N = 51$ K (Nd_5Ge_3) and 32 K (Er_5Ge_3) [1]. In a hexagonal Mn_5Si_3 -type crystal structure (space group $P6_3/mcm$) Nd or Er occupy ($4d$) and ($6g$) positions. Two rare-earth sublattices promote the formation of low-temperature magnetic structures of the spin-wave type with the magnetic moment directed along the c axis [2,3]. Temperature and magnetic field significantly influence physical characteristics of these compounds that reveals the involvement of structural, charge, and spin degrees of freedom.

In this work we investigate magnetic properties and electronic structure of Nd_5Ge_3 and Er_5Ge_3 within the LSDA+U method. This theoretical method combines local spin-density approximation (LSDA) with the correction for electronic correlation effects (U) in the 4f shell of the rare-earth ions. Antiferromagnetic ordering of the rare-earth ions with spin moment of $3 \mu_B$ was found to be the ground state in agreement with experimental data. Low-temperature magnetic properties of Nd_5Ge_3 and Er_5Ge_3 were investigated within the LDA+U+SO method accounting for spin-orbital coupling and exchange interaction of the 4f-electrons. The type of low-temperature ordering of the rare-earth magnetic moments along the c axis experimentally obtained in neutron studies [2,3] was found as the ground state for both intermetallics. The calculated LSDA+U densities of states were analyzed and used to estimate the theoretical interband part of optical conductivity. The later was compared with the experimental curve also measured in this work. Optical properties of Nd_5Ge_3 and Er_5Ge_3 were studied in the wavelength range $k = 0.22$ – $15 \mu m$ by ellipsometric method. From the measured refractive index n and absorption coefficient k the frequency dependence of optical conductivity was obtained.

Summarizing, we report the investigations of magnetic properties and electronic structure of Nd_5Ge_3 and Er_5Ge_3 within the *ab initio* LSDA+U and LDA+U+SO methods, as well as experimental optical measurements [4]. Features of the optical conductivity were interpreted based on the theoretical results. The calculated magnetic moments and directions were found in good agreement with available experimental data.

Support by RFBR (project 13-02-00256-a), the Presidential Program of Grants in Science (project SP-506.2012.2) and the Dynasty Foundation is acknowledged.

[1] B. Maji, K.G. Suresh, A.K. Nigam, *Europhys. Lett.*, **91** (2010) 370071-370076.

[2] A.P. Vokhmyanin, B. Medzhi, A.N. Pirogov, A.E. Teplykh, *Phys. Solid State*, **56** (2014) 34-38.

[3] A.P. Vokhmyanin, Yu.A. Dorofeev, *Phys. Solid State*, **45** (2003) 1735-1741.

[4] Yu.V. Knyazev, A.V. Lukoyanov, Yu.I. Kuz'min, B. Maji, K.G. Suresh, *J. Alloys Compd.*, **588** (2014) 725-727.

1PO-P-25

THE TEMPERATURE INTERVAL OF STABILITY OF THE BUBBLE LATTICES IN FERRITE-GARNET FILM

Siryuk Ju.A., Bezus A.V., Smirnov V.V.

Donetsk national university, Universitetskaya str.24, 83001, Donetsk, Ukraine
juliasiryuk@gmail.com

The temperature stability of the bubble lattices has been studied. It was shown that a value of the temperature interval of stability ΔT depends on the structure of domain boundaries of the bubbles. The investigations were carried out on the film of $(TmBi)_3(FeGa)_5O_{12}$ composition with the developed surface $\langle 111 \rangle$ grown by the liquid-phase epitaxy on a gadolinium-gallium substrate, where T_N is the Neel temperature and T_C is the magnetic compensation temperature. The film have the quality factor $Q > 5$ at room temperature. With such quality factor, a pulsed magnetic field H_{puls} (perpendicular to the film plane) creates vertical Bloch lines (VBL) in the domain boundary (DB) [1]. At the same method of forming the bubble lattice, the number of VBL in the DB is dependent on the magnetic characteristics of the film at given temperature, in particular, the saturation magnetization. The saturation magnetization is low near T_N and T_C (fig.1); because of this a small number of VBL are formed in the bubble domain boundary. The hexagonal bubble

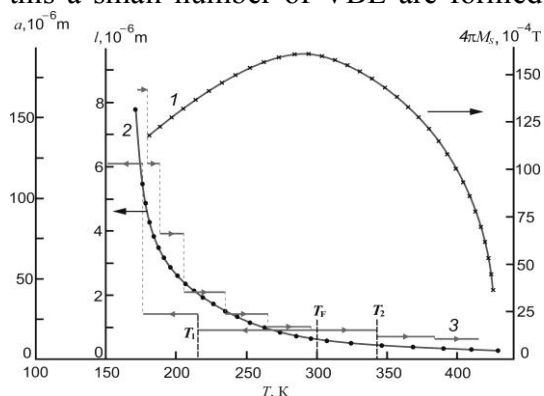


Fig. 1. Temperature dependences of (1) the saturation magnetization $4\pi M_S$, (2) the characteristic length l , and (3) the bubble parameter a of film.

lattice is formed by H_{puls} ; such lattice is equilibrium in the T forming. When the film temperature is changed, the bubble lattice formed at a certain temperature T_F is retained (although it is already nonequilibrium) in the temperature range $\Delta T = T_1 - T_2$ (fig.1). In this case the number of VBL remains in the DB of bubble. As the T_2 is approached, the number of VBL in the domain boundary sharply decreases [2], which causes the the first-order phase transition (PT) in the domain boundary, and, as a result, the bubble lattice undergoes the first-order PT to the two-phase structure [3]. As the T_1 is approached, the bubble lattice undergoes the first-order PT with decreasing number of domains [3]. The width of the domain boundary increases. The number of the

VBL decreases by their untwisting, i.e., a second-order PT occurs in the DB. The temperature interval of stability of the hexagonal bubble lattice formed by H_{puls} near T_N , i.e., with a small number of the VBL, is maximal. The experimental and theoretical studies show that the hexagonal bubble lattice cannot exist near the critical points (i.e., the T_N and the T_C). At these temperatures are approached, an amorphous bubble lattice is observed. The amorphous lattice is formed not only near T_N and T_C . It can be formed at any T , acting on the hexagonal bubble lattice by a planar field that undoes the VBL in the domain boundary interior. The experiments show that any amorphous bubble lattices have the widest temperature range of stability.

Thus, the temperature stability of the bubble lattices depends on the number of vertical Bloch lines in the domain boundary of bubble.

[1] A.Malozemoff, J.Slonczewski, *Mir*, Moscow (1982).

[2] F.G.Bar'yakhtar, A.I.Linnik, A.N.Prudnikov, E.F.Khodosov, *Fiz.Tverd.Tela.*, **27**(1985)8,2503.

[3] Ju.A.Siryuk, A.V.Bezus, *Fiz.Tverd.Tela.*, **55** (2013) 3, 547.

1PO-P-26

HIGH-COERCIVITY STRONTIUM HEXAFERRITE BY GLASS CRYSTALLIZATION

Gorbachev E.A.¹, Trusov L.A.¹, Kazin P.E.²

¹ Department of Materials Science, Moscow State University, Moscow, Russia

² Chemistry Department, Moscow State University, Moscow, Russia

basketevgeny@gmail.com

Hard magnetic ferrites are widely used for permanent magnet production, information storage and millimeter-wave applications. Their inherent magnetic properties could be tuned by element substitution or microstructure control. It's known, that substitution of iron ions by aluminum should result in considerable rise of coercivity. However the reaction of aluminum introduction into hexaferrite crystal structure generally requires very high temperatures and particle size exceeds single domain limits. The promising technique enabling both compositional and microstructure management is crystallization of glasses in the SrO-Fe₂O₃-Al₂O₃-B₂O₃ system.

The glasses with nominal compositions 13SrO–5.5Fe₂O₃–4.5Al₂O₃–nB₂O₃ (n = 3 – 5.5) (1) and 17SrO–(6-m)Fe₂O₃–mAl₂O₃–8B₂O₃ (m = 1 – 3) (2) were prepared by rapid cooling of melts from 1250 – 1400°C. The glasses were heat treated at 600 – 970°C to produce glass ceramic samples. Strontium hexaferrite fine particles were extracted by dissolution of non-magnetic matrix by diluted hydrochloric acid. The chemical composition of the samples was confirmed by ICP-MS.

The phase analysis revealed that the only boron-containing crystalline phase Sr₂B₂O₅ forms in the wide composition range. Thus, this phase could be considered as inert matrix, which doesn't affect the phase relations between metal oxides in the equilibrium state. This assumption simplifies the prediction of the phase composition of glass ceramics and substitution degree in strontium hexaferrite. In addition to borate phase, the samples contain crystalline phases in accordance with ternary SrO-Fe₂O₃-Al₂O₃ diagram. The substitution degree in SrFe_{12-x}Al_xO₁₉ varies from 1 to 5 in dependence on synthesis conditions. More complete introduction of aluminum was observed at high temperatures close to the melting points of glass ceramics.

According to electron microscopy, below 750°C strontium hexaferrite tends to crystallize as platelet nanoparticles with diameters below 100 nm and thickness about 5 nm. At higher temperatures hexaferrite forms submicron particles below the melting point, and further an intensive particle growth occurs resulting in large particles, which are several micrometers in diameter. We developed a two-stage heat treatment technique to obtain mostly single-domain particles with lower size distribution.

Magnetic properties measurements showed that aluminum introduction leads to decrease of saturation magnetization. The coercivity strongly depended on both the substitution and the microstructure – H_c values sharply increased in single-domain particles simultaneously with substitution degree. The highest (BH)_{max} value was obtained for sample with x = 2, H_c = 12500 Oe, M_s = 36.5 eme/g and mean particle diameter 350 nm.

This research was funded by Russian Foundation for Basic Research, grant No. 14-03-31598.

Wednesday

2 July

09:30-11:00

plenary lectures
2PL-A

2PL-A-1

SPINTRONICS – IMPLICATIONS FOR ENERGY, INFORMATION AND MEDICAL TECHNOLOGIES*

Bader S.D.[§]

Materials Science Division and Center for Nanoscale Materials, Argonne National Laboratory,
Argonne, Illinois 60439

Department of Physics and Astronomy, Northwestern University, Evanston, Illinois 60208 USA

[§]bader@anl.gov

Spintronics encompasses the ever-evolving field of magnetic electronics.[1,2] Fields such as spintronics hold the potential to extend the information technology revolution as the semiconductor roadmap reaches its end. A major issue with present day electronics is in its demand for increased power. Spintronics offers the possibility to communicate via pure spin currents as opposed to electric charge currents. The talk provides a brief perspective of recent developments to switch magnetic moments by spin-polarized currents, electric fields and photonic fields. Developments in the field of spintronics continue to be strongly dependent on the exploration and discovery of novel nanostructured materials and configurations. An array of exotic transport effects dependent on the interplay between spin and charge currents have been explored theoretically and experimentally in recent years. The talk highlights promising areas for future investigation, and, features recent work at Argonne on ferromagnetic-superconducting multilayers, [3] including, most strikingly, in the realm of medical applications.[4]

Work supported by the U.S. Department of Energy, Office of Science, Basic Energy Sciences, under contract No. DE-AC02-06CH11357.

- [1]. S. D. Bader and S. S. P. Parkin, “Spintronics,” in *Annual Reviews of Condensed Matter Physics*, **1** (2010) 71-88.
- [2]. S. D. Bader, *Rev. Mod. Phys.*, **78** (2006) 1-15.
- [3]. Leyi Zhu, Yaohua Liu, F.S. Bergeret, J.E. Pearson, Suzanne G.E. te Velthuis, S.D. Bader, J.S. Jiang, *Phys. Rev. Lett.*, **110** (2013) 177001.
- [4]. Dong-Hyun Kim, Elena A. Rozhkova, Ilya V. Ulasov, S. D. Bader, Tijana Rajh, M. S. Lesniak, V. Novosad, *Nature Materials*, **9** (2010) 165-171.

2PL-A-2

SPIN DYNAMICS DRIVEN BY PURE SPIN CURRENT*Demidov V.E.¹, Demokritov S.O.^{1,2}, Urazhdin S.³, Tiberkevich V.⁴, Slavin A.N.⁴*¹ University of Muenster, Corrensstrasse 2-4, 48149 Muenster, Germany² Institute of Metal Physics, Ural Division of RAS, Yekaterinburg 620041, Russia³ Emory University, Atlanta, GA 30322, USA⁴ Oakland University, Dept. of Physics, Rochester, MI, USA

demokrit@uni-muenster.de

In the last years pure spin currents generated by the spin Hall effect have been utilized to suppress noise caused by thermal fluctuations in magnetic nanodevices [1], amplify propagating magnetization waves [2], and to reduce the dynamic damping in magnetic films [3]. Moreover, recently it was shown that the effect of the pure spin current can be strong enough to completely compensate the magnetic damping and can lead to the generation of coherent magnetic auto-oscillations.

Here, we report on the study of nano-devices driven by pure spin currents generated due to the spin Hall effect in a Pt electrode, and locally injected into an extended Permalloy film [4]. By using micro-focus Brillouin light scattering (BLS) spectroscopy, which is capable of dynamic magnetization measurements with the spatial resolution of 250 nm, we demonstrate that in our devices the initial enhancement of incoherent magnetization fluctuations caused by the spin current is followed by a transition to a single-mode coherent auto-oscillation regime. This transition is accompanied by the formation of a new strongly-localized dynamic mode, whose characteristics are reminiscent of the nonlinear stationary spin-wave “bullet” [5] with the spatial dimensions of approximately 100 nanometers [6].

We show that the suggested spin-Hall nano-oscillators (SHNOs) exhibit single-mode coherent auto-oscillations at moderate current densities of about 10^8 A/cm². The spectral linewidth of the auto-oscillations lies in the megahertz range, while their central frequency can be tuned from 5 to 10 GHz by the variation of static magnetic field, without a significant increase in the onset current. We present the results of the micromagnetic simulations, which are in good agreement with the experimental findings and provide additional information about the spatial characteristics of the auto-oscillation mode. Moreover, we show that the studied SHNOs are capable of efficient synchronization to external microwave signals, which opens additional possibilities for the development of novel spintronic devices [7].

Our findings suggest a route for the implementation of novel magnetic nano-oscillators that have significant advantages over conventional spin-torque nano-oscillators (STNOs), whose geometry and structure are limited by the requirement that the spin current is accompanied by the electric current flowing through the ferromagnet.

[1] V. E. Demidov et al., Phys. Rev. Lett., **107** (2011) 107204.

[2] V.E. Demidov et al., to appear in Appl. Phys. Lett.

[3] V. E. Demidov et al., Appl. Phys. Lett., **99** (2011) 172501.[4] V. E. Demidov et al., Nature Mater., **11** (2012) 1028.[5] A. Slavin & V. Tiberkevich, Phys. Rev. Lett., **95** (2005) 237201.[6] H. Ulrichs et al., Appl. Phys. Lett., **102** (2013) 132402.[7] V.E. Demidov, et al. Nat. Commun, **5** (2014) 3179 doi: 10.1038/ncomms4179.

Wednesday

2 July

11:30-13:15

14:30-17:15

oral session

2TL-A

2RP-A

2OR-A

**“Spintronics and
Magnetotransport”**

2TL-A-1

NANOWIRE SPIN TORQUE OSCILLATOR DRIVEN BY SPIN ORBIT TORQUES

Krivorotov I.N.¹, Duan Z.¹, Smith A.¹, Young L.¹, Youngblood B.¹

¹ Department of Physics & Astronomy, University of California, Irvine, USA
ilya.krivorotov@uci.edu

Recently, spin torque oscillators (STOs) based on pure spin currents arising from spin Hall effect were demonstrated in the planar nanoconstriction [1, 2] and nanopillar [3] geometries. In all STOs studied to date, magnetization self-oscillations were excited within a nanoscale active region, in which the negative effective damping from spin torque exceeded the positive Gilbert damping of the ferromagnet. In this talk, I will describe an STO with a micrometer-scale active region thereby showing that self-oscillatory spin torque dynamics can be induced in spatially extended ferromagnets. The oscillator is a 190 nm wide nanowire patterned from a Ni₈₀Fe₂₀(5 nm)/Pt(5 nm) bilayer as shown in Fig. 1. The active region of the nanowire oscillator placed between two thick gold leads is 1.8 μm long. Above a critical bias current, the oscillator emits microwave power originating from persistent self-oscillations of magnetization that are transduced into the electrical microwave signal via anisotropic magneto-resistance of Ni₈₀Fe₂₀ (see Fig. 1). This nanowire STO exhibits two types of self-oscillatory modes that directly arise from the edge and bulk spin wave eigenmodes of the Ni₈₀Fe₂₀ nanowire. Our work suggests that geometric confinement of the spin wave spectrum in the nanowire (1D) geometry limits the phase space for nonlinear magnon scattering compared to the thin film (2D) geometry and thereby enables STOs with a micrometer scale active region. I will also present micromagnetic simulations of magnetization dynamics driven by pure spin current in the nanowire geometry and compare these simulation results to our experimental observations. Support by NSF as well as the FAME Center, one of six centers of STARnet, a Semiconductor Research Corporation program sponsored by MARCO and DARPA is acknowledged.

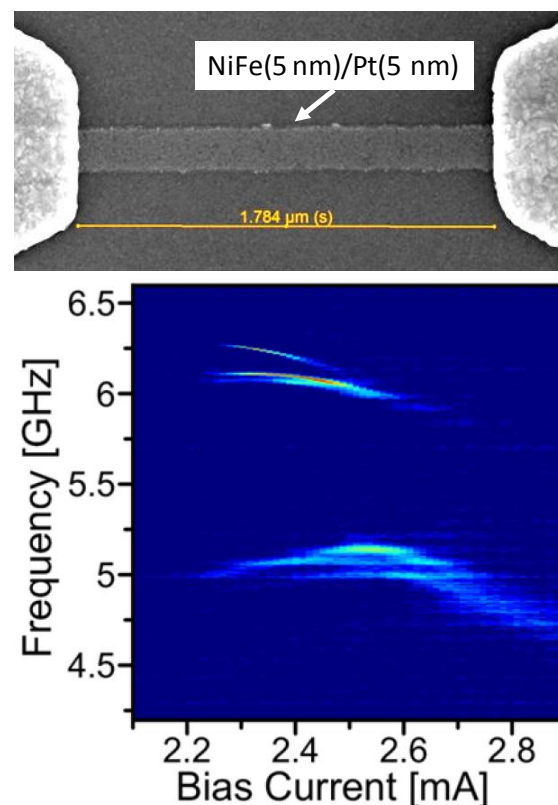


Fig. 1. (Top) Scanning electron micrograph of a Pt(5 nm)/Ni₈₀Fe₂₀(5 nm) nanowire device. (Bottom) Microwave emission spectrum of the device as a function of direct current bias applied to the nanowire.

[1] V. E. Demidov, *et al.*, *Nature Mater.*, **11** (2012) 1028.

[2] R. H. Liu, W. L. Lim, and S. Urazhdin, *Phys. Rev. Lett.*, **110** (2013) 147601.

[3] L. Liu, C.-F. Pai, D. C. Ralph, and R. A. Buhrman, *Phys. Rev. Lett.*, **109** (2012) 186602.

2TL-A-2

ROBUST SYNCHRONIZATION OF 1D AND 2D ARRAYS OF SPIN-TORQUE-BASED VORTEX NANOOSCILLATORS

Berkov D.V.¹, Erokhin S.G.²

¹ General Numerics Research Lab, Jena, Germany

² Innovent Technology Development, Jena, Germany
d.berkov@general-numeric-rl.de

Magnetization oscillations induced in nanoelements by a spin-polarized current (SPC) is at present one of the hottest topics in solid state physics. Synchronization of several spin-torque driven nanooscillators (STNO) is very interesting from the fundamental point of view and highly desirable for numerous applications, because it would result in a large output power and narrow spectral lines required to develop novel spintronic devices. However, such a synchronization still remains a major challenge. In this talk we present a new concept allowing to synchronize not only pairs, but also arbitrarily large 1D and 2D arrays of STNOs without introducing the phase shift between adjacent oscillators, so that a perfect scaling of the oscillation power with the number of oscillators N is observed.

Our concept employs STNOs based on square-shaped nanoelements with magnetization vortices inside, which gyration is driven by SPC injected via point contacts in the nanosquare centers. Our simulations predict that synchronization of two such STNOs placed side-to-side demonstrates a very high dynamical stability due to the strong coupling between them (coupling energy up to 1000 kT for two 500 x 500 nm² nanosquares can be obtained). We show that the origin of such a high coupling constant is the spatial distribution of magnetic surface and volume 'charges'. Both 'in-phase' and 'out-of-phase' locking regimes can be realized in our system. Further, we prove that inclusion of thermal fluctuations does not disturb the synchronization.

The main advantage of this our concept is the possibility to synchronize any number of STNOs, arranged as 1D or 2D arrays. We substantiate this feature by analysing two examples: (a) synchronization of 10 nanooscillators arranged in a 1D chain and (b) a perfect phase locking in a 2D system of 6 x 6 STNOs arranged as a square lattice of nanoelements. We point out that a robust synchronization can be achieved even when the nanocontacts in the system have a broad distribution of diameters, what is very important in technological applications, because the manufacturing of identical nanocontacts remains the major bottleneck by production of STNOs.

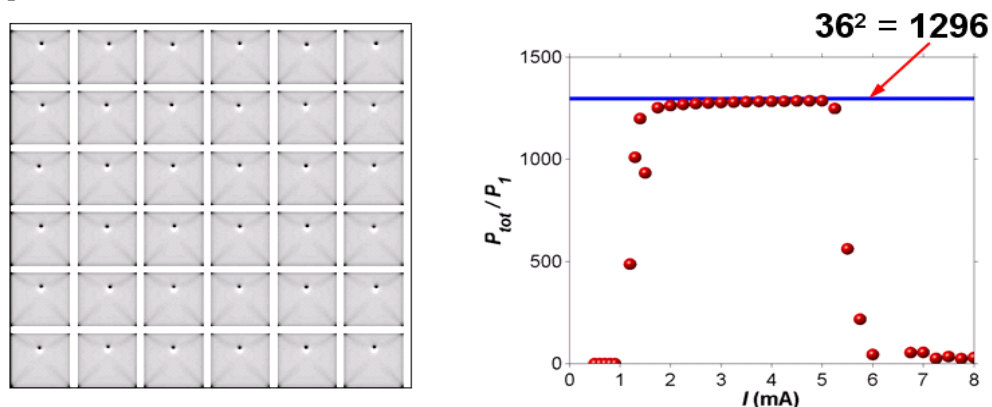


Fig. 1. Left: Vortex configuration (out-of-plane magnetization projection) for the lattice of 6 x 6 STNOs in the synchronized regime. Right: Total oscillation power (normalized to the power of one STNO) of in-plane m -components inside the contact areas demonstrating the exact quadratic power scaling with the number of oscillators.

2OR-A-3

TEMPERATURE DEPENDENCE OF MAGNETIC PROPERTIES OF NiFe/Cu/NiFe/IrMn AND NiFe/IrMn THIN FILMS STRUCTURE

Kupriyanova G.¹, Rodionova V.^{1,2}, Chechenin N.³, Dzhun I.³, Ay F.⁴, Rameev B.^{4,5}

¹ Immanuel Kant Baltic Federal University, 236041 Kaliningrad, Russia

² National University of Science and Technology "MIS&S", Moscow 119049, Russia

³ Skobeltsyn Institute of Nuclear Physics, Lomonosov Moscow State University, 119991 Moscow, Russia

⁴ Department of Physics, Gebze Institute of Technology 41400 Gebze-Kocaeli/Turkey

⁵ Kazan Physical Technical Institute, 420029 Kazan, Russian Federation
galkupr@yandex.ru

Ferromagnetic (FM)/nonmagnetic (NM)/FM multilayers and ferromagnetic/antiferromagnetic (AFM) bilayers have been intensively studied because of physical interest and important applications, which use the giant magnetoresistance (GMR) effect of FM/NM/FM multilayers and exchange bias effect of FM/AFM bilayers [1-3]. We have investigated two types of thin film structures: NiFe/IrMn bi-layers and NiFe/Cu/NiFe/IrMn spin-valves. The thickness of antiferromagnetic layer is the same for all samples and equals 15 nm. The thicknesses of the Cu and NiFe layers are from 2 nm to 10 nm and from 5 to 15 nm, respectively. The samples were prepared by DC magnetron sputtering using a magnetron system ATC ORION-5 produced by AJA INTERNATIONAL, at 3×10^{-3} Torr argon pressure during the deposition with 10^{-6} Torr base pressure. The compositions of the IrMn and NiFe targets were checked by the Rutherford backscattering and the X-ray energy dispersive analysis. The compositions of the targets are Ni₆₅Fe₃₅ and Ir₂₉Mn₇₁. The deposition times and rates for the layers were preset basing on dummy calibrating samples thicknesses measured by the Rutherford backscattering technique. The magnetic field of 400 Oe was applied in the sample plane during the deposition to induce the uniaxial anisotropy. The magnetic properties of the samples were studied by using two systems: Lake Shore Vibrating Sample Magnetometer (System 7404) in a temperature range of 100-450 K and in magnetic fields up to 12 kOe and Quantum Design Physical Property Measurement System (PPMS) with the 9T superconducting solenoid and EverCool system. The hysteresis loops and temperature dependence of the magnetization, coercive fields were investigated in the temperature range of 10-400K. Anisotropic properties, exchange interaction between AFM and FM layers have been studied by ferromagnetic resonance. It was found that the effect of exchange bias in NiFe/Cu/NiFe/IrMn depends on the temperature with a noticeable increase below 70 - 80 K. The factors affecting the temperature dependence of the exchange bias in two and three layer structures are considered. The conditions of the functionality of the spin gate for AFM/FM/NM/FM structures and its temperature dependence were obtained on the basis of proposals for structural stability both in a magnetic field, and without it.

[1] A.E. Berkowitz, K. Takano, *J. Magn. Magn. Mater.*, **200** (1999) 552.

[2] M. Ali, C.H. Marrow, B.J. Hickey, *Phys. Rev. B*, **67** (2003) 172405.

[3] R.D. McMichael, M.D. Stiles, P.J. Chen, W.F. Egelhoff, *Phys. Rev. B*, **58** (1998) 8605.

2OR-A-4

SPIN PUMPING AND SPIN-TRANSFER TORQUES IN ANTIFERROMAGNETS

*Ran Cheng*¹, *Jiang Xiao*², *Qian Niu*^{1,3}, *Arne Brataas*⁴

¹ Department of Physics, University of Texas at Austin, Austin, Texas 78712, USA

² Department of Physics, Fudan University, Shanghai 200433, China

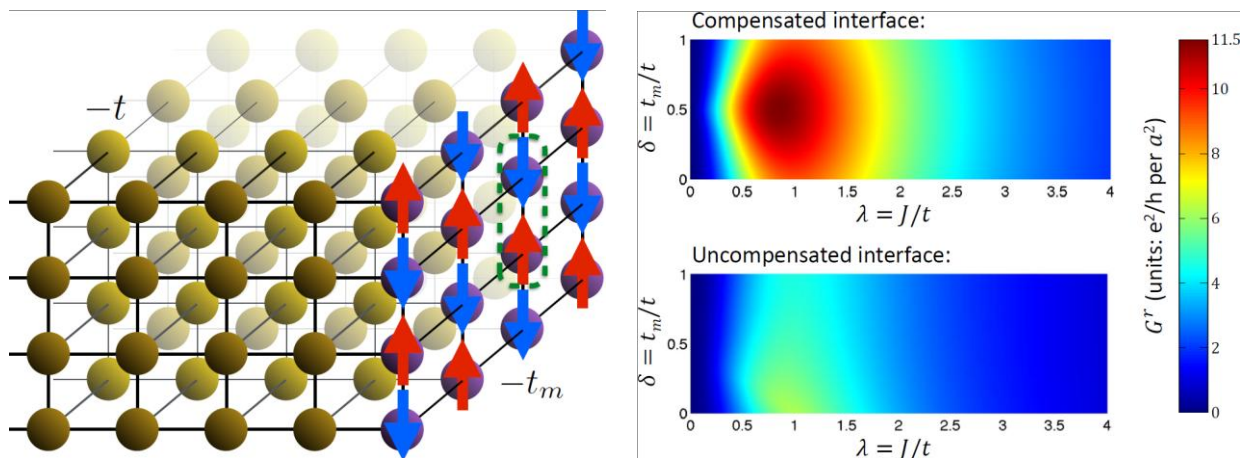
³ International Center for Quantum Materials, Peking University, Beijing 100871, China

⁴ Department of Physics, Norwegian University of Science and Technology, NO-7491 Trondheim, Norway

rancheng@utexas.edu

Spin pumping and spin-transfer torques are two widely studied reciprocal phenomena in ferromagnets. However, pumping phenomena in homogeneous antiferromagnets and their relations to current-induced torques have not been explored. By calculating how electrons scatter off a normal metal-antiferromagnetic interface, we derive pumped spin and staggered spin currents in terms of the staggered field, the magnetization, and their rates of change. For both compensated and uncompensated interfaces, spin pumping is large and of a similar magnitude with a direction controlled by the microwave polarization. The pumped currents are connected to current-induced torques via Onsager reciprocity relations.

The work is supported by DOE, NSF, and the Welch foundation.



[1] R. Cheng, J. Xiao, Q. Niu, and A. Brataas, *arXiv:1404.xxxx*.

2OR-A-5

HYBRID MEMRISTOR OPERATED BY SPIN POLARIZED CARRIERS*Dediu V.¹, Riminucci A.¹, Calbucci M.¹, Cecchini R.¹, Graziosi P.¹, Bergenti I.¹, Prezioso M.²*¹ ISMN-CNR, Bologna, Italy² University of California, Electrical & Computer Engineering, Santa Barbara, USA

v.dediu@bo.ismn.cnr.it

Information and communication technology (ICT) is calling for solutions enabling lower power consumption, further miniaturization and multifunctionality requiring the development of new device concepts and new materials. A fertile approach to meet such demands is the introduction of the spin degree of freedom into electronics devices, an approach commonly known as spintronics. This already led to a revolution in the information storage (GMR readheads) in the last decades. Nowadays, the challenge is to bring spintronics into devices dedicated to logics, communications and storage within the same material technology [1].

In this context the electric control of the magnetoresistance represents one of the most promising issues enabling both further miniaturization and multifunctional operation of spintronic devices. Likewise, also the electronics community is committed to follow the Moore's law, and one of the promising approaches is the use of arrays of crossbar memristors capable of information processing and storing ('stateful' logic) [2].

We show that an electrically controlled magnetoresistance can be achieved in organic devices [3] combining magnetic bistability (spin-valve) and resistance switching effects. In such devices the GMR effect can be turned ON and OFF by a programming bias that sets the device in low or high resistance state respectively. The magnitude of the GMR depends on the bias history and can be recovered up to the pristine value [4]. Such devices operate like a magnetically modulated or spintronic memristor (SPM). SPMs can be operated in both memory and logic gate applications - two logic gates AND and IMP have been experimentally realized on the basis of a single SPM. We believe that devices merging together spintronic and electronic approaches pave the road to new future information processing paradigms [5].

Support by HINTS and IFOX EC projects is acknowledged.

[1] D. D. Awschalom, & Flatte, M. E. *Nature Physics*, **3** (2007) 153.

[2] J. Borghetti, et al. *Nature*, **464** (2010) 873.

[3] V. A. Dediu, et al. *Nature Materials*, **8** (2009) 707.

[4] M. Prezioso, et al. *Advanced Materials*, **25** (2013) 534.

[5] S. Sanvito & V. A. Dediu, *Nature Nanotechnology*, **7** (2012) 696.

2TL-A-6

ULTRAFAST LOCAL AND NON-LOCAL MAGNETIZATION DYNAMICS

Uwe Bovensiepen¹

¹ University Duisburg-Essen, Faculty of Physics and Center for Nanointegration,
47057 Duisburg, Germany
uwe.bovensiepen@uni-due.de

Ultrafast magnetization dynamics allows the real time analysis of a magnetically ordered system which is responding to an optical broadband stimulus according to its elementary excitations accessible on pico- and femtosecond time scales. These excitations comprise spin-dependent electronic excitations which propagate in real space as ballistic carriers with the Fermi velocity v_F until their energy and / or momentum is changed by interaction with phonons, further electrons, and spin waves. We probe ultrafast magnetization dynamics by a various optical and x-ray pump-probe experiments and analyze the processes underlying the laser-induced loss of the magnetic moment localized in the ferromagnet, the transport-mediated redistribution of spin polarization within the sample's extension in real space, and the non-local transfer dynamics from a ferromagnet into an adjacent layer of a noble metal. For the lanthanides Tb and Gd [1], as well as their alloys [2] we find two separate timescales at which the magnetization is changed. An ultrafast, subpicosecond one is found to be independent of the material. It is assigned to spin-dependent relaxation of the optically excited $5d$ valence electrons. The slower picosecond time scale is found to become faster with the increasing content of Tb which we explain by direct spin-lattice coupling mediated by the anisotropic $4f^8$ orbital distribution in Tb compared with the isotropic $4f^7$ one in Gd. In epitaxial layers of transition metal ferromagnets Fe and Co we probe the spatial redistribution and propagation dynamics of spin polarized excited electrons and holes by methods sensitive to the spatial profile of the transient spin polarization as well as to the spin current propagation. In Fe/Au layer stacks it is found that the spin current density and the propagation velocity depend on the majority or minority character of carriers. This is understood as a consequence of the different scattering rates and binding energies in the spin-polarized subbands, respectively [3]. In Co films we investigate the thickness dependent magnetization profile and explain our observations by an ultrafast spatial redistribution of spin polarization.

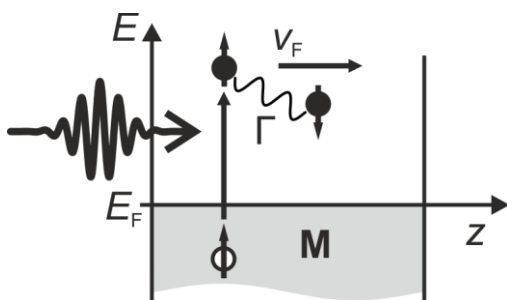


Fig. 1: Schematic optical excitation of a metallic ferromagnet with magnetization M and the dynamic competition of spin-polarized ballistic electrons propagating at the Fermi velocity v_F with spin-flip scattering at a rate \square along a real space direction z .

We conclude that spin dependent scattering resulting in a change of the local magnetic moment and spin dependent transport effects have to be accounted for on an equal footing to obtain a reliable description of ultrafast magnetization dynamics.

Support by the Deutsche Forschungsgemeinschaft, the Mercator Research Center Ruhr, and the German Federal Ministry of Education and Research is gratefully acknowledged.

- [1] M. Wietstruk et al., *Phys. Rev. Lett.*, **106** (2011) 127401.
 [2] A. Eschenlohr et al., *submitted* (2014).
 [3] A. Melnikov et al., *Phys. Rev. Lett.*, **107** (2011) 076601.

2TL-A-7

ULTRA-FAST DOMAIN WALL DYNAMICSKläui M.^{1,2}¹ Institute of Physics, Johannes Gutenberg University Mainz, 55099 Mainz, Germany² Graduate School of Excellence Materials Science in Mainz, 55099 Mainz, Germany

Klaeui@uni-mainz.de

Since conventional approaches of manipulating magnetization using magnetic fields exhibit unfavourable scaling and results in limited switching speed, alternative approaches based on spin-currents have emerged.

The transfer of angular momentum (“spin transfer torque effect”) leads for instance to current-induced domain wall motion (CIDM), which has become the focus of intense research in the last few years. We have comprehensively investigated CIDM and determined the acting adiabatic and non-adiabatic torque terms [1]. We find that the previously neglected diffusive torque term [2] can play an important role for vortex core displacement. For out-of-plane magnetized Co/Pt a large non-adiabatic torque is found, while in Co/Ni the adiabatic torque dominates [3]. Concurrently we also measure the domain wall magnetoresistance effect in nanoconstrictions and correlate the observed large effects with the structure [4].

By separating charge and spin transport we can generate pure diffusive spin currents with no associated net charge current. Using such diffusive spin currents we find large efficiencies for domain wall displacement due to strong spin accumulation absorption [5]. To increase the spin diffusion length, we use robust turbostratic graphene and find spin injection across transparent contacts. Using Free Electron Laser sources we measure the ultra-fast magnetization dynamics due to superdiffusive spin currents [6] using x-ray holography [7].

Finally we also show that using perpendicular fields, multiple domain walls can be displaced synchronously and fast [8].

[1] L. Heyne et al., *Phys. Rev. Lett.*, **105** (2010) 187203.

M. Eltschka et al., *Phys. Rev. Lett.*, **105** (2010) 056601.

[2] A. Manchon, W.-S. Kim, and K.-J. Lee, *arXiv:1110.3487*.

[3] J. Heinen et al., *J. Phys. Cond. Mat.*, **24** (2012) 24220.

[4] A. von Bieren, *et al.*, *Phys. Rev. Lett.*, **110** (2013) 67203.

[5] D. Ilgaz, et al., *Phys. Rev. Lett.*, **105** (2010) 076601.

[6] B. Pfau, *et al.*, *Nature Comm.*, **3** (2012) 1100.

[7] J. Geilhufe, *et al.*, *Nature Comm.*, **5** (2014) 3008.

[8] J.-S. Kim, *et al.*, *Nature Comm.*, **5** (2014) 3429.

2RP-A-8

ELECTRONIC TRANSPORT OF HALF-METALLIC FERROMAGNETIC HEUSLER ALLOYS

Marchenkov V.V.¹, Kourov N.I.¹, Belozerova K.A.¹, Viglin N.A.¹, Weber H.W.²

¹ Institute of Metal Physics, 620990 Ekaterinburg, Russia

² Atominstitut, Vienna University of Technology, 1020 Vienna, Austria

march@imp.uran.ru

Materials that exhibit half-metallic ferromagnetism (HMF) are potential candidates for application in spintronics [1]. Some of the Heusler alloys were predicted to be in a half-metallic state [2-5]. The main feature of the electronic structure of HMF is the presence of an energy gap at the Fermi level in one spin sub-band and a metallic character of the density of states in the other. This can lead to 100% spin polarization of the charge carriers, which can be used for spintronic devices. The depth and the width of the energy gap can vary quite strongly in different HMF. This feature of the electron spectrum is usually predicted by *ab initio* band structure calculations and is experimentally observed by measurements of the optical properties. Due to significant changes in the electronic spectrum it should manifest itself also in other electronic properties at the transition from the ferromagnetic to the paramagnetic state. In particular, we would expect the presence and a manifestation of the "gap" peculiarities in the electronic transport properties.

We studied the electroresistivity ρ , the galvanomagnetic properties and the thermopower S of bulk and film Heusler alloys X_2YZ ($X = Co, Fe, Ni$; $Y = Cr, Mn, Fe, Ni, Ti, V, Nb$; $Z = Al, Ga, Si, Sn$) in the temperature range from 4.2 to 800 K and in magnetic fields of up to 15 T. The bulk alloys were prepared by arc and induction melting methods. The films were synthesized by magnetron sputtering using mosaic targets [6].

It was experimentally demonstrated that in contrast to the usual metallic behavior of $\rho(T)$ and $S(T)$, e.g., in ferromagnetic Ni_2MnGa , an abnormal behavior is observed in high-resistive HMF Heusler alloys, i.e., a negative slope at $T < T_C$ and a minimum of ρ near T_C as well as an additional linear contribution to $S(T)$ (T_C is Curie temperature). These anomalies can be explained by a two-current conduction model that takes into account the presence of an energy gap near the Fermi level in the electronic spectrum for electrons with spin down (minority).

The results are in a good agreement with calculations of the electronic band structure and can be used for the development of materials and devices for spintronics.

This work was partly supported by the UB RAS Program (project No 12-T-2-1011), RFBR (project No 12-02-00271) and by the Scientific School Program (grant No NSh-1540.2014.2).

- [1] Koichiro Inomata, Naomichi Ikeda et al., *Sci. Technol. Adv. Mater.* **9** (2008) 014101.
- [2] V.Yu. Irkhin, M.I. Katsnel'son, *Phys. Usp.* **37** (1994) 659–676.
- [3] R.Y. Umetsu, K. Kobayashi et al., *Appl. Phys. Lett.*, **85** (2004) 2011.
- [4] J. Kuebler, G.H. Fecher and C. Felser, *Phys. Rev. B*, **76** (2007) 024414.
- [5] B. Balke, S. Wurmehl et al., *Sci. Technol. Adv. Mater.*, **9** (2008) 014102.
- [6] N.A. Viglin, V.V. Marchenkov, M.A. Milyaev et al., *The Physics of Metals and Metallography*, **12** (2013) 1003-1008.

2RP-A-9

INVESTIGATION OF CURRENT DRIVEN DOMAIN WALL MOTION IN RE-TM MAGNETIC WIRE

*Hiroyuki Awano*¹

¹ Toyota Technological Institute (TTI), Nagoya, Japan
awano@toyota-ti.ac.jp

A magnetic wire memory has been paying much attention as a future low power consumption storage devices. The data patterns can be recorded by using a magnetic recording head, and those are reproduced by a TMR (Tunnel Magnetic Resistance) head. When someone requests a data recall, the corresponding data in the magnetic wire will be displaced towards the readout head position by applying pulse current along the wire. This domain displacement technique is named as a spin torque transfer effect. In 2004, the first experimental result has been reported by using an in-plane magnetized FeNi wire. However, the critical current density for driving domain walls was $1 \times 10^8 \text{ A/cm}^2$. It is too large value. In order to reduce the critical current density, perpendicular magnetized Co/Ni multilayer wire was improved and it was successfully reduced to $3 \times 10^7 \text{ A/cm}^2$. Furthermore, by using TbFeCo amorphous magnetic wire, it was more reduced to $4 \times 10^6 \text{ A/cm}^2$ [1].

The experimental result of TbFeCo magnetic wire is shown in Fig.1. The magnetic wire width is 800nm and the wire thickness is 20nm. SEM image of the experimental setup is shown in Fig.1(a). When the nucleation current pulse is applied into the Ti/Al electrode, it generates an Oersted field around the left hand side of the TbFeCo wire, and a magnetic domain can be recorded at the left side of the wire. Using this method, 2 separate domains were recorded in both TbFeCo wires. Fig.1(b) shows a Polar Kerr polarized microscope image of the TbFeCo wires. When the driven pulse current is applied into the TbFeCo wire, all recorded domains were shifted in unison to the right hand side. Those domain wall are moved in the opposite direction to the current flow because of spin torque transfer effect. The critical current density was $4 \times 10^6 \text{ A/cm}^2$. This value is much smaller than those of FeNi, and Co/Ni wires.

This work was partially supported by the Ministry of Education, Strategic Research Foundation at Private University (2009-2013) and KAKENHI's No.24656219 (2012-2013) and No.24360126 (2012-2014)

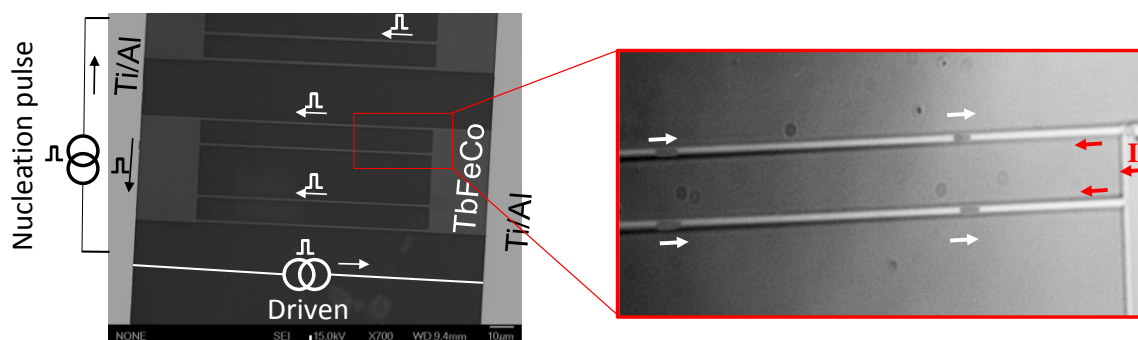


Fig.1 (a) SEM image of the experimental setup. When the nucleation current pulse into the Ti/Al wire is applied, a magnetic domain can be generated in the left hand side of the TbFeCo wire. Then, the recorded domain can be displaced by using the driven pulse current. (b) When 2 domains in each TbFeCo wires are recorded, all domains can be shifted to right hand side by applying the driven pulse current.

[1] D.T. Ngo, K. Ikeda, H. Awano, *Appl. Phys. Express*, **4** (2011) 093002.

2RP-A-10

HIGH SENSITIVITY GMR MAGNETIC SENSORS

Iwata S.¹, Kato T.¹, Wang G.A.¹

¹ Nagoya University, Furo-cho, Chikusa-ku, Nagoya, 464-8603, Japan
iwata@nuee.nagoya-u.ac.jp

Giant magneto-resistance (GMR) magnetic sensors have been developed and widely used in many applications such as field, linear position and rotary angle sensing. Most of the spin-valve type GMR sensors utilize the resistance variation when free-layer magnetization rotates from the direction of pinned layer by the external magnetic field. In this report, we present the GMR sensors employing new sensing methods, where the magnetization direction or the domain wall position of the free-layer is modulated by AC magnetic field[1,2]. The AC modulation contributes enhancement of sensitivity, suppression of temperature drift and detection of strain.

The GMR sensor element, Ta (5 nm)/(Co₉₀Fe₁₀)₉₂B₈(10 nm)/Cu(2.2 nm)/Co₉₀Fe₁₀(3nm)/MnIr(20 nm), was prepared on a thermally oxidized Si substrate by sputtering method. The GMR element was microfabricated to 30 μm width line (length:200 μm). Onto the element, insulation layer of Al₂O₃ (200 nm) and a top Al wire (200 nm thick and 100 μm in width) were fabricated. Figure 1 shows an example of experimental setup. The GMR element was connected to a bridge circuit and the bridge output was amplified by a low-noise instrumentation amplifier and then was sent to a lock-in amplifier (LA). The LA output and the 5 kHz AC signal were added and amplified and the amplified signal was transmitted through the Al conducting wire to generate a feedback field H_{ac} on the GMR element. Since the DC component of the current cancels the external field H_{ext} by negative feedback, the DC output of LA corresponds the H_{ext} . By this circuit, temperature drift was suppressed because the output voltage does not depend on MR ratio of the GMR element.

The GMR strain sensor was also developed by utilizing magnetostrictive effect. The GMR elements with a line shape were microfabricated onto 0.15 mm thick cover glass and the direction of free layer magnetization was modulated by AC field. The change of AC output voltage was detected by bending GMR element shown in Fig.2. This implies that the effective magnetic anisotropy of the free layer was changed by inverse magnetostrictive effect.

[1] G. Wang, S. Nakashima, S. Arai, T. Kato, S. Iwata, *J. Appl. Phys.*, **107** (2010) 09E709-1-3.

[2] G. A. Wang, S. Arai, T. Kato, and S. Iwata, *J. Phys. D: Appl. Phys.*, **44** (2011) 235003-1-5.

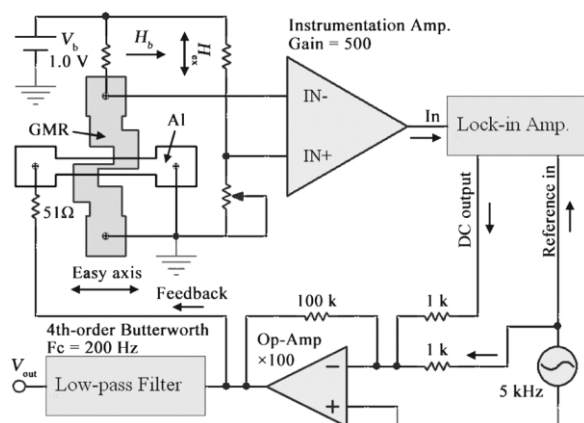


Fig 1. Sample configuration and feedback circuit.

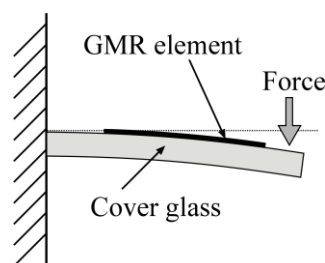


Fig.2 Schematic drawing of the GMR strain sensor.

2OR-A-11

MAGNETORESISTANCE AND MAGNETIC PROPERTIES $Ce_xMn_{1-x}S$ *Aplesnin S.S.^{1,2}, Sitnikov M.N.², Romanova O.B.¹, Eremin E.V.^{1,2}, Sokolov V.V.³, Pichugin A. Yu.³*¹ Kirensky Institute of Physics, Russian Academy of Sciences, Siberian Branch, 660036 Krasnoyarsk, Russia² Siberian State Aerospace University, 660014 Krasnoyarsk, Russia³ Nikolaev Institute of Inorganic Chemistry, Russian Academy of Sciences, Siberian Branch, 630090 Novosibirsk, Russia
apl@iph.krasn.ru

The materials that exhibit the correlation of the electrical and magnetic properties attract attention of researchers as promising candidates for application in microelectronics and spintronics. The compounds with variable valence undergo metal-insulators and magnetic phase transitions, when the magnetic characteristics of the materials can change without variation in magnetic symmetry. Ce ions are characterized by non-integral valence because of the strong hybridization of 4*f* electrons with conduction electrons and these phenomena may be observed on the cation-substituted $Ce_xMn_{1-x}S$ ($0 < x < 0.1$) compounds based on the antiferromagnetic semiconductor manganese monosulfide. Magnetic moment and magnetization curves of the $Ce_xMn_{1-x}S$ solid solutions have been experimentally studied at temperatures (4 – 300) K in magnetic fields up to 9 T. Magnetic ordering induced by Ce ion was found at $T \leq 5$ K. The hysteresis $M(H)$ for $X=0.01$ and nonlinear field behavior of the magnetization at $X = 0.05$, the sharp Curie temperature drop were found.

The sharp maxim in the temperature dependence of resistivity (Fig.1) was observed for all compounds. The maximum temperature was shifted from $T=238$ K to $T=170$ K at Ce ion concentration increasing. This effect may be attributed by incoherent Kondo scattering or orbital electron correlation arising from Jan-Teller effect. The peak in resistivity was also shifted in magnetic field $H=0.8$ T. The magnetoresistivity $[\rho(H)-\rho(0)]/\rho(0)$ changes sign from positive to negative at the heating.

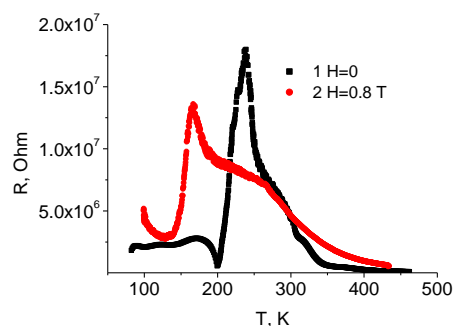


Fig. 1. Resistance of $Ce_xMn_{1-x}S$ for $x=0.01$ versus temperature in magnetic field $H=0$ (1), $H=0.8$ T(2).

Support by the Russian Foundation for Basic Research project № 12-02-00125-a; № 14-02-90010_Бел_a.

2OR-A-12

**FREE-STANDING FLAT SILICENE NANOCRYSTALS
STABILIZED WITH PERFLUOROPHENYL LIGANDS:
EXPERIMENT AND AB INITIO RESEARCH**

Aslanov L.A.¹, Kudryavtsev I.K.¹, Zakharov V.N.¹, Kulatov E.T.², Uspenskii Yu.A.³

¹ Faculty of Chemistry, Lomonosov Moscow State University, Moscow, Russia

² Prokhorov General Physics Institute of RAS, Moscow, Russia

³ Tamm Theory Department, Lebedev Physical Institute of RAS, Moscow, Russia

kulatov@nsc.gpi.ru

Silicon (Si) is currently the basis of most of nanodevice technology, therefore ultrathin materials based on Si would have the great advantage of easy integration into existing circuitry. While the first monoatomic silicon layers were synthesized in 2010, their strong spontaneous deformation was observed [1]. It was found that the stabilization of silicene layers by phenyl (Ph) ligands is not sufficient to solve this problem. First flat silicon nanocrystals have been obtained with perfluorophenyl (PFPh) ligand coating [2]. The size of these particles varies from 15 to 50 nm. Their thickness evaluated with the atomic force microscopy was about 3.3 nm. It is probable that the flatness of nanocrystals was caused by special interaction between PFPh ligands, which makes particles resistant to deformation.

In this presentation we study in details a mechanism for the stabilization of silicene sheets by PFPh ligands. For this aim we investigate the structural, electronic and magnetic properties of single buckled layer Si stabilized by PFPh or Ph ligands, as well as the silicene layers doped by transition metal interstitials. Basing on *ab initio* DFT calculations at the generalized-gradient approximation (GGA) level we investigate the geometries and electronic structures of free-standing PFPh or Ph-stabilized 2D-silicene in order to see if such systems have promising electronic properties. We use a cubic supercell with periodic boundary conditions and with the vacuum spacer of approximately 16 Å. Electronic structures were calculated after geometry relaxation throughout which no symmetry constraints were imposed on the system.

We also examined the effect of doping PFPh-stabilized 2D-silicene by the Mn interstitial placed in the centre of hexagonal ring of Si atoms. We find that the Stoner criteria in non-magnetic state is fulfilled, and the ferromagnetic state with 3 μ_B per Mn has large preference over the non-magnetic one. We therefore consider that the 2D-silicene systems stabilized with perfluorophenyl ligands and doped by transition metal interstitials are a possible candidate material for future nanoscale spintronic devices with very desirable electronic and magnetic properties.

Support by RFBR 13-02-00655 and Programs of the RAS is acknowledged.

[1] Y. Sugiyama, H. Okamoto, T. Mitsuoka, T. Morigawa, K. Nakanishi, T. Ohta, H. Nakano, *J. Am. Chem. Soc.*, **132** (2010) 5946-5947.

[2] A.S. Orekhov, S.V. Savilov, V.N. Zakharov, A.V. Yatsenko, L.A. Aslanov, *J. Nanopart. Res.*, **16** (2014) UNSP 2190, DOI 10.1007/s11051-013-2190-4.

2OR-A-13

ANHYSTERETIC MAGNETIC REVERSAL OF MACRO- AND MICRO-SIZE PATTERNED SPIN VALVES WITH CROSSED ANISOTROPY CONFIGURATION

Milyaev M.A.¹, Naumova L.I.¹, Bannikova N.S.¹, Proglyado V.V.¹, Ustinov V.V.¹

¹ Institute of Metal Physics, Ural Branch of Russian Academy of Sciences, Ekaterinburg, Russia
naumova@imp.uran.ru

A basic spin valve (SV) encloses two ferromagnetic layers, referred to as “pinned” and “free”, which are separated by a nonmagnetic layer. The pinned layer is coupled with an adjacent antiferromagnetic layer by an exchange interaction, and its hysteresis loop is shifted. The displacement H_J of the free layer hysteresis loop arises from the interlayer coupling between ferromagnetic layers. The SVs with negligible free layer coercivity can be used in various analogue devices. An effective way to reduce the coercivity is the formation of crossed orientation of the free layer easy axis (EA) and the pinning direction (PD). In this work the nearly crossed anisotropy configuration (with an angle between the PD and EA of 85 - 90°) was formed in SV films and micro-sized SV meanders. The coercivity reduction for this anisotropy configuration has been studied taking into account the interlayer coupling, the samples macro or micro sizes and an applied magnetic field (MF) direction.

The Ta/NiFe/CoFe/Cu/CoFe/MnIr/Ta SVs with different relation between H_J and the free layer anisotropy field H_A were prepared by DC magnetron sputtering. The free layer coercivity H_c was evaluated as the full width at half maximum of a hysteresis loop. For the sample with strong interlayer coupling ($H_J/H_A > 1$) the creation of nearly crossed anisotropy configuration and the subsequent deviation of the MF from PD by a fixed angle Θ results in $H_c = 0$, keeping the GMR-effect value of 10.5 %. In case of weak coupling ($|H_J/H_A| < 1$) the same treatment did not lead to the same reduction of H_c for any of macroscopic sized samples. But for the meander the H_c was reduced from 16.3 to 1 Oe with an unchanged high GMR value (Fig. 1). The $H_c(\Theta)$ dependences were interpreted in accordance with the phase diagram [1, 2]. The angle intervals of hysteretic (A and B) and anhysteretic (C) reversal modes are shown in Fig 1. Thus, the H_c was reduced by variations of the angle between PD, EA and MF in micro-sized meanders just as in macro-sized samples. In case of $|H_J/H_A| < 1$ the absence of mode C for macro-sized samples can be explained in terms of local fluctuations of magnetization in a film plane.

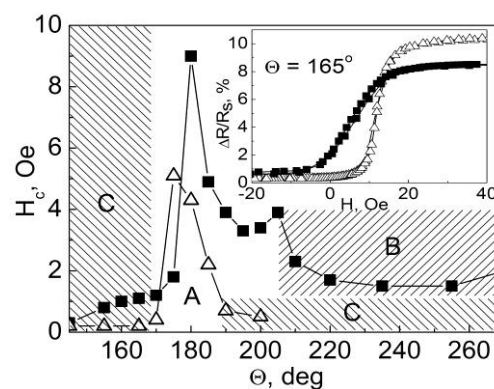


Fig. 1. $H_c(\Theta)$ dependences for strong coupled SV and weak coupled meander (empty and solid symbols respectively). The insert shows low field parts of magnetoresistive curves.

Support by RFBR (project №13-02-00749), Presidium RAS (projects No. 12-P-2-1051 and 12-2-2-009-“Arctica”) and grant SS-1540.2014.2 is acknowledged.

[1] M. Labruno et al, *J. Magn. Magn. Mater.*, **171** (1997) 1-15.

[2] L. Naumova et al, *The Phys. Met. Metallogr.*, **115** (2014) 4, 350–357.

2OR-A-14

RESONANCE AMPLIFICATION OF AZIMUTHAL MODES IN VORTEX SPIN-TORQUE NANO-OSCILLATOR BY SPIN-POLARIZED RF CURRENT

Belanovsky A.D.¹, Skirdkov P.N.¹, Zvezdin K.A.¹, Zvezdin A.K.¹, Ivanov B.A.², Slavin A.N.³

¹ A. M. Prokhorov General Physics Institute, RAS, Vavilova, 38, 119991 Moscow, Russia and Moscow Institute of Physics and Technology, Institutskiy per. 9, 141700 Dolgoprudny, Russia

² Institute of Magnetism, Ukrainian Academy of Science, 36-b Vernadsky Blvd, Kiev, 03142, Ukraine

³ Department of Physics, Oakland University, Rochester, Michigan 48309, USA
abelanovsky@gmail.com

The 2D magnetic solitons (vortexes, domain walls, scyrmions) in ferromagnetic multilayer structures have drawn much attention in the last decades because of its possible applications and interesting fundamental phenomena. The recent experimental and theoretical works devoted to the magnetic vortex dynamics in nanodots have shown that this dynamics has two types of excitations. The first one is the gyrotropic motion of the vortex core with frequency of the hundreds of MHz [1,2], the second excitation correspond to azimuthal and radial spin waves (SW) related to magnon-soliton interaction [3-5]. Most of these works are dealing with excitation of high-frequency modes by external magnetic field, however the influence of spin-polarized current in current-perpendicular to the plane geometry (CPP) on the vortex core ultra-fast dynamics remains unstudied.

In this work we investigate numerically the influence of rf spin-polarized current on high-frequency modes. The results show that current with resonance frequencies corresponding to azimuthal spin-waves modes (in GHz range) can amplify these oscillations, see FIG. 1.

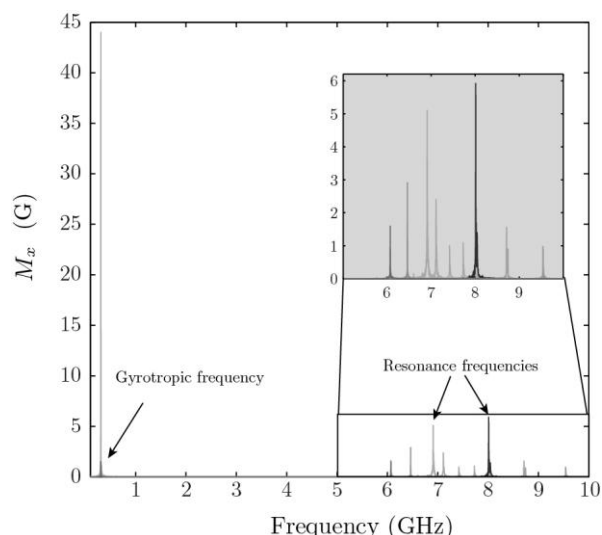


Fig. 1. Resonance amplification of high frequency oscillations by rf spin-polarized current.

Support by Dynasty Foundation and RFBR grant 13-02-90502.

[1] A.Dussaux, B.Georges, J.Grollier, V.Cros, A.Khvalkovskiy, A.V.Fukushima, M.Konoto, H.Kubota, K.Yakushiji, S.Yuasa, K.Zvezdin, K.Ando, A.Fert, *Nature Communications*, **1** (2010).

[2] K.Y. Guslienko, B.A. Ivanov, V.Novosad, Y.Otani, H.Shima, K.Fukamichi, *J. Appl. Phys.*, **91** (2002) 8037.

[3] F.G. Mertens, H.J. Schnitzer, A.R. Bishop, *Phys. Rev. B* **56**, 2510 (1997).

[4] K.Y. Guslienko, W.Scholz, R.W. Chantrell, V. Novosad, *Phys. Rev. B*, **71** (2005) 144407.

[5] J. P. Park and P. A. Crowell, *Phys. Rev. Lett.* **95** (2005) 167201.

Wednesday

2 July

11:30-13:00

14:30-17:00

oral session

2TL-B

2TL-LT

2RP-LT

2OR-LT

**“Magnetism and
Superconductivity”**

2TL-B-1

SPIN IMBALANCE IN A MESOSCOPIC SUPERCONDUCTOR*Quay C.H.L.¹, Aprili M.¹, Chevalier D.¹, Dutreix C.¹, Bena C.²*¹ Laboratoire de Physique des Solides (CNRS), Bât. 510, Université Paris-Sud, 91405 Orsay, France² Institute de Physique Théorique, CEA Saclay 91190 Gif-sur-Yvette, France
marco.aprili@u-psud.fr

Injecting spin-polarized electrons or holes into a superconductor and removing Cooper pairs creates both spin and charge imbalances. A dynamic equilibrium between continuous injection and relaxation leads to constant-in-time spin and charge accumulation proportional to their respective relaxation times, t_s and t_0 .

Using a mesoscopic "absolute" spin-valve [1], we inject spin polarised carriers into superconducting aluminium. Measuring the non-local voltage gives us the chemical potential difference between quasiparticles and Cooper pairs. We observe that spin (charge) accumulation dominates at low (high) injection current [2]. Thus, we generate spin-charge separation within few hundred nanometers from the injecting electrodes as theoretically first predicted by Kivelson and Rokhsar [3]. From the spin accumulation we estimate the spin relaxation time ($t_s \approx 15$ ns), which turns out to be much longer than the charge relaxation time ($t_0 \approx 10$ ps).

To explore the dynamics of spin imbalance, we then create a time-dependent out-of-equilibrium magnetisation in the aluminium by micro-wave spin injection. We obtain the spin relaxation time from frequency domain measurements and find $t_s = 20$ ns, consistent with results from constant current injection. The bias and frequency dependence of the non-local spin signals is well-described by a theoretical model that couples injection from a tunnelling contact with spin relaxation in the superconductor.

These experiments allow us to explore transport scenarios in which spin and charge degrees of freedom are separately addressed.

*Current address : Instituut-Lorentz, Universiteit Leiden, P.O. Box 9506, 2300 RA Leiden
Support by European Research Council Starting Independent Researcher Grant (NANO-GRAPHENE 256965), C'NANO grant (DYNAH) from the Ile-de-France region and ANR grants (DYCOSMA & MASH) from the French Agence Nationale de Recherche, is acknowledged.

- [1] Daniel Huertas-Hernando, Yu. V. Nazarov, and W. Belzig, *PRL*, **88** (2002) 047003-1.
[2] S.A. Kivelson, and D.S. Rokhsar, *PRB*, **41** (1990) 11693–11696.
[3] C.H.L. Quay et al., *Nature Physics*, **9** (2013) 84-88.

LONG RANGE SPIN-POLARIZED QUASIPARTICLE TRANSPORT IN NANOSCALE SUPERCONDUCTORS

Wolf M.J.¹, Hübler F.^{1,2}, Kolenda S.¹, von Löhneysen H.^{2,3}, Beckmann D.¹

¹ KIT, Institute of Nanotechnology, Karlsruhe, Germany

² KIT, Institute of Solid State Physics, Karlsruhe, Germany

³ KIT, Physikalisches Institut, Karlsruhe, Germany

detlef.beckmann@kit.edu

We report on nonlocal transport in superconductor hybrid structures, with ferromagnetic as well as normal-metal tunnel junctions attached to a central superconducting wire (see Fig. 1). In these experiments, we observe both charge and spin imbalance. In the presence of a strong Zeeman splitting of the density of states, we find signatures of spin transport over distances of several μm [1], exceeding other length scales such as the coherence length, the normal-state spin-diffusion length, and the charge-imbalance relaxation length. The relaxation length of the spin signal shows a strong increase with magnetic field, hinting at a freeze-out of relaxation by the Zeeman splitting. Using a combination of ferromagnetic and normal-metal contacts, we demonstrate spin injection from a normal metal, and show a complete separation of charge and spin imbalance [2].

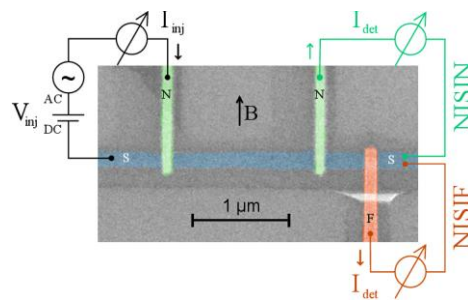


Fig. 1. False-color SEM image of a typical sample and measurement scheme.

[1] F.Hübler, M.J.Wolf, D.Beckmann, H.V.Löhneysen, *Phys. Rev. Lett.*, **109** (2012) 207001.

[2] M. J. Wolf, F. Hübler, S. Kolenda, H.V.Löhneysen, D. Beckmann, *Phys. Rev. B*, **87** (2013) 024517.

2TL-B-3

ELECTRON REFRIGERATION IN SUPERCONDUCTOR/SPIN-FILTER DEVICES

Kawabata S.¹, Ozaeta A.², Vasenko A.S.³, Kashiwaya S.¹, Hekking F.W.J.³, Bergeret F.S.^{2,4}

¹ National Institute of Advanced Industrial Science and Technology (AIST), Tsukuba, Japan

² Centro de Física de Materiales (CFM-MPC), Centro Mixto CSIC-UPV/EHU, Spain

³ LPMMC, Université Joseph Fourier and CNRS, Grenoble, France

⁴ Donostia International Physics Center (DIPC), San Sebastián, Spain

s-kawabata@aist.go.jp

The electric current flow in N/I/S (Normal metal/Insulator/Superconductor) tunnel junctions is accompanied by heat transfer from N into S. This phenomenon arises due to selective tunneling of high-energy quasiparticles out of N which is induced by the superconducting energy gap D . Such a heat transfer through N/I/S junctions can be used for the realization of microcoolers [1].

However a serious limitation of the performance of an N/I/S microcooler arises from the intrinsic multi-particle nature of current transport in N/I/S junctions which is governed not only by single-particle tunneling but also by two-particle processes due to the Andreev reflection [1]. While the single-particle current and the associated heat current are due to quasiparticles with energies $E > D$, at low temperatures or high junction transparencies the charge transport in N/I/S junctions is dominated by the Andreev reflection. The Andreev current does not transfer heat through the N/S interface but rather generates the Joule heating. At low enough temperatures this heating exceeds the single-particle cooling [2].

In order to reduce the Andreev current, it was suggested to use ferromagnetic metals where the Andreev reflection is suppressed [3]. On the other hand, it is also possible to suppress the Andreev reflection by the spin-filtering effect [4,5] in N/spin-filter(SF)/S junction.

In this talk, we propose novel micro-cooler based on clean and diffusive N/SF/S junctions and show that the cooling power is dramatically enhanced by the suppression of the Andreev reflection due to the spin-filter effect [6]. Our results strongly indicate the usefulness of the spin-filter effect for effectively cooling sensors, detectors, as well as quantum devices.

[1] F. Giazotto, T. T. Heikkilä, A. Luukanen, A. M. Savin, J. P. Pekola, *Rev. Mod. Phys.*, **78** (2006) 217.

[2] A. Bardas and D. Averin, *Phys. Rev. B*, **52** (1995) 12873.

[3] F. Giazotto, F. Taddei, R. Fazio, and F. Beltram, *Appl. Phys. Lett.*, **80** (2002) 3784.

[4] S. Kawabata, Y. Asano, Y. Tanaka, A. A. Golubov, S. Kashiwaya, *Phys. Rev. Lett.*, **104** (2010) 117002.

[5] S. Kashiwaya, Y. Tanaka, N. Yoshida, and M. R. Beasley, *Phys. Rev. B*, **60** (1999) 3572.

[6] S. Kawabata, A. Ozaeta, A. S. Vasenko, F. W. J. Hekking, and F. S. Bergeret, *Appl. Phys. Lett.*, **103** (2013) 032602.

2TL-LT-1

PHASE DIAGRAMS OF Fe BASED SUPERCONDUCTORS

Büchner B.^{1,2}

¹ Institut für Festkörperforschung, IFW Dresden

² Institut für Festkörperphysik, TU Dresden

The magnetic/electronic phase diagrams of several classes of iron pnictide superconductors have been studied using a broad spectrum of experimental techniques, such as NMR, μ SR, ARPES, magnetometry, thermodynamics, x-ray diffraction, and transport measurements. For most of the systems the well-known intimate interplay between antiferromagnetism and superconductivity is apparent. There are, however, qualitative differences in the phase diagrams, which could be related to details of the structural/nematic order. For example, measurements of the electrical field gradient by NQR in underdoped $\text{LaO}_{1-x}\text{F}_x\text{AsFe}$ (and other 1111 type materials) yield clear-cut evidence for a nanoscale order of charges and/or orbitals which is absent in other systems. The role of this local order for the unusual electronic/magnetic properties of underdoped 1111 systems will be discussed.

In addition we will present detailed studies of LiFeAs showing superconductivity without doping. From our measurements on the pristine material as well as hole and electron doped compounds we do not find any evidence for strong antiferromagnetic correlations. Instead, measurements of NQR, μ SR, magnetisation and neutron diffraction reveal a weak ferromagnetic order in hole doped LiFeAs . Based on our determination of the phase diagram and the results from spectroscopic studies the possible relationship between this unusual ferromagnetic state and superconductivity in stoichiometric LiFeAs is discussed.

2TL-LT-2

FERROELECTRICITY, ELECTRON AND TRANSPORT PROPERTIES OF CUPRATE SUPERCONDUCTORS

Kusmartsev F.V.¹, Saarela M.²

¹ Department of Physics, Loughborough University, Loughborough, LE11 3TU, UK

² Department of Physics, University of Oulu, Oulu, FIN-90014, Finland

F.Kusmartsev@lboro.ac.uk

We show that doping of hole charge carriers induces formation of electric dipolar moments in cuprates. A single dipole moment is created between the dopant ion outside the CuO plane and a bound cluster of four holes in the CuO plane. The binding energy of the cluster determines the activation energy of the two-fluid model and the pseudogap temperature [1]. Such dipoles may form a disordered state of dipolar glass or an ordered state such as stripes depending on the preparation of the sample. The lowest energy of the ordered system corresponds to a local antiferroelectric ordering. The mobility of dipoles is very low at low temperatures and they prefer first to bind themselves into dipole-dipole pairs. Electromagnetic radiation interacts strongly with electric dipoles and when the sample is subjected to it, the mobility changes significantly. This leads to a fractal growth of dipolar clusters. The existence of electric dipoles reveals a series of new phenomena such as ferroelectricity or a pronounced light and microwave absorption as well as may be related to the phenomenon of the field induced superconductivity.

[1] M. Saarela, F.V. Kusmartsev, *Nanoscience and Engineering in Superconductivity* (Springer-Verlag, Berlin, Heidelberg, 2010) 211-229.

2TL-LT-3

HIGH TEMPERATURE SUPERCONDUCTIVITY WITHIN t - J AND HUBBARD MODELS: COMPARISON TO EXPERIMENT

Spalek J., Kaczmarczyk J.

Marian Smoluchowski Institute of Physics, Jagiellonian University, Reymonta 4, 30-059 Krakow,
Poland
ufspalek@if.uj.edu.pl

We have formulated both the statistically consistent Gutzwiller approximation (SGA) [1], as well as the systematic diagrammatic expansion of the Gutzwiller wave function (DE-GWF) for both the Hubbard [2] and the t - J models [3]. The latter method leads to a proper doping independence of the Fermi velocity in the nodal direction. Both approaches provide a dome-like behavior of the superconductivity appearance in a semiquantitative manner, as well as the doping dependence of extended the d -wave gap in the antinodal direction. The results coming from both models are critically overviewed [4].

The work was partly supported by the projects TEAM (Foundation for Polish Science) and MAESTRO (from National Science Centre).

[1] J. Jedrak, J. Spalek, *Phys. Rev. B*, **83** (2011) 104512.

[2] J. Kaczmarczyk et al., *Phys. Rev. B*, **88** (2013) 115127.

[3] J. Kaczmarczyk, J. Bunemann, J. Spalek, *New. J. Phys.* (2014), in press.

[4] J. Spalek, *Phil. Mag. B* (2014), in press.

2TL-LT-4

EMERGENCE OF SUPERCONDUCTIVITY AND VORTEX CONFINEMENT IN SUPERCONDUCTOR/FERROMAGNET HYBRIDS

Karapetrov G.¹, Iavarone M.², Moore S.A.², Fedor J.², Ciocys S.T.¹, Pearson J.³, Novosad V.³,
Bader S.D.³

¹ Physics Department, Drexel University, Philadelphia, PA 19104, USA

² Physics Department, Temple University, Philadelphia, PA 19122, USA

³ Materials Science Division, Argonne National Laboratory, Argonne, IL 60439, USA
goran@drexel.edu

Magnetically coupled superconductor-ferromagnet hybrids offer advanced routes for nanoscale control of superconductivity. We will show that scanning tunneling microscopy and scanning magnetic force microscopy coupled to magneto-transport measurements reveal rich vortex phase diagram.

The stray field of the ferromagnet induces a non-uniform superconducting state characterized by a local superconducting critical temperature T_c and a non monotonic behavior of T_c vs H close to the critical temperature [1,2]. When the experimental parameters of the superconductor and the ferromagnet are properly tuned such S/F structures are attractive model systems that offer the possibility to control the superconductor inhomogeneity, i.e. the strength and the location of the superconducting nucleus.

We studied Pb/[Co/Pd] systems and we visualized the emergence of superconductivity in regions above the separation between adjacent magnetic domains, as well as reverse domain wall superconductivity. Deep in the superconducting state vortices of opposite polarity are induced by the stray field of the ferromagnet in zero applied external field and they are strongly confined by the stripe of the same polarity.

In those systems with narrower stripe domains, the conditions are not met to support generation of vortices in zero applied field and vortex nucleation can be induced only through the application of an external magnetic field. These results provide direct evidence of the possibility of superconducting order parameter manipulation in S/F hybrid systems.

Work at Temple University was supported by the U.S. Department of Energy, Office of Basic Energy Sciences, Division of Materials Sciences and Engineering under Award DE-SC0004556. The work at Drexel U. was supported by Award No. OISE-14-60109-0 of the U.S. Civilian Research & Development (CRDF). Work at Argonne National Laboratory was supported by UChicago Argonne, LLC, Operator of Argonne National Laboratory (“Argonne”). Argonne, a U.S. Department of Energy Office of Science laboratory, is operated under Contract No. DE-AC02-06CH11357.

[1] Yang Z., Lange M., Volodin A., Szymczak R., Moshchalkov V.V., *Nature Mater.*, **3** (2004) 793.

[2] Aladyshkin A. Yu., Buzdin A. I., Fraerman A.A., Melnikov A.S., Ryzhov D.A., Sokolov A.V., *Phys. Rev. B*, **68** (2003) 184508.

2RP-LT-5

QUANTUM FLUCTUATIONS IN SUPERCONDUCTING NANOSTRUCTURES

Arutyunov K.Yu.^{1,2,3}, Lehtinen J.S.¹, Rantala T.¹

¹ University of Jyväskylä, Department of Physics, NanoScience Centre, 40014 Jyväskylä, Finland

² Moscow Institute of Physics and Technology, Dolgoprudny, 141700, Russia

³ National Research University Higher School of Economics, 101000, Moscow, Russia

The topic of quantum fluctuations in quasi-1D superconductors, also called *quantum phase slips* (QPS), has attracted the significant attention [1]. It has been shown that the phenomenon is capable to suppress zero resistivity of ultra-narrow superconducting nanowires at low temperatures $T \ll T_c$ [2-4] and quench persistent currents in tiny nanorings [5] due to coherent superposition of QPS [6].

A superconducting nanowire in the regime of QPS is dual to a Josephson junction, reflecting the fundamental similarity between these two systems. Here we demonstrate that imbedded in a high-impedance environment, the I-V characteristic of such a QPS nanowire demonstrates pronounced Coulomb blockade with particular back-bending shape (“Bloch nose”) [7]. Application of external RF radiation leads to appearance of steps on the I-V characteristic. The phenomenon is dual to the well-known Shapiro effect: the voltage steps for a Josephson junction are substituted by the current steps for a QPS wire. The position of the n -th step follows the relation $I_n = n \times (2e) \times f_{RF}$, where f_{RF} is the frequency of external RF radiation and $2e$ is the charge of a Cooper pair. Additionally to the substantial significance for fundamental research, the effect is expected to lead to the important metrological application - the quantum standard of electric current [7].

We have also demonstrated that the same phenomenon – quantum fluctuations – is responsible for smearing of superconducting energy gap and finite noise well below the critical temperature and/or critical current in extremely narrow superconducting channels.

The observed effects indicate that the ‘textbook’ attributes of superconductivity are severely violated at reduced dimensions. The studies are of extreme importance for understanding the quantum coherence phenomena at nanoscales.

[1] K. Yu. Arutyunov, D. S. Golubev, A.D. Zaikin, *Phys. Rep.* **464** (2008) 1.

[2] M. Zgirski, K.-P. Riikonen, V. Touboltsev, K. Arutyunov, *NanoLett.* **5** (2005) 1029.

[3] M. Zgirski, et.al., *Phys. Rev. B.*, **77** (2008) 054508.

[4] J. S. Lehtinen, et.al., *Phys. Rev. B*, **85** (2012) 094508.

[5] K. Yu. Arutyunov et.al., *Nature: Sci. Rep.*, **2** (2012) 293.

[6] O. V. Astafiev et.al., *Nature* **484** (2012) 355.

[7] J. S. Lehtinen, K. Zakharov, K. Arutyunov, *Phys. Rev. Lett.*, **109** (2012) 187001.

2RP-LT-6

THERMOPOWER IN SFN HETEROSTRUCTURES

Kalenkov M.S.^{1,2}

¹ P.N. Lebedev Physical Institute, 119991 Moscow, Russia

² LCN, Nizhny Novgorod State Technical University n.a. R.E. Alekseev
kalenkov@lpi.ru

We study electron transport in superconductor/normal metal (SN) structure with spin-active interface (Fig. 1). It was shown that interplay of the Andreev reflection and spin-dependent interface scattering produces large asymmetry in the scattering rates of the electron- and hole-like excitations.

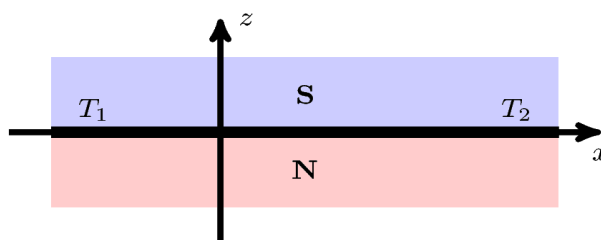


Fig. 1. SN bilayer with spin-active interface.

This asymmetry may result in a drastic enhancement of the thermocurrent in these systems. We calculate thermocurrent flowing along the SN interface within the quasiclassical theory of superconductivity and show that under certain conditions magnitude of the thermocurrent may be much larger than its value in the normal state.

2OR-LT-7

COPPER OXIDE SUPERCONDUCTING/ANTIFERROMAGNETIC INTERFACE

Kislinskii Yu.V.^{1,4}, *Constantinian K.Y.*¹, *Ovsyannikov G.A.*^{1,2}, *Shadrin A.V.*^{1,5}, *Khaydukov Yu.N.*³,
Sheyerman A.E.^{1,5}, *Vasiliev A.L.*⁶

¹ Kotel'nikov IRE RAS, 125009 Moscow, Russia

² Chalmers University of Technology, SE-41 296 Gothenburg, Sweden

³ Max-Planck Institute for Solid State Research, 70 569 Stuttgart, Germany

⁴ Shubnikov Institute of Crystallography, 119333 Moscow, Russia

⁵ Moscow Institute of Physics and Technology, Dolgoprudny, Russia

⁶ Kurchatov National Research Center, Moscow, Russia

yulii@hitech.cplire.ru

Carrier transport and capacitance studies of Nb/Au//Ca_{1-x}Sr_xCuO₂/YBa₂Cu₃O_{7-δ} (Nb/Au/CSCO/YBCO) mesa-structures (MS) reveal a huge conductance rise extended up to 50 nm depth of CSCO film adjacent to the CSCO/YBCO interface. The X-ray, neutron scattering, transmission electron microscopy of Au/CSCO/YBCO MS show sharp enough CSCO/YBCO interface, and relatively rough for the Au/CSCO. The CSCO films grown on the (110)NdGaO₃ behave as Mott insulator. The products of normal resistance by area, R_{NA} , increase with CSCO thickness d_M from 10^{-6} to 10^{-2} Ωcm^2 . Samples with $d_M=20$ and 50 nm demonstrate resistance drop at T_c of Nb indicating presence of superconducting current I_C . Note, $I_C=0$ for $d_M=80$ nm.

For MS with $d_M=50$ and 80 nm we observe an increase in conductivity with temperature for $T=4 \div 60$ K. Differential conductance σ_d of MS have singularity at $V \approx 1$ mV due to Nb superconducting energy gap [1]. Both phenomena points on presence a barrier at the CSCO/Au interface. The barrier

may appear due to low work functions of the metals $\Phi_{Au}=4.3$ eV, $\Phi_{Nb}=4$ eV in comparison with $\Phi_{YBCO}=5-6$ eV [2]. Resistance at the barrier could be caused also by difference in Fermi velocities of YBCO and Au [3]. Capacitance per area, C/A , decreases for large thickness d_M . By the C/A dependence we assume that metallic CSCO layer 20 nm in thickness is formed in MS due to charge doping from YBCO [4].

For relation $\Phi_{Nb} < \chi_{CSCO} < \Phi_{YBCO}$, where χ_{CSCO} is electron affinity, the charge doping can be explained by a model of semiconducting ohmic contact with p^+ YBCO layer and p CSCO layer. A band diagram of the MS is proposed. Dependence of C/A versus d_M , dependencies of the σ_d singularity and $I_C R_N$ products versus temperature are discussed.

We acknowledge the support by RAS, Russian Ministry of Education, RFBR 14-07-00258, Scientific School Grant NSh-4871.2014.2, Visby program of Swedish Institute.

[1] G.A. Ovsyannikov, I.V. Borisenko et al, *JETP Lett.*, **84** (2006) 262.

[2] M. Van Zalk, A. Brinkman et al, *Physical Rev. B*, **82** (2010) 134513.

[3] P.V. Komissinskii, G.A. Ovsyannikov et al, *Physical Rev. B*, **78** (2008) 024501.

[4] K.Y. Constantinian, Yu. V. Kislinskii et al, *Physics of the Solid State*, **55** (2013) 461.

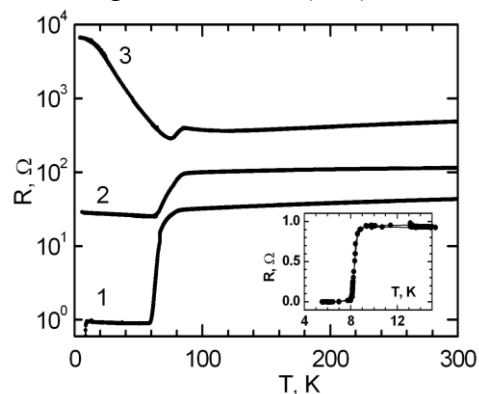


Fig. 1. Temperature dependence of meso-heterostructures resistances with thicknesses (1) - $d_M=20$ nm, (2) - 50 nm, (3) - 80 nm. Inset is given for curve (1).

2TL-LT-8

INFLUENCE OF FLUCTUATIONS ON THE COEXISTENCE PHASE OF SUPERCONDUCTIVITY AND ANTIFERROMAGNETISM IN CERIUM COMPOUNDS

Val'kov V.V.¹, Zlotnikov A.O.¹

¹ L.V. Kirensky Institute of Physics, Krasnoyarsk, Russia
vzv@iph.krasn.ru

In certain compounds of cerium and uranium intermetallics the coexistence of antiferromagnetic phase and superconducting phase has been observed [1, 2]. It is believed that such coexistence can be homogeneous inducing microscopic coexistence phase of antiferromagnetic order and superconductivity, for example in CeRhIn₅ [3]. One of the main features of Ce_nT_mIn_{3n+2m} compounds (T = Rh, Pt; n = 1, 2; m = 1, 2) is that superconductivity appears in the vicinity of the quantum critical point where the long-range antiferromagnetic order is destroyed under pressure [4].

On the basis of the extended periodic Anderson model a theory has been developed which can explain the origin of the superconducting state near the quantum critical point in heavy-fermion systems. It has been shown that Cooper instability and antiferromagnetic ordering in the coexistence phase can be caused by effective exchange interaction between 4f-electrons. Depending on pressure the regions of ground-state stability for the antiferromagnetic ordering, superconductivity and spatially homogeneous coexistence of superconductivity and antiferromagnetism have been found. At a critical pressure P_c the long-range antiferromagnetic order is destroyed by quantum phase fluctuations. At pressures $P < P_c$ the coexistence phase of superconductivity and antiferromagnetism is realized. We have found that a "kink" in the dependence of the superconducting order parameter at P_c is due to the long-range antiferromagnetic order. The influence of thermodynamic fluctuations on the coexistence phase has also been analyzed in the same framework.

The proposed model can also explain an anomalous increase of the electron mass and a Fermi surface change which have been observed in the de Haas-van Alphen experiments on CeRhIn₅ [5]. It has been shown that the transition from small to large Fermi surface occurs and the divergence of the effective electron mass is realized near the quantum critical point. Such behaviors are due to destroying long-range antiferromagnetic order and heavy-fermion band reconstruction.

In this work a detailed description of the rich phase diagram of CeRhIn₅ will be given.

This work was partly supported by the Russian Foundation for Basic Research (project Nos. 13-02-00523, 13-02-98013) and the Presidium of the Russian Academy of Sciences (Program "Quantum mesoscopic and disordered structures"). One of the authors (Z.A.O.) acknowledges the support of the President of the Russian Federation (project MK-526.2013.2).

- [1] C. Pfleiderer, *Rev. Mod. Phys.*, **81** (2009) 1551-1624.
- [2] J.D. Thompson, Z. Fisk, *J. Phys. Soc. Jpn.*, **81** (2012) 011002.
- [3] S. Kawasaki M. Yashima, T. Mito et al., *J. Phys.: Condens. Matter*, **17** (2005) S889-S893.
- [4] T. Park, F. Ronning, H.Q. Yuan et al., *Nature*, **440** (2006) 65-68.
- [5] H. Shishido, R. Settai, H. Harima, Y. Ōnuki, *J. Phys. Soc. Jpn.*, **74** (2005) 1103-1106.

2TL-LT-9

SPIN - FLUCTUATION MECHANISM OF HIGH -TEMPERATURE SUPERCONDUCTIVITY

*Plakida N.M.*¹, *Oudovenko V.S.*²

¹ JINR, Dubna, Russia

² Rutgers University, New Jersey, USA

plakida@theor.jinr.ru

In recent resonant inelastic x-ray scattering experiments in a large family of cuprate superconductors antiferromagnetic (AF) paramagnon excitations with the dispersion and spectral weight similar to those of magnons in undoped cuprates were observed. This suggests that the spin-fluctuation mechanism of high-temperature superconductivity (HTSC) plays the major role while the conventional electron-phonon interaction (EPI) is less important.

To prove this, we consider the extended Hubbard model which takes into account the intersite Coulomb repulsion V and EPI [1]. In the limit of strong correlations appropriate for cuprates (Hubbard $U \gg t$ – hopping parameter) the conduction band splits into two Hubbard subbands of singly and doubly occupied electronic states. In this case, the Hubbard operators (HOs) for these subbands must be introduced. The complicated commutation relations for the HOs result in the so-called kinematic interaction which leads to the spin-fluctuation pairing mechanism. We derived the Dyson equation for the normal and pair Green functions for two Hubbard subbands with the self-energy evaluated in the self-consistent Born approximation. We found the d -wave pairing with high- T_c mediated by spin fluctuations induced by the strong kinematic interaction with a coupling constant of the order of the electronic bandwidth $4t \sim 1.6$ eV, much larger than the AF exchange interaction $J \sim 0.4t$. Contributions coming from the intersite Coulomb repulsion $V \sim 0.5t$ and EPI turned out to be small since only $L=2$ components of the interactions contribute to the d -wave pairing (see Fig.1). We consider also a large intersite Coulomb repulsion V [2]. It was found that the pairing can be suppressed for $V > 3t$, of the order of the kinematic interaction, which proves the spin-fluctuation mechanism. Since the kinematic interaction is specific for strongly correlated electronic systems, as cuprates, we believe that this mechanism is the relevant one for HTSC.

[1] N. M. Plakida, V. S. Oudovenko, *Europ. Phys. Jour.*, **86** (2013) 115 (1-15).

[2] N. M. Plakida, V. S. Oudovenko, *arXiv*: 1402.4934 (2014) (1-11) (to be published in JETP).

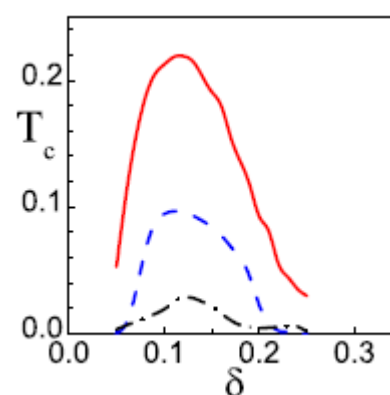


Fig. 1. Superconducting T_c dependence on hole concentration δ induced by all interactions (red solid line), by spin-fluctuations (blue dashed line) or by phonons (black dash-dotted line).

2RP-LT-10

TOPOLOGICAL ANDREEV BOUND STATES IN SPIN-TRIPLET SUPERCONDUCTOR Sr_2RuO_4

Tanaka Y.¹, Yada K.¹, Sato M.¹, Yamakage A.¹

¹ Department of Applied Physics, Nagoya University, Nagoya, Japan
ytanaka@nuap.nagoya-u.ac.jp

Superconducting Sr_2RuO_4 is believed to be a spin-triplet p-wave superconductor where plenty of topological quantum phenomena are expected [1]. The presence of surface Andreev bound state has been experimentally reported[2]. Preexisting theories of tunneling spectroscopy by chiral edge state are based on single band model [3-4] and the role of spin-orbit coupling in many band systems has not been clarified. Here, we present a more realistic theory of tunneling spectroscopy available of this material. Here, We calculate surface density of states (SDOS) and tunneling conductance in normal metal / Sr_2RuO_4 junction in the framework of the recursive Green's function method taking account of orbital degrees of freedom including spin-orbit interaction with realistic material parameters[5]. In Sr_2RuO_4 , there are two bands α and β originating from quasi-one-dimensional orbitals d_{yz} and d_{zx} and a two-dimensional band originating from d_{xy} orbital. We discuss contributions of various electronic bands to LDOS and the influence of atomic spin-orbit interaction (SOI). In the light of our calculations, quasi-one-dimensional model with dominant pair potentials in α and β bands is consistent with conductance measurements in Au/ Sr_2RuO_4 junctions.

We argue that superconductivity in Sr_2RuO_4 hosts a topological phase transition to a topological crystalline SC, which accompanies a d-vector rotation under a magnetic field along the c axis. Taking all three bands and spin-orbit interactions into account, symmetry-protected MFs in the topological crystalline SC are identified [6].

[1] Y. Maeno, et. al, *J. Phys. Soc. Jpn.*, **81** (2012) 011009.

[2] S. Kashiwaya, et.al., *Phys. Rev. Lett.*, **107** (2011) 077003.

[3] M. Yamashiro, Y. Tanaka, and S. Kashiwaya, *Phys. Rev.B*, **56** 7847 (1997).

[4] K. Sengupta, et. al., *Phys. Rev. B*, **63** (2001) 144531.

[5] K. Yada, K. Yada, Y. Tanaka and A.A. Golubov and S. Kashiwaya, *arXiv*: 1311.4682

[6] Y. Ueno, A. Yamakage, Y. Tanaka, and M. Sato, *Phys.Rev. Lett.*, **111** (2013) 087002.

Wednesday

2 July

11:30-13:00

oral session

2TL-C

2RP-C

**“Diluted Magnetic
Semiconductors”**

2TL-C-1

MECHANISM OF LARGE POSITIVE HOPPING MAGNETORESISTANCE IN DILUTE MAGNETIC SEMICONDUCTORS

*Nenashev A.V.¹, Jansson F.², Wiemer M.³, Petznick S.⁴, Klar P.J.⁴, Dvurechenskii A.V.¹,
Hetterich M.⁵, Gebhard F.³, Baranovskii S.D.³*

¹ Institute of Semiconductor Physics and Novosibirsk State University, 630090 Novosibirsk, Russia

² Section Computational Sciences, University of Amsterdam, Amsterdam, The Netherlands

³ Department of Physics, Philipps-University, D-35032 Marburg, Germany

⁴ Institute of Experimental Physics I, Justus-Liebig-University Giessen, D-35392 Giessen, Germany

⁵ Institute of Applied Physics and DFG CFN, KIT, D-76131 Karlsruhe, Germany

baranovs@staff.uni-marburg.de

We suggest a mechanism causing large positive magnetoresistance (MR) in dilute magnetic semiconductors when hopping via nonmagnetic donor impurities dominates the conductivity. The effect is due to the increase in the characteristic width σ of the donor energy distribution with increasing magnetic field B , caused by exchange interactions between magnetic Mn atoms and the electrons localized on nonmagnetic Cl donor impurities.

Using general scaling arguments based solely on the dependencies of hopping rates on temperature and on the energies of hopping sites we show that this broadening of the donor energy distribution alone is sufficient to account for the experimentally observed MR effects in n-type $\text{Zn}_{1-x}\text{Mn}_x\text{Se:Cl}$. We suggest a method for extracting the dependence of σ on magnetic field from the MR data.

The mechanism explains the experimentally observed universal dependence of the MR effect on the ratio B/T at different temperatures T under the premise that transport is due to the nearest-neighbour or Mott hopping mechanism [1]. Theoretical results are supported by straightforward computer simulations of the hopping transport processes.

[1] A. V. Nenashev, F. Jansson, M. Wiemer, *et al.*, *Phys. Rev. B*, **88** (2013) 115210.

2TL-C-2

CARRIER SPIN POLARIZATION IN HYBRID STRUCTURE SEMICONDUCTOR/FERROMAGNETIC GaMnAs

Korenev V.L.¹, Akimov I.A.^{1,2}, Zaitsev S.V.³, Sapega V.F.^{1,4}, Langer L.², Yakovlev D.R.^{1,2}, Danilov Yu. A.⁵, Bayer M.^{1,2}

¹ Ioffe Physical-Technical Institute, RAS, 194021 St. Petersburg, Russia

² Experimentelle Physik 2, Technische Universität Dortmund, D-44227 Dortmund, Germany

³ Institute for Solid State Physics, RAS, 142432 Chernogolovka, Moscow region, Russia

⁴ Spin Optics Laboratory, St. Petersburg State University, 198504 St. Petersburg, Russia

⁵ Physico-Technical Research Institute of Nizhny Novgorod State University, 603950 Nizhny Novgorod, Russia
sapega.dnm@mail.ioffe.ru

Magnetic semiconductors such as GaMnAs have been attracting considerable interest during the last decade, because they combine ferromagnetic and semiconductor properties in such materials. Those two kinds of properties of ferromagnetic semiconductors make possible processing and storing information in a single electronic (spintronic) device. However the poor optical properties restrict the application of this material for the optical methods of information recording and read-out. However, this problem can be overcome in a hybrid structure, consisting of a quantum well (QW) and neighboring ferromagnetic GaMnAs δ -layer.

We studied the exchange interaction in a hybrid structure composed of a nonmagnetic semiconductor QW and ferromagnetic semiconductor δ -layer of GaMnAs located near the QW [1]. It has been demonstrated that spin polarization of the QW carriers is determined not only by external magnetic field but also by their strong exchange coupling with ferromagnetic δ -layer of GaMnAs. Therefore the QW photoluminescence polarization exhibits properties typical for a ferromagnet, i.e. hysteresis loop and magnetization saturation even in low magnetic fields. We have demonstrated unambiguously that this QW PL polarization behavior is explained by dynamic polarization of the QWs nonequilibrium electrons due to spin-dependent electron transfer to the GaMnAs ferromagnet. Because of spin-dependent electron capture from the QW into the ferromagnetic layer, nonequilibrium spin-polarized electrons accumulate in the QW. This spin-separation effect disappears above the Curie temperature, so that it is directly connected with the ferromagnetic ordering in the GaMnAs layer. The important advantage of this hybrid structure is related to its good optical properties due to high efficiency of radiative recombination of carriers in a QW. This gives unique opportunity to read-out optically the ferromagnetic layer magnetization and to control nonequilibrium spin polarization of carriers in a nonmagnetic QW.

Support by RFBR is acknowledged.

[1] V.L. Korenev, et al., *Nature Communications*, **3** (2012) 959.

2RP-C-3

RESONANT INDIRECT EXCHANGE INTERACTION

Rozhansky I.V.^{1,2,3}, *Krainov I.V.*¹, *Averkiev N.S.*¹, *Lahderanta E.*²

¹ Ioffe Physical Technical Institute, St.Petersburg, Russia

² Lappeenranta University of Technology, Finland

³ St. Petersburg State Polytechnic University, Russia

rozhansky@gmail.com

We discuss a new mechanism of ferromagnetism in dilute magnetic semiconductor heterostructures, namely the resonant enhancement of indirect exchange interaction between paramagnetic centers via remote conducting channel.

The standard method for calculating the indirect exchange is Ruderman-Kittel-Kasuya-Yosida (RKKY) theory which predicts oscillatory nature of the indirect exchange interaction as a function of distance [1]. The RKKY theory as perturbation theory has certain limitations. It is not applicable in the case of the strong exchange interaction which resembles a complex many-body problem and requires taking into account the spin dynamics of ions. There is, however an important practical case when the spin dynamics of ions is negligible, but the solution requires going beyond perturbation theory. This situation relevant to the low-dimensional structures arises for the resonant hybridization of a bound state at the paramagnetic ion with the continuum of delocalized states mediating the indirect exchange. An example of such a system is the delta layer of Mn located in a vicinity of a quantum well (QW) in InGaAs based heterostructure [2]. The Mn ion act as acceptor and creates a bound state for a hole with a binding energy comparable to the QW depth. Thus, the tunneling between the bound hole state and the continuous spectrum of 2D holes in the is of a resonance character and cannot be accounted for in the framework of RKKY theory. We use a different approach based on the scattering theory [3] and calculate the indirect exchange interaction energy of the two magnetic ions via the remote 2D conducting channel with account of the resonant tunneling. We demonstrate that in the resonant case when the bound state energy ϵ_0 lies below the Fermi level E_F of the continuum states the resonant hybridization leads to a strong enhancement of the indirect exchange (Fig.1). While analogously to RKKY our theory is valid for weak coupling (the exchange constant $j \ll E_F$), it qualitatively describes the vanishing of the ferromagnetic order in the strong coupling regime as known from the double-impurity Kondo problem.

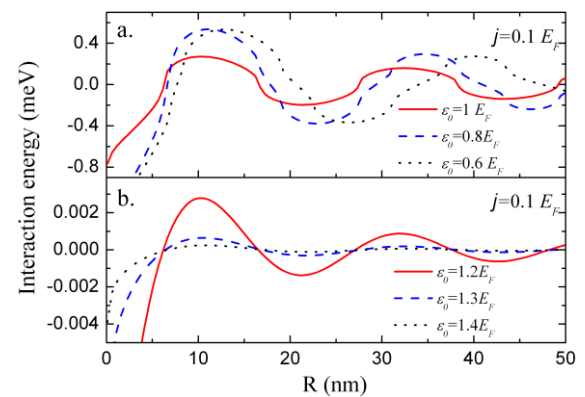


Fig. 1. Enhancement of the indirect exchange in the resonant case (a) as compared to non-resonant RKKY case (b)

[1] M. A. Ruderman, C. Kittel, *Phys. Rev.* **96** (1954) 99.

[2] B.Aronzon, et.al., *J. Phys.: Conf. Ser.*, **456** (2013) 012001.

[3] I. V. Rozhansky, I. V. Krainov, N. S. Averkiev, E. Lahderanta, *Phys. Rev. B*, **88** (2013) 155326.

2RP-C-4

MAGNETIZATION IN HETEROSTRUCTURES GaAs/InGaAs/GaAs LOCALLY DOPED WITH ATOMIC Mn δ -LAYER

*Moiseev K.D.¹, Nevedomsky V.N.¹, Zolotareva R.V.¹, Charikova T.², Kudriavstev Yu.³,
Escobosa A.³, Gallardo S.⁴, Lopez M.⁴*

¹ Ioffe Institute, St Petersburg, Russia

² Institute of Metal Physics RAS, Ekaterinburg, Russia

³ Dep. Ingenieria Eléctrica - SEES, Cinvestav- IPN, México

⁴ Dep. Física, Cinvestav-IPN, Mexico

mkd@iropt2.ioffe.ru

Last decade cooperative phenomena based on spin exchange interactions between carriers and local magnetic moments have long been studied. The mainstream studies of spin-electronic materials based on III-V semiconductors consist of ferromagnet/semiconductor heterostructures, magnetic alloy semiconductors and locally doped heterostructures with Mn δ -layer [1,2]. Advances in epitaxial growth technology, such as molecular beam epitaxy (MBE), have made it possible to grow a variety of semiconductor heterostructures with atomically controlled layer thicknesses and abrupt doping profiles, in which the wave function of carriers can be controlled in artificially designed potentials. Unlike the random alloy system, δ -layer of Mn in GaAs provides the doping profile along the growth direction which can be approximated by Dirac's δ -function. Inherent advantages of δ -doping are locally high dopant concentration and high carrier concentration, which can lead to high Curie temperature T_C . We here report the study of molecular beam epitaxy (MBE) growth, structural, and transport properties of the GaAs/InGaAs/GaAs quantum well heterostructure with Mn d-doped GaAs barrier. The samples were grown on semi-insulating GaAs (001) substrates by MBE at the growth temperatures $T_S=600-200$ °C. The abruptness of the δ -doped Mn profiles and the extent of formation of crystal defects such as dislocations and clusters as well as the degree of localization of the Mn dopants were studied by cross-sectional transmission electron microscopy (TEM), secondary ion mass spectroscopy (SIMS) and X-ray standing wave studies, while the surface morphology was studied by atomic force microscopy (AFM). Abrupt and dislocation-free Mn sheets are formed at h_{Mn} with sub-ML concentrations ($h_{Mn} < 1$ ML), and only a few dislocations are formed with the well-defined interface at 1 ML. Formation of dislocations became observable at 2 ML. SIMS depth profile analyses also indicate abrupt localization of Mn dopants at the sub-ML concentrations without diffusion and segregation. Transport properties were measured in a Hall-bar configuration under a low magnetic field. The local peak on the resistivity dependence at around 90 K indicates its Curie temperature T_C . Superconducting quantum interference device (SQUID) magnetization measurements indicate that the structures are ferromagnetic, and can be thus named digital ferromagnetic heterostructures. We also investigated the temperature dependences of the remanent magnetization in the range $T=2-300$ K. The obtained data pointed out that the combination of localized magnetic ions in a δ -doped profile and presence of low-dimensional carrier channel induced ferromagnetism in GaAs based structures.

[1] A.M. Nazmul, T. Amemiya, Y. Shuto, S. Sugahara, M. Tanaka, *Phys. Rev. Lett.*, **95** (2005) 017201.

[2] Yu.V. Vasilieva, Yu.A. Danilov, A.A. Ershov, B.N. Zvonkov, E.A. Uskova, A.B. Davydov, B.A. Aronzon, S.V. Gudenko, V.V. Rylkov, A.B. Granovsky, E.A. Ganshina, N.S. Perov, A.N. Vinogradov, *Semicond.*, **39** (2005) 87-91.

2 July

Wednesday

11:30-13:00

oral session
2TL-D

“Magnetophotonics”

2TL-D-1

X-RAY MAGNETIC CIRCULAR DICHROISM UNDER HIGH MAGNETIC FIELD

Rogalev A.¹, Wilhelm F.¹

¹ European Synchrotron Radiation Facility (ESRF), Grenoble, France
rogalev@esrf.fr

Discovery of X-ray Magnetic Circular Dichroism (XMCD) ushered in a new era of magnetism research with objectives that previously would have been unattainable. Because of their inherent element and orbital specificity and ability to probe extremely small sample volumes, these spectroscopies have become an indispensable experimental method in studying the magnetism of complex materials. Moreover, derivation of magneto-optical sum rules has greatly strengthened the XMCD, offering a unique capability to deduce from the experimental spectra the orbital and spin contributions to the total magnetic moment carried by the absorbing atom. So far, XMCD has been extensively used to investigate mainly ferro- or ferromagnetic materials, and only very few studies have been performed on paramagnetic compounds. Fields of 1-2 T are generally used for conventional XMCD experiments. However, a high magnetic field could be the essential parameter to explore new phenomena in materials with important magnetic degrees of freedom.

In order to achieve this goal, the external magnetic field has to be comparable with magnitude of the basic magnetic interaction energies. This typically requires magnetic fields above 10 T.

In this contribution we describe a new experimental station dedicated to high field XMCD that has been installed at the ESRF beamline ID12 [1]. This station is based on a high vacuum ($< 10^{-7}$ mbar) 52mm cold bore solenoid producing a horizontal magnetic field of 17 Tesla. The magnet is equipped with two access ports along the field axis, one for the incoming x-ray beam and detector insert and another one for the sample cryostat. The superconducting solenoid coil is built by Cryogenic Ltd whereas the Helium continuous flow cryostat was built by the ESRF Sample Environment Support Group to be "amagnetic". The temperature on the sample can be set in the range 2.05 K to 325 K with a stability $\Delta T/T < 10^{-3}$. All spectra are measured using total fluorescence yield detection mode. A Si photodiode with an oblong hole is mounted on a liquid nitrogen shield of the magnet and collects the fluorescence photons in "backscattering" geometry over a large solid angle.

This new high field experimental station becomes a unique experimental platform for basic research on magnetism and its performances are illustrated with few selected examples:

1. Spin fluctuations of paramagnetic pure metallic Rh clusters with 1.6nm average diameter [2].
2. Strong Paramagnetism of pure Gold Nanoparticles Deposited on a *Sulfolobus acidocaldarius* S Layer [3].
3. Quantification of the magnetic exchange via element-selective high-field magnetometry: Co-doped ZnO epitaxial films [4].

[1] A. Rogalev *et al* in: *Magnetism and Synchrotron Radiation, Lectures Notes in Physics*, **565** (Springer, Berlin, Heidelberg New York 2001) 60-86.

[2] V.M.T.S. Barthem *et al*, *Phys. Rev. Lett.*, **109** (2012) 197204.

[3] J. Bartolomé *et al*, *Phys. Rev. Lett.*, **109** (2012) 247203.

[4] A. Ney *et al*, *Phys. Rev. B*, **85** (2012) 245202.

2TL-D-2

A CLOSE LOOK AT MAGNETIC MULTILAYERS AND NANOMAGNETS WITH X-RAY MICROSCOPY

Nolting F.¹

¹ Paul Scherrer Institut, Villigen PSI, Switzerland
frithjof.nolting@psi.ch

Bringing different materials in contact at the nanoscale opens the door to improving or creating new functionalities by tuning the properties of the resulting nanointerfaces. Employing photoemission electron microscopy (PEEM) and the X-ray magnetic circular dichroism (XMCD) their magnetic properties can be studied. Using recent results I will explain the technique and its possibilities.

One example is the study of the magnetic properties and scaling laws of nanoparticles, where we studied the magnetic properties of individual iron nanoparticles with sizes ranging from 20 nm down to 8 nm. While the magneto-crystalline anisotropy of bulk iron suggests superparamagnetic behavior in this size range, ferromagnetically blocked particles are also found at all sizes (Fig. 1). Spontaneous transitions from the blocked state to the superparamagnetic state are observed in single particles and suggest that the enhanced magnetic energy barriers in the ferromagnetic particles are due to metastable, structurally excited states with unexpected long life times [1]. A second example will be the demonstration of in situ 90 degree electric field-induced uniform magnetization rotation in single domain submicron Ni ferromagnetic islands grown on PMN-PT ferroelectric single crystal. The reorientation occurs by the strain-induced magnetoelectric interaction between the ferromagnetic nanostructures and the ferroelectric crystal. The ferroelectric domain structure plays a key role in determining the response of the structure to the applied electric field [2]. Further examples will be about patterned magnetic nanostructures and how the magnetization of ferromagnetic systems can be manipulated by ultrashort laser pulses studied with time resolved measurements [3].

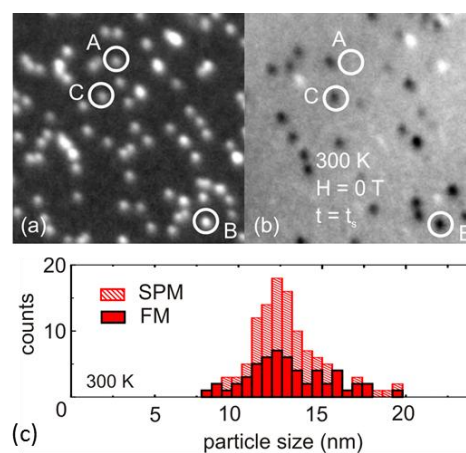


Fig. 1. (a), (b) Elemental and magnetic contrast images of the nanoparticles. (c) Size distribution of the ferromagnetic and superparamagnetic particles (adapted from [1]).

Support by EU's 7th Framework Program and the Swiss Nanoscience Institute is acknowledged.

- [1] A. Balan, P.M. Derlet, A. Fraile-Rodríguez, J. Bansmann, R. Yanes, U. Nowak, A. Kleibert, and F. Nolting, *Phys. Rev. Lett.* accepted (2014).
- [2] M. Buzzi, R. V. Chopdekar, J. L. Hockel, A. Bur, T. Wu, N. Pilet, P. Warnicke, G. P. Carman, L. J. Heyderman, and F. Nolting, *Phys Rev. Lett.*, **111** (2013) 027204.
- [3] L. Le Guyader, S. El Moussaoui, M. Buzzi, R. V. Chopdekar, L. J. Heyderman, A. Tsukamoto, A. Itoh, A. Kirilyuk, Th. Rasing, A. V. Kimel, F. Nolting, *App Phys. Lett.*, **101** (2012) 022410.

2TL-D-3

INVESTIGATION OF THE DOMAIN STRUCTURE IN MAGNETIC MULTILAYERS AND ALLOYS USING RESONANT MAGNETIC SOFT X-RAY SCATTERING

*Weier C.¹, Adam R.¹, Frömter R.², Bach J.², Beyersdorff B.², Bagschik K.², Rudolf D.¹, Grychtol P.⁴,
Winkler G.², Müller L.³, Schleitzer S.³, Berntsen M.H.³, Kobs A.², Grübel G.³, Oepen H.P.², Kapteyn
H.C.⁴, Murnane M.M.⁴, Schneider C.M.¹*

¹ Peter Grünberg Institut, PGI-6, Forschungszentrum Jülich, Jülich, Germany

² Institut für Angewandte Physik, Universität Hamburg, Hamburg, Germany

³ Deutsches Elektronen-Synchrotron (DESY), FS-CXS, Hamburg, Germany

⁴ Department of Physics and JILA, University of Colorado, Boulder, CO, USA
r.adam@fz-juelich.de

Understanding and controlling magnetic domain structures on a nanometer length scale in complex magnetic alloys and magnetically coupled layers requires an experimental technique that allows imaging of magnetic domains with nanometer lateral resolution. This can be achieved using resonant scattering of soft X-rays from a domain pattern acting as two-dimensional magnetic grating.¹ The relative simplicity of the technique allows for detailed studies of magnetic domain dynamics on ultrafast time scales.

Recently, extremely short soft X-ray pulses produced by free-electron lasers,¹ femtosecond slicing,² as well as table-top HHG light sources^{3,4} opened the door to such dynamical studies with the additional benefit of element-selectivity. The latter feature has been achieved by tuning energy of soft X-rays to the absorption edges of the elements explored. Up to date, only few experiments have been designed to resolve the dynamics of magnetic domains temporally and laterally, within femtoseconds and nanometers, simultaneously.

To address this question, we studied the magnetic domain structure of (Co/Pt) multilayers as well as CoPd and FePd thin films using resonant magnetic scattering of soft X-rays. Applying in-situ magnetic fields resulted in surprisingly pronounced changes in the domain structure that were clearly observed in the scattering patterns. Our samples were grown on top of 50 nm thin Si₃N₄ substrates to allow measurements in transmission geometry. By tuning the light to the absorption edges of iron or cobalt we recorded scattering images of the domain structure, corresponding to chosen elements. Our analysis of both magnetic multilayers and alloys provides insight into the formation of domains under small magnetic field perturbations and paves the way to a better understanding of the transient changes expected in magneto-dynamic measurements.

The authors acknowledge DFG funding under the project SCHN 353/17.

Parts of this research were carried out at the light source PETRA III at DESY, a member of the Helmholtz Association (HGF). We thank Jens Viefhaus for assistance in using beamline P04. Additional support by BMBF under 05K10GU4 within "FSP 301 - FLASH" and from the Hamburg Centre for Ultrafast Imaging and the Knut and Alice Wallenberg Foundation is acknowledged.

[1] S. Pfau *et al.*, *Nature Commun*, **3** (2012) 1100.

[2] I. Radu *et al.*, *Nature*, **472** (2011) 205.

[3] C. La-O-Vorakiat *et al.*, *Phys. Rev. Lett.*, **103** (2009) 257402.

[4] D. Rudolf *et al.*, *Nature Commun*, **3** (2012) 1037.

Wednesday

2 July

11:30-13:00

14:30-17:00

oral session

2TL-E

2RP-E

2OR-E

2RP-H

2OR-H

“Theory”

2TL-E-1

IMPURITY AND MAGNETIC FIELD EFFECTS IN KITAEV AND KITAEV-HEISENBERG SYSTEMS

Tripathi V.¹, Das Sitikantha²

¹ Department of Theoretical Physics, Tata Institute of Fundamental Research, Homi Bhabha Road, Mumbai 400005, India

² The Shoenberg Laboratory for Quantum Matter, Department of Physics, Cavendish Laboratory, University of Cambridge, J. J. Thomson Avenue, Cambridge CB3 0HE, United Kingdom
vtripathi@theory.tifr.res.in

The alkali iridates $A_2\text{IrO}_3$ ($A = \text{Li, Na}$) have recently attracted a lot of attention because of the promise they hold for the realization of Kitaev or Kitaev-Heisenberg physics in solid-state systems. The spin-1/2 honeycomb Kitaev model has a quantum spin-liquid ground state with extremely short-ranged spin correlations and low-energy emergent excitations that are dispersing Majorana fermions. In the presence of a sufficiently strong competing Heisenberg interaction between neighbouring spins, the spin-liquid state can give way to a stripy or zigzag order of the spins [1], and the latter is observed in the alkali iridates. We study here a number of effects associated with introducing external magnetic impurities or magnetic fields to such models using analytical and exact-diagonalization approaches. For the Kitaev model to which an external spin is coupled antiferromagnetically, an unusual Kondo effect takes place where an unstable fixed point, corresponding to an intermediate value of the impurity coupling strength, separates two phases with different topology [2]. Our analysis explicitly shows that the change of topology and screening of impurity spin happen at the same point. For ferromagnetic coupling of the magnetic impurity, we find no change of topology while going from the weak coupling to the strong coupling limit. When multiple magnetic impurities are present, the dispersing Majorana fermions mediate a non-dipolar indirect exchange interaction between the impurities. For the Kitaev-Heisenberg model, we find step-like features in the magnetization and oscillations in the torque as a function of the external magnetic field.

[1] J. Chaloupka, G. Jackeli and G. Khaliullin, *Phys. Rev. Lett.*, **110** (2013) 097204.

[2] K. Dhochak, R. Shankar and V. Tripathi, *Phys. Rev. Lett.*, **105** (2010) 117201.

2RP-E-2

CORRELATION EFFECTS AND NON-COLLINEAR MAGNETISM IN THE DOPED HUBBARD MODEL

Igoshev P.A.¹, Timirgazin M.A.², Arzhnikov A.K.², Irkhin V.Yu.¹

¹ Institute of Metal Physics, Ekaterinburg, Russia

² Physical-Technical Institute, Izhevsk, Russia

valentin.irkhin@imp.uran.ru

The ground-state magnetic phase diagram is treated for the two- and three-dimensional (2D and 3D) t - t' Hubbard model. We take into account commensurate ferro- and antiferromagnetic, as well as incommensurate (spiral) magnetic phases. The formalism applied takes into account phase separation (PS) into magnetic phases of different types, which was usually missed in previous investigations. We trace the influence of correlation effects on stability of both spiral and collinear magnetic order by employing (i) the generalized non-correlated mean-field (Hartree-Fock) approximation [1] and (ii) the slave-boson approach by Kotliar and Ruckenstein (correlation effects being included).

We found that in the approximation (ii) the spiral states and especially ferromagnetism are strongly suppressed up to non-realistic large Hubbard U , provided that t'/t is not close to $1/2$. In the hole-doped case ($n < 1$) variety of types of spiral states is destroyed and critical U is renormalized by 2-3 times. In electron-doped case ($n > 1$) stripe-like structures with corresponding PS survive in a vicinity of half-filling. The ratio t'/t is the most crucial parameter determining the actual physical picture: being even small but non-zero it makes phase diagram strongly asymmetric, especially in the approximation (ii).

The results imply possible interpretation of the unusual behavior of magnetic properties of 3D and 2D transition metal compounds (e.g., layered cuprates and ruthenates) in terms of first- or second-order phase transition between collinear and spiral magnetic phases.

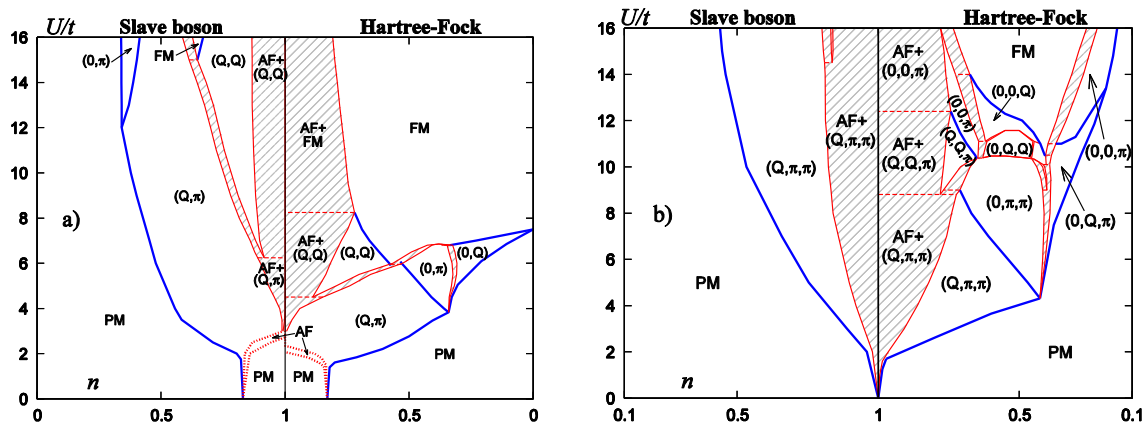


Fig.1 Ground-state phase diagram of the Hubbard model for electron density $n < 1$ (hole doping) in the Hartree-Fock and slave-boson approximations: (a) square lattice with $t'/t=0.2$ (b) simple cubic lattice at $t'=0$. Spiral phases are denoted by their wave vectors. Dashed region “ P_1+P_2 ” denotes phase separation of P_1 and P_2 phases.

[1] P. A. Igoshev, M. A. Timirgazin, A. A. Katanin, A. K. Arzhnikov, and V.Yu. Irkhin, *Phys. Rev. B*, **81** (2010) 094407.

2RP-E-3

GENERALIZED SPIN-FLUCTUATION THEORY OF ANHARMONIC ITINERANT ELECTRON MAGNETS

Solontsov A.^{1,2}

¹ Center for Fundamental and Applied Research, N.L. Dukhov Research Institute for Automatics, Sushevskaya str., 22, 127055, Moscow, Russia

² State Center for Condensed Matter Physics, M. Zakharova str., 6/3, 115569, Moscow, Russia
asolontsov@mail.ru

Spin fluctuations (SF) are known to play a dominant role in itinerant electron magnets and novel superconductors. However, the role of SF in these systems still remain unclear and present a fundamental problem for both magnetism and superconductivity. A conventional theory of spin fluctuations (SF) in itinerant electron magnets known as the self-consistent renormalized (SCR) theory is worked out by many authors, mainly by the groups of Moriya [1], who presents a theory violating spin invariance, and of Lonzarich [2] who improves the SCR theory by taking into account spin rotational invariance. However, the SCR theory has serious drawbacks, namely: i) it completely neglects effects of zero-point SF which may essentially influence both the ground-state and thermal properties and ii) is based on a perturbative approach assuming weak SF coupling, whereas itinerant magnets possess giant strongly coupled SF. Another approach is worked out by Takahashi [3] who takes into account temperature-dependent amplitudes of thermal and zero-point SF assuming that their temperature dependencies compensate each other giving rise to a sum rule: the total squared amplitude of SF including the zero-point and thermal contributions is a conserved quantity. The approach [3] seems to have a limited applicability related to nearly Heisenberg magnets. The joint feature of all approaches [1-3] is that they are based on the random phase approximation (RPA) and have a perturbative character making them applicable to weakly anharmonic magnets. However, in most of itinerant magnets the dimensionless spin anharmonicity parameter induced by zero-point SF is of order unity, and the amplitude of zero-point SF is considered to be giant. So, perturbative approaches are hardly applicable for a description of SF in real materials. Giant zero-point SF and caused by them strong spin anharmonicity are described within a generalized approach of the soft-mode (SM) theory suggested by Solontsov and Wagner [4]. Within the SM theory the zero-point and thermal SF are treated on the same footing, and the free energy is calculated within a self-consistent non-perturbative variational procedure instead of using the RPA.

In the present report a generalized theory (GT) of SF is presented accounting for zero-point and thermal SF, and strong spin anharmonicity in a wide temperature range in ferro-, antiferro-, and paramagnetic phases, extending the SM theory [4]. The previous approaches [1-4] are shown to follow from the GT in different spin anharmonicity limits and temperature regions. The GT is applied to consider effects of zero-point SF on the ground state of magnetoresistive manganites and their polarizations. These effects are shown to impose quantum limitations on their possible 100% polarization and half-metallicity. The effects of zero-point SF are also shown to influence the temperature dependence of the specific heat and affect the Fermi-liquid vs non-Fermi-liquid behaviors in strongly correlated electron systems.

[1] T. Moriya, *Spin Fluctuations in Itinerant Electron Magnetism* (Springer, Berlin, 1985).

[2] G.G. Lonzarich and L. Taillefer, *J. Phys. C: Solid State Phys.*, **180** (1985) 4339.

[3] Y. Takahashi, *Theory of Spin Fluctuations in Itinerant Electron Magnetism*, (Springer, Berlin, 2013).

[4] A.Z. Solontsov and D. Wagner, *Phys. Rev. B*, **51** (1995) 12410.

2OR-E-4

LOW-TEMPERATURE SPIN FLUCTUATIONS BEYOND SPIN WAVES

Melnikov N.B.¹, Reser B.I.²

¹ Lomonosov Moscow State University, Moscow, Russia

² Institute of Metal Physics of the RAS, Ekaterinburg, Russia

melnikov@cs.msu.su

We have developed a low-temperature dynamic spin-fluctuation theory (LDSFT) of ferromagnetic metals [1]. The thermal spin fluctuations are treated by the functional integral method for the multiband Hubbard Hamiltonian [2] without mapping of the itinerant electron system onto an effective Hamiltonian with classical spins [3, 4]. The theory takes into account nonlocal

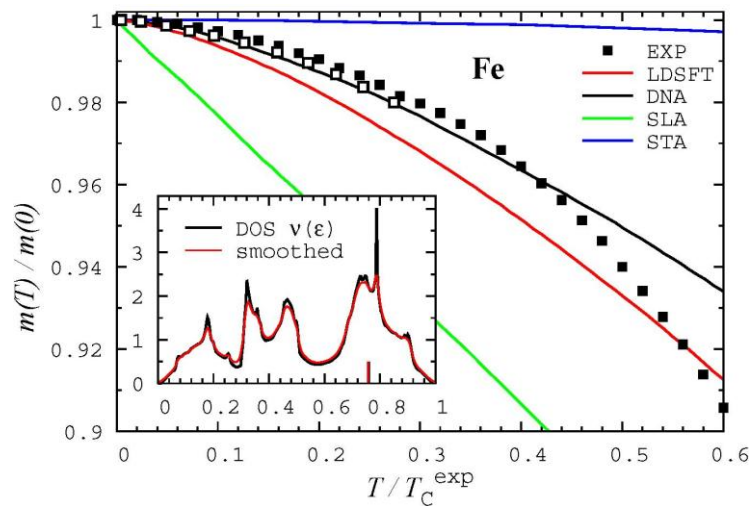


Fig. 1. Magnetization $m(T)$ of Fe calculated in the LDSFT, and three approximations of the spin-fluctuation theory: static local (SLA), dynamic nonlocal (DNA), and Stoner (STA). Squares are the experimental data (EXP). The inset shows the initial DOS at $T=0$; the energy is in units of the bandwidth $W=7.16$ eV, and the vertical line indicates the position of the Fermi level.

interactions, band degeneracy and spherical symmetry of spin fluctuations. At each temperature, we solve a system of three equations, which is only a little more complicated than the one in Stoner theory. It has been shown that the present theory becomes accurate in the low-temperature limit, exactly reproducing the $T^{3/2}$ law for the magnetization. At the same time, the calculated magnetization in Fe is in good agreement with experiment over the interval from zero to $0.6T_C^{\text{exp}} \approx 600$ K, which is about 20 times larger than the interval where the $T^{3/2}$ law is valid (Fig. 1). The calculated spin-wave stiffness $D_0 = 200 \text{ meV}\text{\AA}^2$ and Curie temperature $T_C = 1654$ K for Fe are found in reasonable agreement with experimental data and results of previous calculations. For the $Fe_{0.65}Ni_{0.35}$ Invar, we obtained $D_0 = 110 \text{ meV}\text{\AA}^2$ and $T_C = 546$ K, which are in excellent agreement with experiment. We argue that the present theory can be successfully applied to other ferromagnetic metals and alloys, where the longitudinal fluctuations are small compared to the transverse ones.

This work was carried out as a part of the Program of the Presidium of the Russian Academy of Sciences (project no. 12-П-2-1041).

[1] N.B. Melnikov, B.I. Reser, *Phys. Rev. B*, (2014) submitted.

[2] N.B. Melnikov, B.I. Reser, V.I. Grebennikov, *J. Phys.: Condens. Matter*, **23** (2011) 276003.

[3] A.I. Lichtenstein, M.I. Katsnelson, G. Kotliar, *Phys. Rev. Lett.*, **87** (2001) 067205.

[4] P.-W. Ma, S.L. Dudarev, *Phys. Rev. B*, **86** (2012) 054416.

2RP-H-6

PHASE SEPARATION OF ANTIFERROMAGNETIC GROUND STATES IN SYSTEMS WITH IMPERFECT NESTING

Rakhmanov A.L.¹, Rozhkov A.V.¹, Sboychakov A.O.¹, Nori F.¹

¹ Institute for Theoretical and Applied Electrodynamics RAS, Moscow, Russia

² Advanced Science Institute, RIKEN, Wako-shi, Saitama, Japan
alrakhmanov@mail.ru

We analyze the phase diagram for a system of weakly coupled electrons having an electron- and a hole-band with imperfect nesting [1]. Namely, both bands have spherical Fermi surfaces, but their radii are slightly different, with a mismatch proportional to the doping. Such a model is used to describe the antiferromagnetism of chromium and its alloys, pnictides, AA-stacked graphene bilayers, as well as other systems. Here we show that the uniform ground state of this model is unstable with respect to electronic phase separation in a wide range of model parameters [2]. Physically, this instability occurs due to the competition between commensurate and incommensurate antiferromagnetic states and could be of importance for other models with imperfect nesting [2-4].

[1] T.M. Rice, *Phys. Rev. B*, **2** (1970) 3619.

[2] A.L. Rakhmanov, A.V. Rozhkov, A.O. Sboychakov, F. Nori, *Phys. Rev. B*, **87** (2013) 075128.

[3] A.L. Rakhmanov, A.V. Rozhkov, A.O. Sboychakov, F. Nori, *Phys. Rev. Lett.*, **109** (2012) 206801.

[4] A.O. Sboychakov, A.L. Rakhmanov, A.V. Rozhkov, F. Nori, *Phys. Rev. B*, **87** (2013) R121401.

[5] A.O. Sboychakov, A.V. Rozhkov, K.I. Kugel, A.L. Rakhmanov, F. Nori, *Phys. Rev. B*, **88** (2013) 195142.

2OR-H-7

THE EFFECT OF THE PARTICLE SIZE ON THE MAGNETIC PROPERTIES OF NANOSIZED ε -Fe₂O₃ PARTICLES ON A SILICA SUPPORT

Dubrovskii A.A.¹, Balaev D.A.^{1,2}, Shaykhutdinov K.A.^{1,2}, Yakushkin S.S.³, Bukhtiyarova G.A.³,
Martyanov O.N.³

¹ Kirensky Institute of Physics, Russian Academy of Sciences, Siberian Branch, Krasnoyarsk, 660036 Russia

² Siberian Federal University, Krasnoyarsk, 660041, Russia

³ Borekov Institute of Catalysis, Russian Academy of Sciences, Siberian Branch, Novosibirsk, 630090 Russia.

dabalaev@iph.krasn.ru

Among structural modifications of Fe³⁺ iron oxide the ε -Fe₂O₃ polymorphic modification was identified for the first time in 1998 [1]. A number of studies revealed that ε -Fe₂O₃ can be considered as a canted ferrimagnet [2,3] with the Curie temperature of ~ 500-585 K. This system demonstrate large coercivity ($H_C \sim 20$ kOe) at the room temperature, while below the magnetic transition at $T \sim 110$ K the H_C value drastically decreases. Due to its low surface energy, the ε -Fe₂O₃ phase exists in the form of particles 25–100 nm in size, so most of the available data were obtained on such particles (see for example, [2,3]).

The technique for fabricating ε -Fe₂O₃ in a silica gel matrix reported in [4] allows to obtain particles with an average size of few nanometers. In this study the magnetic properties of ε -Fe₂O₃/SiO₂ samples with the particle size varying from ~ 3 nm to ~ 15–25 nm are reported.

The data obtained show that the ε -Fe₂O₃ particles exhibit superparamagnetism with the blocking temperatures within the range from ~20 to ~100 K, depending on a particle size. Estimation of the particle magnetic moment from magnetization curves obtained above the blocking temperature proves that ferrimagnetic ordering (with $T_C \approx 500$ K) in 4–8 nm ε -Fe₂O₃ particles is responsible for the superparamagnetic behavior [5]. The effective magnetic moment per Fe³⁺ atom μ_{eff} is about 0.3 μ_B which is in consistent with the literature data [2]. However for the particles with the size of ~ 3 nm the specific magnetization is considerably higher than that for the 25–100-nm particles [2]. The μ_{eff} value is about 0.76 μ_B , which was attributed to the effect of uncompensated planes of ferrimagnetically ordered particles with such a small size [6].

Additionally, in the samples where the particle size is no smaller than 15 nm, the anomaly in temperature dependences of the magnetic moment at ≈ 110 K corresponding to the magnetic transition in ε -Fe₂O₃ is observed. Authors [7] attributed this magnetic transition to the change in the sublattice canting angle (analogously to the Morin point in a weak ferromagnet). In the samples with the particles smaller than 8 nm, this anomaly is not observed down to 4.2 K.

We demonstrate that with decreasing particle size and increasing fraction of surface atoms, the contribution of the paramagnetic subsystem forming by the Fe³⁺ ions in the smallest (< 4 nm) particles' shell occurs.

- [1] E. Tronc, C. Chaneac, and J.P. Jolivet, *J. Solid State Chem.*, **139** (1998) 93-104.
- [2] E. Tronc, C. Chaneac, J. P. Jolivet, and J. M. Greneche, *J. Appl. Phys.*, **98** (2005) 053901.
- [3] S. Ohkoshi, S. Sakurai, J. Jin, K. Hashimoto, *J. Appl. Phys.*, **97** (2005) 10K312.
- [4] G.A. Bukhtiyarova, et al, *J. Nanopart. Res.*, **13** (2011) 5527–5534.
- [5] S.S. Yakushkin, A.A. Dubrovskiy, D.A. Balaev, et al, *J. Appl. Phys.*, **111** (2012) 044312.
- [6]. D.A. Balaev, A.A. Dubrovskiy, et al, *J. Appl. Phys.*, **114** (2013) 163911-5.
- [7]. M. Kurmoo, J.-L. Rehspringer, A. Hutlova, et al, *Chem. Mater.*, **17** (2005) 1106.

2OR-H-8

ANOMALOUSLY LARGE DAMPING OF LONG-WAVELENGTH MAGNONS INDUCED BY DIPOLAR FORCES IN CUBIC ANTIFERROMAGNETS

Batalov L. A.¹, Syromyatnikov A. V.^{1,2}

¹ Petersburg Nuclear Physics Institute NRC "Kurchatov Institute", Gatchina, St. Petersburg 188300, Russia

² Department of Physics, Saint Petersburg State University, 198504 St. Petersburg, Russia
zlokor88@gmail.com

The concept of elementary excitations or quasiparticles is one of the most powerful tools in discussion of low-energy properties of strongly interacting many-body systems [1]. According to this concept a weakly excited state of a system can be represented as a collection of propagating weakly interacting quasiparticles which carry quanta of energy $\varepsilon_{\mathbf{k}}$ and momentum \mathbf{k} . Elementary excitations, being wave packets of stationary states, have finite lifetime (or damping $\Gamma_{\mathbf{k}}$) which is interpreted as a result of quasiparticles spontaneous decay and interaction between. According to the quasiparticle concept supported by quite a general line of argument (not considering, however, long-range interactions in a system), long-wavelength elementary excitations are well defined (i.e., $\Gamma_{\mathbf{k}} \ll \varepsilon_{\mathbf{k}}$).

We discuss here the spin-wave interaction in 3D Heisenberg cubic antiferromagnets (AFs) with dipolar forces at small temperature $T \ll T_N$ using $1/S$ expansion. A comprehensive analysis is carried out of the first $1/S$ corrections to the spin-wave spectrum. We observe a number of quite unusual phenomena: the spin-wave gap caused by spin-wave interaction and anomalously large damping of long-wavelength magnons in 3D AF.

We demonstrate that the spin-wave interaction leads to a small gap $\Delta \sim \omega_0$ in the spectrum $\varepsilon_{\mathbf{k}}$ that renormalizes greatly the bare gapless spectrum at small momenta k , where ω_0 is the characteristic dipolar energy. This effect is of the "order-by-disorder" origin. An infinite degeneracy of the classical ground state is removed by thermal and quantum fluctuations making an edge of the cube to be easy direction and leading to the gap.

We show that dipolar forces remove the double degeneracy of the magnon spectrum. It is the spectrum splitting that leads to the magnon damping in the first order in $1/S$ at finite T . We obtain that $\Gamma_{\mathbf{k}}/\varepsilon_{\mathbf{k}} \sim (T/D)^4 (\omega_0/\Delta)^2$ at $k \sim \Delta/D$ and $T \ll T_N$, where D is the magnon stiffness. This value is small because $D \sim T_N$ at $S \sim 1$ but an anisotropy competing to the dipolar anisotropy can reduce Δ and lead to a very large damping in a range of small but finite k . This situation is discussed for $\text{TiMn}_{1-x}\text{Co}_x\text{F}_3$ for $x \sim 0.0001$ [2].

Notice that the similar effect of long-wavelength magnons instability was observed also in cubic ferromagnets with dipolar forces [3,4]. Unfortunately an experimental verification of our predictions is difficult due to very small typical values of momenta of overdamped magnons.

Support by the Dynasty foundation and RFBR grant 12-02-01234 is acknowledged.

[1] A.A. Abrikosov, L.P. Gor'kov, and I. E. Dzyaloshinskii, *Quantum Field Theoretical Methods in Statistical Physics* (Dover, New York, 1963).

[2] D.E. Eastman et al., *J. Appl. Phys.*, **38** (1967) 5209.

[3] A.V. Syromyatnikov, *Phys. Rev. B*, **77** (2008) 144433.

[4] A.V. Syromyatnikov, *Phys. Rev. B*, **82** (2010) 024432.

2OR-H-9

ELEMENTARY EXCITATIONS IN QUANTUM SPIN LIQUIDS WITH DEFECTS

Utesov O.I.¹, Sizanov A.V.^{1,2}, Syromyatnikov A.V.^{1,2}

¹ Petersburg Nuclear Physics Institute NRC "Kurchatov Institute", Gatchina, St. Petersburg 188300,
Russia

² Department of Physics, Saint Petersburg State University, 198504 St. Petersburg, Russia
utiosov@gmail.com

Quantum spin liquids (QSLs) with defects and quantum phase transitions (QPTs) in such systems have attracted much attention recently. This interest has been particularly stimulated by a possibility to observe QPT to a Bose-glass phase which was predicted many years ago for dirty boson systems [1,2]. Two kinds of QSL have been extensively discussed in this respect recently: spin-1/2 dimer systems and magnets with integer spin and large single-ion easy-plane anisotropy. Two types of disorder have been considered in these systems: site dilution (i.e., substitution of magnetic atoms by non-magnetic ones) and disorder on peripheral sites involved in superexchange interaction that leads to exchange constants changing [1,2].

The last kind of disorder is in the focus of the present work. Despite considerable amount of experimental data, we can mention only a few theoretical papers devoted to QSL with disorder far from QPT points. In particular, spin-1/2 bilayer with quenched disorder is considered in [3] numerically using a generalized bond operators approach. We propose a unified theoretical discussion of disorder in 1D, 2D and 3D spin-1/2 dimer systems and magnets with integer spin and large single-ion easy-plane anisotropy. We use the standard T-matrix approach [4] to calculate corrections to elementary excitations spectrum $\varepsilon_{\mathbf{k}}$ and density of states in the first order in defects concentration c . Numerical calculations using quantum Monte-Carlo method and exact diagonalization of finite clusters show reasonable agreement with our analytical results.

In particular, we find that $\Gamma_{\mathbf{k}}/\varepsilon_{\mathbf{k}} \sim c/k$ in magnetic field near the phase transition to the ordered phase, where $\Gamma_{\mathbf{k}}$ is the elementary excitations damping. Although the damping remains small in the range of this expression validity, $1 \gg k \gg c$, this result should be contrasted to corresponding findings in ordered magnets in which $\Gamma_{\mathbf{k}}/\varepsilon_{\mathbf{k}}$ can reach only the value of c for some kinds of defects.

Support by the Dynasty foundation and RFBR grant 12-02-01234 is acknowledged.

[1] R. Yu, L. Yin, N. S. Sullivan et al., *Nature*, **489** (2012) 379.

[2] A. Zheludev and T. Roscilde, *C. R. Physique*, **14** (2013) 740.

[3] M. Vojta, *Phys. Rev. Lett.*, **11** (2013) 097202.

[4] Y. A. Izyumov and M. Medvedev, *Magnetically Ordered Crystals Containing Impurities* (Consultants Bureau, New York, 1973).

2OR-H-10

SPIN FLUCTUATIONS IN DISORDERED METALLIC FERROMAGNETIC ALLOYS

Grebennikov V.I.¹, Radzivonchik D.I.¹

¹ Institute of Metal Physics UD RAS, Yekaterinburg, Russia
greben@imp.uran.ru

We propose a theory for the quantitative description of the thermodynamic, magnetic and electronic properties of disordered alloys of transition and normal metals, for example, the system Fe-Al, as obtained from the melt and in the form of metastable states produced by mechanical action. We consider a system of itinerant 3d-electrons with strong intra-atomic exchange interaction $-u_j s_j^2$, where s_j stands for electron spin density at the site with the number j . The magnitude of the coupling constants u_j takes several different values with probability c_j depending on the site type, which is determined by its nearest-neighbor. Our goal is to calculate the thermodynamic characteristics of the electronic subsystem (entropy, heat capacity) at an arbitrary temperature find the values of the local magnetic moments on the atoms of different types, the resulting magnetization and its variation in the magnetic field, describe the magnetic phase transitions. The problem is solved by the dynamical theory of electron spin density fluctuations [1], and involves the calculation of the spin fluctuations values and their correlation length. The single-site Green function $g(E)$ and its self-energy part $\Sigma(E)$ provide information on the spectrum of elementary excitations, damping of states at the Fermi level and, in particular, allow us to calculate the electrical resistivity due to scattering by spin fluctuations.

The partition function for the system with electron-electron interaction is written as the partition function of electrons in a fluctuating (in space and "thermodynamic time" $\tau \in [0, \hbar/k_B T]$, T – temperature) exchange field $V_j(\tau)$ by the Stratonovich–Hubbard transformation. The principal new feature of this task compared with the standard fluctuating field theory in ferromagnetic materials is the presence of several types of sites with different interactions u_j . Instead of a single equation, a system of equations arises for determining the mean field values and the electron spin densities values for different sites. This system has several ferrimagnetic solutions, transitions between which give variety to the temperature dependence of magnetic properties of disordered alloys.

Figure 1 shows the magnetic moments of the two site types (points and triangles) versus temperature calculated for the FeAl density of states. Squares show the average magnetization. The alloy has four magnetic states (with parallel and antiparallel orientation). Transitions between them describe the unusual temperature behavior of the magnetic properties of the Fe-Al system.

Support by RFBR (grant 14-02-00080) and UD RAS (grant 12-Y-2-1002) is acknowledged.

[1] N.B. Melnikov, B.I. Reser, V.I. Grebennikov, *J. Phys.: Condens. Matt.*, **23** (2011) 276003.

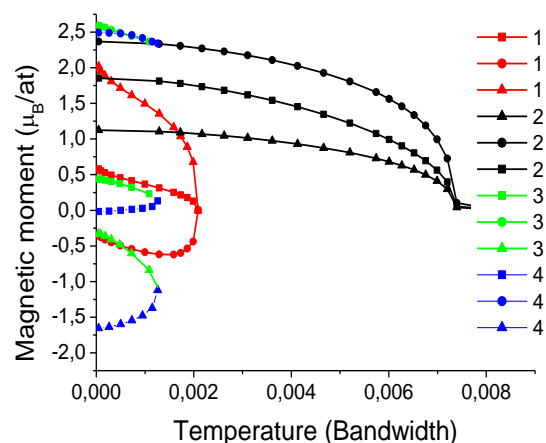


Fig. 1. Magnetic phase diagram for diluted Fe-Al alloy: $u = 0.132 \ 0.120 \ 0$; $c = 0.2 \ 0.3 \ 0.5$.

2OR-H-11

MODELLING OF STRIPE DOMAIN STRUCTURE DRIFT IN ALTERNATING MAGNETIC FIELD

*Pamyatnykh L.A.¹, Shmatov G.A.¹, Lysov M.S.¹, Pamyatnykh S.E.¹, Mehonoshin D.S.¹,
Agafonov L.Y.¹*

¹ Ural Federal University, Lenin Av. 51, Yekaterinburg, 620083, Russia

Lidia.Pamyatnykh@usu.ru

A model of stripe magnetic domain structure (DS) motion in a sample plate with uniaxial anisotropy (quality factor $Q > 1$) in sinusoidal spatially uniform magnetic field, applied perpendicular to the plate's surface, was developed. The model was constructed within the framework of approach developed in [1,2] and includes energy of external magnetic field, magnetostatic energy and attenuation. Numerical simulations show that in case of homogeneous initial conditions a drift of stripe magnetic DS takes place in the presence of spatially inhomogeneous magnetic field. It's shown that the direction of the drift is determined by the sign of the magnetic field gradient. The drift direction is reversed with the change of sign of the field gradient.

The results of numerical modelling are compared to the experimental study of the domain walls (DW) drift in uniaxial (111) iron garnet $(\text{TbErGd})_3(\text{FeAl})_5\text{O}_{12}$ plate in sinusoidal magnetic field, oriented perpendicular to the surface of the plate. Domain structure was revealed by means of magneto-optic Faraday effect and was captured by high speed digital camera at the rates up to 2000 fps. It was compared to the shape of magneto-optic hysteresis loops measured in the range of alternating fields up to amplitude $H_0 = 500$ Oe. Dependencies of DW drift speed from field amplitude for frequencies between 250 and 1000 Hz were obtained. Fig. 1a shows the dependence of the drift speed from H_0 at the field frequency $f = 250$ Hz, which is well approximated by linear function. Fig. 1b shows the dynamic magnetisation curve built based on the tops of individual magneto-optical hysteresis loops. It was established that with increasing field amplitude the value of the coercive force H_c increases smoothly to 18 Oe. At the same time the relative area of hysteresis loops S/S_s sharply increases (here S_s is the area of limit hysteresis loop) (Fig. 1c). The increase of hysteresis losses is indicated by dependence of the coercive force and of the area of the hysteresis loops on the field frequency at 385 Oe amplitude (Fig. 1d).

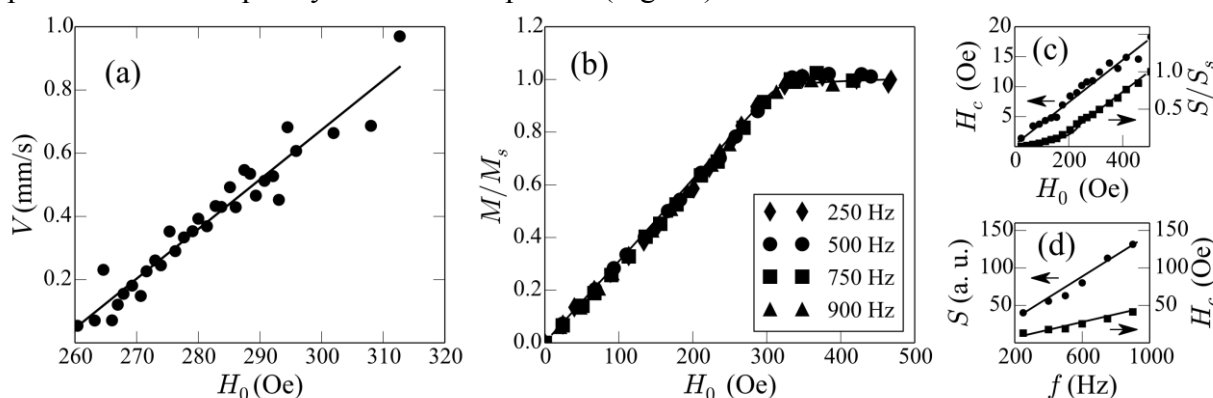


Fig. 1. (a) Dependence of drift speed on field amplitude; (b) dynamic magnetization curve; dependence of area of hysteresis loops and coercive force on amplitude (c) and frequency (d).

[1] M.M. Solov'ev, B.N. Filippov, *Fiz. Met. Metalloved.*, **98** (2004) 12.

[2] L.A. Pamyatnykh, A.V. Druzhinin, M.S. Lysov, S.E. Pamyatnykh, G.A. Shmatov, *Bull. Russ. Acad. Sci. Phys.*, **77** (2013) 1231-1234.

2OR-H-12

NON-LANDAU DAMPING OF MAGNETIC EXCITATIONS IN SYSTEMS WITH LOCALIZED AND ITINERANT ELECTRONS

Efremov D.V.¹, Betouras J.², Chubukov A.V.³

¹ IFW-Dresden, Dresden, Germany

² Department of Physics, Loughborough University, Loughborough, UK

³ Department of Physics, University of Wisconsin-Madison, Madison, USA

d.efremov@ifw-dresden.de

We discuss the form of the damping of magnetic excitations in a metal near a ferromagnetic instability. The paramagnon theory predicts that the damping term should have the Landau form $\gamma(q, \omega) \propto \omega/v_F q$. However, the experiments on uranium metallic compounds UGe₂ and UCoGe showed non-Landau damping $\gamma(q, \omega) \propto \omega/\Gamma$, with $\Gamma = \text{const}$ for small q. It would violate the spin conservation in systems with one type of fermions. Recently it has been conjectured that this non-Landau damping can arise due to the presence of both localized and itinerant electrons in these materials, with ferromagnetism involving predominantly localized spins. We present microscopic analysis of the damping of near-critical localized excitations due to interaction with itinerant carriers. We show explicitly how the presence of two types of electrons breaks the cancelation between the contributions to Γ from self-energy and vertex correction insertions into the spin polarization bubble.

[1] *Phys. Rev. Lett.*, **112** (2014) 037202.

2OR-H-13

GENERALIZED STONER-WOHLFARTH MODEL FOR PSEUDO-SINGLE FERROMAGNETIC PARTICLES

Cimpoesu D.¹, Stoleriu L.¹, Stancu A.¹

¹ Department of Physics, Alexandru Ioan Cuza University of Iasi, Iasi 700506, Romania
cdorin@uaic.ro

The performance of devices based on magnetic structures relies on their switching characteristics that are in many cases simulated with the Stoner-Wohlfarth (SW) model [1]. The magnetization switching can be also described using the concept of critical curve (CC) [2,3], CC being the locus of in-plane fields at which the irreversible magnetization reversal occurs. CC is not only a theoretical concept, but also an important technological parameter.

In this paper we propose a generalized SW type model to describe various experimentally observed angular dependencies of the switching field in non-single-domain magnetic particles. Because the nonuniform magnetic states are generally characterized by complicated spin configurations with no simple analytical description, we maintain the macrospin hypothesis and we phenomenologically include the effects of nonuniformities only in the anisotropy energy, preserving as much as possible the elegance of SW model, the concept of critical curve and its geometric interpretation [4]. The obtained equation for the switching fields is presented in Fig. 1: ξ describes the ratio between the saturation fields along and perpendicular to easy axis, while r describes the curvature of the magnetization curves. We compare the results obtained with our model with full micromagnetic simulations in order to evaluate the performance and limits of our approach (see Fig. 2). Work was supported by Romanian CNCS-UEFISCDI Grants No. PN-II-RU-TE-2012-3-0439, No. PN-II-RU-TE-2011-3-0211, and No. PN-II-ID-PCE-2011-3-0794.

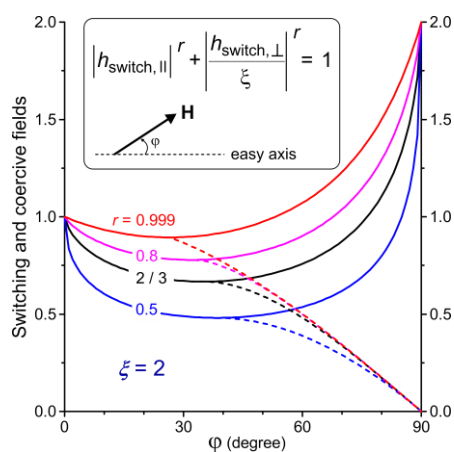


Fig. 1. Angular dependence of the switching (lines) and coercive (dashed) fields for $\xi = 2$ and different values of the parameter r . Inset: the superellipse equation for the switching field, i.e., for the CC.

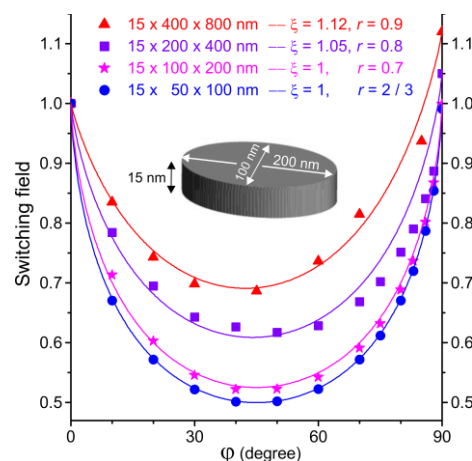


Fig. 2. Switching fields obtained with finite element simulations (symbols) for different elliptical Permalloy disks and the fitting curves (lines).

- [1] E.C. Stoner and E.P. Wohlfarth, *Philos. Trans. R. Soc. London, Ser. A* **240** (1948) 599 (1948); *IEEE Trans. Magn.*, **27** (1991) 3475-3518.
 [2] J.C. Slonczewski, *Research Memorandum R.M.* 003.111.224, IBM Research Center Poughkeepsie, 1956; *IEEE Trans. Magn.*, **45** (2009) 8-14.
 [3] A. Thiaville, *J. Magn. Magn. Mater.*, **182** (1998) 5-18.
 [4] D. Cimpoesu, L. Stoleriu, and A. Stancu, *J. Appl. Phys.*, **114** (2013) 223901-1-6.

2OR-H-14

AUTORESONANT EXCITATION OF SPIN WAVE “DARK” SOLITONS

*Borich M.A.*¹, *Friedland L.*², *Tankeev A.P.*¹, *Shagalov A.G.*¹

¹ Institute of Metal Physics, Ekaterinburg, Russian Federation

² Racah Institute of Physics, Hebrew University of Jerusalem, Israel
shagalov@imp.uran.ru

Dark solitons of spin waves in magnets are studied now both experimentally and theoretically [1,2]. One of the main problem for applications is how to effectively generate dark solitons with prescribed parameters and with smallest remaining perturbations. Excitations by impulse or localized external fields usually are unsuitable to generate pure solitons. Here we propose a method to generate pure dark solitons by a periodic external field, which allows to control amplitude of the excited solitons and period of soliton trains. We consider excitation of solitons in NLS model which is usually employed for studying of nonlinear waves in magnetic films [1],

$$iu_t + u_{xx} - 2(|u|^2 - u_0^2)u = \varepsilon \exp\{i(kx - \int \omega(t)dt)\}, \quad (1)$$

with a special type of wave-like driving of amplitude ε , where the frequency of the driver $\omega(t) = \omega_0 - \alpha t$ slowly varies in time with increment $\alpha > 0$. For example, in easy-axis magnets, ε is proportional to amplitude of an external magnetic field rotating in the plane orthogonal to the easy-axis [3]. If $\varepsilon = 0$, eq.(1) has so-called “dark” solitons, which are similar to localized holes in the homogeneous wave $u(x, t) = u_0 = const$. Our approach to generate dark solitons is based on the effect of autoresonance [4] when the initially small amplitude excited wave is phase-locked by the drive after the frequency $\omega(t)$ crossed the resonant frequency $\omega_{res} = k(k^2 + 4u_0^2)^{1/2}$. It occurs when the driving amplitude is sufficiently large: $\varepsilon > \varepsilon_{cr} = a(k)\alpha^{3/4}$. Moreover, the phase-locking will be conserved when the driving frequency slowly varies which allows one to increase the amplitude of the soliton up to $\sim u_0$.

Fig.1 shows the threshold values of the amplitude of the driving when the autoresonance excitation occurs in comparison of numerical solution of eq.(1) (solid line) with theoretical formula [4] (dashed line). Except of the singular region the numerical values comply with theoretical ones. We have observed that the excitation of dark solitons was a very stable process if the wavelength of the diving was not too small $k > 0.2$. We observed also excitation of trains of the dark solitons which periods are defined by the wavenumber k of the drive.

The research was supported by UD RAS, project No 12-P-2-1045.

[1] M.M. Scott, M.P.Kostylev, B.A. Kalinikos, C.E. Patton, *Phys.Rev. B*, **71** (2005) 174440.

[2] M.A. Borich, V.V. Smagin, A.P. Tankeyev, *Bulletin of the Russian Academy of Sciences: Physics*, **71** (2007) 1571.

[3] S.V. Batalov, A.G. Shagalov, *Phys. Metal and Metall.*, **109** (2010) 3.

[4] L. Friedland, A.G. Shagalov, *Phys.Rev. E*, **71** (2005) 036206.

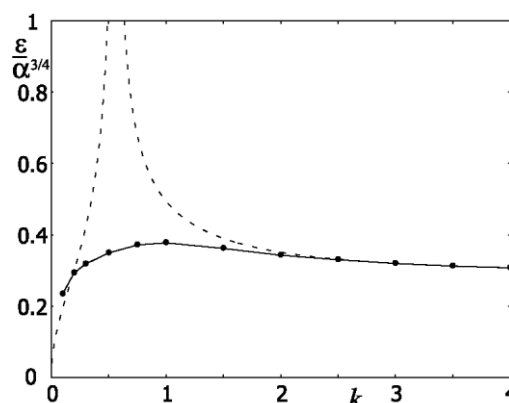


Fig. 1. The dependence the threshold value $\varepsilon/\alpha^{3/4}$ on k for autoresonant excitation of the dark solitons (solid line).

2OR-H-15

SPIN EXCITATIONS IN CHIRAL MODEL OF GRAPHENE

Rybakov Yu.P.¹

¹ Department of Theoretical Physics, PFUR, Moscow, Russia
soliton4@mail.ru

In the chiral model of graphene suggested earlier [1] the unitary matrix was considered as an order parameter, with $\mathbb{1}$ being the unit matrix and the Pauli matrices respectively. Here scalar and vector fields describe the hybridization effect, i. e. and states of the free valence electron in the mono-atomic carbon plane. For the description of spin and quasi-spin excitations in graphene, the latter ones corresponding to independent excitation modes of the two triangular sub-lattices, we introduce the two Dirac spinors and consider the combined spinor field as a new order parameter, where stands for the first column of Ψ . The Lagrangian density of the model includes the standard invariant construction quadratic in derivatives:

$$L = \frac{I}{2} \overline{\Psi} P \partial^\mu \Psi - \frac{\lambda^2}{2} \bar{a}^2 j_\mu j^\mu,$$

where $P = \gamma^\nu j_\nu$ is the projector on the positive energy states and $j_\mu = \overline{\Psi} \gamma_\mu \Psi$, $\mu = 0, 1, 2, 3$, designates the Dirac current. The model contains the two constant parameters: the exchange energy I per lattice spacing and some characteristic length λ . The interaction with the electromagnetic field can be included through the extension of the derivative: $D_\mu = \partial_\mu - ie_0 A_\mu \Gamma_e$, with e_0 being the coupling constant and $\Gamma_e = (1 - \tau_3)/2$ being the charge operator chosen in accordance with the natural boundary condition $a_0(\infty) = 1$. However, the additional interaction term of the Pauli type should be added to the Lagrangian to take into account the proper magnetic moments of the electrons. The resulting Lagrangian reads

$$L = \frac{I}{2} \overline{\Psi} D_\mu P D^\mu \Psi - \frac{\lambda^2}{2} \bar{a}^2 j_\mu j^\mu + i\mu_0 \overline{\Psi} \sigma_{\mu\nu} F^{\mu\nu} \Psi,$$

where $\sigma_{\mu\nu} = [\gamma_\mu, \gamma_\nu]/4$, $F_{\mu\nu} = \partial_\mu A_\nu - \partial_\nu A_\mu$, and μ_0 denotes the Bohr magneton.

The model in question satisfies the correspondence principle, since all previous results [1] follow if one puts $j_\mu j^\mu = 1$, $\psi_i = \text{const}_i$, $A_\mu = 0$. It should also be stressed that the electromagnetic current reads

$$J_\mu = e_0 I \text{Im}(\overline{\Psi} P \Gamma_e \partial_\mu \Psi) - e_0^2 I j_\nu j^\nu (a_1^2 + a_2^2) A_\mu + 2i\mu_0 \partial^\nu (\overline{\Psi} \sigma_{\mu\nu} \Psi)$$

and contains beyond the standard conduction term, the London super-conduction current and the Pauli magnetization-polarization one.

[1] Yu.P. Rybakov, *Solid State Phenomena*, **190** (2012) 59-62.

2 July

Wednesday

11:30-13:00

14:30-17:00

oral session

2OR-F

2TL-B

2RP-B

2OR-B

**“Magnetism of
Nanostructures”**

2OR-F-1

TRANSFORMATION OF MAGNETIC PROPERTIES OF WEAK FERROMAGNET $\text{Pd}_{0.99}\text{Fe}_{0.01}$ NANOFILM UNDER THE MAGNETIC FIELD

Khlostikov I.N.¹, Bolginov V.², Uspenskaya L.S.²

¹ P.L. Kapitza Institute for Physical Problems RAS, 2, ul. Kosygina, Moscow, 119334, Russia

² Institute of Solid State Physics RAS, Chernogolovka, Moscow District, 2 Academician Ossipyan str., 142432 Russia
uspenska@issp.ac.ru

Bulk $\text{Pd}_{1-x}\text{Fe}_x$ alloy is known as the material which gains the ferromagnetic properties because of high magnetic polarization of Pd already at the doping level about 0.1 – 1 %. The effective magnetic moment per Fe atom grows inversely proportional to x and reaches $12 \mu_B$ at $x \sim 0.01$ [1]. Depending on x , ferromagnetic or antiferromagnetic arrangement of magnetization takes place [2]. The spontaneous magnetization of the alloys and the Curie temperature are reduced with the doping decrease and with the reduction of magnetic material volume [3].

The interest to the magnetic properties of weak ferromagnet nanofilms appears a few years ago with the development of cryoelectronics where such a films are suggested to be used as the layer governing electromagnetic properties of hybrid superconductor-ferromagnet-superconductor structures [4].

Herewith we report on the properties of 20 to 40 nanometers thick $\text{Pd}_{1-x}\text{Fe}_x$ films fabricated by rf magnetron sputtering. The experiments were performed by SQUID magnetometry in temperature range 1.4 – 40 K. Temperature dependences of magnetization, coercivity and magnetic permeability were determined. Two types of magnetization loops were found depending on the range of magnetic field sweeping with the threshold value as low as 20 Oe. Large shift of Curie temperature under the applied magnetic field was observed. Huge relaxation of magnetization in all temperature range was revealed. The results are discussed in terms of magnetic aftereffects, desaccommodation and quantum tunneling of magnetic moments.

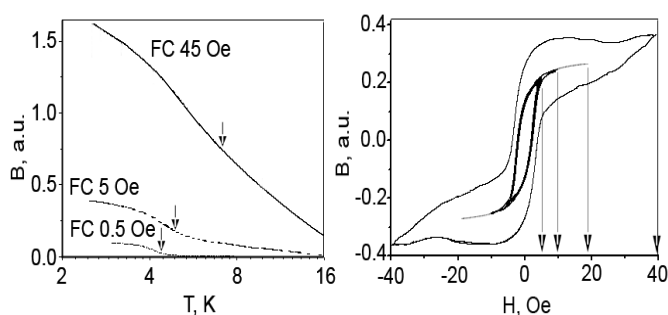


Fig.1. Temperature dependences of magnetization of the film with the thickness about 20 nm obtained at cooling under the magnetic field about 0.5, 5, and 45 Oe (inflection points of the curves are marked by arrows), and variation of the type of magnetization loops if the field exceeds some threshold (field sweeping range is 5, 10, 18, and 40 Oe).

We'd like to thank E. Levchenko and D. Matveev (ISSP RAS) for AFM observation and X-ray microanalysis of the samples.

Support by 12-02-00707 RFBR grant and by the program of the Presidium of Russian Academy of Science "Quantum Mesoscopic and Disordered Systems" is acknowledged.

[1] A.M. Clogston, et al. *Phys. Rev.*, **125** (1965) 541.

[2] Y.Kondo, K.Swieca, F.Pobell, *J. Low Temp. Phys.*, **100** (1995) 195.

[3] T.Shinodara, et al. *J. Magn. Magn. Mat.*, **94** (1999) 196-197.

[4] M.Yu. Kupriyanov, A.A. Golubov, M.Sigel, *Proc. Of SPIE*, **6260** (2006) 62600S.

2OR-F-2

NANOCORRUGATED MAGNETIC FILMS

Sapozynikov M.V.^{1,2}, *Troitski B.B.*³, *Ermolaeva O.L.*^{1,2}, *Nefedov I.M.*¹, *Gusev N.S.*^{1,2}, *Budarin L.I.*²,
*Demidov E.S.*², *Vopilkin E.A.*¹, *Rogov V.V.*¹

¹ Institute for Physics of Microstructures RAS, Nizhny Novgorod, Russia

² N.I.Lobachevskii State University, Nizhny Novgorod, Russia

³ G. A. Razuvaev Institute of Organometallic Chemistry RAS, Nizhny Novgorod, Russia
msap@ipmras.ru

In our report we summarise our investigations of magnetic, transport and optical properties of nanocorrugated ferromagnetic films carried out over the last few years. The 2D ordered ferromagnetic nanostructures are prepared by magnetron sputtering of a thin Co, Ni or Ni₃Fe layers on a surface of the PMMA or SiO₂ colloidal crystal (CC). Preparation of the colloidal crystals is based on self-assembly of monodisperse PMMA or SiO₂ globules suspended in aqueous environment. As the result the surface of the CC is formed by the hexagonally closely packed nanospheres (diameter is 125÷500 nm). CC nanospheres are hemispherically covered with metal (5-120nm) and so the fabricated ferromagnetic film has a strong 2D surface corrugation with a period dictated by the template (Fig. 1). The obtained nanostructured material seems to be very promising for magnetoplasmonics, magnetophotonics and spintronics because its manufacturing does not demand slow and cost ineffective top-down lithographic techniques.

The main results obtained while studying the nanocorrugated magnetic films are summarized here:

- Resonant peculiarities are observed experimentally in reflectance and magneto-optical spectra of the structure in the near UV, IR and visible light range. Their positions are scaled with the structure corrugation period and depend on incident angle. The resonances are theoretically explained both by the surface plasmons excitations and by the interference between light reflected from the colloidal crystal inner 3D structure and from the nanostructured film.

- Magnetization configurations and hysteresis loops of the samples were investigated by magnetic force microscopy and magneto-optic Kerr effect measurements. As the magnetic coupling of the hemispheres which form the nanocorrugated film can be tuned by changing the thickness of the deposited metal, the formation of different magnetic configurations including the frustrated hexagonal lattices of magnetic vortices are observed. The experimental results are complemented by micromagnetic simulations.

- We have found experimentally that the ferromagnetic resonance spectrum depends both on the period of the structure and on the film thickness. The number of observed resonances increases with increasing film thickness up to thicknesses of 70 nm. Observed FMR spectra have the structure usual for spin-wave resonances for the perpendicular and for the longitudinal orientation of the external magnetic field.

- A study of the conductivity on the film thickness is carried out directly in the deposition process. The observed dependencies correspond to different modes of film growth and scaled with the period of the structure.

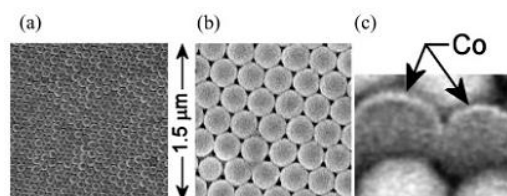


Fig. 1. Scanning electron images of the Co film on the top of the PMMA colloidal crystals with the period 120 (a) and 370 nm (b). (c) Microphotography of the particles cross-section made by focused Ga⁺ ion beam, bright layer is the 30 nm Co coverage.

2OR-F-3

DOMAIN WALL PINNING IN FERROMAGNETIC NANOWIRE BY NANOPARTICLES STRAY FIELDS

Mironov V.L.^{1,2}, Ermolaeva O.L.¹, Skorohodov E.V.¹

¹ Institute for physics of microstructures RAS, Nizhniy Novgorod, Russia

² Lobachevsky State University, Nizhniy Novgorod, Russia

mironov@ipmras.ru

The field-driven motion and pinning of domain walls (DWs) in ferromagnetic nanowires (NWs) are the subjects of intensive researches motivated by promising applications for the development of magnetic logic and data storage systems [1]. The operation of DW based systems requires the controlled DW pinning-depinning for organization of logical calculations, preservation from accidental data erasing and to save the results of intermediate computations. In our work we consider a DW pinning control in combined system consisting of a planar ferromagnetic NW and two elongated ferromagnetic nanoparticles (NPs).

The schematic drawing of NW-NP system is presented in fig. 1. The low-coercive circular pad N is used for the nucleation of domains with opposite orientation, while the NPs are used as a magnetic gate for the controlled DW pinning.

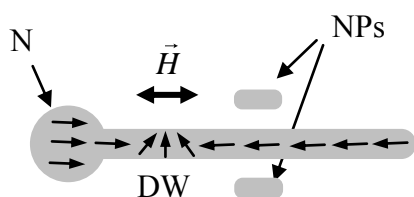


Fig. 1. Schematic drawing of the field-driven NW-NP systems.

The magnetization reversal of NW in an external magnetic field occurs via DW nucleation at the left end and subsequent movement to the right free end. The theoretical estimations and micromagnetic simulations have shown that in dependence on relative orientation of magnetic moments in NW and NPs subsystem there are two variants of DW pinning connected with a potential barrier or a potential well caused by magnetostatic interaction between the DW and local NPs stray field.

In contrast to the previously discussed system with particles placed perpendicular to the nanowire [2], present system has asymmetric DW energy landscape and the magnitude of the pinning potential barrier is twice smaller than the depth of the potential well. This potentially enables the realization of two different logical operation on the same logical element. If the operating magnetic field is less than the depinning field for the potential barrier, this system performs the XOR operation. On the other hand, if the operating magnetic field is more than the depinning field for the potential barrier, but less than the depinning field of the potential well, this system performs the simple OR operation.

The results of experimental magnetic force microscopy investigations of domain wall pinning in NiFe based NW-NPs system are discussed. We also propose the prototype logical cells based on considered NW-NPs system and discuss the algorithm of external magnetic field commutation and independent switching of NPs moments that permits the realization of logical operations.

This work was supported by the Russian Foundation for Basic Research, Presidium of RAS and The Ministry of Education and Science of Russian Federation.

[1] D.A. Allwood, G. Xiong, C. C. Faulkner, et al., *Science*, **309** (2005) 1688.

[2] V.L. Mironov, O.L. Ermolaeva, et al., *Phys. Rev. B*, **85** (2012) 144418.

2OR-F-4

MAXIMUM DENSITY OF MAGNETIC RECORDING

*Meilikhov E.Z.*¹, *Farzetdinova R.M.*²

¹ Kurchatov Institute, 123182 Moscow, Russia
meilikhov@yandex.ru

The principle of the magnetic recording had been discovered 100 years ago. Since then, the medium for magnetic recording became different but the principle remained – the magnetic state of a medium small area is “memorized”. Today, a single bit is written at the area consisting of ~ 100 magnetic granules. It is clear, that the maximum recording density could be reached by writing a bit on a single magnetic granule. To do so one has to prepare some special magnetic medium consisting of regularly placed magnetic nanogranules of identical size, form and orientation (patterned media).

The basic requirement for recording is to make a provision for the information integrity during a long enough period. Usually, they mean duration of about 10 years. In small granules, the general mechanism leading to the magnetic moment overturn (and, hence, to the information loss) is the thermal excitation. To stand against that, the minimum volume should be of $V_{\min} \sim 200 \text{ nm}^3$. For the ellipsoid with semi-axes' ratio of $a/b \sim 5$, that leads to $2a_{\min} \sim 20 \text{ nm}$, $2b_{\min} \sim 4 \text{ nm}$. The smaller cross-section of granules has area $\sim 14 \text{ nm}^2$. Maximum attained density of the data storage, corresponding to their close packing, for granules, staying normally to the disc plane (perpendicular recording), is of $\sim 7 \text{ Tb/cm}^2$.

Is that fantastic figure attainable in practice? One of the points on the road – mostly, technical one – is developing write/read heads. Another and *principal* problem is the magnetic interaction of nearly situated granules that, just as the thermal excitation, could result in shrinking the duration of the information storage. This self-magnetic field presses for overturning the granule magnetic moment. Thus, to compensate the effect of granules' magnetic interaction one needs to enlarge their volume over against the minimum volume V_{\min} .

In doing so the density of bits falls unavoidably. This negative effect should be compensated by the adequate enlarging of granules' volumes. We calculate that in the optimal (in the sense of the recording density) magnetic structure $V_{\text{opt}} = (9/4)V_{\min}$. Representing granules as infinitely thin uniformly magnetized rods one could calculate the total self-magnetic field. The optimal period of the granules' square lattice proves to be equal to $l_{\text{opt}} = 0.76a_{\min} \sim 8.4 \text{ nm}$, and the respective recording density is $\sim 1 \text{ Tb/cm}^2$. This is by 7 times lower than that dictated by the thermal limit, but still very high.

In addition, magnetic interaction between granules results in the broad scattering of external field values needed to switch various granules. We have obtained the *analytical* expression for the relevant distribution.

2OR-F-5

EDGE ROTATIONAL MAGNONS IN MAGNONIC CRYSTALS*Lisenkov I.V.^{1,2,3}, Kalyabin D.V.^{1,2}, Nikitov S.A.^{1,2,4}*¹ Kotelnikov Institute of Radio-engineering and Electronics of RAS, Moscow, Russia² Moscow Institute of Physics and Technology, Dolgoprudny, Russia³ Oakland University, Rochester, USA⁴ Saratov State University, Saratov, Russia

dmitry.kalyabin@phystech.edu

Magnonic crystals (MCs) are counterparts to photonic [1] and phononic [2] crystals for spin waves [3]. Periodic perturbations located along the spin wave propagation path form frequency band gaps within the spin wave spectrum, which were observed [4]. Band gap formation in artificial periodic structures generally relies on two mechanisms, namely Bragg scattering and local Mie-like scattering inside inclusions. Bragg band gaps are formed if the wave-vector inside the crystal is roughly equal to one of the reciprocal lattice vectors. Local resonant band gaps may be formed if resonant scattering conditions, or Mie conditions, are fulfilled inside the inclusions. Generally, local resonant modes are tightly bounded to inclusions, being nearly monochromatic across the Brillouin zone and have zero group velocity [5]. In the present work we consider propagation of forward volume magnetostatic spin waves (FVMSW) [6] in a 2D MC. However, gyrotropic properties of the ferromagnetic medium play an important role in wave scattering, producing an asymmetric helical scattered field, similar to electromagnetic waves in magneto-photonic crystals [7]. Origin of such behavior underlies in time-reversal symmetry breakage in ferromagnetic media. Thus it is expected that surface edge modes of FVMSW may appear by analogy with electromagnetic waves in magneto-photonic crystals, as well as other types of magnonic crystals. We consider a ferromagnetic film (matrix) with the thickness d and the saturation magnetization M_{s0} with embedded cylindrical inclusions of another ferromagnetic material with the same thickness and the value of the saturation magnetization M_{s1} . An external uniform magnetic field is applied normally to the film surface, allowing propagation of FVMSW. We show theoretically that under certain conditions in such structure appear modes with field strongly localized near inclusions. Moreover this field rotates while moving from one inclusion to another. It is also found that under certain conditions the local resonant modes may have negative group velocity, what can be used in signal processing devices.

[1] J. Joannopoulos, S. Johnson, J. Winn, and R. Meade, *Princeton University Press*, (2011).[2] S.A. Nikitov, Y.V. Gulyaev, I.V. Lisenkov, R.S. Popov, A.V. Grigorievskii, and V.I. Grigorievskii, *AIP Conference Proceedings*, (2008) 287-290.[3] S.A. Nikitov, P. Tailhades, C.S. Tsai, *JMMM*, **236** (2001) 320.[4] Y. Filimonov, E. Pavlov, S. Vysotskii, S. Nikitov, *Applied Physics Letters*, **101** (2012) 242408.[5] C. Vandenbem, J.P. Vigneron, *J. Opt. Soc. Am.*, **22** (2005) 1042.[6] A. G. Gurevich and G. A. Melkov, *CRC Press/INC* (1996).[7] A. A. Asatryan, L. C. Botten, K. Fang, S. Fan, R. C. McPhedran, *Physical Review B*, **88** (2013).

2OR-F-6

REVERSIBLE ELASTIC STRESSES AND MAGNETIC ANISOTROPY IN IRON GARNET FILMS, INDUCED BY WATER MOLECULES ADSORPTION

Zubov V.E.¹

¹ Faculty of Physics, M.V.Lomonosov Moscow State University, Leninskie Gory, Moscow,
119991, Russia
zubov@magn.ru

We recently detected and investigated the effect of reversible adsorption that proceeds via hydrogen bond formation mechanism on the domain structure of a magnetic insulator - iron garnet [1]. It is established in particular that in iron garnet films the width of magnetic domains of the labyrinth domain structure decreases after adsorption of water molecules. The decrease of domain width of the films is explained by the reduction of effective magnetic anisotropy constant (K) and effective magnetic anisotropy field (H_k) due to the water molecules adsorption. Measurement of field H_k of iron garnet films in vacuum and in atmosphere of water vapor is carried out in this work.

Iron garnet thin films of (111)-type of composition $(\text{Bi,Lu})_3(\text{Fe,Ga})_5\text{O}_{12}$ with perpendicular magnetic anisotropy are investigated. Thickness of films is $4.5 \mu\text{m}$, $B_s=4\pi I_s=25 \text{ Gs}$ (I_s - magnetization), domain width is $\sim 20 \mu\text{m}$. The content of Ga is 1.2 on formula unit. Samples were placed in an optical vacuum cell connected to a system for pumping out and bleeding in of various gases. Linearly polarized light passed through an iron garnet film perpendicular to the film surface. Faraday rotation of light was measured as a function of magnetic field (H_{\parallel}), which was parallel to a film plane. Magnetization direction deviates from the normal to the film surface in the field H_{\parallel} . Magnetization is rotated at the angle of 90° relative to initial direction if $H_{\parallel}=H_k$ and is directed parallel to a film surface. In this case Faraday rotation equals zero. The described methodology enables to measure the value of H_k in iron garnet films. The measured value of H_k is equal to 1.1 kOe in vacuum and 0.9 kOe in water vapor. The decrease of H_k is equal to about 20% in water vapor compared to vacuum. Using formula $H_k=2K/I_s$, we reach the value of uniaxial magnetic anisotropy constant equal to $K\approx 1100 \text{ erg/cm}^3$ и 900 erg/cm^3 in this two cases accordingly.

Compressive deformation appears on the free surface of the iron garnet film due to the adsorption of water molecules. This deformation induces an addition to uniaxial magnetic anisotropy $\Delta K\sim 200 \text{ erg/cm}^3$, which decreases the initial value of K . Formula $\Delta K\sim(3/2)(\lambda_{111})\sigma$ (where λ_{111} is the constant of magnetostriction, σ – elastic tension in the film induced by water molecules adsorption) can be used for the evaluation of ΔK value. One can get the value of $\sigma\sim 1,3\cdot 10^8 \text{ dyne/cm}^2$ if the value of $\lambda_{111}\sim 1\cdot 10^{-6}$ and $\Delta K\sim 200 \text{ erg/cm}^3$ are substituted in this formula. The value of λ_{111} is received by use of literature data for the investigated iron garnet films. The tension induced by the water molecules adsorption is big enough and is less than the ultimate strength of iron garnets about by one order of magnitude.

[1]. V.E. Zubov, A.D. Kudakov, N.L. Levshin, M.A. Vlasov, *JETP*, **116-5** (2013) 766.

2TL-B-4

LASER CONTROL OF MAGNETISM WITH SUBWAVELENGTH RESOLUTION

*Savoini M.*¹

¹ Radboud University Nijmegen, Institute for Molecules and Materials, Heyendaalseweg 135, 6525 AJ Nijmegen, The Netherlands
m.savoini@science.ru.nl

The interaction of sub-picosecond laser pulses with magnetically ordered materials has developed into a fascinating research topic in modern magnetism. From the discovery of sub-picosecond demagnetization over a decade ago to the recent demonstration of magnetization reversal by a single 40 fs laser pulse, the manipulation of magnetic order by ultrashort pulses has become a fundamentally challenging topic with a potentially high impact for future spintronics, data storage and manipulation [1]. A fundamental issue to be addressed is the spatial resolution. It is of key relevance both scientifically and technologically to be able to control the magnetization at the sub-micron level.

Here we present our results on the magnetization control at the sub-micron level using different approaches. As an example we show that strongly focusing the illuminating pulsed beam can lead to the totally unexpected formation of structures with distinct topological properties that have a high potential for data storage [2].

Moreover, a further reduction of the optically controlled area dimension can be achieved through different methods, namely by patterning the sample to limit the sample area and/or by using plasmonic nano-antennas to further confine the laser excitation. Both approaches are beneficial in the all-optical control of the magnetization. In particular we demonstrated that it is possible to obtain an energy effective and sub-diffraction switching in patterned areas by playing with the shape and the illumination conditions [3].

Finally, all-optical switching of domains as small as 40 nm in diameter has been achieved thanks to the field confining effects of resonant dipolar antennas, see Fig.1.

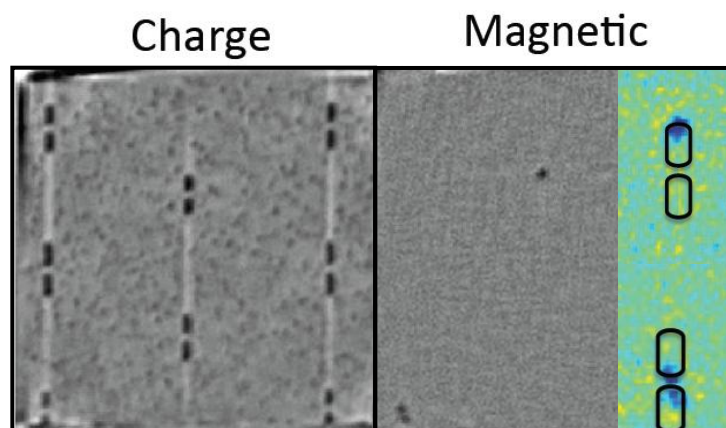


Fig. 1. Charge contrast: X-ray holographic imaging of plasmonic antennas on top of a TbFeCo film. Typical antennas size is 250 nm. Magnetic contrast: Corresponding all-optical magnetization reversal after laser excitation. Insets: Zooms of the magnetic contrast overlaid with the plasmonic antennas position.

- [1] Kirilyuk, A. *et al.*, *Rev. Mod. Phys.*, **82** (2010) 2731.
 [2] Finazzi, M. *et al.*, *Phys. Rev. Lett.*, **110** (2013) 177205.
 [3] Savoini, M. *et al.*, *Phys. Rev. B*, **86** (R) 140404.

2TL-B-5

MAGNETIC PROPERTIES OF CoPt AND FePt NANOPARTICLES

Dupuis V.¹

¹ ILM, UMR 5306 CNRS/Université de Lyon, 69622 Villeurbanne cedex, France
veronique.dupuis@univ-lyon1.fr

Magnetic nanoalloys attract a lot of attention because they offer the possibility to tune the magnetic anisotropy energy (MAE) probably up to the ultimate density storage limit. In particular, an extremely high magnetocrystalline anisotropy is expected from the stacking of pure Co (resp. Fe) and Pt atomic planes in the (001) direction for CoPt (resp. FePt) bulk alloys in the chemically ordered L1₀ phase.

In this paper, we focus our attention on non-trivial structure and magnetic properties obtained on mass-selected CoPt nano-clusters prepared by low energy cluster beam deposition (LECBD) co-deposited in inert carbon matrix [1]. For as-prepared bimetallic nanostructured samples, we have put into evidence from HRTEM the transition from a chemically disordered fcc A1 phase to a chemically ordered L1₀ tetragonal phase upon annealing under vacuum without particles coalescence [2, 3]. From x ray magnetic circular dichroism (XMCD) measurements at the Co and Pt L_{2,3} edge, we have found a significant increase of both Co and induced Pt magnetic moment for CoPt clusters compared to the bulk phase [4]. Moreover thanks to an accurate “triple fit” method which consists in adjusting simultaneously three curves (ZFC, FC and $m(H)$) obtained from SQUID magnetometry measurements, we have put into evidence the fact that the MAE increase in the ordered phase but not in the same proportion that what is expected for bulk CoPt alloys [5, 6].

Finally, we relate such magnetic behaviour to element-specific dependence of the local atomic relaxations in nanoalloys, described from extended x-ray absorption fine structure (EXAFS) experiments at the Co-K and Pt-L edge experiments. Spin-polarized density-functional calculations were carried on using the Vienna ab initio simulation package (VASP) to perform first principles electronic, magnetic and structural optimizations. The calculations fully confirm the experimental trends thus providing a detailed account of the element specific local relaxations which bring back together the experimental results [7]. Some recent results on Iron-based nanoalloys assemblies will be also reported [8, 9].

[1] F. Tournus et al, *JMMM*, **323** (2011) 1868.

[2] N. Blanc et al, *Phys. Rev. B*, **83** (2011) 092403.

[3] F. Tournus et al, *J. Appl. Phys.*, **109** (2011) 07B722.

[4] F. Tournus et al, *Phys. Rev. B*, **77** (2008) 144411.

[5] A. Tamion et al, *Appl. Phys. Lett.*, **95** (2009) 062503.

[6] V. Dupuis et al, *Eur. Phys. J. D* **67**: **25** (2013)

[7] V. Dupuis and A. Tamion, *in press Journal of Physics: Conference Series*

[8] F. Tournus et al. *Phys. Rev. Letters*, **110** (2013) 055501.

[9] A. Hillion et al. *Phys. Rev. Letters*, **110** (2013) 087207.

2TL-B-6

CORE@SHELL MAGNETIC NANOWIRE ARRAYS

Bran C.¹, Ovejero J.G.¹, Palmero E.M.¹, Vazquez M.¹, Contreras M.², Perez J.E.², Vidal E.V.²,
Kosel J.²

¹ Institute of Materials Science of Madrid, CSIC, 28049 Madrid, Spain

² Computer Electrical and Mathematical Sc. & Eng., KAUST, Thuwal 23955, Saudi Arabia
mvazquez@icmm.csic.es

The investigation of magnetism and derived properties of ordered arrays of nanowires and nanotubes is attracting much attention. Such nanostructures are considered nearly-ideal systems to study basic micromagnetic questions and develop applications from magnetic storage and logic devices, to biomedical cell separation or treatments [1]. Template assisted electrochemical growth of nanowires has been proved to be a very successful and cost-efficient way to prepare those nanosystems whose magnetic anisotropy (i.e., NiFe vs. Co) and geometry (diameter and length, interwire/tube distance or nanotube thickness) can be suitably controlled by the electroplating parameters [2].

Recent studies are focusing towards the magnetization reversal process and functionalization of nanowires/nanotubes with compositional multisegmented or diameter modulated structures [3]. In this concern, an interesting goal is the synthesis and characterization of ordered arrays of core@shell nanowires with single or two magnetic phase nature. Their interest for basic magnetic studies lies in the design and characterization of single and bimagnetic core@shell nanowires with complex magnetic interactions between phases (i.e., exchange, magnetoelastic and magnetostatic coupling). In addition, the biomedical functionalization of the external shell is suddenly attracting huge attention owing to their emerging technological potential.

After a general overview of the state-of-the-art of the magnetism and structure of nanowire arrays, we will summarize recent data on the characterization of core@shell magnetic nanowires synthesized by two-step electrodeposition. We introduce the magnetic behavior of nanotubular and core/shell nanowire structures with general composition FeCoNi@Au and Co@Fe. The total diameter of core@shell nanowires was tailored through chemical process between 60 and 80 nm, with shell thickness of around 10 nm, while the interwire distance was kept to 105 nm.

Control of structure and composition of samples was performed by SEM, TEM and EDX analysis. The magnetic analysis was carried out in a VSM magnetometer and it includes the analysis of coercivity and remanence as well as their angular dependence. Furthermore, the magnetic behavior of core@shell nanowire structures is compared to that of single magnetic phase nanowire counterparts.

Such core@shell nanowires can be chemically released from the template for further use. Due to the Au surface layer, such nanowires are excellent candidates for biomedical applications. We will show that the surface layer of FeCoNi@Au nanowires enables the bio-functionalization of the nanowires with antibodies while it reduces the cytotoxicity. This opens new opportunities profiting of the combined magnetic character of the core and the biomedical functionalization of the shell.

[1] X. Kou et al., *Adv. Mater.* **23** (2011) 1393; D. Altwood et al., *Science*, **296** (2002) 2003; J. Bran, *Mater. Today* **15** (2012) 351; D. Magnin et al., *Biomacromolecules*, **9** (2008) 2517.

[2] L.G. Vivas et al., *Nanotechnology*, **24** (2013) 105703; *Appl. Phys. Lett.* **100** (2012) 252405; C. Bran et al., *J. Appl. Phys.*, **114** (2013) 043908.

[3] M.P. Proenca et al., *Phys. Rev. B*, **87** (2013) 134404; M. Salem et al., *Nanoscale*, **5** (2013) 3941; J.I. Minguez et al., *Nanotechnology* (in press); Y. Su et al., *Nanoscale*, **5** (2013) 9709.

2RP-B-7

INTERFACE STUDIES OF IN-PLANE MAGNETIZED EXCHANGE-BIAS SYSTEMS USING X-RAY HOLOGRAPHY AND HERALDO

Jiménez E.¹, Mikuszeit N.², Yakhou-Harris F.¹, Camarero J.³, Vogel J.⁴, Tieg C., Perna P.^{3,5},
 Bollero A.^{3,5}, Rodmacq B.⁵, Gautier E.⁵, Auffret S.⁵, Gaudin G.⁵, Dieny B.²

¹ ESRF, 6 Rue Jules Horowitz, BP 220, 38043 Grenoble, France

² CEA/INAC/SP2M/NM, Grenoble, France

³ IMDEA, 28049, Madrid, Spain

⁴ Institut Néel-CNRS F-38054, Grenoble, France,

⁵ UAM and Instituto Nicolas Cabrera, 28049, Madrid, Spain

Erika.Jimenez@esrf.fr

Studying the origin of the exchange-bias effect is very complicated as it is attributed to interface effects. A technique, hence is required that allow to access magnetic information from a buried interface. One important possibility is the exploitation of x-ray circular dichroism, as soft x-rays penetrate metallic multilayers of several nanometres. A second very important point is the chemical

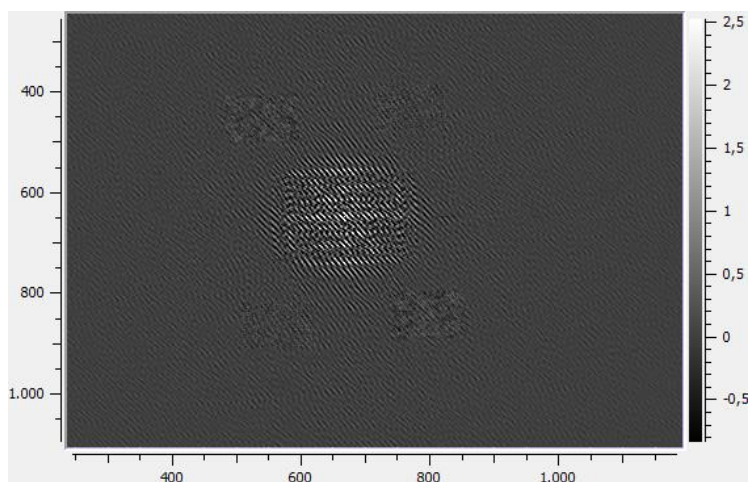


Fig. 1. HERALDO reconstruction of in-plane magnetized exchange-bias system

selectivity, which allows to easily distinguishing between the ferromagnetic and the antiferromagnetic materials, assuming that consist of different elements. Eventually, XMCD can be combined with holography, therefore enabling lensless imaging. This allows not only to quantify the magnetic moments in the interface contributing to the exchange bias effect, but also give special resolution and to determine the according positions, revealing possible correlations between ferromagnetic domains and uncompensated magnetic moments [1].

As the magnetic sensitivity requires a magnetization component in direction of the x-ray beam, XMCD works for out-of-plane magnetization [2]. To overcome the lack of in-plane sensitivity the sample has to be tilted. In case of holography this requires specially prepared reference holes for standard inverse Fourier image reconstruction[3]. To overcome the problem of the restriction of a single tilting angle defined by the reference hole we combine the HERALDO method [4]. As this method uses a slit instead of a hole making use of numerical trick to reconstruct the image, a variety of angles are accessible.

We present studies on the in-plane magnetized exchange bias system Co/IrMn using XMCD holography combined with HERALDO. We show that this technique enables the imaging of inplane domains and at the same time gives access to uncompensated moments in the antiferromagnet.

[1] J. Camarero, *et al. J. Appl. Phys.*, **109** (2011) 07D357.

[2] C. Tieg, *et al. Appl. Phys. Lett.*, **96** (2010) 072503.

[3] D. Stickler, *et al. Appl. Phys. Lett.*, **96** (2010) 042501.

[4] M. Guizar-Sicairos, *et al. Opt. Express*, **15** (2007) 17592.

2OR-B-8

SPIN WAVE PROPAGATING ALONG ULTRA THIN MAGNETIC NANOWIRES IN A TRANSPARENT MATRIX

Roussigne Y.¹, Stashkevich A.¹, Cherif S.-M.¹, Zheng Y.², Vidal F.², Poddubny A.³

¹ LSPM, Villetaneuse, France

² INSP, Paris, France

³ Ioffe Physical-Technical Institute, St. Petersburg, Russia

yves.roussigne@univ-paris13.fr

Self-assembled nanowires of ferromagnetic metals embedded in a dielectric matrix are interesting both for applications and fundamental science. Suffice it to mention ultra-dense magnetic recording media and metamaterials, including recently discovered artificial hyperbolic media.

Contrary to mainstream research in this domain, relying on ferromagnetic structures elaborated by means of a technology, today already conventional, based on electro deposition of metals in a porous alumina matrix [1], we have made use of a novel one. More specifically, it consists in co-deposition, by laser ablation, of the cylinders and the matrix, taking advantage of the natural segregation and of the columnar growth [2]. This alternative way allows fabricating really ultrathin wires with a diameter as small as 2 – 6 nm, which is entirely impossible if the conventional technology is employed (typical diameter varies from 20 nm to 200 nm). The purpose of this paper is the Brillouin Light Scattering (BLS) study of spin-wave modes (thermal magnons) of 5nm wide Co and Ni nano-wires.

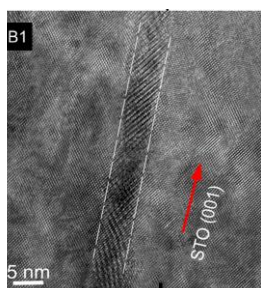


Fig.1. HRTEM image of a Co wire. Fig.2a. “Ferromagnetic” BLS spectrum (Co sample) Fig.2b. “Super-paramagnetic” BLS spectrum (Ni sample)

We would like to call one’s attention to the double-uniqueness of these structures. Magnetically, they can manifest both super-paramagnetic (typically Ni wires) and ferromagnetic behavior (typically Co wires). Optically, metallo-magnetic inclusions are quasi-transparent, their radius being comfortably inferior to the optical skin depth (15 – 20 nm). Moreover, they are placed in a transparent matrix. Not surprisingly, such structures exhibit a number of interesting features, both magnonically and magneto-optically (MO). Some of them are illustrated in Fig.2. Note that the “ferromagnetic BLS spectrum” displays a pronounced, albeit inverted, Stokes/Anti-Stokes asymmetry while the “super-paramagnetic” one is perfectly symmetric. Theoretical explanation, based on propagating spinwave modes localized on individual nano-wires, taking into account the symmetry of MO interaction, has been provided.

[1] U. Ebels et al., *Phys. Rev. B*, **64** (2001) 144421.

[2] P. Schio et al., *Phys. Rev. B*, **82** (2010) 094436.

2OR-B-9

MAGNETIC NANOPARTICLE TRAVELING IN EXTERNAL MAGNETIC FIELD

Usov N.A.¹, Liubimov B.Ya.¹

¹ Pushkov Institute of Terrestrial Magnetism, Ionosphere and Radio Wave Propagation RAS
Troitsk, Moscow, Russia
usov@izmiran.ru

The basic equations describing the motion of a free magnetic nanoparticle in an external magnetic field in a vacuum, or in a medium with negligibly small friction forces are postulated. They explicitly take into account the conservation of the total particle momentum, i.e. the sum of the mechanical and the total spin momentum of the nanoparticle. It has been shown for the first time [1] that the conservation of the total particle momentum leads to important consequences for the quantum tunneling of the magnetic moment of an isolated magnetic nanoparticle. However, the probability of quantum tunneling of the magnetic moment is nonzero only for particles of very small diameters, $D \leq 2-4$ nm. At the same time, the conservation of the total momentum may determine the behavior of a magnetic nanoparticle in a much larger range of sizes. In the present paper it is shown that for a magnetic nanoparticle traveling in a uniform magnetic field there are three different modes of precession of the unit magnetization vector and the particle director, i.e. the unit vector parallel to the particle easy anisotropy axis. These modes differ significantly in the precession frequency. For the high-frequency mode the director points approximately along the external magnetic field, whereas the frequency and the characteristic relaxation time of the unit magnetization vector precession are close to the corresponding values for conventional ferromagnetic resonance. On the other hand, for the low-frequency modes the unit magnetization vector and the director are nearly parallel and rotate in unison around the external magnetic field. The characteristic relaxation time for the low-frequency modes is remarkably long. This means that in a rare assembly of free magnetic nanoparticles there is a possibility of additional resonant absorption of the energy of alternating magnetic field at a frequency that is much smaller compared to the conventional ferromagnetic resonance frequency. The problem of scattering of a beam of magnetic nanoparticles in a vacuum in a non-uniform external magnetic field is also considered taking into account the complicated behavior of the unit magnetization vector and the particle director.

[1] E.M. Chudnovsky, *Phys. Rev. Lett.*, **72** (1994) 3433.

2OR-B-10

MAGNETIC STRUCTURE OF CYLINDRICAL NANOWIRES WITH MAGNETOCRYSTALLINE ANISOTROPY MODULATION

*Ivanov Yu.P.*¹, *Chuvilin A.*^{2,3}, *Kosel*¹

¹ King Abdullah University of Science and Technology, Thuwal, Saudi Arabia

² CIC nanoGUNE Consolider, San Sebastian, Spain

³ IKERBASQUE, Basque Foundation for Science, Spain

ivanov.yup@gmail.com

3D arrays of cylindrical nanowires (NWs) are a promising candidate for realizing a new concept of memory devices – vertical racetrack memories [1]. A key feature of such devices is the controlled manipulation of domain walls (DWs) in periodic potential. In order to realize such potential the local variation of the magnetocrystalline anisotropy can be used. Hcp Co is characterized by a strong uniaxial magnetocrystalline anisotropy. Fcc Ni is a material with a small cubic magnetocrystalline anisotropy. NWs with a high aspect ratio and a diameter from 15 to 200 nm can be prepared by a simple and low cost method using electrodeposition into porous membranes.

Here, we report the studies on magnetic structure of the single crystal hcp Co, fcc Ni and Co/Ni multilayer nanowires by combination of magnetic force microscopy (MFM) technique, Lorentz microscopy and electron holography.

Aluminum oxide templates were by a two-step anodization process of highly pure aluminum disks in oxalic acid, yielding a pore size of 40 nm. Two aqueous electrolytes were used for Co and Ni deposition. Electrodeposition was carried out at room temperature and a bias potential of -1 V (versus Ag/AgCl). The NW length was varied through the deposition time.

Generally, no grain boundaries were observed by transmission electron microscopy for Ni and Co NWs. The NWs have a uniform diameter of about 40 nm, a smooth surface and a single-crystal structure along the entire length. The crystal structure of the Ni NWs is fcc with [220] growth direction, the Co NWs crystal structure is hcp with [100] growth direction which correspond to the direction of the magnetocrystalline anisotropy being perpendicular to the NW axis. Fig. 1 shows the MFM images of the Ni, Co and Ni/Co bilayer NWs at the remanence. The spin configuration of the Ni NW is a single domain state with the magnetization parallel to the NW axis. The MFM image of the Co NW shows an alternating white-black magnetic contrast across the NW diameter. Such MFM contrast corresponds to a magnetic structure consisting of several vortices along the NW with alternating chirality [2]. Ni/Co multilayer NWs demonstrate a periodic domain structure. The quantitative analyse of the electron holograms recorded on single Ni NWs has proved the single domain character of the magnetic structure. Holograms of the Co NWs showed evidence of the complex vortex structure.

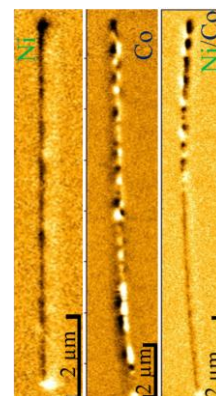


Fig. 1. MFM images of single domain fcc Ni NW, vortex state of hcp Co NW and domain structure of Ni/Co NW.

[1] S. S. P. Parkin et al, *Science*, **320** (2008) 190.

[2] Yu. P. Ivanov et al, *J. Phys. D: Appl. Phys.* **46** (2013) 485001.

Wednesday

2 July

11:30-13:00

14:30-17:00

oral session

2TL-G

2OR-G

**“Magnetic Soft Matter
(magnetic polymers,
fluids and
suspensions)”**

2TL-G-1

LOW TEMPERATURE STRUCTURAL TRANSITIONS IN DIPOLAR HARD SPHERES: THE INFLUENCE ON MAGNETIC PROPERTIES

*Ivanov A.O.*¹, *Kantorovich S.S.*^{1,2}, *Rovigatti L.*³, *Tavares J.M.*⁴, *Sciortino F.*³

¹ Ural Federal University, Ekaterinburg, Russia

² University of Vienna, Vienna, Austria

³ Universita di Roma La Sapienza, Roma, Italy

⁴ Instituto Superior de Engenharia de Lisboa-ISEL, Lisbon, Portugal

Alexey.Ivanov@urfu.ru

We investigate [1], via numerical simulations, mean field, and density functional theories, the magnetic response of a dipolar hard sphere (DHS) fluid at low temperatures and densities, in the region of strong association. The proposed parameter-free theory is able to capture both the density and temperature dependence of the ring-chain equilibrium and the contribution to the susceptibility of a chain of generic length. The theory predicts a nonmonotonic temperature dependence of the initial (zero field) magnetic susceptibility χ , arising from the competition between magnetically inert particle rings and magnetically active chains. Monte Carlo simulation results closely agree with the theoretical findings.

Our study demonstrates that the nonmonotonic temperature dependence of χ in the low-density DHS system is indeed triggered by ring formation, as the average magnetic moment of a ring is zero. The appearance of rings leads to an effective reduction of the magnetically responsive fraction of particles. This mechanism comes into play when both the temperature and the density are very low. For higher densities, the microstructure of the DHS system becomes more complex and simulation studies [2,3] have shown the presence of branched structures which span the entire system. This “gelation”-type crossover, giving rise to structures which could also be characterized by closed magnetic dipole moments, might also lead to the aforementioned effective exclusion of particles and result in the drop of the magnetic susceptibility, also at large densities.

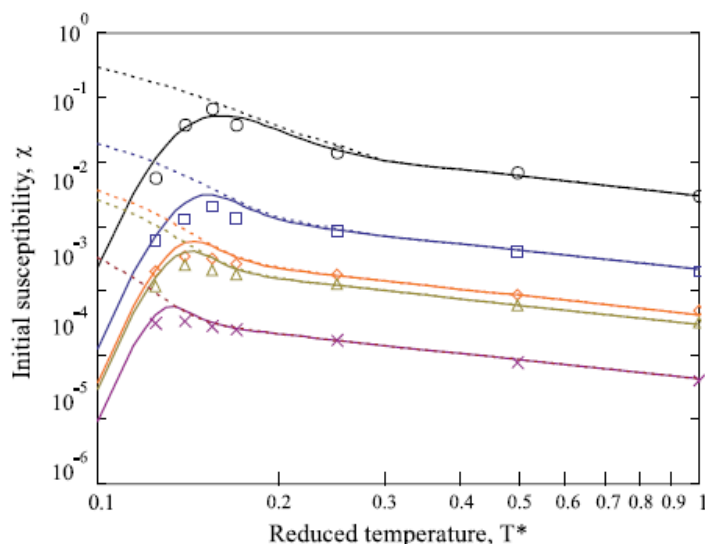


Fig. 1. Initial magnetic susceptibility as a function of reduced temperature for various volume fractions. Simulation data (symbols) and theory (solid lines) are for volume fractions: circles, 0.00367; squares, 0.000262; diamonds, 0.0000524; triangles, 0.0000367; crosses, 0.00000524. Dashed lines: initial magnetic susceptibility for the same range of parameters obtained in theory assuming that only chains (no rings) can form in the system.

Support by RFBR is acknowledged.

[1] S. Kantorovich, et al., *Phys. Rev. Lett.*, **110** (2013) 148306.

[2] L. Rovigatti, J. Russo, F. Sciortino, *Soft Matter*, **8** (2012) 6310.

[3] L. Rovigatti, et al., *J. Chem. Phys.*, **139** (2013) 134901.

2OR-G-2

INITIAL MAGNETIC SUSCEPTIBILITY OF POLYDISPERSE FERROFLUIDS

Elfimova E.A.¹, Ivanov A.O.¹, Camp P.J.²

¹ Ural Federal University (UrFU), Ekaterinburg, 620000 Russia

² University of Edinburgh (UoE), Edinburgh, Scotland

Ekaterina.Elfimova@urfu.ru

Laboratory synthesized dense magnetite-based ferrofluids show high static magnetic susceptibilities $\chi \sim 120$ at low temperatures $T \sim 230$ K [1]. The problem is that no theories predicted these record-breaking values and none has yet described correctly the associated temperature dependence measured experimentally.

In this work we show that the high values of the low-temperature magnetic susceptibility can be explained theoretically on the basis of the second-order modified mean-field approach in combination with a second virial contribution, the latter calculated for a polydisperse ferrofluid modeled as dipolar hard spheres. The resulting expressions are

$$\chi(T) = \chi_L(T) \left[1 + \frac{4\pi\chi_L(T)}{3} \left(1 + \frac{\Lambda(T)}{25} \right) + \frac{(4\pi\chi_L(T))^2}{144} \right], \quad (1)$$

$$\Lambda(T) = \frac{\pi^2 M_0(T)^2}{36k_B T \langle x^6 \rangle_x} \sqrt{\left\langle \left\langle \frac{x^{12} y^{12}}{[(x+y+4l)/2]^6} \right\rangle \right\rangle_{xy}}, \quad \langle \dots \rangle_x = \int_0^\infty \dots f(x) dx,$$

where $\chi_L(T)$ is the Langevin susceptibility, $k_B T$ is the thermal energy, $M_0(T)$ is the saturation magnetization of the ferroparticle bulk magnetic material, l is the thickness of the non-magnetic coating of the particle, and the parameter $\Lambda(T)$ is the polydisperse analogue of the usual dipolar coupling constant. Note that here, the definition of $\Lambda(T)$ contains double averaging of high powers of particle size over the granulometric distribution $f(x)$. For real particle-size distributions, this effective parameter is at least twice as large as the dipolar coupling constant. A comparison has been made between theory (1) and experiments [1, 2]. For that, we chose a reference temperature T_0 as the highest one available in the experiment. Then we bound the theoretical susceptibility to the measured value at this temperature, and then determined the values of $\chi_L(T_0)$ and the parameters of the magnetic-core diameter distribution function $f(x)$ (modeled as a gamma distribution). After that we compared the theoretical predictions with the experimental data over the whole temperature range, taking into account temperature corrections [3], and excellent agreement between theory and experiments was demonstrated even at low temperatures.

To check for consistency of the theory, Monte Carlo computer simulations were performed on monodisperse systems, and polydisperse systems with four discrete particle sizes, at particle volume concentrations of 30% and 40%. It was found that the susceptibility of a polydisperse system is higher than that of a monodisperse system with the same volume fraction and $\chi_L(T)$. Computer simulation data were compared with theory (1) for systems in which $\chi_L(T) < 0.76$, and the agreement was found to be quite good.

[1] Lebedev A.V., Lysenko S.N., *J. Magn. Magn. Mat.*, **323** (2011) 1198-1202.

[2] Pshenichnikov A.F., Lebedev A.V., *private communication*.

[3] Pshenichnikov A.F., Lebedev A.V., *Colloid Journal*, **67** (2005) 189-200.

2OR-G-3

MAGNETIC STRUCTURE OF DIPOLAR CHAINS: NUMERICAL SIMULATION

Kuznetsov A.A.¹, Pshenichnikov A.F.¹

¹ ICMM UB RAS, Perm, Russia

akuzyay@gmail.com

Current literature on ferrofluids draws much attention to single-domain magnetic particle chains. The formation of such objects has been observed in multiple numerical simulations [1] and supported by some experiments [2]. There is a number of analytical works that deal with chain-like aggregates and their impact on the physical properties of dipolar systems [3, 4]. However, the behavior of chains in the region of strong dipole-dipole interactions is still under discussion. For example, the model of quasipolymeric chains [5] predicts the coil–globule transition, which results in chain collapse to the compact formation called globule. It is suggested that globules act as particle condensation nuclei and promote phase stratification in the system. Magneto-dipole interaction energy in the coil-globule transition correlates well with interaction energy in the “gas-liquid” transition. A recent model [6] predicts the ring–chain structural crossover in a weakly-concentrated dipolar system. It is shown, both numerically and analytically, that the higher the energy of dipole-dipole interactions in the system, the stronger the predominance of rings over chains.

In this work, we present the results of Monte-Carlo simulation of dipolar hard sphere chains. Artificial restriction is imposed on the movements of magnetic particles in chains – the distance between the centers of adjacent particles is fixed, and therefore the chains under investigation are indissoluble. This assumption is commonly used in most theoretical studies dealing with chains. It provides opportunities for simulating very long chains consisting of hundreds of particles. In our investigation, two general cases (rod-like chains and flexible chains) are examined in a broad range of dipole-dipole interaction energy. In the first case, the emphasis is placed on the study of self-organization of particle magnetic moments and fluctuations of the average magnetic moment of a single rod-like chain. In the second case, we focus on the structural transformations of flexible chains. The results obtained for a single flexible chain as well as for the system of multiple interacted chains are presented.

This research was supported by the Russian Foundation of Basic Research (under Grants № 13-02-00076 and № 14-01-96007). Calculations were performed using “Uran” supercomputer of IMM UB RAS.

- [1] J.-J. Weis, D. Levesque, *Phys. Rev. Lett.*, **71** (1993) 2729.
- [2] A.F. Pshenichnikov, A.A. Fedorenko, *J. Magn. Magn. Mater.*, **292** (2005) 332–344.
- [3] A.Y. Zubarev, L.Y. Iskakova, *Phys. Rev. E*, **65** (2002) 061406.
- [4] V.S. Mendeleev, A.O. Ivanov, *Phys. Rev. E*, **70** (2004) 051502.
- [5] K.I. Morozov, M.I. Shliomis, *J. Phys.: Condens. Matter*, **16** (2004) 3807.
- [6] S.S. Kantorovich, A.O. Ivanov, L. Rovigatti, *Phys. Rev. Lett.*, **110** (2013) 148306.

2OR-G-4

STUDYING OF MACROSCOPIC PROPERTIES FOR BIDISPERSE MAGNETIC FLUIDS: PRESSURE AND COMPRESSIBILITY FACTOR CALCULATIONS

Novak E.¹, Minina E.^{1,2}, Pyanzina E.¹, Sanchez P.³, Kantorovich S.^{1,3}

¹ Ural Federal University, Ekaterinburg, Russia

² ICP, University of Stuttgart, Stuttgart, Germany (current place of work)

³ University of Vienna, Vienna, Austria

ekaterina.novak@urfu.ru

Industrially synthesized magnetic fluids, systems of magnetic dipolar particles suspended in a nonmagnetic carrier, are usually polydisperse systems with wide distribution over the particle size. One of the first attempts to investigate theoretically how polydispersity influences properties of the magnetic fluids was made for bidisperse systems as the simplest approximation of polydispersity [1]. According to this study, an additional type of dipolar particles of larger or smaller diameter added to the original monodisperse system alters the microstructure dramatically. For example, small particles of the model bidisperse system prevent long chain formation by poisoning effect [1] in contrast to the monodisperse system [2]. Since bidispersity of the system changes the microstructural properties, it has to affect microscopic properties inevitably. To prove the latter we chose osmotic pressure (compressibility factors) and compressibility as targets for the investigation. We perform molecular dynamics (MD) simulations of bidisperse system and compute pressure for a wide range of the total volume fraction of the particles. The MD simulations are done in the simulation package ESPResSo [3]. Besides that, we perform a series of Monte Carlo simulations to extract the isothermal compressibility. In addition, we calculate pressure and compressibility factors for systems of dipolar hard-spheres using the diagrammatic expansion [4]. In all our approaches we fix the total volume fraction of magnetic material. Within these fixed volume fractions we vary the granulometric composition: the system gradually changes from a monodisperse large particle system with the lowest number density to a monodisperse small particles system with the highest number density passing through 5-9 various bidisperse systems.

Comparison of the theoretical results to the simulation data shows that indeed pressure and as a result compressibility factors depend on the granulometric composition of the system. We show, that the dipole-dipole interaction in the range of investigated parameters leads to a qualitative difference in the compressibility factors when comparing to the pure hard-sphere system.

The work was done in the framework of the RFBR Grant No.12-02-33106 mol-a-ved, S.K. has been supported by Austrian Science Fund (FWF): START-Projekt Y 627-N27.

[1] C. Holm et al, *J. Phys.: Condens. Matter*, **18** (2006) S2737-S2756.

[2] S. Kantorovich et al, *Phys. Chem. Chem. Phys.*, **10** (2008) 1883-1895.

[3] H. J. Limbach et al, *Comput. Phys. Commun.*, **174** (2006) 704–727.

[4] E. Novak et al, *J. Chem. Phys.*, **139** (2013) 224905.

2OR-G-5

THERMODYNAMICS OF BIDISPERSE FERROFLUIDS: THEORY AND SIMULATIONS

Solovjova A.Yu.¹, Elfimova E.A.¹

¹ Institute of Mathematics and Computer Sciences, Ural Federal University, Yekaterinburg 620000,
Russia
anita_zy@mail.ru

The thermodynamic properties of the ferrofluids are studied using theory and simulations. The main difficulty is taking into account of the long-range dipole-dipole interparticle interactions. The most common approximation of ferrofluids is the system of dipolar hard spheres (DHS). The real ferrofluids are polydisperse and granulometric distribution significantly affects the properties of these systems. It is possible to approximate very accurately ferrofluids using the bidisperse model which include small and large particle [1]. The choice of a bidisperse system is quite obvious: being, on the one hand, still rather simple, it appears to be the first step on the way to full polydispersity, on the other hand.

The basic method of the theoretical part of this study is the virial expansion of the configuration part of the Helmholtz free energy in term of volume concentration φ . The virial coefficients were calculated as a series expansion in the dipolar coupling constants λ_{ij} , which shows the ratio of the magnetic interaction of two particles at the close contact to the thermal energy. Since the particles of each fraction interact among themselves and with particles of other fraction, we have three different dipolar coupling constants: for two small particles λ_{ss} , for two large particles λ_{ll} and for small and large particle λ_{sl} . As a result, the second and the third virial coefficients was calculated up to 4th and 3rd power of dipolar coupling constants respectively. The equilibrium properties of ferrofluids such as osmotic pressure and the heat were analytically determined as a function of the physico-chemical parameters of the system due to standard methods of statistical thermodynamics.

A series of Monte-Carlo simulations modeling bidisperse DHS fluid were performed for a wide range of system parameters: $\varphi \leq 0.3$ and $\lambda_{ll} \leq 2.7$. The reaction-field method [2,3] was used to handle the long-range dipolar interactions in a cubic box with periodic boundary conditions.

Predictions of thermodynamic functions for dipolar coupling constants $\lambda_{ll} = 2$ show good agreement with simulation result, even for 20 percent of large particles in the system. For higher values of λ_{ll} , there are deviations at high volume fractions and medium content of large particle.

This research project has been supported by UrFU under the Framework Programme of development of UrFU through the «Young scientists UrFU» competition.

[1] A.O. Ivanov, S.S. Kantorovich, *Phys. Rev. E*, **70** (2004) 021401-01-10.

[2] M. Neumann, *Mol. Phys.*, **50** (1983) 841-858.

[3] R. Jia, R. Hentschke, *Phys. Rev. E*, **80** (2009) 051502-02-10.

2TL-G-6

MAGNETIC MICROCONVECTION

Cēbers A.¹, Tatulčenkova A.¹, Kitenbergs G.¹, Ērglis K.¹

¹ University of Latvia, Rīga, Latvia

aceb@sal.lv

Magnetic microconvection arises on the interface of miscible magnetic and non-magnetic liquids due to the action of non-homogeneous ponderomotive forces of self-magnetic field of magnetic liquid [1].

In the Darcy approximation equation of motion of liquids reads

$$-\nabla p - \frac{12\eta}{h^2} \vec{u} - \frac{2M(c)}{h} \nabla \psi_m = 0; \operatorname{div}(\vec{u}) = 0;$$

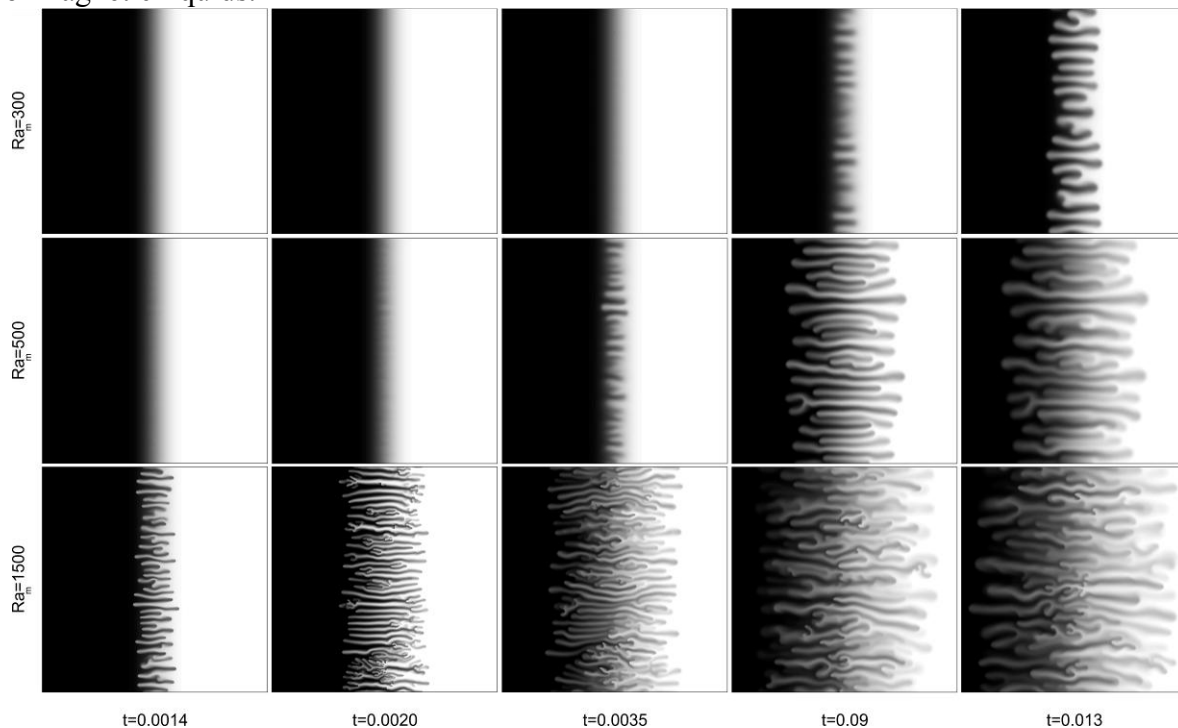
$$\frac{\partial c}{\partial t} + (\vec{u} \nabla) c = D \nabla^2 c.$$

Potential of magnetostatic field ψ_m is given by

$$\psi_m = M_0 \int c(\vec{r}', t) K(\vec{r} - \vec{r}'; h) d\vec{r}',$$

where $K(\vec{r}; h) = 1/|\vec{r}| - 1/\sqrt{\vec{r}^2 + h^2}$ and the magnetization of liquid $M = M_0 c$ is proportional to concentration of magnetic particles c .

The growth increment of perturbation of quiescent state depends on the magnetic Rayleigh number $Ra_m = M_0^2 h^2 / 12D\eta$ and the smearing of the interface between the magnetic and nonmagnetic liquids.



Numerical simulation of development of fingers at magnetic microconvection for several values of the magnetic Rayleigh number is shown in Figure.

[1] K.Ērglis et al, *J.Fluid Mech.*, **714** (2013) 612-633.

2OR-G-7

ISOTHERMAL VORTEX FLOWS NEAR FERRO- AND DIAMAGNETIC CONDENSATION CORES IN MAGNETIC FLUIDS UNDERGOING FIRST ORDER PHASE TRANSITION

Ivanov A.S.^{1,2}, Melenev P.V.^{1,3}

¹ ICMM UB RAS, Perm, Russia

² Perm State National Research University, Perm, Russia

³ Perm State National Research Polytechnic University, Perm, Russia
lesnichiy@icmm.ru

We report a new phenomenon – isothermal vortex flows in magnetic fluids in the vicinity of the localized source of the magnetic field (magnetized sphere) accompanied by the “rain” of drop-like aggregates [1]. The reason of this phenomenon is that exposure of the magnetic fluid to the external magnetic field initiates in the fluid the phase transition of “gas-liquid” type and the formation of the condensed phase – the drop-like aggregates with characteristic dimension of about tens of micrometers elongated along the field lines. A nonhomogeneous spatial distribution of drop-like aggregates leads to inhomogeneity of the ponderomotive force, which is responsible for the formation of vortex flows in the fluid.

The experiments were carried out in the Hele-Shaw cell. A small ferro- and diamagnetic spheres placed at the center of the cavity (condensation core). When exposed to the external magnetic field the sphere was magnetized and generated a homogeneous field in the surrounding space. This evoked phase transition and further segregation of fluid.

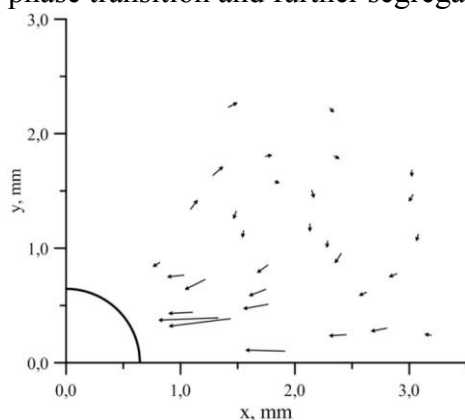


Fig. 1. The drop-like aggregates experimental velocity vector field (only 1 vortex of 4 is shown).

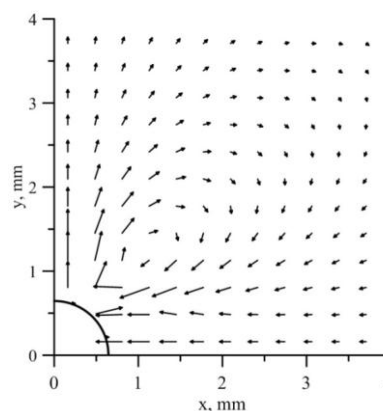


Fig. 2. The drop-like aggregates theoretical velocity vector field, obtained from computer simulation.

Computer simulation was carried out to describe the vortex motion of magnetic fluids. The simulation takes into account the description of phase transition, formation of drop-like aggregates and their influence on the ponderomotive force, leading to mechanical instability of the colloid. Two main equations are the Navier-Stokes equation, describing the fluid’s movement, and the equation for the mass transfer. This equations for stratified magnetic fluids under phase-transition conditions were obtained for the first time and was solved numerically. Good agreement between experiment and simulation is observed (Fig. 1, 2).

The work was supported by the Urals Branch of the RAS (Project No. 12-T-1-1008) and by the Russian Foundation of Basic Research (Grants No. 13-02-00076 and No. 14-01-96007).

[1] A.S. Ivanov, A.F. Pshenichnikov, *Phys. Fluids*, **26** (2014) 012002-9.

2TL-G-8

ANISOMETRIC MAGNETIC COLLOIDS: HOW TO TURN THE RESPONSE*Donaldson J.¹, Pyanzina E.², Novak E.², Prokopieva T.², Weeber R.³, Kantorovich S.S.^{1,2}*¹ University of Vienna, Wien, Austria² Ural Federal University (UrFU), Ekaterinburg, Russia³ Institute for Computational Physics (ICP), Stuttgart, Germany
sofia.kantorovich@univie.ac.at

Magnetic colloids nowadays evolved into an independent branch of dipolar soft matter. Not only the carrier liquids have been tuned to sustain low temperatures or meet medical requirements, but also the particles have been modified in various ways. Here, we present our results on shifted-dipole particles (SD) [1], ellipsoids (EL) [2], Janus particles (MJP) [3] and magnetic cubes (MCB) [4]. We focus on the ground states and magnetic properties of liquids containing such particles. SD. Particles with shifted dipoles represent a toy model of magnetically capped colloids. It is a spherical particle with a dipole moment shifted outwards radially. In this contribution we focus on the influence of an external field on the systems of shifted dipoles [5]. The competition between anti-parallel and ring-like dipole alignments in clusters of shifted dipole particles and an external field leads to a hindered magnetisation behaviour at $T > 0$. The initial susceptibility can fall even below the Langevin value. EL. In this part we focus our attention on the magnetic ellipsoids with the dipole moment pointing or along the main or along the short axes. We show that cluster topology, size-distribution, and average magnetic moment strongly depend on the system parameters. For ellipsoids with dipoles along the long axes we observe the decrease of the initial susceptibility not inherent to the ellipsoids with the dipole along the short axes. MJP. Magnetic Janus particles have already attracted considerable attention in literature [6]. They are half made of a magnetic material, and half silica. Here, we propose a simple toy model in which the spherical particle is divided into two hemispheres one of which contains a point dipole parallel to the division plane. We employ molecular dynamics simulations (MC) and theoretical method of ground-state calculations to understand the influence of the dipolar position and dipole-external field coupling on the cluster topology and cluster-size distributions. MCB. We have used an analytical approach and MC to determine ground state structures of magnetic colloidal cubes allowing for two different dipole orientations: the first aligned along the [100] crystallographic axis, and the second along the [111] axis. For cubes with [100] orientation the ground state is a chain of particles; a ring of cubes (in contrast to dipolar spheres) is always higher in energy. For the cubes with [111] dipolar orientation, we show that the zig-zag chains or "parquet" structures are observed in the ground states. The main conclusion is that the particle shape and structure can be used for bottom-up design of new smart materials.

[1] S. Kantorovich et al., *Soft Matter*, **7** (2011) 5217-5227.[2] S. Kantorovich et al., *Soft Matter*, **9** (2013) 6594-6603.[3] S. Smoukov et al., *Soft Matter*, **5** (2009) 1285-1292.[4] S. Sacanna, D. J. Pine, *Curr. Opin. Colloid Interface Sci.* **16** (2011) 96-105.[5] R. Weeber et al., *J. Chem. Phys.*, **139** (2013) 214901.[6] A. Ruditskiy, *Soft Matter*, **9** (2013) 9174-9181.

2OR-G-9

TWO-DIMENSIONAL LOW ENERGY STRUCTURES OF SUPRAMOLECULAR MAGNETIC FILAMENTS

Sánchez P.A.^{1,4}, Cerdà J.J.², Sintes T.², Kantorovich S.^{1,3}

¹ Computational Physics, University of Vienna, Sensengasse 8/9, 1090 Wien, Austria

² IFISC (UIB-CSIC), Campus UIB, E-07122 Palma de Mallorca, Spain

³ Ural Federal University, Lenin av. 51, Ekaterinburg, 620000, Russia

pedro.sanchez@univie.ac.at

Supramolecular magnetic filaments consist of mesoscopic linear chains of magnetic colloids permanently linked by polymers or other molecules. In difference with molecular magnetic polymers, which have a similar structure at a microscopic scale, magnetic filaments exhibit their magnetic properties at room temperatures and zero external fields, making them a system particularly interesting for many different nanotechnology applications [1]. This potential has just started to be proven in recent years, especially from an experimental perspective thanks to the continuous enhancement of methods for the synthesis of chains of increasing flexibility with colloids of decreasing size. To date most research efforts on magnetic filaments, either experimental or theoretical, have been devoted to their use as artificial magnetic cilia for micro- and nanofluidic applications [2], while other potential applications remain unexplored mainly due to the lack of understanding of the fundamental properties of these systems. In this context, our work is focused on the theoretical study of the fundamental physics of magnetic filaments by means of advanced analytical approaches and computer simulations.

Like in dispersions of free magnetic colloids, to which magnetic filaments are closely related, the equilibrium structural behavior of these systems is primarily governed by the interplay between the magnetic dipolar interaction (a long-range and strongly anisotropic force) and the entropy [3]. However, the existence of the permanent links introduces a structural anisotropy that makes such interplay more complex and suggests the emergence of a distinctive and potentially more rich behavior. In this contribution we discuss the origin and characterization of the multiloop configurations found as low energy structures of magnetic filaments in two dimensions at low temperatures [4], and their connection to the expected athermal ground state structures. In our discussion, we pay a special attention to the similarities and differences with respect to the structural behavior of dispersions of free magnetic colloids.

[1] H. Wang, et al., *Nano*, **6** (2011) 1-17.

[2] A. Cēbers, *Curr. Opin. Colloid. Interface Sci.*, **10** (2005) 167-175; Z. Zhou, et al., *ACS Nano*, **3** (2009) 165-172; J.J. Benkoski, et al., *Soft Matter*, **6** (2010) 602-609; S.N. Khaderi, et al., *Lab Chip*, **11** (2011) 2002-2010; C.-Y. Chen, et al., *Lab Chip*, **13** (2013) 2834-2839.

[3] P.A. Sánchez, et al., *J Chem Phys*, **139** (2013) 044904.

[4] P.A. Sánchez, et al., *Soft Matter*, **7** (2011) 1809-1818.

2OR-G-10

TEMPERATURE DEPENDENCE OF NANOPARTICLE MAGNETIC MOMENTS AND THEIR DIPOLE INTERACTION IN MAGNETIC FLUIDS

Lebedev A.V.¹¹ Institute of Continuous Media Mechanics UB RAS, Perm, Russia

lav@icmm.ru

It is known from an experiment that magnetization of bulk magnetite has the following temperature dependence $m = m_0(1 - \alpha T^2)$, $\alpha = 8 \cdot 10^{-7} \text{ K}^{-2}$. The $m(T)$ dependence for particles of nanometer size is currently the subject of debate. Investigation of the susceptibility of magnetic fluids allows one to get the answer to this question.

The susceptibility measurements of magnetic fluids with low interparticle interactions were performed in a wide temperature range. The fluid samples were stabilized with typical (fatty acids) and original (polypropylene glycol, tallow acids) surfactants. The magnitude of the temperature coefficient α was determined from the condition of the best fit of the measured and calculated values of susceptibility. Thermal expansion of the carrier liquid and interparticle dipole interaction in terms of Ivanov model [1] were taken in to account. Thermal expansion data of the used carrier liquids was obtained by density measurements.

The obtained values of temperature coefficients are correlated with solidification temperature T_S of the magnetic fluids. For fluids with low solidification temperature the coefficient α coincides with the value for bulk magnetite.

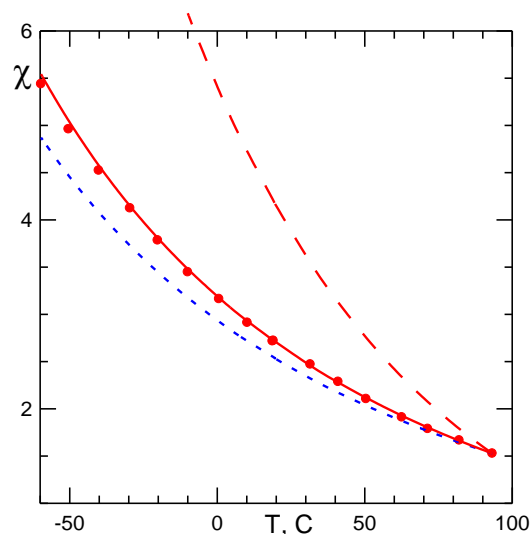


Fig. 1. Susceptibility temperature dependence of sample 1 for different values of temperature coefficient of nanoparticle magnetization: $\alpha = (8; 12; 30) \cdot 10^{-7} \text{ K}^{-2}$.

N	χ	M_∞ , kA/m	$\langle m \rangle$, 10^{-19} Am ²	Surfactant	Carrier liquid	α , 10^{-7} K^{-2}	T_S , C
1	3.065	49.20	2.08	Oleic acid	Isooctane	12	-60
2	1.005	25.58	1.23	Oleic acid	Vacuum oil	12	-60
3	1.549	37.47	1.35	Oleic acid	Isooctane	11	-60
4	3.058	48.07	1.67	Linoleic acid	Isooctane	10	-100
5	0.744	23.87	1.43	Lauric acid	Isooctane	12	-59
6	1.291	22.50	1.67	Stearic acid	Isooctane	13	14
7	4.544	41.27	1.78	Tallow acids	Isooctane	8	-110
8	2.732	29.30	1.71	Polypropylene glycol	Propylene oxide	8	-115

This work was supported by project UB RAS № 12-T-1-1008, and RFBR grants № 13-01-96041 and № 14-01-96007.

[1] A. O. Ivanov and O. B. Kuznetsova, *Phys. Rev. E* **64** (2001) 041405.

2OR-G-11

THE THERMAL RELAXATION OF MAGNETIZATION OF MAGNETIC FLUID IN LOW MAGNETIC FIELD IN ACOUSTOMAGNETIC EFFECT

Storozhenko A.M.¹, Polunin V.M.¹, Ryapolov P.A.¹

¹ Southwest State University, Kursk, Russian Federation

Storozhenko_s@mail.ru, Polunin-vm1@yandex.ru

When a sound wave propagates in magnetized magnetic fluid (MF) variable electromotive force appears in the inductance coil adjacent to a sound beam boundary. This effect is called acoustomagnetic [1-2]. In the adiabatic sound wave magnetic nanoparticles make ultrasmall thermal oscillations. This leads to the perturbation of magnetization of MF. Study of the effect of thermal relaxation of the magnetization allows us to estimate the rotational mobility of nanoparticles, which extends conception of rheology of MF.

The curve of acoustomagnetic effect is the dependence of amplitude of the electromotive force in the coil on the magnetic field. The initial part of the curve is linear. Its inclination to the x-axis is

$$\operatorname{tg}\theta_A = (\chi/M_S) \left[\left(1 + k' \frac{T}{\chi} \cdot \frac{\partial \chi}{\partial T} \right) (1 + N_d \chi)^{-1} + (\omega\tau)^2 \right] / [1 + (\omega\tau)^2],$$

where χ is initial magnetic susceptibility, M_S is saturation magnetization, N_d is the dynamic demagnetization factor [3], ω is the circular frequency of oscillation, τ is the relaxation time of the magnetic moment, $k' = qc^2/C_p$, c is sound speed in MF, q is thermal expansion coefficient, C_p is specific heat capacitance at constant pressure.

The initial part of the magnetization curve is characterized by $\operatorname{tg}\theta_M = \chi/M_S$. Therefore, we have:

$$\frac{\operatorname{tg}\theta_M}{\operatorname{tg}\theta_A} = \frac{1 + (\omega\tau)^2}{\left(1 + k' \frac{T}{\chi} \cdot \frac{\partial \chi}{\partial T} \right) (1 + N_d \chi)^{-1} + (\omega\tau)^2}.$$

Using Langevin theory of paramagnetism, we obtain:

$$\frac{\operatorname{tg}\theta_M}{\operatorname{tg}\theta_A} = \frac{1 + (\omega\tau)^2}{\frac{1 - k''}{1 + k''/3} + (\omega\tau)^2},$$

where $k'' = N_d \mu_0 M_S m^* / (k_0 T)$, μ_0 is the magnetic constant, m^* is the magnetic moment of a nanoparticle, k_0 is the Boltzmann constant.

The last expression contains the dependence $\operatorname{tg}\theta_M/\operatorname{tg}\theta_A$ on acoustic oscillations frequency ω and the relaxation time of the magnetic moment τ . We compare this function with the experimental results. Lines in Fig. 1 show the theoretical values, and the points are experimental results. Frequency range 20-60 Hz includes the area of thermal relaxation of the magnetization.

Based on Fig. 1 we can conclude that the thermal relaxation of the magnetization of MF in conditions of ultra-small thermal oscillations in low magnetic fields is missing. In other words, the process occurs in the area before relaxation. Consequently, the surrounding nanoparticle carrier fluid shows properties of non-Newtonian fluid with a special relationship between the strain rate and stress.

We are grateful for funding of this work via the Grant of the President of the Russian Federation for support of young researchers № 14.124.13.5498-MK "The Details of Mechanisms of magnetization disturbance of magnetic fluid in a sound wave".

[1] N.S. Kobelev, V.M. Polunin, et al, *Magnetohydrodynamics*, **46** (2010) 31–40.

[2] V.M. Polunin, A.M. Storozhenko, *Acoustical Physics*, **58** (2012) 180-186.

[3] V.M. Polunin, A.O. Tantsyura, et al, *Acoustical Physics*, **59** (2013) 662–666.

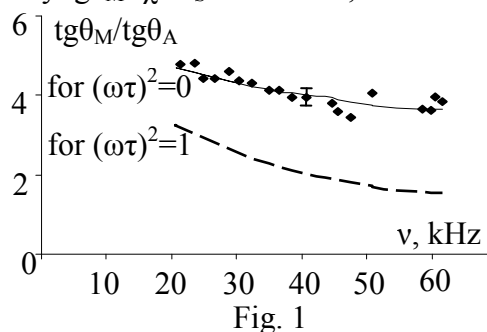


Fig. 1

2OR-G-12

INFLUENCE OF THERMAL NOISE ON MAGNETIC MICROPARTICLE ROTATION RATE IN EXTERNAL MAGNETIC FIELD

Skryabina M.N.¹, Lyubin E.V.¹, Khamidov D.¹, Fedyanin A.A.¹

¹ Lomonosov Moscow State University, Moscow, Russia

fedyanin@nanolab.phys.msu.ru

Magnetic microobjects under action of external rotating magnetic field show complicated dynamical behaviour which is interesting from both fundamental and technological sides. Regarding the practical aspect, one of the most popular examples is a microvortex allowing to mix liquids on the microscales.

This motion have typical transition from uniform rotation mode (rotation with the same frequency with field) to nonlinear microobjects rotation mode[1]. The frequency of transition between two modes is named critical frequency. The value of critical frequency depends on liquid media properties, like viscosity, temperature and presence of solvents, also it depends on the strength and configuration of magnetic field and on the form of microobject. It allow creating a physiochemical microsensor for characterisation of local properties of liquid in volume about picoliters [2]. One of the fascinating application is biosensor for monitoring the growth and drug susceptibility of individual bacteria [3]. Application of optical tweezers enables to study nonlinear rotation of microobject without influence of substrate. In recent studies [4] the influence of occasional perturbation on the motion of birefringent cylinder optically rotated with the frequencies slightly lower then critical. However the question how the thermal fluctuation affects on the rotation of micro-object is still open and the behaviour of rotating microparticles near the critical point is unclear.

In the present work the influence of Brownian fluctuation on the rotation of magnetic spherical microparticle is determined using optical tweezers technique. Microparticles rotation was achieved using external rotating magnetic field with frequencies near the critical. In the experiment the dependance of the mean frequencies of microparticle rotation was measured as a function of rotation frequency of magnetic field. Numerical simulation of microparticle rotation in presence of thermal noise was made using Monte-Carlo method. The results of simulation are in excellent agreement with the experiment.

Support by the RFBR and the Ministry of Education and Science of the Russian Federation.

[1] Helgesen, Geir, Piotr Pieranski, and Arne T. Skjeltop., *Phys. review letters* **64.12** (1990) 1425.

[2] McNaughton, Brandon H., et al., *J. Phys. Chemistry B*, **110.38** (2006) 18958-18964.

[2] Kinnunen, Paivo, et al. , *Biosensors and Bioelectronics*, **26.5** (2011) 2751-2755.

[4] Pedaci, Francesco, et al., *Nature Physics*, **7.3** (2010) 259-264.

2 July

Wednesday

11:30-13:15

oral session

2TL-H

2RP-H

2OR-H

“Multiferroics”

2TL-H-1

MAGNETISM AND MAGNETOELASTIC EFFECTS IN LiMPO_4 ($M = \text{Mn, Ni, Co}$)

Klingeler R.¹, Dietl C.¹, Wallbaum L.¹, Wang K.¹, Maljuk A.², Blum C.G.F.², Jähne C.¹, Neef C.¹, Rudisch C.², Grafe H.-J.², Giebeler L.², Meyer H.-P.³, Wurmehl S.², Büchner B.²

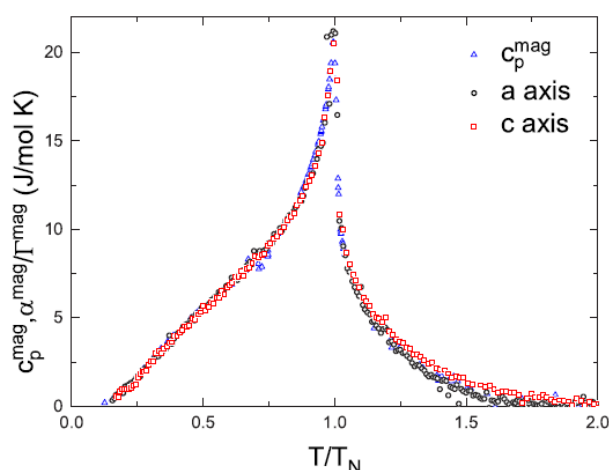
¹ Kirchhoff Institute for Physics, Heidelberg University, 69120 Heidelberg, Germany

² Leibniz Institute for Solid State & Materials Research IFW Dresden, 01171 Dresden, Germany

³ Institut für Geowissenschaften, Heidelberg University, 69120 Heidelberg, Germany

klingleer@kip.uni-heidelberg.de

While the olivine phosphates LiMPO_4 ($M = \text{Mn, Fe, Co, or Ni}$) exhibit complex ordering phenomena and large magnetoelectric effects, the interest in these materials has been further boosted by their high applicability for electrochemical energy storage in Li-ion batteries. In order to study the fundamental properties we have grown $\text{LiMn}_{1-x}\text{Ni}_x\text{PO}_4$ single crystals by the travelling-solvent floating-zone method as well as polycrystalline LiMPO_4 ($M = \text{Mn, Ni, Co}$), including solid solutions with combinations of different transition metal ions. Thermal expansion studies on $\text{LiMn}_{1-x}\text{Ni}_x\text{PO}_4$ ($x = 0, 0.05$) along the crystallographic axes by means of capacitive dilatometry imply strong magnetic-elastic coupling. The onset of long-range magnetic order is associated with pronounced lambda-like anomalies in the a - and c -axis thermal expansion and the magnetic specific heat. The data show a strong positive hydrostatic pressure dependence of T_N and a large fluctuation regime. The effect of Ni-doping on the magnetic anisotropy as probed by the spin-flop field is discussed. Studies of ^7Li - and ^{31}P -NMR in the paramagnetic and antiferromagnetic phase of LiMnPO_4 allow to determine the spin directions in the field-induced spin-flop phase. In LiCoPO_4 , NMR shows pronounced fluctuations. A new tetrahedrally coordinated LiCoPO_4 phase is found where the spin-lattice relaxation rate reveals quite different nature of the spin dynamics in the paramagnetic state including evidence for strong geometrical spin frustration which may lead to the incommensurate magnetic ordering.



Grüneisen scaling of magnetic contribution to linear thermal expansion coefficient α in a - and c -direction and specific heat c_p .

- [1] S.-H. Baek et al., *ArXiv*:1402.3082.
- [2] N. Wizen et al., *J. Cryst. Growth*, accepted.
- [3] K. Wang et al., *J. Cryst. Growth*, (2014) 16-21.
- [4] C. Rudisch et al., *Phys. Rev. B*, **88** (2013) 054303.
- [5] C. Neef et al, *Langmuir*, **29** (2013) 8054–8060.
- [6] C. Jähne et al., *J Materials Chem.*, **1** (2013) 2856-2862.

2TL-H-2

MULTIFERROIC AND MAGNETOELECTRIC METAL-ORGANIC FRAMEWORKS

Stroppa A.^{1*}, *Barone P.*¹, *Jain P.*², *Perez-Mato J.M.*³, *Picozzi S.*¹

¹CNR-SPIN Via Vetoio, 67100, L'Aquila (Italy)

²Los Alamos National Lab, 30 Bikini Atoll Rd Los Alamos, NM 87545-0001 (505) 664-5265

³Departamento de Fisica de la Materia Condensada, Facultad de Ciencia y Tecnologia, UPV/EHU, Bilbao (Spain)

* alessandro.stroppa@spin.cnr.it

Metal-organic frameworks (MOFs) show increasing promise as candidates for different applications. Of particular interest are MOFs with the perovskite topology showing hydrogen bonding-related multiferroic phenomena. By using state-of-the-art-ab-initio calculations, we predict that in $[\text{C}(\text{NH}_2)_3]\text{Cr}(\text{HCOO})_3$ MOF, interaction between Berry pseudo-rotations (i.e cooperative antiferro-distortive Jahn-Teller distortions) and the $\text{C}(\text{NH}_2)_3$ cations breaks the inversion symmetry through hydrogen-bonding and induces a ferroelectric polarization. Interestingly, the polar behavior arises due to a trilinear coupling between two unstable modes, namely a Jahn-Teller and a tilting mode, and one stable polar mode. Therefore, this compound represents the first example of hybrid improper ferroelectric in the family of metal-organic compounds. Since rotational modes in perovskite-inorganic compounds usually freeze-in at elevated temperatures (300 °K), the trilinear coupling in MOF compounds may provide an interesting route to realize room temperature multiferroic. Last but not least, we show that switching of polarization direction implies the reversal of a large weak ferromagnetic component, thus predicting a magnetoelectric effect in this compound [1-4].

[1] T. Besara, P. Jain, N. S. Dalal, P.L. Kuhns, A.P. Reyes, H.W. Kroto, A.K. Cheetham, *Proc. Natl. Acad. Sci. USA*, **108** (2011) 6828.

[2] P.Jain, V.Ramachandran, R.J.Clark, H.D.Zhou, B.H.Toby, N.S.Dalal, H.W.Kroto, A.K.Cheetham, *J. Am. Chem. Soc.*, **131** (2009) 13625.

[3] A. Stroppa, P.Jain, P. Barone, M.Marsman, J.M. Perez- Mato, A.K. Cheetham, H.W. Kroto, S.Picozzi, *Angew. Chem. Int. Ed.*, **50** (2011) 5847.

[4] A. Stroppa, P.Barone, P.Jain, J.M. Perez-Mato, S. Picozzi, *Adv. Mater.*, **25** (2013) 2284.

2RP-H-3

CRYSTAL-FIELD LEVELS OF TERBIUM IN PYROCHLORE COMPOUNDS*Klimin S.A.*¹¹ Institute of Spectroscopy, Russian Academy of Sciences, Moscow, Troitsk, Russia
klimin@isan.troitsk.ru

Rare-earth (RE) titanates $R_2Ti_2O_7$ (R stands for a RE element) with pyrochlore structure and frustration in the magnetic system attract great attention due to a new magnetic state known as spin ice [1]. This state was found only in two members of the family, namely, in $Dy_2Ti_2O_7$ and $Ho_2Ti_2O_7$. The Ising-type single ion anisotropy is a necessary condition for a realization of the spin-ice state [2]. The Tb^{3+} ion in the terbium titanate meets this condition but the spin ice state is not realized in $Tb_2Ti_2O_7$. The reason for this could be the low-lying crystal-field (CF) levels of Tb^{3+} . The CF splitting of the ground Tb^{3+} multiplet in $Tb_2Ti_2O_7$ was studied by neutron scattering [3] and Raman spectroscopy [4], and the data are somewhat contradictory. This study was undertaken to compare low-lying CF levels of Tb^{3+} observed in $Tb_2Ti_2O_7$, $Y_2Ti_2O_7:Tb1\%$, and $Gd_2Ti_2O_7:Tb10\%$.

The absorption spectra were measured in a broad spectral (1800-8000 cm^{-1}) and temperature (1.7 – 300 K) ranges. The CF energies for the ground multiplet 7F_6 were derived from a temperature-dependent spectroscopic study of the three compounds mentioned above. The difference in the number of levels is discussed in terms of interion interaction between terbium ions that arise in a 100% system ($Tb_2Ti_2O_7$) and is absent in a diluted one. Strong interionic interaction leads to a transformation of the terbium energy spectrum, which is confirmed by a dispersion of CF energies observed recently in neutron scattering experiments on $Tb_2Ti_2O_7$ [5]. This also could explain an appearance of extra energy levels reported by authors of Ref. [4].

Support by Russian Foundation for Basic Research (project No 12-02-00858) is acknowledged.

[1] A.P. Ramirez, *et al.*, *Nature*, **399** (1999) 333.

[2] B. Z. Malkin, A. R. Zakirov, M. N. Popova, S. A. Klimin, E. P. Chukalina, E. Antic-Fidancev, Ph. Goldner, P. Aschehoug, G. Dhalenne, *Phys. Rev. B*, **70** (2004) 075112.

[3] J.S. Gardner, B.D. Gaulin, A.J. Berlinsky, P. Waldron, S.R. Dunsiger, N.P. Raju, J.E. Greedan. *Phys. Rev. B*, **64** (2001) 224416.

[4] T.T.A. Lummen, *et al.*, *Phys. Rev. B*, **77** (2008) 214310.

[5] I. Mirebeau, P. Bonville, and M. Hennion, *Phys. Rev. B*, **76** (2007) 184436.

2OR-H-4

PRONOUNCED COUPLING OF 3d-EXCITONS WITH MAGNETIC PHASE TRANSITIONS IN CuB_2O_4

Boldyrev K.N.¹, Popova M.N.¹, Bezmaternykh L.N.², Pisarev R.V.³

¹ Institute of Spectroscopy, Russian Academy of Sciences, Moscow, Troitsk, Russia

² Institute of Physics, Siberian Branch, Russian Academy of Sciences, Krasnoyarsk, Russia

³ Ioffe Physical-Technical Institute, Russian Academy of Sciences, St. Petersburg, Russia
kn.boldyrev@gmail.com

Copper metaborate CuB_2O_4 possesses a complex crystal structure (SG $I42d$, $Z=12$), in which magnetic Cu^{2+} ions ($S=1/2$) in the unit cell occupy two different crystallographic positions, $4b$ and $8d$. Exchange interactions within these two sublattices and between them lead to an antiferromagnetic ordering at $T_{N1} = 21$ K and the second magnetic transition at $T_{N2} = 9.5$ K. Recent studies of electronic absorption spectra of CuB_2O_4 revealed narrow zero-phonon (ZP) exciton lines for all transitions between the crystal-field-split $3d$ -states of Cu^{2+} ions. Remarkably, the ZP lines are accompanied by an unusually rich and well-resolved vibronic structure [1]. In this presentation, we report results of a detailed study of ZP lines in the vicinity of phase transitions which shows a coupling of excitons with the spin ordering in both sublattices.

In contrast to a rigid behaviour of phonon frequencies with respect to the temperature and magnetic transitions [2], pronounced anomalies at $T_{N1}=21$ K are observed in the behavior of ZP lines corresponding to electronic transitions within the $4b$ sublattice. These lines with a half-width of a few wave numbers at low temperatures have a complicated structure, due to the spin-orbit and magnetic Davydov splitting. When approaching T_{N1} from below, the $4b$ ZP lines show a strong broadening and shift. Different behavior is observed for ZP lines related to the $8d$ sublattice, where the main peculiarities are at $T_{N2} = 8.5$ K. However, weaker but clearly visible features in the $8d$ lines are observed also at T_{N1} , as well as the $4b$ lines show marked changes in the frequency position at T_{N2} (see Fig.1). This demonstrates a mutual coupling between the $4b$ and $8d$ sublattices. Near the first $4b$ ZP line, we observed a broad satellite band in the range between 20 and 60 cm^{-1} , which drastically changes its shape at T_{N2} . This band can, presumably, be assigned to the exciton-magnon transition. Its changes at T_{N2} clearly confirm an opening of a gap in the magnon spectrum. A detailed study of a fine structure of the first $4b$ ZP line shows a splitting of the phase transition at T_{N2} into two transitions separated by ~ 0.2 K. Possibly, a sequence of incommensurate magnetic phases is realized with lowering the temperature. Concluding, we can say that the study of ZP exciton lines evidences a pronounced coupling between $3d$ -excitons and spin ordering in both sublattices, in particular, at magnetic phase transitions at T_{N1} and T_{N2} .

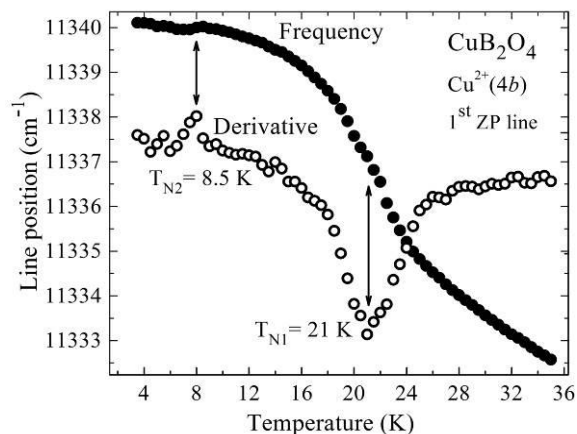


Fig. 1. Temperature dependences of the position of the lowest-frequency $4b$ ZP line and of its derivative.

Support by the President of Russian Federation (K.N.B., project MK-1700.2013.2) and by the Russian Government (R.V.P., project 14.B25.31.0025) is acknowledged.

[1] R. V. Pisarev, A. M. Kalashnikova, O. Schöps, *et al.*, *Phys. Rev.B*, **84** (2011) 075160.

[2] R. V. Pisarev, K. N. Boldyrev, M. N. Popova, *et al.*, *Phys. Rev.B*, **88** (2013) 024301.

2OR-H-5

ELECTROSTATIC PROPERTIES OF LOW-DIMENSIONAL MAGNETIC TOPOLOGICAL DEFECTS

Sergeev A.S.¹, Pyatakov A.P.¹

¹ Lomonosov Moscow State University, Moscow, Russia
ooo.rrdh@gmail.com

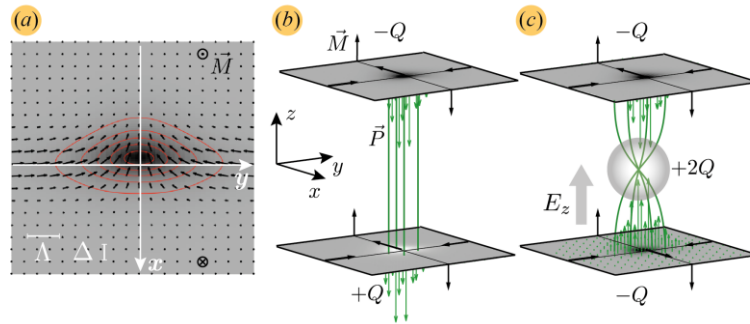


Fig. 1. (a) Magnetization vector (arrows) and electric charge (color) distributions in the vertical Bloch line at the top surface of the film; (b) vertical Bloch line without Bloch point; (c) vertical Bloch line with Bloch point plunged by external electric field from the bottom surface of the film.

Domain walls in magnetically ordered systems are planar objects separating domains – areas of a uniform order parameter distribution. Internal structure of a domain wall can be remarkably complex. In a three-dimensional crystal with vector order parameter there are three possible classes of topological defects: planar (domain walls), linear (vertical Bloch lines) and point-like (Bloch points). A vertical Bloch line separates areas of a domain wall with different chiralities (top view is shown at Fig.1(a)), whereas a Bloch point separates parts of a vertical Bloch line with different magnetization vector orientations. These objects are especially interesting in the light of inhomogeneous magnetoelectric effect, which is a most probable mechanism of domain wall magnetoelectricity studied experimentally in iron garnet films [1].

Idea underlying magnetoelectricity of this kind is that inhomogeneous magnetization distribution causes breaking of inversion symmetry which makes emergence of electric polarization possible. Let us consider vertical Bloch line with micromagnetic structure shown at Fig.1(a). Using expression for electric polarization arising due to inhomogeneous magnetoelectric effect [2] and spatial magnetization vector distribution [3], one can obtain absolute value of total electric charge of the vertical Bloch line at the film surface: $Q = \Gamma\pi^2\Lambda$, where Γ is magnetoelectric coefficient and Λ is vertical Bloch line width. Surface electric charges will have opposite signs on two surfaces of the film (Fig.1(b)). Thus vertical Bloch line has an electric dipole moment which can be reversed by external electric field applied normal to the film. This reversal is likely to be mediated by Bloch point, which has total electric charge of absolute value $2Q$ with sign determined by boundary conditions (Fig.1(c)). Estimation of electric field strength can be done by taking into account energy of Bloch point creation [3] and work against pinning force originating from atomic lattice [4]. For typical values for iron garnet films we obtain $Q = 4e$ and $E_z = 10^7$ V/m, where e is electron charge.

Work is supported by FRBR grants ## 13-02-12443 ofi_m2.

[1] A.P Pyatakov *et al*, *Europhys. Lett.*, **93** (2011) 17001.

[2] M. Mostovoy, *Phys. Rev. Lett.*, **96** (2006) 067601.

[3] A. P. Malozemoff and J. C. Slonczewski, *Magnetic Domain Walls in Bubble Materials*, 1979.

[4] S.Kim and O. Tchernyshov, *Phys. Rev. B*, **88** (2013) 174402.

Wednesday

2 July

11:30-13:00

14:30-17:00

oral session

2TL-O

2OR-O

2TL-C

2OR-C

“Magnetic Oxides”

2TL-O-1

FERROMAGNETISM OF METASTABLE OXIDES CONTAINING DIVALENT EUROPIUM

Tanaka K.¹, Fujita K.¹

¹ Department of Material Chemistry, Graduate School of Engineering, Kyoto University, Katsura, Nishikyo-ku, Kyoto 615-8510, Japan

Stable phases of EuTiO_3 , EuZrO_3 , and EuHfO_3 , which adopt perovskite-type structures, manifest antiferromagnetic transitions at low temperatures due to superexchange interactions among localized magnetic moments of Eu^{2+} ions. Recent experimental and theoretical approaches including those done by our research group have revealed that stress application, lattice volume change, and amorphization, leading to metastable phases of these compounds, can convert the antiferromagnetic into the ferromagnetic structures constructed by the Eu^{2+} spins. In this presentation, we report on our research results about ferromagnetic properties induced by structural change of Eu^{2+} -containing oxides, in particular, perovskite-type oxides.

Figure 1 illustrates temperature dependence of magnetization for EuTiO_3 thin films grown on LaAlO_3 (the data are represented by diamonds), SrTiO_3 (circles), and DyScO_3 (squares) single-crystalline substrates by using a pulsed laser deposition method. The data for bulk EuTiO_3 (triangles), i.e., the stable phase, are also shown for comparison. Ferromagnetic behavior is clearly observed at low temperatures for EuTiO_3 thin films irrespective of the sort of substrates, whereas the bulk EuTiO_3 manifests antiferromagnetic transition as expected. Also, X-ray diffraction analysis indicates that the lattice volume of EuTiO_3 thin film is the largest for the DyScO_3 substrate and the smallest for the LaAlO_3 substrate, correlating with the magnitude of magnetization at low temperatures. This suggests that the lattice volume expansion stabilizes the ferromagnetic rather than the antiferromagnetic states in EuTiO_3 . A theoretical approach can explain this phenomenon in terms of the variation of magnetic interactions among Eu^{2+} ions with the lattice volume.

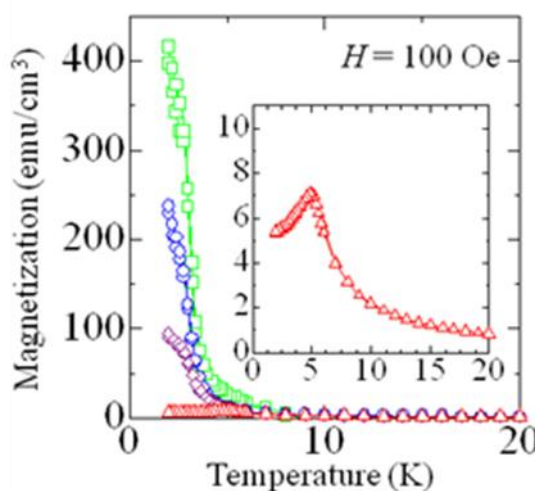


Fig.1 Temperature dependence of magnetization for EuTiO_3 thin films deposited on different crystalline substrates as well as bulk EuTiO_3 .

2OR-O-2

HETEROGENEOUS MAGNETIC STATE ABOVE THE CURRIE TEMPERATURE OF $\text{La}_{0.75}\text{Ca}_{0.25}\text{MnO}_3$ MANGANITE

Lazuta A.V.¹, Ryzhov V.A.¹, Khavronin V.P.¹, Mukovskii Ya.M.², Chichkov V.I.²

¹ Petersburg Nuclear Physics Institute, NRC Kurchatov Institute, 188300, Gatchina, Russia

² National Research and Technology University "MISiS", 119049, Moscow, Russia
alexandr@VL9467.spb.edu

The origination of the ferromagnetic (F) metallic clusters at some temperature T^* above the long – range ferromagnetic ordering temperature (T_C) in the hole doped manganites with the F ground state has been well established. However, a reason of its appearance and properties of this state remain the subject of much discussion. We present here the results of investigation of the clustered state in the $\text{La}_{0.75}\text{Ca}_{0.25}\text{MnO}_3$ single crystal. The studies included the data on the transport and magnetic properties (the linear and nonlinear second and third order ($|M_3|$) susceptibilities). Measurements of the second harmonic of the magnetization in the parallel small ac and steady (H) magnetic fields ($M_2(H, T, \omega)$, $H < 300$ Oe, $\omega/2\pi = 15.7$ MHz) allows one to control T -evolution of the clustered state. This compound reveals the orthorhombic $Pbnm$ (O^*) space group. It does not exhibit the Jahn – Teller distortions and has the metallic ground state with temperature metal – insulator transition $T_{MI} = 240.3$ K. It is found that $\text{Re}\chi(T)$ and $|M_3(T)|$ correspond to $T_C \sim 200$ K $< T_{MI}$. According to the $M_2(H, T)$ data, the development of the F clustered state proceeds into three stages. On cooling, during the first stage, the F clusters nucleate at the preferential sites that are likely produced by variation in oxygen and doping stoichiometry. The second stage is characterized by sharp increasing the concentration of the isolated F clusters on cooling. This is the process of the homogeneous nucleation. A coalescence of the isolated F clusters into some large-scale complexes containing some amount of the domains is associated with the third stage. It is the typical behavior observed at a first order phase transition. The stages clearly seen from $\text{Im}M_2$ data. The first one proceeds from $T^* \approx 292$ K down to $T^\# \approx 270$ K where $\text{Im}M_2(H) \approx -5 \cdot 10^{-8}$ emu/g at $H_{ext} \approx -5$ Oe. Nucleation of the isolated F clusters occurs from $T^\#$ down to $T_{COAL} \approx 230$ K ($> T_C$) where the signal strongly grows but its form does not change. Then isolated clusters start to coalesce and the form of signal starts to change, leading to a percolative type origination of F and insulator to metal transition. The $\text{Im}M_2(0)$ and $\text{Im}M_2(H_{ext})$ reach the maximum at T_C . The cluster signal concentrates at $H < 100$ Oe. The $\text{Re}M_2(H = 200 \text{ Oe}) \propto \tau^{-\gamma_2}$ with $\gamma_2 \approx 4.6$ ($\approx 14/3$) at $0.2 < \tau < 0.073$ ($T_C = 205$ K), that corresponds to critical behavior of an isotropic ferromagnet in a weak field. The F clusters above T_C was found in this system previously [1] due to deviation down from Curie-Weiss behavior $1/\chi(T)$. It was explained by domination of a double - exchange interaction over a super-exchange one.

[1] W. Jiang, X.Zh. Zhou et al., *J. Phys.: Condens. Matter*, **21** (2009) 415603.

2OR-O-3

COLOSSAL MAGNETORESISTANCE OF MANGANITES WITH THE ACTIVATION TYPE CONDUCTIVITY

Gudin S.A.¹, Kurkin M.I.¹, Gapontseva N. N.¹, Neifel'd E. A.¹, Korolev A. V.¹, Ugryumova N. A.¹

1 Institute of Metal Physics, Ekaterinburg, Russia

gudin@imp.uran.ru

The temperature dependence of the resistivity and magnetic moment of the single-crystal samples of manganite $La_{0.85}Ba_{0.15}MnO_3$ and $La_{0.85}Sr_{0.15}MnO_3$ was investigated in the temperature range 40-300 K in magnetic fields up to 90 kOe [1, 2]. Analysis of the experimental results shows that the magnetoresistance of lanthanum manganites far from the Curie temperature T_c can be described quantitatively by the $s-d$ model [3] normally used for ferromagnets and taking into account only the exchange interaction between the spins of charge carriers and magnetic moments. These data also shows that the features of lanthanum manganites responsible for colossal magnetoresistance (CMR) are manifested in a narrow temperature interval $\delta T \approx 20$ K near T_c . Our results suggest a CMR mechanism analogous to the mechanism of giant magnetoresistance (GMR) observed in Fe/Cr type multilayers with nanometer layer thickness. The nanostratification observed in lanthanum manganites and required for GMR can be described taking into account the spread in T_c in the CMR range δT . Physical characteristics required of the mechanisms proposed to explain the colossal values of magnetoresistance manganites with the activation type conductivity have been established. It is shown that the proposed mechanism CMR has these features. I.e. CMR mechanism associated with the phase separation near the Curie temperature on ferromagnetic and paramagnetic microregions exists only in the temperature range near T_c and is valid only in magnetic fields $H < 15kOe$.

This study was supported financially by the Russian Foundation for Basic Research (project № 14-02-00260) and by the Presidium of the Russian Academy of Sciences (project № 12-П-2-1041).

- [1] M.I. Kurkin, A. Neifel'd, A. V. Korolev, N. A. Ugryumova, S.A.Gudin, N. N. Gapontseva, *Phys. Solid State*, **55-5** (2013) 974–976.
- [2] M.I. Kurkin, A. Neifel'd, A. V. Korolev, N. A. Ugryumova, S.A.Gudin, N. N. Gapontseva, *JETP*, **143-5** (2013) 948-952 .
- [3] S.V. Vonsovskii, *Magnetism*, Nauka, Moscow, (1971) [in Russian].

2OR-O-4

INVESTIGATION CRYSTAL AND MAGNETIC STRUCTURE Yb_{1-x}Sr_xMnO₃ BY NEUTRON DIFFRACTION

Kunceovich A.A.¹, Kurbakov A.I.¹, Malyshev A.L.¹

B.P. Konstantinov Petersburg Nuclear Physics Institute, NRC “KI”, Gatchina, Russia

Structure of manganites RMnO₃ (where R is lanthanide) transforms from orthorhombic to hexagonal with decreasing ionic radius. Physical properties of these manganites radical change from orthorhombic doped manganites exhibiting colossal magnetoresistance effect to orthorhombic “geometric” ferroelectrics then to hexagonal “magnetic” ferroelectrics. We expect that YbMnO₃ doped by divalent metals allows switch from hexagonal to orthorhombic multiferroics.

We have carried out neutron diffraction studies of Yb_{1-x}Sr_xMnO₃ in temperature range from 2.6 K to room temperature. The crystal structure of Yb_{0.6}Sr_{0.4}MnO₃ corresponds a mixture of perovskite orthorhombic *Pbnm* and hexagonal *P6₃cm* (like for undoped YbMnO₃ [1]) phases at all temperatures. Such complex crystal structure of Yb_{0.6}Sr_{0.4}MnO₃ is explained with a view to the average A-cation size $\langle r_A \rangle = 1.149 \text{ \AA}$ and the local A-cation size mismatch $\sigma^2 = 0.01724 \text{ \AA}^2$ in comparison with the parent compound YbMnO₃ ($r_A = 1.042 \text{ \AA}$, $\sigma^2 = 0$).

Lattice parameters: $a=5.378(3) \text{ \AA}$, $b=7.580(1) \text{ \AA}$, $c=5.384(3) \text{ \AA}$ for orthorhombic phase (*Pbnm*); $a=6.0466(2) \text{ \AA}$, $c=11.3299(6) \text{ \AA}$ for hexagonal phase (*P6₃cm*).

Magnetic ordering of the hexagonal crystallographic phase is revealed at $T \approx 85 \text{ K}$. The phase with orthorhombic crystal structure shows magnetic ordering at $T \approx 130 \text{ K}$. Magnetic structure of *P6₃cm* phase represents canted-spin ordering of Mn magnetic moments in plane of Γ_2 -type. Mn ions form a well-separated triangular layers parallel to (*ab*) plane, with antiferromagnetic exchange interaction between the spins of the most nearest neighbors, which make Mn spin subsystem of low-dimensional and frustrated. In orthorhombic *Pbnm* phase the C-type magnetic structure is formed. Works was carried to clarify the crystal structure of this compounds. The parameters of the magnetic structure and produced representation analysis were carried out also.

Support by RFBR 12-02-00073.

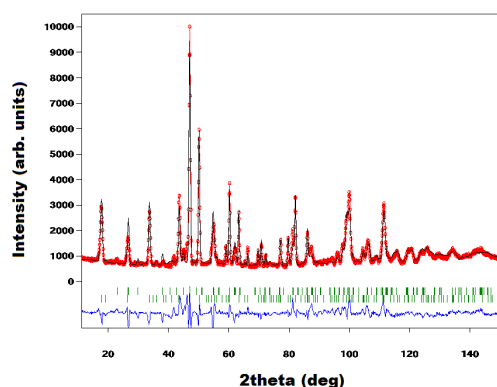


Fig. 1. The refined NPD pattern at 300 K

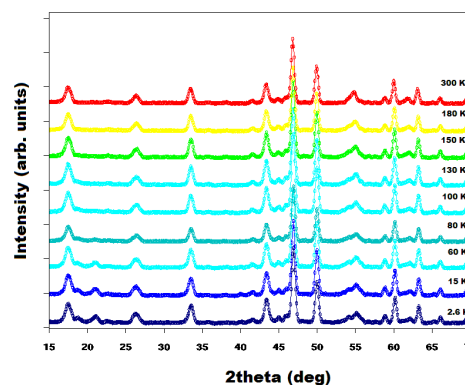


Fig. 2. Fragments of the neutron diffraction patterns $\lambda=1.752 \text{ \AA}$, $T=2.6 - 300\text{K}$.

[1] X. Fabrèges, I. Mirebeau, P. Bonville, S. Petit, G. Lebras-Jasmin, A. Forget, G. André, and S. Pailhès *Phys. Rev. B*, **78** (2008) 214422.

2TL-C-5

OPTICAL CONTROL OF MAGNETISM IN CORRELATED OXIDES

Ishihara S.^{1,2}, *Ohara J.*³, *Kanamori Y.*¹, *Iyoda E.*⁴, *Hashimoto H.*^{1,2}

¹ Department of Physics, Tohoku University, Sendai, Japan

² CREST, Sendai, Japan

³ Department of Physics, Hokkaido University, Sapporo, Japan

⁴ Department of Basic Science, The University of Tokyo, Tokyo, Japan

ishihara@cmpt.phys.tohoku.ac.jp

Optical manipulation of magnetism is one of the recent attractive themes in not only condensed matter physics but also modern nano-technologies. Since electron spins do not couple directly to the electric-field component of light, optical control of magnetism has been done in usual by utilizing the circular polarized light through the spin-orbit coupling. This strategy is applied successfully to the controls of magnetism in metallic magnets and some magnetic semiconductors. Another route for the optical control of magnetism is recently developed in correlated electron systems. There is a possibility to change a magnetic state by modifying the charge state which can be directly controlled by light. In this talk, we introduce recent our theoretical studies for optical manipulation of magnetism in strongly correlated transition-metal oxides.

1) Photoirradiation effects in correlated electrons coupled with localized spins are studied [1]. In particular, we examine melting of an antiferromagnetic (AFM) charge order insulating state by varying the light intensity. When intense light is irradiated, the AFM insulating characteristics are strengthened, rather than change into the ferromagnetic metallic characteristic, which are expected from the conventional double exchange interaction when carriers are introduced by weak light irradiation or chemical doping. This provides a new principle for optically manipulating magnetism.

2) Photo-induced spin-state change in itinerant correlated-electron system is studied [2]. A photon introduced in the low-spin band insulator induces a bound state of the high-spin state and a photo-excited hole. This bound state brings a characteristic peak in the optical absorption spectra in the photo-excited state. The results well explain the recent experimental results of the ultrafast optical spectroscopy in perovskite cobaltites.

We will also briefly touch the optical control of the electron dynamics and electron pair in two dimensional and ladder cuprates [3].

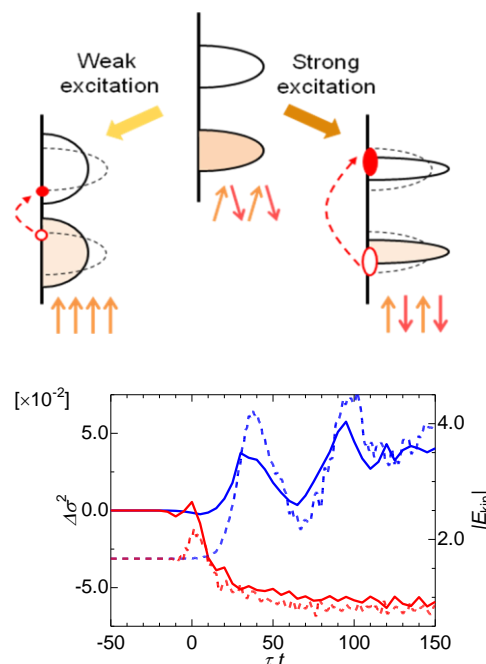


Fig.1 A schematic picture of optical control of magnetism in an charge-spin coupled system. The lower panel shows the time dependence of the electron kinetic energy in weak (blue) and strong (red) photo excitations [1].

[1] J. Ohara, Y. Kanamori, and S. Ishihara, *Phys. Rev. B*, **88** (2013) 085107.

[2] Y. Kanamori, J. Ohara and S. Ishihara, *Phys. Rev. B*, **86** (2012) 045137.

[3] E. Iyoda and S. Ishihara, *Phys. Rev. B* (to be published), and *arXiv:1312.1077*.

2TL-C-6

MAGNETIC AND ELECTRONIC PROPERTIES OF THE 3d COMPOUNDS AT EXTREME CONDITIONS OF HIGH AND ULTRA HIGH PRESSURES

Lyubutin I.S.¹

¹ Shubnikov Institute of Crystallography, Russian Academy of Sciences, 119333 Moscow, Russia
lyubutinig@mail.ru

The high-pressure studies provide additional degree of freedom to control the structural, electronic, optical, and magnetic properties of transition metal compounds which properties are mainly governed by strong electron-electron correlations. The pressure-induced insulator-metal, magnetic and structural phase transitions were predicted in these systems by many theories, however, until recently such effects could not be observed experimentally, since the expected values of necessary pressures exceed 2 Megabar. With the development of the high-pressure diamond-anvil-cell technique, the experimental investigations of such transitions are now possible especially due to the synchrotron radiation facilities [1].

In this report, a short review of several last experiments on the influence of high pressure on the magnetic and crystal structure as well on the electronic and transport properties of 3d metal oxides will be presented. Complex studies have been performed at high pressures up to 250 GPa in diamond anvil cells by several experimental methods including the synchrotron techniques.

At pressures above 50 GPa, the transitions from the magnetic to a nonmagnetic state (magnetic collapse) were discovered in some crystals with 3d ions in octahedral oxygen sites.

The magnetic collapse is associated with the spin crossover in 3d ions which transit from the high-spin (HS) to the low-spin (LS) state. At the same pressures, the structural phase transitions with a sharp drop of the unit cell volume were found. However, the metallization process was very complicated. At pressures of the HS-LS crossover, some crystals transform from the dielectric to a semiconducting state. The direct insulator-metal transition (IMT) was found in $Y_3Fe_5O_{12}$ and $BiFeO_3$ crystals just at the critical pressure P_c of HS-LS crossover, whereas in $FeBO_3$ the metallization does not develop even above 200 GPa. In NiO , the IMT transition was found at $P_c = 240$ GPa. These effects are explained by the extensive suppression of strong $d-d$ electronic correlations in Mott-Hubbard insulators, and new mechanisms of IMT have been suggested [2].

Several minerals important for geophysics were also investigated [3]. As an example, magnesiowüstite $(Mg,Fe)O$ is one of the most abundant minerals of the Earth's lower mantle, and the HS-LS spin transition in the Fe^{2+} ions can dramatically alter the physical and chemical properties of $(Mg,Fe)O$ in the deep mantle, thereby changing our understanding of the Earth's deep interior. To establish a fundamental understanding of the ground electronic state, the electronic and magnetic properties of $(Mg_{0.75},Fe_{0.25})O$ were investigated at high pressures and low temperatures. The results show that the ground electronic state of Fe^{2+} at the critical pressure P_c and close to $T = 0$ is determined by a quantum critical point where the energy difference between the HS and LS states is zero [3]. At $T > 0$, the thermal excitation of the HS or LS states strongly influences the physical properties of the material. In particular, a maximum in the magnetic susceptibility in the low-spin state of $(Mg,Fe)O$ was predicted even at the Earth's lower-mantle depths between 1300 and 1900 km and high temperatures $\sim (1000-3600$ K).

Supports by the Russian Foundation for Basic Researches (Grants #14-02-00483) and by the Russian Academy of Sciences Program "Strongly correlated electronic systems" are acknowledged.

[1] I.S. Lyubutin and A.G. Gavriliuk, *Physics – Uspekhi*, **52** (2009) 989.

[2] I.S. Lyubutin et al., *Phys. Rev. B*, **79** (2009) 085125.

[3] I.S. Lyubutin et al., *PNAS*, **110** (2013) 7142.

2TL-C-7

MAGNETIC AND ELECTRONIC PROPERTIES OF MOTT INSULATORS CLOSE TO SPIN CROSSOVER

*Ovchinnikov S.G.*¹, *Orlov Yu.S.*¹, *Dudnikov V.A.*¹, *Solovyev L.A.*², *Anshits A.G.*²,
*Vereshchagin S.N.*², *Perov N.S.*³

¹ L.V. Kirensky Institute of Physics, Siberian Branch, Russian Academy of Sciences, Krasnoyarsk, 660036, Russia

² Institute of Chemistry and Chemical Technology, Siberian Branch, Russian Academy of Sciences, Krasnoyarsk, 660049, Russia

³ Faculty of Physics, M.V. Lomonosov Moscow State University, Moscow, 119991, Russia
sgo@iph.krasn.ru

A review of unusual magnetic, electronic and structural properties of Mott insulators induced by spin crossover is given. Spin crossover from the high spin (HS) to the low spin (LS) state often is induced by high pressure. Cobaltite LnCoO_3 (Ln is rare-earth element) provide a system with LS of Co^{3+} ion stable in the ground state. A spin gap $\Delta_s = E_{\text{HS}} - E_{\text{LS}}$ is small for LaCoO_3 (150 K) and increases for other Ln due to smaller ionic radius of Ln^{3+} vs La^{3+} . For GdCoO_3 $\Delta_s(T=0) = 2300$ K. The large thermal expansion is equivalent to the negative pressure, both results in $\Delta_s(T)$ decrease. From magnetic susceptibility measurements up to 1000 K we separate the Gd^{3+} and Co^{3+} contributions and found the $\Delta_s(T)$ dependence. We have found that $\Delta_s = 0$ at $T_0 = 800$ K, it means the spin crossover with heating. The volumes of LS and HS states have been calculated by DFT-GGA at $T = 0$. The X-ray diffraction of GdCoO_3 has revealed the phase separation of the HS and LS states at $200 \text{ K} < T < 800 \text{ K}$. In this temperature region the thermal expansion is determined by HS-LS fluctuations. Electronic structure LDA+GTB calculation results in the charge-transfer insulator for LS GdCoO_3 at $T = 0$. With thermal population of HS state the in-gap states appear in the insulator gap and results in the smooth metallization at $T_{\text{MT}} = 780$ K [1].

High pressure induced spin crossover in ferroperricite $\text{Mg}_{1-x}\text{Fe}_x\text{O}$ is discussed. The low temperature P, T phase diagram has the quantum critical point $P = P_c = 55$ GPa at $T = 0$. It was found by the synchrotron Moessbauer spectroscopy [2]. The LDA+GTB calculated phase diagram describes the experimental data [2]. Its extension to the high temperature allows to predict metallization of the ferroperricite at the conditions of the low Earth's mantle and the metallic properties of the Earth's mantle at the depths $1400 \text{ km} < h < 1800 \text{ km}$ [3].

This work was supported by the President of Russia Grant NSh-2886.2014.2, Presidium of RAS (project 2.16), Siberian Branch of Russian Academy of Sciences (project № 38), RFBR Grants 13-02-00358.

[1] Yu.S. Orlov et al, *PRB*, **88** (2013) 235105.

[2] I.S. Lyubutin et al, *PNAS*, (2013) 04827.

[3] S.G. Ovchinnikov et al, *JETP Lett.*, **96** (3) (2012) 135.

2TL-C-8

NEUTRON DIFFRACTION STUDY OF MAGNETISM OF COMPLEX OXIDES

Kurbakov A.I.^{1,2}

¹ Petersburg Nuclear Physics Institute, NRC Kurchatov Institute, Gatchina, Russia

² Faculty of Physics, St.Petersburg State University, St.Petersburg, Russia

kurbakov@pnpi.spb.ru

The results of neutron powder diffraction (NPD) study of the crystal structures and spin configurations in new complex oxides with the layered or chained crystal structure are presented. The complex oxides can be solid electrolytes with very high ionic conductivity, promising electrode materials of the batteries, new high-performance photocatalysts, spintronics materials, etc. Manganites and cobaltites with the perovskite structure, perovskite-type layered structures as the double-layer Aurivillius, Ruddleson-Popper and Dion-Jacobson phases, mixed manganites - multiferroics, new mixed alkali metal - transition metal tellurates and antimonates, new mixed oxides containing 3d-elements in reduced and mixed oxidation states belong to the compounds researched by us. All investigated materials exhibit magnetic ordering of various types at low temperatures. For obtaining more complete, adequate and relevant physical information we always carried out neutron diffraction researches together (and most often after) other physical studies. It was applied the methods of measurement of the temperature and field dependences of magnetic susceptibility and magnetization, specific heat, electrical conductivity, dielectric loss tangent and dielectric susceptibility, polarization, EPR spectra, ⁷Li NMR spectra, ⁵⁷Fe Mössbauer spectroscopy, absorption spectra (NEXAFS), survey spectra of photoelectron spectroscopy (XPS), chemical shift of the x-ray lines etc. During diffraction studies often only neutron powder diffraction is insufficient, and therefore the X-ray and/or synchrotron diffraction measurements were carried out.

The tendency for doped colossal magnetoresistive (CMR) $\text{Sm}_{1-x}\text{Sr}_x\text{MnO}_3$ perovskite manganites to form ordered phase-separated states on crystallographic and, even to a greater extent, on a magnetic level is demonstrated.

The partial hole doping of $\text{Yb}_{1-x}\text{Sr}_x\text{MnO}_3$ manganites-multiferroics allows to pass a range of so-called "geometric" ferroelectrics YMnO_3 -type to "magnetic" ferroelectrics TbMnO_3 -type.

Unique mixed-valence quasi-one-dimensional lithium manganese tellurate system $\text{Li}_{1\pm x}\text{Mn}_{2\pm x}\text{TeO}_6$ with mixed oxidation $\approx 2.5+$, new layered solid electrolyte $\text{Na}_2\text{Ni}_2\text{TeO}_6$, quasi-two dimensional honeycomb oxides $\text{Na}_3\text{Co}_2\text{SbO}_6$, $\text{Li}_3\text{Ni}_2\text{SbO}_6$ and $\text{Na}_3\text{Ni}_2\text{SbO}_6$ were investigated.

The main results of the neutron researches are study of the magnetic phase transitions, the explanation of the magnetic features registered by other physical methods, creation of models of magnetic structures at different temperatures below the magnetic ordering temperatures, the definition of the numerical parameters of these magnetic models.

Also it is shown that NPD in the study of magnetism of complex oxides is very useful, and in many cases simply is a necessary tool of research. At the same time high resolution of neutron diffraction experiment is extremely essential. Its absence may lead to a not quite accurate interpretation of physical phenomena observed in the investigated materials.

Finally it is demonstrated that there is a clear correlation between fine specific features and temperature evolution of crystal structures, the corresponding types of low-temperature spin ordering, and physical properties all researched systems.

Support by RFBR, projects No. 12-02-00073 and 14-03-01122 is acknowledged.

2OR-C-9

NEGATIVE ISOTOPE EFFECT IN STRONG MAGNETIC FIELD

Taldenkov A.N.¹, Snegirev V.V.², Babushkina N.A.¹, Kalitka V.S.², Kaul A.R.²

¹ NRC Kurchatov Institute, Moscow, Russia

² Lomonosov Moscow State University, Moscow, Russia

box-n3@bk.ru

Praseodymium-based ordered manganite RBaMn_2O_6 is the composition in which the FM order of manganese ions is suppressed by developing AFM (and possible CO) ordering with temperature lowering. The large negative oxygen isotope effect in this FM-AFM transition temperature T_{CR} has been observed earlier [1]. The heavy oxygen suppresses FM magnetic state and favors arising of AFM ground state.

The purpose of this study is to investigate the influence of oxygen mass on the processes of magnetization in high magnetic field. The isothermal magnetization is studied at temperature range 300 K-110 K in pulse magnetic field up to the 30 T. Well-defined step-like spin reorientation transition occurs at critical field H_{CR} (Fig.1a). Transition demonstrates a hysteretic behavior. The magnetization saturation value is about $3 \mu_{\text{B}}/\text{Mn}$ that is close to the theoretical limit of $3.5 \mu_{\text{B}}/\text{Mn}$ for fully FM ordered half-doped manganites. The H-T diagram is constructed on the basis of magnetization curves (Fig. 1b). The T_{CR} (H_{CR}) phase boundary has an upward curvature, and isotope shift of T_{CR} is increased with magnetic field. The obtained data coincide well with the results of DC magnetization measurements [1]. The field and temperature dependencies of isotope oxygen exponent α are calculated:

$$\alpha = -\frac{\partial \ln T_{\text{CR}}}{\partial \ln M_{\text{O}}} = -\frac{({}^{16}T_{\text{CR}} - {}^{18}T_{\text{CR}})({}^{16}M_{\text{O}} + {}^{18}M_{\text{O}})}{({}^{16}T_{\text{CR}} + {}^{18}T_{\text{CR}})({}^{16}M_{\text{O}} - {}^{18}M_{\text{O}})}$$

The parametric dependence $\alpha(T_{\text{CR}})$ in accordance with [1] in a wide temperature range obeys the law $\text{abs}(\alpha) = A \cdot \exp(-T_{\text{CR}}/T_0)$, firstly observed in [2]. Note, that α reaches the value of -2.7 at 110 K. Following the main conclusion of [1] one can confirm that large negative isotope effect in AFM transition in half-doped manganites has the same origin as positive oxygen isotope effect in FM transition in optimally doped manganites of different kind. The results are qualitatively interpreted in the frame of model [3].

This work is supported by RFBR grant N1303-01249.

[1] A.N. Taldenkov et al., *Solid State Phenomena*, **190** (2012) 699.

[2]. M. Zhao et al., *Phys. Rev. B*, **60** (1999) 11914.

[3]. N.M. Plakida, *JETP Lett.*, **71** (2000) 493.

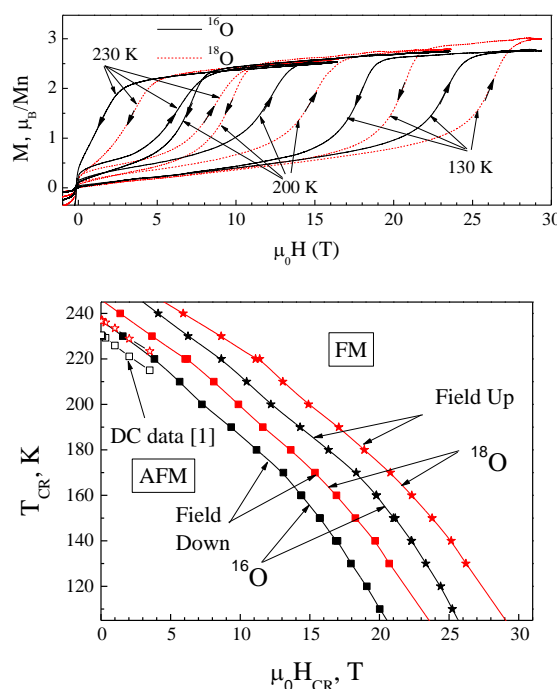


Fig. 1a. M-H curve for $\text{PrBaMn}_{216-18}\text{O}_6$ at different temperatures.

Fig. 1b. H-T diagram for $\text{PrBaMn}_{216-18}\text{O}_6$.

2OR-C-10

MAGNETIC, TRANSPORT, OPTICAL AND STRUCTURAL PROPERTIES OF ELECTRON-DOPED CaMnO_3 WITH Mn-SITE SUBSTITUTION

Mostovshchikova E.V.¹, Zainullina R.I.¹, Solin N.I.¹, Naumov S.V.¹, Telegin S.V.¹, Arbutova T.I.¹, Loshkareva N.N.¹

¹ Institute of Metal Physics, Ural Division of RAS, Ekaterinburg, Russia
mostovsikova@imp.uran.ru

Doped manganites are attractive due to reach phase diagrams and close interrelation between structural, magnetic and charge subsystem [1, 2]. Parent CaMnO_3 is the insulator with antiferromagnetic (AF) ordering of G-type and orthorhombic structure. The electron doping can be obtained by nonisovalent substitution or oxygen nonstoichiometry. Nonisovalent doping in $\text{Ca}_{1-x}\text{A}_x\text{MnO}_3$ where A is trivalent ions like La, Sm or tetravalent ions Ce and others or in $\text{CaMn}_{1-x}\text{M}_x\text{O}_3$ where M is penta- or hexavalent ions like Ru, V, Mo, or W influences the transport, magnetic and crystal structure: the resistivity decreases and at some concentration of Mn^{3+} ions the phase with AF state of C-type and monoclinic crystal structure with orbital/charge ordering is revealed. Because of significant difference between ionic radii of Ca and La, Sm or Ce, in $\text{Ca}_{1-x}\text{A}_x\text{MnO}_3$ the structural distortion takes place and can cause the increase of the charge carriers' localization. The ionic radii of Mn and Mo or W are close to each other, so, the crystal distortion in $\text{CaMn}_{1-x}\text{M}_x\text{O}_3$ is lesser. On the other hand, substitution of Mn-ions by nonmagnetic ions, for example Mo or W, results in switching off the double exchange in that sites which also can increase the localization of the charge carriers.

The aim of the present work is the complex study of the properties of electron doped manganites $\text{CaMn}_{1-x}\text{M}_x\text{O}_3$ with $\text{M}=\text{Mo}$ or W , $x < 0.15$ and comparing with that of manganites with Ca-site doping to reveal the role of structure deformation caused by difference in ionic radii and magnetic dilution in the peculiarities of charge subsystem.

The transport and optical data show that at low doping level, when the concentration of Mn^{3+} in lower than 0.04, in $\text{CaMn}_{1-x}\text{M}_x\text{O}_3$ the degree of the localization of the charge carriers is lesser than that in $\text{Ca}_{1-x}\text{La}_x\text{MnO}_3$ indicating that the crystal distortions play the key role in the transport. At higher concentration of Mn^{3+} ions the charge carriers are more localized in Mn-site doped manganites pointing that the break of Mn-O-Mn bond plays the most significant role.

The magnetic data obtained for our $\text{CaMn}_{1-x}\text{M}_x\text{O}_3$ manganites are close to that in literature [2] and shows only one phase transition. In the same time, the study of the elastic properties has detected the existence of additional phase transition which we have ascribed to appearance of the phase with AF ordering of C-type and monoclinic structure. The presence of this phase in G-AF phase with orthorhombic structure was expected from the comparison with the magnetic data of manganites with Ca-site doping with close concentration of Mn^{3+} [2]. The antiferromagnetic phase of C-type with monoclinic structure is manifested in magnetic data of Mn-substituted manganites at higher doping level ($x=0.07$ for Mo) [3].

The magnetic data of $\text{CaMn}_{1-x}\text{M}_x\text{O}_3$ manganites with $\text{M}=\text{W}$ and $x=0.10, 0.125$ indicate the orbital ordering near room temperature. The transport and optical data of these manganites are also studied and discussed.

The work was supported by grants of Presidium of RAS and RFBR (No. 12-02-00208).

[1] A. Maignan, C. Martin, F. Damay, B. Raveau, *Chem. Mater.*, **10** (1998) 950.

[2] N. N. Loshkareva and E. V. Mostovshchikova, *Phys. Metals and Metallogr.*, **113** (2012) 19.

[3] A. Maignan, C. Martin, C. Autret, M. Hervieu, B. Raveau, J. Hejtmanek, *J. Mater. Chem.*, **12** (2002) 1806.

Wednesday

2 July

11:30-13:00

oral session

2TL-Q

2RP-Q

2OR-Q

**“Magnetic Shape
Memory and
Magnetocaloric Effect”**

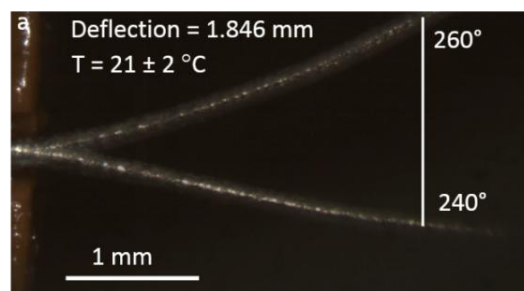
2TL-Q-1

ACTUATION THROUGH HETEROGENEOUS MAGNETIC-FIELD-DRIVEN DEFORMATION OF MAGNETIC SHAPE-MEMORY ALLOYS

Müllner P.¹

¹ Department of Materials Science and Engineering, Boise State University, Boise, ID, USA
 petermullner@boisestate.edu

In the low-symmetry martensite phase, magnetic shape-memory alloys exhibit strong magneto-structural coupling. This coupling, when combined with a low twinning stress, enables large magnetic-field-induced deformation. Local control of twinning via variable inhomogeneous magnetic fields initiates local reversible deformation. The material morphs into different shapes. We demonstrated this concept by moving a narrow neck along a Ni-Mn-Ga single crystal without changing the length of the crystal [1]. We also applied this concept to build a valve-less micropump consisting of a Ni-Mn-Ga single crystal, a casing, and a rod magnet [2]. The micropump successfully pumped fluid in opposite directions when the magnet was turned at 1000 rpm clockwise and counter clockwise. The pumping precision was one discrete gulp, in this particular case 260 nl. At 1000 rpm, the pump moved 16 gulps per second or 4.2 $\mu\text{l/s}$ with a precision of 0.26 μl for any given volume. We further demonstrated magnetic-torque induced bending as a second example for heterogeneous magnetically induced shape change [3]. For a polycrystalline Ni-Mn-Ga wire with diameter of 250 μm , a variable magnetic field bent the wire to a radius of curvature of 8 mm, corresponding to a surface strain of 1.5%. The curvature was reversed via a change in the magnetic field direction. Bending amplifies the actuation stroke and produces displacements in the order of the element length. In both examples, the magnetic shape memory element was rigidly fixed at one end (wire) or both ends (micropump) without constraining the actuator's operation. Localized magnetic-field-driven deformation provides actuator solutions not attainable with homogeneous deformation.



Bending is one example of heterogeneous deformation which can be achieved with magnetic fields. The picture shows two overlapped images of a wire exposed to a magnetic field oriented at 240 and 260° to the horizon. [3]

Support from the National Science Foundation under DMR-1207192 and the Department of Energy, Office of Basic Energy Sciences under contract DEFG-02-07ER46396 is acknowledged.

[1] A. Smith, J. Tellinen, P. Müllner, K. Ullakko, *Scripta Materialia*, **77** (2014) 68-70.

[2] K. Ullakko, L. Wendell, A. Smith, P. Müllner, G. Hampikian, *Smart Materials and Structures*, **21** (2012) 115020.

[3] P. Zheng, N. Kucza, C. L. Patrick, P. Mullner, D. C. Dunand, *subm. to Acta Mater.* (2014).

2RP-Q-2

STRUCTURAL AND MAGNETIC PROPERTIES OF Mn_2NiGa MAGNETIC SHAPE MEMORY ALLOY

*Singh Sanjay*¹, *Rawat R.*¹, *Muthu S.E.*², *D'Souza S.W.*¹, *Ranjan R.*³, *Suard E.*⁴, *Rajput P.*⁵, *Senyshyn A.*⁶, *Arumugam S.*², *Schlagel D.L.*⁷, *Lograsso T.A.*⁷, *Banik S.*¹, *Chakrabarty A.*⁸, *Barman S.R.*¹

¹ UGC-DAE Consortium for Scientific Research, Khandwa Road, Indore 452001, India

² School of Physics Bharathidasan University, Tiruchirappalli 620024, India

³ Department of Materials Engineering, Indian Institute of Science, Bangalore 560012, India

⁴ Institut Laue-Langevin, BP 156, 38042 Grenoble Cedex 9, France

⁵ European Synchrotron Radiation Facility, 6 rue Jules Horowitz, F-38000 Grenoble, France

⁶ Forschungsneutronenquelle Heinz Maier-Leibnitz FRM-II, Technische Universität München, Lichtenbergstrasse 1, 85747 Garching bei München, Germany

⁷ Division of Materials Science and Engineering, Ames Laboratory, Ames, Iowa 50011, USA

⁸ Raja Ramanna Centre for Advanced Technology, Indore 452013, India

sanju8419@gmail.com

Magnetic shape memory alloys have emerged as an important class of smart material in recent years because they exhibit interesting physics as well as properties of technological importance such as large magnetic field induced reversible strain, magnetoresistance and magnetocaloric effect. Recently it has been reported that Mn_2NiGa single crystal shows 1.7% magnetic field induced strain (MFIS). [1] Mn_2NiGa has high magnetic transition temperature (588 K) and martensite transition close to room temperature (270 K). The existence of modulation and ferrimagnetism in the martensite phase of Mn_2NiGa have been observed from x-ray and neutron diffraction, respectively.[2,3] In Mn_2NiGa antiferromagnetic coupling between two types of Mn atoms gives rise to interesting physical properties. The spin-valve-like asymmetric magnetoresistance has been observed Mn_2NiGa at room temperature.[3] The asymmetry in magnetoresistance persists down up to 5K. The antisite disorder between Mn and Ga gives rise to the ferromagnetic nano-cluster in the Mn_2NiGa ferrimagnetic matrix which causes asymmetry in magnetoresistance with change in the direction of field. The inverse magnetocaloric effect across martensite transition is also observed in Mn_2NiGa . [4]

[1] G. D. Liu *et al.*, *Appl. Phys. Lett.*, **87** (2005) 262504.

[2] Sanjay Singh *et al.*, *Appl. Phys. Lett.*, **96** (2010) 081904.

[3] Sanjay Singh *et al.*, *Phys. Rev. Lett.*, **109** (2012) 246601.

[4] Sanjay Singh *et al.*, *Appl. Phys. Lett.*, **104** (2014) 051905.

2OR-Q-3

APPLICATION OF FERROMAGNETIC SHAPE MEMORY ALLOYS IN MEMS-NEMS TECHNOLOGY

Irzhak A.V.¹, Dilmieva E.T.², Kamantsev A.P.^{2,4}, Koledov V.V.^{2,4}, Kuchin D.S.², Albertini F.³,
Fabricci S.³, von Gradowski S.V.², Shavrov V.G.²

¹ NUST MISIS, Moscow, Russia

² Kotelnikov Institute of Radio-engineering and Electronics of RAS, Moscow, Russia

³ Instituto dei Materiali per l'Electronica ed il Magnetismo IMEM-CNR, Parma, Italy

⁴ International Laboratory of High Magnetic Field and Low Temperatures, Wroclaw, Poland

shavrov@cplire.ru

Ferromagnetic shape memory alloys (FSMA) represent a new class of materials possessing a unique combination of their mechanical, thermal, magnetic and electric properties. Of special interest is the small scale application of FSMA in MagMEMS because they offer large energy output of $\sim 10^7$ J m⁻³ large compared to that of classical electrodynamic devices having poor scaling of this parameter [1]. Kohl et al. [1] recently gave an analysis of the scaling properties and their influence on the thermo-mechanical and magneto-mechanical coupling effects in Ni-Mn-Ga alloys related to the development of some practical constructions. In the present work we focus our attention on the experimental verification of the magnetic-field-controlled actuation of submicron size elements not demonstrated in the previous studies.

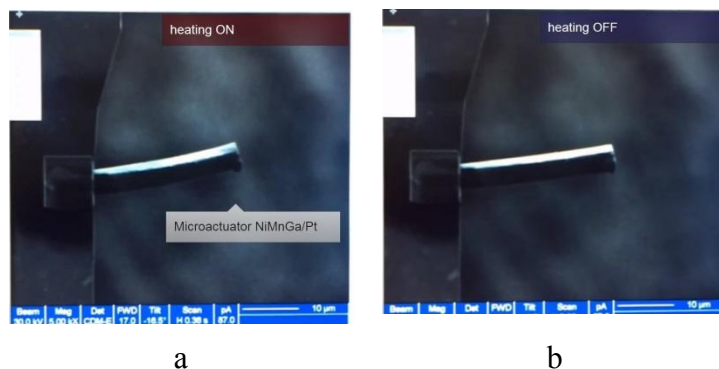


Fig. 1. Composite microactuator based on Ni-Mn-Ga melt-spun ribbon. (a) austenite, (b) martensite state

Melt-spun 30- μ m thick ribbons with nominal composition of Ni₅₃Mn₂₄Ga₂₃ were prepared by melt spinning. Some pieces of ribbons were annealed in vacuum at 800°C for 5 and 72 hours. At room temperature all samples were in the ferromagnetic and martensitic state. Composite NiMnGa/Pt micro-actuators of size 25×2.3×1.7 μ m were prepared. Omniprobe micromanipulator was used to transfer the micro-actuator elements from the surface of the ribbon and to attach them to Si substrates (Fig. 1) by FIB-CVD process (details of composite

technology are given in [2]). The layered composite structure was formed by 900 nm layer of Pt and 800 nm active layer of Ni₅₃Mn₂₄Ga₂₃. The experiments on magnetic actuation have been carried out in a 8 T Bitter coil magnet. The long term relative bending strain controlled by temperature or magnetic field at constant temperature T = 56 °C was found to be 1,2%.

Support by RAS-CNR Joint Research Program, RFBR 12-08-01043, 12-07-00811, 12-07-00676, 12-07-00656, 13-07-12130, CRDF RUP1-7028-MO-11 is acknowledged.

[1] M. Kohl, M. Schmitt, A. Backen, L. Schultz, B. Krevet, S. Fahler, *Appl. Phys. Lett.* **104**, 043111 (2014); doi: 10.1063/1.4863667.

[2] D. Zakharov, G. Lebedev, A. Irzhak et. al., *Smart Mater. Struct.* **21**. № 052001 (2012); doi: 10.1088/0964-1726/21/5/052001.

2OR-Q-4

MAGNETOCALORIC EFFECT IN ALTERNATING MAGNETIC FIELDS UP TO 25 Hz

*Aliev A.M.¹, Batdalov A.B.¹, Gamzatov A.G.¹, Kamilov I.K.¹, Koledov V.V.², Shavrov V.G.²,
Taskaev S.V.³, Buchelnikov V.D.³, Tereshina I.S.⁴*

¹ Amirkhanov Institute of Physics of DSC RAS, 367003 Makhachkala, Russia

² Kotelnikov Institute of Radio Engineering and Electronics of RAS, 125009 Moscow, Russia

³ Chelyabinsk State University, 454001 Chelyabinsk, Russia

⁴ Baikov Institute of Metallurgy and Material Science RAS, 119991 Moscow, Russia

lowtemp@mail.ru

The creation of magnetic refrigerators remains an actual and alluring idea. Today the compact sources of high magnetic fields exist; the alloys with large values of magnetocaloric effect (MCE) are obtained. But an important questions is scarcely explored. The magnetocaloric materials in refrigerators will be affected by external alternating magnetic field. But it is not clear how will the magnetocaloric effect behave under alternating magnetic fields. Whether a magnetocaloric material will have time to exchange energy with surrounding heat exchanger under such conditions?

In this work we present the modulating method of the direct measurement of magnetocaloric effect, alternating magnetic field source, and experimental results of magnetocaloric effect in different materials, including gadolinium, some manganite compositions, and Heusler alloys under alternating magnetic fields up to 25 Hz.

In some of the studied materials no significant dependence of the MCE on frequency of magnetic field change is observed (Fig. 1). In some Heusler alloys and manganite compounds, MCE strongly depends on the frequency of magnetic field changes, and can even vanish at high frequencies (Fig.2).

Possible reasons for the frequency dependence of MCE are discussed. The results show that for the choice of materials for magnetic refrigerators the frequency dependence of MCE should be considered.

This work was supported by the Branch of Physical Sciences of the Russian Academy of Sciences within the framework of the program “Strongly Correlated Electrons in Solids and Structures,” RFBR (Grant Nos. 14-02-01177 and 12-02-96506).

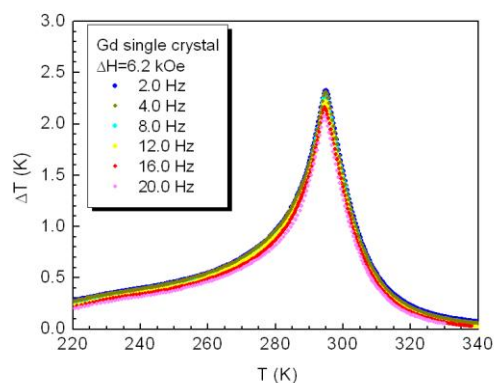


Fig.1. MCE of Gd single crystal in alternating magnetic fields

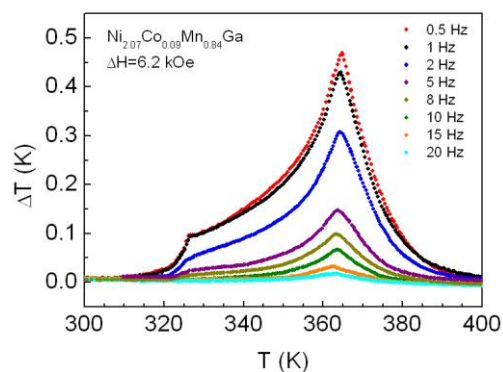


Fig.2. MCE of Ni-Co-Mn-Ga Heusler alloy in alternating magnetic fields

2OR-Q-5

GIANT MAGNETOCALORIC EFFECT OF Gd IN HIGH MAGNETIC FIELDS*Koshkid'ko Yu.S.^{2,3}, Ivanova T.I.^{1,3}, Nikitin S.A.¹, Miller M.³, Rogacki K.³, Cwik J.³*¹ Physics Department of Moscow State University 119992, Moscow, Russian Federation² VŠB-Technical University of Ostrava, Ostrava-Poruba, Czech Republic³ International Laboratory of High Magnetic Fields and Low Temperatures, Wroclaw, Poland

ivanova@phys.msu.ru

It is known that a rare-earth element gadolinium is the most promising material for exploitation as a refrigerant for magnetic refrigerator, because it has a high value of magnetization and Curie temperature near room temperature [1], [2].

Despite a large number of publications on magnetocaloric effect (ΔT) of gadolinium, there is no data on the MCE measurement of Gd in a high static magnetic field.

The aim of our work is:

1. The measurement of the MCE gadolinium by direct method in high magnetic fields. Until now the MCE study of Gd was performed in magnetic fields only up to 9 T. As a result of our work an experimental device has been developed and constructed that allows measurements of the MCE in magnetic fields up to 14 T and in temperature range of 77 K to 350 K by method of input (output) of sample in the magnetic field. We have found that the Gd exhibits a giant value of MCE equal to 19.5 K in field 14 T. The experimental curves of the MCE temperature dependence show maximum near the phase transition (Fig.1).

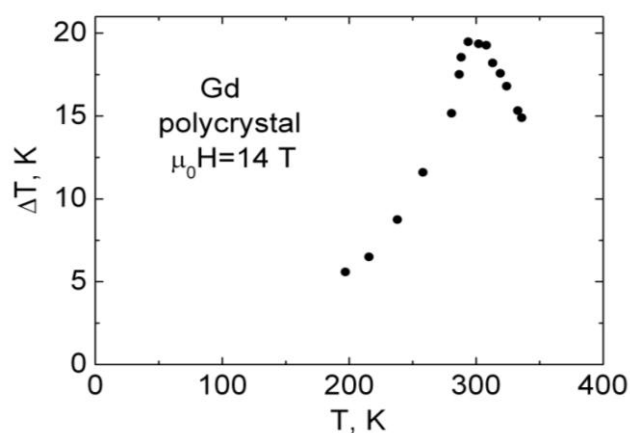


Fig.1. The Gd MCE vs. T in magnetic field 14 T.

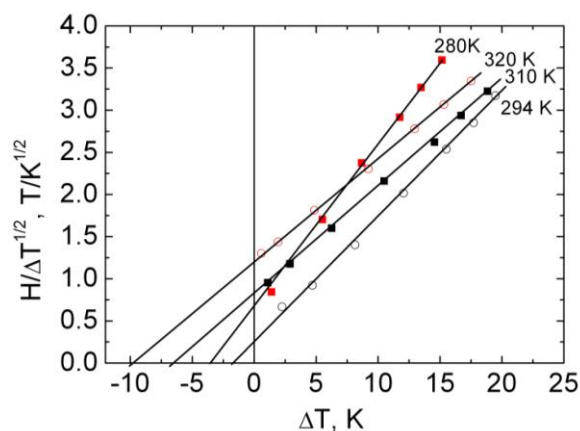


Fig.2. The $H/\Delta T^{1/2}$ vs. ΔT

2. The magnetic field dependencies of MCE gadolinium were obtained in the area of paraprocess near the Curie point. We tried to interpret these experimental curves within the framework of the thermodynamic Landau theory. The magnetic field dependencies of ΔT near Curie point can be described by equations of state follows from Landau thermodynamic. The dependence of the $H/\Delta T^{1/2}$ value vs ΔT is shown in Figure 2. Note that experimental points fall on a straight line. It should be pointed out that thermodynamic Landau theory yields inaccurate results in Curie point, because it does not take into account the effect of spin fluctuations.

Support by RFBR Grant 13-02-90049 and RFBR Grant 13-02-00916 ; CZ.1.07/2.3.00/30.0016 and CZ.1.05/2.1.00/01.0040.

1. A. Tishin and Y. Spichkin, *The Magnetocaloric Effect and its Applications*, Institute of Physics, Bristol (2003).

2. A.S. Andreenko, K.P. Belov, S.A. Nikitin, A.M. Tishin, *Sov. Phys. Usp.*, **32** (1989) 649–664.

2 July

Wednesday

14:30-17:00

oral session

2TL-D

2RP-D

2OR-D

“Magnetoplasmonics”

2TL-D-4

OPTICAL AND MAGNETO-OPTICAL SPECTROSCOPY IN 2D MAGNETOPLASMONIC NANOGRATINGS

Chetvertukhin A.V.¹, Musorin A.I.¹, Grunin A.A.¹, Dolgova T.V.¹, Uchida H.², Inoue M.³,
Fedyanin A.A.¹

¹ Lomonosov Moscow State University, Moscow, Russia
fedyanin@nanolab.phys.msu.ru

² Tohoku Institute of Technology, Sendai, Japan

³ Toyohashi University of Technology, Toyohashi, Japan

Magneto-optical effects can be greatly enhanced in periodic nanostructured materials due to plasmonic, photonic and other resonant effects [1, 2]. One of the modern techniques to observe magnetoplasmonic effects is the use of magnetoplasmonic crystals. Periodic nanostructuring of magnetoplasmonic crystals allows one to control propagation of surface plasmon polaritons (SPP) by the use of diffraction maxima to satisfy fulfill phase-matching for incident light and SPP. 2D-periodicity provides the opportunity of spectral tuning of the phase-matching conditions via superposition of two vectors of the reciprocal lattice. In some materials there is an ability to simultaneously excite two intersecting magnetoplasmons providing opportunity to form a standing plasmonic wave that leads to formation of plasmonic band gap [5]. As local as propagating surface plasmons were used to control the magneto-optical signal of nanoparticles and multilayered structures [3, 4]. In this work, the transversal magneto-optical Kerr effect (TKE) is studied in two-dimensional magnetoplasmonic crystals. Resonant enhancement of the Kerr effect is observed and can be attributed to the resonant excitation and the interaction between magnetoplasmonic modes, waveguide modes and effects that are emerging when diffraction maxima lays into the plane of structure.

The sample is 2D square lattice of Au disks placed on 1-mm-thick quartz substrate. 100-nm-thick Bi:YIG layer covers the structure. The sample is characterized by an atomic force microscopy (Fig.1). The period of the lattices is 600 nm. The Au disks height is about 60 nm and their diameters are about 100 nm. According to vibrating sample magnetometry measurements the saturation field is 1 kOe.

Optical and magneto-optical spectra of the sample were measured at different azimuthal angles and polarizations. There is a distinct correlation between the spectral positions of plasmonic resonances and the resonances in TKE spectra.

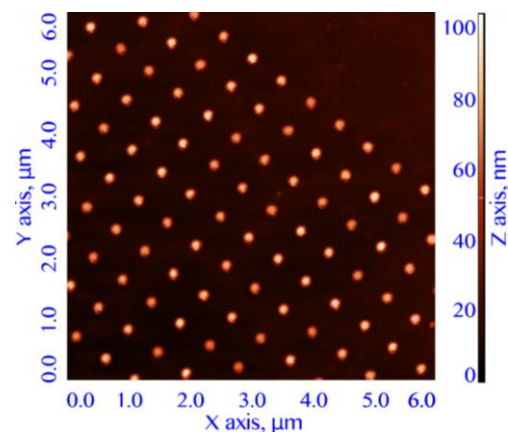


Fig. 1. AFM-image of the 2D magnetoplasmonic nanostructured sample.

- [1] M. Inoue, et al. *J. Phys. D*, **39** R151, (2006).
- [2] V.I. Belotelov et al., *Nature Nanotech*, **6** (2011) 370.
- [3] H. Uchida, et al., *J. Magn. Magn. Mat.*, **321** (2009) 843.
- [4] A.A. Grunin et al., *Appl. Phys. Lett.*, **97** (2010) 261908.
- [5] A.V. Chetvertukin et al., *J. Appl. Phys.*, **113** (2013) 17A942.

2TL-D-5

MAGNETOOPTICAL EFFECTS IN HYBRID PLASMONIC CRYSTALS*Akimov I.A.*^{1,2}, *Kreilkamp L.E.*¹, *Yakovlev D.R.*^{1,2}, *Bayer M.*¹, *Belotelov V.I.*^{3,4,5}, *Zvezdin A.K.*^{4,5,6}¹ Experimentelle Physik 2, Technische Universität Dortmund, 44221 Dortmund, Germany² A.F. Ioffe Physical-Technical Institute, RAS, 194021 St. Petersburg, Russia³ Lomonosov Moscow State University, Leninskie gori, 119991 Moscow, Russia⁴ Russian Quantum Center, 143025 Skolkovo, Moscow Region, Russia⁵ Prokhorov General Physics Institute, RAS, 119991 Moscow, Russia⁶ Moscow Institute of Physics and Technology (State University), 117303 Moscow, Russia

ilja.akimov@tu-dortmund.de

The key object of plasmonics is the surface plasmon polariton (SPP) - the coupled oscillation of the electromagnetic field and the electron plasma in metals. The excitation of a SPP leads to significant electromagnetic energy localization near the metal surface and thereby enhances nonlinear effects and light-matter interaction. Current state-of-the-art criteria in telecommunication require plasmonics to be active, i.e. a possibility for control by means of an external stimulus must be provided in the timescale of several nanoseconds or shorter. This talk presents an overview on experimental studies of magneto-optical intensity effects in plasmonic crystals, which are formed by patterning the noble metal film (gold) with a period comparable to the SPP wavelength. To become relevant for magneto-optics, the plasmonic structure is patterned at the top of ferromagnetic layer of rare-earth iron-garnet (BiIG).

First, it is demonstrated that there is a significant enhancement of transverse magneto-optical Kerr effect (TMOKE) at photon energies close to the resonances corresponding to SPP at the interface between magnetic and metallic layers [1,2]. The application of a magnetic field modifies the permittivity tensor of the magnetic film, which is covered with plasmonic crystal. As the result the propagation constant of SPP at the metal-dielectric interface changes and the resonance experiences the spectral shift. The latter defines the strength of TMOKE, which is proportional to the gyration vector component directed along the slits of the plasmonic crystal. In addition TMOKE magnitude changes its sign for SPPs traveling in opposite directions. A unique property of the transverse Kerr effect in transmission, which makes it different from all the other magneto-optical effects, is that it arises solely from the magnetic film boundary conditions and does not depend on the bulk component. Second, apart from enhancing established magneto-optical effects magneto-plasmonic structures can also be used for investigation of new phenomena. Recently longitudinal magneto-optical effect has been revealed [3]. It describes the influence of longitudinal magnetization on the optical transmission of light in the magneto-photon structure, which comprises the plasmonic crystal at the top of magnetic BiIG waveguiding layer. The magnetization modifies the eigenmodes of the waveguiding layer allowing for excitation of the otherwise "dark" anti-symmetric quasi-TE mode by the TM-polarized illumination. This kind of switching between the "bright" and "dark" modes initiated by external magnetic field is manifested in modification of transmission and reflection spectra in the far field radiation.

[1] V.I. Belotelov et al., *Nature Nanotechnology*, **6** (2011) 370.[2] M. Pohl et al, *New J. Phys.*, **15** (2013) 075024.[3] V.I. Belotelov et al., *Nature Communications*, **4** (2013) 2128.

2RP-D-6

MAGNETIC AND MAGNETOOPTICAL PROPERTIES OF BISMUTH IRON GARNET PREPARED BY MOD TECHNIQUE

Nobuyasu Adachi¹, Kazunari Hayashi¹, Yuusaku Kiba¹, Toshitaka Ota¹

¹ Advanced Ceramics Research Center, Nagoya Institute of Technology, Tajimi, Japan
nadachi@nitech.ac.jp

For the development of the imaging sensor of high frequency electromagnetic field [1] or the application of the spatial light modulator [2], the thermally non-equilibrium $\text{Bi}_3\text{Fe}_5\text{O}_{12}$ films have been investigated. The films were prepared by metal organic decomposition (MOD) technique. The $\text{Bi}_3\text{Fe}_5\text{O}_{12}$ (BIG) films were prepared on GGG single crystal substrate and glass substrate.

From the point of view of industrial application, the substrate using rare earth compounds has an disadvantage. For the crystallization of the BIG films on glass substrate, three kinds of buffer layers (BFL: $\text{Bi}_1\text{Y}_2\text{Fe}_5\text{O}_{12}$, $\text{Bi}_1\text{Nd}_2\text{Fe}_5\text{O}_{12}$ and $\text{Nd}_1\text{Y}_2\text{Fe}_5\text{O}_{12}$) were inserted and the magnetic and magneto-optical properties of BIG/BFL/Glass were compared each other.

The buffer layer with 10 times coating on glass showed the polycrystalline garnet structures. The secondary phase (Fe_2O_3 , YFeO_3 , etc) was also observed in the films. The SEM micrograph shows the smooth surface of the $\text{Nd}_1\text{Y}_2\text{Fe}_5\text{O}_{12}$ film although cracks or dislocations were also observed. Whereas, the crystal grains were observed for the Bi-substituted buffer layers of $\text{Bi}_1\text{Y}_2\text{Fe}_5\text{O}_{12}$, and $\text{Bi}_1\text{Nd}_2\text{Fe}_5\text{O}_{12}$ buffer layer. The Faraday rotations of the BIG films with 10 times coating showed the largest values for the case of $\text{Nd}_1\text{Y}_2\text{Fe}_5\text{O}_{12}$ buffer layer and this value is almost the same as the film on GGG substrate. The lattice parameter of $\text{Nd}_1\text{Y}_2\text{Fe}_5\text{O}_{12}$ is the most close to that of the BIG. Both the small lattice mismatch and the smooth surface of the buffer layer may improve the crystal growth condition of BIG film.

For the another application of magneto-optical spatial light modulator, the BIG and the piezoelectric composite films have been investigated. As the piezoelectric materials, we expect the BiFeO_3 (BFO) materials. This material is famous for the multiferroic materials. By adding the bismuth organic solutions, we prepared the BFO film on glass and GGG substrate. The XRD analysis showed that MOD solutions with the non-stoichiometric composition ratio of Bi to Fe is better to crystallize BFO phase. The crystallizing temperature can be also decreased to 480 degreeC which is the crystallizing temperature of BIG film and we can prepare the BIG and BFO multilayer on GGG substrate at the same growing temperature.

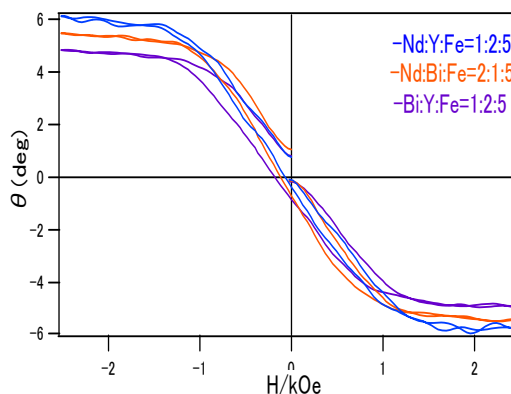


Fig. 1. Faraday rotation @ 635 nm of BIG films on BiYIG, BiNdIG and NdYIG buffer layers on glass substrates.

[1] M. Takahashi, H. Ota, N. Adachi, K. Arai, *IEICE Tech. Rep.*, **106** 2(007) 77-82.

[2] S. Mito, H. Takagi, P. B. Lim, A. V. Baryshev and M. Inoue, *J. Appl. Phys.*, **109** (2011) 07E313.

[3] N. Adachi, K. Yogo, T. Ota, M. Takahashi, K. Ishiyama, *Journal of Applied Physics*, **109**(7) (2011), 07A506/1-07A506/3.

2OR-D-7

NONLINEAR OPTICAL EFFECTS IN Au/GARNET 1D MAGNETOPLASMONIC CRYSTALS

Krut'yanskiy V.L.¹, Chekhov A.L.¹, Stognij A.I.², Murzina T.V.¹

¹ Department of Physics, Moscow State University, Moscow, Russia

² Institute of Solid State and Semiconductor Physics, Minsk, Belarus
chekhov@shg.ru

Optics of the magnetoplasmonic crystals (MPC) have been actively developing in the last decade. This interest is caused by unique properties of such structures, which allow for the resonant enhancement of optical and magneto-optical effects due to the excitation of waveguide modes (WM) and surface plasmon-polaritons (SPP) at the boundary of the magnetic medium. Metal perforated films with a spatial periodicity support the excitation of SPP and WM, which should result in an amplification of optical fields for definite angular-frequency spectral regions. Linear transmission spectra and magnetic response of such structures were reported recently, while the spectroscopy of nonlinear optical and magneto-optical effects has not been studied up to now. In this paper we present the first results on the spectroscopic studies of optical second harmonic generation (SHG) and nonlinear magneto-optical effects in 1D MPC composed of a gold grating on a garnet layer.

The structure under study is the 1D MPC consisting of an array of gold stripes with spatial period of 720 nm deposited on bismuth iron garnet (BIG) film, epitaxially grown on a gallium gadolinium garnet. The thickness of Au and BIG layers was 30 nm and 2 μm , respectively. Such an MPC was shown to support the excitation of three types of modes: two SPP modes on air/Au and Au/BIG interfaces, and WM in the BIG film, the latter two were shown to contribute to an enhancement of the transverse magneto-optical effect up to $4 \cdot 10^{-3}$.

The SHG and nonlinear magneto-optical Kerr effect (NOMOKE) were studied using a femtosecond Ti-sapphire laser tunable in the spectral range from 730 nm to 860 nm, for the angles of incidence from 0° to 15° . Transversal saturating magnetic field was applied along the stripes of the MPC, and the SHG intensity was registered in transmission through the structure.

Fig. 1 shows the SHG intensity and NOMOKE spectra versus the pump wavelength. Three SHG maxima at longer wavelengths correspond to the resonant excitation of the waveguide modes, while the maximum near 775 nm is attributed to the Au/BIG SPP excitation at the fundamental wavelength. The NOMOKE spectrum shows a complicated behavior and changes the sign in the vicinity of the SPP resonance and some of the WMs, the largest NOMOKE value being about 10%. We show that the spectral maxima of SHG intensity and NOMOKE are shifted with respect to each other, which stems probably from complicated resonant shapes of the SHG resonances and from phase relations between different nonlinear contributions to the SHG field under the excitation of various resonant modes in the MPC. A phenomenological model of these effects is discussed.

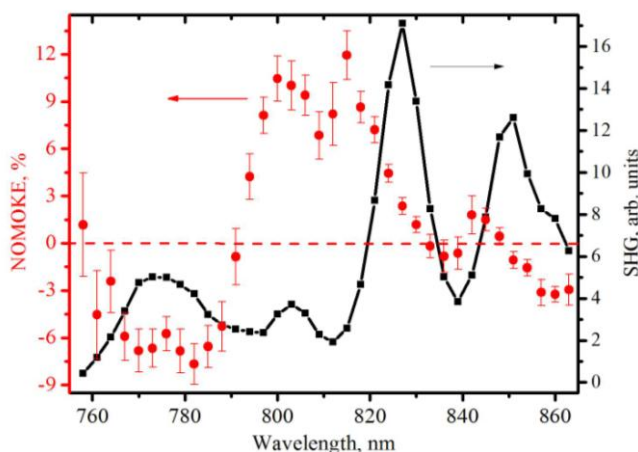


Fig. 1. The SHG (solid) and the NOMOKE (dots) spectra versus the pump wavelength.

MAGNETOOPTICAL DISPLAY CONTROLLED BY DOMAIN WALLS MOTION IN ASYMMETRICAL ANTIDOT GARNET STRUCTURE

Skidanov V.A.¹, Vetoshko P.M.²

¹ Institute for Design Problems in Microelectronics RAS, Moscow, Russia

² Kotel'nikov Institute of Radio Engineering and Electronics RAS, Moscow, Russia

skidanov@zelnet.ru

Bi-substituted epitaxial garnet films with uniaxial anisotropy and high Faraday rotation are expected for years to be used for spatial light modulator (MOSLM) development. Two basic problems were met: 1) high pixel switching field and 2) wide spread of switching field values in a pixel array [1,2]. It was shown previously [3] that bridge between two garnet half-planes with opposite directions of magnetization demonstrates rectangular hysteresis loop with reproducible switching field H_c . H_c can be controlled by garnet magnetization M , film thickness h and the shape of the pixel in film plane. Its value is defined by magnetostatic barrier formed by inhomogeneous stray field of garnet film edges for single straight domain wall (DW) inside bridge. On the contrary to DW repulsion from edges in quadratic element DW inside bridge suffers increasing attraction from nearest half-plane edge when shifted from bridge centre. Traditional quadratic element with single DW is magnetized by reversible manner and can't be used for MOSLM matrix whereas bridge is magnetized irreversibly and maintains one of two saturated states in zero external field. H_c is inversely proportional to bridge width.

Antidot-like structure was etched in garnet film to fabricate an array of bridges. Vertical and horizontal garnet stripes were made with different widths (15 and 40 μm). Wider stripe parts serve as matrix pixels. Matrix columns are separated by narrow stripes. Rows are separated by hollows in garnet.

Array of seeds with reverse magnetization was formed in a chess desk order in initially monodomain structure. Seeds occupy crossings between wide and narrow strips as shown in upper photo in Fig. 1. Different stripe widths are used to prevent switching by DW motion in vertical direction in array. Garnet magnetization is $4\pi M = 50$ G, film thickness is $h = 3$ μm . Switching amplitude of external magnetic field $H_c = 1.5$ Oe was achieved for DW jumping in horizontal direction. The spread of switching field values between pixels does not exceed $\Delta H_c \sim 0.3$ Oe.

DW moves with saturated speed ~ 1 m/s in external field $H \geq H_c$ so that MOSLM consisted of 10 μm long bridges can operate at ~ 100 kHz.

[1] J.H. Park, J.H. Kim, J.K. Cho, K. Nishimura, H. Uchida, M. Inoue, *JMMM* **272-276** (2004) 2260-2262.

[2] J.H. Park, H. Takagi, D. H. Lee and J. K. Cho, K. Nishimura, H. Uchida and M. Inoue, *J. Appl. Phys.*, **93** (2003) 8522-8525.

[3] V. Skidanov, P. Vetoshko, A. Stempkovskiy. *J. of Phys.: Conf. Series*, **266** (2011) 012125.

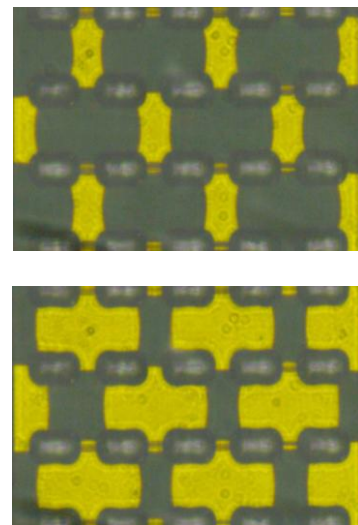


Fig. 1. Microphotographs of two stable states of magneto-optical pixels in antidot structure in external field: upper $H = -1.5$ Oe, lower $H = +1.5$ Oe.

2RP-D-9

ONE-DIMENSIONAL PHOTONIC-MAGNONIC CRYSTALS*Klos J.W.¹, Krawczyk Y.¹, Dadoenkova Yu.S.², Dadoenkova N.N.², Lyubchanskii I.L.^{2,3}*¹ Faculty of Physics, Adam Mickiewicz University, Poznan, Poland² Donetsk Physical and Technical Institute of the National Academy of Sciences of Ukraine,
Donetsk, Ukraine³ Faculty of Physics and Technology, Donetsk National University, Donetsk, Ukraine

We investigate the properties of a photonic-magnonic crystal, a complex multifunctional one-dimensional structure with magnonic and photonic band gaps in the GHz and PHz frequency ranges for spin waves and light, respectively. The system consists of periodically distributed dielectric magnetic slabs of yttrium iron garnet and nonmagnetic spacers with an internal structure of alternating TiO₂ and SiO₂ layers which form finite-size dielectric photonic crystals. We show that the spin-wave coupling between the magnetic layers, and thus the formation of the magnonic band structure, necessitates a nonzero in-plane component of the spin-wave wave vector. A more complex structure perceived by light is evidenced by the photonic miniband structure and the transmission spectra in which we have observed transmission peaks related to the repetition of the magnetic slabs in the frequency ranges corresponding to the photonic band gaps of the TiO₂/SiO₂ stack. Moreover, we show that these modes split to very high sharp (a few THz wide) subpeaks in the transmittance spectra. The proposed novel multifunctional artificial crystals can have interesting applications and be used for creating common resonant cavities for spin waves and light to enhance the mutual influence between them [1].

[1] J.W. Klos, M. Krawczyk, Yu.S. Dadoenkova, N.N. Dadoenkova and I.L. Lyubchanskii, *J. Appl. Phys.*, **115** (2014) 174311.

2RP-D-10

GIANT MAGNETOTRANSMISSION AND MAGNETOREFLECTION IN FERROMAGNETIC MATERIALS

Telegin A.V.¹, Sukhorukov Yu.P.¹, Loshkareva N.N.¹, Mostovshchikova E.V.¹, Bebenin N.G.¹, Gan'shina E.A.², Granovsky A.B.²

¹ Institute of Metal Physics UD of RAS, 620990, Ekaterinburg, Russia

² Moscow State University, 119991, Moscow, Russia

telegin@imp.uran.ru

In this report, we review our last experimental results on the giant magnetotransmission and magnetoreflexion in the ferromagnetic single-crystalline semiconductors $\text{Hg}_{1-x}\text{Cd}_x\text{Cr}_2\text{Se}_4$ ($0 \leq x \leq 1$) [1-4], the single crystals of the ferromagnetic rare earth manganites $\text{A}_x\text{B}_{1-x}\text{MnO}_3$ ($\text{A}=\text{La}, \text{Pr}; \text{B}=\text{Ca}, \text{Sr}, \text{Ba}, \text{Ag}, \text{Na}, \text{K}$) with perovskite structure [5-9], thin films and heterostructures on the base of the manganites. We studied magnetic properties, resistivity, magnetoresistance, transverse Kerr effect, optical properties for the same samples in a wide temperature range. The reflectance and transmittance of the unpolarized light were measured in magnetic fields of up to $H=4$ kOe applied parallel to the sample surface and up to $H=8$ kOe applied perpendicular to the sample surface, respectively.

The magnetoreflexion and magnetoreflection effects are nongyrotropic and in the infrared range are due to the optical response to magnetoresistance, their absolute values in manganites exceed significantly the linear magneto-optical Faraday and Kerr effects in a wide spectral range from middle infrared to ultraviolet. Besides, the resonance-like contribution to the magnetoreflexion spectra of manganite films has been observed in the vicinity of the phonon bands

It is demonstrated how the effects can be used for studying the process of phase separation, i.e. the co-existence of regions with different magnetic and resistivity properties [5, 6]. The possible applications [10-14] of the effects investigated are also discussed.

The work was supported by Russian government grant № 2013-220-04-350; RFBR grant 13-02-00007 and grant of Presidium of RAS № 12-P-2-1034.

- [1] Yu.P. Sukhorukov, A.V. Telegin, N.G. Bebenin, et al., *JETP Letters*, **98** (2013) 313-316.
- [2] M. Auslender, E.V. Barsukova, N.G. Bebenin, et al., *Sov. Phys. JETP*, **68** (1989) 139-142.
- [3] M.I. Auslender, N.G. Bebenin, *Sol. State Commun.*, **69**(7) (1989) 761.
- [4] N.N. Loshkareva, Yu.P. Sukhorukov, et al., *Fiz. Nizk. Temp.*, **18**(S1) (1992) 127-130.
- [5] A. Granovsky, Yu. Sukhorukov, E. Gan'shina, A. Telegin., In book «Magnetophotonics: From Theory to Applications», Springer, Berlin, New-York, (2013) 580.
- [6] E. Gan'shina, N. Loshkareva, Yu. Sukhorukov, et al., *JMMM*, **300** (2006) 62-66.
- [7] E.V. Mostovshchikova, N.N. Loshkareva, et al., *J. Appl. Phys.*, **113** (2013) 043503.
- [8] Yu.P. Sukhorukov, et al., *J. Spintronics and Magn. Nanomaterials*, **1** (2012) 139-146.
- [9] Yu.P. Sukhorukov, et al., *Phys. Met. and Metallography*, **107** (2009) 579-587.
- [10] Yu.P. Sukhorukov, et al., *Patent of RF № RU2346315*, **4** (10.02.2009).
- [11] Yu.P. Sukhorukov, et al., *Patent of RF № RU2439637*, **1** (10.01.2012).
- [12] A.V. Telegin, et al., *Patent of RF № RU2497166*, **30**, (27.10.2013).
- [13] E.V. Mostovshchikova, et al., *Patent of RF № RU129665*, **18**, (27.06.2013).
- [14] Yu.P. Sukhorukov, et al., *Patent of RF № RU88165*, **30**, (27.10.2009).

2OR-D-11

MAGNETO-OPTICAL SENSORS BASED ON MAGNETOPLASMONIC CRYSTALS

Grunin A.A.¹, Mykha I.R.¹, Chetvertukhin A.V.¹, Fedyanin A.A.¹

¹Lomonosov Moscow State University, Moscow, Russia

grunin@nanolab.phys.msu.ru

Commonly level magneto-optical (MO) effects is small and does not allow them to be used for various applications. In recent years several topics of magnetophotonic researches were targeted on study of new magnetophotonic materials with enhanced MO properties. One of these is magnetoplasmons crystals which can demonstrate simultaneously both increased MO effects and the excitation of surface plasmon-polaritons (SPP). The enhancement of MO effects in this case appears due to dependence of SPP dispersion law on the magnetization. On the other hand one of the main traditional applications of SPP resonance is biosensors and optical sensors based on SPP. Magnetoplasmonic crystals allow to excite SPP without of additional optical schemes that makes them attractive for optical sensors. Another feature of the magnetoplasmonic crystals in the optical sensors application is the ability to detect changes in the refractive index not only by optical response but also by the MO response in SPP resonance area. This is possible due to the strongly resonant spectral dependence of MO in vicinity of SPP resonance. Recently in the number of papers [1-3] was shown that the using of MO detection method with excitation of SPP in Kretschmann scheme can increase the sensitivity and resolution of the optical sensors in several times. The approach presented in this paper combine the advantages of the MO response detection method in transversal configuration and convenience of SPP excitation in magnetoplasmonic crystals. The optical and MO properties of silver/iron based magnetoplasmonic crystals were studied in the context of sensors application. The possibility of detection of refractive index changes in real time mode using MO method and magnetoplasmonic crystals was experimentally studied and these results are shown in comparison with traditional optical method in Fig.1.

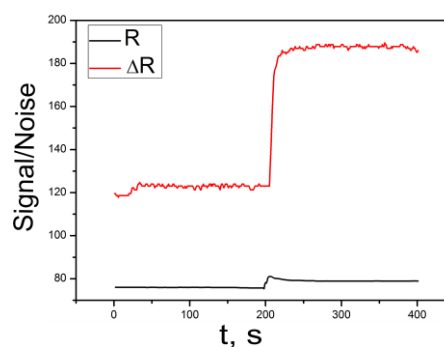


Fig1. Comparison of the signal/noise ratios for the two methods of detection (R - for optical, ΔR - for MO methods) in real time regime

- [1] B. Sepulveda, A. Calle, L. M. Lechuga, G. Armelles, *Opt. Lett.*, **31** (2006) 1085–1087.
- [2] D. Regatos, D. Farina, A. Calle, A. Cebollada, B. Sepulveda, G. Armelles, L. M., *J. Appl. Phys.*, **108** (2010) 054502–054502.
- [3] M.G. Manera, et al., *J. Mater. Chem.*, **21** (2011) 16049–16056.

2 July

Wednesday

14:30-17:00

oral session

2TL-E

2OR-E

**“High Frequency
Properties and
Metamaterials”**

2TL-E-5

EVOLUTION OF UNDERSTANDING OF COUPLING MECHANISMS IN MAGNETIC METAMATERIALS

*Radkovskaya A.A.*¹

¹ M.V. Lomonosov Moscow State University, Faculty of Physics, Moscow, Russia
a_radkovskaya@mail.ru

Magnetic metamaterials usually consist of small resonant elements of circular shape called meta-atoms with strong magnetic response to the electromagnetic waves. An advantage over naturally occurring materials is that it is possible to design electromagnetic properties of metamaterials by choosing the shape of the constituent elements and the way they are arranged within the structure. Interestingly, metamaterials comprising the same type of elements can exhibit quite different properties. The reason is the inter-element coupling which can affect the effective parameters of metamaterials by giving rise to slow waves. The coupling mechanisms in magnetic metamaterials operating at MHz, GHz and THz frequencies differ quite dramatically. Slow waves propagating in metamaterials by virtue of inter-element coupling were introduced in 2002 under the name of magnetoinductive (MI) waves, the name which emphasized the mechanism of coupling via magnetic inductance in structures comprising capacitively loaded loops of cm diameter in the MHz frequency range [1,2]. Depending on the mutual orientation of the elements, the coupling coefficient can be positive or negative resulting in forward or backward MI waves. At higher frequencies coupling between split ring resonators can have both a magnetic and an electric part. The magnetic coupling of two elements occurs as the ac current flowing in an element induces a magnetic field which threads the neighboring element and excites a current in it. Similarly, the electric coupling is due to the ac charge distribution in the first element inducing an electric field which results in a charge distribution in the second element. Generally, both electric and magnetic coupling constants can be complex due to the retardation effects. Even if retardation is negligible, the coupling anisotropy means that both the relative position and the orientation of the elements strongly influence the value and the sign of the coupling [3,4]. At THz frequencies another dramatic change in coupling mechanisms comes to light: the coupling coefficients become strongly affected by the kinetic inductance due to electron's inertia [4].

This talk provides an overview of advances in understanding coupling mechanisms between "meta-atoms" in magnetic metamaterials covering a wide frequency range from low frequencies up to the visible range.

- [1] E. Shamonina, V.A. Kalinin, K.H. Ringhofer, L. Solymar, *J. Appl. Phys.*, **92** (2002) 6252-6261.
- [2] L. Solymar, E. Shamonina, *Waves in Metamaterials*, Oxford University Press, Oxford, 2009.
- [3] E. Tatartschuk, N. Gneiding, F. Hesmer, A. Radkovskaya, and E. Shamonina, *J. Appl. Phys.*, **111** (2012) 094904-1-9.
- [4] A.A. Radkovskaya, G.S. Pal'vanova, E.I. Lebedeva, V.N. Prudnikov, O.A. Kotel'nikova, P.N. Zakharov, A.F. Korolev, A.P. Sukhorukov, *Bulletin of the Russian Academy of Sciences: Physics*, **77** (2013) 1401-1406.

2OR-E-6

MAGNETOINDUCTIVE WAVES IN METAMATERIALS WITH STRONG INTER-ELEMENT COUPLING IN MHz RANGE

Radkovskaya A.A.¹, Palvanova G.S.¹, Prudnikov V.N.¹, Kotelnikova O.A.¹, Petrov P.S.¹, Zakharov P.N.¹, Korolev A.F.¹, Sukhorukov A.P.¹

¹ M. V. Lomonosov Moscow State University, Faculty of Physics, Moscow, Russia
anna@magn.ru

Magnetic metamaterials (MM) consist of "meta-atoms" such as split-ring resonators (SRRs) exhibiting a strong magnetic response. Their electromagnetic properties are strongly affected by the inter-element coupling which gives rise to slow magnetoinductive (MI) waves [1]. One of practical applications of MI waves is a low-loss waveguide capable of guiding signals on a subwavelength scale [2]. To keep the insertion loss low, the elements comprising the MI waveguide have to be closely packed, resulting in strong interactions between remote elements [3,4].

In this paper we study experimentally how the dispersion of MI waves in axial magnetic metamaterials is affected by structure parameters and coupling coefficients.

We use a set of identical capacitively-loaded SRRs (23 mm in diameter) with the resonant frequency $f_0=50.22$ MHz. The coupling coefficient κ is varying in a wide range from 0.1 to 1 depending on the distance between meta-atoms. We show that, depending on the density of SRRs, not only nearest-neighbour interactions but also interactions between remote elements (2nd order coupling, 3rd order coupling etc.) have to be taken into account. Figure 1 shows the variation of the MI passband width, $\delta\omega$, with the coupling coefficient κ . An analytical model including only nearest neighbour interactions predicts the passband width increasing unrealistically fast with the coupling strength, whereas incorporation of also the 2nd order interactions results in an unrealistically narrow passband. However, taking interactions up to the 3rd order yields a good agreement with the experimental data.

We conclude that although reducing the distance between elements results in smaller insertion losses, in order to be able to correctly describe properties of MI waveguides higher order interaction have to be included in the model, thus enabling accurate design of metamaterials with desired properties.

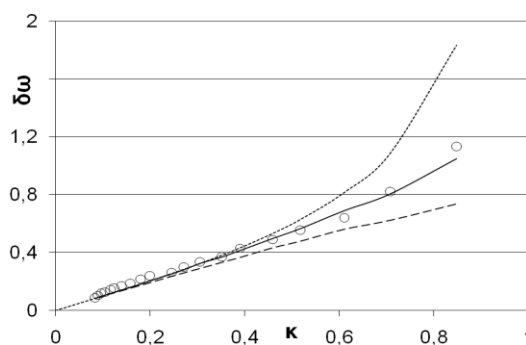


Fig. 1. Normalized to ω_0 passband width of MI waves $\delta\omega$ vs. coupling coefficient κ . Circles: experimental data. Curves: analytical results including coupling for nearest neighbours only (dotted), up to next nearest neighbours (dashed) and up to 3rd order coupling (solid).

- [1] L.Solymar, E.Shamonina, *Waves in Metamaterials*, Oxford University Press, Oxford (2009).
- [2] R.A. Syms, I.R. Young, L. Solymar, *J. Phys. D: Appl. Phys.*, **39** (2006) 3945–3951.
- [3] O. Sydoruk., A. Radkovskaya, O. Zhuromskyy, E. Shamonina, M. Shamonin, C. Stevens, D.J. Edwards, G. Faulkner, L. Solymar, *Phys. Rev. B*, **73** (2006) 224406–1–12.
- [4] R.A. Syms, O.Sydoruk, E. Shamonina, L. Solymar, *Metamaterials*, **1** (2007) 44–51.

2TL-E-7

RADIATIVE PROPERTIES OF METAMATERIAL DIMERS*Shamonina E.¹, Radkovskaya A.², Solymar L.³*¹ University of Oxford, Department of Engineering Science, Oxford, UK² M.V. Lomonosov Moscow State University, Faculty of Physics, Moscow, Russia³ Imperial College London, EEE Department, London, UK

ekaterina.shamonina@eng.ox.ac.uk

In this talk we review our recent progress in achieving superdirectivity in subwavelength metamaterial structures with inter-element coupling. In the traditional approach, sharp radiation patterns from phased dipole-antenna linear arrays result from constructive interference with radiation produced by the elements of the array adding up in phase in the selected direction; the maximum end-fire directivity achievable increases with the number of elements N as $D=1.5N$; the optimum inter-element distance being around half-wavelength means large structure sizes. However, if the structure is required to be small, then the advantage of using many elements in the array ceases. The solution is offered by the so-called superdirective arrays, based on the opposite physical principle of destructive interference. The radiation produced by individual elements has to cancel out in all directions but cancels out least in the chosen direction. The maximum end-fire directivity achievable increases with the number of elements as N^2 as the separation between the elements tends to zero, offering a noticeable advantage already for 2 elements. The practical challenge is to impose a rapidly varying current distribution required for destructive interference. For a dimer of two dipole antennas the currents have to be almost in anti-phase [1].

Following our previous studies [4] which have demonstrated that magnetically coupled dimers of split rings can produce superdirective patterns, we extend in this paper our analysis to electric coupling [5]. The physical mechanism is propagation of slow waves (magneto-inductive or electro-inductive) on arrays of meta-atoms by virtue of coupling [2,3], which offer a possibility to impose rapidly varying current distribution required for superdirectivity. We deduce rigorous analytical conditions for achieving superdirectivity in terms of structure parameters (the distances between meta-atoms, their quality factors and impedances, and the values of the mutual coupling), and demonstrate that the maximum directivity of $D=5.3$ is achievable at frequencies in the vicinity of the antisymmetric mode of the coupled dimer. We verify our predictions numerically and experimentally thus proposing a number of practically feasible designs. Our results might pave the way to the first realization of genuine superdirective metamaterials.

Financial support by the DFG is gratefully acknowledged.

- [1] E. Shamonina, K.H. Ringhofer, L. Solymar, *AEÜ: Int. J. Electron. Comm.*, **56** (2002) 115-119.
- [2] E. Shamonina, V.A. Kalinin, K.H. Ringhofer, L. Solymar, *J. Appl. Phys.*, **92** (2002) 6252-6261.
- [3] L. Solymar, E. Shamonina, *Waves in Metamaterials*, Oxford University Press, Oxford, 2009.
- [4] E. Shamonina and L. Solymar, Abstracts of 7th Int. Cong. on Advanced Electromagnetic Metamaterials in Microwaves and Optics, Sept. 16-21, Bordeaux, France (2013).
- [5] A.A. Radkovskaya, G.S. Pal'vanova, E.I. Lebedeva, V.N. Prudnikov, O.A. Kotel'nikova, P.N. Zakharov, A.F. Korolev, A.P. Sukhorukov, *Bulletin of the Russian Academy of Sciences: Physics*, **77** (2013) 1401-1406.

2TL-E-8

ANALYSIS OF TRANSMISSION LINES LOADED WITH PAIRS OF COUPLED RESONANT ELEMENTS AND APPLICATION TO SENSORS

Naqui J.¹, Su L.¹, Mata J.¹, Martín F.¹

¹ GEMMA/CIMITEC, Departament d'Enginyeria Electrònica, Universitat Autònoma de Barcelona, 08193 Bellaterra (Barcelona), Spain
Ferran.Martin@uab.es

This paper is focused on the analysis of transmission lines loaded with pairs of coupled resonators. We have considered two different structures: (i) a microstrip line loaded with pairs of stepped impedance resonators (SIRs), and (ii) a coplanar waveguide (CPW) transmission line loaded with pairs of split ring resonators (SRRs). It is found that, as compared to lines loaded with single resonators, the considered lines (loaded with coupled resonator pairs) exhibit a different fundamental resonant frequency. This also occurs when the resonators are different (asymmetric structure), namely, the resulting resonance frequencies are different than those corresponding to the individual resonators (that coincide with the resonance frequencies of lines loaded with uncoupled resonators). In spite that the considered lines and loading resonators are very different and are described by different lumped element equivalent circuit models, the phenomenology associated to the effects of coupling is exactly the same, and the resonance frequencies are given by analogue expressions.

As an example, Fig. 1 shows three microstrip lines loaded with pairs of shunt connected SIRs. The structure of Fig. 1(a) is symmetric, whereas the other structures (b) and (c) are obtained from the original structure by increasing or decreasing the capacitive patch of one of the SIRs, as indicated. Fig. 2 compares the frequency response of the structures of Fig. 1 with those of Fig. 1 with only one SIR. As can be seen the above mentioned phenomenology arises.

These structures are of potential interest in microwave sensors/comparators based on symmetry properties [1] because a small level of asymmetry causes significant split in the resonance frequencies.

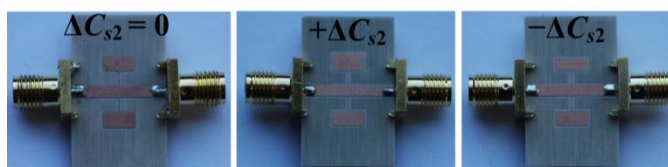


Fig. 1. Microstrip line loaded with (a) a symmetric SIR pair, (b,c) asymmetric SIR pairs.

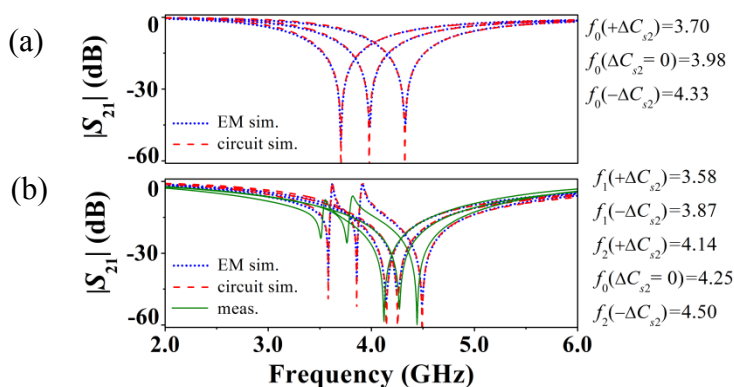


Fig. 2. Frequency responses. (a) with one SIR; (b) with two SIRs.

[1] J. Naqui *et al.* *IEEE Int. Microwave Symposium (IMS 2014)*, accepted.

2OR-E-9

NON-DIPOLE INTERACTION OF INCLUSIONS IN METAMATERIALS WITH ARTIFICIAL MAGNETISM

Starostenko S.N.¹, Rozanov K.N.¹

¹ ITAE RAS, Moscow, Russia

To develop a metamaterial for microwave applications one needs to optimise the shape and concentration of artificial inclusions. We concentrate on vitreous (unordered) metamaterials with inclusions with ring conductivity (spirals) that display artificial magnetism. The research aim is to analyse a relation between the shape of a spiral inclusion (a self-capacity loaded resonant coil [1]) and the magnetic and reflectivity responses of a composite layer filled with these inclusions.

In case of a composite filled with permeable particles, the magnetic response monotonously increases with volume fraction of these particles, while the spiral inclusions display mutual inductance that decreases the magnetic response of neighbouring inclusions. The mutual inductance increases with filling factor making the concentration dependence of the magnetic response of metamaterial more complicated. To study this dependence we use the calculation technique based on 1) Maxwell's solution for inductance of neighbouring loops; 2) Wheeler's approximation for Lorenz formula for loop or cylindrical solenoid inductivity [1]; and 3) calculations of magnetic susceptibility of a conductive ellipsoid [2]. Experimental technique is based on 1) measurements of near-field transmission gain between coils at frequencies below 100MHz; 2) microwave magnetic response of a coil (similar to [3]) and assembly of coils, and 3) reflectivity response of model metamaterials.

Studying the frequency dependence of magnetic response of a system of coils on a single permeable core we optimise the coil parameters (wiring and coil shape) taking into account the interaction between coils (intercoil distance) and develop a metamaterial cord that can be applied to improve electromagnetic compatibility for example.

The reflectivity response (Fig.1) of model metamaterial is measured with several $\sim 0.5 \times 5 \times 40$ mm laminated cores placed on a metal surface; each core has 2 symmetrically wound short coils. The combined inclusions (cores with coils) cover about 25% of metal surface.

The solid black curve corresponds to the optimal positioning of spiral inclusions on the cores. The dashed lines illustrate the performance deterioration due to non-dipole interaction of artificial inclusions if the coil concentration is higher or lower than the optimal one. The light-gray curve corresponds to the performance of metamaterial made of the same permeable core (laminates of 0.2mm-thick permalloy films) without the spiral coils. As the absorbing layer is electrically thin (~ 0.5 mm with wiring), the reflectivity response is proportional to the shape of absorption line of artificial permeability.

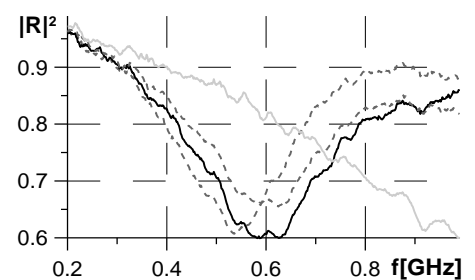


Fig.1

Support by RFBR grants No 13-08-12112 and No 12-08-00954 is acknowledged.

[1] Knight D.W., *An introduction to the art of Solenoid Inductance Calculation*, (2012-2013).

<http://www.g3ynh.info/>

[2] K.S, Lee, *Dikewood Corp.report, L-A* (1974).

[3] O. Acher, Permeability enhancement of soft magnetic films through metamaterial structures, *J. Magn. Magn. Mater.*, **320-23** (2008) 3276-3281.

2TL-E-10

THz POLARIZATION CONTROL USING CHIRAL METAMATERIALS

Kafesaki M.¹, Kenanakis G.¹, Economou E.N.¹, Soukoulis C.M.¹

¹ Foundation for Research and Technology Hellas (FORTH), Heraklion, Crete, Greece, and
University of Crete, Greece
kafesaki@iesl.forth.gr

The design and development of THz metamaterials, which will enable the realization of a variety of THz optical components, is becoming recently a task of continuously increasing attention. This is due to the fact that the majority of natural materials do not show strong response in the THz radiation, and thus they are not offered for the realization of THz manipulation components, along with the large technological importance of the THz radiation, especially in domains like imaging, security and sensing.

THz chiral metamaterials, due to their strong chiral response exceeding that of natural chiral materials by several orders of magnitude, can offer unique capabilities in the control of the THz wave polarization, enabling the realization of a variety of polarization control components, including polarization filters, wave-plates, polarizers, etc.

In this talk we will review our recent work on THz chiral metamaterials. In particular we will discuss a variety of THz chiral structures which show very large optical activity, circular dichroism and negative refractive index response for both left and right-handed circularly polarized waves. The structures are planar, fabricated on flexible substrates, and their basic element is a pair of conductors mutually twisted, as shown in Fig. 1, as to give the chiral response.

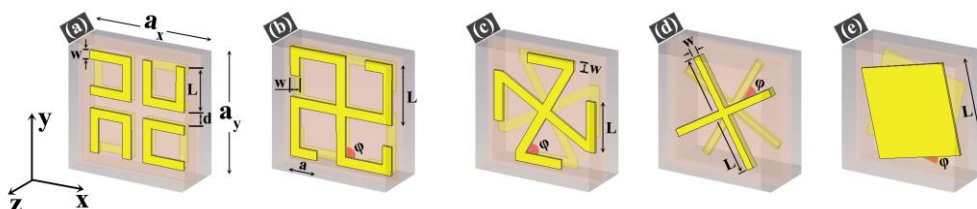


Fig. 1. Schematic of the unit cell of the main chiral metamaterials under consideration: (a) two relatively rotated layers of four U-shaped split-ring-resonators, (b) and (c) two relatively rotated layers of Z-type crosses with $\varphi=90^\circ$ and $\varphi=60^\circ$, respectively, (d) two relatively rotated layers of cross-wires and (e) design based on two relatively rotated squares. The metal is indicated by the yellow-color and the dielectric substrate and superstrate by light-grey.

Moreover, introducing properly in specific parts of the structures photoconducting Si, which can be transformed from an insulating to a conducting state upon illumination, we demonstrate the realization of switchable and tunable chiral response, which will enable a variety of active THz polarization control components, like switchable polarizers, polarization modulators etc.

2 July

Wednesday

14:30-17:00

oral session

2TL-O

2OR-O

**“Low Dimensional
Magnetism”**

2TL-O-5

NEUTRON SCATTERING STUDIES OF SPIN CHAINS AND LADDERS*Lake B.¹, Notbohm S.¹, Tennant D.A.^{1,2}, Caux J.-S.³, Tsvelik A.M.⁴, Barthel T.⁵, Schollwöck U.⁵,
Frost C.D.⁶, Perring T.G.⁶, Sekar C.⁷, Krabbes G.⁷, Büchner B.⁷*¹ Helmholtz Zentrum Berlin für Materialien und Energie, Berlin, Germany² Oak Ridge National Laboratory, Oak Ridge, U.S.A.³ University of Amsterdam, Amsterdam, The Netherlands⁴ Brookhaven National Laboratory, U.S.A.⁵ Ludwig-Maximilians-University, Munich, Germany⁶ ISIS Facility, Rutherford Appleton Laboratory, Chilton, U.K.⁷ Leibniz-Institut für Solid State and Material Research, IFW-Dresden, Germany
Bella.lake@helmholtz-berlin.de

Quantum magnetism studies the behaviour of magnetic materials where quantum fluctuations are strong and give rise to exotic ground states and unusual excitations that are not found in conventional magnets. It is possible to make model materials engineered to exhibit specific quantum features which can then be investigated using neutron scattering. This presentation will discuss a number of different quantum magnets.

An example is the one-dimensional, spin-1/2, Heisenberg antiferromagnet which lies at the Luttinger Liquid quantum critical point where quantum fluctuations prevent the development of long-range magnetic order. The excitations are known as spinons and have fractional spin quantum number $S=1/2$ and thus must be created in multiple pairs which are observed as a spinon continuum. Although this problem was first tackled in 1931 it has only recently been solved theoretically for zero temperature using integrability-based methods and at finite temperature using DMRG calculations. We have verified the accuracy of these solutions by comparison to experimental data from the compound KCuF_3 [1]. Small perturbations from the ideal spin-1/2, Heisenberg antiferromagnetic chain lead to departures from this behavior. An example is the spin-ladder which consists of two parallel antiferromagnetic spin-1/2 chains which form the legs of the ladder, that are coupled to each other via the rungs of the ladder. Strong rung coupling completely alters the spectrum from that of the chain and the fundamental excitations are magnons rather than spinons which have an integer spin quantum number of $S=1$, as observed in $\text{La}_4\text{Sr}_{10}\text{Cu}_{24}\text{O}_{41}$. On the other hand in the case of weak rung coupling the fundamental excitations remain spinons. At low energies the spinons are bound while at high energies they are still free. An example is CaCu_2O_3 where the additional perturbation of ring exchange drives the system gapless and our work shows that it CaCu_2O_3 close to the Wess-Zumino-Novikov-Witten quantum critical point [2].

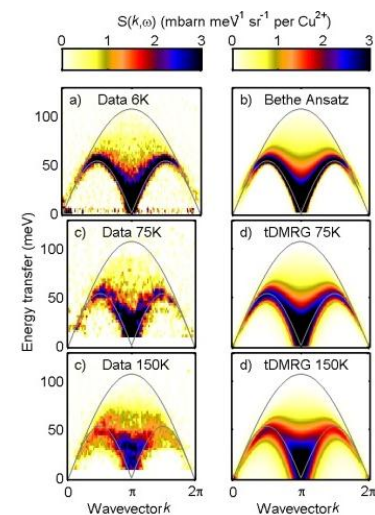


Fig. 1. Spinon continuum of KCuF_3 at various temperatures compared to theory.

[1] B. Lake, D.A. Tennant, J.-S. Caux, T. Barthel, U. Schollwöck, S.E. Nagler, C.D. Frost, *Phys. Rev. Lett.*, **111** (2013) 137205.

[2] B. Lake, A.M. Tsvelik, S. Notbohm, D.A. Tennant, T.G. Perring, M. Reehuis, C. Sekar, G. Krabbes, B. Büchner. *Nature Physics*, **6** (2010) 50-55.

2TL-O-6

RECENT RESULTS FROM THE HIGH MAGNETIC FIELD LABORATORY DRESDEN: PROBING THE 1D OR 2D NATURE OF $M^{2+}Ta_2O_6$ ($M^{2+}=Ni,Co$)

Law J.M.¹, Koo H.-J.², Whangbo M.-H.³, Pomjakushin V.⁴, Kremer R.K.⁵

¹ Dresden High Magnetic Field Laboratory (HLD), Helmholtz-Zentrum Dresden-Rossendorf, D-01314 Dresden, Germany

² Department of Chemistry and Research Institute of Basic Science, Kyung Hee University, Seoul 130-701, Korea

³ Department of Chemistry, North Carolina State University, Raleigh, North Carolina, U.S.A.

⁴ Laboratory for Neutron Scattering, Paul Scherrer Institut, CH-5232 Villigen, Switzerland

⁵ Max-Planck-Institut für Festkörperforschung, Heisenbergstr. 1, D-70569 Stuttgart, Germany
j.law@hzdr.de

Herein, we present recent advances at the high magnetic field laboratory, with relevance to probing the spin exchange interactions of $M^{2+}Ta_2O_6$ ($M^{2+}=Ni,Co$).

The magnetic properties of MTa_2O_6 were investigated by magnetic susceptibility, specific heat, neutron powder diffraction and pulse field magnetization measurements. In a previous finding both $NiTa_2O_6$ and $CoTa_2O_6$ were argued to be 2D in nature with weak inter-plane coupling leading to long range magnetic order at 10 and 6.5K, respectively.[1]

By using a combined study of *ab-initio* DFT calculations, experimental findings and computational simulations we clearly show that $NiTa_2O_6$ must be described as a quasi-1D Heisenberg $S = 1$ spin chain system with a nearest-neighbor only anti-ferromagnetic spin-exchange interaction of 18.9 K. Inter-chain coupling is about two orders of magnitude smaller. As evidence by our comparison between quantum Monte Carlo and experimental observables shown in figure 1.

Likewise we show $CoTa_2O_6$ to be a non-Heisenberg XXZ-type spin chain, with a dominant anti-ferromagnetic nearest neighbor spin exchange $J_{zz}=9K$. By applying a combined study of DFT and t-DMRG calculations, and experiment measurements on single crystals.

The authors would like to thank HLD at HZDR, a member of the European Magnetic Field Laboratory (EMFL) for the high-field measurements. The work at NCSU was supported by the HPC Center of NCSU for computing resources.

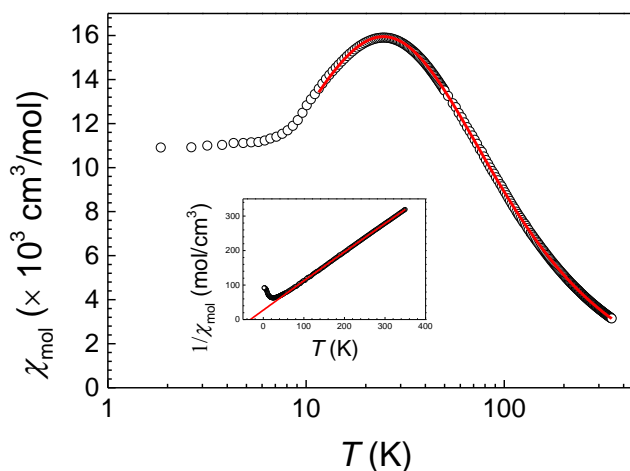


Figure 1 - The magnetic susceptibility of $NiTa_2O_6$. Solid (red) line represents a fit to the data using our Pade approximation to the susceptibility of a $S = 1$ Heisenberg AFM with nn SEI.[3] Inset: The reciprocal magnetic susceptibility versus temperature. Solid (red) line is a Curie-Weiss fit to the data.

[1] E. G. Santos, *et al.*, *Journal of Physics: Condensed Matter*, **22** (2010) 496004.

[2] J. M. Law, *et al.*, *Phys. Rev.*, **B 89** (2014) 014423

[3] J. M. Law, *et al.*, *Journal of Physics: Condensed Matter*, **25** (2013) 065601.

2OR-O-7

CROSSOVER BETWEEN SPINONS AND MAGNONS IN A TRIANGULAR LATTICE ANTIFERROMAGNET

Smirnov A.I.¹, Soldatov T.A.¹, Povarov K. Yu.¹

¹ P.L. Kapitza Institute for Physical Problems RAS, Moscow 119334, Russia
smirnov@kapitza.ras.ru

The $S=1/2$ antiferromagnet Cs_2CuCl_4 is a quasi 2D magnet with a distorted triangular lattice. The ordering at $T_N=0.62$ K is strongly delayed with respect to Curie-Weiss temperature $T_{CW}=4$ K and greatly reduced by zero-point fluctuations. In the temperature range $T_N < T < T_{CW}$ there is a correlated spin-liquid state with a continuum of magnetic excitations, which may be considered as a continuum of $S=1/2$ chain [1]. Our electron spin resonance study is performed in the frequency range $9 < f < 350$ GHz. In the spin-liquid phase, it reveals a fine structure of the spinon spectrum in the Brillouin zone center in form of a resonance doublet. This doublet is a signature of the spinon continuum of $S=1/2$ chains with the uniform Dzyaloshinskii-Moriya interaction [2]. At cooling down to $T=0.05$ K, for $f=60\text{--}120$ GHz this spinon doublet is found to survive deep in the ordered phase. On the other hand, at $f < 50$ GHz the doublet is transformed to an antiferromagnetic resonance (AFMR) signal, indicating a low field crossover from spinons to magnons.

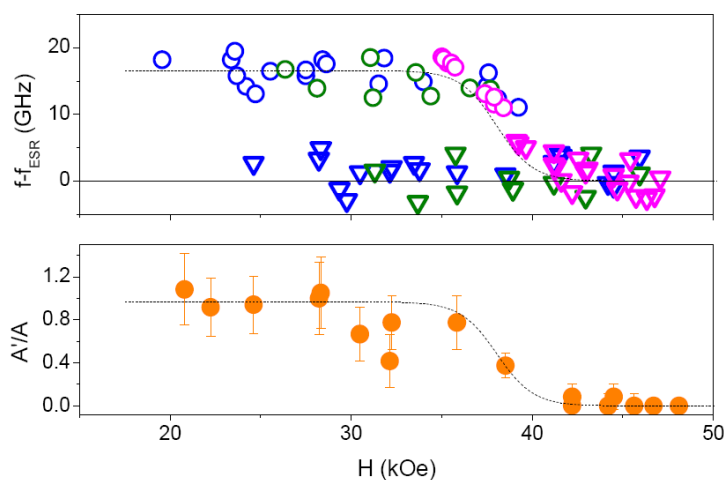


Fig.1. Collapse of the spinon doublet in a magnetic field at $T=0.5$ K. Upper panel: field dependence of the shift from the Larmor frequency for two components of the doublet. Lower panel: ratio of amplitudes of the doublet components vs magnetic field.

The coexistence of AFMR and of a spinon mode may be ascribed to the proximity of a quantum critical point, where oscillations of an order parameter and spinons coexist. At the increase of the frequency and, hence, of the magnetic field, the spinon doublet collapses at about a half of the saturation field. Further increase of the magnetic field causes magnetic saturation and reveals a new spectrum of $q=0$ excitations in form of intensive Larmor precession, coexisting with a much weaker mode of the exchange origin. This high-frequency crossover to a doublet of another kind is due to the transition from the fluctuating spin liquid to a fully polarized saturated phase.

[1] R. Coldea et al., *Phys. Rev. B.*, **68** (2003) 134434.

[2] K. Yu. Povarov et al., *Phys.Rev. Lett.*, **107** (2011) 037204.

2OR-O-8

A NOVEL SPIN- $\frac{1}{2}$ HEISENBERG ANTIFERROMAGNETIC CHAIN (NO)[Cu(NO₃)₃] WITH FRUSTRATED INTERCHAIN COUPLING

Balz C.¹, Lake B.¹, Guidi T.², Luetkens H.³, Deeva E.⁴, Morozov I.⁴, Volkova O.⁴, Vasiliev A.⁴

¹ Helmholtz-Zentrum Berlin, Berlin, Germany

² ISIS Facility, Didcot, UK

³ Paul Scherrer Institut, Villigen, Switzerland

⁴ Moscow State University, Moscow, Russia

christian.balz@helmholtz-berlin.de

Low-dimensional and frustrated antiferromagnets with low spin values are characterized by the suppression of long-range magnetic order and exotic excitations. A well-known example is the Spin- $\frac{1}{2}$ Heisenberg Antiferromagnetic Chain (S- $\frac{1}{2}$ HAFC) which fails to develop long-range magnetic order and is characterized by spinon excitations. Spinons are fractional particles with spin= $\frac{1}{2}$, which are observed as a multi-spinon continuum. Most physical realisations of the S- $\frac{1}{2}$ HAFC have weak nearest neighbour interchain coupling (J') that gives rise to long-range order at a suppressed but finite temperature. More complex behaviour occurs when the interchain interactions are competing e.g. in the case of an antiferromagnetic J' , an additional next-nearest neighbour interchain interaction (J_2) would give rise to frustration (“confederate flag” model). For the special case $J'=2J_2$ which corresponds to the Nersesyanyan-Tsvetlik model, the interchain interactions effectively cancel completely suppressing long-range order and the ground state is predicted to be a resonating valence bond [1]. (NO)[Cu(NO₃)₃] is a S- $\frac{1}{2}$ HAFC with potentially frustrated interchain interactions. The crystallographic structure [2] suggests that the spin- $\frac{1}{2}$ Cu²⁺ ions are coupled by strong antiferromagnet exchange interactions along the b -axis and these chains are weakly coupled in the b - c plane by J' and J_2 . Inspection of the exchange paths suggests that $J'=2J_2$ [3]. We report inelastic neutron scattering (INS), heat capacity and muon spin spectroscopy (μ SR) studies of (NO)[Cu(NO₃)₃]. INS shows by the presence of a spinon continuum that (NO)[Cu(NO₃)₃] is a 1D S- $\frac{1}{2}$ HAFC. From these measurements the intrachain exchange constant was found to be $J=142(3)$ K. A transition to incommensurate sinusoidal magnetic order with a very small ordered moment of $m=7\cdot 10^{-4}\mu_B$ was found by μ SR measurements at $T_N=0.585(5)$ K corresponding to the temperature where a lambda type transition is found in the specific heat. The suppressed ordering temperature with respect to the intrachain coupling ($T_N/J=0.4\%$) as well as the small ordered moment imply that (NO)[Cu(NO₃)₃] is highly one-dimensional and/or frustrated. Furthermore incommensurate magnetism is usually due to frustrated interactions suggesting that the interchain interactions in (NO)[Cu(NO₃)₃] are competing and are thus consistent with the Nersesyanyan-Tsvetlik model.

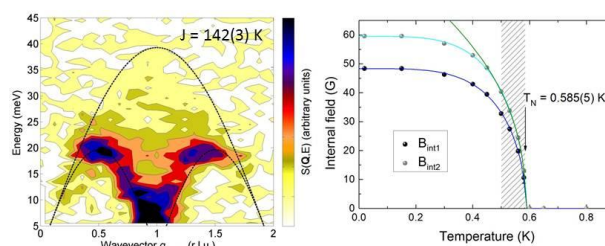


Fig. 1. (left) Inelastic neutron data at 5.5 K. Black lines show upper and lower boundary of the spinon continuum for $J = 142$ K. (right) Transition into long-range magnetic order from muon spectroscopy. Two internal fields are observed. Green line is a fit to the critical exponent in the shaded region.

[1] A. Nersesyanyan and A. Tsvetlik, *Phys. Rev. B* **67** (2003) 024422.

[2] K. Znamenkova, I. Morozov, and S. Troyanov, *Russ. J. Inorg. Chem.* **49** (2004) 172.

[3] O. Volkova, I. Morozov, A. Vasiliev, *et al.*, *Phys. Rev. B* **82** (2010) 054413.

2OR-O-9

MAGNETIC BEHAVIOUR OF THE HONEYCOMB ANTIFERROMAGNET $\text{BaNi}_2\text{V}_2\text{O}_8$

Klyushina E.S.^{1,2}, *Lake B.*^{1,2}, *Islam A.T.M.N.*¹, *Klemke B.*¹, *Schneidewind A.*³, *Park J.*³, *Mansson M.*⁴

¹ Helmholtz-Zentrum Berlin, Berlin, Germany

² Technical University Berlin, Berlin, Germany

³ Forschungs-Neutronenquelle Heinz Maier-Leibnitz, Garching, Germany

⁴ Paul-Scherrer Institut, Villigen PSI, Switzerland

Ekaterina.Klyushina@helmholtz-berlin.de

A number of unconventional magnetic phenomenon are predicted for low-dimensional magnets with antiferromagnetic exchange interactions and quantum spin values ($S=1/2,1$). One example is the Berezinsky-Kosterlitz-Thouless transition (BKT) which is a topological magnetic phase transition proposed for 2D XY magnetic systems [1] that was initially found in superfluid and superconducting films [2]. However, recent theoretical research indicated that BKT behaviour can be also expected for 2D Heisenberg systems with a small easy-plane XY anisotropy [3].

In present work we introduce our recent investigations of a spin-1 honeycomb antiferromagnetic $\text{BaNi}_2\text{V}_2\text{O}_8$, which is considered as a potential candidate for a 2D antiferromagnet with XY anisotropy and BKT behaviour. Indeed, the magnetic structure is ordered below $T_N=47\text{-}50\text{K}$: the spins of the Ni^{2+} mostly lie within the honeycomb planes and are aligned antiferromagnetically with their nearest neighbours while the crystal structure (R-3 space group symmetry $a=b=5.0375 \text{ \AA}^{-1}$, $c=22.3300 \text{ \AA}^{-1}$) suggests that the magnetic exchange interaction between the nearest neighbours within the honeycomb planes will be dominant [4].

Our inelastic neutron scattering measurements of a $\text{BaNi}_2\text{V}_2\text{O}_8$ single crystal in the honeycomb plane (a-b plane) at 4K reveal that magnetic excitation spectra extend from 0.3—26 meV and consist of two anisotropy-split gapped excitation modes with gaps 0.3 meV and 3.3meV which can be associated with anisotropy within the a-b plane and XY anisotropy respectively (fig 1a). Both modes are found to be completely dispersionless in the out-of-plane direction suggesting negligible interplane coupling (fig 1b). The excitations agree well with simulations based on linear spin - wave theory [5].

The values of intra-and out plane magnetic exchange interactions extracted from simulations, confirm that magnetic properties of the system are mainly determined by the first neighbour antiferromagnetic interactions of Ni ions within the honeycomb layers while the interlayers interaction can be neglected. That makes the $\text{BaNi}_2\text{V}_2\text{O}_8$ an ideal model compound for explore of 2D Heisenberg magnetic system with XY anisotropy.

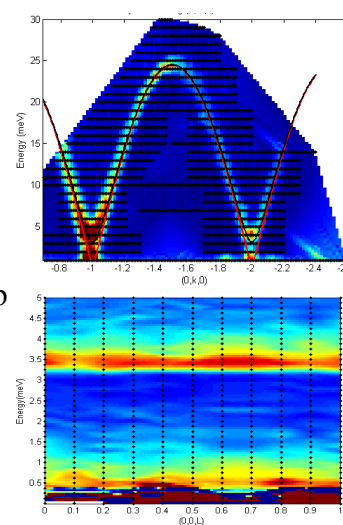


Fig1. Energy dispersion within the a-b plane (a) and out-of-plane (b) directions

[1] J. M. Kosterlitz, D.J. Thouless *J. Phys.*, C **6** (1973) 1181.

[2] P. Minnhagen, *Rev. Mod. Phys.*, **59** (1987) 1001.

[3] A. Cuccoli et al., *Phys. Rev. B*, **67** (2003) 104414.

[4] N. Rogado et al. *Phys. Rev. B*, **65** (2002) 144443.

[5] <http://wiki.helmholtz-berlin.de/spinw/index.php5/SpinW>.

2OR-O-10

QUANTUM BICRITICALITY IN $\text{Mn}_{1-x}\text{Fe}_x\text{Si}$ SOLID SOLUTIONS

Demishev S.V.¹, Lobanova I.I.¹, Glushkov V.V.¹, Ischenko T.V.¹, Sluchanko N.E.¹, Grigoriev S.V.²

¹ Prokhorov General Physics Institute of RAS, Moscow, Russia

² Konstantinov Nuclear Physics Institute, Gatchina, Russia

demis@lt.gpi.ru

The study of the magnetic susceptibility and magnetization together with the analysis implying polarized small angle neutron scattering data [1] allowed reconstructing the T - x magnetic phase diagram of $\text{Mn}_{1-x}\text{Fe}_x\text{Si}$ solid solutions [2], which includes both regions of long-range and short-range magnetic orders (Fig. 1,a). The boundary $T_s(x)$ limiting short-range (or chiral spin liquid [2]) phase is described analytically within suggested simple model accounting both classical critical (CF) and quantum critical (QF) magnetic fluctuations together with effects of disorder (Fig. 1,b). It is found that $\text{Mn}_{1-x}\text{Fe}_x\text{Si}$ may be treated as quantum *bicritical* system driven by two successive quantum phase transitions. The first underlying quantum critical (QC) point at $x^* \sim 0.11$ is surrounded by the phase with short-range order and corresponds to the disappearance of the spiral long-range magnetic order, $T_c(x^*)=0$ [1,2]. The second QC point $x_c \sim 0.24$ has topological nature and corresponds to the percolation threshold in magnetic subsystem of $\text{Mn}_{1-x}\text{Fe}_x\text{Si}$ [2]. Above x_c the transition into chiral spin liquid phase is suppressed and magnetic subsystem becomes separated

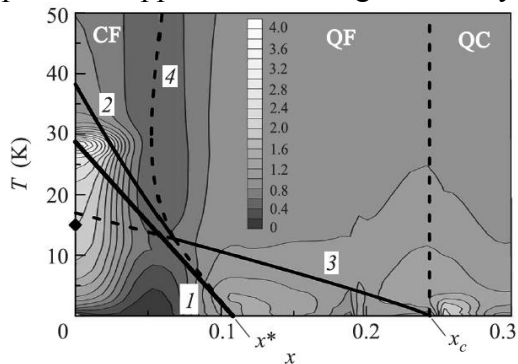


Fig. 2. Resistivity exponent map. Solid lines correspond to LRO transition (1) and SRO transition (2,3). Dashed line 4 is a crossover between classical and quantum critical fluctuations.

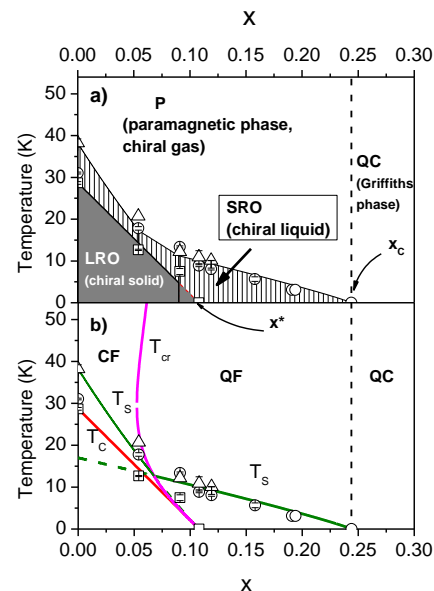


Fig. 1 Experimental magnetic phase diagram of $\text{Mn}_{1-x}\text{Fe}_x\text{Si}$ (a) and its theoretical description (b).

into spin clusters, which result in observation of the disorder-driven QC Griffiths phase characterized by anomalously divergent magnetic susceptibility $\chi \sim 1/T^{0.5}$. The theory developed for description of the magnetic phase diagram [2] predicts a crossover line between classical and quantum fluctuations in the paramagnetic phase, $T_{cr}(x)$. This new phenomenon was observed experimentally as a broad minimum of the resistivity exponent $\alpha(x, T)$ defining low temperature resistivity asymptotic $\rho(T) = \rho_0 + AT^\alpha$ (Fig. 2). We argue that “visualization” of this unusual line in the T - x plane is a consequence of the magnetic scattering effects recently discovered in MnSi [3]. This work is supported by the Program of RAS “Strongly correlated electrons” and by RFBR grant 13-02-00160.

[1] S.V. Grigoriev, et al., *Phys. Rev. B*, **83** (2011) 224411.

[2] S.V. Demishev, et al., *JETP Letters*, **98** (2013) 829-833.

[3] S.V. Demishev, et al., *Phys. Rev. B*, **85**, (2012) 045131.

2OR-O-11

HIGH FIELD ESR STUDY OF FRUSTRATED ANTIFERROMAGNETS

Okubo S.¹, Ohya H.^{1,2}, Nakata R.², Takahashi N.², Shimokawa T.³, Sakurai T.⁴, Zhang W.¹,
Okuta K.⁵, Hara S.⁴, Sato H.⁵

¹ Molecular Photoscience Research Center, Kobe University, Kobe, Japan

² Graduate School of Science, Kobe University, Kobe, Japan

³ Center for Collaborative Research and Technology Development, Kobe University, Kobe, Japan

⁴ Center for Supports to Reserach and Education Activites, Kobe University, Kobe, Japan

⁵ Department of Physics, Chuo University, Bunkyo, Tokyo, Japan

hohta@kobe-u.ac.jp

Frustrated antiferromagnets, especially the kagome antiferromagnets, have attracted much interest recently [1]. However, the high quality single crystal is essential to study the magnetic anisotropy of the system, and the existence of Dzyaloshinsky-Moriya (DM) interaction is unavoidable in kagome antiferromagnets due to their crystal symmetry. Moreover, high field ESR measurements turned out to be the powerful means to study the magnetic anisotropy [2].

Recently Okuta *et al.* succeeded in synthesizing high quality single crystals of Cr-jarosite ($\text{KCr}_3(\text{OH})_6(\text{SO}_4)_2$) without defects of Cr ions and large enough to measure the magnetic anisotropy [3]. Using these high quality single crystals we have performed high field ESR measurements of Cr-jarosite. First the anisotropic g-values are determined at 265 K, which turned out to be typical for the Cr^{3+} ion. Moreover, antiferromagnetic resonances (AFMR) are observed at 1.9 K, which is below the Neel temperature 4.5 K, in the frequency region from 80 to 481 GHz using the pulsed magnetic field. The analyses of AFMR by the molecular field theory clearly suggested the existence of DM interaction and the DM interaction is estimated. Moreover, the obtained DM interaction can also interpret the weak ferromagnetism observed in the magnetization measurement quantitatively. As the the ground state of kagome lattice antiferromagnet depends strongly on the DM interaction from the Monte Carlo simulations [4], the possible ground state will be discussed from the obtained DM interaction and the nearest neighbor exchange interaction.

[1] Special Topics Section “Novel States of Matter Induced by Frustration”, *J. Phys. Soc. Jpn.*, **79** (2010).

[2] S. Okubo *et al.*, *Phys. Rev. B*, **86** (2012) 140401/1-5.

[3] K. Okuta *et al.*, *J. Phys. Soc. Jpn.*, **80** (2011) 063703/1-4.

[4] M. Elhajal, B. Canals and C. Lacroix, *Phys. Rev. B*, **66** (2002) 014422.

Wednesday

2 July

17:30-18:30

poster session

2PO-I1

**“Magnetic
Nanostructures and
Low Dimensional
Magnetism”**

2PO-I1-1

MAGNETIC PROPERTIES AND METASTABLE STATES OF Co-Rh SOLID SOLUTION NANOPARTICLES

*Artemiev E.M.*¹, *Shubin U.V.*², *Yakimov L.E.*³

¹ Siberian Federal University, Krasnoyarsk, Russia

² Nikolaev Institute of Inorganic Chemistry SB RAS, Novosibirsk, Russia

³ Siberian State Aerospace University, Krasnoyarsk, Russia

aem49@yandex.ru

To clarify the phase diagram of CoRh systems and their crystalline structure we studied the structure and magnetic properties of CoRh nanoparticles. They were obtained chemically in the process of thermolysis of metal complexes. The metal complexes have different temperature stabilities so the reduction of metals happened at different temperatures, which was an important factor in producing the systems.

The high-resolution microscope JEM-2100 was used to study crystalline structure, phase and composition of produced particles. Results show that nanoparticles have 3–5 nm size regions with various lattice parameters. They are mainly fcc or hcp. Also, photos show many lattice defects and disordered areas. It is obvious that fcc and hcp structures are close-packed layered ones differing

only in the way the layers are aligned. Probably the energy of defect formation

is very low in such close-packed systems so disordered areas appear among fcc and hcp regions.

Nanoparticles of solid solutions $\text{Co}_{65}\text{Rh}_{35}$ – $\text{Co}_{25}\text{Rh}_{75}$ were studied. Magnetic measurements in the temperature range of 3K – 300 K were made using SQUID magnetometer. Saturation magnetization with its temperature dependence and coercive force were measured for all produced systems.

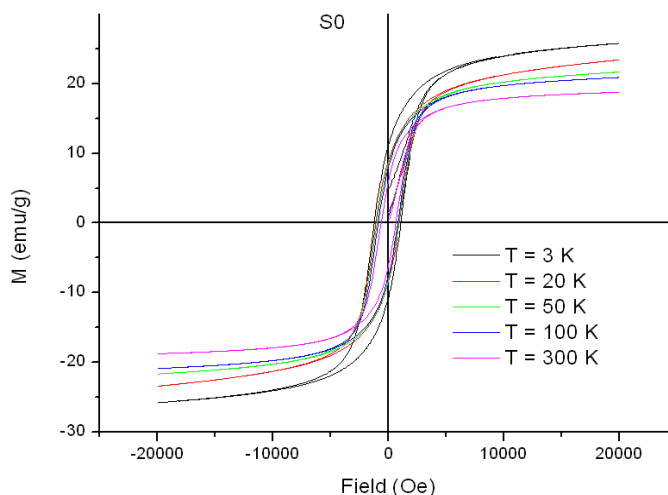


Fig 1. Hysteresis loops for $\text{Co}_{50}\text{Rh}_{50}$ at $T=3\text{--}300\text{K}$.

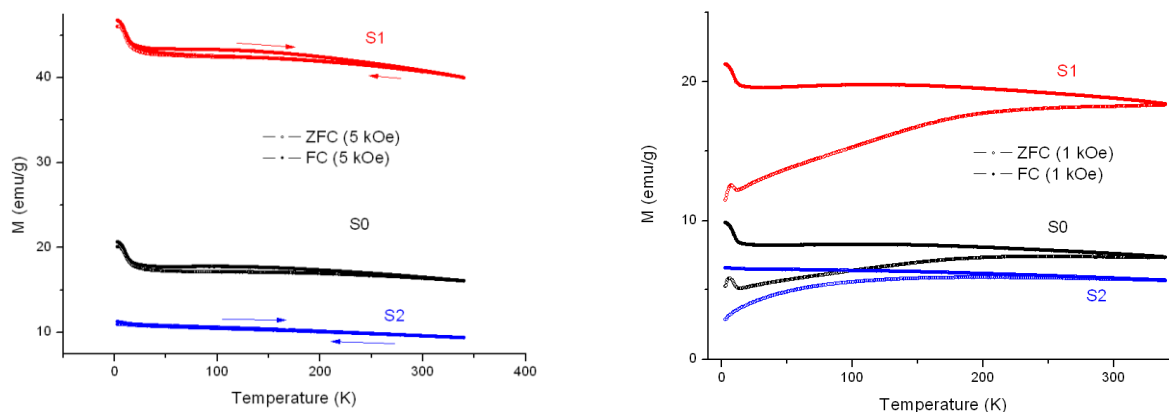


Fig 2. Temperature dependence of particles' magnetization with (left) and without (right) magnetic field for $\text{Co}_{60}\text{Rh}_{40}$ (S1), $\text{Co}_{50}\text{Rh}_{50}$ (S0), $\text{Co}_{25}\text{Rh}_{75}$ (S2) systems.

2PO-I1-2

FERRITE NANOPARTICLES IN BORATE GLASS MATRIX: STRUCTURE AND MAGNETIC PROPERTIES

*Trofimova N.N.¹, Zubavichus Y.V.¹, Edelman I.S.², Ivanova O.S.^{2,3}, Velikanov D.A.^{2,3},
Petrakovskaya E.A.², Zaikovskij V.I.⁴*

¹NRC "Kurchatov Institute", 123182 Moscow, Russia

²L.V. Kirensky Institute of Physics, SB RAS, 660036 Krasnoyarsk, Russia

³Siberian Federal University, 660036 Krasnoyarsk, Russia

⁴Boreskov Institute of Catalysis, SB RAS, 630090 Novosibirsk, Russia
ise@iph.krasn.ru

Magnetic nanoparticles of different morphology (Fig. 1) are formed in borate glasses co-doped simultaneously with Fe and one or two of larger radius ions (Tb, Dy, Gd, Ho, Pb, Sm, Bi, Y) in the process of glass additional thermal treatment. XRD data show peaks of nanocrystalline maghemite, $\gamma\text{-Fe}_2\text{O}_3$, for all glass samples independently of the kind of co-doping elements and their concentrations. The average nanoparticles size varies from 12 to 23 nm depending, as a rule, on the thermal treatment conditions. The EXAFS data show two Fe-O bond distances, 1.88 and 2.05–2.10 Å, related, respectively, to tetrahedral and octahedral sites in the spinel structure. The peaks corresponding to Fe...Fe interatomic distances, at ca. 3.0 and 3.5 Å, values are also quite consistent with the spinel-type structure. The EXAFS results for the larger radius ions, in contrast to those for iron, discern no apparent further coordination shells. The EDXA spectra for several samples indicate that both iron and the larger ion radius elements are gathered, predominantly, in the region of the particles. In order to explain some discrepancy between XRD and EDXA data, one can suggest that while Fe ions enter inside the particles, the larger radius ions concentrate, mainly, at the particle surface contributing to form a more or less disordered "spin glass" shell.

Magneto-optical measurements confirmed the assignment of nanoparticles structure to $\gamma\text{-Fe}_2\text{O}_3$ and, what is the most important, showed that maghemite is the only magnetic phase in all glasses.

Magnetization FC and ZFC temperature dependences demonstrated superparamagnetic state of particles with the blocking temperature in a range of 150-250 K for different samples. EMR data showed significant contribution of the nanoparticles surface to their anisotropy.

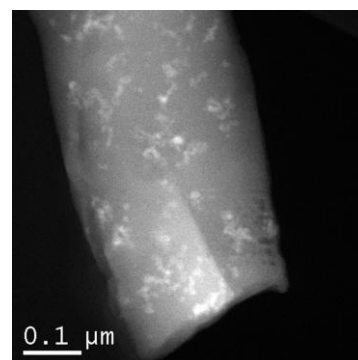


Fig. 1. HAADF-STEM image glass doped simultaneously with Fe, Bi and Y. Iron ferrite nanoparticles 10-20 nm in size is obvious as elongated chains of a white color.

Support by RFBR Grants No 14-02-01211_a and the President of Russia Grant No. NSh-2886.2014.2 is acknowledged.

2PO-I1-3

MAGNETIC PROPERTIES OF SPUTTER-DEPOSITED NANOCUSTER AGGREGATIONS IN SUPERLATTICE Fe/Co/Mo

*Senina V.A.*¹, *Antipov S.D.*¹, *Gorunov G.E.*¹, *Kornilov A.A.*¹, *Smirnitskaya G. V.*¹, *Grishina A.E.*¹,
*Pivkina M.N.*¹

¹ M.V. Lomonosov Moscow State University, GSP-1, Leninskie Gory, build.2, Physics Department,
Moscow, Russia
Vera_sen@mail.ru

It is known that nanoclusters are aggregates containing N atoms or molecules ($N=10-10^6$). They are characterized by: a) unlike molecules they do not have a fixed size or composition, b) they can be homogenous or heterogenous, c) they may be neutral or charged, d) they are finite small objects and do not possess of translational symmetry, e) they have nanocrystalline structure (icosahedra and decahedra are best known).

In this paper we report the results of the investigation of magnetic behavior of nanosized clusters aggregation in the three-components superlattice $[\text{Fe}(10\text{\AA})\text{Co}(7.8\text{\AA})\text{Mo}(23\text{\AA})]*100$. Magnetic superlattice (MSL) Fe/Co/Mo have been synthesized by cathode sputtering from two opposed cathodes on mica substrates (muscovite) at 70°C temperature in Kr atmosphere at the working gas pressure 10^{-5} torr.

According XRD investigation the sample is in nanocrystalline (amorphous) phase. The studies of ESR and XPA spectra bring about conclusion that in process of sputtering the transition metal complexes with Kr [1] were formed.

Scanning tunneling microscopy measurements were performed to characterize the deposited clusters aggregations of clusters, resulting the island structure on mica substrate. Basic magnetic properties were measured along and across the planes of samples MSL at different temperatures. Magnetic measurements were carried out using VSM with $2*10^{-7}$ emu sensitivity in magnetic fields $\pm 8\text{kOe}$.

We observed the stepped shape of the hysteresis loops for MSL $[\text{Fe}(10)\text{Co}(7.8)\text{Mo}(23)]*100$, which is typical for quantum resonant tunneling between the spin levels with s , where s - ground spin level, n - exited spin levels ($n=1\div s$). The temperature dependence of magnetization measured in external field of 5 Oe indicates the transition type spin crossover from low spin (LS) to high spin (HS) states of ions with increasing of temperature from 70 to 300K the temperature shows the spin crossover type behavior (transition LS-HS) for ions Fe^{2+} from the 70 to 300 K. Mechanisms underlying the spin crossover phenomenon in such nanocluster aggregations were discussed.

[1] F. Grandinetti, *European Journal of Mass Spectrometry*, **17** (5) (2011) 423–463.

2PO-I1-4

SPIN-WAVE SPECTRUM FORMATION IN MULTILAYERED MAGNONIC STRUCTURES WITH HIGH MAGNETOCRYSTALLINE ANISOTROPY

Grigoryeva N.Yu.¹, Kalinikos B.A.¹

¹ Saint-Petersburg Electrotechnical University (LETI), Saint-Petersburg, Russia
natallygri69@gmail.com

In the last years different planar structures consist of dielectric and ferrite layers with high magnetocrystalline anisotropy (e.g. hexaferrites) have been studied extensively [1-2]. This study is associated with a demand of micro- and nanoelectronics for signal processing devices, operating in subterahertz frequency range. Due to the high magnetocrystalline anisotropy the frequency range for spin waves in hexaferrite films is shifted to subterahertz frequencies at reasonable bias magnetic fields. This makes them very good candidates as information carriers for subterahertz applications.

The presented work is devoted to the theoretical analysis of the influence of the strength and orientation of uniaxial magnetocrystalline anisotropy on the spectrum of normal electromagnetic-spinwave modes propagating in multilayered structure consisting of several hexaferrite films separated with nonmagnetic spacer (Fig 1). The two types of hehaferrite films are examined separately: the M-type hexaferrite and Y-type hexaferrite. The previously elaborated theory [3] was extended to the case of multilayered structure. The considered model takes into account the dipole-dipole and exchange interaction inside the ferromagnetic films, the interlayer dipole-dipole interaction, and also includes the influence of volume and surface anisotropy field.

The obtained spectrum of hybrid electromagnetic-spin waves shows a strong dependence of the dispersion characteristics on the mutual orientation of the anisotropy axes in different layers. It is shown that for some cases of mutual orientation of the anisotropy axes in hexaferrite films and the external magnetic field the propagating hybrid waves can change their behaviour from surface to backward volume waves by changing only the strength of the external magnetic field. Thus the type of the propagating hybrid electromagnetic-spin waves can be controlled during spin-wave propagation.

Some peculiarities of electromagnetic-spinwave propagation in multilayered structures with “easy axis” and “easy plane” types of uniaxial anisotropy are pointed out.

Support by RFBR is acknowledged.

- [1] M.A. Popov, I.V. Zavislyak, G. Srinivasan, V.V. Zagorodnii, *J. Appl. Phys.*, **105** (2009) 083912.
[2] A. B. Ustinov, A. S. Tatarenko, G. Srinivasan, A. M. Balbashov, *J. Appl. Phys.*, **105** (2009) 023908.
[3] N.Yu. Grigoryeva, R.A. Sultanov, B.A. Kalinikos, *El.Lett.*, **47** (2011) 35-36.

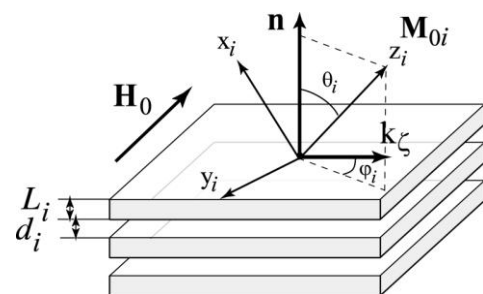


Fig. 1. Structure geometry.

2PO-I1-5

PEIERLS "WASHBOARD" CONTROLS DYNAMICS OF THE DOMAIN WALLS IN MOLECULAR FERRIMAGNETS

Kirman M.V.¹, Talantsev A.D.¹, Morgunov R.B.¹

¹ Institute of Problems of Chemical Physics RAS, Chernogolovka, Russia
kirmanm@yandex.ru

Molecular based magnets have weaker exchange interactions and larger lattice constants in comparison with inorganic magnets early explored to study domain walls dynamics. Therefore, molecular magnet seems to be proper to study dynamics of the "narrow" domain walls in the periodical Peierls relief.

Frequency and temperature dependence of the real and imaginary parts of the magnetic susceptibility of two chiral ferrimagnets (Yellow Needle $[\text{Mn}\{\text{R/S-pn}\}]_2 [\text{Mn}\{\text{R/S-pn}\}_2(\text{H}_2\text{O})] [\text{Cr}(\text{CN})_6]$ and Brown Needle $[\text{Mn}^{\text{II}}(\text{H}(\text{R/S-pn})(\text{H}_2\text{O}))][\text{Mn}^{\text{III}}(\text{CN})_6] \cdot 2\text{H}_2\text{O}$) were obtained by SQUID magnetometer MPMS 5XL Quantum Design. Frequency of AC magnetic field was 0.01 - 1400 Hz, its amplitude was 4 Oe, temperature range was 1.8 - 300 K. We have analyzed Cole -Cole diagrams that are dependencies of the imaginary part of the magnetic susceptibility on the its real part in the both Yellow and Brown Needle samples. Four modes of domain walls motion were distinguished: Debye relaxation, creep, slide and above-barrier motion (switching). In the Brown Needle racemic crystals transitions between «creep» and «relaxation» regimes occur at higher temperatures than in the chiral crystals of the same chemical composition. We have recognized and studied the contribution of the Peierls relief to the low-frequency spin dynamics of chiral and racemic samples. Sensitivity of the domain walls dynamics to the Peierls periodical potential was evaluated as a temperature shift of the AC- maximum in chiral crystals in comparison with racemic crystals. This relative shift was compared with the relation between the domain wall width W and the period of the crystal lattice a , i.e. W/a value was accepted as a key parameter controlling Peierls relief contribution. It was established that damping of the domain walls is controlled by both Peierls relief and structural defects. Domination of the damping mechanisms depends on the W/a value. Peierls regime dominates below $W/a = 4.2$ value.

Thus, we have studied the low-frequency magnetic properties of Yellow Needle and Brown Needle molecular ferrimagnets. Analysis of regimes of motion of domain walls, as well as the comparison racemic and chiral crystals allows us to conclude contribution of the Peierls relief to the dynamics of domain walls.

Support by RFBR № 14-02-31022 is acknowledged.

[1] F. Mushenok, O. Koplak, R. Morgunov, *Eur. Phys. J. B*, **84** (2011) 219 - 225.

[2] F.B. Mushenok, R.B. Morgunov, O.V. Koplak, M.V. Kirman, *Physics of the Solid State(rus)*, **54** (2012) 709 - 714.

2PO-I1-6

THE INFLUENCE OF THE SIZE DISTRIBUTION AND ORIENTATIONS OF PARTICLES ON THE FMR CHARACTERISTICS OF THE COMPOSITE FILMS

Kotov L.N.¹, Vlasov V.S.¹, Turkov V.K.¹, Ustyugov V.A.¹, Kalinin Yu. E.², Sitnikov A.V.², Golubev E.A.³

¹ Department of Radiophysics and Electronics, Syktyvkar State University, Syktyvkar, Russia

² Department of Solid State Physics, Voronezh State Technical University, Voronezh, Russia

³ Institute of Geology, Komi Scientific Center of UB RAS, Syktyvkar, Russia
kolovln@mail.ru

The research is devoted to the studying of the size distribution function and orientations of metal granules in the composite films derived from the images obtained using the atomic force microscope (AFM).

The composite films were obtained by the ion beam sputtering method in the argon atmosphere with the compositions: $\{(Co_4-Fe_4-Zr_{0.7})_x+(Al_2O_3)_{1-x}\}$, $\{(Co_1-Nb_{0.2}-Ta_{0.05})_x+(SiO_2)_{1-x}\}$, $0.2 < x < 0.7$. The effective size distributions of the metallic granules are studied for the different concentrations of the metallic phase and the different annealing temperatures. Assuming that the granules have the ellipsoidal shape, by the effective size we mean ellipsoid radius in the plane of the film. We found that by the increasing of the concentration of the metal phase in the composite the amount of small size particles decreases. The annealing the composite film lead to the decrease of surface roughness of the film due to the alloying of the metal fine granules and structure relaxation of the dielectric phase. This decreases the relative proportion of the particles with the small effective size. This gives rise to the large-sized particles that exceeds the maximum size of the particles observed in the not annealed films. The purpose of this work is to study the relationship between the structure granules composite films and their microwave magnetic properties, as well as in the construction of the theoretical model to describe the magnetic properties of the composite structures in the framework of micromagnetics.

On the basis of the obtained data the microwave magnetic properties (FMR line width and the resonance field) of composite films are calculated. We assume that the granules system in the composite film may be described as the regular array of the identical single-domain particles. The chosen model gives the satisfactory results in the range of the middle concentrations. The discrepancy between theory and experiment at the low x of the metal due to the limitation the scope of the chosen model. In the real films with the low metal x , there is the significant spread of particle shape and size, as well as their the random arrangement of the granules in the film volume. At the high concentrations x of the metal particles may form the complex shape clusters, which also remains outside the applicability of the model.

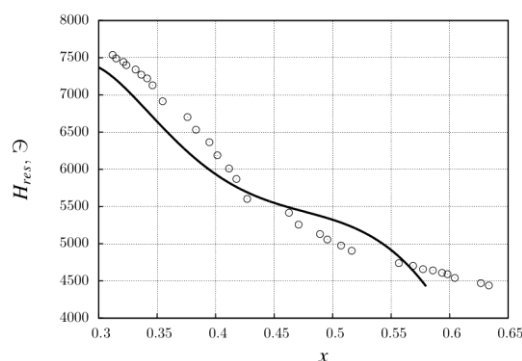


Fig. 1. The resonance field of the composite films with the various concentrations of the metal phase (circles – experiment, solid line – model).

Research is supported by RFBR (grant №13-0201401-a).

2PO-I1-7

CHIRAL SPIN LIQUID AND LIFSHITZ POINT IN 2D XY HELIMAGNET

Sorokin A.O.^{1,2}, *Korshunov S.E.*³

¹ Saint Petersburg State University, Saint Petersburg, Russia

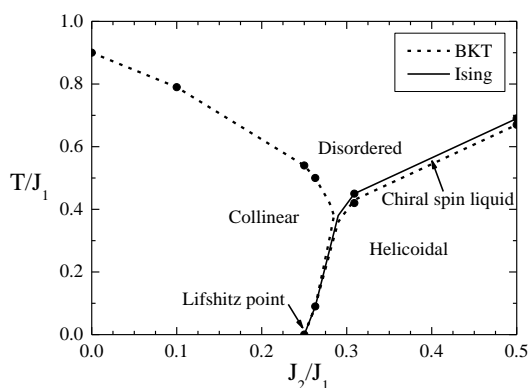
² Petersburg Nuclear Physics Institute NRC Kurchatov Institute, Gatchina, Russia

³ Landau Institute for Theoretical Physics, Chernogolovka, Russia
aosorokin@gmail.com

Two-dimensional helimagnets with planar (XY) spins have non-trivial thermal and critical properties due to the coexistence of the magnetic quasi-long-range and chiral long-range orderings. Using Monte Carlo simulations, we study the model on a simple square lattice with the ferromagnetic exchange interaction (J_1) between nearest spins and the additional antiferromagnetic exchange (J_2) between next-to-nearest neighbours along one direction of the lattice.

Well above the zero-temperature Lifshitz point $J_2/J_1=0.25$, two successive phase transitions occur with the temperature increasing [1]: the first one is a Berezinskii-Kosterlitz-Thouless (BKT) type transition, and the second one is of the Ising type associated with the chiral (discrete) symmetry restoration. Such a behavior is in agreement with the arguments [2] based on the analysis of the mutual influence of the topological excitations (domain walls, conventional and fractional vortices) present in an analogous system.

Closer to the Lifshitz point ($0.28 < J_2/J_1 < 0.35$), large domains of the opposite chiralities crossing the system in the direction perpendicular to a helix appear in the simulations on small-size lattices at relatively low temperatures, which has led the authors of Ref. 3 to the conclusion on the reversal of the phase transition sequence. We show that this is an artifact of small lattice sizes. Investigating large lattices ($L > 120$), we observe the usual sequence of the transitions.



At $J_2/J_1 < 0.28$, after the destruction of the helical ordering due to the thermal renormalization of the effective couplings, the system behaves itself as the set of almost non-interacting ferromagnetic chains without even quasi-long-range order. With further increase in temperature, one observes the appearance of the phase with the collinear (ferromagnetic) quasi-long-range order, and then the BKT-transition to the disordered phase (see Fig. 1). Such a behavior has been predicted in Refs. 4 and 5.

Fig. 1. Phase diagram.

- [1] A.O. Sorokin, A.V. Syromyatnikov, *Phys. Rev. B*, **85** (2012) 174404.
- [2] S.E. Korshunov, *Phys. Rev. Lett.*, **88** (2002) 167007.
- [3] F. Cinti, A. Cuccoli, and A. Rettori, *Phys. Rev. B*, **83** (2011) 174415.
- [4] Y. Okwamoto, *J. Phys. Soc. Jpn*, **53** (1984) 2613.
- [5] H. Schenck, V.L. Pokrovsky, and T. Nattermann, ArXiv: 1308.0823.

2PO-I1-8

INFLUENCE OF BIAS FIELD ON DYNAMIC DOMAIN STRUCTURES AND ANGER-STATE OF FERRIT-GARNET FILMS

*Rusinova E.A.*¹, *Rusinov A.A.*²

¹ Urals State University of Railway Transport 620034 Ekaterinburg, Russia

² Ural Federal University 620002 Ekaterinburg, Russia
earusinova@mail.ru

It is known [1] a constant bias field H_b influences strongly on view and behavior of dynamic domain structures (DDS), originating in "anger state" (AS) of ferrit-garnet films. Investigation of DDS at field $H = H_0 \sin 2\pi f t$ with frequencies $f = 10^2 - 10^5$ Hz and field H_b , oriented along the normal to the film, are continued in this work.

It shown for the first time, that lifetimes T_g of dynamic spiral domains (SD) decreases, but wait times T_w increases ($T_w \rightarrow \infty$) with growth of H_b . The SD quite not arises ($T_g = 0$) at H_b , exceeding some critical value. Thus new mechanism of AS destruction, different from known earlier [1] has been revealed.

Influence of field H_b on DDS of "leading centre" (LC) type [2] has been studied. It is shown, that number of rings in the system of concentric ring domains going to zero with growth of H_b , that is the LC are destroyed under field H_b . The destruction of LC starts either from periphery or from within depending on H_b values (at $f, H_0 = \text{const}$).

It has been revealed, that bias field may induce AS as well as destroy it. It appears that new gain-frequency (H_0 - f) regions of AS are occurred when H_b is applied. We named it as induced anger state (IAS). The SD properties in different (H_0 - f) regions of IAS differ each from other essentially.

Research of formation and destruction of dynamic spiral domains proceeds [3].

The work has been supported by RFFR.

[1] G.S.Kandaurova, A.E.Sviderskiy, *Zh.Eksp.Teor.Fiz.*, **97** (1990) 1218-1229.

[2] G.S.Kandaurova, Yu.V.Ivanov, *Fiz.Met.Metalloved.*, **76** (1993) 49-61.

[3] G.S.Kandaurova, A.A.Rusinov, V.Kh.Osadcheko., **392** (2003) 618-622.

2PO-I1-9

MAGNETIC RESONANCE IN CuCr_2S_4 NANOCCLUSERS AND NANOCRYSTALS

Pankrats A.I.^{1,2}, *Vorotynov A.M.*¹, *Tugarinov V.I.*¹, *Zharkov S.M.*^{1,2}, *Abramova G.M.*¹,
*Zeer G.M.*², *Gupta A.*³, *Ramasamy K.*³

¹ Kirensky Institute of Physics SB RAS, Krasnoyarsk, 660036, Russia

² Siberian Federal University, Krasnoyarsk, 660041, Russia

³ MINT Center, University of Alabama, Tuscaloosa, USA

pank@iph.krasn.ru

Magnetic materials with critical dimensions on the order of nanometer scale display unique properties such as superparamagnetism, high field irreversibility and high saturation field due to surface anisotropy contributions. Among the chalcospinel, Cu- and Cr-based systems are unique in that they are ferromagnetic metals at room temperature.

It was shown [1] that if oleylamine (OLA) or octadecylamine (ODA) are used as a solvent, pure-phase CuCr_2S_4 spinel can be obtained in the form of nanoclusters composed of smaller particles or cube-shaped nanocrystals, respectively. Both type of nanopowder samples were examined by transmission electron microscopy and by magnetic resonance in the frequency range 9.6÷80 GHz and at temperatures down to 4.2 K.

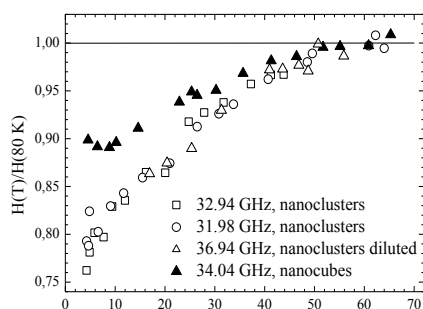


Fig. 1. Temperature dependencies of the resonance fields of clusters and cubic crystals normalized to $T=80$ K

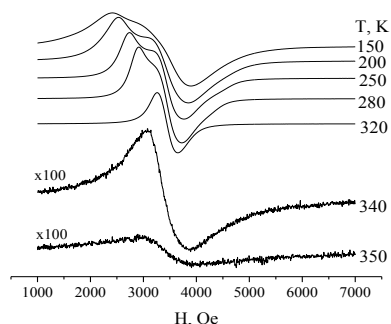


Fig. 2. Temperature evolution of the X-band spectrum in nanoclusters

A decrease of the resonance field (see Fig.1) and broadening of the resonance lines are observed below ~ 50 K in both nanocluster and nanocube samples. These phenomena are typical for superparamagnetic particles and are explained by the freezing of magnetic moments of particles (nanocubes and nanoclusters constituting smaller particles) due to the magnetic anisotropy. The effective field of averaged magnetic anisotropy is estimated to be ~ 2.4 kOe at 4.2 K for both nanopowder samples.

Nanoclusters have shown additional blocking behavior around 300 K, which is likely due to the freezing of the magnetic moment of the cluster as a whole. Below this blocking temperature, an additional low-field resonance line was found in the resonance spectra of nanoclusters (Fig. 2) at X-band due to the additional dipolar field acting at the boundaries of interacting constituent smaller nanoparticles. Interestingly, this disappeared after grinding with magnesium carbonate. As follows from the TEM study, most of the clusters are destroyed by such treatment, being transformed into single particles. The additional resonance line was not observed for nanocubes.

Support by CRDF – SB RAS, RUP1-7054-KR-11, N 16854 is acknowledged.

[1] K. Ramasamy, D. Mazumdar, Z. Zhou, Y.-H. A. Wang, and A. Gupta, *J. Am. Chem. Soc.*, **133** (2011) 20716–20719.

2PO-I1-10

ISING ANTIFERROMAGNET WITH NEAREST-NEIGHBOR AND NEXT-NEAREST- NEIGHBOR INTERACTIONS ON A SQUARE LATTICE

Murtazaev A.K.^{1,2}, Ramazanov M.K.^{1,3}, Badiev M.K.¹, Kurbanova D.R.^{1,2}

¹ Institute of Physics, Daghestan Scientific Center, Russian Academy of sciences, Makhachkala,
367003 Daghestan, Russia

² Daghestan state universities, Makhachkala, 367025 Daghestan, Russia

³ Dagestan State Pedagogical University, Makhachkala, 367003 Dagestan, Russia
m_zagir@mail.ru

We seek to determine the accurate values of critical parameters of Ising model in square lattice with next-nearest-neighbors interactions using a reliable and checked scheme, special replete algorithm of Monte-Carlo (MC) method, and keeping to the united technique. Research of this Ising model allows to clarify an influence of next-nearest-neighbors interaction on features and a character of critical behavior.

An Ising model on a square lattice with interactions between nearest neighbors is exactly solvable and almost any its properties are known [1]. An inclusion of the interaction between the next-to-nearest neighbors results in appearance of frustration that complicates the solution.

In recent years, intensive experimental and theoretical investigations of critical behavior of this model are being carried out. In Refs. [2] it has been shown that in an antiferromagnetic Ising model on a square lattice with interactions between the next-to-nearest neighbors the second order phase transition takes place. And this model can have “anomalous” critical exponents. Furthermore, a dependence of critical exponents on the ratio $k=J_2/J_1$, where J_1 and J_2 are constants of an exchange interaction the nearest and next-to-nearest neighbors, respectively, has been found.

According to the phase diagram of this model appeared in Ref. [3], for $k<0.5$ and $k>0.95$ the second order phase transitions is observed. The case $k=0.5$ is of particular interest because of strong degeneracy of a ground state.

The frustrated Ising model is described by the classical Hamiltonian:

$$H = -J \sum_{\langle ij \rangle} (\vec{S}_i \cdot \vec{S}_j) - J_1 \sum_{\langle il \rangle} (\vec{S}_i \cdot \vec{S}_l)$$

where the summations are over nearest-neighbor (nn) and next nearest-neighbor (nnn) pairs with J_1 and J_2 interactions, respectively. Calculations were carried out for systems with periodic boundary conditions (PBC) and linear dimensions $L \times L = N$, $L=20 - 150$. The ratio of the exchange interaction of the next-to-nearest and nearest neighbors $k=J_2/J_1 = 0 \div 0.9$. For calculation of static critical exponents of specific heat α , susceptibility γ , ordering parameter β , and correlation radius ν , we used the relations of the finite-size scaling theory [4].

The work has been supported by the grant of RFBR (project № 12-02-96504; project № 13-02-00220), the grant of RFBR (project № 12-02-31428), and by the grant Ministry of education and science of Russia, project 14.B37.21.1092.

[1] R. Baxter, *Exactly Solvable Model in Statistical Mechanics*, Mir, Moscow (1985).

[2] K. Minami and M. Suzuki, *J. Phys. A* **27** (1994) 7301.

[3] Rosana dos Anjos, J. Roberto Viana, and J. Ricardo de Sousa, *Phys. Lett.*, **372** (2008) 1180.

[4] A. K. Murtazaev, M. K. Ramazanov, M. K. Badiev, *Low temperature physics*, **37** (2011) 12.

2PO-I1-11

THERMODYNAMIC PROPERTIES OF FRANCISITES $\text{Cu}_3\text{Ln}(\text{SeO}_3)_2\text{O}_2\text{Cl}$ (Ln = Y, La)

Berdonosov P.S.¹, Kuznetsova E.S.¹, Zakharov K.V.¹, Markina M.M.¹, Vasiliev A.N.^{1,2}

¹ Moscow State University, Moscow 119991, Russia

² Ural Federal University, Ekaterinburg 620002, Russia

Francisites $\text{Cu}_3\text{Ln}(\text{SeO}_3)_2\text{O}_2\text{Cl}$ (Ln = Y, La) having orthorhombic structure (space group Pmmn) represent a new class of layered compounds. The carriers of the magnetic moment - Cu^{2+} ions form a distorted kagome-type lattice within each layer [1], which causes frustration of the magnetic exchange interactions.

It was found that the temperature dependence of reduced magnetization $\chi = M/H$ of $\text{Cu}_3\text{Y}(\text{SeO}_3)_2\text{O}_2\text{Cl}$ shows a sharp peak at the Néel temperature $T_N = 36.5$ K (fig. 1.), that may be related to antiferromagnetic ordering in the subsystem of transition metal. The existence of phase transition is also confirmed by measuring the temperature dependence of specific heat. Surprisingly, this transition is

suppressed even by weak magnetic field of 4 T.

The temperature dependence of reduced magnetization in the case of $\text{Cu}_3\text{La}(\text{SeO}_3)_2\text{O}_2\text{Cl}$ was somewhat different (data not shown). Besides the antiferromagnetic transition at $T_N = 31.2$ K the anomaly at $T^* = 60.4$ K was observed for this compound presumably due to a structural transition.

The field dependences of the magnetization of $\text{Cu}_3\text{Ln}(\text{SeO}_3)_2\text{O}_2\text{Cl}$ (Ln = Y, La) have clearly defined metamagnetic transition in magnetic field of about 2.5 T and at temperatures below

T_N (Fig. 2).

This work was supported by Russian Foundation for Basic Research grants 13-02-00174, 14-02-00245, 14-02-92693.

[1] P. S. Berdonosov and V. A. Dolgikh, *Russian Journal of Inorganic Chemistry*, **53** (9) (2008) 1353–1358.

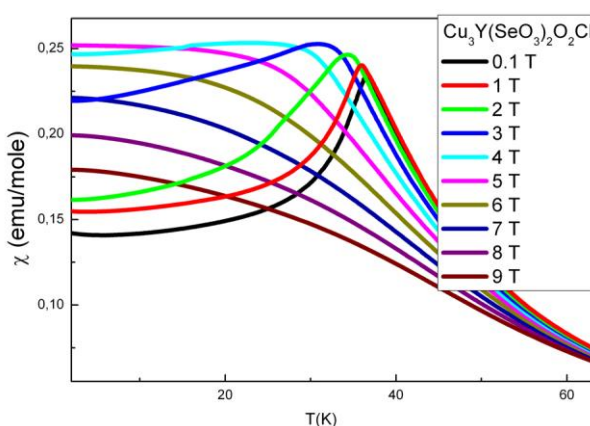


Fig. 1. The temperature dependences of reduced magnetization of $\text{Cu}_3\text{Y}(\text{SeO}_3)_2\text{O}_2\text{Cl}$

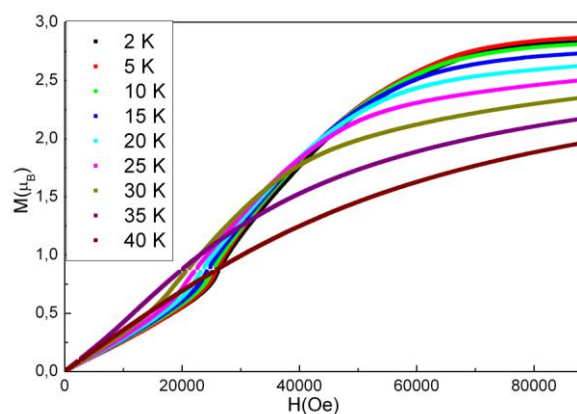


Fig. 2. The field dependences of magnetization of $\text{Cu}_3\text{Y}(\text{SeO}_3)_2\text{O}_2\text{Cl}$

2PO-I1-12

THE INVESTIGATION OF CRITICAL PROPERTIES OF THE TRANSITION FROM MODULATED PHASE INTO PARAMAGNETIC PHASE

Murtazaev A.K.^{1,2}, Ibaev Zh.G.¹

¹ Institute of Physics DSC RAS, Makhachkala, Yaragskogo 94, Russia

² Dagestan State University, Makhachkala, Gadjieva 43a, Russia

ibaev77@mail.ru

In addition to simple magnetic orderings (ferromagnetic, antiferromagnetic, and ferrimagnetic), in nature, is also available a modulated ordering. Such type of magnetic ordering occurs in the systems with the exchange interaction competition irrespectively of the physical nature of this interaction [1].

In practice, the systems, in which a magnetic modulated ordering is possible, are described using different models. The simplest and most effective model is anisotropic Ising model with competing interactions (ANNNI-model, Fig. 1).

ANNNI-model was developed in the statistical physics in the latter half of the 20th century to describe a helical magnetic ordering in high-density rare-earth metals. The Hamiltonian for this model in a regular cubic lattice is:

$$H_{ANNNI} = -J \sum_{i,j} s_i s_j - J_1 \sum_i s_i s_{i+1}, \quad (1)$$

where $s_i = \pm 1$, J denotes the parameter of the exchange interaction of neighbor spin pairs, $J_1 < 0$ denotes the parameter of the antiferromagnetic interaction of next nearest neighbors along Z axis.

According to literature data, when increasing the temperature, the ANNNI model undergoes a second order transition from the paramagnetic state into the nearest ordered state, and a transition “ferromagnetic-modulated phase” is a first order transition [1].

A simulation is made by the Monte-Carlo method for values $|J_1/J| = 0, 1 \div 1, 0$ including the multicritical region of Lifshitz point. Critical parameters of second order transitions from the ferromagnetic state into the paramagnetic state are calculated. The multicritical behavior of the system near the Lifshitz point is described.

In recent work [2], the ANNNI-model was studied in a modulated region by the Monte-Carlo methods using an averaged amplitude value of a modulated structure as an order parameter. Derived results showed that the phase transition from the modulated state into the paramagnetic state was the second order transition. In present work, we report the results on study of the critical properties of anisotropic Ising model with competing interactions at the transition from the modulated phase into the paramagnetic one.

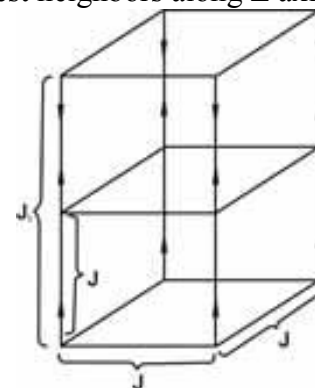


Fig. 1. ANNNI – model

Support by grant RFBR № 12-02-96504.

[1] Yu.A. Izumov, V.M. Siromiatnikov, *Science*, (1984) 241.

[2] A.K. Murtazaev, Zh.G. Ibaev, *JETP.*, **116** (2013) 266–271.

2PO-I1-13

MICROMAGNETIC CALCULATION OF NEEL DOMAIN WALL STRUCTURE

Semenov V.S.¹

¹ V.A. Trapeznikov Institute of Control Sciences of Russian Academy of Sciences, Moscow, Russia
vsemsem@mail.ru

In thin magnetic films which thickness is less than 50 nm, the domains of opposite magnetization are separated by 180° Neel domain walls (DW). Magnetization of such DW rotates in the film plane. In uniaxial anisotropic films, one-dimensional Neel wall magnetization distribution is characterized by directional cosines $m_x(x)$, where x is perpendicular to easy axis of the film. In thin magnetic films having small quality factor $Q = K / M_s^2$ ($M_s = |\vec{M}|$ is saturated magnetization of the film, K is anisotropy constant), magnetostatic energy is of the main influence on the domain walls structures. It is precisely the decrease in or the complete absence of magnetostatic energy that leads to vortex-like closed magnetization structure in Bloch domain walls and the narrow central zone (core) with very wide side zones (tails) in Neel walls. Calculating magnetostatic energy is of main and the greatest difficulty in Bloch and Neel domain walls structures determination.

Brown and La Bonte [1] substituted continuous one-dimensional magnetization change in 180° DW by discrete distribution permitting exact computation of magnetostatic energy. Minimal total energy conditions for the discrete distribution are found by variation method with effective field expressions; these expressions are used to find fine magnetization structure of 180° DW and to determine the energy corresponding to that structure. By this method, exact magnetization distribution for one-dimensional 180° Bloch DW was found, however the computation of magnetization distribution for DW was of no success because of very wide tails and insufficient computer velocities of those days. This paper presents 180° Neel DW structure and energy investigations by numerical method [1].

Fig. 1 demonstrates changing directional cosine $m_x(x)$ for film thickness meaning $2D=10$ nm. The computations were executed on the base of CUDA architecture using the program language CUDA C.

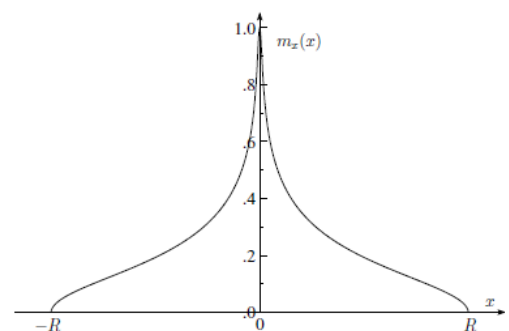


Fig. 1. Changing directional cosine $m_x(x)$ in one-dimensional Neel DW.

[1] Brown W.F., Jr., La Bonte A.E., *Journal of Applied Physics*, **36** (1965) 1380-1386.

2PO-I1-14

HEAT TRANSFER IN BOILING MAGNETIC FLUID IN A MAGNETIC FIELD

Yanovskiy A.A.¹, Simonovskii A.Ya.², Kholopov V.L.³, Chuenkova I.Yu.²

¹ Stavropol State Agrarian University, 12 Zootekhnicheskii per., 355017 Stavropol, Russia

² North Caucasian Federal University, 2 Kulakova ave., 355029 Stavropol, Russia

³ Institute of Mechanics, Lomonosov MSU, 1 Michurinskiy ave., 119192 Moscow, Russia
aa.yanovskiy@yandex.ru

The thermal processes in boiling magnetic fluid in applied magnetostatic uniform field were experimentally studied earlier [1]. In this work we investigated heat transfer processes in boiling magnetic fluid with different concentration of magnetic phase on unlimited horizontal surface in magnetostatic uniform field. The physical model of this process was developed. Our experiments showed that the magnetic field could more than twice intensify the heat transfer process in boiling magnetic fluid. Corresponding equations described the intensity of heat transfer process in boiling magnetic fluid under applied magnetic field. The equations considered all forces acting the vapor bubble in magnetic field. The proposed method used for measuring the frequency of steam bubbles formation in boiling opaque fluids. This method used the technique of double-layer media. It gave us the dependence of the formation frequency of steam bubbles in boiling magnetic fluid on unlimited horizontal surface from the wall heater temperature and the intensity of the applied magnetic field. At the same time, we investigated the influence of the magnetostatic uniform field on heat transfer in boiling two layers of magnetic-nonmagnetic fluids on the unlimited horizontal surface with a point heat source. It was shown that the magnetic field effected on the heat transfer process in two-layered fluids in 1,5 - 2 times less than on boiling single-layer magnetic fluid. Experimental and theoretical modeling of the form, volume and formation frequency of steam bubbles in boiling magnetic fluid on unlimited horizontal surface in magnetostatic field were performed. The proposed physical model explained observed changes of heat flows in boiling magnetic fluid in magnetic field.

Work has been done at financial support of RFBR (grant № 14-01-00056).

[1] M.A. Kobozev, A. Ya. Simonovskii, *Technical Physics*, **52** (2007) 1422-1428.

2PO-I1-15

PHASE TRANSITION IN FRUSTRATED ISING ANTIFERROMAGNET ON A BODY-CENTERED-CUBIC LATTICE WITH NEXT- NEAREST NEIGHBOR INTERACTIONS

Murtazaev A.K.^{1,2}, Ramazanov M.K.¹, Kurbanova D.R.^{1,2}

¹ Institute of Physics, Dagestan Scientific Center, RAS, Makhachkala, Russian Federation

² Dagestan State University, Makhachkala, Russian Federation
sheikh77@mail.ru

The study of phase transitions and critical phenomena in frustrated spin systems is one of the fundamental problems in statistical physics [1]. Recent advances in understanding phase transitions and critical phenomena in frustrated systems have largely been achieved by applying of Monte Carlo (MC) methods, because most attempts to calculate the critical exponents and characterize the mechanisms of the critical behavior of such systems by conventional theoretical and experimental methods are confronted by serious difficulties [2,3].

The problem of frustrations and phase transitions in Ising model on body-centered-cubic (BCC) lattice is explored in a great many works [4,5].

In the given work, we attempt whenever possible, with maximum accuracy, with observance of a uniform technique, and with a reliable and tested scheme, based on a replica exchange algorithm of the MC method, to determine the value of the critical parameters of the frustrated Ising model on a BCC lattice with allowance for next-nearest neighbor interactions.

The Hamiltonian of the Ising antiferromagnetic model can be represented in a following form:

$$H = -J_{NN} \sum_{\langle i,j \rangle} (S_i \cdot S_j) - J_{NNN} \sum_{\langle i,l \rangle} (S_i \cdot S_l), \quad (1)$$

where $S_{i,l} = \pm 1$ is the Ising spin. The first term in the Equation (1) accounts for the exchange interaction of nearest neighbors by the value of $J_{NN} < 0$, and the second term considers second nearest neighbors by $J_{NNN} < 0$. This model is schematically shown in Fig. 1.

The competition between the J_{NN} and J_{NNN} interactions gives rise to a helical ordering along the Z axis. This Ground State is characterized by the turn angle A between spins belonging to two adjacent planes perpendicular to the Z axis. A is given by the formula $\cos(A) = -J_{NNN}/J_{NN}$ and A decreases slowly as function of the temperature.

Similar model has been studied by Diep and Loison [4,5].

The static magnetic exponents specific heat α , susceptibility γ , magnetization β , correlation length ν were calculated by using the finite-size scaling theory [2,3].

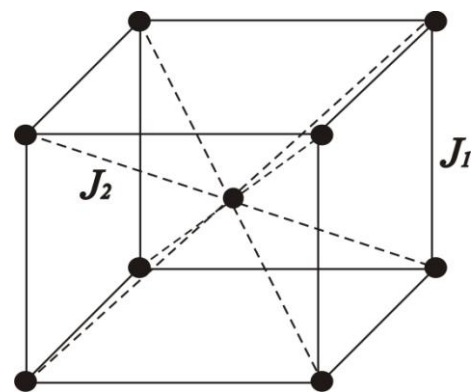


Fig. 1. Schematic representation of the antiferromagnet on a body-centered-cubic lattice.

[1] Vik.S. Dotsenko, *Usp. Fiz. Nauk*, **165** (1995) 481.

[2] A.K. Murtazaev, M.K. Ramazanov, *Phys. Rev. B*, **76** (2007) 174421.

[3] A.K. Murtazaev, M.K. Ramazanov, M.K. Badiev, *JETP*, **105** (2007) 1011.

[4] H.T. Diep, *Phys. Rev. B*, **39** (1989) 397.

[5] D. Loison, *Physics A*, **275** (1999) 207.

2PO-I1-16

EASY AXIS FLOP IN ϵ -PHASE IRON (III) OXIDE NANOWIRESDmitriev A.I.¹, Namai A.², Tokoro H.², Ohkoshi S.², Morgunov R.B.¹¹ IPCP RAS, Chernogolovka, Russia² Department of Chemistry, School of Science, University of Tokyo, Tokyo, Japan
aid@icp.ac.ru

Polymorphic ϵ -modification of iron (III) oxide (ϵ -Fe₂O₃) has giant coercive force (up to 2.34 T) at room temperature. Coercive force is one of the important criteria of applicability of a material in magnetic memory engineering and spintronics. In addition, the ϵ -Fe₂O₃ phase exhibits magnetoelectric properties and is known to be a good absorber of millimetre electromagnetic waves [1]. The ϵ -Fe₂O₃ nanoparticles absorb microwaves below 182 GHz frequencies in zero external magnetic field, i.e. they possess “natural” ferromagnetic resonance. The resonant microwave frequency can be controlled by admixture of various impurities (Al, Ga, In) in the sample [2]. These reasons as well as possibility to use the oxide for spin battery engineering stimulated our interest to magneto-crystalline anisotropy and its contribution to the magnetization of ϵ -In_{0.24}Fe_{1.76}O₃ diluted magnetic compounds.

This work reports on a study of magnetic properties of ordered arrays of ϵ -In_{0.24}Fe_{1.76}O₃ nanowires possessing a room-temperature coercive force of 6 kOe. Well certified arrays of oriented ϵ -In_{0.24}Fe_{1.76}O₃ nanowires doped with indium and containing no inclusions of other polymorphic modifications of iron oxide were used in experiments.

1. We have separated contributions of the high-temperature hard-magnetic and the low-temperature soft phases of ϵ -In_{0.24}Fe_{1.76}O₃ nanowires.
2. Magnetic resonance response to the magnetic phase was studied.
3. The types of magnetic ordering in the high- and low-temperature magnetic phases were determined.
4. Recognizing of the spin-flop transition of anisotropy easy axis was identified.
5. Lines related to the high-temperature and low-temperature phases have been identified in ferromagnetic resonance spectra of the nanowires. A line lying near zero magnetic field and evolving from “natural” ferromagnetic resonance has also been detected. Lowering the temperature below 190 K brings about a sharp decrease of the coercive force and magnetization of nanowires driven by the spin-flop transition [3].

Supported by the Grant of the President of Russian Federation MK-1598.2014.3.

[1] S. Ohkoshi, S. Kuroki, S. Sakurai, K. Matsumoto, K. Sato, S. Sasaki, *Angew. Chem.*, **46** (2007) 8392-8395.

[2] S. Sakurai, S. Kuroki, H. Tokoro, K. Hashimoto, S. Ohkoshi, *Adv. Funct. Mater.*, **17** (2007) 2278-2282.

[3] A.I. Dmitriev, O.V. Koplak, A. Namai, H. Tokoro, S. Ohkoshi, R.B. Morgunov, *Physics of the Solid State*, **55** (2013) 2252-2259.

2PO-11-17

TEMPERATURE DEPENDENCE OF ELECTRONIC AND MAGNETIC PROPERTIES OF $(\text{DOEO})_4[\text{HgBr}_4]\cdot\text{TCE}$ SINGLE CRYSTALS

Chernenkaya A.^{1,2}, Kotov A.³, Medjanik K.², Gloskovskii A.⁴, Nagel P.⁵, Merz M.⁵, Schuppler S.⁵, Morgunov R.³, Yagubskii E.³, Elmers H.J.², Schönhense G.²

¹ Graduate School Materials Science in Mainz, Staudinger Weg 9, 55128, Mainz, Germany

² Institut für Physik, Johannes Gutenberg-Universität, Staudinger Weg 7, 55128, Mainz, Germany

³ Institute of Problems of Chemical Physics, Russian Academy of Science, 142432 Chernogolovka, Russia

⁴ Deutsches Elektronen-Synchrotron DESY, Notkestr. 85, 22607 Hamburg, Germany

⁵ Karlsruhe Institute of Technology, Institut für Festkörperphysik, Hermann-v.-Helmholtz-Platz 1, 76344 Eggenstein-Leopoldshafen, Germany
chernenk@uni-mainz.de

We investigated $(\text{DOEO})_4[\text{HgBr}_4]\cdot\text{TCE}$ crystals that were synthesized in Prof. Yagubskii group (Chernogolovka, Russia) using SQUID magnetometry as well as using synchrotron techniques like near-edge X-ray adsorption fine structure (NEXAFS) and hard X-ray photoelectron spectroscopy (HAXPES).

We found evidence of an antiferromagnetic phase that exists in $(\text{DOEO})_4[\text{HgBr}_4]\cdot\text{TCE}$ below 40 K. We characterize occupied and unoccupied electronic states in the crystals. We observed Sulfur 2s and Chlorine 2p HAXPES core-level spectra at different temperatures (Fig. 1). They provide evidence of electron density redistribution in DOEO layers upon cooling and correlations between phase transition and electronic states in the crystals. Furthermore we investigated Sulfur 2p and Oxygen 1s NEXAFS edges and found fingerprints of charge carrier redistribution and localization at $T < 50$ K. Based on temperature dependences of magnetic susceptibility, transport properties [1], electron spin resonance study [2] and electron density distribution we propose an ambient pressure phase diagram of $(\text{DOEO})_4[\text{HgBr}_4]\cdot\text{TCE}$.

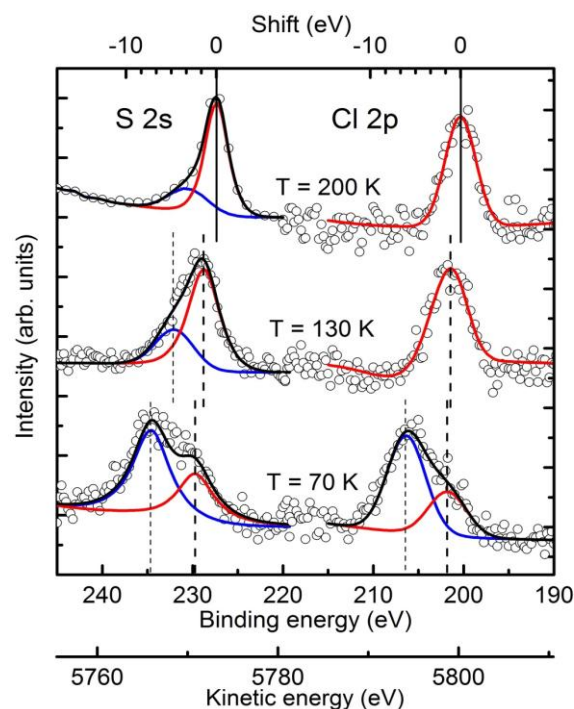


Fig. 1. S2s and Cl2p HAXPES core-level spectra of $(\text{DOEO})_4[\text{HgBr}_4]\cdot\text{TCE}$. The solid lines denote the decomposition of the spectra by a least squares fit.

The project is funded through Transregio SFB TR 49 (Frankfurt, Mainz, Kaiserslautern) and Graduate School of Excellence MAINZ.

[1] A. Bardin et. al., *Coord. Chem.*, **32** (2006) 88.

[2] A. Chernenkaya, et. al., *Phys. Sol. St.* **54** (2012) 2391.

2PO-I1-18

STRUCTURE AND MAGNETIC PROPERTIES OF FeNi/Ti MULTILAYERED FILMS GROWN BY MAGNETRON SPUTTERING

Svalov A.V.^{1,2}, *Vas'kovskiy V.O.*², *Larrañaga A.*³, *Kurlyandskaya G.V.*^{1,2}

¹ Depto. Electricidad y Electrónica, Universidad del País Vasco (UPV/EHU), Bilbao, Spain

² Dept. Magnetism and Magnetic Nanomaterials, Ural Federal University, Ekaterinburg, Russia

³ SGIker, Universidad del País Vasco (UPV/EHU), Bilbao, Spain

andrey.svalov@ehu.es

Permalloy thin films are widely used in magnetoelectronic devices due to their favourable soft magnetic properties. Non-magnetic metal thin layers are typically used as an encapsulation material for permalloy films in magnetoresistive sensors, in patterned nanomagnetic structures [1]. Titanium is also used as a non-magnetic component layer in multilayered structures. In particular, the sputtered FeNi/Ti multilayers were successfully used for development of thin film structures with high value of giant magnetoimpedance [2]. However, adjacent non-magnetic layers can strongly influence the properties of a magnetic layer. In this work, the microstructure and magnetic properties of FeNi/Ti multilayers prepared by magnetron sputtering were studied.

The thickness of the FeNi layers (L_{FeNi}) in $[\text{FeNi}/\text{Ti}]_n$ ($n = 8$ or 16) multilayered structures were varied in the interval of 1.5 nm to 50 nm. The thickness of Ti layers was kept constant (6 nm). A magnetic field of 250 Oe was applied parallel to the film plane during deposition in order to induce a uniaxial magnetic anisotropy. Magnetic properties were studied by vibrating sample magnetometer. Magnetic domain structure was studied by Bitter and magneto-optical Kerr effect techniques.

It was found that the FeNi magnetization saturation value (M_s) decreases with the decrease in magnetic layer thickness (Fig. 1, dots). This could be explained in terms of the interfaces' variable composition with reduced magnetization. A probable cause of the interface formation is interlayer mixing. The depths for mixed interfaces is estimated to be as high as 1 nm. A simple model for the description of the interface formation was proposed. The calculation agrees satisfactorily with the experimental $M(L_{\text{FeNi}})$ dependence (Fig. 1, line). The presence of (FeNi)Ti phase formed by the interdiffusion of FeNi and Ti layers was confirmed by x-ray diffraction measurements.

The coercive force of multilayers (H_c) increases strongly at small values of L_{FeNi} . It was shown that a decrease in M_{FeNi} makes a dominant contribution to the coersivity increase. This assumption was confirmed by the lineal dependence of the H_c on $(M_{\text{FeNi}})^{-1}$.

This work has been supported by the Spanish Government grant MAT2011-27573-C04 and the Actimat project of the EtorTek programme of the Basque Government.

[1] G.N. Kakazei, *et al.*, *Appl. Phys. Lett.*, **99** (2011) 052512-3.

[2] G.V. Kurlyandskaya, *et al.*, *IEEE. Trans. Magn.*, **48** (2012) 1375-1380.

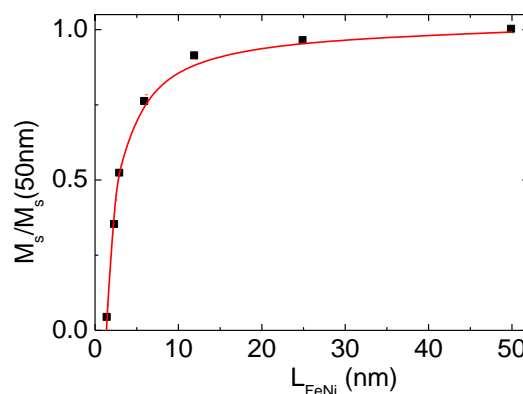


Fig. 1. Dependence of normalized magnetization on the FeNi layer thickness.

2PO-I1-19

REDUCTION OF NOISE INTENSITY IN SYSTEM OF FERROMAGNETIC NANOPARTICLES UNDER ASYMMETRIC STOCHASTIC RESONANCE CONDITIONS

*Isavnin A.G.*¹

¹ Kazan (Volga region) federal university, - Naberezhnye Chelny – RUSSIA
isavnin@mail.ru

Effect of stochastic resonance means previous quite sharp increase and subsequent gradual decay of response of a multistable system to a weak periodic modulation as internal noise of the system goes up [1]. Generally external periodic signal is assumed to be weak, so without noise any transitions between stable states of the system are impossible. At a certain noise intensity regular part of dynamics of the system increases, that is the transformation of stochastic energy into coherent one occurs. At greater noise intensities the coherency of signal and noise fails and the response goes down.

Single-domain magnetic particles with «easy axis» anisotropy are bistable elements with steady states associated with two opposite directions of easy axis. In previous papers stochastic resonance was considered in fine magnetic particles for thermal [2] and tunneling [3,4] modes of magnetization reversal. Obtained results displayed specific non-monotonous dependence of the response to radiofrequency signal on the noise level. Values of signal-to-noise ratio and components of dynamic magnetic susceptibility derived within the two-state approximation were verified by means of numerical calculations [5], based on a Fokker-Planck equation with periodic drift term.

Here we consider the influence of additional external magnetic field applied at arbitrary angle to the easy axis on output thermal noise power as stochastic resonance rises. The field distorts symmetry of double-well potential and results in inequality of the Kramers escape rates from two minima. The discrete-orientations approximation is used in the calculations. Power spectrum of the system as Fourier transform of the autocorrelation function displays Lorentzian background associated with stochastic dynamics and delta-spike describing regular motion of the magnetic moment vector at the frequency of external signal.

As well, we consider underbarrier mode of magnetization reversal due to the macroscopic quantum tunneling effect [3,4] at different directions of the auxiliary constant field in the regime of stochastic resonance.

Output power of the system can be derived by means of power spectrum integrating over frequency. So we have obtained analytical expressions describing dependence of thermal noise intensity on some external and internal parameters of the system of ferromagnetic nanoparticles, including value and direction of additional permanent magnetic field, under conditions of stochastic resonance. The ratio of output power of the modulated system to output power of the non-modulated system reveals non-monotonous dependence on temperature with a distinct minimum.

1. B. McNamara, K. Wiesenfeld, *Phys.Rev.A*, **39** (1989) 4854-4869.
2. E.K. Sadykov, A.G. Isavnin, *Hyperfine Interactions*, **99** (1996) 415-419.
3. E.K. Sadykov, A.G. Isavnin, A.B. Boldenkov, *Phys. of the Solid State*, **40** (1998) 474-476.
4. A.G. Isavnin, *Physics of the Solid State*, **43** (2001) 1263-1266.
5. A.G. Isavnin, *Russian Physics Journal*, **45** (2002) 1110-1114.

2PO-I1-20

ASYMMETRIC EXCHANGE BIAS DRIFT AT ROOM TEMPERATURE IN CoFe/FeMn BILAYERS

Jiménez E.¹, Cavicchia D.², Mikuszeit N.³, D'Orazio F.⁴, Rossi L.⁴

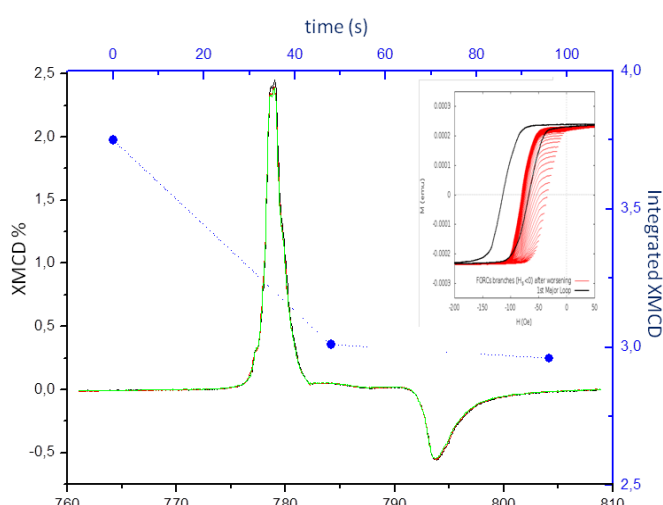
¹ ESRF ID08, Grenoble, France

² Institut für Angewandte Physik, Universität Hamburg, Germany

³ Cea Grenoble INAC/SP2M/NM, Grenoble, France

⁴ Dipartimento di Scienze Fisiche e Chimiche, Università di L'Aquila, Italy

Erika.Jimenez@esrf.fr



XMCD signal at Co-edge decrease when under applied external magnetic field, the temporal evolution of the XMCD area is shown by the symbols. Inner graph show the Forc measurements performed by MOKE.

mT coercive field. Periodic hysteresis measurements, i.e. first order reversal curves (FORC) [3] at room temperature, however, reduce the EB field significantly. Reversing the applied field procedure does not result in the initial state. This behavior is confirmed by XMCD measurements. The element specific XMCD measurements allow to study the uncompensated moments of the antiferromagnet and their evolution in time when applying an external magnetic field. The amount of uncompensated moments decreases with time. The stronger the applied field the more pronounced the decrease. The variation of uncompensated moments is in good agreement with the variation of EB field. Different layer thicknesses show the same behavior, supporting the interfacial nature of the effect.

The possibility of easy field control of EB enables new insights in the microscopic details of exchange bias.

[1] J. Nogues, and I. K. Schulle, *J. Magn. Magn. Mater.*, **192** (1999) 203.

[2] E. Jiménez, *et al.*, *Phys. Rev. B*, **80** (2009) 014415.

[3] C. R. Pike. *et al.*, *J. Appl. Phys.*, **85** (1999) 6660.

With respect to exchange bias systems it is mainly agreed on that pinned and unpinned uncompensated moments at the interface play an important role [1,2], while the full picture of all underlying microscopic mechanisms yet has to be developed. The amount and nature of the uncompensated moments depend among others on the interface quality. This influences coercivity enhancement, maximum exchange bias field, and the accordingly required field cooling procedure.

We present results on in-plane magnetized CoFe films on antiferromagnetic FeMn grown by rf magnetron sputtering at room temperature. Magnetic characterization has been done using the magneto-optic Kerr effect (MOKE) and X-ray circular dichroism (XMCD) measurements. After a field cooling procedure of 50 mT MOKE results show a very large negative exchange bias (EB) of 10 mT, compared to 0.7

2PO-I1-21

FOURFOLD MAGNETIC ANISOTROPY OF CoPd ALLOY, OBTAINED BY SOLID STATE REACTIONS IN EPITAXIAL Pd/hcp-Co AND Pd/fcc-Co BILAYERS

Myagkov V.G.¹, Bykova L.E.¹, Zhigalov V.S.¹, Bondarenko G.N.²

¹ Kirensky Institute of Physics, Russian Academy of Sciences, Siberian Branch, Krasnoyarsk, 660036 Russia

² Institute of Chemistry and Chemical Technology, Russian Academy of Sciences, Siberian Branch, Krasnoyarsk, 660049 Russia
miagkov@iph.krasn.ru

Multilayers with perpendicular magnetic anisotropy (PMA) continue to attract attention and are intensively investigated for practical applications as a medium for perpendicular recording media, bit-patterned media, and magnetic random access memory [1]. The Co/Pd multilayer samples have PMA $\sim 8 \cdot 10^5$ J/m³ [2], which is slightly less than in high uniaxial magnetocrystalline anisotropy materials [3]. Experimental observations show that a heating to ~ 400 °C does not change the magnetic properties of Co/Pd multilayers. However, annealing at temperatures above 400 °C causes the degradation of PMA and the in-plane direction becomes the easy axis of magnetization. It may be explained by the fact that heating causes mixing and alloying at the originally sharper Pd/Co interfaces [4-6].

In this work we have compared the structural and magnetic evolutions of the Pd/hcp-Co (110) and Pd/fcc-Co (001) bilayers with 1Co:1Pd composition as functions of the annealing temperature. No significant intermixing of the layers occurs at annealing temperatures below 400 °C in the bilayers and no compounds are formed. After annealing at 450 °C the disordered solid solution fcc-Co_xPd_{1-x} is formed on the Pd/hcp-Co (110) and Pd/fcc-Co (001) interfaces. After annealing at 650 °C the synthesis of the fcc-Co_xPd_{1-x} phase is completely finished. Lack of (001) superstructure reflex argues that the formed CoPd is a disordered phase. The disordered fcc-CoPd phase has lattice parameter $a = 0.37135$ (4) nm. Epitaxial relationships $\text{CoPd (110)} \langle -111 \rangle \parallel \text{MgO(001)} \langle 100 \rangle$ and $\text{CoPd(001)} \langle 100 \rangle \parallel \text{MgO(001)} \langle 100 \rangle$ between the nucleated disordered phase CoPd and the substrate MgO(001) were determined for Pd/hcp-Co (110) and Pd/fcc-Co (001) bilayers, respectively. CoPd(110) and CoPd(001) orientations of synthesized crystallites inherit orientations of the hcp-Co (110) and fcc-Co (001) initial layers. With increasing annealing temperature, the fourfold in-plane magnetic anisotropy constants change in accordance with changes in the phase composition of Pd/hcp-Co (110) and Pd/fcc-Co (001) bilayers. The first magnetocrystalline anisotropy constants for the (110) and (001) orientations of the disordered phase CoPd have values close to $K_1^{\text{CoPd}} = - (1.8 \pm 0.4) \cdot 10^4$ J/m³. A possible mechanism for solid-state synthesis of the fcc-Co_xPd_{1-x} solid solution is discussed.

[1] B.D. Terris, *J. Magn. Magn. Mater.* **321** (2009) 512.

[2] Z. Liu, et al., *J. Magn. Magn. Mater.* **323** (2011) 1623.

[3] D. Weller, et al., *IEEE Trans. Magn.* **36** (2000) 10.

[4] K. Yakushiji, et al, *Appl. Phys. Lett.* **97** (2010) 232508.

[5] M. Gottwald, et al., *Appl. Phys. Lett.* **102** (2013) 052405.

[6] A. Murdoch, et al., *Surf. Sci.* **608** (2013) 212.

2PO-I1-22

MICROMAGNETIC KINETICS OF MAGNETIZATION REVERSAL OF PATTERNED SOFT FERROMAGNET THIN FILMS

Kabanov Yu.P.¹, Gornakov V.S.^{1,2}, Shull R.D.², Chen P.J.², Dennis C.L.², Nikitenko V.I.^{1,2}

¹ Institute of Solid State Physics, RAS, Chernogolovka, 142432, Russia

² National Institute of Standards and Technology, Gaithersburg, MD 20899 USA

kabanov@issp.ac.ru

Soft nanomagnets such as thin-film Permalloy (Py) are the subject of intense fundamental and applied scientific research. The magnetization reversal in this material with restricted lateral sizes is mostly governed by the magnetostatic fields, localized in the edges. Depending on the Py film thickness, a domain structure with three types of domain walls (DWs) – Bloch wall, cross-tie structure, and Néel wall – may be realized in such films [1]. The reversal of these films is controlled by the formation and motion kinetics of the DWs. In micrometre and submicrometre scale materials, their size and shape play a significant role [2]. In our report, we present both experimental and simulation results of the magnetization distribution and transformation during the reversal of microstructured Py thin films having various lateral geometries and sizes.

The effect of shape and edges in the magnetic elements with reduced dimensions on the magnetization reversal of a cross and a square-mesh shaped film of Ni₈₁Fe₁₉ (30nm) were studied. The stripes of the patterned structures had ~3, 10, 15, and 30 μm widths and either 10 or 85 μm lengths. Details of the remagnetization in these structures were visualized by the magneto-optical indicator film (MOIF) technique. The hysteresis loops were measured in a vibrating sample magnetometer.

The MOIF imaging revealed that magnetostatic fields, which are formed on the edges perpendicular to the applied field during the sample magnetization reversal, induce a canted state of the spins exclusively along the stripe edges. With decreasing field, the spins rotate parallel to the edge in order to minimize the magnetostatic energy near the edge. Due to the FM exchange interaction, the spins further from the edge also rotate with decreasing field toward the edge spin direction. When the spin deviations near the two opposite edges become perpendicular to the interior spins one or two Néel domain walls will appear, depending upon whether the spin canting directions near the opposite edges of the stripes are respectively the same or not. This work established that the magnetization switching of such stripes occurs through the formation of a cross-tie structure followed by its transformation and annihilation, simultaneously with the homogeneous rotation of the spins inside the domains. The reversal process in the parallel to applied field stripes is quite different; it occurs separately for each stripe. In this case, the magnetization switching of stripes occurs by the nucleation and motion of unusual magnetization fronts, which consist of a number of coupled vortices located along both edges. The experimental results are in good agreement with simulation results.

[1] A. Hubert and R. Schafer, *Magnetic Domains*, 3th ed. Berlin, Springer, Germany (2008).

[2] L.A. Fomin, I.V. Malikov, S.V. Pyatkin, et al., *J. Magn. Magn. Mat.*, **322** (2010)851-857.

2PO-I1-23

FINITE SIZE EFFECTS IN MAGNETIC MULTILAYERS INDUCED BY INTERACTION WITH THE SUBSTRATE

Kostyuchenko M.V.¹

¹ Yaroslavl State Technical University, Yaroslavl, Russia
mkspin@mail.ru

Striking physical properties of the magnetic multilayers and the inviting prospects of their applications have recently attracted a great deal of research interest. It has been repeatedly mentioned that the substrate and the overlayer exert influence on the magnetic properties of the multilayers [1]. In this work the technique of finite difference equations [2] was used to analytically investigate the influence of the substrate on the distribution of the magnetization in magnetic multilayers within the framework of the model of the strong coupling with the substrate for a small-angle deflection of the magnetization vector in the boundary layer towards the easy axis. In this issue the external magnetic field was applied along the easy axis. The multilayer with equal magnetic layers and the ferrimagnetic multilayer were considered. Heisenberg and biquadratic exchange interactions and the uniaxial anisotropy were taken into account. The analytical dependencies of the total magnetization on the external magnetic field were obtained for the finite multilayer with an arbitrary number of equal magnetic layers and for the ferrimagnetic multilayer in the odd and the even cases. It was shown that the asymptotic stability condition of the ferromagnetic phase towards such boundary disturbances for the finite multilayer coincides with the stability condition for the infinite multilayer. The total magnetization of the finite multilayer with equal magnetic layers doesn't reach the saturation at a finite magnitude of the field, but verges towards the saturation with the increase of the field. This result is in a qualitative agreement with the experimental data [3]. The total magnetization of the ferrimagnetic multilayer exhibits a significant difference in the odd and the even cases. Finite size effects are appeared both in the finite multilayer with equal magnetic layers (Fig.1) and in the ferrimagnetic multilayer due to the dependence of the tilting angle of magnetization vector of n th-layer φ_n on the total magnetic layer number $N+1$ (φ_n and φ_0 are the tilting angles of magnetization vector of n th-layer and of 0-layer, h_c is a critical field value of the stability condition of the ferromagnetic phase).

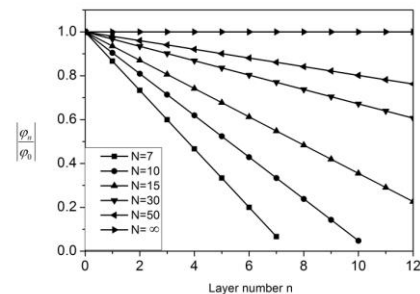


Fig. 1. The dependence of φ_n on n at $h = h_c$ for various values N .

[1] M.E.Backley, F.O.Schumann and J.A.C.Bland, *Phys.Rev.B* **52** (1995) 6596.

[2] V.V.Kostyuchenko, *Solid State Phenomena*, **152-153** (2009) 245.

[3] A.Schreyer, J.F.Ankner, T.Zeidler, H.Zabel, M. Schäfer, J.A.Wolf, P.Grünberg, C.F.Majkrzak, *Phys.Rev.B* **52** (1995) 16066.

2PO-I1-24

THERMODYNAMICS OF FRUSTRATED MAGNETS: HIGH-TEMPERATURE EXPANSION REVISITED

*Schmidt H.-J.*¹, *Richter J.*², *Lohmann A.*²

¹ Universität Osnabrück, Fachbereich Physik, Germany

² Institut für Theoretische Physik, Universität Magdeburg, Germany
Johannes.Richter@Physik.Uni-Magdeburg.DE

We present the high-temperature expansion (HTE) up to 10th order of the specific heat C and the uniform susceptibility χ for Heisenberg models with arbitrary exchange patterns and arbitrary spin quantum number s . We encode the algorithm in a C++ program provided at <http://www.uni-magdeburg.de/jschulen/HTE10/> which allows to get explicitly the HTE series for concrete Heisenberg models [1,2]. We use our HTE scheme to study the specific heat and the susceptibility of frustrated quantum magnets. In particular, we consider magnetic systems with highly degenerate classical ground states, such as the kagome, the checkerboard, the square-kagome, the J1-J2, as well as the pyrochlore antiferromagnets. We investigate to what extent strong frustration is evident at moderate and high temperatures. Moreover, we discuss the influence of the spin quantum number s on the thermodynamic properties and compare this way quantum and classical systems.

[1] H.-J. Schmidt, A. Lohmann, and J. Richter, *Phys. Rev. B*, **84** (2011) 104443.

[2] A. Lohmann, H.-J. Schmidt and J. Richter, *Phys. Rev. B*, **89** (2014) 014415.

2PO-I1-25

MAGNETIC PROPERTIES OF NANOCOMPOSITES METAL-CARBON*Aleshnikov A.A.¹, Al Azzavi H.C.M.¹, Kalinin Yu.E.¹, Sitnikov A.V.¹, Tarasova O.S.¹*¹ Voronezh State Technical University, 394026, Voronezh, Russia

sitnicov04@mail.ru

The films of heterogeneous systems based on ferromagnetic alloy and C were produced with the help of ion-beam sputtering of the composite target. The synthesized compounds $(\text{Co}_{40}\text{Fe}_{40}\text{B}_{20})_x(\text{C})_{100-x}$, $(\text{Co}_{84}\text{Nb}_{14}\text{Ta}_2)_x(\text{C})_{100-x}$, $(\text{Co}_{45}\text{Fe}_{45}\text{Zr}_{10})_x(\text{C})_{100-x}$, $(\text{Ni})_x(\text{C})_{100-x}$, $(\text{Co})_x(\text{C})_{100-x}$ in a wide range of concentrations of the metal phase.

The study of the structure of obtained composites showed that the latter represent a heterogeneous system of metal granules size 2-4 nm in amorphous carbon matrix.

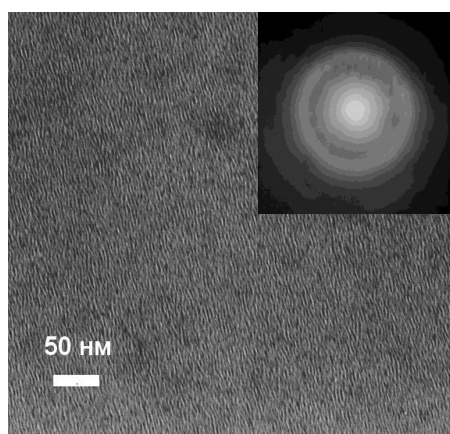


Fig.1 - Microphotography and electronic diffraction composite $(\text{Co}_{40}\text{Fe}_{40}\text{B}_{20})_{70,7}(\text{C})_{29,3}$

The analysis of the concentration dependences of electric resistivity, showed that the percolation threshold investigated composites shifted towards greater concentration of the metal phase compared with the theoretically calculated values. It is assumed that the formation of the heterogeneous structure is uniform coverage of the surface of metal granules carbon atoms (Table 1).

Low specific electrical resistance of nanocomposites are investigated before and after the course is associated with low specific electrical resistance of a carbon matrix.

Table 1

Composites	X _{III} , at. %	The range of change x, at. %	The range of change ρ , $(10^{-6}) \text{ Ohm}\cdot\text{m}$
$(\text{Co})_x(\text{C})_{100-x}$	62	38 - 70	1-8
$(\text{Ni})_x(\text{C})_{100-x}$	70	22 - 90	0,6 - 3,8
$(\text{Co}_{40}\text{Fe}_{40}\text{B}_{20})_x(\text{C})_{100-x}$	62	48-72	0,6 - 3,6
$(\text{Co}_{45}\text{Fe}_{45}\text{Zr}_{10})_x(\text{C})_{100-x}$	55	20-59	2 - 300
$(\text{Co}_{84}\text{Nb}_{14}\text{Ta}_2)_x(\text{C})_{100-x}$	59	42-72	2-20

The conducted research of magnetostatic and magnetodynamic properties of heterogeneous metal-carbon showed that compounds $(\text{Co})_x(\text{C})_{100-x}$ $(\text{Co}_{40}\text{Fe}_{40}\text{B}_{20})_x(\text{C})_{100-x}$ $(\text{Co}_{45}\text{Fe}_{45}\text{Zr}_{10})_x(\text{C})_{100-x}$ after the percolation threshold have good soft magnetic properties. Thermal processing of these composites reduces coercive force, increases the magnetic permeability and significantly increases the value of complex magnetic permittivity at frequency of 50 MHz.

Composite $(\text{Ni})_x(\text{C})_{100-x}$ after the percolation threshold high coercive force, what is the reason of the low values of complex magnetic permittivity at frequency of 50 MHz. In composite $(\text{Co}_{84}\text{Nb}_{14}\text{Ta}_2)_x(\text{C})_{100-x}$ was significantly perpendicular magnetic anisotropy, which may be related to structural peculiarities of the heterogeneous structure.

This work was supported by RFBR (project number 13-02-97511-r_tsentr_a).

2PO-I1-26

SURFACE MODIFICATION OF THIN IRON FILMS IN AROMATIC SOLVENTS AT AMBIENT CONDITIONS

*Zalbidea Arechaga I.¹, Chlenova A.A.², Kurlyandskaya G.V.^{1,2}, Safronov A.P.³, Larrañaga A.⁴,
Fernandez S.⁴, Lepalovskij V.N.²*

¹ Dept. Electricity and Electronics, Basque Country University UPV-EHU, Bilbao, Spain

² Dept. Magnetism and Magnetic Nanomaterials, Ural Federal University, Ekaterinburg, Russia

³ Dept. Macromolecules, Ural Federal University, Ekaterinburg, Russia

⁴ SGIKER, Basque Country University UPV-EHU, Bilbao, Spain

anniaally@gmail.com

Many modern magnetic materials from magnetic sensors through bioactive surfaces and microwave absorbers require surface modification and functionalization. Recently we reported interesting phenomenon, the condensation reaction of aromatic organic compounds resulting in formation of irregular polycyclic structures on the surface of Fe or Ni nanoparticles immersed in toluene at ambient temperature [1]. The mechanism of carbon self-assembly at the elevated temperatures is well understood [2]. The mechanism of liquid-phase carbon deposition at ambient temperature onto the metal surface is different from the high temperature case. The objectives of the present work were to test the possibility of ambient deposition of carbon on the surface of Fe film, to study the kinetics of the deposition, to characterize the structure of the deposits by scanning electron microscopy, SEM (including energy dispersive analysis) and X-ray diffraction (Fig. 1). 300 nm iron films prepared by rf-sputtering were placed into toluene immediately after deposition. Periodic structural and magnetic measurements (vibrating sample magnetometer and magneto-optical Kerr effect) were performed on the dry samples just taken out of toluene. We observed that carbonaceous layers on the Fe surface are formed rather fast – they can be initially detected after about one week treatment. At the same time both surface and bulk magnetic properties are almost non-affected by the treatment up to 120 days. Surface modified iron films with carbonaceous deposits show high stability with respect to atmospheric oxygen and therefore such a treatment can be used for metallic surfaces protection.

Support by ETORTEK-ACTIMAT and CRDF and UB RAS RUE2-7103-EK-13 grant is acknowledged.

[1] I.V. Beketov, A.P.Safronov, A.V. Bagazeev, A. Larrañaga, G.V. Kurlyandskaya, A.I. Medvedev, *J. All. Comp.*, **586** (2014) S483–S488.

[2] Y. Saito, *Carbon*, **33** (1995) 979-988.

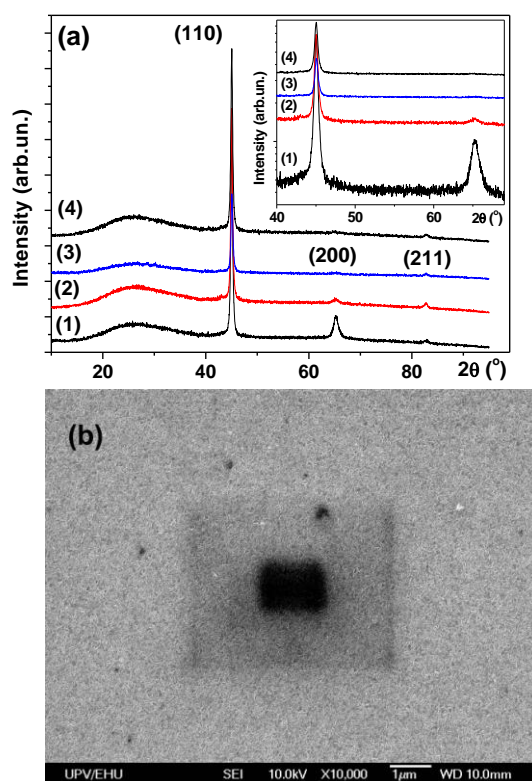


Fig. 1. XRD spectra of thin Fe film surface modified in toluene for 7 (1), 19 (2), 66 (3) and 112 (4) days; Bragg positions are also indicated (a). SEM image of the surface of iron film: two black areas clearly indicate the scanning track due to re-distribution of the carbon deposited during surface modification in toluene for 112 days.

2PO-11-27

MAGNETIC AND MAGNETOTRANSPORT PROPERTIES OF Fe-NbO SYSTEM

Tregubova T.N.¹, Semenenko K.I.¹, Grebennikov A.A.¹, Stognei O.V.¹

¹ Voronezh State Technical University, Voronezh, Russia
konst199i@yandex.ru

New composite system $\text{Fe}_x(\text{NbO})_{100-x}$ ($13 \leq x \text{ at.}\% \leq 79$) has been synthesized. Electrical, magnetic and magnetoresistive properties of these new $\text{Fe}_x(\text{NbO})_{100-x}$ composite materials have been investigated. Thin film composite samples were prepared by ion beam sputtering of iron and niobium oxide in argon and depositing of the material on a pyroceramic substrate.

Comparison of the formation enthalpy values of iron oxide and niobium oxide shown the large probability of nanogranular composite formation in the $\text{Fe}_x(\text{NbO})_{100-x}$ system. According to X-ray diffraction the obtained material actually contains two phases: an amorphous niobium oxide and a fine-grained bcc-iron (according to estimation the X-ray data the iron grain size is 2-3 nm in $\text{Fe}_{48}(\text{NbO})_{52}$ composite).

Concentration dependence of the electrical resistance of the $\text{Fe}_x(\text{NbO})_{100-x}$ samples is typical for metal/dielectric composites with a sharp resistance decrease at the percolation threshold. However, the position of the percolation threshold ($\sim 65 \text{ at.}\% \text{ Fe}$) is substantially displaced in a region with a high iron content, as compared with Fe-AlO or Fe-SiO composites.

The pre-percolation composites exhibit superparamagnetic properties near the threshold. When the iron concentration exceeds the 65 at. % the samples magnetization curves take the form typical for the ferromagnetic state. The coercive force of the composites is almost concentration independent and is equal to 4 - 7 Oe. Complex permeability of the composites (both imaginary and real parts), measured at 50 MHz, shows a sharp increase when the iron concentration becomes a bit larger than the percolation threshold (66 - 68 at. %), which is also typical for ferromagnetic/dielectric nanocomposites.

Despite the fact that all physical properties of the $\text{Fe}_x(\text{NbO})_{100-x}$ composites confirm the composite structure of the samples the magnetoresistive effect (one of the most striking effects of the ferromagnetic/dielectric nanocomposites) does not observed in the studied system.

Thermal annealing of the $\text{Fe}_x(\text{NbO})_{100-x}$ composites at 650 °C leads to a change of their properties. Firstly, the ferromagnetic properties begin to appear even at low iron concentrations (fig.1) and coercive force reaches quite large values (300 – 360 Oe). Concentration dependence of the coercive force passes through a maximum, which is probably due to the change of the iron grain size (increasing with Fe concentration) and can be explain within the randomly anisotropy model.

Secondly, tunneling isotropic magnetoresistance appears in the annealed composites at room temperature. Absolute values of magnetoresistance are small (less than 1 %) but it is observed in wide concentration range in spite of ferromagnetism.

Support by Russian Science Foundation (grant № 14-13-00403) is acknowledged.

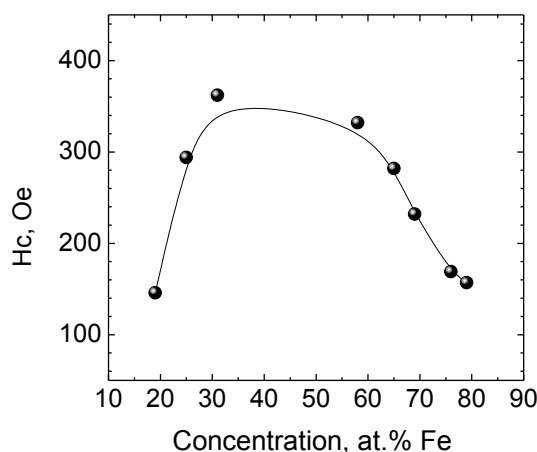


Fig. 1. Concentration dependence of the coercive force of $\text{Fe}_x(\text{NbO})_{100-x}$ composites annealed at 650 C.

2PO-I1-28

SYNTHESIS AND PHYSICAL PROPERTIES OF MULTILAYER MAGNETIC FILMS IN Co-Ni-P SYSTEM

Patrin K.G.^{1,2}, Kiparisov S.Ya.¹, Patrin G.S.^{1,2}, Shiyan Ya.^{1,2}, Yurkin G.Yu.^{1,2}

¹ L.V. Kirensky Institute of Physics, Siberian Branch of Russian Academy of Sciences, Krasnoyarsk, 660036, Russia

² Siberian Federal University, prospect Svobodny, 79, Krasnoyarsk, 660041, Russia
patrin@iph.krasn.ru

Appreciable interest to systems with spin-valve effect is caused by their practical use in devices of spin electronics. Here the problem of creation spin-polarized electrons is put in the forefront. The film systems with effect of exchange bias are convenient object for solution of this task. The interlayer coupling in such system is responsible for forming magnetic state. Namely the study of mechanisms of magnetization in multilayer magnetic films with alternate layers of soft and hard magnetic layers is the principal purpose of this report.

The $(\text{CoNiP}_{\text{soft}}/\text{NiP}/\text{CoP}_{\text{hard}})_n$ films were prepared by chemical deposition method. The phosphorus content in every magnetic layer was 8 %. In hard magnetic layer the CoP was in hexagonal polycrystalline state, and in soft magnetic layer the CoP was in amorphous state. The thickness of every magnetic layer was $t = 4$ nm. Interlayer NiP layer was in amorphous state and nonmagnetic. Such layer composition was chosen because the sharp change of structure on interface is absent when conjugation of layers takes place. For individual soft magnetic layer the temperature behavior of magnetization loops has character typical for soft magnetic ferromagnet, the coercive force ($H_C(T = 77.4 \text{ K}) \cong 15 \text{ Oe}$) decreases more than order with temperature increasing from nitrogenous temperature up to room one. The in-plane anisotropy of film is absent. For individual hard magnetic CoP layer the behavior is also ferromagnetic, but in this case ($H_C(T = 77.4 \text{ K}) \cong 950 \text{ Oe}$) and the change of H_C is half as much with temperature increasing from nitrogenous temperature up to room one [1]. The situation is noticeably changed when the sandwich is formed from such layers. The result is not algebraic sum of initial curves, here the inner loop is broadened as compared with initial curve of soft magnetic layer and the outer curve is appreciably shrunk. More one interesting point is connected with behavior of saturation field (H_S) of magnetization in dependence on n , notably, the saturation field for films with odd number of layers is higher than for films with even number of layers, and it has form of decaying oscillations.

With the view of control of interlayer coupling the films with nonmagnetic amorphous NiP interlayer were studied. For series of films with $t_{\text{NiP}} = 2$ nm it was found that the increase of layer number conduces to more strong appearance of step, which is arisen from hard magnetic layer, but the decrease of coercive force and saturation field take place. For films with large number n (> 20) the temperatures changes are weaker than for films with small n .

To study interlayer interactions the measurements of electron magnetic resonance parameters were made. It was found that resonance curve is superposition of three resonance lines where two lines belong to soft and hard magnetic layers, and the third line, apparently, belongs to phase formed on $\text{CoP}_{\text{hard}} - \text{NiP}$ interface.

This study was supported by Russian Foundation of Basic Researches, project № 14-02-00238.

[1] G.S. Patrin, M.G. Palchik, D.A. Balaev, S.Ya. Kiparisov, *Izvestiya RAN. Seriya fizicheskaya*, (in Russia) **77** (2013) 1230-1231.

2PO-I1-29

Cu(Qnx)(Cl_{1-x}Br_x)₂ AS A TUNABLE QUANTUM SPIN LADDER

Povarov K. Yu.^{1*}, Lorenz W. E. A.¹, Xiao F.²⁺, Landee C. P.², Krasnikova Y.^{3,4}, Zheludev A.¹

¹ Neutron Scattering and Magnetism, Laboratory for Solid State Physics, ETH Zurich, Switzerland

² Department of Physics, Clark University, Worcester, Massachusetts 01610, USA

³ P. L. Kapitza Institute for Physical Problems, RAS, 119334 Moscow, Russia

⁴ Moscow Institute for Physics and Technology, 141700 Dolgoprudny, Russia

* Previous address: P. L. Kapitza Institute for Physical Problems, RAS, 119334 Moscow, Russia

+ Present address: Department of Physics, Durham University, South Road, Durham, DH1 3LE, United Kingdom

povarovk@phys.ethz.ch

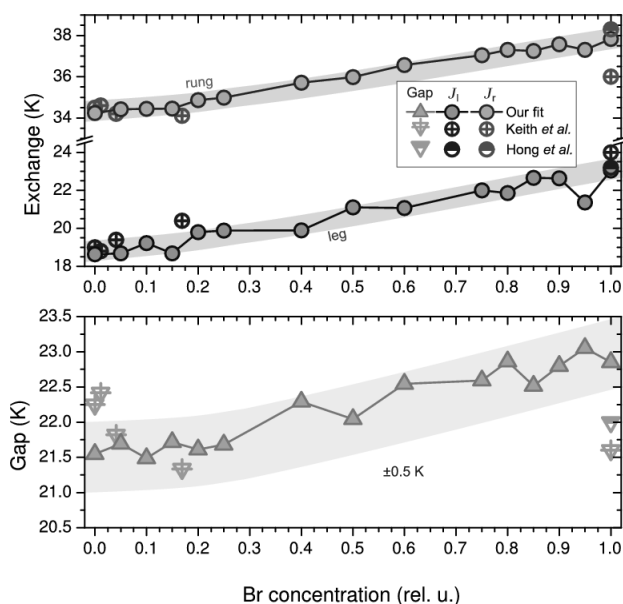


Figure 1: Spin Hamiltonian parameters and energy gap versus Br concentration x as determined by data analysis.

comparing the experimental data on susceptibility and magnetization to quantum Monte-Carlo simulations. The results are shown in Fig. 1 together with the data from preceding studies [1, 2]. As the ESR measurements show the g -factor of impurities to be precisely equal to g -factor of the ladder spins, we suppose the impurities to be the consequence of structural defects resulting in a broken ladder ends.

Support by Swiss National Fund, Division 2 and RFBR grant 12-02-31220 is acknowledged.

[1] B. Keith, F. Xiao, C. Landee, M. Turnbull, A. Zheludev, *Polyhedron*, **30** (2011) 3006.

[2] T. Hong, M. Kenzelmann, M. Turnbull et al., *Phys. Rev. B*, **74** (2006) 094434.

We report magnetic susceptibility, low-temperature magnetization and ESR measurements on a series of $S=1/2$ spin ladder compounds Cu(Qnx)(Cl_{1-x}Br_x)₂ (CQX) [1]. An important feature of this material family is that they all belong to the same structure type for any $0 \leq x \leq 1$. Thus, chemical substitution opens a route to creating spin ladders with continuously tunable exchange constants and magnetic properties. We demonstrate that this is indeed true, and undesirable effects due to structural disorder and potential randomness of magnetic interactions are negligible in CQX. Down to $T=2$ K all the observables can be described by the spin ladder model with about 1% of $S=1/2$ impurities in the background, which are present even in a nominally pure Cu(Qnx)Cl₂ and Cu(Qnx)Br₂, for the whole range of $0 \leq x \leq 1$. We extract leg and rung ladder exchange constants $J_l(x)$ and $J_r(x)$ as well as the gap value $\Delta(x)$ by

2PO-I1-30

MAGNETIC PROPERTIES OF Fe_2CoO_4 IN SHELLS OF HOLLOW CAPSULES STUDIED BY MOSSBAUER SPECTROSCOPY

Lin C.-R.¹, Gervits N.E.², Wang C.-C.¹, Lyubutin I.S.², Gippius A.A.³

¹ Department of Applied Physics National Pintung University of Education, Pintung City, Pintung County 90003, Taiwan

² Shubnikov Institute of Crystallography, RAS, Moscow 119333, Russia

³ Lomonosov Moscow State University, Moscow 119991, Russia
ngervits@gmail.com

Poly(MMA-co-MAA) microspheres were used as a core template to synthesize the hollow $\text{SiO}_2/\text{CoFe}_2\text{O}_4$ composite spheres using chemical co-precipitation, followed by the sol-gel method and then calcination. It was found that the polymer cores are completely removed from the hollow spheres after calcination at 450°C . Size control of the CoFe_2O_4 nanoparticles has been achieved through the variation of the calcined temperature T_{cal} from 300 to 900 C. The process of synthesis and morphology of the composites were controlled by X-ray diffraction, field emission scanning (FESEM) and transmission (TEM) electron microscopy, and the magnetic properties were investigated by Mössbauer spectroscopy and magnetic measurements.

It was shown that the monodisperse $\text{CoFe}_2\text{O}_4/\text{SiO}_2$ hollow magnetic spheres can be obtained (Fig. 1). The Co-ferrite nanoparticles in the shells gain the spinel crystal structure, and their size varies from 2 to 10 nm with increasing in the T_{cal} value.

It was found from the Mössbauer spectroscopy that the distribution of Fe and Co ions over octahedral (B) and tetrahedral (A) sites in the spinel structure is changed with variation of T_{cal} , which essentially influences the magnetic properties of the CoFe_2O_4 nanoparticles. The low-temperature Mössbauer spectra recorded between 10 and 300 K reveal superparamagnetic behavior of the particles, and the spin blocking temperature increases simultaneously with the T_{cal} value. This result correlates with the particle size of and magnetic measurements.

The magnetic properties of monodisperse $\text{CoFe}_2\text{O}_4/\text{SiO}_2$ hollow magnetic spheres can be tuned with relatively high accuracy at the stage of calcination. Magnetic measurements indicate that some of the samples exhibit ferromagnetic behavior with coercivity up to 375 Oe. The highest saturation magnetization value in this series was observed for the $T_{\text{cal}} = 900\text{C}$ sample, and it was about 40 emu/g which is 50% of bulk value.

This work is supported by the Presidium RAS program #24.3.1-“Nanodiagnostics”, by Russian Scientific Foundation and by the National Science Council of Taiwan (NSC96-2112-M-218-001-MY3).

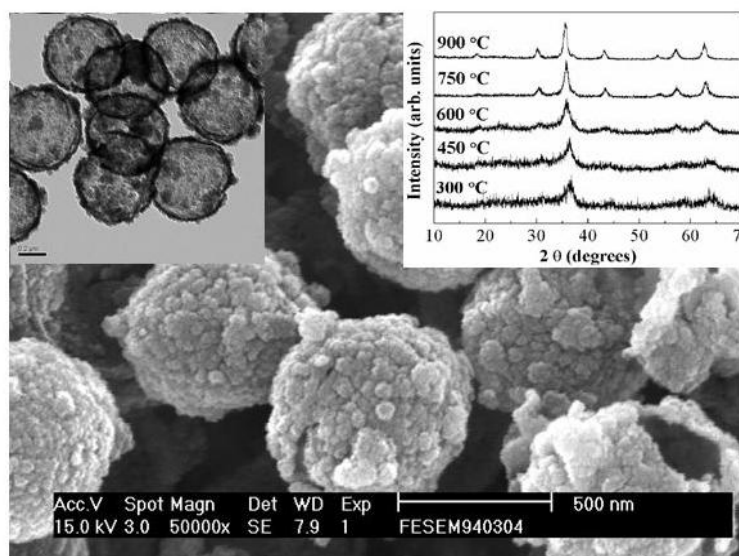


Fig. 1. The FESEM and TEM images and X-ray patterns of the $\text{SiO}_2/\text{CoFe}_2\text{O}_4$ nanocomposites.

2PO-I1-31

MORPHOLOGY AND MAGNETIC PROPERTIES OF AMORPHOUS Co-P AND Co-Ni-P FILMS

Chzhan A.V.^{1,2}, Seredkin V.A.¹, Patrin G.S.^{1,2}, Zablude V.N.¹, Zubavichaus Ya.V.³, Rudenko R.Yu.²

¹ Kirensky Institute of Physics, Siberian Branch of RAS, , Krasnoyarsk, 660036 Russia

² Siberian Federal University, Krasnoyarsk, 660041 Russia

³ National Research Center “Kurchatov Institute”, Moscow, 123182 Russia

avchz@mail.ru

One of the key issues in the development of spintronic devices based on sandwich structures comprising magnetic and nonmagnetic layers is the formation of sharp interfaces between layers. As was established in [1] for trilayers consisting of amorphous and polycrystalline Co-P alloys and a nanometer nonmagnetic Ni-P spacer, embedding of Ni atoms in the amorphous Co-P alloy significantly improves the quality of the interface between layers, which manifests itself in spacer thickness dependences of coercivity and field that shifts the hysteresis loop center in the magnetically soft layer.

The aim of this study was to investigate the morphology of amorphous Co-P films and their magnetic properties with and without nickel atoms.

Co-P and Co-Ni-P thin films were prepared by chemical deposition of ions onto glass substrates in a dc magnetic field. The phosphorous content in the Co-P films was 5.5 weight%. In the Co-Ni-P films, the cobalt content was 69.5; the nickel content, 25; and the phosphorous content, 5.5 weight%. The EXSAFS spectrum indicates the absence of a crystal phase in the films of both compositions. Embedding of Ni reduces the size of grains that occur due to the film growth features (Fig. 1) and roughness. The occurring structural variations are reflected on the magnetic properties of the films. The presence of Ni enhances the induced anisotropy constant and reduces its angular dispersion and coercivity.

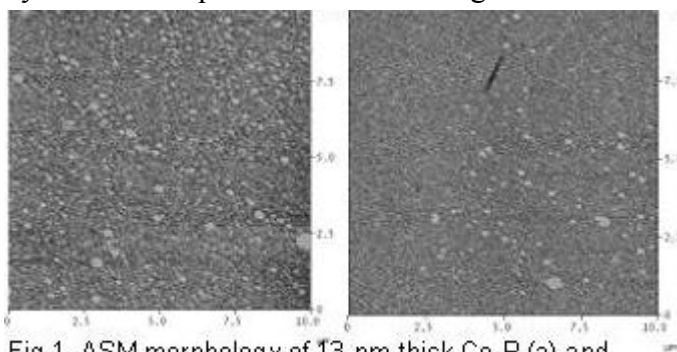


Fig.1. AFM morphology of 13-nm-thick Co-P (a) and Co-Ni-P (b) films.

[1] A.V. Chzhan, V.A. Seredkin, S.Ya. Kiparisov, and G.S. Patrin, *Bulletin of RAS. Physics*, **77** (2013) 1210-1212.

2PO-I1-32

ANISOTROPIC MAGNETORESISTANCE AND WEAK LOCALIZATION IN GRANULAR SYSTEM Ni-MgO

Grebennikov A.A.¹, Stognei O.V.¹

¹ Voronezh State Technical University, Voronezh, Russia
anton18885@yandex.ru

Magnetoresistive effect of $\text{Ni}_x(\text{MgO})_{100-x}$ (x : 21-48 at.%) granular composites has been investigated. Samples were obtained by ion-beam sputtering of composite Ni-MgO target. After preparation the samples were heat treated in a vacuum ($\sim 10^{-3}$ Pa) at 500 °C.

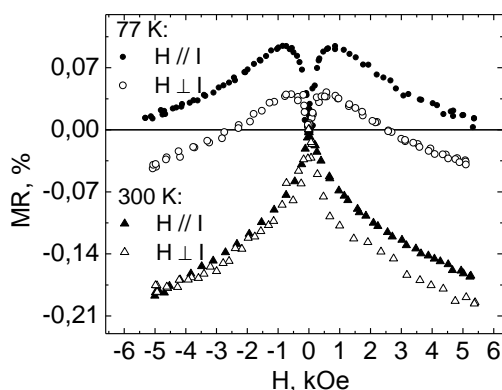


Fig. 1. Magnetoresistance of $\text{Ni}_{27}(\text{MgO})_{73}$ sample after air plasma processing

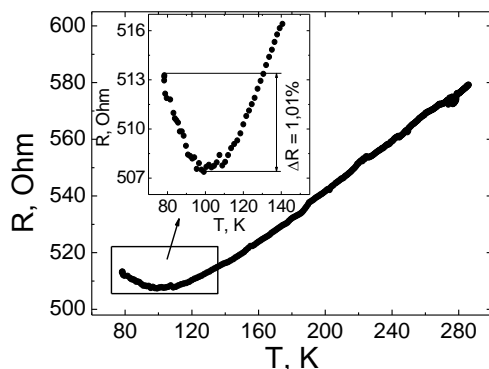


Fig. 2. Temperature dependence of resistance of $\text{Ni}_{27}(\text{MgO})_{73}$ sample

It is found by TEM that the structure of $\text{Ni}_x(\text{MgO})_{100-x}$ samples after heat treatment include two main phases: Ni (fcc, $a = 0,352 \pm 0,001$ nm) and MgO (fcc, $a = 0,421 \pm 0,001$ nm). The percolation threshold (x_C) in these composites is observed at 27 at.% of Ni concentration according to the analysis of the temperature dependences of the resistance measured in the range of 77-280 K.

The samples with Ni concentration below x_C do not show a magnetoresistance (MR) at room temperature. However at 77 K tunnel magnetoresistance (TMR) is observed in it. One can assume that the absence of TMR at 300 K is due to the low value of Curie temperature (T_C) in studied nanocrystalline Ni.

Anisotropic magnetoresistance (AMR) is observed in the samples with Ni concentration larger than 33 at.%. The AMR is due to the presence of volume percolation nickel clusters showing ferromagnetic properties at 300 K.

The weak localization is observed in the samples with Ni concentration of 27-29 at.%. The isotropic MR has been observed in these samples at 300 K. However at 77 K the positive MR arises (fig. 1). The temperature coefficient of resistance also changes its sign from positive to negative in these samples at 100 K (fig. 2): in the range of 100-280 K the sample resistance decrease with decreasing temperature, below 100 K the sample resistance increase with temperature decreasing. Increasing the value of the

resistance in the range of 77-100 K is typical for samples which exhibit weak localization (fig. 2, insert). Probably the weak localization is due to the large number of defects in the samples structure which are the centres of the electron scattering. The electron spin is not conserved in the scattering at temperature more than 100 K so weak localization is not observed. Below 100 K the elastic electron scattering with spin conservation occurs. Therefore weak localization is observed below 100 K.

Support by the Russian Science Foundation (Grant No 14-13-00403) is acknowledged.

2PO-I1-33

MAGNETIC ANISOTROPY IN Co-SUBSTITUTED MgFeBO₄ WARWICKITE

Platunov M.S.¹, Bayukov O.A.¹, Ivanova N.B.², Kazak N.V.¹, Bezmaternykh L.N.¹, Knyazev Yu.V.², Arauzo A.³, Bartolomé J.³, Ovchinnikov S.G.¹

¹ Kirensky Institute of Physics SB of RAS, Krasnoyarsk, Russia

² Siberian Federal University, Krasnoyarsk, Russia

³ Universidad de Zaragoza, Zaragoza, Spain

platunov.iph@krasn.ru

Mg_{1-x}Co_xFeBO₄ ($x = 0.0, 0.5, 1.0$) are mixed warwickites with orthorhombic structure (*Pnam* space group). The needles like single crystals were grown by flux method [1]. The XRD study was carried out in work [1]. The monotonic changes of the lattice parameters were observed with Co content. The present work is devoted to the magnetic study.

The magnetic measurements were carried out in wide intervals of the temperatures and applied magnetic fields and at the different orientations of the applied field regarding to the crystallographic axes (Fig. 1). All samples demonstrate a spin-glass behavior with a increasing of the transition temperature as a cobalt content increase ($T_{SG} = 10, 20, 22$ K).

The magnetic anisotropy is negligible for sample with $x = 0.0$. In contrast, anisotropy is found in the $x = 0.5$ compound, though it is small (Fig. 1b) and reaches maxima for the sample with $x = 1.0$ (Fig. 1c). So, the Co²⁺ ions induce uniaxial magnetic anisotropy (*b* is easy magnetization axis).

Spin-glass state is predicted by the superexchange interactions calculations and can be explained by the presence of the high level magnetic frustrations.

Support by RFBR № 12-02-00175, 14-02-31051-mol-a, 13-02-00958, 13-02-00358-a. the programs Leading Scientific Schools NSch 2886.2014.2

[1] A. Arauzo, N.V. Kazak, N.B. Ivanova, et al., Be published in 2014.

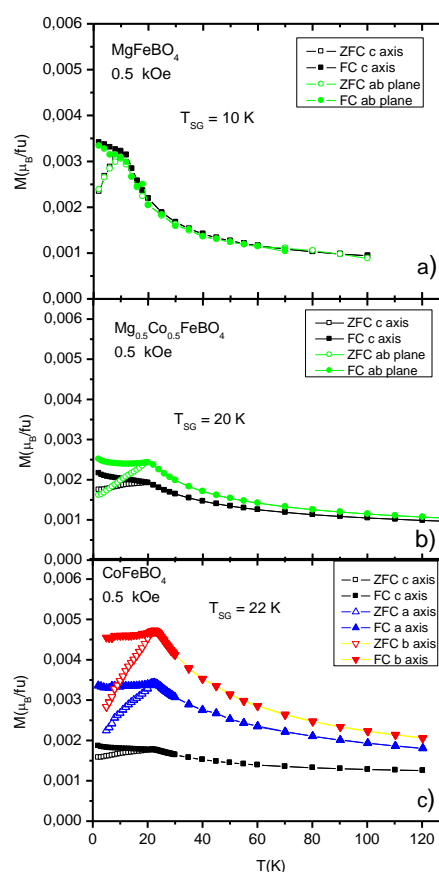


Fig. 1 Magnetization temperature dependence, showing a spin-glass transition

2PO-I1-34

THE PECULIARITIES OF MAGNETIC MICROSTRUCTURE OF THE TERNARY ORDERED Fe-Al-B ALLOYS

*Voronina E.V.*¹, *Yelsukov Eu.P.*², *Korolyov A.V.*³, *Maslennikova A.E.*¹, *Rusakov V.S.*⁴

¹ Institute of Physics, KFU, Kazan, Russia

² Physical-Technical Institute of UrB RAS, Izhevsk, Russia

³ Institute of Metal Physics UrB RAS, Ekaterinburg, Russia

⁴ Lomonosov Moscow State University, Moscow, Russia

evoronina2005@yandex.ru

Nanoscale magnetic phases such as incommensurate spin spiral structures are candidates for spintronics, because this kind of nanostructures provides a way for a control of electron transport by an external magnetic field. The number of systems, in which incommensurate spin spiral waves are observed, constantly grows, an amount of experimental data and theoretical concepts increases. But there is no yet common point of view on the origin of spin spiral wave and spin density wave, and to distinguish these magnetic structures with unsophisticated experimental methods is still not possible. The ordered Fe_{100-x}Al_x alloys (25<x<35 at.%) attract great attention to the present day in the magnetic interactions and magnetic structure aspect. Being a natural magnetic lamellar, these alloys exhibit abnormal magnetic characteristics for the Al concentration from 27 to 35 at.%. Investigations of the magnetic properties anomalies gave rise controversial conceptions of their magnetic structure: mictomagnetic, reentrant spin glass, sperimagnetic, antiferromagnetic with ferromagnetic clusters. In Ref.[1] the magnetic properties of these alloys were interpreted from the incommensurate spin density waves conception.

The study is directed to examination of the effect of boron admixture in the Fe₆₅Al₃₅ alloy on magnetic characteristics by magnetometry and Mössbauer spectroscopy.

The binary alloy and ternary quasiordered materials Fe₆₅Al₃₅, Fe₆₅Al_{35-x}B_x (x =5,10 at.%) have been produced by a special heat treatment of the originally disordered nanocrystalline alloys synthesized by mechanochemistry. According to the X-ray-diffraction data, the Fe₆₅Al_{35-x}B_x alloys have a DO₃-type structure. The magnetization curves do not show saturation in external magnetic fields of up to $H_{ext} < 5.0$ T. The ZFC and FC curves of all alloys are peaked curves having a maximum whose position depends on the applied external field. ZFC and FC curves of all alloys display hysteresis in low (0.05–0.1 T) fields and no hysteresis in higher external fields. The results of the analysis of the Fe₆₅Al_{35-x}B_x (x =5,10 at.%) Mössbauer spectra in the model of different local configuration in the DO₃ superlattice and magnetic phase separation are discussed.

Comparison of the boron-doped alloys with the initial alloy showed the considerable increase of all magnetic parameters T_C - from 340K to 630K, the Fe atom average magnetic moment $\bar{\mu}_{Fe}$ -from 0.34 μ_B to 1.12 μ_B , ⁵⁷Fe (T=5K) average hyperfine magnetic field - from 14.0 to 20.0 T, for Fe₆₅Al₃₅ and Fe₆₅Al₃₀B₅ alloys, respectively. The interpretation of the results in terms of localized Heisenberg model and magnetic phase separation is discussed.

Support by RFBR (Grant № № 12-02-01316-a) is acknowledged.

[1] D.R.Noakes et al, *Phys.Rev.Let.*, **91** (2003) 217201-1-4.

2PO-11-35

THE HIGH RESOLUTION ELECTRON MICROSCOPY FOR INVESTIGATION $\text{Fe}_{86}\text{Mn}_{13}\text{C}$ FILMS

*Abylkalykova R.B.*¹, *Kveglis L.I.*^{1,2}, *Dzhes A.V.*³, *Volochaev M.N.*⁴, *Cherkov A.G.*⁵, *Gorev M.V.*⁶

¹ EKSU, Ust-Kamenogorsk, Kazakhstan

² SFU, Krasnoyarsk, Russia

³ EKSTU, Ust-Kamenogorsk, Kazakhstan

⁴ SibSAU, Krasnoyarsk, Russia

⁵ NSU, Novosibirsk, Russia

⁶ Kirensky Institute of Physics SB RAS

rabykalykova@mail.ru

The aim of this work was to investigate features of the structure transformation formed during plastic deformation in bulk and thin-film alloy samples. Thin discs of $\text{Fe}_{86}\text{Mn}_{13}\text{C}$ alloy, cut from bulk samples using the electric spark method, were thinned by jet polishing. Films of the same alloy were obtained by thermal deposition on NaCl substrates and coating glass at a of 10^{-5} Torr in a VUP-4 vacuum installation. Internal stresses and deformations in film and bulk samples were induced through their multiple immersion into liquid nitrogen, due to the strong temperature gradient. Thinned bulk and film samples were investigated by electron microscopy on JEOL-2100. Fig.1 shows the image in a high-resolution transmission electron microscope of the film $\text{Fe}_{86}\text{Mn}_{13}\text{C}$ subjected to cryomechanical processing in liquid nitrogen (on the left); of the magnetic cluster (on the right). A striate contrast as shown is formed in the dark area after some seconds of focusing an electron beam onto this area. The electron beam deviates the magnetic field of the magnetic cluster. The dark area was formed as a result of the lack of electrons. Surplus electrons formed the light areas.

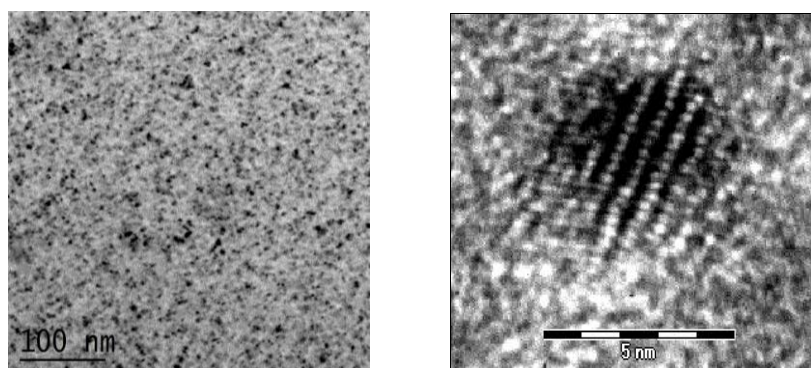


Fig. 1. The image in a high-resolution transmission electron microscope of the film $\text{Fe}_{86}\text{Mn}_{13}\text{C}$ subjected to cryomechanical processing in liquid nitrogen (on the left); fragment of dark area (magnetic cluster) after an exposition under an electron beam (on the right).

It was shown using high resolution transmission electron microscopy that deformation martensite is formed in local regions of bulk and film samples of the $\text{Fe}_{86}\text{Mn}_{13}\text{C}$ alloy during plastic deformation, leading to the formation of structural and magnetic inhomogeneities.

This work was supported by Grant 278/2013 of the Ministry of Education and Science of the Republic of Kazakhstan

2PO-I1-36

MAGNETIC AND MAGNETORESONANCE STUDIES OF COMPOSITE MULTILAYER FILMS WITH DIFFERENT KINDS OF INTERLAYERS

Shipkova I.G.¹, Chekrygina Iu.I.¹, Lebedeva Ye.V.², Syr'ev N.E.², Vyzulin S.A.³

¹National Technical University "Kharkov Polytechnic Institute", Kharkov, Ukraine

²Lomonosov Moscow State University, Moscow, Russia

³Krasnodar University of the Ministry of the Interior of Russia, Krasnodar, Russia

niksyr@mail.ru

Magnetic composite multilayer films belong to the new materials that are very promising for microwave electronic devices. Here we have studied multilayer nanostructures containing magnetic $\text{Co}_{40}\text{Fe}_{40}\text{B}_{20}\text{-SiO}_2$ composite with layers separated by nonmagnetic dielectric interlayers of silicon oxide (SiO_2) and by semiconductors of two kinds, namely, amorphous hydrogenated silicon (a-Si:H) and amorphous silicon carbide (a-SiC:H). The samples were obtained in Voronezh State Technical University by ion-beam sputtering. In all the samples the compositions of magnetic layers and their thickness were nearly the same. The concentration of CoFeB component was 50 at.% (~20 vol.%), the thickness of magnetic layers was 4.5–5 nm, the thickness of the nonmagnetic interlayers varied from 1 to 2.5 nm.

Hysteresis loops and magnetic moments of the films were measured by vibrating sample magnetometer in the fields up to 5 kOe. Magneto-resonance investigations were carried out at 9.15 GHz in magnetic fields applied parallel and perpendicularly to the film plane. Insertion of the nonmagnetic interlayers was found to lead to essential changes in magnetic properties and resonance fields in comparison with the compact composite films, these changes depending on the interlayer type. The films with SiO_2 and a-SiC interlayers have magnetization curves typical for superparamagnetic state and are adequately approximated by Langevin function (Fig. 1a) if we assume the magnetic phase concentration in the composite layers being 19.6 vol.% and 21.2 vol.% and the volume of individual granules 45 nm³ and 86 nm³ for SiO_2 and SiC interlayers, respectively. In contrast, a steep sharp part is observed in the hysteresis loops of the films with the a-Si:H interlayers (Fig. 1b). This is an evidence of the ferromagnetic interaction. Moreover, the mean magnetic moment of the films with a-Si:H interlayers was smaller than with SiO_2 and a-SiC ones. The joint analysis of magnetostatic and resonance data have shown that the observed differences of magnetic properties of these films can be explained by different sizes and shapes of the granules as well as the interface chemical reactions.

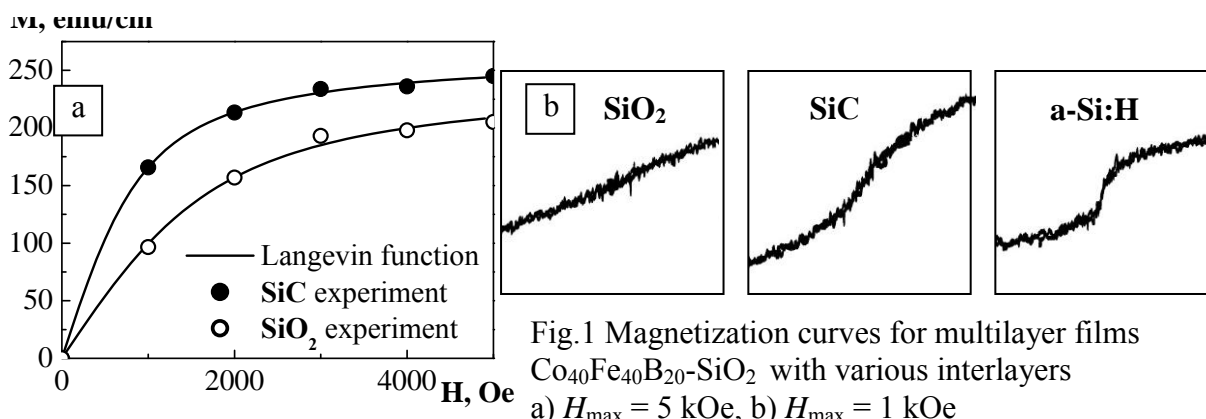


Fig.1 Magnetization curves for multilayer films $\text{Co}_{40}\text{Fe}_{40}\text{B}_{20}\text{-SiO}_2$ with various interlayers
a) $H_{\text{max}} = 5$ kOe, b) $H_{\text{max}} = 1$ kOe

2 July

Wednesday

17:30-18:30

poster session

2PO-I2

**“Magnetophotonics
(linear and nonlinear
magnetooptics,
magnetophotonic
crystals)”**

2PO-I2-1

MAPPING OF ELEMENTARY TOPOLOGICAL CONFIGURATIONS OF INHOMOGENEOUS MAGNETIC FIELDS BY MAGNETO-OPTICAL IMAGES

Ivanov V.E.

Ural Federal University, Yekaterinburg, Russia
vladimir.ivanov@usu.ru

Application of magnetic metal films with in-plane anisotropy for the visualization of inhomogeneous magnetic fields makes it possible to obtain information on the distribution of the vertical (H_z) and plane (H_x , H_y) components of the magnetic field in the plane of the indicator film [1]. Global structure of three-dimensional magnetic fields of complex configuration includes null points, spine curve and fan surface [2]. The projection of such a vector field on any section plane generally leads to an increase in the number of singular points due to the appearance of zero points, which are in the topological sense "sources" (S_o) and "sinks" (S_i). If the section plane perpendicular to the separator of three-dimensional field, the projection will include saddle singular point (S_a), near which the field lines are hyperbolas.

In this article we analyze the topology mapping of elementary topological configurations of an inhomogeneous magnetic field by magneto-optical (MO) images arising in indicator magnetic metal films with in-plane anisotropy. If the magnetization of indicator film is parallel to the plane component field, the singular points of the MO-images have the characteristic appearance of the light sector (or multiple sectors) with vertex at the singular point. MO-images of S_a -points differ from the image points S_o and S_i when you change the orientation of the plane of incidence of the light beam. Analysis of compliance MO-images topological structure of the field shows that the presence in MO-image one singular point corresponds to the presence of total dipole moment of magnetic field sources and the distance between them is less than the distance to the observation plane.

If the dipoles lie in a plane parallel to the display plane of the film, the magneto-optical image include the singular points the type S_i ($\gamma = 1$), S_o ($\gamma = 1$) and S_a ($\gamma = -1$). Sum of the indexes of all singular points [3] is invariant with respect to the distance from the source system to the plane of observation and is characterized by presence ($\gamma = 2$) or absence of the resulting dipole moment. This is evident in the MO-images as a simplification of their structure with increasing the distance from the sources.

[1] V.E. Ivanov, *J. Magn. and Magn. Mater.*, **324** (2012) 2572-2578.

[2] E.R. Priest, T.N. Bungey, V.S. Titov, *Geophysical and Astrophysical Fluid Dynamics*, **84** (1997) 127-163.

[3] D.Milnor, A.Uolles. *Differential topology*, New-York, (1968) 280 P.

2PO-I2-2

MAGNETIZATION DYNAMICS IN FERRIMAGNETIC GARNET FILMS STUDIED BY A TWO-PULSE FEMTOSECOND LASER TECHNIQUE

Shelukhin L.A., Pavlov V.V., Kalashnikova A.M., Pisarev R.V.

Ioffe Physical-Technical Institute, Russian Academy of Sciences, St. Petersburg Russia
utroma@yandex.ru

During the last decade the ultrafast optical manipulation of the spin systems became a subject of intense research in the condensed matter physics [1]. An enhanced attention of researchers in this field was motivated by interesting fundamental processes resulting from interaction of strong femtosecond pulses with magnetically-ordered media as well as by possible technological applications for high-speed magnetic memory devices. Only few reports were published on interaction of femtosecond laser pulses with ferrimagnetic garnet films, most of them being devoted to films with the in-plane orientation of magnetization, see, e.g. [2].

Here we report on coherent manipulation of magnetization in ferrimagnetic garnet films of an uniaxial type. The study was performed using a femtosecond two-pulse laser technique, where two collinear pulses were nearly identical with the intensity similar to the intensity of the pump pulse in the conventional pump-probe experiments. Optical parametric amplifier was used as a source of femtosecond laser pulses with time duration 150 fs, repetition rate 5 kHz, wavelength 690 nm, averaged power 2 mW, and spot diameter 100 μm . Experiments were done in transmission geometry and the Faraday rotation of the polarization of both laser pulses was measured as a function of delay between them.

Figure shows results for an epitaxial garnet film $(\text{YPrLuBi})_3(\text{FeGa})_5\text{O}_{12}$ grown on a substituted $\text{Gd}_3\text{Ga}_5\text{O}_{12}$ substrate with the (210)-orientation. The film is characterized by an uniaxial magnetic anisotropy with an angle of 16° between the easy axis of the magnetization and surface normal [3]. In contrast to conventional pump-probe experiments the observed variation of the rotation in our experiments is symmetric for the (\pm) time delay with respect to the zero delay when both pulses overlap.

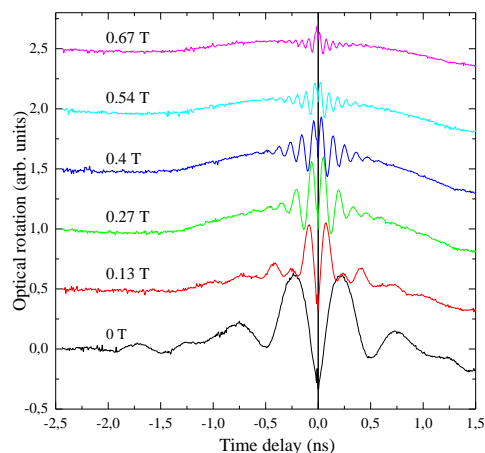
The data in Figure clearly show the decaying oscillatory signal which varies as a function of the applied magnetic field. This behavior is a good prove of the magnetic origin of the signal. In zero field the observed signal represents the ferromagnetic resonance mode in the anisotropy field. Evidently, the resonance frequency increases when the applied field is increased (see Figure). Interestingly, at fields below 0.13 T it is possible to resolve two frequencies of the magnetization precession probably due to the complex anisotropy of the (210)-type film. We note that the damping factor of magnetization precession in this film is rather large in comparison with previously observed photo-induced precession in (001)-type garnet films with in-plane magnetization [2]. Along with the magnetization precession a slow varying incoherent dynamics is observed on a nanosecond time scale which most probably is related to the laser-induced demagnetization.

This work is supported by the Russian Government project #14.B25.31.0025 and in part by the RFBR project #13-02-00754.

[1] A. Kirilyuk, A. V. Kimel, Th. Rasing, *Rev. Mod. Phys.* **82**, 2731 (2010).

[2] F. Hansteen, A.V. Kimel, A. Kirilyuk, and Th. Rasing, *Phys. Rev. Lett.* **95**, 047402 (2005).

[3] B. B. Krichevstov, V. V. Pavlov, R. V. Pisarev, *JETP Lett.* **49**, 535 (1989).



2PO-I2-3

MAGNETIC PROPERTIES OF NI- AND FE-BASED MAGNETOPLASMONIC CRYSTALS WITH DIFFERENT THICKNESSES

Belyaev V.¹, Grunin A.², Fedyanin A.², Rodionova V.^{1,3}

¹ Immanuel Kant Baltic Federal University, Kaliningrad, Russia

² Lomonosov Moscow State University, Moscow, Russia

³ National University of Science and Technology "MIS&S", Moscow, Russia

v.k.belyaev@gmail.com

Small values of magneto-optical (MO) effects strongly restrict their practical applications and in recent years several topics of photonic researches were targeted on development of new types of small and reliable biosensors. Sensitivity of MO sensors can be enhanced by creating them on base of magnetoplasmonic crystals (MPC). This way can demonstrate that in such systems, it is possible both to enhance the MO activity of the system via surface plasmon excitation, and to modulate the plasmon properties via application of a magnetic field [1].

We investigated magnetic and MO properties of MPC structures, based on embossed substrates with different spatial profiles, and magnetic properties of structures on smooth *Si/SiO₂* substrates which were created by ion plasma deposition. Spatial profiles of the MPC were obtained by atomic-force microscopy (AFM). The samples of magnetoplasmonic crystals were fabricated by using polymer templates of commercial digital discs. The polymer spiral gratings inside the Blu-ray disc (BD), DVD, and CD have declared periods of 320, 740, and 1600 nm, respectively. First, protective layer of the digital disc's surface was mechanically removed. Then, metals (Ag and Ni) were sputtered on the polymer gratings with thicknesses from 80 to 100 nm and from 5 to 100 nm respectively. In the end structures were covered by SiO₂ layer to prevent oxidation.

Magnetic properties of all structures were investigated by vibrating sample magnetometer by LakeShore and it appeared that they greatly depend on thickness of ferromagnetic layer. For samples *DVD//Ag(80nm)/Ni(10nm)/SiO₂(30nm)* and *BD//Ag(100nm)/Ni(100nm)/SiO₂(30nm)* a step-like behavior of hysteresis loops in dependence of the magnetic moment versus magnetic field in case of transverse plasmon propagation way (along the direction of substrate battlements) was observed. At the same time, measurements along the plasmon propagation way showed near-rectangular hysteresis loops typical for Ni-based thin films. Thin films of nickel and iron with same thicknesses on *Si/SiO₂* substrates were sputtered during same sputtering cycles and in-plane anisotropy was found in case with Ni-based thin films. All Fe-based structures had isotropic in-plane magnetic properties. AFM images of surface of structures based on digital discs showed that nickel and iron had partly covered sides of the substrate battlements. Thus, the anisotropy of the magnetic properties of MPC can be explained by the magnetostatic interaction between the different factions of nickel. Anisotropy of magnetic properties for nickel thin films on *Si/SiO₂* substrates can be explained by its magnetostriction properties of Ni. Last result can explain difference in magnetic properties of Fe-based and Ni-based MPC.

MO response of MPC structures was measured by setup which consists of halogen lamp with a monochromator as a light source, and a photomultiplier tube with a lock-in amplifier as detector and enhancement of transversal Kerr effect and magneto-optical activity in the narrow spectral range of the surface plasmon-polaritons excitation was observed.

We determined the optimum thickness of ferromagnetic layer (from the submitted samples) for enhancing MO response. We need to continue investigation of MPC based on digital discs to improve the quality factor of plasmons and to find a way to control properties of MPC for creating sensible biosensors.

[1] A. Grunin, A. Fedyanin, et. al., *Appl. Phys. Lett.*, **97** (2010) 261908 - 261908-3.

2PO-I2-4

OPTICS AND MAGNETO-OPTICS OF 3d-METAL OXIDES: A THEORETICAL CONSIDERATION

Zenkov A.V.

Ural Federal University, Ekaterinburg, Russia

zenkow@mail.ru

In the cluster approach, for the whole series of 3d transition metal oxides, we consider the peculiarities of charge-transfer (CT) states and CT $O\ 2p \rightarrow Me\ 3d$ transitions in the octahedral (MeO_6) complexes, where Me stands for a 3d-metal (Ti, V, Cr, Mn, Fe, Co, Ni) [1, 2]. We have computed the reduced matrix elements of electric-dipole transition operator on many-electron wave functions — the initial and final states of CT transitions. We have parameterized the obtained results and computed the relative intensities of various allowed CT transitions in the absence of the mixing of CT configurations having the same symmetry. Using the Tanabe-Sugano technique, we have taken into account this mixing and obtained the energies of many-electron CT transitions and their actual intensities as well.

We have also allowed for the Coulomb interaction between the 2p-electrons of the O^{2-} ligands and the 3d-electrons of the central Me ion in the (MeO_6) cluster. This interaction proved insignificant for the optic spectra.

We have modeled the optic and magneto-optic spectra of 3d-oxides. Modeling the optic spectra has yielded a complicated CT band consisting of many lines, the total extent of the CT band in all cases being about 10 eV. The model spectra are in satisfactory agreement with experimental data, which shows the limited validity of the generally accepted notion of a simple structure of CT spectra.

For an example of our results, see the Fig 1 [2].

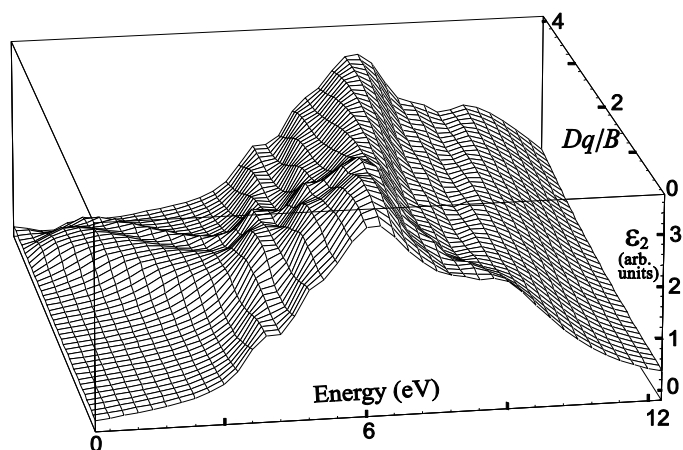


Fig. 1. Theoretical simulation of O2p–Cr3d CT band in a model chromite. The spectral dependence of all electric-dipole allowed CT transitions contribution to the imaginary part ϵ_2 of the diagonal component of the permittivity tensor is shown as a function of crystal field strength. Variation of Dq causes not merely the relative change of peaks height, but also the restructuring of the whole spectrum.

[1] A.V. Zenkov, *Int. J. of Quant. Chem.*, **111** (2011) 3864–3872.

[2] A.V. Zenkov, *Opt. and Spectr.*, **114** (2013) 581–589.

2PO-I2-5

COLORIZATION OF MAGNETO-OPTIC THREE DIMENSIONAL DISPLAYS USING OPTICAL SPACE DIVISION METHOD

Nakamura K., Kudo K., Goto T., Takagi H., Lim P.B., Inoue M.

Toyohashi University of Technology, Toyohashi, Japan

k_nakamura@spin.ee.tut.ac.jp

The holographic display can show real three-dimensional (3D) images without any special glasses [1]. A key characteristic of holographic displays is a viewing angle of reconstruction images. Submicron scale pixels of spatial light modulators (SLMs) are required for the reconstruction of 3D images with wide-viewing-angle. Recently, we developed magneto-optic 3D displays (MO-3D displays), substantialized by the submicron scale magnetic pixels. Using this MO-3D display, the 3D images were reconstructed with magnetic holograms. The reconstruction images had the wide viewing angle of ~ 20 degrees. However, the colors of the reconstruction images were only green whose wavelength was 532 nm. For full color 3D display, three primary colors are needed to be reconstructed. Thus, in this study, we represent the yellow (intermediate color between red and green) images reconstructed by the MO-3D displays. To represent yellow images, the optical space division method was used, which can synthesize several-colored images.

The light intensity of 3D images reconstructed from the magnetic holograms depends on the optical efficiency that is a ratio of reconstructed light intensity and incident light intensity. According to Haskal's equations [2], the optical efficiency depends on the transmissivity and the Faraday rotation angle of MO films in the case of that the linearly polarized light (reference beam) goes vertically to magnetic grating. Then, polycrystalline BiDyYFeAlG ($\text{Bi}_{1.3}\text{Dy}_{0.85}\text{Y}_{0.85}\text{Fe}_{3.8}\text{Al}_{1.2}\text{O}_{12}$) films with perpendicular magnetization were used for their high transmissivity and large Faraday rotation angle. These MO properties have wavelength dependence; the thickness of MO film was tuned so that the optical efficiencies for both wavelengths of 532 nm and 633 nm are close. The optical efficiencies of 1.1- and 2.6- μm -thick MO films were $2.5 \times 10^{-2} \%$ at 532 nm and $2.8 \times 10^{-2} \%$ at 633 nm, respectively.

We demonstrated the reconstruction of magnetic holographic images comprising yellow, red and green lights. The red and green images reconstructed by BiDyYFeAlG films showed three spheres. The hologram patterns for the red and green images were prepared by computer generated hologram (CGH) method. The wavelengths of the used light sources were 532 nm and 633 nm. Diameters of these spheres were 0.8 mm. The distance between the closest two spheres was 2.7 mm. Figure 1 shows the synthesized 3D image presented by the MO-3D display with optical space division method. The center sphere was yellow; top two spheres are green, bottom two spheres are red. To change the tones of this intermediate color (yellow), the intensities of red and green lights were changed from 0 to 300 μW with 50 μW step. The number of tone levels of the intermediate colors was 36. These results showed the possibility of full color MO-3D display can represent colored images.

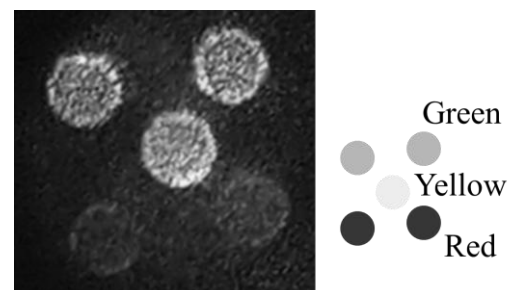


Fig. 1. Synthesized three-dimensional image.

[1] P. St-Hilaire, S. A. Benton and M. Lucente, *J. Opt. Soc. Am. A*, **9** (1992) 1969-1977.

[2] H. M. Haskal, *IEEE Trans. Magn.*, **6** 3 (1970) 542-545.

2PO-I2-6

FABRICATION OF MAGNETOPHOTONIC CRYSTAL FOR MAGNETO-OPTICAL IMAGING

Hashimoto R.¹, Yonezawa T.¹, Sakaguchi K.¹, Goto T.¹, Takagi H.¹,
Endo H.², Nishimizu A.², Inoue M.¹

¹ Toyohashi University of Technology, Toyohashi, Aichi 441-8580, Japan

² Hitachi Research Laboratory, Hitachi Ltd., Hitachi, Ibaraki 319-1221, Japan
inoue@ee.tut.ac.jp

Non-destructive testing (NDT) is an important technology for life of safety. The magneto-optical (MO) imaging can visualize the magnetization distribution corresponding to the stray fields originated from defects on metal surface [1]. Therefore, the MO imaging is one of the advantageous methods for high speed NDT of metal surface. The MO imaging for NDT requires MO imaging films which can provide a high-spatial resolution and a high-contrast image. The spatial resolution depends on the magnetic domain width. The monocrystalline yttrium iron garnet (YIG) films are used for the MO imaging commonly. However, the magnetic domain width of the monocrystalline YIG is too large to obtain high-spatial resolution MO images. In contrast, polycrystalline YIG has small magnetic domains. Thus, we used the polycrystalline YIG films for the MO imaging [2].

The MO image contrast depends on the Faraday rotation angle of MO media. To obtain a high-contrast MO image, we focused on the magnetophotonic crystal (MPC) which can enhance the Faraday rotation angle based on the Fabry-Perot resonance [3]. In this study, we fabricated MPC to obtain a high-spatial resolution and a high-contrast MO image.

The fabricated MPC was composed of three materials (YIG, SiO₂ and Ta₂O₅). Bismuth, dysprosium and aluminum substituted YIG (Bi:YIG) was deposited as a polycrystalline YIG using a radio frequency ion beam sputtering. SiO₂ and Ta₂O₅ were deposited by electron beam evaporation as Bragg mirrors. The MPC structure was SGGG substrate/(Ta₂O₅/SiO₂)^{2 pair}/(Bi:YIG)^{350 nm}/(SiO₂/Ta₂O₅)^{4 pair}. Also, Bi:YIG film was prepared to compare the Faraday rotation angle. Bi:YIG film's thickness was about 350 nm, same as the Bi:YIG layer of MPC. The domain width of Bi:YIG, measured by the magnetic force microscope, was about 50 nm. Thus, Bi:YIG provided a high-spatial resolution MO imaging film.

We demonstrated the MO imaging of metal with micro cracks (Fig. 1(a), 1 and 2) using MPC. The dc magnetic field applied by the electric magnet to magnetize the metal. The applied field was about 450 Oe (in-plane direction) that was larger than the coercive force of Bi:YIG. The MPC showed a high-contrast MO image (Fig.1(b)) because of that the Faraday rotation angle of the MPC was 9 times larger (17 deg.) than that of polycrystalline Bi:YIG film. As a result, MPC provided a high-contrast MO image.

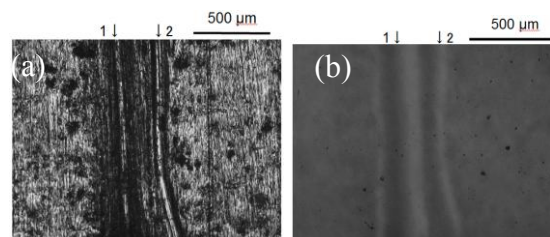


Fig.1. (a) Optical image of metal surface. (b) Experimental MO image on metal surface taken with MPC.

[1] Z. Zeng, X. Liu, Y. Deng, et al., *IEEE Trans. Magn.*, **42** 3737 (2006).

[2] S. Mito, et al., *J. Appl. Phys.*, **111** 07A519 (2012).

[3] M. Inoue, et al., *J. Phys. D: Appl. Phys.*, **39** R151 (2006).

2PO-I2-7

VOLUMETRIC MAGNETIC HOLOGRAM MEDIA USING FERROMAGNETIC GARNET-BASED MAGNETOPHOTONIC CRYSTALS

*Isogai R., Kobayashi K., Goto T., Takagi H., Nakamura Y., Lim P.B., Inoue M.**

Toyohashi University of Technology, Tempaku, Toyohashi 441-8580, Japan

*inoue@ee.tut.ac.jp

Hologram memory is a promising data storage technology with a high recording density and fast data-transfer rate. As a candidate for rewritable hologram media, magnetic films such as transparent magnetic material, bismuth substituted yttrium iron garnet (SYIG) films have been studied [1]. However, the diffraction efficiency of a monolayer SYIG film was not sufficient to apply to data storage devices. To improve the diffraction efficiency, Faraday rotation angle should be increased. A way to increase the rotation angle is use of magnetophotonic crystal (MPC), where a magnetic layer is sandwiched between two Bragg mirrors (BMs). In this work, we demonstrate a high diffraction efficiency using MPC media by numerical calculation.

The diffraction efficiencies of the SYIG monolayer film and MPC medium were evaluated with finite element method (COMSOL Multiphysics). The structure of the MPC media used for the simulations was substrate / $(\text{Ta}_2\text{O}_5 / \text{SiO}_2)^2$ / SYIG / $(\text{SiO}_2 / \text{Ta}_2\text{O}_5)^2$. The BMs were optically designed so that the center wavelength of the photonic band gap was 532 nm. The thickness of the SYIG layer, t_{SYIG} , and the average light energy density for writing were varied.

Figure 1 shows the calculated diffraction efficiency and the typical shape of magnetic fringe. The diffraction efficiency of the monolayer SYIG film was saturated about 0.09% at the thickness larger than 3 μm because the effective fringe depth was limited due to the connection near the surface. On the other hand, the diffraction efficiency of the 2-pair MPC medium with $t_{\text{SYIG}} = 3.88 \mu\text{m}$ were 0.36%, which was 4 times larger than that of the monolayer film. The enhanced specific rotation angle per unit length in MPCs brings such a high diffraction efficiency as expected. In addition, the effective depth of magnetic fringe was longer than that of monolayer film probably due to the multipath reflection between the BMs. This multipath reflection formed periodic island-shaped fringes in the depth, and avoided the heat concentration near the surface to reduce the connection of the fringes. This deep fringe was also the reason for high diffraction efficiency. However, the connection of fringes still existed in the MPC media as shown in Fig. 1; this means that the diffraction efficiency will be improved by reducing this connection. To suppress this connection of fringe, the insertion of heat sink layers like alumina into garnet media is proposed to diffuse the excess heat into the heat sink layers, and this may suppress heat localization in the garnet. At the conference, we will discuss the effect of this hybrid media composed of the MPC structure with heat sink layers to achieve high-performance as magnetic hologram media.

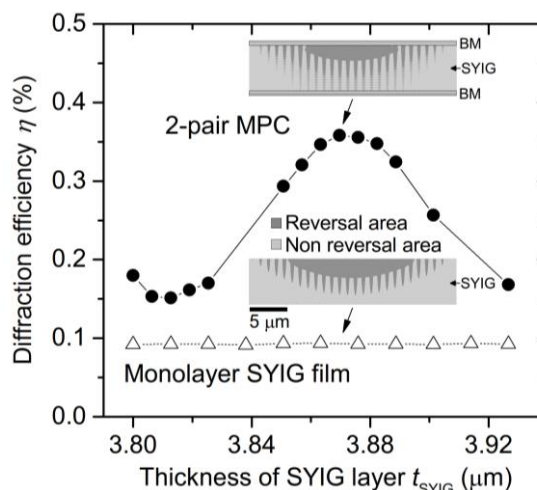


Fig. 1. SYIG thickness dependence of diffraction efficiency and the typical magnetic fringes for the monolayer SYIG film and 2-pair MPC medium.

This work was supported in part by the Grants-in-Aid for Scientific Research (A) 23246060 and Grant-in-Aid for Japan Society for the Promotion of Science (JSPS) Fellows No. 25-8942.

[1] S. Baek, H. Sakurai, et al., *IEICE Technical Report*, **111** (2011) 21–25.

2PO-I2-8

NONRECIPROCAL TRANSMISSION SHIFT OF OPTICAL ISOLATOR WITH VACUUM ANNEALED CERIUM SUBSTITUTED YTTRIUM IRON GARNET

Goto T.¹, Inoue M.^{1*}, Ross C.A.^{1*}

¹ Toyohashi University of Technology, Toyohashi, Japan

² Massachusetts Institute of Technology, Cambridge, USA

* goto@ee.tut.ac.jp

The integration of magneto-optical components on non-garnet substrates has been challenging work because of the difficulty in growth of the rare-earth substituted yttrium iron garnets. However, recently we demonstrated the large Faraday rotation angle and high transmissivity in near-infrared region with cerium substituted yttrium iron garnets (CeYIGs), which showed single polycrystalline x-ray patterns on silicon, silica, and silicon on insulator (SOI) substrates. This CeYIGs' figure of merit defined with Faraday rotation angle multiplied by absorption at the wavelength of 1550 nm was close to that of the epitaxially grown CeYIGs. Such CeYIGs were prepared by vacuum annealing after the deposition. The vacuum anneal controlled the valence state of Fe in CeYIG, which was relatively important for CeYIG than other garnets (well-known crystallization processes of garnets have been done in air pressure). Then, the improvement of the conventional magneto-optical component was strongly expected.

In this paper, we fabricated the optical isolator comprising vacuum annealed CeYIG, and compared with other optical isolators.

First the optical waveguide was fabricated with the e-beam patterning and dry etching. Its width was 450 nm and the height was 250 nm. These parameters were tune for the wavelength of 1550 nm. To yield the resonance, the waveguide has a 200 μm diameter ring with 200 nm distance from the straight line, shown in Fig. 1. On this device, the films of 80 nm thick CeYIG were deposited by rf sputtering, followed by annealing at high temperature in vacuum for crystallization, resulting in formation of a polycrystalline garnet phase. The transmission peak was measured with opposite external magnetic field (~ 1 kOe), resulting in the nonreciprocal shift of TM mode peak. However the isolation ratio was not large as the estimation. In the symposium, the detail of the structures and the reason of the difference will be shown.

This work was partly supported by the JSPS Postdoctoral Fellowships for Research Abroad.

[1] Taichi Goto, Yu Eto, Keiichi Kobayashi, Yoji Haga, Mitsuteru Inoue and C. A. Ross, *J. Appl. Phys.*, **113** (2013) 17, 17A93.

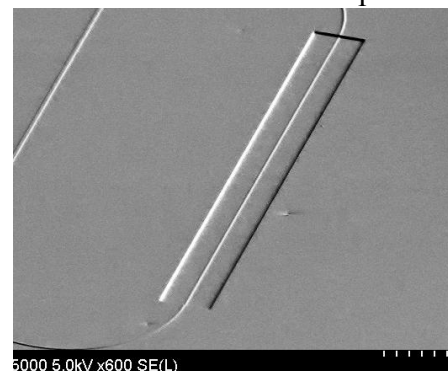


Fig. 1. The ring resonator covered with CeYIG. The rectangular shows the waveguide contacting to the CeYIG directly without the 1- μm -thick SiO₂ layer.

2PO-I2-9

THE TOTAL NON-REFLECTION OF SPIN WAVES ON AN ARRAY OF ANTIDOTS IN THIN GARNET FILMS

Bessonov V.D.^{1,2}, Gieniusz R.¹, Guzowska U.¹, Stognij A.I.³, Maziewski A.¹

¹ Faculty of Physics, University of Białystok, Białystok, Poland

² Institute of Metal Physics, Ural Division of RAS, Yekaterinburg, Russia

³ Scientific-Practical Materials Research Center at NAS of Belarus, Minsk, Belarus

bessonov@uwb.edu.pl

A thin yttrium iron garnet (YIG) film with its characteristic low damping parameter which allows spin wave propagation to the longer distance serves as an excellent model medium to demonstrate many effects. In the YIG film, wavelength of the magnetostatic surface spin waves (MSSW) is much smaller than the linear size of the typical samples. By utilizing above parameter the magnetostatic waves can be treated like light waves propagating in a transparent medium in such samples.

In the present work we have studied the phenomenon of total non-reflection of the spin wave in YIG film monocrystalline patterned by antidots. YIG films with a thickness of $t = 4.5 \mu\text{m}$ were epitaxially grown along the (111) crystallographic axis on transparent gadolinium gallium garnet substrates were studied. The arrays of antidots were chemically etched, with $67 \mu\text{m}$ diameters or widths, and with round or square shapes. The line of antidots can be used as an edge to produce the phenomenon of total non-reflection of the spin wave in YIG film. The total non-reflection phenomenon of the spin waves is edge wave arises at the critical angle between the reflective boundary of the medium and the external magnetic field. The edge wave propagates along the reflective boundary and the reflected waves are absent for all possible incidence angles of spin wave. A high-intensity beam of spin waves moving along the line of antidots is observed at the critical angle between the line of antidots and the magnetic field. Potentially one can generate continuous or periodic spin wave beams by changing the periods of the antidot arrays. The results of the OOMMF simulations are consistent with the experimental results, while the isofrequency curves provide a tool for clear interpretation of the experimental data[1].

Supported by the SYMPHONY project operated within the Foundation for Polish Science Team Programme co-financed by the EU European Regional Development Fund, OPIE2007–2013 and by the program Megagrant No. 2013-220-04-329.

[1] R. Gieniusz, V.D. Bessonov, U. Guzowska, A. Maziewski, A.I. Stognij, *Appl. Phys. Lett.*, **104** (2014) 0824.

2PO-I2-10

OPTICAL AND MAGNETOOPTICAL SPECTROSCOPY OF MAGNETOPLASMONIC CRYSTALS BASED ON THIN YIG LAYER

Shaymanov A.N.^{1}, Chekhov A.L.¹, Stognij A.I.², Murzina T.V.¹*

¹ Physics Department, M.V. Lomonosov Moscow State University

² Institute of Solid State and Semiconductor Physics, Minsk, Belarus

*shaymanov.aleksey@physics.msu.ru

Magneto-plasmonic crystals (MPC) are intensively studied nowadays as they reveal a number of exciting effects like high concentration of optical field in the vicinity of surface plasmon-polaritons (SPP) modes, efficient tunability of their transmission and reflection spectra. Introduction of magnetic materials in plasmonic structures allows to control over the SPP and light propagation through magneto-optical effects [1]. One of the ways to make an MPC is to fabricate a gold grating on the top of a magneto-optical dielectric, e.g. yttrium-iron garnet (YIG). Such a structure allows the excitation of two SPP modes that are localized on the air/Au and Au/YIG interfaces. A promising task remains to decrease the thickness of the magnetic dielectric layer, which may diminish the MPC optical losses while remaining high quality of MPC structure. In this work, we present the results on the SPP excitation in MPC structures based on thin YIG film and with varied parameters of the MPC structure.

MPC were fabricated by a combined ion-beam etching process described in detail elsewhere [2]. The samples with the spatial period of the gold gratings of 500-700 nm and the width of the slits of 60-200 nm were studied, the thickness of the gold layer being 100 nm. YIG layer of the thickness 100-250 nm was epitaxially grown on a gallium gadolinium garnet substrate. Optical properties of the MPC were studied in the spectral region from 630 to 950 nm using a collimated p-polarized beam of a halogen lamp as the light source. Magneto-optical (MO) effects were studied in transmission through MPC as the transversal magnetic field of 3 kOe was applied parallel to the stripes.

Fig. 1 shows the frequency-angular transmission spectrum of a Au/garnet based MPC with the period of 686 nm, the thickness of the YIG layer being 250 nm, the slits are 150 nm wide. Transmission minima are attributed to the excitation of SPP with the wavevector k_{SPP} determined by the phase matching condition $k_0 \sin \Theta + mD = k_{SPP}$, where D is the lattice reciprocal vector, Θ is the angle of incidence, m is the order of the corresponding mode, k_0 is wave vector of the incident light. Black lines on Fig.1 correspond to the Au/air interface with $m = \pm 1$, and white lines to Au/YIG interface with $m = -2, 2$. We show that spectra of the MO contrast reveals the maxima with the value up to $5 \cdot 10^{-3}$ near the SPP excitation at Au/garnet interfaces, MO contrast being odd with respect to Θ and tunes on the frequency-angular scale. Importantly, such high values of MO effects are achieved in MPC with rather thin YIG layer. Besides, small YIG thickness restricts the excitation of waveguide modes. MPC structures with other values of the period and slits width reveal similar behavior for the corresponding spectral ranges.

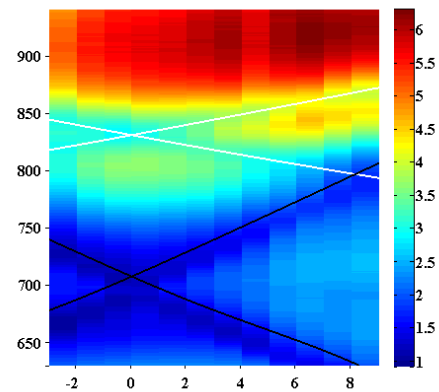


Fig.1 Frequency-angular transmission spectra of a Au/garnet based MPC

[1] V.I. Belotelov et al., *Nature Nanotechnology*, **6** (2011) 370 - 376.

[2] A.I. Stognij et.al., *Inorganic materials*, in press (2014).

2PO-I2-11

MAGNETO-OPTICAL PROPERTIES OF MULTILAYER NANOSTRUCTURES WITH COMPOSITE MAGNETIC LAYERS NEAR PERCOLATION TRESHOLD

Buravtsova V.¹, Gan'shina E.¹, Kalinin Yu.², Sitnikov A.², Zubakin D.¹

¹ Moscow State University, Faculty of Physics, Moscow, 119991, Russia

² Voronezh State Technical University, Voronezh, 394026, Russia

daniilzubakin@gmail.com

In this report we present the results of magnetic and magneto-optical (MO) studies of $[(\text{Co}_{45}\text{Fe}_{45}\text{Zr}_{10})_{46}(\text{Al}_2\text{O}_3)_{54}(X)/\alpha\text{-Si}(Y)]_n$ multilayers (ML), where the granular composite based on $\text{Co}_{45}\text{Fe}_{45}\text{Zr}_{10}$ with concentrations near the percolation threshold was used as a magnetic layer. ML structures with different thicknesses of magnetic ($X=1.76 - 2.21$ nm) and non-magnetic ($Y=0.72 - 3.31$ nm) layers and different X to Y ratio were investigated.

It was found that the Transversal Kerr Effect (TKE) spectra of ML films strongly depends not only on semiconductor and composite interlayer thickness, but also on values of applied magnetic field. For the ML with $X < 2$ nm TKE spectra at $H=2.1$ kOe were similar to the spectra of bulk metal-insulator nanocomposite [1]. For the $X > 2.14$ nm TKE value was positive throughout the wavelength range (0.5-4.2 eV) and the TKE spectra were similar to the $\text{Co}_{45}\text{Fe}_{45}\text{Zr}_{10}/\text{Si}$ ML spectra. The increase of magnetic layers thickness induces the similar spectra's shape evolution as in ML based on nanocomposite with less metal phase concentration [2].

TKE field dependences $\delta(H)$ were studied in near IR and visible photon energy ranges. It was found that $\delta(H)$ curves for all ML are considerably different for various energy ($E=1.3$ and 3.06 eV). Anomalies on $\delta(H)$ curves such as TKE sign changing and presence of local maximums at $H < 500$ Oe were revealed for some ML. In several cases TKE value in a large field less, than in a small field. TKE spectra measured in small and large fields were essentially different.

On the isoenergetic dependences $\delta(Y)$ two maximums were observed: 1st – near $Y_1=1.3$ nm; 2nd – near $Y_2=2,3$ nm. The first maximum of TKE corresponds to the beginning of resistivity falling on $\rho(Y)$ curve. This pattern was observed for ML with similar chemical composition, but with less metal phase concentration in nanocomposite layers [2]. Analogically [2] it can be explained by formation of new composite $\text{CoFeZr}+(\text{Si}$ and/or silicides) with metal phase concentration dependend on X and Y . Presence of the second maximum on $\delta(Y)$ curves for studied ML, may be associated with completion of silicide formation process on interface and beginning of the Si interlayer growth. At the same time in composite formed on interface metal phase concentration may shift to the percolation threshold area, and TKE value increase as the result. Further semiconductor thickness increase weakens the interaction between adjacent layers of nanocomposite and reduces the TKE value.

Anomalous behavior in the nearest IR range most probably relates to a competition between two contributions from (CoFeZr)- Al_2O_3 and (CoFeZr)- silicides + Si composites that have opposite sign of TKE in this spectral range.

This research was supported by the Russian Foundation for Basic Researches (grant No 13-02-90491).

[1] V.E.Buravtsova, V.S.Guschin, Yu.E.Kalinin, et al.: *CEJP*, **2** (2004) 566.

[2] E.Gan'shina, V.Buravtsova, A.Novikov, et al.: *Sol. State Phenomena*, **190** (2012) 361-364.

2PO-I2-12

THE FEATURES OF SOLVING THE INVERSE ELLIPSOMETRIC PROBLEM FOR FERROMAGNETIC NANOSTRUCTURES

Maximova O.A.¹, Kosyrev N.N.¹, Ovchinnikov S.G.^{1,2}

¹ Kirenskiy Institute of Physics of the SB RAS, Krasnoyarsk, Russia

² Siberian Federal University, Krasnoyarsk, Russia

maximo.a@mail.ru

It is currently important to develop high-precision and user-friendly control methods of synthesis and diagnostics of nanofabricated structures properties. Hence a new technique of magneto-optical ellipsometry has been lately evolved for studying magnetic materials. It combines in situ measurements of the magneto-optical Kerr effect and the potential of the ellipsometric method, which gives an opportunity to completely define all elements of the dielectric tensor, where diagonal tensor elements are responsible for refractive and absorbance indexes, off-diagonal tensor elements are related to magneto-optical effects. Magneto-optical ellipsometry has some distinct advantages. It can be used for nondestructive, simultaneous, precise, in situ control of magnetic, structural, and optical properties of nanomaterials in the process of deposition in the high-vacuum chamber.

In this paper the features of the ferromagnetic samples ellipsometric measurement under the influence of an external magnetic field in the equatorial magneto-optical Kerr effect configuration are shown. For the first time the relationship of the ellipsometric parameters ψ and Δ with a proportional to magnetization magneto-optical parameter Q is obtained, the ellipsometric angles corrections ($\delta\psi$ and $\delta\Delta$) are evaluated due to the equatorial surface magneto-optical Kerr effect. As a result, it becomes possible to measure the magnetic characteristics of the layered nanostructures, such as the hysteresis loop and coercivity with the conventional ellipsometric apparatus [1]. The values of refractive (n) and absorbance indexes (k) of the ferromagnetic metal, as well as the values of real (Q_1) and imaginary parts (Q_2) of magneto-optical parameter Q can be obtained from the deduced expressions for the model of a homogeneous semi-infinite medium with the use of the ellipsometric and magneto-ellipsometric measurements data.

To check our method Fe films were synthesized on the surface of single-crystalline Si with a SiO₂ buffer layer. The process of a Si substrate primary chemistry is specified in [2]. The spectral dependences of the ellipsometric parameters ψ and Δ under Fe film growth were obtained, magneto-optical Kerr effect was analyzed by data of in situ measurements for the wavelength $\lambda = 577\text{nm}$ under Fe film growth and after the deposition. The results of magneto-optical Kerr effect measurements for $\lambda = 577\text{nm}$ and for $\lambda = 633\text{nm}$ were compared according to the sample orientation. In situ and ex situ spectral dependences of the magneto-optical Kerr effect were compared for the deposited Fe film. The values of refractive and absorbance indexes of Fe film, the values of real and imaginary parts of magneto-optical parameter Q were obtained from the ellipsometric and magneto-ellipsometric in situ and ex situ measurements data.

Support by the President of Russia Grant No. NSh-2886.2014.2, and RFBR Grant No. 13-02-01265 is acknowledged.

[1] O.A. Maximova, S.G. Ovchinnikov, U. Hartmann, N.N. Kosyrev, S.N. Varnakov, *Vestnik SibGAU*, **3** (2013) 212-217.

[2] N.V Volkov, A.S. Tarasov, E.V. Eremin and al., *J. Appl. Phys.*, **109** (2011) 123924.

2PO-I2-13

MAGNETO-OPTICAL PROPERTIES OF $\text{Bi}_{12}\text{GeO}_{20}$ NANOCOMPOSITE WITH Ni AND Co INCLUSIONS

Kozhaev M.A.¹, Belotelov V.I.^{1,2}, Mrozek M.³, Gawlik W.³, Gajc M.⁴, Klos A.⁴, Pawlak D.A.⁴

¹ Russian Quantum Center, Skolkovo, Moscow Reg., Russia

² Lomonosov Moscow State University, Moscow, Russia

³ Institute of Physics, Jagiellonian University, Cracow, Poland

⁴ Institute of Electronic Materials Technology, Warszawa, Poland

mikhail.kozhaev@gmail.com

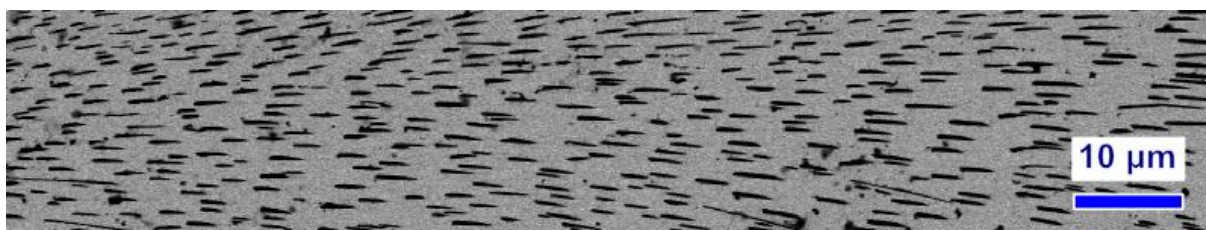


Fig. 1. Microstructure of a composite made by doping $\text{Bi}_{12}\text{GeO}_{20}$ single crystal with nanoparticles based on Co (Scanning electron microscope picture).

One of the modern ways to develop computing technologies is photonics. Therein information carrier is light instead of electrons. Modulation of different light characteristics is necessary for optical computing realization. Magneto-optical effects allow to control light polarization, phase and intensity through a magnetic field. Thus, structures with a strong Faraday and Kerr effects have both fundamental and practical importance.

Recently, a lot of attention has been given to study nanocomposites containing para- and ferromagnetic material properties. Such structures show resonant optical and magneto-optical properties associated with the included nanosized ellipsoids and cylinders [1-3]. Dr. Pawlak et al. developed a methodology for creating $\text{Bi}_{12}\text{GeO}_{20}$ with elongated nanoparticles based on Co and Ni (Fig. 1). The method is based on similar idea as recently developed NanoParticle Doping method enabling manufacturing of dielectric materials doped with various nanoparticles [4].

In this work we study experimentally and theoretically the influence of the ellipsoidal nanosized inclusions in the dielectric host on the magneto-optical properties of the nanocomposite. It is found that the Faraday effect in $\text{Bi}_{12}\text{GeO}_{20}/\text{Ni}(\text{Co})$ nanocomposites is increased by an order of magnitude. Different reasons for the enhanced Faraday effect are discussed: light scattering on nanoparticles increases light path; plasmon emergence leads to field redistribution; admixing material with different optical properties to the host modifies composite effective permittivity. Resonant features for optical and magneto-optical spectra are demonstrated.

[1] M. Abe, T. Suwa, *Phys. Rev. B*, **70** (2004) 235103.

[2] V. Myroshnychenko, et al., *Opt. Express*, **20** (2012) 10879-10887.

[3] V. Gasparian, Zh. S. Gevorkian, *Phys. Rev A*, **87** (2013) 053807.

[4] M. Gajc, et al., *Adv. Funct. Mater.*, **23** (2013) 3443.

2PO-I2-14

TEMPERATURE DEPENDENCE OF MAGNETO-OPTICAL ACTIVITY IN ErAl₃(BO₃)₄, ErFe₃(BO₃)₄ AND HoFe₃(BO₃)₄ CRYSTALS

*Sukhachev A.L.**, Malakhovskii A.V., Sokolov V.V., Gudim I.A., Sokolov A.E.

L.V. Kirensky Institute of Physics, Siberian Branch of Russian Academy of Sciences,
660036 Krasnoyarsk, Russian Federation

*sunya@iph.krasn.ru

Compounds containing rare earth ions are widely studied because of their great importance for optical applications. Investigation of optical and magneto-optical properties of these compounds gives information both about ground and excited states of $4f$ ions.

In the present work, optical absorption and magnetic circular dichroism (MCD) spectra of some f - f transitions were studied in ErAl₃(BO₃)₄, ErFe₃(BO₃)₄ and HoFe₃(BO₃)₄ single crystals in temperature range 90-293 K. From these measurements, temperature dependences of the paramagnetic magneto-optical activity (MOA) of the electric dipole forbidden f - f transitions were obtained as the ratio of zero moments of MCD and absorption bands:

$$c = \langle \Delta k(\omega) \rangle_0 / \langle k(\omega) \rangle_0 = C \frac{\mu_B H}{k(T - \Theta)}. \quad (1)$$

According to Ref. [1], the MOA should be proportional to the paramagnetic susceptibility. It was revealed that, in contrast to allowed transitions, temperature dependences of the MOA of some f - f transitions substantially deviate from the Curie-Weiss law (1). Parity forbidden f - f transitions are partially allowed due to odd components of crystal field (CF), which mix states of different parity. There are several contributions in MOA and the ratio of these contributions can depend on the population of the components of the CF split ground state [2]. Therefore, intensity and magneto-optical properties of these transitions are very sensitive to the local environment of the $4f$ ion and temperature dependence of MOA can deviate from the Curie-Weiss law. Even for isostructural crystals ErAl₃(BO₃)₄ and ErFe₃(BO₃)₄ temperature dependences of the MOA of the same transitions revealed different behavior up to opposite signs of MOA.

It is possible to calculate theoretical MOA of f - f transitions at room temperature [2]. MOA of f - f transition is provided by allowed transitions from the ground state to admixed states. These transitions should satisfy the total angular-momentum selection rule $\Delta J = 0, \pm 1$. For Ho³⁺ ions the theoretically possible values of MOA are obtained as -5.6, -0.6 and +5 (in units of $\mu_B H/kT$). Experimentally observed MOA (Table) are combinations of the theoretical ones.

Transition	⁵ I ₈ →	E (cm ⁻¹)	C
D	⁵ F ₅	15300	-0,39
E	⁵ S ₂ + ⁵ F ₄	18500	-2,20
F	⁴ F ₃	20500	-6,27
G	⁴ F ₂	21050	-3,28
H	³ K ₈	21350	-0,72

Experimental MOA (C) of f - f transitions in Ho³⁺ ions in HoFe₃(BO₃)₄ crystal (in units $\mu_B H/kT$)

[1] J.H. Van Vleck, M.H. Hebb, *Phys. Rev.*, **46** (1934) 17.

[2] A.V. Malakhovskii et al., *Physics of the Solid State*, **49** (2007) 701.

2PO-I2-15

NANOSCALE DOMAIN WALL DYNAMICS IN GARNET FILMS

Gerasimov M.V.¹, Logunov M.V.¹, Nikitov S.A.², Loginov N.N.¹, Spirin A.V.¹

¹National Research Ogarev Mordovia State University, 430005 Saransk, Russia

²Kotel'nikov Institute of Radio Engineering and Electronics of RAS, 125009 Moscow, Russia
logunovmv@bk.ru

A study of quasistatic domain wall movements in nanometer scale necessitates development of experimental methods for increasing the sensitivity of instrumentation [1-2].

In this report, we present the magneto-optical system for the measurement of nanoscale dynamics of dynamic domain walls in magnetic films. The system works by using Faraday effect. We used method of optical signals spatial filtering in the diffraction patterns of the domain structure to increase the sensitivity, and electronic techniques: modulation of photo-detector, time shift, storage and averaging of signals. As a result, we achieved spatial resolution of ~ 1 nm at registration of dynamic domain wall movements.

Magneto-optical system was used for the study of domain wall dynamics in uniaxial garnet films. Some results of the study in pulse fields H (pulse duration 0.1 - 0.5 μ s, fig. 1) are shown on fig. 1. Dependence of "ballistic" effect ΔX on pulse field amplitude at domain walls movement was observed. This dependence was quasiperiodic. It may be caused by periodic inhomogeneity of magnetic film properties with spacing 100-200 nm.

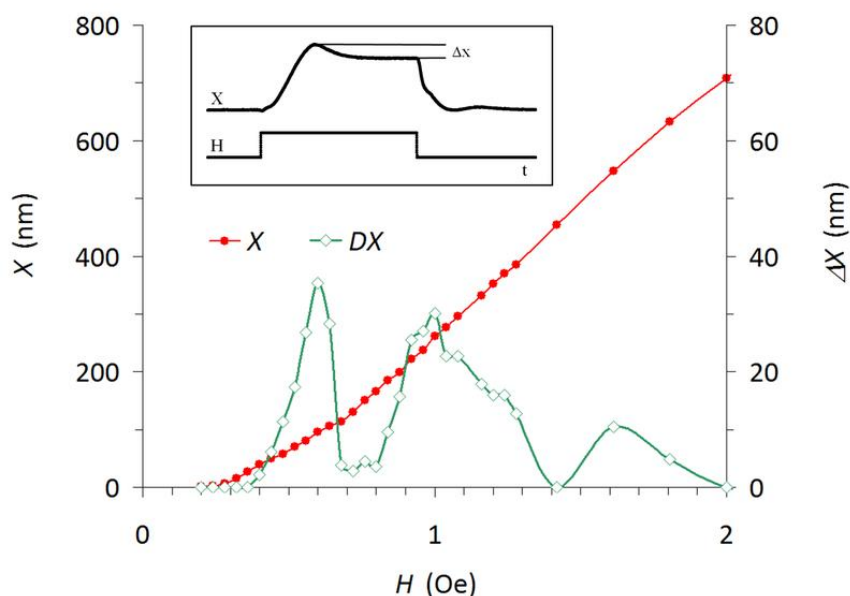


Fig. 1. Changes of maximal domain wall displacement X with pulse magnetic field H , and corresponding value of the "ballistic" effect ΔX .

Support by Ministry of Science and Education of Russia is acknowledged.

[1] D.A. Christian, K.S. Novoselov, and A.K. Geim, *Phys. Rev. B*, **74** (2006) 064403.

[2] V.V. Khotkevych, M.V. Milosevic, and S.J. Bending, *Rev. Sci. Instrum.*, **79** (2008) 123708.

2PO-I2-16

SURFACE PROPERTIES OF NANOSCALE IRON GARNET FILMS

*Kosykh T.B.*¹, *Prosyakov A.S.*¹, *Pyatakov A.P.*¹, *Shaposhnikov A.N.*², *Prokopov A.R.*², *Sharay I.V.*³

¹ M.V.Lomonosov Moscow State University, Moscow

² Taurida National V.I.Vernadsky University, Simferopol

³ Institute of Magnetism, NASU and MESU, Kiev

kosykh@phys.msu.ru

Interest to thin and ultrathin iron garnet films have grown significantly due to their potential in spintronics and magnonics application [1, 2]. For these purposes, it is very important to know the surface state of these films. In this work the surface properties of ultrathin (thickness h ranging from ~ 6 to ~ 90 nm) highly bismuth-substituted iron garnet films were investigated. These films were prepared by reactive ion beam sputtering of the target of nominal composition $\text{Bi}_{2.5}\text{Gd}_{0.5}\text{Fe}_{4.2}\text{Al}_{0.8}\text{O}_{12}$ on (111) $\text{Gd}_3\text{Ga}_5\text{O}_{12}$ substrates in an argon-oxygen mixture and subsequent crystallized by annealing in air at 680°C for 20 min with heating rate $\sim 40^\circ/\text{min}$ [3]. Before the film deposition the substrates were pretreated during 2 min by either an Ar^+ ion beam with ion energy of 1 keV (A-films) or 5 keV (B-films) and current density of $2.5 \text{ mA}\cdot\text{cm}^{-2}$. The film thickness was estimated based on the sputtering velocity of 6–8 nm per minute.

Surface properties of the films were investigated by AFM with a FemtoScan microscope. Size of the taken frames was $5 \times 5 \mu\text{m}$, or 512×512 pixels, that provides spatial resolution of about 10 nm. Each film was scanned in several (three or more) places.

Topography of the films was analyzed using FemtoScan software for image processing. Five parallel cross-sections were built at an arbitrary angle for each frame, and the average width and height of the grains were determined. The data in the Figs. 1 and 2 are additionally averaged over several (from 4 to 7) frames taken in different places of the film. Fig. 1 represents the dependence of the grains height on the film thickness and Fig. 2 is the analogues dependence for the grains width. The study revealed that all the films obtained by sputtering have a granular structure, and the roughness increases with increase of h . It was also found that both height and width of the grains in B-films are more than in A-films for all available thicknesses. The observed roughness increase in B-films is caused by appearance of additional lattice defects on the substrate surface under high-energy ion bombardment. It was found that the roughness of the films could be reduced by decreasing the heating rate of annealing up to $\sim 2^\circ/\text{min}$.

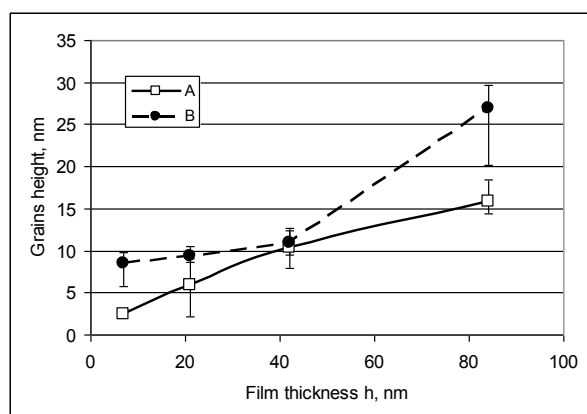


Fig. 1 Dependence of the grains height on the film thickness for A- and B-films.

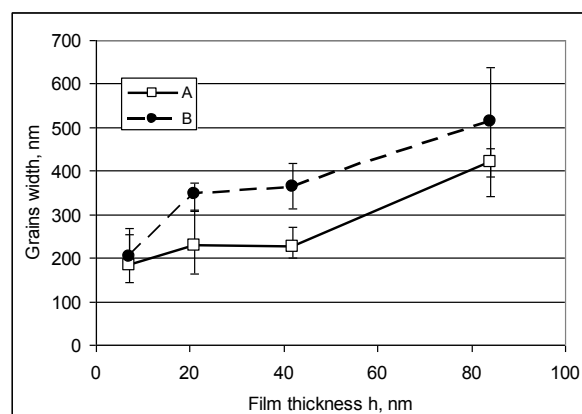


Fig. 2. Dependence of the grains width on the film thickness for A- and B-films.

[1] Y.Kajiwara et al., *Nature* **464**, 262 (2010).

[2] Y.Sun et al., *Appl. Phys. Lett.* **101**, 152405 (2012).

[3] V. Berzhansky et al., *Functional Materials*. **17** (2010), No 1, 120–126.

2PO-I2-17

THE EVANESCENT SHEAR ACOUSTIC WAVE AMPLIFICATION NEAR THE SURFACE OF SEMI-INFINITE FERROMAGNET (ANTIFERROMAGNET)

Prikhodko O.¹, Sukhorukova O.¹, Tarasenko S.¹, Shavrov V.²

¹ Donetsk Institute for Physics and Engineering of the National Academy of Sciences of Ukraine,
83114, R.Luxemburg Str.,72, Donetsk, Ukraine E –mail: s.v.tarasenko@mail.ru

² Kotel'nikov Institute of Radio Engineering and Electronics of the Russian Academy of Sciences,
125009, Mokhovaya Str.,11-7 Moscow
shavrov32@mail.ru

One of the key points in evaluating the possible applications of composite magnetic media as a special class of acoustic metamaterials is the analysis of the possibility of the elastic evanescent wave amplification at the interface between the magnetic (in particular, ferromagnetic) and nonmagnetic media. In this case, imposing a static external magnetic field is considered as a promising way of fine-tuning the dynamic characteristics of magneto-acoustic metamaterials [1–3]. Since the fundamental work by Parekh [4], the calculation of the spectrum of a shear surface acoustic wave propagating along the mechanically free surface of an easy axis ferromagnet magnetized by the external static magnetic field \mathbf{H}_0 is traditionally conducted with the mere inclusion of the magnetoelastic interaction.

Our investigation shows that a traditional approach to the calculation of a Parekh wave [4] only on the base of magnetoelastic and magnetodipole interaction inadequately describes the spectrum of the surface elastic wave in the high-frequency range. It is determined that the magnetostriction plays an important role for high-frequency surface magnetoelastic dynamic of ferromagnet or antiferromagnet. The necessary conditions for existence of the "new" Parekh wave and for amplification of evanescent SH wave and leaky Parekh wave are derived

According to the general concepts of the theory of wave processes in layered media one can find the amplitude transmittance of the bulk shear wave with $\mathbf{u} \parallel \mathbf{H}_0 \parallel OZ$ incident from the interior of an elastically isotropic nonmagnetic media on the surface of an easy axis ferromagnetic (antiferromagnetic) half -space ($\mathbf{k} \in XY$, $n \parallel OX$, \mathbf{n} – normal to the boundary between magnetic and nonmagnetic half –spaces, \mathbf{k} -wave vector) under the conditions of total internal reflection:

$$T = \frac{2\tilde{Z}}{\tilde{Z} + Z} \quad (1)$$

where \tilde{Z} and Z – the surface acoustic impedance of the upper and low half –space respectively for case of shear wave. In the complex plane the pole in Eq. (13) specifies the dispersion relation of the surface acoustic SH wave for the acoustically continuous interface of two half -spaces occupied by ferromagnetic(antiferromagnetic) and non - magnetic media, respectively. The condition $Z = 0$ specifies the dispersion relation of the above shear Parekh surface acoustic wave specified at the mechanically free surface of the ferromagnetic (antiferromagnetic) media. The peculiarities of the Shoch effect for above case are established.

[1] O. B. Matar, J.F. Robillard, J. O. Vasseur, et al., *J. Appl. Phys.* **111** (2012) 054901.

[2] J. O. Vasseur, O. B. Matar, J. F. Robillard, et al., *AIP Adv.* **1** (2011) 041904.

[3] J. F. Robillard, O. B. Matar, J. O. Vasseur, et al., *Appl.Phys. Lett.* **95** (2009) 124104.

[4] J.P.Parekh, *Electron.Lett* **6** (1969) 322 .

2PO-I2-18

LASER-INDUCED SOUND-DRIVEN MAGNETIC DYNAMICS IN WEAK FERROMAGNET FeBO_3

*Afanasiev D.¹, Razdolski I.¹, Skibinsky K.M.², Bolotin D.², Yagupov S.V.², Strugatsky M.B.²,
Kirilyuk A.¹, Rasing Th.¹, Kimel A.V.¹*

¹Radboud University, Nijmegen, Netherlands

²Taurida National University, Simferopol, Ukraine
strugatsky@crimea.edu

Here we report that femtosecond laser pulses trigger coherent oscillations of the magnetic anisotropy in magnetic easy-plane antiferromagnet with weak ferromagnetism FeBO_3 (D_{3d}^6). The oscillations are driven by optically excited lattice vibrations strongly coupled to the magnetic system. Unlike the spin resonances this mode is characterized by a very small damping ratio and can be easily pushed into an anharmonic regime [1].

We found that lattice vibrations are longitudinal standing acoustic waves ($\mathbf{k} \parallel C_3$) at the conditions of size resonance. Optical control of the magnetic anisotropy in FeBO_3 was studied employing a typical optical pump-probe technique. The laser-induced magnetization dynamics was monitored with mechanically delayed probe pulse measuring the pump-induced Faraday rotation. We used a series of iron borate single crystals with thicknesses of $4 \mu\text{m}$ to $40 \mu\text{m}$, synthesized by us. Dependences of the Faraday rotation on time-delay had an oscillating character for all the tested samples.

We theoretically describe experimental field dependences (Fig.1, points) of the 1st and the 2nd harmonics of the spin oscillations (Fig.1, solid lines) taking into account dynamical contributions $\delta d_{\text{dyn}} = G_4 \cdot u_{zz}$ and $\delta e_{\text{dyn}} = G_6 \cdot u_{zz}$ to effective constants of in-plane magnetic anisotropy (u_{zz} is a dynamic part of the strain tensor component; G_4 , G_6 are magnetoelastic fit parameters).

The constructed theory is the following. Based on the condition for spin oscillations frequency in our case $\omega \ll \omega_{\text{FMR}}$ we assume that the magnetic oscillations follow acoustic ones in a quasi-equilibrium manner [2]. Minimizing thermodynamic potential of the crystal with respect to in-plane orientation of the antiferromagnetic vector, we can find how the equilibrium orientation of the vector depends on the dynamical strains and external magnetic field. In particular, we show that the dynamical strain oscillating at frequency f leads to a strongly anharmonic response of the magnetization and generation of the second harmonic, in particular.

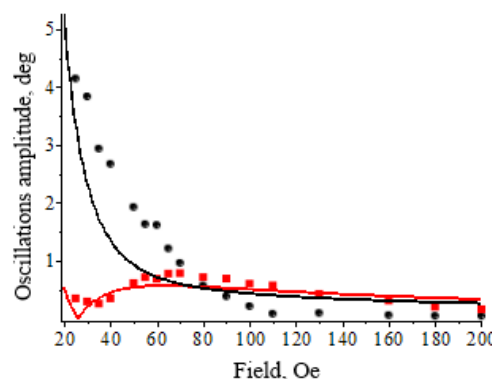


Fig. 1. Field dependences (Fig.1, points) of the amplitudes of the 1st and the 2nd harmonics of spin oscillations:
points – experiment,
solid lines – theory.

[1] D.Afanasiev, et al. *Phys. Rev. Lett.* (2014) (in press).

[2] Yu. N. Mitsay, et al., *JMMM*, **219** (2000) 340-348.

2PO-I2-19

DIAMAGNETIC METALLIC INCLUSIONS EXITATIONS IN GLOBULAR PHOTON CRYSTAL

Yurasov N.I.

BMSTU, Moscow, Russia

nikyurasov@yandex.ru

On the basis of a method of the connected waves the dispersive equation (DE) of excitations of a photon crystal (PC) was found. We have been considered the approach of two forbidden zones. Three components of decomposition of dielectric function of PC have been used: $\varepsilon_{-1}, \varepsilon_0, \varepsilon_1$. DE had the following form $K^6 - a_2 K^4 + a_4 K^2 - a_6 = 0$, where $K = ka/2\pi$, k – wave vector of excitation, a – lattice parameter of PC in a direction of propagation of excitations, a_2, a_4, a_6 – functions of frequency $\Omega = \omega a/2\pi$, $\hbar\omega = E$ – an energy of excitation, c – a velocity of light, ω – cyclic frequency of the electromagnetic wave falling normally on a surface of PC. Dielectric function of PC depends on dielectric functions of components of PC structure and structure of surface. The skeleton of PC was formed bcc by structure of spheres. For the purpose of studying of electromagnetic reaction in visible area it was accepted, that diameter of a sphere of an order 100 nm and it consists of an amorphous silicon oxide. The irradiated surface of PC was a plane (111).

Modeling components of dielectric function with the account of surface structure PC and the diamagnetic inclusions having negative material dielectric permeability has been executed.

The analytical condition of occurrence of crossing of dispersive branches in the form of the reference in zero of the function F depending on a_2, a_4, a_6 has been found. As generally a_2, a_4, a_6

are complex numbers the condition of crossing of branches looks like system of the equations for energy of photons, $F_1(E) = 0 \cup F_2(E) = 0$. By means of computer modeling the system has been investigated. In case of the free PC it has been received $F_1(E) > 0 \cup F_2(E) = 0$. If inclusions are diamagnetic nanoparticles of metal (gold) [1] we have found fixed performance of a condition of crossing of the branches, corresponding two various excitations. In calculations it was supposed, that diameter глобул D PC is in the range from 200 to 300 nm. The diameter of particles of gold was set in limits from 1 to 32 nm. Energy of photons in the field of crossing of dispersive branches laid in a range from 3.3 to 2.4 eV (length of a wave 378-485 nm), and volume concentration of gold was in the range of 18-24 % (D=200nm) and 11-18 % (D=300nm). Recent experiments with particles of gold have revealed appreciable changes of reflexion at its introduction in PC c the help of a suspension in water [2]. These changes are in settlement area of change of energy of photons.

[1] U. Kreibig., *J. Phys. France.*, **38** (1977) Suppl. N 7 C2.97-C2.103.

[2] V.S. Gorelik, V.V. Filatov, *Inorganic Materials*, **48** (2012) N 4,361-367.

2PO-I2-20

SURFACE AND BULK MAGNETIZATION IN X-RAY MAGNETIC CIRCULAR DICHROISM SPECTROSCOPY

Kuznetsova T.V.¹, Grebennikov V.I.¹, Zainullina R.I.¹, Buling A.², Kuepper K.²

¹Institute of Metal Physics UD RAS, Yekaterinburg, Russia

²Department of Physics, University of Osnabrück, D-49069 Osnabrück, Germany

kuznetsova@ifmlrs.uran.ru

X-ray magnetic circular dichroism (XMCD) is a very powerful tool to investigate the internal magnetic structure of compounds in question, including the unique possibility to separate the magnetic moments into their spin and orbital contributions. However XMCD lines often have a complex shape and direct application of the sum rules does not give reasonable values for the magnetic moments of the component compounds. Our report provides a method of obtaining information about the magnitude of the local atomic moments on the surface and in the bulk.

For example, we consider the $\text{La}_{0.5}\text{Pr}_{0.2}\text{Ca}_{0.3}\text{MnO}_3$. In Fig. 1 the XMCD difference of Mn $L_{2,3}$ -edges spectra, recorded with left and right circular polarized x-rays measured in magnetic field 6.9 T at 2 K, are presented as a green curve. The dichroic curve changes sign at 645 eV in L_3 region, therefore standard application of the XMCD sum rules gives very small total magnetic moment of $0.69 \mu_B$ on Mn atom. We suggest that magnetic moments in surface layers (TEY depth 10 nm) have two opposite orientations: with and against the bulk magnetization. Therefore, we propose to expand the observed complex signal into two contributions from atoms with different orientations of the magnetic moments. Fitting procedure gives two curves: dashed-dot for moments up and dot line for down. Applying the sum rules for each curve separately we find the values for the up and down magnetic moments in the surface layer (see Table 1). Sum of absolute values of the received moments gives values in the bulk. This results of a maximal total magnetic moment of $3.30 \mu_B$ in good agreement with magnetic measurements. We conclude that in surface layers (TEY depth) at 6.9 T only 62% moments stand along magnetization direction and 38% opposite.

The Pr $M_{4,5}$ spectra also contain the two signals from atoms with up and down magnetic moments. The above analysis gives the praseodymium magnetic moment $-3.81 \mu_B$ in the bulk (directed antiferromagnetically relatively manganese). At the surface 55% Pr atoms have down direction and 45% have up direction.

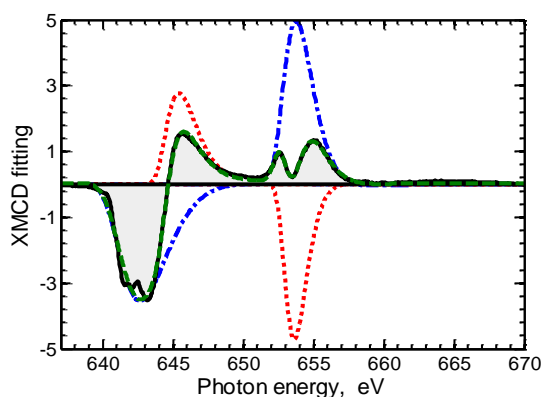


Fig. 1. The Mn $L_{2,3}$ XMCD spectrum (solid) and its fitting (dashed) by contribution from up magnetic moments (dashed-dot) and down (dots).

Table 1. The magnetic moments of the iron atoms in Bohr magnetons

Magn. moment	up	down	Surface sum	Bulk up-down
spin	2.00	-1.30	0.69	3.30
orbital	0.06	0.04	0.10	0.02
total	2.06	-1.26	0.79	3.32

Support by RFBR (grant 14-02-00080 and 13-02-96046-Ural) is acknowledged.

2PO-I2-21

ULTRAFAST DYNAMICS OF FARADAY ROTATION IN MAGNETOPHOTONIC CRYSTALS

Sharipova M.I.¹, Musorin A.I.¹, Dolgova T.V.¹, Inoue M.², Fedyanin A.A.¹

¹ Faculty of Physics, Lomonosov Moscow State University, Moscow, Russia

¹ Toyohashi University of Technology, Toyohashi, Japan

sharipova@nanolab.phys.msu.ru

Faraday effect is a phenomenon widely used for light propagation control. The effect is non-reciprocal and proportional to the thickness of a magnetic medium. Thus, it can be enhanced in multilayered structures with artificial dispersion and group delay, such as magnetophotonic crystals. In case of short femtosecond laser pulse its front part interacts with the structure less effectively than the rear one, so the latter one should rotate stronger and, due to that, Faraday rotation will grow

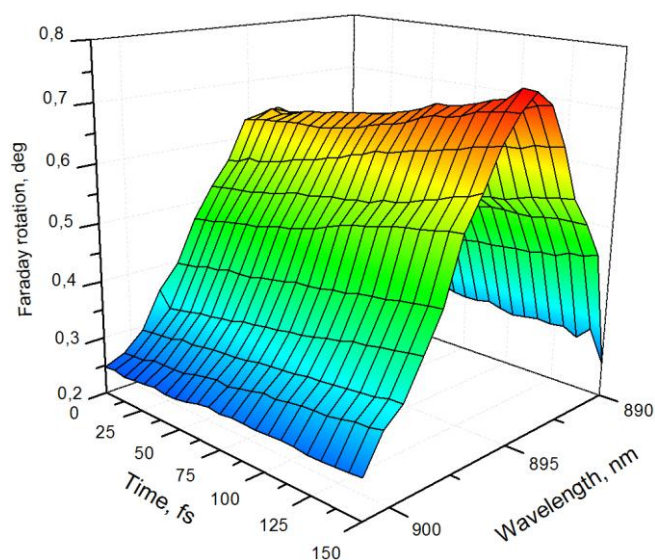


Fig. 1. Faraday rotation inside Bi-YIG magnetophotonic microcavity versus time and pulse' central wavelength. The effect always increases with time; maximum growth is observed at wavelength which equals to the center of the microcavity mode.

In other words, the closer pulse central wavelength to the center of the microcavity mode, the stronger is the growth with time.

To conclude, ultrafast Faraday rotation dynamics in a magnetophotonic microcavity has been detected. It is caused by the pulse self-interference inside its layers. The character of dynamics strongly depends on spectral position of the pulse central wavelength due to the strong artificial dispersion of the medium. The time derivative of Faraday rotation is the greatest when pulse central wavelength is at the center of microcavity mode and much less when it's in the vicinity of this point.

[1] A.V. Chetvertukhin *et al.*, *J. Appl. Phys.*, **111** (2012) 07A944.

[2] A.I. Musorin *et al.*, *Bulletin of the Russian Academy of Sciences: Physics*, **78** (2014) 43-48.

2PO-I2-22

MAGNETIZATION PROCESSES STUDY IN THE IMPLANTED GARNET FILMS USING THE SECOND HARMONIC GENERATION EFFECT

Bonda A.¹, Uba S.¹, Uba L.¹

¹ Institute of Computer Science, University of Białystok, Lipowa 41, PL-15-424 Białystok, Poland
a.bonda@uwb.edu.pl

The work concerns the study of magnetic properties of inhomogeneous systems using the methods of nonlinear optics. In particular, magnetization-induced second-harmonic generation (MSHG) effect has been applied in order to investigate the implantation effects in thin magnetic garnet film. The studies were performed on classical material of $(\text{YSmLuCa})_3(\text{FeGa})_5\text{O}_{12}$ garnet film, grown epitaxially on (111)-oriented gallium gadolinium garnet (GGG) substrate, implanted with H_2^+ ions of $1.5 \times 10^{16} \text{ cm}^{-2}$ dose and 60 keV energy. The total film thickness was 950 nm and the range of implantation was estimated to be 300 nm. In the implanted volume of the film large changes in uniaxial anisotropy have been observed as a result of radiation defects associated with strain in the crystal structure, and chemical effects of hydrogen ions influence occurring along the implantation depth [1]. Changes of the anisotropy in implanted film volume from the out-of-plane to the in-plane involve redistribution of the film magnetization. The measurements of the MSHG effect were performed in transmission as a function of amplitude and direction of external magnetic field [2]. The results show the complexity of the remagnetization processes for the garnet film subjected with hydrogen implantation. The MSHG intensities were measured as a function of the magnetic field providing insight into the nature of film magnetization distribution induced by implantation. Theoretical model of the MSHG effect has been developed which allows to perform decomposition of measured dependences on separate contributions originating from magnetization components for implanted and unimplanted film volume, respectively. It has been shown that the experimental techniques based on nonlinear MSHG effect are more informative as compared to the conventional methods of linear magneto-optics and enable to obtain complementary information about implantation effects which are the subject of the present study.

[1] P. Gerard, *Thin Solid Films*, **114** (1984) 3.

[2] A. Bonda, S. Uba, and L. Uba, *Phys. Rev. B*, **87** (2013) 024426.

2PO-I2-23

MAGNETOOPTICAL PROPERTIES OF Cd DOPED HgCr₂Se₄

Sukhorukov Yu.P.^{1,a}, Telegin A.V.¹, Mostovshchikova E.V.¹, Bebenin N.G.¹, Zainullina R.I.¹,
Gan'shina E.A.², Zykov G.S.², Fedorov V.A.³, Menschikova T.K.³

¹ Institute of Metal Physics UD of RAS, 620990, Ekaterinburg, Russia

² Moscow State University, 119991, Moscow, Russia

³ Kurnakov Institute of General and Inorganic Chemistry of RAS, Moscow 119991, Russia

^a suhorukov@imp.uran.ru

The goal of the work is to establish the effect of the band structure change in ferromagnetic semiconductors of Hg_xCd_{1-x}Cr₂Se₄ on the magneto-optical properties, namely, transversal Kerr effect (TKE), magnetotransmission $\Delta t/t_0 = (t_H - t_0)/t_0$ and magnetoreflexion $\Delta R/R_0 = (R_H - R_0)/R_0$, where t_0 , R_0 and t_H , R_0 are the transmission and reflection coefficients without and in a magnetic field, respectively.

The single-crystals of spinels (space group *Fd3m*) Hg_{1-x}Cd_xCr₂Se₄ ($0 \leq x \leq 1$) of size 4x4x3 mm³ were grown by the chemical transport reaction method described in detail in [1]. The TKE spectra of the spinels (Fig.1) above 2.5 eV originates likely from the overlapping of Se 4*p* → Hg 3*d* (Cd 3*d*) and Cr 3*d* transitions, below 2.5 eV they can be ascribed to the intra-atomic *d-d* transition of the Cr³⁺ ion in the octahedral environment. The difference in TKE spectra of doped Hg_{1-x}Cd_xCr₂Se₄ is likely connected with difference between the Se 4*p* → Hg 3*d* and Se 4*p* → (Cd 3*d*) transitions. The complex forms of $\Delta R/R_0$ and $\Delta t/t_0$ spectra for the spinels (Fig.2) are connected with (1) the “red” shift of absorption edge, (2) change of the interaction of light with free charge carriers, (3) change in the transitions in complexes that are formed by Cr²⁺ ions and Se vacancies in a magnetic field, and (4) type of conductivity.

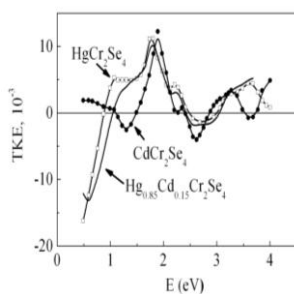


Fig.1

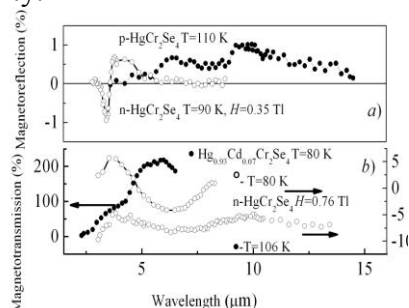


Fig.2

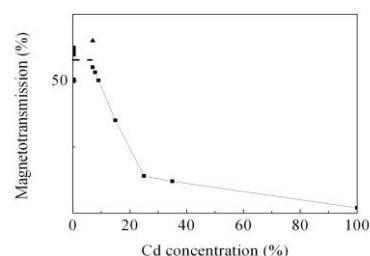


Fig.3

The substitution of Hg by Cd ions results in the decrease of the magnitude of magnetotransmission from ~60 % to 15 % for $0.1 < x < 0.25$ down to $\Delta t/t_0 \sim 2$ % for $x=1$ (Fig.3). Significant decrease in the $\Delta t/t_0$ value due to increase in Cd concentration is connected with the change in the band structure proposed in [2, 3]. The giant magneto-optical effects in Hg_{1-x}Cd_xCr₂Se₄ spinel can be used in magneto-optoelectronics.

The work was supported by Russian Government Mega-grant № 2013-220-04-350; RFBR grant № 13-02-00007 and project of DPS of RAS № 12-T-2-1005.

[1] Harald Schäfer, *Verlag Chemie*. (1962), 194.

[2] Yu.P. Sukhorukov, A.V. Telegin, N.G. Bebenin, et al., *JETP Letters*, **98** (2013) 313-316.

[3] M.I. Auslender, N.G. Bebenin, *Sol. State Commun.*, **69** (1989) 761-765.

2PO-I2-24

ORIENTATIONAL PHASE TRANSITION INTO A MODULATED MAGNETIC STATE IN THE SOME MAGNETICS

Djuarev D.R., Niyazov L.N., Fayziev Sh.Sh.

Bukhara State University, M.Iqbol, 11, 200000, Uzbekistan, Bukhara
djuraev2002@mail.ru

The magnetic linear birefringence of an $\text{FeBO}_3:\text{Mg}$ crystal is investigated as a function of the magnetic field strength and its orientation. The structure of the inhomogeneous magnetic phase of this weak ferromagnet is determined by analyzing the experimental results obtained. It is shown that, in an inhomogeneous magnetic state, the ferromagnetic moment does not deviate from the basal plane of the crystal and the angle of its deviation from the direction of the applied magnetic field is described by a one-dimensional function of the spatial coordinate along the axis of magnetization.

The transition from a homogeneous into a modulated magnetic state in weak ferromagnet $\text{FeBO}_3:\text{Mg}$ is studied by a magneto-optic method. At $T < 135\text{K}$, the application of a magnetic field in the weak plane of the crystal is shown to excite the modulation of its magnetic order parameter, which manifests itself in a periodic deviation of the local ferromagnetism vector from the magnetization direction. The modulation period and the azimuthal angle specifying the local ferromagnetism vector direction in the modulated magnetic state of the crystal are studied as a function of temperature and magnetic field. The results obtained are discussed in terms of the theory of «magnetic ripple».

The domain structure transformation and the technical magnetization process of $\text{Tb}_{0,26}\text{Y}_{2,74}\text{Fe}_5\text{O}_{12}$ single crystal has been studied by magneto-optic method in temperature region of spontaneous spin flip phase transition (SPT). It has been found that SPT occurs in a finite temperature interval where one has the coexistence of low- and high-temperature magnetic phase domains. We have observed the anomalies of temperature dependences of the coercive force and magneto-optic susceptibility related with the crystal domain structure transformation under spin flip. Interpretation of our experimental results has been carried out within the framework of SPT theory for a cubic crystal. It has been demonstrated that the existing theory describes consistently the evolution of $\text{Tb}_{0,26}\text{Y}_{2,74}\text{Fe}_5\text{O}_{12}$ garnet domain structure at spontaneous spin flip of easy magnetization axis.

The domain structure behavior of the plane-parallel plate of the ferrite-garnet $\text{Ho}_3\text{Fe}_5\text{O}_{12}$ in the temperature range nearby the magnetic compensation temperature T_K have been investigated by the magneto-optical method. The value of $T_K = (131 \pm 1)\text{K}$ have been determined from investigation of the temperature dependence of Faraday's effect. It has been shown that nearby T_K the essential modification of the domain width has been observed; the domain width increases near T_K and reaches the maximum. The stable «nondomain» state of the crystal exists in temperature range 129–132 K. The experimental results have been interpreted within the existing theory of the strip domain structure.

Experimental researches of influence of radial stresses and stresses C_3 of symmetry on domain structure Iron-Borate are executed and is shown, that stresses arising in a crystal lead to essential change of its domain structure and the basic magnetic characteristics (coercive force, an initial magnetic susceptibility, the form of the hysteresis loops). It is shown, that besides well-known influence of mechanical stresses on the basic magnetic properties of the magnetic, under certain conditions non-uniform mechanical stresses can lead to change of type of its magnetic ordering. The theoretical description of the revealed laws of influence of mechanical stresses on domain structure and magnetic properties Iron-Borate is executed

This research was supported by the Basic Research Foundation of Uzbekistan under grant No. $\Phi 2-\Phi A-0-83921/\Phi 2-\Phi A-\Phi 0383$.

2PO-I2-25

PROBLEMS OF ULTRAFAST MAGNETIC DYNAMICS INDUCED BY FEMTOSECOND LASER PULSES

Kurkin M.I.¹, Orlova N.B.²

¹ Institute of Metal Physics UrB RAS, Ekaterinburg, Russia

² Novosibirsk State Technical University, Novosibirsk, Russia

kurkin@imp.uran.ru

The processes of ultrafast magnetic dynamics with the characteristic times in the interval

$$10^{-14} \text{ s} < \tau_{uf} < 10^{-11} \text{ s} \quad (1)$$

are encountered by the means of femtosecond magneto-optics with the pulse durations of $\tau_p = 10^{-13}$ s [1]. In this report we consider the problems of description of ultrafast magnetic dynamics in ferromagnetics. The peculiarity of ferromagnetics is that the exchange interaction V_{ex} cannot alter their spin states. This follows from the properties of the full spin operator \mathbf{S}

$$\mathbf{S} = \sum_j \mathbf{S}_j, \quad (\mathbf{S})^2 V_{ex} - V_{ex} (\mathbf{S})^2 = 0, \quad S^z V_{ex} - V_{ex} S^z = 0$$

The interactions weaker compared with V_{ex} limit the characteristic time of spin dynamics τ_s by the value

$$\tau_s > 10^{-10} \text{ s} \quad (2)$$

The inequality

$$\tau_s \gg \tau_{uf} \quad (3)$$

is considered to be the main problem of the description of ultrafast magnetic dynamics processes in ferromagnetics. Three options to solve this problem are suggested:

- (i) the existing theory of spin magnetism has its internal limitations and the significance of the (2) inequality should not be overestimated;
- (ii) the optical pump is able to change the scale of τ_s from nanoseconds to femtoseconds;
- (iii) ultrafast magnetic dynamics is the property of the orbital magnetism L rather than spin S unquenched by the optical pump.

In this report we suppose to discuss the advantages of the third option and problems that appear with its application. The answers to the following questions will be suggested:

1. Why the electric field excitation can affect magneto-optical phenomena?
2. Why the ultrafast magnetic dynamics requires the excitation by femtosecond rather than more long pulses?
3. Why the quenching time of non-equilibrium orbital momenta τ_L can be more than τ_s ?
4. Why the rate of the angular momentum transmission from spins S via L to the lattice (τ_s^{-1}) can appear to be larger than the rate of its transmission (τ_L^{-1}) during the quenching of L ?

The answers to these questions justify the application of the option (iii) for the description of the observed processes of ultrafast magnetic dynamics.

The work is performed under the financial support of Russian Foundation for Basic Research (project 14-02-00260).

[1] A. Kirilyuk, A. Kimel and Th. Rasing, *Rev. Mod. Phys.*, **82** (2010) 2731.

2PO-I2-26

CORRELATION BETWEEN MAGNETIC AND MAGNETO-OPTICAL PROPERTIES OF Sr DOPED PrMnO₃ POLYCRISTALLINE FILMS

Greben'kova Yu.E.^{1}, Edelman I.S.¹, Sokolov A.E.¹, Stepanova E.A.²,
Andreev N.V.³, Chichkov V.I.³*

¹ L.V. Kirensky Institute of Physics, SB RAS, Krasnoyarsk, Russia

² Ural Federal University, Ekaterinburg, Russia

³ National University of Science and Technology "MISiS", Moscow, Russia

* uliag@iph.krasn.ru

Magnetic properties and visible magnetic circular dichroism (MCD) were investigated in Pr_{1-y}Sr_yMnO₃ polycrystalline films with y=0.2 and 0.4. Samples of 20–150 nm in thickness were prepared with the dc magnetron sputtering. Single-crystal zirconium oxide stabilized by yttrium was used as the substrate.

Field dependences of magnetization were very close for the both compounds as well as their low-temperature magnetization values. Temperature dependences of these samples magnetization measured in magnetic fields up to 3 kOe demonstrate both a various behavior and a difference in the low-temperature value of the magnetization.

MCD spectral dependences of the films with various Sr concentrations are characterized by several maxima with different intensities: very strong one in range 3.25–3.4 eV and a broad essentially weaker band near 2 eV (Fig.1). An additional maximum of opposite sign arises at 2.33 eV in the spectrum of the Pr_{0.6}Sr_{0.4}MnO₃ samples with the temperature decrease. Intensity of the high-energy MCD maximum increases strongly when coming from Pr_{0.8}Sr_{0.2}MnO₃ to Pr_{0.6}Sr_{0.4}MnO₃, while the MCD value in the low-energy interval remains almost the same for the both compounds. Experimental MCD spectra were decomposed to several Gaussian components, and temperature dependences of their amplitudes were analyzed in comparison with that of the samples magnetization. In the case of insulating Pr_{0.8}Sr_{0.2}MnO₃, the amplitude temperature course of each component is identical and corresponds to the temperature dependence of the films magnetization. In the case of metal Pr_{0.6}Sr_{0.4}MnO₃ the observed picture is more complex, since five maxima revealed in different spectral intervals demonstrate various temperature dependences of their amplitudes.

Thus, we met with a peculiar situation: the concentration dependence of the high-energy MCD maximum intensity doesn't correspond to the concentration behavior of the magnetization. The difference between MCD characteristics of two compounds and their relation to the magnetization are considered taking into account the different nature of electron transitions responsible for MCD.

The work was supported partly by the Russian Foundation for Basic Researches, Grant No. 14-02-01211 and 12-02-00717, and Grant of President of Russian Federation No.NSh-2886.2014.2.

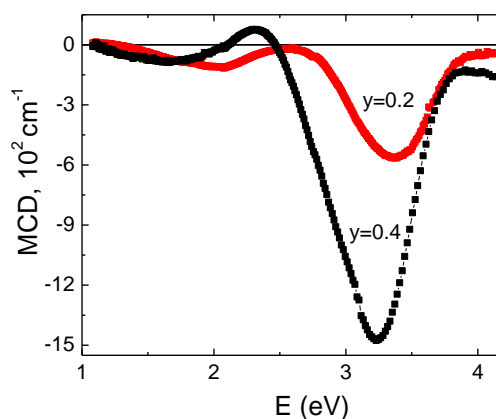


Fig. 1. MCD spectra of the Pr_{0.8}Sr_{0.2}MnO₃ and Pr_{0.6}Sr_{0.4}MnO₃ films reduced to the thickness. T=100 K, H=3 kOe

2PO-I2-27

EFFECT OF TETRADIC MAGNETOPOLARONS ON A MAGNETOOPTICAL ARB-SORPTION OF LIGHT IN A QUANTUM WELL IN A STRONG MAGNETIC FIELD

Eshpulatov B.¹, Kuvodikov Sh.², Eshniyazov O.², Xujanjva D.¹

¹ Samarkand branch of Tashkent University of Information Technologies, Samarkand, Uzbekistan

² Samarkand State University, Samarkand, Uzbekistan

After the pioneer works of Johnson and Larsen, [1][2] the magnetopolaron effect has attracted a great deal of attention from both theoretical and experimental groups. The magnetopolaron features in transport and optical phenomena have been intensely investigated. During the last years, a new wave of attention to this very interesting phenomenon has been stimulated by investigations of low-dimensional structures where the magnetopolaron effect is increased because of size-quantized character of both electronic and vibrational excitations. The Johnson-Larsen effect [1][2] appears when the condition $\omega_0 = j \omega_{eH}$ is satisfied, where the cyclotron frequency $\omega_{eH} = |e|H/(m_e c)$, j is an integer, e the charge of the electron, H the magnetic field, m_e the electron effective mass, and c the speed of light. Resonant coupling between pure electronic and mixed electron-phonon states light the degeneracy at all crossing points of dispersion branches for bare excitations. Double, triple and tetradic polaron splitting appear in the vicinity of points where two, three and four branches cross at $\omega_0 = \omega_{eH}$, respectively. Although the double, triple magnetopolarons has been investigated in detail for both bulk and low-dimensional structures, the crossing point of three and four energy branches, situated higher in energy, has not received much attention [3][4][5]. We show in this paper that there are a number of features that make the tetradic magnetopolaron (TMP) and his effect on a magneto-optical absorption of light in a quantum well in a strong magnetic field.

The one-particle Green function is calculated and the spectrum is derived for an electron in a magnetic field at zero temperature by taking into account interaction with polarization phonons. At magnetic field strengths corresponding to magnetophonon resonance the spectrum consists of four branches separated by an energy gap defined by the coupling constant. Damping of the higher energy branches of the spectrum is derived and the cut-off point of the branches is determined. The interband magneto-optical absorption of the light coefficient in the magneto-phonon resonance region is calculated. It is shown that in this region the magneto-optical absorption coefficient has four maxima, the distance between them being of the order of the distance between electron spectrum branches in the conductivity band.

In our calculations we did not take into account the Coulomb interaction between electrons and holes. The change of the energy spectrum due to Coulomb force is small. Thus, our theory of the tetradic magnetopolaron is relevant for the case when the deviation from equidistant energy separation of the four lower Landau levels is smaller than the tetradic magnetopolaron splitting.

The work was supported by the fundamental Investigation grant of SCST of the Republic of Uzbekistan (Project No.F2 FK-0-47 339 F2-015).

[1] D.M. Larsen et al., *J. Phys. Soc. Jpn. Suppl.*, **21** (1966) 443.

[2] E.J. Johnson and D.M. Larsen, *Phys. Rev. Lett.*, **16** (1966) 655.

[3] L.I. Korovin et al., *Fiz. Tverd. Tela Leningrad*, **13** (1971) 842, *Sov. Phys. Solid State* **13** (1971) 695.

[4] I.G. Lang et al., *Phys. Rev.B*, **56** (1997) 6880.

[5] B. Eshpulatov, E. Arzikulov, *American Journal of Analytical Chemistry*, **4** (2013) 457.

2PO-I2-28

MODELING OF A MINIATURE MAGNETO-OPTICAL CURRENT SENSORS*Safronova E.S.¹*¹ VNIIA, Moscow, Russian Federation
elnsafronova@gmail.com

For monitoring and diagnosis of electrical circuits, electrical fault detection, etc. different types of current sensors are applied. Recent developments have shown that among of the possible configurations of a pulse current sensor - magneto – optical sensors are compact, not subject to electromagnetic interference and require low power supply. In order that the sensors can be suitable for direct incorporation into an electrical circuit it's requires considerable size reduction. Reducing size of the sensors reduces the sensitivity as a function of the length of the optical path of the light signal through the magneto - optical material .

This study presents the results of numerical modeling of a miniature magneto-optical current sensor that can be embedded in a coaxial cable MPIEP/0.15-K. The modeling have been performed in the software package Comsol Multiphysics. According to the results of the theoretical research, it was found that the tailoring magneto-optical sensors suitable for monitoring high amplitude pulse current.

2PO-I2-29

FEMTOSECOND-SCALE TIME-DEPENDENT TRANSVERSE MAGNETO-OPTIC KERR EFFECT IN ONE-DIMENSIONAL MAGNETOPLASMONIC CRYSTALS

Frolov A.Yu., Vabishchevich P.P., Shcherbakov M.R., Dolgova T.V., Fedyanin A.A.
Faculty of Physics, Lomonosov Moscow State University, Moscow, Russia
frolov@nanolab.phys.msu.ru

We demonstrate the nontrivial evolution of the transverse magneto-optic Kerr effect (TMOKE) within 45-fs pulses reflected from an iron-based magnetoplasmonic crystal. The effect takes place for resonant surface plasmon-polariton (SPP) excitation, has opposite signs of the time derivative for different slopes of the SPP resonance, and is addressed to the magnetization-dependent dispersion relation of SPPs.

SPP is a short-living excitation spanning for up to several hundreds of femtoseconds. Interaction of a femtosecond laser pulse with plasmonic nanostructures recently emerged as a topic for research bringing about, to name a few, polarization shaping [1] with plasmonic media. On the other hand, it was shown that external quasi-static magnetic field can be used to control the dispersion of SPP in magnetic media [2]. However, the femtosecond laser pulse modification by SPP in an external magnetic field has not been demonstrated so far.

Measurements of the femtosecond-scale time-dependent TMOKE were performed for a sample of one-dimensional magnetoplasmonic crystal based on a commercially available digital versatile disk polycarbonate template having periodic corrugation with the depth of approximately 50 nm and the period of 750 ± 10 nm. The dielectric template was covered by a 100 nm layer of the polycrystalline iron deposited by magnetron sputtering and protected by a 20 nm-thick silica layer from the top.

Time-dependent TMOKE $\delta(t)$ is defined as:

$$\delta(t) = \frac{I(\vec{M}, t) - I(-\vec{M}, t)}{I(0, t)},$$

where $I(t)$ – is the envelope function of the pulse. In order to obtain the information about $\delta(t)$, a cross-correlation function (CCF) measurement setup was used. The difference of the CCFs in two opposite directions of the sample magnetization was measured instead of the $\delta(t)$ value:

$$\Delta(\tau) = \frac{I_{cf}(\vec{M}, \tau) - I_{cf}(-\vec{M}, \tau)}{I_{cf}(0, \tau)},$$

where τ is the time delay between the reflected and reference pulses, $I_{cf}(0, \tau)$ is the measured CCF of the reflected pulse without a sample magnetization.

We found that the $\Delta(\tau)$ -value has non-trivial behavior on the femtosecond time scale within the femtosecond laser pulse reflected from the magnetoplasmonic crystal. The femtosecond TMOKE $\Delta(\tau)$ has either increasing or decreasing character depending on the position of the incident pulse's carrier wavelength λ_c with respect to the slope of the SPP resonance.

[1] M.R. Shcherbakov, P.P. Vabishchevich, V.V. Komarova, T.V. Dolgova, V.I. Panov, V.V. Moshchalkov, A.A. Fedyanin, *Phys. Rev. Lett.*, **108** (2012) 253903.

[2] K.W. Chiu, and J.J. Quinn, *Il Nuovo Cimento B*, **10** (1972) 1-20.

2PO-I2-30

INFLUENCE OF THE INHOMOGENEITY ON MAGNETOREFLECTION AND MAGNETOTRANSMISSION IN MANGANITES

Yurasov A.N.¹, Gan'shina E.A.², Kaul A.R.², Korsakov I.E.², Sukhorukov Yu.P.³, Telegin A.V.³

¹ Moscow State Technical University of Radioengineering, Electronics and Automation, Moscow, Russia

² Moscow State University, Moscow, Russia

³ Institute of Metal Physics, Ural Division of RAS, Ekaterinburg, Russia
alexey_yurasov@mail.ru

The magnetorefractive effect (MRE) is a high frequency analogy of magnetoresistance (MC) and consists in variations of the coefficients of reflection, transmission and absorption of electromagnetic waves of samples with GMR, TMR or CMR under magnetization (see [1,2] and references therein). Thin films of manganites with the large values of Kerr and magnetorefractive effect are a promising magneto-optical material in the infrared and visible range. We present the results of investigations influence of the inhomogeneity on magnetoreflexion and magnetotransmission in manganites such as $\text{La}_{1-x}\text{Ca}_x\text{MnO}_3$, $\text{La}_{1-x}\text{Sr}_x\text{MnO}_3$ and $\text{La}_{1-x}\text{K}_x\text{MnO}_3$. It is shown that magnetic and charge inhomogeneity strongly influences on the magneto-optical effects in films. Our calculations of MRE in manganites bulk crystals and thin films have made in the framework of the effective medium approach (EMA) supposing that manganites consist of low and high resistivity phases with volume fractions depending on the magnitude of an applied magnetic field [2]. It was shown that the sign, magnitude, frequency dependencies of MRE in reflection and transmission modes are very sensitive to the model parameters and a sample thickness. The experimental data for compositions close to optimally doped films are in good agreement with the data calculated in the framework of a theory developed for manganites[3-4] and there is no good agreement in the case of low doping. In this case it is possible to unite the developed theory with an effective medium approach. This way has allowed to explain the experimental data.

This work was supported by the Russian Foundation for Basic Research № 12-02-33158.

- [1]. A.B. Granovsky, E.A. Ganshina, A.N. Yurasov, et al. *J. Commun. Technol. Electron.*, **52** (2007) 1065-1071.
- [2] A.N. Yurasov, T.N. Bakhvalova, A.V. Telegin, Yu.P. Sukhorukov *Functional materials*, **2** (2012) 178-181.
- [3] Yu.P. Sukhorukov, A.V. Telegin, A.B. Granovskii et al. *J. of Exp. and Theor. Phys.*, **114** (2012) 141-149.
- [4] A.B. Granovskii, Yu.P. Sukhorukov, A.V. Telegin, et al. *J. of Exp. and Theor. Phys.*, **112** (2011) 77-86.

2 July

Wednesday

17:30-18:30

poster session
2PO-J

**“Magnetic Soft Matter
(magnetic polymers,
fluids and
suspensions)”**

2PO-J-1

SIMULATION OF MAGNETODIELECTRIC EFFECT IN MAGNETORHEOLOGICAL ELASTOMERS

Isaev D.A.¹, Semisalova A.S.¹, Khajrullin M.F.¹, Loginova L.A.¹, Kramarenko E.Yu.¹, Perov N.S.¹

¹ Faculty of Physics, Lomonosov MSU, Moscow, Russia

isaev.danil@gmail.com

For the first time the effect of a uniform magnetic field on the permittivity of magnetorheological elastomers (MREs) has been simulated. The effective permittivity of MRE filled with conductive particles was shown to be strongly dependent on the applied magnetic field (magnetodielectric effect (MDE), or magnetocapacitance effect in MRE). The model has been developed to give the qualitative explanation of the experimental results obtained earlier in our group – we studied the change of the capacity of plane capacitor filled with magnetorheological elastomers and observed the increase of effective dielectric permittivity of MRE based on Fe, Fe₃O₄ and NdFeB [1].

Here we present the model for computer simulation of MDE and results on the influence of particles concentration, orientation of magnetic field, matrix elasticity on the studied effect obtained within this model. The behavior of spherical equally sized magnetic particles uniformly distributed in elastic matrix under the applied magnetic field was simulated, we considered the dipole-dipole interactions, the interaction of particles magnetic moments with external field and elastic stresses caused with matrix deformations. The particles were shown to tend to the formation of chain-like structures when magnetic field is applied (Fig. 1), and the displacement of particles and, therefore, the value of magnetodielectric effect, was shown to be dependent on the elastic properties of matrix and intensity of magnetic field. The results of modeling are in good qualitative agreement with experiment (Fig. 2). The observed field-induced phenomena evidence the attractiveness of MREs as novel promising materials in family of composite multiferroics.

Supported by RFBR (grants 13-03-00914, 13-02-90491, 13-02-12443).

[1] A.S. Semisalova, N.S. Perov, G.V. Stepanov, E.Yu. Kramarenko and A.R. Khokhlov, *Soft Matter*, **9** (2013) 11318-11324.

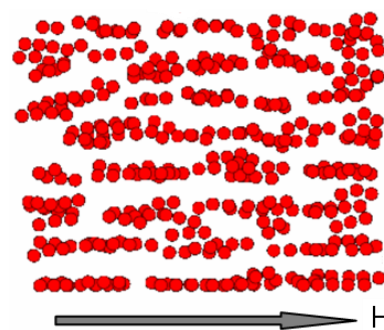


Fig. 1. Formation of chain-like structures in MRE under applied magnetic field.

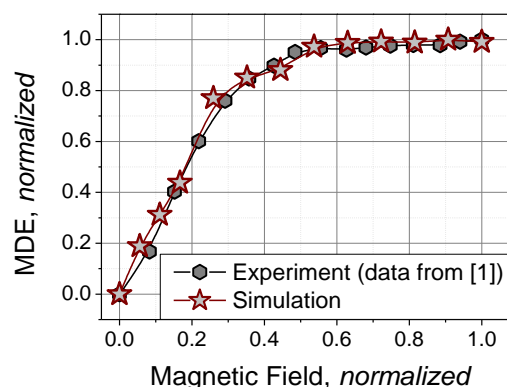


Fig. 2. Relative change of MRE effective dielectric permittivity (normalized) vs. applied magnetic field (normalized) dependence – comparison between experiment and simulation. Experimental data were taken from field dependence of effective permittivity of Fe-based MRE (size of particles – 2-5 μm , mass concentration – 73%) [1].

2PO-J-2

MAGNETIC PROPERTIES OF MAGNETIC HYDROGELS*Nikitin L.V.¹, Gladkov A.A.¹, Korovushkin A. E.¹*¹ Moscow State University, Physical department, Moscow, 119899, Russia

Hydrogels - solidlike disperse systems, characterized by the formation of the structure, which gives them the mechanical properties of solids. Unlike ordinary hydrogels magnetic hydrogels possess magnetic properties inherent for clusters of small magnetic particles. Magnetic hydrogels are quite new smart nanocomposites with a wide prospect for application. In particular, these soft magnetic materials are intended to be used as humidity and temperature sensors and actuators of many kinds in microfluidics and medicine. Due to that, their investigation is an issue of progressively growing interest for chemists, physicists and engineers.

This paper investigates magnetic hydrogels and their magnetic properties. In this work polyacrylamide hydrogel has been used as a source to create a magnetic hydrogels. This hydrogel has been chosen as the common and well-researched. Also this hydrogel have a good repeatability of the samples.

In our experiments we have prepared magnetic hydrogels with different mass concentration of magnetic particles. Also we studied changing of the magnetic characteristics of magnetic hydrogel samples during their drying. We obtained hysteresis loops, magnetization of saturation and susceptibility patterns. Experiments have shown that the mass concentration of magnetic particles has serious influence on the magnetic properties of the magnetic hydrogel. In both cases was marked nonlinear dependence of the magnetic characteristics from the mass concentration of magnetic particles.

Despite the fact that the magnetic hydrogels are completely new materials, there are already proposals for their use. It is supposed to use them as new composite materials, humidity sensors and for new devices in medicine.

2PO-J-3

GRADIENT DIFFUSION IN FERROCOLLOIDS WITH CHAIN AGGREGATES

Muratova A.B.¹, Ivanov A.O.¹, Kantorovich S.S.^{1,2}

¹ Ural Federal University (*UrFU*), Ekaterinburg, Russia

² University of Vienna, Wien, Austria

alla.muratova@urfu.ru

Ferrofluids are the systems consisting of single-domain magnetic particles (a particle of dispersed phase) suspended in a carrier liquid. Over time, magnetic fluids received wide application. Among these applications, the ones in medicine are the most promising. Thus, for example, a ferrofluid can be used to direct transport of drugs or contrast imaging. Of course, one of the most important medical applications of magnetic fluids is the treatment of cancer, so called hyperthermia. It is worth saying that the majority of medical applications rely on diffusion properties of magnetic fluids. For the correct application of magnetic fluids one needs to know how to describe both self-diffusion coefficients, and the coefficient of the gradient diffusion (when concentration and field gradients are formed in the system). The complex microstructure of magnetic colloids makes the study of diffusion rather complicated. There were several attempts to study diffusion [1] – [5], but the detailed theoretical description is still missing.

We investigate two systems: monodisperse and bidisperse ferrofluids with chain aggregates. Microstructure of the monodisperse system can be represented by one topological class of chains (different length) whereas it consists of three main classes of the chains in the bidisperse case. Weakly interacting small particles do not form chains without large ones, so we consider also single small particles in the bidisperse model. Also we study the three-dimensional and quasi-two-dimensional samples (also called monolayers). The quasi-two-dimensional ferrofluids are more complex because its microstructure contains more chain aggregate classes.

We present the results on the mobility and diffusion coefficients in the systems of magnetic dipolar particles. In the study we firstly investigated the influence of chain formation, polydispersity of particles, and geometric constraints on self-diffusion and gradient diffusion. We have approximated chain aggregates by ellipsoids and computed mobility of systems. We have used the Density Functional Approach and direct calculations to elucidate why the formation of chains leads to the average decrease of mobility in bulk monodisperse systems, but in the case of a bidisperse particle size distribution (in a bulk) the particle mobility becomes a function of the fractional composition. As the second step we calculated the diffusion coefficients using the mobility coefficients obtained before for both mono- and bidisperse systems of magnetic particles.

The research was supported by the Act 211 Government of the Russian Federation № 02.A03.21.0006, Ural Federal University development program with the financial support of young scientists (№ 1.2.2.2-14/40), RFBR Grants (№ 12-02-33106 and № 14-02-31698), and FWF START-Projekt Y627-N27.

- [1] Yu.A. Buyevich et al., *Physica. A*, **190** (1992) 276.
- [2] K.I. Morozov, *Phys. Rev. E* **53** (4) (1992) 3841.
- [3] P.Ilg, *Phys. Rev. E*, **71** (2005) 051407.
- [4] P.Ilg et al., *Phys. Rev. E*, **72** (2005) 031504.
- [5] J. Jordanovic et al., *Phys. Rev. Lett.*, **106** (2011) 038301.

2PO-J-4

MAGNETIC FLUID BRIDGE BETWEEN COAXIAL CYLINDERS WITH A LINE CONDUCTOR IN CASE OF WETTING

Vinogradova A.S.^{1,2}, Naletova V.A.¹, Turkov V.A.¹

¹ Lomonosov Moscow State University, Moscow, Russia

² National Research University Higher School of Economics (HSE), Moscow, Russia
vinogradova.msu@gmail.com

The shape of the free surface of a magnetic fluid (MF) may change spasmodically in the magnetic field of a line conductor while the current is slowly changing. In [1] the break-up of a MF bridge between coaxial cylinders with a line conductor was investigated theoretically for both cases of wetting and non-wetting, but the problem about formation of the MF bridge after its break-up was solved only for case of non-wetting. A MF drop appears on a line conductor after the MF bridge breaks up. In [2] the spreading of a MF drop along a wire in case of wetting for small magnetic fields was studied theoretically and observed in the experiment. The behaviour of a MF drop on a line conductor was developed in [3] for arbitrary magnetic fields.

In the present paper we consider a heavy, incompressible, homogenous, isothermal MF between two coaxial cylinders in case of wetting. There is a line conductor with current on the axis of these cylinders (Fig. 1). The MF is immersed in a non-magnetic liquid with the same density. We use the Langevin law to describe a MF magnetization. We get the general analytical solution for any axially symmetric shape of the MF free surface in any axisymmetric magnetic field from the hydrostatic equation and the boundary condition on the free surface.

It is shown that in case of wetting a break-up of the MF bridge between cylinders into two volumes occurs when the current increases from zero to some break-up value. The problems of a MF drop on line conductor and of a MF volume on outer cylinder are solved. The volumes of the MF which appear on cylinders and a break-up current are calculated numerically. There is also a critical value of current for which the MF bridge

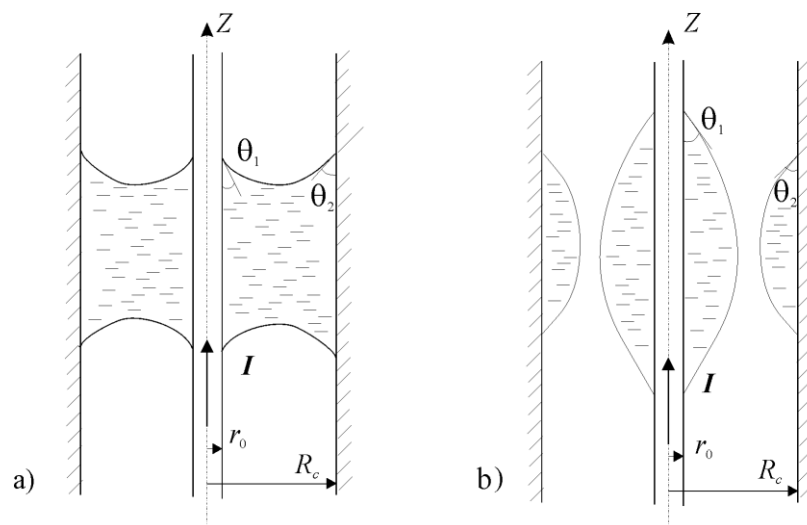


Fig. 1. The MF in case of wetting a) before and b) after break-up.

between cylinders cannot exist. The problem of formation of the MF bridge between two cylinders after its break-up when the current decreases from the break-up value to zero is solved. The minimal volume of the MF for which the MF bridge appears is found. This work is supported by Russian Foundation for Basic Research (projects 13-01-00703, 14-01-90003 and 14-01-31146).

[1] V.A. Naletova, V.A. Turkov, A.S. Vinogradova, *Physics Procedia*, **9** (2010) 68-73.

[2] J.C. Bacri, C. Frenois, R. Perzynski, D. Salin, *Rev. Phys. Appl.*, **23** (1988) 1017-1022.

[3] A.S. Vinogradova, V.A. Naletova, V.A. Turkov, A.G. Reks, *Magnetohydrodynamics*, **49** (2013) 119-126.

2PO-J-5

MAGNETOMECHANICAL ANISOTROPY OF FeGa/PU HYBRID NANOCOMPOSITE VIA PARTICLE CONCENTRATION AND SPATIAL ORIENTATION

Kiseleva T.Yu¹, Zholudev S.I.¹, Novakova A.A.¹, Smarjevskaya A.I.¹, Gendler T.S.², Grigorieva T.F.³

¹ Faculty of Physics, Lomonosov MSU, Moscow, Russia

² Institute of the Physics of the Earth RAS, Moscow, Russia

³ ISSC MC SB RAS, Novosibirsk, Russia

Kiseleva.TYu@gmail.com

Composites with magnetic fillers dispersed in a polymer matrix represent a system with physical and chemical properties that are influenced by the powder fillers and polymer matrix characteristics as well as by the interaction at the particle-polymer interface. The ability of taking the advantage of particular properties of particles as the constituent materials and its orientation in the matrix is the most important motivation for the development of magnetically anisotropic metal-polymer functional hybrids. The present work has been undertaken to research effects of structure, morphology, volume fraction, spatial arrangement of magnetostrictive intermetallic FeGa alloy particles in modified polyurethane matrix. Particles of FeGa alloy were used as perspective magnetostrictive material sensitive to mechanical stress and inverse magnetostrictive effect. Particles have been obtained by means of developed mechanochemical technology for producing particular phase composition [1]. Mechanochemically induced lattice distortions and stress possess increase the own particles magnetostriction [2]. Anisotropy of magnetization acquired during the composite preparation and composite magnetostriction via FeGa particles concentration, temperature and applied field were carried out. Correlation of composite magnetic properties with structure and anisotropy of their mechanical properties have been obtained by scanning electron microscopy, conversion electron Mossbauer spectroscopy, X-ray diffraction and dynamical mechanical analysis. Anisotropic structures of formed particles chains [3] with different interparticle interactions were observed. The increase of the magnetostrictive response with tailor-made magnetic anisotropy induced by magnetic particles volume fraction has been demonstrated. Support by RFBR Grant 13-00-838 is acknowledged.

[1] T.Grigoryeva, T.Kiseleva, et al. *Physics of Metals and Metallography*, **113** (2012) 575-582.

[2] T. Kiseleva, S. Zholudev, et al. *Tech. Phys. Letters.*, **39** (2013) 1110.

[3] A.Novakova, et al., *JMMM*, **258** (2003) 354–357 .

2PO-J-6

MACROPROPERTIES OF THE MAGNETIC SYSTEMS WITH ANISOTROPIC MICROSTRUCTURAL UNITS

Pyanzina E. S.¹

¹ Ural Federal University, Ekaterinburg, Russia
Elena.Pyanzina@urfu.ru

System with anisotropic microstructural units in the last several years became an independent fast-emerging branch of dipolar soft matter research. There are magnetic anisotropic particles (e.g. ellipsoids or rods) with different orientation of magnetic moments (along/perpendicular to the main axis), chains from magnetic particles in ferrofluids and etc. Shape of their units leads to the orientation-dependent steric interparticle interaction. The magnetic part of the interaction will be characterised by simple magnetic dipole–dipole interaction.

We present the theoretical study of the magnetic and some thermodynamic (structure factor and diffusion coefficient) properties for the systems of ellipsoidal magnetic particles with different dipole orientation, partially investigated in our previous work [1]. We focus our attention on the theoretical description of the magnetisation and initial susceptibility. We have developed a theoretical model for calculating magnetic properties (using modified mean field theory [2]) and also obtained preliminary results for structure factor and diffusion coefficients. An extensive comparison of our theoretical model to the results of molecular dynamics simulation for a wide range of system parameters demonstrated good quantitative and qualitative agreement. As a result, macroscopic responses of the systems drastically change with microstructural unit anisotropy. Using particle anisotropy as a control parameter the system structure can be altered without changing the value of the saturation magnetisation. This may prove to be very important in various medical and industrial applications, where a bottom up design of materials plays a crucial part and strong magnetic response of particles should be combined with the absence of strong cluster formation.

- [1] Kantorovich S., Pyanzina E., Sciortino F., *Soft Matter*, **9** (2013) 6594–6603.
[2] Ivanov A.O., Kuznetsova O.B., *Physical Review E*, **64** (2001) 041405-01-12.

2PO-J-7

**EXACT SOLUTIONS, INEQUALITIES AND APPROXIMATIONS
IN THE PROBLEM OF ACCELERATION OF SHOCK WAVES
IN THE MAGNETIC FIELD**

Golubiatnikov A.N.¹, Kovalevskaya S.D.¹

¹ Institute of Mechanics of Moscow State University, Moscow, Russia
golubiat@mail.ru

A class of magnetohydrodynamic problems describing the motion of a perfectly conducting gas with plane waves in a given homogeneous gravitational field is investigated. The solution involves a piston-driven shock wave which moves over the initially equilibrium background with decreasing density (and with a finite mass per unit area). Such phenomena are observed, in particular, in heated or ionized areas of atmospheres of planets and stars. The analysis is restricted to the Newtonian mechanics, although in the description of chromospheric solar flares the particle velocity can be as high as 0.8 of the speed of light, so the effects of relativity should be taken into account. Physically, two factors play a role here: the acceleration of the medium due to the decrease in inertia (L.I. Sedov, 1951) and the unlimited growth of the initial speed of sound. The external gravity force, which forms the initial state and restrains the acceleration, is a significant inhibiting factor here. In the absence of gravity, various blow-up effects associated with the finite time of shock wave's motion to infinity (Golubiatnikov A.N., Kovalevskaya S.D., 2012-2013) arise.

There exist some classes of exact solutions: self-similar solutions and solutions associated with separation of variables. An exact solution with an arbitrary function of the Lagrangian variable and solid-state gas motion behind the shock wave will be presented and investigated. The previously proposed method of integral inequalities (Golubiatnikov A.N., 1978) will be used for both analyzing the general one-dimensional case and qualitative investigation of particular solutions. The method makes it possible to derive and explicitly solve two-sided differential estimates for integral characteristics of the gas motion and, in particular, for the law of the shock wave motion. The method can be generalized to the presence of gravitational and frozen-in magnetic fields.

The work was supported by the RFBR (grant 14-01-00056).

2PO-J-8

PAIR CORRELATIONS IN A BIDISPERSE FERROFLUID IN THE ABSENCE OF A MAGNETIC FIELD

Nekhoroshkova Y.E.¹, Elfimova E.A.¹

¹ Ural Federal University (*UrFU*), Ekaterinburg, Russia
julechka.n@gmail.com

The pair distribution function $g(r)$ for a ferrofluid modeled by a bidisperse system of dipolar hard spheres is calculated. The influence of polydispersity on $g(r)$ and the related structure factor is studied. The calculation is performed by diagrammatic expansion methods within the thermodynamic perturbation theory in terms of the particle number density and the interparticle dipole-dipole interaction strength. Analytical expressions are provided for the pair distribution function to within the first order in number density and the second order in dipole-dipole interaction strength. The constructed theory is compared with the results of computer (Monte Carlo) simulations [1] to determine the range of its validity. The scattering structure factor is determined using the Fourier transform of the pair correlation function $g(r) - 1$. The influence of the granulometric composition and magnetic field strength on the height and position of the first peak of the structure factor that is most amenable to an experimental study is analyzed. The data obtained can serve as a basis for interpreting the experimental small-angle neutron scattering results and determining the regularities in the behavior of the structure factor, its dependence on the fractional composition of a ferrofluid, interparticle correlations, and external magnetic field.

[1] Yu. E. Nekhoroshkova, O.A. Goldina, P.J. Camp, E.A. Elfimova, A.O. Ivanov, *JETP*, **118** (2014) 442-456.

2PO-J-9

EFFECTS OF A SUPERPARAMAGNETIC STATE OF PARTICLES OF A PARAFFIN BASED MAGNETIC COLLOID

Dikansky Yu.I.¹, Ispiryayn A.G.¹, Kunikin S.A.¹, Radionov A.V.²

¹ North-Caucasian Federal University, Stavropol, Russia

² Ferrohydrodynamics, Nikolaev, Ukraine

Kunikin_S_A@rambler.ru

One of the parameters which investigation allows to carry out the analysis of relaxation peculiarities of a magnetic moment of nanoparticles' is the magnetic susceptibility which functional relationships were repeatedly explored by many authors. Interesting result in this field is the experimentally ascertained maximum of the temperature dependence of the susceptibility which presence was related to the loss of orientation degrees of freedom of hard magnetic one-domain particles at a solidification of a dispersion medium [1], and with the magnetic phase transition of system into a so-called state of "a dipolar glass" [2]. In the present work similar investigations are made for the magnetic colloidal nanosystems which dispersion medium transition from a liquid state to a solid state can be carried out at room temperatures.

As the object of investigation two samples of paraffin based magnetic fluid with magnetite particles with saturation magnetization 28 and 80 kA/m have been used. It has appeared that temperature dependence of a magnetic susceptibility of both samples has similar character, thus there are two maximums, one of which corresponds to the solidification point of a dispersion medium (fig. 1, curve 1), and another one is more flat and corresponds to a solid state of the sample. Additional constant magnetic field does not influence the temperature of the first maximum, but it translocates the second maximum to the lower temperatures (curve 2). It has been revealed that after solidification of the sample of colloid in a constant magnetic field, its magnetic susceptibility was essentially increased ($\approx 20\%$), besides, it maintains some remanent magnetization, which time dependence is not exponential and not power function. It has been concluded that the sharp maximum of temperature dependence of the magnetic susceptibility observed at paraffin melting

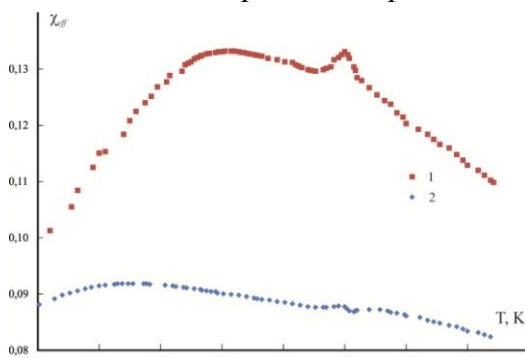


Fig. 1. Temperature dependence of ac susceptibility of paraffin based ferrofluid

point is really related to the blocking of Brownian degrees of freedom of a part of the largest magnetite particles which magnetic moment is rigidly related to a solid matrix. The presence of the basic flat maximum corresponding to a solid state of the sample, is not related to the magnetic phase transition, and explained by transition of a part of smaller particles at the decreasing temperature from a superparamagnetic state into the stable state. of conclusions the results of analysis of the dependence of remanent magnetization of the paraffin based colloid and the temperature dependence of the paste of magnetite particles are presented. The analysis of the peculiarities of a superparamagnetic state of the real magnetic colloid, related to a particle size distribution and

a period of a measuring field is also carried out.

Acknowledgements. Support by The Ministry of Education and Science of the Russian Federation and RFBR (project № 14-03-00312 a).

[1] S. A. Kunikin, Yu. I. Dikanskii, *Technical Physics*, **55** (2010) 866-870.

[2] S. Nakamae et al., *J. Appl. Phys.*, **105** (2009) 07E318.

2PO-J-10

ROSENSWEIG INSTABILITY UNDER TILTED MAGNETIC FIELD

Kazhan V.A.¹, Korovin V.M.²

¹ Moscow State University of Environmental Engineering, 127550 Moscow, Russia

² M.V. Lomonosov Moscow State University, Research Institute of Mechanics, 119192, Moscow, Russia

The hypothesis of field-independent susceptibility is frequently used in ferrohydrodynamics. In particular, origin of sharp peaks on a flat interface between a magnetic fluid and nonmagnetic one (or gas) submitted to a perpendicular magnetic field of supercritical intensity (Rosensweig instability) and following formation of steady patterns of different symmetries has been studied in numerous papers within the framework of this approach. Initiation and subsequent development of the instability are explained by an action of bulk and surface magnetic forces.

Of course, the Rosensweig instability can arise also due to tilted field. It is well known that in this case after onset the instability the longitudinal component of the field exerts an essential influence on the formation of surface structures at either (linear or nonlinear) magnetization. On the other hand, in the case of linear magnetization the longitudinal component of an applied tilted field does not affect the critical value M_{pc} of perpendicular magnetization M_p . Initiation of the Rosensweig instability occurs if $M_p > M_{pc}$. The expressions M_{pc} for both cases of linear as well as nonlinear magnetization for ferrofluids placed in a perpendicular field can be found in [1]. One has to notice here that for the case of nonlinear magnetization the obtained expression for M_{pc} is in fact a (not solved) nonlinear algebraic equation with respect to the critical value of magnetic field intensity in ferrofluid. In case of nonlinearly magnetizable ferrofluids under tilted field an expression M_{pc} has never been obtained before.

We report the derivation of a dispersion equation of linear inviscid surface waves on a deep ferrofluid of nonlinear magnetization submitted to a tilted magnetic field. Using the obtained dispersion equation we introduce some auxiliary function $Q=Q(k_x, k_y)$ of wave vector components k_x, k_y . The components of magnetization vector, the gravity acceleration and physical properties of the considered ferrofluid are parameters of this function. Modular surface $Q=Q(k_x, k_y)$ is symmetrical about the coordinate planes $k_x = 0$, $k_y = 0$. In contrast to [1], the calculation of critical wave number k_c of Rosensweig instability is reduced to searching the point of minimum of $Q=Q(k_x, k_y)$. Making use of $Q=Q(k_x, k_y)$, k_c and applying the magnetization law a nonlinear algebraic equation for M_{pc} is derived. Numerical calculations in the case of Langevin's magnetization curve show an essential stabilizing effect due to longitudinal component of the field.

This work was supported by RFBR (project 14-01-00056).

[1] R. E. Rosensweig, Ferrohydrodynamics (Cambridge Univ., Cambridge, 1985).

2PO-J-11

OPTICAL PROPERTIES OF AGGREGATED MAGNETIC FLUID: BIREFRINGENCE AND LIGHT SCATTERING

Yerin C.V.¹

¹ North Caucasian Federal University, Stavropol, Russia
exiton@inbox.ru

Aggregates of particles present in the magnetic fluids have a significant impact on their magnetic, optical and electrical properties [1]. Optical methods are among the most effective for the study of particle aggregates in magnetic fluids. Allocate the optical properties of colloids in the absence of external fields (static and dynamic light scattering, light absorption) and the effects of optical anisotropy under the influence of external fields (birefringence, dichroism).

Investigation of static and dynamic light scattering (SLS and DLS) [2] allow not only to determine the size of particles in a magnetic colloid, but also to study the dynamics of aggregation processes.

Effects of optical anisotropy in magnetic colloids in AC or pulsed external fields also allow to define the particle size, as well as explore their electrical and magnetic properties.

In this paper we present the results of studies of the optical properties of kerosene based magnetic fluids on with different concentrations of magnetite. Dynamic light scattering indicates the presence in the samples in addition to the size of individual particles and aggregates of 10-20 nm particle size of 60-120 nm.

Figure 1. Light scattering is a diagram of two samples of magnetic fluids with concentrations of 0.001% and 0.01%. As can be seen, significant differences between the charts no.

Fig. 2 shows the birefringence relaxation curves for four samples with concentrations between 10% and 0.01%. Effect of the samples with a concentration lower than 0.1% is virtually indistinguishable.

Thus we can conclude that the same mechanism of optical anisotropy in dilute magnetic fluids. The size of these aggregates is virtually independent of particle concentration units by the interaction apparently absent.

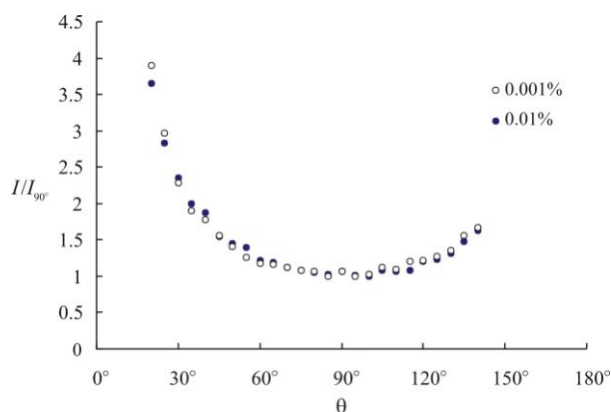


Fig.1 Angular diagram of SLS

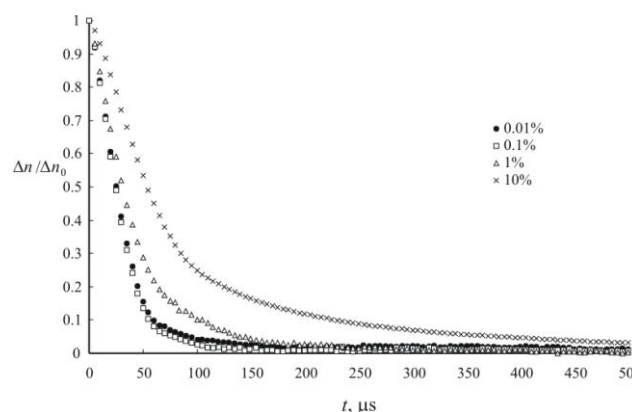


Fig. 2. Birefringence relaxation curves

Support by Russian Foundation for Basic Researches.

[1] W. Reed, J.H. Fendler // *J. Appl. Phys.* **59** (1986) 2914-2924.

[2] C. Yerin, V. Padalka // *J. Magn. Magn. Matter.* **289** (2005) 105-107.

2PO-J-12

SANS STUDY OF CoFe_2O_4 /LAURIC ACID/DDC- $\text{Na}/\text{H}_2\text{O}$ FERROFLUID STRUCTURE

BalasoIU M.^{1,2}, Ivankov O.¹, Soloviov D.^{1,3}, Lysenko S.⁴, Yakushev R.⁴, BalasoIU-Gaina A.M.^{1,5,6}, Burlui V.⁶, Lupu N.⁷

¹ Joint Institute for Nuclear Research, Dubna, Russia

² Horia Hulubei National Institute for Physics and Nuclear Engineering, Bucharest, Romania

³ Taras Shevchenko University, Kiev, Ukraine

⁴ Institute of Technical Chemistry Ural Branch of RAS, Perm, Russia

⁵ CMCF, Moscow State University, Moscow, Russia

⁶ University Apollonia, Iasi, Romania

⁷ Technical Physics Institute, Iasi, Romania

balas@jinr.ru; alexandra@balasoIU.com

In the present paper results on a new CoFe_2O_4 /lauric acid/DDC- $\text{Na}/\text{H}_2\text{O}$ ferrofluid sample investigation by means of small angle neutron scattering (SANS), high resolution transmission electron microscopy (HRTEM) and selected area electron diffraction (SAED) are presented.

High-resolution TEM (HRTEM) analysis was carried out on a LEO 912 AB OMEGA transmission electron microscope with an accelerating voltage of 120 kV (Advanced Technology Centre, Moscow). SANS experiments were performed at the time-of-flight YuMO spectrometer in function at the high flux pulse IBR-2 reactor, JINR Dubna.

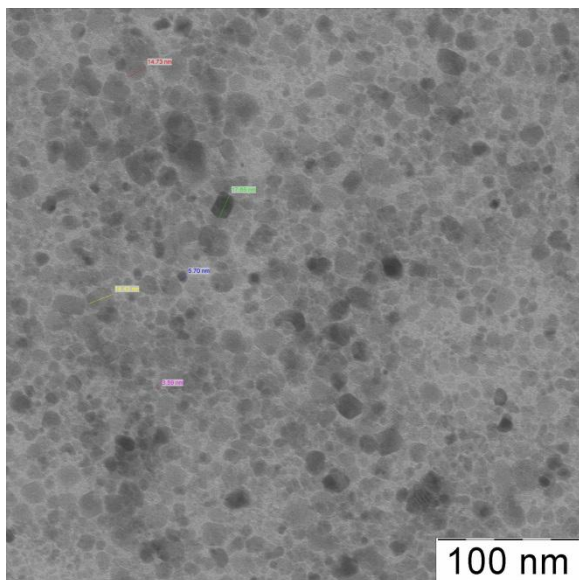


Fig.1 HRTEM image of a 3% particle vol. concentration CoFe_2O_4 /lauric acid/DDC- $\text{Na}/\text{H}_2\text{O}$ ferrofluid.

2PO-J-13

DYNAMIC MAGNETIC AND ELECTRICAL PROPERTIES OF MAGNETIC ELASTOMERS

Loginova L.A.¹, Khajrullin M.F.¹, Kramarenko E.Yu.¹, Stepanov G.V.², Perov N.S.¹

¹Lomonosov MSU, Faculty of Physics, Moscow, 119991, Russia

² State Research Institute of Chemistry and Technology of Organoelement Compounds, Moscow, 111123, Russia

la.loginova@physics.msu.ru

Magnetic elastomers or magnetoreological elastomers (MRE) are composite materials, which consist of polymer matrix and filler magnetic particles. The mechanical properties of magnetic elastomers change significantly under external magnetic field. It seems to be obvious that their magnetic and electrical properties can be varied with magnetic fields also, so the investigation of these materials is promising.

Previously it was shown that applying external magnetic field to the capacitor filled with MRE between plates led to change of its capacity due to MRE permittivity change (magnetodielectric effect) [1] in the frequency range from 1 to 200 kHz. The value of the magnetodielectric effect strongly depends on the type, size and concentration of MRE magnetic filler.

In this work the result of investigation of dependences of the magnetic and electrical properties of MRE based on silicon rubber matrix and various filler magnetic particles (Fe, NdFeB, Fe₃O₄) with different sizes and concentrations are presented. The magnetoelectric conversion factor's studies in the presence of induced electrical polarization are analyzed.

Also the dependences of magnetic susceptibility on frequency and external magnetic field were investigated. The magnetic field up to 0.5 T was applied to the coils with MRE core perpendicularly to their axes. The magnetic susceptibility components were calculated from the differences between the empty coil inductance and inductance of the coil with core. Measurements were carried out both the toroidal and cylindrical coils. It was found the difference between data for two types of coils. The found dependencies are discussed.

The work was financially supported by RFBR (grants No 13-02-12443, 13-03-00914, 13-02-90491).

[1] A.S. Semisalova, N.S. Perov, G.V. Stepanov, E.Yu. Kramarenko and A.R. Khokhlov, *Soft Matter*, **9** (2013) 11318-11324.

2PO-J-14

STRUCTURAL ORGANIZATION IN MAGNETIC FLUIDS WITH MAGNETIZED AGGREGATES IN ROTATING MAGNETIC FIELD

Gladkikh D.V.¹, Dikansky Yu.I.¹, Kolesnikova A.A.¹

¹ Institute of Mathematics and Natural Sciences, North-Caucasus Federal University, 355009
Stavropol, Russian Federation
gladkikhdv@gmail.com

Magnetic fluids (MF), being magnetic colloidal nano-systems, remain a field of interest attracting the attention of researchers due to the discovery of new aspects of their physical properties. The possibility of long-range magnetic ordering emergence in a system of colloidal single-domain particles has been considered previously, however, so far the problem remains unclear.

We have found a well-developed system of magnetized aggregates in kerosene-based magnetic liquids in certain conditions [1, 2]. Note that a typical feature of the magnetized aggregates is that, being exposed to the external magnetic field, they trigger the formation of long enough filamentary structures.

We have also found the emergence of structural organization in the system of magnetized aggregates under the concurrent action of crossed steady and alternating magnetic fields, a system of mutually perpendicular filament structures is formed, which periodically split up in a number of tiny fluctuating needle-like aggregates. (Fig. 1).

Structural organization has also been found under the action of the thin layer of magnetic colloid, which contains such aggregates, elliptically polarized rotating magnetic field, directed perpendicularly to the layer. In this case, aggregates rotating perpendicular to the plane of the layer form long filaments, which larger assembly can travel along (Fig. 2a). In this case sufficient regularity of formed lattice allows the observation of a diffraction image appearing on the screen when a laser beam goes perpendicularly to the MF layer. Additional action of steady magnetic field, directed perpendicular to the plane of rotation of the original (elliptically polarized) field significantly alters the properties of formed structural lattice (Fig. 2b, c).

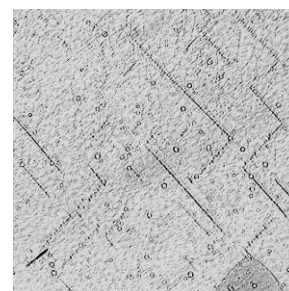


Fig. 1. Structure of the magnetized aggregates in the steady magnetic field ($H = 2 \text{ kA/m}$) and additionally imposed alternating magnetic field ($f = 30 \text{ Hz}$).

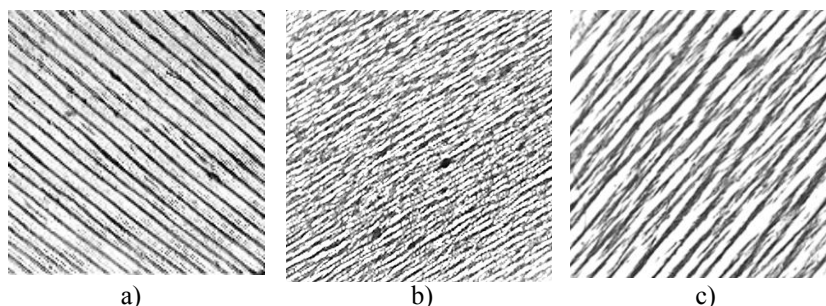


Fig. 2. Structural organization in the system of magnetized aggregates in elliptically polarized rotating magnetic field ($f = 3 \text{ Hz}$), directed perpendicularly to the layer (a), and transformation of a structure under additional action of steady magnetic field directed perpendicular: (b) $H = 650 \text{ A/m}$, (c) $H = 2000 \text{ A/m}$.

This work was supported by The Ministry of Education and Science of the Russian Federation and Russian Foundation for Basic Research (project № 14-03-00312 a).

[1] Yu.I. Dikanskii et al., *Colloid Journal*, **67** (2005) 134-139.

[2] Yu.I. Dikansky et al., *Magneto hydrodynamics*, **48** (2012) 493-501.

2PO-J-15

TO THE THEORY OF HYPERTHERMIA EFFECT INDUCED BY MAGNETIC NANOPARTICLES

Zubarev A.Yu.¹, Abu-Bakr A.F.²

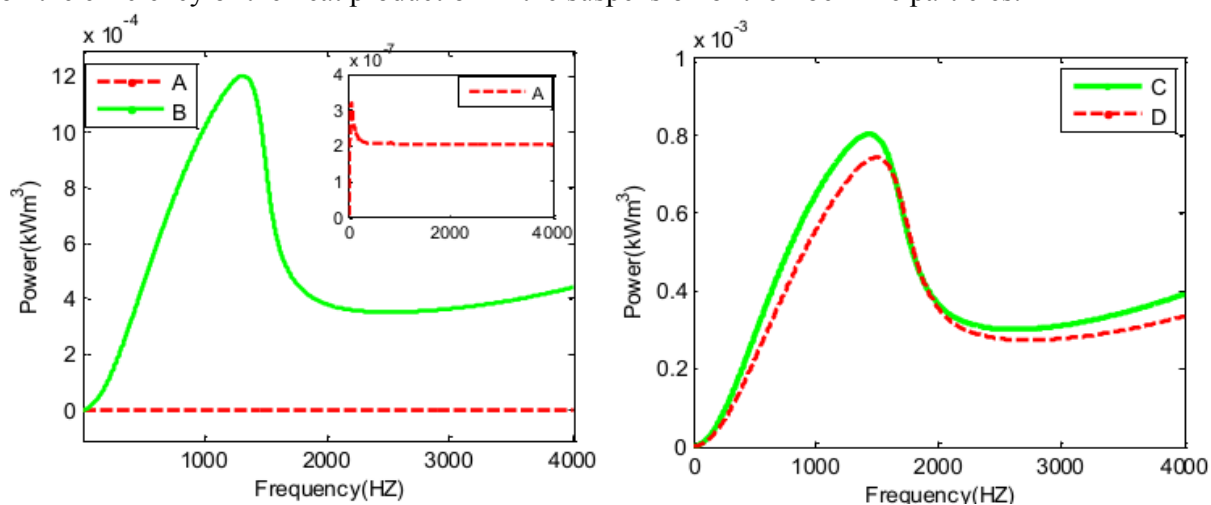
¹ Ural Federal University, Lenina Ave 51, 620083, Yekaterinburg, Russia

² Menoufiya University, Shebin El-Koom, 32511, Egypt
alibakr@yahoo.com

Magnetic nanoparticles placed in alternating magnetic field can be used for destruction of cancer cells due to heat production, resulted by the particle remagnetization, and mechanical damage of the cell membrane caused by oscillation motion of the particle as well. The majority of works on the magnetic hyperthermia effect deal with the spherical ferro-magnetic nanoparticles. The recent experiment of [1] have shown that the usage of the fiber-like ferromagnetic particles with the length about 100nm and diameter about 10nm can be very efficient for the both ways of the tumor cells destruction – the heating and mechanical damage of the cell membrane. The size of the particles is near the threshold size between the single - and multi domain state. Experiments [1] indicate that these particles experience internal remagnetization and, simultaneously, have some finite permanent magnetic moment.

We present results of theoretical modeling of the ellipsoidal particle rotating and the heat production under the alternating magnetic field. According to the experiments of [1], we suppose that in the magnetic field the particle experience the nonlinear (with saturation) magnetization and they have a permanent magnetic moment.

Mathematically, this model includes the equations of the particle rotating and remagnetization under the alternating field. These equations have been solved numerically; intensity of the power production in suspension of the particles has been calculated. The figures show the results of calculations of the power production of suspensions of the iron particles in water as a function of the frequency of the field oscillations. A) Calculations for the particles with a permanent moment, determined in experiments of [1]; B) same, when the particle has the permanent moment and, additionally, experiences nonlinear magnetization C) for magnetizable ellipsoidal particles with the aspect ratio 5.2 and D) same with the aspect ratio 3.7. These results demonstrate effect of the particle internal remagnetization and its shape on the efficiency of the heat production in the suspension of the fiber-like particles.



[1] Biran WANG, PhD dissertation, Universite de Nice-Sophia Antipolis - UFR Sciences, France. (2012) (under Georges Bossis).

2PO-J-16

EFFECTS OF MAGNETIC FIELDS ON THE STRUCTURE AND ON SURFACE TENSION OF FERROFLUID-VAPOUR INTERFACES

Zhukov A.V.¹

¹ Institute of Mechanics, Moscow State University, Moscow, Russia
az@imec.msu.ru

The structure of a flat equilibrium interphase boundary between a magnetic suspension (e.g., ferrofluid) and the vapour phase is investigated within the framework of the model of a two-component medium taking the dependence of the free energy of the system on the gradients of magnetic particle volume fraction, of carrier-fluid density and of magnetization into account. This dependence is found via simplified version of density functional theory [1]. The additional terms in the expression for the free energy describe the repulsive interaction between magnetic particles and molecules of the carrier-fluid and take into account the effect of magnetic particles on the carrier-fluid free energy similarly to “excluded volume” model. Although in the vapour region the magnetic particle volume fraction is mathematically nonzero for the considered equation of state, it can be made negligible for a fairly large value of the particle-fluid interaction parameter and, therefore, the penetration of magnetic particles into the vapour region is almost eliminated. The similar three-component model of the interface between magnetic and conventional fluids was developed in [2].

It is shown that for certain values of the constitutive parameters the bulk magnetic particle concentration increases significantly inside the interfacial layer, i.e., the particles are significantly adsorbed on the interface. For other values of parameters, however, this concentration is mainly spatially monotonic. In the case of strong particle adsorption the dependence of the surface tension on the magnetic particle concentration in the bulk (in the neighbourhood of the interface) is significantly nonlinear.

A refined model of the interface as a two-dimensional continuum with surface magnetization is constructed. Constitutive equations, conditions on the interface, and necessary stability conditions are obtained. The surface values of extensive parameters are determined as excess values associated with the Gibbs dividing surface. The surface tension tensor is anisotropic and depends on the location of the dividing surface. Various possible choices of the position of the dividing surface are considered.

The dependence of the surface tension tensor on the magnetic field strength is determined. It is shown that for certain problem parameters this dependence qualitatively corresponds to that obtained experimentally for ferrofluid-water interface and described in the phenomenological theory [3].

Applications of the proposed model to magnetic fluid boiling problems [4] are discussed.

Support by the Russian Foundation for Basic Research (projects Nos. 13-01-00035 and 14-01-00056) is acknowledged.

[1] P.I. Teixeira, M. M. Telo da Gama, *J. Phys.: Cond. Matter*, **3** (1991) 111-125.

[2] A.V. Zhukov, *Fluid Dynamics*, **48** (2013) 599-611.

[3] A.N. Golubyatnikov, G.I. Subhankulov, *Magnetohydrodynamics(Engl.Transl.)*, **22** (1986) 62.

[4] M.A. Kobozev, A.Ya. Simonovskii, *Technical Physics*, **52** (2007) 1422-1428.

2PO-J-17

THE MOVEMENTS OF AN ELLIPSOID WITH MAGNETIZABLE MATERIALS ALONG THE VESSEL BOTTOM IN THE UNIFORM ROTATING MAGNETIC FIELD

Pelevina D.A.^{1,2}, Turkov V.A.², Lukashevich M.V.², Kalmykov S.A.², Naletova V.A.^{1,2}

¹ Lomonosov Moscow State University, Moscow, Russia

² Institute of Mechanics, Lomonosov Moscow State University, Moscow, Russia
pelevina.daria@gmail.com

Magnetic fluid (MF) drop in uniform rotating magnetic fields can rotate and move progressively. In [1] the progressive motion of MF drop, wetting the smooth horizontal substrate, in a rotating magnetic field for different values of surface tension is investigated experimentally. It is shown that for small values of the surface tension the drop rolls as in the case of solid rolling, but at a higher value of the surface tension drop moves in the opposite direction. In this paper, we investigate experimentally the motion of the MF drop in a viscous non-magnetic fluid near the rough bottom of a rectangular vessel in a rotating uniform magnetic field. The progressive average velocity of the drop for different frequencies and amplitudes of the applied field is studied. Non-monotonic dependence of average velocity on the magnetic field frequency is received. Drop can move progressively towards solid rolling or in the opposite direction depending on the frequency and amplitude of the magnetic field, see Fig. 1.

In [2] theoretically and experimentally the motion of an elongated cylindrical body with a magnetizable polymer in a traveling magnetic field is considered. In this paper, we investigate experimentally the ellipsoid made of magnetizable polymer in a rotating uniform magnetic field. The dependence of the ellipsoid average velocity on frequency and amplitude of the magnetic field for different prolate of ellipsoid and environments is studied. Non-monotonic dependence (with one maximum) of average velocity on the frequency of the magnetic field is obtained. At a certain frequency of the magnetic field body stops.

A comparison of motion of a magnetizable polymer body and MF drop is made, see Fig. 2.

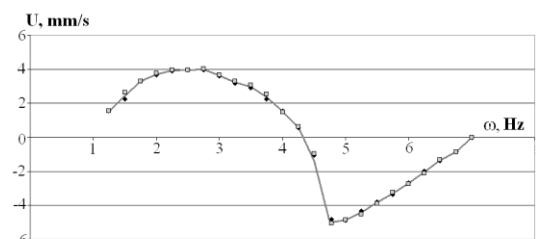


Fig. 1. Dependence of the average velocity U of the MF drop on the field frequency ω at $H = 100$ Oe

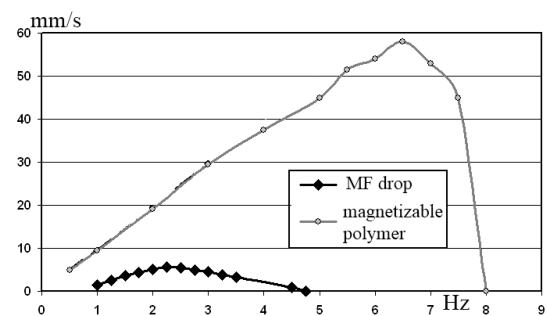


Fig. 2. Dependence of the average velocity U on the frequency of the magnetic field ω at $H = 150$ Oe

Support by RFBR (projects 14-01-31146, 14-01-91330) is acknowledged.

[1] A. Zakinyan, O. Nechaeva, Yu. Dikansky. *Experimental Thermal and Fluid Science*, **39** (2012) 265–268.

[2] S.A. Kalmykov, V.A. Naletova, V.A. Turkov. *Fluid Dynamics*, **48** (2013) 1, 4–13.

2PO-J-18

FERROFLUIDS BASED ON HARD MAGNETIC HEXAFERRITE NANOPARTICLES

Anokhin E.O.¹, Trusov L.A.¹, Vasilyev A.V.¹

¹ Moscow State University, Moscow, Russia
anokhin.evgeny@gmail.com

Ferrofluids containing hard ferrite particles are of great interest because of their distinctive features – high magnetocrystalline anisotropy of the material and platelet-like anisotropic particle shape. Such colloidal solutions can be used as material for production of magnetic coatings, films, nanocomposites, and nanostructures and they are also perspective for biomedical applications, e.g. magnetic hyperthermia, drug delivery and visualization. However, preparation of hexaferrite-based magnetic fluids is hindered by strong inter-particle magnetic interactions that lead to their agglomeration and subsequent sedimentation.

In this work we describe synthesis and peculiar properties of stable colloidal solutions of strontium hexaferrite single crystal nanoparticles with large spontaneous magnetization and coercivity by employing glass-ceramics in the SrO-Fe₂O₃-Al₂O₃-B₂O₃ system as a source of non-aggregated nanoparticles.

According to TEM, colloidal particles have platelet-like shape with thickness about 5 nm and diameter of 30 – 200 nm, depending on the synthesis conditions. XRD analysis confirmed that particles possess a strontium hexaferrite structure, where 10% of iron atoms are substituted by aluminum. Magnetic measurements of dried powders showed that particles exhibit hard-magnetic behavior with a saturation magnetization of 25 – 50 emu/g and a coercivity of 1200-5600 Oe. Comparison of specific magnetization of the colloids and respective extracted particles allows calculation of magnetic phase content. Estimated concentration of strontium hexaferrite in colloidal solutions is about 400 mg/l.

Stability of strontium hexaferrite aqueous colloidal solutions was investigated by dynamic light scattering in dependence on pH values, ionic strength, morphology and magnetic properties of the particles. It was found that colloidal solutions are stable at pH = 1.5 – 5 and electrolyte concentrations up to 100 mmol/l (NaCl).

Since colloidal particles carry considerable permanent magnetic moment, the solutions have a high sensitivity to magnetic field. Thus, 50% and 95% of the saturation values are achieved at 5 and 150 Oe, respectively. Due to tough coupling of particle magnetic moment to crystal axes in hexaferrite structure the particles align in magnetic field which results in a magnetic field dependent optical transmission of the colloids. The changes in transmission are clearly detectable even at very low magnetic field right down to 4 Oe. The AC measurements showed that optical modulation could be achieved at frequencies up to 1000 Hz.

Also the colloidal particles can be transferred to non-aqueous solvents (chloroform, heptane). It was demonstrated that strontium hexaferrite present there in the form of large aggregates (over 400 nm in diameter) and high stability can be achieved by using proper surfactants.

This research was funded by Russian Foundation for Basic Research, grant No. 14-03-31598.

2PO-J-19

INFLUENCE OF ROTATION ON THE MAGNETIZATION OF DILUTE SUSPENSIONS OF MAGNETIC PARTICLES

Tyatyushkin A.N.¹

¹ Institute of Mechanics, Moscow State University, Moscow, Russia
tan@imec.msu.ru

Non-equilibrium magnetization of a suspension of magnetic dipoles in oscillating [1] and rotating [2] magnetic fields was theoretically studied with the use of the Fokker–Plank equation. Within the frame of this approach, the influence of the rotational Brownian motion of the magnetic dipoles is taken into account, but the inertial effects are neglected. The influence of the inertial effects on the non-equilibrium magnetization of an immovable dilute suspension of spherical magnetic particles was theoretically investigated in [3] and [4]. The goal of this work is to investigate theoretically the influence of rotation on the magnetization of a suspension of spherical magnetic particles in a uniform magnetic field with taking into account the inertial effects. The radii and magnetic dipole moments of the particles are regarded as the same. The volume concentration of the suspension is regarded as so small that the magnetic and hydrodynamic interactions of the particles can be neglected.

A rotation of a single spherical non-Brownian particle with an embedded magnetic moment under action of a rotational flow of the ambient liquid in an applied uniform magnetic field is considered. The system of equations is obtained that determines the rotation of the particle and the instant orientation of its magnetic dipole moment. A uniform rotation in a constant magnetic field and an oscillatory rotation in a sufficiently weak alternating magnetic field are investigated.

The magnetization vector of a suspension of non-Brownian spherical magnetic particles rotating in a uniform magnetic field is found for the case of the equilibrium magnetization in a constant magnetic field and for the case of the non-equilibrium magnetization in a sufficiently weak alternating magnetic field.

The system of equations is obtained for the function of the distribution over the orientations of the magnetic dipole moments for a suspension of Brownian spherical magnetic particles rotating in a uniform magnetic field. The obtained system of equations takes into account both the inertia of the particles and that of the dispersion liquid of the suspension. The solution to this system of equations is obtained for a suspension rotating in a sufficiently weak alternating magnetic field. With the use of this solution, the magnetization vector of the suspension is found.

The magnetization vector of a suspension rotating with angular velocity Ω in a sufficiently weak uniform alternating magnetic field with intensity $H_a \cos(\omega t)$, where H_a and ω are the amplitude and circular frequency of the oscillations and t is the time, is established to have the form

$$\mathbf{M} = \chi' \cdot \mathbf{H}_a \cos(\omega t) + \chi'' \cdot \mathbf{H}_a \sin(\omega t) + \tau' \Omega \times \mathbf{H}_a \cos(\omega t) + \tau'' \Omega \times \mathbf{H}_a \sin(\omega t),$$

where the in-phase and out-of-phase components of the magnetic susceptibility tensor, χ' and χ'' , and the time-dimension coefficients, τ' and τ'' , are calculated for both suspension of non-Brownian particles and that of Brownian ones, and \times denote the contraction and vector product.

Support by RFBR grants 13-01-00035 and 14-01-00056 is acknowledged.

- [1] Yu.L. Raikher and V.I. Stepanov, *J. Magn. Magn. Mat.*, **320** (2008) 2692.
- [2] Yu.L. Raikher and V.I. Stepanov, *Phys. Rev. E*, **83** (2011) 021401.
- [3] A.N. Tyatyushkin, *Solid State Phenom.*, **152-153** (2009) 167.
- [4] A.N. Tyatyushkin, *Solid State Phenom.*, **190** (2012) 657.

2PO-J-20

MAGNETIC SUSCEPTIBILITY OF THE POLYDISPERSE FERROFLUID EMULSION

*Subbotin I.M.*¹

¹ Institute of Mathematics and Computer Sciences, Ural Federal University, 51 Lenin Av., 620000 Ekaterinburg, Russia
i.m.subbotin@gmail.com

Experimental study of the static magnetic properties of ferrofluid emulsions has demonstrated the nonmonotonic field dependence of the emulsion magnetic permeability. In a weak magnetic field the emulsion permeability rapidly grows and reaches maximum, and then it decreases slowly in stronger fields. We suggest the theoretical description of the effect based on the following idea. Weak field growth of the emulsion magnetic permeability is caused by the droplet elongation and the resulting reduction of demagnetizing field under the constant value of ferrofluid magnetic susceptibility. Subsequent decrease of the emulsion magnetic permeability in stronger magnetic field is explained by the decay of ferrofluid magnetic susceptibility under the approximately constant degree of droplet elongation.

The influence of droplet polydispersity on the emulsion magnetic susceptibility is investigated on the basis of iterative scheme similar to that described in [1]. This procedure allows us to calculate the internal field and the elongation for each class of droplets of different size. For the case of weak magnetic field the emulsion magnetic susceptibility χ_e is obtained as:

$$\chi_e = \chi_0 \left[1 + \frac{(4\pi\chi_0)^3 (1-\varphi)^2 H_0^2 \langle R^4 \rangle}{120 \varphi^3 \sigma \langle R^3 \rangle} \right],$$

$$\chi_0 = \frac{\chi_f \varphi}{1 + \frac{4\pi}{3} \chi_f (1-\varphi)},$$

where the angle brackets are used for notation of the mean value over the droplet size distribution, R is the droplet radius, φ stands for the total droplet volume fraction, H_0 has a meaning of the applied field strength, σ is the interfacial tension, and χ_0 is the initial (zero-field) magnetic susceptibility, which is independent on the droplet polydispersity.

So, in weak magnetic field the ferrofluid emulsion magnetic susceptibility increases parabolically with field strength. Concerning the influence of droplet polydispersity, we have to say that the emulsion susceptibility is weakly dependent on the polydispersity degree, since it depends on the ratio of the mean values of the forth power of droplet radius and the third power, that is $\langle R^4 \rangle / \langle R^3 \rangle$.

This research was carried out under the financial support from the Russian Foundation for Basic Research and the Government of Sverdlovsk Region, grant No. 13-01-96032_r_ural.

[1] A.O. Ivanov, O.B. Kuznetsova, I.M. Subbotin, *Magnetohydrodynamics*, **49** (2013) 191–196.

2PO-J-21

MAGNETOACTIVE ELASTOMER AND IT'S PROPERTIES

Stepanov G. V.¹, Kramarenko E. Yu.²

¹ GNIChTEOS 105118, Moscow, Russia

² Physics Department, Moscow State University, 119992 Moscow, Russia
gstepanov@mail.ru

There has passed 20 years since Lord Corp. and Ford Co. patented the magnetorheological elastomer (MRE) and damping devices on its basis. The rheological properties of the material were described in a number of articles [1]. Over a long period of time the research was conducted in the direction of the magnetoelasticity of the elastomer expected to be capable of changing its viscoelasticity in the magnetic field. Simultaneously with the MRE, there were done studies of magnetic gels by M. Zrínyi and magnetoelastics by L. Nikitin and G. Stepanov [2]. In their work attention was mainly focused on the magnetodeformational effect based on the field-induced elongation of the elastomeric sample placed in inhomogeneous magnetic fields. As the set of fascinating properties of the composite was becoming more and more extensive, the spectrum of names attributed to the material was getting wider, which is indicative of the number of features reversibly changeable under the influence of magnetic fields. Featuring a typical “smart material” the magnetoactive elastomer (MAE) exhibits the following bevy of properties:

Magnetorheological effect – the unique ability to exhibit significant quick and controllable changes in the viscoelastic properties when influenced with magnetic fields; Magnetoelctorheological effect – exhibition of changes in the viscoelasticity under simultaneous influence of magnetic and electric fields; Magnetodeformational effect – capability to demonstrate quick and controllable large-scale deformations in gradient magnetic fields; Magnetostriction effect – capability to exhibit modest (up to 10%) quick and controllable deformations in homogeneous magnetic fields; Shape memory effect or magnetic-field-induced plasticity – a property based on the ability to retain the new shape acquired as a result of mechanical stimulation when under the influence of a magnetic field and restitution of the initial geometrical configuration after the field has been off; Magneto-resistive effect – magnetic-field-induced change in the electroconductivity; Piezoresistive effect – external-pressure-induced change in the electroconductivity; Magnetopiezoresistive effect – superadditive change in the electroconductivity under the simultaneous influence of mechanical pressure and magnetic field; Magneto-optical effect – magnetic-field-induced change in the optical transmission; Magnetodielectric effect – magnetic-field-induced change in the electric permeability and magnetic susceptibility; Magnetoacoustic effect – change of the speed of acoustic waves propagating in the material under the influence of magnetic field; Piezoelectric effect – the capability of the material to generate an electric impulse as a result of a mechanical impact. Thus the area of investigations to be done on the properties of the MAE is very extensive. Currently intensive work is conducted on designing and patenting a broad spectrum of devices employing elastomers of the given kind. What is the specific mechanism leading to such a rich set of features? It is a known fact that a magnetic field induces magnetization of the particles of the magnetic filler resulting in their attractive interaction. As long as the particles are placed in the elastic polymer matrix, they overcome the elastic forces of the polymer and drift towards each other, which results in the formation of a chain-like structure and in the whole a new anisotropic arrangement. The given structure remains stable until the external magnetic field is off. Then the particles of the magnetic filler drift back to the primary positions in the polymer matrix, which leads to the restitution of the initial features.

[1] M. R. Jolly, J. Carlson, B. Munoz, T. Bullions, J. *Intell. Mater. Syst. Struct.*, **7** (1996) 613.

[2] L. Nikitin, L. Mironova, G. Stepanov, *Polymer Science, Ser. A.*, **43** (4) (2001) 443.

2PO-J-22

THE INSTABILITY OF FERROFLUID LAYER ON A LIQUID SUBSTRATE IN VERTICAL MAGNETIC FIELD

Bushueva C.A.¹, Kostarev K.G.¹

¹ Institute of Continuous Media Mechanics, Perm, Russia
bca@icmm.ru

The formation of ordered systems of drops resulting from the disintegration of a horizontal ferrofluid layer on a liquid substrate under the action of a uniform vertical magnetic field is investigated experimentally. The use of liquid substrate allows us to rupture ferrofluid layers which deformation on the solid substrate manifests itself only in periodic surface perturbation in the same range of field intensity [1]. The quantity and size of drops depend on the initial thickness of ferrofluid layer and the time necessary to achieve the critical intensity of the magnetic field (fast or slow rising magnetic field). The experiments show that the critical field strength increases with the initial layer thickness and decreases with increasing magnetic susceptibility of the ferrofluid.

The distribution of droplets' size and spatial period of their location relative to each other was built. The experimental results were compared with the theoretical works on the instability of the ferrofluid layer's free surface. The experimental data for dimensionless critical values of the magnetic field intensity H and for spatial period k of the ferrofluid surface instability are in a good agreement with the theoretical description of the magnetic fluid layer decay to drops designed for "magnetic fluid sandwich structures" [2] (fig. 1).

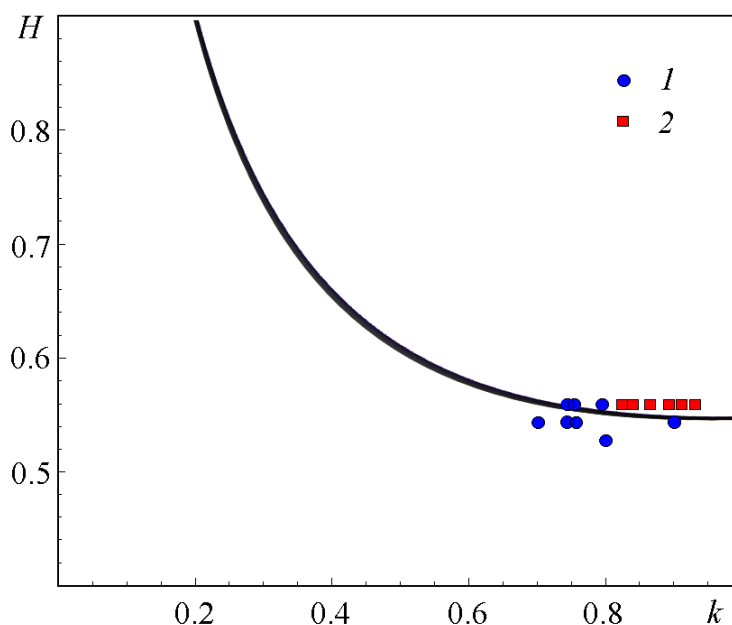


Fig. 1. Dimensionless critical value of the magnetic field intensity H versus dimensionless spatial period k . Full line – theory, experiment: 1 – slow rising field, 2 – fast rising field.

The work was supported by the grant of the research program of the Ural Branch of RAS No. 12-T-1-1008 and the RFBR project No. 13-01-96041.

[1] M.D. Cowley, R.E. Rosensweig, *J. Fluid Mech.*, **30** (1967) 671–688.

[2] D. Rannacher, A. Engel, *Phys. Rev. E.*, **69** (2004) 066306 (1–8).

2PO-J-23

CHOOSING BIDISPERSE APPROXIMATION USING EXPERIMENTS FOR DESCRIBING REAL-WORLD POLYDISPERSE FERROFLUIDS

Minina E.S.^{1,2}, *Novak E.V.*¹, *Pyanzina E.S.*¹, *Avdeev M.V.*³, *Kantorovich S.S.*^{1,4}

¹ Ural Federal University, Ekaterinburg, Russia

² University of Stuttgart, Stuttgart, Germany (current place of work)

³ Joint Institute for Nuclear Research, Russia

⁴ University of Vienna, Wien, Austria

eminina86@gmail.ru

Ferrofluids are stable colloidal suspensions of ferromagnetic nanoparticles of typical diameter 10–20 nm. The ferrofluid properties are strongly dependent on its microstructure. The latter may be described by the pair correlation function, which means the probability density for the mutual position of two randomly chosen ferroparticles, the magnetic moments of which are averaged over all their orientations. The pair correlation function describes the interparticle correlations, which are responsible for the differences between the properties of a magnetic fluid and those of an ideal paramagnetic gas. Experimentally the structure properties of ferrofluids may be investigated with the small-angle neutron scattering technique [1]. Scattering measurements allow obtaining the so-called structure factor, which is actually the Fourier transform of the pair correlation function of the ferroparticle system. Thus, for correct processing of experimental data it is necessary to develop a theoretical model for calculating the pair correlation function. Ferroparticles are distributed in sizes in real magnetic fluids, and the particle polydispersity needs to be taken into account. We chose bidisperse system as the first step to allow for polydispersity when studying thermodynamics of magnetic fluids in the paper [2].

Using molecular dynamics simulations, we calculated polydisperse structure factor and compared it to a model bidisperse structure factor, with the bidisperse parameters chosen in such a way that the initial susceptibility and the saturation magnetization of a poly- and bidisperse systems are the same. It turned out that even though the position of the first peak is the same, the peak height of a bidisperse structure factor is higher than that of a truly polydisperse system for about 10%. This pushed us to the important conclusion: the bidisperse approximation based on matching the magnetic properties is not appropriate for the description of the structure factor in polydisperse systems. Thus, the primary task is to figure out how to choose the parameters of a bidisperse system to obtain not only a qualitative agreement but also the quantitative one.

Here, we present one of the possible approaches to solve this problem, taking into account carefully form-factors always used in real experiments. We took as the basis real experiment [3], where were examined the suspension of magnetite in benzene with oleic acid, volume concentrations varied between 0.01, 0.019, 0.038, 0.075, 0.15. The sample did not contain any aggregates. In this work we present our attempt to develop a bidisperse model to describe the existing experimental data for various volume concentrations using fixed form-factors.

Here, we also answer a very crucial question: Is there a bidisperse system suitable to describe structure factors of real ferrofluids, or one has to unavoidably use multi-fractional models.

The work was done in the framework of the RFBR Grant No.12-02-33106 mol-a-ved, S.K. has been supported by Austrian Science Fund (FWF): START-Projekt Y 627-N27.

[1] M. V. Avdeev, E. Dubois, G. Mériduet, E. Wandersman, V. M. Garamus, A. V. Feoktystov, and R. Perzynski, *J. Appl. Crystallogr.*, **42** (2009) 1009–1019.

[2] E. Novak, E. Minina, E. Pyanzina, S. Kantorovich, A. Ivanov, *J. Chem. Phys.*, **139** (2013) 224905.

[3] private communication.

2 July

17:30-18:30

Wednesday

poster session
2PO-K

“Multiferroics”

2PO-K-1

EFFECT OF CORONA TREATMENT ON MAGNETIC PROPERTIES OF NANOSCALED MULTIFERROIC FILMS BiFeO_3 , $(\text{BiLa})\text{FeO}_3$ AND $(\text{BiNd})\text{FeO}_3$

Kostishin V.G.¹, Krupa N.N.², Panina L.V.¹, Nevdacha V.V.², Chitanov D.N.¹, Truhan V.M.³, Yudanov N.Yu.¹

¹ National University of Science and Technology "MISIS" (MISIS) Moscow, Russia

² Institute of Magnetism, NAS of Ukraine, Kyiv, Ukraine.

³ Institute of Solid State Physics and Semiconductors, NAS of Belarus, Minsk, Belarus
denchitanov@mail.ru

We have fabricated multiferroic films of BiFeO_3 , $(\text{BiLa})\text{FeO}_3$ and $(\text{BiNd})\text{FeO}_3$ with various concentration of ions of Bi, La and Nd in dodecahedral sublattice utilising a number of technological methods: sputtering in transverse high frequency discharge, vacuum laser ablation and chemical deposition from gaseous phase of metalloorganic compounds on monocrystalline substrates of (001) SrTiO_3 , (100) MgO and (100) Al_2O_3 . Magnetic properties of the obtained films were investigated. Doping of Bi-ferrites by P3-ions La(Nd) results in a shift in Neel temperature T_N towards higher values, an increase in magneto capacitance and ME-effect, an increase in magnetisation saturation, an increase in optical absorption and Faraday rotation. It is suggested that the observed effects are related with increase in magnetic crystalline anisotropy due to doping by rare-earth ions (REI). The symmetry of crystalline field around Fe^{3+} ions is distorted by REI which causes changes in the value of the anisotropy constant. As a result, a spatially modulated structure (SMS) typical of BiFeO_3 becomes energetically unfavourable. Suppression of SMS leads to growth of magnetic and magnetoelectric parameters and change in magnetic structure is responsible for a shift in T_N .

Conclusion

Corona treatment results in

- Essential growth in magnetisation saturation (34-35%), coercive force (up to 8 times);
- Optical absorption, but Faraday rotation changes only slightly;

Giant change in coercive force after treatment in corona discharge was investigated previously for thin epitaxial films of magnetic garnets.

The observed changes are due to induced electret state formed by corona treatment. A physical model is proposed to explain the changes in magnetic and optical parameters.

The observed effects could be useful for information recording.

2PO-K-2

MAGNETIC HYPERFINE INTERACTIONS OF ^{57}Fe IN AFeO_3 ($A = \text{Sc, Al}$) MULTIFERROICS

Sobolev A.V.¹, Belik A.A.², Presnyakov I.A.¹

¹ Lomonosov Moscow State University, Moscow, Russia

² National Institute for Materials Science (NIMS), Tsukuba, Japan

alex@radio.chem.msu.ru

^{57}Fe Mössbauer spectra of AFeO_3 ($A = \text{Sc, In}$) samples, measured in a magnetically ordered temperature range ($T < T_N$) have a magnetic structure, which reveals the transformation into a Zeeman sextet with broadened components with decreasing temperature. Analysis of the parameters of the distributions $p(H_{\text{Fe}})$ profiles allows us to make some preliminary conclusions (as an example: for ScFeO_3 see fig. 1):

Mean values of isomer shifts $\langle \delta T \rangle$ relate with the range of values of "+3" oxidation state high-spin iron cations.

It is important to note that over the entire temperature range ($77 \leq T \leq 300$ K) the quadrupole shift $\langle \varepsilon \rangle$ values remain almost unchanged. Thus, we can assume the absence of the Morin transition in the AFeO_3 sample (or its substantial decrease in comparison with Fe_2O_3). This result is consistent with the results of the investigations of $\text{Fe}_{2-x}\text{Al}_x\text{O}_3$ solid solutions [1], when the introduction of a small amount of diamagnetic Al^{3+} cations leads to a sharp decrease in the temperature of the Morin transition (e.g., $T_M \approx 120$ K for $x \approx 0.16$).

As a result of such description, $T_N = 408 \pm 15$ K was estimated and its value is in good agreement with magnetic measurements data. The Neel temperature decreased by almost half of this value in comparison with the corresponding value for the unsubstituted $\alpha\text{-Fe}_2\text{O}_3$ oxide ($T_N = 956$ K) and this value semi-quantitatively agreed with rather crude, but also very physically intuitive model of the Weiss molecular field.

The temperature dependence of partial hyperfine fields at low temperatures was fitted in terms of Weiss molecular field and gave the values of the superexchange integrals.

At the high temperature region ($T > 120$ K) model spectra deconvolution revealed not satisfactory χ^2 -criteria and, thus, all spectra were fitted by distribution of spin-lattice relaxation frequency (Ω) model. This procedure showed a strong positive correlation of intensities of higher frequencies and temperature.

This study was supported in part by the Russian Foundation for Basic Research, project no. 14-03-00768.

[1] J.K. Srivastava and R.P. Sharma, *Phys. Stat. Sol. (b)*, **49** (1972) 135.

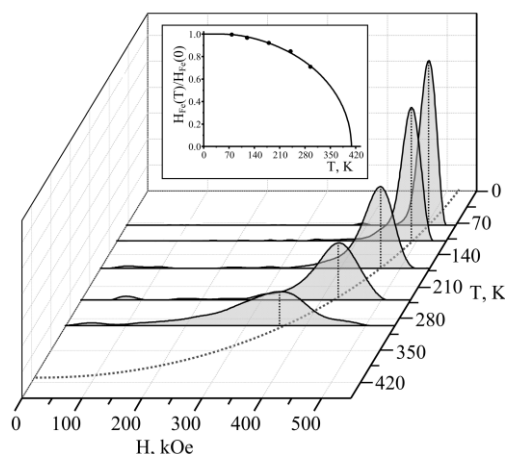


Fig. 1 Temperature dependence of ^{57}Fe hyperfine fields (H_{Fe}) distributions and temperature dependence of the mean value of reduced H_{Fe} versus temperature (inset).

2PO-K-3

PECULIARITIES OF MAGNETOELECTRIC RESPONSE IN MULTILAYER HETEROSTRUCTURES Ni-Zn FERRITE AND PZT NEAR THE RESONANCES

Karpenkov D. Yu.¹, Ivanov P.N.¹, Bogomolov A.A.¹, Solnyshkin A.V.¹, Karpenkov A.Yu.¹,
Pastushenkov A.G.¹

¹ Tver State University, Tver, Russia
karpenkov_d_y@mail.ru

In the last decade, much attention was paid to the magnetoelectric (ME) effect in multilayered composite structures containing layers of magnetostrictive Ni-Zn ferrite (NZFO) and piezoelectric (PZT) materials. This interest is caused by the great value of the ME coefficient in multilayered structures and potential applications in magnetic field sensors and solid-state voltage converters as well as the relatively easy manufacturing process of multilayered composites. However, reproducibility of ME parameters is not adequate, that prevents widespread application of the devices based on the layered heterostructures. Furthermore, achieving high ME coefficient values requires a good mechanical coupling, as well as chemically nonreactive phases of the composite.

In this paper, we propose a new preparatory method for ME structures consisting from NZFO and PZT layers. This method eliminates the voltage drop across the dielectric layers of magnetostrictive ceramics, and also allows the combination of layers of PZT ceramics electrically in series, which subsequently increases the efficiency of the composites. The results of systematic investigations of the ME effect for the samples produced by the proposed method are presented. The ME voltage coefficient is determined in wide ranges of applied magnetic fields, frequencies, and temperatures.

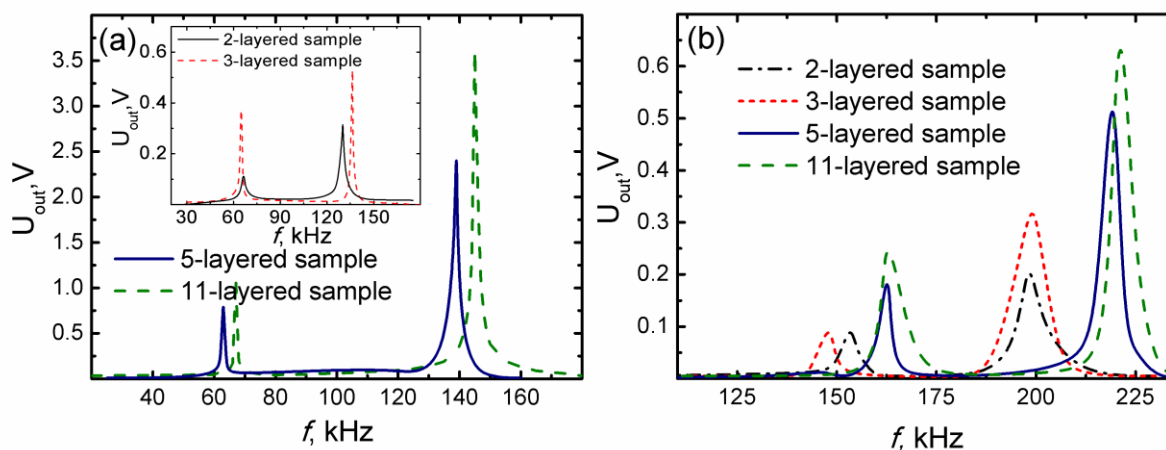


Fig. 1. The frequency dependence of ME voltage for: (a) rectangular-shaped samples, or (b) disk-shaped samples.

The preparation method of magnetoelectric multilayered ceramic heterostructures was suggested, and series of the rectangular and disk shape samples were produced on the base of this method. The maximum value of a magnetoelectric voltage coefficient $\alpha_E = 35 \text{ V}/(\text{cm} \times \text{Oe})$ was observed for the eleven-layered rectangular specimen at the electromechanical resonance frequency $f_r = 144 \text{ kHz}$, $H_{DC} = 84 \text{ Oe}$, and $H_{AC} = 2.5 \text{ Oe}$. The sensitivity to static magnetic fields is equal to $3.5 \times 10^{-2} \text{ Oe}$, and the alternating field sensitivity is equal to $8 \times 10^{-3} \text{ Oe}$ (see Fig. 1).

2PO-K-4

MONTE-CARLO MODELING OF MULTIFERROICS ON TWO-DIMENSIONAL LATTICE

Lamekhov S. J.¹, Bychkov I. V.¹, Kuzmin D. A.¹, Shavrov V. G.²

¹ Chelyabinsk State University, 454001, Chelyabinsk, Br. Kashirinykh str., 129, Russia

² Kotel'nikov Institute of Radio Engineering and Electronics of RAS, 125009, Moscow, Mokhovaya str., 11-7, Russia
sjlamekhov@gmail.com

Monte-Carlo method is widely used in many areas of physics, including modeling of phase-transitions in materials with magnetic structures, for example in multiferroics [1].

In current work the properties of multiferroic with collinear order of polarization (P) and magnetization (M) on two-dimensional lattice with 20×20 size were studied. Aim of modeling is to obtain temperature dependency of polarization, magnetization and susceptibilities (dielectric, magnetic and magnetoelectric) of multiferroic in external electric and magnetic fields with various values of magnetoelectric coupling factor.

Model is based on two-dimensional Ising's model and includes Hamiltonians: magnetic (1), elastic (polarization) (2) and magnetoelectric (3).

$$H^m = - \sum_{\langle i,j \rangle} J_1 s_i s_j - \sum_{[i,j]} J_2 s_i s_j - \sum_i H s_i \quad (1)$$

$$H^e = \sum_i \left(-\frac{A}{2} u_i^2 + \frac{B}{4} u_i^4 \right) - \sum_{\langle i,j \rangle} U_1 u_i u_j - \sum_i E u_i \quad (2)$$

$$H^{em} = - \sum_{\langle k,i \rangle \langle k,j \rangle} \varepsilon_{ij} g u_k^2 s_i s_j - \sum_{[i,j]} \varepsilon_{ij} k E s_i s_j \quad (3)$$

J_1 and J_2 – exchange integrals for first and second coordination spheres, A and B – parameters for double-well potential, U_1 – strength constant, g – magnetoelectric coupling factor.

For forming configurations of lattice Metropolis algorithm was used with this values of Hamiltonian's constants:

$$J_1=1, J_2=0.5, A=0.1, B=0.1, U_1=0.1, k=1.$$

Modeling was performed with values of g 0, 10 and 100.

Simulated results showed that increasing of magnetoelectric coupling factor leads to proportionally to g right shift of polarization and magnetization of lattice (fig. 1 and 2) and to increasing of magnetoelectric susceptibility (fig. 3).

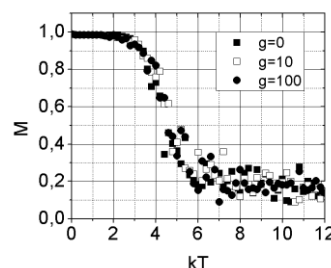


Fig. 1. The temperature dependence of magnetization in case of H=0.

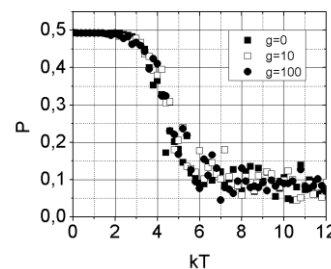


Fig. 2 The temperature dependence of polarization in case of H=0.

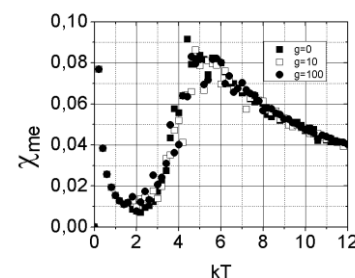


Fig. 3. The temperature dependence of magnetoelectric susceptibility in case of H=0.

[1] Q. C. Li, J.-M. Liu, *Phys. Rev. B*, **75** (2007) 06441.

2PO-K-5

A NEW MULTIFERROIC - $\text{SmCr}_3(\text{BO}_3)_4$: MAGNETIC PHASE TRANSITIONS AND CRYSTAL-FIELD PARAMETERS

Boldyrev K.N.¹, Dobrecova E.A.¹, Popova E.A.², Malkin B.Z.³, Popova M.N.¹

¹ Institute of Spectroscopy, Russian Academy of Sciences, Moscow, Troitsk, Russia

² National Research University "Higher School of Economics", Moscow, Russia

³ Kazan Federal (Volga region) University, Kazan, Russia

kn.boldyrev@gmail.com

Rare-earth (RE) borates with the general formula $RM_3(\text{BO}_3)_4$ ($R = \text{Y, La-Lu}$; $M = \text{Al, Ga, Fe, Cr, Sc}$) have non-centrosymmetric huntite-type structure (SG R32). The most studied crystals from this family are aluminum and iron borates. Recent investigations have shown that many of them are multiferroics. So, $\text{SmFe}_3(\text{BO}_3)_4$ shows the greatest magneto-electric effect from all RE iron borates. At the same time, properties of the borates with another magnetic M-ion, chromium, are little known. Up to now, only magnetization, specific heat, and spectroscopic studies of $\text{NdCr}_3(\text{BO}_3)_4$ single crystals were reported [1,2], some preliminary spectroscopic data on $\text{SmCr}_3(\text{BO}_3)_4$ were published [2], the magnetic susceptibility, specific heat, and lattice parameters of polycrystalline $\text{EuCr}_3(\text{BO}_3)_4$ were studied [3].

In the present work, a comprehensive study of $\text{SmCr}_3(\text{BO}_3)_4$ single crystals, both pure and doped with Er^{3+} or Nd^{3+} ions, was undertaken. Spectroscopic data, as well as specific heat and magnetic susceptibility measurements show that $\text{SmCr}_3(\text{BO}_3)_4$ undergoes three phase transitions, at temperatures $T_1 = 8.0$ K, $T_2 = 6.7$ K, and $T_3 = 4.3$ K (see Fig.1). A splitting of Sm^{3+} and Er^{3+} spectral lines that starts at T_1 points to a magnetic ordering phase transition. An observed quasi-soft-mode behaviour at T_2 of the phonon line 185 cm^{-1} is, possibly, connected with an (anti)ferroelectric ordering. The

first-order phase transition at T_3 is, most probably, associated with a spin reorientation of the Cr^{3+} magnetic moments. Investigation

of Sm^{3+} crystal-field levels by optical spectroscopy and crystal-field calculation allowed us to compare the crystal-field parameters for Sm^{3+} in $\text{SmCr}_3(\text{BO}_3)_4$ with those in $\text{SmFe}_3(\text{BO}_3)_4$ [4].

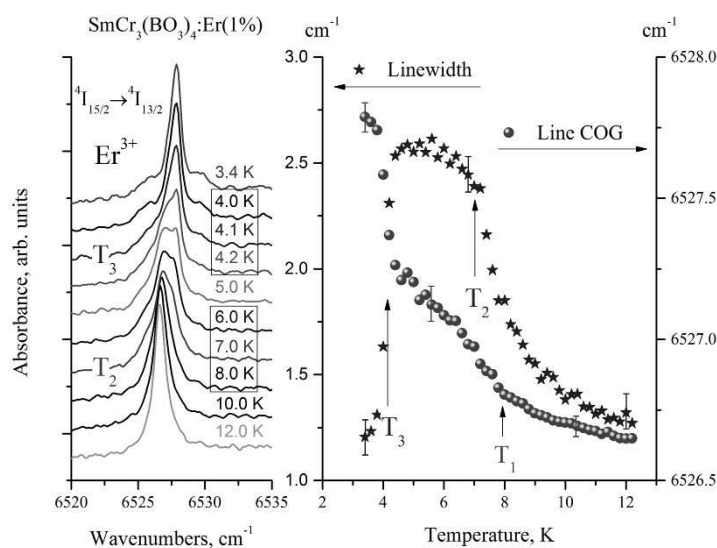


Fig.1. Absorption spectrum of $\text{SmCr}_3(\text{BO}_3)_4:\text{Er}$ in the region of Er^{3+} transition ${}^4I_{15/2} \rightarrow {}^4I_{13/2}$ and temperature dependences of the linewidth and line's center of gravity (COG).

Support by the President of Russian Federation (K.N.B. project MK-1700.2013.2) and by the Russian Foundation for Basic Research (grant No 13-02-00787-a) is acknowledged.

[1] E.A. Popova, N.I. Leonyuk, M.N. Popova, et.al, *Phys. Rev.*, **B 76** (2007) 054446.

[2] K.N. Boldyrev, E.P. Chukalina, N.I. Leonyuk, *Solid State Phys* **50** (2008) 1617.

[3] L. Gondek, A. Szytula, J. Przewoznik, et.al, *J. Solid State Chem.*, **210** (2014) 30.

[4] M.N. Popova, E.P. Chukalina, B.Z. Malkin, D.A. Erofeev et.al, *JEPT* **118** (2014) 111.

2PO-K-6

INTERFACE MAGNETOELECTRIC EFFECT IN Co/PZT/Co HETEROSTRUCTURES

Stognij A.I.¹, Novitskii N.N.¹, Poddubnaya N.N.¹, Sharko S.A.¹, Sazanovich A.², D'yakonov V.P.²,
Szymczak H.²

¹ Scientific-Practical Materials Research Centre NAS of Belarus, Minsk, Belarus

² Institute of Physics, Polish Academy of Science, Warsaw, Poland

stognij@ifftp.bas-net.by

The ion-beam sputter deposition technique (IBSD) allows to form the artificial composites consisting of materials differ in chemical and physical properties, for example, such as layered ferromagnetic / ferroelectric composites possess the room temperature magnetoelectric (ME) effect [1]. In particular, formation of the temperature-stable plane-parallel ferromagnetic metal / ferroelectric ceramics interface by the IBSD permits to refuse of traditionally used ways of mechanical connection [2] of specified heterogeneous materials. The thermostable interfaces provide the scaling of the layered heterostructures in microsensor devices producing.

The IBSD used for formation of Co (d) / PZT / Co (d) ME-heterostructures in which the thickness of the ferromagnetic cobalt layer varied from 0.5 to 9 μm and that of the ferroelectric ceramics on a basis of lead zirconate-titanate (PZT) was within 100...400 μm .

According to [1], a ferromagnetic cobalt layer with thickness in the range from 2 to 3 μm deposited onto the planarized surface of the ferroelectric substrate possesses the maximum saturation magnetization and induces the maximum mechanical stresses in ferroelectric substrate. Due to ME interaction there is a maximum on dependence of ME voltage coefficient α upon thickness d of a ferromagnetic layer (Fig.).

The results obtained show that in the heterostructures formed by the IBSD a known condition of rough equality of volume fractions of the ferromagnetic and ferroelectric components for realization of the maximum ME-effect [2] is not necessary. The small volume fraction of a ferromagnetic material compared by that of a ferroelectric one allows suggesting the interface origin of ME-properties in the mentioned structures.

The IBSD composites exhibit the quasistatic ME-effect (beyond the resonance) typical for that of the known composites but have the thermostable ferromagnetic/ ferroelectric interfaces and are available for application as magnetic field microsensors.

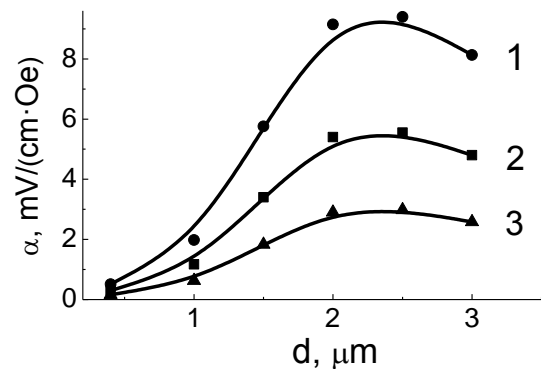


Fig. Longitudinal ME voltage coefficient α versus Co layer thickness d in Co (d) /PZT /Co (d) heterostructures in magnetic field 50 Oe and frequency 100 Hz. PZT thicknesses are 100 (1), 280 (2), and 400 μm (3).

[1] A. Stognij, N. Novitskii, A. Sazanovich, N. Poddubnaya, S. Sharko, V. Mikhailov, V. Nizhankovski, V. Dyakonov, and H. Szymczak, *Eur. Phys. J. Appl. Phys.* **63**. Issue 02 (2013) 21301-1-7.

[2] C.-W. Nan, M. Bichurin, S. Dong, D. Viehland, G. Srinivasan, *J. Appl. Phys.* **103** (2008) 031101-1-35.

2PO-K-7

MAGNETOELECTRIC EFFECTS IN $\text{HoAl}_3(\text{BO}_3)_4$ *Freydman A.L.¹, Balaev A.D.¹, Eremin E.V.¹, Dubrovsky A.A.¹, Temerov V.L.¹, Gudim I.A.¹*¹ L.V. Kirensky Institute of Physics of Siberian Branch of Russian Academy of Sciences,
Krasnoyarsk, Russia
fss4@yandex.ru

In recent years materials, which simultaneously possess (anti)ferromagnetism and ferroelectricity, called multiferroics, were the subject of intensive research. In these materials there is strong correlation between the magnetic and ferroelectric subsystems. The general method of investigating of magnetoelectric properties is measurement of polarization induced by magnetic field (ME_H -effect). In present work the reversal magnetoelectric effect (ME_E -effect) of singlecrystalline $\text{HoAl}_3(\text{BO}_3)_4$ is measured for the first time. By using of this approach is possible to investigate magnetoelectric response as function of electric field, magnetic field and temperature. Also it makes possible to separate contribution of piezoelectric effect and electrostriction. As was mentioned by other authors [1], in this compound the giant magnetoelectric effect was found. The peculiarity of this compound is that, this crystal is paramagnetic [2] and consequently is not multiferroic, but crystal shows the magnetoelectric properties.

On the figure 1 the susceptibilities of ME_H - and ME_E -effect are present (α and β respectively). It is good seen the correlation between these two dependences. The maximum of the ME_E -effect is exploring in terms of reorientation of magnetic moments of Ho atoms in applied oscillating electric field. At increasing magnetic field the magnetic moment of the sample grows according to paramagnetic type-magnetization. The ME_E -effect also grows, since magnetoelastic effect increases. After the maximum point magnetic field stabilizes the magnetic moment of Ho atoms strongly, and amplitude of oscillations of magnetic moments decreases. Due to this the value of ME_H -effect decreases.

At low temperatures the maximum of the ME_H -effect is corresponds to the ME_E -effect maximum point. But at increasing of temperature maximum of ME_E -effect is moved in strong magnetic field area more rapidly than ME_H -effect maximum.

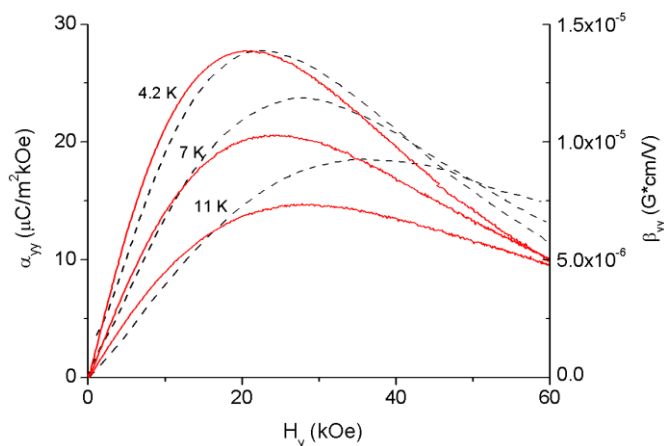


Fig. 1. Magnetoelectric susceptibilities of ME_H - (α) and ME_E -effect (β). The dotted and solid lines corresponds to α , to β respectively.

[1] K.-C. Liang et. al., *Phys. Rev. B*, **83** (2011) 180417(R).

[2] D. Neogy et al., *J. Magn. Magn. Mater.*, **154** (1996) 127-132.

2PO-K-8

MAGNETIC AND STRUCTURAL PHASE TRANSITIONS IN BiFeO_3 MULTIFERROIC FILMS AND SINGLE CRYSTALS

Soloviov S.V.¹, Popkov A.F.¹, Kulagin N.E.², Zvezdin A.K.³, Gareeva Z.V.⁴

¹ National Research University of Electronic Technology (MIET), Zelenograd, Moscow, Russia

² State University of Management, Moscow, Russia

³ A.M. Prokhorov General Physics Institute, Russian Academy of Sciences, Moscow, Russia

⁴ Institute of Molecular and Crystal Physics, Russian Academy of Sciences, Ufa, Russia

sv.soloviov@yandex.ru

Magnetoelectric properties of multiferroics attract a wide attention due to a lot of its possible applications. In this aspect, BiFeO_3 (BFO) antiferromagnet should be distinguished as a material with outstanding magnetoelectric properties at room temperature. Doped compounds and film heterostructures based on BFO allow a film engineering for some applications.

Investigation of magnetic and electric phase transitions allows one to determine a details of exchange and magnetoelectric interactions of magnetic subsystem with a crystal structure, and of a phase transitions mechanisms in both subsystems (magnetic and electric) under external influence. A significant part of researches of BFO's magnetoelectric properties is based on a phenomenological approach using space invariants for ferroelectric rhombohedral phase of BFO.

In this work we study phase structural transformations and magnetic changes in a single crystal and films of BFO-like multiferroic in dependence on magnetic and electric fields, and variations of induced magnetocrystalline anisotropy. Reorientation of the polarization P and of the angle ω of oxygen octahedrons rotation in external electric field is investigated using the Landau theory of phase transitions in an analogy to the Ref [1]. Critical fields E_{c1} and E_{c2} at which a sharp change of P and ω happens are determined and compared with ab initio calculations [2]. Furthermore, we got concomitant changes of magnetization and antiferromagnetic vector depending on electric field when magnetic field is high. Reorientation of a plane of spin cycloidal structure in the crystal is demonstrated at fields close to the critical values. Additionally, a magnetic ground state of BFO-like multiferroic is analyzed for the constant P and ω taking into account a specificity of film structures for several substrate orientations. Energy diagrams of magnetic states which determine the stability regions of homogeneous and inhomogeneous phases under variation of magnetic anisotropy and magnetic field are obtained for the case of (001)-oriented substrate. Differences in behavior of magnetic subsystem between cases of (001)- and (111)-oriented films are established.

This work is supported by the Russian Foundation for Basic Research, project 13-07-12405 ofi_m2.

[1] V.B. Shirokov, Yu.I. Yuzyuk, and V.V. Lemanov, *Phys. of the Solid State*, **51** (2009) 047204.

[2] S. Lisenkov, D. Rahmedov, and L. Bellaiche, *Physical Review Letters*, **103** (2009) 1025.

2PO-K-9

SPECIFIC HEAT AND MAGNETOCALORIC EFFECT IN $\text{LuFe}_{2-x}\text{Mn}_x\text{O}_{4-\delta}$

*Gamzatov A.G.¹, Aliev A.M.¹, Batdalov A.B.¹, Mukhuchev A.A.¹,
Markelova M.N.², Burunova N.A.², Kaul A.R.²*

¹ Amirkhanov Institute of Physics of DSC RAS, Makhachkala, Russia

² Department of Chemistry, Moscow State University, Moscow, Russia
Gamzatov_adler@mail.ru

In recent years there has been taken a big upsurge in interest in materials with large values of a magnetocaloric effect. This interest is caused by prospects for creation of high-effective solid refrigerating machines. The analysis on the current state of searches of effective materials for such machines shows that more likely the design of effective solid refrigerators will require the combination of different caloric effects, in particular, magneto- and electrocaloric effects. In multiferroics, the considerable in value muticaloric effects can be observed due to the co-existence of magnetic and electric ordering.

In this work we present the experimental results of the heat capacity and the direct measurements of magnetocaloric effect (MCE) of $\text{LuFe}_{2-x}\text{Mn}_x\text{O}_{4-\delta}$ ($x=0; 0.01; 0.3$) in the magnetic fields from 500 Oe to 18 kOe.

Ceramic $\text{LuFe}_{2-x}\text{Mn}_x\text{O}_{4-\delta}$ ($x=0; 0.1; 0.3$) were prepared by chemical homogenization technique from nitrates and sintered at 1000°C for 30 h with the presence of FeO/Fe₃O₄ getter in an evacuated silica ampoule. Single phase $\text{LuFe}_{2-x}\text{Mn}_x\text{O}_{4-\delta}$ were obtained and characterized by XRD. It was shown that the increasing of Mn content affect mainly at *c* cell parameters. A cerium based titration was used for determination of δ .

Fig. 1 shows the results of direct measurements of magnetocaloric effect for $\text{LuFe}_{2-x}\text{Mn}_x\text{O}_{4-\delta}$ ($x=0; 0.1; 0.3$) in the magnetic field of 18 kOe. The maximum value of MCE is observed for the sample with $x=0$ (LuFe_2O_4) and achieves value $\Delta T=0.21\text{K}$ at 18 kOe with maximum at $T=245\text{K}$. The addition of manganese leads to significant decrease of MCE value (for $x=0.10$ the MCE decreases approximately 4 times) and to the displacement of the maximum temperature towards lower temperatures at increasing manganese concentration. Authors of work [1] reported about the strong suppression of magnetization and monotone decrease in T_N at increasing of Mn concentration for samples $\text{YbFe}_{2-x}\text{Mn}_x\text{O}_4$. As follows from Figure, a small break in the temperature curve of MCE is observed in samples $\text{LuFe}_{2-x}\text{Mn}_x\text{O}_{4-\delta}$ ($x=0; 0.1$) at temperatures about 200 K. The same behaviour for LuFe_2O_4 was observed by authors of work [2].

This work was supported by the Branch of Physical Sciences of the Russian Academy of Sciences within the framework of the program “Strongly Correlated Electrons in Solids and Structures,” RFBR (Grant Nos. 14-02-01177, 13-03-01249 and 12-02-96506).

[1] K. Yoshii et al. *Journal of Solid State Chemistry*, **182** (2009) 1611-1618.

[2] M.H. Phan et al. *Solid State Communications*, **150** (2010) 341-345.

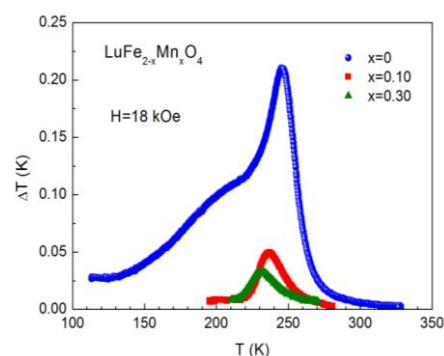


Fig. 1. Temperature dependence of the MCE for $\text{LuFe}_{2-x}\text{Mn}_x\text{O}_{4-\delta}$.

2PO-K-10

MAGNETIC FIELD INDUCED PHASE TRANSITIONS IN MULTIFERROIC Mn_{1-x}Co_xWO₄ SINGLE CRYSTALS

Urcelay-Olabarria I.¹, Ressouche E.², Ivanov V.Yu.³, Mukhin A.A.³,
Popov Yu.F.⁴, Vorob'ev G.P.⁴, Balbashov A.M.⁵, Skumryev V.⁶, García-Muñoz J. L.⁷

¹ BCMaterials, 48160 Derio, Spain

² Institute Laue-Langevin, 15638042 Grenoble Cedex 9, France

³ Prokhorov General Physics Institute of the Russian Acad. Sci., 119991, Moscow, Russia

⁴ Faculty of Physics, M.V. Lomonosov Moscow State University, 119992 Moscow, Russia

⁵ Moscow Power Engineering Institute, 105835, Moscow, Russia

⁶ Institut Català de Recerca i Estudis Avançats (ICREA), Barcelona, Spain; and Departament de Física, Universitat Autònoma de Barcelona, Bellaterra 08193, Spain

⁷ Instituto de Ciencia de Materiales de Barcelona, CSIC, E-08193 Bellaterra (Barcelona), Spain
BalbashovAM@mpei.ru

Natural mineral Hummerite MnWO₄ with the monoclinic crystal structure (space group P2/c) is regarded as one of the best examples of magnetically induced multiferroic system with spiral magnetic structure. Due to strong frustration the magnetic order in MnWO₄ is very sensitive to small perturbations, thus giving rise to a rich magnetic phase diagram which can be readily modified by external field or by chemical substitution [1-4]. In this work we present results of complex (magnetic, magnetoelectric and neutron diffraction) investigations of field induced phase transitions in single crystalline Mn_{1-x}Co_xWO₄ samples (0 ≤ x ≤ 0.2) in static and pulsed magnetic fields up to 25 T.

The magnetic structure of the high field phase of MnWO₄ with a flopped to *a* axis electric polarization induced by magnetic field (~10.5 T) along *b* axis from the ferroelectric (*P*||*b*) cycloidal AF2 structure has been identified as reoriented cycloidal spin structure, AF2'. Unlike for usual magnetic field induced spin-flop transitions, the high field flopped phase does not directly develop from the low field one but emerges via the non-polar collinear commensurate AF1 phase, which creeps in between. Investigations of Mn_{0.95}Co_{0.05}WO₄ in magnetic field applied along the *b* axis has revealed that the ferroelectric phase with spin-cycloid structure AF2 in the *εb* plane and with polarization along *b* undergoes a continuous transition from the *εb* plane to the *εω* plane, *ε* and *ω* being the easy and the hard magnetic direction in the *ac*-plane. The electric polarization undergoes a similar behavior: it rotates continuously from the *b* axis to the *ac* plane so *P_b* and *P_a* coexist in this doped composition.

Various field induced phase transitions have been observed in the Mn_{0.8}Co_{0.2}WO₄ where the conical antiferromagnetic ferroelectric structure exists at temperature below T_{FE}~8.6 K [1]. When *H*||*b* and *H*||*ω* the rotation plane of the magnetic moments flops perpendicular to the *H* or the transition to the paraelectric phase takes place at the critical field ~15 T at 2 K. This transition is accompanied by the disappearance of the electric polarization *P_b*. The parameters of this high field structure and its evolution from the zero field state have been determined by neutron diffraction. If the external field is applied along the easy *ε*-axis, it is likely that the conical structure transforms to a pure cycloidal one with the electric polarization along *b*-axis.

This work was partially supported by RFBR (12-02-01261).

[1] K. Taniguchi, et al., *Phys. Rev. Lett.*, **97** (2006) 097203, *Phys. Rev. B* **77** (2008) 064408.

[2] A. H. Arkenbout, et al., *Phys. Rev.*, **B 74** (2006) 184431.

2PO-K-11

PECULIARITIES OF DOMAIN WALL STRUCTURE IN FERRITE-GARNET CRYSTALS WITH FLEXOMAGNETOELECTRIC EFFECT

Vakhitov R.M.¹, Kharisov A.T.¹, Iskhakova R.R.¹

¹ Institute of Physics and Technology, Bashkir State University, Ufa, Russia
VakhitovRM@yahoo.com

The magnetic materials which display magnetoelectric properties acquire topicality at present in view of their possible applications in various devices of magnetic storage devices and spintronics [1, 2]. Belonging to the magnets of this kind are ferrite-garnet crystals in which the effect of the domain wall (DW) shift under the influence of an inhomogeneous electric field at room temperature has been recently discovered [2]. An explanation of the phenomenon observed presented in the same paper was based on the mechanism conditioned by the occurrence in these materials of inhomogeneous magnetoelectric interaction (IMEI). Another explanation of the experimentally obtained data was offered in [3] which stated that a strong inhomogeneous electric field generated by a pointed electrode induced inhomogeneous anisotropy in the DW location. This anisotropy can be regarded as a defect which, depending on its variety (a "potential hole" or a "barrier" [4]), will attract or repel the DW.

The paper [5] presented a theoretical investigation into the influence of an electric field on the DW structure in a uniaxial ferromagnet with IMEI. It follows from the results obtained that the flexomagnetolectric mechanism provides a presentation which does not contradict to the phenomenon observed in [2]. It should be stated however that a portion of experimental data did not receive an explanation due to a limited nature of the model discussed in [5].

This paper looks into the contribution of cubic anisotropy to the structure and properties of 180°-DW in ferrite-garnet films with IMEI. The films with the orientations of the developed surface of the (111) and (010) types are discussed. The studies have demonstrated that with no IMEI present, a 180°-DW with the quasi-Bloch structure is realized in the (111)-oriented films at certain values of material parameters. Such a DW features an exit of magnetization from the wall plane, this exit being characterized by the angle $\varphi(y)$, where y is the coordinate [6]. According to the calculations, $\varphi(y)$ is an uneven function. Notably, this dependence remains the same when IMEI is brought into picture. As a result, the flexomagnetolectric mechanism creates a double electric layer in such DW, the vector of the resulting polarization \mathbf{P} in this layer being equal to zero. A different situation is observed in the (011)-oriented film. Here, the DW also features an exit of magnetization from the plane. In this case, however, $\varphi(y)$ is an even function which is not disturbed if IMEI is present. Correspondingly, charges appear in such DW and it is due to these charges that the wall will interact with the source of the electric field. The results obtained agree well with the experimental data [2].

[1] A.P. Pyatakov and A.K. Zvezdin, *Physics – Uspekhi*, **55** (2012) 557-581.

[2] A.S. Logginov et. al. *Appl. Phys. Lett.*, **93** (2008) 182510 (3).

[3] A.F. Kabychenkov, F.V. Lisovskii, E.G. Mansvetova, *JETP Lett.*, **97** (5) (2013) 265-269.

[4] A.I. Mitsek, S.S. Semyannikov, *Sov. Phys. Solid State*, **11** (5) (1969) 899-907.

[5] R.M. Vakhitov, A.T. Kharisov, Yu.E. Nikolaev, *Doklady Physics*, **59** (3) (2014) 119-121.

[6] M.A. Shamsutdinov, A.T. Kharisov, Yu.E. Nikolaev, *Phys. Met. Metallogr.*, **111** (2011) 451-457.

2PO-K-12

HYPERFINE INTERACTIONS OF ^{57}Fe ATOMS IN MULTIFERROIC CuCrO_2 Rusakov V.S.¹, Presniakov I.A.¹, Gapochka A.M.¹, Sobolev A.V.¹, Matsnev M.E.¹, Lekina Yu.O.¹¹ Lomonosov Moscow State University, Moscow, 119991 Russia

al-gap@physics.msu.ru

Delafossite oxide CuCrO_2 is one of quasi two-dimensional antiferromagnetic triangular-lattice compounds, and it is of great interest as magnetoelectric multiferroic material. Magnetic order in CuCrO_2 is in the form of an incommensurate proper-screw spiral, with a propagation vector of the moments of $(q, q, 0)$, where $q = 0.329$ [1]. Individual spins rotate in the $(HH0)$ plane. According to the latest high-resolution neutron spectroscopy only true magnetic phase transition occurs at $T_N = 23.5$ K [2]. This work presents the results of detailed Mössbauer studies of ^{57}Fe doped CuCrO_2 powder sample in the temperature range, including the Neel temperature of magnetic phase transition. For processing and analysis of the Mossbauer spectra we used methods of recovery of hyperfine magnetic field H_n distributions and fitting in the incommensurate proper-screw spiral type model implemented in the SpectrRelax program [3].

The Mössbauer spectra of $\text{CuCr}_{0.99}\text{Fe}_{0.01}\text{O}_2$ measured in the paramagnetic range ($T > T_N$) consist of one quadrupole doublet with isomer shift value $\delta(33\text{K}) = 0.485 \pm 0.003$ mm/s corresponding to the high spin Fe^{3+} state. The quadrupole shift value $\varepsilon(33\text{K}) = 0.300 \pm 0.003$ mm/s is rather high for Fe^{3+} ions, which can indicate that oxygen octahedra (FeO_6) are significantly distorted. The spectra obtained in the temperature range $4.96 \text{ K} \leq T < T_N$ consist of asymmetric Zeeman sextet with inhomogeneous line broadenings. From the temperature dependencies of the mean magnetic field $\langle H_n \rangle$ of the resulting $p(H_n)$ distributions, we determined the temperature 24.5 ± 1.0 K at which the magnetic hyperfine structure of the spectra completely disappears. Line broadenings and spectrum asymmetry in the case incommensurate modulated helicoid type magnetic structure of CuCrO_2 arise from the modulation of the electric hyperfine interactions as the Fe^{3+} magnetic moment rotates with respect to the principal axis (Z) of the electric field gradient (EFG) tensor, and from the anisotropy of the magnetic hyperfine interactions at the Fe^{3+} sites along the helicoid propagation vector (x):

$$\varepsilon(\vartheta(x)) = \varepsilon_{\text{lat}}(3\cos^2 \vartheta(x) - 1)/2, \quad H_n(\vartheta(x)) = H_{\text{is}} + H_{\text{an}}(3\cos^2 \vartheta(x) - 1)/2.$$

Here ε_{lat} – quadrupole shift caused by the EFG created by surrounding the nucleus of charge distribution in the lattice, H_{is} and H_{an} – isotropic and anisotropic contributions to the H_n , $\vartheta(x)$ – the angle between the direction of the hyperfine magnetic fields H_n and axis Z has been described by the equation: $\cos \vartheta(x) = \text{sn}((\pm 4K(m)/\lambda)x, m)$,

where $\text{sn}(x, m)$ is the Jacobian elliptic function, m is its parameter, $K(m)$ is the complete elliptic integral of the first kind. As a result of fitting the spectra, it was found that the value of anharmonicity parameter (0.58 ± 0.03) practically no change with temperature in the range of 5-21 K. At isotropic contribution $H_{\text{is}} = 482.4 \pm 0.3$ kOe a relatively large anisotropy is observed: $H_{\text{an}} = 19.2 \pm 0.6$ kOe (at 4.96 K). Part of the H_{an} can be ascribed to the field $H_{\text{an}}^{\text{dip}}$ arising from the external magnetic dipole moments. From the lattice sum, using $\mu_{\text{Cr}} = 3\mu_{\text{B}}$ per Cr^{3+} ion, we found that $H_{\text{an}}^{\text{dip}} \approx 12$ kOe. The anisotropic part of the hyperfine field only partly results from dipolar effects and seems to involve an electronic intrinsic contribution.

This work is supported by the RFBR grant No. 14-03-00768a and partially No. 14-02-01109a.

[1] M. Soda, K. Kimura, T. Kimura et al. *J. Phys. Soc. Jpn.*, **78**, No. 12 (2009) 124703.

[2] G. Ehlers, A.A Podlesnyak, et al. *J. Phys.: Condens. Matter*, **25** (2013) 496009.

[3] M.E. Matsnev and V.S. Rusakov. *AIP Conference Proceedings*, **1489** (2012) 178-185.

2PO-K-13

TERAHERTZ SPECTROSCOPY OF $\text{TmAl}_3(\text{BO}_3)_4$ MAGNETOELECTRICS

Kuzmenko A.M.¹, Mukhin A.A.¹, Ivanov V.Yu.¹, Bezmaternykh L.N.², Gudim I.A.²

¹ A.M. Prokhorov General Physics Institute of the RAS, 119991 Moscow, Russia

² Institute of Physics SB RAS, 660036 Krasnoyarsk, Russia

artem.m.kuzmenko@gmail.com

Rare-earth aluminum borates $\text{RAl}_3(\text{BO}_3)_4$ are a new family of magnitoelectrics with non-centrosymmetrical trigonal crystal structure. These compounds exhibit interesting magnetic, magnetoelectric and optical properties which strongly depend on the rare-earth (R) ion.

This work is devoted to terahertz study of the low-energy crystal field states of Tm^{3+} ions in $\text{TmAl}_3(\text{BO}_3)_4$ aluminum borate. The observed increase of the field induced electric polarization in $\text{TmAl}_3(\text{BO}_3)_4$ at low temperatures [1] indicates the prevailing contribution of the low energy crystal field Tm^{3+} states not only into magnetic but also magnetoelectric properties of the crystal.

The polarization measurements of transmission spectra of single crystalline *a*-cut and *c*-cut $\text{TmAl}_3(\text{BO}_3)_4$ plates were carried out by a submillimeter quasi-optical backward-wave-oscillator technique at the frequency range 8-35 cm^{-1} at the temperatures 3-300 K. Intensive resonance absorption was observed at $\sim 28 \text{ cm}^{-1}$ (Fig. 1) for ac electro-magnetic field polarizations with the magnetic component \mathbf{h} perpendicular to the trigonal axis *c* and independently on the electric component polarization \mathbf{e} . This line was identified as magnetic dipolar crystal-field transition from the ground singlet to the next excited doublet within the ground multiplet 3H_6 of Tm^{3+} ions occupying sites of D_3 symmetry in aluminum borates.

A fine structure of the observed transition was revealed at low temperatures. The appearance of the distinct components of the transition could be explained by distortions of the crystal field due to defects, likely Bi impurities in R-sites. These features of the Tm^{3+} ground state were also confirmed by the measurements of transmission spectra in external magnetic fields up to 7 T. In particular, the magnetic field $\mathbf{H} \parallel c$ splits the doublet.

An explanation and quantitative description of the observed temperature and magnetic field dependencies of resonance mode parameters have been performed. Matrix elements of magnetic transitions have been extracted. The contributions of magnetic (electric) dipolar transitions into static magnetic (dielectric) properties have been also analyzed.

This work was supported by RFBR (12-02-31461).

[1] R. P. Chaudhury, B. Lorenz, Y. Y. Sun *et al.*, *Phys. Rev. B*, **81** (2010) 220402(R).

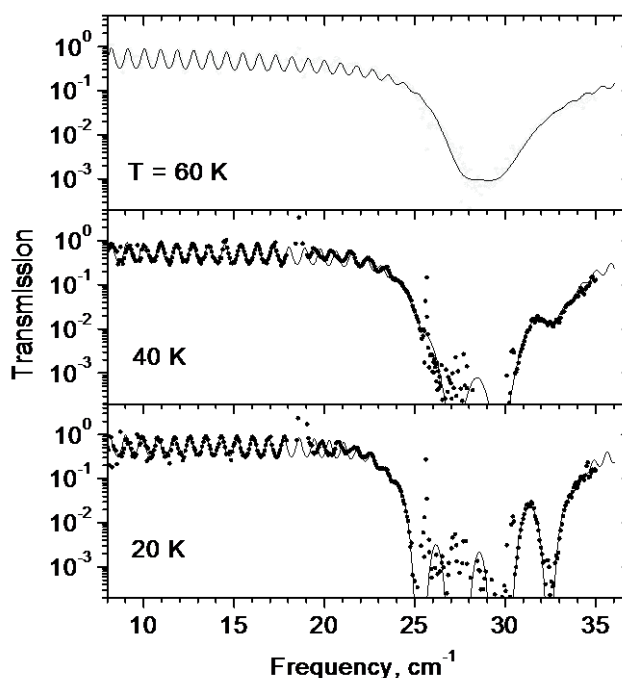


Fig. 1. Transmission spectra of $\text{TmAl}_3(\text{BO}_3)_4$ a-cut plate for ac magnetic field $\mathbf{h} \parallel \mathbf{b}$ -axis. Points – experiment, solid line – fit.

2PO-K-14

NONLINEAR PHASE SHIFTERS BASED ON SPIN-ELECTROMAGNETIC WAVES

Ustinov A.B.¹, Kalinikos B.A.¹

¹ St.Petersburg Electrotechnical University, St.Petersburg, 197376 Russia
ustinov-rus@mail.ru

In recent years there is a strong interest to ferrite-ferroelectric (FF) structures (see e.g. [1]. In particular, the linear properties of spin-electromagnetic waves (SEWs) propagating in FF layered structures have been studied and a number of linear ferrite-ferroelectric devices have been designed and suggested [2-6]. This work reports the first experimental results on a nonlinear FF device, namely, SEW nonlinear phase shifter. A principle of operation of the device is based on the dual control of the phase shift of the hybrid spin-electromagnetic waves propagating in the FF bilayer. The specific experiments were carried out for the phase shifter structure similar to that described in [3]. The layered structure was composed of 5.7- μm -thick single crystal yttrium iron garnet film and a 500- μm -thick barium strontium titanate slab. Two microstrip transducers separated by 8 mm were used for the excitation and detection of the SEW. A bias voltage in the range of $U = 0\text{-}1000$ V was applied across the BST slab. The prototype device was placed between the poles of electromagnet. The bias magnetic field in the range of $H = 1100\text{-}1400$ Oe was applied in-plane of the YIG film parallel to the antennae.

In the experiment, S-parameters as a function of frequency f and as a function of input microwave power P_{in} were measured for different H and U . The device demonstrated a dual-function performance with a nonlinear phase shift up to 250 degrees for $P_{\text{in}} = 17$ dBm and electric field induced differential phase shift up to 330 degree for $U = 1000$ V. The nonlinear phase shift increased with frequency whereas the differential phase shift decreased with frequency. Therefore, the nonlinear phase shift and electric field induced differential phase shift are competing characteristics for the surface SEW nonlinear phase shifters. The device could find different applications. In particular, it could be used for development of the microwave logic gates, nonlinear interferometers, and nonlinear directional couplers.

This work was supported in part by the Russian Foundation for Basic Research, the Ministry of Education and Science of Russia, and by the grant of the National Research University of Information Technologies, Mechanics and Optics.

- [1] U. Ozgur, Ya. Alivov, H. Morkoc, *J. Mater. Sci.: Mater. Electron.*, **20** (2009) 911.
- [2] V.E. Demidov, B.A. Kalinikos, P. Edenhofer, *J. Appl. Phys.*, **91** (2002) 10007.
- [3] A.B.Ustinov, G. Srinivasan, B.A. Kalinikos, *Appl. Phys. Lett.*, **90** (2007) 031913.
- [4] A.B. Ustinov, B.A. Kalinikos, V.S. Tiberkevich, A.N. Slavin, G. Srinivasan, *J. Appl. Phys.*, **103** (2008) 063908.
- [5] M.A. Popov, I.V. Zavislyak, G. Srinivasan, *J. Appl. Phys.*, **110** (2011) 024112.
- [6] I.V. Bychkov, D.A. Kuzmin, V.G. Shavrov, *J. Magn. Magn. Mat.*, **329** (2013) 142.

2PO-K-15

SYMMETRY AND MAGNETOELECTRIC EFFECTS IN GARNET CRYSTALS AND FILMS

Popov A.I.^{1,2}, Plokhov D.I.¹, Zvezdin A.K.^{1,3}

¹A.M. Prokhorov General Physics Institute of Russian Academy of Sciences, Moscow, Russia

²National Research University of Electronic Technology, Zelenograd, Moscow, Russia

³Moscow Institute of Physics and Technology, Dolgoprudny, Russia

dmitry.plokhov@gmail.com

Continued expansion in research on physical properties of magnetically ordered crystals and films requires exploring a wide spectrum of magnetic phenomena, including magnetoelectric ones. Such cross-correlated phenomena have attracted considerable attention in recent years because of novel physics and great potential for practical applications.

A family of garnets provides a fascinating field of science and technology because of versatile functions that could be attained by introducing different ions. Studies of several years show that doping, creation of thin films, multilayer structures and composites based on the yttrium iron garnet leads to strengthening a number of effects, as well as discovery of fundamentally new phenomena in these materials.

Garnet crystals $R_3M_5O_{12}$, where R stands for a rare-earth or yttrium ion and M stands for a metal ion (such as Fe, Al, Ga, etc.), have a complicated cubic crystallographic structure, described by the space group. While a primitive cell contains four $R_3M_5O_{12}$ units, a unit crystal cell contains eight of them. Rare-earth ions are located in the positions with a dodecahedral environment of oxygen ions with no inversion center (the so-called *c*-positions of the D_2 symmetry).

Meanwhile, there are known several garnets of odd magnetic structures with respect to spatial inversion, for example, the most investigated dysprosium-aluminum garnet. In this work, we investigate it and show that despite the antisymmetric magnetic structure, the linear magnetoelectric effect in it is prohibited by the spatial symmetry. This means that the condition of the magnetic structure antisymmetry is only a necessary condition for the effect to exist, not sufficient one.

We also show that, despite the absence of the linear magnetoelectric effect in the garnet, there is a number of new other magnetoelectric effects, sensitive to an external magnetic field, such as linear in the magnetic field antiferroelectric, piezoelectric, piezomagnetic effects, etc.

An interesting situation takes place in epitaxial films of mixed garnets $R1_{3-x}R2_xM_5O_{12}$, where R1 and R2 stand for different rare-earth ions and M denotes Al or Fe. The uniform distribution of the rare-earth ions by their nonequivalent positions in the unit cell of the crystal in this case is disturbed, which results in the electric polarization occurrence in them.

In this report, we will describe in detail the structure of garnet crystals, provide the magnetoelectric Hamiltonian of rare-earth ions in the garnets, discuss the ferroelectric structure induced by magnetic fields in the dysprosium aluminate garnet and the holmium-yttrium iron garnet, and describe the linear magnetoelectric effects in a single crystal (in an inhomogeneous magnetic field) and also in epitaxial thin films.

Support by the Russian Scientific Foundation and the Russian Foundation for Basic Research is acknowledged.

2PO-K-16

LOCAL STATES OF IRON ATOMS IN MULTIFERROIC

$\text{Bi}_{0.815}\text{Eu}_{0.085}\text{La}_{0.1}\text{FeO}_3$

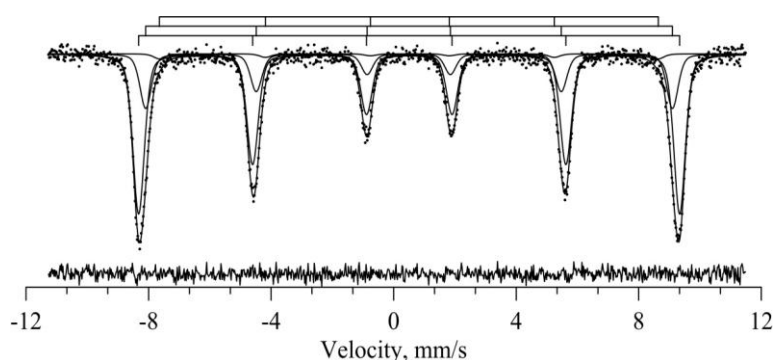
Pokatilov V.S.¹, Rusakov V.S.², Sigov A.S.¹, Pokatilov V.V.¹

¹ Moscow State Institute of Radio Engineering, Electronics, and Automation (Technical University),
Moscow, Russia

² Lomonosov Moscow State University, Moscow, Russia
pokatilov@mirea.ru

It is known that substitution of Bi ions with rare-earth ions in multiferroics on the basis of BiFeO_3 results in the magnification of electrical polarization and magnetization. However local magnetic and valence states of Fe ions which spot electrical and magnetic properties in these compounds are practically not explored. The purpose of this study is examination of the valence and magnetic states of Fe ions in multiferroic $\text{Bi}_{0.815}\text{Eu}_{0.085}\text{La}_{0.10}\text{FeO}_3$ by methods of Mössbauer spectroscopy in the field of temperatures 5 – 700 K. The investigated sample was synthesized by the solid-state ceramic technology. X-ray studies of the crystal structure and phase state revealed that the sample was single-phase and had a rhombohedral structure with lattice parameters: $a = 0.5556 \pm 0.0005 \text{ \AA}$ and $c = 1.3770 \pm 0.0005 \text{ \AA}$. The temperature of the magnetic phase transition (Neel point) $T_N = 635 \pm 2 \text{ K}$ was determined. Techniques of recovery of hyperfine magnetic field H_n distribution $p(H_n)$ and model fitting based on the SpectrRelax program [1] in the temperature range $5 \text{ K} \leq T < T_N < 700 \text{ K}$ were used for processing and analysis of the spectra.

The spectrum at 700 K represents the symmetrical quadrupole doublet with parameters: isomer $\delta = 0.106 \pm 0.007 \text{ mm/s}$, quadrupole shifts $\varepsilon = 0.080 \pm 0.006 \text{ mm/s}$ and width of resonance lines $\Gamma = 0.313 \pm 0.012 \text{ mm/s}$. These data show that Fe atoms are in one crystallographic position in multiferroic $\text{Bi}_{0.815}\text{Eu}_{0.085}\text{La}_{0.10}\text{FeO}_3$. For all temperatures $T < T_N$ hyperfine field distributions $p(H_n)$ consist at least of three local maxima for three most probable various magnetic states of Fe atoms. According to results of recovery of distributions $p(H_n)$ model fitting of spectra was performed in the form of superposition of three partial Zeeman sextets for all temperatures $T < T_N$. As an instance, the model fitting of the spectrum measured at 87 K is shown in figure. It was found that at each temperature for three states of Fe atoms the shifts δ of subspectra were equal, quadrupole shifts were also equal and $\varepsilon = 0.00 \pm 0.01 \text{ mm/s}$, but fields H_n were essentially different. At room temperature for three various magnetic states of Fe atoms the shifts were equal $\delta = (0.40 \pm 0.02) \text{ mm/s}$, and hence, in $\text{Bi}_{0.815}\text{Eu}_{0.085}\text{La}_{0.10}\text{FeO}_3$ Fe atoms are in high spin trivalent state in an octahedral oxygen environment. Thus hyperfine magnetic fields for three states of Fe atom have appeared equal: $501.10 \pm 0.20 \text{ kOe}$, $488.67 \pm 0.35 \text{ kOe}$ и $462.9 \pm 1.8 \text{ kOe}$. The relation of intensities of subspectra for these states of Fe atoms equals 61:36:3 accordingly. We assume that first of all observable effects are caused by the essential difference of ionic radiuses: $R(\text{Bi}^{3+}) = 1.45 \text{ \AA}$, $R(\text{La}^{3+}) = 1.37 \text{ \AA}$, $R(\text{Eu}^{3+}) = 1.23 \text{ \AA}$ and $R(\text{Eu}^{2+}) = 1.44 \text{ \AA}$ in a 12-oxygen environment.



This work is supported by the RFBR grant № 12-02-00977.

[1] M.E. Matsnev and V.S. Rusakov. *AIP Conference Proceedings*, **1489** (2012) 178-185.

2PO-K-17

MAGNETOELECTRIC EFFECT IN FERRITE-PIEZOELECTRIC DUAL-PHASE STRUCTURE

Petrov R.V.¹, Petrov V.M.¹, Bichurin M.I.¹

¹ Novgorod State University, Veliky Novgorod, Russia
initra@yandex.ru

This manuscript devotes to the investigation of magnetoelectric (ME) coupling at longitudinal modes in a dimensionally graded magnetostrictive-piezoelectric bilayer. The measured value of magnetoelectric voltage coefficient is optimized by adjusting the geometry of layers. Theoretical estimates for the bilayer of PZT and single-crystal $\text{Zn}_{0,3}\text{Ni}_{0,7}\text{Fe}_2\text{O}_4$ are in satisfactory agreement with data. The obtained results are expected to facilitate observation of enhanced ME coupling at overlapping of electromechanical and magnetic resonance due to energy transfer between spin waves and phonons. Previously we have discussed the case of magnetoelectric coupling at thickness shear modes in bilayer of single-crystal YIG as magnetostrictive phase and Y-cut langatate (LGT) as piezoelectric phase [1]. ME effect has reached in this case 2,66 V/(cm·Oe).

To form a bilayer, PZT and ZNFO layers are bonded together with epoxy glue with thickness of 15 μm . PZT and ZNFO have dimensions of 20x5x0,5 mm³ and 8x5x0,2 mm³, correspondingly. A dc bias magnetic field was applied to (110) ZNFO parallel to the sample plane to enable exciting the longitudinal vibrations in free standing ZNFO plate by in-plane ac magnetic field (H_{ac}).

The H_{ac} was provided by a Helmholtz coil driven by a Network Analyzer Obzor-304. To excite longitudinal vibrations in free standing PZT plate, electrodes are connected to Network Analyzer. As this takes place, the longitudinal mode frequency equals 350 kHz for free standing both PZT and ZNFO layer. The ME voltage coefficient α_E of the longitudinal-mode heterostructure is measured as the ratio of induced ac electric field across the piezoelectric layer to applied ac magnetic field of 0.25 Oe. The ac magnetic field is produced by a Helmholtz coil driven by a signal generator and induced electric field is measured by an oscilloscope. The maximum ME voltage coefficient of 0,5 V/(cm·Oe) is observed at optimal $H_{dc}=340$ Oe (fig.1).

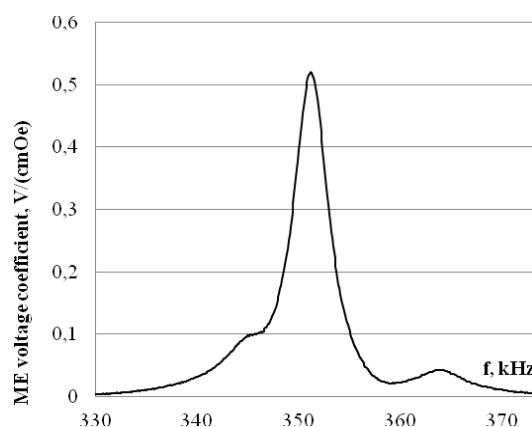


Fig. 1. Frequency dependence of ME voltage coefficient.

This work was supported by RFBR research project #13-02-98801.

[1] M.I. Bichurin, R.V. Petrov, and V.M. Petrov, *Appl. Phys. Lett.*, **103** (2013) 092902.

2PO-K-18

MAGNETIC FIELD TUNABLE ELECTROMECHANICAL RESONANCE PROPERTIES OF MAGNETOELECTRIC BILAYER

Petrov R.V.¹, Petrov V.M.¹, Kovalenko D.V.¹, Bichurin M.I.¹

¹ Novgorod State University, Veliky Novgorod, Russia
initra@yandex.ru

The present paper focuses on the study of spectrum of a magnetolectric (ME) dimensionally graded ferrite-piezoelectric bilayer at electromechanical resonance (EMR) in piezoelectric and magnetoelastic resonance in ferrite which exist simultaneously. Theoretical estimates of ME coefficient at EMR in ME composites was reported recently [1]. Experimental study of ME coupling in ferrite-piezoelectric bilayer at thickness shear mode was discussed in our earlier work [2]. The present study enables to solve several problems of the feasibility of control by a signal spectrum passing through ME bilayer by means of magnetic field and determine the adjustment characteristics.

The design of studied prototype consists of solenoid with the inside ME element. Bias magnetic field was implemented with an external electromagnet with the field value up to 340 Oe. ME element is a dual-phase structure consisting of a single-crystal $Zn_{0,3}Ni_{0,7}Fe_2O_4$ (NZFO) and piezoelectric lead zirconate-titanate (PZT). PZT and NZFO have dimensions of $20 \times 5 \times 0,5 \text{ mm}^3$ and $8 \times 5 \times 0,2 \text{ mm}^3$, correspondingly. The output voltage across the piezoelectric layer is measured by using the electrodes that are placed on planar surfaces of piezoelectric layer. Coupling at the interface is provided by gluing. Bilayer structure is formed so that the magnetoelastic resonance frequency in ferrite layer coincides with EMR frequency in the piezoelectric material. Frequencies of both resonances are about 350 kHz and primarily depend on linear dimensions. DC magnetic field H is necessary for magnetic layer to provide non-zero piezomagnetic coefficient and achieve the resonant characteristics. The measurements were carried out on Network Analyzer Obzor-304.

The frequency spectrum of the studied prototype is presented by the resonance curve at frequency 350 kHz. The measurement data are shown in Fig. 1. One can see that the value of transmission coefficient equals approximately -83 dB in the absence of DC magnetic field and -44 dB in the field of 340 Oe. Thus, applying the DC field enables to obtain the transmission coefficient control range of 39 dB for the investigated structure. The obtained results can be further used in practical applications.

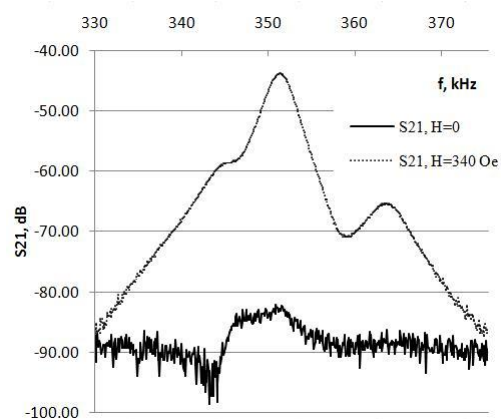


Fig. 1. Frequency dependence of transmission coefficient S_{21} .

This work was supported by RFBR research project #13-02-98801.

- [1] M. Bichurin, V. Petrov, R. Petrov, and S. Priya. *Solid State Phenomena*, **189** (2012) 129-143.
[2] M.I. Bichurin, R.V. Petrov, and V.M. Petrov, *Appl. Phys. Lett.*, **103** (2013) 092902.

2PO-K-19

HIGH-FIELD MAGNETIZATION AND MAGNETIC PHASE DIAGRAMS OF $R\text{Fe}_{11}\text{Ti}$ AND $R\text{Fe}_{11}\text{TiH}$

Kostyuchenko N.^{1,2}, *Tereshina I.*^{3,4}, *Skourski Y.*⁵, *Tereshina E.*⁶, *Doerr M.*⁷,
*Pelevin I.A.*⁴, *Drulis H.*⁸, *Zvezdin A.K.*^{1,2}

¹ A. M. Prokhorov General Physics Institute of Russian Academy of Sciences, Moscow, Russia

² Moscow Institute of Physics and Technology, Dolgoprudny, Russia

³ Lomonosov Moscow State University, Moscow, Russia

⁴ Baikov Institute of Metallurgy and Materials Science RAS, Moscow, Russia

⁵ Hochfeld-Magnetlabor Dresden, Helmholtz-Zentrum Dresden-Rossendorf, Dresden, Germany

⁶ Institute of Physics, ASCR, Prague, Czech Republic

⁷ Technische Universität Dresden, Dresden, Germany

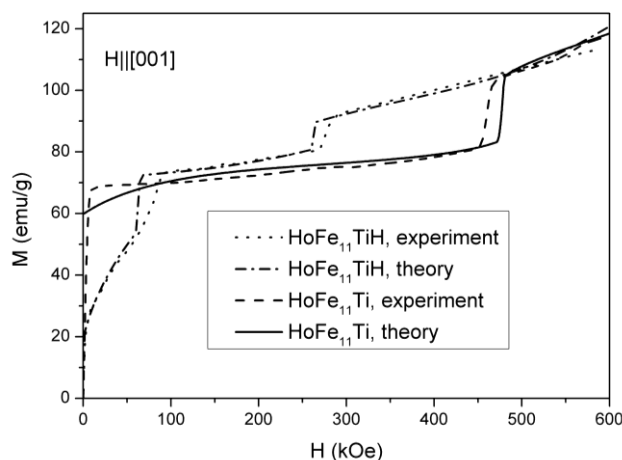
⁸ Institute of Low Temperature and Structure Research, Wroclaw, Poland

nvkost@gmail.com

Due to recent major progress in developing methods for the high-field magnetization studies, experiments in very strong (up to 100 T) magnetic fields became feasible. This has demonstrated that some theoretical models used previously to describe the magnetization behavior were inaccurate, in particular, the crystal-field parameters have been reported with the insufficient precision [1,2]. This work reports on the high-field magnetization study of the rare earth (*R*) intermetallics $R\text{Fe}_{11}\text{Ti}$ and their hydrides $R\text{Fe}_{11}\text{TiH}$, which have attracted a great deal of attention in the past decades during the search for new permanent magnet materials. The compounds are interesting also from the fundamental viewpoint, as in contrast to the famous $R_2\text{Fe}_{14}\text{B}$ and $R_2\text{Fe}_{17}\text{N}_3$, they have a single rare-earth position and three positions for iron.

The $R\text{Fe}_{11}\text{Ti}$ single crystals were obtained and subsequent hydrogenation of the samples was performed. Mild hydrogenation conditions have ensured the preserved single-crystalline structure of $R\text{Fe}_{11}\text{TiH}$. The magnetization curves of $R\text{Fe}_{11}\text{TiH}$ and $R\text{Fe}_{11}\text{Ti}$ were measured along different crystallographic directions at 4.2 K in pulsed fields up to 60 T. To describe the experimental data obtained, we have performed calculations that allowed us to determine the crystal field parameters in the parent and hydrogen-charged $R\text{Fe}_{11}\text{Ti}$ compounds. As seen in Fig. 1, the magnetization behavior is well reproduced by the curves obtained theoretically both in the low and high-field regions. Phase diagrams constructed demonstrate a strong influence of hydrogen on magnetic properties of $R\text{Fe}_{11}\text{Ti}$.

Support by RFBR, pr. No. 13-03-00744, 14-03-31395 and by the Czech Science Foundation under Grant No. P204/12/0150, by HLD at HZDR, member of the European Magnetic Field Laboratory (EMFL). Part of measurements has been performed in MLTL (<http://mltl.eu>), which is supported within the program of Czech Research Infrastructures (project no. LM2011025).



[1] C. Piquer et al., *J. Phys.: Condens. Matter*, **18** (2006) 221–242.

[2] C. Abadia et al., *J. Phys.: Condens. Matter*, **10** (1998) 349–361.

2PO-K-20

NONRESONANT MAGNETOELECTRIC FREQUENCY DOUBLING IN A METGLAS - PZT-FIBER STRUCTURE

Fedulov F.A.¹, Fetisov L.Y.¹, Fetisov Y.K.¹

¹ Moscow State Technical University of Radio Engineering, Electronics and Automation, Russia
fetisov@mirea.ru

Nonlinear magnetolectric (ME) effects of the frequency doubling [1] and magnetic fields mixing [2] in the structures consisting of ferromagnetic (FM) and piezoelectric (PE) layers arise due to nonlinearity of the FM layer magnetostriction $\lambda(H)$. Up to now these effects were studied mainly in a resonance regime, when a frequency of generated signal coincided with a frequency of acoustical resonance of the structure.

This paper describes a nonresonant wideband ME frequency doubling which was observed in a structure comprising a layer of amorphous ferromagnet FeBSiC (Metglas Corp.) and a PZT (lead zirconate titanate)-fiber composite (Smart Material Corp.). The FM metglas layer had in-plane dimensions of 10 mm x 50 mm and thickness of 75 μm . The PE composite had in-plane dimensions of 10 mm x 50 mm, it contained ~ 30 μm diameter PZT fibers and interdigital electrodes. The layers were bonded with a fast dry epoxy. The structure was placed in a dc bias magnetic field $H = 0$ -200 Oe and ac excitation field $h\cos(2\pi ft)$ with a frequency of $f = 0$ -25 kHz and magnitude h up to 20 Oe. Both the fields were applied along the long side of the structure. The ME voltage u generated by the PZT-fiber composite was measured as functions of f , h and H .

Fig. 1 shows measured dependences of excitation field $h(t)$ with frequency $f = 2$ kHz and ME voltage $u(t)$ with double frequency 4 kHz. The voltage reaches maximum at $H = 0$, when the nonlinear piezomagnetic coefficient $p = \partial^2 \lambda / \partial H^2$ is maximum, and turns out to zero at $H = 40$ Oe, when $p = 0$ while the linear piezomagnetic coefficient $q = \partial \lambda / \partial H$ is maximum. Fig.2 shows frequency dependences of the structure's ME sensitivity u/h for the nonlinear frequency doubling regime ($H=0$) and for the linear ME effect ($H = 40$ Oe). It is seen that the nonresonant ME frequency doubling may be used to design the wideband ac magnetic field sensors which operate without dc bias magnetic field. Sensitivity of such sensors may reach ~ 20 -50 mV/Oe.

The research was supported by the Ministry of Education and Science of Russian Federation and the Russian Foundation for Basic Research.

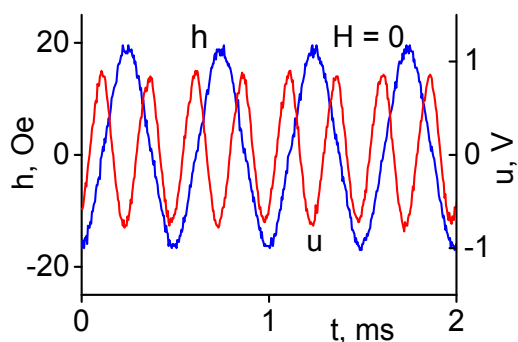


Fig. 1

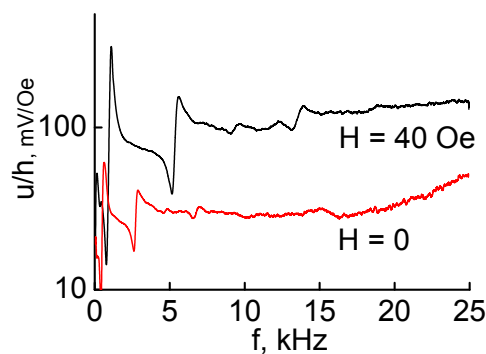


Fig. 2

- [1] K.E. Kamentsev, Y.K. Fetisov, and G. Srinivasan, *Appl. Phys. Lett.*, **89** (2006) 142510.
[2] D.A. Burdin, D.V. Chashin, N.A. Ekonomov et al, *JMMM*, **358-359** (2014) 98.

2PO-K-21

**PECULIARITIES OF MAGNETIC PROPERTIES OF THE
Bi_xLa_{1-x}MnO₃ (0.2 ≤ x ≤ 0.6) SYSTEM: CONNECTION WITH THE
SYNTHESIS CONDITIONS**

*Tarasenko T.N.¹, Kravchenko Z.F.¹, Mazur A.S.¹, Kamenev V.I.¹, Pismenova N.E.¹,
Demidenko O.F.², Ignatenko O.V.², Makovetskii G.I.², Panasevich A.M.², Yanushkevich K.I.²,
Tovstolytkin A.I.³, Pogorily A.M.³, Polek T.I.³*

¹ Donetsk Institute for Physics and Engineering named after O.O. Galkin, NAS of Ukraine,
Donetsk, Ukraine

² Scientific-Practical Materials Research Center, NAS of Belarus, Minsk, Belarus

³ Institute of Magnetism NASU and MES of Ukraine, Kyiv, Ukraine

Solid solutions based on BiMnO₃ and LaMnO₃ are examples of the systems with a strong relationship of the magnetic and electrical properties. Both manganites have a perovskite structure: BiMnO₃ is a multiferroic with the temperature of ferromagnetic ordering $T_C = 100$ K, the temperature of ferroelectric ordering $\sim 750\text{--}780$ K and monoclinic structure, and LaMnO₃ is an antiferromagnetic ($T_N = 140$ K) with orthorhombic structure.

The synthesis of polycrystalline compounds of the Bi_xLa_{1-x}MnO₃ system ($x = 0.2, 0.4$ and 0.6) with the dispersion of powder grains up to ~ 90 nm was performed by co-precipitation of the hydroxides. The powders of the compounds with the concentration $x = 0.2, 0.4, 0.6$ (sample I) have been pressed at 0.2 GPa and calcinated at 800°C (20 h). The powders of the same compounds (samples II) have been compacted at 1000°C and $P = 4$ GPa (60 s). X-ray diffraction studies showed that all compounds had distorted perovskite structure. The crystal structure of the solid solutions with $x = 0.2$ and 0.4 is identified as the $Pm\bar{3}m$ pseudocubic space group, and $x = 0.6$ is associated with the $C2$ monoclinic one (like BiMnO₃).

The results of magnetic (measurements of specific magnetization and magnetic susceptibility) and resonance (electron spin resonance (ESR)) tests have demonstrated the absence of magnetically ordered phase in samples I. With increasing temperature, the intensity of the ESR resonance absorption is reduced, which is typical for paramagnetics. The value of the resonant field (≈ 3400 Oe) does not change with increasing concentration x and is not practically dependent on the temperature. The width and the position of the resonance line is the same for the perpendicular and parallel orientations of the magnetic field. The value of the paramagnetic Curie temperature was estimated on the basis of the temperature dependences of inverse intensity of ESR. Processing conditions II of initial nanopowders have been voted optimal for composition Bi_{0.4}La_{0.6}MnO₃. The value of the specific magnetization of the Bi_{0.4}La_{0.6}MnO₃ compact ($T_C = 105$ K) is about 100 times more than the value of specific magnetization of the rest of compounds. The presence of ferromagnetic clusters in the $T_C < T < T_N$ temperature range is assumed [1].

[1] E. Dagotto, T. Hotta, and A. Moreo, *Phys. Rep.*, **344** (2001) 1.

2 July

Wednesday

17:30-18:30

poster session
2PO-M

**“High Frequency
Properties and
Metamaterials”**

2PO-M-1

GREEN'S FUNCTIONS OF SPIN AND ELECTROMAGNETIC WAVES IN THE SINUSOIDAL SUPPERLATTICE

Ignatchenko V.A.¹, Tsikalov D.S.¹
¹ L.V. Kirensky Institute of Physics SB RAS, Krasnoyarsk, 660036, Russia
 d_tsikalov@iph.krasn.ru

The problem of finding the Green's function of the scalar wave equation with a sinusoidal modulation of the medium parameters is considered. In this case, the equation has the form

$$\nabla^2 G(\mathbf{r}, \mathbf{r}_0) + [\nu - 2\eta \cos(qz + \psi)] G(\mathbf{r}, \mathbf{r}_0) = -\delta(\mathbf{r} - \mathbf{r}_0), \quad (1)$$

where $q = 2\pi/l$, l is the superlattice period and ψ is a phase. For electromagnetic waves in a medium with an inhomogeneous permittivity ε $\nu = \varepsilon(\omega/c)^2$ and $2\eta = \Delta\varepsilon(\omega/c)^2$. For spin waves $\nu = (\omega - \omega_0)/\alpha g M_0$, where $\omega_0 = g[H + (\beta - 4\pi)M_0]$ is the frequency of a uniform ferromagnetic resonance, g is the gyromagnetic ratio, α is the exchange constant, β is the value of the uniaxial anisotropy, M_0 is the magnetization and 2η is the amplitude of the magnetic parameters modulation in the superlattice. The homogeneous equation corresponding to Eq. (1) (the Mathieu equation) has been well investigated (see, e.g. [1]). The Green's function of waves in the superlattice is much less studied. In the work [2] the approximate expressions have been found for the function in the \mathbf{r} space. The purpose of this work is to obtain a general expression for the Green's function in the \mathbf{k} space. Applying to Eq. (1) the Fourier transformation and using the method of presenting solutions of linear equations with tridiagonal matrix in the form of continued fractions [3], we found an analytical expression for the spectral Green's function

$$\tilde{G}(\mathbf{k}, z_0) = -\frac{\exp(-ik_z z_0)}{(2\pi)^3} \frac{1 + \eta [e^{i\psi} P_1^+ + e^{-i\psi} P_1^-]}{\nu - k^2 - \eta^2 \left[\frac{1}{L_1^+} + \frac{1}{L_1^-} \right]}. \quad (2)$$

Here P_1^\pm are ascending continued fractions defined by recursion formulas $P_n^\pm = [\exp(\pm inqz_0) + \eta \exp(\pm i\psi) P_{n+1}^\pm] / L_n^\mp$, $L_n^\pm = \nu - k_\rho^2 - (k_z \mp nq)^2 - \eta^2 / L_{n+1}^\pm$ are ordinary continued fractions, $k = \sqrt{k_\rho^2 + k_z^2}$ is the wave number, $k_\rho = \sqrt{k_x^2 + k_y^2}$ is its radial projection and k_z is the longitudinal projection. The spectral Green's function also was represented as a Fourier series in the terms of the source coordinate z_0

$$\tilde{G}(\mathbf{k}, z_0) = -\frac{1}{(2\pi)^3} \sum_{n=-\infty}^{\infty} g_n \exp[-i(k_z - nq)z_0]. \quad (3)$$

The coefficients g_n were determined by the expressions $g_{\pm n} = [\eta \exp(\pm i\psi)]^n / L_n^\pm / L_{n-1}^\pm / \dots / L_0$, where L_0 is the denominator of Eq. (2). In the case of the one-dimensional problem the Green's function $G(z, z_0)$ has been found by numerical inverse Fourier transformation taking into account a small intrinsic attenuation. Thus found the Green's function is in a good agreement with the numerical solution of Eq. (1) by the finite-difference method on a finite space interval with non-reflective boundary conditions at the edges of the computational domain.

[1] L. Brillouin, et al., *Wave propagation in periodic structures*, IIL, M. (1959) 457.

[2] E.V. Aksenova, et al., *Optika i Spektroskopiya*, **104** (2008) 440-473.

[3] P.K. Korneev, *Vestnik Stavropol State University*, **38** (2004) 69-72.

2PO-M-2

GREEN'S FUNCTION OF MAGNETOELASTIC WAVES

Ignatchenko V.A.¹, Polukhin D.S.¹

¹ L.V. Kirensky Institute of Physics SB RAS, Krasnoyarsk, 660036, Russia
polukhin@iph.krasn.ru

The dispersion law of magnetoelastic waves is theoretically well studied [1]. Green's function in the vicinity of the crossing resonance of spin and elastic waves for both homogeneous and inhomogeneous medium also has been obtained [2] but in the framework of the model problem. The purpose of this work is to derive and study the Green's function for magnetoelastic waves in a homogeneous medium, taking into account both the dynamic dipole-dipole interaction, and the difference in speed of transverse and longitudinal elastic waves. Unlike [2], where the Green's

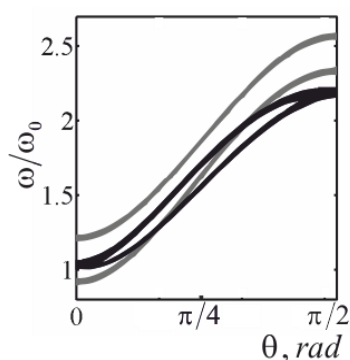


Fig. 1.

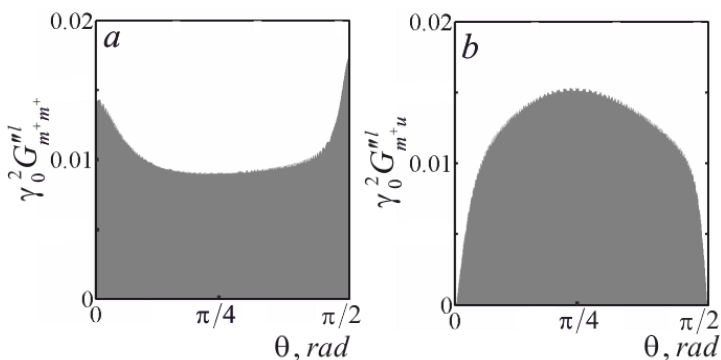


Fig. 2.

function is described by a 2x2 matrix, in this case the Green's function has the form of a 5x5 matrix. Magnetoelastic resonances and the corresponding gaps $\Delta\omega_t$ and $\Delta\omega_l$ appear in two points of the spectrum (ω_t, k_t) and (ω_l, k_l) , corresponding to the intersection of the spin wave spectrum with the spectra of transversal and longitudinal elastic waves. Dependences of the boundary frequencies of the gaps ω_{\pm} on the angle of wave propagation θ are shown in Fig. 1. The gaps offset to higher frequencies with θ increasing is due to shifting the entire spectrum of spin waves with increasing the dynamic dipole-dipole interaction. The gap width $\Delta\omega_t$ is with almost no change

(gray curves in Fig. 1). Quite a different picture is observed for the gap $\Delta\omega_l$ corresponding to the interaction between the spin and the longitudinal elastic waves (black curves). At both $\theta=0$ and $\theta=\pi/2$, the gap width $\Delta\omega_l=0$ and reaches a maximum at $\theta=\pi/4$. Fig. 2 shows the dependence of the diagonal $G_{m^+m^+}^l$ (a) and off-diagonal $G_{m^+u}^l$ (b)

elements of the matrix Green's function at the points corresponding to the magnetoelastic resonance of spin and longitudinal elastic waves. We see that when $\theta=0$ and $\theta=\pi/2$ the value $G_{m^+m^+}^l$ reaches a maximum, and by the middle of this range decreases. This is due to the emergence of interaction and the redistribution of energy between the magnetic and elastic vibrations. At the same time the value of the off-diagonal element $G_{m^+u}^l$ that characterizes the mutual exchange of energy between the magnetic and elastic system increases to the point of maximum interaction $\theta=\pi/4$.

[1] A.I. Akhiezer, V.G. Bar'yakhtar, S.V. Peletminskii, *Spin waves*, Nauka, Moscow (1967).

[2] V.A. Ignatchenko, D.S. Poluhin, *Zh.Eksp.Theor.Fiz.* **143** (2013) 238-256; **144** (2013) 972-989.

2PO-M-3

SPIN-WAVE OSCILLATIONS IN TRANSVERSELY MAGNETIZED ELLIPTIC WIRES

Golovach G.P.¹, Zavislyak I.V.¹, Popov M.A.¹, Stashkevich A.A.², Roussigné Y.²

¹ Taras Shevchenko National University of Kyiv, Kyiv, Ukraine

² Université Paris 13, Villetaneuse, France

zav@univ.kiev.ua

Let us consider an infinitely long ferromagnetic elliptical cylinder, with semiaxes a and b , made from ferrite with saturation magnetization $4\pi M$ and biased to saturation with external static magnetic field \vec{H}_0 , applied along cylinder larger semiaxis. In order to solve the Walker equation we shall introduce modified elliptical coordinate system (ρ, φ) [1]. In these coordinates the magnetostatic potential in the ferrite is given by $\Psi_1(\rho, \varphi) = \sum_{k=1}^{\infty} (M_k U^k(\rho, \varphi) + N_k V^k(\rho, \varphi)) + M_0$, where

$U(\rho, \varphi) = \left(\rho + \frac{c^2}{4\rho}\right) \cos \varphi + \frac{1}{\sqrt{-\mu}} \left(\rho - \frac{c^2}{4\rho}\right) \sin \varphi$, $V(\rho, \varphi) = \left(\rho + \frac{c^2}{4\rho}\right) \cos \varphi - \frac{1}{\sqrt{-\mu}} \left(\rho - \frac{c^2}{4\rho}\right) \sin \varphi$, and μ is the diagonal part of tensor magnetic permeability; whereas outside $\Psi_2(\rho, \varphi) = \sum_{k=1}^{\infty} \frac{1}{\rho^k} (E_k \cos k\varphi + F_k \sin k\varphi)$. After applying standard electrodynamic boundary

conditions at the lateral boundary of the cylinder we get a pair of secular equations:

$$\left((1 - i\sqrt{-\mu}) \left(a + \frac{ib}{\sqrt{-\mu}} \right)^k + (1 + i\sqrt{-\mu}) \left(a - \frac{ib}{\sqrt{-\mu}} \right)^k \right) = 0, \quad \left(-(i + \sqrt{-\mu}) \left(a + \frac{ib}{\sqrt{-\mu}} \right)^k + (i - \sqrt{-\mu}) \left(a - \frac{ib}{\sqrt{-\mu}} \right)^k \right) = 0 \quad (1)$$

After solving (1) for $\mu^{(nk)}$, the spin modes eigenfrequencies can be calculated according to

$$\omega^{(nk)} = \gamma \sqrt{\left(H_0 - 4\pi M \frac{b}{a+b} \right) \left(H_0 - 4\pi M \frac{b}{a+b} + \frac{4\pi M}{1 - \mu^{(nk)}} \right)}$$

The presented theory was applied to explain the experimental results, published in [2]. In that work the dependence of the spin-wave modal frequency on the intensity of the magnetic field applied normal to the rod axis has been measured using Brillouin light scattering technique for the array of nickel nanowires with length $L=175$ nm, radius $R=35$ nm and packing density 0.15. In order to provide better agreement, the demagnetizing dipole field due to interaction between nanowires as well as exchange interaction term were added to the internal field. Transversal wavevector component was extracted from the peak value of the spatial Fourier transformation for the mode dynamic magnetization.

The results are presented on Fig. 1. From it we can draw a conclusion that experimentally observed spin-wave modes correspond to the two lowest non-uniform oscillations of cylindrical nanowire.

[1] I.V. Zavislyak, G.P. Golovach et al, *J. of Comm. Tech. and Electronics*, **51** (2006) 203-211.

[2] A.A. Stashkevich, Y. Roussigné, P. Djemia et al., *Phys. Rev. B*, **80** (2009) 144406-1-13.

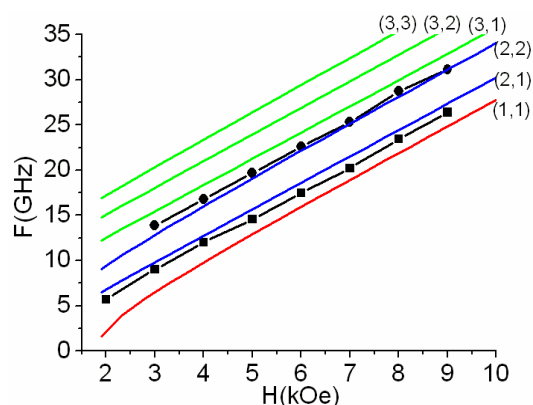


Fig. 1. The theoretical (solid lines) and experimental values (filled symbols) of resonance frequencies vs. the intensity of magnetic field applied normally to the axis of a Ni nanorod

2PO-M-4

ATTENUATION OF NONCOLLINEAR SURFACE MAGNETOSTATIC WAVES

Annenkov A. Yu.¹, Gerus S. V.¹

¹ Kotel'nikov Institute of Radio Engineering and Electronics, Fryazino Branch,
Russian Academy of Sciences, 141190, Fryazino, Russia
svg318@ire216.msk.su

The attenuation of magnetostatic surface waves (SMSW) propagating at an arbitrary angle to the bias field on the plane of the ferrite film was investigated. Decaying plane waves in the form $Ae^{i(\mathbf{k}\mathbf{r}-\omega t)-\mathbf{q}\mathbf{r}}$ were considered, where the frequency ω depends on the parameters of the film, on the bias field and on 2-d wave vector \mathbf{k} , \mathbf{r} - 2-d radius vector on the yz plane of the film. Bias field vector is directed along the axis z . Directions of phase and group velocities of these waves are different, so they are called non-collinear. As is known [1], the attenuation of the ferrite medium can be considered by formally adding the imaginary term $i\alpha\omega/\gamma$ to the value of the bias field in the dispersion equation for MSSW [2], where α - attenuation coefficient, γ - gyromagnetic ratio. Vector \mathbf{q} describes the attenuation of the wave in the minimal losses direction, which is calculated directly from the dispersion equation for SMSW. Characteristic dependences of the normalized vector magnitude $|\mathbf{q}|$ and its angle ψ_q from the angle φ of the phase velocity are shown in Fig. 1 and 2. The angles are measured from the axis y . Fig. 3 shows the iso-frequency curves of SMSW. In all figures, the dashed line shows the graphs for the film with the small attenuation factor α , and the solid line - for the film with the large one.

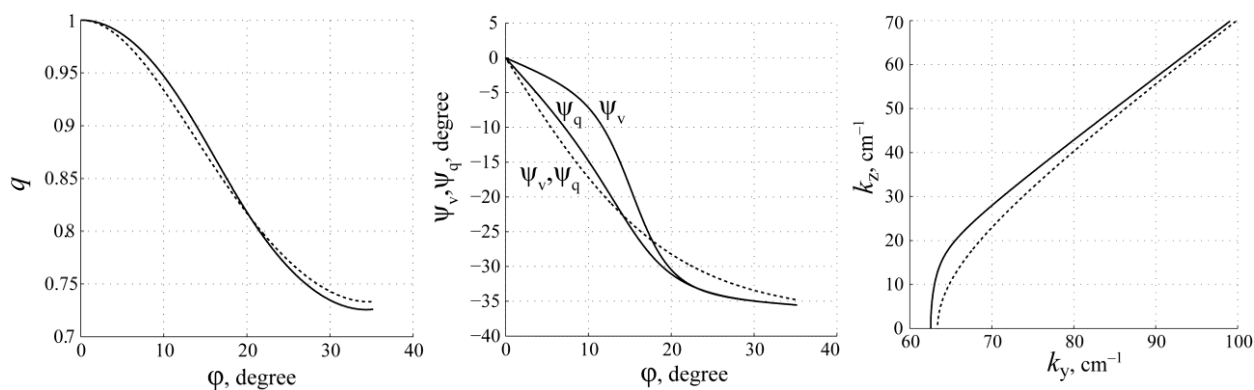


Fig. 1. Dependence of the attenuation coefficient $|\mathbf{q}|$ from the angle φ of the phase velocity.

Fig. 2. Dependences of the angle ψ_q of the decay vector \mathbf{q} and the angle ψ_v of group velocity vector from the angle φ of the phase velocity.

Fig. 3. Iso-frequency curves showing possible values of the wave vector \mathbf{k} at a given frequency ω .

In low attenuation films the vector \mathbf{q} is directed along the group velocity (Fig. 2). With increasing of the attenuation these vectors cease to be parallel, iso-frequency curves become deformed (Fig. 3).

This work was supported by RFBR grant № 14-07-00332.

[1] A.G. Gurevich and G.A. Melkov, Magnetization Oscillations and Waves (CRC Press, Boca Raton, FL 1996).

[2] Yu.I. Bespyatyh, V.I. Zubkov, V.V. Tarasenko, *ZhTF*, **50** (1980) 140-146.

2PO-M-5

INVESTIGATION OF NONLINEAR DYNAMICS OF MAGNETOELASTIC OSCILLATIONS IN NORMAL MAGNETIZED FERRITE PLATE

*Pleshev D.A.¹, Vlasov V.S.², Kotov L.N.², Asadullin F.F.¹, Poleshikov S.M.¹, Shavrov V.G.³,
Shcheglov V.I.³*

¹ Saint-Petersburg state forest technical university named after S.M. Kirov, St-Petersburg, Russia

² Syktyvkar State University, Syktyvkar, Russia

³ Institute of Radioengineering and Electronics of the Russian Academy of Sciences, Moscow, Russia

dpleshev@gmail.com

In one of the previous papers [1] the system of ordinary differential equations was obtained which described the electromagnetic excitation of nonlinear magnetoelastic oscillations in the normally magnetized ferrite plate when the parametric excitation of spin waves was blocked. The angles of the magnetization precession can be up to few tens degrees. The present work deals with investigation of the features of the magnetization vector nonlinear precession and the elastic displacement close to ferromagnetic resonance.

The case of only first elastic mode excitation was considered. The alternating circular polarized magnetic field was oriented in the plane of the plate. The system of ordinary differential equations [1] was solved numerically by the Runge-Kutta 7-8 orders method with control of the integration at every step length.

The time evolution of magnetic and elastic oscillations caused by the alternating field was analyzed. The dependences of magnetoelastic oscillation relaxation time on magnitudes of dc and alternating magnetic fields, saturation magnetization, magnetoelasticity constant, magnetic and elastic relaxation parameters were determined. Magnetoelastic coupling efficiency in particular is determined by the ratio of the relaxation times of magnetic and elastic subsystems was revealed. The resonance curves of magnetic and elastic oscillations were built in the nonlinear regime of the excitation. We show that increasing of excitation amplitude on two orders excited hypersound amplitude in nonlinear regime may exceed the same amplitude in linear regime 70 times. When the dc field is less than the demagnetization field we can obtain the second order magnetization precession. In this paper some peculiarities of the second order magnetization precession near to the condition of elastic resonance were investigated. Several regimes of precession changing each other by increase of the alternating field amplitude were identified. It was found that the magnetoelastic interaction changed the character of the observed precession regimes especially in the condition of the elastic resonance.

In case of detuning the eigenfrequency of the magnetic and elastic resonances, chaotic oscillation modes took place. The boundaries between regular and chaotic oscillations depending on the magnetic dissipation parameter, frequency and amplitude of the alternating field were determined.

The work is supported by Russian Foundation of Basic Research (grant №12-02-01035-a).

[1] V.S. Vlasov, L.N. Kotov, V.G. Shavrov, V.I. Shcheglov, *J. Comm. Tech. El.*, **54** (2009) 821-832.

2PO-M-6

NONLINEAR PROPERTIES OF MAGNETOSTATIC SURFACE SPIN WAVES ONE-PORT FABRY-PEROT RESONATOR

Pavlov E.S.¹, Filimonov Yu.A.¹, Vysotskiy S.L.¹, Nikitov S.A.²

¹ Kotel'nikov SBIRE RAS, Zelenaya str., 38, Saratov, Russia

² Kotel'nikov IRE RAS, Mokhovaya str., 11-7, Moscow, Russia

gekapavlov@gmail.com

Magnetostatic waves (MSW) technology is well known for providing frequency tunable filters and oscillators for linear and nonlinear microwave signal processing [1]. Properties of nonlinear Fabry-Perot (F-P) resonator for surface magnetostatic waves (MSSW) were theoretical studied in [2]. We present experimental results on investigation of influence a three-magnon (3M) and four-magnon (4M) parametric processes on formation of MSSW resonances F-P resonator. F-P resonator design consist of two Bragg mirrors lattice R1 and R2 made of etched grooves have the width $w_g \approx 80 \mu\text{m}$ and the depth $\delta d \approx 1.8 \mu\text{m}$ with the period $\Lambda \approx 150 \mu\text{m}$ at the surface of a epitaxial YIG film with the thickness $d \approx 14.7 \mu\text{m}$ with resonator gap between them $L_R \approx 2 \cdot \Lambda \approx 300 \mu\text{m}$ fig.1(a). The resonator is excited by a microstrip transduced, which locate on resonator gap. The modulus and phase of the reflection coefficient $S_{11} = P_{\text{ref}}/P_{\text{in}}$ at the different input power levels P_{in} was measured. At the input power $P_{\text{in}} \approx -30 \text{ dBm}$ in the spectra of MSSW on the frequency f_R F-P resonator excitation is formed with quality $Q \approx 4000$ (fig.1(a)). This resonance is the effect of interaction between MSSW reflected from the mirrors R1 and R2 and the formation of a standing wave. At input power $P_{\text{in}} \approx -29 \text{ dBm}$ on the frequency f_R an increase abruptly "stage" of F-P resonance is destroyed. Magnitude of the input threshold power P_{in} lower than magnitude of the input threshold power 3M processes for typical YIG film. Fig.1(c) shows influence 4M processes at P_{in} in the range $P_{\text{in}} \approx -10 \dots +20 \text{ dBm}$ which leads to nonlinear shift down frequency of f_R as a function of P_{in} and destroyed F-R resonance. These dependences are caused by the effect of local amplification of amplitude of MSSW in the resonator gap and decrease of magnitude of the threshold input power of parametric instability.

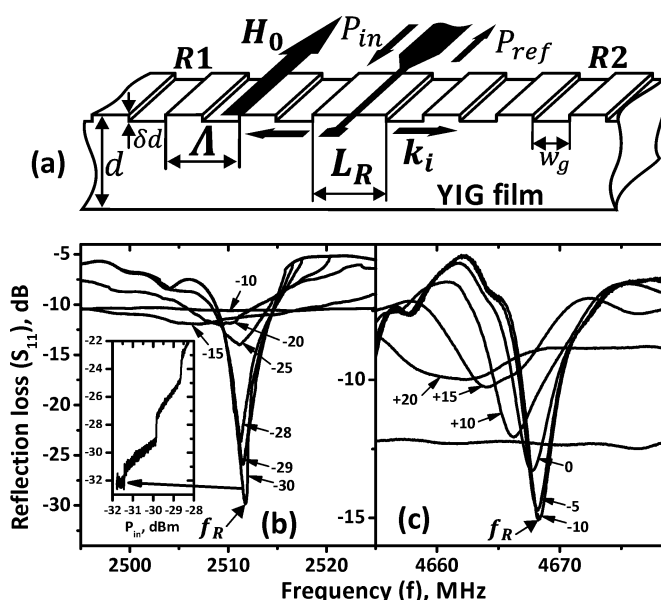


Fig. 1. (a) MSSW Fabry-Perot resonator schematic. Dependence of reflection loss S_{11} MSSW spectrun the value of the input power P_{in} at $H_0 \approx 238 \text{ Oe}$ (b) $H_0 \approx 910 \text{ Oe}$ (c).

Supported by RFBR (grants № 13-07-12421, 13-07-00941, 14-07-00896).

[1] R. Marcelli, S.A. Nikitov C.D. Eee, F.G. Hhh, *Signal processing; Nonlinear optics; Microwave devices; Congresses* (1996) 507.

[2] A. D. Boardman, Yu. V. Gulyaev, and S. A. Nikitov, *Sov. Phys. JETP.*, **68** (1989) 1238-1243.

2PO-M-7

INFLUENCE OF THE MAGNETIC PROPERTIES OF COMPOSITE FILMS ON RF AND MICROWAVE COMPLEX CONDUCTIVITY

Lasek M.P.¹, Kotov L.N.¹, Kirpicheva O.A.¹, Kalinin Yu. E.², Sitnikov A.V.²

¹ Syktyvkar State University (SyktSU), Syktyvkar, Russia

² Voronez State Technical University (VorSTU), Voronez, Russia

mplasek@yandex.ru

Spectra of complex conductivity and magnetic spectra of composite thin films with magnetic metal phase have been investigated in this work. They have been explained by structures and magnetic properties of the thin composite films. Electrical model of the composite films has been proposed. The model describes influence of magnetic properties of the composite films on behavior of the spectra of the complex conductivity.

The films contained particles of ferromagnetic metals Co and Fe in the insulating matrix. Composite films compositions were: $(\text{Fe}_7+\text{Co}_7+\text{Zr}_2)_x(\text{Al}_2\text{O}_3)_{1-x}$, $0,25 < x < 0,66$. The composite films were prepared by ion beam sputtering method in the argon atmosphere with the pressure 0.04 Pa. Chemical compositions and thicknesses of the composite films were determined by scanning electron microscope JSM-6400. Thicknesses of the films were 250 ± 0.350 nm.

Spectrum analyzer (INSTEK GSP-7830), sweep-frequency generator and element of coaxial cable were used to study the spectra of the complex conductivity of the magnetic composite films in RF and microwave ranges. The films were put in the rupture of center conductor of coaxial cable. The coaxial cable was connected with the sweep-frequency generator and the spectrum analyzer. The spectra of the power dissipation of the current in the films were measured and the spectra of the complex conductivity were investigated. All measurements were obtained at room temperature. Usable frequency range was from 100 kHz to 3 GHz. The magnetic spectra were measured by Q-meter E4-11 at room temperature in the 50-160 MHz range with amplitude of alternating field 1 mOe.

It has been determined that the real part of the magnetic permeability μ' does not depend on the frequency before the percolation threshold in the composite films. It can be explained that films have super paramagnetic state and interaction energy of magnetic particles was less than heat energy. μ' increases proportionally the frequency after the percolation threshold. It decreases with increasing of concentration of the magnetic metal phase. The imaginary part of the magnetic permeability μ'' decreases with increasing of the frequency before the percolation threshold. It increases proportionally square root to frequency after the percolation threshold. μ'' increases with increasing of concentration of the magnetic metal phase. The complex conductivity increases with increasing of the frequency and decreases with increasing of the magnetic metal phase before the percolation threshold, because magnetic losses are small and the complex conductivity increases between the metal particles in insulating matrix. The complex conductivity decreases proportional the square root to frequency after the percolation threshold. Behavior of the complex conductivity was connected with skin effect. Model of the composite films has been obtained to explain behavior of spectra of the complex conductivity.

The work was supported by RFBR (№ 13-02-01401).

2PO-M-8

THE TEMPERATURE DEPENDENCE OF THE SPIN-WAVE RESONANCE MODE LINE WIDTHS IN THREE-LAYER MAGNETIC FILM

Zyuzin A.M.¹, Bazhanov A.G.¹

¹ Mordovia State University, Saransk, Russia
bajanovag@mail.ru

The effect of temperature on the line width of the spin-wave modes in two series of three-layer iron garnet films under the dominant mechanism of action of a dissipative spin pinning in the parallel orientation of the external magnetic field \vec{H} relative to the film plane. In the samples of the first series of the middle layer $Y_{2.98}Sm_{0.02}Fe_5O_{12}$ is a layer of excitation of standing harmonic modes (SW-modes), the lower and upper layers have a composition $(SmEr)_3Fe_5O_{12}$ and layers were spin pinning. In the second series of samples, the middle and upper layers were the same as in the first series of samples, and the lower layer had a composition $(YSmLuCa)_3(FeGe)_5O_{12}$. In both sets of samples at room temperature was carried symmetric spin pinning. As can be seen from the experiment, there is a significant difference in the behavior of the line widths SW-modes $2\Delta H_n(T)$ in the first and second series of the samples. In the first series of samples in a temperature range from 20 to 200⁰C $2\Delta H_n$ is practically independent from temperature. Number of SW-modes in this temperature range does not change. At higher temperatures, the number and width of the lines of all SW-modes decrease monotonically. Near the Curie point $T_K \approx 270$ ⁰C of the excitation and pinning layers the SW-modes cease to be excited in the spectrum. Dependence $2\Delta H_n(T)$ on the second series of samples a sharp reduction near the temperature $T \approx 150$ ⁰C. Thus the number of SW-modes in the spectrum on the contrary increased about two times. In this paper we calculated the SW-mode line width $2\Delta H_n$, taking into account the impact on $2\Delta H_n$ the field of spin-wave attenuation in the pinning layer [1]. The calculation showed that the observed behavior $2\Delta H_n(T)$ is due to several factors. In the first series of samples availability portions where the $2\Delta H_n$ is virtually independent of T due on one hand to decrease the damping parameter in the layer, and on the other hand, increasing the penetration depth of the spin waves in this layer. Marked decrease $2\Delta H_n$ at temperatures above 200⁰C ~ associated with the predominant influence of the first factor. The sharp decrease in the line widths in the second series of samples near the temperature 150 ⁰C due to the fact that the lower pinning layer has a Curie temperature $T_K \approx 150$ ⁰C. At this point, designated layer becomes paramagnetic state and securing spins on one of the borders completely disappears. As a result, the contribution to the line width of this layer decreases sharply and the line width is reduced accordingly. Reduction of fixing on one of the boundaries of the three-layer film results in that the number of SW-modes increases about twice.

[1] A.M. Zyuzin, A.G. Bazhanov. *Phys. Stat. Sol.*, **42** (2000) 1279-1286.

2PO-M-9

STUDY OF THE TORQUE ACTING ON THE MAGNETIZATION DURING 90° PULSED REVERSAL PROCESS IN FERRITE-GARNET FILMS WITH IN-PLANE ANISOTROPY

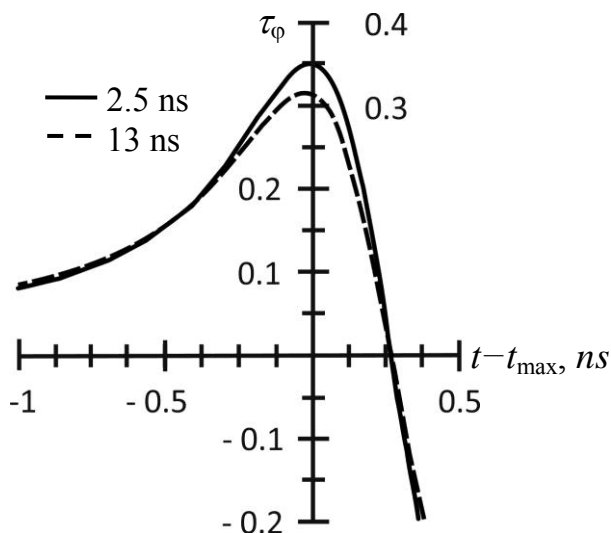
Kolotov O.S.¹, Matyunin A.V.¹, Nikoladze G.M.¹, Polyakov P.A.¹

¹ MSU, Faculty of Physics, 1-2 Leninskiye Gory, GSP-1, Moscow, 119991, Russia
physphak@mail.ru

To calculate the torque acting on the magnetization vector during the process of 90° pulsed magnetization in real ferrite-garnet films, in which besides in-plane anisotropy biaxial anisotropy is present, the method based on the analysis of the trajectory of an operating point is used. As the coordinates of the operating point the azimuthal angle φ and the torque component T_m caused by the pulsed magnetizing field are used [1]. It has been shown that the exciting of the nonlinear magnetization oscillations takes place within the narrow time interval $\Delta t \leq 1$ ns including the moment $t = t_{\max}$, at which the maximum of the resulting torque T_φ is observed. Here the normalized value of the torque $\tau_\varphi = T_\varphi / (M_S \cdot H_{K2})$ is used, where M_S is the saturation magnetization, H_{K2} is the biaxial anisotropy field.

It has been also found that within the time interval Δt the shape of the time dependence of the resulting torque is weakly depended on the pulse front duration τ_f . To provide a more precise comparison of the time torque dependences obtained for different values of τ_f we used the value $t - t_{\max}$ as the argument of these dependences. Figure shows the two curves $\tau_\varphi(t - t_{\max})$ calculated respectively for $\tau_f = 2.5$ ns ($t_{\max} = 3.8$ ns) and $\tau_f = 13$ ns ($t_{\max} = 14.6$ ns). It is seen that a rather significant increase in the front duration should result only in a slight decrease in the values of the torque τ_φ . Figure also shows that within the time interval under consideration both curves have similar forms. Thus the change in τ_f should not result in any essential change in the spectral composition of the function $\tau_\varphi(t)$. These results account for the slight dependence of the magnetization oscillation intensity on the front duration. This feature of real ferrite-garnet films was found experimentally in [2].

The performed analysis has also shown that with decrease in the value of τ_f to 0.3 – 2.5 ns there should appear an additional maximum on the initial part of the curve $\tau_\varphi(t)$. This appearance has been confirmed by the observation of the experimental magnetizing signals.



[1] O.S. Kolotov, A.V. Matyunin, G.M. Nikoladze, P.A. Polyakov, *Izvestiya RAN. Seriya fizicheskaya*, **77** (2013) 1429-1431.

[2] E.I. Il'yashenko, O.S. Kolotov, A.V. Matyunin, O.A. Mironets, *Physics of the Solid State*, **48** (2006) 297-302.

2PO-M-10

RESEARCH OF NONLINEAR EXCITATION OF HIGH-FREQUENCY AND MICROWAVE MAGNETOELASTIC OSCILLATIONS IN THE THREE-LAYER STRUCTURE

Dianov M.Yu.¹, Vlasov V.S.¹, Kotov L.N.¹, Shavrov V.G.², Shcheglov V.I.²

¹ Syktyvkar State University, Syktyvkar, Russia

² Institute of Radio Engineering and Electronics of RAS, Moscow, Russia
Dianovmy@yandex.ru

The work is devoted to study of elastic RF and microwave oscillations excitation in a three-layer structure in the most general nonlinear case without limit of the exciting signal power. The geometry of the problem was following. The external dc magnetic field was directed perpendicularly to the plane of multilayer plate and alternating circularly polarized magnetic field was directed in the plane of the plate. Elastic properties of all the layers were the same. However, the layers have different magnetic properties, cubic crystallographic symmetry and thickness. To describe the magnetoelastic oscillations we used Landau-Lifshitz equation in the form of Gilbert and the equation for the elastic displacements. The solution for elastic displacements was a sum of linear functions of the coordinate and the deviation from this linear function. The solution was sought in the form of an expansion in a series of functions that are solutions of the homogeneous equation with homogeneous boundary conditions. Coupling between the layers in our model was carried out by the zero terms of Fourier series. For simplicity we consider only zero and the first terms in the decomposition. The system for describing of excitation of magnetoelastic oscillations contains 11 first-order equations for the first and the third layer, and 7 first-order equations for the second (central) layer. We have 7 equations for the second layer because 2 equations for zero terms in Fourier decomposition are absent.

The resulting system of equations was solved numerically by the 4-5 orders Runge-Kutta method. For the calculations the parameters of the yttrium iron garnet were used. The curves of the magnetization components dependence on time were plotted. At the same time, the parameters of the material were chosen as with the absence of magnetoelastic coupling in the case of linear ferromagnetic resonance and the first mode of elastic oscillations eigen frequencies were equal. Plotted graphs were compared with the similar cases for a single-layer and double-layer structures. The calculation models for single-layer and double-layer structures were described earlier in works [1, 2]. For comparison of the three-layer and the single layer structures the three-layer structure thicknesses are chosen arbitrarily and the thicknesses of all layers are equal to the thickness of single layer structure. In the simulation almost the same data for the three-layer and single-layer structures were obtained which means a good agreement with the one-layer model. Also the resonance curves were plotted for the cases of linear and nonlinear oscillations. The excitation of elastic oscillations on combination frequencies of individual layers was investigated. The time dependences of the magnetization and the elastic displacements were plotted for this case.

The work was supported by RFBR (grants №12-02-01035-a).

[1] V.S. Vlasov, L.N. Kotov, V.G. Shavrov, V.I. Shcheglov, *J. Comm. Tech. El.*, **54** (2009) 821-832.

[2] V.S. Vlasov, V.G. Shavrov, V.I. Shcheglov, *Journal of Radio Electronics*, **2** (2013). URL: <http://jre.cplire.ru/jre/feb13/10/text.pdf>.

2PO-M-11

HYPER SOUND EXCITATION IN THE FERRITE PLATE BY IMPULSE MAGNETIZATION REVERSAL

*Vlasov V.S.¹, Pleshev D.A.², Kotov L.N.¹, Shavrov V.G.³, Shcheglov V.I.³, Asadullin F.F.²,
Poleshchikov S.M.²*

¹ Syktyvkar State University, Syktyvkar, Russia

² Saint-Petersburg state forest technical university named after S.M. Kirov, St-Petersburg, Russia

³ Institute of Radioengineering and Electronics of the Russian Academy of Sciences, Moscow,
Russia

vlasovv78@mail.ru

Dynamic behavior of a magnetization vector on the reorientation transition in normal magnetized ferrite plate from the direction antiparallel to the dc magnetic field through the plane of the plate to the parallel direction was considered. The plate has magnetoelastic properties. A change in orientation of the magnetization vector is accompanied by its precession around the field direction. In this case before passing through the plane of the plate of the magnetization vector the precession frequency is determined by the sum of the applied field and the demagnetization field, and after passing through the plane - their diminution. Changing orientation of magnetization due to magnetostriction causes the excitation of intense hypersound elastic oscillations whose frequency corresponds to the frequency of magnetization vector precession in a switching magnetic field.

The computation of the magnetic and elastic oscillations amplitudes was performed on the base of the system of ordinary differential equations obtained in the paper [1]. The system of the equations was solved numerically by the Runge-Kutta method.

The studies showed that the amplitude of elastic oscillations in the orientation of the magnetization vector beyond from the plane of the plate is proportional to the amplitude of the precession and passing through the plane magnetization is equal to zero. Rotation of the magnetization vector and development of elastic oscillations, does not begin immediately at the switching field time but with the delay time. The delay time is correlated by with direct dependence to the relaxation time of magnetic oscillations and with the inverse dependence with the magnitude of the initial deviation of magnetization vector with the direction of the dc field. At a small value of elastic oscillation damping parameter development can also be delayed relative to the development of magnetic oscillations defined by its relaxation time. The decrease in time both magnetic and elastic oscillations after field switching occurs with time delay caused by the decrease of force, which rotates the magnetization vector when the angle from dc field and magnetization vector decrease.

Two models are offered to explain the observed phenomena: empirical model describing the development of magnetic and elastic oscillations based on exponential approximation and vector model which is based on the mechanism of quasistatic rotation of the magnetization vector relative to the field direction.

In case of yttrium iron garnet use the amplitude excited hypersound elastic oscillations in the microwave range can rise up to 10^{-9} cm, which exceeds the level corresponding to their traditional nonlinear excitations two times as large, and the level of linear excitation by more than three to four orders of magnitude [1].

The work is supported by Russian Foundation of Basic Research (grant №12-02-01035-a).

[1] V.S. Vlasov, L.N. Kotov, V.G. Shavrov, V.I. Shcheglov, *J. Comm. Tech. El.*, **54** (2009) 821-832.

2PO-M-12

MICROWAVE MAGNETIC INDUCTION STRUCTURE OF THE SURFACE SPIN WAVE IN FERRITE FILM.

Lock E.H.¹

¹ Kotel'nikov Institute of Radio Engineering and Electronics of Russian Academy of Sciences (Fryazino branch), 141190, Vvedensky sq.1, Fryazino, Moscow region, Russia
edwin@ms.ire.rssi.ru

Surface spin wave, named also magnetostatic surface wave, were investigated firstly in magnetostatic approximation [1]. It may seem that all properties of this wave are well known. However, the structure of the microwave magnetic induction \mathbf{b} isn't studied yet.

Calculations, based on Maxwell's equations, show that the vector lines of magnetic induction represent vortices localized near both surfaces of the ferrite film (Fig. 1a), while the vector lines of the magnetic field, calculated earlier [1, 2] don't form a vortex structure (Fig. 1b). Calculations were carried out for the next parameters: $H_0 = 300$ Oe, $4\pi M_0 = 1750$ Gs, $\varepsilon = 15$, $s = 10$ μm , $k = 1000$ cm^{-1} , $\lambda = 2\pi/k$, $f = 3167$ MHz. It should be noted that inside the ferrite film the vectors \mathbf{b} and \mathbf{h} are directed oppositely in general, while \mathbf{b} and \mathbf{h} fields structures coincide in vacuum half-spaces surrounding ferrite film (see Fig. 1). It is also evidently, that in accordance with Maxwell's equations magnetic induction vortices must create a microwave electric field \mathbf{e}_z : the upper-left and lower-right vortices in Fig. 1a create the field \mathbf{e}_z , directed along z axis (in accordance with right-hand screw rule), and the lower-left and upper-right vortices in Fig. 1a create the field \mathbf{e}_z , directed opposite to z axis (z -axis is directed from the reader to the plane of Fig.1). Mention must be made that, calculations of microwave magnetic induction structure agree with obtained previously calculations of the microwave electric field structure for spin wave. In particular, it was found in [3, 4], that dependence of electric field amplitude \mathbf{e}_z has two maxima along x axis (normal to the film plane): maxima are localized on the film surfaces, one of them is higher than the other and their signs are opposite.

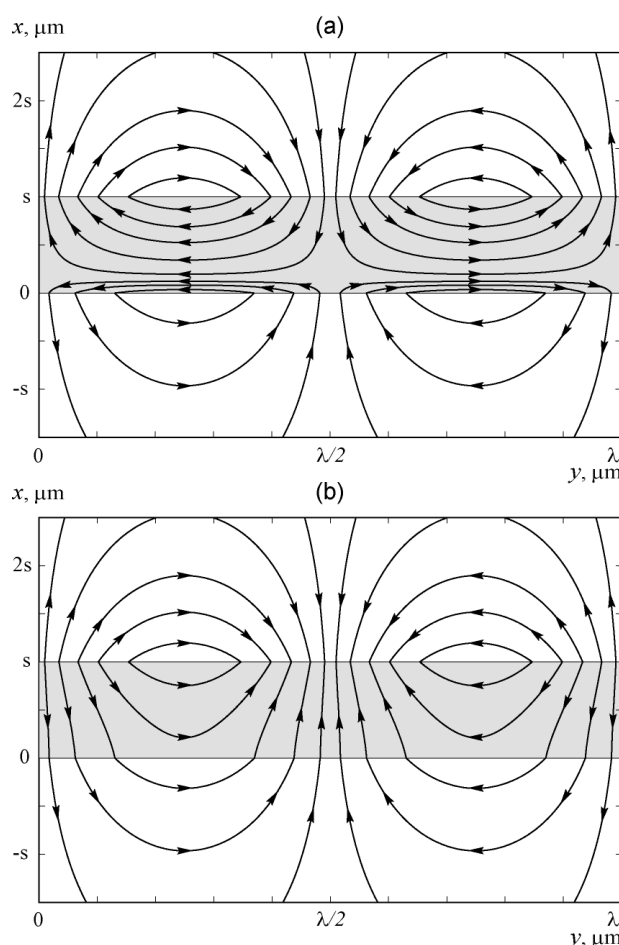


Fig. 1. Microwave magnetic induction \mathbf{b} (a) and magnetic field \mathbf{h} (b) structures for spin wave, propagated along y axis in tangentially magnetized ferrite film with thickness s . Magnetic bias field \mathbf{H}_0 is parallel to z axis.

[1] Damon R. W., Eshbach J. R. *J. Phys. Chem. Solids*, **19** (1961) 308 - 320.

[2] Gurevich A. G., Melkov G. A. *Magnetization Oscillations and Waves*. M.: Nauka (1994).

[3] Lokk E. G. *J. Comm. Techn. Electron.*, **50** (2005) 67-74.

[4] Vashkovsky A. V., Lock E. H. *Physics-USpekhi*, **54** (2011) 281 - 290.

2PO-M-13

FERROMAGNETIC RESONANCE IN AN ARRAYS OF MAGNETIC FeNi MICROSTRIPES

Skorohodov E.V.^{1,2}, Mironov V.L.^{1,2}, Vdovichev S.N.^{1,2}, Skopin E.V.², Budarin L.I.², Gorev R.V.¹

¹ Institute for physics of microstructures RAS, Nizhniy Novgorod, Russia

² Lobachevsky State University, Nizhniy Novgorod, Russia

evgeny@ipmras.ru

The significant efforts have been focused in recent years on the fundamental investigations of static and dynamic properties of ferromagnetic nanostructures because of their perspective applications including magnetic memory, data storage and logic devices [1]. One of a powerful technique for measuring the dynamic properties of magnetic structures is the ferromagnetic resonance (FMR) spectroscopy [2]. In our work we investigated the influence of magnetostatic interaction on ferromagnetic resonance spectra in arrays of rectangular microstripes FeNi. The arrays of one-layer (thickness 30-40 nm) and multilayer (thickness of magnetic layers 15 nm, thickness of non-magnetic layers 5 nm) ferromagnetic stripes with lateral dimensions 3000×500 nm were fabricated over an area 2×2 mm² on silicon substrate using electron-beam lithography and lift-off process. The ferromagnetic resonance spectra were investigated by EPR spectrometer Bruker EMXPlus-10/12. The frequency of microwave magnetic field was 9.5 GHz. The static magnetic field was changed up to 1.5 T.

We have investigated the variation of FMR spectrum depending on the arrangement and density of microstripe array. The typical scanning electron microscopy (SEM) images of microstripe arrays are presented in Fig. 1(a, b). As the example, the dependences of FMR amplitude (arbitrary units) on the value of an external uniform magnetic field for one-layer and two-layer stripes are presented in Fig. 1(c, d). The effect of nonuniform mode suppression due to magnetostatic interlayer interaction is clearly seen comparing Fig. 1c and Fig. 1d. The effects of magnetostatic interaction in the arrays of one-layer and multi-layer stripes are discussed.

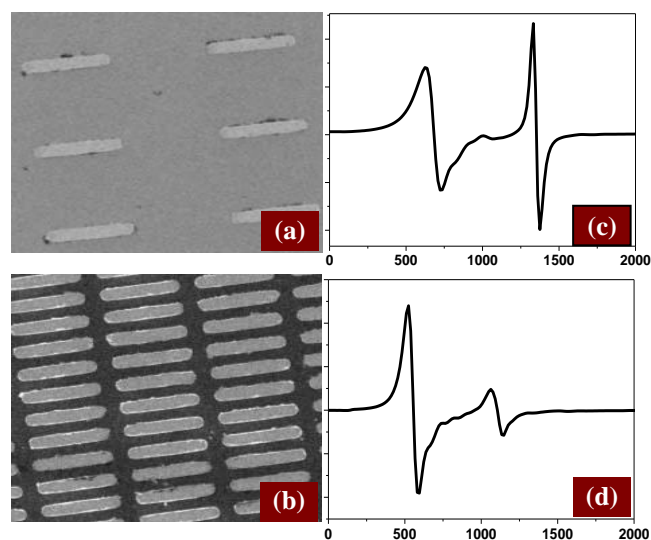


Fig. 1. (a,b) are SEM images of microstripes arrays. (c,d) are the FMR spectra for one-layer (c) and two-layer (d) microstripes arrays (the values of magnetic field are given in Oe).

This work was supported by the Russian Foundation for Basic Research, Presidium of RAS and The Ministry of Education and Science of Russian Federation.

[1] S. Tehrani, et al, *J. Appl. Phys.*, **85** 5822 (1999).

[2] X. Kou, et al, *Appl. Phys. Lett.*, **94** 112509 (2009).

2PO-M-14

SURFACE MODIFIED Ni NANOPARTICLES PRODUCED BY THE ELECTRICAL EXPLOSION OF WIRE

*Safronov A.P.^{1,2}, Kurlyandskaya G.V.^{2,3}, Bhagat S.M.⁴, Beketov I.V.^{1,2}, Murzakaev A.M.¹,
Volodina N.S.^{1,2}, Orue I.³, Larrañaga A.³*

¹ Institute of Electrophysics, RAS, Urals Branch, Ekaterinburg, Russia

² Ural Federal University, Ekaterinburg, Russia

³ University of the Basque Country UPV-EHU, Bilbao, Spain

⁴ University of Maryland, College Park, USA
galina@we.lc.ehu.es

Spherical nickel nanoparticles (MNPs) were prepared by the electric explosion of wire (EEW) [1]. The as-prepared MNPs were modified immediately after fabrication at room temperature in order to provide tunable surface properties with focus on the development of MNPs containing composites. Following modifiers were used: hexane (Ni-I), toluene (Ni-II) and the solution of polystyrene in toluene (Ni-III). In Ni-IV the surface covering consisted of carbon solution in Ni as a result of hydrocarbon injection. According to the X-ray diffraction data the average size of the MNPs was about 30-40 nm and unit cell parameters were close to 0.351 nm for all samples except N-IV. For Ni-IV core-shell structure was observed: shell with width of about 10 nm, the unit cell of 0.354 nm and core of 30 nm with the unit cell of 0.352 nm. The specific surface was determined by low temperature nitrogen adsorption: mean diameter of about 50 nm was obtained in all cases under consideration. Transmission electron microscopy was performed using JEOL JEM2100 microscope. Magnetic measurements at room and cryogenic temperatures were done by VSM and a SQUID: the highest saturation magnetization of 52 emu/g (at room temperature) was observed for Ni-I MNPs. Microwave resonant (FMR) and zero-field absorption was studied by the microwave techniques based on usage of a conventional homodyne spectrometer for the frequency of about 9 GHz. All MNPs exhibited a sizable loss at a zero-field. The position of the FMR corresponds well to that one expected for spherical nickel MNPs ($H_{\text{res}} \approx 2.7$ kOe) in all cases except N-IV. For N-IV case $H_{\text{res}} \approx 2.4$ kOe. The observed shortfall of about 0.3 kOe can be understood by invoking stresses created by the carbon containing shell.

This work was supported by SAIOTEK-REMASEN grant and by a grant CRDF – UB RAS RUE2-7103-EK-13 from the U.S. Civilian Research & Development Foundation (CRDF Global) with funding from the United States Department of State. The opinions, findings and conclusions stated herein are those of the author(s) and do not necessarily reflect those of CRDF Global or the United States Department of State. Selected measurements were done in UPV-EHU SGIKER Services.

[1] G.V. Kurlyandskaya, S.M. Bhagat, A.P. Safronov, I.V. Beketov, A. Larrañaga, *AIP Advances*, **1** (2011) 042122.

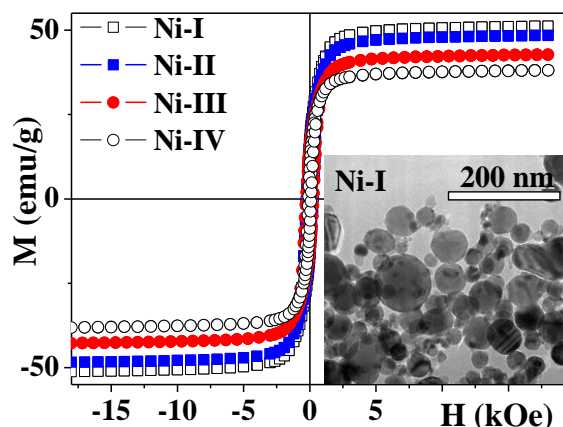


Fig. 1. Hysteresis loops and TEM image of Ni MNPs measured at room temperature, inset show Ni-I MNPs obtained by the electrical explosion of wire method.

2PO-M-15

HIGH-FREQUENCY PROPERTIES OF MULTILAYER SYSTEMS BASED ON THE $(\text{Co}_{41}\text{Fe}_{39}\text{B}_{20})_x(\text{SiO}_2)_{100-x}$ AND $(\text{Co}_{45}\text{Fe}_{45}\text{Zr}_{10})_x(\text{Al}_2\text{O}_3)_{100-x}$ NANOCOMPOSITES

Al Azzavi H.C.M.¹, Kalinin Yu.E.¹, Sitnikov A.V.¹, Tarasova O.S.¹

¹ Voronezh State Technical University, 394026 Voronezh, Moscovski prospekt, 14 oksanchik2603@mail.ru

In this paper we consider the possibility of changing the growth of perpendicular anisotropy composites $(\text{Co}_{41}\text{Fe}_{39}\text{B}_{20})_x(\text{SiO}_2)_{100-x}$ and $(\text{Co}_{45}\text{Fe}_{45}\text{Zr}_{10})_x(\text{Al}_2\text{O}_3)_{100-x}$ due to formation of the multilayer structure and the impact of structural changes on the magnetic properties of the films.

Ion-beam sputtering a composite target were synthesized samples of 3D composites $(\text{Co}_{41}\text{Fe}_{39}\text{B}_{20})_x(\text{SiO}_2)_{100-x}$, $(\text{Co}_{45}\text{Fe}_{45}\text{Zr}_{10})_x(\text{Al}_2\text{O}_3)_{100-x}$ and multilayer structures $\{[(\text{Co}_{41}\text{Fe}_{39}\text{B}_{20})_x(\text{SiO}_2)_{100-x}]/[(\text{Co}_{41}\text{Fe}_{39}\text{B}_{20})_x(\text{SiO}_2)_{100-x}+\text{O}_2]\}_{178}$, $\{[(\text{Co}_{45}\text{Fe}_{45}\text{Zr}_{10})_x(\text{Al}_2\text{O}_3)_{100-x}]/[(\text{Co}_{45}\text{Fe}_{45}\text{Zr}_{10})_x(\text{Al}_2\text{O}_3)_{100-x}+\text{O}_2]\}_{300}$. The multilayers structure of alternating layers composite were obtained under argon, and the composite was obtained under argon and oxygen. The layer thickness is several nanometers.

Changes magnetostatic properties of films and multilayer composites of heterogeneous structures affect the frequency dependence of the real (μ') and imaginary (μ'') parts of the complex magnetic permeability.

Composite $(\text{Co}_{41}\text{Fe}_{39}\text{B}_{20})_{66,2}(\text{SiO}_2)_{33,8}$ has a broad peak dependence of $\mu''(f)$. The maximum value of μ'' is observed at a frequency of 500 - 600 MHz (f_{res}). The real part of the complex magnetic permeability is decreases in the frequency range 500-1300 MHz. For composite films $(\text{Co}_{45}\text{Fe}_{45}\text{Zr}_{10})_{61}(\text{Al}_2\text{O}_3)_{39}$ $f_{\text{res}} \approx 600$ MHz. However, the composite $(\text{Co}_{45}\text{Fe}_{45}\text{Zr}_{10})_{61}(\text{Al}_2\text{O}_3)_{39}$ has low values μ' and μ'' for frequencies below f_{res} . A considerable width of the maximum $\mu''(f)$ due to the dispersion of local magnetic anisotropy field, for 3D composites.

For a film $\{[(\text{Co}_{41}\text{Fe}_{39}\text{B}_{20})_{67,4}(\text{SiO}_2)_{32,6}]/[(\text{Co}_{41}\text{Fe}_{39}\text{B}_{20})_{67,4}(\text{SiO}_2)_{32,6}+\text{O}_2]\}_{178}$ value was $f_{\text{res}} \approx 2,5$ GHz, the magnitude $\mu' \approx 250$ for frequencies below f_{res} . For multilayer heterogeneous structure $\{[(\text{Co}_{45}\text{Fe}_{45}\text{Zr}_{10})_{61}(\text{Al}_2\text{O}_3)_{39}]/[(\text{Co}_{45}\text{Fe}_{45}\text{Zr}_{10})_{61}(\text{Al}_2\text{O}_3)_{39}+\text{O}_2]\}_{300}$ natural ferromagnetic resonance frequency was ~ 800 MHz, but the values of μ' and μ'' were increased substantially relative to 3D composite ($\mu' \approx 40$ for frequencies below f_{res} and $\mu''_{\text{max}} \approx 40$).

These results are showing that the new heterogeneous multilayer structure $\{[(\text{Co}_{41}\text{Fe}_{39}\text{B}_{20})_{60}(\text{SiO}_2)_{40}]/[(\text{Co}_{41}\text{Fe}_{39}\text{B}_{20})_{60}(\text{SiO}_2)_{40}+\text{O}_2]\}_{176}$ have a good high frequency magnetic properties for various practical applications.

This work was supported by RFBR (project number 13-02-97511-r_tsentr_a).

2PO-M-16

HIGH FREQUENCY ELECTRON SPIN RESONANCE IN $\text{Mn}_{1-x}\text{Fe}_x\text{Si}$

Demishev S.V.¹, Samarin A.N.¹, Semeno A.V.¹, Lobanova I.I.¹, Glushkov V.V.¹, Samarin N.A.¹,
Sluchanko N.E.¹, Grigoriev S.V.²

¹ Prokhorov General Physics Institute of RAS, Moscow, Russia

² Konstantinov Nuclear Physics Institute, Gatchina, Russia

sasha@lt.gpi.ru

We report results of the first systematic study of high frequency (60 GHz) low temperature (1.8–60 K) electron spin resonance (ESR) in $\text{Mn}_{1-x}\text{Fe}_x\text{Si}$ solid solutions in the concentration range $x < 0.3$. In the limit of weak magnetic field $B \rightarrow 0$ the T - x magnetic phase diagram of $\text{Mn}_{1-x}\text{Fe}_x\text{Si}$ is driven by two subsequent quantum phase transitions located at $x^* \sim 0.11$ and $x_c \sim 0.24$ [1]. First quantum critical point (QCP) x^* separates regions with long-range ($x < x^*$) and short range ($x > x^*$) magnetic orders, whereas the second QCP marks disappearance of any type of magnetic order and onset of the Griffiths-type singularity of the magnetic susceptibility [1]. The magnetic phase diagram of $\text{Mn}_{1-x}\text{Fe}_x\text{Si}$ in a magnetic field corresponding to ESR absorption maximum $B_{res} \sim 2$ T changes substantially (Fig. 1,a). Following technique suggested in [2], it is found that strong magnetic field suppresses phases with short range magnetic order and T - x magnetic phase diagram is formed by paramagnetic (P) and spin polarized (ferromagnetic) phases separated by well-defined transition temperature $T_{SP}(x)$. For studying of the ESR, we have used the original method which allows finding the full set of spectroscopic parameters including oscillating magnetization M_0 , g -factor and line width W [2,3]. Magnetic resonance in $\text{Mn}_{1-x}\text{Fe}_x\text{Si}$ is characterized by a strong broadening of the line width of x and for $x > x_c$ the ESR line becomes undetectable. At the same time, the parameter M_0 coincides with the static magnetization at the resonant field $M(B_{res})$ and g -factor equals $g = 1.95 \pm 0.02$ for any x and does not depend on temperature. Analysis of the $W(T)$ temperature dependence shows that except selected concentrations x^* and x_c line width scales as $W(T)/W(T_{SP}) = 1 + a \cdot (T - T_{SP})^2$ for $T > T_{SP}$ and $W(T)/W(T_{SP}) \approx \text{const}$ for $T < T_{SP}$ (Fig. 1,b). The deviations from the universal behavior demonstrate existence of anomalous spin relaxation at QCPs in $\text{Mn}_{1-x}\text{Fe}_x\text{Si}$ solid solutions. This work is supported by the Program of RAS “Strongly correlated electrons” and by RFBR grant 13-02-00160.

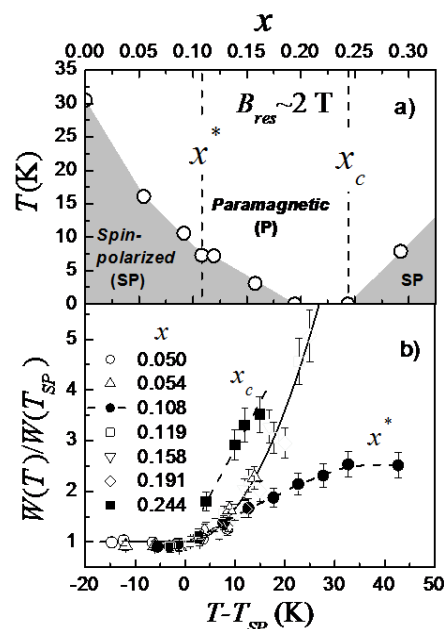


Fig. 1. Magnetic phase diagram (a) and scaling behavior of the ESR line width (b). Solid line in panel (b) corresponds to square dependence described in the text.

[1] S.V. Demishev, et al., *JETP Letters*, **98** (2013) 829-833.

[2] S.V. Demishev, et al., *Phys. Rev. B*, **85** (2012) 045131.

[3] S.V. Demishev, et al., *Phys. Rev. B*, **80** (2009) 245106.

2PO-M-17

FMR STUDY OF SPIN EXCITATIONS IN $\text{Cr}_{1/3}\text{NbS}_2$ HELIMAGNET

Mushenok F.B.¹

¹ Institute of Problems of Chemical Physics, Chernogolovka, Russia
mushenokf@gmail.com

Incommensurate magnetic structures are intriguing objects of the solid state physics. The pressing problem is the influence of the magnetic anisotropy on a magnetic phase diagram and a spectrum of the spin excitations. The aim of the present work is to establish how magnetocrystalline anisotropy influences on spin excitation in the chiral “easy-plane” helimagnet $\text{Cr}_{1/3}\text{NbS}_2$.

High frequency spin excitations were studied by ferromagnetic resonance (FMR) method [1]. At low temperature ($T < 50$ K) FMR spectra consist of two lines with different temperature dependences of resonance fields H_{res} (Fig. 1). The line I with “usual” ferromagnetic temperature dependence of resonance field corresponds to homogeneous ($q = 0$) magnetization precession in a helical phase. The resonance field of the line I is determined by uniaxial magnetocrystalline anisotropy K_2 .

The line II with “abnormal” temperature dependence of resonance field corresponds to the Goldstone mode with a wave factor $q = \pm Q$ (Q is wave vector of the modulated magnetic structure). The finite value of the Goldstone mode energy $q = \pm Q$ is due to magnetocrystalline anisotropy in basal ab plane. Unusual temperature dependence of the resonance field is explained by decreasing of anisotropy constant K_6 with temperature increasing. For the first time, it has been shown experimentally that effective excitation of the Goldstone mode is realized only when microwave magnetic field vector h is perpendicular to magnetic structure modulation vector Q .

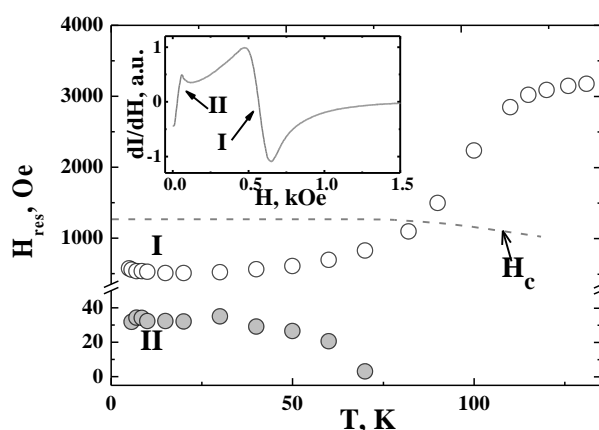


Figure 1. Temperature dependences of resonance fields of lines I and II for $\text{Cr}_{1/3}\text{NbS}_2$ single crystal, $H \perp c$ ($\perp Q$). Critical field of transition to ferromagnetic state is shown by dashed line. FMR spectra at $T = 5$ K is shown on inset.

Support by grant of President of Russia MK-1474.2014.3 is acknowledged.

[1] F.B. Mushenok, *J.Eur. Phys. Journ. B*, **86** (2013) 1-4.

2PO-M-18

STATIK AND MICROWAVE MAGNETIC PROPERTIES OF NiCoZn SPINEL FERRITES

Stergiou C.A.¹, Zezyulina P.A.², Rozanov K.N.²

¹ Lab. of Inorganic Materials, Centre for Research and Technology Hellas, Thessaloniki, Greece

² Inst. for Theoretical and Appl. Electromagn., Russian Acad. of Sci., Moscow, Russian Federation
stergiou@cperi.certh.gr

In this work we have studied the effect of heat treatment on the magnetic properties of NiCoZn ferrites, with a view to high frequency applications.

To this end, we have synthesized samples of spinel ferrite structure with the basic composition $\text{Ni}_{0.25}\text{Co}_{0.50}\text{Zn}_{0.25}\text{Fe}_2\text{O}_4$ through the conventional solid-state reaction method. This includes the calcination of the precursor mixtures followed by an intermediate ball-milling step. The prefired powders were then pressed to the proper shape and finally sintered in air.

Deliberate differences in microstructure have been attempted by applying different temperatures during prefiring or sintering processes. The morphological variations have been verified with observation by means of SEM. However, the analysis of the respective powder samples with X-ray diffraction has highlighted the formation of single phase specimens in all cases.

The static magnetic properties, saturation magnetization M_S and coercive field H_C , of the prepared ferrite materials were recorded with a vibrating sample magnetometer. Small ring samples were used for the electromagnetic characterization in the frequency range from 10 MHz to 20 GHz. This has allowed us to investigate the complex permeability $\mu^*(f)$ dispersion spectra, where two distinct mechanisms seem to occur. The reasons for these dynamic effects are discussed in the presentation and associated with the samples microstructure and dc magnetic properties.

2PO-M-19

ESR PROBING OF THE SYMMETRY OF Ce^{3+} STATE IN ANTIFERROQUADROPOLAR PHASE OF CeB_6

Semeno A.V.¹, Gilmanov M.I.¹, Samarin A.N.¹, Filipov V.², Shitsevalova N.Yu.², Demishev S.V.¹

¹ Prokhorov General Physics Institute RAS, Moscow, Russia

² Frantsevich Institute for Problems of Materials Science NASU, Kiev, Ukraine

semeno@lt.gpi.ru

The recent discovery of electron spin resonance (ESR) in heavy fermion compound YRh_2Si_2 [1] resulted in intensive study of the origin of ESR in Kondo systems. The main reason of the interest is that the basic physical considerations contradict to the possibility of the observation of a resonance behavior in the corresponding group of materials. In contrast to other studied compounds where ferromagnetic correlations dominate, CeB_6 is antiferromagnetic and the observation of ESR in it [2] requires a separate theoretical explanation [3]. Here we present high-frequency (60 GHz) ESR measurements of heavy fermion system CeB_6 provided for high-symmetry directions [100], [110] and [111] (fig.1). It's found that for directions [110] and [111] g -factors coincide ($g=1.6$) while for [100] g -factor value is $g=1.74$. This experimental result contradicts to theoretical calculation done for Γ_8 state of Ce^{3+} ion [3] both in absolute g -factor values and in their anisotropy. From the other hand ESR results corresponds very well to CeB_6 in antiferroquadrupolar phase magnetization data [4].

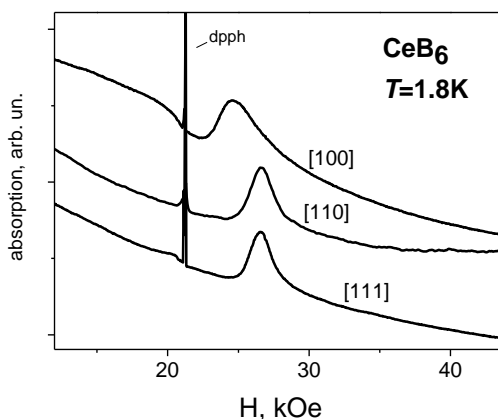


Fig. 1. ESR spectra of CeB_6 taken for three directions of magnetic field.

Support by RFBR (14-02-00800) is acknowledged.

- [1] J. Sichelschmidt et. al., *Phys.Rev.Lett.*, **91** (2003) 156401.
- [2] S.V. Demishev et. al., *Phys.Rev.B*, **80** (2009) 245106.
- [3] P. Schlottmann, *Phys.Rev.B*, **86** (2012) 075135.
- [4] M. Kawakami et.al., *Solid State Comm.*, **36** (1980) 435-439.

3 July

Thursday

09:30-11:00

plenary lectures

3PL-A

3PL-A-1

STRUCTURE AND COMPOSITION DRIVEN FUNCTIONALITY IN MAGNETIC NANOPARTICLES

Farle Michael

Center of Nanointegration Duisburg-Essen (CENIDE)
Faculty of Physics, University of Duisburg-Essen, 47057 Duisburg, Germany

Magnetism in structures with dimensions on the few - nanometer scale have been the center of many investigations ranging from topics in spin-torque and spin-injection dynamics and interactions in biomedical applications to the creation of new types of hard, soft or multi-functionalized materials. Such nanostructured “building blocks” offer new exciting possibilities to create new artificial materials. In biological and medical technologies magnetic hybrid or functionalized particles find applications in site-targeted therapy, diagnosis, cell separation and water purification. While most of this work does not require a detailed understanding of the intrinsic magnetism of the nanoparticle, future nanotechnological devices based on *one* single nanoparticle require the knowledge of local crystal as well as of the electronic and magnetic structure and surface composition and their induced changes when interacting with the environment.

The hysteresis and magnitude of the magnetization of a single ferro- (superpara-) magnetic nanoparticle is determined by its morphology, shape, composition, and crystal structure [1,2]. In nanoparticles competing energies originating from strain, chemistry, surface and defects change their relative importance and new structures become stable or metastable. Such structures can stabilize magnetic properties which cannot be achieved in volume materials and open new routes to tailoring magnetism for innovations in energy related materials (Rare-Earth free permanent magnets) and processes (spin logic) as well as in biomedical applications. In this talk I will review some examples illustrating the sensitivity of magnetic properties to strain, surface and also intraparticle interface effects between surface (shell) layers and the core: 1) Tuning magnetism in Co nanoparticles due to the formation of oxidic shells [3,4] and by light. 2) The ageing effects in FeAg dumbbell particles [5], 3) Strain and surface effects leading to a loss of hard-magnetic properties in bimetallic FePt nanoparticles[6,7]. It is demonstrated that many “surprising” properties reported in nanoparticles can be simply understood by referring to crystal field theory.

Work performed within EU- networks SyntOrbMag, REFreePerMag, IMAGINE and DFG,SFB 445.

- [1] C. Antoniak, et al., *Intrinsic Magnetism and Collective Magnetic Properties of Size-Selected Nanoparticles* in A. Lorke et al. (eds.), *Nanoparticles from the Gas Phase, NanoScience and Technology*, p. 273, © Springer-Verlag Berlin Heidelberg 2012.
- [2] M. E. Gruner, G. Rollmann, P. Entel, and M. Farle, *Phys. Rev. Lett.* **100** (2008) 087203.
- [3] U. Wiedwald, et al., *ChemPhysChem*, **6** (2005) 2522.
- [4] N. Fontaina-Troitano et al., *Nanoletters*, **14** (2014) 640.
- [5] A. Elsukova, et al. *Phys. Status Solidi A*, **208**(2011)2437–2442 .
- [6] Rongming Wang, et al, *Phys. Rev. Lett.*, **100** (2008) 017205.
- [7] Zi-An Li et al., *Phys. Rev. B*, **89** (2014) 161406(R) .

3PL-A-2

MAGNETIC MICROPARTICLES IN SOFT MATRICES: IDEAS, EXAMPLES AND MODELS

Raikher Yu.L.¹

¹ Institute of Continuous Media Mechanics, Ural Branch of RAS, Perm, Russia
Corresponding author: raikher@icmm.ru

Soft polymeric networks and gels, when filled with fine magnetic particles turn into smart materials, which combine equilibrium elasticity with a strong response to magnetic fields of moderate (~ 1 kOe) strength. High magneto-mechanical sensitivity of these composites—we generally term them “soft magnetic elastomers” (SMEs)—makes them attractive for developing unique devices and techniques. This calls for reliable models of the behavior of SME elements under mechanical loads and magnetic fields. The natural way to do so is to reduce full theory to a set of a few continuum magneto-mechanical equations to be solved for any particular case.

To the general framework comprising the conservation laws, theory of elasticity, and Maxwell equations, one has to add the equations of state, which specify the material properties of a particular SME. These relations imply the knowledge of the composite reaction at mesoscopic level. The latter means treating a SME as a heterogeneous medium: a viscoelastic matrix, where the particles are embedded in and linked to. A magnetic field, changing the interparticle forces, makes the particles to move. This arises elastic stresses in the matrix, forcing the sample to find its equilibrium by way of macroscopic deformation.

At the scale of interparticle distances the non-uniformity of the applied field does not matter, but essential is the short-range spatial distribution of the local field inside the assembly of magnetized particles. The works reviewed in the talk deal right with this fundamental issue.

Two types of problems are highlighted. First is the analytical / numerical modeling of the particle displacements under application of a uniform field. It turns out that short-range spatial order strongly affects both small- and large-scale magneto-mechanical behavior of SMEs. For example, a SME filled with isolated particles shrinks under the action of a field, while under the same field a SME with aggregated particles elongates.

The problems of another type concerns modification of the point dipole-dipole potential widely used to describe the interparticle interaction in SMEs. The point is that the filler phase in most popular polymeric SMEs is formed by magnetically soft microparticles, e.g. iron carbonyl. These particles, when positioned at close distances (of the order of their diameter), magnetize each other non-uniformly. When this is accounted for by using high-order multipole expansions, the resulting interparticle forces differ greatly from those rendered by the standard approach. In particular, the balance between the attraction / repulsion forces changes making attraction to considerably dominate. This fact has important consequences for the theory of SMEs.

Support by RFBR grants # 13-01-96056 and 14-02-96003, Ural Branch of RAS Programme #10 (12-P-01-108) and project MIG S26/617 from Ministry of Education and Science of Perm Region is acknowledged.

3 July

Thursday

11:30-13:30

oral session

3OR-A

**“Spintronics and
Magnetotransport”**

3OR-A-1

ZERO-FIELD SPIN TRANSFER OSCILLATORS COMBINING IN-PLANE AND OUT-OF-PLANE MAGNETIZED FREE LAYERS

Fowley C.¹, Sluka V.¹, Bernert K.^{1,2}, Lindner J.¹, Fassbender J.^{1,3}, Rippard W.H.⁴, Pufall M.R.⁴, Russek S. E.⁴, Deac A.M.¹

¹ Helmholtz-Zentrum Dresden-Rossendorf, 01328 Dresden, Germany

² Institute for Materials Science, TU Dresden, 01069 Dresden, Germany

³ Institute for Physics of Solids, TU Dresden, 01069 Dresden, Germany

⁴ National Institute of Standards and Technology, Boulder, CO 80305, U.S.A.

c.fowley@hzdr.de

Excited magnetization dynamics in a spin-valve device consisting of an in-plane polarizer and an out-of-plane free layer were studied numerically. Such devices hold promise for nanoscale wireless transmitters operating at gigahertz frequencies, compatible with current technologies [1]. We solve the Landau Lifschitz-Gilbert-Slonczewski equation taking into account the spin-transfer-torque asymmetry.

This asymmetry is directly responsible for the appearance of excited dynamics in this specific geometry as it leads to a *net* spin transfer torque over one precession cycle. Unfortunately, when the free layer lacks any in-plane anisotropy components, i.e. is circular in shape and possesses purely uni-axial perpendicular magnetic anisotropy, a finite external field is required to generate steady-state dynamics, in agreement with previous reports[2][3].

We demonstrate that this constraint can be removed and precession can be stabilized in zero applied field by introducing an additional in-plane anisotropy axis, in this case an elongation of the free layer in the direction of the injected spin polarized current. Moreover, the in-plane anisotropy offers an additional degree of freedom for tuning the frequency response of the device[4].

The shape anisotropy introduces a variable in-plane magnetic field whose direction is dependent on the exact location of the magnetisation of the free layer around the precession trajectory. The field induced by the shape anisotropy is sufficient to balance the action of the spin transfer torque and leads to steady state precession in suitably shaped devices. The frequency dependence, frequency spectra as well as a selected precession orbit for a 90nmx80nm free layer at zero applied field are shown in the figure to the right.

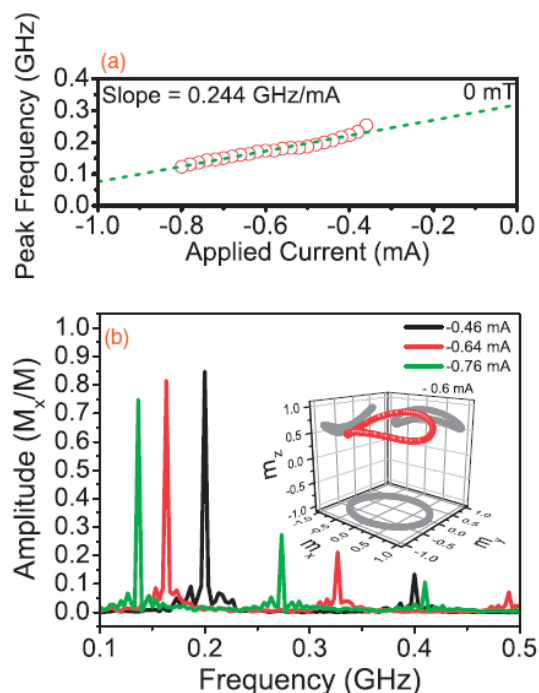
Our results show that the use of an intrinsic shape anisotropy is beneficial for spin transfer oscillators in order to achieve consistent high-power, zero-field, out-of plane precessional states without any initial magnetization direction dependence.

[1] S. I. Kiselev et al., *Nature* **425**, 380 (2003).

[2] W. H. Rippard et al., *Phys. Rev. B* **81**, 014426 (2010).

[3] S. M. Mohseni et al., *Phys. Status Solidi: Rapid Res. Lett.* **5**, 432 (2011).

[4] C. Fowley et al., *Applied Physics Express* **7**, 043001 (2014).



3OR-A-2

SPIN POLARONS AND COLOSSAL MAGNETORESISTANCE IN Ca-DOPED EuB₆

Glushkov V.V.^{1,2}, *Anisimov M.A.*¹, *Baybakov R.F.*³, *Bogach A.V.*¹, *Demishev S.V.*¹, *Filipov V.B.*⁴,
*Flachbart K.*⁵, *Gabáni S.*⁵, *Ivanov V.Yu.*¹, *Kuznetsov A.V.*³, *Levchenko A.V.*⁴, *Sluchanko N.E.*¹

¹ Prokhorov General Physics Institute of RAS, Moscow, Russia

² Moscow Institute of Physics and Technology, Dolgoprudny, Moscow Region, Russia

³ National Research Nuclear University "MEPhI", Moscow, Russia

⁴ Frantsevich Institute for Problems of Materials Science NASU, Kiev, Ukraine

⁵ Institute of Experimental Physics, Slovak Academy of Sciences, Košice, Slovak Republic
glushkov@lt.gpi.ru

Magnetic scattering of itinerant electrons from spin fluctuations is suggested to be responsible for large colossal magnetoresistance (CMR) of manganese pyrochlores and doped magnetic semiconductors [1-2]. In these low-density electron systems ($k_F a \ll 1$, k_F – the Fermi wave vector, a – the lattice parameter) the concentration of charge carriers n defines low-field magnetoresistance near Curie temperature ($T > T_C$): $-\Delta\rho/\rho = C(M/M_0)^2$, $C \sim n^{-2/3}$ (M_0 – the saturation magnetization) [2]. So it is of particular interest to recognize the role of self-trapping effects, which lead to formation of magnetic polarons and could significantly modify the amplitude of CMR in doped ferromagnetic semiconductors and semimetals [2-3].

Here we analyze the transport and magnetic properties of $\text{Eu}_{1-x}\text{Ca}_x\text{B}_6$ ($0 \leq x < 0.4$) solid solutions measured on the single crystals at temperatures 1.8–300 K in magnetic fields up to 8 T. A universal dependence of the CMR amplitude on the squared magnetization is established in the paramagnetic phase of these compounds (see $\Delta\rho/\rho = f((M/M_0)^2)$ graph for $x=0$ in Fig.1). In low-field limit ($M/M_0 \ll 1$, $T > T_C$) this relationship is reduced to $-\Delta\rho/\rho = C(M/M_0)^2$ with the parameter, which decreases under Ca doping from $C(x=0) = 20 \pm 2$ to $C(x=0.08) = 6 \pm 2$ (inset in Fig.1) and rises up to $C \approx 60-100$ in the insulating state of $\text{Eu}_{1-x}\text{Ca}_x\text{B}_6$ ($x > x_{\text{MIT}} \approx 0.2$) [4-5]. We argue that the low-field CMR effect enhances due to spin splitting of the conduction band under strong $s-f$ exchange ($J \sim 0.1$ eV). The comparison between the estimated values of C and the scaling law $C \sim n^{-2/3}$ earlier reported for CMR compounds [2] proves the common origin of the CMR effect in these compounds, which is related to the delocalization of electrons trapped in the spin-polaronic potential under applying of magnetic field.

Support by RFBR 11-02-00623 is acknowledged.

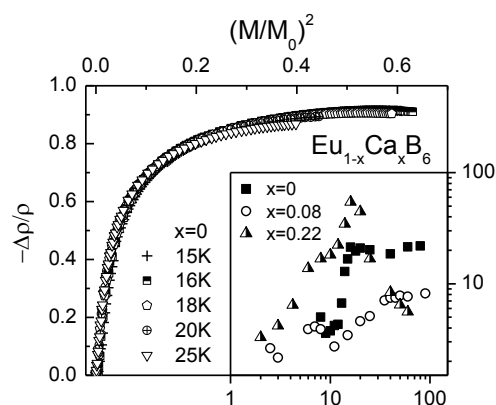


Fig. 1. Magnetoresistance as a function of the squared reduced magnetization in the paramagnetic phase of EuB_6 . Inset shows the $C(T)$ dependence for selected $\text{Eu}_{1-x}\text{Ca}_x\text{B}_6$ compounds.

[1] P. Majumdar, P. Littlewood, *Phys. Rev. Lett.*, **81** (1998) 1314-1317.

[2] P. Majumdar, P. Littlewood, *Nature*, **395** (1998) 479-481.

[3] S. Süllo et al., *J. Appl. Phys.*, **87** (2000) 5591-5593.

[4] V.V. Glushkov et al., *JETP*, **111** (2010) 246-250.

[5] V.V. Glushkov et al., *phys. stat. sol. B*, **250** (2013) 618-620.

3OR-A-3

MAGNETORESISTANCE OF MAGNETIC POINT CONTACTS ACCOUNTING FOR GRADIENTS OF CHEMICAL POTENTIAL

Useinov N., Tagirov L.

Institute of Physics, Kazan Federal University, Kazan, Russia
Niazbeck.Useinov@kpfu.ru

The quantum and macroscopic performances of magnetic point contacts (PC's) have been intensively studied both experimentally and theoretically (see, for example, Refs. [1, 2]). In the present work a model of the PC between two ferromagnetic metals with different conduction properties of the spin sub-bands is considered. The PC is simulated by a nanosized circular hole of the radius a made in a membrane, which divides the space on two half-spaces, occupied by single-domain ferromagnetic metals. A model of a linear domain wall has been used to account for the finite contact length. The electron motion on the both sides of the contact can be described by transport equations for quasi-classical Green functions (GF's) [3]. These GF's are symmetrical and antisymmetrical with respect to z projection of the quasiparticle momentum and satisfy Boltzmann equations in the τ approximation. We develop a theory of electric transport through magnetic PC's taking into account gradient terms in the series expansion of GF's. The theory covers the ballistic $l > a$ and diffusive $l < a$ regimes (l is the mean free path) to explain the variety of observed experimental data.

Results of magnetoresistance (MR) calculations for different ferromagnetic metals are shown in Fig. 1. Domain wall thickness between the magnetic domains is assumed to be equal $L = 10 \text{ \AA}$. The solid curve is calculated with gradient terms in the series expansion of GF's, and the dashed line – without gradient terms. Moreover, we investigated mean-free path effects on MR. In some cases the MR monotonously decreases as the PC cross-section increases. For some cases with a large difference in spin sub-band mean-free paths, the calculated MR shows non-monotonous behavior in the region where the radius of the contact becomes comparable with the mean-free path of electrons. We attribute this effect to the gradual change of conduction regimes in vicinity of the PC upon changing the contact cross-section size. The theoretical dependence of MR on the contact size can be used in interpreting the experimental data on MR of PC's of Fe-Co, Ni-Mumetall and tunnel structures of CoFeB/MgO/CoFe.

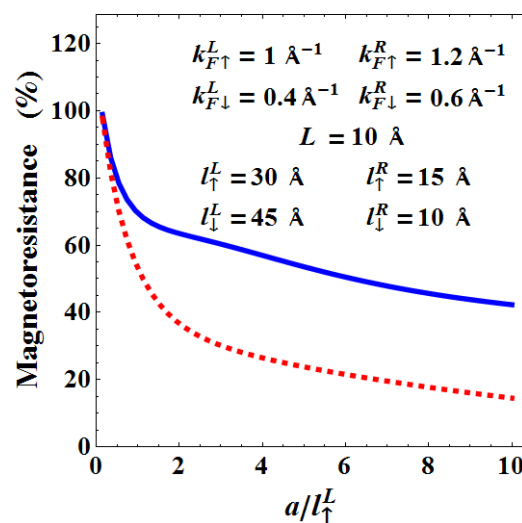


Fig. 1. Dependence of MR on the ratio of the radius to mean free path of conduction electrons with spin up of the left magnetic domain.

The reported study was partially supported by RFBR, research project No.14-02-00348 a.

- [1] A. Fernández-Pacheco, L.E. Serrano-Ramón *et al*, *Nanotechnology* **23** (2012) 105703.
[2] B Doudin, M Viret, *J. Phys.: Condens. Matter* **20** (2008) 083201.
[3] L.R. Tagirov, B.P. Vodopyanov, K.B. Efetov, *Physical Review B*, **63** (2001) 104428.

3OR-A-4

SIMULTANEOUS LOCALIZATION OF ELECTRONS IN DIFFERENT Δ VALLEYS IN Ge/Si QUANTUM DOT STRUCTURES

Zinovieva A.F.¹, Stepina N.P.¹, Dvurechenskii A.V.¹, Kulik L.V.², Mussler G.³, Moers J.³, Gruetzmacher D.³

¹ Institute of Semiconductor Physics SB RAS, 630090 Novosibirsk, Russia

² Institute of Chemical Kinetics and Combustion SB RAS, 630090 Novosibirsk, Russia

³ Peter Gruenberg Institute, Forschungszentrum Julich and Julich-Aachen Research Alliance
aigul@isp.nsc.ru

Quantum dot (QD) semiconductor system is one of the best candidates for realization of quantum computation ideas and spintronics devices. Recent theoretical study of Ge QDs grown on Si(001) has shown that two electrons with different g-factors can be localized nearby the same Ge QD that might provide the selective access to individual qubit for implementation of one-qubit and two-qubit operations. The g-factor difference is provided by different strain distribution in the Si vicinity of Ge QD. Uniaxial compression near QD apex allows to realize an electron localization in the Δ^{001} valley, while strain in the vicinity of QD base edge can promote the electron localization in the Δ^{100} valley. Localization in different Δ valleys can be confirmed by characteristic angular dependence of g-factor.

In the present work the possibility of simultaneous localization of two electrons in Δ^{100} and Δ^{001} valleys in ordered structures with Ge/Si quantum dots was verified experimentally by electron spin resonance (ESR) method. Structures under study contain ten layers of QDs grown on prepatterned substrates by molecular beam epitaxy at temperature $T=525^\circ\text{C}$.

Fig. 1 demonstrates the change of ESR spectra under illumination. ESR spectrum in the dark consists of two lines with $g_1=1.9997$ and $g_2=1.9988$. The first ESR line (not related to QDs) does not change under illumination, while the intensity of the second ESR line increases. Angular dependence of g_2 indicates that this ESR signal comes from the electrons in Δ^{100} valley localized at the QD base edges. Light illumination causes the appearance of a new ESR line ($g_3=1.9993$), attributed to the electrons in Δ^{001} valley localized at the QD apexes.

These results can be explained as follows. The potential well at the QD base edge is deeper than the potential well at the QD apex. Thus in the dark electrons are mainly localized at the QD base edges in Δ^{100} valley. Under the illumination, photogenerated holes are trapped by Ge QDs; the Coulomb attraction to the hole makes the potential well at the QD apex strong enough to provide electron localization. Thus, new ESR line with $g_3=1.9993$, responsible for the electron in Δ^{001} valley will be appeared simultaneously with the ESR line from electrons in Δ^{100} valley. The observed simultaneous localization of electrons with different g-factors in QD system can greatly facilitate the organization of one- and two-qubit operations and promotes the quantum computing realization in the future.

Support by RFBR (Grant 13-02-12105), SB RAS integration project No. 83 and DITCS RAS project No. 3.5 and Project ERA-NET-SB RAS (Grant 186) is acknowledged.

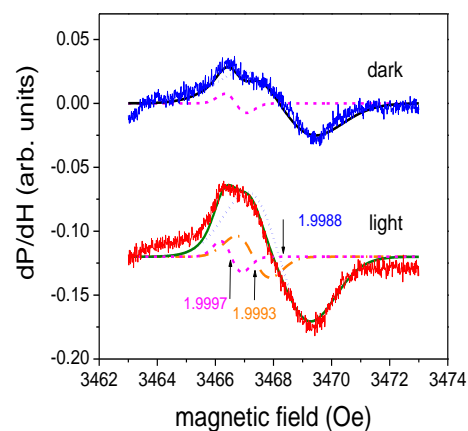


Fig. 1. ESR spectra of electrons localized in the structures with ordered QD array with (without) illumination.

3OR-A-5

MODELLING OF GMR CURVES IN SPIN-VALVES

Kurenkov A.S.^{1,2}, *Chernykh P.N.*¹, *Chechenin N.G.*^{1,2}

¹ Skobeltsyn Institute of Nuclear Physics, MSU, Moscow, Russia

² Faculty of Physics, Lomonosov Moscow State University, Moscow, Russia

kurenkov@physics.msu.ru

We report on observation and analysis of shapes of magnetoresistance (MR) curves in spin-valve structures with composition ferromagnetic – spacer – ferromagnetic – antiferromagnetic. Though asymmetries of MR curves are often observed in spin-valve GMR measurement, there is still no classification and satisfactory explanation for them. In order to classify and interpret this phenomenon, a modelling method has been developed. It is based on a compact theoretical model of electron scattering, where the magnetoresistance is a function of the angle φ between FF and PF magnetization vectors, \mathbf{M}_{FF} and \mathbf{M}_{PF} , respectively:

$$R(H) = R_0 + \Delta R_{GMR} \cos(\varphi), \quad (1)$$

where φ is the angle between magnetization vectors of FF and PF. Angle φ can be estimated as:

$$\varphi = \arccos(M_{FF}^{ext}) - \arccos(M_{PF}^{ext}), \quad (2)$$

assuming a constant length of the magnetization vector (M_{FF}^{ext} and M_{PF}^{ext} are projections of magnetization vector of FF and PF, respectively, on the axis, parallel to external field). Thus:

$$R(H) = R_0 + \Delta R(H), \quad \Delta R(H) = \Delta R_{GMR} \cos(\arccos(M_{FF}^{ext}) - \arccos(M_{PF}^{ext})). \quad (3)$$

We apply Eq. (3) to construct MR curves. For that, we take M_{FF}^{ext} and M_{PF}^{ext} values from assumed $M(H_{ext})$ hysteresis loops for FF and PF. Vice versa, when deriving hysteresis loops from MR curves, we vary parameters of hysteresis loops in order to adjust calculated MR curves to experimental ones (see Fig. 1 for example).

The method is used to construct MR curves from magnetisation hysteresis loops of composing F layers and to decompose the measured MR curves to obtain the FF and PF hysteresis loops. It allows predicting properties of spin-valve starting from the hysteresis loops for composing layers. Five types of asymmetry, comprehensively describing all shapes of MR curves, are found and discussed.

3OR-A-6

**OBSERVATION OF POWER-LAW SCALING BEHAVIOR IN
FERROMAGNETIC FILMS WITH UNIDIRECTIONAL ANISOTROPY***Shashkov I.V.¹, Gornakov V.S.¹, Lebyodkin M.A.²*¹ Institute of Solid State Physics, Russian Ac. Sci., 142432 Chernogolovka, Russia² LEM3, CNRS/Université de Lorraine, UMR 7239, Ile du Saulcy, 57045 Metz, France

e-mail: shav@issp.ac.ru

During the last two decades the mechanisms of magnetization reversal in exchange coupled ferromagnetic (FM) / antiferromagnetic (AFM) heterostructures were intensively studied. It is known that nucleation and evolution of magnetic domains in such coupled systems are usually associated with the penetration of a partial domain wall (exchange spring) into the AF layer [1]. As a consequence, this exchange spring leads to asymmetry in the domain wall (DW) mobility during magnetization reversal. One can expect that this asymmetry will influence on the statistics of DW motions due to different defects acting as DW pinning centers during the forward and backward branches of the hysteresis loop. It is important to note that DW motions in ferromagnet materials usually display intermittent behavior with nontrivial magnetization jumps statistics. In particular, it was found that distributions of durations and sizes of magnetization jumps obey power-law statistics. Such scale-free behavior indicates a critical avalanche-like character of magnetization reversal in ferromagnet materials.

Here we investigate the intermittent nature of the domain wall motion during magnetization reversal in epitaxial NiFe/NiO bilayers grown on single-crystal MgO (001) substrates. The use of the magneto-optical indicator film technique let us to observe evolution of the magnetic domain structure in the FM layer. The measured magneto-optical response is processed using statistical analysis. Power-law statistics is found for magnetization jumps, thus indicating a nonstochastic nature of DW motions. Moreover, the power-law indices are close to each other for both branches of the hysteresis loop. This result leads to a suggestion that the statistics of the magnetization avalanches depends on the overall distribution of pinning centers within the sample. Alongside with the statistical analysis of the magnetization jumps, multifractal analysis is applied to uncover the possible time correlations in the DW dynamics.

[1] C.L. Chien, V.S. Gornakov, V. I. Nikitenko *et al.*, *Phys. Rev. B*, **68** (2003) 014418.

3OR-A-7

INDIRECT THERMODYNAMIC MAGNETIZATION MEASUREMENTS IN TWO-DIMENSIONAL SYSTEMS

*Kuntsevich A. Yu.*¹

¹ P.N. Lebedev physical institute of the RAS, Moscow, Russia
alexkun@lebedev.ru

Two dimensional systems(2DS) (metal-insulator-semiconductor structures, semiconducting heterostructures, graphene, etc) contain $n=10^9$ - 10^{13} electrons (or holes) per square centimeter. Magnetometry of such systems suffers from huge substrate contribution and can only be done at low temperatures in quantizing magnetic field, where magnetization of the 2DS oscillates[1].

We develop an alternative approach to magnetization measurements in gated 2DS. Voltage across a gated structure is the difference of the electrochemical potentials of the gate electrode and the 2DS. It has a thermodynamic component μ (Fermi energy). Using the Maxwell relation $d\mu/d\mathbf{B}=-d\mathbf{M}/dn$ (here \mathbf{B} is magnetic field, \mathbf{M} is a magnetization per unit area) and modulating the magnetic field \mathbf{B} we can measure the magnetization per electron $d\mathbf{M}/dn$. Such measurements are sensitive to 2D gas solely without substrate contribution.

The sensitivity of the method allows one to resolve not only oscillatory effects in Si-MOS, and GaAs heterostructures[2] but also Pauli paramagnetism in 2D Si-MOS[3] in magnetic fields parallel to 2D plane. Our measurements[4] revealed superparamagnetic spin droplets(total spin ~ 2) on top of paramagnetic Fermi-liquid. The droplets are result of strong electron-electron correlations. Melting of droplets was shown to be intimately related to 2D metal-to-insulator transition.

I will also review our recent measurements of low-field diamagnetic properties of 2DSs, limitations and development of chemical potential related methods.

The work is supported by Russian Ministry of Science and Education grant M-4208.2013.2.

[1] Usher, Elliott, *J. Phys.: Condensed Matter*, **21** (2009) 103202.

[2] V. M. Pudalov, et al, *ZhETF*, **89** (1985) 1870 [*JETP*, **62** (1985) 1079]; R.T. Zeller et al, *Phys. Rev. B*, **33** (1986) 1529(R); S.Anissimova et al, *Phys. Rev. Lett.*, **96** (2006) 046409; V.I. Nizhankovskii, *Hindawi Publ. Corp. Phys. Research Int.* (2011), Article ID 742158.

[3] O. Prus et al, *Phys. Rev. B*, **67** (2003) 205407; A.A. Shashkin et al, *Phys. Rev. Lett.*, **96** (2006) 036403.

[4] N. Tenen et al; *Phys. Rev. Lett.*, **109** (2012) 226403.

3OR-A-8

COMPOSITE ANTIFERROMAGNETS FOR TA-MRAM APPLICATIONS

Akmaldinov K.^{1,2,*}, *Ducruet C.*², *Portemont C.*², *Alvarez-Hérault J.*², *Vidal J.*², *Joumard I.*¹,
*Prejbeanu I.L.*¹, *Dieny B.*¹, *Baltz V.*^{1,*}

¹SPINTEC, Uni. Grenoble Alpes / CNRS / INAC-CEA, F-38000 Grenoble, France

²CROCUS Technology, F-38000 Grenoble, France

* vincent.baltz@cea.fr ; kamil@crocus-technology.com

Spintronics devices and in particular thermally assisted magnetic random access memories (TA-MRAM) [1] require a wide range of ferromagnetic/antiferromagnetic (F/AF) exchange bias properties and subsequently of AF materials in order to fulfil diverse functionality requirements for the reference and storage. For the reference layer, large exchange bias energies and high blocking temperature (T_B) are required. In contrast, for the storage layer, mostly moderate T_B is needed. Tunability of T_B is also desirable to minimize the write power consumption while insuring proper functioning on the device temperature operating range. One of the present issues is to find a storage layer with properties intermediate between those of IrMn and FeMn and in particular: i) with a T_B larger than FeMn for better stability at rest-T but lower than IrMn to reduce power consumption at write-T and ii) with improved magnetic interfacial quality, i.e. with reduced interfacial glassy character for lower properties dispersions [2-4]. To address this issue, the exchange bias properties of F/AF based stacks were studied for various mixed [IrMn/FeMn] AFs. In addition to exchange bias loop shifts, the F/AF magnetic interfacial qualities and the AF grains thermal stability are probed via measurements of the low- and high-temperature contributions to the blocking-temperature distributions, respectively. Regarding the magnetic interfacial quality, the smaller the low-temperature contribution, the less glassy the interface [2]. A tuning of the above mentioned exchange bias parameters was observed when evolving from IrMn to FeMn via [IrMn/FeMn] repetitions. In addition, it is expected that the better the F/AF sheet films interfacial qualities, the lower the cell to cell exchange bias properties dispersions for the corresponding nanofabricated devices. Therefore, these results for sheet films were compared to data obtained for the corresponding nanofabricated devices.

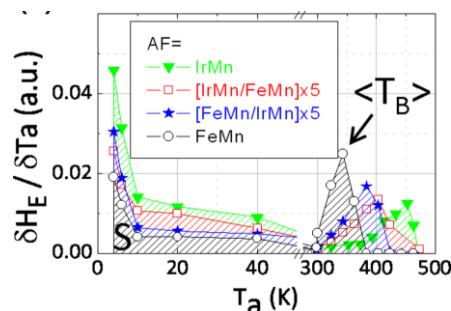


Fig. 1. Typical blocking temperature distributions for TA-MRAM stacks with various antiferromagnetic (AF) layers [4].

[1] R. C. Sousa and I. L. Prejbeanu, *CR Physique*, **6** (2005) 1013.

[2] V. Baltz, B. Rodmacq, A. Zarefy, L. Lechevallier, B. Dieny, *Phys. Rev. B*, **81** (2010) 052404.

[3] K. Akmaldinov, S. Auffret, I. Joumard, B. Dieny and V. Baltz, *Appl. Phys. Lett.*, **103** (2013) 042415.

[4] K. Akmaldinov, C. Ducruet, C. Portemont, I. Joumard, I. L. Prejbeanu, B. Dieny and V. Baltz *J. Appl. Phys.*, **115** (2014) 17B718.

3 July Thursday

11:30-13:45

oral session

3TL-B

3RP-B

3OR-B

3TL-LT

3RP-LT

3OR-LT

**“Magnetism and
Superconductivity”**

3TL-B-1

DOMINANT SECOND HARMONIC IN THE JOSEPHSON CURRENT-PHASE RELATION: MANIFESTATION OF THE LONG RANGE SPIN-TRIPLET PROXIMITY EFFECT IN FERROMAGNETIC BILAYERS

Radović Z.

University of Belgrade, Department of Physics, 11158 Belgrade, Serbia
zradovic@ff.bg.ac.rs

We have predicted a pure second harmonic current-phase relation, $I(\phi) \propto \sin(2\phi)$, in SFF'S Josephson junctions with conventional (s-wave) superconductors and two highly unequal ferromagnets with noncollinear magnetizations [1], see Fig. 1(a). This is a characteristic manifestation of the long range spin-triplet proximity effect in ferromagnetic bilayers where the first harmonic is suppressed [2] and the phase coherent transport of two Cooper pairs becomes dominant [3,4]. Effect is also accompanied by distinctive two-peak structure in energy dependence of electronic density of states [5], see Fig. 1(b), which can be used for a detection of the long range spin-triplet proximity effect by tunneling spectroscopy. Although we have considered clean and moderately diffusive ferromagnets, the effect exists in diffusive systems as well [6], and has been observed recently [7]. The half-periodicity of $I(\phi)$, like at $0 - \pi$ transitions, can be used for "silent" quantum interferometers (SQUIDS) which exhibit the superposition of macroscopically distinct quantum states in the absence of an external magnetic field.

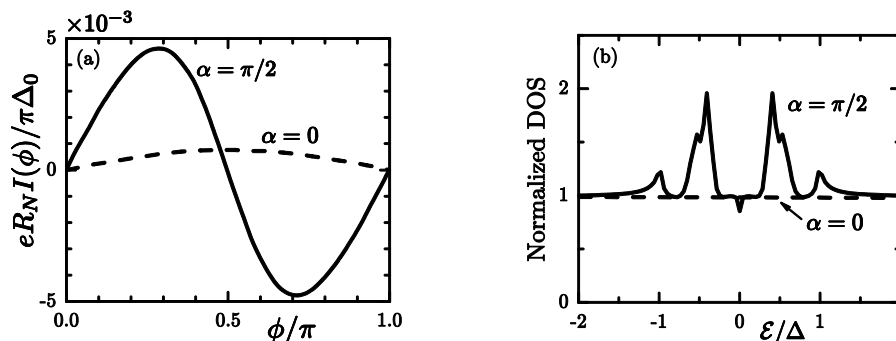


Fig. 1. (a) The Josephson current – phase relation for an asymmetric (magnetic influence ratio 1:100) SFF'S junction with parallel ($\alpha = 0$, dashed line) and orthogonal ($\alpha = \pi/2$, solid line) magnetizations [1]. (b) Normalized electronic density of states in the middle of the thick (strong) F' layer as a function of energy near the Fermi level [5]. Moderately diffusive case is shown (electronic mean free path in ferromagnets $l = 200k_F^{-1}$) at low temperatures ($T/T_c = 0.1$).

- [1] L. Trifunovic, Z. Popović, and Z. Radović, *Phys. Rev. B*, **84** (2011) 064511.
- [2] L. Trifunovic and Z. Radović, *Phys. Rev. B*, **82** (2010) 020505(R).
- [3] L. Trifunovic, *Phys. Rev. Lett.*, **107** (2011) 047001.
- [4] A. Mel'nikov, A. Samokhvalov, S. Kuznetsova, and A. Buzdin, *Phys. Rev. Lett.*, **109** (2012) 237006.
- [5] M. Knežević, L. Trifunovic, and Z. Radović, *Phys. Rev. B*, **85** (2012) 094517.
- [6] C. Richard, M. Houzet, and J. Meyer, *Phys. Rev. Lett.*, **110** (2013) 217004.
- [7] A. Pal, Z. Barber, J. Robinson, and M. Blamire, *Nature Commun.*, **5** (2014) 3340.

3OR-B-2

REALIZATION OF A JOSEPHSON SPIN VALVE

Iovan A., Golod T., Krasnov V.M.

Department of Physics, Stockholm University, AlbaNova University Center, SE-10691 Stockholm, Sweden

In this work we study nano-scale superconducting spin-valve devices, in which a spin valve structure is implemented as a barrier in a Josephson junction. $\text{Cu}_{0.4}\text{Ni}_{0.6}/\text{Cu}/\text{Cu}_{0.5}\text{Ni}_{0.5}$ (thicknesses 10/6nm /10nm /10nm) spin valve is sandwiched between two thick Nb electrodes (thickness ~ 200 nm). The Nb/CuNi/Cu/CuNi/Nb multilayer was deposited by magnetron sputtering in a single deposition cycle without breaking vacuum. The CuNi films were deposited by co-sputtering from Cu and Ni targets. This allows easy variation and control of composition. The two ferromagnetic layers in the spin-valve had different concentrations of Ni in order to achieve different coercive fields. Nano-scale junctions with sizes down to 150 nm were patterned by photolithography, reactive ion etching and three-dimensional nano-sculpturing using focused ion beam, as described in Ref. [1]. Small dimensions were necessary both for mono-domain switching of spin valves and for enhancement of junction resistances to comfortably measurable values.

Figure 1 shows experimental characteristics of a junction $250 \times 500 \text{ nm}^2$ in area as a function of in-plane magnetic field applied perpendicular to the long side of the junction. Panel (a) shows ac-resistance measured with a small bias current $I=50 \text{ }\mu\text{A}$ for increasing (black) and decreasing (red) magnetic fields. This graph represents Fraunhofer modulation of the Josephson critical current $I_c(H)$. To show this more clearly we reversed the scale of the vertical axis. A regular Fraunhofer modulation indicates a good homogeneity of the Josephson current through the spin valve.

Panel (b) shows the high bias resistance, measured at $I \gg I_c$. It represents a pure spin valve magneto-resistance with minima and maxima at parallel and antiparallel orientations of magnetizations in the two ferromagnetic layers, respectively.

Thus we have successfully realized a superconducting spin-valve, exhibiting both the spin valve effect and a Josephson supercurrent. We discuss properties of such a Josephson spin valve and demonstrate tunability of the Josephson current depending on the orientation of magnetization in the spin valve.

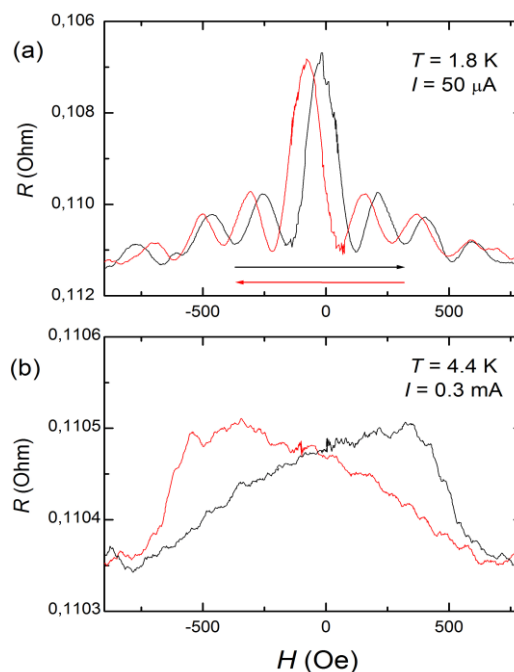


Fig. 1. Low (a) and high (b) bias resistance of a Nb/CuNi/Cu/CuNi/Nb Josephson spin-valve as a function of the in-plane magnetic field. Modulation in (a) reflects Fraunhofer oscillation of the Josephson current, in (b) the spin valve magnetoresistance.

[1] T. Golod, A. Rydh, and V.M. Krasnov, *Phys. Rev. Lett.*, **104** (2010) 227003.

3OR-B-3

INHOMOGENEOUS SUPERCONDUCTIVITY AT OXIDE INTERFACES WITH STRONG RASHBA SPIN-ORBIT INTERACTION

Caprara S.¹, Bucheli D.¹, Grilli M.¹

¹ Department of Physics - Sapienza University, Rome, Italy
sergio.caprara@roma1.infn.it

The two-dimensional electron gas formed at the the LaAlO₃/SrTiO₃ or LaTiO₃/SrTiO₃ oxide interfaces becomes superconducting when the carrier density is tuned above a certain threshold by means of gating. The measured resistance, superfluid density, and tunneling spectra reveal an inhomogeneous superconductivity resulting from percolation of filamentary structures of superconducting "puddles" with randomly distributed critical temperatures, embedded in a non-superconducting matrix [1]. Following the evidence that superconductivity is related to the appearance of high-mobility carriers, we model intra-puddle superconductivity by a multi-band system within a weak coupling BCS scheme. The microscopic parameters, extracted by fitting the transport data with a percolative model, yield a consistent description of the dependence of the average intra-puddle critical temperature and superfluid density on the carrier density [2].

As a possible mechanism for electron inhomogeneity, we propose that the sizable and density dependent Rashba spin-orbit coupling measured in these systems can induce electronic phase separation [3]. The resulting phase diagram is characterized by a quantum critical point, which turns into a line of quantum critical points in the presence of a magnetic field parallel to the interface [4].

Financial support from University Research Project of the University of Rome Sapienza, No. C26A125JMB, is acknowledged.

- [1] D. Bucheli, S. Caprara, C. Castellani, and M. Grilli, *New Journal of Physics* **15**, (2013) 023014.
- [2] S. Caprara, J. Biscaras, N. Bergeal, D. Bucheli, S. Hurand, C.Feuillet-Palma, A. Rastogi, R. C. Budhani, J. Lesueur, and M. Grilli, *Physical Review B* **88**, (1023) 020504(R).
- [3] S. Caprara, F. Peronaci, and M. Grilli, *Physical Review Letters* **109**, (2012) 196401
- [4] D. Bucheli, M. Grilli, F. Peronaci, G. Seibold, and S. Caprara, preprint.

3RP-B-4

SPIN-TRIPLET SUPERCONDUCTING CORRELATION IN EPITAXIAL HYBRID OXIDE HETEROSTRUCTURE

Ovsyannikov G.A.^{1,2}, *Constantinian K.Y.*¹, *Sheyerman A.E.*¹, *Shadrin A.V.*¹, *Kislinski Yu.V.*¹,
*Khaydukov Yu.*³, *Mustafa L.*³, *Kalbukhov A.*², *Winkler D.*²

¹ Kotel'nikov IRE RAS, Russian Academy of Sciences, Moscow, Russia

² MC2, Chalmers University of Technology, Gothenburg, Sweden

³ Max-Planck Institute for Solid State Research, Stuttgart, Germany

gena@hitech.cplire.ru

We present experimental investigation triplet superconducting correlation in the magnetic interlayer of mesa-structure with the linear size in plane 10-50 μm made from hybrid heterostructures Nb-Au/La_{0.7}Sr_{0.3}MnO₃/SrRuO₃/YBa₂Cu₃O_x (Nb-Au/LSMO/SRO/YBCO). No superconducting critical current was observed in the heterostructures with either a LSMO or a SRO interlayer with thickness larger than 10 nm. In thinner heterostructures, the observed critical current was attributed to the presence of pinholes [1]. A critical current was observed in the mesa-structure with the LSMO/SRO bilayer with total thicknesses up to 60 nm. Magnetic, SQUID and neutron measurements indicate on the presence of magnetization misorientation on the angle that depended on the external magnetic field. The presence of second harmonic in current-phase relation of mesa-structure was confirmed by the subharmonic Shapiro steps. Obtained results are discussed in terms of generation of a long-range triplet superconducting current component at superconductor/ferromagnetic interfaces consisting of ferromagnetic materials with non-collinear magnetization [2-4].

Partially support by RAS, RFBR 14-07-00258, Scientific School Grant 4871.2014.2 are acknowledged.

[1] A.M. Petrzhik, et al, *JEPT*, **112** (2011) 1043.

[2] A.V. Zaitsev, *JEPT Lett*, **83** (2006) 277.

[3] F. S. Bergeret et al, *Rev. Mod.Phys.*, **77** (2005) 1321.

[4] G.A. Ovsyannikov, et al, *JEPT Lett*, **97** (2013) 145.

3RP-B-5

MEMORY EFFECT IN SUPERCONDUCTOR/FERROMAGNET NANOSTRUCTURES Co/CoO_x/CuNi/Nb/CuNi

*Morari R.^{1,2}, Zdravkov V.I.^{1,3}, Obermeier G.³, Lenk D.³, Seidov Z.^{3,4}, Krug von Nidda H.-A.³,
Müller C.³, Kupriyanov M.Yu.⁵, Sidorenko A.S.¹, Horn S.³, Tidecks R.³, Tagirov L.R.^{2,3}*

¹ Institute of Electronic Engineering and Nanotechnologies ASM, 2028 Kishinev, Moldova

² Solid State Physics Department, Kazan Federal University, 420008 Kazan, Russia

³ Institut für Physik, Universität Augsburg, D-86159 Augsburg, Germany

⁴ Institute of Physics, Azerbaijan National Academy of Science, AZ-1143 Baku, Azerbaijan

⁵ Skobeltsyn Institute of Nuclear Physics, Moscow State University, Moscow 119992, Russia
anatoli.sidorenko@kit.edu

The theory of superconductor-ferromagnet (S-F) heterostructures with two and more ferromagnetic layers predicts generation of long-range, odd-in-frequency triplet pairing at non-collinear alignment of magnetizations of the F-layers ([1] and references therein). Based on ideas of the superconducting triplet spin-valve [2,3] we observed switching of the Co/CoO_x/Cu₄₁Ni₅₉/Nb/Cu₄₁Ni₅₉ proximity type heterostructures between normal and (almost) superconducting states [4].

The Co/CoO_x/Cu₄₁Ni₅₉/Nb/Cu₄₁Ni₅₉ ultrathin heterostructure was prepared by magnetron sputtering on a commercial silicon substrate covered by a silicon buffer layer prior the heterostructure deposition. The Co/CoO_x composite layer provided strong exchange biasing (~ 1800 Oe) of the adjacent hard ferromagnetic Cu₄₁Ni₅₉ alloy layer, while the outer soft Cu₄₁Ni₅₉ alloy layer could be remagnetized by a weak external magnetic field creating controllable alignments with respect to the hard interior Cu₄₁Ni₅₉ alloy layer and the metallic Co layer as well. The thickness of the Cu₄₁Ni₅₉ alloy layers was varied between 0 and 25 nm, the Nb layer thickness was about 12 nm.

Upon cycling the in-plane magnetic field in the range ± 6 kOe and the temperature close to the superconducting transition a memory effect has been observed [4]. If the magnetic field was dropped to zero from the initial field-cooling direction at 10 kOe, the system resistance dropped down to the almost superconducting low-resistive state. Changing polarity of the field, raising its magnitude to -6 kOe and dropping the field to zero again brought the system to the resistance at the normal conducting state. The bistability was repeatedly reproduced upon further cycling along the full magnetic hysteresis loop of the heterostructure. The both low- and high-resistive states at zero magnetic field were determined solely by pre-history of the field cycling and did not need biasing field to keep them steady.

We refer the observed memory effect to generation of the triplet pairing at non-collinear magnetic configurations in the studied system.

The support by DFG, and RFBR, grants Nos. 14-02-90018 (M.Yu.K) and 14-02-00793-a (L.R.T.), is gratefully acknowledged.

1. F.S. Bergeret, A. F. Volkov, and K.B. Efetov, *Rev. Mod. Phys.*, **77** (2005) 1321.
2. Ya.V. Fominov, *et al.*, *JETP Lett.*, **77** (2003) 510.
3. Ya.V. Fominov, *et al.*, *JETP Lett.*, **91** (2010) 308.
4. V.I. Zdravkov, *et al. Appl. Phys. Lett.*, **114** (2013) 0339903.

3TL-B-6

SPIN-DIFFUSION AND SPIN-INJECTION IN HYBRID S-N/F-S-STRUCTURES*Ryazanov V.V., Golikova T.E., Batov I.E.*Institute of Solid State Physics RAS, Chernogolovka, Moscow Distr. Russia
valery.ryazanov@gmail.com

We have realized planar Josephson S-(N/F)-S junctions proposed firstly in [1]. They enable spin-diffusion and spin-injection in Josephson normal-metal barrier.

Recently we have observed a double-peak peculiarity in differential resistance of the Al-(Cu/Fe)-Al structure at a bias voltages corresponding to the superconducting gap and minigap [2]. We claim that this effect (the splitting of the minigap) is due to an electron spin polarization in the copper layer which is induced by the single-domain iron sublayer.

Our new results are related to spin-injection to banks and barrier of planar Josephson junctions. Support by RFBR and RSF is acknowledged.

[1] T. Yu. Karminskaya, A. A. Golubov, M. Yu. Kupriyanov, and A. S. Sidorenko, *Phys. Rev. B*, **81** (2010) 214518.

[2] T.E. Golikova, F. Hübler, D. Beckmann, I.E. Batov, T.Yu. Karminskaya, M.Yu. Kupriyanov, A.A. Golubov, and V.V. Ryazanov, *Phys. Rev. B*, **86** (2012) 064416.

3RP-B-7

**SUPERCONDUCTIVITY R&D OVERVIEW IN TURKEY IN VIEW OF
"CENTER OF EXCELLENCE FOR SUPERCONDUCTIVITY RESEARCH
(CESUR), VISION, MISSION AND ROADMAP WITH INTERNATIONAL
COLLABORATION OPPORTUNITIES"**

Turkoz S.

Ankara University, Center of Excellence for Superconductivity Research, Ankara, Turkey
turkoz@science.ankara.edu.tr

Turkey as a country with no long tradition of low temperature physics before 90s, some scientific studies were only limited to a few university laboratories with no significant contribution to the worldwide efforts in the field. In this talk, we will focus on the research papers trial from 1990 until 2014 along with Turkey's state initiatives to develop the science and technology in the country. Needless to say, the aim of this plenary talk is not to give a full account of R&D progress of the country, rather it is to give a brief understanding of scientific publication trial in terms of statistics and funding raise with more emphasis on superconductivity over the last decade and expectations and extrapolation over the next decade.

With the initiatives of a group of scientists back in 2007 headed by myself, following a submission of joint project proposal, Turkish Ministry of Development granted an infrastructural research funding in 2010 to Ankara University together with other 7 different participating universities under the coordination of Ankara University to establish a national center of excellence in Superconductivity Research. The center (CESUR) has been officially approved in 14th June, 2012 and has eventually become an official host for ICSM conferences. (ICSM conference has grown to be truly international with participation of over 1100 from about 60 countries.) The center composes of four technical and four administrative divisions. The technical ones are Fundamental Superconductivity Research, Small-scale Applications, Large-scale Applications and Materials Development Units. Educational out-reach and Public Relations, Innovation, Financial Affairs and Workshop/Device Construction Units are administrative ones. The central laboratory building houses 8 different divisions to be specialized with state of the art facilities needed in relevant research directions.

In view of the center's vision, mission and roadmap for the next 10 years, Turkey has a targeted vision of 2023, by the centenary of the Republic to increase exports to the level of 1/3 of Germany totaling above 500 billion dollars of exports, with GDP of above 2 trillion dollars and together with R&D investment of around 50-60 billion dollars annually. In this targetable approach, an active research center in superconductivity can be a driving force in related research areas such as materials science, chemistry, electronics, electrical engineering, information technology, energy sector, renewable energy, transportation sector. Sustainability of the center will be realized through contribution of member institutions and by dynamic character of research activities both at national and international level (funding via projects).

A detailed roadmap of superconductivity together with a national program subject to approval, activities of participating research groups will be presented with international scientific collaboration opportunities.

3RP-LT-1

VORTEX STRUCTURE AND NORMAL PROPERTIES BSLCO (2201) SINGLE CRYSTALS

Vinnikov L.Ya.¹, Zverev V.N.¹

¹ ISSP RAS, Chernogolovka, Russia
vinnik@issp.ac.ru

Family compounds Bi –based high-Tc superconductors $\text{Bi}_2\text{Sr}_{2-x}\text{La}_x\text{CuO}_y$ (2201), where Sr partially substituted by La, with one cuprate plane are subject of high interest .

Vortex structure, magnetic and resistive properties in normal state for $\text{Bi}_2\text{Sr}_{1.65}\text{La}_{0.35}\text{CuO}_{6+\delta}$ single crystals has been studied. Vortex structure has been studied at tilted magnetic fields by use the decoration technique[1]. Observation of vortex chains structures in basal ab cuprate (CuO_2) plane (Fig.1) allowed to measure penetration depth ratio $\gamma_s = \lambda_{\perp} / \lambda_{\parallel} = 460 \pm 40$ using Koshelev's model [2].

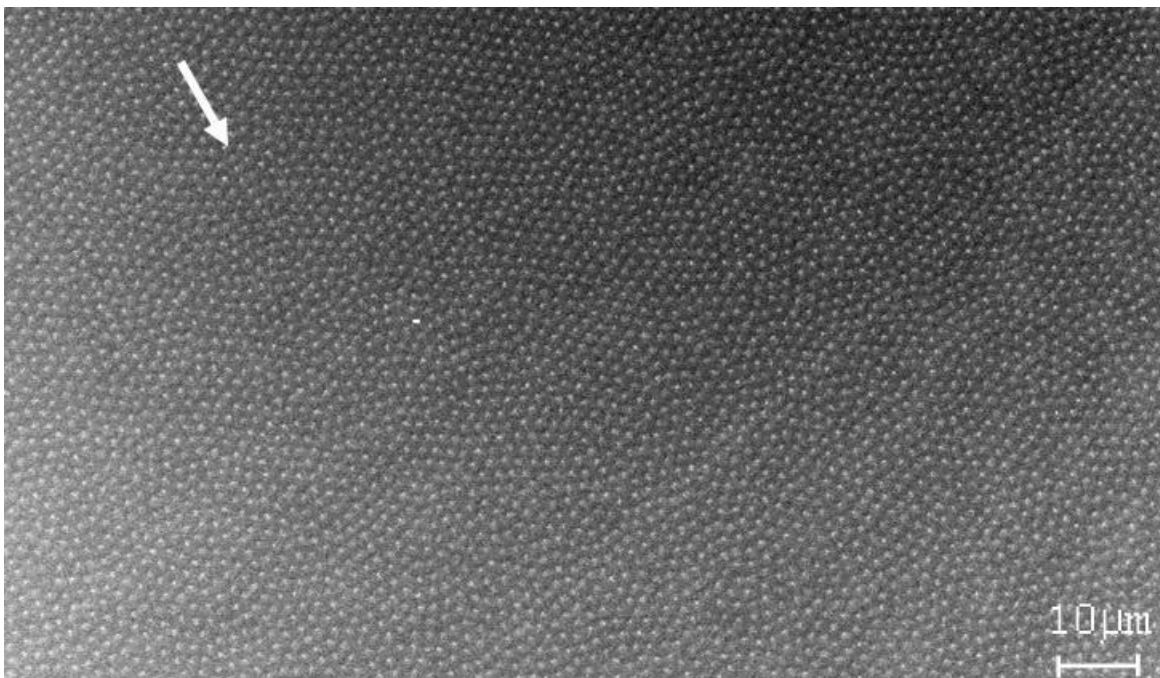


Fig.1 Vortex structure in $\text{Bi}_2(\text{Sr}_{1.65}\text{La}_{0.35})_2\text{CuO}_y$ single crystals at tilted magnetic field $H_{\parallel}=15$ Oe, $H_{\perp}=4$ Oe.

Ratio of specific resistances $\rho_{\perp}/\rho_{\parallel} = 3.2 \cdot 10^5$, was measured near T_c in normal state by Montgomery method . Comparison of anisotropy parameters in superconducting state γ_s and in normal state $\epsilon_N \sim \sqrt{\rho_{\perp}/\rho_{\parallel}} = \sqrt{3.2 \cdot 10^5} = 570$ seems to be reasonable.

Support by RFBR 12-02-91055 is acknowledged.

[1] L.Ya.Vinnikov, L.A.Gurevich, I.V.Grigor'eva, *Springer series in Material Science*, **23** (1993) 89-109

[2] A.E. Koshelev, *Phys. Rev. Lett.*, **83** (1999) 187.

3OR-LT-2

ULTRAFAST INFRARED RESPONSE IN TOPOLOGICAL INSULATORS

*Luo C.W.*¹, *Tu C.M.*¹, *Chen H.-J.*¹, *Tzeng W.Y.*¹, *Lin J.-Y.*¹, *Wu K.H.*¹, *Juang J.Y.*¹, *Sankar R.*²,
*Chou F.C.*², *Kokh K.A.*³, *Gu G.D.*⁴,

¹ Department of Electrophysics, National Chiao Tung University, Hsinchu 300, Taiwan

² Center for Condensed Matter Sciences, National Taiwan University, Taipei 106, Taiwan

³ Institute of Geology and Mineralogy, SB RAS, Novosibirsk, Russia

⁴ Condensed Matter Physics and Materials Science Department, Brookhaven National Laboratory,
 Upton, New York 11973, United States
 cwluo@mail.nctu.edu.tw

This study shows that a THz wave can be generated from Bi₂Se₃, Bi₂Te₃ and Cu-doped Bi₂Se₃ single crystals using 800 nm femtosecond pulses, as shown in Fig. 1. The generated THz power is strongly dependent on the carrier concentration of the crystals [1]. An examination of this dependence reveals that Dirac fermions are indispensable for two-channel free carrier absorption. Dirac fermions in Bi₂Se₃ are significantly better absorbers of THz radiation than bulk carriers at room temperature. Moreover, the ultrafast dynamics of Dirac fermions in the surface state of Bi₂Se₃ is significantly different from that in bulk state, which was investigated using optical pump mid-infrared probe spectroscopy [2]. The rising time and decay time of the negative component in transient reflectivity changes, assigned to carrier relaxation in Dirac cone, are ~1.62 ps and ~20.5 ps, respectively. The measured relaxation time of Dirac fermions was used to estimate the Dirac fermion-phonon coupling strength which is ~0.08 near Dirac point.

This project is financially sponsored by the National Science Council (grant no. NSC 98-2112-M-009-006-MY3, NSC 98-2112-M-009-008-MY3 and NSC 101-2112-M-009-016-MY2) and the Ministry of Education (MOE ATU program at NCTU) of Taiwan, R.O.C.

[1] C.W. Luo, H.-J. Chen, C.M. Tu, C.C. Lee, S.A. Ku, W.Y. Tzeng, T.T. Yeh, M.C. Chiang, H.J. Wang, W.C. Chu, J.-Y. Lin, K.H. Wu, J.Y. Juang, T. Kobayashi, C.-M. Cheng, C.-H. Chen, K.-D. Tsuei, H. Berger, R. Sankar, F.C. Chou, H.D. Yang, *Advanced Optical Materials*, **1** (2013) 804-808.

[2] C.W. Luo, H.J. Wang, S.A. Ku, H.-J. Chen, T.T. Yeh, J.-Y. Lin, K.H. Wu, J.Y. Juang, B.L. Young, T. Kobayashi, C.-M. Cheng, C.-H. Chen, K.-D. Tsuei, R. Sankar, F.C. Chou, K.A. Kokh, O. E. Tereshchenko, E.V. Chulkov, Yu.M. Andreev, G.D. Gu, *Nano Letters*, **13** (2013) 5797-5802.

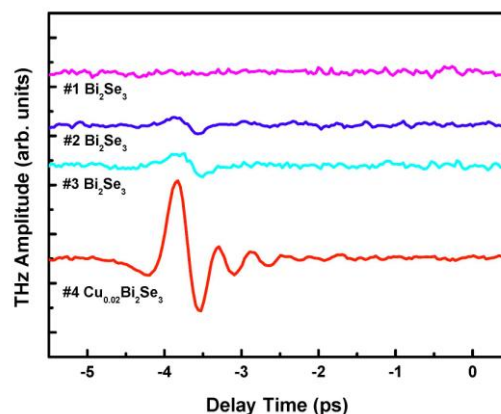


Fig. 1. THz waveform generated from various Bi₂Se₃ and Cu_{0.02}Bi₂Se₃ single crystals.

3OR-LT-3

EVOLUTION OF MAGNETISM IN Co SUBSTITUTED FeGa₃ PROBED BY NUCLEAR MAGNETIC RESONANCE

Gippius A.A.^{1,2}, *Verchenko V.Yu.*³, *Tkachev A.V.*^{1,2}, *Gervits N.E.*², *Lue C.S.*⁴,
*Buettgen N.*⁵, *Kraetschmer W.*⁵, *Baenitz M.*⁶, *Shevelkov A.V.*³

¹ Department of Physics, Moscow State University, 119991, Moscow, Russia

² A.V. Shubnikov Institute of Crystallography, 119333, Moscow, Russia

³ Department of Chemistry, Moscow State University, 119991, Moscow, Russia

⁴ Department of Physics, National Cheng Kung University, 70101, Tainan, Taiwan

⁵ Experimental Physics V, University of Augsburg, 86159, Augsburg, Germany

⁶ Max Planck Institute for Chemical Physics of Solids, 01187 Dresden, Germany
gippius@mail.ru

Solid solutions based on FeGa₃ attracted much interest because of their prospective thermoelectric applications and an intriguing low-temperature magnetic behavior. The parent binary compound FeGa₃ is a rare representative of non-magnetic and semiconducting Fe-based intermetallic compounds akin to the small gap semiconductors FeSi and FeSb₂ [1,2]. Solid solutions Fe_{1-x}Co_xGa₃ exhibit a metal-insulator transition at $x \sim 0.025$. Our *ab-initio* band structure calculations have shown that Co doping shifts the Fermi level position within conduction band enabling precise tuning of the power factor $PF = S^2\sigma$ [3].

Spin-lattice relaxation (SLR) $1/T_1$ of ^{69,71}Ga nuclei was investigated in the temperature range 2 - 300 K for compounds with $x = 0.0, 0.5$ and 1.0 .

In the parent compound FeGa₃ the ^{69,71}Ga spin-lattice relaxation rate $1/T_1(T)$ reveals an unexpected huge maximum at low T with an essentially magnetic relaxation mechanism indicating the existence of the in-gap states. The opposite end member, CoGa₃, is a band metal. It demonstrates the metallic Korringa behavior of the spin-lattice relaxation with $1/T_1 \sim T$. In the intermediate Fe_{0.5}Co_{0.5}Ga₃ compound $1/T_1(T)$ is strongly (by ~ 2 orders) enhanced due to spin fluctuations with $1/T_1 \sim T^{1/2}$ in perfect agreement with Moriya's spin-fluctuation theory for itinerant magnetic systems [4]. Such a SLR behavior is a unique feature of weakly and nearly AF metals. The Fe_{1-x}Co_xGa₃ compounds with $x \sim 0.5$ seem to be very close to magnetic ordering which is prohibited probably by strong spin fluctuations and structural disorder in T-T dumbbells (T=Fe, Ga).

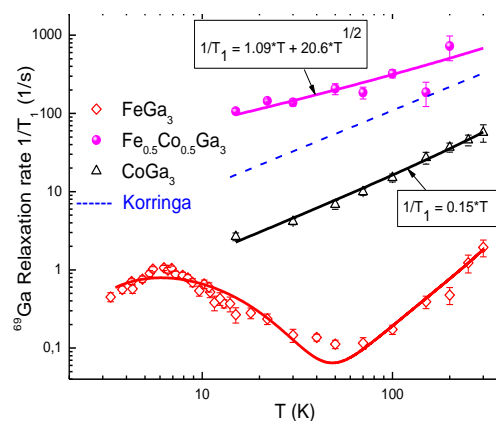


Fig. 1. ⁶⁹Ga SLR $1/T_1$ for FeGa₃, CoGa₃ and Fe_{0.5}Co_{0.5}Ga₃.

Support by RFBR Grants 12-03-92002-NSC_a and 14-03-31181 is acknowledged.

[1] D. Mandrus et al., *Phys. Rev. B*, **51** (1995) 4763.

[2] C. Petrovic, J. W. Kim, et al. *Phys. Rev. B*, **67** (2003) 155205.

[3] V.Yu. Verchenko, et al., *Journal of Solid State Chemistry*, **194** (2012) 361-368.

[4] T. Moriya, *JMMM*, **14** (1979) 1.

3OR-LT-4

THE THEORY OF CHARGE TRANSPORT EXPERIMENTS FOR DETERMINING OF THE ORDER PARAMETER SYMMETRY IN MULTIORBITAL SUPERCONDUCTORS.

Devyatov I.A.¹, Burmistrova A.V.^{1,2}

¹ Lomonosov Moscow State University Skobeltsin Institute of Nuclear Physics, Moscow, Russian Federation

² Moscow State Pedagogical University, Moscow, Russian Federation
igor-devyatov@yandex.ru

Investigations of the charge transport in contacts with unusual superconductors allows to obtain the crucial information about the type of symmetry of the order parameter in them. Type of the symmetry of the order parameter in unusual superconductor sheds light on the type of superconducting pairing in them. Many new unusual superconductors, such as Fe-based superconductors (FeBS), Sr_2RuO_4 , doped superconducting insulators $\text{Cu}_x\text{Bi}_2\text{Se}_3$, are multiband metals with several bands, which intersect their Fermi surface. However, there is currently no consistent theory of coherent charge transport in contacts with them.

In this paper, we present a consistent microscopic theory of charge transport in contacts of multiband superconductors with a normal metal and an usual s-type superconductor and break junctions. In our calculations we for the first time take into account crystal structure of multiband superconductors, the size of the Fermi surfaces, sign-changing and an anisotropy of the order parameter, the misorientation angle of the boundary, as well as interband and intervalley scattering at the interface. Our general theory we apply to a specific analysis of the charge transport in contacts with FeBS, described by the two-orbital model, with a possible s_{++} , s_{+-} symmetry of the order parameter in them.

As a result of microscopic calculations, we demonstrated the ability to distinguish between the symmetry of the order parameter in FeBS in above-listed tunneling experiments. We demonstrate that in experiments on tunneling transport in S_p -I-N (FeBS-Insulator-Normal metal) contacts it is necessary to use contacts with transport in the a-b plane with zero angle of misorientation and a large Fermi surface of a normal metal (N) [1]. In such experiments s_{++} and s_{+-} symmetry of the order parameter in FeBS can be distinguished by the presence or absence of undergap features. In Josephson experiments to distinguish the symmetry of the order parameter of FeBS should be used S-I- S_p (usual s-type Superconductor-Insulator-FeBS) contacts with transport in c direction with a large Fermi surface of usual s-type superconductor (S). We demonstrate that it is necessary to investigate the difference between current-phase relations of S-I- S_p Josephson junctions with and without long oxide layer. We demonstrate that in order to distinguish the symmetry of the order parameter in FeBS it is necessary to investigate break junctions with transport the a-b plane.

The suggested approach can be applied for the theoretical investigation of current transport in structures with mysterious Majorana fermions.

Support by the Russian Foundation for Basic Research, projects N 13-02-01085-a, 14-02-31366-mol_a and by the Ministry of Education and Science of the Russian Federation is acknowledged.

[1] A.V. Burmistrova, I.A. Devyatov, A.A. Golubov *et al.*, *J. Phys. Soc. Jpn.*, **82** (2013) 034716.

3OR-LT-5

THE MICROSCOPIC INVESTIGATION OF THE ELECTRON COHERENT TRANSPORT IN STRUCTURES, CONTAINING MULTIBAND SUPERCONDUCTORS

Burmistrova A.V.^{1,2}, Devyatov I.A.¹

¹ Scobeltsyn Institute of Nuclear Physics Lomonosov Moscow State University, Moscow, Russia

² Moscow State Pedagogical University, Moscow, Russia

burmangelina@gmail.com

Determination of the symmetry of the order parameter of new unconventional superconductors is one of the very important tasks after their discovery, because the type of the symmetry of the order parameter in them contains an important information about the mechanism of superconducting pairing. The phase-coherent tunneling experiments, such as experiments to study current-voltage characteristics of a junction of a normal metal with a new superconductor or experiments on the Josephson tunneling in superconducting junction with a new superconductor, provide a necessary information about the symmetry of the order parameter in them [1]. The common property of many new unusual superconductors as Sr₂RuO₄, Fe-based superconductors (FeBS), doped superconducting insulators Cu_xBi₂Se₃ is that all of them are multiband metals with several bands which intersect a Fermi surface. Thus, it is necessary to create a consistent microscopic theory of charge transport in structures with multiband materials.

Microscopic theory of dc Josephson current in contacts between multiband superconductor with unusual type of the symmetry of the order parameter (FeBS or Sr₂RuO₄) and spin-singlet s-wave superconductor was created. The basis of the method is the construction of a coherent temperature Greens function of the system in the framework of the tight-binding model. The phase dependencies of the Josephson current for different directions of current relative to the crystallographic axes of multiband superconductor and different length of an insulator layer and temperature dependencies of the critical Josephson current were calculated. The obtained results allow to formulate the ultimate experiment to determine the symmetry of the order parameter in Fe-based superconductors and in Sr₂RuO₄.

This work was supported from the Russian Foundation for Basic Research, project N 13-02-01085 and N 14-02-31366 and partly supported by the Ministry of Education and Science of the Russian Federation, contract N 14.B25.31.0007 of 26 June 2013.

[1] D. A. Wollman, D. J. Van Harlingen, W. C. Lee, D. M. Ginsberg, and A. J. Leggett, *Phys. Rev. Lett.* **71**, 2134 (1993).

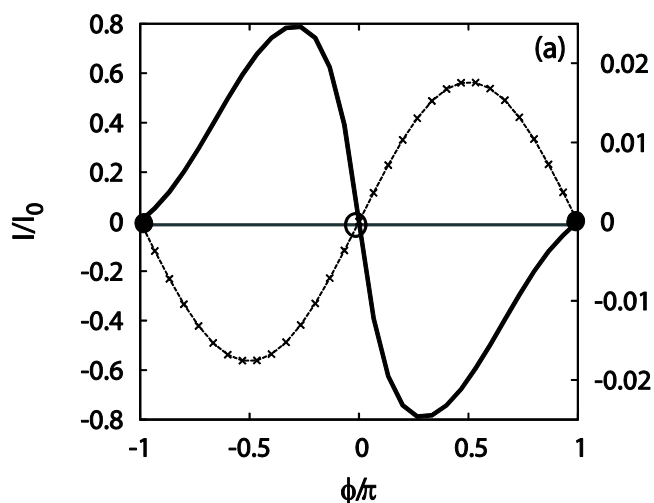


Fig. 1. The phase dependencies of the Josephson current in the S/I/Sp junction along z-axis for s+_z model of the superconducting pairing in FeBS. Solid line and left axis correspond to atomically sharp boundary, line with crosses and right axis correspond to the case of insulating layer containing N = 3 atoms,

3OR-LT-6

Fe-BASED HTSC: MAGNETIC (AF SDW) PHASE TRANSITION, PRECEDING SC ONE. UPPER CRITICAL MAGNETIC FIELD $H_{c2}(0)$

*Mazov L.S.*¹

¹ Institute for Physics of Microstructures RAS, Nizhny Novgorod 603600 Russia
mazov@ipm.sci-nnov.ru

The parent, undoped Fe-based compounds exhibit the magnetic (AF SDW) phase transition at $T \sim 140$ K, depending on compound. On the other hand, in literature there are often claimed that at doping this transition disappears and is replaced by transition to superconducting (SC) state. Such conclusion permits consider Fe-based HTSC as systems with only SC order parameter(s) when magnetic phase (H - T) diagram comprises only two characteristic regions: SC and normal-state ones. Moreover, at present, these compounds are considered as most prospective for high-field applications since value of their upper critical magnetic field $H_{c2}(0)$ (in geometry $H // c$) is claimed in literature as essentially high.

There, it is demonstrated that SC transition in Fe-based HTSC is preceded by in-plane magnetic phase transition from spin-disordered state to the state of modulated magnetic structure (like spin density wave (AF SDW)). This normal-state transition occurs in temperature region of pseudogap regime ($T_c(H) < T < T^*(H)$). Such conclusion is obtained on the basis of detailed analysis of magnetoresistive data for perfect single crystals of Fe-based HTSC (see, e.g. Fig.1). In transverse magnetic field ($H // c$) the resistive transition in Fe-based HTSC is broadened and the “shoulder” (“kink”) appears at resistive transition curve $\rho(T)$. As its seen from Fig.1, these “shoulder” points fall exactly at some regular curve (dashed curve), which (as follows from analysis performed) follows the Bloch-Gruneisen curve, which, as known, is characteristic for resistive contribution $\rho_{ph}(T)$ due to phonon scattering of mobile charge carriers (MCC) in most metals, including magnetic ones (here estimated Debye temperature $\theta_D \sim 270$ K). (At this analysis, the residual contribution $\rho_{res}(T)$ (dash-dotted line) to the total resistivity $\rho(T)$ was subtracted). From such a picture, it follows that shaded part of resistivity above the dashed curve corresponds to the scattering of MCC via AF spin fluctuations, persisted in the system under doping, i.e. it is the magnetic contribution $\rho_m(T)$ to resistivity. (Note that such decomposition procedure of resistivity is usual for magnetic metals). Similar decomposition was performed also for in-plane $\rho(H)$ curves [1].

The results demonstrate that disappearance of $\rho_m(T)$ in “shoulder” points indicates to formation AF SDW-like order in the system. On the other hand, these points correspond to the onset of SC transition and being plotted at (H, T)-plane form a dependence $H_{c2}(T)$, which appears to be linear in as in BCS and GL theories. The value of $H_{c2}(0)$ being estimated in parabolic approximation is of the order of only 25 T rather than ~ 70 T, claimed in literature. It is here demonstrated that 70 T corresponds rather to the $H^*(0)$, characteristic for magnetic (AF SDW) phase transition. The comparison with theory of metal-insulator transition and with picture for cuprates is performed.

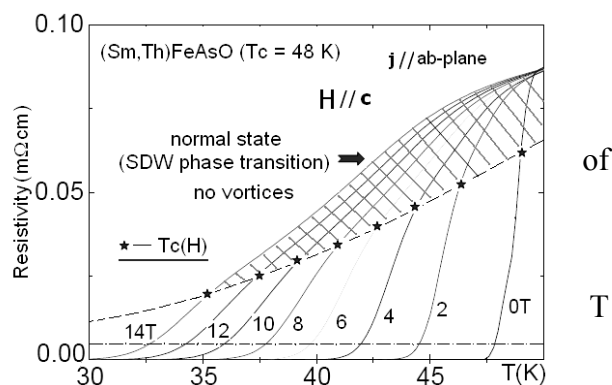


Fig.1. The in-plane resistivity vs. T [1].

[1] L.S. Mazov, *J. Supercond. Nov. Magn.*, **27** (2014) (in press, April).

3OR-LT-7

COLLECTIVE SPIN EXCITATIONS IN HTSC CUPRATES. THEORY AND NMR, NEUTRON AND RIXS DATA

Eremin M.V., Shigapov I.M.

Institute of Physics, Kazan Federal (Volga region) University, Kazan, Russia
meremin@kpfu.ru

Starting from the generalized t-J-G model, we analyze the dynamical spin susceptibility of superconducting cuprates taking into account both local and itinerant spin components which are coupled to each other self-consistently. Dispersion of collective spin excitations were calculated as a solution to the equation: the denominator of the dynamical spin susceptibility is equal to zero. Frequency plots along the route $(0,0) - (0,\pi) - (\pi,\pi) - (0,0)$ in the Brillouin zone for the normal state (dashed line) and superconducting one (solid line) are displayed in Fig. 1. Tight-binding parameters and Fermi surface were taken in accordance with the angle-resolved photoemission spectroscopy data.

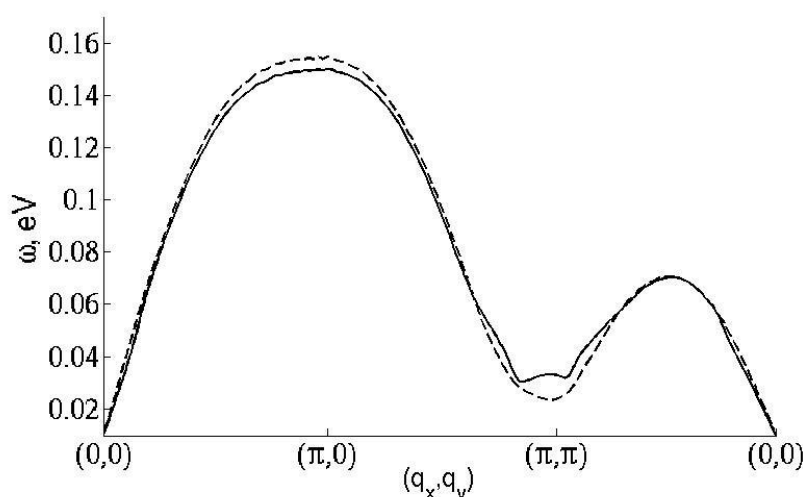


Fig. Collective spin excitation spectra along triangle contour in Brillouin zone.

Intensity plot of the imaginary part along this contour shows a strong maximum near (π,π) point. This result corresponds to neutron scattering data. Up-ward dispersion can be interpreted in favor of magnon-like excitations, but these excitations are freezing out inside the superconducting gap at $T < T_c$. The so-called hour-glasses picture is reproduced successfully [1]. It is formed as result of competition between spin-gap in magnon-like excitations spectrum and superconducting gap. The calculated frequencies along the line $(0,0) - (0,\pi)$ are in agreement with positions of the absorption peaks in the spectra of inelastic x-rays scattering. We also find that the imaginary part of susceptibility along the $(0,0) - (0,\pi)$ direction shows an additional splitting, which is enhanced at $T < T_c$. This observation strongly supports the idea that this branch of spin excitations is rather paramagnon-like mode related to itinerant spin subsystem than magnon-like excitations, which is originates from short range order effect in subsystem of local spins at Cu sites.

Support by RFBR Grant 13-02-00492_a is acknowledged.

[1] M. V. Eremin, I. M. Shigapov, Ho Thi Duen Thuy, *J. Condens. Matter*, **25** (2013) 345701.

3OR-LT-8

**ENHANCED FRACTIONAL MATCHING IN SUPERCONDUCTING FILM
WITH A SQUARE LATTICE OF ANTIDOTS***Kamran M.^{1,2}, He S.K.¹, Qiu X.G.¹*¹ Beijing National laboratory of Condensed Matter physics, Institute of physics, Chinese Academy of Sciences P. O. Box 603, Beijing 100190, PRC² Department of Physics, COMSATS Institute of Information Technology, Islamabad, Pakistan
muhammad_kamran@comsats.edu.pk

Nano engineered square antidot array has been fabricated over a micro-bridge of NbN superconducting thin film by electron beam lithography and lead to vortex matching phenomena at commensurate fields. The strength of the vortex pinning depends on the geometrical characteristics of the antidote lattice, coherence length and penetration depth. In this experiment there are two scenarios, multi integer and enhanced fractional matching fields. These integer and enhanced fractional matching fields are temperature and current dependent. Sharp peaks are observed at integer matching fields, first to sixth order and enhanced fractional matching fields, including $1/2$, $1/3$, $2/3$, $3/2$, $5/2$etc, appear first integer matching field to 6th order integer matching field. We present our experimental results on superconducting Nb film antidot arrays.

3TL-LT-9

MAGNETIC PROPERTIES OF FeSe(Te) SUPERCONDUCTORS: PRESSURE EFFECTS

*Grechnev G.E.¹, Panfilov A.S.¹, Pashchenko V.A.¹, Fedorchenko A.V.¹, Desnenko V.A.¹,
Gnatchenko S.L.¹, Chareev D.A.², Mitrofanova E.S.³, Volkova O.S.^{3,4}, Vasiliev A.N.^{3,4}*

¹ B.Verkin Institute for Low Temperature Physics, National Academy of Sciences of Ukraine,
Kharkov 61013, Ukraine

² Institute of Experimental Mineralogy, Russian Academy of Sciences, Chernogolovka, Moscow
District 142432, Russia

³ Faculty of Physics, Moscow State University, Moscow 119991, Russia

⁴ Theoretical Physics and Applied Mathematics Department, Ural Federal University, Ekaterinburg,
620002, Russia
grechnev@ilt.kharkov.ua

For the most families of recently discovered Fe-based superconductors the emergence of superconductivity with doping or under pressure is accompanied by suppression of the magnetic ordering. It is also believed that spin fluctuations play an important role in formation of the Cooper pairs. So the close interplay of magnetism and superconductivity determines the importance of further studying of magnetic and superconducting properties and their evolution under variations of composition, pressure, etc. for understanding superconducting mechanism in the new class of iron compounds. One of representatives of this class is the system of FeSe_{1-x}Te_x chalcogenides, which possesses the simplest crystal structure among iron-based superconductors, that favors to studying the effects of chemical substitution and high pressures on its properties. Here we present the results of the experimental study of magnetic properties of FeSe_{1-x}Te_x superconductors ($0 \leq x \leq 1$), which were supplemented by appropriate *ab initio* DFT calculations of the electronic structure and magnetic characteristics of the system.

Magnetic susceptibility χ of FeSe_{1-x}Te_x superconductors was studied in the normal state at temperatures up to 300 K and appeared to increase gradually with Te content by about ten times. The calculated values of χ for FeSe, FeTe and FeSe_{0.5}Te_{0.5} compounds support basically the itinerant nature of their magnetism closely related to magnetic instability. For parent compounds Fe_{1+y}Te in AFM state below $T \approx 70$ K, the measured value of magnetic anisotropy $\Delta\chi = \chi_{\parallel} - \chi_{\perp}$ was found to be the same in magnitude but different in sign depending on the small variations of the excess iron y in Fe_{1+y}Te samples. Our *ab initio* calculations of electronic structure and magnetic susceptibilities of AFM FeTe have revealed a possibility of frustrated AFM orderings of Fe moments along [100] and [001] axes, which would explain the observed peculiarity.

Magnetic susceptibility of parent compounds FeSe and FeTe was also studied in the normal state under pressures, and at $T = 78$ K a large *positive* pressure effect was observed for both compounds. The calculated strong dependence of χ on the structural parameters – volume V and especially the height Z of chalcogen species from the Fe plane – allowed to explain the puzzling pressure effects on χ in terms of the $V(P)$ and $Z(P)$ dependences, the latter determines the dominating positive contribution.

The influence of pressures on the superconducting transition temperature T_c was studied for FeSe_{1-x}Te_x system. For the first time, we observed a change in sign of the pressure effect on T_c when going to tellurium rich FeSe(Te) alloys. Comparison of the observed results with our experimental and calculated data on pressure dependence of χ for FeSe(Te) systems in the normal state demonstrates a competing interplay between superconductivity and magnetism in tellurium rich FeSe_{1-x}Te_x compounds.

3 July

Thursday

11:30-13:15

oral session

3TL-C

3RP-C

3OR-C

“Magnetophotonics”

3RP-C-1

MAGNETIC RAMAN SCATTERING IN NICKEL BORATE $\text{Ni}_3\text{B}_2\text{O}_6$ Pisarev R.V.¹, Davydov V.Yu.¹, Smirnov A.N.¹, Babkin R.Yu.², Pashkevich Yu.G.²¹ Ioffe Physical-Technical Institute, Russian Academy of Sciences, St. Petersburg, Russia² A.A. Galkin Donetsk Phys.-Tech. Institute, NAS of Ukraine, Donetsk, Ukraine
pisarev@mail.ioffe.ru

Nickel orthoborate $\text{Ni}_3\text{B}_2\text{O}_6$ crystallizes in the orthorhombic space group $Pn\bar{m}n$ (#58, $Z=2$) where Ni^{2+} ions ($S=1$) occupy two types of non-equivalent positions $2a$ and $4f$ in the unit cell with the parameters $a(x)=5.396$, $b(y)=8.297$, $c(z)=4.459$ Å [1]. Ni^{2+} spins order antiferromagnetically below the Néel temperature $T_N=46$ K and recent measurements on single crystals showed strong anisotropy of the magnetization with the spins oriented along the y -axis [2]. In this talk we present results of our investigation of magnetic Raman scattering in $\text{Ni}_3\text{B}_2\text{O}_6$. Single crystals were grown by a gas-transport method in evacuated quartz ampoules and had dimensions up to $2 \times 1 \times 4$ mm³. Raman spectra were measured in the range from 10 to 300 K in the back-scattering configuration with all geometry/polarization settings being applied.

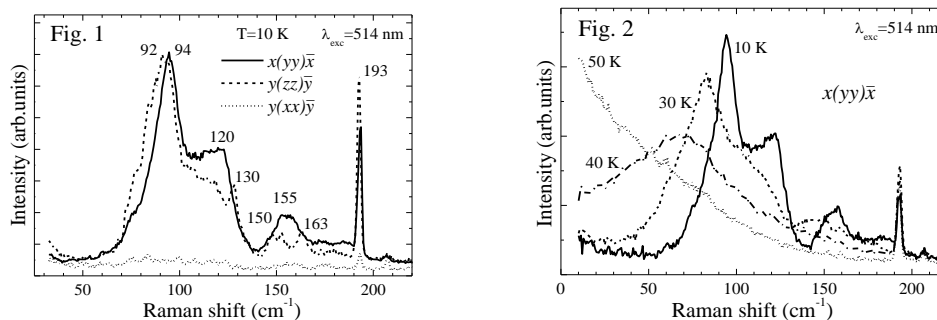


Figure 1 shows the low-frequency Raman spectra at $T=10$ K for the three main diagonal polarizations. A 193 cm⁻¹ feature is attributed to the lowest frequency phonon mode. Below this mode no features were observed in the (xx) -polarization at low temperature. In contrast, strong scattering signals of complicated structure were observed in the (yy) - and (zz) -polarizations in the range up to ~ 200 cm⁻¹. Undoubtedly, the scattering features must be attributed to the magnetic Raman scattering though they radically differ from the magnetic scattering spectra previously observed [3,4]. Our assignment is strongly supported by the temperature dependence measurements shown in Fig. 2. When approaching $T_N=46$ K from below the scattering features experience frequency shift, become broader, and finally in the close vicinity of T_N the broad band with a maximum disappears. However, a magnetic “inelastic tail” survives in the range up to 180 cm⁻¹ gradually decreasing in intensity and remaining observable up to about 180 - 200 K.

The polarization of the scattering spectra evidences highly anisotropic nature of magnetic excitations in $\text{Ni}_3\text{B}_2\text{O}_6$ which we relate with the quasi-chain atomic structure along the x -axis with the spins oriented perpendicular to the chains. The broad and gap-like maxima can be assigned with two-magnon scattering processes which involve the so called “optic magnons” [3]. Such excitations are intrinsic for ions with $S=1$. Our conclusions are based on characteristic temperature dependences and theoretical estimates of the energies of the observed features.

Support by the Russian Ministry of Education and Science (project 14.B25.31.0025) and a partial support by the RFBR (project 12-02-00130a) are acknowledged.

[1] H. Effenberger und F. Pertlik, *Zeit. Krist.*, **166** 129 (1984).

[2] L.N. Bezmaternykh, S.N. Sofronova, *et al.*, *Phys. Stat. Solidi B*, **249** (2012) 1628.

[3] M.G. Cottam and D.J. Lockwood, *Light Scattering in Magnetic Solids*, Wiley (1986).

[4] P. Lemmens, G. Güntherodt, and C. Gros, *Phys. Rep.*, **375** (2003) 1.

3TL-C-2

OPTICAL CONTROL AND DETECTION OF THREE DIMENSIONAL MAGNETIC OSCILLATIONS IN YMnO_3

Satoh T.¹

¹ Department of Physics, Kyushu University, Fukuoka, Japan
satoh@phys.kyushu-u.ac.jp

We demonstrate optical control and detection of three magnetic oscillation modes, where modes and initial phases of the oscillations are independently triggered and measured by tailoring optical polarization states in a pump-probe measurement. Two in-plane modes and an out-of-plane mode (Fig. 1) are triggered by linearly and circularly polarized light pulses via the inverse Cotton-Mouton effect and the inverse Faraday effect, and detected by circularly and linearly polarized ones via the Cotton-Mouton effect and the Faraday effect, respectively, in a hexagonal antiferromagnet YMnO_3 with three-sublattices. The control and detection represent a bijection of quantum information from polarization of pump pulse to magnetic oscillation and toward polarization of probe pulse. Also, the two-dimensional vector control of magnetic oscillation of YMnO_3 was realized by a pair of optical pulses with different polarizations.

This work has been performed in collaboration with R. Iida, T. Higuchi, M. Fiebig, and T. Shimura. Support by JST-PREST and KAKENHI (23104706) is acknowledged.

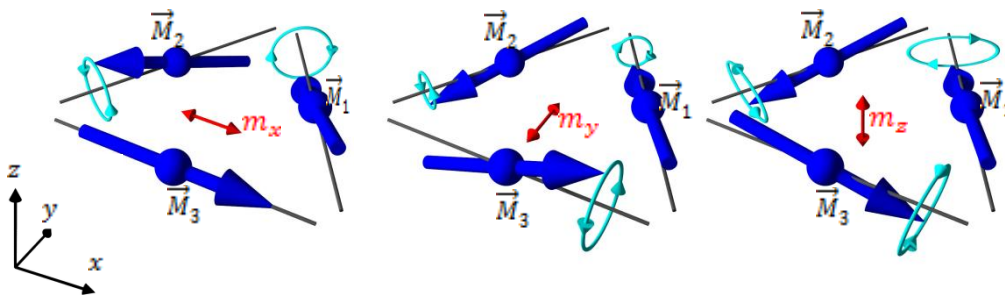


Fig. 1. Magnetic oscillation eigenmodes in YMnO_3 .

3OR-C-3

EFFECTS OF CRYSTALLOGRAPHIC BIREFRINGENCE ON ULTRAFAST LASER-INDUCED SPIN DYNAMICS

de Jong J.A.¹, Kalashnikova A.M.², Pisarev R.V.², Balbashov A.M.³, Kirilyuk A.¹, Kimel A.V.¹, Rasing Th.¹

¹ Radboud University Nijmegen, IMM, Nijmegen, The Netherlands

² Ioffe Physical Technical Institute, St. Petersburg, Russia

³ Moscow Power Engineering Institute, Moscow, Russia

kalashnikova@mail.ioffe.ru

Magneto-optical pump-probe techniques have become a primary tool for studying spin dynamics induced by femtosecond laser pulses and the further progress in this field of research relies to the great extent on correct interpretation of the results of such experiments. In typical experiments, detailed information about the response of the spin system to the pump pulse is obtained from changes of the probe pulse polarization. However, since most solids possess one or another type of optical anisotropy, the polarization of the probe pulse propagating through the medium excited by the pump pulse can experience additional changes due to circular or linear birefringence effects not related to the changes in magnetic ordering. The situation becomes even more intricate when the excitation of the spin system depends on the pump pulse polarization. There have been a few attempts to tackle the problem of adequate interpretation of the results of the pump-probe experiments in an anisotropic medium, however effects of optical anisotropy on the polarization state of either pump or probe pulses were considered separately so far [1,2].

We have studied experimentally and by means of calculations the laser-induced spin dynamics in single-crystal orthoferrites ($\text{Sm}_{0.5}\text{Pr}_{0.5}\text{FeO}_3$ and $(\text{Sm}_{0.55}\text{Tb}_{0.45})\text{FeO}_3$), possessing weak and strong crystallographic linear birefringence, respectively. The coherent spin precession has been excited either via a laser-induced spin-reorientation phase transition, independent on the pump polarization [3], or via the ultrafast inverse Faraday effect (IFE), sensitive to the helicity of the pump pulses [4]. The excited precession has been detected by measuring the rotation of the probe pulse polarization in both cases. In the case of spin precession excited due to a spin reorientation phase transition the probe polarization rotation was found to be significantly reduced in the sample with strong birefringence. Surprisingly, the probe polarization rotation due to the spin precession excited via the IFE appeared to be weakly dependent on the birefringence value. We show that the latter results from the fact that, while propagating through the medium, the pump and probe polarizations experience the same changes due to birefringence, which effectively diminishes the influence of the birefringence on the outcome of the experiment [5].

We conclude that an appropriate interpretation of the magneto-optical pump-probe experiments requires taking into account the effects of birefringence on propagation of both pump and probe pulses. Furthermore, the proper choice of pump and probe wavelength ensures similar birefringence values and thus allows suppressing the obscuring effects of birefringence on the experimental results. This should be taken into account especially in experiments performed in the vicinity of optical absorption resonances, where birefringence exhibits strong dispersion.

Partial support by FOM, NWO, ERC, EU FP7 (Femtospin and IFOX) is acknowledged. A.M.K. and R.V.P. thank the Russian Government (grant #14.B025.0031.25) and RFBR for a support.

[1] S. R. Woodford *et al.*, *J. Appl. Phys.*, **101** (2007) 053912.

[2] R. Iida *et al.*, *Phys. Rev. B*, **84** (2011) 064402.

[3] A. V. Kimel *et al.*, *Nature*, **429** (2004) 850.

[4] A. V. Kimel *et al.*, *Nature*, **435** (2005) 655.

[5] J. A. de Jong *et al.*, *in preparation*.

3OR-C-4

FEMTOSECOND PHOTO-INDUCED PHENOMENA IN MULTIFERROIC HEXAGONAL MANGANITE YMnO_3

Pavlov V.V.¹, Gridnev V.N.¹, Pisarev R.V.¹, Pohl M.², Akimov I.A.^{1,2}, Yakovlev D.R.^{1,2}, Bayer M.²

¹Ioffe Physical-Technical Institute, Russian Academy of Sciences, St. Petersburg, Russia

²Experimental Physics 2, Technical University, Dortmund, Germany

pavlov@mail.ioffe.ru

Ultrashort pulsed lasers have opened new opportunities for implementing high-speed control of electronic and spin states in matter [1, 2], which is important for applications in fields as diverse as information processing, optoelectronics and spintronics.

The hexagonal manganite YMnO_3 is a multiferroic binary oxide with ferroelectric Curie temperature $T_C = 913$ K and antiferromagnetic Néel temperature $T_N = 75$ K. We report on transient optical anisotropy in the hexagonal manganite YMnO_3 excited by linearly and circularly polarized laser pulses in the temperature region 10-300 K. The transient optical anisotropy was studied by a pump-probe technique based on a femtosecond Ti:sapphire laser generating optical pulses at the photon energy of 1.55 eV. Using different transmission filters applied to the laser beam, generated by a liquid crystal pulse shaper, it was possible to cover the photon energy range from 1.460 to 1.636 eV.

Figure 1 shows temporal variations of the photo-induced rotation and ellipticity excited by linearly and circularly polarized laser pulses with 17 and 34 fs duration. These dependencies were analyzed using a theory describing ultrafast population and relaxation processes near the interband transition from the hybridized O-Mn states to the Mn ($3d_{3z^2-r^2}$) at ~ 1.6 eV. Ultrashort relaxation time of ~ 10 fs has been determined solving numerically the optical Bloch equations.

The observed photo-induced phenomena are attributed to the optical alignment and orientation with a Raman coherence time of ~ 10 fs between the excited $\Gamma^5|x\rangle$ and $\Gamma^5|y\rangle$ states and a relaxation time of ~ 500 fs between the $\Gamma^5|x,y\rangle$ and $\Gamma^1|g\rangle$ states for the electronic transition $\Gamma^1 \rightarrow \Gamma^5$ [3]. It is interesting to compare spin relaxation time of 30–50 fs observed in the strongly correlated Mott insulators $R_2\text{CuO}_4$ ($R = \text{Pr}, \text{Nd}, \text{Sm}$) [4]. Relaxation processes in the Mott insulators $R_2\text{CuO}_4$ and hexagonal manganite YMnO_3 are on the same time scale. The observed photo-induced phenomena in the hexagonal manganite YMnO_3 may have a technological potential for novel all-optical devices based on the nonlinear interaction of light.

Supports by the Russian Foundation for Basic Research (13-02-00754), the Government of Russia (14.B25.31.0025) and the Deutsche Forschungsgemeinschaft are acknowledged.

[1] A. J. Ramsay, *Semicond. Sci. Technol.*, **25** (2010) 103001.

[2] A. Kirilyuk, A. V. Kimel, *T. Rasing, Rev. Mod. Phys.*, **82** (2010) 2731.

[3] M. Pohl, V. V. Pavlov, I. A. Akimov, et al., *Phys. Rev. B*, **88** (2013) 195112.

[4] V. V. Pavlov, R. V. Pisarev, V. N. Gridnev, et al., *Phys. Rev. Lett.*, **98** (2007) 047403.

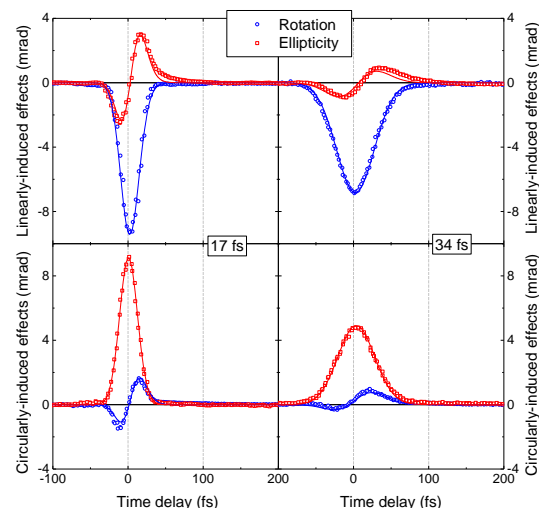


Fig. 1. Photo-induced rotation and ellipticity for linearly and circularly polarized pump excitation at 1.531 eV. Dots are experimental data, lines show theoretical calculations.

3RP-C-5

MAGNETOOPTICAL TIME-RESOLVED STUDY OF Eu^{2+} SPIN DYNAMICS IN $\text{EuFe}_2(\text{As}_{1-x}\text{P}_x)_2$ Pnictide SUPERCONDUCTOR

Pogrebna A.¹, Mertelj T.¹, Vaskivskiy I.¹, Xu Z.A.³, Cao G.³, Mihailovic D.^{1,2}

¹ Complex Matter Department, Jozef Stefan Institute, Jamova 39, SI-1000 Ljubljana, Slovenia

² Center of Excellence on Nanoscience and Nanotechnology – Nanocenter (CENN Nanocenter), Jamova 39, SI-1000 Ljubljana, Slovenia

³ Department of Physics, Zhejiang University, Hangzhou 310027, People's Republic of China
tomaz.mertelj@ijs.si

We investigated temperature and magnetic field dependent photoexcited electron and spin relaxation in $\text{EuFe}_2(\text{As}_{0.81}\text{P}_{0.19})_2$ (EuP-122) pnictide superconductor [1] and parent nonsuperconducting EuFe_2As_2 (Eu-122) by means of optical pump-probe femtosecond spectroscopy.

In both samples we observe an emergence of a slow anisotropic transient reflectivity ($\Delta R/R$) component concurrent with Eu^{2+} spin ordering at $T_N \sim 18$ K, which shows a risetime of ~ 1 ns in Eu-122 and ~ 100 ps in EuP-122. The magnetic field dependence of the slow component in the superconducting EuP-122 is different than in the nonsuperconducting Eu-122. In Eu-122 we observe switching of the in-plane optical-transient anisotropy with increasing magnetic field attributed to a field-induced antiferromagnetic (AFM) to ferromagnetic (FM) phase transition. [2]

In the superconducting EuP-122 a large coherent magnon oscillation is observed in $\Delta R/R$ on the low-field side of a similar metamagnetic transition at $\mu_0 H \sim 0.5$ T. The oscillatory part of $\Delta R/R$ is isotropic in the ab plane. Another mode with higher oscillation frequency is observed in the transient magneto-optical Kerr response measured along the c axis.

The slow risetime of the Eu^{2+} magneto-optical transients indicates that the coupling between the photoexcited quasiparticles in Fe- d derived bands to Eu^{2+} spins is rather weak. The isotropic transient-reflectivity magnon response is discussed in the context of proposed Eu^{2+} -spin orderings. [3]

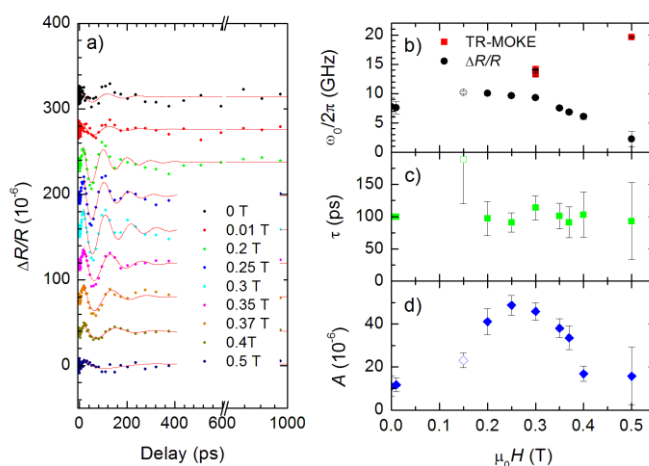


Fig. 1. The oscillatory part of the isotropic $\Delta R/R$ component in EuP-122 at low magnetic fields (a). The frequency (c), decay time (d) and amplitude (e) of the oscillations as functions of the magnetic field. The red squares in (b) are frequencies obtained from TR-MOKE fits.

[1] Z. Ren et al., *Phys. Rev. Lett.*, **102** (2009) 137002.

[2] Y. Xiao et al., *Phys. Rev. B*, **81** (2010) 220406.

[3] I. Nowik, et al., *Journal of Physics: Condensed Matter*, **23** (2011) 065701; S. Zapf et al., *Phys. Rev. B*, **84** (2011) 140503(R); S. Nandi et al., *Phys. Rev. B*, **89** (2014) 014512.

3OR-C-6

HIGH FIELD XMCD STUDIES IN UCoGe FERROMAGNETIC SUPERCONDUCTOR

Taupin M.¹, Brison J.-P.¹, Aoki D.¹, Sanchez J.-P.¹, Wilhelm F.², Rogalev A.²

¹ Univ. Grenoble-Alpes, INAC-SPSMS, CEA Grenoble, France

² European Synchrotron Radiation Facility (ESRF), Grenoble, France

wilhelm@esrf.fr

True coexistence of a homogeneous ferromagnetic state with superconductivity at ambient pressure has been found up to now only in two, strongly correlated, uranium based systems: URhGe and UCoGe. In both systems, the Curie temperature ($T_C = 9\text{K}$ and 2.8K respectively) is higher than the superconducting temperature ($T_S = 0.25\text{K}$ and 0.5K respectively), and the anticipated ordered moment on the uranium is substantially reduced, compared to the free ion U^{3+} or U^{4+} values: $0.4\mu_B$ in URhGe, $0.07\mu_B$ in UCoGe. They are both orthorhombic, with an Ising-like anisotropy of the magnetization, **c** being the easy axis, **a** the hard axis and **b** intermediate. A striking point is the large upper critical field H_{c2} exceeding the Pauli paramagnetic limit, and reaching record values of H_{c2}/T_S [1]. Moreover, when the field is applied very precisely along the **b**-axis, a field re-entrant superconducting phase, with T_S higher than in zero field, appears in URhGe, whereas an unusual S-shaped H_{c2} curve is observed in UCoGe. These phenomena seem to be closely related to the ferromagnetic instabilities, as T_C is reduced under magnetic field and collapses at the enhanced superconducting phase. This suggests a new pairing mechanism, intimately related to the magnetism of the systems.

We have performed a thorough high field XMCD study of magnetic properties on well-characterized high quality single crystal of UCoGe. First we have concentrated on XMCD measurements at the $M_{4,5}$ edges of Uranium and at the K-edge of Co at 3.1 K and 17 Tesla applied along the **c** axis. A sizeable XMCD signal observed at the Uranium M-edges unambiguously confirms that U 5f states are carrying a magnetic moment. Using magneto-optical sum rules we deduce that magnetism of U is dominated by orbital component of $\sim 0.68\mu_B$ at 17 Tesla. The spin component is aligned antiparallel to the orbital one and equals to $-0.29\mu_B$ at 17 Tesla. The total magnetic moment of Uranium 5f states is $0.39\mu_B$ which has to be compared with the total magnetization of $0.44\mu_B$ at 17 Tesla. This observation seems to indicate that Co atoms do not carry a sizeable magnetic moment in UCoGe. This result is confirmed by a rather weak XMCD signal at the Co K-edge. Moreover, its field dependence is following exactly the U magnetization. The results of high field XMCD are nicely confirmed by the measurements performed at 1 Tesla field. The total U 5f magnetization is about $0.075\mu_B$ whereas the total magnetization of the crystal along the **c** axis is equal to $0.08\mu_B$. The ratio of the orbital-to-spin moment is about -2.31 ± 0.03 in both high and low field cases. Secondly, we tried to record XMCD spectra at the Uranium $M_{4,5}$ -edges along the **b**-axis of the crystal. The magnetic moment on Uranium induced by 17 Tesla field, is again dominated by the orbital component of $0.163\mu_B$ whereas the spin moment amounts to $-0.079\mu_B$. The total 5f Uranium moment is only $0.084\mu_B$ which is again of $0.05\mu_B$ smaller than the total magnetization value. Surprisingly, the orbital-to-spin moment along the **b** axis equals to -2.06 which is very much different from the value along the **c** axis. This is the first time that a difference in magnetic anisotropy in actinide compounds manifests itself through huge changes in μ_L/μ_S ratio.

[1] D.Aoki *et al.* *J. Phys. Soc. Japan*, **78** (2009) 113709.

3 July

Thursday

11:30-13:15

oral session

3TL-D

3RP-D

3OR-D

**“Magnetism of
Nanostructures”**

3TL-D-1

2D AND 3D ORDERED ARRAYS OF MAGNETIC NANOWIRES

Prida V.M.¹, García J.¹, Vega V.¹, Rosa W.O.², Caballero-Flores R.¹, Iglesias L.¹, Hernando B.¹

¹ Depto. Física, Universidad de Oviedo, Oviedo, Spain

² Centro Brasileiro de Pesquisas Físicas, Rio de Janeiro, Brazil

vmpp@uniovi.es

Magnetic nanowires and their ordered arrays have gained increasing scientific interest over the last decades due to their exciting magnetic, magneto-optic, magneto-resistive and magneto-thermoelectric properties [1,2]. Template-assisted synthesis methods based on a smart combination of nanoporous alumina membranes together with low-cost electrodeposition techniques have provided a flexible and high yield approach to produce large scale arrangements of magnetic nanowires with tuneable geometrical parameters, such as their diameter and length, composition, multisegmented structure and symmetry of the ordered arrays. Furthermore, the development of heterogeneous nanostructured materials as multi-layers or core-shell structures also allows us to modify its physicochemical properties, which is relevant in many fields as opto-electronics and magnetic materials research. While planar arrays of nanowires are ideal systems to study magnetic phenomena at the nanoscale, other geometries like cylindrical arrays of magnetic nanowires surrounding a conductive/non-magnetic core lead to a 3D spatial arrangement of nanowires, which can be of great interest for applications based in magneto-transport, electromagnetic filters at microwave antennas, magnonics, etc. An accurate control of the nanowire arrangements allows tuning the effective magnetic anisotropy and thus the overall magnetic behaviour of the nanowire array. The use of different alloys and/or heterostructures offers an additional strategy to modify the magnetic response of the nanowires. In this regard, electroplating of Co-based alloys enables to control the crystalline structure by adjusting the electrodeposition conditions and tuning the magneto-crystalline anisotropy between that of fcc or hcp structures, thus counterbalancing the shape anisotropy of the nanowires [3,4].

Here we provide a comprehensive review on both planar (2D) and cylindrical (3D) arrays of nanowires with different compositions based on ferromagnetic transition metal alloys and heterogeneous structures. The main magnetic features are discussed from hysteresis loop measurements, and First Order Reversal Curve (FORC) analysis, being correlated with the crystallographic and morphologic characterization.

Support by MINECO under research project MAT-2010-20798-C05-04 is acknowledged

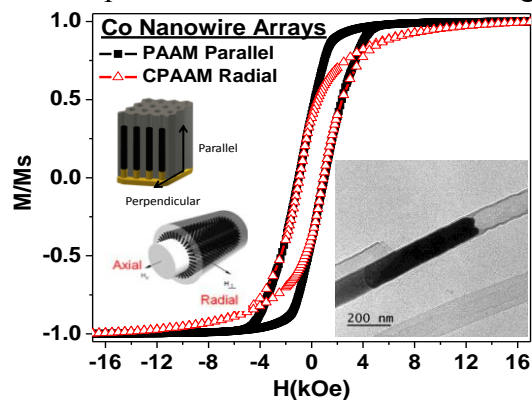


Fig. 2. Magnetic hysteresis loops of 2D and 3D arrays of Co nanowire. Inset shows a TEM image of a Co nanowire.

- [1] J.B. González-Díaz, et al., *Adv. Mater.*, **19** (2007) 2643-2647.
- [2] T. Böhnert, et al., *Appl. Phys. Lett.*, **103** (2013) 092407.
- [3] W.O. Rosa, et al., *J. Magn. Magn. Mater.*, **324** (2012) 3679.
- [4] V. Vega, et al., *Nanotechnology*, **23** (2012) 465709.

3TL-D-2

**MICRO-MAGNETIC PROPERTIES OF FEPT NANO-DOTS
PATTERNED WITH SELF-ASSEMBLED POLYMER MASK***Kikitsu A., Maeda T., Yamamoto R., Kamata Y.*

Toshiba Corp., Corp. R&D Center, Kawasaki, Japan

akira.kikitsu@toshiba.co.jp

Promising candidate for future high-density magnetic recording media is a bit-patterned media (BPM), where isolated magnetic dots are aligned precisely as data bits and servo control bits [1]. Challenging issues for BPM are fabrication process and a reduction of switching field distribution (SFD). For the fabrication process, a directed self-assembly (DSA) process, where self-assembled di-block copolymer is used as an etching mask, was developed [2, 3]. A BPM made of FePt ordered phase with feature size of 12nm-pich (5 Tdots/in^2) was successfully fabricated. However, the SFD of the FePt-BPM was far beyond the system specification. In this paper, micro-magnetic properties of the FePt dots were investigate to reduce SFD.

Details of the fabrication process are shown in the previous papers [2, 3]. Film stack was NiTa (25nm) / Cr (5nm) / Pt (10nm) / Fe₅₀Pt₅₀ (5nm) / C (5nm). Substrate was heated at about 250 C during FePt deposition. Polystyrene (PS) – polydimethylsiloxane (PDMS) was used as a self-assembled etching mask. PDMS dot pattern was transferred to a carbon hard mask with RIE, and FePt layer was etched with Ar ion milling. SFD was estimated using the delta-theta method.

Figure 1 shows an angle dependence of switching field for FePt BPM and CoPt BPM fabricated with similar PS-PDMS mask. CoPt BPM shows the coherent motion type angle dependency, which is typical for ideal isolated magnetic dots. On the other hand, FePt BPM shows domain wall (DW) motion type regardless of the dot size. A dark field TEM analysis revealed that a portion of FePt dots was disordered phase. This means that the anisotropy energy is partially reduced to almost zero. Micro-magnetic simulation revealed that this situation resulted in a reduction in switching field and DW motion type angle dependency. Non-uniform etching damage caused such a disordered portion and gave large SFD. Crystal orientation of ordered FePt also had distribution (delta-theta-50 was 6.9 deg.), though no in-plane hysteresis loop was observed. This easy axis distribution may also contribute to the large SFD.

3RP-D-3

NUCLEAR RESONANCE REFLECTIVITY FOR DEPTH-RESOLVED SPIN REORIENTATION STUDY IN $[\text{Fe}/\text{Cr}]_n$ MULTILAYERS

Andreeva M.A.

Faculty of Physics, M.V. Lomonosov Moscow State University, Moscow, Russia
Mandreeva1@yandex.ru

Layer-by-layer magnetization reorientation in antiferromagnet/ferromagnet [F/AF] multilayers under the external field application has been extensively treated theoretically [1-3] but has not yet got a reliable experimental prove [4-6]. Nuclear resonance reflectivity (NRR) is the most advanced method for such investigations supplying the depth resolution less than 1 nm and exclusive sensitivity to the magnetic hyperfine field values and orientation [7].

Our experiment was carried out for $^{57}\text{Fe}/\text{Cr}]_n$ samples at Japanese synchrotron SPring-8 [8]. At each step of the gradually increasing external field the measurements of the delayed reflectivity curves and time spectra of reflectivity have been performed. The data treatment has been done by our REFTIM program package [9]. The measured time spectra of reflectivity are quite different at different Bragg angles. The fit gives the depth profiles of the hyperfine field values and its orientation \mathbf{B}_{hf} . We prove that the partially coherent averaging over surface domains can explain the results of the preferable orientation of magnetic in the absence of the external field. The pronounced superstructure maxima (1/2 and 3/2) are observed on the delayed NRS reflectivity curves. That confirms the doubling of the magnetic period. At the external field about 600 Oe these magnetic maxima show the decrease in the L-geometry, but the essential increase in the T-geometry. Qualitatively it means that the magnetization rotates perpendicularly to the external field. However, the fit of the time spectra of reflectivity measured at these maxima gives more complicated noncollinear magnetic structure: in the central layers the magnetization orientation is preferably perpendicular to the external field, where as the magnetization in the top and bottom layers has a tendency to be along external field [10]. At the highest field 1500 Oe the data gives evidence that the magnetization in all ^{57}Fe layers aligns almost parallel to the direction of the external field.

The direct comparison of the obtained results with the theoretical predictions [1-3] is not simple. The theory deals with the ideal single domain models. In reality we have 1) the complicated picture of lateral domains; 2) the distribution of the magnetic hyperfine fields (i.e. magnetic moment values) for ^{57}Fe atoms (so their interaction with external field is different for interfaces and central part of each ^{57}Fe layer); 3) the central, top and bottom ^{57}Fe layers are not identical, due to the influence of substrate (or buffer layer) and covering layer.

Our investigation demonstrates that this research area has substantially benefited from the unique opportunities offered by NRR method.

Support by RFBR (No. 12-02-00924-a and No. 13-02-00760-a) is acknowledged.

- [1] A.I. Morosov, A.S. Sigov, *Uspekhi Fizicheskikh Nauk* **180**, No.7 (2010) 709-722.
- [2] J. Meersschant C. L'abbé, F. M. Almeida *et al.*, *PRB* **73** (2006) 144428-1-7.
- [3] V.V. Ustinov, <http://www.imp.uran.ru/UserFiles/File/dostizhenia/Ustinov.pdf>
- [4] V. Lauter-Pasyuk, H.J. Lauter, B.P. Toperverg, *et al.*, *PRL* **89** (2002) 167203-1-4.
- [5] V.V. Ustinov, M.A. Milayev, L.N. Romashev *et al.*, *JMMM* **300**, e281-e283 (2006).
- [6] T. Diederich, S. Couet, R. Röhlberger, *PRB* **76** (2007) 054401-1-5.
- [7] M.A. Andreeva, B. Lindgren, *PRB* **72** (2005) 125422-1-22.
- [8] <https://user.spring8.or.jp/apps/experimentreport/detail/9616/en>.
- [9] M.A. Andreeva, *Hyperfine Interactions*, **185** (2008) 17-21.
- [10] M. Andreeva, A. Gupta, G. Sharma, S. Kamali, K. Okada, Y. Yoda, *PRB*, submitted.

3OR-D-4

TEMPERATURE DEPENDENCE OF THE ISOTROPIC FMR FIELD SHIFT IN FERRITE NANOPARTICLES

Stepanov V.I.¹, Raikher Yu.L.¹, Silva F.G.², Aquino R.², Tourinho F.A.², Depeyrot J.², Perzynski R.³

¹Institute of Continuous Media Mechanics, Ural Branch of RAS, Perm, Russia

²Universidade de Brasília, Brasília DF, Brazil

³Université Pierre et Marie Curie, Laboratoire PHENIX, Paris, France

stepanov@icmm.ru

The origin of the exchange-bias effects is attributed to the interactions emerging at the interface, where a ferro- or ferrimagnetically ordered structure abuts on a layer of uncompensated spins. In thin films the latter is usually provided by sandwiching a ferromagnet and an antiferromagnet. In a fine particle, formation of a shell of uncompensated spins is favoured by the very topology of the object: a quasi-sphere “cut out” from a translationally symmetric lattice. Due to utter finiteness of a nanograin, the spin arrangement of its outer layer cannot be clearly attributed to any of the conventional patterns inherent to large-scale structures like an antiferromagnet or a spin-glass. However, qualitatively, this uncertainty does not matter for the occurrence of the exchange bias (EB) as such.

The EB effect brings in additional contributions to the magnetic anisotropy energy of a nanoparticle, which are termed *exchange-bias* and *rotatable* (RA) anisotropies. Until now, the orientation symmetry of these contributions is a questionable issue. In particular, the rotational anisotropy energy density w_{RA} is taken either in unidirectional form as $K_{RA}(\mathbf{e} \cdot \mathbf{l})$ or in bidirectional form as $K_{RA}(\mathbf{e} \cdot \mathbf{l})^2$, depending on the problem considered, here \mathbf{e} and \mathbf{l} are unit vectors along the directions of the particle magnetic moment and direction of the effective RA field, respectively.

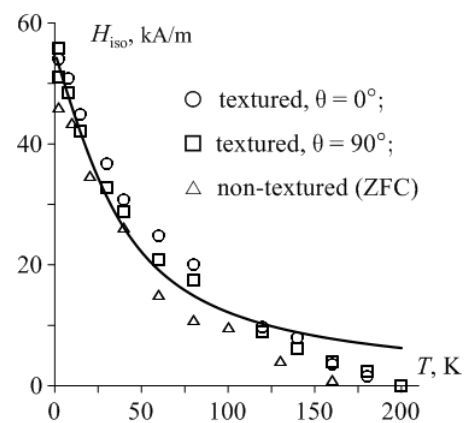
In this work we apply the once developed kinetic model [1] to describe the RA-induced isotropic shift H_{iso} of the FMR resonance field in a superparamagnetic particle. We find that the dependencies $H_{iso}(T)$ are qualitatively different for alternative w_{RA} symmetries. Namely, the unidirectional w_{RA} does not cause any additional temperature dependence of H_{iso} , while the bidirectional w_{RA} makes H_{iso} to decrease $\propto [1/L(\xi) - 3/\xi]$ where L is the Langevin function and $\xi = mH/T$ with m being the particle magnetic moment and H the magnetizing field in FMR measurements.

The model is applied to the FMR data obtained on solidified magnetic fluids with $MnFe_2O_4$ particles of the mean size 3.3 nm [2]. An example of fitting with our model is shown in the figure. As seen, it clearly evidences that the encountered RA anisotropy is of bidirectional type.

Support by RFBR grants # 12-02-00897 and #14-02-96002 and project MIG S26/617 from Ministry of Education and Science of Perm Region is gratefully acknowledged, together with CAPES/COFECUB # 714/11, PICS # 5939, and Brazilian agencies CAPES, FAP/DF and CNPq.

[1] Yu.L. Raikher, V.I. Stepanov, *J. Exp. Theor. Phys.*, **75** (1992) 764-771.

[2] F.G. Silva, PhD Thesis, UPMC-UnB (2013).



3OR-D-5

MAGNETIZATION AND FMR STUDIES OF Fe/Cr/Gd MULTILAYERS

Drovosekov A.B.^{1*}, *Kreines N.M.*¹, *Savitsky A.O.*^{1,2}, *Kravtsov E.A.*³, *Blagodatkov D.V.*³,
*Ryabukhina M.V.*³

¹ P.L.Kapitza Institute for Physical Problems RAS, Moscow, Russia

² Moscow Institute of Physics and Technology, Dolgoprudny, Russia

³ Institute of Metal Physics UD RAS, Ekaterinburg, Russia

*drovosekov@kapitza.ras.ru

The work is devoted to investigations of interlayer coupling between ferromagnetic Fe and Gd layers through a Cr spacer in Fe/Cr/Gd multilayer structures. Magnetic properties of Fe/Gd multilayers are well known at present [1–3]. Due to a strong AFM coupling at the interface and essentially different Curie temperatures of the Fe and Gd layers (1043K and 290K respectively) the Fe/Gd system exhibits ferrimagnetic properties. Recently it was reported that the presence of thin Cr spacer between Fe and Gd layers should change the AFM ordering of the magnetic layers to the FM one [4, 5]. The purpose of this work was to study the dependence of the interlayer coupling in Fe/Cr/Gd system on the Cr spacer thickness.

We investigated a set of [Fe(35Å)/Cr(t)/Gd(50Å)/Cr(t)]₁₂ superlattices with different Cr spacer thicknesses $t = 4 - 30\text{Å}$. The samples were prepared by magnetron sputtering on Si as well as on glass substrates and had polycrystalline structure. The low-angle X-ray reflectometry showed well defined layered structure of the samples. The magnetic properties of the samples were studied by SQUID magnetometry and ferromagnetic resonance technique (FMR) in the 4 – 300K temperature range.

The obtained experimental data show that the interlayer coupling is strongly dependent on the Cr spacer thickness and temperature [6]. For the samples with relatively thin Cr spacers ($t < 10\text{Å}$), the low temperature magnetization curves as well as FMR spectra demonstrate the presence of AFM interlayer coupling $\sim 1\text{ erg/cm}^2$ that is comparable with that in Fe/Cr structures. The strength of the interlayer coupling diminishes as temperature rises. The evolution of magnetization curves and FMR spectra with temperature is described qualitatively in the frame of mean field model taking into account biquadratic contribution to the interlayer exchange energy and nonhomogeneous magnetization profile within Gd layer. Magnetic H – T phase diagrams are obtained.

As spacer thickness increases, the interlayer coupling decays rapidly. The samples with thick Cr spacers ($t \geq 10\text{Å}$) demonstrate FM hysteresis loops with no indications of interlayer coupling. Nevertheless the FMR data demonstrate the presence of a weak interlayer interaction $\sim 0.01\text{ erg/cm}^2$.

The resonance spectra for samples with $t = 10 - 15\text{Å}$ show peculiarities that can be ascribed to small FM coupling. The sample with $t = 20\text{Å}$, on the contrary, demonstrates weak AFM coupling. The observed behavior probably indicates the presence of long period oscillations of the interlayer coupling associated with RKKY exchange through metallic Cr spacer. Such oscillations are well known to take place in classical Fe/Cr/Fe systems [7].

- [1] R.E. Camley and R.L. Stamps, *J. Phys: Condens. Matter*, **5** (1993) 3727.
- [2] M. Sajieddine, Ph. Bauer, K. Cherifi, et al., *Phys. Rev. B*, **49** (1994) 8815.
- [3] D. Haskel, G. Srajer, J.C. Lang, J. Pollmann, et al., *Phys. Rev. Lett.*, **87** (2001) 207201.
- [4] B. Sanyal, C. Antoniak, T. Burkert, et al., *Phys. Rev. Lett.*, **104** (2010) 156402.
- [5] C. Ward, G. Scheunert, W.R. Hendren, et al., *Appl. Phys. Lett.*, **102** (2013) 092403.
- [6] A.B. Drovosekov, N.M. Kreines, A.O. Savitsky, et al., *Spin Waves 2013*, (2013) 65.
- [7] S.S.P. Parkin, N. More, K.P. Roche, *Phys. Rev. Lett.*, **64** (1990) 2304.

3OR-D-6

MFM INVESTIGATION OF MAGNETIC PROPERTIES OF NANOWIRES AND NANOPARTICLES AT HIGH TEMPERATURE

Nurgazizov N.I.¹, Bukharaev A.A.^{1,2}, Bizyaev D.A.¹, Khanipov T.F.¹

¹ Zavoisky Physical Technical Institute, 420029, Russian Academy of Sciences, Kazan, Tatarstan, Russia

² Kazan (Volga Region) Federal University, 420008, Kazan, Tatarstan, Russia
niazn@mail.ru

Magnetic properties and resistance of the ferromagnetic metals may significantly change at heating. The variation of magnetic properties can be estimated from change of sample magnetization. A micromagnetic structure of nanoobjects can be visualized by magnetic force microscope (MFM). It is also possible to estimate changes of magnetic properties from measurements of macroscopic parameters of the sample, for example, by measuring of the resistance dependence on temperature.

In this work we present the experimental results of the changing of magnetic properties of the isolated permalloy nanoparticles (NP) during the heating. Magnetic properties of the nanowire (NW) (made from permalloy and Ni) was also studied. In particular, a domain wall moving by high density current was investigated. The NP and NW were created on non-conducting substrates (SiO₂/Si) by scanning probe nanolithography.

The magnetic reversal of the permalloy NP in a constant external field 100–800 Oe at the temperature range 300–800 K was investigated by Solver HV device. Solver HV allowed to heat sample in external magnetic field at high vacuum condition (for prevent sample oxidation) and allowed to visualize of the NP magnetization by MFM. It is shown that the switching field of the NP was decreased to several times when the sample temperature was increased. Based on analysis of experimental results it was concluded that the behavior of a NP magnetization depending on a temperature increasing was successfully described by the Heisenberg model.

The Curie temperatures of single NWs formed on SiO₂/Si surface were found by two techniques. According first technique, the whole sample was thermal heated and a moment of the ferromagnetic – paramagnetic transition was fixed by analysis of the dependence of the wire resistance on temperature. According second technique, the wire was heated up by a high density current pulse. For that the sawtooth pulse of voltage was applied to the NW and the current in the wire was measured (I-V measurement was carried on). Then the sample was heated up on some tens degrees, and the I-V measurement was made again. After the lot of I-V measurement at different reference temperatures the Curie's temperature was calculated by analysis of the obtained data. It was shown the Curie temperature of NWs with cross-section 8x200 nm and more were close to the Curie temperature of solid.

After the voltage pulse the magnetic structure of a NW was investigated by MFM. It was showed a magnetic domain distribution in the NW was essentially changed after heating wire higher that the Curie temperature. It was also registered the switching of a magnetization direction of one domain after applying the current pulse insufficient to heat a wire to the Curie temperature. This magnetization change was caused by spin transfer torque. The switching of a domain direction was started at current density more 70% the current density necessary for heating the NWs up to the Curie temperature.

This work was partly supported by RFBR (project no. 12-02-00820) and RAS.

3OR-D-7

EFFECT OF INTERLAYER COUPLING ON THE DOMAIN WALL DYNAMICS IN ULTRATHIN Co/Pt/Co TRILAYER

Iunin Y.L.¹, Nikitenko V.I.^{1,2,3}, Shull R.D.², Chien C.L.³

¹ Institute of Solid State Physics, RAS, Chernogolovka, 142432 Russia

² National Institute of Standards and Technology, Gaithersburg, MD 20899, USA

³ The Johns Hopkins University, Baltimore, MD 21218, USA

iunin@issp.ac.ru

Investigations of the nucleation and motion of domain walls in multilayers with perpendicular anisotropy, which are composed of ultrathin magnetic layers separated by nonmagnetic spacers, are of great fundamental and technological importance. In addition to the features of magnetization reversal in single layers, manifestations caused by the interlayer coupling can be revealed in the multilayers. Up to now only few experimental [1–3] and theoretical [4] studies have been devoted to the study of the effect of interlayer coupling on the domain wall dynamics. In this work we investigated the elementary events of magnetization reversal in the perpendicular magnetic field of an ultrathin Co/Pt/Co structure, having Co layers of equal thickness (0.6 nm) and a varying thickness Pt spacer (0–10 nm) using magneto-optical Kerr microscopy.

A surprising spin-reorientation transition from the out-of-plane to in-plane anisotropy with decreasing Pt spacer thickness below 1.6 nm has been found. For Pt thicknesses greater than 1.6 nm, the Co layers have a perpendicular to the surface magnetization as their ground state configuration. In this region two distinct modes of domain wall formation and motion have been observed. With spacer thicknesses in the range 1.6–5.4 nm domain nucleation occurred in both Co layers in a correlated manner and the subsequent motion of domain walls in the individual layers proceeded as though bound together. In addition, a great increase in domain wall velocity (by more than six orders of magnitude) was observed as the spacer thickness increased. This unusual velocity increase is due to reduction in the domain wall pinning strength because of the change in the magnetostatic coupling between the Co layers. The theory for bound domain wall dynamics [4] fails to explain this phenomenon.

For Pt spacer thicknesses above 5.4 nm an abrupt transition to layer-by-layer reversal with uncorrelated domain wall nucleation and unbound motion has also been observed. In this region the domain wall velocities in the bottom and top Co layers differ by almost an order of magnitude. In addition, the velocities exhibit an oscillatory dependence on the spacer thickness. The nature of effects revealed is discussed.

Support by the program for basic research “New Materials and Structures” of the Division of Physics, Russian Academy of Sciences is acknowledged.

[1] P. J. Metaxas, et al., *J. Magn. Magn. Mater.*, **320** (2008) 2571-2575.

[2] P. J. Metaxas, et al., *Phys. Rev. Lett.*, **104** (2010) 237206.

[3] L. San Emeterio Alvarez, et al., *J. Magn. Magn. Mater.*, **322** (2010) 2529-2532.

[4] P. Politi, et al., *Phys. Rev. B*, **84** (2011) 54431.

3 July Thursday

11:30-14:00

oral session

3TL-E

3RP-E

3OR-E

**“High Frequency
Properties and
Metamaterials”**

3TL-E-1

MICROWAVE TUNABLE PROPERTIES OF POLYMER COMPOSITES CONTAINING FERROMAGNETIC MICROWIRES

*Peng H.X.*¹, Luo Y.¹, Qin F.X.^{1,2}, Panina L.V.³, Ipatov M.⁴, Zhukov A.⁴*

¹ Advanced Composite Centre for Innovation and Science, University of Bristol, UK

² 1D Nanomaterials Group, National Institute for Materials Science, Tsukuba, Japan

³ School of computing, Communication and Electronics, University of Plymouth,
Drake Circus, Plymouth, Devon, PL4 8AA, UK

⁴ Dept. Material Physics, Chemistry Faculty University of the Basque Country, San Sebastián, Spain

* hxpengwork@gmail.com

In the context of developing multi-functional composites [1], our efforts have been devoted in exploring ideal functional fillers that could meet the criteria: (i) a likely omnipotent functional filler that will ensure the realization of multi-functionalities and a relatively simple composite architecture, and (ii) a fine geometry and large susceptibility to external fields that will warrant a low and effective loading of fillers. Soft ferromagnetic amorphous glass-coated microwires with singular giant magneto-impedance (GMI) and/or giant stress-impedance (GSI) effect are promising candidate materials. With relatively small diameter (1-30 μm), high mechanical strength ($\sim 10^3$ MPa), reasonable electrical conductivity ($\sim 6 \times 10^3$ S/cm) and high magnetic permeability ($\sim 10^4$), these microwires can be incorporated into polymer-based composites to provide a variety of functionalities with minimum physical perturbation to the matrix.

In the present talk, microwave tuneable properties and associated peculiarities of electromagnetic spectra are analysed in the presence of low (\sim up to 30Oe) and high dc magnetic field (up to 3kOe) and stress field. The composites containing continuous Co- and/or Fe-based ferromagnetic microwires have also been shown to possess metamaterial characteristics [2] and microwave absorption capability. Our recent investigation on a hybridized parallel Fe- and Co-based microwire arrays revealed a dual-band left-handed feature in the frequency bands of 1.5 ~5.5 GHz and 9~17 GHz as indicated by two transmission windows [3]. With a discussion on the underlying physics of the influence of composite architecture such as material parameters of microwires and microwire periodicity on the performance of resultant composites, useful insights are provided for the design of smart composites for specific engineering applications such as structural health monitoring, stress sensing, invisible cloaking and microwave absorption applications.

Support by UoB/CSC Scholarship (YL) and JSPS Fellowship (FXQ) is acknowledged.

[1]F.X. Qin, H.X. Peng, *Prog. Mater. Sci.*, **58** (2013) 183-259.

[2]Y. Luo, H.X. Peng, F.X. Qin, et al. *Appl. Phys. Lett.* **103** (2013) 251902.

[3]Y. Luo, H.X. Peng, F.X. Qin, et al. *Appl. Phys. Lett.* (under preparation).

3TL-E-2

MICROWAVE RESPONSES OF META-MOLECULES WITH MAGNETISM AND CHIRALITY

Tomita Satoshi

Nara Institute of Science and Technology, Ikoma, Nara 630-0192, Japan
tomita@ms.naist.jp

Electromagnetic metamaterials consist of artificial units, called *meta-atoms*, which are much smaller than the wavelength of electromagnetic waves. In an analog to condensed matter physics, a couple of meta-atoms corresponds to a *meta-molecule*, which is the smallest constituent showing intriguing properties of the metamaterials [1]. For obtaining physical insight into the metamaterials, single meta-molecule spectroscopy is indispensable. In this talk, we report the X-band microwave responses of two types of meta-molecules with magnetism and chirality: magneto-chiral (MCh) meta-molecules and ferromagnetic-metal chiral meta-molecule.

The directional birefringence, which is independent of the polarization of light, is called MCh effects [2]. The MCh effect is a key phenomenon in creating an effective magnetic field for electromagnetic waves [3]. We prepared a meta-molecule consisting of a copper (Cu) chiral structure combined with a ferrite rod. When a dc magnetic field was applied to the single meta-molecule, space-inversion and time-reversal symmetries were simultaneously broken. This resulted in the emergence of the artificial MCh effect at a frequency of resonant optical activity of the Cu chiral structure. The MCh effect was induced by a very weak magnetic field of 1 mT, which is of great advantage in the realization of an artificial gauge field for electromagnetic waves.

The second part of my talk is devoted to chiral meta-molecules made of ferromagnetic-metals. We fabricated arrays of micrometer-sized, three-dimensional chiral structures (chiral meta-molecules: CMMs) made of cobalt (Co) by using a strain-induced self-coiling technique [4]. The Co CMMs were fixed on a silicon substrate and aligned in the same direction. We investigated spin-wave resonance of the arrays with varying angles of the external dc magnetic field. The Co CMM arrays showed an angle-independent resonance signal at a much lower field than the Kittel mode of uniform ferromagnetic resonance. The signal is likely to be caused by structural resonance by the CMM. The coupling between spins and chirality via electromagnetic waves in the meta-molecule is an attractive topic also in terms of a classical analog of topological spin textures like skyrmion [5]. The present works thus open a door to *meta-condensed-matter physics*, a new physics of metamaterials.

The author acknowledges T. Ueda, K. Sawada, T. Kodama, N. Hosoi, and H. Yanagi for valuable contributions. Financial supports by MEXT KAKENHI (No. 22109005) and JSPS KAKENHI (No. 23654124) are also acknowledged.

- [1] D. R. Smith et al, *Science*, **305** (2004) 788.
- [2] L. D. Barron and J. Vrbancich, *Molecular Physics*, **51** (1984) 715.
- [3] K. Sawada and N. Nagaosa, *Phys. Rev. Lett.*, **95** (2005) 237402.
- [4] E. J. Smith et al., *Phys. Rev. Lett.*, **107** (2011) 097204.
- [5] X. Z. Yu et al., *Nature*, **465** (2010) 901.

3TL-E-3

SWITCHING DYNAMICS OF Co/Pt NANODOTS UNDER THE ASSISTANCE OF RF FIELD

Okamoto S.¹, Kikuchi N.¹, Furuta M.¹, Kitakami O.¹, Shimatsu T.^{2,3}

¹ IMRAM, Tohoku University, Sendai 980-8577, Japan

² FRIS, Tohoku University, Sendai 980-8578, Japan

³ RIEC, Tohoku University, Sendai 980-8577, Japan

Microwave assisted switching (MAS) of magnetization has been expected as a key technology for future ultra-high density magnetic recording [1,2]. In this switching mode, large amplitude precessional motion of magnetization excited by applying an rf field with GHz frequency range promotes the magnetization switching even in a much smaller field than the coercivity. We have systematically studied the MAS effect on perpendicular magnetic Co/Pt multilayer nanodots [3-5]. From our elaborated experiments, it is found that the non-uniform magnetization precession such as spin wave significantly enhances the MAS effect.

The Co/Pt dots with diameter ranging from 50 nm to 330 nm were lithographically fabricated on a cross-shaped Pt electrode for anomalous Hall effect (AHE) measurement. The rf field was generated from a Cu strip line with 2 μm in width fabricated just above the dot with insertion of an insulating layer. Fig. 1(a) shows the switching field H_{sw} of a single Co/Pt dot of 120 nm in diameter as a function of rf frequency f_{rf} for various rf field amplitude h_{rf} . For $h_{\text{rf}} = 450$ Oe, the H_{sw} significantly decreases from 5.5 kOe to 2.1 kOe with increasing the f_{rf} until the critical frequency. In the range above the critical frequency, the H_{sw} steeply increases and coincides with the value obtained in the absence of rf field. It should be addressed that this significant reduction of switching field is much more profound than the theoretical prediction based on the single macrospin model. To elucidate the switching mechanism, dot size dependent switching behaviors are studied as shown in Fig. 1(b). H_{sw} gradually decreases with increase in the dot diameter. In this figure, simulation results based on two different models, that is, single macrospin and finite cell models, are also plotted. It is very interesting that H_{sw} for larger and smaller dots agree with the finite cell and single macrospin simulation results, respectively. The finite cell simulation reveals that the this largely enhanced MAS effect for larger dot is resulted from the excitation of non-uniform magnetization precession. This size dependent switching behaviors are well explained by the spin wave dispersion theory for a magnetic disk.

This work was partially supported by Grant-in-Aid for Scientific Research from MEXT, the Management Expense s Grants for National Universities Corporations from MEXT, Strategic Promotion of Innovative Research and Development from JST, and the Storage Research Consortium in Japan.

[1] C. Thirion et al., *Nature Mater.*, **2** (2003) 524.

[2] S. Okamoto et al., *APL*, **93** (2008) 102506.

[3] S. Okamoto et al., *APEX*, **5** (2012) 093005.

[4] S. Okamoto et al., *PRL*, **109** (2012) 237209.

[5] M. Furuta et al., *APEX*, **6** (2013) 053006.

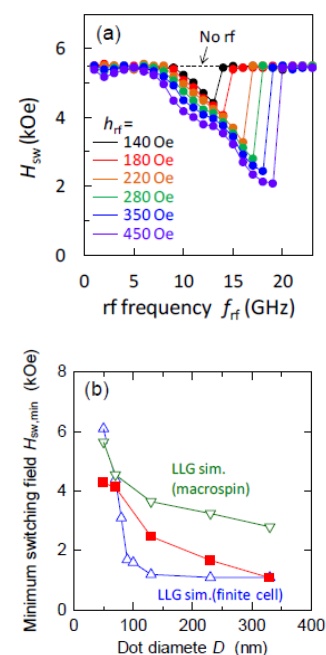


Fig. 1 (a) H_{sw} of a single Co/Pt dot of 120 nm in diameter as a function of f_{rf} and (b) H_{sw} as a function of dot diameter. In (b), simulation results based on single macrospin model and finite cell model are also plotted.

3RP-E-4

IN-SITU MICROWAVE CHARACTERIZATION OF FERROMAGNETIC MICROWIRES-FILLED POLYMER COMPOSITES

Qin F.X.^{1,2}, Tang J.¹, Peng H.X.², Brosseau C.³*

¹ 1D Nanomaterials Group, National Institute for Materials Science 1-2-1 Sengen, Tsukuba, Ibaraki 305-0047, JAPAN

² Advanced Composite Centre for Innovation and Science, Department of Aerospace Engineering, University of Bristol, University Walk, Bristol, BS8 1TR, UK

³ Université Européenne de Bretagne, Université de Brest, Lab-STICC, CS 93837, 6 Avenue Le Gorgeu, 29238 Brest Cedex 3, France

* faxiang.qin@gmail.com

In the present talk, we will present the most recent progress on the microwave tunable wire-composites in terms of their electromagnetic behaviours sensitively modulated by the external stimuli [1]. Specifically, the effects of magnetic field, tensile stress and dc current will be discussed on the electromagnetic properties of several sets of composites with differing wires, matrices and mesostructure, such as continuous-wire against short-cut wire, periodical against random. Two kinds of wires have been adopted as fillers, namely, glass-coated microwires prepared by Taylor-wire technique and the melt-extraction microwires prepared by the melt-extraction method. These composites were tested by a modified frequency-domain microwave spectroscopy which is capable of accurate measurement of the permittivity and permeability under external stimuli, i.e., in-situ microwave characterization. The emphasis is placed upon the presentation and analyses of the roles of dc magnetic field [2], tensile stress (strain) [3] and dc current [4] on the formulation of the electromagnetic spectra via delineating the relations between microstructure/mesostructure-macroscopic properties. We have shown here some unique dielectric characteristic such as cross-over phenomenon conditioned by specific geometry or microstructure and wide range of magnetic field, which are supported by the coupling between magnetostatics and electrodynamics of microwire(s). On the same footing, the mechanism accounting for the complex stress dependence of permittivity and unusual current effect are discussed. The special role of polymer matrix and interface is also analysed to account for some unexpected features in the electromagnetic spectra. Apart from these insights into basics, the application significance in the domains of e.g., high-performance sensing and microwave devices are concluded in the end corresponding to the discussed functionalities. Collectively, this talk purposes to provide some general principles in designing, fabricating and characterizing such kind of polymer composites filled by elongated magnetic fillers and inspire the advance of next-generation multifunctional microwave devices.

[1] F.X. Qin and H.X. Peng. *Prog Mater Sci*, **58** (2013) 183.

[2] F. X.Qin et al. *Appl. Phys. Lett.*, **100** (2012) 192903; *ibid* 101 (2012) 152905; *ibid* 102 (2013) 122903.

[3] F. X.Qin et al. *Appl. Phys. Lett.*, **97** (2010) 153502; *ibid* 99 (2011) 252902.

[4] F. X.Qin et al. *Appl. Phys. Lett.*, **104** (2014) 012901.

3RP-E-5

TUNABLE PERMEABILITY OF MAGNETIC WIRES AT MICROWAVES

Panina L.V.^{1,2}, Morchenko A.T.¹, Makhnovsky D.P.³

¹ National University of Science and Technology (MISIS), Moscow, Russia

² Institute for Design Problems in Microelectronics RAS, Moscow, Russia

³ School of Computing & Mathematics, University of Plymouth, UK

lpanina@plymouth.ac.uk

Artificial materials containing ferromagnetic microwires have generated a considerable interest because they make it possible to tune the electromagnetic response in the microwave frequency band. Typically, the effect of the wire magnetic polarization on the effective dielectric function in diluted composites is considered [1]. In this context, the ac permeability of wires may strongly contribute to the dielectric losses owing to the magnetoimpedance (MI) effect, resulting in unusual dependence of the effective permittivity on the external magnetic or mechanical stimuli. This work presents the investigation into microwave magnetic activity of the magnetic wires and their composites demonstrating that for wires with specific helical anisotropy the effective permeability is relatively large for relatively low concentration (less than 10%). We also demonstrate the possibility to design the wire media with a negative index of refraction utilizing natural magnetic properties of wires.

The problem is approached by solving the electrodynamic problem for a single wire coupled with the Landau Lifshitz equation for the magnetization dynamics. Because of a very high aspect ratio of magnetic elements, the effective permeability could be approximated by averaging the wire magnetic polarization for a system of magnetically non-interacting wires. For a wire with a near circular anisotropy the demagnetization effects are reduced with respect to the excitation magnetic field along the wire. This results in the relatively large longitudinal permeability for frequencies up to few GHz. Such composites can be used as effective microwave absorbers.

A number of topologies for magnetic wire composites was considered to generate highly dispersive characteristics for both dielectric and magnetic functions. Firstly, we considered a system of continuous parallel wires spaced relatively densely to achieve volume concentration of 5-10 percent. This system can be supplemented with orthogonal wire-array with large spacing to generate dielectric response. For a proper magnetic anisotropy of wires, the effective permeability has negative values in a wide frequency band which overlaps the frequency region where the effective permittivity is negative (due to plasmonic behavior). We also compared the obtained refractive index spectra with those for a system of short-cut wires where the magnetic response is generated due to conduction currents in wire-pairs [2-4]. The negative refraction is seen in a much narrower frequency band comparing the system with natural magnetic resonances. In both cases, a very strong dependence on the external magnetic field is observed.

[1] D.P. Makhnovskiy, L.V. Panina, C. Garcia, A.P. Zhukov, J. Gonzalez, *Phys. Rev. B*, **74** (2006) 064205.

[2] L.V. Panina, A.N. Grigorenko, D.P. Makhnovskiy, *Phys. Rev. B*, **66** (2002) 155411.

[3] S.N. Burokur, A. Sellier, B. Kanté, A. de Lustrac, *Appl. Phys. Lett.*, **94** (2009) 201111.

[4] A. Sellier, S.N. Burokur, B. Kanté, A. de Lustrac, *Opt. Express*, **17** (2009) 6301.

3OR-E-5

GIANT MAGNETO-IMPEDANCE SENSOR FOR MEASURING OF LOCAL MAGNETIC FIELDS

Gudoshnikov S.A.^{1,2}, *Liubimov B.Ya.*¹, *Nozdrin A.G.*³, *Serebryakova O.N.*¹, *Skomarovsky V.S.*^{1,2},
Usov N.A.^{1,2}

¹ IZMIRAN, Troitsk, Moscow, Russia

² MaCryEl systems Ltd, Troitsk, Moscow, Russia

³ MIREA, Moscow, Russia

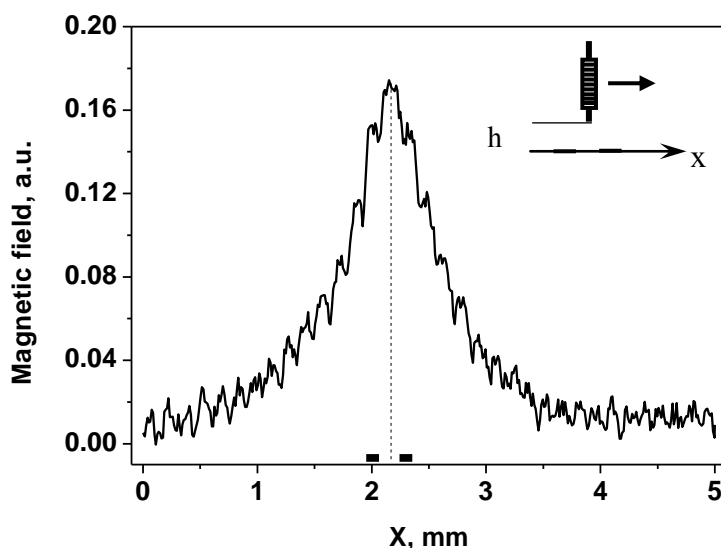
gudosh@izmiran.ru

Recently developed technique for measuring and imaging of local stray magnetic fields near a sample surface is promising for investigation of different objects. The important characteristics of this technique are the magnetic sensitivity, spatial resolution and minimal return influence of a measuring instrument on the sample. These parameters are determined by the magnetic sensor used, such as Hall probe, SQUIDS, MFM sensor and others. In this work a sensor based on the effect of a giant magneto-impedance (GMI-sensor) is developed and tested for magnetic microscopy. In our case the GMI-sensor consists of a 8 mm long piece glass-coated amorphous microwire, having a ferromagnetic Co Fe Ni Si B Mo core with diameter $d \sim 20 \mu\text{m}$ [1] and a receiving pick-up coil of 85 turns wound around the microwire.

During the measurements, the GMI-sensor is placed perpendicular to the sample surface so that the distance between the microwire's tip and the sample surface h is of order of 100-500 μm (see inset in Fig.1). A specialized electronic circuit with feedback loop is used to register GMI-sensor signals [2]. Measurements are carried out within a magnetic shield to reduce the effects of external magnetic fields. Movement of the sample relative to the sensor is carried out by means of a nonmagnetic positioner. As

an example, Fig. 1 shows a magnetic scan measured across a two-wires 100 μm line which carries a DC current of 2 mA. These data indicate that the GMI-sensor can detect small and highly localized magnetic fields. Features and characteristics of the GMI-sensor developed for the magnetic microscopy will be presented in this work.

Fig. 1. The magnetic scan measured across a two-wire line.



[1] V. Zhukova, A. Chizhik et al., *IEEE Trans. Magn.*, **38** (2002) 5, 3090.

[2] S.Gudoshnikov, N.Usov et al., *Phys. Status Solidi (A)* (2014) 1-6, DOI 10.1002/pssa.201300717.

3OR-E-6

BIAS CURRENT EFFECT ON SECOND HARMONIC IN ASYMMETRIC MAGNETOIMPEDANCE RESPONSE IN AMORPHOUS MICROWIRES

*Buznikov N.A.*¹, *Antonov A.S.*², *Granovsky A.B.*³

¹ Scientific-Research Institute of Natural Gases and Gas Technologies – GAZPROM VNIIGAZ, 142717 Razvilka, Leninsky District, Moscow Region, Russia

² Institute for Theoretical and Applied Electrodynamics, Russian Academy of Sciences, 125412 Moscow, Russia

³ Faculty of Physics, M.V. Lomonosov Moscow State University, 119992 Moscow, Russia
n_buznikov@mail.ru

The giant magnetoimpedance (GMI) effect consists in a strong dependence of impedance of a magnetic conductor on an external magnetic field. The effect has been observed in different soft magnetic materials [1]. Amorphous microwires with nearly zero magnetostriction stand out among GMI materials due to their magnetic softness and favorable geometry. The GMI effect has attracted a great interest in connection with the development of magnetic-field sensors. The linearity and the sensitivity for the magnetic field are the most important parameters in practical applications of the GMI. To improve the linear characteristic of the GMI response and to suppress the hysteresis effect, the asymmetric GMI is very promising. Recently, the asymmetric GMI due to bias current has been studied intensively in amorphous microwires [2,3]. The asymmetry in the field dependence of the impedance is caused by the combination of a helical magnetic anisotropy with the circular field produced by the bias current and is ascribed to the asymmetry in the axial magnetization loop.

The majority of the GMI studies are carried out at sufficiently low amplitudes of the exciting current, when the voltage response across the sample is sinusoidal. At higher current amplitudes, distortions appear in the voltage resulting in the generation of higher harmonics in the response. This mode is often referred to as the nonlinear magnetoimpedance. It has been shown that this effect may be promising for applications, since the second harmonic has extreme sensitivity to the external magnetic field [4,5].

In this work, the appearance of asymmetry in the nonlinear magnetoimpedance in an amorphous microwire arising due the bias current is analyzed. A model to calculate the voltage response of the microwire with a helical anisotropy in the low-frequency range is proposed. The frequency spectra of the voltage are analyzed as a function of the external magnetic field, current amplitude and the value of the bias current. Generation of higher harmonics in the voltage response is related to the magnetization reversal of a surface layer of the microwire. The application of the bias current leads to the asymmetry in the magnetization reversal process and, as a result, the field dependences of harmonic amplitudes become asymmetric. It is shown that in the nonlinear mode, the second harmonic is more sensitive to the external field in comparison with other harmonics. The ranges of the current amplitude and bias current to achieve maximal field sensitivity of the second harmonic are found. The results obtained may be useful for applications in magnetic-field sensors.

- [1] M.-H. Phan, H.-X. Peng, *Prog. Mater. Sci.*, **53** (2008) 323.
- [2] M. Ipatov, V. Zhukova, A. Zhukov, J. Gonzalez, A. Zvezdin, *Phys. Rev. B*, **81** (2010) 134421.
- [3] M. Ipatov, V. Zhukova, A. Zhukov, J. Gonzalez, *J. Appl. Phys.*, **113** (2013) 203902.
- [4] J.G.S. Duque, et al., *Appl. Phys. Lett.*, **83** (2003) 99.
- [5] D. Seddaoui, D. Ménard, P. Ciureanu, A. Yelon, *J. Appl. Phys.*, **101** (2007) 093907.

3 July Thursday

11:30-13:45

oral session

3TL-F

3RP-F

3OR-F

“Multiferroics”

3TL-F-1

MAGNETO-ELECTRIC COUPLING IN GRANULAR MULTIFERROICS

Udalov O.G.^{1,2}, Chtchelkatchev N.M.^{1,3}, Beloborodov I.S.¹

¹ Department of Physics and Astronomy, California State University Northridge, Northridge, CA 91330, USA

² Institute for Physics of Microstructures, Russian Academy of Science, Nizhny Novgorod, 603950, Russia

³ L.D. Landau Institute for Theoretical Physics, Russian Academy of Sciences, 117940 Moscow, Russia

oleg.udalov@csun.edu

Currently composite multiferroics – materials with strong coupling between electric and magnetic degrees of freedom are the main topic of research in condensed matter physics and materials science. These materials show non-trivial fundamental physical properties and are promising candidates for numerous applications. In this report we will discuss a new mechanism for magneto-electric coupling appearing in granular multiferroics due to the interplay of ferroelectricity and magnetism via Coulomb blockade effects. This mechanism leads to the unusual magnetic phase diagram with the ordered magnetic phase appearing at higher temperatures than the magnetically disordered phase (see Fig. 1(a)). The mechanism allows the electric field to control the magnetic properties and magneto-transport in composite multiferroics. Even magnetic phase transition can be driven by electric field (see Fig. 1(b)).

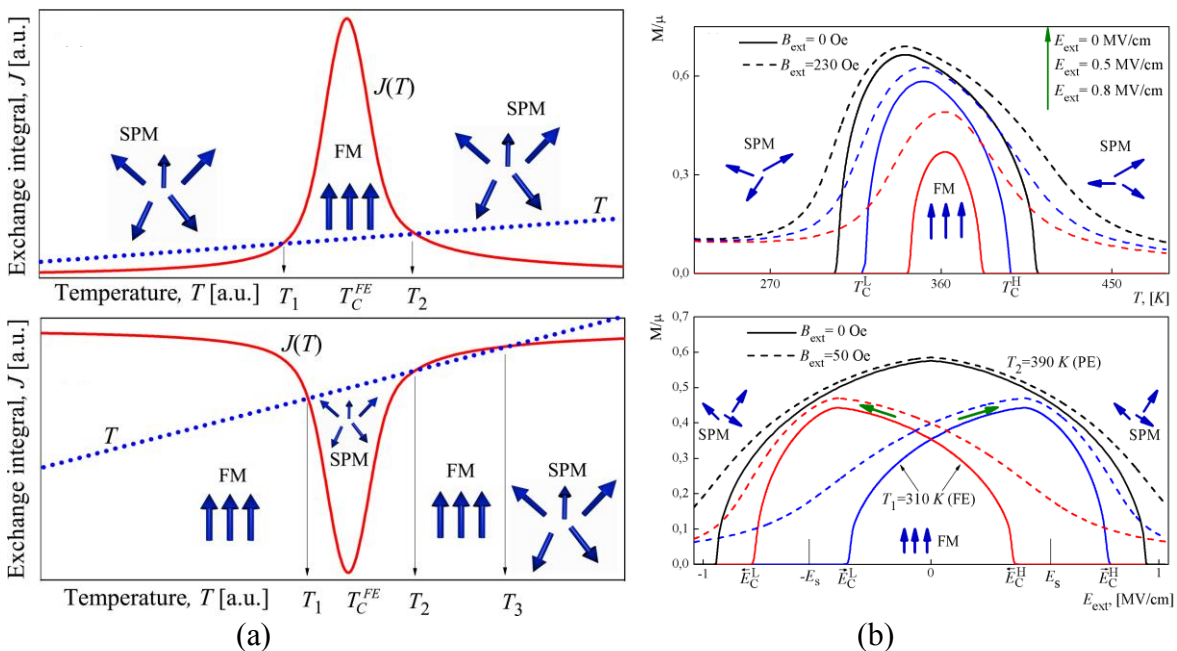


Fig. 1. (a) Exchange coupling constant J in granular multiferroic as a function of temperature T (solid line). Dotted line is the temperature T . Intersections of exchange constant and temperature correspond to magnetic phase transitions. Upper and lower panels show J for systems with different parameters. (b) Magnetization of granular multiferroic M as a function of temperature T (upper panel) and external electric field E (lower panel).

3OR-F-2

INTERPLAY OF FERROELECTRICITY AND MAGNETISM IN MULTIFERROIC Co/BaTiO₃ THIN FILMS

Jedrecy N.¹, von Bardeleben J.¹, Stanescu D.², Magnan H.², Barbier A.²

¹ Institut des Nano Sciences de Paris, UPMC-Sorbonne Universités, CNRS-UMR7588,
75005 Paris, France

² CEA Saclay, DSM, IRAMIS, SPCSI, F-91191 Gif Sur Yvette, France
jedrecy@insp.jussieu.fr

Heterostructures made of ferroelectric and ferromagnetic layers are very promising for the development of novel nanometric memories, in particular, in view of a possible control of magnetization by electric voltage. We have studied the system formed by ferromagnetic Co layers (5–40 nm) grown on epitaxial, single-crystalline (001)-oriented, ferroelectric BaTiO₃ layers (about 15 nm). Thanks to the nearly ideal monodomain electric polarization of our BaTiO₃ thin films, and which is oriented along the surface normal, we give evidence of a strong magnetoelectric coupling at room temperature between the BaTiO₃ polarization and the Co magnetization.

We have used different techniques to characterize the system and establish the coupling effect: magnetometry, piezoresponse force microscopy, and ferromagnetic resonance spectroscopy. In the latter case, a clear dependence of the resonance magnetic field on the orientations of polarization and magnetization is observed [1]. The resonance field at room temperature significantly shifts depending on whether the polarization and magnetization are aligned parallel or anti-parallel. This observation made in zero electric field conditions allows excluding any indirect effects such as magneto-striction or external electric field influence. Complementary experiments under external voltage will also be presented.

By lowering the temperature and going through the tetragonal versus orthorhombic phase transition of BaTiO₃, we observe a progressive reduction of the resonance shift, corresponding to a reduction of the polarization. By contrast, the resonance field is not affected at all by the temperature when orienting the magnetization perpendicular to the polarization. We also show that the magnetoelectric coupling modifies notably the magnetic anisotropy of the system. Despite the polycrystalline nature of the Co thin film, a notable remanent magnetization may be obtained perpendicular to the film plane.

[1] N. Jedrecy, H.J. von Bardeleben, V. Badjeck, D. Demaille, D. Stanescu, H. Magnan, A. Barbier, *Phys. Rev. B*, **88** (1999) 121409(R).

[3] V.N. Men'shov, V.V. Tugushev, S. Caprara, *Phys. Rev. B*, **83** (2011), 035201.

[4] V.V. Rylkov, S.N. Nikolaev, K.Yu. Chernoglazov et al., *JETP Lett.*, **96** (2012) 255.

[5] V.V. Rylkov, E.A. Gan'shina, O.A. Novodvorskii et al., *Europhys. Lett.*, **103** (2013) 57014.

3OR-F-3

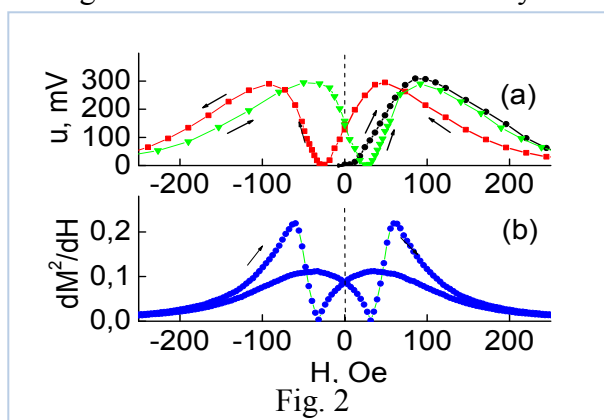
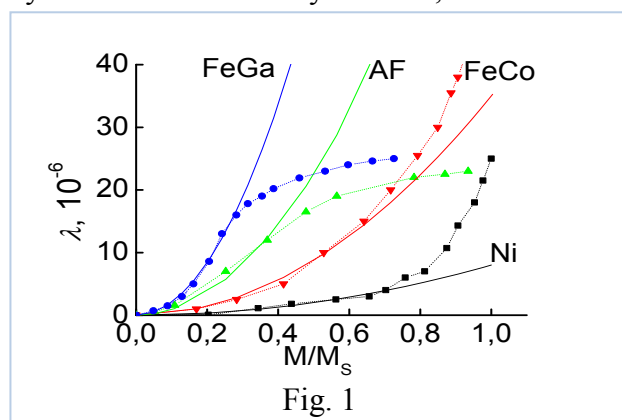
RELATION BETWEEN MAGNETOELECTRIC AND MAGNETIC CHARACTERISTICS OF MULTIFERROIC STRUCTURES

Fetisov L.Y., Chashin D.V., Ekonomov N.A., Burdin D.A., Fetisov Y.K., Kulikov A.G.
 Moscow State Technical University of Radio Engineering, Electronics and Automation,
 Moscow, Russia
 fetisovl@yandex.ru

Characteristics of magnetolectric (ME) interactions in multiferroic structures containing ferromagnetic (FM) and ferroelectric (FE) layers are determined by the magnetostriction of the FM layer. It was shown that magnetostriction of a ferromagnet λ is connected with its magnetization as $\lambda \sim M^2$ [1]. This relation can be used to investigate and predict ME characteristics of the structures by measuring their magnetic properties.

The aim of this paper is to demonstrate a connection between ME and magnetic characteristics of multiferroic structures. The bilayer structures consisting of a FM plate with dimensions of 30 x 7 mm² (made of nickel - Ni, permendur - FeCo, galfenol - FeGa, or amorphous ferromagnet FeBSiC - AF), bound to the langatate plate of the same dimensions were used in measurements. The dependences of magnetization $M(H)$ and magnetostriction $\lambda(H)$ on dc tangential field H for the FM layers have been measured using a vibration sample magnetometer and a strain gauge. The data obtained were used to draw dependences $\lambda(M/M_s)$ (where M_s is the saturation magnetization), depicted with points in Fig.1 The lines in Fig. 1 show quadratic approximations. It is seen, that $\lambda \sim (M/M_s)^2$ in rather wide interval of M . For all the structures the field dependences of ME voltage $u(H)$ have been measured. Figure 2a shows an example of $u(H)$ dependence for the Ni-langatate structure excited with a field $h \sim 1$ Oe at acoustic resonance frequency $f = 70$ kHz.

It is well known, that ME voltage $u \sim d_{31}ph$, where d_{31} is the piezoelectric module of the PE layer and $p = \partial\lambda/\partial H$ is the piezomagnetic coefficient of the FM layer. By using the measured dependence $M(H)$ and the relation $\lambda \sim M^2$, the dependence $p(H) = \partial M^2/\partial H$ shown in Fig.2b have been calculated. One can see a good qualitative coincidence of the curves. The voltage u and the derivative p turn out to zero when $M = 0$, both of them do not equal to zero at $H = 0$ due to hysteresis of the Ni layer. Thus, measurement of magnetization curves for the FM layer allows



describing field dependence of the ME voltage, generated by composite multiferroic structures. The research was supported by the Ministry of Education and Science of Russian Federation and the Russian Foundation for Basic Research.

[1] Kikuchi Y. *Ultrasonic transducers*. Tokyo: Corona publishing Company, Ltd, (1969) 424.

3OR-F-4

NONLINEAR OPTICS OF MULTIFERROIC HETEROSTRUCTURES

Buryakov A.M., Grishunin K.A., Mishina E.D., Sherstyuk N.E.

Moscow State Technical University of Radioengineering, Electronics and Automation
Moscow, Russia
mishina@mirea.ru

The properties of planar and perforated multiferroic structures obtained by "engineered epitaxial stress" and their connection with ferroelectric and magnetic subsystems are of great interest of modern solid state physics and nanotechnology. This paper is aimed on the study of nature and characteristics of nonlinear optical response in such structures as a measure of magnetism, ferroelectricity and magnetoelectric effect.

Multilayered structures of $(\text{BiFeO}_3/\text{BaSrTiO}_3)_n$, $(\text{LaSrMnO}_3/\text{BaSrTiO}_3)_n$ with the layer thickness in the range of 1-20 nm and $n=1-35$ were studied by optical second harmonic generation (SHG). All samples reveal SHG parameters dependence on electric field applied in in-plane geometry, i.e. dielectric polarization switching at room temperature. In the same time SHG dependence on magnetic field was not found although magnetization hysteresis was confirmed by different techniques. The shape of hysteresis loops depends on composition of ferroelectric layers. Interestingly, strontium concentration in BST films, providing the sharpest dielectric hysteresis in heterostructures falls in the range of paraelectric phase for the phase diagram of bulk material.

For $(\text{YFeO}_3/\text{LaFeO}_3)_5$ heterostructures consisting of nanolayers (from one to five atomic layers) of centrosymmetric and therefore non-polar materials, appearance of a polar non-centrosymmetric ordering was found. This property was first predicted theoretically, and then confirmed by various experimental techniques: X-ray diffraction (pole figures), atomic force microscopy in piezomode [1]. Nonlinear optical experiment played crucial role for a proof of the symmetry change, since significant increase of the SH intensity was found for superlattices accompanied by a change of polarization and azimuthal dependences of SHG intensity for this structures in comparison with pure material. Magnetic field induced SHG was found in this material as well. In this way we proved construction of new multiferroic composite material.

Perforated BST films (photonic crystals) in in-plane polarization geometry were studied experimentally by SHG microscopy. This allows to map ferroelectric polarization distribution in the vicinity of cylindrical void. These data correlate with electric field distribution calculated for the same structures using COMSOL software.

The work is supported by Russian Foundation for Basic Research and the Ministry of Education and Science of RF.

[1] J. Alaria, P. Borisov, M.S. Dyer, T.D. Manning, S. Lepadatu, M.G. Cain, E.D. Mishina, N.E. Sherstyuk, N.A. Ilyin, J. Hadermann, D. Lederman, J.B. Claridge, M.J. Rosseinsky. *Chemical Science*, **5** (2014) 1599-1610.

3RP-F-5

MAGNETORESISTIVE MEMORY WITH RECORDING BY ELECTRIC FIELD: IS THE WEAK FERROMAGNETISM NECESSARY?*Morosov A.I., Sigov A.S.*

Moscow State Technical University of Radioengineering, Electronics
and Automation, Moscow, Russia
morosov@mirea.ru

Possible approaches to creating a magnetoresistive memory with recording by electric field (MERAM) are considered. The memory based on a particular geometry of multiferroic BiFeO₃ is shown to be the most promising. The relatively small values of the weak ferromagnetic moment and linear magnetoelectric coupling constant in BiFeO₃ are not significant obstructions for creation of such a MERAM. The key factors are the coupling between electrical polarization and the antiferromagnetism vector in the multiferroic (not between polarization and magnetization vectors), as well as the exchange coupling between the antiferromagnetism vector and the ferromagnet layer magnetization caused by the spin-flop orientation of the latter two vectors at the interface. Electric field induces rotation of the polarization vector and of the related vector of antiferromagnetism in the multiferroic layer, which, in its turn, brings about rotation of the ferromagnet layer magnetization vector through $\pi/2$ due to the exchange interaction at the ferromagnet-multiferroic interface. This is inherently an antiferromagnetic-ferroelectric device mechanism.

3RP-F-6

PHYSICS OF DIMENSIONALLY GRADED MAGNETOELECTRIC ENERGY HARVESTER

Petrov R.V.¹, Petrov V.M.¹, Bichurin M.I.¹, Soloviev I.N.¹, Soloviev A.N.¹, Zhou Y.², Priya S.²

¹ Novgorod State University, Veliky Novgorod, Russia

² Virginia Tech, Blacksburg, Virginia 24061, USA

initra@yandex.ru

Since the magnetoelectric (ME) composites combine piezoelectric and magnetostrictive phases, a possibility emerges for using the ME composites in energy-harvesting applications due to summation effect for both mechanical and magnetic energies. The energy collection and conversion effectiveness are expected to be enhanced under magnetic and mechanical excitation. We report a theoretical model for a magnetoelectric energy harvester structure that can simultaneously scavenge magnetic and vibration energy. The structure considered is designed by combining a Ni unimorph and bilayer of piezoelectric microfiber composite (MFC) and Ni in a cantilever configuration [1].

Theoretical modeling rests on the assumption that the sample undergoes the superposition of axial and bending strain. These strains can be calculated by solving the elastodynamic equations for Ni unimorph and bilayer of MFC and Ni. The found solutions for unimorph and bilayer are joined. Then the strain components can be expressed in terms of stress components with the aid of elasticity law. To obtain the expression for the induced voltage, we substitute the found stress components into the open circuit condition.

The stress and magnetic field energy could be converted into electric charges in the piezoelectric layer through a direct piezoelectric effect and ME effect, correspondingly. Under the external vibration of clamped end of the structure, oscillation of the cantilever can directly create strain in the piezoelectric layer and produce electrical voltage.

3OR-F-7

NEW SPIN-DRIVEN MULTIFERROICS $\text{Sc}_2\text{NiMnO}_6$ AND $\text{In}_2\text{NiMnO}_6$

*Belik A.A.*¹, *Yi W.*¹, *Liang Q.F.*², *Matsushita Y.*³, *Tanaka M.*³, *Terada N.*⁴, *Suzuki H.S.*³, *Tsujii N.*³,
*Sobolev A.A.*⁵, *Presnyakov I.A.*⁵

¹ International Center for Materials Nanoarchitectonics (WPI-MANA), National Institute for Materials Science (NIMS), 1-1 Namiki, Tsukuba, Ibaraki 305-0044, Japan

² Department of Physics, University of ShaoXing, Shaoxing 312000, P. R. China

³ NIMS, 1-2-1 Sengen, Tsukuba, Ibaraki 305-0047, Japan

⁴ Rutherford Appleton Laboratory, ISIS, University of Oxford, Harwell Oxford, UK

⁵ Department of Chemistry, Moscow State University, Moscow 119991, Russia

Alexei.Belik@nims.go.jp

Multiferroic materials, where ferroelectric order and (any) magnetic orders coexist, form an interesting class of materials and have been extensively studied in recent years. Tremendous efforts by many researchers resulted in the discovery of many new multiferroic materials and the identification of new mechanisms of ferroelectricity. Among different multiferroic materials, spin-driven multiferroics attract special interest because ferroelectricity is induced by magnetic ordering and, therefore, the coupling between different order parameters is usually very strong. Ferroelectric and dielectric properties can easily be controlled by magnetic fields in such spin-driven multiferroics. Spin-driven ferroelectricity appears from spin frustration, in general, or more specifically from spiral and cycloid spin orders, exchange striction, and spin-direction dependent metal-ligand hybridization.

Ferroelectricity from spiral and cycloid spin orders was found, for example, in RMnO_3 ($R = \text{Tb}, \text{Dy}, \text{Eu}_{1-x}\text{Y}_x$), $\text{Ni}_3\text{V}_2\text{O}_8$, MnWO_4 , LiCu_2O_2 , CuO , and $\text{Sr}_3\text{Co}_2\text{Fe}_{24}\text{O}_{41}$. Ferroelectricity from the metal-ligand hybridization was suggested to appear in $\text{Ba}_2\text{CoGe}_2\text{O}_7$ and CuB_2O_4 . Ferroelectricity from the exchange striction appears in RMnO_3 ($R = \text{Ho-Lu}$), RMn_2O_5 ($R = \text{Y}$ and Tb-Lu), GdFeO_3 , and $\text{Ca}_3\text{CoMnO}_6$.

3OR-F-8

X-RAY MEASUREMENT OF THE SIGN OF THE DZYALOSHINSKII-MORIYA INTERACTION IN HEMATITE Fe_2O_3

*Ovchinnikova E.N.*¹, *de Bergevin F.*², *Rogalev A.*², *Wilhelm F.*², *Kokubun J.*³, *Dmitrienko V.E.*⁴

¹ Moscow State University, Moscow, Russia

² ESRF, Grenoble, France

³ Tokyo University of Science, Japan

⁴ Institute of Crystallography (RAS), Moscow, Russia
ovtchin@gmail.com

The Dzyaloshinskii-Moriya (DM) interaction [1,2] is the key element in the physics of multiferroics, that's why so many efforts are devoted to its theoretical and experimental studies. Recently a method has been developed [3] for the DM sign measurement in weak ferromagnets and applied for FeBO_3 . It is based on the interference between charge and magnetic contributions to resonant X-ray scattering.

In this report, we present a novel experimental technique which enables the determination of the sign of the DM interaction. We use the interference between multiple-wave diffraction (which acts as a reference wave) and non-resonant magnetic scattering. For both scattering channels very reliable and model-independent calculations have been performed. However the signal is quite small and requires very stable and highly sensitive experimental set-up.

This new technique was applied to study the hematite Fe_2O_3 (space group $R-3c$). Hematite is antiferromagnetic in which DM interaction leads to a small canting of Fe magnetic moments (weak ferromagnet). Owing to the crystal symmetry, the DM vector is directed along threefold axis but its absolute value and direction depend on details of the spin-orbit interaction.

The experiment was carried out at the ID12 beamline of the ESRF (Grenoble, France). We measured the diffracted intensities for the 111_{rh} forbidden reflection in hematite recorded with right-handed and left-handed circularly polarized X-rays at photon energy of 5521 eV (well below the K absorption edge of Fe) which corresponds to $\Theta_{\text{Bragg}} = 14.67^\circ$. The asymmetry ratio of this reflection $(I_{\text{left}} - I_{\text{right}}) / (I_{\text{left}} + I_{\text{right}})$ was measured which depend on the azimuthal deviation from the multiple diffraction position for the optimal angular settings suitable for the observation of the desirable interference. An external magnetic field were applied to saturate the weak ferromagnetism of hematite and obtain a single-domain state. Direction of the magnetic field was changed in the easy 111_{rh} plane to vary the value and sign of non-resonant magnetic scattering.

The obtained experimental results are in very good agreement with preliminary calculations and demonstrate strong difference between reflection intensities for right-handed and left-handed circularly polarized X-rays. Analysis of the experimental data using rather simple phenomenological calculations allowed us to determine the sign of the Dzyaloshinskii-Moriya interaction in hematite. The latter is compared with the DM vectors in hematite calculated in [4] using very sophisticated ab-initio method.

[1] I. Dzyaloshinsky, *Sov. Phys. JETP* **5**, (1957) 1259; *J. Phys. Chem. Solids*, **4** (1958) 241.

[2] T. Moriya, *Phys. Rev. Lett.* **4**, (1960) 228; *Phys. Rev.*, **120** (1960) 91.

[3] V. E. Dmitrienko, E. N. Ovchinnikova, S. P. Collins, G. Nisbet, G. Beutier, Y. O. Kvashnin, V. V. Mazurenko, A. I. Lichtenstein, M. I. Katsnelson, *Nature Physics*, **10** (2014) 202.

[4] V. V. Mazurenko and V. I. Anisimov, *Phys. Rev. B*, **71** (2005) 184434.

Author Index

A

Abakumova N.N.	164	Allia P.	357
Abashev D.M.	593	Al-Maliki A.J.	550
Abdel-Hafiez M.	152, 153	Almasy L.	418
Abedini-Nassab	355	Al-Qahtani M.	515
Abouhaswa A.S.	171	Alshammari M.	515
Abramova G.M.	752	Alshetwi Y.A.	515
Abrudan R.	374	Altynbayev E.V.	54
Abu-Bakr A.F.	828	Alvarez-Herault J.	306, 891
Abylkalykova R.B.	778	Ambaye H.	370
Acet M.	139, 503	Amelichev V.A.	61
Adachi Nobuyasu	720	Amirzadeh P.	482
Adam R.	648	Amonov B.U.	597
Adanakova O.A.	460	Ando K.	115
Afanasiev D.	799	Andreenko A.S.	442
Afremov L.L.	141, 156, 161	Andreev A.V.	173, 407, 592
Agafonov L.Y.	659	Andreev N.V.	261, 593, 807
Aguilera-Granja J.F.	372	Andreev V.G.	562
Agzamova P.A.	509	Andreeva M.A.	922
Ahmadvand H.	482	Andrianov T.	243
Aiev A.M.	482	Andriichuk M.A.	206, 234
Airiyani E.L.	473, 474, 494	Anikin M.S.	478
Akaki M.	392	Anisimov M.A.	237, 238, 885
Akdoğan N.	251	Anisimov N.V.	223
Akimov I.A.	641, 719, 915	Anisimov S.V.	156
Akmaldinov K.	891	Anitas E.M.	255
Aköz M.E.	251	Annaorazov M.P.	486
Akterskiy A.Yu.	445	Annenkov A.Yu.	863
Akzyanov R.S.	125	Anokhin E.O.	831
Al Azzavi H.C.M.	768, 874	Anshits A.G.	706
Albertini F.	345, 714	Antipov S.D.	145, 746
Albisetti E.	247	Antonov A.	226
Alekhin A.	382	Antonov A.N.	220
Alekseev A.V.	453	Antonov A.S.	934
Aleshnikov A.A.	768	Anwand W.	106, 107, 211
Alexeev A.V.	130	Aoki D.	917
Alfehaid S.	515	Apalkov D.	19
Ali N.	344, 493	Aplesnin S.S.	513, 542, 620
Aliev A.M.	715, 846	Aprili M.	626
Alisultanov Z.Z.	488	Aquino R.	923
		Arauzo A.	447, 776
		Arbuzova T.I.	510, 511, 709
		Ari-Gur P.	349, 484
		Arima T.	44

Arkhipov V.E.	58	Balbikhina O.V.	494
Arnold Z.	345	Bali R.	82
Aronov A.V.	523	Baltz V.	891
Aronzon B.A.	109, 110, 215, 366, 514	Balymov K.G.	460
Artemiev E.M.	744	Balz C.	466, 739
Arumugam S.	713	Bandiera S.	306
Arutyunov K.Yu.	632	Banerjee N.	556
Aryal A.	344	Banik S.	713
Arzhnikov A.K.	448, 651	Bannikova N.S.	622
Asadullin F.F.	565, 566, 864, 870	Baran M.	409
Asai H.	31	Barandiaran J.M.	495
Ashizawa Y.	389	Baranov D.A.	136, 204, 467
Aslanov L.A.	621	Baranov D.G.	116
Atkinson R.	371	Baranov N.V.	171, 289, 485, 589
Attanasio C.	25	Baranovskii S.D.	640
Attane J.P.	15, 16	Barbier A.	937
Audinet P.	306	Baretzky B.	108
Auffret S.	352, 675	Barman S.R.	713
Avdeev M.V.	327, 836	Barmin Yu.V.	283
Aver'yanov D.V.	365	Barnes C.H.W.	354
Averkiev N.S.	519, 642	Barone P.	695
Avvakumov I.L.	177	Barrera G.	357
Awano Hiroyuki	618	Barthel T.	736
Azarevich A.	313	Bartolomé J.	447, 776
Azarevich A.N.	252	Bartov D.	553
<hr/>			
B			
Babaev A.B.	197	Barulin A.V.	131
Babkin R.Yu.	912	Baryshev A.	115
Babkina I.V.	555	Baryshnikov A.Y.	223
Babushkina N.A.	708	Baryshnikov K.A.	519
Bach J.	648	Bataev D.S.	336, 480, 481
Baco V.	89	Batalov L.A.	656
Baczewski L.T.	84	Bataronov I.L.	283
Badelin A.G.	205	Batdalov A.B.	482, 715, 846
Bader S.D.	606, 631	Batov I.E.	899
Badiev M.K.	753	Battiato M.	383
Badini-Confalonieri G.A.	64	Baturin V.S.	458
Baehz C.	107	Bauch J.	82
Baenitz M.	903	Bauer A.	22
Bagschik K.	648	Baulin R.	211
Bai Jianmin	132	Baybakov R.F.	885
Bakirov M.M.	453	Bayer M.	641, 719, 915
Bakurskiy S.V.	186, 323, 326	Bayukov O.A.	208, 225, 226, 447, 521, 776
Balaev A.D.	446, 517, 844	Bazarov V.V.	151, 176
Balaev D.A.	225, 226, 655	Bazhanov A.G.	867
Balasoïu M.	416, 418, 825	Bazhanov D.I.	162, 443
Balasoïu-Gaina A.M.	825	Beach G.	49
Balatsky A.F.	122	Bebenin N.G.	39, 522, 724, 804
Balbashov A.M.	847, 914	Becca F.	123
		Beckmann D.	627
		Bee A.	414
		Begunov A.I.	275
		Behrenz S.	390

Beigne C.....	15	Bobrikov I.....	255
Beketov I.V.....	353, 873	Bobrov A.I.....	253
Belanovsky A.D.....	236, 546, 623	Bocharova O.A.....	223
Belik A.....	258	Bogach A.....	313
Belik A.A.....	839, 942	Bogach A.V.....	160, 175, 237, 238, 252, 885
Belik A.V.....	259, 260	Bogdanov A.E.....	350
Belikov V.V.....	183	Bogdanov S.G.....	265
Belliveau H.....	370	Bogomazova O.B.....	241
Beloborodov I.S.....	936	Bogomolov A.A.....	840
Belotelov V.I.....	119, 149, 719, 794	Boldyrev K.N.....	275, 697, 842
Belozerova K.A.....	491, 617	Bolginov V.....	666
Belyaev V.....	784	Bollero A.....	675
Belzig W.....	319	Bolotin D.....	799
Bena C.....	626	Boltalin A.I.....	182
Bending S.J.....	88	Bolyachkin A.S.....	294
Berdonosov P.S.....	754	Bonda A.....	803
Berestovaya A.A.....	202	Bondarenko G.N.....	764
Bergenti I.....	614	Bondarev A.V.....	283
Berger H.....	22	Bondarev I.A.....	536, 537, 548
Bergeret F.S.....	325, 628	Bonetti S.....	556
Berkov D.....	85	Borich M.A.....	278, 662
Berkov D.V.....	611	Boucher R.....	82
Bern F.....	378	Bouravleuv A.D.....	111
Bernert K.....	884	Bovensiepen U.....	382, 615
Berntsen M.H.....	648	Bowlan J.....	35
Bersuker I.B.....	519	Bozhko A.....	168
Bertacco R.....	247	Božović I.....	73
Berzhansky V.N.....	68, 119	Bragina V.A.....	361
Bespalov V.A.....	554	Bran C.....	674
Bessonov V.D.....	790	Brataas Arne.....	613
Betouras J.....	660	Brener S.....	387
Beyersdorff B.....	648	Breunig O.....	94
Bezmaternykh L.N.....	208, 279, 394, 447, 516, 697, 776, 850	Brisson J.-P.....	917
Beznosikov D.S.....	565	Brosseau C.....	931
Bezus A.V.....	602	Brovko O.O.....	373, 376
Bhagat S.M.....	873	Brück E.....	42
Bibikov S.B.....	562	Brusentsov N.A.....	223
Bica I.....	418	Brusentsova T.N.....	223
Bichurin M.I.....	854, 855, 941	Brüssing F.....	374
Biller A.M.....	417	Bucatco I.V.....	287
Bilych I.V.....	273	Bucheli D.....	896
Bischoff M.....	580	Buchelnikov V.D.....	40, 336, 341, 479, 480, 481, 496, 501, 585, 715
Bizyaev D.A.....	925	Büchner B.....	96, 146, 152, 212, 401, 589, 629, 694, 736
Blagodatkov D.V.....	924	Budarin L.I.....	667, 872
Blamire M.G.....	24, 556	Buettgen N.....	903
Blanco J.M.....	63	Bugaev A.S.....	365
Blinov I.....	334	Bukharaev A.A.....	925
Blinov I.V.....	451	Bukhtiyarova G.A.....	655
Bludov A.N.....	273	Bukreev D.A.....	235, 545, 579
Blum C.G.F.....	694	Bukreeva T.V.....	224
Bobin S.B.....	234		

Buling A.....	801	Charikova T.B.....	190
Bulka B.R.....	311	Chashin D.V.....	263, 938
Buravtsova V.....	792	Chatterjee R.....	346
Burdin D.A.....	263, 938	Chebotkevich L.A.....	88, 134, 436, 560, 590
Burkhanov G.S.....	490	Chechenin N.G.....	137, 138, 439, 612, 888
Burlui V.....	825	Chekanova L.A.....	154, 438, 452, 463, 464, 469
Burmistrov I.S.....	430	Chekhov A.L.....	721, 791
Burmistrova A.V.....	904, 905	Chekrygina Iu.I.....	779
Burova L.I.....	508	Chen H.-J.....	902
Bürstel D.....	382	Chen J.M.....	321
Burunova N.A.....	846	Chen P.J.....	765
Buryakov A.M.....	939	Cheng Ran.....	613
Buschhorn S.....	374	Chepulskyy R.....	19
Bushueva C.A.....	835	Cherif S.-M.....	676
Butler W.....	19	Chérif S.-M.....	371
Butrim V.I.....	384	Cherkasskii M.A.....	573
Butterling M.....	106, 107, 211	Cherkov A.G.....	558, 778
Buttgen N.....	454	Chernenkaya A.....	760
Buzdin A.....	303	Chernenko V.A.....	495
Buzdin A.I.....	324	Chernenkov Yu.P.....	170
Buznikov N.A.....	934	Chernikov R.V.....	588
Bychkov I.V.....	475, 489, 569, 841	Chernoglazov K.Yu.....	365, 520, 553
Bykov D.A.....	119	Chernova M.A.....	141
Bykova L.E.....	764	Chernykh P.N.....	888
<hr/>			
C			
Caballero-Flores R.....	920	Chernyshev V.A.....	509
Cabassi R.....	345	Chervonova U.V.....	80
Calbucci M.....	614	Chetkin M.V.....	559
Calemczuk R.....	352	Chetvertukhin A.V.....	718, 725
Camarero J.....	675	Chevalet J.....	414
Camp P.J.....	681	Chevalier D.....	626
Cantoni M.....	247	Chichay K.....	63, 69, 138, 168
Cao G.....	916	Chichkov V.I.....	98, 261, 424, 701, 807
Cao Jiangwei.....	132	Chicu L.I.....	287
Caprara S.....	896	Chien C.L.....	926
Carley R.....	35	Chigarev S.G.....	549
Caron L.....	42	Chikov A.A.....	177
Carriere M.....	352	Chinenkov M.Y.....	554
Carva K.....	383	Chirikov D.N.....	420
Caux J.-S.....	736	Chistyakov O.D.....	490
Cavicchia D.....	763	Chistyakova N.I.....	221
Cēbers.....	685	Chitanov D.N.....	838
Cecchini R.....	614	Chizhik A.....	586
Cerdà J.J.....	688	Chlenova A.A.....	59, 769
Cesari E.....	495	Cho V.....	94
Chakrabarty A.....	713	Chou F.C.....	902
Chakrabarty T.....	454	Chshiev M.....	312
Chareev D.A.....	155, 909	Chhtchelkatchev N.M.....	936
Charikova T.....	643	Chu Y.H.....	321
		Chuang Yi-De.....	321
		Chubanov A.A.....	232
		Chubova N.M.....	547
		Chubukov A.V.....	660

Chudnovskiy A.L.	431	Dediu V.	614
Chuenkova I.Yu.	757	Deeva E.	739
Chuev M.A.	337	Deeva E.B.	466
Chueva T.R.	65	del Pino P.	358
Chukalina E.P.	279	Delbecq M.R.	28
Chulkov E.	432	Demidenko O.F.	542, 858
Chulkov E.V.	428, 433	Demidov A.A.	192, 275
Churyukanova M.	66, 584	Demidov E.S.	112, 379, 667
Chuvilin A.	678	Demidov V.E.	607
Chzhan A.V.	774	Demin G.D.	231
Chzhan V.B.	490	Deminov R.G.	328
Cimorra C.	354	Demirci E.	251
Cimpoesu D.	661	Demishev S.	313
Ciocys S.T.	631	Demishev S.V. ..	131, 160, 175, 237, 238, 252, 547, 741, 875, 878, 885
Cirlin G.E.	111	Demokritov S.O.	607
Coïsson M.	357	Demyanov S.E.	272
Comtesse D.	40	Denisova E.A.	154, 452, 462, 463, 464
Conraux Y.	306	Dennis C.L.	765
Constantinian K.Y.	181, 329, 634, 897	Depeyrot J.	923
Contreras M.	674	Deranlot C.	15
Corbetta M.	376	Derevyanko M.S.	235, 545
Cornei N.	255	Deryushkin V.V.	234
Cornelius S.	106, 107, 211	Desnenko V.A.	909
Cottet A.	28	Deutsch M.	52
Craus M.-L.	255	Devishvili A.	477
Creuzet C.	306	Devyatov I.A.	904, 905
Cros V.	236, 546	Dianov M.Yu.	869
Cugini F.	345	Dias T.J.	358
Cwik J.	240, 497, 505, 716	Dieguez O.	274
<hr/>			
D			
D'Orazio F.	763	Dieleman D.	377
D'Souza S.W.	713	Dieny B.	312, 352, 675, 891
D'yachenko A.I.	179	Diesing D.	382
Dadoenkova N.N.	723	Dietl C.	694
Dadoenkova Yu.S.	723	Dietsch T.	352
Danilov Yu.A.	203, 233, 242, 253, 367, 641	Dikansky Yu.I.	822, 827
Dartiailh M.C.	28	Dilmieva E.T.	348, 497, 714
Darton N.J.	362	Djuarev D.R.	805
Das Sitikantha	650	Djuzhev N.A.	554
Dasa T.R.	373	Dmitrienko V.E.	943
Davydenko A.V.	134, 590	Dmitriev A.	110, 213
Davydov A.B.	514	Dmitriev A.I.	759
Davydov V.Yu.	912	Dmitrieva N.V.	599
de Bergevin F.	943	Dmitrieva T.V.	457
de Jong J.A.	914	Dobrecova E.A.	842
de la Fuente M.J.	358	Dobrogowski W.	84
de Oliveira A.J.A.	87	Dobrowolski W.	523
De Teresa J.M.	16	Doerr M.	332, 856
Deac A.M.	884	Dolgova T.V.	718, 802, 810
		Domański T.	311
		Domracheva N.E.	80
		Donaldson J.	687

Doppelt P.....	572
Dorgiev V.V.....	465
Dorofeev N.V.....	536, 537
Dorokhin M.V.....	233, 242, 253
Dramicanin M.D.....	166
Drobosyuk M.O.....	480, 481
Drovosekov A.B.....	525, 924
Drozdov Yu.N.....	203
Drulis H.....	332, 856
Duan Z.....	610
Dubenko I.S.....	344, 493, 502
Dubois E.....	414
Dubovik M.N.....	587
Dubrovsii A.A.....	225, 655
Dubrovsy A.A.....	844
Dubuis G.....	73
Ducruet C.....	306, 891
Dudnikov V.A.....	706
Dupuis V.....	372, 673
Dutreix C.....	626
Dvurechenskii A.V.....	640, 887
Dyadkin V.A.....	54
D'yakonov V.P.....	843
Dzhes A.V.....	558, 778
Dzhumaliev A.S.....	582
Dzhun I.....	138, 612
Dzhun I.O.....	137, 439
Dziom V.....	394

E

Eckstein M.....	386
Economou E.N.....	733
Economov N.A.....	263
Edelman I.S.....	745, 807
Efimov V.N.....	218
Efremov D.V.....	660
Eggers T.....	370
Eisterer M.....	491
Ekomasov A.E.....	164, 535
Ekomasov E.G.....	164, 241, 535
Ekomasov E.G.....	576
Ekonomov N.A.....	938
Elfimova E.A.....	681, 684, 821
Elin A.S.....	127
Eliseev A.A.....	163
Elkhova T.M.....	219
Elmers H.J.....	760
Elsukova A.....	90
Emelyanova S.M.....	491
Endo H.....	787

Entel P.....	40, 341
Eremeev S.V.....	428, 433
Eremin E.V.....	267, 271, 273, 275, 462, 469, 513, 516, 521, 620, 844
Eremin I.S.....	441
Eremin M.V.....	907
Eremina R.M.....	98
Ērglis.....	685
Eriksson O.....	377
Erkovan M.....	251
Ermolaeva O.L.....	379, 667, 668
Ermolov A.S.....	152
Ernst A.....	428, 432
Erofeev D.A.....	279
Erokhin S.....	85
Erokhin S.G.....	611
Eschrig M.....	318, 319
Escobosa A.....	643
Eshniyazov O.....	808
Eshpulatov B.....	808
Estemirova S.Kh.....	205
Eubank M.....	344
Evstigneeva M.....	153

F

Fabbrici S.....	345
Fabricci S.....	714
Facsko S.....	82
Farag L.A.....	359
Farle M.....	90, 139, 880
Farzetdinova R.M.....	669
Fassbender J.....	82, 884
Fayziev Sh.Sh.....	805
Fayzullin R.R.....	501
Fazlizhanov I.I.....	98
Fedor J.....	631
Fedorchenko A.V.....	909
Fedorchenko I.....	110, 213
Fedorchenko I.V.....	109, 523
Fedorov V.A.....	804
Fedorov V.V.....	136, 204, 467
Fedulov F.A.....	857
Fedyanin A.A.....	117, 691, 718, 725, 784, 802, 810
Felner I.....	349
FengH.-L.....	152
Fernandez S.....	769
Fernandez-Diaz M.T.....	52
Fernando G.W.....	122
Ferré J.....	84

Fert A.	15, 16
Fetisov L.Y.	572, 857, 938
Fetisov Y.K.	263, 857, 938
Filimonov Y.A.	564, 582
Filimonov Yu.A.	570, 865
Filipov V.	878
Filipov V.B.	175, 237, 238, 885
Filippov B.N.	587, 599
Filippov V.	313
Filippov V.B.	160, 252
Fisher T.	441
Flachbart K.	160, 237, 252, 313, 885
Fomicheva L.N.	52
Fominov Ya.V.	328, 330
Fowley C.	884
Fox A.M.	515
Fraerman A.A.	21, 118, 195, 379
Freydman A.L.	844
Friedland L.	662
Frielingsdorf J.	94
Frietsch B.	35
Frolov A.Yu.	810
Frolov K.V.	183, 184
Frömter R.	648
Frost C.D.	736
Fujita K.	700
Fujiyama K.	405
Fukunaga H.	405
Funtov K.O.	224, 457
Furuta M.	930
Futamoto M.	302

G

Gabani S.	160, 237, 252, 313, 885
Gabriels K.S.	555
Gaidukova I.Yu.	477
Gaifullin R.R.	328
Gajc M.	794
Galimov D.M.	91
Galindo-González C.	414
Galkin A.S.	135
Gallardo S.	643
Gamzatov A.G.	482, 715, 846
Gan'shina E.	792
Gan'shina E.A. ...	106, 165, 168, 365, 367, 444, 495, 500, 724, 804, 811
Ganeev V.R.	132, 144
Gapochka A.M.	260, 849
Gapontseva N.N.	702
García J.	920

García-Muñoz J.L.	847
Gareeva Z.V.	274, 845
Garel O.	288
Garst M.	22
Gastev S.V.	136
Gaudin G.	675
Gautier E.	675
Gaviko V.S.	43, 290, 297, 598
Gavriliuk A.A.	446, 578, 579
Gavrilkin S.Yu.	183, 252
Gavrilova T.P.	98
Gawlik W.	794
Gebhard F.	640
Gehring G.A.	515
Gendler T.S.	220, 292, 818
Geondzhian A.Y.	588
George J.M.	15
Gerasimov E.G.	43, 290, 297
Gerasimov M.V.	796
Gerber A.	553
Gerus S.V.	863
Gervits N.E.	773, 903
Geydt P.V.	295
Gheorghe D.G.	378
Giebeler L.	694
Gieniusz R.	790
Gierak J.	84
Gilmanov M.I.	131, 878
Gilmutdinov V.F.	448
Gimaev R.R.	595, 596
Gippius A.A.	182, 276, 454, 773, 903
Gladkikh D.V.	827
Gladkov A.A.	815
Glavic A.	370
Glazkov V.N.	97, 400
Glazkova Ia.S.	258, 259, 260
Gloskovskii A.	760
Glushkov V.V. ...	160, 175, 237, 238, 252, 313, 547, 741, 875, 885
Gnatchenko S.L.	909
Goering E.	108
Goikhman A.	472
Goldobin E.	27, 30
Golik L.L.	367
Golikova T.E.	899
Golod T.	895
Golov A.V.	566
Golovach G.P.	862
Golovanov A.N.	155, 476
Golub V.	168
Golubev E.A.	459, 749
Golubiatnikov A.N.	820

Hashimoto R.	787	Iniguez J.	274
Hatakeyama K.	103	Inishev A.A.	290
Havela L.	335	Inoue M. 117, 568, 718, 786, 787, 788, 789, 802	
Hayashi Kazunari	720	Ionescu A.	354, 362
He S.K.	908	Iovan A.	895
Heidarian A.	82	Ipatov M.	63, 69, 347, 584, 928
Heim D.M.	30	Iqbal Ya.	123
Heinemann A.	54	Irkhin V. Yu.	409, 531, 651
Heinrich G.	415	Irzhak A. V.	714
Hekking F.W.J.	325, 628	Isaev D.A.	814
Helm M.	212	Isavnin A. G.	762
Hendry E.	386	Isayenko L.I.	580
Hernando B.	343, 347, 348, 500, 920	Ischenko T.V.	741
Hetterich M.	640	Ishchenko L.A.	225, 226
Hiertz M.	94	Ishibashi T.	114
Higgs T.D.C.	556	Ishihara S.	704
Holm C.	76, 78	Ishio S.	144
Hong J.-Il.	83	Ishiyama K.	356
Horn S.	26, 898	Iskhakov R.F.	462
Hou Y.	352	Iskhakov R.S. 154, 225, 226, 438, 446, 452, 455, 463, 464, 469	
Hrubovčák P.	157	Iskhakova R.R.	848
Hu Can-Ming	18	Islam A.T.M.N.	740
Hu Xing Hao	355	Isogai R.	788
Huang Shih-Wen.	321	Ispiryan A.G.	822
Hübler F.	627	Iss C.	352
Hübner R.	82	Ito T.	392
Hwang Jong-Soon.	196	Ito W.	340
<hr/>			
I			
Iakovleva M.F.	212	Iunin Y.L.	926
Iakubov I.T.	101	Iusipova I.A.	551
Iavarone M.	631	Ivaneyko D.	415
Ibaev Zh.G.	755	Ivankov O.	825
Ibrahim P.N.G.	289, 589	Ivanov A.A.	190
Ichkitidze L.P.	222	Ivanov A.O.	680, 681, 816
Idzikowski B.	62	Ivanov A.S.	686
Iglesias I.	284	Ivanov B.A.	384, 623
Iglesias L.	920	Ivanov D.A.	330
Ignatchenko V.A.	860, 861	Ivanov O.A.	583
Ignatenko A.N.	531	Ivanov O.V.	360
Ignatenko O.V.	858	Ivanov P.N.	840
Ignatiev M.S.	454	Ivanov V.E.	782
Ignatiev P.	376	Ivanov V. Yu. 262, 394, 395, 547, 847, 850, 885	
Ignatov M.S.	360	Ivanov Yu.P.	678
Igoshev P.A.	651	Ivanova N.B.	208, 447, 776
Il'yushin A.S.	490	Ivanova O.S.	745
Il'ichev E.V.	186	Ivanova T.I.	716
Iliushin I.G.	156	Ivasishin O.M.	240
Ilkovic S.	499	Ivicheva S.N.	176
Ingale B.	346	Iwasieczko W.	476
		Iwata S.	619

Iyoda E.	704
Jaffres H.	15

J

Jähne C.	694
Jain P.	695
Jakina E.S.	524
Jalink J.	377
Jamet M.	16
Janjan S-M.	134
Jansson F.	640
Jedrecy N.	937
Jeng Horng-Tay.	321
Jiménez E.	675, 763
Joisten H.	352
Joumard I.	891
Jovanovic D.	166
Juang J.Y.	902

K

Kabanov Yu.P.	765
Kaczmarczyk J.	630
Kafesaki M.	733
Kagalovsky V.	431
Kainuma R.	168, 340
Kalabukhov A.	329
Kalanda N.A.	272
Kalashnikova A.M.	783, 914
Kalbukhov A.	897
Kalenkov M.S.	633
Kalenov D.V.	475, 489
Kalenteva I.L.	233
Kaletina Yu.V.	491
Kalinikos B.A.	268, 747, 851
Kalinin Yu.E.	270, 444, 456, 459, 539, 553, 555, 566, 749, 768, 792, 866, 874
Kalish A.N.	149
Kalitka V.S.	708
Kalmykov I.A.	287
Kalmykov S.A.	830
Kaloshkin S.	66, 584
Kaluzhnaya G.A.	185
Kalyabin D.V.	670
Kamancev A.P.	489
Kamantsev A.P.	347, 348, 475, 497, 501, 714
Kamarad J.	345
Kamata Y.	921
Kameli P.	482

Kamenev V.I.	858
Kameneva M.Yu.	442
Kamilov I.K.	715
Kammouni R.E.	284
Kamran M.	908
Kamynina I.A.	162, 443
Kamzin A.S.	132, 144, 227
Kanamori Y.	704
Kanazawa N.	568
Kanomata T.	340
Kantorovich S.	683, 688
Kantorovich S.S.	76, 680, 687, 816, 836
Kapelnitsky S.V.	525
Kapteyn H.C.	648
Karapetrov G.	631
Karashtin E.A.	118, 195
Karavainikov A.V.	119
Kargin N.I.	441
Karimov O.I.	597
Karminskaya T.Yu.	323, 328
Karmous F.	572
Karo H.	359
Karpasyuk V.K.	205
Karpenkov A.Yu.	473, 474, 494, 504
Karpenkov D.Yu.	473, 474, 494, 504, 505, 840
Karpenkov A.Yu.	840
Karzanov V.V.	112
Kasagi T.	103
Kashchenko M.A.	277
Kashina N.V.	136
Kashirin M.A.	270, 539
Kashiwaya S.	628
Kassan-Ogly F.A.	58, 124, 492
Kataev V.	212, 401, 422
Kataev V.A.	295
Katanin A.A.	531
Kato T.	619
Katsnelson M.I.	377, 386, 387
Kaul A.R.	508, 708, 811, 846
Kawabata S.	31, 325, 628
Kaya D.	370
Kazak N.V.	208, 447, 776
Kazakov S.M.	183
Kazei Z.A.	442
Kazhan V.A.	823
Kazin P.E.	603
Keimer B.	329
Keller T.	329
Kenanakis G.	733
Ketsko V.A.	308
Khadra G.	372

Khaidukov Y.	534	Kiseleva T.Yu.	818
Khajrullin M.F.	814, 826	Kisilev N.I.	544
Khalid M.	212	Kislinskii Yu.V.	181, 329, 634, 897
Khamidov D.	691	Kitakami O.	930
Khanipov T.F.	925	Kitenbergs.	685
Kharchenko Yu.M.	119	Klar P.J.	640
Kharisov A.T.	848	Kläui M.	616
Kharlamova A.M.	65, 165	Klein P.	64
Kharmouche A.	67	Kleiner R.	27, 30
Kharrasov M.Kh.	126	Kleinerman N.M.	43, 296, 598
Khatsaiuk V.V.	68	Klekovkina V.V.	191
Khavronin V.P.	170, 424, 701	Klemke B.	740
Khaydukov Yu.	897	Klenov N.V.	186, 323, 326
Khaydukov Yu.N.	329, 634	Kliava J.	575
Khivintsev Y.V.	564	Klimin S.A.	135, 146, 277, 696
Khivintsev Yu.V.	570	Klimov A.Yu.	379
Khlustikov I.N.	666	Klimovskikh I.I.	246
Khlybov E.P.	184	Klingeler R.	146, 694
Khmelevskoi D.V.	109	Klos A.	794
Khohlov A.R.	223	Klos J.W.	723
Khokhlov N.E.	119	Klyuchnikova M.A.	496
Kholopov V.L.	757	Klyushina E.S.	740
Khomitsky D.V.	232	Knotko A.V.	214
Khomskii D.I.	74, 422	Knyazev Yu.V.	208, 447, 601, 776
Khoroshilov A.	313	Kobayashi K.	788
Khoroshilov A.L.	160	Kobs A.	648
Khovaylo V.V.	168, 336, 346, 348, 480, 481, 498	Kobyakov A.V.	557
Khrebtov A.I.	111	Kocharian A.N.	122
Khvalkovskiy A.	19	Kochura A.	110, 213, 215
Khvalkovskiy A.V.	535	Kochura A.V.	109
Kiba Yuusaku.	720	Koelle D.	27, 30
Kikitsu A.	921	Kohlstedt H.	27
Kikoin K.	310	Kokh K.A.	902
Kikuchi N.	930	Kokorin V.V.	348
Kilanski L.	523	Koksharov Yu.A.	409
Kim CheolGi.	355	Kokubun J.	943
Kim Dong-Hyun.	272	Koledov V.	349, 484
Kim Kee Hoon.	395	Koledov V.V.	347, 348, 475, 483, 489, 497, 714, 715
Kim Kun Woo.	355	Kolenda S.	627
Kim S.H.	356	Kolentcova O.S.	441
Kim Y.K.	134	Kolesnikov A.G.	436, 560
Kimel A.V.	11, 378, 386, 799, 914	Kolesnikova A.A.	827
Kiparisov S.Ya.	771	Kolesnikova E.M.	516
Kirillova M.M.	540	Kolker A.M.	80
Kirilyuk A.	377, 378, 799, 914	Kolland G.	94
Kirman M.V.	748	Kolmychek I.A.	118
Kirpicheva O.A.	866	Kolotov O.S.	868
Kirschner J.	376, 432	Komogortsev S.V.	88, 154, 309, 446, 452, 455, 463, 464, 469
Kirushev M.S.	571	Konakov A.A.	232
Kiryukhantsev-Korneev Ph.V.	591	Konev V.V.	178
Kiselev I.A.	91, 170		

Konig E.J.	430	Kovalyuk Z.D.	240
Kononenko V.V.	179	Kozeeva L.P.	442
Konoplyuk S.M.	348	Kozhaev M.A.	794
Kontos T.	28	Kozhanov A.	441
Koo H.-J.	96, 737	Kozlov A.G.	590
Kopeliovich D.B.	596	Kozlov V.I.	299
Koplak O.	110, 213, 518	Kozulin A.S.	232
Korenev V.L.	641	Krabbes G.	736
Kornilov A.A.	145, 746	Kraetschmer W.	454, 903
Korobova J.G.	162, 443	Krainov I.V.	642
Korolev A.F.	729	Kramarenko E.Yu.	419, 814, 826, 834
Korolev A.V.	58, 178, 511, 702	Krasikov A.A.	225
Koroleva L.I.	524	Krasnikova Y.	772
Korolyov A.V.	777	Krasnikova Yu.V.	400
Korostelin Yu.V.	519	Krasnorussky V.N.	175
Korostil A.	230	Krasnov V.M.	895
Korotaev E.V.	450	Kravchenko E.A.	209
Koroteev Yu.M.	428	Kravchenko Z.F.	858
Korotin M.A.	423	Kravtsov E.A.	924
Korotkov N.Yu.	183, 184, 224	Krawczyk Y.	723
Korovin A.M.	204	Kreilkamp L.E.	719
Korovin V.M.	823	Kreines N.M.	525, 924
Korovushkin A.E.	815	Kremer R.K.	737
Korsakov I.E.	811	Krichevtsov B.B.	467
Korshunov A.S.	440	Krinitsina T.P.	451
Korshunov S.E.	750	Krivenkov M.S.	292
Kosel	678	Krivorotov I.N.	610
Kosel J.	674	Krivtsov I.V.	580
Koshelev A.V.	155	Kronast F.	82
Koshkid'ko Yu.S.	716	KrounbiM.	19
Kostarev K.G.	835	Krug von Nidda H.-A.	26, 898
Kostishin V.G.	838	Kruglyak V.V.	386
Kostishyn V.	230	Krugvon Nidda H.-A.	98
Kostishyn V.G.	562	Krupa M.	230
Kostitcyana E.	584	Krupa N.N.	838
Kostyuchenko M.V.	766	Krupskaya Y.	401
Kostyuchenko N.	856	Krutyanskiy V.L.	118, 721
Kosykh T.B.	248	Krylov V.I.	173
Kosykh T.B.	797	Krynetskii I.B.	185
Kosyrev N.N.	793	Ksenevich T.I.	361
Kotelnikova O.A.	41, 729	Kuchin A.G.	43
Kotov A.	760	Kuchin D.S.	475, 489, 714
Kotov L.N.	456, 459, 565, 566, 571, 749, 864, 866, 869, 870	Kudasov Yu.B.	269, 440
Kourov N.I.	617	Kudo K.	786
Kováč J.	157	Kudrevatykh N.V.	285, 478
Kovalenko D.V.	855	Kudriavstev Yu.	643
Kovalenko V.I.	185	Kudrin A.V.	203, 233, 253, 367
Kovalev A.S.	437	Kudryashov V.Y.	153
Kovalev L.V.	272	Kudryavtsev I.K.	621
Kovalev V.I.	367	Kudryavtsev R.V.	164
Kovalevskaya S.D.	820	Kuepper K.	801
		Kugel K.I.	425

Kuhns P.L.....	402	Lagarkov A.N.	101
Kulagin N.E.	845	Lahderanta E.	109, 110, 213, 215, 366, 523, 642
Kulatov E.T.....	216, 365, 621	Lähderanta E.	91, 295
Kulbachinskii V.A.	185, 210, 508, 514	Lahova M.B.	333
Kulesh N.A.....	140, 460	Lake B.	466, 736, 739, 740
Kulik L.V.	887	Lamekhov S.J.....	841
Kulikov A.G.....	938	Lamonova K.V.....	208
Kulikovskiy A.V.	193	Landee C.P.	772
Kun Fang.....	122	Landman A.I.	519
Kun'kova Z.E.....	367	Langer L.....	641
Kuncevich A.A.....	703	Langer M.C.....	321
Kunikin S.A.	822	Lapa P.N.	370
Kuntsevich A.Yu.....	890	Larin V.S.....	287
Kuo C.N.	198	Larrañaga A.	761, 769, 873
Kuo Y.K.	198	Laschitzky P.....	94
Kupriyanov M.Yu. 26, 30, 186, 323, 326, 328, 898		Lasek M. P.....	459
Kupriyanova G.S.....	147, 239, 612	Lasek M.P.	866
Kuratieva N.V.	449, 450	Lashkul A.V.....	91
Kurbakov A.I.	91, 703, 707	Lau J.T.	86
Kurbanova D.R.	753, 758	Lauter V.	370
Kurbatova Yu.N.	559	Lavrenova L.G.	449, 450
Kurenkov A.S.....	888	Law J.M.	335, 737
Kurkin M.I.	702, 806	Lazuta A.V.....	170, 701
Kurlyandskaya G.V.....	59, 165, 761, 769, 873	Le Trong H.....	89
Kurlyandskaya G.V.....	545	Lebedev A.V.	689
Kushnir V.N.....	174	Lebedeva Ye.V.	779
Kusmartsev F.V.	629	Lebedeva E.V.....	167
Kuvandikov O.K.....	597	Lebyodkin M.A.....	889
Kuvodikov Sh.	808	Lee J.M.	321
Kuwahara H.	392	Lehtinen J.S.	632
Kuz'min Yu.I.	601	Lekina Yu.O.....	849
Kuzmenko A.M.....	394, 850	Lekina Yu.V.....	260
Kuzmichev S.A.	182	Lenk D.	26, 898
Kuzmicheva T.E.....	182	Lepalovskij V.N.....	254, 461, 769
Kuzmin D.A.	475, 489, 569, 841	Lepalovsky V.N.....	295
Kuznetsov A.A.	682	Lepeshkin S.V.....	458
Kuznetsov A.R.	300	Leskova Yu.V.	509
Kuznetsov A.V.....	237, 238, 885	Lesnikov V.P.	112, 203
Kuznetsov V.D.....	223	Leulmi S.....	352
Kuznetsova E.S.....	754	Levchenko A.....	313
Kuznetsova T.V.	801	Levchenko A.V.....	238, 885
Kuzovnikova L.A.....	462, 463	Levchenko G.G.....	574
Kveglis L.I.	558, 778	Levchenko G.V.....	175
Kytin V.G.....	508	Li J.	153
Kyzyrgulov I.R.....	126	Li O.A.....	463, 469
<hr/>		Li Z.-A.....	139
L		Liang Q.F.....	942
Laczkowski P.	15, 16	Lichtenstein A.I.	387
Ladygina V.P.	225, 226	Liébana-Viñas S.....	90
		Lim Byeonghwa.....	355
		Lim P.B.....	786, 788

Lin C.-R.	773
Lin Chun-Rong	457
Lin J.-Y.	153, 321, 902
Lindner J.	82, 884
Lipman A.	27
Lipsanen H.	111
Lisenkov I.V.	670
Lisunov K.G.	91, 109, 215
Lisyansky A.A.	116
Liu H.F.	198
Liu M.	182
Liubimov B.Ya.	677, 933
Livache T.	352
Llandro J.	354, 362
Lobanova I.I.	547, 741, 875
Lobov I.D.	540
Lock E.H.	871
Lodewijk K.J.	59
Loginov N.N.	796
Loginova L.A.	418, 814, 826
Lograsso T.A.	713
Logunov M.V.	796
Lohmann A.	767
Loidl A.	98
Lombard L.	306
Lonchakov A.T.	206, 234
Lopez M.	643
Lorenz T.	94
Lorenz W.E.A.	772
Los A.S.	240
Loshkareva N.N.	709, 724
Lotin A.A.	520
Lou G.	114
Love D.M.	354
Lozovik Yu.E.	429
Lue C.S.	182, 198, 903
Lue C.S.	198
Lue C.Y.	198
Luetkens H.	739
Lukashevich M.V.	830
Lukitsa I.G.	133
Lukoyanov A.V.	601
Lukshina V.A.	599
Luo C.W.	902
Luo Y.	928
Lupu N.	825
Lutsev L.V.	204, 308, 565
Lyadov N.M.	176
Lyange M.	168
Lyange M.V.	498
Lyapilin I.I.	250
Lysenko I.A.	224

Lysenko S.	825
Lysov M.S.	659
Lyubchanskii I.L.	723
Lyubin E.V.	691
Lyubina J.	45
Lyubutin I.S.	183, 184, 224, 276, 457, 705, 773

M

Machon P.	319
Mackay K.	306
Madiligama A.S.B.	349, 484
Maeda T.	921
Magnan H.	937
Magnitskaya M.V.	216
Mahajan A.V.	454
Maignan A.	51
Makagonov V.A.	539, 550
Makarova A.O.	207
Makarova O.L.	52
Makhnev A.A.	512
Makhnovsky D.P.	932
Maklakov S.A.	61, 101, 600
Maklakov S.S.	61, 600
Makovetskii G.I.	542, 858
Maksimova K.Y.	204
Malakhovskii A.V.	795
Malekhonova N.V.	253
Maljuk A.	694
Malkin B.Z.	191, 279, 842
Maltsev V.K.	557
Malyarenko P.	187
Malyshev A.L.	703
Malyshev A.Y.	596
Malysheva E.I.	253
Mamedov D.V.	98
Mamonova M.V.	158, 159
Mamsurov I.V.	189
Mamsurova L.G.	189
Mangin S.	36
Manna S.	432
Mansson M.	740
Mansurova M.	390
Marchenko I.V.	224
Marchenkov V.V.	491, 617
Marenkin S.	213
Marenkin S.F.	109, 523
Markelova M.N.	846
Markin Yu.V.	367
Markina M.M.	214, 754

Martin C.	51	Merentsov A.I.	171
Martín F.	731	Meriakri V.V.	489
Marty A.	15, 16	Merkulova A.M.	466
Martyanov O.N.	655	Merkulov D.I.	205
Martyshko P.S.	130	Mertelj T.	916
Maruschenko E.A.	557	Mertig I.	432
Mashirov A.	349	Merz M.	760
Mashirov A.V.	348, 497, 501	Meutzner F.	82
Mashkovtseva L.S.	580	Meyer H.-P.	694
Maslennikova A.E.	777	Meyerheim H.L.	432
Maslov D.A.	269, 440	Miao X.F.	42
Mata J.	731	Michałek G.	311
Matsko N.L.	148, 375, 458	Michels A.	85, 404
Matsnev M.E.	259, 260, 266, 849	Mihailovic D.	916
Matsushita Y.	942	Mikhailov G.G.	580
Matsuura M.	543	Mikhailov G.M.	549
Matukhin V.L.	402	Mikhailova T.V.	119
Matveev V.V.	79, 91	Mikhailovsky Yu.	106
Matyunin A.V.	868	Mikhailovsky Yu.O.	553
Maximova O.A.	793	Mikhalevsky V.	213
Mayer M.	419	Mikhailitsyna E.A.	295
Mazalski P.	84	Mikhashenok N.V.	517
Maziewski A.	84, 307, 388, 586, 790	Mikhaylovskiy R.V.	386
Mazilkin A.A.	108	Miki H.	498
Maznichenko I.V.	432	Mikuszeit N.	675, 763
Mazov L.S.	906	Mill B.V.	135
Mazur A.S.	858	Miller C.W.	370
Mazurkin N.S.	554	Miller M.	716
Mc Cord J.	84	Milyaev I.M.	298
Mc Millen M.	371	Milyaev M.A.	451, 540, 622
Medjanik K.	760	Minina E.	683
Medvedev A.I.	353	Minina E.S.	836
Medvedev M.V.	492	Mints R.	27
Medvedeva M.A.	127, 529	Mirebeau I.	52
Mehonoshin D.S.	659	Mirlin A.D.	430
Meilikhov E.Z.	669	Mironov V.L.	379, 668, 872
Mel'nikov A.S.	324	Mishina E.D.	939
Melenev P.V.	77, 78, 686	Mistonov A.A.	163
Melnik D.D.	508	Mitrofanov V.Ya.	130
Melnikov A.	382	Mitrofanova E.S.	909
Melnikov N.B.	653	Miura S.	20
Melnikov Y.P.	596	Miyake A.	392
Melnikova S.V.	154	Moers J.	887
Men'shenin V.V.	55	Mohseni K.	432
Menschikova T.K.	804	Moiseev A.A.	235, 545
Menschikova T.V.	428	Moiseev K.D.	643
Menshov V.N.	428, 433	Mokeev M.V.	91
Mentink J.H.	386	Mokhovikov A.Yu.	578, 579
Menushenkov A.P.	588	Molkanov P.L.	91, 170
Menushenkov V.P.	282, 581	Möller A.	401
Menzel D.	54, 163	Molokanov V.V.	65
Mercone S.	572	Molokeev M.S.	271, 513, 521

Monakhov A.M.	519
Monkman G.	419
Montejano-Carrizales J.M.	372
Moore S.A.	631
Moosaeva S.M.	145
Morari R.	26, 898
Morchenko A.T.	562, 563, 932
Morcrette M.	352
Morgunov R.	110, 213, 518, 760
Morgunov R.B.	366, 748, 759
Moria A.	20
Morimoto Y.	406
Moros M.	358
Morosov A.I.	940
Moroz O.Yu.	133
Morozkin A.V.	350
Morozov A.S.	524
Morozov I.	739
Morozov I.V.	182, 466
Morozova N.V.	578, 579
Moshchalkov V.V.	152, 252
Moskvin A.S.	177, 178
Moskvin E.V.	54
Mostovshchikova E.V.	709, 724, 804
Motomura K.	405
Moulin J.	288
Movchan N.N.	567
Mrozek M.	794
Muduli P.	24
Muenzenberg M.	390
Mukhin A.A.	262, 394, 395, 847, 850
Mukhin A.N.	165
Mukhuhev A.A.	846
Mukovskii Ya.M.	261, 424, 522, 593, 701
Müller C.	26, 898
Müller L.	648
Müllner P.	712
Mulyukov R.R.	483
Munekata H.	34
Münzenberg M.	382
Murai S.	44
Murakami Y.	44
Murata H.	32
Muratova A.B.	816
Murnane M.M.	648
Murphy A.P.	371
Murtazaev A.K.	197, 753, 755, 758
Murtazaliev R.A.	197
Murtazin R.R.	164, 241, 576
Murzakaev A.M.	353, 873
Murzina T.V.	118, 721, 791
Musabirov I.I.	483

Mushenok F.B.	876
Mushnikov N.V.	43, 290, 296, 297, 407, 592
Musorin A.I.	718, 802
Mussler G.	887
Mustafa L.	329, 534, 897
Muthu S.E.	713
Muzaffarov A.	597
Myagkov V.G.	764
Mykha I.R.	725

N

Naboko A.S.	61, 600
Nagel P.	760
Nakagawa K.	389
Nakamura K.	786
Nakamura Y.	788
Nakano M.	405
Nakata R.	742
Nakatani R.	20
Nalbandyan V.B.	96, 152, 153
Naletova V.A.	817, 830
Namai A.	759
Nanto Dwi.	272
Nanto Dwi.	196
Napolskii K.S.	163
Naqui J.	731
Nasirpouri F.	88
Nasirpouri Farzad	134
Nasirpouri Forough	134
Naumov P.G.	183
Naumov S.V.	249, 510, 511, 512, 709
Naumova L.I.	622
Nazarov V.N.	576
Nechaev I.A.	428
Neef C.	694
Nefedov I.M.	667
Nehoroshkova Y.E.	821
Neifel'd E.A.	702
Nemrava S.	580
Nemtsev I.V.	154, 464
Nenashev A.V.	640
Netesova N.P.	194
Neudert A.	82
Nevdacha V.V.	838
Nevedomskiy V.N.	111
Nevedomsky V.N.	643
Neverov V.N.	190
NhungDinh T.H.	288
Niebergall L.	376
Niedner-Schatteburg G.	377

Niewa R.....	580
Nigam A.K.....	342
Nii Y.....	44
Nikiforov A.E.....	509
Nikiforov V.N.....	409
Nikitenko V.I.....	765, 926
Nikitenko Yu. V.....	21
Nikitin A.A.....	268
Nikitin L.V.....	286, 815
Nikitin M.P.....	223, 361
Nikitin P.I.....	223, 361
Nikitin S.A. 350, 474, 476, 487, 504, 505, 716	
Nikitin V.	19
Nikitov S.A.	564, 570, 670, 796, 865
Nikoladze G.M.....	868
Nikolaev A.B.	248
Nikolaev S.N.....	365
Nikolaeva E.P.....	248
Nikolaychuk G.A.	133
Nikulin Y.V.....	582
Nishi T.....	114
Nishimizu A.	787
Niu Qian.....	613
Niyazov L.N.....	805
Nizamov F.A.....	176
Nizhankovskii V.I.	208
Nižňanský D.....	142
Nolting F.	647
Nomerovannaya L.V.....	512
Nomura H.....	20
Nori F.	125, 425, 654
Nosov A.P.....	265
Notbohm S.	736
Notin C.....	15
Novak E.....	683, 687
Novak E.V.....	836
Novakova A.A.	220, 292, 818
Novikov A.....	106, 168, 367, 444
Novikov A.I.....	495, 500
Novitskii N.N.....	308, 843
Novodvorskii O.....	110, 213
Novodvorskii O.A.....	365, 366
Novosad V.....	631
Nozdrin A.G.....	933
Nugumanov A.G.....	126
Nurgaliev T.C.....	172
Nurgazizov N.I.....	925
Nurimov U.E.....	597
Nuzhdin V.I.....	151

O

Obermeier G.	26, 898
Oepen H.P.....	648
Oganov A.....	334
Ogimoto H.	406
Ognev A.V.....	88, 134, 436, 560
Oh Suhk Kun	272
Oh Suhk-Kun.....	196
Ohara J.....	704
Ohishi T.	32
Ohkoshi S.....	759
Ohldag H.....	556
Ohta H.....	742
Ohtake M.	302
Ohtsuka M.....	168
Oka H.....	376
Okamoto S.	930
Okorokov M.S.	250
Okubo A.....	168
Okubo S.	742
Okulov V.I.	234
Okulov B.I.	206
Okuta K.....	742
Ong C.K.....	100
Onufrieva F.....	322
Oppeneer P.M.....	383, 384
Orlov A.	106, 211
Orlov A.V.	361
Orlov Yu.S.....	706
Orlova A.	147
Orlova N.B.....	806
Ortiz G.....	352
Orue I.	873
Osadchenko V.H.....	478
Osin Yu.N.....	151
Osipov A.V.....	101, 600
Ostrovskaya N.V.....	551
Ostrovsky P.M.	330, 430
Ota Toshitaka.....	720
Otrokov M.M.....	428
Otsuka M.....	498
Ouazi S.....	376
Oudovenko V.S.....	636
Ovchenkov E.A.....	350
Ovchenkov Y.A.	182
Ovchenkova I.A.....	350, 487
Ovchinnikov S.G.	208, 309, 315, 447, 706, 776, 793
Ovchinnikova E.N.	943
Ovejero J.G.....	674

Oveshnikov L.N.	210, 514
Ovsyannikov G.A.	181, 329, 534, 634, 897
Oyartzun S.	16
Ozaeta A.	325, 628
Ozherelyev V.V.	283
Öztürk M.	251
Öztürk O.	251

P

Pal A.	24
Palmero E.M.	674
Palvanova G.S.	729
Pamyatnykh E.A.	234
Pamyatnykh L.A.	130, 659
Pamyatnykh S.E.	659
Panasevich A.M.	858
Panchenko V.Ya.	365
Pandey S.	344
Panfilov A.S.	909
Panina L.V.	562, 563, 838, 928, 932
Pankov M.A.	520
Pankratov N.Yu.	504, 505
Pankratova M.L.	437
Pankrats A.I.	192, 517, 521, 752
Pankrstov A.L.	186
Paranchich L.D.	206, 234
Park J.	740
Park S.	370
Parkhomenko M.P.	489
Parlak U.	251
Parshina L.	110
Parshina L.S.	520
Pashchenko V.A.	273, 909
Pashkevich Yu.G.	912
Pastushenkov A.G.	333, 840
Pastushenkov Yu.G.	333, 474, 494
Patrakov E.I.	249, 491
Patrin G.S.	264, 557, 771, 774
Patrin K.G.	557, 771
Paukov M.	335
Pavlochev S.Y.	493, 502
Pavlov D.A.	253
Pavlov E.S.	865
Pavlov V.N.	440
Pavlov V.V.	783, 915
Pavlova I.O.	583
Pavlukhina O.O.	585
Pavuna D.	73
Pawlak D.A.	794
Pearson J.	631
Pechnikov V.S.	143
Peighambari S.M.	88
Pelevin I.A.	332, 335, 856
Pelevina D.A.	830
Pellenen A.P.	336, 480, 481
Peng H.X.	928, 931
Pereira E.C.	87
Pereira J.	306
Perez J.E.	674
Perez-Mato J.M.	695
Perl J.	90
Perna P.	675
Perov N.S.	106, 365, 366, 591, 706, 814, 826
Perring T.G.	736
Perunov I.V.	183
Pervakov K.S.	184
Perzynski R.	414, 923
Pestov A.E.	379
Peters L.	377
Petit S.	52
Petrakovskaya E.A.	745
Petrenko A.V.	21
Petrenko O.A.	97
Petrik M.V.	300
Petrov A.A.	161
Petrov P.S.	729
Petrov R.V.	854, 855, 941
Petrov V.M.	854, 855, 941
Petrov V.P.	509
Petrzhik A.M.	534
Petti D.	247
Petukhov D.A.	552
Petukhov D.S.	190
Petukhov V.Yu.	453
Petznick S.	640
Pfeuty P.	322
Pfleiderer Ch.	22
Phuoc N.N.	100
Pichugin A.Yu.	620
Picozzi S.	247, 695
Pigalskiy K.S.	189
Pilipenko D.V.	158, 159
Pilipets E.S.	566
Pimenov A.	394
Pirogov A.N.	265
Pirogov Y.A.	223
Pisarev R.V.	386, 697, 783, 912, 914, 915
Pismenova N.E.	858
Pitimova E.A.	203
Pivkina M.N.	746
Plakida N.M.	636
Platonov E.P.	491

Raikher Yu.L.	77, 78, 416, 417, 418, 881, 923
Rajput P.	713
Rakhmanov A.L.	125, 425, 654
Ramasamy K.	752
Ramazanov M.K.	753, 758
Rameev B.	612
Randhawa B.S.	411
Ranjan R.	713
Rantala T.	632
Rasing Th.	377, 378, 386, 799, 914
Rawat R.	713
Razdolski I.	378, 799
Razmyslov I.N.	150
Reddy Venu.	355
Reiffers M.	499
Repko A.	142
Reser B.I.	653
Ressouche E.	847
Reukova O.V.	508
Reyes A.P.	402
Reyren N.	15
Rhen F.M.F.	380
Richardson D.	380
Richter J.	399, 767
Riminucci A.	614
Rippard W.H.	884
Rivera S.	358
Robinson J.W.A.	24, 25, 556
Rodary G.	376
Rodin V.V.	185
Rodionov I.D.	344, 493, 495, 502
Rodionov V.V.	486
Rodionova V.V.	63, 69, 137, 138, 168, 284, 472, 486, 612, 784
Rodmacq B.	675
Rogacki K.	716
Rogalev A.	646, 917, 943
Rogov V.V.	379, 667
Rojas-Sanchez J.C.	15, 16
Romachevskii K.E.	227
Romanova O.B.	542, 544, 620
Romashev L.N.	540
Rosa W.O.	343, 920
Rosenfeld Ye.V.	407
Roshchin I.V.	370
Roslova M.V.	182
Ross C.A.	236, 546, 789
Rossi L.	763
Roussigne Y.	676
Roussigné Y.	371, 572, 862
Rovigatti L.	680
Roy S.	432
Roazanov K.N.	101, 102, 732, 877
Rozhansky I.V.	642
Rozhkov A.V.	125, 425, 654
Rudenko R.Yu.	774
Rudenok A.A.	563
Rudisch C.	694
Rudolf D.	648
Rudoy Yu.G.	41
Ruiz-Diaz P.	373
Rumyantseva S.S.	224
Rungger I.	382
Runov V.V.	170
Rusakov V.S.	207, 221, 259, 260, 266, 296, 777, 849, 853
Rusinov A.A.	751
Rusinova E.A.	751
Russek S.E.	884
Ryabinkina L.I.	544
Ryabukhina M.V.	924
Ryapolov P.A.	690
Ryazanov V.V.	899
Ryba T.	499
Rybakov Yu.P.	663
Rybkin A.G.	246
Rybkina A.A.	246
Rylkov V.V.	365, 525, 553
Ryzhanova N.	243, 245, 316
Ryzhikov I.A.	61, 101, 600
Ryzhkov A.V.	77, 78
Ryzhov A.V.	170
Ryzhov V.A.	91, 424, 701

S	
Saarelad M.	629
Sablina K.A.	517, 521
Sabon P.	352
Sadakov A.V.	184
Saeid S.	242
Safronov A.P.	353, 545, 769, 873
Safronova E.S.	809
Saha-Dasgupta T.	398
Saito H.	115
Saito S.	117
Saito T.	543
Sakaguchi K.	787
Sakharov V.K.	564
Sakhratov Yu.A.	402
Sakurai T.	742
Salakhova R.T.	219
Salamat H.	482

Saleheen A.	344	Schottenhamel W.	589
Saletsky	128	Schuppler S.	760
Salgueiriño V.	90	Schütz G.	108
Salikhov R.	374	Schwarze Th.	22
Samanta T.	344	Sciortino F.	680
Samardak A.S.	88, 134, 436, 560	Score D.S.	515
Samarin A.N.	131, 875, 878	Secchi A.	386, 387
Samarin N.A.	160, 238, 875	Sechin D.A.	248
Samatov O.M.	353	Sechovský V.	173
Samokhvalov A.V.	324	Sedova M.V.	600
Samsonenko Yu.B.	111	Seidov Z.	26, 898
Sanchez J.-P.	917	Sekar C.	736
Sanchez P.	683	Sekiguchi Koji	14
Sánchez P.A.	688	Selezneva N.V.	171, 289, 589
Sander D.	376	Seleznyova K.	575
Sankar R.	902	Semenenko K.I.	770
Sanvito S.	382	Semeno A.V.	131, 875, 878
Sanyal B.	377	Semenov A.A.	268
Sapega V.F.	111, 641	Semenov A.G.	318
Saphiannikova M.	415	Semenov A.L.	578, 579
Sapoletova N.A.	163	Semenov S.V.	225
Sapozhnikov M.V.	112, 118, 195	Semenov V.S.	756
Sapozynikov M.V.	667	Semenova E.M.	333, 473, 474
Sarychev M.N.	519	Semirov A.V.	235, 545
Sasada I.	359	Semisalova A.S. 106, 365, 366, 520, 580, 591, 814	
Sato H.	742	Semkin M.A.	265
Sato M.	637	Senina V.A.	145, 746
Satoh T.	307, 913	Senyshyn A.	713
Savchenko A.S.	574	Serebryakova O.N.	468, 933
Savchenko E.S.	282	Seredkin V.A.	774
Savel'ev S.	31	Sergeev A.S.	53, 698
-Savero-Torres W.	15, 16	Serikov V.V.	43, 296, 598
Savin A.	111	Seryotkin Yu.V.	516
Savin P.A.	254, 461	Shabanova N.P.	185
Savitsky A.O.	924	Shadrin A.V.	181, 329, 534, 634, 897
Savoini M.	672	Shadrov V.G.	570
Saxena S.S.	72	Shafeev R.R.	576
Sazanovich A.	843	Shagalov A.G.	662
Sazhina E.Yu.	291	Shahosseini I.	288
Sboychakov A.O.	125, 425, 654	Shakarov H.O.	597
Schäpers M.	401	Shakin A.A.	593
Scharffe S.	94	Shakirova O.G.	449, 450
Scherbakov A.V.	385	Shalygin A.N.	65
Schlagel D.L.	713	Shalygina E.E.	65, 165
Schleitzer S.	648	Shamonina E.	730
Schmidiger D.	400	Shamonine M.	419
Schmidt H-J.	767	Shanova E.I.	439
Schneider C.M.	648	Shapaeva T.B.	241, 559
Schneidewind A.	740	Shapkin A.A.	221
Schoenlein R.W.	321	Shaposhnikov A.N.	119, 797
Schollwöck U.	736	Sharafullin I.F.	126
Schönhense G.	760		

Sharay I.V.	797	Sidorov V.A.	52
Sharipova M.I.	802	Siegfried S.-A.	54
Sharko S.A.	843	Sigov A.S.	207, 266, 853, 940
Shashkov I.V.	889	Silhanek A.V.	152, 153
Shatruk M.	588	Silva F.G.	923
Shavrov V.G.	347, 348, 349, 475, 484, 489, 497, 565, 569, 571, 574, 714, 715, 798, 841, 864, 869, 870	Simkin V.	255
Shaykhutdinov K.A.	655	Simonovskii A.Ya.	757
Shaymanov A.N.	791	Singh R.	346
Shcheglov V.I.	565, 571, 864, 869, 870	Singh Sanjay	713
Shchegoleva N.N.	598	Sintes T.	688
Shcherbakov M.R.	810	Sinyukhin A.	147
Sheftel E.N.	70, 591	Siruguri V.	46
Shegolev A.E.	186	Siryuk Ju.A.	602
Shelukhin L.A.	783	Sitnikov A.V.	270, 444, 456, 459, 539, 550, 553, 555, 566, 749, 768, 792, 866, 874
Shelushinina N.G.	190	Sitnikov M.N.	513, 620
Sherendo T.A.	130	Sizanov A.V.	528, 657
Sherstobitova E.A.	485	Skibinsky K.M.	799
Sherstyuk N.E.	939	Skidanov V.A.	293, 551, 722
Shevchenko A.D.	240	Skipetrov E.P.	214
Shevelkov A.V.	182, 903	Skipetrova L.A.	214
Shevyrtalov S.	168	Skirdkov P.N.	236, 246, 546, 623
Sheyerman A.E.	181, 329, 634, 897	Skokov K.P.	333, 336, 473, 474, 480, 481, 487, 494
Shigapov I.M.	907	Skomarovsky V.S.	933
Shikin A.M.	246	Skopin E.V.	872
Shimatsu T.	930	Skorohodov E.V.	118, 379, 668, 872
Shimokawa T.	742	Skoropata E.	370
Shimura T.	307	Skorupa W.	212
Shin Kwang Woo	395	Skourski Y.	407, 592, 856
Shindo D.	44	Skryabina M.N.	691
Shipkova I.G.	779	Skulkina N.A.	583
Shishkin D.A.	289, 599	Skumryev V.	847
Shishkin I.S.	163	Skvortsov M.A.	330
Shitsevalova N.Yu.	160, 175, 237, 238, 252, 313, 878	Slavin A.N.	607, 623
Shiyan Ya.	771	Sluchanko N.E.	160, 175, 237, 238, 252, 313, 547, 741, 875, 885
Shlapakov M.S.	167	Sluka V.	884
Shmatov G.A.	659	Slynko E.I.	214
Shmyreva A.A.	79	Slynko V.E.	214
Shodiev Z.M.	597	Smagin V.V.	278
Shokri R.	432	Smarjevskaya A.I.	818
Shorokhova A.V.	365	Smarzhevskaya A.I.	476
Shreder E.I.	244	Smekhova A.	106, 107, 211
Shubakov V.S.	581	Smelova	128
Shubin U.V.	744	Smirnitskaya G.V.	145, 746
Shull R.D.	765, 926	Smirnov A.I.	738
Shulyatev D.A.	593	Smirnov A.N.	912
Shuvaev A.	394	Smirnov A.V.	350
Shuvaeva E.	584	Smirnov I.A.	473
Sickinger H.	27	Smirnov O.P.	170
Sidorenko A.S.	26, 898	Smirnov V.M.	133

Smirnov V.V.	602	Stasinopoulos I.	22
Smith A.	610	Stebliy M.E.	134, 436, 560
Smolyakov D.A.	315, 538, 541, 548	Stepanov A.L.	151
Snegirev V.V.	442, 477, 708	Stepanov G.V.	419, 826, 834
Śniadecki Z.	62	Stepanov S.V.	535
Sobolev A.A.	942	Stepanov V.I.	923
Sobolev A.V.	260	Stepanova E.A.	461, 583, 807
Sobolev A.V.	258, 259, 839, 849	Stepanyuk V.	376
Soh Wee Tee	100	Stepanyuk V.S.	373
Sokolov A.	477	Stepina N.P.	887
Sokolov A.E.	795, 807	Stergiou C.A.	877
Sokolov N.S.	136, 204, 467	Stognei O.V.	550, 770, 775
Sokolov V.V.	620, 795	Stognij A.I.	308, 721, 790, 791, 843
Sokolovskaya Y.A.	479	Stolbov O.V.	416, 417
Sokolovskiy V.V.	40, 341, 479, 496, 585	Stoleriu L.	661
Soldatov T.A.	738	Stolyar S.V.	225, 226, 438
Soldusova A.P.	127	Storozhenko A.M.	690
Solin N.I.	249, 709	Straumal B.B.	108
Solnyshkin A.V.	840	Straumal P.B.	108
Solonetskiy R.V.	410	Strelkov N.	243, 245
Solontsov A.	652	Strelsov S.V.	152
Solovev A.A.	214	Streltsov S.V.	74
Soloviev A.N.	941	Strikhanov M.N.	441
Soloviev I.I.	186, 323, 326	Stroppa A.	153, 247, 695
Soloviev I.N.	941	Strugatsky M.	575
Soloviov D.	825	Strugatsky M.B.	799
Soloviov S.V.	845	Stupakiewicz A.	307, 388, 586
Solovjova A.Yu.	684	Su L.	731
Solovyev L.A.	706	Su Y.	503
Solymar L.	730	Suard E.	713
Solzi M.	345	Subbotin I.M.	833
Somova V.M.	291	Subkhangulov R.R.	378
Sorella S.	123	Sugimoto S.	543
Sorokin A.O.	750	Suhetsky A.A.	231
Sorokin V.V.	419	Sukhachev A.L.	795
Sosin S.S.	97	Sukhorukov A.P.	729
Soukoulis C.M.	733	Sukhorukov Yu.P.	724, 804, 811
Spalek J.	630	Sukhorukova O.	798
Spasova M.	90	Sukovatitsina E.V.	88, 134
Spichkin Y.I.	38, 595, 596	Suleimanov N.M.	176
Spirin A.V.	796	Sulyanov S.N.	224
Srinivasan G.	567	Suñol J.J.	343
Stadler S.	344	Suturin S.M.	204
Stakhanova S.V.	108	Suzuki H.S.	942
Stamenova M.	382	Svalov A.V.	165, 254, 761
Stancu A.	661	Svechkina N.B.	202
Stanescu D.	937	Sviridova T.A.	261
Starchikov S.S.	224, 457	Svistov L.E.	95, 402
Starostenko S.N.	101, 732	Svyazhin A.D.	244
Stashkevich A.	371, 572, 676, 862	Syr'ev N.E.	167, 779
Stashkov A.N.	291	Syromyatnikov A.V.	445, 528, 656, 657
Stashkova L.A.	291, 598	Szajek A.	62

Szymczak H.843

T

Tafeenko V.A.466
 Tagirov L.886
 Tagirov L.R.26, 144, 328, 552, 898
 Tailhades Ph.89
 Takagi H.786, 787, 788
 Takagi T.498
 Takahashi N.742
 Takezawa M.406
 Talaat A.63, 584
 Talantsev A.110, 213
 Talantsev A.D.748
 Talbot D.414
 Taldenkov A.N.708
 Tamion A.372
 Tan X.588
 Tanaka K.700
 Tanaka M.942
 Tanaka S.32
 Tanaka Y.637
 Tang J.931
 Tanigaki T.44
 Tankeev A.P.662
 Tankeyev A.P.278
 Tarasenko A.S.574
 Tarasenko S.V.574, 798
 Tarasenko T.N.858
 Tarasov A.S.315, 536, 537, 548
 Tarasov E.N.478
 Tarasova O.S.768, 874
 Tarenkov V.Yu.179
 Taskaev S.V.336, 480, 481, 715
 Tatarsky D.A.21
 Tatulčenkova685
 Taupin M.917
 Tavares J.M.680
 Tedzhetov V.A.591
 Teichmann M.35
 Telegin A.V.724, 804, 811
 Telegin S.V.511, 512, 709
 Telegina I.332
 Temerov V.L.192, 267, 271, 844
 Tennant D.A.736
 Teplykh A.E.265
 Terada N.942
 Terekhov A.V.240
 Terentev P.B.43, 290, 297
 Tereshina E.A.332, 335, 490, 856

Tereshina I.S.332, 335, 490, 497, 715, 856
 Tezuka N.543
 Thanh Tran Dang272
 Tiberkevich V.607
 Tiberto P.357
 Tidecks R.26, 898
 Tieg C.675
 Tietze Th.108
 Tihomirova K.A.236
 Tikhonov E.V.148, 375
 Timirgazin M.A.448, 651
 Tishin A.M.38, 595, 596
 Titkov A.N.91
 Titov I.S.344, 495, 503
 Titova A.O.591
 Titova M.S.245, 316
 Tkachenko I.A.449
 Tkachev A.V.276, 454, 903
 Toal B.371
 Togulev P.N.176
 Tokoro H.759
 Tokunaga M.392
 Tomita S.929
 Torelli P.50
 Toshchevnikov V.415
 Tourinho F.A.923
 Tournus F.372
 Tovstolytkin A.I.858
 Tra V.T.321
 Tregubova T.N.770
 Tretiakov O.A.314
 Trifonov A.S.182
 Tripathi V.650
 Trofimova N.N.745
 Troitski B.B.667
 Tronov A.A.112
 Troyanchuk I.O.170
 Troyanov S.I.466
 Truhan V.M.838
 Trukhanov P.A.591
 Trusevich N.G.189
 Trusov L.A.603, 831
 Tsikalov D.S.860
 Tsindlekht M.I.349
 Tsirkin S.S.428
 Tskhadadze G.A.487
 Tsujii N.942
 Tsutaoka T.103
 Tselik A.M.736
 Tsvyashchenko A.V.52, 54
 Tsymbal E.Y.17
 Tsysar128

Tu C.M.	902
Tufatullina M.A.	341
Tugarinov V.I.	192, 752
Tugushev V.V.	365, 428, 433, 525
Tumanov V.A.	180
Turchenko V.	255
Turkov V.A.	817, 830
Turkov V.K.	150, 456, 459, 749
Turkoz S.	900
Turpanov I.A.	557
Tusche C.	432
Tyatyushkin A.N.	832
Tyukova I.S.	353
Tzeng W.Y.	902

U

Uba L.	803
Uba S.	803
Uchida H.	117, 718
Udalov O.G.	21, 936
Udod L.V.	513
Ugryumova N.A.	702
Ulyanov M.N.	336, 480, 481
Umetsu R.Y.	168, 340
Umnov P.P.	65
Umnova N.V.	65
Ünal A.A.	82
Ünlü G.	139
Urazhdin S.	607
Urcelay-Olabarria I.	847
Uribe-Laverde M.A.	329
Urs N.O.	84
Urusova N.V.	265
Useinov N.	886
Useinov N.Kh.	552
Ushakov A.V.	152
Usov N.A.	468, 677, 933
Uspenskaya L.S.	172, 666
Uspenskii Yu.A.	148, 216, 375, 458, 621
Ustinov A.B.	268, 851
Ustinov V.V.	39, 58, 451, 522, 540, 622
Ustinova I.A.	573
Ustygov V.A.	565
Ustyugov V.A.	749
Utesov O.I.	657

V

Vabishchevich P.P.	810
--------------------	-----

Vacková T.	142
Vakhitov R.M.	410, 848
Valeev V.F.	151, 453
Valencia S.	82
Valenti R.	153
Valiullin A.A.	132, 144
Val'kov V.V.	635
Valldor M.	94, 212
van den Brink J.	320
Van Haesendonck C.	261
van Lierop J.	370
Vanaken J.	252
Varga L.K.	346
Varga R.	64, 499
Vargova Z.	499
Varnakov S.N.	309, 315
Varyukhin V.N.	179
Vas'kovskiy V.O.	254, 761
Vasenko A.S.	325, 628
Vasil'evskii I.S.	441
Vasiliev A.	739
Vasiliev A.L.	224, 366, 634
Vasiliev A.N.	96, 146, 152, 153, 182, 465, 466, 754, 909
Vasiliev V.G.	419
Vasilyev A.V.	831
Vaskivskiy I.	916
Vasuhno N.V.	235
Vasyukov D.M.	183
Vavilova E.L.	153, 212, 401
Vazhenin V.A.	130
Vazhenina I.G.	438
Vazquez M.	64, 284, 674
Vdovichev S.N.	21, 379, 872
Vdovin V.G.	130
Vedeneev A.S.	365
Vedyaev A.	243, 316
Vedyaev A.V.	245
Vega V.	920
Vejpravová J.	142
Velikanov D.A.	154, 192, 264, 452, 521, 745
Veniaminova Y.	371
Verbetsky V.N.	476
Verchenko V.Yu.	903
Vereshchagin S.N.	706
Vergazov R.M.	562
Vergnaud C.	16
Vergniory M.	428
Vergniory M.G.	432
Vershinin A.V.	43, 296
Vetoshko F.P.	293
Vetoshko P.M.	293, 722

Vidal E.V.	674
Vidal F.	676
Vidal J.	306, 891
Viennot J.J.	28
Viglin N.A.	617
Vikhrova O.V.	203, 233, 367
Vila L.	15, 16
Vilkov E.A.	549
Vinnik D.A.	580
Vinnikov L.Ya.	901
Vinogradov A.P.	116
Vinogradova A.S.	817
Vishnev A.A.	189
Vlasov V.S.	150, 459, 565, 566, 571, 749, 864, 869, 870
Vlasova N.I.	598
Vogel J.	675
Volegov A.S.	285, 289, 294, 589
Volkov D.V.	275, 465
Volkov N.V.	267, 271, 315, 517, 536, 537, 538, 541, 548
Volkova E.G.	599
Volkova O.	739
Volkova O.S.	155, 466, 909
Volochaev M.N.	558, 778
Volodin A.P.	261
Volodina N.S.	873
Vompe T.A.	298
von Bardeleben J.	937
von Dreifus D.	87
von Gratowski S.V.	489, 714
von Löhneysen H.	627
Vopilkin E.A.	667
Vopson M.M.	48
Vorob'ev G.P.	262, 395, 847
Vorobeve V.E.	80
Voronina E.V.	777
Vorotynov A.M.	521, 542, 752
Vrejoiu I.	378
Vylegzhanin A.G.	219
Vymazalova A.	155
Vysotskiy S.L.	865
Vysotsky S.L.	570
Vyzulin S.A.	167, 779

W

Wagner A.	106, 107, 211
Waizner J.	22
Wallbaum L.	694
Wang C.-C.	773

Wang G.A.	619
Wang K.	694
Wang R.L.	491
Wang X.	556
Wawro A.	84
Weber H.W.	491, 617
Weeber R.	76, 77, 687
Wehling T.	382
Wei Fulin	132
Weides M.	27
Weides M.P.	29
Weier C.	648
Weinelt M.	35
Werner P.	111
Werwiński M.	62
Weschke E.	212
Whangbo M.-H.	96, 737
Wiemer M.	640
Wiesendanger R.	10
Wilhelm F.	646, 917, 943
Winkler D.	329, 897
Winkler G.	648
Wintz S.	82
Wolf M.J.	627
Wolter A.U.B.	589
Wolter-Giraud A.U.B.	401
Wosnitza J.	407, 592
Woytasik M.	288
Wray A.L.	321
Wu K.H.	902
Wurmehl S.	694
Wysokiński K.I.	311

X

Xiao F.	772
Xiao Jiang	613
Xu Z.A.	916
Xujanjva D.	808

Y

Yada K.	637
YagubskiiE.	760
Yagupov S.	575
Yagupov S.V.	799
Yakhou-Harris F.	675
Yakimov L.E.	744
Yakovchuk V.Yu.	438
Yakovlev D.R.	641, 719, 915

Yakovleva E.....	215	Zaikovskij V.I.....	745
Yakushechkina A.K.....	219	Zainullina R.I.....	39, 522, 709, 801, 804
Yakushev R.....	825	Zaitsev R.O.....	199
Yakushkin S.S.....	655	Zaitsev S.V.....	641
Yamakage A.....	637	Zakharov K.V.....	214, 754
Yamamoto R.....	921	Zakharov M.A.....	466
Yamamoto S.....	103	Zakharov P.N.....	729
Yamaura K.....	152, 153	Zakharov V.N.....	621
Yanai T.....	405	Zalbidea Arechaga I.....	769
Yang C.P.....	491	Zaleski A.J.....	240
Yang H.X.....	312	Zamoranskaya M.V.....	204
Yanovskiy A.A.....	757	Zamyatin D.A.....	130
Yanushkevich K.I.....	542, 858	Zaporojan S.I.....	287
Yarmdich M.V.....	272	Zaripova L.D.....	132, 144, 227
Yaroslavtsev A.A.....	588	Zarubin A.V.....	492
Yaroslavtsev R.N.....	452, 463	Zavarzina D.G.....	221
Yasin S.....	407, 519, 592	Zavislyak I.V.....	567, 862
Yastremskii I.A.....	384	Zayats A.....	371
Yatsyk I.V.....	98	Zayets V.....	115
Yellen BenjaminB.....	355	Zdoroveishev A.V.....	242
Yelsukov E.P.....	60, 777	Zdoroveushev A.V.....	253
Yerin C.V.....	824	Zdravkov V.I.....	26, 898
Yi W.....	942	Zeer G.M.....	752
Yibole H.....	42	Zelevák V.....	157
Yildirim O.....	106, 107, 211	Zeleváková A.....	157
Yonezawa T.....	787	Zenkevich A.V.....	365
Yoshida T.....	114	Zenkov A.V.....	785
Yoshimine I.....	307	Zezyulina P.A.....	101, 102, 877
Young L.....	610	Zhang W.....	742
Youngblood B.....	610	Zhang Y.....	32
Yu Seong-Cho.....	196, 272	Zharkov S.M.....	752
Yuasa S.....	115	Zhekov K.R.....	273
Yudanov N.A.....	563	Zheludev A.....	772
Yudanov N.Yu.....	838	Zheludev A.I.....	400
Yumaguzin A.R.....	410	Zheng Y.....	676
Yunin P.A.....	203	Zherebtsov D.A.....	580
Yurasov A.N.....	811	Zherlitsyn S.....	407, 519, 592
Yurasov N.I.....	800	Zhevstovskikh I.V.....	519
Yurkin G.Yu.....	771	Zhigalov V.S.....	764
Yurov A.S.....	554	Zhilna T.N.....	221
Yurtaeva S.V.....	218	Zhilova O.V.....	555
Yushkov V.I.....	557	Zhizhaev A.M.....	452
<hr/>			
Z			
Zabel H.....	374	Zholudev S.I.....	818
Zablotskii V.....	586	Zhou H.D.....	402
Zabluda V.N.....	309, 774	Zhou S.....	212, 364, 365, 525
Zagoskin A.....	31	Zhou Y.....	941
Zagrebin M.A.....	341, 479, 496	Zhukov A.....	63, 66, 69, 584, 586, 928
Zaikin A.D.....	318	Zhukov A.V.....	223, 829
		Zhukova V.....	63, 66, 69, 584
		ZhukovM.V.....	501
		Zhuravlev M.Ye.....	245, 316
		Ziese M.....	378

Zilberman P.E.	549
Zingsem B.	90
Zinin A.V.	478
Zinovieva A.F.	887
Zlotnikov A.O.	635
Znoyko S.L.	361
Zolotareva R.V.	643
Zotova O.V.	286
Zubakin D.	792
Zubarev A.Yu.	420, 828
Zubavichaus Ya.V.	774
Zubavichus Y.V.	745
Zubin A.Y.	239
Zubov V.E.	671
Zuev Yu.N.	58
Zverev V.I.	38, 395
Zverev V.N.	901
Zverev V.V.	587
Zvereva E.A.	96, 152, 153, 155
Zvezdin A.K.	53, 149, 236, 246, 274, 395, 546, 623, 719, 845, 852, 856
Zvezdin K.A.	236, 246, 535, 546, 623
Zvonkov B.N.	203, 233, 253, 367
Zvonov A.I.	504, 505
Zvyagin A.A.	273
Zvyagina G.A.	273
Zykov G.S.	168, 367, 444, 804
Zyuzin A.M.	867

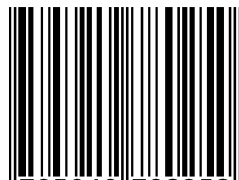
Notes

Notes

Notes

PRINTHOUSE
.LETO

ISBN 978-5-91978-025-0



9 785919 780250

Изготовлено PrintLETO.ru
г. Москва, Нижняя Сыромятническая д. 10/4, этаж 1
Тел. + 7(495) 728-09-42, Офис +7(495) 995-09-39
Тираж 300 экз.